



CTU REPORTS

Proceedings of
WORKSHOP 2005

Part A

CZECH
TECHNICAL
UNIVERSITY
IN PRAGUE

SPECIAL ISSUE

March 2005
Volume 9

These are the Proceedings of the Thirteenth Annual university-wide seminar WORKSHOP 2005 which took place at the Czech Technical University in Prague from 21st to 25th March, 2005.

The aim of the seminar is to present and discuss the latest results obtained by researchers especially at the Czech Technical University in Prague and at collaborating institutions.

The organizing committee has selected a total of 514 contributions divided into 15 different areas of interest:

• **Part A:**

- mathematics
- physics
- informatics and automation engineering
- electrical engineering and instrumentation
- materials engineering

• **Part B:**

- mechanics and thermodynamics
- mechanical engineering
- production systems, technology and technological processes automatisaton
- energetics and power engineering
- nuclear engineering
- chemistry
- biomedical engineering
- civil engineering
- architecture, town planning, geodesy and cartography
- transportation, logistics, economy and management

Organizing committee:

Chairman: Bohuslav Říha

Members (in alphabetical order):

Karel Andrejsek, Tomáš Brandejský, Vítězslava Drtinová, Jiří Houkal, Libor Husník, Zbyněk Kabelík, Květa Lejčková, Milan Němec, O^a tlc'R^a tqx^a . 'Markéta T flk nqx^a . 'Ondřej Rypar , Bohuslav Říha, Jana Schneiderová, Ida Skopalová, Rcxgn'Smřčka, Rcxgn'Uxqdfc. 'Jan Šístek, Eva Šmídová, Jaroslav Zeman

Prague, March 2005

ISBN 80-01-03201-9

This book was prepared from the input files supplied by the authors. No additional English style corrections of the included articles were made by the compositor.

Published by the Czech Technical University in Prague. Printed by CTU Publishing House.

CONTENTS

1. MATHEMATICS

Multilevel Additive and Multiplicative Schwarz Method	22
<i>I. Pultarová</i>	
A Method of Inverse Kinematics Solution for a 6R Robot Manipulator	24
<i>C. Hao</i>	
Geometry for Shell Constructions	26
<i>J. Černý, J. Vecková</i>	
Mathematical Modelling of an Aquifer Contaminated by Organic Compounds II.	28
<i>J. Mikyška</i>	
Three Ways to GPS Altimetry Problem Solution.....	30
<i>M. Kočandrlová, S. Olivík</i>	
Modelling a MOSFET: Speed vs. Accuracy	32
<i>T. Zahradnický, R. Lorencz</i>	
Methods for Binary Image Processing Based on Approximation of Surface Diffusion by Cahn-Hilliard Equation and Their Numerical Analysis	34
<i>V. Chalupecký</i>	
Linear Systems with Uncertain Data	36
<i>J. Koničková</i>	
Computations of Stationary Probability Vectors of a Reducible Stochastic Matrix	38
<i>P. Mayer</i>	
Further Development of Fermat's Ideas in Connection with Applied Mathematics in Engineering	40
<i>A. Šolcová</i>	
Learning Geometry with Maple.....	42
<i>Š. Voráčová</i>	
Improvement of the Course Game Theory and Optimal Decisions.....	44
<i>M. Hykšová</i>	
Support of Individual Education at Bachelor's Stage of Study	46
<i>M. Hykšová</i>	
Support and Development of Active Approach to Mathematical Education.....	48
<i>M. Hykšová</i>	

2. PHYSICS

Improvement of Physics Teaching Based on Student Laboratory Work at Faculty of Transportation Sciences and Photodocumentation of Laboratory Exercises for www.....	52
<i>Z. Malá, D. Nováková, T. Polcar</i>	

Support of Physics Practical Education at the Faculty of Transportation Sciences of CTU .. 54 <i>Z. Malá, D. Nováková, T. Polcar</i>	
Numerical Modelling of the Origin and Evolution of Plasma Instabilities 56 <i>D. Škandera</i>	
Application of Modern Optical Methods in Physical Laboratory Training at Faculty of Transportation Sciences 58 <i>D. Nováková, Z. Malá, T. Polcar</i>	
Support for Laboratory Practise in Physics – Tests of Knowledge 60 <i>D. Nováková, Z. Malá, T. Polcar</i>	
Satellite Laser Ranging Normal Point Precision Limit 62 <i>K. Hamal, I. Procházka, G. Kirchner, F. Koidl</i>	
Measurement and Interpretation of Soft X-ray Emission Spectra from Nitrogen Capillary Discharge 64 <i>M. Vrbová, A. Jančárek, P. Vrba, A. Fojtík, L. Scholzová, R. Havlíková</i>	
Mathematical Methods in the Physics of Microworld 66 <i>J. Tolar</i>	
Neutron Production at PF 1000 68 <i>P. Kubeš, J. Kravárik, D. Klír, P. Barviř</i>	
Neutron Production at S-300 70 <i>P. Kubeš, J. Kravárik, D. Klír, P. Barviř</i>	
Plasma Technologies for Ecological Applications 72 <i>S. Pekárek, J. Khun</i>	
Temperature Dependence of the Photoluminescence and Scintillation Decay of Yb-doped YAlO ₃ 74 <i>J. Pejchal, V. Můčka, M. Nikl, N. Solovieva, J. Shim, A. Yoshikawa, T. Fukuda, A. Voloshinovskii, A. Vedda, M. Martini, D. Yoon</i>	
Determination of Lifetime of Carriers in Semiconductors InP and CdTe from Photoconductivity and Seebeck effect 76 <i>S. Vacková, D. Tischler, V. Gorodynskyy, J. Oswald, F. Karel, K. Žďánský, L. Pekárek, K. Vacek</i>	
Experimental Results from Z-Pinch Z-150 at CTU 78 <i>D. Klír, P. Kubeš, J. Kravárik</i>	
Optical Absorption Loss at Nano-Rough Silver Back Reflector of Thin Film Silicon Solar Cells 80 <i>L. Hodakova, J. Springer, A. Poruba, M. Vanecek, Z. Brykhar, O. Kluth, B. Rech</i>	
Intensive Course Concepts of Postmodern Physics 82 <i>L. Drška</i>	
Analysis of X-Ray Spectra Using a GA Code 84 <i>P. Adámek, L. Drška, O. Renner</i>	

Measurement of Optical Systems using Shack-Hartmann Sensor.....	86
<i>J. Novák, P. Novák, A. Mikš</i>	
Modern Evaluation Techniques in Optical Testing.....	88
<i>J. Novák, A. Mikš, P. Novák</i>	
Hyperchromatic Optical Systems	90
<i>J. Novák, P. Novák, A. Mikš</i>	
Aberration Analysis in Optical Imaging Systems.....	92
<i>J. Novák, A. Mikš, P. Novák</i>	
Investigation of Phase Evaluation Techniques in Optical Measurement Methods.....	94
<i>A. Mikš, P. Novák, J. Novák</i>	
Evaluation Techniques in Microwave Phase Interferometry	96
<i>A. Mikš, J. Novák</i>	
Mathematical Simulation of Optical Forces	98
<i>A. Mikš, J. Novák</i>	
New Laboratory Experiments in Physics.....	100
<i>A. Mikš, J. Novák, P. Novák, P. Semerák</i>	
Investigation of Optical Measurement Methods for Nondestructive Testing	102
<i>A. Mikš, J. Novák, P. Novák</i>	
Laser Interactions with Low-Density Foams.....	104
<i>J. Limpouch, M. Kálal, R. Liska, M. Šiňor, E. Krouský, K. Mašek, A. Kasperczyk, T. Pisarczyk, N. Demchenko, S. Guskov</i>	
Possible Applications of Goos-Hänchen Effect in Optical Measurement Systems.....	106
<i>P. Novák, J. Novák, A. Mikš</i>	
Polyester Fabric Hydrofobicity Modification with Atmospheric Corona Discharge.....	108
<i>J. Píchal</i>	
Dynamics of Isolated Spherical Bubble in Incompressible Fluid.....	110
<i>V. Sopko, L. Samek</i>	
Measurement of Sub-12-fs Laser Pulses by a Light Emitting Diode	112
<i>M. Smrž, M. Divoký, P. Straka</i>	
Powder Neutron Diffraction Study of Lithium Titanium-based Li-ion Conductors (part II).....	114
<i>S. Vratislav, M. Dlouhá, M. Martinez, L. Mestres</i>	
Laser Annealing of Bi ₂ Te ₃ Thin Film Prepared by Pulsed Laser Deposition.....	116
<i>L. Cudzik, M. Jelínek, V. Studnička, M. Pavelka, P. Atanasov</i>	
Computer Simulation of Magnetron Target Erosion.....	118
<i>T. Kubart, R. Novák</i>	
Development of Arbitrary Lagrangian-Eulerian (ALE) Methods in Plasma Physics.....	120
<i>M. Kuchařík, R. Liska, P. Bureš</i>	

Ozone Generation in Electrical Discharge.....	122
<i>V. Scholtz</i>	
Verification of Method for Description of Secondary Sound Field	124
<i>I. Bláhová, J. Zendulka</i>	
Waves in Pinch Generated by Z-150.....	126
<i>V. Kaizr</i>	
Deposition of Thin Layers by Matrix Assisted Pulsed Laser Evaporation	128
<i>J. Remsa, M. Jelínek,, T. Kocourek, R. Christescu</i>	
Computational Meshes for Plasma Physics and Fluid Dynamics.....	130
<i>P. Váchal, R. Liska</i>	
Numerical Modeling of Radiative Processes in Plasma Fibre.....	132
<i>D. Břeň</i>	
The Use of Radiofrequency and Microwave Discharge for Textile Modification.....	134
<i>J. Koller</i>	
Pulse Stretcher for Chirped Pulse Amplification with High Power – and Spectral – Transmissions.....	136
<i>M. Divoký, M. Smrž, P. Straka</i>	
Transient Absorption of a Bichromophoric Molecule	138
<i>M. Dvořák, J. Zerbs, M. Michl, P. Wagener, Z. Surovec, D. Pánek, J. Schroeder, M. Nepraš, V. Fidler</i>	
Laser Induced Fluorescence for Water Surface Pollution Detection	140
<i>D. Koňářík, J. Blažej, I. Procházka</i>	
Low Background Spectrometer TGV II for Measurement of Double Beta Decay of Cd106 and Ca48	142
<i>P. Čermák, I. Štekl</i>	
Experimental System for Plasma Surface Modification	144
<i>L. Aubrecht</i>	
Secondary Sound Field Around Cylindrical Obstacle	146
<i>I. Bláhová, O. Jiříček, J. Zendulka, M. Brothánek</i>	
Influence of Pleasantness on the General Impression of Tested Sounds	148
<i>R. Jurč, O. Jiříček</i>	
The Automatic Data Acquisition System for Calibrations with Remote Access.....	150
<i>V. Vacek, M. Dione, M. Galuška, M. Doubrava</i>	
Radon Trapping Factory for Low Background Experiments.....	152
<i>I. Štekl, P. Jeanneret, J. Vuilleumier, K. Ciahotný</i>	
Study of the flow through capillary-tube	154
<i>V. Vínš, V. Vacek</i>	
Committing of the Atlas Inner Detector Cooling System in the SR1 Building.....	156
<i>V. Vacek</i>	

Discharge at atmospheric pressure.....	158
<i>P. Barvir, P. Kubes, J. Kravarik, D. Klir</i>	
Observation of Optical Waveguides Arising from Dark Photovoltaic Soliton Propagation in LiNbO ₃	160
<i>M. Bodnár, P. Hříbek</i>	
Radiation Defect Profiles Created by High Energy Protons and Alphas: Simulation of Their Influence on Silicon Power Diodes.....	162
<i>V. Komarnitskyy, P. Hazdra</i>	
Hybrid Plasmachemical System for VOC Decomposition.....	164
<i>S. Pekárek</i>	
Experimental Study of de-NO _x Processes in Non-Equilibrium Electrical Discharges.....	166
<i>S. Pekárek</i>	

3. INFORMATICS AND AUTOMATION ENGINEERING

Implementation of Control in Redundant Parallel Robotic Structures.....	170
<i>K. Belda, J. Böhm, M. Valášek</i>	
Control of Distributed Parameters System by MPC Controller.....	172
<i>J. Roubal, V. Havlena</i>	
Design and Analysis of Model Based Predictive Controllers.....	174
<i>J. Pekař, V. Havlena</i>	
Colour Rough Textures Modelling.....	176
<i>J. Filip, M. Haindl</i>	
Architecture Dependent Linear Code Optimizations.....	178
<i>P. Tvrđík, I. Šimeček</i>	
Software Cache Analyzer.....	180
<i>P. Tvrđík, I. Šimeček</i>	
Possibilities of GPU Computing.....	182
<i>I. Šimeček</i>	
Semi-sparse Cholesky Factorization.....	184
<i>I. Šimeček</i>	
Radiation and Disturbance Caused by PLC Systems.....	186
<i>P. Vančata</i>	
Qualitative Aspects of Image Compression Methods in Multimedia Systems.....	188
<i>M. Klíma, M. Bernas, L. Husník, P. Páta, K. Roubík</i>	
The Research of Copper Pairs Characteristics on High Frequency and their Theoretical Limits for Digital Signal Transmission.....	190
<i>J. Vodrážka</i>	

Load and Memory Balancing of Parallel Envelope Solver of Large Sparse Linear Systems of Equations.....	192
<i>O. Medek, P. Tvrđík</i>	
Placement and Routing for Dynamic Reconfiguration of FPGAs.....	194
<i>M. Daněk, J. Kadlec, R. Matoušek</i>	
Bypass Routing in Survivable Trees.....	196
<i>V. Dynda</i>	
BR(τ) Scheme for Tree Failure Recovery: Applications.....	198
<i>V. Dynda</i>	
Fragment Reconnection in Failed Partially Ordered Trees.....	200
<i>V. Dynda</i>	
Two-Dimensional Pattern Matching.....	202
<i>T. Polcar, B. Melichar</i>	
Rating Information Systems.....	204
<i>K. Hartman</i>	
Adaptation of Intelligent Agents in Artificial Life Domain.....	206
<i>P. Nahodil, D. Kadleček</i>	
SD Card File System for Atmel FPSLIC.....	208
<i>P. Honzik, R. Matoušek, J. Kadlec</i>	
Development of an E-learning Course in Fundamentals of the Linux Operation System.....	210
<i>P. Soukup</i>	
Telecommunication Network Optimization Algorithms.....	212
<i>O. Hudousek</i>	
Design of Self-Testing Circuits Using Parity Codes.....	214
<i>P. Kubalík, H. Kubátová</i>	
Gossiping Algorithms.....	216
<i>M. Šoch</i>	
The Reliability and Safety Modelling for Safety Critical Application.....	218
<i>R. Dobiáš, H. Kubátová</i>	
E-learning Course Development to Support Teaching of Programming Tools.....	220
<i>M. Fejtová, P. Smrčka</i>	
Simulation of Selected Part of Artificial Life Domain.....	222
<i>K. Kohout, P. Nahodil, J. Altmann, F. Duda, L. Foltýn, D. Kadleček, M. Mach, D. Řehoř, J. Svoboda, A. Svrček, O. Fiala</i>	

Image Quality Testing and Comparison for Selected Perspective Image Compression Formats	224
<i>J. Dušek</i>	
Exploitation of the Open Source Relational Database with Spatial Extension for GIS Needs	226
<i>V. Honzík, M. Bořík</i>	
Two-Dimensional Pattern Matching Using Finite Automata.....	228
<i>J. Žďárek, B. Melichar</i>	
Innovation of subject “Communication in Data Networks”	230
<i>P. Bezpálec</i>	
Implementation Signaling Gateway in Next Generation Network	232
<i>J. Baloun, V. Lojík</i>	
Network Attached Storage	234
<i>O. Smíšek</i>	
Ethernet for Real-Time Applications	236
<i>O. Dolejš</i>	
Coordinate Systems in PostGIS and Results of the Transformations	238
<i>M. Bořík, V. Honzík</i>	
Location Methods in GSM.....	240
<i>M. Frýda</i>	
Simulation of Fuzzy Control of Belt Drive Driven by DC Motor.....	242
<i>R. Havlíček</i>	
Hardware for Solving Sets of Linear Conguences	244
<i>J. Hlaváč, R. Lórencz</i>	
Pattern Matching in Compressed Text	246
<i>J. Lahoda, B. Melichar</i>	
Using of VHR and Radar Satellite Data for Environmental Changes Monitoring.....	248
<i>L. Halounová, K. Pavelka</i>	
Update Propagation and Merging in GFS.....	250
<i>P. Rydlo, V. Dynda</i>	
Objective Quality Evaluation of Compressed Video Sequences	252
<i>R. Javůrek</i>	
Codesign in Celoxica DK3	254
<i>M. Kuneš</i>	
Matrix Converter Control	256
<i>J. Lettl, S. Fligl</i>	
Design Retiming in HDL.....	258
<i>L. Kafka, R. Matoušek</i>	

Combustion Engine's Running Roughness Measuring and Utilization for Fault Diagnosis	260
<i>M. Čambál, J. Chyský, M. Novák, I. Uhlíř</i>	
Algorithm Acceleration in Programmable System on Chip	262
<i>M. Bečvář, T. Brabec</i>	
Searching for Regularities in Strings using Finite Automata.....	264
<i>M. Voráček, B. Melichar</i>	
Quantum Technologies for Trust and Security	266
<i>M. Dobšíček, J. Kolář, R. Lórencz</i>	
Searching for Repetitions in the Set of Strings.....	268
<i>P. Matyáš</i>	
Multiple Path Interference and Its Impact on System Design	270
<i>J. Burcik</i>	
Control Design Using Bypass for Sliding Mode Applied to Time Delay Systems	272
<i>J. Fišer, P. Zítek</i>	
Throughput Modelling of Symmetrical Digital Subscriber Lines	274
<i>P. Jareš</i>	
File Integrity Checking in GFS.....	276
<i>P. Rydlo</i>	
Transmission Parameters Analysis of the Low Voltage Power Lines.....	278
<i>T. Hubený, J. Vodrážka</i>	
High Precision Computing through Interval Arithmetic Paradigm	280
<i>T. Brabec, R. Lórencz</i>	
GF(p) Montgomery Multiplication for Cryptosystems on FPGA.....	282
<i>J. Buček, R. Lórencz</i>	
Building Automation in the Education of Control Systems.....	284
<i>P. Burget, V. Vozár, B. Kirchmann</i>	
Data Mining and Visualization Tools.....	286
<i>L. Nováková</i>	
Analysis of GPS Flight Data.....	288
<i>S. Kroupa, D. Pachner, Z. Pech</i>	
Some Internal Structures of the Execution Engine.....	290
<i>M. Dráb, L. Kalvoda, S. Vratislav, M. Dlouhá</i>	
Investigation of Cellular Automata for Diagnostic Purposes	292
<i>J. Schmidt</i>	
Inovation of subject Switching systems I	294
<i>D. Jandera, P. Koloros</i>	
Applications of Genetic Algorithms	296
<i>J. Kubalík, P. Pošík, L. Lhotská, J. Kléma</i>	

Fundamentals of Computer Literacy	298
<i>M. Fejtová, J. Fejt, L. Lhotská</i>	
Image Attributes for Comparison Process	300
<i>M. Čadík</i>	
Kernel-Level Communication Library for Linux	302
<i>M. Kačer, D. Langr</i>	
Timeout-Based Protocol for Monitoring Workstation Clusters	304
<i>M. Kačer</i>	
Authentication Protocol Resistant To Online Dictionary Attacks	306
<i>T. Vanek</i>	
Internet Texbook SARI and Remote Scale Models	308
<i>J. Fuka, M. Kutil</i>	
Gloom of Modern Econometrics and Impacts of Prescott's Nobel Price 2004 Work	310
<i>J. Trinkewitz</i>	
Efficient Number Representation for Floating-Point Operations	312
<i>P. Štukjunger, M. Bečvář</i>	
Verification of CAN Bus Behaviour in Real-Time Systems.....	314
<i>J. Krákora</i>	
Laboratory Model "Bathyscaph"	316
<i>M. Hofreiter</i>	
Modelling and Control of Linear Combustion Engine	318
<i>P. Němeček, O. Vysoký</i>	
Iterative Detection and Turbo-Coding Methods in Spatial Diversity MIMO System	320
<i>J. Včelák, M. Kníže</i>	
Inovation of "Coupled Drives" Laboratory Model.....	322
<i>F. Vaněk, J. Fuka</i>	
Robust Control and Reference Tracking for Nonlinear Uncertain Systems	324
<i>B. Rehák, S. Čelikovský</i>	
Multi-Modal Modeling by Sketching	326
<i>R. Ženka, P. Slavík</i>	
Sensitivity Analysis of Inverse Kinematics Problem Solved by Extended Jacobian Inversion Method	328
<i>M. Šoch, R. Lórencz</i>	
Course on Dynamics of Multidisciplinary and Controlled Systems in a Virtual Lab	330
<i>H. Mann</i>	
Graphical User Interface for Robust Control.....	332
<i>P. Urban</i>	
Data Source Aggregation in Semantic Web.....	334
<i>M. Švihla, I. Jelínek</i>	

TEMCON - Transmission Electron Microscope Control	336
<i>Z. Hurák, M. Hromčík</i>	

4. ELECTRICAL ENGINEERING AND INSTRUMENTATION

Calibration Procedure at Shanghai Satellite Laser Ranging Observatory	340
<i>P. Bendová, K. Hamal, I. Procházka, J. Blažej, Y. Fumin, H. Peicheng, Z. Zhongping</i>	
Solid State Detector for Space Applications	342
<i>I. Procházka, K. Hamal, J. Blažej</i>	
Improvement of Laboratory of Microprocessor Applications	344
<i>J. Novák</i>	
The Application of Platinum Silicide in Power Semiconductor Devices	346
<i>D. Kolesnikov, J. Vobecký</i>	
Ultrathin MOVPE Grown InAs Layers in GaAs Characterized by Photomodulated Reflectance Spectroscopy	348
<i>P. Hazdra, J. Voves, E. Hulicius, J. Pangrác</i>	
Education of the Digital Signal Processing in Telecommunication Engineering	350
<i>P. Zahradník</i>	
Digital Audio Signal Processing	352
<i>F. Kadlec, L. Husník, Z. Bureš</i>	
Radiation Defect Profiles Created by High Energy Protons and Alphas: Simulation of Their Influence on Silicon Power Diodes	354
<i>V. Komarnitsky, P. Hazdra</i>	
Optimal Control of Active Magnetic Bearing	356
<i>L. Šynek</i>	
Control of Platinum Profiles in Silicon by Radiation Enhanced Diffusion	358
<i>P. Hazdra, J. Vobecký</i>	
Transfer Functions of Elementary Transducers as Filters of Digital Signal in Acoustic Systems with Direct D/A Conversion	360
<i>L. Husník</i>	
8th International Student Conference on Electrical Engineering POSTER 2004	362
<i>L. Husník, L. Lhotská, T. Bílek, Z. Škvor</i>	
3D Prediction of Electromagnetic Wave Propagation for Wideband Systems Working in MM Band	364
<i>S. Zvánovec</i>	
Communications over DC Power Lines	366
<i>M. Purkert, M. Trnka</i>	
Scientific Facility for Space Research Model of Electromagnetic Vibration Damping	368
<i>J. Masarik, M. Plihal, J. Zdenek</i>	

A New Concept of PTP Vector Network Analyzer	370
<i>V. Závodný, K. Hoffmann, Z. Skvor</i>	
The Utilization of an In-System Programmable Analog Circuit for Education.....	372
<i>M. Havlan, P. Kosek, O. Hudousek</i>	
3-D Components in Microwave Planar Structures	374
<i>V. Sokol</i>	
Objective Image Quality Evaluation Using Artificial Neural Network	376
<i>K. Fliegel</i>	
SYNTFIL – Synthesis of Electric Filters in Maple software	378
<i>J. Hospodka</i>	
Measuring Optical Losses of the Planar Waveguides Fabricated by Ion Exchange of Ag+ -- NA+ and Li+ -- Na+	380
<i>K. Bušek, J. Schröfel</i>	
Measuring System for Verification of Contactless Measurement Methods that Use CCD Cameras	382
<i>T. Radil, J. Fischer, R. Dvořák, J. Kučera</i>	
Analysis and Filtering of Ultrasonic signal	384
<i>V. Matz, M. Kreidl, R. Šmíd</i>	
Design of the Electronic Evaluation Circuits for the Pressure Sensors	386
<i>A. Bouřa, M. Husák, P. Kulha, M. Seidenglanz</i>	
Bistable Laser Diode with a Multiple-Divided Contact Stripe	388
<i>V. Jeřábek</i>	
Overview of the Experimental GNSS Software Receiver Design Issues	390
<i>P. Puričer, J. Špaček, P. Kovář, L. Seidl</i>	
Advanced Methods of Description of Imaging Systems	392
<i>J. Hozman</i>	
Sensors and Microsystems with Thin-Film Piezoresistive Layers for Measurement of Mechanical Values at High Temperatures.....	394
<i>P. Kulha, M. Husák, Z. Výborný, F. Vaněk</i>	
Quantum Devices Transport Simulation.....	396
<i>T. Třebický, J. Voves</i>	
Inovation of Control Systems Education	398
<i>P. Burget, J. Pšenička, J. Bayer, B. Kirchmann</i>	
Modelling of Special Types of Acoustic Receivers	400
<i>P. Honzík, M. Lukeš, D. Kovář</i>	
LC Network for Generation of Solitons.....	402
<i>T. Martan</i>	
Verification of CAN Bus Behaviour in Real-Time Systems.....	404
<i>J. Krákora</i>	

Signal Acquisition and Tracking Methods in GNSS	406
<i>L. Seidl, P. Kovář, P. Puričer, J. Špaček, M. Vičan, P. Kačmařík, F. Vejražka</i>	
Modeling of IR Image Sensors	408
<i>S. Vitek</i>	
Bistable Laser Diode with a Multiple-Divided Contact Stripe	410
<i>V. Jeřábek</i>	
Educational Microcontroller at The Faculty of Transportation Sciences CTU in Prague	412
<i>M. Leso, V. Fáběra</i>	
Navigation System with Magnetometers and Accelerometers	414
<i>J. Včelák, P. Kašpar</i>	
Peripheral Circuits for the Silicon MEMS Microphones.....	416
<i>M. Seidenglanz, M. Husák, P. Kulha, A. Bouřa</i>	

5. MATERIALS ENGINEERING

Inverse Analysis of Coupled Water and Salt Transport in Porous Materials Using a Diffusion-Advection Model	420
<i>R. Černý, Z. Pavlík</i>	
Basic Hygric and Thermal Properties of Two Self-Compacting Concrete Mixtures.....	422
<i>E. Mňahončáková, M. Jiříčková, R. Černý</i>	
Experimental Setup for Monitoring Coupled Water and Salt Transport in Building Materials	424
<i>M. Jiříčková, Z. Pavlík, R. Černý</i>	
Basic System of Experimental Methods for Testing and Quality Evaluation of New Building Materials	426
<i>R. Černý, Z. Pavlík</i>	
Thermal and Hygric Characteristics of Composite Materials on the Basis of Alkali-Activated Slag.....	428
<i>L. Friedlová, R. Černý</i>	
Effect of Admixtures on the Properties of FGD Gypsum.....	430
<i>P. Tesárek, R. Černý</i>	
Lime Plasters with Pozzolan Admixtures: a Perspective Material for Building Renovation	432
<i>V. Tydlitá, P. Tesárek, R. Černý</i>	
Tensile Properties of Neutron Irradiated Reactor Pressure Vessel Steel.....	434
<i>P. Haušild, M. Kytka, M. Karlík, P. Pešek</i>	
Influence of Neutron Fluence on Ductile Crack Growth in Reactor Pressure Vessel Steel..	436
<i>P. Haušild, M. Kytka, M. Karlík, P. Pešek</i>	
Innovation of Computer Graphics Stream at the CTU FEE	438
<i>I. Jelinek</i>	

Study and Development of CrN Layers Prepared by the Multiplex IBAD/CVD Technology	440
<i>D. Tischler, S. Semenko, O. Pacherová, J. Gurovič</i>	
Study and Prepared Cr(N) Layers as Anticorrosive Protection.	442
<i>T. Horaždovský, D. Tischler, S. Semenko, S. Vacková, J. Gurovič, V. Chmelik</i>	
The Variations of Thermal Conductivity and Porosity of Cementitious Composites Due to the Thermal Load	444
<i>J. Toman, E. Mňahončáková, P. Rovnaníková, R. Černý</i>	
Yield Strength of Low Carbon Cast Steels	446
<i>K. Macek, J. Cejp, G. Pluphrach</i>	
Research of Technology Used for Fabrication of Active and Passive Waveguides on Semiconductor Base.....	448
<i>V. Prajzler, I. Hüttel, J. Špirková, J. Oswald, V. Peřina, J. Haměček, V. Machovič, Z. Burian</i>	
Polymer Optical Planar Waveguides Containing Erbium Ions	450
<i>V. Prajzler, M. Prajer, I. Hüttel, J. Špirková, J. Ondráčková, J. Oswald</i>	
Measurement of Optical Losses in Gallium Nitride Layers	452
<i>V. Prajzler, M. Skalský, I. Hüttel, J. Špirková, J. Stejskal, V. Drahoš, Z. Burian</i>	
Textural Fractography of Fatigue Failures under Variable Cycle Loading – Direct Solution.....	454
<i>H. Lauschmann, J. Šumbera, F. Šiška, I. Nedbal</i>	
Elastic Properties of NiTi and CuAlNi Shape Memory Alloys in the Vicinity of Martensitic Transformation	456
<i>P. Sedlák, H. Seiner, M. Landa, V. Novák, P. Šittner</i>	
Influence of High Temperature Degradation on Fatigue Crack Growth in Cr-Mo Tube Steels	458
<i>J. Kunz, J. Siegl, P. Kopřiva, J. Kudrman</i>	
Basic Methodology for the Assessment of Production Technology of Cement Composites with Non-Metallic Fiber Reinforcement.....	460
<i>J. Němečková, R. Černý, P. Padevět, L. Kopecký, J. Němeček</i>	
Detection Possibility of Microstructure of Steel by Eddy Current	462
<i>J. Hořejší, J. Pitter, P. Tichý, L. Vokurka, J. Cejp</i>	
Properties of PVD Coatings for Cutting Tools	464
<i>A. Winklerová, J. Měřejovský, J. Cejp</i>	
Continuous Casting Technologies for Production of Aluminium Alloy Sheets for Transportation Applications.....	466
<i>M. Karlík, M. Slámová, Z. Juříček, K. Sejk, Y. Birol, M. Dündar</i>	
Solution of Heat and Moisture Transport in a System with Interior Thermal Insulation Using the Computer Code TRANSMAT	468
<i>J. Maděra, M. Pánek, R. Černý</i>	

TRANSMAT – a Computer Simulation Tool for Modeling Coupled Heat and Moisture Transport in Building Materials	470
<i>J. Maděra, R. Černý</i>	
Water and Water Vapor Transport Properties of Hydrophilic Mineral Wool	472
<i>P. Michálek, M. Jiříčková, Z. Pavlík, R. Černý</i>	
A Comparison of Hygric Properties of Three Different Insulation Materials	474
<i>Z. Pavlík, M. Jiříčková, P. Tesárek, M. Gazdo, R. Černý</i>	
Experimental Assessment of Thermal Properties of Thermal Insulation Materials as a Basis for Their Proper Technical Utilization	476
<i>Z. Pavlík, M. Jiříčková, P. Tesárek, M. Gazdo, R. Černý</i>	
Thermal and Hygric Properties of Ceramic Brick: Reference Data Measurements for Application in Modeling Coupled Moisture and Heat Transport	478
<i>Z. Pavlík, M. Jiříčková, P. Tesárek, P. Rybár, R. Černý</i>	
Inverse Modeling of Water and Salt Transport in Building Materials: The Choice of a Proper Model	480
<i>Z. Pavlík, R. Černý</i>	
Experimental Setup for Measuring Moisture Profiles in Building Materials Using Time-Domain Reflectometry	482
<i>Z. Pavlík, M. Jiříčková, R. Černý</i>	
Application of Fractal Geometry in Textural Fractography of Fatigue Failures	484
<i>Z. Sekerešová, H. Lauschmann</i>	
Computational Simulation of Hygrothermal Performance of Building Envelopes on Modified FGD Gypsum Basis	486
<i>P. Tesárek, J. Maděra, M. Pánek, R. Černý</i>	
Measurement of Basic Material Parameters of High Performance Concrete Using SORPTOMATIC 1990	488
<i>D. Stoklasová, M. Jiříčková, R. Černý</i>	
Microstructure of Fe-3wt. %Si Monocrystal Close to the Fracture Surface	490
<i>M. Karlík, P. Haušild, M. Landa</i>	
Fracture of Fe ₃ Al-Zr Intermetallic Alloy at Elevated Temperatures	492
<i>J. Prah, P. Haušild, M. Karlík, J. Crenn</i>	
Neutron Diffraction Texture Investigations of Zircaloy-4 Tubes	494
<i>M. Dlouhá, S. Vratislav, L. Kalvoda, A. Chichev</i>	
Image Analysis of Cement Paste	496
<i>K. Forstová, J. Němeček</i>	
Improvement of Application Properties of Gypsum	498
<i>A. Vimmrová, L. Svoboda</i>	
Strain Energy Density and Crack Rate along the Curved Fatigue Crack Front	500
<i>T. Denk, V. Oliva, A. Materna</i>	

FEM Simulation of Plastic Zone in Front of the Fatigue Crack with Shear Lips.....	502
<i>A. Materna, V. Oliva, T. Denk</i>	
Project ITER: FEM Simulation of Mechanical Tests of a Primary First Wall Panel Attachment System	504
<i>V. Oliva, T. Denk, A. Materna</i>	
Structure Changes of Concrete Due to Gamma Radiation	506
<i>V. Sopko, L. Samek</i>	
The 3D Reconstruction of Fracture Morphology by Means of a Metallographic Microscope.....	508
<i>M. Ponec, I. Karovičová, H. Lauschmann</i>	
Texture Analysis of poly(Vinyl Chloride) Foils.....	510
<i>L. Kalvoda, M. Dlouhá, P. Sedlák, S. Vratislav</i>	
Novel Sensors of Alkali Metal Ions Based on Optical Fibers	512
<i>R. Klepáček, L. Kalvoda</i>	
Quantitative Texture Analysis of Grain-Oriented Steel Sheets.....	514
<i>S. Vratislav, M. Dlouhá, L. Kalvoda, A. Grišín</i>	
Chemisorbed Zeolitic Catalysts Studied by Powder Neutron Diffraction and 13C MAS NMR	516
<i>S. Vratislav, M. Dlouhá, A. Chichev, A. Balagurov, V. Bosáček</i>	
Hygric and Thermal Properties of a Cracked High Performance Concrete.....	518
<i>E. Mňahončáková, M. Jiříčková, R. Černý</i>	
Microstructure and Mechanical Properties of the Accumulative Roll Bonded AA 8006 Alloy	520
<i>P. Homola, M. Karlík, M. Slámová</i>	
Pozzolanic Admixtures in Lime Plasters – Mechanical Stress Caused by Temperature and Moisture Changes.....	522
<i>A. Kunca, V. Tydlitát, R. Černý, P. Rovnaníková</i>	
Influence of Materials on Wear of Blade Impellers	524
<i>D. Čuprová, I. Fořt, J. Cejp, T. Jirout, F. Rieger</i>	
Residual Stress Analysis of Steel Surfaces after Progressive Methods of Machining	526
<i>N. Ganev, I. Kraus</i>	
Grain Size of Ferrite in Low Carbon Microalloyed Cast Steels	528
<i>G. Pluphrach</i>	
Study and Preparation of CrN, CrCN and Cr(x)C(y) Layers as a Protection against Corrosion. Testing of Mechanical Properties.....	530
<i>L. Berka, N. Murafa, D. Tischler</i>	
Consortium for R&D of Tribological Coatings	532
<i>R. Novák, T. Kubart, D. Nováková, T. Polcar, T. Vítů</i>	
Microscopic Analysis of Hardness of a Material Surfaces and Evaporated Layers	534
<i>N. Murafa, L. Berka, O. Bláhová, I. Štěpánek</i>	

A Few Comments on Life Time of Automobile Components	536
<i>J. Zýka</i>	
Electro-Osmotic Flow in Building Materials III.....	538
<i>L. Balík, L. Svoboda</i>	
Changes of Material Characteristics of Concrete under the Freeze-Thaw Loading.....	540
<i>T. Doležal, P. Konvalinka</i>	
Fracture Behaviour of Functionally Graded Materials	542
<i>J. Bensch</i>	
Heat Treatment of Wind Power Station Shafts	544
<i>K. Dalíková, Z. Nový, D. Kešner</i>	
X-ray Diffraction Analysis of Zr-Based Alloys Oxidized in Steam at 1000 °C	546
<i>G. Gosmanová</i>	

Section 1

MATHEMATICS

Multilevel Additive and Multiplicative Schwarz Method

I. Pultarová

ivana@mat.fsv.cvut.cz

Department of Mathematics, Faculty of Civil Engineering, Czech Technical University,
Thákurova 7, 166 27 Prague 6, Czech Republic

The estimate of the C.B.S. constant

Multiplicative and additive Schwarz methods belong to a group of multilevel methods, which represent the existing trend in numerical computing. We have studied the multilevel approach to solution of partial differential equations, namely with the use of multilevel wavelet algorithms. But wavelet methods used in this area are important mainly from the theoretical point of view and they can be hardly applied to the solution of very large scaled real-life problems. The need of some more simply applicable sets of functions leads to hierarchical finite element bases. At present, these functions are mostly used in two level algorithms, which exploit the properties of Schur complement. The condition number of the matrix of the resulting preconditioned system of linear equations arising from finite element discretization, depends on the relation of two subspaces of functions, belonging to the finer and to the coarser finite element grid. More precisely, this relation can be expressed by the strengthened Cauchy-Bunyakovski-Schwarz (C.B.S.) inequality constant γ . The condition number κ of the resulting preconditioned system can be estimated by relation $\kappa \approx \frac{1}{1-\gamma^2}$. Let a denote the symmetric positive definite bilinear form according to the problem and let us consider two level hierarchical finite element spaces. Let us denote U and W the spaces of finite element functions belonging to the coarser grid and to the finer grid, respectively. Then the strengthened C.B.S. inequality is $|a(u, w)| \leq \gamma \sqrt{a(u, u)} \sqrt{a(w, w)}$ and it holds for any $u \in U$ and $w \in W$.

The first of the two results of the grant project is the establishing the estimate of the strengthened C.B.S. inequality constant γ made for the elliptic partial differential equation of two variables with nonconstant coefficients and for two level hierarchical bilinear finite elements with rectangular support [1]. We have derived the upper bound for γ and we have shown that the estimate is sharp, i.e. there exist circumstances under which the equality matches in C.B.S. inequality with γ equal to its upper bound. The value of γ is $\sqrt{3/4}$ for anisotropic case, which is the same quantity as for the linear finite elements with triangular support. As for the isotropic case, the constant γ equals to $\sqrt{3/8}$. This value is lower than that in the case of linear finite elements with triangular support, which yields the value γ equal to $\sqrt{1/2}$. This result qualifies the problems discretized by bilinear finite elements to be preconditioned effectively by multilevel methods, the isotropic problems admit even better properties for rectangular than for triangular elements. We have also computed some estimates of the C.B.S. constant for two level bilinear finite elements with varying size of the sub elements [2]. But these results have not been completed yet. Some computational aspects for highly varying coefficients and for multilevel approach can be found in [3].

Multilevel method for stochastic matrices

As a second result of the grant project, a contribution to the convergence theory of the two level iterative algorithm, called iterative aggregation-disaggregation (IAD) method of finding stationary probability vector of a stochastic matrix, is presented. Let us suppose that B is a column stochastic matrix. Then it is to find a vector x such that $Bx = x$ and $\|x\| = 1$. Matrix B is supposed to be irreducible and not cyclic. Then B is known to have only one eigenvalue equal to 1 and the other eigenvalues are less than 1 in magnitude. A sufficient condition for the local convergence of IAD method and the corresponding rate of convergence have been established. The core of IAD methods consists of repeating two main steps. In the first step, the events are partitioned into aggregation groups. Thus the original problem is transformed to the smaller size problem in the manner described e.g. in [1], considering only the relations between groups. The corresponding collapsed matrix is also column stochastic. The first step finishes by computing its eigenvector corresponding to the Perron eigenvalue 1. In the second step, the obtained eigenvector is projected to the original size of the problem and several correcting iterations are performed. Correction can be done using variety of methods: power method, block Jacobi method, block Gauss-Seidel method, etc. In the end of the second step, the convergence is tested and the algorithm is either stopped or it continues with step 1. There are lots of results available on the convergence of IAD method using partition into only two aggregation group. Concerning the multidivision, some convergence analysis results are presented in literature, but they cannot be used in order to decide whether IAD algorithm for particular data will converge or not. We have established [1,3] the local convergence sufficient condition for such an IAD algorithm, when the correction is done by one iteration of power method. When the original matrix B involves at least one positive row, then the IAD algorithm converges locally and the error descents like the powers of $(1-\delta)^{1/2}$, where δ is the minimal element of that row. In addition to it, when $B \geq \delta P$ then the errors drop like the powers of $(1-\delta)$. Here P is the Perron projection matrix of B . The example, in which IAD method doesn't converge even locally, is presented in [4].

References:

- [1] I. PULTAROVÁ: *The Strengthened C.B.S. Inequality Constant for Hierarchical Bilinear Finite Element Functions*, Proceedings of conference Iterative Methods, Preconditioning and Numerical PDEs, 2004, pp. 110-118.
- [2] I. PULTAROVÁ: *The Strengthened C.B.S. Inequality Constant for Second Order Elliptic Partial Differential Operator and for Hierarchical Bilinear Finite Element Functions*, submitted to Application of Mathematics, 2004.
- [3] I. PULTAROVÁ: *Multilevel bases for second order elliptic partial differential equations with variable coefficients*, accepted for publication in International Journal of Computational Engineering Science, 2003.
- [4] I. MAREK, I. PULTAROVÁ: *Two Notes on Local and Global Convergence Analysis of Iterative Aggregation-Disaggregation Method*, submitted to Linear Algebra and its Applications, 2004.

This research has been supported by CTU grant No. CTU0200111.

A Method of Inverse Kinematics Solution for a 6R Robot Manipulator

C. Hao

haochaoyang@yahoo.com

Department of Mathematics and Physics, Faculty of Mechanical Engineering, Czech Technical University, Karlovo nam. 13, Prague 2, Czech Republic

This paper deals with the positioning problem of inverse kinematics for a 6R serial robot manipulator, which can be solved by using the technique of inverse transformation in a pure algebraic way and facilitate it by means of the computer algebra system- MAPLE. In contrast to other methods, the proposed algorithms in this paper is more simple.

The task to be performed and the trajectory to be followed by an industrial robot during motion planning is of primary importance in a real-time control problem. The motion takes place in Cartesian space, but most of the industrial robots are controlled in their own joint spaces. In order to execute a motion, a kinematic transformation between the Cartesian space and joint space is needed. Unfortunately, inverse kinematics problem that consists of determination of each joint variable by using the Cartesian space data does not guarantee a closed form solution. The inverse kinematic transformation is nonlinear, and depends on its configuration and structure. Only certain classes of industrial robots such as, Staubli RX series, PUMA series, ABB IRB series, Kawasaki U and J series have closed-form solutions for the inverse kinematics problem [1], [2].

A six-revolute-joint robot manipulator ($O_{i-1} \perp O_i$) which is shown in schematic representation in Fig. 1. This case violates Pieper's conditions, since it does not have a spherical wrist, there is no closed-form inverse kinematic solution. The kinematic model of the manipulator is obtained by using the Denavit and Hartenberg approach. The inverse analysis is the determination of the manipulator parameters $\theta_1, \theta_2, \theta_3, \theta_4, \theta_5$ and θ_6 , given the sixth frame position and orientation T with respect to the base frame.

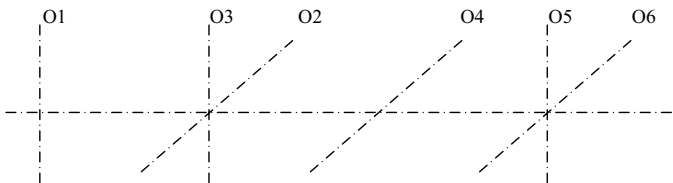


Figure 1: The schematic representation of the six axes

From the forward kinematics equation of this case, we get:

$${}^0T_6 = A_1 A_2 A_3 A_4 A_5 A_6 = (A_1 A_2 A_3)(A_4 A_5 A_6) = (\text{arm motion})(\text{wrist motion}).$$

$${}^0T_6 = {}^0T_3 {}^3T_6; \quad {}^0T_3 = T_{\text{arm}} = T_a = A_1 A_2 A_3; \quad {}^3T_6 = T_{\text{wrist}} = T_w = A_4 A_5 A_6.$$

Since, ${}^0T_6 = T$, so we get: ${}^3T_6 = ({}^0T_3)^{-1} T$.

The value of T and t_w can be computed by software MAPLE, as the follows:

>T := matrix(4,4,[-3/7,6/7,2/7,2/7,-2/7,-3/7,6/7,8/7,6/7,2/7,3/7,5/7,0,0,0,1]);

>t_w := multiply(inverse(matrix(Ta),T).

Since, $T_w = t_w$, we compare the left side and right side of this equation, elements (2,4), (1,3), (1,4), (3,3) and (3,4) from both sides are equated as:

>tw24 - Tw24 = 0;

>-2/7 cos(θ 1) cos(θ 2) sin(θ 3) + 2/7 sin(θ 1) cos(θ 3)- 8/7 sin(θ 1) cos(θ 2) sin(θ 3) - 8/7 cos(θ 1) cos(θ 3) - 5/7 sin(θ 2) sin(θ 3) + cos(θ 2) sin(θ 3) = 0.

>tw13 = Tw13;

2/7 cos(θ 1) cos(θ 2) cos(θ 3)+ 2/7 sin(θ 1) sin(θ 3)+ 6/7 sin(θ 1) cos(θ 2) cos(θ 3)- 6/7 cos(θ 1) sin(θ 3) + 3/7 sin(θ 2) cos(θ 3) = cos(θ 4) sin(θ 5).

>tw14 = Tw14;

2/7 cos(θ 1) cos(θ 2) cos(θ 3)+ 2/7 sin(θ 1) sin(θ 3)+ 8/7 sin(θ 1) cos(θ 2) cos(θ 3)- 8/7 cos(θ 1) sin(θ 3) + 5/7 sin(θ 2) cos(θ 3)- cos(θ 2) cos(θ 3) = cos(θ 4) + 1.

>tw33 = Tw33;

2/7 cos(θ 1) sin(θ 2) + 6/7 sin(θ 1) sin(θ 2)- 3/7 cos(θ 2) = sin(θ 4) sin(θ 5).

> tw34 = Tw34;

2/7 cos(θ 1) sin(θ 2) + 8/7 sin(θ 1) sin(θ 2)- 5/7 cos(θ 2) - sin(θ 2) = sin(θ 4).

Making the following substitutions, and then substituting it to the above five equations:

cos(theta1):=(1-x^2)/(1+x^2); sin(theta1):=2*x/(1+x^2); cos(theta2):=(1-y^2)/(1+y^2);
sin(theta2):= 2*y/(1+y^2); cos(theta3):= (1-z^2)/(1+z^2); sin(theta3):= 2*z/(1+z^2).

We get the four solutions for z:

-3.200596800, -.3124417296, .2999515448, 3.333871811.

If z := -.3124417296, then we can get the six solutions for y:

-2.612486108, .4092927378, 1.714386279, 9.716919132, 10.34442952, 35.16161745.

If y := 10.34442952, then we can get the two solutions for x:

-6.979499051, -.3336145159.

If x := -.3336145159, we can get one of the final solution:

cos(θ 1):= (1-x^2) / (1+x^2) = .7996962462; sin(θ 1):= 2*x / (1+x^2) = -.6004047920.

cos(θ 2):= (1-y^2) / (1+y^2) = -.9814827198; sin(θ 2):= 2*y / (1+y^2) = .1915507004.

cos(θ 3):= (1-z^2) / (1+z^2) = .8221245076; sin(θ 3):= 2*z / (1+z^2) = -.5693077328.

sin(θ 4):= tw34 = .4218371117.

cos(θ 5):= tw[2,3] = -.4979332053.

tan(θ 6):= -tw[2,2] / tw[2,1] = 1.082318740.

References:

- [1] T. BALKAN, M. K. OZGOREN, M. A. SAHIR ARIKAN, H. MURAT BAYKURT: *A method of inverse kinematics solution including singular and multiple configurations for a class of robotic manipulators*, Mechanism and Machine Theory, 35, 2000, pp.1221-1237.
- [2] C. Hao, M. Kargerova: *Analysis of Geometry of a RRP RR Robot Manipulator*, The 23rd Conference of Geometry and Computer Graphics, Czech Republic, 2003, pp. 71-76, ISBN 80-7082-943-5.

Geometry for Shell Constructions

J. Černý, J. Vecková

cerny@mat.fsv.cvut.cz

Department of Mathematics, Faculty of Civil Engineering

The contemporary development of architectural design involves both the possibility of free form surfaces (e.g. Dancing House in Prague), and the classic geometrically defined shapes represented by well known surfaces (quadrics, ruled surfaces, envelopes, etc., e.g. the Glass Footbridge over Corporation Street in Manchester). One of our goals in the grant mentioned below is the studies of geometrical structures – surfaces, which can be applied to the new constructions, see [2], [3]. These papers deal with classical shapes (HP surface, domes, etc.) and their generalizations as well. A classical generalization of the hyperbolic paraboloid is the Hacar surface, which can be found in the papers published some fifty years ago, see e.g. [1].

Our research can be divided into two directions. The first goal is a generalization of HP surfaces using a collinear mapping instead of an affine one. We will speak about a generalized Hacar surface. The notion of this „Collinear Surface“ can be found in several works of Russian mathematicians, see Harant., F. *O kolineačnich plochách*, PhD thesis, 1961, for more information. We try to find a family of suitable surfaces which can be used in practice. The second goal of our work will be the study of these surfaces by means of the theory of small deformations and the membrane theory as well. We suppose that we will follow the paper [4].

The next illustration shows two types of generalized Hacar surfaces. Let $k(t)$ be a curve in the yz -plane and let $h(u)$ be a curve in the xz -plane. Consider an arbitrary plane α_0 with the equation $x=x_0$, where $x_0 \neq 0$. We suppose the existence of the intersection point of the plane α_0 and the curve $h(u)$. We denote it by $H=h(u_0)$. We translate the plane by the vector $(-x_0, 0, 0)$. The translated plane α_0 is the yz -plane, the image of the point H is the point H_p .

Let φ be a central collineation with the centre $S \in k(t)$ and let y be its axis. We suppose there exists a intersection point $K \in k(t)$ of the line SH_p and the curve $k(t)$ such that $K \notin y$. Then the pair of points $\{K, H_p\}$ is a pair of corresponding points in φ . Using an inverse translation on the curve $\varphi(k)=k_p$ we obtain a parameter curve of the surface in the plane α_0 . This procedure can be applied for all suitable x_0 .

The simplest case shows a generalized Hacar surface ρ (type parabola-parabola) generated by a parabola k in the yz -plane with the vertex $V=[0, 0, z_V]$, $z_V > 0$, and passing through the point $P=[0, y_P, 0]$, $y_P > 0$. Its parameterization is $k(t) = \left[0, t, -\frac{z_V}{y_P^2} t^2 + z_V \right]$. Let the second curve director be the parabola h in the xz -plane, with the vertex V and passing through the point $Q=[x_Q, 0, 0]$, $x_Q > 0$. A parameterization of this parabola is $h(u) = \left[u, 0, -\frac{z_V}{x_Q^2} u^2 + z_V \right]$.

The central collineation has the centre $S=[0, 0, z_S]$, $z_S > z_V$. A pair of corresponding points is the pair $\{H=h(u_0), V\}$. If we choose suitable parameters, $x_Q=4$, $y_P=5$, $z_V=3$, the surface is parameterized by the following equation

$$\rho(t, u) = \left[u, 25 \frac{(3u^2 + 64)t}{1600 + 3t^2u^2}, 12 \frac{-25u^2 - 16t^2 + u^2t^2 + 400}{1600 + 3t^2u^2} \right].$$

We have obtained different types of surfaces using this procedure. More examples can be found in [3], where pictures are also provided.

We have obtained interesting examples in the case where the centre S of the collineation is placed in the point $[0, y_s, z_s]$, $z_s > 0$, $y_s \neq 0$. This surface in the case parabola – parabola is presented in the paper [3]. The analytic description of this type of surfaces is in general complicated.

An interesting class of surfaces represent surfaces of the type sinus – sinus. Let a curve director k is a sinus curve in yz -plane parameterized by the equation $k(t) = [0, t, z_v \cos(t)]$. The second director h lies in the xz -plane, $h(u) = [u, 0, z_v \cos(u)]$. The generalized Hacar surface (for suitable parameters) is then parameterized by the function ε

$$\varepsilon(t, u) = \left[u, - \frac{(2 \cos(u) - 7)t}{-2 \cos(t) - 2 \cos(u) + 2 \cos(u) \cos(t) + 7}, 10 \frac{\cos(u) \cos(t)}{-2 \cos(t) - 2 \cos(u) + 2 \cos(u) \cos(t) + 7} \right].$$

The intersection of the plane $z = 0$ is a family of lines, and the surface or its suitable part (and also all surfaces we have presented here) includes a horizontal rectangle, see Fig. 8, 9 in [3]. This condition was a principal condition in the process of generalization of HP surface to a Hacar surface.

References:

- [1] HAVEL, V.: *O plochách klinových I, II* Časopis pro pěstování matematiky 1955 pp. 51-59, 308 - 316.
- [2] ČERNÝ, J. – KOČANDRLOVÁ, M.: *Trojúhelníkové sítě na hyperbolickém paraboloidu* Proc. Int. Symp. on Computational Geometry 2004 pp. 26 - 32
- [3] VECKOVÁ, J.: *Zobecněné klínové plochy* Proc. Int. workshop 2004 2004 pp. 123 - 128
- [4] VELIMIROVIČ, L. *Analysis of hyperbolic paraboloids at small deformations* Facta Univ. Niš 1998 pp. 627 - 636

This research has been supported by MSM 210000010.

Mathematical Modelling of an Aquifer Contaminated by Organic Compounds II.

J. Mikyška

`mikyška@kmlinux.fjfi.cvut.cz`

Department of Mathematics, Faculty of Nuclear Science and Physical Engineering, Czech Technical University in Prague, Trojanova 13, 120 00 Praha 2

Organic compounds belong to the most often encountered contaminants in the groundwater. Many kinds of these contaminants are only weakly soluble in water and behave as Non Aqueous Phase Liquids (NAPL's). These chemicals are often used in the industry, e.g. as industrial solvents like TCE or PCB's, and despite of their low solubilities they usually are highly toxic even in small concentrations and pose the problem for the groundwater quality when they enter the subsurface. Because of their high viscosities and low solubilities their movement is very slow and that is the reason for which the NAPL's usually represent long-time source of the contamination.

Depending on NAPL's density, one can distinguish between the so-called DNAPL's and LNAPL's. DNAPL is a NAPL whose density is higher than the density of water whilst LNAPL is a NAPL whose density is lower than the density of water. When a LNAPL enters the subsurface it percolates down in the direction of gravity through the unsaturated zone until it reaches the water table. Since the LNAPL is lighter than water it spreads along the water table. Unlike the LNAPL, DNAPL infiltrating through the unsaturated zone advances across the water table and continues to percolate down in the direction of gravity through the saturated zone.

Full description of NAPL infiltration through the unsaturated zone requires three phase equations, which describe movement of the three phases (water, NAPL, and air) in the subsurface. If we are interested only in the dynamics of a DNAPL in the saturated zone, we can use the two-phase equations in the so-called pressure-saturation formulation, for details see [1].

These equations supplemented by suitable initial and boundary conditions have been numerically solved using the Control Volume Finite Element Method (CVFE) for discretization in space and implicit Euler discretization in time. Stability of the numerical scheme is achieved by upwinding the relative permeability coefficients. This scheme leads to a system of non-linear algebraic equations which is linearized using modified Newton's method. As a result, this procedure leads to solution of large sparse systems of linear algebraic equations with a non-symmetric matrix. These systems are solved using the stabilized biconjugate gradient method with the multigrid preconditioning. The developed codes can use advantage of the adaptive timestepping which is a very essential feature which is necessary to use for simulation of the real-world problems and is very handy even for computations of some simplified problems.

The developed codes have been tested on the McWhorter - Sunada problem which is a simplified one-dimensional degenerated parabolic problem with a well-known quasi-analytical solution. Since the developed code is two-dimensional, simulations were carried out using the CVFE scheme in a rectangular domain of a long thin stripe shape. Triangular mesh was constructed in such way that the long axis of the stripe is constituted by triangle edges only,

and thus direct comparison of the values of NAPL saturation on the stripe axis with the corresponding values of the quasi-analytical solution was possible. Numerical simulations have been repeated with several settings of numerical parameters. The code has been run on different meshes and with several timesteps. These comparisons with the quasi-analytic solution establish experimentally convergence of the numerical solution towards the exact solution in norms of several function spaces, see [3] for details. During these numerical experiments it was found out that the original McWhorter-Sunada solution admits some generalizations. For details on the original McWhorter-Sunada solution and its possible generalization see [4] and the references in there. Another problem which we used for validation of our code was the Buckley-Leverett problem in which the capillary pressure is neglected. In this case the saturation is driven by a first-order hyperbolic equation. Again, the experiments verified convergence of the numerical solutions towards the physically correct exact solution, see [3] for details.

This multiphase flow model has then been applied to several model problems, in which we have simulated percolation of a dense non-aqueous phase liquid into a heterogeneous aquifer, which was initially fully saturated by water. The aquifer domain is composed of two different sands which are separated by a sharp inclined interface. Main attention has been paid to the complex behaviour of the non-aqueous phase liquid at the interface. We have also addressed the question of importance of the slope of the interface. These simulations used realistic input data and their results can be compared to results of carefully driven laboratory experiments, see [2] for details. The next question considered was the model sensitivity with respect to its input parameters. We have chosen a two-dimensional homogeneous problem and we have solved this problem and compared its solution to the solutions of several perturbed problems. Every perturbed problem differed from the original reference problem in only one parameter whose value was changed by 1%, 5%, 10% and 20 %. Results of this analysis allow us to assess importance of all input parameters and to give indication, which parameters must be measured very accurately if the model should be used for simulations of real-world problems.

References:

- [1] MIKYŠKA, J.: *First Steps Towards Formulation of Surfactant Enhanced NAPL Dissolution Problem* technická zpráva MMG 4-02, 2002.
- [2] MIKYŠKA, J., ILLANGASEKARE T. H.: *Application of a Multiphase Flow Model for Simulations of NAPL Behaviour at Inclined Material Interfaces* to appear in the proceedings of the Czech-Japanese Seminar in Applied Mathematics, conference webpage: <http://geraldine.fjfi.cvut.cz/cjs2004/cjs.php>, 2004.
- [3] MIKYŠKA J., BENEŠ M., ILLANGASEKARE T. H.: *Development and Validation of a Multiphase Flow Model for Applications to NAPL Behaviour in Highly Heterogeneous Aquifer Formations* in proceedings of FEM_MODFLOW 2004 2004 215–218.
- [4] BENEŠ M., FUČÍK R., MIKYŠKA J., ILLANGASEKARE T. H.: *Generalization of the Benchmark Solution for Two-Phase Flow* in proceedings of FEM_MODFLOW 2004 2004 181–184

This research has been supported by the Internal Grant of the Czech Technical University, code number CTU 0410714.

Three Ways to GPS Altimetry Problem Solution

M. Kočandrlová, S. Olivík

olivik@mat.fsv.cvut.cz

Department of Mathematics, Faculty of Civil Engineering, Czech Technical University
in Prague, Thákurova 7, 166 29 Praha 6, Czech Republic

Satellite altimetry is a tool for determining the geoid model. It uses one satellite as a sender and also as a receiver of reflected radar signal. Idea of bistatic (GPS) altimetry is to use one satellite as a receiver and another as sender. Senders can be GPS (Global Positioning System) satellites that gravitate at the high earth orbit (HEO), at the altitude of 20.200 kilometers. As a receiver can be used satellite that gravitates at the low earth orbit (LEO). That means altitude of 300 to 470 kilometers. Bistatic radar altimetry on the ocean surface with two satellites was presented in 1993 by Rubaškin. His model used one LEO satellite as a sender and another satellite at Geosynchronous Orbit as a receiver. In the same year, Martin-Neira suggested and described a system of bistatic altimetry with GPS satellites.

This paper describes three geometric models for bistatic altimetry. All three models produce the reflecting point on an ellipsoid.

The first model uses three rotational quadrics – two ellipsoids and one cone. The first ellipsoid Q_0 is the fully defined geocentric reference ellipsoid WGS 84. The second ellipsoid Q_1 is an ellipsoid of reflecting points. It results from positions of satellites as foci and the semi-axes derived from the length of reflected radar signal. The third rotational quadric Q_2 is the straight circular cone that results from the position of the LEO satellite, the velocity vector of this satellite and the angle between the velocity vector and reflected ray vector.

In the first step we compute the intersection of ellipsoid Q_1 and cone Q_2 . The intersection curve consists of two ellipses in two planes (ρ_1 and ρ_2). These planes are from a beam of quadrics determined by the quadrics Q_1 and Q_2 . We find these planes and identify one of them, where lies intersection points of three quadrics. We sign this plane as ρ . Now we compute the intersection of plane ρ and quadrics Q_0 and Q_1 . On the plane ρ we find the intersection ellipse Q'_1 . Its center O' and vectors of its axes define a local coordinate system S' . In this coordinate system we try to find equations $f_2(x) = 0$ and $g_2(x) = 0$ of the conic sections Q'_0 and Q'_1 , where $Q'_0 = Q_0 \cap \rho$. In the last step we find the reflecting point P . The reflecting point is one of common points of Q'_0 and Q'_1 that fulfill the Fermat principle.

The second model uses two rotational ellipsoids. Ellipsoids Q_0 and Q_1 are the same as in the first model.

In this model we are looking for the points $X_0^* \in Q_0$ and $X_1^* \in Q_1$ such that $|X_0^* X_1^*| = \inf\{|X_0 X_1|; X_0 \in Q_0, X_1 \in Q_1\}$. When ellipsoids Q_0 and Q_1 touch each other, then the point $X_0^* = X_1^*$ is evidently the reflecting point P . We evaluate points X_0^* and X_1^* by the sequence of successive approximations. In the zero approximation are the points X_0 and X_1 intersection points of the corresponding ellipsoid and the line segment between centre points of ellipsoids. Then we make unit normal vectors \mathbf{n}_0 and \mathbf{n}_1 in these points. If a dimension of space $V = \langle X_0 - X_1, \mathbf{n}_0, \mathbf{n}_1 \rangle$ is one, then the pair (X_0, X_1) will be the solution. If a dimension of the space V is greater than one, we choose normal section of ellipsoid Q_0 in

the point X_0 including the point X_1 . Then we determine the centre of curvature of selected normal section. We repeat this process also for the ellipsoid Q_1 . Now we determine the next approximation of points X_0 and X_1 according to determination of initial approximation. The line segment goes now from one centre of curvature to the second. The points X_0 and X_1 are intersection points of the corresponding ellipsoid and this line segment.

The third model uses two rotational ellipsoids. Ellipsoids Q_0 and Q_1 are the same as in the first two models.

In this model we determine the ellipsoid homothetic to the reference ellipsoid Q_0 so that the new ellipsoid touches the ellipsoid Q_1 . The point, where are these ellipsoids touching each other, is the reflecting point P . The homothetic ellipsoid has the same polar flattening as the reference ellipsoid Q_0 . We express ellipsoid Q_1 in geocentric frame. Then we express one ellipse, whose rotation forms the ellipsoid Q_1 . By stepwise derivation we obtain the equation of ellipsoid Q_1 in uniform coordinates. In the affinity, which transform the reference ellipsoid Q_0 to the sphere, we determine an image of the ellipsoid Q_1 - the non-rotational ellipsoid Q'_1 . This transforms the initial problem to the problem how to find a point on ellipsoid Q'_1 nearest to the reference ellipsoid Q_0 , also on the adequate sphere. We solve this problem with the method of stepwise approximation. First we label the intersection of ellipsoid Q'_1 and line segment between midpoints of Q_0 and Q'_1 as a point P' . In this point we compute normal and tangent vectors \mathbf{n} and \mathbf{t} of Q'_1 oriented inward and normal curvature radius r' in direction of \mathbf{t} . Now we determine new position of one end of line segment from the first step. It is a normal curvature centre $O = P' + r'\mathbf{n}$. The next steps are similar to the described process. To the point P' we designate a point P on the ellipsoid Q_1 and an intersection point P_r of the line segment O_0P and the reference ellipsoid Q_0 in an inverse affinity. The point O_0 is a midpoint of the reference ellipsoid Q_0 .

The first geometric model solution is the most dependent on the input data precision. The next two models give comparables results.

References:

- [1] KOČANDRLOVÁ M.: *Geometrický model úlohy GPS-altimetrie*, Sborník 27. konference VŠTEZ, JČMF, 2002, pp. 110–113.
- [2] OLIVÍK S.: *Reflecting point of bistatic altimetry – geometric model with three quadrics* Sborník 3. matematický workshop, FAST VUT v Brně 2004, [CD-ROM].
- [3] MARTIN-NEIRA, M: *A passive reflectometry system: Application to ocean altimetry*, ESA Journal 17, 1993, pp. 331–356.
- [4] WAGNER, C., KLOKOČNÍK, J: *The value of ocean reflections of GPS signals to enhance satellite altimetry: data distribution and error analysis*, J. Geod., 77, 2003, pp. 128–138.

This research has been supported by MŠMT grant No. MSM 21 0000 10.

Modelling a MOSFET: Speed vs. Accuracy

T. Zahradnický, R. Lorencz

{zahradt|lorencz}@cslab.felk.cvut.cz

Department of Computer Science and Engineering, Faculty of Electrical Engineering,
Czech Technical University, Karlovo nám. 13, 121 35, Praha 2, Czech Republic

Parameter extraction algorithms extensively evaluate some form of a mathematical model function which presents the dependency of output data on the input data. In the case of MOSFET transistor parameter extraction, mathematical model forms the dependency of drain-source current on drain-, base-, gate-source voltages including set of approximately 30 other parameters. The task of parameter extraction process is to find out values for some subset of parameters of the parameter set with respect to the data measured. Our parameter extraction process uses a modified version of least squares approximation and is solved by Marquardt's method [1]. Since Marquardt's method requires Jacobi's matrix, a numerical derivative algorithm is necessary. The numerical derivative algorithm we use needs mathematical model be evaluated 5 times for each data point per variable. Since there are 15 extracted parameters and 1500 data samples, the number of model evaluations is as high as 112500 evaluations per a single iteration step. An analysis was performed to find out what percentage of the total extraction time is spent during model's evaluation. We used code analysis tool Shark 4.0 running on Mac OS X 10.3.7 with sample rate of 1 ms to find out how frequently model gets called. The time profile shows that out of 8.9 minutes, 6.5 minutes – approximately 73 per cent of the whole is spent in a function which evaluates the value of MOSFET mathematical model. Improving the evaluation of mathematical model seems to be very promising way to speed up the extraction process. The extraction algorithm extracts about 15 parameters out of 30 and therefore we can use the aspects of dynamic programming and pull the remaining (independent) parameters out of the model's evaluation to cache them. Cached results are then used where possible and an improved version of the mathematical model is then obtained. The improved version of the mathematical model is ~ 37 per cent faster than the old one. We can use Amdahl's law to calculate the overall expected speedup.

Since the overall speedup is approximately 25 per cent, we can be satisfied with this improvement. After changing the extraction algorithm to employ the improved version of mathematical model, a dramatic change happens. The extraction process runs 10.4 minutes instead of 6.5 minutes. The paradox of slowing down instead of speeding up is caused by *rounding and truncation*. After a cross compare of the values of mathematical model at given points, we have found out that they differed due to different approaches used to evaluate them. Since floating point arithmetic is finite, rounding and some form of truncation is inevitable. The form of floating point numbers used in computers is defined by IEEE 754 standard [4] and is widely used. IEEE 754 standard defines two kinds of precision called single and double precision, rounding modes, floating point exceptions and more. The first source of problems was found during the evaluation of the following equation:

$$\phi = 2temp \log \left(\frac{N_{SUB}}{ni} \right). \quad (2)$$

Since ni and $temp$ did not depend on the input parameters nor parameters being extracted and we knew that neither of them could be negative, we could freely split the logarithm into two logarithms. The modified equation was $\phi = 2temp \log(N_{SUB}) - 2temp \log(ni)$ instead. Since a

portion of first and the entire second part of the equation could be cached, the equation evaluated during the model's evaluation simplified to

$$\phi = \phi_{C1} \log(N_{SUB}) - \phi_{C2}, \quad (3)$$

where $\phi_{C1} = 2temp$ and $\phi_{C2} = 2temp \log(ni)$. The problem that appeared was that eq. (2) gave different results from eq. (3) and their results differed by an ulp (unit in the last place). The error analysis [2] of BSD libm log function proved that error of the log function was about a round-off unit. Mathematics software Waterloo Maple was used to find out the more precise approximation of the eq. (2) and found that the correct value up to 17 significant digits was $\phi = 0.79710802480330416$. Once we took ϕ and have it bound it by the error of log function, we found out that we could get three different results that fit into the bounds specified by log function. The result, $\phi_1 = 0.79710802480330412$ (0x3FE981E7B03D1961) is closer to the approximation given by Maple and has relative error $E_1 = 5.36 \cdot 10^{-17}$, and the second result $\phi_2 = 0.79710802480330423$ (0x3FE981E7B03D1962) returned by eq. (3) with a relative error $E_2 = 8.44 \cdot 10^{-17}$ was farther from the approximation. This was, however for a single line of MOSFET's mathematical model. The entire MOSFET model has over 100 lines of C code and is beyond the limits of this text to analyze it.

Rounding errors and especially their accumulation caused mathematical model's value to end up with a last six significant digits different. Such errors happened in each line and it beyond the limits of this article to fully explain what happened and what caused it. The inaccuracy in model's evaluation lead to oscillation of extraction algorithm due to the overall extraction time increase up instead of its reduction. The solution to this problem is to perform the error analysis of the entire mathematical model and use the results to improve model's evaluation. The essential thing is to avoid divide operation and critical cancellation as much as possible. Division is the lengthiest instruction of the entire FPU instructions and is rarely pipelined therefore takes a huge number of cycles and often causes pipeline RAW hazards. It is important to keep in mind that speed *has* to be traded for accuracy.

References:

- [1] MARQUARDT, D. W.: *An algorithm for least squares estimation of nonlinear parameters*. Journal of Society of Industrial and Applied Mathematics, 1963, pp. 341–344.
- [2] HIGHAM, N.: *Accuracy and Stability of Numerical Algorithms*. SIAM, 1996.
- [3] LORENCZ, R.: *A novel extraction method for BJT-parameters*. Journal of Electrical Engineering, Vol. 51, No. 1-2, 2000, pp. 21–29.
- [4] IEEE STANDARD 754: *IEEE Association*, 1985.

Methods for Binary Image Processing Based on Approximation of Surface Diffusion by Cahn-Hilliard Equation and Their Numerical Analysis

V. Chalupecký

chalupec@kmlinux.fjfi.cvut.cz

Department. of Mathematics, Faculty of Nuclear Sciences and Physical Engineering,
Czech Technical University, Trojanova 13, 120 00 Prague 2, Czech Republic

Phase separation is a physical process at micro scale taking place when a binary alloy in thermal equilibrium is undercooled under a critical temperature. Homogeneous state with single phase becomes unstable and the system will try to reach thermodynamical equilibrium. At this point, phase separation will take place and the solution will separate into regions rich in one component and poor in the other. This process can progress in two different ways: as nucleation (nuclei of one component appear randomly and grow) or as spinodal decomposition (the whole solution nucleates at once, periodic structures appear).

Cahn-Hilliard equation with degenerate mobility is a partial differential equation of fourth order used to model isothermal phase separation in two component system [1]. Cahn-Hilliard theory is based on Ginzburg-Landau free energy functional. Minimizing this functional under the constraint of mass conservation yields the division of the domain into regions rich in one of the components and poor in the other, which are separated by a thin interface. This minimizing is realized by evolving the Cahn-Hilliard equation with degenerate mobility. The role of the mobility function is to enhance diffusion on the interface. Important property of the solution of the Cahn-Hilliard equation is the conservation of mass. Existence of the weak solution has been proved by Yin (1992) in one-dimensional case and by Elliot, Garcke (1996) for dimensions higher than one. As for the uniqueness, no results are known so far.

Vast majority of papers treating this equation numerically deals only with the case, when the mobility function is constant and thus non-degenerate. Finite element method for the degenerate case has been proposed by Barrett, Blowey, Garcke in [2].

Besides the mass conservation property the Cahn-Hilliard equation has another property which makes it very useful also for applications other than the simulation of phase decomposition. If we scale the equation properly [3], the thin interface will move according to a motion law called surface diffusion. It is a geometric motion law for curves, which is mass conserving and curve shortening. Here appears the important difference between the constant and degenerate mobility cases. Constant mobility Cahn-Hilliard equation leads to the so called Mullins-Sekerka problem, where nonintersecting interfaces are coupled. Degenerate mobility case leads to surface diffusion, where such interfaces evolve independently. These properties of surface diffusion can be successfully used for applications in image processing, e.g. [4].

In this project, we solve the degenerate Cahn-Hilliard equation by method of lines, discretizing the equation by central finite differences in space and leaving the time variable continuous. The resulting system of ODEs is then solved by an embedded 4th order Runge-Kutta Cash-Karp method with 5th order error estimate, which enables adaptive changes in time step while maintaining the required accuracy. Zero Neumann boundary conditions are treated by reflecting the solution at the boundary.

We have computed a number of numerical experiments and have obtained both the nucleation case as well as the spinodal decomposition case of phase separation. The

numerical experiments also demonstrate that the numerical scheme keeps the property of conserving the mass.

We have justified the theoretical results by measuring the experimental order of convergence of the proposed scheme. Since there are no analytical solutions at our disposal, we used the so called double mesh principle, where we compare the error between solutions on a set of gradually finer meshes. This way, the experimental order of convergence suggests that the scheme is first order accurate.

In order to recover the thin interface layer where the solution changes rapidly, a fine grid has to be used which leads to high computational demands. Therefore, a parallel implementation is necessary in order to be able to execute large amount of computational experiments. We have implemented such parallel version of the proposed numerical scheme using the MPI standard. The computational grid is divided in patches and each process is designated one patch. During the computation, each process updates only its own patch. Values of boundary nodes are computed either from boundary conditions or they are obtained from communication with neighboring processes. All-to-one communication is necessary for I/O operations only and it is kept to minimum. For parallel experiments we used the computational resources provided by Computing and Information centre of CTU (Altix).

Image processing by degenerate Cahn-Hilliard equation

One of the important steps in image processing pipeline is image segmentation, which yields binary image with several objects with possibly distorted or unnecessarily complicated boundaries. The goal is to remove the noise and smooth the edges. This process is called shape recovery. Noise creates interfaces with high curvature, therefore, if we move them according to some curvature-dependent motion law, the noise disappears quickly while dominant features are preserved. This motion law can be for example surface diffusion. It is mass conserving and operates on two different scales (small scale – noise at the boundaries, large scale – shape of the objects). For approximating the motion by surface diffusion, we use the indirect approach – we define the curve of interest as a level set of some higher dimensional function and then use this function as an initial condition for a partial differential equation. In our approach, this function is represented by the segmented image which is used as the initial condition for the degenerate Cahn-Hilliard equation and the boundaries of objects will automatically evolve according to the surface diffusion motion law.

This proposed algorithm has been verified by numerous computational experiments to yield the desired results, both on artificial as well as natural images.

References:

- [1] CAHN, J.W.: *On spinodal decomposition* Acta Met., 1961, pp. 795–801.
- [2] BARRETT, J.W. – BLOWEY, J.F. – GARCKE, H.: *Finite element approximation of the Cahn-Hilliard equation with degenerate mobility* SIAM J. Numer. Anal., 1999, pp. 286–318.
- [3] CAHN, J.W. – HILLIARD, J.E. – NOVICK-COHEN, A.: *The Cahn-Hilliard equation with concentration dependent mobility* Eur. J. Appl. Math., 1996, pp. 287–301.
- [4] BENEŠ, M., – CHALUPECKÝ, V., – MIKULA, K.: *Geometrical image segmentation by the Allen-Cahn equation* Applied Numerical Mathematics, 2004, pp. 187–205.

This research has been supported by CTU grant No. CTU0410514.

Linear Systems with Uncertain Data

J. Koničková

konicko@fsv.cvut.cz

Department of Mathematics, Faculty of Civil Engineering, Czech Technical University,
Thákurova 7, 166 29 Prague 6, Czech Republic

In many practical problems which lead to systems of linear equations, the input data are not known exactly. Usually these are the result of measurements, rounding errors, etc. One of the simplest ways of representation of uncertain or inexact data, as well as inexact computations on them, is based on the so-called interval arithmetic, called also interval analysis. In this approach, an uncertain real number is represented by an interval (a continuous bounded subset) of real numbers which presumably contains the unknown exact value of the number. Vector and matrices whose elements are intervals are called interval vectors and interval matrices, respectively. We consider a system of interval linear equations with a nonsingular interval matrix. The solution set X of this system is connected and bounded (if the interval matrix is nonsingular), it is generally nonconvex, it constitutes an n -dimensional polyhedron which is a sum of at most 2^n convex polyhedrons.

We study a system of interval linear equations $A^l x = b^l$, where $A^l = \{A; \underline{A} \leq A \leq \bar{A}\}$ is a nonsingular interval matrix, $A \in R^{n \times n}$, $b^l = \{\underline{b} \leq b \leq \bar{b}\}$ is an interval vector, $b \in R^n$. The matrix A^l can be written in the form $A^l = [\underline{A}, \bar{A}] = [A_c - \Delta, A_c + \Delta]$, where A_c is the center matrix of A^l , Δ is the radius of A^l . The interval vector b^l is defined analogously: $b^l = [\underline{b}, \bar{b}] = [b_c - \delta, b_c + \delta]$. Under the system $A^l x = b^l$ we understand the family of systems of linear equations $Ax = b$ for all A and b satisfying $A \in A^l$, $b \in b^l$. The solution set of the system $A^l x = b^l$ is defined by $X = \{x; \exists A \exists b Ax = b\}$. We have to find the bounds $\underline{x}_i = \min\{x_i; x \in X\}$, $\bar{x}_i = \max\{x_i; x \in X\}$. We call the interval vector $x^l = [\underline{x}, \bar{x}]$ interval solution (interval hull of the solution set, too). We denote by R_z^n the orthant $R_z^n = \{x; T_z x \geq 0\}$, where T_z is the diagonal matrix with the sign vector z on the diagonal, $z_i \in \{-1, 1\}$.

Many methods are known for calculating interval hull of the solution set. The convex hull of the solution set can be calculated by Rohn's sign-accord algorithm, for calculating the interval hull there can be used the interval Gaussian algorithm, interval Gauss-Seidel method and number other methods. Most of these methods calculate the enclosure of the interval hull instead of the exact interval hull of the solution set.

We present a new method for computing the enclosure of the interval hull of the solution set. We give the algorithm for calculating the enclosure of $X \cap R_z^n$. We will show that the interval hull of the union of these enclosures is the interval hull of the solution set, denoted by x^l . There are presented new formulas, which enable to calculate the enclosure of $X \cap R_z^n$ using iterative computation of two matrices, which are unique solutions of the matrix equations described below. In the case, when the solution set intersects one orthant only, two matrices must be computed only. In the general case, when the solution set intersects all 2^n

orthants, all 2^n enclosures of $X \cap R_z^n$ must be computed. Frequently, the solution set intersects only a few orthants, and the method works efficiently. Using presented method we can compute the interval hull x^I with the prescribed precision. The proofs of presented theorems can be found in [1].

The following theorem can be proved using the theorem given by Rohn [3]. Let A^I be a nonsingular interval matrix. Then the matrix equations $QA_cT_z + |Q|\Delta = E$, $QA_cT_z - |Q|\Delta = E$ have unique solutions Q, Q' .

In the formulae for exact bounds of interval solution x^I we use the interval vector x_z^I defined by

$$\begin{aligned} (\underline{x}_z)_i &= \begin{cases} (Qb_c - |Q|\delta)_i & \text{for } z_i = 1, \\ -(Q'b_c + |Q'|\delta)_i & \text{for } z_i = -1, \end{cases} \\ (\bar{x}_z)_i &= \begin{cases} (Q'b_c + |Q'|\delta)_i & \text{for } z_i = 1, \\ -(Qb_c - |Q|\delta)_i & \text{for } z_i = -1, \end{cases} \end{aligned}$$

where the matrices Q, Q' are the respective solutions of the matrix equations given above. The proof of the following relations for the interval vectors x^I, x_z^I is presented in [1]:

$$X \cap R_z^n \subset x_z^I, \quad \underline{x}_i = \min_z \{(\underline{x}_z)_i\}, \quad \bar{x}_i = \max_z \{(\bar{x}_z)_i\}$$

The algorithm for computing matrices Q, Q' is presented in [1], [2]. This algorithm is derived from the matrix equations given above.

This algorithm can be used in the numerical methods of structural mechanics. Limit load states of reinforced concrete slabs and shells are solved by discretization and linearization using finite element method and linear programming. The input data (staf thickness, reinforcement location and material constants) are known to lie within some real intervals. The interval of the limit load states can be computed using this new algorithm.

References:

- [1] J. KONÍČKOVÁ: *On the Hull of the Solution Sets of Interval Linear Equations*, in Scientific Computing, Validated Numerics, Interval Methods (edited by Walter Kraemer and Juergen Wolff v. Gudenberg), Kluwer, Boston/Dordrecht/London, 2001, pp. 91-102.
- [2] J. KONÍČKOVÁ: *Interval Solutions of Interval Linear Systems*, in Proceedings of the International Conference Mathematical and Computer Modelling in Science and Engineering in honour of the 80th birthday of K. Rektorys, Prague, 2003, pp. 186-191.
- [3] J. ROHN: *Systems of Linear Interval Equations*, Linear Algebra and Its Applications 126, 1989, pp. 39-78.

This research has been supported by MSM 210000003.

Computations of Stationary Probability Vectors of a Reducible Stochastic Matrix

Petr Mayer

pmayer@mat.fsv.cvut.cz

Department of Mathematics, Faculty of Civil Engineering, Czech Technical University
Prague, Thákurova 7, 166 29 Prague 6, Czech Republic

Our goal is to find all steady states of homogeneous discrete time Markov chain. One of motivations for the study of homogeneous reducible Discrete Time Markov Chain (DTMC) is a quantitative risk and reliability analysis for Railways signaling systems see [2]. A natural property of the risk model is a presence of several independent sets of persistent - absorbing states. The sets represent the fundamental classes of the system hazards. For chains with large amount of states is open question, how to find these sets.

Homogenous Finite Discrete Markov Chain is described by nonnegative matrix T and sum of elements of each row is equal to one: $T \geq 0$ and $T^T e = e$, where $e = (1, K, 1)^T$. Such matrix is called **stochastic**. The element T_{ij} of the matrix T is the probability of transition from the state i to state j . The state of Markov chain is described by a vector, whose i -th element is probability that the process is in the state i .

For any stochastic matrix, the number 1 is largest eigenvalue in magnitude. The corresponding eigenvector describes the long time behavior of Markov Chain. When the matrix T describing Markov chain is irreducible the eigenvalue 1 is single and the equation $Tx = x$, $e^T x = 1$ has one solution which is strictly positive. When the matrix T is reducible the eigenvalue 1 has multiplicity larger than 1 and the number of linearly independent eigenvectors is multiplicity of eigenvalue 1.

Any stochastic matrix T can be permuted to the Romanovski canonical form, i.e. there is a permutation matrix P such that

$$P^T T P = \begin{pmatrix} F_0 & 0 & 0 & \Lambda & 0 \\ F_1 & G_1 & 0 & \Lambda & 0 \\ F_2 & 0 & G_2 & 0 & M \\ M & M & 0 & 0 & 0 \\ F_p & 0 & \Lambda & 0 & G_p \end{pmatrix},$$

Such that G_1, Λ, G_p are irreducible stochastic matrices, and spectral radius of matrix F_0 is less than one. The number of irreducible blocks is the multiplicity of eigenvalue 1. The eigenvectors $u_k, k = 1, K, p$ defined by $u_k = (0, 0, K, 0, \tilde{u}_k^T, 0, K, 0)^T$ where $G_k \tilde{u}_k = \tilde{u}_k$ and \tilde{u}_k is on the k -th block position in vector u_k are **extremal stationary distributions**. The problem is to find all blocks G_k and all extremal eigenvectors.

For the case, when matrix T is irreducible the Iterative Aggregation/Disaggregation (IAD) method is good approach for computing this vector, see [2],[3]. In more general situation, when the matrix is reducible the eigenvector for the eigenvalue 1 is not unique. It can be shown, that IAD method may not converge. One approach is in first step analyze graph of matrix T , and then use standard approach to find all extremal eigenvectors separately. But it is impossible when the matrix T is not available elementwise, but just as some formula. It happens for example, when we use for modeling approach of stochastic automata networks. In this situation the matrix T is given as sum of tensor products. We show that problem of

finding all extremal eigenvectors can be solved by analysis of zero/nonzero structure of computed limits by power method with special initial approximations.

We present modification of IAD which is significantly faster than power method, but which preserves the same zero/nonzero structure behavior of computing solution which is necessary for analysis of block structure of matrix T . We prove global convergence for presented modification of IAD method. In special situation, when the non diagonal blocks of matrix T are of small rank, we can prove convergence to exact solution after first iteration. We finish with some numerical examples which demonstrates behavior of presented method.

References:

- [1] KEMENY, J. G. - SNELL, J. L.: *Finite Markov Chains*, Van Nostrand, New York, 1960
- [2] KLAPKA, Š. – MAYER, P.: *Aggregation/Disaggregation method for safety models*, Applications of Mathematics, 2002, pp. 127-137.
- [3] MAREK, I - MAYER, P.: *Convergence analysis of an aggregation-disaggregation iterative method for computation stationary probability vectors of stochastic matrices* Linear Algebra With Applications, 1998, pp. 253-274.
- [4] STEWART, W. J.: *Introduction to the Numerical Solution of Markov Chains*, Princeton University Press, 1994

Further Development of Fermat's Ideas in Connection with Applied Mathematics in Engineering

A. Šolcová

solcova@mbbox.cesnet.cz

Dept. of Mathematics, Faculty of Civil Engineering, Czech Technical University, Prague

We examine Pépin's test for the primality of the Fermat numbers

$$F_m = 2^{2^m} + 1 \text{ for } m = 0, 1, 2, \dots$$

We show that $D_m = (F_m - 1)/2 - 1$ can be used as a base in Pépin's test for $m > 1$.

Some other bases are proposed as well.

Keywords: Fermat primes, Mersenne numbers, law of quadratic reciprocity, primitive roots, quadratic nonresidues.

AMS Subject Classification: 11A07, 11A15, 11A51

In 1640 Pierre de Fermat incorrectly conjectured that all the numbers

$$F_m = 2^{2^m} + 1 \text{ for } m = 0, 1, 2, \dots \quad (1.1)$$

are prime. The numbers F_m are called *Fermat numbers* after him. If F_m is prime, we say that it is a *Fermat prime*. The first five members of sequence (1.1) i.e.,

$$F_0 = 3, F_1 = 5, F_2 = 17, F_3 = 257, F_4 = 65537, \quad (1.2)$$

are really primes. However, in 1732 Leonhard Euler proved that F_5 is composite by showing that $641 \mid F_5$. For a detailed historical account about this affair we refer to [1].

We examine admissible bases for the well-known Pépin's test, which is a sophisticated necessary and sufficient condition for the primality of F_m . It was discovered in 1877 by the French mathematician Jean François Théophile Pépin (1826 –1904). He surely would have been surprised by how many mathematicians will have used his test for more than one hundred years until now. For instance, in 1905 J. C. Morehead and independently A. E. Western found by computing the Pépin residue that the 39-digit number F_7 is composite without knowing any explicit nontrivial factor. Morehead and Western also manually calculated that F_8 with 78 digits is composite. Later F_{10} , F_{13} , F_{14} , F_{20} , and F_{22} were found to be composite by Pépin's test and by the use of electronic computers (the associated literature is given in [1]).

Moreover, very recently the twenty-fourth Fermat number F_{24} , which has over 5 million decimal digits, was shown to be composite by Pépin's test (see [1]). This was the biggest computation ever done to obtain a simple "yes-or-no" answer. It required 10^{17} computer operations. The computational complexity of Pépin's test is discussed in [1]. Note that J. F. T. Pépin entered to the Jesuit Order in 1846. Therefore, some of his papers were published under the name: *le P. Pépin, S. J.*, which means: *Pater Pépin, Societatis Jesu*.

Although hundreds of factors of the Fermat numbers and many necessary and sufficient conditions for the primality of F_m are known, no one has been able to discover a general principle that would lead to a definitive answer to the question whether F_4 is the largest Fermat prime.

Which Fermat numbers can stand as a base in Pépin's test?

Pépin's test. *Let $m \geq 1$. Then*

$$F_m \text{ is prime} \Leftrightarrow 3^{(F_m-1)/2} \equiv -1 \pmod{F_m}.$$

Pépin, in his original paper of 1877, used the base 5 for $m > 1$ rather than the base 3 (see [4]). The base 3 was later suggested by François Proth (1852–1879) see for further references or [1] for the proof. Pépin also noted that the base 10 could be used instead of the base 5 in his test. This fact is generalized.

Classification of Tests

Finding efficient primality tests with a low arithmetic number of operations has been a research area for mathematicians for a long time. This research has gone parallel with the search for the 'largest known prime number'. With the invention of computers, it is now possible to tackle numbers consisting of thousands of digits. Limiting factors are computer memory and machine time. The goal would be to find an algorithm which is of polynomial type, that is where the number of operations increases as a polynomial in n , where n is the number of digits to be tested.

Criteria for the classification of the tests are:

- A. Tests which can be applied to any integer.
 - B. Tests which can be applied to integers of a particular given form, like Pépin's test.
- A. Deterministic tests.
 - B. Probabilistic tests.

Some tests are based on elementary results of the theory of congruences and the theory of quadratic residues. Their historical roots are connected with famous personalities in mathematics as L. Euler, J. Legendre, C. F. Gauss, being based on ancient theories, improved through time, and still today the object of current research (see [2], [3]).

References:

- [1] KŘÍŽEK, M., LUCA, F., SOMER, L.: *17 Lectures on Fermat Numbers: From Number Theory to Geometry*, CMS Books in Mathematics, Vol. 9, Springer-Verlag, 2001, pp.541–549.
- [2] KŘÍŽEK, M. – ŠOLCOVÁ, A. : *Marin Mersenne a jeho prvočísla (Marin Mersenne and his primes*, Matematika, fyzika, informatika, 2002 pp. 204–212.
- [3] KŘÍŽEK, M. – ŠOLCOVÁ, A. : *Prvočíslo 11 v kódování (The prime number 11 v kódování*, Rozhledy mat.–fyz., 79/2004, v tisku.
- [4] PÉPIN, P: *Sur la formule $2^{(2^n)} + 1$* , C. R. Acad. Sci. Paris, 85/1877, pp. 329–331.

This research has been supported by CTU grant No. CTU0400211.

Learning Geometry with Maple

Š. Voráčová

`voracova@fd.cvut.cz`

CTU, Faculty of Transportation Sciences, Dept. of Applied Mathematics,
Na Florenci 25, Prague 1, Czech Republic

The main goals of the project Learning Geometry with Maple were the reinvents education on the Faculty of Transportation, specifically in the subject “Geometry”. The application of suitable software allows creating the spatial imagination of the students and helps them understand quickly and better. Partial tasks could be divided in to three parts:

- Introduce Maple into the Geometry curriculum – study the theoretical background for the practical application and create a list of examples appropriated for the Maple use.
- Set the short learning guide and training materials for the students. Materials present some elementary methods for analytical modeling and visualization of curves and surfaces.
- Improving methods of education in the subject “Geometry”. Each day’s class would be a combination of traditional lecture and problem solving, along with examples using Maple demonstrated to the class as a whole, or worked out on individual workstations

Symbolic manipulations programs, such as Mathematica and Maple are very useful tool for differential geometry. Computations, those are very complicated to do by hand can frequently be performed with ease in suitable Computer Algebra System (CAS). Maple 9 is the environment of choice for scientific and engineering problem solving, mathematical exploration, data visualization and technical authoring. Maple consists of a kernel, a library written in the language of Maple and an interface. The kernel executes most of the basic operations. The library contains commands (procedures) that work in interpretation mode. Built-in programming language support for writing our own procedures allows us to build on the basic capabilities of Maple. Writing code in Maple does not require expert programming skills, so it is ease to start on many of the basics – such as arithmetic computation, solving equations, simplifying expressions and making graphs. Used imaginatively, Maple can help students learn better and faster, and help prepare them using the mathematics technology that they will need throughout their professional lives.

Since using CAS require, except theoretical training, also practical computer training for which only limited time is enabled in the course of training, the project solution was addressed for creation of the Web Interface accessing training materials in electronic form. All results created in the framework of the project can be found on the page. <http://fd.cvut.cz/department/k611/pedagog/K611GM.htm>.

Covering materials include step-by step problem solving; with hints (in Czech) and simple plot commands to illustrate concepts of theme. This pilot project was focused on the individual work of the group of students. We have two goals: to expose the students to modern mathematical software and to learn geometric ideas using the software in ways not possible on the blackboard.

The geometry course was rapidly changed last year to reflect the requirements of the future engineers of transportation sciences. All lectures are available in electronic version (pdf) on <http://fd.cvut.cz/department/k611/pedagog/K611GM.htm>.

Curriculum is divided in to three theoretical parts.

1. Descriptive geometry- parallel and central projection

2. Cartography- basic azimuthal projections – stereographic, gnomonic, orthographic and equal area projections. Cylindrical and conical projection. Plotting a map using Maptools library (available at <http://www.maplesoft.com>)
3. The geometry of curves and surfaces –plane curves in rectangular coordinates, tangent line, arc length parameterization, Frenet formulas, calculating curvature of curves, curves in technical use – the envelope of the system of curves, evolute and involute, clothoid. Regular parametrized surface, methods of generating surface, tangent planes and normal line, ruled surface, surfaces of revolution and helical surfaces.

There are presented both classical methods of descriptive geometry and analytical ones. Produced materials include worked examples – provides students with fundamentals models and illustrations of important concepts and many of suitable exercises. Previous experience with scientific computing is not a prerequisite. In general, simple forms are given, which readers with computer experience can refine and amplify. Example worksheets contain some basic application of Maple to the differential geometry of curves and surfaces. In particular, there are procedures for computing fundamental geometrical invariants. Using the techniques described in proposed materials students can understand concepts geometrically by plotting curves and surfaces on a monitor. The effect of changes in parameters can be strikingly portrayed.

References:

- [1] ROVENSKI, V.: *Geometry od Curves and Surfaces with Maple* Birkhauser 1999, pp. 360.
- [2] NĚMEČEK, A.: *Computer Algebra Systems(CAS)-New Ways in Mathematical Teaching Workshop 98*, ČVUT Praha, 1998 pp. 44-43.
- [3] NĚMEČEK, A.: *Matematika přijemněji*, Sborník 25. konference VŠTEZ, JČMF 1998 pp. 181-184.
- [4] HŘEBÍČEK, J. – PEŠL, J., RÁČEK, J.: *Úvod do Maplu 7* výukový text, Masarykova univerzita, 2002, 74 stran.

This research has been supported by MSM 68/2004.

Improvement of the Course Game Theory and Optimal Decisions

M. Hykšová

hyksova@fd.cvut.cz

Department of Applied Mathematics, Faculty of Transportation Sciences,
Czech Technical University, Na Florenci 25, 110 00 Prague 1, Czech Republic

As the time is passing, the need to motivate students for mathematical education increases. Moreover, due to significant reductions of the extent of mathematical lessons, as well as frequent prejudice against this subject (not only from student's side), it is necessary to search various ways how to "slip" mathematics into the studies and how to convince those prejudiced

of the necessity, usefulness, importance and even attractiveness of mathematics. One of the best opportunities to carry out this purpose is represented by game theory. In a mathematical sense, game is a model of any decision situation, the result of which depends on the decision of at least two different individuals or subjects. Since such situations can be found in almost all fields related to our lives, the field of applications of game theory is exceptionally broad and rich and most problems can be formulated in a very attractive manner. Since the „players“ can be financial houses, creditors, business companies, factories, motorists, users of an information network, troops, fighters, submarines, countries, nations, politicians, political parties, lovers of the same lady, males in rut, genes, etc., the application domain covers economics, industry, transportation, telecommunication, warfare, political and social sciences, biology, ethics and many other branches. On the other hand, game theory leads mathematicians and technicians to such fields as ethology, evolutionary biology, political sciences, sociology, psychology, ethics, etc., that would otherwise remain marginal for many of them.

The facultative course Game Theory and Optimal Decisions taught at the Faculty of Transportation Sciences is the only one at the Czech Technical University, which is solely devoted to this subject. Due to the support by the CTU grant for the year 2004, it was possible to improve the Internet propagation and presentation of the course stressing the interesting and important applications mentioned above, extend the collection of problems for homeworks and create an interactive study text and the collection of practical examples, both written exclusively for students of the technical university with their special needs in mind. The Internet pages of the course are accessible to everyone at the address:

http://euler.fd.cvut.cz/predmety/teorie_her

Compared with the first announcement in the year 2002, the number of participating students has substantially increased; the course is recommended to all students of the economical branch of study and many students from other branches attend it, too, with a positive response.

As far as the content of the course is concerned, the lectures are devoted to the fundamental concepts and solution methods in the fields of non-cooperative and cooperative game theory. After the historical introduction and the foundations of the decision theory, the course starts with basic models used in game theory: explicit form game and normal form game. Main solution concepts are introduced, both zero-sum and non-zero-sum games are discussed. Considerable place is devoted to repeated games, too. Then the cooperative game theory is

investigated with the special interest to the core, shapley value and nucleolus and their mutual comparison. Finally decisions under risk and uncertainty, decisions in conflicts with p-intelligent players and utility theory are explored. To make the theory most accessible to students, each lesson combines the theoretical exposition with the detailed discussion of practical applications, both to motivate new concepts before their introduction and to practise the explained theory. The stress is put on the active approach of students and on their independent work, to be able to use the knowledge gained through the course later in practise.

To illustrate the utilization of game theory in technical domains, let us mention interesting applications in transportation. Game-theoretical models are used for solving problems of the transport network management (whether the network consists of roads, pipelines, sea lanes or flight routes; whether the means of transport is by land, sea, air, or electro-magnetic fields, and whatever goods are being transported), traffic routing and control, traffic allocation, scheduling, transport economics or walker behaviour modelling, to name only few.

As it was mentioned in the introduction, except technical and economic problems, game theory has exceptionally rich applications in many other branches, whose inclusion into the course serves both for motivation and for broadening students' general knowledge. For example, the theory of games is used in political sciences for modelling of various situations related to international relations, elections, legislature, politics of interest groups, lobbies, bargaining, etc. Not only facilitates it to solve particular problems, it provides the exact terminology and methods – what is an underbelly of all social sciences. Although game theory is not a "cure-all" and it can't offer an optimal solution to all problems, it is a strong tool for analysis and it induces the decision-maker to think rationally and without emotions; this, in itself, often yields a general acceptable solution. Probably the most remarkable application domain is biology: game theory is the main tool for the investigation of conflict and cooperation of animals and plants. It is used for the analysis, modelling and understanding the fight, cooperation and communication of animals, coexistence of alternative traits, mating systems, conflict between the sexes, offspring sex ratio, distribution of individuals in their habitats, etc., among botanical applications we can find the questions of seed dispersal, seed germination, root competition, nectar production, flower size, sex allocation, etc. It shall be pointed out that game theory represents the foundations of modern and generally accepted evolution theory – and getting to the heart of our lives is an exceptionally exciting experience.

References:

- [1] HYKŠOVÁ, M.: *Teorie her – prezentace a motivace*, In: *International Conference Presentation of Mathematics*. Technical University Liberec, 2003, pp. 35–42.
- [2] HYKŠOVÁ, M.: *Game Theory and Life*. Slovak University of Technology Bratislava, 2004, pp. 495–500.
- [3] HYKŠOVÁ, M.: *Several Milestones in the History of Game Theory*, In: *VII. Österreichisches Symposium zur Geschichte der Mathematik*. Technische Universität Wien, 2004, pp. 49–56.
- [4] HYKŠOVÁ, M.: *Game Theory – Motivation for Mathematical Education*. Mathematica Montisnigri, to be published in 2005, 8 pp.

This research has been supported by CTU grant No. 0418816.

Support of Individual Education at Bachelor's Stage of Study

M. Hykšová

hyksova@fd.cvut.cz

Department of Applied Mathematics, Faculty of Transportation Sciences,
Czech Technical University, Na Florenci 25, 110 00 Prague 1, Czech Republic

In 2002 the newly organized structure studies at the Faculty of Transportation Sciences of the Czech Technical University were accredited and in the last school year the first students of this system started their education. Among the subjects taught in the first – it means bachelor's stage of study, Mathematical Analysis I (winter semester, 2 lecture hours, 3 hours of tutorials) and Mathematical Analysis II (summer semester, 2+2) can be found. Up to the school year 2002/03, the number of tutorial hours devoted to practical exercises of the theoretical exposition was substantially higher: 4 hours in both semesters. Even worse situation is in the "Distance Learning" consisting of lectures only. For many students it is difficult to understand the theoretical subject matter from textbooks without its detailed investigation at tutorials. The only way how to compensate the loss of hours is the maximal support of individual independent work of each student.

Due to the support by the Universities Development Fund of the Czech Republic, grant FRV 2107f1/2004, it was possible to start the work on the above mentioned aim. New Internet pages of the subjects Mathematical Analysis I and II were created:

"<http://euler.fd.cvut.cz/predmety/mta1>" and "<http://euler.fd.cvut.cz/predmety/mta2>"

A lot of study material is now available at these addresses: newly created study text including theoretical exposition together with the collection of theoretical and practical examples and applications which serve for motivation purposes and which shall help the students to understand the subject matter and computing methods. Moreover, other information on the mentioned subjects, recommended and additional literature, etc., are given there.

Since the necessity is steadily increasing to motivate students for the mathematical education and to show them how useful, interesting and attractive mathematics can be and how important its deep knowledge is, it was necessary to find various applications from many different fields. Including such applications in the course serves for the deeper insight into particular themes, too.

The best experience and the greatest motivation success were achieved with optimization problems that can be solved by the tools of mathematical analysis. In the second semester of their bachelor's stage, students have to attend the obligatory course Microeconomic Theory. A part of this course is devoted to the investigation of total-cost function $TC(q)$, where q denotes the number of units of a product that is produced and marketed, total-revenue functions $TR(q)$ and corresponding marginal-cost and marginal-revenue functions. It is important for students to know, that the rate of change of TC , *marginal cost*, which is often introduced verbally as "the approximate cost of one additional unit of output", is simply the derivative of the total-cost function TC with respect to the amount of the product q :

$$MC = \frac{d TC}{d q},$$

and the rate of change of TR , *marginal revenue*, which is often introduced verbally as “the approximate revenue received from selling one additional unit of output”, is simply the derivative of the total-revenue function TR with respect to q :

$$MR = \frac{d TR}{d q}.$$

It is easy for students to imagine that firms need to solve the problem of revenue maximization or costs minimization and hence that the methods for finding extremes of functions are really important in practice. Similarly, microeconomic theory investigates the properties of demand and supply functions, utility functions, etc. – and these discussions are much more obvious when we can use the concepts of mathematical analysis. In general, the mentioned maximization and minimization problems concern one-variable, as well as multivariable calculus.

From another domain, let us mention a model of traffic flow on a lane of a freeway. The number of cars the lane can carry per unit time is given by

$$N = \frac{-2a}{-2a_1 + v - \frac{2al}{v}},$$

where a is the acceleration of a car when stopping ($a < 0$), t_r is the reaction time to begin braking, v is the average speed of the cars, and l is the length of a car (for the sake of simplicity, we may assume that these values are constant). To find how many cars a lane can carry at most, we need to find the speed v that maximizes N .

Besides optimization problems, interesting applications concern definite integrals which cover – in addition to finding the area of a region – consumer’s and producers’ surplus, total expenditures, fluid flow, inventory, center of gravity, static moments, volumes, etc. It is not necessary to continue in the enumeration of all applications which are convenient for illustration of fundamental concepts and for students’ motivation. The aim of this contribution was only to point out the importance of these matters and to mention the efforts made in this field at the Faculty of Transportation Sciences.

References:

- [1] HYKŠOVÁ, M.: *Matematika v praxi*, In: *Kombinované studium na VŠCRHL, 1. semestr [Textbook on CD-ROM]*. VŠCRHL Praha, 2003, 37 pp.
- [2] HYKŠOVÁ, M.: *Modul Matematika - dle Jar-66*. CERM, Brno, 2003, 114 pp. [Textbook].
- [3] HYKŠOVÁ, M.: *Game Theory – Motivation for Mathematical Education*. Mathematica Montisnigri, to be published in 2005, 8 pp.

This research has been supported by the Universities Development Fund of the Czech Republic, grant FRV 2107f1/2004.

Support and Development of Active Approach to Mathematical Education

M. Hykšová

hyksova@fd.cvut.cz

Department of Applied Mathematics, Faculty of Transportation Sciences,
Czech Technical University, Na Florenci 25, 110 00 Prague 1, Czech Republic

Teachers of mathematical analysis at technical universities are often faced with the problem of rather passive approach of student to their mathematical education and with perpetual attempts to memorize formulas and use them without a deeper understanding – and therefore in a wrong way or in a short examination time only, without the ability to apply them to real problems. Although the university education should differ from the secondary one in treating the students (it deals with adults, no more adolescents), it is still necessary to motivate them to work continuously during the whole semester, since in most cases it is not possible to understand properly the whole subject matter in a relatively short examination period. As the number of students is increasing and the number of hours devoted to tutorials decreasing, it is essential to move students to an active approach to their study and to make them work, in addition to school lessons, individually on solving problems which require more than a mere set of formulas or a “cookbook”, as it is often called, and which gradually lead them to understand the whole subject matter.

To carry out this purpose, the sets of exercises were prepared for the courses on mathematical analysis taught at the Faculty of Transportation Sciences of the Czech Technical University, consisting both of solved problems used for motivation of students and for explaining the basic principles, and unsolved problems that are used for students’ homeworks. Students receive them in batches, according to particular topics, and for each batch there is a fixed term when it must be handed in. The works are evaluated, and by a random selection it is checked during tutorial lessons whether particular students understand the problems they solved (thus, of course, whether they did it themselves). The second way of control are tests, the evaluation of which is also included in the total score for the credit.

The sets of exercises concern the courses Mathematical Analysis I, II and Differential and Difference Equations, taught in the first, second and third semester respectively. The selected solved examples are available at the Internet pages of particular courses, namely:

- Mathematical Analysis I: <http://euler.fd.cvut.cz/predmety/mta1>
- Mathematical Analysis II: <http://euler.fd.cvut.cz/predmety/mta2>
- Differential and Difference Equations: <http://euler.fd.cvut.cz/predmety/ddr>

This project was connected to the project *Support of Individual Education at Bachelor's Stage of Study* whose main aim was to create a study text for the courses Mathematical Analysis I and II for a better understanding the subject matter explained in textbooks and during the lectures and tutorial lessons. The project discussed in this contribution was mainly aimed at the concrete database of practical and theoretical examples, huge enough to generate different batches for different students.

Each batch contains usual exercises formulated mathematically to practise the calculation techniques of particular topics, as well as practical problems formulated in a common language, the solution of which require a proper understanding of the text (which seems itself difficult for many students – although they graduated from the secondary school), to think about the problem in question and the core that shall be solved, to introduce convenient variables and notation, to construct mathematical expression of the practical problem in question, and finally to use the mathematical solution for the correct answer to the original problem. The computation itself is often relatively simple in these practical exercises, but they are important for the development of the ability to apply the knowledge of theoretical concepts to practical problems and hence for better understanding of the theory. Moreover, they have a strong motivation power and show to students that many concepts they are learning in other subjects have a close connection to mathematics and are often nothing more than – for example – derivatives or primitive functions. In this sense, a rich field is micro-economy (obligatory course for all students) with its total-cost and marginal-cost functions, total-revenue and marginal-revenue functions, total-utility and marginal-utility functions, etc.

Let us finish the contribution with two examples, both devoted to some optimization problem. In the field of one variable analysis, a simple but illustrative application is the following one from the transportation domain: “A common transportation enterprise of the city of Chelm is searching an optimal price of a quarterly ticket. Now it costs 1600 CZK and 60 000 people are buying it. A marketing survey reveals that each decrease of 1 CZK in the quarterly charge will result in 30 new customers, and each increase of 1 CZK will result in a loss of 30 customers. What increase or decrease will maximize the monthly revenue, and what is the largest possible monthly revenue?” Similarly with other revenue maximization or costs minimization problems, as well as with optimization problems from various technical branches.

In the field of two variables, for example, interesting examples concern a monopoly: “Suppose a monopolist is practicing price discrimination in the sale of a product by charging different prices in two separate markets. In market A the demand function is $p_A = 100 - q_A$, and in B it is $p_B = 84 - q_B$, where q_A and q_B are the quantities sold per week in A and B , and p_A , p_B are the respective prices per unit. If the monopolist’s cost function is $c = 600 + 4(q_A + q_B)$, how much should be sold in each market to maximize profit? What selling prices give this maximum profit? Give the maximum profit.” Of course, this problem can be arbitrarily modified by changing monopolist’s cost function as well as the demand functions representing the behaviour of the markets in question.

References:

- [1] HYKŠOVÁ, M.: *Matematika v praxi*, In: *Kombinované studium na VŠCRHL, 1. semestr [Textbook on CD-ROM]*, VŠCRHL Praha, 2003, 37 pp.
- [2] HYKŠOVÁ, M.: *Modul Matematika - dle Jar-66*, CERM, Brno, 2003, 114 pp. [Textbook].

This research has been supported by the Ministry of Education grant MSM 75/2004.

Section 2

PHYSICS

Improvement of Physics Teaching Based on Student Laboratory Work at Faculty of Transportation Sciences and Photodocumentation of Laboratory Exercises for

WWW

Z. Malá, D. Nováková, T. Polcar

mala@fd.cvut.cz

Department of Applied Mathematics, Faculty of Transportation Sciences, Czech Technical University, Na Florenci 25, 110 00 Praha 1, Czech Republic

Laboratory practice in Physics I and II has been newly built up at Faculty of Transportation Sciences of ČVUT since 2000. It was used for the first time in the academic year of 2003/04 as part of the Bachelor Studies Program. 230 students on average attend laboratory practices, for 2 hours a week for 2 terms. Laboratory Practise in Physics I and Physics II includes 12 laboratory exercises, and students do the measurements in pairs. Laboratory practice has become even more important after the introduction of structured studies as laboratory practice in physics is one of few possibilities where students can apply and enhance their practical skills in basic types of measurements and where they can also learn methodology of measurement and basic methods of data processing.

During the existence of laboratory practice in physics at Faculty of Transportation Sciences, we managed to build up this practice to an adequate technical level, using Faculty's funds and above all funds provided from grants. All measurement worksites are equipped with new personal computers, the laboratory has its own internal network and the laboratory is connected to the Faculty network. The laboratory has a network-connected printer. Routine processing of measured results is no longer required, data from some measurements are recorded directly through a PC; all the students have to do is to process and evaluate the data. Users programs for processing of the measured dependencies using the least squares method and for processing of repetitive measurements are available to the students.

Level of preparation of students for measurement is one of persistent problems we keep running up against in laboratory practice. Without a good preparation for the measurement, students mechanically follow the recommended sequence of operations, mechanically entering the measured quantity values in formulas listed in the instructions for the laboratory exercises measurement.

We often experience situations where students see drawings and verbal descriptions of individual devices in the instructions for the laboratory practise exercise but cannot imagine what these devices look like. This is probably caused by the fact that our practise is the first instance where students see measuring devices. For many students this is the first time they see even such basic measuring devices as a slide ruler or a micrometer.

We therefore decided, following an example of other faculties, to photo-document individual laboratory exercises and individual devices used in relevant laboratory exercises.

Students can access the photo-documentation on the website for Physics that is located on the Applied Mathematics Department server Euler (<http://euler.fd.cvut.cz/new>).

The photo-documentation will be available to students as of the winter term of the academic year of 2004/05. It is expected that this will make it easier both for students and for teachers as they will not need to explain, at the beginning of practise, that this is for example a device called voltage supply used to control voltage, etc.

Over 100 years ago E.H. Hall discovered that when a magnetic field is applied perpendicular to the direction of a current flowing through a metal a voltage is developed in the third perpendicular direction. This is well understood and is due to the charge carriers within the current being deflected towards the edge of the sample by the magnetic field.

It seems that Hall Effect must be well known for one century. However, in 1985 Klaus von Klitzing won the Nobel Prize for discovery of the quantized Hall Effect. In a two-dimensional metal or semiconductor the Hall Effect is also observed, but at low temperatures a series of steps appear in the Hall resistance as a function of magnetic field instead of the monotonic increase. What is more, these steps occur at incredibly precise values of resistance which are the same no matter what sample is investigated. The resistance is quantized in units of h/e^2 divided by an integer. This is the Quantum Hall effect. Nevertheless, we included in our laboratory exercises Hall Effect measurement in classical form.

We obtained the laboratory set for measuring of Hall Effect in our laboratories. We can measure Hall Effect with variation of magnetic field or current. Moreover, there is possibility to change the temperature of germanium slide, thus, we can demonstrate the temperature dependency of Hall bias. Students will measure Hall bias as a function of increasing magnetic field and/or current and showing that the bias increases with magnetic field or current linearly using linear regression.

References:

- [1] NOVÁKOVÁ, D. – MALÁ, Z.: *Laboratorní cvičení z Fyziky I* ČVUT, Praha, 2002.
- [2] NOVÁKOVÁ, D. – MALÁ, Z.: *Laboratorní cvičení z Fyziky II* ČVUT, Praha, 2004.
- [3] NOVÁKOVÁ, D. - MALÁ, Z., - POLCAR, T.: *Laboratory practise in bachelor studies at Faculty of transportation sciences CTU NTF 2004* Brno 11. - 12.11.2004 p. 338 - 341

This research has been supported by grant CTU0418916.

Support of Physics Practical Education at the Faculty of Transportation Sciences of CTU

Z. Malá, D. Nováková, T. Polcar

`mala@fd.cvut.cz`

Department of Applied Mathematics, Faculty of Transportation Sciences, Czech Technical University, Na Florenci 25, 110 00 Praha 1, Czech Republic

The Physics I, Physics II and Precision of Measurement and Data processing subjects are important, if not fundamental, part of bachelor study at Faculty of Transportation Sciences, CTU in Prague. Laboratory exercises (2 hours per week, 2 semesters) are integrated into physics education for all study programs, while Precision of Measurement is a component of Engineering and technology in transportation. This subject will start in winter semester of 2005/2006 with laboratory exercises of 1 hour per week.

Laboratory practice in Physics I and II has been newly built up at Faculty of Transportation Sciences of ČVUT since 2000. It was used for the first time in the academic year of 2003/04 as part of the Bachelor Studies Program. 230 students on average attend laboratory practices, for 2 hours a week for 2 terms. Laboratory Practice in Physics I and Physics II includes 12 laboratory exercises, and students do the measurements in pairs. Laboratory practice has become even more important after the introduction of structured studies as laboratory practice in physics is one of few possibilities where students can apply and enhance their practical skills in basic types of measurements and where they can also learn methodology of measurement and basic methods of data processing.

During the existence of laboratory practice in physics at Faculty of Transportation Sciences, we managed to build up this practice to an adequate technical level, using Faculty's funds and above all funds provided from grants. All measurement worksites are equipped with new personal computers, the laboratory has its own internal network and the laboratory is connected to the Faculty network. The laboratory has a network-connected printer. Routine processing of measured results is no longer required, data from some measurements are recorded directly through a PC; all the students have to do is to process and evaluate the data. Users programs for processing of the measured dependencies using the least squares method and for processing of repetitive measurements are available to the students.

Batchelor study programs lay stress on practical education and new subject Precision of Measurement will include some novel themes for laboratory exercises dealing with large data collecting. Faculty supposes that the number of students will steadily increase; therefore, we have to obtain measuring devices in appropriate quantity. However, our aim is to retain the same high level of subject quality independently of mentioned rise in students.

Principal executives of Faculty of Transportation Sciences have recognized the importance of physics laboratory exercises and, as a consequence, have agreed with our plan to transfer laboratories to new rooms, which meet all our demands. Thanks to mentioned transfer we have the possibility to prepare more exercises, but it insists new laboratory equipment. Moreover, there is other important factor. Because of high utilize of all equipment,

probability that such equipment will need urgently repair increases. In order to prevent from omission of laboratory exercise we must have sufficient backup in measuring devices.

The aim of this project was obtaining of such backup of equipment. Nevertheless, many measuring devices will be used for improvement of actual exercises, e.g. laser diodes, thermometers, blenders, etc. New laboratory exercise was realized for subject Precision of Measurement and Data processing (in cooperation with the financial support of grant FRV 2102/2004).

References:

- [1] NOVÁKOVÁ, D. – MALÁ, Z.: *Laboratorní cvičení z Fyziky I* ČVUT, Praha, 2002.
- [2] NOVÁKOVÁ, D. – MALÁ, Z.: *Laboratorní cvičení z Fyziky II* ČVUT, Praha, 2004.

This research has been supported by grant FRV 2108/2004.

Numerical Modelling of the Origin and Evolution of Plasma Instabilities

D. Škandera

skanded@fel.cvut.cz

Department of Physics, Faculty of Electrical Engineering, Czech Technical University, Technická 2, 166 27 Prague 6, Czech Republic

In this paper, a present status in the development of the new numerical code is reported. The code is considered for simulations of fluid flows. The finite volume approach is adopted for solving standard fluid equations. They are treated in a conservative form to ensure a correct conservation of fluid quantities. Thus, a nonlinear hyperbolic system of conservation laws is numerically solved. The code uses the Eulerian description of the fluid and is designed as a high order central numerical scheme. The central approach employs no (approximate) Riemann solver and is less computationally expensive. The high order WENO strategy is adopted in the reconstruction step to achieve results comparable with more accurate Riemann solvers. A combination of the central approach with an iterative solving of a local Riemann problem is tested and behavior of such numerical flux is reported. An extension to three dimensions is implemented using a dimension by dimension approach, hence, no complicated dimensional splitting need to be introduced. The code is fully parallelized with the MPI library. Several standard hydrodynamic tests in one, two and three dimensions were performed and their results are presented.

A numerical investigation of various plasma systems and phenomena is a necessary part of modern plasma physics. Plasmas can be described in different approximations; one of the most common is a magnetohydrodynamical (MHD) treatment appropriate for cases when plasma behaves as an electrically conducting fluid. The main part of MHD equations consists of nonlinear hyperbolic partial differential equations, which express conservation laws of physical quantities. Of course, other additional (e.g. parabolic) terms can be there. The difficulty is that nonlinear advective terms can cause a generation of discontinuities from initially smooth flows [1]. Thus, this first part of the work presented here is focused on the treatment of the hyperbolic system, at first, of Euler equations. Euler equations are simpler since their solution does not consist of as many waves as the MHD case. However, a finite volume method in the semidiscrete form [2] is chosen for solving the set, so the code can be later extended in a very straightforward manner.

Due to the fact that central schemes are less accurate than upwind ones, some high order reconstruction procedure must be employed, to achieve results comparable with upwind schemes. The reconstruction procedure should satisfy several basic requirements, e.g. conservation, accuracy, shape preserving. In our case, two different procedures were implemented.

The semidiscrete equation set is in the form of an ODE and can be solved with any appropriate method. In the present version of the code, this ODE is solved with one from the family of standard Runge-Kutta schemes. The 3rd, 4th and the 5th order Runge-Kutta schemes are implemented there. As a rule, the discretization error in the temporal domain dominates the overall error of high order (spatial) numerical schemes, especially in long time evolution runs. During last years strong stability preserving modifications of Runge-Kutta schemes appear in the literature [3]. Implemented schemes of the 3rd and the 4th order are this case.

Multidimensional results were obtained using a dimension by dimension approach, hence, no dimensional splitting was involved. Definitions of several presented test problems are extensively described in Liska & Wendroff [4].

The present status in the development of the new code is reported and its preliminary results are discussed. Several modern techniques were implemented and their various combinations were tested. The high order WENO reconstruction overcomes the other methods, especially in the resolution of the contact, which is usually the deficit of central schemes. Although the reconstruction step in the WENO scheme is more expensive, in the framework of the central scheme is acceptable, gives better results and preserves the simplicity, which is the main point for a further applicability. Additional extensions are planned (e.g. MHD).

References:

- [1] LIU X. D., TADMOR E.: *Third order nonoscillatory central scheme for hyperbolic conservation laws* Numerische Mathematik, 1998, 397–412.
- [2] KURGANOV P. A., NOELLE S., PETROVA G.: *Semi-discrete central-upwind scheme for hyperbolic conservation laws and Hamilton-Jacobi equations* SIAM Journal on Scientific Computing, 2001, 707–720.
- [3] GOTTLIEB S., SHU CH. W., TADMOR E.: *Strong Stability Preserving High-order Time Discretization Methods* NASA/ICASE Report, 2000, No.200-15.
- [4] LISKA R., WENDROFF B.: *Comparison of several difference schemes on 1D and 2D test problems for the Euler equations* SIAM Journal on Scientific Computing, 2003, 995–1115.

This research has been supported by CTU grant No. CTU0406313, by GA ČR grant No. GD202/03/H162, by the research program No J04/98:212300017 "Research of Energy Consumption Effectiveness and Quality" of the Czech Technical University in Prague, by the research program INGO No. LA055 "Research in Frame of the International Center on Dense Magnetized Plasmas" and "Research Center of Laser Plasma" LN00A100 of the Ministry of Education, Youth and Sport of the Czech Republic.

Application of Modern Optical Methods in Physical Laboratory Training at Faculty of Transportation Sciences

D. Nováková, Z. Malá, T. Polcar

novakova@fd.cvut.cz

CTU, Faculty of Transportation Sciences, Dept. of Applied Mathematics,
Na Florenci 25, Praha 1

It was the objective of the project funded from FRVS to support practical lessons for students in the bachelor program by means of laboratory practice in Physics at Faculty of Transportation Sciences of ČVUT (Czech Technical University).

Laboratory practice in Physics I and II has been newly built up at Faculty of Transportation Sciences of ČVUT since 2000. 230 students on average attend laboratory practices, for 2 hours a week for 2 terms. 12 laboratory exercises are installed in the laboratory practice in Physics I and Physics II so that students can carry out measurements in couples. Laboratory practice has become even more important after the introduction of structured studies. Laboratory practice in physics is one of few possibilities where students can apply and deepen their practical skills in basic types of measurements and where they can also learn methodology of measurement and basic methods of data processing. During the course of existence of laboratory practice in physics at Faculty of Transportation Sciences, i.e. during the period of 2000 – 2004, we managed to build up this practice at the adequate technical level, using Faculty's funds and above all funds provided from grants. It is one of the biggest achievements that we managed to equip all measurement worksites with new PCs, a server and a printer controlled from the network. Routine processing of measured results is no longer required and some measurements are carried out and recorded directly through a PC. Also, user programs for processing the measured dependencies using the least squares method and for processing repetitive measurements are available to the students. It is possible to print the measured and processed dependencies straight away. Finally, students can send the data and their measured dependencies to their e-mail address for further processing.

When bachelor program was introduced in the academic year of 2003/04, justified need to make practical lessons in those subjects where practical form of teaching is possible more intense and also to improve the lessons emerged.

Funds from the project were therefore directed to applications of physical knowledge that students may use in practice. Optics is one of these areas. Currently, modern optical methods are being used more and more frequently in technical practice; however the level of knowledge students get in this area at high-schools keeps getting poorer. Funds from the grant were used to buy for example a laser interferometer that will be used for the laboratory exercise "Check of Drift Indicator Accuracy". Experimental configuration and attachment of the drift indicator are being prepared. Students will be able to get familiar with one of modern optical methods, laser interferometry. Laboratory exercise "Determination of the Diffraction Intensity at Slit and Double Slit Systems" is already in operation. In this exercise, students see diffraction phenomena in an illustrative way and they carry out graphic and numeric evaluation of these phenomena. The text below is an example – it is part of the instructions for this laboratory exercise specifying tasks for students that they are meant to accomplish in the laboratory practice. The instructions are available to students at the department web pages.

Determination of the diffraction intensity at slit and double slit systems

Problems:

1. Determination of the intensity distribution of the diffraction patterns due to two slits of different widths.
The corresponding width of the slit is determined by means of the relative positions of intensity values of the extremes.
Furthermore, intensity relations of the peaks are evaluated.
2. Determination of location and intensity of the extreme values of the diffraction patterns due to two double-slits with the same widths, but different distances between the slits.
Widths of slits and distance between the slits must be determined as well as the intensity relations of the peaks.

Theory and evaluation

If monochromatic light of wavelength λ impinges on a system of parallel and equidistant slits, the luminous intensity I of the beam diffracted in the direction φ is given through

$$I(\varphi) \approx b^2 \frac{\sin^2\left(\frac{\pi}{\lambda} b \sin \varphi\right)}{\left(\frac{\pi}{\lambda} b \sin \varphi\right)^2} \cdot \frac{\sin^2\left(\frac{p\pi}{\lambda} g \sin \varphi\right)}{\sin^2\left(\frac{\pi}{\lambda} g \sin \varphi\right)}, \quad (1)$$

b is width of the slit, p is number of slits and g is distance between slits.

Set-up and procedure

Slit and double slit systems are illuminated with laser light. The corresponding diffraction patterns are measured by means of a photodiode which can be sifted, as a function of location and intensity.

Inaccuracy of results is determined mainly by uncertainties in determination of location of maxima and minima, and also by the fact that the values of voltage measured (photodiode current) is affected by lights in the room.

Determination of intensity distribution for a single slit and a double-slit system (slits of the same width) is affected by uncertainties in measurement of relative intensities. Double-check measuring showed that relative uncertainty in determining intensity in zero maximum is approximately 8 %.

References:

- [1] NOVÁKOVÁ, D.-MALÁ, Z.: *Laboratorní cvičení z Fyziky I*, ČVUT Praha, 2001 .
- [2] NOVÁKOVÁ, D.-MALÁ, Z.: *Laboratorní cvičení z Fyziky II*, ČVUT Praha, 2002 .

This research has been supported by FRVS 2102.

Support for Laboratory Practise in Physics - Tests of Knowledge

D.Nováková,Z.Malá,T.Polcar

novakova@fd.cvut.cz

CTU, Faculty of Transportation Sciences, Dept. of Applied Mathematics,
Na Florenci 25, Praha 1

Level of preparedness of students for measurement is one of persistent problems we keep running up against in laboratory practice. If a student does not get well prepared for the measurement, and the process of preparation, of course, also includes understanding of the principles of physics the laboratory exercise is based on, he/she only mechanically follows the recommended sequence of operations, mechanically entering the measured quantities values in formulas listed in the instructions for the laboratory exercises measurement.

Clear, concise rules have been defined for students' written home preparation for measurements in laboratory practice in physics. Abiding by these rules regarding the preparation content and form should ensure good preparation of students for measurements and it should also enable simple checking on the preparation quality. Unfortunately it seems that it is easy for students to obtain an already existing PC version of a study, including the preparation, from another student or, in other cases, to copy a part of instructions from a textbook. Such written preparation does not serve its purpose in either of the above cases and the quality of preparation therefore needs to be checked.

A new computer-aided system of verification of students' preparation for laboratory practice was therefore created in 2003. Checks of home preparations were carried out previously, through testing of individual students before measurements. This method, however, was a particularly time-consuming activity for teachers. Students had to be tested immediately before commencement of measurements otherwise the test would lack purpose. There are between 8 – 12 students per a teacher in laboratory practice, and the testing of all students would take at least 15 – 25 minutes which is unacceptable as teacher's primary role is to commence all measurements with students as soon as possible, without any delays so that students have enough time to complete the exercise.

So far, 30 – 50 questions have been prepared for all laboratory exercises and students are to decide whether they are right or wrong. The contentions include statements regarding the following: definition of the quantities measured, dimensions and units of measurements for the quantities sought, measurement principle, measurement process, measurement methods, measurement accuracy estimates, general relationships for uncertainties. Questions for particular tests were randomly selected. Nine questions were selected for each test, three on each of the three sheets. The choice of answers is "yes," "no", "I don't know" and students have 5 minutes to complete all nine answers. A test example is given below. The limit for successful completion of a test is six correct answers out of nine. The answer "I don't know" is assessed as a wrong answer. An example of a particular test is shown at the end of this text.

After laboratory practice commencement, teacher used his/her PC that also serves as a server to generate tests for individual laboratory exercises on all 12 student PCs. Each laboratory couple completed the test on their PC collectively, and the couple were also assessed collectively. In the case of another student joining the laboratory exercise on an alternative

date due to them previously been denied a measurement, a test could be generated for the student later on.

The program package to test students' knowledge necessary for laboratory exercises contains 3 programs created in Visual Basic in Excel that is part of MS Office. They are these programs:

- Setting up of the PC for the test
- Generating the test
- Actual test

The students' opinion of the new method of testing was mostly positive. There were some inaccuracies in wording of the questions and some of them were not very clearly worded; we are improving on this on an ongoing basis. Students appreciated in particular random selection of the questions included in tests. The test time limit – 5 minutes – proved to be sufficiently long to answer the questions. There were no objections to test results, even though a failure meant that the student (the couple) had to repeat the measurement on an alternative date, and that he/she scored a mark 4 (failed) for his/her overall rating. Rate of success of the test in the course of one term when they were used was approximately 80 %.

For the time being, after just one term, it is difficult to say whether computer-aided testing of students at the beginning of each laboratory practice contributed to better preparation of students. However, the tests definitely shut out from measurement those students who did not get prepared for laboratory practice at all or prepared just formally. For teachers, this method of testing resolves the critical situation at the beginning of laboratory practice where there is not enough time to test all students individually.

References:

- [1] NOVÁKOVÁ,D.-MALÁ,Z.: *Laboratorní cvičení z Fyziky I*, ČVUT Praha, 2001 .
- [2] NOVÁKOVÁ,D.-MALÁ,Z.: *Laboratorní cvičení z FyzikyII*, ČVUT Praha, 2002 .

This research has been supported by grant MSMT 33/2004.

Satellite Laser Ranging Normal Point Precision Limit

K. Hamal, I. Procházka, G. Kirchner*, F. Koidl*

blazej@troja.fjfi.cvut.cz

Department of Physical Electronics, Faculty of Nuclear Sciences and Physical Engineering,
Czech Technical University, Břehová 7, 115 19 Prague 1, Czech Republic

* Observatory Lustbühl, Austrian Academy of Sciences, Graz, Austria

The Satellite Laser Ranging (SLR) is a highly accurate measuring technique providing the accurate range to the retroreflector equipped Earth satellites. It operates on a classical radar principle. Measuring the time interval between the pulse transmission and reception, considering the speed of light and the way of its propagation, the target distance may be evaluated. The picosecond laser pulses together with highly precise timing systems and optical detectors enable resolution and accuracy of the entire ranging system in the range of several millimeters. The results of SLR are used, among others, for the determination of terrestrial reference frame and the product of the universal gravitational constant and the Earth mass, which represent one of the fundamental constants in physics [1]. In this view, the SLR serves as a fundamental technique to calibrate other measurements. That is why, the precision and accuracy of the SLR data itself is a critical issue. To reduce the requirements on data transfer and archiving and to simplify the data analysis procedures, the individual SLR measurements are compressed into so-called normal points. The data time series are divided into time slots – time bins of pre defined size of 5 to 300 seconds, depending on the satellite orbit altitude. The individual ranging data within one bin are fitted and averaged and on the end are represented by a single range called normal point.

The goal of this paper is to find out the ultimate precision of the satellite laser ranging normal points and to identify the error sources limiting the normal point precision.

The main factors limiting the normal point precision are: the overall stability of the laser ranging chain and the precision of the data reduction and fitting procedure. The laser ranging hardware and its stability has been characterized by means of a Portable Calibration Standard [2] in numerous missions. The best laser ranging stations achieve the system bias stability of the order of picoseconds in time, what corresponds to 0.1 mm in range. The precision of the data reduction, fitting and normal point forming procedure has been tested by the following experiment. The SLR raw ranging data have been processed; fitted and normal points formed using two different and independent algorithms. The data processing procedures used:

1. Graz SLR data reduction, consisting of IRVINT integrator providing 1 minutes x,y,z coordinates, 8-points Lagrange interpolation and topocentric conversion, optional manual range and time bias tuning, polynomial fitting, standard scheme, degree 5-10, data screening and manual editing,
2. Portable Calibration Standard data reduction package, consisting of orbit integration using Herstmonceux RGO scheme providing 1 minutes x,y,z coordinates, 8-points Lagrange interpolation and topocentric conversion, automated range and time bias and DUT tuning procedure, iterative polynomial fitting with fully automated data editing. In this data reduction package, the processing consists of several individual programs, the data are passed from one to another one via formatted data file with the least significant digit of 1 picosecond, thus the rounding is implemented 3 to 5 times consequently.

The data from SLR station Graz, Austria have been used. The segments of the ERS-2 ranging with the data rate 750 echoes per second, acquired October 2003 to January 2004 have been

selected. The echoes from the closest corner retroreflector have been selected to eliminate the influence of the target influence completely from the process. The single shot precision achieved in the tested data series was 18 to 20 picoseconds rms, what corresponds to 2.5 to 3.0 mm range precision.

The range residuals of individual ranges have been compared for all individual measurements. The difference between the computed ranging residuals on a shot by shot basis indicates the estimate of the data processing procedure. The computed differences have the following characteristics: the slowly varying component with the period about 15 second and the amplitude ± 3 picoseconds and the random spread within ± 2 picoseconds. The slowly varying component has been attributed to the interpolation, the random component to the numerical noise of the computation and to the rounding process.

The normal points have been formed for different bin width. Varying the bin width, the number of individual measurements compressed into one normal point is changing. Considering the normal data distribution and its properties, the internal consistency - the precision of these normal points - should increase with a square root of the number of individual measurements compressed in one normal point. The deviation from this behavior should indicate the limits of the normal point precision. The numerical experiments showed the deviation from the ideal model in the case, when about 75 individual ranges are compressed into one normal point with the corresponding normal point precision 2.5 ps. The second break point occurred when compressing more than 2000 points with the corresponding normal point accuracy of 1 ps. These two break points correspond perfectly to the two limiting factors identified as the interpolation and rounding errors.

The completed experiment demonstrates the ultimate normal point precision at the level of 2.5 picoseconds, what corresponds to 0.37 mm in range of the retroreflector equipped satellite in space. The key contributor to this value is the interpolation used in the orbit modeling procedure.

References:

- [1] DEGNAN, J. J: *Millimeter Accuracy Laser Ranging: A Review*, Contributions of Space Geodesy to Geodynamics: Technology (Geodynamics Series), vol. 25, 1993. pp. 133-162.
- [2] HAMAL, K. – PROCHAZKA, I. – BLAZEJ, J. – KIRCHNER, G. – SCHREIBER, U. – RIEPL, S. – SPERBER, P. – GURTNER, W. – APPLEBY, G. – GIBBS, P. – YANG FUMIN – NEUBERT, R. – GRUNWALDT, L., *Satellite Laser Ranging Portable Calibration Standard Missions 1997-2002*, In *Abstract Book 'Geophysical Research Abstracts' Volume 5, 2003*, EGS - AGU - EUG Joint Assembly 2003, Nice, France, April 2003, p. 243.
- [3] KRAL, L. – PROCHAZKA, I. – BLAZEJ, J. – HAMAL, K., *Satellite Laser Ranging Precision Ultimate Limit*, In *Proceedings of SPIE 5240*, 2003, pp. 26–30.
- [4] PROCHAZKA, I. – KIRCHNER, G.: *Numerical Noise in Satellite Laser Ranging Data Processing*, 14th International Laser Ranging Workshop, San Fernando, Spain, June 7-11, 2004, published in Boletín ROA No. 4/2004, Real Instituto Observatorio de la Armada, en San Fernando, ISSN 1131-5040, edited by J.M.Davila, 2004.

This research has been supported by grant GA205/03/0314.

Measurement and Interpretation of Soft X-ray Emission Spectra from Nitrogen Capillary Discharge

M. Vrbová, A. Jančárek, P. Vrba*, A. Fojtík, L. Scholzová, R. Havliková

vrbova@troja.fjfi.cvut.cz

Department of Physical Electronics, Faculty of Nuclear Science and Physical Engineering,
Czech Technical University, Brehova 7, 115 19 Prague 1, Czech Republic

*Institute of Plasma Physics, AS CR, Na Slovance 2, 182 21 Prague 8, Czech Republic

Our aim is to realize soft X-ray laser recombination pumping during the pinch decay and to get lasing on Balmer alpha transition of N^{6+} ions. To this purpose plasma should be enough heated during the pinch collapse and then quickly cooled during the pinch decay. We look for the optimum experimental arrangement that results in proper capillary plasma pinch. Spectral diagnostics is used as a principal diagnostic tool.

Our system is manually controlled by dual channel pulse generator, which triggers a two stage Marx generator and diagnostic system. The Marx generator stage capacity is 15 nF and it is charged up to 40 kV. Capacitor bank of 7.5 nF is charged with 0.5 kV/ns rate until capillary self-breakdown takes place. Capillaries with 1 or 3 mm diameter made from RF alumina have been used. Nitrogen pressure inside the capillary may be varied within 0.5-15 mbar. Capillary voltage profile corresponds to under critically damped RLC circuit with the quarter period of 50 ns and current peak value about 10 kA. Time integrated EUV emission spectra in the range 10 – 24 nm are studied by means of the Jobin -Yvon monograph PGM-PGS 200 and a Reflex BICCD camera RXBIC512c in many repetitive shots.

We have observed many spectral lines in the studied spectral range. These lines should belong to three or more times ionized nitrogen atoms. Their intensities vary if the initial filling pressure is varied and if the capillary diameter is changed. To identify the spectral lines observed we have estimated the time dependence of plasma electron temperature by means of the MHD code [1] and then evaluated ion abundances by means of FLY code [2]. Unfortunately, the last code cannot be used for evaluation of N^{3+} spectral lines that may be also observed in the investigated spectral range. To identify all lines we chosen the SAPPHERE code [3].

The measured current pulse shape is approximated as $I(t) = I_1 \sin(\pi t / 2t_1) \exp(-t/t_2)$. The optional experimental parameters for the code are capillary radius R_0 , initial filling pressure p_0 (or atom concentration N_0), electric current amplitude I_1 and quarter period t_1 . It has been shown that the pinch dynamics is very sensitive namely on pressure variations. From the calculated results, which correspond to our experimental conditions we can see that the pinch compression ratio is rather small and the highest plasma electron temperature is about 30 eV. Plasma reflection from the wall is not taken into account and the results are valid only on the limited time interval till the plasma reaches the capillary wall.

Files containing the temporal history of axial plasma electron temperature $T_e(0,t)$ and electron density $N_e(0,t)$, are used as input history files for the FLY code [2]. At the very beginning of the current pulse the plasma ionization is small. During the pinch compression the ionization stage of plasma is quickly changed. The densities of forth and five times

ionized atoms quickly grow and achieve their peak values approximately at the pinch time $t_p = 57$ ns. During the pinch expansion stage the helium-like ions N^{5+} prevail. Time dependences of population densities of energy levels and line intensities corresponding to selected quantum transitions for N^{6+} , N^{5+} and N^{4+} may be evaluated using the subprogram FLYSPEC. All these lines have steep increase of the intensities at the time of the pinch. These time dependencies were observed during our measurements in the UV spectral range (200- 300 nm). Steep increase of their intensities is a principle feature of the pinch.

To identify the quantum transitions, corresponding to the spectral lines observed in experiment in the EUV range from 10 to 23 nm, and also UV range from 200 to 300 nm synthetic spectra separately for helium-, lithium- and beryllium-like ions were generated by means of the SAPPHIRE code [3]. In this case we have taken into account the plasma equilibrium temperature 30 eV as it follows from the MHD code. As it is well known the lines with wavelength shorter than 13 nm may belong to helium- and hydrogen- like ions only, whereas in the range 13-16 nm also lithium- like lines may be observed. For even longer wavelengths also the lines belonging to the N^{3+} should be judged. The identified quantum transitions, corresponding to the most intensive lines observed in our time-integrated spectra, are summarized in Table 1.

Table 1: EUV quantum transitions
Table 2: UV quantum transitions

λ [nm]	E_L [eV]	Ion	L. L. Config.	U. L. Config.
11.7	426.3	N^{5+}	1s(2S)2p	1s(2S)5d
13.0	426.33	N^{5+}	1s(2S)2p	1s(2S)4d
14.0	0.00	N^{4+}	[He]2s	[He]6p
15.0	9.976	N^{4+}	[He]2p	[He]8d
17.3	426.42	N^{5+}	1s(2S)2s	1s(2S)3p
17.5	0.00	N^{3+}	[He]2s2s	[He]2s6p
18.5	430.70	N^{5+}	1s(2S)2p	1s(2S)3d

λ [nm]	E_L [eV]	Ion	Lower Level Config.	Upper Level Config.
248	63.8	N^{3+}	[He]2s4d	[He]2s5f
265	64.1	N^{3+}	[He]2s4f	[He]2s5g
288	84.1	N^{4+}	[He]5p	[He]6d
297	38.3	N^{2+}	[He]2s2p3p	[He]2s2p3d

Conclusion:

Practical realization of recombination laser pumping scheme is conditioned by a fine careful tuning of all system parameters. To this purpose detail spectral diagnostics but time resolved should be developed.

References:

- [1] N. A. BOBROVA ET AL.: Plasma Physics Reports 22 , 1996, pp. 387-402.
- [2] R.W. LEE, J. T. LARSEN: J.Q.S.R.T. 56, 1996, pp. 535-556.
- [3] CODE: *Sapphire Professional, version 1.0.3.2*, Cavendish Instruments, Ltd. 2003

This work was supported by grants from the Ministry of Education Youth and Sports CR under contracts MSM 210000022, INGO-IP2004 and IPP AVK research grant 2790 05.

Mathematical Methods in the Physics of Microworld

J. Tolar

jiri.tolar@fjfi.cvut.cz

CTU, Faculty of Nuclear Sciences and Physical Engineering, Dept. of Physics
Břehová 7, 115 19 Praha 1

The research group of 7 collaborators from the Department of Physics of CTU-FNSPE (G. Chadzitaskos, L. Hlavatý, I. Jex, P. Jizba, V. Svoboda, L. Šnobl and J. Tolar) and 7 from the Department of Mathematics of CTU-FNSPE (Č. Burdík, M. Havlíček, M. Krbálek, Z. Masáková, E. Pelantová, S. Pošta and P. Šťovíček) carried out research in 2004 in the framework of the long term research plan MSM210000018 in mathematical physics. The research was devoted, among other topics, to generalized symmetries connected with the physics of microworld, the associated algebraic and geometric structures, and their applications to classical and quantum systems, especially the integrable or chaotic systems. In this connection, special models were studied in terms of the corresponding Schroedinger operators as well as via the solution of the Schroedinger equation and the Hamilton equations. The investigations by the participating qualified researchers were performed in direct collaborations with the students and doctoral students of Mathematical Engineering at FNSPE. They are given below under each research theme together with our foreign collaborators.

The research topics were the following:

(1) Quantum groups and related algebraic structures, their representations; quantum integrable models were studied by Burdík, Havlíček, Hlavatý, Pošta, Šnobl, Šťovíček together with Doc. O. Navrátil (CTU) and students of FNSPE (Marek Filan, Ing. Vít Jakubský, Ing. Václav Kavka, Ing. Hynek Lavička).

(2) Gradings and graded contractions of Lie algebras were investigated by Havlíček, Pelantová, Tolar together with Prof. Jiří Patera (Université de Montréal) and PhD. students of FNSPE (Ing. Jiří Hrivnák, Ing. Petr Novotný, Ing. Milena Svobodová). Our research group specializing on this mathematical topic related to symmetries in physics is unique worldwide in its broad experience with related problems. Among other results of our common long term research we concluded in 2004 a large three-year project on graded contractions of $sl(3, \mathbb{C})$ [2], [3], for which the system for symbolic computations MAPLE 8 was an indispensable tool.

(3) Quantization and quantum mechanics in finite-dimensional Hilbert spaces, applications in quantum optics (coherent states) and quantum information theory were subject of investigations by Chadzitaskos, Jex, Šťovíček, Tolar together with Prof. G. Alber (Darmstadt), Dr. E. Andersson (Glasgow), Prof. S.M. Barnett (Glasgow), Prof. V. Bužek (Bratislava), Dr. A. Delgado (Ulm), Prof. A. Odziejewicz (Bialystok) and students of FNSPE (Vojtěch Košťák, Ing. Petr Luft, Mgr. Michaela Kryšková, Ing. Jaroslav Novotný, Ing. Stanislav Petráš, Ing. Martin Štefaňák, Ing. Jan Vymětal). Prof. I. Jex was awarded in 2004 the prize of first degree of the rector of CTU for excellent scientific results related to the subject of manipulating quantum information obtained in international collaboration.

(4) Mathematical models of quasicrystals and their applications to wavelets, coding and pseudorandom number generators were studied by Burdík, Masáková, Pelantová, together with Prof. Ch. Frougny (Paris VII), Prof. J.-P. Gazeau (Paris VII), Dr. L.-S. Guimond (Paris VII), Prof. Jiří Patera (Montréal), Prof. R. Twarock (London) and students of FNSPE (Ing.

Miroslav Andrlé, Ing. Jan Patera, Petr Ambrož, Petr Baláži, Lubomíra Balková, Petra Kocábová, Ondřej Turek). E. Pelantová and Z. Masáková obtained in 2004 the prize of second degree of the rector of CTU for excellent scientific results related to the subject of mathematical description of quasicrystals obtained in collaboration with Université Paris VII.

(5) Schrödinger operators periodically dependent on time, solutions of Schrödinger equation and Hamilton equations for special models, classical and quantum chaotic systems were studied by Burdík, Jex, Krbálek, Svoboda, Šťovíček together with Prof. P. Duclos (Toulon), Prof. R. Kerner (Paris VII), Doc. L. Krlín (ÚFP AV ČR), Prof. P. Šeba (FzÚ AV ČR), Prof. M. Vittot (Toulon) and students of FNSPE (Ing. Ondřej Lev, Ing. Ondřej Mareš, Ing. Karel Maršálek, Ing. Petr Vytřas). Ing. O. Mareš, PhD. defended in 2004 his PhD. under double supervision agreement with Université Paris VII.

Quantum properties of matter are becoming increasingly important in modern technological applications. This leads to the necessity to investigate quantum or classical models which yield qualitative as well as quantitative view of the observable characteristics of physical systems. We have used simplifying assumptions on symmetry or geometry which allowed us to derive typical models possessing at the same time physically relevant properties of real systems, and to solve them in a mathematically rigorous way. In this manner such mathematical models have served as suitable laboratories for the study of fundamental properties of microsystems.

References:

- [1] TOLAR, J.: *Výzkumné zprávy "Matematické metody ve fyzice mikrosvěta" (MSM 210000018, část I)*, http://www.fjfi.cvut.cz/katedra_fyziky, 2000 - 2003.
- [2] HRIVNÁK J. - NOVOTNÝ P. - PATERA J. - TOLAR, J.: *Graded contractions of the Pauli graded $sl(3,C)$. 180 SOLUTIONS OF THE CONTRACTION SYSTEM*, preprint submitted to Journal of Mathematical Physics (USA), 2004, 23 pp.
- [3] NOVOTNÝ P. - HRIVNÁK J. - PATERA J. - TOLAR, J.: *Graded contractions of the Pauli graded $sl(3,C)$. IDENTIFICATION OF CONTRACTED LIE ALGEBRAS*, preprint submitted to Journal of Mathematical Physics (USA), 2004, 16 pp.
- [4] TOLAR, J.: *Souhrnná výzkumná zpráva "Matematické metody ve fyzice mikrosvěta" (MSM 210000018, část I)* http://www.fjfi.cvut.cz/katedra_fyziky, 2004.

This research has been supported by the Ministry of Education of the Czech Republic under the research plan MSM 210000018.

Neutron Production at PF 1000

P. Kubeš, J. Kravárik, D. Klír, P. Barviř

kubes@fel.cvut.cz

ČVUT FEL Praha

The plasma focus discharges are studied due to high efficiency of the x-ray emission and the neutron production if the deuterium is in the load. This research is concentrated on a comprehensive x-ray and neutron diagnostics with the temporal spatial and spectral resolution of the phase of the plasma focus evolution [1-3]. Nowadays, the fusion reaction mechanism and the acceleration of high energy electrons and deuterons in z-pinches are still under discussion [4]. This paper presents the results of observations of the temporal correlation of the visible radiation, x-rays, electrons and neutrons produced during the implosion of the deuterium plasma sheath obtained in 2004.

The discharges were carried out at the PF-1000 facility with current amplitudes ranging 2 MA. A set up of diagnostics with spatial, temporal, and spectral resolution were used – the filtered Ne102a scintillator for soft x-rays, 4-stripes soft x-ray detector using microchannel-plate, three frame cameras in visible spectral range, visible streak camera, two Cherenkov detectors for fast electrons, two scintillation probes for time-resolved measurements of the hard x-ray and neutron emission in upstream (7 and 35 m) and one probes in side-on (7 m) directions. The neutron yield was measured with the silver-activation counters.

The results obtained in the sequence of the shots 4000-4200 we can describe from the view of the temporal correlation of signals. The pinch phase corresponds to the minimum pinch diameter and to the minimum of the current derivative and it is characterized with an intensive XUV emission and with the first peak of soft x-rays, axial electrons and hard x-rays. After the first peak we can often observe the second peak, in this shot it is recorded 100-120 ns after the first peak at the time of pinch disintegration and instability development, usually without emission of XUV and without extreme of the current derivative. The waveforms of x-rays and upstream electrons show a good temporal correlation. Partial difference of the profiles seems to be caused by a sequence of few their sources and by different ranges of energies in each peak and source. It is observed the shorter duration and a fast decrease of the fast axial electrons together with a marked anisotropy of the axial and radial directions. The side-on electrons are emitted during relatively long time of 300-400 ns with minimum at the maximum of axial electrons.

As well the waveforms of x-rays and neutrons show two peaks the same distance of peaks of ~ 100 ns. The energy of neutrons in the upstream direction was calculated from positions of the maximum of neutron peaks registered at the distance of 7 and 35 m from the center of the plasma focus using the time of flight method. We have two reasons for this assumption - the same distance of maximum inducing the similar energy distribution in both peaks and the same distance of the onsets of both peaks. For example in the shot 4197 the calculated neutron energy of 2.7 MeV is higher then the thermal value of 2.45 MeV. The value of the energy enabled an estimation of the 40-60 ns time delay of neutron maximum after the hard x-rays and energy of side-on neutrons 2.5 MeV. The duration ~ 50 ns (the same as hard x-rays) of neutron production was estimated by extrapolation of the FWHM measured at both distances 7 and 35 m. When we assume the production of neutrons at the time of hard x-rays, than for waveform at 7 m the peak of neutrons in distance 35 m should be 400-500 ns after the observed peak. It seems, that acceleration of deuterons and electrons depends very

close, but it follows. Anisotropy of fast electrons (and ions) in comparison with isotropy of neutrons and x-rays may be caused by existence of B_z field at the time of the fast particles acceleration [1].

At the pinch phase of the plasma focus the production of soft- and hard x-rays are in good temporal correlation, as well onset of x-rays and fast electrons. Energy of upstream neutrons is in range 2.6-3 MeV, energy of side-on electrons 2.4-2.5 MeV. Onset of neutrons started probably at the time of decrease of fast electrons and x-rays and maximum of neutron peak was ~ 50 ns after maximum of x-rays. Neutrons were produced at the time of disintegration of the pinch phase. Fast axial electrons were observed at the time of minimum of side-on electrons. When the anisotropy of electrons (and deuterons) is much higher than anisotropy of x-rays and neutrons, then the direction of charged particles should be influenced by internal B_z field. These preliminary results will be tested by using of 7 scintillators in axial and radial direction during next half of year.

References:

- [1] JAEGER, U. – HEROLD, H.: *Nuclear fusion* 27, 1978, p. 407.
- [2] SCHOLZ, M. ET AL.: *Czech. J. Phys.* 50, 2000, p. 150.
- [3] KARAKIN, M.A., KHANTIEV, E.Y., KRAUZ, V.I.: *Czech. J. Phys.* 52 2002, p. D255.
- [4] BATUNIN, A.V. ET AL: *Plasma Physics Reports* 16, 1990,, p. 1027.

This research has been supported by the research program MSMT No 1P04LA235 .

Neutron Production at S-300

P. Kubeš, J. Kravárik, D. Klír, P. Barviř

kubes@fel.cvut.cz

ČVUT FEL Praha

Wire-array z-pinchs are nowadays the most intensive laboratory sources of soft x-ray radiation, and this is also the main reason why they are studied. The application of z-pinchs as neutron sources has struggled with some difficulties as early as z-pinch research began. The fundamental questions that have been studied were the origin of neutrons and the scaling of neutron yield with the current. In order to solve these questions and to achieve higher neutron yield, various types of z-pinch configurations and deuterium loads have been tried from that time on. In this presentation we would like to show results from the implosion of a wire array z-pinch onto a deuterated fiber.

The implosion of a wire array z-pinch onto a deuterated fiber was studied on S-300 device (4 MA, 700 kV, 100ns; RRC Kurchatov Institute, Moscow). The experiments were performed at a peak current of ≈ 2 MA with a rise time of ≈ 100 ns. An aluminum wire array of 1 cm in diameter was used as a load. Each wire array consisted of 30)60 aluminum wires of 15 μm in diameter and 1 cm in length. The deuterated polyethylene $(\text{CD}_2)_n$ fibers with diameters between 80 and 120 μm were placed on the axis of the array. The preliminary results and results from neutron diagnostics were published in [1] and [2], respectively. In this article, the comparison between shots with and without a central fiber will be presented.

In order to observe z-pinch dynamics, we employed an comprehensive set of diagnostics tools: e.g. an optical streak camera (radial mode), a 4-frame x-ray pinhole camera (2 ns gate, 10 ns separation, 24 μm Be filter) a differentially filtered time integrated pinhole camera (without a filter, and with 5 μm and 24 μm mylar), a 11-channel soft x-ray polychromator (channels: 50, 80, 120, 180, 270, 370, 600, 800, 1000, 1200, and 1900 eV), and 5-frame laser shadowgraphy (2 ns exposure, 10 ns separation, 532 nm). The neutron emission was measured with an indium activation counter (neutron yield measurement) and two SSDI-8 scintillators (at the distance of 2.70 m and 7.45 m downstream, time of flight analysis).

We carried out a series of 13 shots with an Al wire array and a $(\text{CD}_2)_n$ fiber as a load. The power of soft x-rays (above 100 eV) reached 90)230 GW with the FWHM of (30)50 ns. The total radiated energy varied from 3 to 8 kJ. The maximum spectral power density of ≈ 1 GW/eV was measured at the photon energy of 120 eV. The radiation was close to the radiation of the blackbody with the temperature of 40 eV. The energy radiated in the carbon Ly- α line was 15)60 J whereas the energy emitted in K-shell lines of aluminum exceeded 250 J. Similar values were obtained during the implosion without a central fiber (220 GW power, 10 kJ energy). The shot-to-shot variation seemed to be more important than the presence of a deuterated fiber in the center of a wire array.

Noticeable differences were seen in streak and pinhole images. Comparing images of both diagnostics we can see that when a central fiber was used, the stagnation lasted much longer (> 20 ns), the diameter of the pinched plasma determined from pinhole images was greater (2)3 mm), and the most intensive hot spots were observed predominantly on the surface.

We detected neutrons from the D-D reaction in 6 cases over a series of 13 shots. The peak neutron yield reached 2×10^8 . The maximum yield was achieved in the case of 48 Al wires (264 $\mu\text{g/cm}$), and the shortest rise time of the current ($t_{10\%90\%} \approx 70$ ns). Two SSDI-8

scintillators detected several x-ray pulses (usually more than two) and one neutron pulse. For example the result from shot no. 030603-1 show that the x-ray pulses from both scintillators were placed over each other. The first x-ray pulse appeared early in the discharge and was caused probably by electron flux leakages in the vacuum concentrator. The second x-ray pulse was emitted during the stagnation when the peak of soft x-rays was observed. We determined from time-of-flight analysis (“peak-to-peak” as well as “onset-to-onset” method) that the neutron pulse was not related to the dominant second x-ray pulse but to the third pulse. In half of all the shots in which neutrons were detected, neutrons were emitted after the stagnation, during the expansion stage. At this point we would like to emphasize that a neutron pulse was in each shot coincident with one of x-ray pulses but the corresponding x-ray pulse was usually not the dominant one.

In all the shots, the mean energy of neutrons detected in the axial direction (downstream) was shifted from 2.45 MeV.

The implosion of an aluminum liner onto a deuterated polyethylene fiber was studied at the S-300 machine. The peak power of soft x-rays exceeded 200 GW and the total emitted energy was 28 kJ. The radiation was close to the radiation of the blackbody with the temperature of 40 eV. The neutron yield from the D-D reaction reached 2×10^8 per shot. The mean energy of neutrons determined from time-of-flight analysis in the axial direction (downstream) was shifted from 2.45 MeV towards higher energies. Although the shift was not remarkable huge, it indicated that the beam-target mechanism played an important role in neutron production.

References:

- [1] KLÍR, D., KUBEŠ, P., KRAVÁRIK J. ET AL: *Fusion Science and Technology*, 2005, in print.
- [2] KUBEŠ, P ET AL: *Czech J. Phys* 54, 2004, pp. C298–C302.

This research has been supported by MŠMT grant 1P04ME761.

Plasma Technologies for Ecological Applications

S. Pekárek, J. Khun

pekarek@feld.cvut.cz

Czech Technical University, Faculty of Electrical Engineering, Department of Physics,
Technická 2, 166 27 Prague 6, Czech Republic

Pollutant emission is an important problem of the environment. Besides existing technologies such as thermal incineration, catalytic oxidation or adsorption, the importance of plasma technologies for these purposes is increasing. Critical parameters of all above-mentioned technologies are the energy consumption and the removal efficiency. Traditional thermal and thermo-catalytic methods for gas cleaning operate very efficiently when the concentration of volatile compounds is high enough. However at low concentrations alternative methods are required.

Plasma technologies can be distinguished according to the relation between the temperature of electrons and ions. In case of thermal plasma, the temperature of electrons is approximately the same as the temperature of ions. On the other hand if the temperature of electrons is higher than the temperature of ions we are talking about the non-thermal plasma.

Thermal plasma can be generated e.g. by following ways [1,2]:

- DC, AC arc discharges,
- plasma torches,
- RF discharges – inductive and capacitive coupling discharges,
- microwave discharges.

The generation of the non-thermal plasma can be performed among others by:

- electron beam,
- DC corona discharge,
- pulse corona discharge,
- dielectric barrier discharge,
- silent discharge,
- gas flow enhanced discharge.

The advantage of the non-thermal plasma with respect to the thermal plasma is a direct utilization of the energy delivered to the discharge for generation of highly energetic electrons and little energy loss for the heating of the gas.

Non-thermal plasma decomposition processes can proceed in several ways:

- Electrical discharge produces various kinds of radicals by electron impact reactions. The radicals may react with pollutants to either complete or incomplete oxidative forms. In the last case many secondary products are generated. Radicals produced by electrical discharges in air at atmospheric pressure include O, O₃, OH etc.
- Electrons of suitable energy can react directly with pollutant compounds.
- Light emission produced in plasma, especially UV radiation decomposes pollutants.

Frequently used non-thermal electrical discharge for pollutant decomposition is the DC corona discharge that involves many electrode geometries such as wire-cylinder, pin-to-plate or needle-to-plate. Since the corona is relatively low-power discharge for ecological applications its power must be enhanced with the simultaneous discharge stabilization. For

these purposes a mixture of air with volatile organic compounds (VOC) can be supplied either perpendicularly (as in case of multi crenelated pin-to-crater electrode geometry) or parallel to the discharge axis (as in case of multi hollow needle-to-plate electrode geometry) [3]. Because of different methods of delivering mixture of air with toluene to the discharge the glow and streamer character of the discharge was obtained in the first and in the second case respectively. To compare these two different ways of the mixture supply to the discharge the dependence of removal or remaining fraction of toluene as a function of specific input energy *SIE* can be used. The *SIE* is defined in the following way:

$$SIE = \frac{P}{Q} \quad [\text{J/L, W, L/min}],$$

where P is a discharge power and Q is a flow of mixture of air with VOC. From this comparison we obtained that for the toluene decomposition the same energy efficiency of about $14 \text{ g}_{\text{toluene}} \text{ kWh}^{-1}$ for both experiments [3] is required.

As it was mentioned before one of the products generated by non-thermal electrical discharges at atmospheric pressure in air is ozone. Ozone is very strong oxidizing and disinfecting agent and therefore it is suitable for many applications. Production of ozone by two hollow needles to plate electrical discharges enhanced by the airflow was studied and compared with production of ozone by single needle to plate discharge at the same conditions [4]. This study was performed for needles biased negatively. The distance between needles was kept constant. It was found that:

- Ozone concentration as well as ozone production yield reached a maximum for the smallest distance between the tips of the needles and the plate. They were the same for a single needle to plate discharge as well as for the both needles to plate simultaneous discharges operation. In the last case the two discharges worked as two separate discharges due to the large distance between the needles in comparison with the distance between the needles tips and the plate.
- For increasing distance between the needles tips and a plate the ozone concentration as well as the ozone production yield decreased due to the increased power delivered to the discharge and consequently gas heating.

References:

- [1] CHANG, J-H.: *Recent Development of Plasma Pollution Control Technology: A Critical Review* Science and Technology of Advanced Materials, 2001, pp. 571–576.
- [2] ODA, T.: *Non-Thermal Plasma Processing for Environmental Protection: Decomposition of Dilute VOCs in Air* Journal of Electrostatic, 2003, pp. 293–311.
- [3] NEIRYNCK, D. – KHUN, J.: *Electrical Discharges in Flowing Medium* In Proceedings of the Fourth International Workshop and School [CD-ROM] Warsaw: IPPLM, 2004, pp. 677–684.
- [4] PEKÁREK, S. – ROSENKRANZ, J. – KHUN, J.: *Ozone Generation from Two Hollow Needles to Plate Electrical Discharges Enhanced by Airflow* In Proc. 12th International Congress on Plasma Physics. Paris: CEA, 2004, pp.1–6.

This research has been supported by MEBV 2004-2005-03.

Temperature Dependence of the Photoluminescence and Scintillation Decay of Yb-doped YAlO₃

J. Pejchal¹, V. Múčka¹, M. Niki², N. Solovieva², J. B. Shim³, A. Yoshikawa³, T. Fukuda³,
A. Voloshinovskii⁴, A. Vedda⁵, M. Martini⁵, D. H. Yoon⁶

pejchal@fzu.cz

¹Faculty of Nuclear Sciences and Physical Engineering, Břehová 7, 115 19 Praha 1, Czech Republic

²Institute of Physics, AS CR, Cukrovarnicka 10, 16253 Prague, Czech Republic

³IMRAM, Tohoku University, 2-1-1 Katahira, Aoba-ku, Sendai 980-8577, Japan

⁴I. Franko National University of Lviv, Physics Faculty, Kyryla and Mefodiya 8, Lviv, Ukraine

⁵INFN and Dipartimento di Scienza dei Materiali dell' Università di Milano "Bicocca,"
Via Cozzi 53, 20 125 Milano, Italy

⁶Department of Advanced Materials Engineering, Sungkyunkwan University, Suwon 440-746, Korea

Single crystals of Yb doped YAlO₃ (YAP) have become a subject of interest in recent years because of its possible usage as neutrino detectors in high energy physics. Favorable characteristics of Yb³⁺ charge transfer (CT) luminescence, such as very fast response, reasonable high light yield, possibility of their temperature tuning and suitable emission spectrum position from UV to green region make this material a promising candidate for fast scintillators even in other applications [1,2].

In this work more systematic investigation of temperature dependence of scintillation and photoluminescence decay parameters is performed to complete further the studies reported until now in the literature [1,2].

Two Czochralski-grown single crystals of Yb_xY_{1-x}AlO₃ were studied, the values of x were either 0.02 or 0.3 in the melt.

Photoluminescence decay measurements were performed with modified spectrofluorimeter 199S by Edinburgh instruments using single photon counting method at various temperatures in the range from that of liquid helium up to room temperature (RT). Luminescence was excited by steady state hydrogen lamp using 230 nm wavelength. Pulsed x-ray tube was used for excitation of radioluminescence in scintillation decay measurements, which were performed at temperatures varying from that of liquid nitrogen to room temperature. Resulting decay curves were decomposed into sum of exponentials with Ames Photonics' SpectraSolve computer program using deconvolution procedure to obtain true decay times.

Our previous measurements revealed that photo- and radioluminescence spectra of Yb-doped YAP samples resemble each other, which means that both photoluminescence and scintillation are governed by the CT luminescence.

For the sample with x=0.02 the photoluminescence decay curve was approximated by two exponential components. The slow one was almost negligible. The decay time of the fast dominant component is about 90 ns up to 100K, then it starts to decrease down to about 1 ns at RT. This is caused by previously reported thermal quenching [1]. The slow tail component decay parameters do not show a stable trend with temperature because of the component's very low intensity and consequent difficulties of stabilizing the parameters during the run of computer programme. In the scintillation decay also two components, the fast and dominant and the slower and less intensive, were found. The decay time of the fast one are about two times shorter in the temperature region from 100 to 200 K when compared to the decay time of the photoluminescence fast component. The relative amplitudes of both scintillation decay components are almost comparable in the range between 80 and 100K, above 150 K the

slower one almost vanishes with increasing temperature favouring the faster one. This is probably caused by shallow trapping levels already proved by thermoluminescence below 150K, which cause slow-down in the scintillation response at lower temperatures.

For the highly doped sample with $x=0.3$, at the temperatures below 250K, all the decay time dependences are shifted to lower values with respect to the sample with $x=0.02$. This is due to concentration quenching, which causes decay nonexponentiality and already has been reported in this material [1]. That is why in the photoluminescence decay curve fits three components had to be used at lower temperatures. The decay time of the fastest one decreases similarly with temperature as the fast component in the sample with $x=0.02$. The calculated parameters of the slowest component are not stable due to its very low intensity. The slowest components in photoluminescence in both samples have probable origin in photoionization, as was recently proposed for Yb^{3+} CT luminescence [3]. Let us compare only the two most intensive ones. Interestingly, at lower temperatures the relative intensity of the fast component is significantly lower than the intermediate one. This is not observed for the sample with $x=0.02$, where the fast component is always dominant or at least comparable. At 100K the intensities are the same and above 180K the intensity of the fastest component reaches about 90%. For this heavily doped sample two main components were found in the scintillation decay, fast and dominant one and slow one with low intensity. This is similar to the sample with low Yb concentration. Also the relative intensities of both components change with temperature the similar way as for the other sample. The decay time values for the fast component almost follow the values of photoluminescence decay time from 140K to RT, but at lower temperatures under 140K they are significantly higher and the scintillation decay is significantly slowed down. This is probably caused by trapping states which have been evidenced by thermoluminescence measurements under 80K [2].

Concluding, in both samples, the relative intensity of the fast component is at least 90% above 180K irrespectively on the excitation source (UV, X-ray) and the corresponding decay times are of the order of nanoseconds. At this temperature the radioluminescence intensities reach 50% of BGO scintillator for highly doped sample and 30% of BGO for the other one. At room temperature scintillation response is considerably faster (decay time almost 1 ns) in both samples, while the radioluminescence intensities are 8% of BGO for heavily doped sample and 4% for the other one.

References:

- [1] SHIM, J.B., YOSHIKAWA, A., FUKUDA, T., PEJCHAL, J., NIKL, M., SARUKURA, N., YOON, D.H.,: *Growth and charge transfer luminescence of Yb^{3+} -doped YAlO_3 single crystals*, Journal of Applied Physics Vol.95, No.6, 2004, pp. 3063–3068.
- [2] NIKL, M., SOLOVIEVA, N., PEJCHAL, J., SHIM, J.B., YOSHIKAWA, A., FUKUDA, T., VEDDA, A., MARTINI, M., YOON, D.H.,: *Very fast $\text{Yb}_x\text{Y}_{1-x}\text{AlO}_3$ single-crystal scintillators*, Applied Physics Letters Vol.84, No.6, 2004, pp.882–884.
- [3] VAN PIETERSON, L., HEEROMA, M., DE HEER, E., MEIJERINK, A.: *Charge transfer luminescence of Yb^{3+}* , Journal of Luminescence 91, 2000, pp.177–193.

This research has been supported by Czech GA AV Project no. A1010305 and MSMT Project KONTAKT no. 1P2004ME716

Determination of Lifetime of Carriers in Semiconductors InP and CdTe from Photoconductivity and Seebeck effect

S. Vacková*, D. Tischler*, V. Gorodynskyy**, J. Oswald***, F. Karel***, K. Žďánský**, L. Pekárek***, K. Vacek****

vackova@fsid.cvut.cz

*Department of Physics, Faculty of Mechanical Engineering, Czech Technical University in Prague, **Institute of Radio Engineering and Electronics AV CR, Praha 8, *** Institute of Physics AV CR, Praha 6, ****MFF, Charles University in Prague

It is known, that the lifetime of carriers represents an important parameter of radiation detectors. Generation and recombination phenomena involving electron and holes are very important processes in any nonequilibrium thermodynamics. Our experimental work is concentrated on the application of the new model of generation and recombination processes of charge carriers. Comparison of two methods of determination of lifetime – photoconductivity measurements and Seebeck effect is presented.

The following transport coefficients were measured on all samples: temperature dependence of d.c. electrical conductivity, Hall and Seebeck coefficients. The samples (15 x 4 x 1.5) mm³ in size were squeezed between two copper blocks with an electrical heater inside each block. Temperature was measured by two Cu-constantan thermocouples; the Cu wires were simultaneously used for voltage measurements. On the same samples we measured also the photoconductivity. The main idea of calculation process: Experimental curve is „limited“ by two curves marked - α_n , and α_p . Curve α_p is calculated from experimental values obtained in Hall effect (at a given temperature one can define the position of Fermi level from known concentration of holes and by means of it the theoretical value of α_p). The curve ($-\alpha_n$) is obtained from electron concentration n which is calculated from known relation $n \cdot p = n_i^2$. This formula is valid only under the assumption that equilibrium statistics is applied for electrons and holes. But due to the violation of equilibrium owing to temperature gradient, yields theory [1] expressions for nonequilibrium carriers. It brings not only the formula for

their new distribution but gives directions on fitting of experimental dependence α_{exp} . Gurevich introduces lifetime of carriers analogically to photoconductivity measurement with the assumption that nonequilibrium carriers can recombine. The distance of calculated curve α_p and $(-\alpha_n)$ from experimental curve α_{exp} reflect the size of non-equilibrium and lifetime can be found through fitting of theoretical curve with the experimental one.

Table 1. Comparison of two methods of determination of lifetime of carriers. In p-CdTe the role of surface recombination is not included, so the differences are greater [2, 3, 4].

LIFETIME (s)	from photoconductivity 300 K	from photoconductivity 77 K	From Seebeck effect 300 K
InP semiisol.	2×10^{-3}	71×10^{-6}	2×10^{-5}
InP $p = 8,9 \times 10^{15} \text{cm}^{-3}$			$1,1 \times 10^{-4}$
CdTe $p = 8 \times 10^{15} \text{cm}^{-3}$	$9,3 \times 10^{-5}$	$13,9 \times 10^{-5}$	$1,3 \times 10^{-5}$
CdTe $p = 8 \times 10^8 \text{cm}^{-3}$	$8,7 \times 10^{-6}$	110×10^{-6}	4×10^{-3} with phonon drag effect $6,5 \times 10^{-4}$ without phonon drag

References:

- [1] GUREVICH YU ET AL.: *The role of non-equilibrium Carriers in the formation of Thermo-E.M.F. in bipolar Semiconductors*, phys. stat. sol. (b), vol.231, No.1, 2002, pp. 278 - 293.
- [2] VACKOVÁ S. ET AL *Workshop 2004* CTU in Prague 2004
- [3] VACKOVÁ S., ŽDÁNSKÝ K., VACEK K., SCHERBACK L., FEJCHOUK P., ILASCHOUK M., *Phonon Drag effect in Cd1-xZnxTe in Dependence on x: Minimum at x=0,04* phys. stat. sol. (a) vol. 177, 2000 pp263 - 265.
- [4] VACKOVÁ S., GORODYNSKYY V., OSWALD J., PEKAREK L., ŽDÁNSKÝ K., KAREL F., VACEK K., *Lifetime of Carriers and Seebeck Coefficient in InP Semiconductors*, send to phys. stat sol. 2005

Experimental Results from Z-Pinch Z-150 at CTU

D. Klír, P. Kubeš, J. Kravářík

klird1@fel.cvut.cz

Department of Physics, Faculty of Electrical Engineering, Czech Technical University,
Technická 2, 166 27 Prague 6, Czech Republic

The aim of this article is to present some important results of the z-pinch research at the Department of Physics at Faculty of Electrical Engineering, CTU in Prague. The primary objective of our research is a detailed description of a fibre z-pinch. We believe that our findings will help us to get deeper insight into the processes of generation of x-ray radiation and charged particles in dense z-pinch – the processes that have not yet been fully understood but seem to be a key to further and wider z-pinch applications.

During the past four years, a variety of fibre z-pinch experiments has been performed on a small device Z-150 at the Czech Technical University in Prague. The generator used to drive the last experiments consisted of one capacitor with the capacitance of 3 μF . In the case of a 20 kV charging voltage, the current was peaking at 70 kA with a quarter period of 850 ns. The z-pinch was formed from carbon fibres of 15 μm diameter and of 9 mm length [1,2].

In order to observe plasma dynamics, comprehensive diagnostics was implemented and used:

- (i) The circuit dI/dt was monitored with a Rogowski coil placed near the cathode.
- (ii) Two filtered PIN diodes (0.8 μm Al foil, and 15 μm Be filter) detected temporal evolution of XUV and soft x-ray radiation.
- (iii) Fibre scintillator and HAMAMATSU photomultiplier were used to detect hard x-rays above 8 keV.
- (iv) The spectral characteristics of radiation were recorded by a gated XUV spectrograph. The useful spectral ranges of the XUV Rowland-circle grating spectrometer of 2÷10 nm, 7÷25 nm, and 25÷60 nm were achieved with the gratings of 1200, 600, and 300 gr./mm, respectively.
- (v) The spatial characteristics of radiation were detected by a gated VUV pinhole camera. The gated pinhole camera was used either without any filter for detection of VUV ($\lambda < 200$ nm) radiation or with a filter (Al or Be) for the detection of XUV or soft x-ray emission. The temporal resolution of the gated spectrometer and pinhole camera was carried out with two 4 frame MCP detectors with the exposure time of 2 ns and the time delay between exposures of 10 ns.
- (vi) A time-integrated x-ray pinhole camera was differentially filtered. The filters (1.5 μm Al foil, and 15 μm Be filter) were chosen according to filters used with PIN diodes.
- (vii) The laser probing enabled the visualisation of the electron density gradient (schlieren method). The beam of a frequency doubled Nd-YAG laser (530 nm, 3 ns FWHM) was separated into two beams and one of them was delayed by 10 ns with respect to the other.

This comprehensive set of diagnostic tools was synchronized in such a way, that an XUV spectrum, a pinhole image and a schlieren image were taken simultaneously.

This diagnostic set-up, and by extension the results obtained from it, enabled us to observe the evolution that can be summarized as follows:

The carbon fibre z-pinch driven by a slow current generator consisted of two apparently different stages:

- (i) The first stage could be shortly described as “plasma on fibre”. We expect that the low density (coronal) plasma is formed during the breakdown. Due to the fact that the conductivity of a carbon fibre is very low, the electric current is flowing through the coronal plasma. The coronal plasma is expanding and when the current has built up, the implosion of the low density plasma onto a fibre occurs. The XUV pulses are generated when the coronal plasma has imploded onto a dense fibre. The maximum electron temperature and electron density of the “hottest” region were estimated to be 80 eV and 10^{19} cm^{-3} respectively. Although the presence of a fibre did not significantly suppress MHD instabilities, they are not disruptive.
- (ii) The second stage begins when a part of a fibre has been already ablated. After that, the discharge is realized mostly in the vapour of electrodes. In this phase the x-ray radiation is generated when an $m = 0$ instability has developed.

On the basis of our experimental results we can conclude that the combination of a small current generator and low-Z dielectric load (such as carbon fibre) allows us to study key-issues of z-pinches: the snowplough implosion of the coronal plasma, the zipper effect, the development of MHD instabilities, the generation of x-ray radiation, the low density plasma as a very good conductor, etc.

Moreover, the unique comprehensive diagnostics, part of which was tested at Z-150 device in Prague, were also used on more powerful devices in Moscow [3] and Warsaw [4].

References

- [1] KLÍR, D., KUBEŠ, P., KRAVÁRIK, J.: *Carbon Fiber Z-Pinch Driven by Microsecond-Long Capacitive Discharge*, CZECH. J. PHYS. 54 C (2004), pp. 264-273.
- [2] KLÍR, D., KUBEŠ, P., KRAVÁRIK, J.: *XUV Emission from Small Fibre Z-Pinch X-Ray Lasers 2002*, 8th International Conference on X-Ray Lasers, American Institute of Physics, 2002, pp. 447-450.
- [3] KLÍR, D. – ET AL: *XUV and Soft X-Ray Emission from Fast Z-Pinch Discharge* 3rd International Conference on Inertial Fusion Sciences and Applications, Monterey, California, 2003, pp. 735-738.
- [4] KUBEŠ, P. – ET AL: *Influence of CD2 Fiber on the Compression in the PF-1000 Facility* CZECH. J. PHYS. 54 C (2004), pp. 285-290.

This research has been supported by the research program LN00A100 "Research Center of Laser Plasma", the Ministry of Education, Czech Republic.

Optical Absorption Loss at Nano-Rough Silver Back Reflector of Thin Film Silicon Solar Cells

L. Hodakova*, J. Springer**, A. Poruba**, M. Vanecek**, Z. Brykнар*, O. Kluth,
B. Rech*****

mulle@fzu.cz

**ČVUT, Trojanova 13,
CZ-120 00, Prague 2, Czech Republic*

***Institute of Physics, Academy of Sciences of the Czech Republic, Cukrovarnicka 10,
CZ-16253, Prague 6, Czech Republic*

****Institute of Photovoltaics, Forschungszentrum Jülich GmbH, D-52425 Jülich, Germany*

Rough silver back reflector (BR) is used in thin film silicon solar cells to reflect and scatter light, which was not absorbed during the first path through the very thin solar cell. The roughness on a scale of 20-200 nm (root mean square, rms, value) serves to scatter the light, in order to increase the optical path of weakly absorbed light in the cell [1]. In combination with the light trapping effect in medium (silicon) with a high index of refraction, it increases the current generated in thin film silicon solar cells, leading to efficiencies over 14 % in the amorphous Si/microcrystalline Si tandem [2].

The experiments cover the range 4–150 nm of rms roughness which was determined by atomic force microscopy. Two series of silver back reflectors (one covered with thin ZnO layer) were investigated. The investigated samples (nano-textured back reflectors) were prepared in three or four steps. First, the ZnO film was deposited on glass by sputtering. This film, initially “flat”, (rms roughness below 15 nm) develops a surface texture upon etching in diluted HCl. In the next step, the surface roughness was varied by varying the etching time. Then, such textured ZnO films were coated by 500 nm thick silver layers also prepared by sputtering, which maintained surface texture of ZnO. Thus the rms roughness of the silver films ranges between 14 and 150 nm. Finally, samples of “type 2” were covered by a sputtered thin (30 nm) ZnO film without an oxygen exposure before the sputtering. Additionally, we prepared two samples with a smooth silver surface as a reference: silver sputtered directly on the Corning glass (rms roughness = 4.2 nm) and silver sputtered on a thin (30 nm) non-etched ZnO film (rms roughness = 5.5 nm).

Optical properties of thin film silicon solar cells with nano-rough interfaces were modeled [3-4]. These models ask for the accurate optical constants of materials used in the solar cells. They are well known for different forms of silicon (amorphous, microcrystalline, crystalline) and ZnO with various doping level, but no precise spectral study has been done for the rough silver surface, covered by a thin ZnO layer – the best back reflector for thin film silicon solar cells.

The spectra of the total absorption loss (absorptance A) of nano-rough silver surfaces were measured with high accuracy. Instead of the measurement of total reflectance R and calculation of $A=(1-R)$, we measure A directly, using the Photothermal deflection spectroscopy (PDS) [4], which is more accurate for A below approximately 20 %. The PDS measurement [4] was done in CCl_4 , which is transparent in the UV region and its refractive index strongly varies with temperature. This helps us to increase the precision of measurement for the most important case of weak absorption losses. The range 4-150 nm of

rms roughness is covered in our experiment. Roughness is determined by Atomic force microscopy (AFM).

The results show that the absorbance A is not a simple function of the rms roughness. The lowest absorption loss in 500-1100 nm region is for the silver layer deposited directly on a glass substrate. Absorbance is already higher for silver deposited on "smooth" (rms roughness < 15 nm) ZnO layer and increases for silver deposited on rough ZnO. A similar trend is for silver covered by 30 nm ZnO layer. For the roughness larger than approximately 35 nm (rms) the absorbance saturates for both series.

To conclude, we directly measured absorption losses in rough silver back reflectors, with a high precision in the spectral region of interest for silicon thin film solar cells. Absorption loss did not scale directly with an increasing surface roughness and the saturation is observed. Photothermal deflection spectroscopy, as presented here, proved to be a useful tool for this study. According to our modeled results, short circuit current reduction due to surface plasmon absorption is about 0.5 mA/cm² for thin μ -Si cells.

References:

- [1] PORUBA, A. – FEJFAR, A. – REMES, Z. – SPRINGER, J. – VANECEK, M. – KOCKA, J. – MEIER, J., TORRES, P. – SHAH, A.: *Optical absorption and light scattering in microcrystalline silicon thin films and solar cells*, J. Appl. Phys. 88, 2000, pp. 148-161 .
- [2] SHAH, A.V. – SCHADE, H. – VANECEK, M. – MEIER, J. – VALLAT-SAUVAIN, E. – WYRSCH, N. – KROLL, U. – DROZ, C. – BAILAT, J.: *Thin-film silicon solar cell technology*, Progress in Photovoltaics 12, 2004, pp. 113- 142.
- [3] YAMAMOTO, K. – NAKAJIMA, A. – YOSHIMI, M. SAWADA, T. - FUKUDA, S. – HAYASHI, K. – SUEZAKI, T. – ICHIKAWA, M. – KOI, Y. – GOTO, M. – TAKATA, H. – TAWADA. Y.: *Accurate Evaluation of Minority Carrier Diffusion Length in Thin Film Single Crystalline Silicon Solar Cells*, In Proceedings of the 29th IEEE PVSC, New Orleans, LA, 2002, 1110.
- [4] SPRINGER, J. – PORUBA, A. – VANECEK, M. – FAY, S. – FEITKNECHT, L. – WYRSCH, N. – MEIER, J. – SHAH, A. – REPMANN, T. – KLUTH, O. – STIEBEG, H. – RECH, B.: *Improved Optical Model for Thin Film Silicon Solar Cells*, In Proceedings of the 17th E-PVSEC, Munich, Germany, 2002, 2830.

This research has been supported by the project DOIT of European Communities, contract ENK6-CT2000-00321, by the Czech research program K1010104, and by FRV grant No. 2098/2004.

Intensive Course Concepts of Postmodern Physics

L. Drška

drska@antu.fjfi.cvut.cz

Department of Physical Electronics, Faculty of Nuclear Sciences and Physical Engineering,
Trojanova 13, 120 00 Prague 2, Czech Republic

Knowledge of modern physics and its current trends at the beginning of the 21st century is an indispensable part of the training of any engineer and physical scientists. That is because virtually all novel technology is based, at least in part, on this knowledge. This contribution describes development and concepts of a concise course devoted to selected problems in high-tech physics. Modern pedagogical approach, relevant to the presented topics, is emphasized.

The objectives of the course “Concepts of Postmodern Physics” are as follows: (1) To present an overview of methods, selected topics and trends in contemporary physics with emphasis on potential applications in future high-tech engineering. (2) To show the key role of information technology in research and application of novel physics. (3) To demonstrate an extensive evaluated collection of printed / electronic resources for the study of contemporary physics.

TAB. 1. DEVELOPMENT TOOLS FOR THE COURSE

Development Tasks	Presentation Set Standard Software	Website Set A/B
Office work	Office 2003	Office 2003
	POWERPOINT 2003	PowerPoint 2003
Package integration	CAPTIVATE	STUDIO MX 2004 WITH
Conversion & capture	- Flash Paper 2	FLASH PROFESSIONAL
Course authoring	Mozilla Composer	- Dreamweaver MX 2004
	/ Netscape Composer	- Fireworks MX 2004
Website authoring	Contribute 3	- Flash MX 2004
	/ NetObject Fusion*	Professional
Graphics	Photoimpact 10	- Course Builder
	/ Paint Shop Pro 9	- Learning Site*
Animation	GIF Animator 5	Contribute 3
Multimedia	Videostudio*	Captivate
	/ Pinnacle Studio*	-----
Assessments Tests	Respondus 2	Premiere Pro 1.5*
	Hot Potatoes 6	Respondus 2
Special Software		
Formulas Symbolic computing Scientific graphics	CALCULATION	MATHEMATICA 5.2
	CENTER 2	WEBMATHEMATICA 2 / MAPLE 9.5
Numeric calculation Simulation	Java Applets	MAPLENET 2.5*
	Physlets	----- MathType 5.2 Matlab 7
Special assessments, tests	Spotter 2*	MAPLE T.A. 1.5*
<i>Comment:</i> * Software tools with a limited use in the first version of the course.		

TAB. 2. CONCEPTS OF POSTMODERN PHYSICS	
1st Day	1. Introduction. 2. Postmodern Physics Features: Classical, Modern and Postmodern Physics. Information Science and Contemporary Physics. <i>Comp Lab 1:</i> Introduction to the Work in the Computational Laboratory. Electronic Resources for the Course.
2nd Day	3. Methods: Integrated Computing Systems (ICS). Intensive Computing and Visualization. Emerging Concepts: AI, GA, PSE. <i>Comp Lab 2:</i> Practical Use of ICS in Physics.
3rd Day	<i>Cultural / European Dimension Program.</i>
4th Day	4. Selected Topics: High-Energy and High-Intensity Lasers. Soft X-Ray Sources and X-Ray Lasers. Physics of Extreme Systems. <i>Comp Lab 3:</i> Some Relevant Complex Codes.
5th Day	5. Applications: Subpicosecond / Superstrong Field Photonics. Laser and Plasma Nucleonics, ICF. Computational and Laboratory Astrophysics. <i>Laboratory Visit:</i> Research Center for Laser Plasmas (PALS) and Institute of Physics. 6. Conclusion: Contemporary Physics and High-Tech Engineering. Study and Research Possibilities at the CTU. <i>Final E-Test.</i>

To achieve these goals effectively, the course is presented in Twin-Learning Mode (TLM course); substantial part of the course is delivered in a computational laboratory. Active participation of the students in the education process is required, appropriate skills for individual work in a computational laboratory and using e-documents are expected.

In order to develop this course sophisticated development methods have been tested / used. A concise survey of development software is presented in **TAB. 1**. More information is available in [1],[2]. The experiences from the work have been exploited for designing a new, workshop-like course “Technologies for ICT-Based Knowledge Transfer“ (Prospectus 2005, 12TPL).

A short syllabus of the course “Concepts of Postmodern Physics” in the version offered for the Program ATHENS (2005) is shown in **TAB. 2**. More details are available in [3]. An example of materials for a selected lecture in the course can be found in [4]. Some parts of the courseware have been tested in lectures and seminars of the curriculum “Information Physics” at the FNSPE CTU. The courseware will be used also for a reconstruction of the obligatory course “Fundamentals of Computational Physics I” (Prospectus 2005, 12MPF1).

References:

- [1] DRŠKA, L.: *E-Learning for Information Physics..* Workshop CTU 2004.
<http://vega.fjfi.cvut.cz/docs/w2004/>
- [2] DRŠKA, L.: *Concepts of Postmodern Physics. Addendum.* Workshop CTU 2005.
<http://vega.fjfi.cvut.cz/docs/w2005add/>
- [3] DRŠKA, L.: *Concepts of Postmodern Physics. Detailed Information.* ATHENS, Spring 2005, <http://vega.fjfi.cvut.cz/docs/athens2005/>
- [4] DRŠKA, L.: *Laser and Plasma Nucleonics. Short Free Version.*
<http://vega.fjfi.cvut.cz/docs/athens2005/lpnshort.htm>

This research has been supported by CTU grant No. CTU0418714 .

Analysis of X-Ray Spectra Using a GA Code

P. Adámek*, L. Drška* , O. Renner**

drska@antu.fjfi.cvut.cz

*Department of Physical Electronics, Faculty of Nuclear Sciences and Physical Engineering, Trojanova 13, 120 00 Prague 2, Czech Republic

**Institute of Physics, AS CR, Na Slovance 2, 182 21 Prague 8, Czech Republic

Genetic Algorithms (GA), Optimization Problems in Physics Research: Genetic algorithms are computer procedures that employ the mechanics of natural selection and natural genetics to evolve solutions to problems. They are most appropriate for complex non-linear models where location of global optimum is a difficult task. In the study of physics of high energy densities (HED) such problems are typical. Analysis of X-ray spectra emitted by high-parameter plasmas can be quoted as a very important example. This contribution presents some concrete software and applications of GA in this area and suggests potential use of evolutionary computation in more sophisticated studies.

GA Tool Development, Program GASpeD 2 [1]: Our main application of GA focuses mainly on the spectroscopic diagnostics of laser-produced high parameter plasmas. A new robust approach to spectral decomposition has been developed. The method is based on a genetic algorithm using tournament selection and a simple elitist scheme. Problem-dependent representation and special genetic operators are used. Several modifications improving the convergence have been applied; the Levenberg- Marquardt (L.-M.) method can be turned on to refine the final fit.

The method was implemented as GASpeD 2 - a specialized program designed to perform spectral decomposition. The code was created using the Borland C++ Builder 6, the genetic algorithm is however independent of graphics user interface and can be compiled using common ANSI compatible C++ with minimum changes. The program works under Windows 98/2000/XP operating systems with at least 32 MB of RAM. A high-resolution display is recommended.

GASpeD 2 offers two different fitting modes, depending on number of parameters the user wants to control. It enables to perform an interactive fitting of spectra with only a minimal user input, most of the parameters and constraints can be set automatically. In the automated fit (suitable for the basic analysis of spectra or for fitting a simple data, 2 – 3 profiles), the only input required is the following: (a) Type of fitting curves: Gauss, Lorentz, pseudo-Voigt. (b) Type of background: none, constant, 2nd to 4th order polynomial, Gauss. (c) Approximate number of curves in the spectrum > +/- 50 %. In contrast, the advanced fit allows the user to control all the parameters of the algorithm, including the constants describing the constraints, parameters of individual genetic operators, etc.

User-friendly GUI for basic visual analysis of the spectra is also available. The program was successfully tested on both simulated and real experimental data, it produces good parameterizations of given spectra, even in the case of severe noise.

GA in Dense Plasma Spectroscopy, Other and Future Applications: Main applications of the program GASpeD include analysis of X-ray spectra of laser-produced plasma measured in experiments of several authors. Some typical results of this work can be quoted. Most interesting application include spectral line decomposition and frequency shifts in He-alpha group emission in dense Aluminum plasma [2],[3]. Detailed investigation of the profiles and frequency shifts in both optically thin and thick plasma media with advanced, high-resolution X-ray spectrometers for collection of precise benchmark data for testing the theoretical models was primary goal of these studies. The case-based model emphasizing aggregate satellite shifts has been used.

The program GASpeD proved to be a robust and effective tool in these studies.. The advanced fit has been applied in this work. Pseudo-Vogt profiles line profiles have been accepted. Some concrete code characteristics used in this study are as follows: (1) Genome size: 26 - 38 parameters. (2) Population: 250 - 500 genomes. (3) Number of operators tailored for spectral decomposition: 8. (4) Number of generation: ~1000. (5) Refined final fit: L-M method.

Other successful (unpublished) applications of the program are as follows: (1) Verification study of quiet Sun spectrum measured by SOHO satellite. (2) Interpolation of X-ray ablation spectrum, fitting the soft X-ray spectrum of Xe-He gas puff target irradiated by the PALS laser (Létal, 2004). (3) Decomposition of PIXE spectra (data kindly provided by J. Král), comparison with the output of GUPIX - the most popular program in this area.

New version of the GASpeD code will include the possibility of the analysis of multi-exponential, weak and strongly noisy decay sources, a very important feature for evaluation of HED experiments related to laser nucleonics and laboratory astrophysics. Application in nuclear excitation and transmutation studies are planned. Our studies should consider also potential applications of GA and evolutionary algorithms for solving multi-objective problems (MO-GA) in the design and evaluation of HED studies related to these areas [4].

References:

- [1] ADÁMEK, P.: *Application of Genetic Algorithms to Analysis of High-Parameter Plasma. Diploma Thesis.* Faculty of Nuclear Sciences & Physical Engineering, Czech Technical University, Prague, 2004.
- [2] RENNER, O. – KROUSKÝ, E. – ADÁMEK, P. – AT AL.: *Plasma Induced Line Shifts in Emission of Aluminum He-alpha Group.* In: 17th International Conference on Spectral Line Shapes, Paris, France, June 21 - 25, 2004.
- [3] RENNER, O. – ADÁMEK, P. – KROUSKÝ, E. – AT AL.: *Spectral Line Decomposition and Frequency Shifts in Al He-alpha Group Emission from Laser Produced Plasma.* In: 11th International Workshop on Radiative Properties of Hot Dense Matter, Santa Barbara, CA , 1 - 5 Nov., 2004. To be published in Journal of Quantitative Spectroscopy & Radiative Transfer.
- [4] DRŠKA, L.: *Nucleoreactive Plasmas: Future Trends and Some Potential Experiments.* In: International Workshop on Physics of High Energy Density in Matter, Hirschegg, Austria, Jan. 30 - Feb. 4, 2005.

This research has been supported by MŠMT grant No. MSM LN00A100.

Measurement of Optical Systems using Shack-Hartmann Sensor

J.Novák, P.Novák, A.Mikš

novakji@fsv.cvut.cz

Department of Physics, Faculty of Civil Engineering, Czech Technical University,
Thákurova 7, 166 29 Prague 6, Czech Republic

Various measurement methods [1,2] can be implemented for testing optical systems in practice. Interferometric techniques [1] are most frequently used in industrial practice. These methods permit to measure the wave-front shape with respect to a specified reference wavefront (mostly planar or spherical) with specially designed interferometers, either Fizeau or Twyman-Green type. The shape of the tested wavefront is then evaluated using phase analysis of the interference field [1-3]. These measurement devices (interferometers) may obtain a very high measurement accuracy. However, the interferometers are very expensive and relatively very complicated measurement systems that cannot be used in most cases in industrial conditions. Interferometric techniques have several important drawbacks, especially a large sensitivity to environmental conditions (e.g. vibrations) and a limited measurement range. In comparison to interferometric methods, which determine the wavefront aberration using phase analysis of the interference field, one can use the methods that enable to measure the wavefront slope (phase gradients) [2,4], and consequently calculate the wave-front aberration. Such measurement techniques have several advantages in comparison to above-mentioned interferometric methods. These are simpler, less expensive, do not need a coherent source of light, are practically insensitive to mechanical vibrations of the measurement environment, and even wavefronts with large aberrations can be tested.

Our research deals with the design and testing of the Shack-Hartmann sensor for wave-front shape measurements. It was proposed, designed and fabricated the lenslet array objective that is based on the Shack-Hartmann method for wave-front evaluation. The Shack-Hartmann method [3,4] uses the microlens array and the CCD sensor for wave-front evaluation. The Shack-Hartmann sensor estimates the wave-front local slopes (wave-front gradient) at points located in a regular grid. The tested wavefront is spatially sampled by the microlens array and the sampled wavefront impinges on the CCD sensor, which is most usually situated in the focal plane of the microlens array. The area of the CCD sensor is divided virtually in many subdetectors. The size and the number of subdetectors correspond to the size and number of microlenses. The incident (tested) wave-front that impinges on the array of microlenses has a general shape, and the normal to the wave-front has a different direction for different positions (different microlenses). The microlenses focus the light into their focal plane, where the CCD detector is placed. The spot array obtained in the focal plane of the microlens array is detected.

The detected "spots" correspond to the intensity distribution after sampling by the sub-apertures of the microlens array. A position of the spot on the sensor is given by the direction of the main normal corresponding to a specific microlens and the focal length of the microlens. The main normal of each microlens is a normal to the wave-front, which passes through the center of the microlens. In order to calculate the deformation of the tested wavefront using wave-front gradient measurements, we must determine a deviation of the spot of a given beam, which is specified by the size of the correspondent microlens and by the direction of the main normal, from a position of the spot in the case of a reference wave-front (usually flat wavefront). In the case of a test wave-front, which impinges on the microlens

array, the spots of beams from individual microlenses will be detected in certain parts of the detector. The spots of individual beams have a relatively difficult intensity profile that depends on the wavelength of light, size, shape, focal length, and aberrations of microlenses. The centre of the spot must be determined very accurately in order to achieve high measurement accuracy. Several methods can be used for spot detection, e.g. the spot can be calculated as a centre of gravity of the detected intensity profile. These intensity spots form a specific grid, which is named the Hartmann pattern. The position of each spot is dependent on the slope of the part of the wavefront, which impinges on the corresponding microlens. The displacements of the spot positions can be measured with respect to the reference position and the wave-front can be numerically reconstructed from the values of the spot displacements using various mathematical procedures [3,4], e.g. by integration or by approximation using polynomials. In our work, we investigated various methods for approximation of the wavefront from a discrete set of wave-front gradients

We proposed, designed, and fabricated the lenslet array objective that consists of the lenslet array (20x20 microlenses with the diameter 0,3 mm and the focal length 40 mm, made from fused silica) and the CCD sensor (resolution 768x576 pixels and pixel size 6 μm .). The array objective, which represents one of key elements of the measurement system, has been tested in a setup with an autocollimator that generates plane wave. We performed several experiments that enable to verify the measurement and evaluation method by comparison with the theoretical analysis of experiments. It was shown a very good agreement between the experimental data and expected theoretical results. The measurement range of the sensor is limited by diffraction of light and the ability to detect the corresponding intensity spots. However, the accuracy of the designed sensor is higher than $\lambda/20$, where λ is the wavelength of light. Such accuracy is comparable to common interferometric techniques in optical industry, and it is sufficient for testing of optical elements and systems. Moreover, together with Meopta Optika, a.s., several experiments were made for testing optical systems in UV and visible light using our wave-front sensor. The effective computation algorithms were proposed for automatic computer analysis of the tested wavefronts. These evaluation algorithms were implemented into the software for wave-front analysis that was used for primary experiments with the wave-front sensor. Further work will be devoted to calibration and completion of the whole measurement system, completion of the evaluation software for wave-front analysis, improvement of measurement accuracy, and making more experiments on optical system testing.

References:

- [1] MIKŠ, A.: *Interferometrické metody vyhodnocování sférických ploch v optice*. Jemná mechanika a optika, roč. 46 , č. 1, (2001) p.29-35.
- [2] NOVÁK, J. - MIKŠ, A.: *Modern Techniques for Evaluation of Phase of Wave Field*. Proceedings of the conference New trends in physics. Brno 2004, pp.250-253.
- [3] NOVÁK, J.: *Five-step phase-shifting algorithms with unknown values of phase shift*. Optik, Vol. 114, No. 2 (2003), pp.63-68.
- [4] MIKŠ, A. - NOVÁK, J.: *Evaluation of Gradient of Wave Field in Optical Testing*. MATLAB 2002. VŠCHT, Prague 2004, pp.319-322.

This research has been supported by GA ČR grant No. GA 103/03/P001.

Modern Evaluation Techniques in Optical Testing

J. Novák, A. Mikš, P. Novák

novakji@fsv.cvut.cz

Department of Physics, Faculty of Civil Engineering, Czech Technical University,
Thákurova 7, 166 29 Prague 6, Czech Republic

A basic task in optical production is to design and fabricate surfaces of optical elements with specified tolerances in order to satisfy production requirements, i.e. the shape and accuracy of optical surfaces must correspond to tolerances given by drawings and other documentation. It is much simpler to satisfy tolerances of optical elements with planar or spherical surfaces than optical elements with aspherical surfaces. In the case of fabrication of optical elements with planar or spherical surfaces, deviations from the nominal shape are determined by comparison of the fabricated optical surface (flat or spherical) with the reference surface that is flat or spherical. The optical element with a reference optical surface of a defined shape is called a calibre (calibration surface) [1]. The fabricated optical surface has a perfect shape if no interference fringes can be seen between the optical surface and the calibre, which is put in contact with the fabricated surface. In the case of fabrication of optical elements with aspherical surfaces, it is much more difficult to fabricate the calibre corresponding to a given aspherical surface. In practice, the aspherical surface is most frequently tested using a spherical surface that is similar to the tested surface. Interference pattern occurs between the tested aspherical surface and the spherical surface of the calibre. Interference fringes characterize the shape of the aspherical surface only in the case that the tested surface and the calibre are properly mutually positioned, e.g. they are concentric and have a defined axial distance in the case of rotationally symmetric aspherical surfaces. The mentioned conditions can be hardly fulfilled during optical testing in practice. Nowadays, the process of testing of aspherical optical surfaces is a difficult problem that can be solved by several ways. It can be designed for every aspherical surface the so-called null-lens based on the diffractive optical element, but it is a very tedious and financially demanding process. Substantially better results can be obtained using interferometers, mostly Fizeau or Twyman-Green types [1]. The interferometers use the principle of interference of the reference and tested wavefront. Aberrations of the tested optical surface can be evaluated by a proper analysis of the detected interference pattern using various computer phase evaluation techniques [1,2]. The accuracy of such measurement techniques is very high. However, these interferometric methods have several drawbacks, especially sensitivity to mechanical vibrations and heat fluctuations of the measurement environment, relatively complicated design, limited measurement range, and high acquisition costs.

In comparison to interferometric methods, which determine the wavefront aberration using phase analysis of the interference field, one can use methods that enable to measure the wavefront slope, and consequently calculate the wave-front aberration. Such techniques have several advantages. These methods are more simple, less expensive, do not need a coherent source of light, are practically insensitive to vibrations, and even wavefronts with large aberrations can be tested. In practice, the most widely used measurement method is the Shack-Hartmann method that uses the microlens array and the CCD sensor for wave-front evaluation. However, this method has also some limitations.

The aim of our work was to propose new and simple evaluation methods that enable to remove disadvantages and limitations of above-mentioned methods and speed up the testing process of optical surfaces and optical elements. We focused on the problems of testing surfaces of optical elements using two-beam interferometry. It was shown how to perform a

computer simulation of various types of optical surface deformations for various optical elements. Interference patterns that correspond to required tolerances of fabricated optical elements can be generated using suitable computer programs, and the shape of interference fringes is known in advance. Such information is very helpful in practical optical testing. We proposed two evaluation methods for optical testing. The proposed methods do not require to make a detail analysis of the interference field, i.e. determination of shape and orders of interference fringes or classical phase analysis as it is necessary with existing interferometric methods. The proposed methods can be used for testing the quality of optical surfaces and optical elements in practice.

The first method can be used for testing a shape of general optical surfaces (i.e. flat, spherical or aspherical surfaces). The method is based on the correlation analysis and mathematical optimization techniques [3]. It is a relatively simple evaluation method that enables to speed up the process of optical surfaces testing. The deviation of the tested surface from its nominal shape is characterized by the correlation coefficient between the tested wave field and reference wave field that corresponds to the nominal shape of surface. By maximization of the correlation coefficient, one can obtain information about the deviation of the tested optical surface from its nominal shape, i.e. it is possible to evaluate whether the tested optical surface fulfils the tolerance requirements. The proposed method is universal and can be used for testing of flat, spherical or aspherical optical surfaces. The second method can be used for evaluation of small phase variations using shearing interferometry. This evaluation technique uses the interference of polychromatic light and the colorimetric analysis of the interference pattern [4]. The wave-front aberration is determined directly from the colour of the interference field, because even a small phase change has effect on the colour of the interference pattern. If the tested optical system is aberration free, then the field of view will be uniformly coloured because the path difference between sheared wavefronts is constant. However, if the tested wavefront is aberrated, then the field of view will be uniformly coloured no longer. Colour interference fringes or a nonuniformly coloured field of view occur because the path difference between sheared wavefronts is not constant. The phase change that represents the wave-front deformation has effect on the colour of the interference pattern, and it can be evaluated using colorimetric methods. We proposed a technique, which enables an automatic evaluation of the detected interference pattern. The proposed method offers very accurate results and it is suitable for practical utilization in optical industry.

References:

- [1] MIKŠ, A.: *Interferometrické metody vyhodnocování sférických ploch v optice*. Jemná mechanika a optika, roč. 46 , č. 1, (2001) p.29-35.
- [2] NOVÁK, J.: *Five-step phase-shifting algorithms with unknown values of phase shift*. Optik, Vol. 114, No. 2 (2003), pp.63-68.
- [3] NOVÁK, J. - MIKŠ, A.: *Korelační analýza interferogramů*. MATLAB 2004 - Sborník příspěvků 12. ročníku konference. Praha: VŠCHT, 2004, pp. 411-414.
- [4] NOVÁK, J. - MIKŠ, A. - NOVÁK, P.: *Colorimetric Analysis of Small Phase Changes of Wave Field*. Proceedings of the conference New trends in physics, Brno 2004, pp. 242-245.

This research has been supported by GA ČR grant No. GA 103/03/P001.

Hyperchromatic Optical Systems

J. Novák, P. Novák, A. Mikš

novakji@fsv.cvut.cz

Department of Physics, Faculty of Civil Engineering, Czech Technical University,
Thákurova 7, 166 29 Prague 6, Czech Republic

Generally, optical lens systems consist of several lenses that are made from different kinds of optical glass. The lens optical systems have always chromatic aberration due to a dependence of the refraction index of optical glass on the wavelength of light [1]. The chromatic aberration has a negative effect in imaging optical devices, because it reduces the imaging quality of optical systems and it is necessary to correct this type of aberration very well. Optical systems that are used for imaging in optical instruments, e.g. in binoculars, microscopes, cameras and projectors, have chromatic aberration corrected very well in order not to reduce the imaging quality. By a proper choice of optical glass types, it is possible to correct chromatic aberration for several wavelengths.

However, it is sometimes necessary to design optical systems with relatively large chromatic aberration in practice. Such optical systems are called hyperchromats (hyperchromatic optical systems) [2]. Our work solves the problems of calculation of design parameters for hyperchromats that consist of several thin lenses in contact. These hyperchromatic optical systems have a linear dependence of the longitudinal chromatic aberration on the wavelength of light. General equations were derived for calculation of powers of individual lenses of such optical systems. Moreover, general equations were derived for calculation of powers of hyperchromats with a specified range of longitudinal chromatic aberration and a linear dependence of longitudinal chromatic aberration on the wavelength. Examples were shown for calculation of hyperchromatic doublets and triplets with the linear dependence of longitudinal chromatic aberration on the wavelength. Such hyperchromatic optical systems can find their application area especially in 3D imaging (topography of surfaces), spectroscopy, and confocal microscopy.

We focused our research on possible application of hyperchromatic optical systems in systems for topography measurement. The problems of topography of surfaces are very important in various parts of science and engineering. Several approaches exist for surface figure and roughness measurement [3,4]. The measurement methods can be divided into two distinct categories, contact and non-contact techniques. Contact techniques use mainly linear sensors for measurement, e.g. dial indicators based either on a mechanical principle (sprockets and geared transmission) or on the principle of sensing mechanical probe movement using measurements of electromagnetic induction (inductive sensors), capacitance (capacitive sensors), resistance (resistive sensors), and using contact optical sensing systems. Main disadvantage of contact methods is the possibility of damaging the investigated surface with the mechanical sensor. The accuracy of measurement with contact sensors is mainly within the range $0.1 - 1 \mu\text{m}$. On the other hand, non-contact methods are mainly based on the principle of optical non-contact sensing systems or measurements of the change of capacitance. Interferometric methods are most frequently used for very accurate measurements of surface topography. With these methods, one can obtain the accuracy up to 0.1 \AA . Further methods that can be used for topography of surfaces are techniques AFM (Atomic Force Microscopy) and STM (Scanning Tunneling Microscope). AFM can work either in contact or in non-contact mode. The accuracy that can be reached with these

methods is within the range of nanometers. However, such measurement systems are very expensive, can be applied only to special specimens, and their dynamic range is limited.

We proposed a relatively simple method for topography measurements that uses special optical systems (hyperchromats) with a linear dependence of longitudinal chromatic aberration on the wavelength of light. The aim of this work was to show a possible application of hyperchromats, i.e. optical systems with a large chromatic aberration for topography of surfaces. The advantages of this method are relatively low costs, large dynamic range of measurement, simple experimental arrangement, and relative simple analysis.

Our work describes a basic analysis of parameters of hyperchromats, i.e. optical systems with large longitudinal chromatic aberration that is in our case linearly dependent on the wavelength of light. On the basis of the performed analysis, such optical systems can be designed that permit to perform measurements of topography of surfaces, i.e. determine a figure or roughness of surfaces. We proposed an optical system for measurements of topography of surfaces using hyperchromats. Polychromatic light from the source of light is focused into a little circular pinhole in the aperture stop using the condenser. After passing through the pinhole, the light is reflected by semitransparent mirror and transformed by the hyperchromatic objective lens. The image of the pinhole is formed by the hyperchromat in different distances with respect to the wavelength of light. After reflection from the tested surface, the light goes back through the semi-transparent mirror and impinges at the second aperture stop with a pinhole. The intensity of light, which propagates through the pinhole, will be maximal only for light of a specific wavelength that corresponds to a minimal diameter of ray bundle in the plane of the second aperture stop (for wavelength λ_0). For other wavelengths, different from wavelength λ_0 , will be the intensity of light behind the pinhole very low. A concave diffractive grating splits the transmitted light into a spectrum and a position of the maximum of intensity, corresponding to wavelength λ_0 , can be determined using a CCD sensor. The surface can be scanned with such a sensor. If the shape of the tested surface changes within the measurement range of the proposed hyperchromatic sensor, we obtain maxima of intensity on the CCD sensor for a number of wavelengths. Then, one can relatively simply determine the topography of the investigated surface using the known linear relationship between wavelength and the longitudinal chromatic aberration of the hyperchromatic lens. It was also proposed modification of the measurement system that uses optical fibres and spectrometer for quantitative evaluation. Further research will be devoted to designing, fabrication, and application of chosen hyperchromatic doublets and triplets for topography measurements.

References:

- [1] MIKŠ, A.: *Aplikovaná optika*. Vydavatelství ČVUT, Praha 2000.
- [2] MIKŠ, A. - NOVÁK, J. - NOVÁK, P.: *Application of Hyperchromats for Topography Measurements*. Proceedings of International Workshop: Research Activities of Physics Departments of Civil Engineering Faculties in the Czech and Slovak Republics. Brno: Akademické nakladatelství CERM, 2004, pp. 82-87.
- [3] MICHALKO, O. – MIKŠ, A. – SEMERÁK, P. – KLEČKA, T.: *Fyzikální a mechanické zkoušení stavebních materiálů*. Vydavatelství ČVUT, Praha 1998.
- [4] MIKŠ, A. - NOVÁK, J. - NOVÁK, P.: *Zjišťování drsnosti povrchu pomocí speklu*. Defektoskopie 2004, ČNDT, Praha 2004, pp.139-144.

This research has been supported by GA ČR grant No. GA 103/02/0357.

Aberration Analysis in Optical Imaging Systems

J. Novák, A. Mikš, P. Novák

novakji@fsv.cvut.cz

Department of Physics, Faculty of Civil Engineering, Czech Technical University,
Thákurova 7, 166 29 Prague 6, Czech Republic

Our research was focused on a theoretical analysis of aberrations of various elements in optical imaging systems in industrial practice. The first part of the work analyses an influence of the Goos-Hänchen effect in optical imaging systems. Optical systems that are used in various types of optical instruments consist of reflecting planar optical elements, namely reflecting prisms, in many practical cases. These reflecting prisms are used for changing a direction of an incident bundle of rays in optical instruments, e.g. in telescopes and binoculars. The change of the direction of the bundle of rays is mainly performed by total internal reflection of rays on the surfaces of the prism. It is well-known from the theory of reflection of light that total reflection is observed in the case of the propagation of light from the higher-index material into the lower-index material and that the so-called Goos-Hänchen effect occurs during total reflection of linearly polarized waves at the boundary surface between two different optical media. The Goos-Hänchen effect describes the spatial shift of the reflected ray with respect to a point, where the incident intersects the boundary (so-called Goos-Hänchen shift). The light penetrates through the interface into the second medium and propagates parallel to the boundary (evanescent wave). The penetration depth is very small. However, the law of reflection is still valid, i.e. the angle of incidence is equal to the angle of reflection. This evanescent wave depends on two parameters: the incident polarization state and the incident angle. Our work describes an influence of the Goos-Hänchen effect on the imaging properties of planar optical systems and it was derived a differential equation of a wave-front meridian that corresponds to a reflected bundle of rays. It was shown that the wave-front can be described by d'Alambert differential equation. This equation make possible to determine the coordinates of individual points on the wave-front meridian. Moreover, the Strehl definition, which describes the imaging quality, was calculated for the bundle of rays after its total reflection and it was shown the influence of total internal reflection on the value of Strehl definition. It can be concluded that the Goos-Hänchen shift may affect the imaging quality (resolving power and image contrast) of optical systems in the optical systems that use reflecting prisms with several reflective surfaces (multiple total reflection).

Furthermore, it was thoroughly analysed the case of thin oscillating mirrors that can be used for designing optical measurement and imaging systems. Vibrating thin flat mirrors are used in various areas of science and engineering, e.g. in optical measurement and imaging systems. The mirror vibration is closely related to the dynamic wave aberration of the wave-front, reflected from the mirror. The consequence of the wave aberration is a spatially inhomogeneous frequency shift of the light reflected from the vibrating mirror. The influence of the wave aberration on the frequency shift was studied theoretically in our work [1], and equations were derived for the frequency shift and dynamic wave aberration.

We have also presented the work that deals with the influence of the decentricity of individual optical elements in optical imaging systems on aberrations of such systems [2]. It was shown that a specific position of an axial object point can be found for every optical element, where the spherical aberration is either zero or minimal. It can be used for testing of centricity of very precise optical elements in optical imaging systems, because one can simply detect unsymmetry of the point spread function that is caused by the decentricity of the tested

optical element. It was also derived a simple theoretical equation for calculation of the coefficient of third order coma that corresponds to the decentricity of the optical surface due to a tilt of the surface with respect to the optical axis.

Our work also deals with an influence of aberrations of optical systems that are used in optical information processing systems [3,4]. We carried out a detailed analysis of the influence of aberrations on the image formed by the optical system. The work describes the theory of imaging using a diffraction limited optical system and the optical system with aberrations for the case of coherent radiation. Furthermore, the effect of aberrations of the wave field, which illuminates the object, was also studied. A theoretical analysis was carried out using the third order aberration theory. It was shown that the effect of aberrations is substantial in both cases and leads to the image degradation. We have also proposed a method for removing the spherochromatic aberration of optical imaging systems. Formulas for calculation of the thickness of thin aspherical layers were derived in our work. The proposed method seems to be especially suitable for correcting optical systems with zero chromatic aberration in the paraxial space. The elimination of the spherochromatic aberration is perfect in this case and the optical system is almost identical with the ideal optical system. Deposited thin aspherical layers also act as antireflective coatings. One may achieve three effects simultaneously with the proposed correction method: elimination of spherical aberration, elimination of spherochromatic aberration, and decreasing the reflectance of the optical system. The described method represents an advanced trend in correction of optical systems.

The last part of our work deals with the influence of object position on the image quality that is directly related to the measurement accuracy of optical measurement systems and the image quality of imaging optical systems. On the basis of the third-order aberration theory, it was shown that the change in the position of object leads to the change of aberrations of the optical system, and this change affects negatively the measurement accuracy or the imaging quality. The described effect cannot be removed. The mentioned effect was theoretically described in terms of both geometrical and diffraction theory of optical imaging. On the basis of the aberration theory, it was shown that the change of the object position with respect to the measurement instrument leads to the change of aberrations of the optical system, and this change affects negatively the measurement accuracy. The equations for determination of the relative measurement error were also derived. It was shown that the error must be taken into account in practical measurements and the correction must be calculated.

References:

- [1] MIKŠ, A. - NOVÁK, J. - NOVÁK, P.: *Frequency Shift of Light Reflected from Vibrating Mirror*. Proceedings of SPIE Vol. 5457, Washington 2004, pp. 292-299.
- [2] MIKŠ, A. - NOVÁK, J.: *Testing Centricity of Optical Elements Using Point Spread Function*. Proceedings of SPIE Vol. 5457, Washington 2004, pp.421-427.
- [3] MIKŠ, A. - NOVÁK, J.: *Four-Element Optical System for Fourier Transform*. Proceedings of SPIE Vol. 5457, Washington 2004, pp.284-291.
- [4] MIKŠ, A. - NOVÁK, J.: *Influence of Aberrations in Optical Information Processing*. Proceedings of SPIE Vol. 5457, Washington 2004, pp. 428-438.

This research has been supported by MSM research project J04/98:210000022.

Investigation of Phase Evaluation Techniques in Optical Measurement Methods

A.Mikš, P.Novák, J.Novák

miks@fsv.cvut.cz

Department of Physics, Faculty of Civil Engineering, Czech Technical University,
Thákurova 7, 166 29 Prague 6, Czech Republic

The research deals with modern methods for phase evaluation of investigated optical wave fields that are based on intensity measurements at the set of chosen points in space. The computer aided methods were studied, which use for evaluation of the phase of wave fields various principles, e.g. interference of light, measurements of the wave-front gradient, and the equation for transport of energy in electromagnetic field.

In practice, various optical methods are used for making measurements of different quantities, e.g. shape, static and dynamic deformation of surfaces, roughness, etc. These methods use the interaction of the optical (object) wave field with the investigated object for quantitative analysis. Physical properties (amplitude, phase, frequency, polarization) of the object wave are modified after the interaction. A very important class of such methods are phase techniques that use evaluation of the phase change. From these phase values, one can obtain corresponding physical and geometrical quantities. Our work focuses on modern methods for phase evaluation in optical measurement techniques that are based on measurements of light intensity at the set of chosen points in a space. We proposed new phase evaluation methods and algorithms in order to improve present phase evaluation and measurement techniques, especially by simplification of the measurement devices and evaluation technique, lower sensitivity to mechanical vibrations, etc.

Interferometric methods cover a large number of different measurement and evaluation techniques. These methods use the principle of interference of light for evaluation of phase differences between the reference and object wave field. The phase change of the object wave corresponds to the measured physical or geometrical quantity (shape, deformation, roughness, etc.). The research deals especially with new phase evaluation algorithms that enable to make fully automatic analysis of the interference field in quasi-real time [1,2]. We have proposed several new phase-shifting algorithms and several improvements in algorithms for preprocessing of interference patterns.

New method was proposed for computer evaluation of very small phase changes in optical testing [3]. One possible way how to determine the phase of the tested wave field (or wave-front deformation) is the use of the method of shearing interferometry that is based on the principle of interference of two spatially sheared wave-fronts. These wavefronts originate from a tested wavefront. The shear is performed by a proper shearing element, which forms two images of the tested wavefront that are separated by a mutual radial shift, lateral shift or rotation. We used a compact shearing interferometer with the Wollaston prism as a shearing element that is situated between two polarizers. A uniformly illuminated slit is imaged into the plane of localization of interference fringes in the Wollaston prism. Due to birefringence the tested wave field is divided into two wave fields. The interference pattern can be observed by an additional objective either visually or by a CCD camera. The shearing interferometer enables to determine the residual wave aberration of the tested optical system. The device is characterized by very small dimensions, which provide its easy portability. It is practically insensitive to vibrations and the mechanical design is also very simple.

The measurement instrument (interferometer) is suitable for practical testing of the imaging quality of optical systems. The mentioned method uses interference of polychromatic light and the phase change is determined from the colour of the interference field, because even a small phase change has effect on the colour of the interference pattern. If the tested optical system is aberration free, then the field of view will be uniformly coloured because the path difference between sheared wavefronts is constant. However, if the tested wavefront is aberrated, then the field of view will be uniformly coloured no longer. Colour interference fringes or a nonuniformly coloured field of view occur because the path difference between sheared wavefronts is not constant. Every colour in the interference pattern can be assigned to a specific phase change and it can be evaluated using colorimetric methods. We proposed a theoretical approach, which enables an automatic evaluation of the detected interference pattern. The evaluation method offers very accurate results and it can be used for practical testing in optical industry (e.g. microscope objectives and camera lenses).

Other phase evaluation techniques that were thoroughly investigated are methods that evaluate the phase gradient and subsequently calculate the phase change by an approximation. The phase change usually corresponds to the deformation of tested wavefront with respect to some ideal (reference) case. Perhaps the most important testing technique is the Shack-Hartmann [4] method that is based on the spatial sampling of the tested wavefront by the lenslet array. It estimates the wavefront local slopes (phase gradient). The sampled wavefront impinges on the detector that is usually situated in the focal plane of the microlens array and the specific intensity distribution (Hartmann pattern) is detected. Detected "spots" correspond to the intensity distribution after sampling by the sub-apertures of the microlens array. The position of each spot is dependent on the slope of the part of the wavefront that impinges on the corresponding microlens. One can determine the displacement of the spot positions with respect to the reference position that corresponds to an ideal (reference) wavefront. Phase values can be calculated from the measured phase gradient either by integration or by approximation using polynomials, e.g. Zernike or Legendre polynomials.

The last group of methods, which were studied in our work, is based on the application of equations for transport of energy in electromagnetic field [1]. We derived theoretically equations for determination of the phase of the wave field from several measurements of intensity of the wave field.

References:

- [1] NOVÁK, J. - MIKŠ, A.: *Modern Techniques for Evaluation of Phase of Wave Field*. Proceedings of the conference New trends in physics. Brno 2004, pp. 250-253.
- [2] NOVÁK, J.: *Five-step phase-shifting algorithms with unknown values of phase shift*. Optik, Vol. 114, No. 2 (2003), pp.63-68.
- [3] NOVÁK, J. - MIKŠ, A. - NOVÁK, P.: *Colorimetric Analysis of Small Phase Changes of Wave Field*. Proceedings of the conference New trends in physics. Brno 2004, pp. 242-245
- [4] MIKŠ, A. - NOVÁK, J.: *Evaluation of Gradient of Wave Field in Optical Testing*. MATLAB 2002. VŠCHT, Prague 2004, pp.319-322.

This research has been supported by GA ČR grant No. GA 103/02/0357.

Evaluation Techniques in Microwave Phase Interferometry

A.Mikš, J.Novák

miks@fsv.cvut.cz

Department of Physics, Faculty of Civil Engineering, Czech Technical University,
Thákurova 7, 166 29 Prague 6, Czech Republic

Nowadays, various measurement methods are used for analysis of physical and deformation properties of structural materials in mechanical and civil engineering [1]. These methods can be divided into two distinct groups: contact and noncontact techniques. The main disadvantage of contact methods is their contact character. On the other hand, noncontact methods are nondestructive and the measurement can be carried out very quickly and almost automatically without any mechanical interaction between the tested object and the measurement instrument. Various optical measurement methods are used in practice [2], e.g. holographic interferometry, speckle metrology, moiré techniques, geodetical methods, etc. Another method that can be used for determination of physical properties of materials in civil and mechanical engineering is the technique based on application of X-rays and projection techniques. X-ray computer tomography, which is based on the different absorption of X-rays in different materials, is rapidly developed in recent years.

Microwave measurement techniques are also used for measurements of structural materials. Compared to optical methods, their main advantage is the possibility to investigate the properties of opaque materials, i.e. most of structural materials. Compared to optical frequencies, the microwave frequency band enables to carry out technically the larger variability of measurements. Measurements can be not only scalar, but also directly vectorial. Measurements can be carried out in a wide and successively tunable bandpass with microwaves. It enables to apply various types of correction methods, which significantly improve the measurement accuracy. One can also obtain information about spatial orientation of vectors of the electromagnetic field. Therefore, it can be expected that microwave frequency bandpass offers the considerable area for further development and application of measurement methods, originally developed for optical frequencies. It concerns especially phase-shifting interferometry [3], which is used in optical metrology over thirty years.

The aim of our research project is to develop a mathematical model of the microwave phase-shifting interferometer for evaluation of the wavefront shape of the investigated microwave wave fields, propose suitable mathematical algorithms for measurement evaluation, design the laboratory model of the microwave phase-shifting interferometer, and perform subsidiary experiments, which verify our measurement and evaluation methods, in frequency bandpass from 10-100 GHz (wavelengths 30-3 mm). Regarding to used wavelengths, the research and the experimental verification of the method is not simple, because measuring instruments needed for measurements are not commonly accessible and some of them must be designed and constructed.

For a practical application of various measurement methods in optics or microwave engineering, an important task is determination of the wave-front shape (or phase of wave field). Several different methods exist for microwaves and various measuring instruments are available for vectorial and scalar measurements of microwave field. However, those methods are relatively time consuming and can be hardly used for measurements of dynamic effects. The research project is focused on a quite new method for evaluation of microwave fields. Our work deals with suitable methods for wave-front shape evaluation in microwave range. The evaluation is carried out by measurement and analysis of the interference field that

originates from interference of the reference microwave field with the investigated (object) wave field. The phase of investigated microwave field can be then determined from values of squared amplitude of the electric field intensity using appropriate phase evaluation techniques [3]. The advantage of the proposed method is the fact that the method is based only on scalar measurements of microwave field. In the theoretical part of the project, we firstly consider the transfer of the phase-shifting interferometry into the microwave area along with investigating the possibility of improving the mentioned technique with respect to the availability of tunable frequencies, vectorial correction measurement methods, and other technical possibilities in microwave frequency bandpass.

The analysis of the interference field will be carried out using the array microwave detector (analogy to CCD detectors in optics). We proposed an array microwave scalar detector that can perform field measurements in a relatively short time. From values of the intensity, one can determine simply the phase change of the microwave field using special evaluation techniques that are well adopted for interferometric methods in optics. Advantages of microwaves over light can lead to proposal of novel measurement techniques for nondestructive testing [4]. The wavelength of microwaves is approximately thousand times longer than the wavelength of light and one can carry out nondestructive measurements in the range that is impossible with light. Introducing the controlled change of the phase of investigated wave field, we obtain interference signals as the output from every point of the array detector. Evaluating these interference signals with suitable phase evaluation techniques, we obtain the phase values at every point of the investigated wave field. Various physical properties of investigated materials can be determined from the phase values. The described method will be used for design and application of new microwave measurement systems for evaluation of physical properties of structural materials in civil and mechanical engineering. Taking into account physical properties of microwaves, we obtain absolutely new diagnostic method for analysis of material properties. The proposed method will be widely applicable in many areas of science and engineering.

The main advantage of the proposed evaluation methods with respect to present methods is the fact that one must perform only scalar measurements of the microwave field and the field is evaluated at every element of the array microwave detector simultaneously. Measurements can be carried out practically in the real time, the measurement accuracy is high, and one can measure both static and dynamic events, which is either impossible or difficult with current measuring methods in the microwave frequency band.

References:

- [1] MICHALKO, O. – MIKŠ, A. – SEMERÁK, P. – KLEČKA, T.: *Physical and mechanical testing of building materials (in Czech)*. CTU Publishing House, Prague 1998.
- [2] NOVÁK, J. - MIKŠ, A.: *Modern Optoelectronic Methods for Non-Contact Deformation Measurement in Industry*. Journal of Optics A: Pure and Applied Optics, 2002, vol. 4, no. 6, pp.413-420.
- [3] NOVÁK, J.: *Five-step phase-shifting algorithms with unknown values of phase shift*. Optik, 2003, Vol. 114, No. 2, pp. 63-68.
- [4] MIKŠ, A. - NOVÁK, J. - NOVÁK, P.: *Určování defektu stavebních materiálů pomocí fázové mikrovlnné interferometrie*. Defektoskopie 2004, ČNDT, Brno 2004, pp.145-150.

This research has been supported by GA ČR grant No. GA 102/04/0898.

Mathematical Simulation of Optical Forces

A.Mikš, J.Novák

miks@fsv.cvut.cz

Department of Physics, Faculty of Civil Engineering, Czech Technical University,
Thákurova 7, 166 29 Prague 6, Czech Republic

The field of microtechnologies and micromechanisms, which are based on several different physical principles, starts to develop nowadays. One of the most perspective scientific areas is to be the principle of using light as a source of force fields that react with the dielectric objects found in these force fields. At present the research all over the world is focused particularly on micromanipulation with the microorganisms in molecular biology, genetics and microbiology [1]. Recently, the research results in the described areas of research led to the development of optical micromanipulators that are able to choose and manipulate (move) with microobjects, e.g. with bacteria and similar small microorganisms without their damaging. The problem needs to model an appropriate field of force with a laser beam, which is transformed using a standard optical setup.

With present techniques it is not possible to generate an arbitrary force field, but only very specialized type of a force field. This is a restrictive property of the present techniques and it is desirable to develop a general theory that make possible to design optical systems that generate the force field of known physical properties. These problems are not solved in the world yet and therefore it is necessary to pay increasing attention to them, because the proposed technique becomes a basic part of modern microtechnologies.

Our research focuses on mathematical simulation of optical forces that are caused by optical beams with various spatial energetic profiles. The energy of the optical beam, which is transformed by appropriate optical system, is spatially redistributed in dependence on properties of the optical system.

It is well-known that the transformed optical beam has force effects on a dielectric object in this field. The light that impinges on mass objects evokes forces (the pressure of light), which may draw the object either in or out of the light field. If we are able to design such optical systems that can transform the energy of the beam in a predetermined way, then it will be possible to model a force field of the required properties in a very small volume. The force field can be either static or dynamic, temporally and spatially. It will be possible to model, for example, rotational force field in an area of several micrometers that can be used as a non-contact micromotor in the micromechanisms, i.e. mechanisms with the size of several micrometers. The different area of using the proposed techniques is molecular biology and genetics, where the described force fields can be used for manipulation with the microobjects.

We tried to derive a general theory of force fields of power redistributed optical beams and a theory of optical systems that transform the standard optical beam with known distribution of energy to the beam with the redistributed profile of energy that generates force fields of the required properties, either static or dynamic.

The problems were solved at two levels, partly with the classical theory of electromagnetic field based on Maxwell's equations, partly with the theory of quantum electrodynamics (photon theory) [2,3]. Our work describes both the photon [4] and electromagnetic theory of optical forces that affects objects with dimensions larger than the wavelength of light. Equations were derived for calculation of the force and the moment of force that is caused by the light. Objects in the optical force field can be modelled and one can calculate the total force and total moment of force that have effect on the microobject. If all

forces (optical, gravitational, viscous, etc.) and moments of forces are balanced, then the object is in equilibrium. According to properties of the optical field, the object and environment, the object can levitate, can be caught by the optical field or can be forced out of the optical field.

For a simple spatial distribution of generated force field were derived general analytic equations that provide a deeper view of the solved problems, and for more difficult distributions of the force fields were proposed suitable numerical procedures that enable to perform a computer simulation and visualisation of the spatial distribution of the investigated force fields.

Furthermore, we worked on the theory of optical systems that transform the standard optical beam with the known distribution of energy to the beams with the redistributed profile of the beam energy. These beams generate the force fields of the required physical properties. The results will lead to the design of several non-classical optical systems that can be applied with some modifications in the different areas of science and engineering.

The proposed solution includes several quite original procedures, especially in the theoretical part. The result is a general theory of optical force fields of the required properties that are generated by suitable optical systems. On basis of the developed theory it is possible to carry out a computer simulation of the solved problem and to design corresponding optical systems.

In our research the emphasis was placed on the theoretical analysis and computer simulation of the problem. There was carried out a complex analysis of the investigated problem. Further, we developed the theory of the force fields of power redistributed optical beams. On the basis of some theoretical results, we can numerically simulate various force fields with respect to physical properties of the optical beam.

References:

- [1] GREULICH, K.O.: BIRKHAUSER (ARCHITECTURAL), 1999: *Micromanipulation by light in biology and medicine: The laser microbeam and optical tweezers*. Birkhauser, 1999.
- [2] MIKŠ, A.: *Fyzika 28 (Elektromagnetické pole)*. Vydavatelství ČVUT, Praha 1999.
- [3] MIKŠ, A.: *Aplikovaná optika 10*. Vydavatelství ČVUT, Praha 2000.
- [4] MIKŠ, A. – NOVÁK, J.: *Photon theory of optical forces*. Proceedings of International Workshop: Research Activities of Physics Departments of Civil Engineering Faculties in the Czech and Slovak Republics., Akademické nakladatelství CERM, Brno 2004, pp. 94–97.

This research has been supported by GA ČR grant No. GA 202/02/0314.

New Laboratory Experiments in Physics

A.Mikš, J.Novák, P.Novák, P.Semerák

`miks@fsv.cvut.cz`

Department of Physics, Faculty of Civil Engineering, Czech Technical University,
Thákurova 7, 166 29 Prague 6, Czech Republic

Nowadays, it is very important to introduce students to modern experimental and evaluation methods for measurement of physical properties of construction materials and structures that are widely used in practice [1]. Within the scope of education of physics, we made an innovation and modernization of existing standard laboratory experiments in physics.

The purpose of the project was innovation and modernization of education in experimental physics and metrology, improvement of practical physical experiments using computers and modern digital measuring instruments and devices. The innovation of practical experiments in physics at the Faculty of Civil Engineering originated in new laboratory experiments (mechanical, electrical, and optical measurements) with the possibility of computer analysis of the measurement results. Measurements that are carried out in laboratory experiments support lectures from a basic course of physics [2-4].

The aim of the project was to propose such experiments and experimental methods that can be performed by students with the help of a teacher. The proposed experiments were focused on measurements of important physical properties of building materials using modern digital measuring instruments and computers that will lead to the simplification of the measurement and evaluation process. The modernization of laboratory experiments using computers also enables to introduce students to computer modelling of solved physical and engineering problems that will lead to deeper understanding of solved physical problems and creative invention of students.

The simplification of the measurement process using digital measuring instruments and computers enables to extend the spectrum of measurement methods that can be used for evaluation, and students will be introduced to various practical measurement methods. The advantage of such approach is that the students can simply compare the results using different experimental methods, and they can decide independently, which method is most appropriate for the solved problem. It was also carried out a corresponding support of new physical experiments on the web sites of the department. Moreover, several subsidiary computer programs were developed for effective processing of measured data using proposed measurement techniques.

Our student laboratories were equipped with several new measurement devices that enable to measure various physical properties of building materials. New laboratory experiments can be divided into the following sections: measurement of elastic physical properties of building materials, measurement of noise and mechanical vibrations, topography measurement, measurement of thermophysical properties of building materials, measurement of photometric properties of light sources, and measurement of optical parameters of materials. In the experiments for measurement of elastic physical properties of building materials, students measure Young's modulus from the deflection of the rods that have various geometrical parameters (cross-section) and are made from different materials (metals, wood). Other methods that are used for determination of elastic, strength and deformation parameters of materials are ultrasonic method, and Schmidt hammer method.

The experiments for measurement of noise and mechanical vibrations use the sound-level meter for noise measurement and accelerometer for vibration measurement. Students can measure different noise sources and compare the results. The experiments for measurement of thermophysical properties of building materials enable to determine heat and temperature conductivity, and heat capacity of chosen building materials (concrete, bricks, porous concrete, wood, polyethylen, etc.). The students can also measure the dependence of the heat conductivity on the moisture of the porous material. The experiments are carried out using ISOMET device for measurement of thermophysical properties of materials and by the calorimetric method. The experiments for measurement of topography of surfaces permit to measure the shape of spherical and generally aspherical surfaces using contact methods (using spherometer or coordinate measuring device). In our laboratory experiments that are focused on optical measurements, students become familiar with basic methods for measurement of photometric characteristics of various light sources (e.g. light bulbs, lamps, photodiodes, etc.) and optical elements (lenses, prisms, optical filters, etc.) that can be used for the design of illumination system, which fulfils requirements on the level of irradiation and spectral composition of light. For our student laboratory experiments were designed the photogoniometer (made by MEOPTA Optika a.s.), which is an optical instrument that is mainly predetermined for making measurements of radiation characteristics of light sources. The students can simply measure radiation characteristics of several light sources (light bulbs, halogen bulbs, and LED diodes) using the photogoniometer and spectral radiation of light sources with the spectrometer. The experiments for measurement of optical parameters of materials are carried out using a spectrometer. The students can measure spectral transmittance and reflectance of various materials (different types of glass, window-glass, optical filters, reflection and antireflection foils, etc.). As a source of light, it is used LS-1 source from Ocean Optics for wavelength range $\lambda = 360 \text{ nm} - 2000 \text{ nm}$. The analysis of measurements is performed using spectrophotometer USB2000 (range 200 nm – 850 nm) and optical fibres from Ocean Optics. The measurement results can be analysed and visualized using computer software.

Described laboratory experiments are used from the winter term 2004. It can be concluded that the modernization of student laboratories made possible an implementation of modern digital instruments and measurement methods that are used in practice.

References:

- [1] MICHALKO, O. – MIKŠ, A. – SEMERÁK, P. – KLEČKA, T.: *Physical and mechanical testing of building materials (in Czech)* CTU Publishing House, Prague 1998.
- [2] TOMAN, J. – SEMERÁK, P.: *Fyzika 10 Praktická cvičení*. Vydavatelství ČVUT, Praha 2001.
- [3] KAPIČKOVÁ, O. – VODÁK, F.: *Fyzika 10 (Mechanika)*. Vydavatelství ČVUT, Praha 2000.
- [4] KAPIČKOVÁ, O. – VODÁK, F.: *Fyzika 20 (Termodynamika)*. Vydavatelství ČVUT, Praha 2002.

This research has been supported by grant FRVŠ A 1909 MŠMT.

Investigation of Optical Measurement Methods for Nondestructive Testing

A.Mikš, J.Novák, P.Novák

miks@fsv.cvut.cz

Department of Physics, Faculty of Civil Engineering, Czech Technical University,
Thákurova 7, 166 29 Prague 6, Czech Republic

The research deals with an analysis and a design of several nondestructive optical methods for measurement of physical properties of various structural materials. We focused on optical methods for measurement of moisture of building materials, detection of material defects, and measurement of surface roughness. It is very important to test and analyse the physical properties of various building materials in building industry. The trend in recent years shows a tendency to apply widely nondestructive testing methods and measurements, which can be relatively simply carried out and analysed practically in real time.

A very important physical property of building materials is the moisture. The building materials built in structures, generally absorb water. It is possible to use a wide spectrum of measurement methods, e.g. gravimetric, capacitive or microwave method. One possibility of non-contact moisture measurement of building materials is also testing of building materials using surface optical methods. We have proposed a relatively simple non-destructive technique for analysis of moisture in building materials using application of fluorescent dyes. The moisture can be determined on the basis of detection of fluorescent radiation that occurs after interaction of excitation light with the tested sample [1]. The measured sample of absorptive building material is insulated by a layer that is waterproof, but optically transparent. The bottom part of the sample is dipped into the water with fluorescent dye. Due to absorbability of the material, we can observe different moisture levels in different parts of the sample. We can illuminate the sample by the light with the excitation wavelength λ_B and image the sample using the optical filter and telecentric optical system onto the CCD camera. Because the optical filter has the transmittance $T(\lambda_B) = 0$, the detected intensity of fluorescence light will correspond to moisture of the sample. This method permits the determination of the spatial distribution of moisture in the sample of tested building materials.

We also investigated two measurement methods for diagnostics of inner material defects. The first method uses the fact that microwaves can penetrate samples of building materials with a relatively large thickness. Microwave nondestructive testing belongs to a very perspective field of defectoscopy. One can determine the defects of such materials from the phase change of microwave wave field. We proposed an interferometric microwave method for nondestructive testing of building materials [2]. The evaluation is carried out by measurement and analysis of interference field that originates from interference of reference microwave field with investigated wave field. The phase of investigated microwave field is then determined from values of squared amplitude of the electric field intensity that is detected by the proposed array microwave detector, which can perform field measurements in a relatively short time. The described measurement method is very sensitive on the change of phase of the interfering microwaves, and enables to determine inner material defects that cause the phase change of transmitted electromagnetic wave. Our work also deals with the problems of detection of inner material defects of engineering components. The principle of the method is based on the modal analysis of investigated objects [3]. If the tested component is fabricated without defects, then it is characterized by a specific spectrum of eigenfrequencies. On the contrary, the spectrum of eigenfrequencies will change in the

presence of material defects and different frequencies will appear in the spectrum. One can determine relatively simply eigenfrequencies of the sample for samples with simple geometrical shape (sphere, rectangular parallelepiped, cylinder, etc.). Then, the spectrum of eigenfrequencies can be compared with the test sample of the same shape. By proper analysis of the spectrum, we can determine the defects of the tested object. One can also use prefabricated samples with given shape and different inner defects of various size for experimental analysis of the influence of various material defects on eigenfrequencies.

Every surface in industrial practice is characterized by the surface roughness that can affect importantly functionality of fabricated mechanical elements, especially in mechanical engineering. In practice, various roughness requirements are specified for different fabricated mechanical elements. Therefore, it is very important to measure and analyse not only surface figure, but also surface roughness. The methods for measurements of surface roughness belong to an important part of engineering metrology and defectoscopy. We also focused our research on the problem of application of modern optical methods for surface roughness measurement [4]. It was proposed and investigated optical measurement method that uses the evanescent wave field for determination of a very small surface roughness. The proposed method uses total reflection at the boundary of two different optical media, where the so-called Goos-Hänchen effect occurs, and the evanescent wave field penetrates the second media into a very small depth under the boundary. This evanescent wave interacts with a rough surface, and the light is scattered at the surface. The scattered wave field can be detected with a suitable optical system and the surface roughness can be analysed. Due to the fact that the penetration depth of evanescent wave field is very small, it is possible to visualize only very small roughness of the investigated surface. Another technique that was studied uses evaluation of the speckle pattern. When an optically rough surface is illuminated with a coherent light, the incident wave field is scattered in all possible directions from the surface. The scattered wave distribution displays a random spatial variation of intensity called a speckle pattern. Information about the roughness of the tested surface can be determined by correlation analysis of the speckle pattern. The method is not experimentally difficult and gives good results for a specific range of roughness.

The work shows that it is possible to use several different optical measurement techniques for nondestructive testing in civil and mechanical engineering, which differ in their approach to evaluation and in complexity of the experimental measurement device.

References:

- [1] MIKŠ, A. - NOVÁK, J. - NOVÁK, P.: *Zjišťování vlhkosti stavebních materiálů fluorescenční metodou*. Defektoskopie 2004, ČNDT, Brno 2004, pp. 151-153.
- [2] MIKŠ, A. - NOVÁK, J. - NOVÁK, P.: *Určování defektu stavebních materiálů pomocí řázkové mikrovlnné interferometrie*. Defektoskopie 2004, ČNDT, Brno 2004, pp. 145-150.
- [3] MIKŠ, A. - NOVÁK, J. - NOVÁK, P.: *Určování vnitřních vad konstrukčních prvků metodou modální analýzy*. Defektoskopie 2004, ČNDT, Brno 2004, pp. 129-132.
- [4] MIKŠ, A. - NOVÁK, J. - NOVÁK, P.: *Zjišťování drsnosti povrchu pomocí speklu*. Defektoskopie 2004, ČNDT, Brno 2004, pp. 139-144.

This research has been supported by MSM research project J04/98:210000022.

Laser Interactions with Low-Density Foams

J. Limpouch, M. Kálal, R. Liska, M. Šňor, E. Krouský*, K. Mašek*, A. Kasperczuk**,
T. Pisarczyk**, N.N. Demchenko***, S. Yu. Gus'kov***

limpouch@siduri.fjfi.cvut.cz

CTU, Faculty of Nuclear Sciences and Physical Engineering, Dept. of Physical Electronics,
V Holešovičkách 2, 180 00 Praha 8

*Institute of Physics of AS CR, Na Slovance 2, 182 21 Praha 8

**Institute of Plasma Physics and Laser Microfusion, 23 Hery St., Warsaw, Poland

***P.N.Lebedev Physical Institute, RAS, Leninsky Ave. 53, 117 924 Moscow, Russia

Interactions of sub-nanosecond pulses of kJ-class iodine laser "PALS" with low-density foams and acceleration of Al foils by the pressure of the heated foam matter are investigated here, both experimentally and theoretically. X-ray streak camera is used for evaluation of the speed of energy transfer through the porous foam material. The shock-wave arrival on the rear side of the target is monitored by optical streak camera. Accelerated foil velocities, measured by three-frame optical interferometry and shadowgraphy, reach up to 10^7 cm/s. The accelerated foil shape is smooth without any signature of small-scale structures. Conversion efficiencies as high as 14 % of the laser energy into the kinetic energy of accelerated Al foil are derived. Experimental results compare well with our two-dimensional hydrodynamics simulations and with an approximate analytical model.

A very smooth ablation pressure profile (typically up to a few percent) is required in the direct-drive laser fusion experiments to suppress the onset and a subsequent growth of Rayleigh-Taylor instability, which might disrupt the target compression. As it is generally very difficult to meet the required uniformity level in the ablation pressure by an improvement of the illumination scheme as such, other smoothing mechanisms have been proposed, which are based on a modification of the laser-target interaction process. One of these methods employs a low-density porous matter as a voluminous absorber of laser radiation in ICF targets [1], another method uses laser prepulse to enhance transverse thermal smoothing in expanding plasma corona [2].

The main goal of this work is to study energy transport through the low-density foam and to demonstrate a sufficient efficiency of thin foil acceleration together with a substantial smoothing effect of the low-density foam absorber. Experiments were conducted on the PALS iodine laser facility in Prague. The laser provided 400 ps (FWHM) pulse with the energy up to 600 J at the basic harmonic ($\lambda_1 = 1.32 \mu\text{m}$). Laser was incident normally on the target; the target was placed out of the best focus and the laser spot radius $R_L \approx 150 \mu\text{m}$ was used. Laser irradiances were varied from $I \approx 10^{14}$ W/cm² up to $I \approx 10^{15}$ W/cm².

Several types of foam target were used. Most experiments were done with polystyrene foam with density in range 8–10 mg/cm³ and typical pore diameter $D_p \approx 50$ –70 μm . Polystyrene foam with $\rho \approx 30$ mg/cm³, $D_p \approx 10 \mu\text{m}$, and with $\rho \approx 20$ mg/cm³, $D_p \approx 5 \mu\text{m}$, and PVA foam with $\rho \approx 5$ mg/cm³, $D_p \approx 5 \mu\text{m}$ were also used. Aluminum layer 2 μm or 0.8 μm thick was placed at the foam rear side in the majority of foam targets.

The target self-emission was imaged with eleven-fold magnification on the x-ray streak camera entrance slit through 50 μm wide slit providing spatial resolution along the target depth. Only photons of energy above 1.7 keV could propagate with less than 80% absorption through the recording channel. As plastic foams containing only light elements were used, the amount of x-ray emission was rather low. The only usable pictures (weak, but significantly above x-ray streak sensitivity limit) were recorded for the foams with the largest

pore diameter (50–70 μm). From such record the upper estimate of the laser penetration depth is the thickness of about 120 μm of the immediately heated layer. Later, heat wave propagates into the foam material with velocity of approximately $\sim 1.4 \times 10^7$ cm/s. Though the x-ray signal lasts for nearly 3 ns, the x-ray emitting zone covers only about two thirds of the 400 μm foam thickness and no emission near the Al foil at the target rear side is detected.

Optical diagnostics employing interferometry and shadowgraphy was carried out by means of 3-frame polari-interferometric system with automated image processing technique. Maximum velocities of the accelerated Al layer up to 10^7 cm/s have been measured. For 400 μm -thick polystyrene foams, the shock wave reaches the foil only 2-4 ns after the laser pulse, and the delay decreases with laser energy. The above delay is larger by about 2 ns than in simulations for homogeneous material of the same density as the foam, and the difference is tentatively explained by foam homogenization process [3].

In order to verify feasibility of measurement of the time and of the form of the shock wave arrival on the target rear side, we have conducted preliminary experiment where self-emission in the normal direction from the target rear side was imaged with magnification of 10 on the entrance slit of an optical streak camera [4]. Shock wave arrival delay grows smoothly with the distance from the central point. No macroscopic spatial features are registered, which is also consistent with smooth shape of the accelerated part of the foil observed in optical interferometry.

Velocities of the accelerated foil at the target rear side, measured by 3-frame optical interferometry, are in a good agreement with our two-dimensional hydrodynamic calculations and with an analytical model. However, a delay in the shock wave propagation in the foam is observed in our experiments in comparison with our theoretical calculations that do not take foam structure into account. This delay may influence laser imprint mitigation.

References:

- [1] DUNNE, M. – BORGHESI, M. – IWASE, A. – JONES, M.W. – TAYLOR, R. – WILLI, O. – GIBSON, R. – GOLDMAN, S.R. – MACK, J. – WATT, R.G.: *Evaluation of a Foam Buffer Target Design for Spatially Uniform Ablation of Laser-Irradiated Plasmas*. Phys. Rev. Lett. 75, 1995, pp. 3858–3861.
- [2] ISKAKOV, A.B. – TISHKIN, V.F. – LEBO, I.G. – LIMPOUCH, J. – MAŠEK, K. – ROHLENA, K.: *Two-dimensional model of thermal smoothing of laser imprint in a double-pulse plasma*. Phys. Review E 61, 2000, pp. 842–847.
- [3] LIMPOUCH, J. – DEMCHENKO, N.N. – GUS'KOV, S.YU. – KÁLAL, M. – KASPERCZUK, A. – KONDRASHOV, V.N. – KROUSKÝ, E. – MAŠEK, K. – PISARCZYK, P. – PISARCZYK, T. – ROZANOV, V.B.: *Laser interactions with plastic foam—metallic foil layered targets*. Plasma Phys. Control. Fusion 46, 2004, pp. 1831–1841.
- [4] LIMPOUCH, J. – DEMCHENKO, N.N. – GUS'KOV, S.YU. *et al.*: *Laser Interactions with Low-Density Plastic Foams*. XXVIII ECLIM Roma September 6-10, 2004, oral contribution Fr/O1/2/O, Laser and Particle Beams (accepted for publication).

This research has been supported by the Ministry of Education, Youth and Sports of the Czech Republic under project No. LN00A100 "Laser Plasma Research Centre". Partial support by INTAS (Project No. 01-0572) is gratefully acknowledged.

Possible Applications of Goos-Hänchen Effect in Optical Measurement Systems

P. Novák, J. Novák, A. Mikš

xnovakp9@fsv.cvut.cz

Department of Physics, Faculty of Civil Engineering, Czech Technical University,
Thákurova 7, 166 29 Prague 6, Czech Republic

Various optical effects and processes find their application area in optical imaging and measurement systems, e.g. total internal reflection at the boundary between two different optical media is such an optical effect that can lead to the development of many practical optical systems in microscopy, topography of surfaces, etc. In case of total reflection [1] at the boundary surface between two different optical media, the ray reflected at the boundary is spatially shifted with respect to a point, where an incident ray intersects the boundary. The light penetrates into the second medium and the evanescent electromagnetic wave propagates along the boundary.

It is well-known from the theory of reflection of light that total reflection is observed in the case of the propagation of light from the higher-index material into the lower-index material and that the so-called Goos-Hänchen effect occurs during total reflection of linearly polarized waves at the boundary surface between two different optical media [2]. Taking into account that the penetration depth of radiation in the second optical medium is very small and is comparable to the wavelength of incident light, one can use the mentioned effect for investigation of fine structures, e.g. in biology, medicine or industry.

We proposed applications of the Goos-Hänchen effect in optical microscopy, and topography measurements. Our work describes the Goos-Hänchen effect and basic equations are shown for the Goos-Hänchen shift and the depth of penetration of the evanescent wave in the case of total reflection at the boundary between two different optical media. We propose methods for investigation of very fine surface structures using the Goos-Hänchen effect. The methods use the fact that the reflected light penetrates into the second medium and the evanescent electromagnetic wave propagates along the boundary. Because of a very small penetration depth of evanescent wave field (fraction of the wavelength of light), it is possible to visualize very small structures. The size of structures, which can be observed with the Goos-Hänchen effect, can be even smaller than a classical value of the resolving power for optical systems that are used for their observation. The Goos-Hänchen effect can be advantageously used in optical microscopy and one can observe very small objects that are situated just under the boundary, where the light undergoes a total internal reflection. The light will interact only with objects that are situated within the range of the evanescent field that penetrates the investigated specimen.

It was described a method for microscope investigation of biological specimens [2]. The specimen, which is modified by a fluorescent dye, is deposited on the glass slide. This specimen is illuminated by the beam (e.g. by a laser beam) that undergoes total internal reflection at the side of the prism. The bottom part of the illuminant prism adjoins to the upper part of the specimen. Due to total internal reflection at the side of the prism, the beam penetrates a small part of the specimen that is in proximity of the side of the prism. Biological objects that are located in this part of the specimen will start to fluoresce, i.e. they will start to emit the light with larger wavelengths than the wavelength of the illuminant beam (the Stokes rule). Objects that are situated in proximity of the side of the prism will fluoresce more strongly than objects that lie at the border of active area of the evanescent wave. By a proper

microscope objective lens, one can image the above-mentioned objects onto the detector. If we place an eye-piece behind the image plane of the objective lens, then we can observe the objects by a human eye. Due to the fact that the penetration depth of evanescent wave field is very small, it is possible to visualize very small objects that are under the resolving power of microscope objective lenses, which are used for observation, and one can obtain a superresolution.

Our work also proposes a method for investigation of surface structures that is based on the Goos-Hänchen effect in case of total reflection at a boundary surface between two different optical media [3,4]. Our work describes possibilities of applications of the Goos-Hänchen effect for investigation of surface roughness. It uses the fact that the reflected light penetrates into the second medium and the evanescent electromagnetic wave propagates along the boundary. It has been shown that the penetration depth of the evanescent wave into the second medium is very small (usually several hundreds of nanometers) and its magnitude depends on the angle of incidence. This fact can be applied advantageously in investigation of very fine surface structures. One can investigate very fine structures that are situated just under the boundary, where the light undergoes a total internal reflection, because the light will interact only with objects that are within range of the evanescent field. An optical system has been proposed that enable to apply the technique in practice, i.e. an optical system that can be used for investigation of a very fine surface roughness. The specimen is illuminated by the beam that undergoes total internal reflection at the side of the illuminant prism. The bottom part of the illuminant prism adjoins to the upper part of the specimen. Due to total reflection at the side of the prism, the light penetrates into a very small distance under the prism surface. The evanescent wave is then scattered at the surface of the specimen. The parts of the specimen, where the light is scattered can be imaged onto the detector and the structure can be analysed. Due to the fact that the penetration depth of evanescent wave field is very small, it is possible to visualize only very small roughness of the investigated surface.

References:

- [1] MIKŠ, A.: *Aplikovaná optika*. Vydavatelství ČVUT, Praha 2000.
- [2] MIKŠ, A. - NOVÁK, J. - NOVÁK, P.: *Application of Goos-Hänchen Effect in Optical Systems for Microscopy*. 2004, Proceedings of International Workshop: Research Activities of Physics Departments of Civil Engineering Faculties in the Czech and Slovak Republics. Brno: Akademické nakladatelství CERM, pp. 88-93.
- [3] NOVÁK, J. - MIKŠ, A.: *Application of Goos-Hänchen Effect for Investigation of Surfaces*. Proceedings of International Workshop: Research Activities of Physics Departments of Civil Engineering Faculties in the Czech and Slovak Republics. Brno: Akademické nakladatelství CERM, 2004, pp.129-131.
- [4] MIKŠ, A. - NOVÁK, J. - NOVÁK, P.: *Užití evanescentních vln pro diagnostiku drsnosti povrchu*. Defektoskopie 2004, Praha 2004, pp.133-138.

This research has been supported by GA ČR grant No. GA 202/02/0314.

Polyester Fabric Hydrophobicity Modification with Atmospheric Corona Discharge

J. Píchal

pichal@fel.cvut.cz

Czech Technical University, Faculty of Electrical Engineering, Department of Physics,
Technická 2, 166 27 Praha 6, Czech Republic

In the textile industry there is permanent search for new methods of technological optimisation and cost-effective production of fabrics. One of mostly used synthetic fabrics is PES (polyester) based on PET (polyethylene terephthalat), with still growing world production.

Since begin of the PET production single-minded effort was paid to the PET hydrophobicity improvement because of the PET low wettability, low adhesion, high oil impurities cohesion and undesirable electric discharge generation. The most reliable way how to change the wettability of the PET is the change of its surface chemical characteristics. The modification can be achieved by different processes, e.g. by enzymatic hydrolysis, low pressure and atmospheric pressure plasma application, chemical grafting or excimer laser application [1].

The most extensive number of potential chemical reactions on the fabric's surface seems to be related with plasma modification. The effect of the surface plasma modification depends on properties of used gas, because of methane, ethylene, ethanol participation in the graftage, oxide, tetrafloromethane (CF₄) and ammonia can be used for sloughing, or noble gases as helium, neon, argon etc. effectivity as admixtures for better chemical processes initialization.

At present fabric modification by low-pressure plasma is among most frequently investigated treatment methods. It seems to be more advantageous than classical chemical methods and offers distinctive advantages, especially easy modification process control (control parameters being e.g. plasma pressure, discharge input power, modification time and distance between electrode and modified fabric), for details see e.g. [2], [3].

On the other hand the low-pressure plasma employment is mostly joined with higher financial expenses due to the necessity of the vacuum equipment application and batch processing. Necessary purchase of the complex equipment also significantly advances the final product price. The disadvantages of the low-pressure plasma employment might be removed with design of the continual modification system exploiting stable atmospheric plasma discharges. Due to relative simplicity of continual modification system exploiting stable atmospheric plasma discharges its operating expenses might be lower than that of the low-pressure equipment. That is why we focused on the applicability of atmospheric corona discharge for PES fabric modification. We studied the relation between corona discharge input power and fabric's hydrophobicity and modification effect aging expressed in the feathering spot size time changes. Results of measurements were compared with values obtained in radio-frequency (RF) low-pressure discharges.

The specimens used in all experiments were made from the polyester fabric "Tesil12". Before modification specimens had to be properly cleaned. The modification was performed in atmospheric corona discharge generated between grounded large plane brass electrode, diameter 45 mm and an electrode matrix (72 × 54) mm, a set of "single point" iron electrodes, each of cylindrical shape, diameter 0.7 mm and spike curvature radius about 25 μm, placed in vertices of rectangular square grid, dimensions of each square being (9 × 9) mm, hence the distance of electrodes was fixed at 9 mm. The electrodes were put into the open cylindrical vessel (diameter 15 cm, height 15 cm). During modification specimens were placed right on the large plane electrode. All experiments were performed in stationary air under atmospheric pressure and room temperature. Stabilized D.C. voltage (7,4-8,4) kV was applied to the

electrodes, typical current values were (50-281) μA . The voltage setting limited spark discharge ignition. Modification time was 600 seconds.

Hydrophobicity was evaluated by means of the drop test [4], 20 μl of distilled water being the test liquid. After start of every experiment the feathering spot size was recorded with a camera until 10 minutes from the start. The area of the spot in the 300th second after start of the test was used as the standard for the evaluation. The experiment was stopped if the drop did not soak into the fabric after 10 minutes from the start.

The time dependence of the fabric moistened and feathering area was growing. Almost linear shapes of 7.1 kV and 7.7 kV curves changed into the polynomial for 8.1 kV and 8.4kV ones. This change of shape might be connected with the rise of fabric modification degree or/and existence of fabric area “modification inhomogeneities” in case of less modified specimens.

The corona discharge column had conical shape. Particles ionised in corona discharge modified the fabric in the close surroundings of their touch points with textile. Final shape of treated area was almost circular. The regions of ionised particle–fabric touch points were not completely joined together in case of low modification intensity and the test drop had to pour over unmodified zones. The time necessary for “unmodified zones overflowing” was relatively long and feathering area seemed to be almost straight time dependent. The modification “irregularities” might be corrected by optimising of the interelectrode distance.

More effective modification expressed by the treated fabric area changes can be achieved by discharge input power rise. For in experiment used input power values the feathering area–time dependence seemed to be exponential, hence small change of input power resulted in greater change of the hydrophobicity. PES fabric hydrophobicity changes were related with number and characteristics of ionised particles, too. Measurements in more intensive corona discharge were impossible due to the spark discharge ignition.

The estimation of the corona PES fabric modification effect aging expressed in the feathering spot size time changes for different discharge input power showed that the feathering spot size and hence modification effectivity had sharply diminished in time. The efficiency drop might be connected with transformation of created hydrophilous function groups on the fabric surface. The transformation might be caused by chemical reactions of created hydrophilous function surface groups with air components. Dipoles orientation might also change backwards in time returning into primary orientation. Four days after modification no important difference in hydrophobicity of modified and unmodified specimens was found.

Results of corona discharge modification were compared with results of the RF discharge modification. There were used specimens of the same PES fabric. The modification process seemed to be more efficient in case of RF discharges, but having in mind the costs of modification process the comparison is more difficult. For detailed comparison of both methods further experiments are necessary.

References:

- [1] WONG, W.–ET AL.: *Journal of Materials Processing Technology* , 103 (2000), pp. 225–229.
- [2] SARMADI, M.: *Text. Chemist and Colorist* , 28/6 (1996), pp. 17–22.
- [3] WAKIDA, T.–ET AL.: *Text. Research J* , 63/8 (1993), pp. 433–438.
- [4] WROBEL, A. M. –ET. AL.: *Polymer* , 19 (1978), pp. 908–912.

This research has been supported by COST grant No. 527.120.

Dynamics of Isolated Spherical Bubble in Incompressible Fluid

V. Sopko, L. Samek

vit.sopko@fs.cvut.cz

Department of Physics, Faculty of Mechanical Engineering, Czech Technical University,
Technická 4, 166 27, Prague 6, Czech Republic

The research deals with an analysis and calculation of radial oscillations of isolated spherical bubble in unlimited incompressible and inviscid liquid. The bubble is filled with gas (vapor) of constant pressure. The bubble with initial radius R_0 is created in immovable liquid. The velocity v of radial flow of liquid is expressed with equation

$$v = \frac{R^2}{r^2} \frac{dR}{dt}; \quad r > R, \quad (1)$$

where R is radius of bubble and dR/dt is velocity of liquid on the surface of the bubble. Under the given conditions is the expansion work A_1 of the gas in the bubble

$$A_1 = p_n \frac{4}{3} \pi (R^3 - R_0^3), \quad (2)$$

equal to sum of kinetic energy of liquid W_k and work A

$$A = p_\infty^o \frac{4}{3} \pi (R^3 - R_0^3), \quad (3)$$

done by pressure p_∞^o which acts on the liquid in infinity, where

$$W_k = \int \frac{1}{2} v^2 dm = \int_R^\infty \frac{1}{2} \left(\frac{dR}{dt} \right)^2 \frac{R^4}{r^4} 4\pi r^2 \rho_0 dr = 2\pi \rho_0 \left(\frac{dR}{dt} \right)^2 R^3. \quad (4)$$

Substituting of equations (1,2,3) in an equation $A_1 = W_k + A$, gives solution for surface velocity of the bubble

$$\left(\frac{dR}{dt} \right)^2 = \frac{2}{3\rho_0} (p_\infty^o - p_n) \left(\frac{R_0^3}{R^3} - 1 \right). \quad (5)$$

This formula determines velocity of the bubble surface. Form eq. (5) we obtain acceleration of the bubble surface

$$\frac{d^2 R}{dt^2} = - \frac{p_\infty^o - p_n}{\rho_0} \frac{R_0^3}{R^4}. \quad (6)$$

Different problems are possible, for example if the bubble is empty, i.e. $p_n = 0$, we find from eq. (5) the velocity contraction of the bubble

$$\frac{dR}{dt} = \left[\frac{2p_\infty^o}{3\rho_0} \left(\frac{R_0^3}{R^3} - 1 \right) \right]^{\frac{1}{2}}, \quad (7)$$

which was derived by Rayleigh [1]. From the eq. (7) and eq. (6) is evident that for $R \rightarrow 0$, the velocity and the acceleration of particles of liquid near the surface of the bubble increasing unlimitedly. In the fact due to various reasons both these quantities gain limited values.

Time interval t^* during that the radius of the bubble decrease from R_0 to R find out with integration of eq. (7).

$$t^* = \left(\frac{3\rho_0}{2p_\infty^0}\right)^{\frac{1}{2}} \int_R^{R_0} \frac{R^{\frac{3}{2}}}{(R_0^3 - R^3)^{\frac{1}{2}}} dR = R_0 \left(\frac{\rho_0}{6p_\infty^0}\right)^{\frac{1}{2}} \int_{\left(\frac{R}{R_0}\right)^3}^1 \frac{x^{-\frac{1}{6}}}{(1-x)^{\frac{1}{2}}} dx, \quad (8)$$

where $x = (R/R_0)^3$. The relation for time τ in which the empty bubble fully implode ($R = 0$), we obtain from eq. (8) in this case the lower integral limit is equal to 0.

$$\tau = R_0 \left(\frac{\rho_0}{6p_\infty^0}\right)^{\frac{1}{2}} B\left(\frac{5}{6}, \frac{1}{2}\right) \approx 0,9146R_0 \left(\frac{\rho_0}{p_\infty^0}\right)^{\frac{1}{2}}, \quad (9)$$

where $B(p,q)$ is function beta (Euler's integral).

The equation for pressure in liquid surrounding empty bubble is derivable from Euler's hydrodynamic equations, which for considered problem with spherical symmetry reduce to one equation, which is

$$\frac{\partial v}{\partial t} + v \frac{\partial v}{\partial r} = -\frac{1}{\rho} \frac{\partial p}{\partial r}. \quad (10)$$

The p is pressure and $\rho = \rho_0$ is density of liquid. On substituting the eq. (8) into eq. (4), the equation becomes

$$\frac{\partial p}{\partial r} = \frac{p_\infty^0}{3} \left[4R_0^4 z^{-4} (z^3 - 1) \frac{1}{r^5} - \frac{R_0}{z} (z^3 - 4) \frac{1}{r^2} \right]; \quad r \geq R, \quad (11)$$

where $z = (R_0/R)$. Integration of eq. (11) with respect to r from r to ∞ we obtain

$$\frac{p(r, z)}{p_\infty^0} = 1 - \frac{1}{3} \left[\frac{R_0^4}{z^4 r^4} (z^3 - 1) - \frac{R_0}{zr} (z^3 - 4) \right], \quad (12)$$

The function (12) gives us information about different stage of implosion. It is visible that in vicinity of collapsing bubble is created pressure wave. The growing of wave amplitude depends on implosion of the bubble. Distance r^* points with maximum pressure in this wave

is obtainable from equation (11) when $\frac{\partial p}{\partial r} = 0$, then

$$r^{*3} = \frac{4R_0^3 z^3 - 1}{z^3 z^3 - 4}. \quad (13)$$

At the end of implosion, when $z = R_0/R \rightarrow \infty$, it will be along equation (12) a (13)

$r^* \approx 4^{\frac{1}{3}} R = 1,587R$ and

$$p_{max} = p_\infty^0 R_0^3 \left(4^{\frac{1}{3}} R^3 \right)^{-1}. \quad (14)$$

References:

[1] RAYLEIGH, L.: *On Pressure Developed in a Liquid during the Collapse of a Spherical Cavity*. Philosophical Magazine, 1917, pp. 94–98.
 [2] BRIGGS, L. J.: *Limiting Negative Pressure of Water*. Philosophical Magazine, 1950, pp. 16–17.
 [3] MINNAERT, M. J.: *Bubbles and the Sounds of Running Water*. Philosophical Magazine, 1933, pp. 235–248.
 [4] NOLTINGK, B.E.–NEPPIRAS, E.A.: *Limiting Negative Pressure of Water*. Philosophical Magazine, 1950, pp. 16–17.

This research has been supported by MSMT grant No. MSM J04/98:210000018.

Measurement of Sub-12-fs Laser Pulses by a Light Emitting Diode

M. Smrž*, M. Divoký*, P. Straka**

smrz@sh.cvut.cz

*Dept. of Physical Electronics, Faculty of Nuclear Sciences and Physical Engineering, Czech Technical University, V Holešovičkách 2, 180 00 Prague 8, Czech republic

**Dept. of Nonlinear Optics, Institute of Physics, AS CR, Na Slovance 2, 182 21 Prague 8, Czech Republic

Pulsewidths of ultrashort laser pulses can be measured by several techniques in both time and frequency domain. There are many useful methods of the measurement involving frequency resolved optical gating (FROG), spectral phase interferometry for direct electric-field reconstruction (SPIDER), and interferometric autocorrelation. The latest one is simple and versatile for an evaluation of the pulsewidths in experiments with ultrashort pulses. New approaches were developed for a full-field reconstruction of pulses from the interferometric autocorrelation, for example PICASO [1].

A second-order autocorrelation is proportional, for example, to a nonlinear second harmonic signal generated in a thin birefringence crystal by two replicas of the measured pulse, which was split in a Michelson interferometer. The signal of the autocorrelation depends on a relative delay of the pulses and can be recorded by a photomultiplier.

The detection of the autocorrelation can be rather simplified using another nonlinear effect, for example, two-photon absorption in a proper semiconductor. Two-photon absorption does not require a fulfillment of a phase-matching condition and is polarization insensitive. A thickness of absorbing material is small and the dispersion can be reduced. A photocurrent is proportional to the autocorrelation and can be recorded easily from a cheap semiconductor. Even 6-fs pulses were measured with a semiconductor photodiode [2] and about 80-fs pulses with a light-emitting diode used as an unbiased photodiode [3].

Single-photon ($E_g < h\nu$) or two-photon ($2h\nu > E_g > h\nu$) absorption in semiconductors generates an electron-hole couple, which can be collected. Here E_g is bandgap energy and $h\nu$ is photon energy. The collected charge is proportional to the pulse intensity I or to I^2 , respectively. A second-order autocorrelation, which is useful for the measurement of pulsewidths, is proportional to I^2 , i.e. to an amount of two-photon absorption. A pure quadratic response of semiconductor on pulse intensity is desirable. Even if two-photon absorption occurs ($E_g > h\nu$), significant residual single photon (i.e. linear) absorption involving intra bandgap transitions on impurities could distort the second-order autocorrelation and hinder the pulse retrieval.

We found several commercial LED (material GaP, $E_g = 2,2$ eV or GaAsP, $E_g = 1,8$ eV) with the quadratic photocurrent response on the peak power of a mode-locked Ti:sapphire laser. The laser had a spectral bandwidth of 700-900 nm and a photon energy between 1,4 and 1,8 eV. Photovoltage at LED was measured with a multimeter. A negligible linear absorption was observed in cw regime of the laser. The LED detector (material GaP) of the autocorrelator had a lower capacitance (35 pF) than most of photodiodes used obviously for the femtosecond pulse measurement. That is why our detector had a faster response and a higher sensitivity, so that no current amplifier was required for the ultrashort pulse measurement.

We built an interferometric autocorrelator for the real-time and full characterization of sub-12-fs laser pulses. We used LED (Agilent Technologies HLMP-K640) as the nonlinear detector of the interferometric autocorrelation. We measured the interferometric autocorrelation of the femtosecond pulses from a Ti:sapphire laser. The amplitude of pulses and their phases were retrieved from the second-order autocorrelation and pulse spectrum using PICASO technique [3]. The duration of the retrieved pulse was $12,6 \pm 0,2$ fs comparable with a calculated fit of the interferometric autocorrelation for a Gaussian pulse with duration of $12,9 \pm 0,1$ fs. A sensitivity of the autocorrelator with our LED was a few pJ per pulse.

The LED detector was also a useful tool for an easy and fast adjustment of pulse compression. The output beam from the pulse compressor (prisms, diffraction gratings, etc.) could be simply focused to any two-photon detector, e.g. when a pulse from one arm of the Michelson interferometer is stopped. The photovoltage measured by a multimeter depended on the separation of diffraction gratings (prisms). The maximum voltage corresponded to the best pulse compression. According to this approach we were able to find the optimal separation of the diffraction gratings (groove density 1200/mm, the Littrow angle of incidence was 27° and off-plane diffraction) with a precision better than ± 45 μm . Therefore pulse compression of a stretched pulse with duration of 360 ps was better than 25 fs which corresponds to theoretical calculations. A further adjustment of the compressor was done with the same detector using the interferometric autocorrelation. Note that the sensitivity of LED decreased significantly for pulses longer than 100 fs

We measured sub-12-fs laser pulses by a light-emitting diode, which was a smart, cheap, sensitive, and reliable quadratic detector of interferometric autocorrelation. Both the pulse and its phase was retrieved by PICASO technique. The detector was also useful for a simple diagnostics of pulse compression with a precision of 25 fs.

References:

- [1] NICHOLSON, J.W. ET AL.: *Full-field characterization of femtosecond pulses by spectrum and cross-correlation measurements* Optics Letters 22, 1999, pp. 1774–1776.
- [2] RANKA, J.K. ET AL.: *Autocorrelation measurement of 6-fs pulses based on two-photon-induced photocurrent in a GaAsP photodiode* Optics Letters 22, 1997, pp. 1344–1346.
- [3] REID, D.T. ET AL.: *Light-emitting diodes as measurement devices for femtosecond laser pulses* Optics Letters 24, 1997, pp. 233–235.

This research has been supported by the Czech Ministry of Education grant #LN00A100 and the Czech Academy of Sciences grant #K2043105.

Powder Neutron Diffraction Study of Lithium Titanium-based Li-ion Conductors (part II)

S. Vratislav*, M. Dlouhá*, M-L.Martinez**, L. Mestres**

stanislav.vratislav@fjfi.cvut.cz

*Department of Solid State Engineering, Faculty of Nuclear Sciences and Physical Engineering, Czech Technical University, Trojanova 13, 120 00 Prague 2, Czech Republic

**Dept. of Inorganic Chemistry, Universitat de Barcelona, Martí i Franqués 1-11, 08028 Barcelona, Spain

Systems containing Bi_2O_3 are now becoming increasingly important in the technology of new materials used by the electronic industry. The binary systems $\text{Bi}_2\text{O}_3/\text{Li}_2\text{O}$, $\text{Bi}_2\text{O}_3/\text{TiO}_2$, and $\text{Bi}_2\text{O}_3/\text{La}_2\text{O}_3$ were described [1]. Structure parameters of perovskites containing system Bi_2O_3 are now becoming increasingly important in the technology of new materials. Recently, the phase diagram of the system $\text{Li}_2\text{O}/\text{La}_2\text{O}_3/\text{TiO}_2/\text{Bi}_2\text{O}_3$ has been studied. A region of perovskite-like solid solutions was obtained when the bismuth content in the general formula $\text{Bi}_y\text{La}_{0.5+x-y}\text{Li}_{0.5-3x}\text{TiO}_3$ was less than $y = 0.10$. These compounds are ionic conductors [2].

In general, the amount of lithium inserted is consistent with the number of vacancies. The knowledge of crystal structure of these compounds is crucial to the understanding of the Li ionic mobility within the La(Bi)-Ti-O framework. In these perovskites, the tilt of the TiO_6 octahedra is a predominant feature that introduces structural distortions affecting Li mobility. In previous paper [3], chemical lithium intercalation was carried out on different compositions of similar systems. The structure determination of these oxides by X-ray diffraction is difficult as the superlattice reflections associated with the tilting of the TiO_6 octahedra arise from the oxygen atoms, weak scattering if compared with La and Ti; hence neutron diffraction measurements [4] are more suitable for these investigations. Lithium ions were electrochemically inserted into perovskite-type $\text{La}_{0.50}\text{Li}_{0.37}\text{TiO}_3$ [2]. The results indicated that lithium ions were inserted into A-site vacancies until they were occupied by lithium ions, then, the new lithium ions were inserted into the largest interstitial space, $3c$ -site, in the cubic perovskite structure.

In this paper, the structure parameters of three members of the $\text{Bi}_{0.04}\text{La}_{0.53}\text{Li}_x\text{TiO}_3$ series ($x = 0.29, 0.45$ and 0.70) has been analysed at 7 K by neutron diffraction. A Li-poor perovskite with composition $\text{Bi}_{0.04}\text{La}_{0.53}\text{Li}_{0.29}\text{TiO}_3$, Li-rich perovskite (occupied all the vacancies) with composition $\text{Bi}_{0.04}\text{La}_{0.53}\text{Li}_{0.45}\text{TiO}_3$ and a third composition with more lithium than A-site vacancies, with general formula $\text{Bi}_{0.04}\text{La}_{0.53}\text{Li}_{0.70}\text{TiO}_3$. The main point of this work is to know the Li position in this new perovskites obtained by chemical insertion. The preparation of samples were described at [5].

Phase purity was checked by X-ray powder diffraction on the Siemens D-500 diffractometer in reflection mode using $\text{Cu-K}\alpha$ radiation.

Complete structural determination was carried out by powder neutron diffraction on the diffractometer KSN-2 located at the LVR-15 research reactor near Prague. The diffraction patterns were taken at $\lambda = 0.1362$ nm over a range $2\theta = 10 - 92^\circ$ in steps 0.1° . The structural refinement was refined by a profile analysis using the GSAS package, taking into consideration the absorption correction for the natural mixture of the lithium isotopes.

Tab. 1: Crystallographic data for $\text{Bi}_{0.04}\text{La}_{0.53}\text{Li}_{0.75(9)}\text{TiO}_3$ at 7 K

Atom	Site	x	y	z	Occupancy
La	4c	0.0123(19)	0.2500	0.9997(14)	0.537(11)
Bi	4c	0.0123(19)	0.2500	0.9997(14)	0.041(7)
Ti	4b	0.5000	0.0000	0.0000	1
O(1)	4c	0.4943(16)	0.2500	0.0202(17)	1
O(2)	8d	0.2345(12)	-0.0241(31)	0.2453(18)	1
LiA	4c	0.0000	0.2500	0.8410(23)	0.217(5)
LiB	4c	0.133(28)	0.2500	0.1348(27)	0.060(10)
LiC	4c	0.0080(22)	0.3710(27)	0.0061(26)	0.163(9)
LiD	4c	-0.1430(25)	0.2500	0.0860(28)	0.142(9)
LiE	4c	-0.2420(24)	0.2500	0.7414(22)	0.165(8)
LiF	4a	0.0000	0.5000	0.0000	0.030(10)

Remarks: a= 5.4619(17) b= 7.7207(14) c= 5.4886(13), space group: Pnma

In order to establish the location of the inserted lithium neutron diffraction studies were carried out. The neutron powder diffraction pattern at room temperature (results are given at [4]) and low temperature (7 K) were collected. Structural parameters at the 7 K temperature were determined in the frame of the Pnma space group and for the composition with $x = 0.70$ (as an example) are given in Tab. 1. The structure contains a three dimensional framework of corner sharing TiO_6 which are almost perfectly regular octahedra and slightly tilted. Lanthanum are placed close the theoretical A-site in all the compounds. In the structures is possible to see the following alignments: the La-LiC-LiF-LiC-La row and the La-LiA-LiE-La one. We can conclude that the results obtained from low temperature measurement are in reasonable agreement with room temperature ones. The occupation of the different sites seems to be sequential as has been observed in a previous paper [5]. The high content of lithium favours the occupation of the LiE and LiF sites which are far from the theoretical A-site. In these positions the coordination of lithium is four.

As the results indicate, in these perovskites the insertion limit not only depends on the A-sites vacancies as well on the possibility of the creation of new lithium sites.

- [1] E.-M. LEVIN, R.- S. ROTH: J. Res. Nat. Bur. Stan. 68A, 1964, pp. 197-206.
- [2] M.-L. MARTINEZ-SARRIÓN, L. MESTRES, M. HERRÁIZ, O. MAQUEDA, A. BAKKALI, N. FERNÁNDEZ: Eur. J. Inorg. Chem. 17, 2002, pp. 94-98.
- [3] M. MORALES, M.-L. MARTINEZ-SARRIÓN: J. Solid State Chem. 140, 1998, pp. 377-381.
- [4] S. VRATISLAV, M. DLOUHÁ, M.-L. MARTINEZ-SARRIÓN, L. MESTRES,: Proc. of the CTU WORKSHOP, vol. 8, part A, 2004, pp. 559-558.
- [5] M. MORALES, L. MESTRES, M. DLOUHÁ, S. VRATISLAV, M.-L. MARTINEZ-SARRIÓN: J. Mater. Chem. 8, 1998, pp. 2691-2694.

This research has been supported by GA ČR grant No. GA 202/03/0981, by MŠMT grant No. MSM210000021 and was partially sponsored by financial support from BQU2002-00619.

Laser Annealing of Bi₂Te₃ Thin Film Prepared by Pulsed Laser Deposition

L.Cudzik*, M.Jelínek**, V. Studnička**, M.Pavelka**, P.A. Atanasov***

L.Cudzik@sh.cvut.cz

* Department of Physical Electronics, Faculty of Nuclear Sciences and Physical Engineering, Czech Technical University, V Holešovičkách 2, 180 00 Prague 8, Czech Republic

**Institute of Physics, Academy of Sciences CR, Na Slovance 2, 182 21 Prague 8

***Institute of Electronics, Bulgarian Academy of Sciences, 72 blv. Tsarigradsko Chaussee, Sofia 1784, Bulgaria

Very thin layers of thermoelectric materials are potential candidates for many applications. Thermoelectric effect and its physical explanation is known since 19th century [1-3]. The ecological problems with cooling medias at the end of 20th meant rapid increase in research of thermoelectric materials. Main application areas for these materials are thus cooling, electric energy generation, sensors and detectors, not only on Earth, but in space either. The most important properties of thermoelectric materials are high Seebeck coefficient, high electric conductivity and low thermal conductivity. These three properties create so called “figure of merit” of thermoelectric material. There is a possibility to improve figure of merit of thermoelectric material by preparation of low-dimension structure (thin film, quantum wire or quantum dot). One of the most interesting materials is Bi₂Te₃. In the past thin layer of Bi₂Te₃ were prepared by various deposition methods. Pulsed laser deposition is a suitable to create thin layer in room temperature with stoichiometry close to bulk Bi₂Te₃.

Pulsed laser deposition (PLD) is a method using laser-solid interaction. High fluence of laser radiation interacts with target. The material of the target evaporates and creates plasma cloudlet, which flies on the substrate. Evaporated material condensates on the substrate. One of disadvantages of this method is forming nanocrystals or droplets on the film surface. It is desirable, if the layer is crystallized. After some PLD conditions the layer are crystallized only partially and another laser treatment is convenient. This laser treatment is called laser annealing. Lower fluence of laser energy is focused on deposited layer and the surface is quickly warmed up. The temperature must be higher than melting point, but lower than evaporating temperature of the material. Once the film is melt, new crystalline layers are formed. Pulse laser are used usually. Whole process is very rapid (in order of ns). Treatment can lead to destruction of the layer, or to forming new texture, finally there is a possibility, that layer freezes in some metastable phase. During this process is necessary to check crystallinity of thin films. For this purpose many methods was developed. One of the favourites, and the one used in this experiment is X-ray diffractometry (XRD). Principle is quite simple. At the beginning of installation there is a source of x-rays. After x-ray source is placed Goeble mirror, this special part changes parabolic beam by parallel one, this improves resolution of whole experimental set-up approximately by factor of ten. Roentgen beam is refracted if the Bragg equation is fulfilled, this means, that exists some crystalline plane, which is parallel to surface. Before detector there are placed some filters. There are three possible tests, the one described is called symmetric scan. It's the simplest one and can reveal only planes collinear to surface, but for our purposes is sufficient. [1]

In laboratories of the Institute of Physics AS CR Bi₂Te₃ films of 500nm thick were prepared on fused silica substrate. KrF excimer laser (248nm) with laser energy density 2-10 J.cm⁻² was used [1]. Crystallinity of films was examined by XRD. Texture of Bi₂Te₃[0 1 5] was found, but quite large amount of amorphous Bi₂Te₃ was present as well.

In the next part of experiment the layers were laser annealed. For annealing was chosen XeCl excimer laser (308nm). Recrystallization of annealed layer depends on various conditions, such as specimen temperature, laser fluence, pressure in vacuum chamber, time of annealing.

Laser fluence varied from 0.03J.cm⁻² to 0.06J.cm⁻², specimen temperature from 300K to 450K, ambient pressure from 5.10⁵Pa to 1.10⁻⁴Pa. Time of annealing was either 1 hour or half an hour. One specimen wasn't annealed and was used as a reference one. Layers were then examined by XRD and compared with reference. All the specimens recrystallized and their quality has improved. Annealing in atmospheric pressure created often texture Bi₂Te₃[0 1 5]. Films annealed in high vacuum emphasized texture Bi₂Te₃[0 0 1]. The best results were reached under these conditions: laser fluence: 0.06J.cm⁻², atmospheric pressure, specimen temperature 450K and time of annealing: 30min.

A theoretical model of laser annealing has been built for future experiments. This model consists of solving one-dimensional heat equation to estimate temperature on the thin film surface in dependence on used laser fluence. This problem was solved in MATLAB by explicit scheme of finite differences method. Validity of the model was tested on described experiment and the results were satisfactory.

References:

- [1] R. ZEPL, M. PAVELKA, M. JELÍNEK, J.CHVAL, P. LOŠŤÁK, K. ŽĎÁNSKÝ, J. VANIŠ, S. KARAMAZOV, S. VACKOVÁ, J. WALACHOVÁ: *Some properties of very thin Bi₂Te₃ layers prepared by laser ablation* phys.stat.sol (c) 2003 pp. 867-871
- [2] A.DAUSCHER, A.THOMY, H. SCHERRER.: *Pulsed laser deposition of Bi₂Te₃ thin film* Thin Solid Films 280 1996 pp.61-66
- [3] R.S. MAKALA, K. JAGANNADHAM, B.C. SALES *Pulsed laser deposition of Bi/sub 2/Te/sub 3/-based thermoelectric thin films* Journal of Applied Physics 2003, pp. 3907-3918.

This research has been supported by Grant Agency of the Czech Republic, projects No.202/02/0098 and No.A1010110.

Computer Simulation of Magnetron Target Erosion

T. Kubart, R. Novák

Tomas.Kubart@fs.cvut.cz

Institute of Physics, Faculty of Mechanical Engineering, Czech Technical University,
Technická 4, Praha 6, 166 07, Czech Republic

DC planar magnetron sputtering is widely used for the deposition of metallic thin films. Taking advantage of the magnetic field, a magnetron operates at much higher power density, lower pressure and lower discharge voltage compared to the simple diode sputtering. The applied magnetic field confines energetic electrons near the cathode creating thus a dense plasma just above the target surface. The target material atoms are then efficiently sputtered off by the ion impingement, diffuse through the working gas and condense on the coated surface where they possibly react with the reactive gas. By sputtering can be deposited coating of high melting point materials as well as nonconducting ceramics films which might be prepared by reactive sputtering, when reactive gas such as nitrogen or oxygen is introduced into the processing atmosphere.

One of the important issues of the magnetron sputtering is related to the target erosion. Its possible non-uniformity decreases the target utilization several times and variations in the deposited layer thickness and composition may appear. The computer simulation of the sputtering rate distribution is used to prevent these harmful effects. When rectangular magnetrons are used, one of the factors limiting the target utilization is intensive erosion that usually occurs in the joint area of the bended end area and the straight part.

Magnetron discharge is a kind of low pressure glow discharge. The plasma density is relatively low with low degree of ionization and the created electrons do not undergo many collisions so they are not in equilibrium. Therefore, the discharge has to be modeled by particle simulations. Self-consistent particle-in-cell (PIC) models completed with Monte-Carlo (MC) collisions are a suitable approach giving full information about the process, but it requires a very long calculation time. To reduce computation costs the more simple method was used, only secondary electrons are traced and their collisions are simulated by MC. The target erosion is determined from the ion impact density assuming constant sputtering yield. The electric field is assumed to be unaffected by the plasma and constant over the whole target surface. The field intensity in the sheath layer corresponds to full voltage applied to the target while in the plasma volume it is supposed to be zero. The thickness of the sheath is considered equal to the Larmor radius of an electron in magnetic. Magnetic field was solved using FEM software Ansys version 5.7. To reduce computation time, symmetries of the problem were utilized and the complete field was obtained by mirroring. The boundary condition on the free surfaces was satisfied by infinite elements, considering the decay of the field to zero far from the magnets.

Equation of motion of a charged particle in ExB field is solved by fourth-order Runge-Kutta method due to its high accuracy. In our model time step in bulk plasma was 50 times longer than in sheath layer in order to avoid numerical heating of electrons in a strong electric field. An electron is traced until its energy decreases below the ionization potential of argon or moves away from the calculation domain. First electron is created in a fixed point and then the emission point is selected randomly according to the ion impingement density on the target surface. New electrons are created at the end of the sheath with the energy equals to applied voltage.

It is tested after each time step if a collision occurs. Only elastic, excitation and single ionization collisions are taken into account. The collision probability is proportional to the

sum of the total cross-sections for each collision type. When a collision occurs, its type is distinguished by individual cross-sections. The energy of electron is decreased by 11.55 eV after excitation, by 15.76 eV after ionization and by 0.3 eV after elastic collision. Since the angular distribution of electrons scattered in argon is similar for all three collisions, the velocity direction after collision is determined according to the differential cross-section of elastic scattering. Trajectories of created ions are affected very little by magnetic field due to their high mass so they were assumed to be unmagnetized. Also collisions of ions with neutral gas were neglected. Therefore the ions created in collisions fell directly to the target without any transverse motion.

As an example of use of our model may serve a design of circular magnetron for sputter deposition of ionic conducting layers based detectors. After several magnetic optimization steps a first configuration of magnetic system was prepared. This was then adjusted according to erosion simulations. The different magnetic system configuration were prepared with different density of substrate ion current. This magnetron was manufactured and introduced into operation without any need of additional adjustment.

Another studied system was rectangular magnetron sputtering source. The most interesting result in that case was a clear asymmetry in the erosion depth in spite of the symmetry of the magnetic field, the erosion rate is the highest at the end (outlet) of the weak region. The asymmetry may be caused by gradients of the magnetic field in the transition zone or by the lost of electrons in the weaker field and this effect will be studied in more details.

We prepared a collisional model of magnetron discharge for simulation of the target erosion. Using the model simulations of erosion were performed. Main result is the asymmetrical erosion in symmetrical magnetic field which probably results from the magnetic field gradients in the bend. Such effect may dramatically influence local erosion rate and decrease the target yield a lot. Our results may be useful for design of the bended end of rectangular magnetrons.

References:

- [1] KUBART, T. - NOVÁK, R. - VALTER, J.: *Computer simulation of MagnetronSputtering Process* Proc. of Conf. New Trends in Physics, BUT, Brno, 2004 pp. 182-185.
- [2] KUBART, T. - NOVÁK, R. - VALTER, J.: *Modelling of Magnetron Sputtering Process*, Czech.J.Phys., 54, 2004 Suppl. C ,pp. 1027-1030

This research was funded by grant MPO No. FD- K3/104 and grant MSM No. MSM 212200008 .

Development of Arbitrary Lagrangian-Eulerian (ALE) Methods in Plasma Physics

M. Kuchařík, R. Liska, P. Bureš

kucharik@karkulka.fjfi.cvut.cz

Department of Physical Electronics, Faculty of Nuclear Sciences and Physical Engineering, Břehová 7, 115 19, Praha 1, Czech Republic

Plasma can be treated as a compressible fluid consisting of ions and electrons. Many problems from plasma physics are modeled by hydrodynamical Euler equations which form conservation laws for mass, momentum in every direction, and total energy. Conservation laws possess discontinuous solutions including shock waves and contact discontinuities which require special numerical treatment. In the approximation of the ideal plasma we use a more suitable equation of state, and include the parabolic term representing heat conductivity to the energy equation. When solving this system of partial differential equations, several approaches can be employed.

The classical Eulerian-type method solves the hydrodynamics equations on the static computational grid, the fluid flows through computational cell boundaries. In the Lagrangian approach, the Lagrangian grid moves together with the fluid movement, there is no mass flux between computational cells. The advantage of the Lagrangian method is a very good resolution of the material interfaces, and it allows the usage of moving boundary conditions. This method is typically used for problems with large changes of computational volume with moving boundaries, in cases of large fluid compression or expansion (as laser plasma target compression or corona expansion), where the Eulerian approach would be problematic. On the other hand, it may happen, that the moving grid loses its regularity, or degenerates in critical regions (e. g. the edges of the cell intersect each other), or some cells become non-convex, so the assumptions of the numerical method do not hold (e. g. some cell volumes become negative). The ALE method is able to treat these problems with distorted moving computational meshes.

The ALE (Arbitrary Lagrangian-Eulerian) method combines the advantages of both mentioned methods. It uses the Lagrangian solver as long as the grid is not too distorted. Now, the Eulerian part comes - we regularize (rezone) the grid by smoothing and conservatively recompute (remap) the values of the conserved quantities to the new, smoother grid [1]. Then, the Lagrangian computation can continue until the next rezoning-remapping step.

We have developed 2D ALE code on logically orthogonal grids which has three main parts – the Lagrangian solver based on support-operator method, the rezoning routine for untangling and smoothing of the computational meshes, and the remapping algorithm for conservative quantity interpolation to the smoothed grid [1]. The Lagrangian solver incorporates several artificial viscosity formulations, which allow the code to behave reasonably also in the critical situations of huge grid deformations. Another type of adding the diffusion to the solution has been developed – the hybrid Lagrangian solver. Instead of adding the artificial viscosity, the diffusion around the discontinuities is added by the affine combination of the numerical fluxes of the high order scheme with the lower order diffusive one. We have developed the general algorithm for 3D remapping of conservative quantities between general unstructured grids [2]. This algorithm is based on the piecewise linear reconstruction, numerical integration of the reconstructed function, and the conservative redistribution of the quantity between neighboring cells. This algorithm is applicable to

general 3D grids and to all conservative quantities and extends the 2D algorithm on logically orthogonal grids [1]. It can be one of the bases of the future general 3D ALE code.

Instead of ideal gas equation of state, we use the quotidian equation of state (QEOS) for plasma simulations. It calculates thermodynamic properties for given conditions by applying Thomas-Fermi theory for electrons, and Cowan model for ions. It gives reasonable results for quite a broad range of plasma densities and temperatures. Thermal conductivity has been added to the code. In the model, it is represented as the parabolic terms in the energy equation. By splitting, we solve the parabolic PDE separately, by using the support operator method with the mimetic discretization. We use the implicit method, which allows choosing the same time step, as in the hyperbolic part of the system. Two different methods for the thermal conductivity coefficient computation are included – the classical Spitzer-Harm and more suitable Rozmus-Offenberger method, which is more appropriate for the laser plasma temperature range.

The presented 2D ALE code was applied to the plasma physics problems inspired by the experiments performed on the PALS laser facility. The laser beam irradiates a small Aluminum disc, which is ablatively accelerated up to a very high speed (up to 150 km/s), and strikes the massive Aluminum target. The crater is formed, the Aluminum evaporates, and the coronal material is launched away. We simulated several situations with different disc impact velocities, thickness, density, or temperature [3, 4]. The crater size and shape is comparable with the experimental data. Standard Lagrangian methods are unable to treat these problems due to extremely high distortion of the computational mesh around the disc edge after the impact. The developed ALE code proved to provide efficient simulation tool for laser plasma simulations. Simulations of high-velocity impact play an important role in the construction of the cosmic aircrafts, and in the inertial confinement fusion research.

References:

- [1] KUCHARÍK, M. – SHASHKOV M. – WENDROFF B.: *An Efficient Linearity-and-Bound-Preserving Remapping Method*, Journal of Computational Physics, Vol. 188, Num. 2, 2003, pp. 462–471.
- [2] KUCHARÍK, M. – GARIMELLA, R. – SHASHKOV M. – WENDROFF B.: *Efficient Algorithm for Conservative Local-Bound-Preserving Remapping in 3D ALE Methods*, Technical Report, Los Alamos National Laboratory, 2005, In preparation.
- [3] KUCHARÍK, M. – LISKA, R. – LIMPOUCH, J. – VÁCHAL, P.: *ALE Simulations of High-Velocity Impact Problem*, Czechoslovak Journal of Physics, Vol. 54, Suppl. C, 2004, pp. 391–396.
- [4] KUCHARÍK, M. – LIMPOUCH, J. – LISKA, R. – HAVLÍK, P.: *ALE Simulations of Laser Interactions with Flyer Targets*, Proceedings of XXVIII ECLIM, 2004, To appear.

This research has been supported in parts by CTU grant No. CTU0410914.

Ozone Generation in Electrical Discharge

V. Scholtz

scholv1@fel.cvut.cz

Department of Physics, Faculty of Electrical Engineering, Czech Technical University,
Technická 2, 166 27 Prague 6, Czech Republic

Ozone as a chemical element becomes to be more and more important in many technical and biological applications. For better improving of industrial devices it is required to describe the mechanisms of ozone generation, transposition and its influence on destination material. In this article, it is described one way of describing the production and transportation of generated ozone in electrical corona discharge. It is based on simplifying of chemical reaction described in [1] and on creation of a hydrodynamical model of air movement in the discharge, based on Fick's law and the conservation of total number of particles.

The chemical reactions describing the ozone generation published in [1] are:

1. $e + O_2 \rightarrow e + O + O$
2. $O + O_2 + O_2 \rightarrow O_2 + O_3$
3. $O + O_3 \rightarrow O_2 + O_2$
4. $O_2 + O_3 \rightarrow O + O_2 + O_2$

and the coefficients of probability are:

$$\begin{aligned}
 k_1 &= 2 \times 10^{-9} \text{ cm}^3 \text{ s}^{-1} \\
 k_2 &= 6.9 \times 10^{-34} \times (300/T)^{1.25} \text{ cm}^3 \text{ s}^{-1} \\
 k_3 &= 1.8 \times 10^{-11} \times \exp(-2300/T) \text{ cm}^3 \text{ s}^{-1} \\
 k_4 &= 7.3 \times 10^{-10} \times \exp(-11400/T) \text{ cm}^3 \text{ s}^{-1}
 \end{aligned}$$

Looking on this reactions, it is obvious that in atmospherical pressure at standard temperature (300K) only first two reactions becomes to be important and for qualitatively studying whole reactions may be simplifying to following equations:

$$\begin{aligned}
 A - Bn_O &= dn_O / dt \\
 B n_O - F(n_{O_3}) &= dn_{O_3} / dt
 \end{aligned}$$

where $A=2n_e n_{O_2} k_0$, $B=n_{O_2}^2 k_1$, where n_e , n_O , n_{O_2} and n_{O_3} are the concentrations of electrons, atomic oxygen, molecular oxygen and ozone. Function $F(n)$ is function describing the decrease of ozone by diffusion and wind speed and for the first approximation may be defined as $F(n_{O_3}) = F^* n_{O_3}$. The result of considering of this equations is, that there is only one stationary state for $n_O=A/B$ and $n_{O_3}=A/F$, which is really stable.

It may be deduced that in the ozone and air stream modelling the electrical discharge may be represented only as a constant source of ozone. Up to now, we have done some numerical simulations considering the diffusion and constant speed of wind with results describing the dynamics of ozone moving. Next, considering the hydrodynamical model of air, we make some numerical simulations of it in some easier configurations of discharge or discharges in some boxes. This same method may be, after using some corrections, used for

ozone generation modelling in electrical field with small electrical gradient, that means not only corona discharge but for barrier or other types of discharges, too. In this case it is needed to remake this discrete source of ozone to continuous source.

References:

- [1] PIGNOLET, P. – HADJ-ZIANE, S - HELD, B. - BENAS, J - COSTE, C.: *Ozone generation by point to plane corona discharge* J. Phys. D: Appl. Phys. 23, 1990, 1069-1072.

This research has been supported by GAČR grant nr. 202-03-H162.

Verification of Method for Description of Secondary Sound Field

I. Bláhová, J. Zendulka

blahova@fel.cvut.cz

Department of Physics, Faculty of Electrical Engineering, Czech Technical University,
Technická 2, 166 27 Prague 6, Czech Republic

Scattering and diffraction are phenomena still frequently discussed in acoustics. In his book "Theory of Sound" published in 1887 Lord Rayleigh provided the analytical description of a secondary sound field for a spherical obstacle and the approximate description for a cylindrical shaped obstacle. Yet since his time, no analytical solution for an obstacle of any other shape has been published. For these obstacles, only the numerical description of the secondary sound field based on experimental results is possible.

We have prepared the method for creating mathematical models of a secondary sound field for different shaped bodies. For preparation of this method, a spherical body was chosen because the comparison between experimental and analytical results is feasible. The obtained numerical description of secondary sound field was compared to descriptions calculated on the basis of analytical formula. A mathematical model of the secondary sound field measured was prepared, and measurements with differently shaped bodies and their mathematical models with respect to our experiences obtained up to now is being prepared.

Measurements were performed in an anechoic room, which is an ideal model of a free field. For testing of the measuring method, a model of a rigid sphere-shaped body was used. The concave sphere-shaped body is made of glass and filled with foam. The diameter of the sphere is 35 cm. During measurements, the body was hung from a rope. The measuring microphone was fixed on the stand towards the sphere. The upper part of the stand is movable, allowing the changing of the position of a measuring microphone in a line. The speaker was placed 5 m towards the measuring body where it is supposed that an incident sound wave is a plane wave for a frequency range used. A sinusoidal logarithmic sweep signal from frequency 100 Hz to frequency 10 kHz and sinusoidal signals with frequencies 500 Hz, 1 kHz, 2 kHz and 4 kHz were generated. The responses were picked up by a measuring microphone. The position of the measuring microphone was changed on lines. For lower frequencies from the surface of the sphere to the distance 60 cm from the surface of the sphere, the step was 1 cm. For higher frequencies from the surface of the sphere to the distance 15 cm from the surface of the sphere, the step was 0,25 cm. These lines cover the plane perpendicular to the sphere and parallel with incidental wave. The polar coordinates with the origin in the centre of the sphere were used. The angle between neighbour lines used for measurement was 15°. A frequency analyzer was used for measuring. Data were processed in the system MATLAB and compared with analytical results.

After the first part of measurements, it was revealed that measurements are affected by the characteristics of the speaker and the anechoic room itself. To avoid this unwanted effect, it was decided to perform every measurement twice - the first time with the measuring object and the second time without it. Then the difference between these two measurements was evaluated. Though there are some reflections between the measuring object and the speaker, for example, they affect the results of our measurements, it is not possible to suppress all these effects totally.

The measurement method for scattering and diffraction on a sphere was proposed, and the first set of measurements with a spherical-shaped body was realized. Results obtained were compared with the analytical solution for a rigid sphere-shaped body. The very good agreement between analytical and experimental results was found. So we can say that our experimental method using a speaker sound excitation is verified.

It is planned to enlarge this measuring method. The pulse method of excitation is planned to be used. A major part of the pulse excitation apparatus is expected to be located outside of the anechoic room, so it is supposed that these measurements going to be less affected by involving measuring apparatus than measurements using the speaker excitation. Obtained results will be compared with results obtained with the previous method of sound excitation. Then the proper sound excitation will be chosen for next measurements.

Future measurements will be focused on scattering on complex bodies particularly on a human body. The results of this measurement will be applied, for example, in active noise control research being performed in our workplace.

References:

- [1] BLÁHOVÁ, I., JIŘÍČEK, O.: *Experimental Method for Measuring Secondary Sound Field for Sphere and Its Comparison with Analytical Results*, Proceedings of ICA 2004, Kyoto, 2004.
- [2] MORSE, P.M.: *Vibration and Sound*, ASA, USA, 1995.
- [3] RAYLEIGH: *Theory of Sound*, Cambridge, 1877.
- [4] SKUDRZIK, E.: *The Foundations of Acoustics*, Springer-Ferlag, New-York, 1971.

This research has been supported by AV ČR grant No. KJB 1120301.

Waves in Pinch Generated by Z-150

V. Kaizr

Kaizr@aldebaran.cz

CTU, Faculty of Electrical Engineering, Department of Physics, Technická 2, 166 27 Prague 6

It is well known that electromagnetic waves cannot propagate in a plasma whose density exceeds critical value deduced from the condition of equality of the electron plasma frequency. But there is a property that waves in special configuration can go through plasma object. We try to find the waves and its conditions to heat up a hot spot. From known parameters device Z-150 we can solve the critical frequency.

The basic parameters device Z-150:

$$I = 10 \text{ kA};$$

$$r = 0,6 \text{ mm};$$

$$\lambda = 1 \text{ mm};$$

$$\rho = m_e n_i = 4 \times 10^{-3} \text{ kg m}^{-3};$$

$$n_e = 6 \times 10^{23} \text{ m}^{-3};$$

$$n_i = 2 \times 10^{23} \text{ m}^{-3};$$

$$B = \frac{\mu I}{2\pi r} = 3,4 \text{ T};$$

$$p_B = \frac{B^2}{2\mu} = 4,59 \text{ MPa};$$

$$kTe = \frac{p_B}{n} = 35,9 \text{ eV}.$$

The waves which can propagate in this plasma.

Plasma elektron frequency: $\omega_{pe} = \left(\frac{n_0 e^2}{\epsilon_0 m} \right)^{\frac{1}{2}} \approx 9\sqrt{6 \times 10^{23}} = 6,97 \times 10^{12} \text{ s}^{-1}.$

Plasma cyklotron gyration: Elektron $\omega_{pe} = \left(\frac{n_0 e^2}{\epsilon_0 m} \right)^{\frac{1}{2}} \approx 9\sqrt{6 \times 10^{23}} = 6,97 \times 10^{12} \text{ s}^{-1}.$

Ion $\omega_{ci} = 3,4 \times 10^7 \text{ s}^{-1}.$

Magnetoacoustic Waves:

Longitudinal: Alfvén's wave: $v_a = \frac{B}{\sqrt{\rho\mu}} = \frac{3,4}{\sqrt{4 \times 10^{-3} \cdot 4\pi 10^{-7}}} = 4,8 \times 10^4 \text{ ms}^{-1}.$

$$\frac{\omega^2}{k^2} = c^2 \frac{v_z^2 + v_a^2}{c^2 + v_a^2};$$

Perpendicular :

$$\frac{\omega^2}{k^2} = 8,2 \times 10^9 \text{ ms}^{-1}$$

Research will focus on find the condition how heat up the „hot spot“ with laser frequency even higher than critical density.

References:

- [1] KULHÁNEK, P.: *Particle and Field Solvers in PM Models*. Czechoslovak Journal of Physics, Vol. 50, Suppl. S3, 2000, pp. 213 – 244.
- [2] TIMOFEEV, A. V.: *Electromagnetic waves in a magnetized plasma near the critical surface*. Physics-Uspekhi, 2004.
- [3] STURROCK, P. A.: *Plasma Physics*. Cambridge University Press, 1995.
- [4] KAIZR, V.: *Low Frequency Waves in Plasma Fibers with Gravitational Filed*. Czechoslovak Journal of Physics, Vol.52, Suppl. D, 2002, pp. 231-234.

This research has been supported by the research program No J04/98:212300017 "Research of Energy Consumption Effectiveness and Quality" of the Czech Technical University in Prague, by the research program INGO No LA 055 "Research in Frame of the International Center on Dense Magnetized Plasmas" and "Research Center of Laser Plasma" LN00A100 of the Ministry of Education, Youth and Sport of the Czech Republic.

Deposition of Thin Layers by Matrix Assisted Pulsed Laser Evaporation

J. Remsa*, M. Jelínek**,***, T. Kocourek**, R. Christescu****

remsa@centrum.cz

*Dept. of Physical Electronics, Faculty of Nuclear Sciences and Physical Engineering, CTU,
V Holešovičkách 2, Praha 8, 180 00

**Institute of Physics, Academy of Sciences of the Czech Republic,
Na Slovance 2, 182 21 Praha 8

***Institute for Biomedical Engineering, CTU, Sítňá 3105, 27201 Kladno

****University of Bucharest, 36-46, M. Kogălniceanu Bd, Sector 5, 70709, Bucharest,
Romania

One of the most important conditions for development of new devices in biomedicine, sensor and drug delivery applications, non-linear optics is the ability to create thin layers of generally large molecules such as polymers and biomaterials. The molecular weight of some common proteins can be larger than 150 000 amu. Biomaterials include a large class of materials which range from simple polymers to enzyme, protein, antibodies, nucleic acids and cells. Very important difference between biomaterials and passive materials, such as dielectrics, is their activity, i.e. they have specific biochemical function. This implies that biomaterial transfer requires preserving molecular functions which is much stricter requirement than the retention of composition in passive materials. The obvious choice for making thin layers of biomaterials was Pulsed Laser Deposition but – except addition type polymers such as PTFE – decomposition of molecules was observed. Given the fact that in these materials the chemical bonds have energies well below the UV photon energies, some degree of photochemical decomposition is expected in PLD process. As solution for this problem new deposition technique was discovered. It was named Matrix Assisted Pulsed Laser Evaporation (MAPLE).

MAPLE is vacuum based physical vapor deposition technique – very similar to PLD. MAPLE differs from conventional PLD by preparation of target, conditions in chamber and energy of laser beam. The target material is cooled to temperatures between -40°C and -190°C. In MAPLE the biomaterial is mixed with large excess of solvent material that strongly absorbs at laser deposition wavelength (ArF* 193 nm, KrF* 248 nm). The word “matrix” is used because low concentration (0.1-5 wt %) of biomaterial in solvent. The beam energy is absorbed by the matrix, material is ejected from target and carried towards substrate and layers composed of large molecules are grown.

We deposited thin films of cryoglobulin, fibrinogen, polyvinyl alcohol (PVA) and pullulan in different matrixes. For deposition KrF* excimer laser with repetition rate 10 Hz was used. The depositions took place in stainless-steel vacuum chamber. In case of fibrinogen and pullulan the nitrogen as background gas (5-15 Pa) was used. We used wide variety of laser fluencies from 100 to 700 mJ/cm². Our substrates were squares of 1x1 cm and 2x2 cm of Si(111). We prepared the targets by immersing copper holder with mixture of the analyte and the solvent in liquid nitrogen (LN). During the whole deposition process was the target cooled by LN. The target-substrate distance was between 3 and 6 centimeters.

In this work we present results of deposition of cryoglobulin. Cryoglobulin is an abnormal blood protein with a molecular weight of approximately 200,000 amu associated with several diseases. These diseases include cancers, infections and autoimmune disorders. It is characterized by its tendency to clump in cold temperatures. Thin layers of cryoglobulin can be used for faster disease sensing than classical analysis. We prepared the target from cryoglobulin solved in sanguine plasma. Deposition conditions are summarized in Table 1.

Vacuum [$\times 10^{-4}$ Pa]	Fluence [mJ/cm ²]	Target- substrate distance [cm]	Number of pulses	Thickness [nm]	Deposition rate [Å/pulse]
1.5	300	3	11,600	100-830	0.72
1.5	200	3	6,000	200-290	0.48
1.5	200	6	6,000	140-140	0.24
2	100	4.5	6,000	90-120	0.20

Table 1. Deposition conditions of cryoglobulin

We can see that the film growth rate was in the region from 0.2 Å/puls to 0.7 Å/pulse. Films were smooth as measured by optical microscopy (magnification 250 x). All substrates surfaces were covered homogeneously. Preliminary results of FTIR (Fourier Transformed Infrared Spectroscopy) measurement show similarity of films bounds to reference film created by drop-in technique.

We can conclude that by MAPLE technique the thin films of large organic molecules can be fabricated.

References:

- [1] REMSA J.: *Rešeršní práce: Laserová depozice tenkých vrstev biomateriálů pomocí technologie MAPLE* ČVUT FJFI KFE, 2004,
- [2] CHRISTESCU R.: *Laser - Matter Interactions: Processing of Polymeric Thin Films for Biomedical Applications* PhD. thesis, Bucharesti 2004
- [3] CHRISEY D.B., PIQUÉ A., MCGILL R., A. HORWITZ J.S., RINGEISEN B.R., BUBB D. M., WU P. K.: *Laser Deposition of Polymer and Biomaterial Films* Chemical Review 103, 2003, 553-576.
- [4] CHRISEY D. B., HUBBLER G. K.: *Pulsed Laser Deposition of Thin Films* John Wiley & Sons, Inc, 1994

The authors thank grant GA AV ČR A 1010110 for support.

Computational Meshes for Plasma Physics and Fluid Dynamics

P. Váchal, R. Liska

vachal@galileo.fjfi.cvut.cz

Dept. of Physical Electronics, Faculty of Nuclear Sciences and Physical Engineering, CTU,
V Holešovičkách 2, 180 00 Praha 8, Czech Republic

The Arbitrary Lagrangian-Eulerian (ALE) methodology is a very promising approach for fluid dynamics simulations. During the computation, the mesh is adapted to keep track with geometry of the physical system under study. Therefore, this method is especially advantageous for modeling of extremely complex phenomena such as metal forming, laser-plasma interactions or hydrodynamic instabilities. The ALE algorithm consists of three stages: a Lagrangian stage, in which the mesh nodes move with the material flow, a rezone stage in which the mesh is modified to improve its quality, and a remapping stage in which the solution is conservatively interpolated from the old mesh to the new, improved one. In purely Lagrangian simulations, the mesh often becomes so heavily distorted, that the computation cannot continue. This is avoided in ALE methods by the rezoning and remapping stages. Here, we focus on mesh rezoning, that is on the issue how to improve the mesh quality in order to keep the computation running by making the next Lagrangian step possible.

There are two ways to rezone the mesh: node repositioning and node reconnection. We believe, that an ideal method has to combine both approaches. However, to gain full control about the rezoning process, one first has to understand and manage each of the two techniques separately. Recently, we suggested a set of methods based on mesh repositioning, without changes of connectivity [1]. The routines combine geometrical analysis with numerical optimization and were designed to rezone even tangled meshes, that is meshes with inverted elements. However, in practical ALE implementations [2], such extreme deformations are rarely the case and a certain amount of smoothing has to be added. Therefore, the sensitivity of proposed procedures can be triggered by a set of parameters.

Let us now follow the other path. Positions of nodes stay fixed and the mesh quality will be improved by changing of the edges between them. For simplicity, let us consider a two-dimensional unstructured triangular mesh, where the process can be simply described by a series of edge “swaps”. Each pair of neighboring triangular cells forms a quadrilateral, split by the common edge. By edge swapping we mean replacement of this edge by the other diagonal of the quadrilateral. Our mesh rezoning algorithm is as follows: Loop through all interior edges. For each edge, compare the quality of the adjacent cell pair to the alternative pair, created by swapping of the current edge. If the new pair is better, keep the edge swapped. Continue with the next cell. Stop if there is no change during the entire loop.

The basic question is how to measure the cell quality. We tested and combined a wide set of criteria, from pure geometrical ones (condition number for particular vertices, average cell areas, etc.) to those more physics related. Here we focus on the latter ones, since our primary objective is to develop a robust and universal mesh rezoning method for ALE simulations. The experience shows, that best results are achieved if the geometrical mesh changes are closely related to physical behavior of the system under study. This can be implemented by utilizing the discrete values of a selected state variable, for example density in fluid dynamics or temperature in plasma physics.

Suppose that the selected state variable is described by a smooth function $f(x,y)$. In each cell, we approximate it by a constant or linear reconstruction. The quality measure will

then be the integral of the reconstruction error over the whole cell. This error is estimated by square of the following terms in Taylor expansion, particularly terms with f_x, f_y for piecewise constant reconstruction or terms with f_{xy}, f_{xx} and f_{yy} for piecewise linear one. However, in practical ALE simulations, a physical quantity will be always described by a set of discrete values rather than by a smooth, differentiable function. In this case, one has to approximate numerically also the derivatives. We first tested an existing approach utilizing Green's theorem and then suggested another method, based on integration of forward differences and minimization of suitable functional.

The proposed method was implemented for analytical underlying function as well as for the discrete values. As expected, the behavior of the mesh was generally the same in all tests. The cells tend to align either parallel or perpendicular to isolines of the function. This effect is more dramatic in the case of piecewise constant reconstruction, since the interpolation error is bigger. With piecewise linear reconstruction, the effect is still strong enough and moreover the cells retain a reasonable shape.

Besides ALE simulations, our mesh reconnection strategy can be applied in other areas of computational physics. Recently, it has been successfully used to modify a program package for solution of elliptic problems [3]. To keep the error small, the original code used the adaptive mesh refinement (AMR) technique, which required a sophisticated and expensive mechanism for storage and management of the mesh structure. Replacement of the AMR module by our edge swapping procedure significantly decreased these costs, while keeping the same level of accuracy. In the previous application, where the mesh was rezoned to allow better interpolation of a state variable, the error was measured by magnitude of the following terms in Taylor expansion. Here the aim of rezoning is to improve a solution of an elliptic problem. For this purpose, a new error estimator has been constructed, based on integration of intercell jumps of the reconstruction. The actual mesh reconnection strategy is problem independent and thus can be used as described above. After extensive testing we concluded that elliptic problems can be solved with significantly higher accuracy on sufficiently fine meshes rezoned by our method.

As mentioned above, the proposed mesh rezoning strategy can be further improved by combining the node repositioning technique with node reconnection. This possibility is currently being studied and preliminary tests yield promising results.

References:

- [1] VÁCHAL, P. – GARIMELLA, R. - SHASHKOV, M.: *Untangling of 2D Meshes in ALE Simulations*. Journal of Computational Physics, Vol. 196, No. 2, 2004, pp. 627-644.
- [2] KUCHARÍK, M. - LISKA, R. - SHASHKOV, M. - VÁCHAL, P.: *Conservative Interpolations in Arbitrary Lagrangian-Eulerian (ALE) Codes*. Journal of Computational and Applied Mathematics, 2004. Submitted.
- [3] BERNDT, M. - VÁCHAL, P. - LIPNIKOV, K. - SHASHKOV, M.: *Mesh Reconnection Method for the Solution of Elliptic Problems*. SIAM Conference on Computational Science and Engineering, February 2005, Orlando, FL, USA. Presentation accepted.

This research has been partly supported by the CTU grant CTU0411014.

Numerical Modeling of Radiative Processes in Plasma Fibre

David Břeň

bren@aldebaran.cz

CTU, Faculty of Electrical Engineering, Dept. of Physics
Technická 2, 166 27 Prague 6, Czech Republic

Introduction

The plasma fibers are the most common structures in both laboratory and space plasma. In the Department of Physics of the FEE CTU the study of plasma fibers has a long tradition. They are studied both experimentally and theoretically. Approximately since 1997 runs the parallel theoretical research in the area of computational simulations. Formally general studies of many body systems and simulation of their behavior by Monte Carlo method, recently the studies of quasineutral systems by Particles in Cells method (PIC). The equilibrium or near-equilibrium state is caused by equality of plasma pressure gradient and Lorentz force (magnetic pressure gradient). This type of equilibrium evolves in famous Bennett profile of particle density. Formally it was calculated for uniform current density, but nowadays the density profiles are known in much general cases.

The plasma current generates magnetic field that is important for the equilibrium. However the current increases fiber temperature via Joule heating. Increasing temperature leads to higher plasma pressure and the equilibrium would be instable. Role of the opposite channel to the Joule heating plays radiation of the fiber. Radiative processes cool the fiber and enable maintenance of the equilibrium. First calculations of radiative equilibrium configuration did Pease and Braginski. They discovered that under some conditions the cooling process can overcome the heating one and the fiber electromagnetically collapses to the axis.

In the Department of Physics of the FEE CTU the study of plasma fibers has a long tradition. They are studied both experimentally and theoretically. Approximately since 1997 runs the parallel theoretical research in the subject of computational simulations. Formally had been made general studies of many body systems and simulation of their behavior by Monte Carlo method, recently are studied quasineutral systems by Particles in Cells method (PIC). The simulation of the plasma pinches is done via PIC method. This program solves the movement of the particles in the external fields, the change of the field as a reaction of the movement of the particles and again the movement of the particles in the forced fields. It does not solve neither the energetic losses caused by peculiar movement of the particles, nor their recombination yet.

The Solution of the Radiation

The radiation of the fibers is very important feature because it is the most efficient channel of energy losses. Detailed synchrotron and bremsstrahlung radiation processes in the plasma fiber will be treated in this paper. The goal of this work is the diagnostics of the plasma pinch in the sphere of the energetic radiation of the charged particle. The radiative fields are visualized on a two-dimensional sphere located far away from the radiation sources.

The code of the program from which the calculations are coming is written in FORTRAN 95. For the translation the compiler and linker from Compaq Visual FORTRAN 6.6 were used.

It is necessary to use the relativistic scheme for the calculation of the bremsstrahlung and synchrotron radiation, dominating during high velocities. Buneman's relativistic scheme was used here. From motion of the charged particle, we can calculate intensity, its time course, and dependence on direction.

There are furthermore radiative processes in the plasma related to recombination and excitation processes in the atomic shell. These processes are treated as global ones, no detailed analysis is included.

Conclusions

The radiative fields are visualized on a two-dimensional sphere located far away from the radiation sources. All the calculations serve as a diagnostic part of the "3D PIC model". We hope to obtain model of the pinch one step nearer to the reality after the inclusion of these results into energetic losses of moving charged particles into PIC model.

Typical directional patterns for radiation of experimentally interesting field configurations were found in this work. As the most interesting situations, the electric double layer, polar region of magnetic dipole, magnetic compression bow-shock, MHD shock and plasma fiber were treated.

References:

- [1] BŘEŇ, D: *Numerical Simulation of Plasma Fibers Energy Losses* Prague: CTU, 2003, pp. 102–103
- [2] BŘEŇ, D: *Numerical Modeling of Energy Losses in z-Pinches* Czechoslovak Journal of Physics, 2002, pp. 226–230.
- [3] KULHÁNEK, P. – BŘEŇ, D. – KAIZR, V. – PAŠEK, J.: *Particle in Cell Simulation of Helical Structure Onset in Plasma Fiber with Dust Grains* Dusty Plasmas in the New Millennium. Melville, New York, 2002, pp. 353–356.
- [4] KAIZR, V. – KULHÁNEK, P. – BŘEŇ, D. – PAŠEK, J.: *Low Frequency Acoustic Waves in Nebulae with Gravitational Field Induced by Dust* Dusty Plasmas in the New Millennium. Melville, New York, 2002, pp. 329–332.

This research has been supported by CTU0413913 and by research program No J04/98:212300017 "Research of Energy Consumption Effectiveness and Quality" of the Czech Technical University in Prague, by the research program INGO No LA 055 "Research in Frame of the International Center on Dense Magnetized Plasmas" and "Research Center of Laser Plasma" LN00A100 of the Ministry of Education, Youth and Sport of the Czech Republic.

The Use of Radiofrequency and Microwave Discharge for Textile Modification

J. Koller

koller@fel.cvut.cz

Katedra fyziky, elektrotechnická fakulta ČVUT,
Technická 2, Praha 6, 166 27

Introduction

PET hydrophobicity improvement was the main goal of our research due to the PET low wettability, low adhesion, high oil impurities cohesion and undesirable electric discharge generation. The most reliable way how to change the wettability of the PET is the change of its surface chemical characteristics. The modification can be achieved [1] by various processes, e.g. by enzymatic hydrolysis, low pressure and atmospheric pressure plasma application, chemical grafting or excimer laser application [2].

Experiments

Treated specimens made from the polyester fabric with trade-description Tesil 12 were modified with MW discharge PC controlled plasma plant equipped with a downstream microwave plasma generator or with RF plasma.

Both experiments were performed in the air and in the oxygen– nitrogen mixtures. All experiments were performed under constant pressure (64 Pa) and constant gas flow rate (100 sccm).

Air was chosen due to its easy availability and low cost. Modification efficiency grew with increasing discharge input power. The maximum modification efficiency corresponds to the input power of 125 W. Further increase of the input power led to the discharge instability and larger dispersion of measured hydrophilicity values. In case of modification maximum efficiency the fabric surface was probably fully saturated with active particles. The hydrophilicity differences in our experiments seems to be related to enhancement of the hydrophilicity due to the etching effect accompanied by microcracks creation on the tested surface. This led both to the tested surface growth and hydrophilic groups binding area enlargement and reorientation of the dipoles on the surface.

Experiments in the (N₂:O₂) mixtures were performed due to the low fabric plasma modification efficiency in the air. If nitrogen or oxygen would distinctively improve the plasma modification efficiency, their admixture with the air should improve the process efficiency without substantial additional cost, too. Used discharge gas mixtures differed in nitrogen–oxygen concentrations (100:0; 80:20; 60:40; 40:60; 20:80; 0:100).

Comparison of modification efficiency

To standardize different characteristics of the RF and MW discharge we introduced the standardized area. The modification efficiency expressed in the standardized feathering spot size for different nitrogen and oxygen concentrations in RF and MW discharges were compared. The modification efficiency of RF discharge decreases with growing concentration of nitrogen. For microwave discharge is the course of dependence similar but in smaller range of values.

RF discharge modification efficiency was evidently higher than that of MW discharge. RF discharge efficiency seems to be higher than expected, probably being dependent on the energy transfer method and on the location of specimen in plasma. The modification

efficiency of MW discharge was strongly influenced with the substrate – MW discharge center spacing.

Air plasma modification effect aging

During first 24 hours the feathering spot size and hence the modification effectivity had sharply diminished. The modification effect highest durability corresponded to the 125 W input power. This efficiency drop might be connected with the transformation of created hydrophilous function groups. Dipoles orientation might also change backwards in time coming into the primary orientation. There was found no important difference in hydrophobicity of modified and unmodified specimens 5 days after modification. Longer modification effect duration seemed to be connected with higher admixtures of oxygen in plasma, for pure oxygen plasma the effect lasted for about 10 days.

Conclusions

1. To obtain comparable PES fabric modification effect either in oxygen and nitrogen plasma, the nitrogen plasma treatment must be longer or higher discharge input power is necessary. The costs/modification efficiency ratio seems to be the most economic in case of air–oxygen mixtures.
2. PES fabric RF plasma modification seems to be more effective than that of the MW plasma.

There was performed a study of the PES fabric modification effect aging expressed in the feathering spot size time changes. Modification effect of pure oxygen plasma evidently lasted for about 48 hours, and then became extinct. Modification effect of pure nitrogen or air plasma vanished after 24 hours, thereafter resulting in almost the same hydrophilicity degree of modified and unmodified PES specimens. In case of air plasma modification with the discharge inputs power the extinguishing of the modification effect lasted two times longer (48 hours).

References:

- [1] PASTORE CH.M., KIEKENS P.: *Surface Characteristics of Fibers and Textiles* DEKKER:, Inc.(2001) 49-52.
- [2] WONG W.,ET ALL: *Surface structuring of poly(ethylene terephthalate) fibres with a UV excimer laser and low temperature plasma* Journal of Materials Processing Technology, 103 (2000), pp. 225–229.

This research has been supported by GA 202/02/D055.

Pulse Stretcher for Chirped Pulse Amplification with High Power- and Spectral- Transmissions

M. Divoký*, M. Smrž*, P. Straka**

divoky@fzu.cz

*Department of Physics, Faculty of Nuclear Sciences and Physical Engineering, Czech Technical University, V Holešovičkách 2, 180 00 Prague 8, Czech Republic

**Institute of Physics, AS CR, Na Slovance 2, 182 21 Prague 8, Czech Republic

Nowadays the leading laser laboratories are on a hunt for the highest power of laser pulses up to petawatts. To gain such a high powers it is necessary to amplify the shortest optical pulse possible, which can be supplied by commercially lasers, i.e. femtosecond pulses ($1 \text{ fs} = 10^{-15} \text{ s}$). To achieve the powers of terawatts (10^{12} W) or even petawatts (10^{15} W), the pulse power must be amplified at least $10^7 \times$. Usual methods of laser amplification, where a beam size is enlarged, are not sufficient for femtosecond pulses. Their high powers after amplification would cause an optical damage of material (even air) by high electric fields ($\sim \text{GV/cm}$).

How then one could amplify the femtosecond pulses to such powers? First, a pulse is stretched in time by dispersion in a system called pulse stretcher to hundreds of picoseconds ($1 \text{ ps} = 10^{-12} \text{ s}$). The pulse becomes frequency modulated, i.e. chirped. Second, the chirped sub-nanosecond pulse is amplified in a usual laser amplifier. Its power is increased, but still remains under the threshold of the optical damage. Third, it is directed to an evacuated chamber, where its power is finally increased to petawatt by a temporal compression of the pulse in a system called pulse compressor. It compresses the pulse back to femtosecond region using the opposite dispersion than the stretcher had. This technique of femtosecond pulse amplification up to petawatt power is called chirped pulse amplification (CPA). The petawatt optical field is then used for an experimental study of its interaction with matter. Such strong optical fields encourage a study of new promising phenomena of laser interaction and their applications, e.g. relativistic acceleration of elementary particles in future compact laser accelerators or a generation of special matter that occurs only in cosmos. Later, the CPA system could be used to ignite an inertial thermonuclear fusion or to create a source of intensive coherent X-Ray radiation (X-Ray laser).

Our task was to build a highly efficient stretcher for a stretching of 10-fs pulses to 300 ps and to recompress the stretched pulses in a pulse compressor. The compressor usually consists of two parallel diffraction gratings, while the stretcher has an additional imaging system between the gratings, which changes the sign of dispersion in comparison to the compressor.

The highest diffraction efficiency of blazed ruled gratings is at the Littrow angle α ($\sin\alpha = \lambda b/2$, where λ is a diffracted wavelength and b is a groove density), when the input beam is diffracted back. For the in-plane diffraction the angle of incidence differs usually from the Littrow angle by $5\text{-}10^\circ$ in usual double-pass compressors. As a result a spectral bandwidth can be reduced and a power transmission can decrease to less than 60% assuming a double-pass compression to less than 20 fs. The imaging system involves additional losses for the stretcher. With such a spectrally broadband pulses, the Littrow angle can be approached better for an incident pulse slightly out of the plane of diffraction (off-plane diffraction), i.e. not perpendicularly to grooves of the grating. However, an attention must be paid to the effect of the conical diffraction.

For our pilot optical parametric CPA system [1], we prepared a new scheme of the double-pass pulse stretcher with small conical (off-plane) diffraction and an imaging Öffner telescope. A beam from a Ti:sapphire laser enters the stretcher under a descend angle of 2° (i.e. off-plane), strikes the diffraction grating at the Littrow angle in the horizontal plane and is diffracted. After passing the Öffner telescope, the beam is diffracted again by the grating to the retroreflector. A similar design using two diffraction gratings has already been reported [2]. Nevertheless, an alignment of our stretcher is simplified when using the single grating. So far, most of the CPA pulse stretchers with the Öffner telescope have used the traditional in-plane diffraction scheme [3]. The complementary compressor is also double-pass with two diffraction gratings and the retroreflector. To ensure the opposite dispersion, the beam enters the compressor under an elevation angle of 2° and at the Littrow angle.

The stretcher and the compressor, both with the off-plane diffraction, were ray-traced and compared with the system [3], which uses the in-plane diffraction. We calculated spectral divergence of the components of the beam (angular chirp), spatial displacement of the spectral components (spatial chirp), and observed focal spots of the beam at the output of the compressors. We found out that the slight conical diffraction is not a serious limit as for the pulse stretching and compression of ultrashort optical pulses of duration approaching 10 fs. Optical aberrations may be even lower than in a comparable design using the in-plane diffraction.

Other important characteristics of the stretcher and the compressor are the power transmission of pulses and the transmission of their spectral bandwidth. We observed a high power transmission of 10-fs laser pulses, which was over 50 % in both the stretcher and compressor. The measured power transmissions are in a good agreement with calculated ones. Calculated values were obtained by a proper multiplication of the measured values of mirror reflectivity and diffraction efficiency, which were averaged over the whole spectrum of the pulse. The full pulse spectrum of 110 nm FWHM (over 210 nm in total) was well transmitted through both systems (transmittance > 98%). We did not observe a significant distortion of spectral shapes. We have not yet found in literature such a high power transmission of the double-pass pulse stretchers for such a short optical pulses. The higher transmission can improve performance of CPA systems and also leads to an easier beam diagnostics and manipulation.

Finally, we stretched ultrashort pulses, with duration of 10 fs and with a high power transmission of the pulse (>50%), to 360 ps. Stretched pulses were measured by 20 GHz sampling oscilloscope and fast photodiode. The pulsewidth of the detection response to an infinitely short (femtosecond) pulse is about 100 ps. Then we recompressed them back to 16 fs without a significant distortion of pulse spectrum. Compressed pulses were measured by use of interferometric autocorrelation.

References:

- [1] STRAKA, P. - ET AL.: *Proposed Upgrades of the Laser System PALS: From a Novel Solid-State Oscillator toward Petawatt*, Czech Journal of Physics, 2002, pp. 368-374.
- [2] ITATANI, J. - ET AL.: *Generation of 13-TW, 26-fs pulses in a Ti:sapphire laser*, Optical Communications, 1997, pp. 134-138.
- [3] CHERIAUX, G. - ET AL.: *Aberration free stretcher design for ultrashort pulse amplification*, Optics Letters, 1996, pp. 414-416.

This research has been supported by Czech Ministry of Education, Youth and Sports (project #LN00A100) and Czech Academy of Sciences (project #K2043105).

Transient Absorption of a Bichromophoric Molecule

M. Dvořák, J. Zerbs*, M. Michl, P. Wagener*, Z. Surovec**,
D. Pánek, J. Schroeder*, M. Nepraš**, V. Fidler

DvorakM@kml.fjfi.cvut.cz

CTU, Faculty of Nuclear Sciences and Physical Engineering, Dept. of Physical Electronics
V Holešovi kách 2, 180 00 Praha 8, Czech Republic

* Universität Göttingen, Institut für Physikalische Chemie, Tammannstr. 6, D-37077
Göttingen, Germany

** University of Pardubice, Faculty of Chemical Technology, Dept. of Organic Technology,
Studentská 95, 532 10 Pardubice, Czech Republic

Intramolecular electronic energy transfer in rigidly linked bichromophoric molecule 2-(3-benzanthronylamino)-4-(1-pyrenylamino)-6-chloro-1,3,5-triazine, (APyTCABa), and corresponding model compounds that closely mimic the photophysical properties of the donor and acceptor sub-units in the bichromophore, were studied.

Electronic energy transfer is a frequent relaxation mechanism of an excited multichromophoric system. It is important to study such process for both understanding of its physical mechanism and for possible application of it in molecular optoelectronics, light harvesting, polymer photophysics, dye laser operation or photochemical synthesis.

The molecule APyTCABa consists of the aminopyrene moiety acting as a donor, the aminobenzanthrone moiety acting as an acceptor and the triazine ring as a spacer. APyTCABa has absorption bands centered at 350 nm and 420 nm resulting from overlapped absorption bands of the donor and acceptor parts, respectively. Model donor APyTAn2 consists of the aminopyrene moiety and two aniline groups linked to triazine ring. Similarly, model acceptor ABaTAn2 consists of aminobenzanthrone moiety and two aniline groups linked to triazine.

Absorption and fluorescence spectra of APyTCABa, their comparison with spectra of model compounds, as well as some theoretical calculations indicate that the lowest electronically excited states are localized on the donor and the acceptor part of the bichromophoric molecule, respectively. After the excitation into the absorption band of the donor part at 350 nm, a fluorescence of the aminobenzanthrone type occurs only, which indicates that an electronic energy transfer happens. The previous fluorescence up-conversion experiments [1] showed that this process occurs on 200 fs timescale.

This contribution illustrates the dynamics of the above described multichromophoric system as seen by transient absorption measurement with 150 fs time-resolution.

An experimental setup based on a commercial Clark – MXR CPA – 2001 Ti:Sapphire laser with 150 fs FWHM pulse at 773 nm, average energy in pulse 880 μ J and 1kHz repetition rate was used. The laser beam was divided into two parts. One part was processed by two-stage NOPA (*Noncollinear Optical Parametric Amplifier*) which produces laser pulses in the range of 460 – 700 nm, as short as <30 fs (after compression) and average pulse energy 7 μ J. After frequency doubling, they were used as pump pulses tunable from 230 nm to 350 nm. The second part of the original laser beam was processed by TOPAS (*Travelling-wave Optical Parametric Amplifier of Superfluorescence* of the Light Conversion company). This device

allowed us to produce probe pulses in the range of 400 – 850 nm by utilizing corresponding set of nonlinear optical processes (SHG, SFG, FHG).

A synchronized chopper blocked every second pump pulse in order to eliminate the influence of eventual slow drifts of the instrumentation as well as of the background absorption. The pump and probe pulses were collinearly focused into the cell with sample. The measured signal was obtained as a difference between the absorbance of the sample after the excitation by the pump pulse and the absorbance without any previous excitation. This whole apparatus provided time resolution 150 fs approximately. All measurements described in this contribution were done in dioxane.

Transient absorption spectra of the model donor APyTAn2 after the excitation at 360 nm were measured in the range of 400 – 730 nm. The resulting spectra show one decreasing and one increasing band. Those could be assigned to a transition from the upper excited state, possibly of a similar character as La state in pure aminopyrene, to a lower state with Lb character. This process occurs on the time scale of a few tens of picoseconds.

Transient absorption spectra of the model acceptor ABaTAn2 after the excitation centered at 473 nm were measured in the range of 510 - 830 nm.

Bichromophoric molecule APyTCABa was excited by pump pulses at 360 nm and 473 nm, which should correspond to a direct excitation of the donor and the acceptor part, respectively. The molecule was probed by pulses in the range of 450 – 850 nm. Although the resulting transient absorption spectra had a similar character as transient spectra of the model acceptor, some differences between the spectra after donor and/or acceptor selective excitation, were observed. Detailed analysis of those differences will extend the knowledge about the energy transfer process.

Transient absorption bands of model donor and model acceptor are partially overlapping. This could complicate a direct observation of the energy transfer in the bichromophore.

[1] FIDLER, V., KAPUSTA, P., NEPRAŠ, M., SCHROEDER, J., RUBTSOV, I. V., YOSHIHARA, K.: *Femtosecond Fluorescence Anisotropy Kinetics as a Signature of Ultrafast Electronic Energy Transfer in Bichromophoric Molecules*. Z. Phys. Chem. **216** (2002) 589-603, München

This research has been supported by MŠMT grants No. MSM J04/98:210000022 and ME 559. Financial support by DFG/SFB 357/B7 and by Max-Planck-Institute of Biophysical Chemistry, Goettingen is gratefully acknowledged.

Laser Induced Fluorescence for Water Surface Pollution Detection

D. Koňářík, J. Blažej, I. Procházka

blazej@troja.fjfi.cvut.cz

Department of Physical Electronics, Faculty of Nuclear Sciences and Physical Engineering,
Czech Technical University, Břehová 7, 115 19 Prague 1, Czech Republic

Our work is focused on detecting of pollution on water surface. For this purpose it uses Laser Induced Fluorescence (LIF) technique. The main advantages of this approach are remote detection due to LIF principle and greater sensitivity in compare with absorption measurements due to inherently lower background. There is no need to have any contact with surface and the measurements can be done for example from the plane and the maps of pollution can be created and dynamically updated. This technique we want to use for detection various pollutants like oil products, detergents, industrial pollution, algae and other organisms. All pollutants concentrated on surface are for this approach more perspective in compare with dissipated in whole volume. Our goal is also usage of 2nd or 3rd harmonic frequency of Nd:YAG not for some special absorption properties but for their technology state, compactness, robustness, and price.

The principle of laser induced fluorescence can be described as following. With laser radiation the atoms or molecules are excited. Laser pulse must have 30 ns duration or shorter¹, this pulse is in matter absorbed and higher energy state is achieved. Than this energy can be lost with various principles but for us is important incoherent spontaneous emission. The atom or molecule can hold this excited state for some time and than it spontaneously emit light with wavelength spectrum dependent on its inner energy states. The frequency is than $f = (\text{energy of higher state} - \text{lower state}) / h$, where h is Planck constant. The frequency of emitted light is lower than of incident light because part of absorbed energy can be transferred into non-radiative transitions. This emitted light has for various materials different temporal and wavelength spectra. These spectra are then used to determine the pollutant. The light dissipated can be detect far from the water surface also near the detector. So we can get lidar like configuration and make remote sensing without any contact with water surface. The energy balance of described experiment is defined by lidar equation²:

$$N_{PE_{REC}} = \left\{ \frac{E_{LAS}}{h\nu} \right\} \cdot \left\{ T_A^2 \right\} \cdot \left\{ \eta_s \right\} \cdot \left\{ \frac{r_{REC}^2}{4R^2} \right\} \cdot \left\{ \eta_{REC} \cdot T_{REC_{OPT}} \right\} \quad (\text{eq. 1})$$

where $N_{PE_{REC}}$ – number of received photoelectrons, $E_{LAS}/h\nu$ – original number of photons emitted by the laser, T_A – transmittance of the atmosphere between surface and detector, η_s – the overall scattering efficiency, including fluorescence efficiency, r_{REC} – radius of circular receiver, R – range, η_{REC} – the receiver efficiency, $T_{REC_{OPT}}$ – transmission of the receiver optics. The availability of the solid state photon counter³ is opening a full spectrum of new possibilities in these type measurements. Obviously, the photon counting enables to register the ultimately weak optical signals, but this is just one of many features. The photon counting principle permits to measure light intensities with high precision and stability. The quantum nature of the light on one hand and the capability to count the number of the light quanta on the other hand enable to measure the analog value – light intensity by a purely digital way.

The analog to digital conversion is carried out by the quantum nature of the light and the detection principle. The absence of analog signal processing: amplification, discrimination and conversion results in extreme measurement stability, linearity, reproducibility etc.

The system can be mounted for example on the plane and when with pollution measurement is also recorded the position of measurement we can easily create the map of pollution. This can be useful and is already used for oil monitoring on seas, but we want to monitor more different types of pollutants and extend the places and application areas where this method can be used.

References:

- [1] DEMTRODER, W., *Laser Spectroscopy: Basic Concepts and Instrumentation*, 3rd Edition, Springer Verlag, 1995.
- [2] HARSDORF, S. - REUTER, R., Laser remote sensing in highly turbid waters: validity of the lidar equation, In *Environmental Sensing and Applications*, edited by Michel Carleer, et al., SPIE, Proc. SPIE Vol. 3821, 1999, pp. 369-277.
- [3] PROCHAZKA, I., HAMAL, K., BLAZEJ, J., KIRCHNER, G., KOIDL, F., Extended Dynamical Range Solid State Photon Counter, In *Photodetectors: Materials and Devices III*, ed. Gail J. Brown, Proc. SPIE Vol. 3287, Apr. 1998, pp. 336-340.

This research has been supported by research framework MSM 210000022.

Low Background Spectrometer TGV II for Measurement of Double Beta Decay of Cd106 and Ca48

P. Čermák, I. Štekl
(for TGV collaboration)

pavel.cermak@utef.cvut.cz

IEAP CTU,
Horská 3a/22, 12800 Prague 2, Czech Republic

The TGV (Telescope Germanium Vertical) project is devoted to the study of double-beta decay processes of ^{106}Cd and ^{48}Ca .

TGV I apparatus [1] (16 HPGe detectors each with diameter 40mm) aimed at the investigation of double-beta decay of ^{48}Ca . Even though the very small natural abundance (0.187%) of ^{48}Ca complicates the production of radioactive sources in sufficient quantities, the large energy of reaction available ($Q_{\beta\beta}=4272$ keV) makes this nucleus suitable for the study of such very rare processes. The total mass of ^{48}Ca inserted into the TGV I detector was 1.08g (1.35×10^{22} atoms). This project was terminated in 2000 and yielding the half-life of the two-neutrino double-beta decay mode of ^{48}Ca ($T_{1/2}(2\nu\beta\beta) = (4.2^{+3.3}_{-1.3}) \times 10^{19}$) years and an estimate on the limit of the half-life of the neutrino-less double-beta decay mode of ^{48}Ca ($T_{1/2}(0\nu\beta\beta) > 1.5 \times 10^{21}$) years [2].

Since 2001 the spectrometer TGV II has been under construction. The main aim of the project is an improvement over the results on ^{48}Ca obtained by TGV I and especially an investigation of double-beta decay processes in ^{106}Cd (with emphasis on EC/EC channel). The EC/EC channel is the most favorable among the $\beta^+\beta^+$ processes due to the largest energy of reaction ($Q_{\text{EC/EC}} = 2778\text{keV}$). Spectrometer TGV II consists of 32 HPGe planar detectors mounted one over another in one common cryostat. The active area of the detector is of diameter 51mm and of thickness 6mm. The radioactive source in the form of a thin foil is inserted between neighbouring detectors. As the TGV II spectrometer is primarily designed to investigate very rare effects, several methods to minimize possible background are used. The cryostat itself is surrounded by passive shielding made of copper and lead. The cryostat and the copper shielding are enclosed in an airtight box against external radon gas contamination. Anti-neutron shielding (16cm thick) made of boron doped polyethylene is used. The experimental facility is located in Modane Underground Laboratory in France (4800 m.w.e.). The data acquisition program runs on Real-Time Linux system. This configuration is stable and allows to operate and control the electronics remotely. Experimental data are recorded event-by-event and processed offline. During data processing only double coincidence signals from neighbouring detectors are treated as candidate events for double-beta decay. Two different electronic setups were constructed for measurements with the TGV II spectrometer. In the case of ^{48}Ca two electrons emitted in double-beta decay are detected. The energy region of interest extends from 2.7MeV (due to the end-point of natural background, 2614.5keV) to 4.2MeV ($Q_{\beta\beta}$). An additional technique for background suppression based on pulse shape analysis is used for the ^{48}Ca measurement. This method (combined with the coincidence technique) allows to suppress background due to gamma events by a factor of 4-9 [3]. The measurement with ^{106}Cd consists in the detection of two X-rays (having energies from 21keV to 24keV) accompanying double-electron capture. In such a low-energy region the most important source of background is microphonic and electronic noise. To suppress such noise, a technique utilizing two spectrometry amplifiers with different shaping times (e.g. 4 μs and 12 μs) is used [4].

The basic run for background determination (for Cd setup) was performed in the period December 03 – February 04 (total time of measurement was 1363 hours, 14312946 events, no radioactive sources). The background level was very low (~231 events/year) in the energy region of our interest. Then, radioactive sources ($13 \times$ enriched ^{106}Cd , $3 \times$ natural Cd) were inserted into the cryostat. The data obtained from the measurement during the following run (March 04 – May 04, 1768 hours, 16531047 events) showed that the radioactive sources contain impurities which give a continuous beta spectrum with the end point at about 600 keV. Consequently, the Cd sources were changed ($12 \times$ enriched ^{106}Cd , $4 \times$ natural Cd) and another experimental data were taken (June 04 – October 04, 2033 hours, 158382662 events). The second measurement confirmed again presence of impurities giving a continuous beta spectrum. Finally the sources made of natural Cd were put into the TGV II detector ($16 \times$ natural Cd). Data taking was started in November 04 and is still in progress. In the near future the data obtained with natural Cd sources will be processed and enriched ^{106}Cd sources will be purified. Preliminary processing of Cd data gives limit on $T_{1/2}(2\nu\text{EC}/\text{EC}, \text{g.s.} \rightarrow \text{g.s.})$ at the level of $10^{17} - 10^{18}$ years. The measurement will continue in the next two years (2005 – 2006). During this period a long term measurement with ^{48}Ca sources is also planned.

References:

- [1] BRIANCON, CH. – BRUDANIN, V.B. – EGOROV, V.G. – JANOUT, Z. – KONÍČEK, J. – KOVALENKO, V.E. – KUBAŠTA, J. – POSPÍŠIL, S. – REVENKO, A.V. – RUKHADZE, N.I. – SALAMATIN, A.V. – SANDUKOVSKY, V.G. – ŠTEKL, I. – TIMKIN, V.V. – TSUPKO-SITNIKOV, V.V. – VOROBEL, V. – VYLOV, TS.: *The high sensitivity double beta spectrometer TGV*, Nucl. Instr. Meth. Phys. Res. A 372, 1996, pp. 222–228.
- [2] BRUDANIN, V.B. – RUKHADZE, N.I. – BRIANCON, CH. – EGOROV, V.G. – KOVALENKO, V.E. – KOVALÍK, A. – SALAMATIN, A.V. – ŠTEKL, I. – TSUPKO-SITNIKOV, V.V. – VYLOV, TS. – ČERMÁK, P.: *Search for double beta decay of ^{48}Ca in the TGV experiment*, Physics Letters B 495, 2000, pp. 63–68.
- [3] ČERMÁK, P. – ŠTEKL, I. – BENEŠ, P.: *Distinguishing between electrons and γ rays in experiment TGV using a pulse rise time*, Czech. J. Phys., vol 52, 2002, pp. 583–587.
- [4] MORALES, J. – GARCIA, E. – ORTIZ DE SOLORZANO, A. – MORALES, A. – NUÑEZ-LAGOS, R. – PUIMEDON, J. – SAENZ, C. – VILLAR, J.A.: *Filtering microphonics in dark matter germanium experiments*, Nucl. Instr. Meth. Phys. Res. A 321, 1992, pp. 410–414.

This research has been supported by GA ČR grant No. 202/02/0157.

Experimental System for Plasma Surface Modification

L. Aubrecht

aubrecht@fel.cvut.cz

Department of Physics, Faculty of Electrical Engineering, Czech Technical University,
Technická 2, 166 27 Prague 6, Czech Republic

This paper deals with phenomena observed during the study of plasma modification of polymer surfaces – effects of atmospheric pressure discharge treatment on surfaces and influence of these phenomena on the physical properties of these surfaces.

In our experiments polymer surfaces by a high-energy barrier discharge and UV radiation were treated. For experiments there were chosen the following materials: polyethyleneterephthalate (PET), polypropylene (PP) and polytetrafluoroethylene (PTFE).

After several experiments the standard and optimal shape of studied samples was found. The laboratory sample is a cut square polymer film with a 15 - 20 mm side, strongly attached to the glass platform with a 600x600 mm side size and 1.5 mm thickness by glue. Polymer and glass platform previously were cleaned with acetone without evaporation residue. Different types of glue were studied, but in light of glue sort uninfluenced to experimental part and measuring the epoxy adhesive generally were used like more preferred glue. The necessity of excellent attaching is required for homogeneous modification and possible subsequent measurements at Atomic Force Microscopy (AFM) and Water Contact Angle Measurement (WCA) setups.

At 50 Hz voltage the average current density is low (in time and in space) and modification rate is low too. Low frequency of applied voltage creates many independent discharge channels and parameters of the discharge are little different. On this device the series of experimental samples were performed.

For the UV treatment of polymer films we used the following setup: the closed glass tube in shape of rectangle with 400x125 mm side sizes and 30 mm diameter was pumped to high vacuum and then filled with Kr (50 Pa) and Hg (1 Pa) and RF low-pressure discharge can be excited. The ultra violet setup works on Hg-lines 253.7 and 185 nm. Power source frequency is 250 kHz. Electrical power directed to the plasma is about 180 W. All UV radiation torch with polymer sample were put inside the glass box and covered by aluminum foil. Distance between treated polymer sample and tube was about 30 – 50 mm.

PP polymer foils [1] were treated in described dielectric barrier discharge setup with two glass barriers with depends on the time of treatment. Investigations show that a small time (several seconds) is enough to observe changes at the sample surface. The modification processes don't change the transparency of polymer film.

Water contact angle measurements of PET films [2] treated in plasma as compared with reference non-treated sample were performed and the AFM scanned images that show the dielectric barrier treatment of PET and PTFE films in artificial air and in argon were obtained. Pure PTFE and PTFE with a graphite inclusions samples after barrier discharge treatment also were studied on contact angle measurements setup. Wettability of mentioned polymer samples distinctly rises. Decreasing contact angle from 90° to 40° was found. However, this modification disappears at pure PTFE after treatment its surface by acetone. The similar process takes place with a composite of PTFE and carbon. Visual effects of plasma treatment are similar in both cases, for PET and PTFE polymers. The surface after modification acquires high roughness. In case of PET film the characteristic artifacts are in

the form of bubbles appeared on the smooth PET surface after the plasma treatment. It is possible that barrier discharge disrupts the chemical bonds on polymer surface.

Samples of PTFE and PTFE-graphite foils with a very rough surface were modified by UV radiation. Strong shaggy surface prevent from AFM measurements. Only rough WCA measurements were performed. Samples of PTFE with a little modification time, about several decade minutes, don't display significant changes. In case of long-time UV treatment, about one month, polymer sample of PTFE was absolutely destroyed at surface region and in the bulk as well. That demonstrates inapplicability UV modification methods to such materials.

In case of PET foils the structure and surface changes present after ultra-violet treatment. PET sample was treated by UV radiation during two days. WCA measurements point the strongly changes in polymer wettability properties. In addition the opposite polymer foil side also changes surface energy. Organic polymers such as polyethylene, polypropylene and polystyrene are difficult to wet, or "hydrophobic". This makes very difficult to apply them for paintings, printing inks and other surface coatings. Conventional approaches to modify polymer surface properties have included plasmas, corona discharge, flame treatment and wet chemical treatments. A more recent approach is using ultraviolet radiation of the polymer surface. This approach reduces the damage to the bulk polymer and can be applied to materials of complex shape, using conventional treatment chambers.

Chemical changes induced by UV exposure are the result of a complex set of processes involving the combined effect of UV and oxygen. Bond dissociation is initiated by the absorption of UV radiation, resulting in chain scission and/or cross-linking; subsequent reactions with oxygen result in the formation of functional groups such as carbonyl (C=O), carboxyl (COOH), or peroxide (O-O). The effects of UV exposure, or photo degradation, are usually confined to the top few microns of the surface. However, in some cases, degradation at the surface of a polymeric component has been shown to affect mechanical properties disproportionately, as flaws that result from surface photodegradation can serve as stress concentrators and initiate fracture at stress levels much lower than those for unexposed specimens. The effect of ultraviolet radiation is also compounded by the action of temperature, moisture, wind-borne abrasives, freeze-thaw and other environmental components.

References:

- [1] S. MEINERS, J.G.H. SHINE, E. PRINZ, F. FÖRSTER: *Surface Modification of Polymer Materials by Transient Gas at Atmospheric Pressure*, Surface and Coating Technology 98, 1998, pp. 1121-1127.
- [2] S. ISHIKAWA, K. YUKIMURA, K. MATSUNAGA, T. MARUYAMA: *The Surface Modification of Poly(tetrafluorethylene) Film Using Dielectric Barrier Discharge of Intermittent Pulse Voltage*, Surface and Coating Technology 130, 2000, pp. 52-56.

This research has been supported by grant COST 527.120.

Secondary Sound Field Around Cylindrical Obstacle

I. Bláhová, O. Jiříček, J. Zendulka, M. Brothánek

blahova@fel.cvut.cz

Department of Physics, Faculty of Electrical Engineering, Czech Technical University,
Technická 2, 166 27 Prague 6, Czech Republic

Secondary sound field is created around an obstacle when incidental wave is scattered and diffracted on the obstacle. Having the description of such a secondary sound field is important from technical point of view. For example measuring microphone, which has a cylindrical shape, affects an acoustical field that is measured. Because of this affection we can, for example, consider correction coefficients which can correct a value measured. We would like to propose different possibilities to obtain a description of secondary sound field around a cylindrical obstacle and prepare them for future usage.

We would like to briefly introduce the analytical solution of the scattering of a sound wave on a cylindrical obstacle. The incidental plane should be expressed in terms of cylindrical waves. During the solution of the wave equation the expression for acoustical pressure should be expressed as the multiplication of two parts; where the first part is a function of a radius only and the second part is a function of an angle only. After that the partial differential equation is separated into two parts where each of them is solved apart.

Solution can be expressed as a linear combination of Bessel and Neumann functions or as a linear combination of Hankel functions of the first and second type. The first type describes the wave spreading from infinity to the source and the second type describes the wave spreading from the source to the infinity. The last task is to find coefficients for members of series. For figuring out of these coefficients the boundary conditions are needed. The convergence of the scattered sound wave is required. The analytical solution exists for a few simple symmetrical bodies only.

For the majority of bodies the analytical description of a secondary sound field does not exist but a satisfied description can be obtained by mathematical modeling. For example program OPENBEM [2] prepared for MATLAB provides numerical modeling of a secondary sound field. This program is based on boundary element method. A very precise net of the surface of an obstacle should be prepared before. An accuracy of the obstacle definition and a proper selection of net elements influence an accuracy of the numerical model of a secondary sound field a lot.

The other possibility to obtain a description of a secondary sound field is a measurement. Measurement is still very important, for example, for a verification of models based on computation. Disadvantage of the description of a secondary sound field based on experimental results is the necessity to do hundreds or thousands of measurements. It is very time-consuming. We would like to be precise (affect the sound field measured less as possible) so we can not use more than one measuring microphone; it means that value in one single point corresponds to one measurement.

Mathematical modeling of complex bodies can be very complicated with respect to their shape and verification of results obtained is helpful. Mathematical models give us more information about a secondary sound field than measurement but sometimes we do not know if these models are correct. Because of that a measurement is still needed. It is not necessary and also it is not possible to compare mathematical model with measurement in every single point, but we have to choose some area where comparison can help us.

References:

- [1] BLÁHOVÁ, I., JIŘÍČEK, O.: *Experimental Method for Measuring Secondary Sound Field for Sphere and Its Comparison with Analytical Results*, Proceedings of ICA 2004, Kyoto, 2004.
- [2] JUHL, P. M.: *The Boundary Element Method for Sound Field Calculations*, The acoustics laboratory, Technical university of Denmark, 1993.
- [3] MORSE, P.M.: *Vibration and Sound*, ASA, USA, 1995.
- [4] REJLEK, J.: *Numerical Modelling of Sound Diffraction by Boundary Element Method*, Diploma Theses, CTU, Prague, 2004.

This research has been supported by GA ČR grant No. GP 202/03/P008.

Influence of Pleasantness on the General Impression of Tested Sounds

R. Jurč, O. Jiříček

`jurcr1@fel.cvut.cz`

Department of Physics, Faculty of Electrical Engineering, Czech Technical University, Technická 2, 166 27 Prague 6, Czech Republic

Many factors (e.g. sound, colour, appearance of product etc.) influence the overall quality of a certain product. Sound quality, as a highly important component of the overall quality, is related to human perceptual reaction to the sound of a product. As the discipline of psychoacoustic investigates the human sense of sound, a knowledge of psychoacoustic results can help research the sound quality of product.

Methods of evaluating sound quality can be divided into two parts – *objective* and *subjective* methods, both of which have their own advantages and disadvantages. The main advantage of the objective methods is the reduction of evaluation time, as they are independent of variation in human perception. However, the sound of each evaluated product is specific and this specificity is not accurately reflected by objective methods, in which event subjective methods can present a better solution.

The advantages and disadvantages of both types of methods, similar to the problem of the product specificity, are described in many papers from important acoustic conferences across the world; some findings of which were used in the research of the present authors.

Several subjective tests were performed in previous research. In these subjective tests, the sounds of several devices (vacuum cleaners, computer fans and hair dryers) were investigated, the results of which were presented in several papers (viz. [1] – [4]). In the tests, the auditory characteristics of sounds were evaluated by human subjects. For each tested device, six characteristics were selected that best describe these evaluated devices. The sounds were then presented to human subjects, who listened and then evaluated these sounds. However, why did the human subjects evaluate only sounds? Several reasons are true:

- The reduction of evaluation time.
- Assuring the same test conditions for all human subjects.
- The easier preparing of tests.
- Eliminating the influence of visual information on the aural perception of the evaluated products.
- Providing evaluations by human subjects of the same sounds, which were then analyzed in following research.

Two auditory characteristics, *pleasantness* and *general impression*, were common for each evaluated devices. Therefore, the influence of pleasantness on the general impression of tested sounds is investigated in this paper. First, the psychoacoustic metrics were calculated, (loudness, roughness and sharpness), which represent the objective methods. The metrics were compared with the results of the subjective tests, especially the characteristics *pleasantness* and *general impression*.

This comparison indicates that psychoacoustics metrics are unlikely to influence the evaluated characteristics of the sounds of the tested devices. The hypothesis that loudness has the same and significant influence at the sense of *pleasantness* for each tested product was not confirmed. Loudness, in fact, has significant influence only in evaluation of vacuum cleaners,

but is insignificant in evaluation of computer fans and hair dryers (see [1]). The influence of other psychoacoustic metrics on human evaluation is also presented in paper [1].

The aim of this contribution is to investigate the dependence between the sense of *pleasantness* and the sense of *general impression* for the evaluated sounds. The results of subjective tests show that the sense of *pleasantness* is closely connected with the sense of *general impression* (the correlation coefficients between evaluated characteristics reaching the highest value – see [1]). It is necessary to say that the sense of *pleasantness* has similar auditory features to the sense *general impression*. Moreover, the sound of a product supplies important information - for example, sound informs the customers if a device is functioning correctly. This informational feature of the evaluated sounds is related to human perception of the *general impression*. Therefore, the test results show the difference between the evaluation of the *pleasantness* and the evaluation of the *general impression*.

These two previous characteristics were compared with such characteristics as greatly influence the previous two characteristics. The evaluation of the sense of sound *familiarity* was compared with the previous characteristics in the test of vacuum cleaners and computer fans. Specifically, the influence of the sense *familiarity* on the sense *general impression* is greater than that of *pleasantness* in the evaluation of the sound of computer fans. The sense of the *familiarity* is related to the information factors of the sound.

Why are the sense of the *pleasantness* and the sense of the *general impression* so similar? The one reason is that the visual factor (e.g. the proportions, appearance, colour of evaluated devices etc.) was absent in the subjective tests, and was not reflected in the human evaluation. As a consequence, *pleasantness* and *general impression* are very dependent on these subjective tests. If human subjects had the visual information, than the sense of the *general impression* would be connected with the overall quality of tested products, nor would *pleasantness* would not so related to the *general impression*.

In this research, the products' sound quality is investigated. Therefore, the visual information must be absent and in addition, the same test conditions must be assured for all human subjects. If these two conditions are fulfilled, the evaluated sounds will be analysed further in upcoming research. In the next stage, the sound quality of several products will be investigated. The aim of the next research will be an investigation of the dependence between subjective methods and objective methods.

References:

- [1] JURČ, R. - JIŘÍČEK, O.: *Psychoacoustic and Objective Testing of Product Sound* Proceedings of Inter-Noise 2004 Prague, Czech Acoustic Society, 2004,
- [2] JURČ, R. - JIŘÍČEK, O.: *Subjektívne testovanie zvukov počítačov* 67. Akustický seminár, Česká akustická společnost, 2003, s7 – 14.
- [3] JURČ, R.: *Porovnanie výsledkov psychoakustických testovaní zvukov vysávačov* Audio Technologies and Processing ATP 2004, VUT v Brně, FEKT, 2004, s. 64-69.
- [4] JURČ, R.: *Testing of loudness produced by compute fan* Poster 2003. Prague: CTU, Faculty of Electrical Engineering , 2003, s. NS7.

This research work has been supported by research program No. J04/98:212300016 "Pollution Control and Monitoring of the Environment".

The Automatic Data Acquisition System for Calibrations with Remote Access

V. Vacek, M. Dione, M. Galuška, M. Doubrava

vacek@fsid.cvut.cz

CTU, Faculty of Mechanical Engineering, Department of Applied Physics,
Technická 4, 16607 Praha 6

The goal of this project was a study and development of an automated data acquisition system for laboratory measurements, namely for calibration measurements of temperature and pressure sensors.

The Department of Applied Physics is cooperating on the development of the cooling system for the ATLAS Inner Detector to be installed in the new LHC particle accelerator at CERN, Geneva. This cooperation naturally led to frequent use of various temperature and pressure sensors, the characteristics of which had to be known for precise measurements. Especially in the case of temperature sensors, the feasibility to perform precise calibrations of them was analyzed.

Previous studies performed at the Department of Applied Physics have shown that, by performing a supplementary calibration on an appropriate calibration set-up, the measuring accuracy of a sensor can be increased in comparison to the accuracy given by the manufacturer. This calibration, however, involving a series of measurements at various conditions (temperatures / pressures), is very time-consuming and difficult to conduct manually – a typical temperature sensor calibration from $-20\text{ }^{\circ}\text{C}$ to $+50\text{ }^{\circ}\text{C}$, the temperature range needed for the CERN cooling system, at a $2\text{ }^{\circ}\text{C}$ step increment can take over 8 hours. To ensure precision and quality of the calibration measurements, an automated procedure became necessary.

The presented system was developed using National Instruments LabVIEW software, communicating over the GPIB (IEEE 488) interface with electronic multimeters Keithley 2000 and Keithley 195A. These multimeters serve for reading the sensors being calibrated and an appropriate referential sensor. Additionally, the system communicates with an appropriate device that regulates the input conditions – pressure or temperature. In case of the temperature calibration set-up, this was the ASL Metal Block Calibrator B140, modified for computer control and liquid bath measurements, connected by a serial port to the PC with the LabVIEW data acquisition system. For the pressure sensor calibration set-up, an electronic pressure regulator would be ideal, but because pressure changes stabilize a lot quicker than temperature changes, pressure regulation is performed manually.

The developed system does not only perform data acquisition, but also its analysis. The portion of the calibration process that is most time consuming is waiting until a new input condition is stable. In the case of pressure, this takes only a few seconds, but the stabilization of a new temperature within the ASL Calibrator takes as much as 15 minutes. The Automated DAQ System continuously reads the reference sensor and monitors how its measurement changes with time. A stability criterion can be set by the user (in the form of selecting the maximum allowable deviation of several consecutive measurements), and only once this criterion is reached, several readings of the sensors to be calibrated are made. The measured values, along with the value of the reference sensor and the time of the

measurement are stored in a data file that can be easily manipulated within common software such as MS Excel.

The only procedure required from the user is the physical preparation of the sensors in the test set-up and configuration of the calibration in the Automated DAQ System LabVIEW interface. After this, there is no need for the user's presence until the end of the calibration. Nevertheless, supervision of the process is sometimes needed or wanted. Using the integrated LabVIEW web-server, remote access to the DAQ System interface was prepared, and allows monitoring or control of the running calibration process from anywhere in the world via the internet and a common web-browser.

The Automated DAQ System allows instantaneous sharing of measured data (for example between the laboratories of the CTU Department and CERN), monitoring long-duration high-precision calibrations that can run for several days from the comfort of home or office, and acquires data of precision never before reached in the standard laboratory environment. As an example of common results, DIN class B temperature sensors with manufacturer-stated precision greater than ± 0.3 °C were calibrated to a precision of ± 0.1 °C.

References:

- [1] VACEK, V. - VINŠ, V. - NOVÁK, R.: *An Upgrade of the Calibration Setups for the DAQ Systems* Proceedings of the Workshop 2003, CTU Reports, Special Issue, Part B February 2003 Prague, pp. 420-442.
- [2] VACEK, V. - VINŠ, V.- DOUBRAVA, M - GALUŠKA, M.: *DAQ and DCS sensors database, Capillary studies and Thermophysical property Database for the C.S. applications at SRI Bldg.* Pixel Mechanics Meeting at CERN, Geneva February 2003, pp. 12 .
- [3] 6. BÍLA, J. - NOVÁK, R. - VACEK, V.: *DAQ Systems Using the Different Platforms for Mechanical Engineering Applications* Workshop 2004 [CD-ROM]. Prague: CTU, 2004 March 2004, pp. 678-679 , ISBN 80-01-02945-X
- [4] VACEK, V. - NOVÁK, R. -BÍLA J.: *Moderní přístrojová technika v inženýrské praxi (in Czech)* CTU Prague, Faculty of Mechanical Engineering, November 2003, pp. 8.

This research has been supported by Grant No.: FRVŠ 1974 - G1.

Radon Trapping Factory for Low Background Experiments

I. Štekl* (for NEMO collaboration),
P. Jeanneret**, J.L. Vuilleumier**, K. Ciahotný***

ivan.stekl@utef.cvut.cz

*Institute of Experimental and Applied Physics, CTU in Prague, Prague, Czech Republic

**University of Neuchâtel, Rue A.L.Breguet 1, CH-2000 Neuchâtel, France

***Institute of Chemical Technology, Technická 5, 166 28 Prague 6, Czech Republic

Neutrinoless double beta decay ($0\nu\beta\beta$) is a problem of great interest in particle physics. One of the most promising experiments is NEMO-3 [1]. It is devoted to the study of double beta decay of different nuclei with the primary objective to look for the $0\nu\beta\beta$ decay of ^{100}Mo . $0\nu\beta\beta$ decay is a very rare process and therefore special attention is devoted to background suppression. The important part of the background inside the NEMO-3 detector is caused by radon [2]. Similar difficulties were faced also by other underground experiments such as Super-Kamiokande detector. In the framework of this experiment the air purification system [3] has been developed. Typical radon concentration in the radon-reduced air is $2\text{--}3\text{ mBq/m}^3$ [3]. Also big attention has been devoted to the purification of gaseous nitrogen from ^{222}Rn [4]. Such system is important for Ge spectrometers operated deep underground. The purification principle is based on the radon adsorption on charcoal at low temperatures (liquid nitrogen). The lowest concentration at the purified nitrogen output achieved was $12\pm 3\text{ }\mu\text{Bq/m}^3$ with the gas flow rate between $0.3\text{--}2.5\text{ m}^3/\text{h}$. The activity of radon in the air of Fréjus underground laboratory is at the level of 15Bq/m^3 . The first step to avoid this radon level in the NEMO-3 detector was to install a airtight tent surrounding the detector (May 2004). To suppress radon further it was decided to build a radon trapping factory providing a continuous flow of air into the NEMO-3 airtight tent. The detailed technical solution of radon trapping factory based on Super-Kamiokande proposal has been performed by the NEMO collaboration. The anti-radon factory was produced in company ATEKO (Czech Republic). At the beginning of October 2004 the system for air purification was installed in the Fréjus underground laboratory by ATEKO team. Radon trapping setup consists mainly of compressor, drier (dew point -70°C), cooling unit (output air temperature $\sim -50^\circ\text{C}$) and two charcoal tanks with 475 kg of charcoal each. Setup is constructed to give $150\text{ m}^3/\text{h}$ of purified air for the purpose of detectors installed in Fréjus underground laboratory. The principle of radon trapping factory is based on radon trapping by cooled charcoal, when trapped radon decays in charcoal. Retention time T (in hours) of radon inside charcoal is given by equation $T = K*(m/f)$, where K (m^3/kg) depends on charcoal type, temperature and pressure; m (kg) is mass of charcoal and f (m^3/hour) is flux of gas. Coefficient K highly changes with temperature ($K = 4$ for $T = 20^\circ\text{C}$; $K = 78$ for $T = -40^\circ\text{C}$; $K = 152$ for $T = -50^\circ\text{C}$) and type of charcoal. Charcoal type K48 made of coconut shells was selected as the best for our purpose ($K = 141$ for $T = -40^\circ\text{C}$). The anti-radon setup is operating fully from the beginning of October 2004. The level of radon in the output air from radon trapping factory is about mBq/m^3 . At present, the factory gives $125\text{ m}^3/\text{h}$ of purified air. The level of radon is measured at several locations (output of the anti-radon factory, upper part of the NEMO tent) using different experimental techniques (Ge detector, electrostatic collection on Si detector). The radon detector based on electrostatic collection on PIN photodiode could reach the radon level $\sim 1\text{ mBq/m}^3$. Such radon level

corresponds to 1.5 count/day registered in PIN photodiode. The Table 1 gives the radon concentration in the upper part of the NEMO tent from 26 of November to 15 of December. During this period some tests and maintenance of anti-radon setup were performed. The first test consisted in the removing of the mylar tightening at the top of the NEMO tent (from 28 of November to 30 of November). One can see (Table 1) gradual increasing of radon level inside the NEMO tent. The second test was carried out with the output of air flow from the lower part of the NEMO tent (December, 2). The lower part of the NEMO tent contains all electronics of the NEMO-3 detector. Output of air from lower part was re-routed out of the tent and not to the upper part of the NEMO tent as before. The level of radon in the upper part of the NEMO tent was decreasing gradually and it reached the lowest level 0.2-0.3 Bq/m³ (see Table 1). On Monday, December 6, the upper part of the NEMO tent has been opened to insert calibration sources into the NEMO-3 detector. During the period from December 7 to December 15 the anti-radon factory was stopped for maintenance. On Table 1 you can see substantial increase of radon level.

Date of measurements	Rn activity [Bq/m ³]							
26.11.2004	0,89	1,03	1,16	1,23	1,37	1,37	1,54	1,46
27.11.2004	1,49	1,38	1,23	1,36	1,61	1,67	1,66	2,08
28.11.2004	2,15	2,82	3,24	3,97	4,06	4,36	4,53	5,34
29.11.2004	5,34	4,95	5,59	5,73	6,58	7,63	8,37	8,58
30.11.2004	5,91	1,85	1,31	1,21	1,61	1,56	2,38	2,18
1.12.2004	1,90	2,01	2,08	1,96	1,91	2,11	2,35	2,18
2.12.2004	2,15	1,62	0,64	0,35	0,39	0,37	0,27	0,37
3.12.2004	0,25	0,29	0,19	0,28	0,28	0,23	0,29	0,33
4.12.2004	0,38	0,32	0,22	0,31	0,21	0,38	0,35	0,21
5.12.2004	0,19	0,22	0,33	0,32	0,28	0,28	0,25	0,16
6.12.2004	0,28	3,88	4,39	0,62	0,30	0,25	0,26	0,43
7.12.2004	5,63	12,53	14,60	14,61	15,41	15,33	17,44	17,13
8.12.2004	15,38	16,99	19,48	17,45	17,02	17,78	20,68	18,25
9.12.2004	14,75	13,89	13,09	13,71	13,91	16,32	18,19	16,18
10.12.2004	12,22	11,49	11,98	12,58	13,02	14,00	14,37	14,96
11.12.2004	12,94	13,85	13,45	16,63	15,29	13,78	14,05	17,18
12.12.2004	19,08	18,73	18,34	19,58	19,28	17,71	18,38	16,10
13.12.2004	16,21	15,68	18,18	16,73	17,97	15,68	15,68	16,19
14.12.2004	15,33	14,84	14,73	15,34	16,40	20,20	20,19	17,21
15.12.2004	5,72	1,22	0,38	0,34	0,28	0,24	0,33	0,33

Table 1. Rn activities in the upper part of the NEMO airtight tent.

References:

- [1] NEMO COLLABORATION: *Nemo-3 Proposal*, LAL preprint 94-29, 1994.
- [2] MARGUET CH. ET AL., Nucl. Phys. B 87, 2000, p. 298.
- [3] TAKEUCHI Y. ET AL., Phys. Let. B 452, 1999, pp. 418-424.
- [4] WOJCIK M. - ZUZEL G., accepted to Nucl Instr. Meth. in Phys. Research A.

This research has been supported by GA ĀR grant No. 202/02/0157.

Study of the flow through capillary-tube

V. Vinš, V. Vacek,

vacek@fsid.cvut.cz ; vaclav.vins@cern.ch

CTU, Faculty of Mechanical Engineering, Department of Applied Physics

Technická 4, 16607 Praha 6

Small diameter (around $0,5 \div 1,5$ mm) capillary tubes are widely used for liquid coolant pressure reduction from high pressure in the condenser to the low pressure of evaporation. Capillary-tube expansion devices are used in refrigeration equipment, especially in small units such as household refrigerators, freezers or room air conditioners.

The Department of Applied Physics has been participating in the design of cooling systems and subsequent measurements on prototypes of Pixel and SCT detectors at the international nuclear research center CERN for several past years. In most cases of these special designed cooling circuits, the combination of the capillary-tube and pressure reduction valve is used. Fluoroinert refrigerants, with chemical structures $C_n F_{(2n+2)}$, were mostly considered according to the specific needs of the cooling systems.

The main goals of our research are the study of all important capillary-tube parameters (inner diameter, length, wall roughness) and theoretical simulations of the flow through a capillary-tube, based mainly on numerical algorithms.

The test stand for measurements of one phase flow through a capillary-tube has been used for experimental determination of the pressure drop along different capillaries. Several methods for the flow friction factor prediction (Coolebrook's, Haaland's, Churchill's eq.) were put into account to get the optimal value of the capillary-tube wall roughness. The short evaluating algorithm was programmed using the software product *Matlab R12*. The Colebrook's equation with the wall roughness value 2.10^{-3} mm was found as the most representative after the analysis of theoretical and experimental data. The average value of the friction factor in one phase region is around $0,03$ and $0,04$.

The knowledge of the precise capillary-tube inner diameter value has a crucial importance both for a proper functioning of theoretical simulations and experimental measurements of the capillary characteristics. Unfortunately the average inner diameter supplied by the manufacturers for each capillary sometimes differs by more than 5% from the real value. The method of weighting the capillary when empty and when filled with water or some fluoroinert (C_6F_{14} , C_8F_{18}) was used to determine the inner diameter.

Several works found in the open literature have focused their attention on experimental and analytical investigations to describe the phenomenology and develop methods to simulate the behavior of the capillary-tube expansion devices.

We have assumed fully adiabatic flow with two main regions in our capillary flow simulations: single phase region of liquid coolant with linear pressure drop and two phase region with increasing vapor quality connected with a rapid pressure drop. The flash point between both assumed regions is reached when the pressure equals saturation pressure. Three different models were studied using *Matlab R12* programmed software. The analytical model [3] can be used just for a simple length prediction both for a single phase and two-phase region.

Two more-sophisticated numerical models are based on Runge-Kutta solution of differential equations. Total pressure and vapor quality are the primary solved variables in the two-phase region. The first numerical model [4] assumes homogeneous flow of vapor and liquid in the two-phase region. The second model [2] takes into account the separated flow of both phases. Numerical models predict, along with pressure and vapor quality, the distribution of the following thermo-physical properties: enthalpy, void fraction, temperature, velocity and density.

All three models for capillary-tube flow simulation were compared with experimental data from the literature. The most benevolent data for optimal capillary length prediction were obtained from the analytical model. Numerical models give shorter two-phase region in which the flow reaches its critical conditions at the capillary outlet.

Programmed models were prepared for the following refrigerants: C₃F₈, C₄F₁₀, R12, R134a and R22. The special equations describing various thermo-physical properties of each refrigerant vary mostly with temperature in the one-phase region and pressure in the two-phase region and were determined with the help of the modified extended BWR equation.

A more complex numerical simulation algorithm, which could solve even non-adiabatic flow through capillary tube, is the next step for the study. A special test stand with pressure and temperature sensors installed along the capillary is being designed in our laboratory. Foreseen measurements, namely in two-phase flow region, could validate some of our hypotheses about the conditions at the capillary outlet, once the outlet pressure is strictly set by a backpressure regulator.

References:

- [1] V. VINŠ, V. VACEK, M. DOUBRAVA, M. GALUŠKA: *Study of the Cooling System with Fluorinert Refrigerants*, Proceedings of Workshop 2004, CTU Reports, Special issue, Part b - Vol. 8, March 2004, pp.640-641.
- [2] T. N.WONG, K. T. OOI: *Adiabatic capillary tube expansion devices: A comparison of the Homogeneous flow and the Separated flow models*, Applied Thermal Engineering Vol. 16, No. 7, 1996, pp. 625-634.
- [3] CHUNLU ZHANG, GUOLIANG DING: *Approximate analytic solution of adiabatic capillary tube*, Elsevier, International Journal of Refrigeration 27, 2004, pp. 17-24.
- [4] S. M. SAMI, C. TRIBES: *Numerical Prediction of Capillary tube behaviour with pure and binary alternative refrigerants*, Applied Thermal Engineering Vol. 18, No. 6, 1998, pp. 491-502.

This work was funded by the Czech Ministry of Education within the framework of the programs INGO for the cooperation with CERN and by VZ MŠMT - J04/98 - 212200008

Commissioning of the Atlas Inner Detector Cooling System in the SR1 Building

V. Vacek

vacek@fsid.cvut.cz

CTU, Faculty of Mechanical Engineering, Department of Applied Physics

Technická 4, 16607 Praha 6

The **Inner Detector (ID)** measures the directions, momentum, and signs of charge of electrically-charged particles produced in each proton-proton collision. It consists of different sensor systems all immersed in a magnetic field parallel to the beam axis. The sensors closest to the collision point are the Pixel detectors. The Semiconductor Tracker (SCT) is the following one. An evaporative cooling system has been chosen for these two detectors to evacuate dissipated energy from the pixel and SCT detectors.

The design of the Atlas Inner Detector cooling system passed several stages of development over the last five years and this paper describes the current status of the design. The Department of Applied Physics has been involved in its design via international cooperation supervised by CERN since 1995

The heat sources in the ATLAS SCT & Pixel detectors are formed by the silicon detectors and hybrids with electronic chips: SCT = 32 550 [W], Pixel = 14 960 [W] and by the thermal enclosures and service panels: SCT = 6 182 [W], Pixel = 4 000 [W]. A total of 57 692 W of heat load will be taken out by the evaporative cooling system using C₃F₈ as the fundamental refrigerant.

The choice of the fluorocarbons was driven by the following reasons

- High dielectric strength
- Good chemical stability under ionizing radiation
- Non-toxic
- Non-flammable
- Zero ozone depletion potential (ODP)
- High degree of compatibility with most of the metals, plastics and other materials
- Contrary to some classical refrigerants (HCFC, or HFC) they do not contain Hydrogen (under ionizing radiation HF acid may be formed so any H donor impurity must be absent),

however, fluorocarbons

- are expensive
- have relatively high global warming potential (GWP) and long atmospheric lifetime.

Besides the final cooling system, a second cooling system had to be designed and constructed for the assembly facilities at CERN in the Bldg. SR1 with cooling power around 22 kW. This cooling system is going to be used during the ID assembly procedure tests and it has to operate in two temperature modes (WARM mode – evaporation at + 15°C; and COLD mode - evaporation at - 25°C). The second task of the system is pilot testing of the components of the final system for the Atlas ID.

Both systems will operate in a similar manner. A coolant vapor returning from the SCT and Pixel detectors is compressed by an oil free compressor and condensed in a water-cooled condenser. The liquid of C_3F_8 coming from condenser is pressurized to 16 bar_a and it is transferred along 120 m pipe to the regulation racks on the platform. A high pressure value is driven by the requirement of keeping the cooling agent above the saturation point along tubes between the condenser and heat exchangers. The maximal liquid temperature expected in the inlet tubes is 40°C. At that temperature the saturation pressure is 12.8 bar_a, thus 13 bar_a is then set as the minimum pressure in the inlet of capillaries.

There are pressure inlet regulators and back pressure regulators on the platforms. The mass flow rate is set by the pressure inlet regulators and could be readjusted during the lifetime of the detector as function of the increasing power dissipation of the electronics. The liquid flows across a recuperative heat exchanger and it is cooled down by a mixture of vapor and liquid returning from cooling channels of the detector. The recuperative heat exchanger between the warm inlet and cold return mixture allows increasing the efficiency of the cycle (sub-cooling refrigerating effect). Over-cooled liquid expands in the capillaries just before the cooling channels and then remains in saturation conditions (boiling) in the detector cooling channels. Thermal resistances in the silicon module imply a coolant temperature of -24°C to keep the silicon module at -7°C. Evaporating temperature is determined by the saturation pressure 1.74 bar_a (set by the back pressure regulator). Mass flow rate of C_3F_8 is set to obtain maximum 0.9 vapor quality on the outlet from cooling channels at maximum heat load produced by the detectors and minimum efficiency of the heat exchanger. The residual liquid in the mixture at the exhaust of the cooling channels is evaporated by means of the power provided by the heater. The heater also raises the temperature of the vapor above the dew-point temperature in the environment. Superheated vapor flows across back pressure regulator on the platform to the cooling plant situated at free access area USA 15.

The Department of Applied Physics has been participating in commissioning of cooling system in SR1 Bldg. at CERN recently and the poster presentation will introduce the results from the tests performed both for WARM and COLD mode operation.

References:

- [1] VACEK, V. - VINŠ, V. - DOUBRAVA, M. - GALUŠKA, M.: *DAQ and DCS sensors database, Capillary studies and Thermophysical property Database for the Cooling applications at SR1 Bldg.* Pixel Mechanics Meeting at CERN, February 2003, Geneva, pp. 12.
- [2] BUDINSKÝ, R., VACEK, V., AND LÍŠAL, M.: *Vapor-liquid equilibria of alternative refrigerants and their binaries by molecular simulations employing the reaction Gibbs ensemble Monte Carlo method* Fluid Phase Equilibria, Volumes 222-223 (2004), pp. 213-220
- [3] OLCESE, M., EINSWEILER, K., KERSTEN, S., VACEK, V. ET.AL.: *Requirements for Pixel Detector Services* Atlas Note - ATL-IP-ES-0007, CERN, 2003, pp. 82
- [4] VACEK, V.: *A Study of the Cooling Facility in Preparation for the ATLAS Inner Detector Testing* Proceedings of Workshop 2003, CTU Reports, Special issue, Part A - Vol. 7, February 2003, Prague pp.100-102.

This work was funded by the Czech Ministry of Education within the framework of the programs INGO Grant for the cooperation with CERN

Discharge at atmospheric pressure

P. Barvir, P. Kubes, J. Kravarik, D. Klir

barvirp@fel.cvut.cz

Department of Physics, Faculty of Electrical Engineering, Czech Technical University,
Technická 2, 166 27 Prague 6, Czech Republic

The study of the high power electric discharge with parameters of the lightning channel was directed to the investigation of possibilities of the ball lightning generation and due to security of the airplane components against the lightning. The properties of the ball lightning are summarized and described in [1]. Experiments were held in the High Power Discharges Laboratory of the Institute of Plasma Physics and Laser Microfusion in collaboration with the International Center for Dense Magnetized Plasmas in Warsaw.

The discharge was supplied with capacitor bank with the total electric charge about 100 C. The average current during discharge reached about 300 A. Duration of the discharge was a few hundreds ms. The electrodes were connected with the copper or aluminum wire of 300 μm diameter before the discharge to enable the breakdown through the horizontal distance of 40 cm. The electrodes were made from aluminum or brass. For capturing plasma channel evolution the high speed CCD cameras were used. Framerate of 2000 pictures per second gave the evolution scale of millisecond.

During the discharge the creating of an interesting structures were observed. The parts of the plasma channels were twisting, spinning and the intensity in visible region of spectra were changeable. The interlacing plasma channel under the appropriate conditions may create a ball-like structure. This structure have a relatively long livetime, after that, the ball can decaying either slow diminishing in time or spread out into an plasmatic channels. At the surface of the channel must be tension responsible for its lifetime a few ms. These ball structures have usually stable brightness similar to the channel and the supposed electron temperature may be about 0.5 eV. Lifetime of these balls increases with its diameter. It is possible to make statistical evaluation, then it can be obviously seen the correlation between the lifetime and the radius of the ball structures. In our experiments were observed the most common diameters about 20 to 30 millimeters with the lifetime 6 to 8 ms.

The radiate intensity of the discharge channel can be divided into three different parts. The first one connected with the electrodes is directed straight to another electrode. The second one connected with the first parts has more complicated structure. It is characterized by fast transforming of direction and wide range of intensities, radiation and diameters (1 \div 30 mm) of the channel. The transition from the first part into the second part is characterized by the rapid change of channel direction and the twisting nearly oposit to the previous direction. The third one is represented by dark space, it is under detection limit of the camera. Appropriate temperature for this area may be about 0.1 eV.

It is possible to determine the parameters of the type of first and second current channels. For the near-electrodes parts with electrical current of 300 A and the mean value of channel diameter of 2 cm we can calculate the current density about 10^6 A/m². Then for the temperature of 0.5 eV the electron density of $6 \cdot 10^{23}$ m⁻³ was evaluated (supposing the magnetic pressure is much smaller than the atmospheric pressure [2,3]). The conductivity ($1.4 \cdot 10^3$ S/m) was calculated from Spitzer formula for temperature 0.5 eV. From the

knowledge of the current density and the conductivity we can estimate the electric field intensity as 700 V/m. On the length of this part (20 cm) the voltage drop is approximately 150 V. We can make a conclusion that the thermal plasma with Spitzer conductivity exists in this part of the channel.

The second part of the channel has wide range of diameters. The narrow form with the smallest diameters of $1 \div 2$ mm radiates more intensive. It usually starts with straight short circuit in the dark part of the channel. Later the evolution of these channels is determined usually by helical instability development. In this form we can estimate the plasma parameters relatively simple (current density $3.7 \cdot 10^8$ A/m², magnetic field 120 mT, magnetic pressure 10^4 Pa, plasma temperature 0.5 eV, electron and ion densities $6 \cdot 10^{23}$ m⁻³ and Spitzer conductivity $1.4 \cdot 10^3$ S/m). But if we assume that the radiated power was 200 kW, then the electric conductivity of $1.2 \cdot 10^5$ S/m can be calculated from equation $\gamma = I^2 / (P \cdot S)$, where I is electric current, P is Joule power, l and S is length and cross-section of radiated area, respectively. It seems that the Spitzer formula cannot be used for the calculation of electric conductivity. Electric field intensity is about 3100 V/m, then the voltage drop in 10 cm length is about 300 V.

Both magnetic and dynamic pressures represent insignificant part of the total pressure in the plasma. It is evident that the plasma pressure, which is equal to atmospheric pressure, has the dominant influence. The magnetic and the dynamic pressures only slowly affect the current channel transformations and enable demonstration of the current channel evolution in scale of ms.

References:

- [1] M. STENHOFF: *Ball Lightning - An Unsolved Problem in Atmospheric Physics*, Kluwer Academic/Plenum Publishers, New York, 1999.
- [2] P. BARVIR: *Diagnostics of high current discharges at atmospheric pressure*, ICDMP, 2003, pp. 410.
- [3] P. BARVIR, P. KUBES, J. KRAVARIK, M. SCHOLZ, L. KARPINSKI, E. SKLADNIK-SADOWSKA, K. MALINOWSKI: *Characteristic of Discharge at Parameters of Lightning Channel*, Czech. J. Phys. 54, pp. C274-C278, (2004).

This research is supported by the research program No 202-03-H162.

Observation of Optical Waveguides Arising from Dark Photovoltaic Soliton Propagation in LiNbO₃

M. Bodnár, P. Hříbek

bodnar@troja.fjfi.cvut.cz

Department of Physical Engineering, Faculty of Nuclear Sciences and Physical Engineering, Czech Technical University, V Holešovičkách 2, 180 00 Prague 7, Czech Republic

Spatial photorefractive solitons have attracted much interest in the past two decades. Their potential applications are in waveguides, directional coupling, electro-optical switching, and frequency conversion. Soliton-induced waveguides are key elements in the development of reconfigurable optical switches and dynamic interconnects. In particular, spatial photorefractive solitons have the advantage to be generated from low-power sources. Moreover, their photo-induced waveguides can be temporarily stored, erased or rewritten or can even be permanently fixed.

At present, several generic types of photorefractive solitons are known: quasi-steady-state solitons, screening solitons, and photovoltaic solitons. Spatial solitons is separated into two basic types: the bright soliton and the dark soliton. The bright soliton, in which a beam of light propagates without change in its transverse profile, occurs when self-focusing due to the light-induced change in the index of refraction balances diffraction. The resulting index of refraction is positive; it is proportional to the intensity of the beam. The dark soliton, in which a dark band, or notch, is superimposed on an otherwise uniform background illumination, occurs when self-defocusing due to a light-induced index change balances the diffraction of the notch. The resulting index of refraction is negative. A dark soliton may be black, in which the intensity minimum is zero, or gray, in which it is nonzero but less than the background intensity.

The optical nonlinearity responsible for soliton formation is due to the transport of electronic charge dominated by the bulk photovoltaic current (for photovoltaic solitons). Electrons are photo excited from impurity centers with momentum preferentially directed along the z axis of a ferroelectric crystal, and are then trapped in different impurity centers. The resulting space-charge distribution gives rise to an index gradient through the electro-optic effect. This index gradient is responsible for the self-guiding needed to generate photovoltaic solitons. These solitons do not necessitate application of an external field.

In this paper we describe one-dimensional dark photovoltaic solitons for generation planar waveguides in iron doped LiNbO₃, which are predicted to occur in a medium with significant photovoltaic effect. The LiNbO₃ have after illumination the negative index of refraction, and this is the reason for the use a dark soliton. We used also LiNbO₃ material, because it is a widely used material for optoelectronics application due to the numerous properties (electro-optic, photovoltaic, pyroelectric, piezoelectric) it offers.

We generate the one dimensional spatial soliton in bulk sample of crystal. When the background illumination is sufficiently broad, this case reduce to the problem of planar solitons in two dimensions: the propagation dimension and the transverse dimension, so we create a planar waveguide in the bulk sample.

The experimental setup consist of a iron doped LiNbO₃, a collimated continuous-wave argon-ion laser beam of 514 nm, a phase mask, and a telescope to image the collimated beam onto the front crystal surface. The dimensions of the crystal are 20mm x 10 mm x 3 mm (x x y x z), and the concentration of iron ions 250ppm (0.25%mol). A laser beam at 514 nm polarized along the z-axis direction, is collimated about 2 mm on the input face of the crystal and propagated along x-axis. The polarization along z-axis is used the biggest electro-optic

coefficient r_{33} and the biggest photovoltaic coefficient β_{33} . This polarization is caused by the biggest index change Δn . Photovoltaic soliton in this type of crystal is needed for generation only 5 mW/cm^2 optical intensity. The phase mask, which is the silicon cover plate, forms a phase step across a beam of circular cross section and imaging it onto the front surface of a sample to produce a narrow dark notch. The dark notch is oriented so that the intensity gradient of the beam is parallel to the z-axis (optical axis). The narrow dark notch has $15 \mu\text{m}$ on the front surface of the sample. The variations in phase and in intensity arising from the phase step occur along the z axis. Before the photovoltaic effect takes place, the dark notch diffracts from $15 \mu\text{m}$ FWHM on the front surface to about $20 \mu\text{m}$ FWHM at the exit surface. As the photovoltaic space charge field builds up (change the index perturbation), the dark notch starts to narrow. The resulting index perturbation forms a waveguide that can be probed by launching a second beam into it.

The beam profile is detected by a charge-controlled device array (CCD) and captured by a computer-controlled frame grabber. For an average background intensity of 5 mW/cm^2 , we obtain steady-state measurements after a 10 min exposure.

After soliton formation we can launch the second beam into this waveguide. The photovoltaic effect is wavelength sensitive, and the iron doped LiNbO_3 is less sensitive on the higher wavelength. Our probe beam is the polarized laser beam at 633 nm . This wavelength isn't caused any refractive change in the crystal. We excite a TE mode in the waveguide.

The experimental setup is the same as for the generation spatial solitons, only we mistake the phase mask for a pinhole. The pinhole has the diameter $10 \mu\text{m}$, and we can launch TE mode into the waveguide by means of the pinhole.

In summary, we have observed dark spatial solitons in a photovoltaic medium, and we have shown that the photovoltaic solitons are capable of guiding beams at less sensitive wavelengths and therefore may be used for producing waveguides in the bulk media.

References:

- [1] BODNÁR, M. – HRÍBEK, P.: *Photovoltaics Properties of Fe:LiNbO₃*, Proseeding Workshop 2003, CVUT, Prague, 2003, pp. 94-95
- [2] BODNÁR, M. – HRÍBEK, P.: *Photovoltaic Solitons*, Proseeding Workshop 2004, CVUT, Prague, 2004, pp. 66-67
- [3] BODNÁR, M.: *Graduated Thesis-Photovoltaic effect in Ferroelectric Materials*, CVUT-Prague, 2002
- [4] COUTON, G.-MAILLOTTE, H.- CHAUVET, M. *Self-formation of multiple spatial photovoltaic solitons* Journal of Optics B: Quantum and Semiclassical Optics Institute of Physics Publishing, vol. 6, 2004 pp. 223-230

This research has been supported by MŠMT grant No. MSM 210000022.

Radiation Defect Profiles Created by High Energy Protons and Alphas: Simulation of Their Influence on Silicon Power Diodes

V. Komarnitskyy, P. Hazdra

komarv1@fel.cvut.cz

Department of Microelectronics, Faculty of Electrical Engineering,
Czech Technical University, Technická 2, 166 27 Prague 6, Czech Republic

New generation of silicon power devices is faced with increasing tasks regarding their switching speed performance. Advanced method of carrier lifetime control have to be used to speed-up device turn-off without substantial deterioration of ON-state losses. For this reason, traditional techniques of lifetime killing, like diffusion of noble metals, were replaced by irradiation with high energy particles. Irradiation with protons and alphas in combination with electron irradiation allows creation of nearly arbitrary carrier lifetime profile [1] and very good controllability and reproducibility of lifetime killing process. In this project, we focused on detailed characterization of radiation defects and their profiles resulting from proton and alpha-particle irradiation in the MeV range. Profile parameters and defect introduction rates were further used for simulation of irradiated structures using modern Technology Computer Aided Design (TCAD) tool to predict the effect of irradiation on device performance.

Radiation defects produced by high energy ions were investigated in the low-doped (phosphorous concentration below 10^{14} cm^{-3}) <100>-oriented FZ silicon substrate forming the n-base of 1.7kV/100A power planar p^+nn^+ chip diodes for power modules from ABB Switzerland Ltd., Semiconductors. The diodes were irradiated with 1.8, 2.8 and 3.6 MeV protons ($^1\text{H}^+$) and 3.6, 8, 12 and 14.5 MeV alphas ($^4\text{He}^{2+}$) using the 5 MeV tandem accelerator in FZ Rossendorf. The irradiation with low fluences ranging from 7×10^9 to $2 \times 10^{10} \text{ cm}^{-2}$ ($^1\text{H}^+$) and 1.4×10^9 to 1×10^{10} ($^4\text{He}^{2+}$) were used for defect characterization. Higher fluences of alphas (up to $5 \times 10^{11} \text{ cm}^{-2}$) were used to modify static and dynamic parameters of investigated diodes.

To fully characterize radiation defects, the following methods were used: the capacitance deep level transient spectroscopy (C-DLTS), I-V profiling, the high voltage current transient spectroscopy (HV-CTS), and C-V measurement.

C-DLTS spectra of proton irradiated samples revealed six electron traps and two holes traps while only three electron trap levels and one hole trap were detected in samples irradiated with helium [2]. The most prominent recombination levels were attributed to the acceptor level of vacancy-oxygen pair VO^{-0} at $E_c-0.167 \text{ eV}$ and the single acceptor level of divacancy V_2^{-0} at $E_c-0.436 \text{ eV}$. While the VO pair set the lifetime at high injection levels, the single acceptor level of divacancy is responsible for the carrier recombination at low injection levels and charge generation in depletion regime.

Profiles of dominant recombination levels measured by HV-CTS and C-DLTS were compared with primary vacancy distributions obtained from simulation using the Monte Carlo code SRIM2000. Results show that divacancy profiles, consisting of a sharp defect peak with a tail extending to the irradiated surface, follow in principle the simulated distributions. The peak depth R_D and its straggle ΔR_D were estimated both for helium and hydrogen irradiation. As we summarized in [3], SRIM simulation exhibited a good agreement with experiment concerning the divacancy peak depth while the measured straggle showed noticeable broadening. For protons and alphas the difference was in the range of 0.6-0.7 μm and 0.7-1.4

μm respectively. The introduction rates of particular defects, which were defined as a fraction of total number of produced defects to total amount of primary vacancies, were established for different ion energies. An example of data received from HVCTS measurement is shown in Table 1 where profile parameters of vacancy-related defects in silicon irradiated with 12 MeV alphas and 2.8 MeV protons are compared.

Table 1. Profile parameters and introduction rates for defects in silicon irradiated with 12 MeV alphas (left) and 2.8 MeV protons (right)

12 MeV He				2.8 MeV H			
Defect	$R_D/\Delta R_D$ [μm]	Introduction rate $\times 10^2$		Defect	$R_D/\Delta R_D$ [μm]	Introduction rate $\times 10^2$	
		Peak	Tail			Peak	Tail
VO^{-0}	91.6 / 1.88	2.9	2.4	VO^{-0}	84.7/2.45	1.6	1.3
V_2^{-0}	92.7 / 2.11	1.1	1.7	V_2^{-0}	84.5/2.98	0.90	1.1
Vacancy	91.9 / 0.98 (simulation)			Vacancy	81.7 / 2.14 (simulation)		

Simulation of unirradiated and irradiated diodes was performed using device simulator ATLAS from Silvaco Inc. The simulator possesses a model of thermal recombination/generation with full trap dynamics and arbitrary distribution of defect levels. Two dominant recombination levels, the acceptor level of vacancy-oxygen pair VO^{-0} and the single acceptor level of divacancy V_2^{-0} were used to simulate the effect of irradiation. The defects were characterized by their profiles, capture cross sections and bandgap positions [4]. To receive realistic magnitudes of defect capture cross sections, we have to extract them from room temperature I-V and Open Voltage Circuit Decay (OCVD) data since the magnitudes measured by DLTS are valid only at cryogenic temperatures. Simulated static and dynamic characteristics of irradiated devices showed a good agreement with experimental ones.

References:

- [1] P. HAZDRA, J. VOBECKÝ, H. DORSCHNER, K. BRAND: *Axial Lifetime Control in Silicon Power Diodes by Irradiation with Protons, Alphas, Low- And High-Energy Electrons*, Microelectronics Journal 35 (3) 2004, pp. 249-257.
- [2] P. HAZDRA, V. KOMARNITSKY, *Accurate Identification of Radiation Defect Profiles in Silicon after Irradiation with Protons and Alpha-Particles in the MeV Range*, Solid State Phenomena 95-96, 2004, pp. 387-392.
- [3] P. HAZDRA, V. KOMARNICKIJ, *Effect of proton and alpha irradiation on advanced silicon power devices: defect profiles and stability*, Proceedings of ASDAM'04, 2004, pp. 223-226.
- [4] V. KOMARNITSKY, P. HAZDRA, *Identification of Radiation Defect Profiles for Accurate Simulation of Power Devices Irradiated with Protons, Alphas and Low-Energy Electrons* Proceedings of ISPS'04, Prague 2004, pp. 177-182.

This research has been supported by the European Community - Access to Research Infrastructure Action of the Improving Human Potential Program project HPRI-1999-00039, the grant No. GAAV 102/03/0456 of the Grant Agency of the Czech Republic, and the MŠMT grant No. MSM 6840770014.

Hybrid Plasmachemical System for VOC Decomposition

S. Pekárek

pekarek@feld.cvut.cz

CTU, Faculty of Electrical Engineering, Department of Physics
Technická 2, 166 27 Prague 6

The non-thermal plasma based technologies are becoming more and more important for destruction of volatile organic compounds (VOC) in air streams because of their energy selectivity and capability for the simultaneous removal of various pollutants. Corona discharge (DC, AC or pulsed) and a dielectric barrier discharge in a confined space have been tested for these purposes. Recently, it has been shown that a combination of non-thermal plasma with catalyst leads to very promising results for the destruction of atmospheric pollutants at relatively low energy cost.

The corona discharge is a relatively low power electrical discharge. Discharge power enhancement and at the same time discharge stabilization can be achieved by applying a gas flow with respect to the active electrode [1]. Another approach to the discharge power enhancement is based on the simultaneous application of ultrasound waves and gas flow through the active electrode [2, 3].

For the purpose of VOC decomposition we performed the study of two hollow-needles-to-mesh atmospheric pressure discharge enhanced by a mixed VOC/air flow through the needle electrode in combination with TiO₂ catalyst [4]. The advantage of this arrangement is that all the mixture passes through the discharge zone and therefore is affected by plasmachemical processes. We studied discharge operational regimes as well as n-heptane decomposition. We used a stainless steel mesh electrode either uncoated, coated by a TiO₂ layer or as base structure for a layer of Aerolyst TiO₂ catalyst globules. We used two needles to increase the energy density and to test possible scaling for future application. For our experiments we choose n-heptane CH₃(CH₂)₅CH₃, a common part of organic solvents and automotive fuels (petrol), which represents a wide group of saturated hydrocarbons.

Results of operational regimes study:

We found that for the optimum interelectrode distance 8 mm, for flow rates from 3.2 to 20.3 slm, coating of the mesh with a layer of TiO₂ decreases discharge voltage in the low currents region. For higher currents the difference between V-A characteristics for coated and uncoated mesh is smaller. Significant difference however exists among V-A characteristics of the discharge with the layer of TiO₂ globules on the mesh, discharge with an uncoated mesh and the mesh coated with the layer of TiO₂. The obtained results reveal that for particular current the discharge with TiO₂ globules requires the smallest voltage.

Results of decomposition efficiencies study:

It was found that the decomposition efficiency increases with increased energy density. It was also found that for particular energy density the decomposition efficiency is the highest for the discharge with the layer of the TiO₂ globules, smaller for the mesh coated with the layer of TiO₂ and the smallest for the discharge with an uncoated mesh. These results can be explained by the effect of photocatalyst TiO₂ on decomposition efficiency. In case of TiO₂ globules the photocatalysts area exposed to the UV emitted from the discharge is higher than for the case of TiO₂ coated mesh, therefore the decomposition efficiency is higher.

Titanium dioxide (TiO₂) is an n-type semi-conductor, biologically and chemically inert, and existing in rutile and anatase phase. A series of its energy levels is associated with covalent

bonding between atoms composing the crystallite (valence band) and a second series of spatially diffuse higher energy levels is associated with conduction in the macromolecular crystallite (conduction band). Both series are strictly separated by a fixed energy gap of 3.2 eV. Incidence of UV light of a higher energy than this band gap, e.g. originating from de-excitation processes in the plasma reactor, can promote electrons from the valence band to the largely vacant conduction band. Simultaneously, a positive hole with strong oxidizing capability is formed. In order for photo catalysis to be productive chemically, electron-hole pair recombination followed by energy dissipation as heat, must be suppressed by fast trapping either of the electrons, or the holes or both, not exceeding the time constant of recombination, which is a fraction of nanoseconds. The anatase TiO₂ is predominantly used, because it has a higher O₂ adsorbing capacity than rutile TiO₂. The contaminating organic substrates themselves can react as adsorbed traps for the photo-generated holes.

Decomposition efficiencies for the discharge with an uncoated mesh and a mesh coated with TiO₂ layer for the different flow rate of the mixture of air with n-heptane and for the inter-electrode distance 8 mm are shown in table 1.

Flow rate [slm]	20.3	10.4	5.2	3.2
Decomposition efficiency [%] Uncoated mesh	20	26	36	--
Decomposition efficiency [%] Coated mesh	24	30	47	37.5*

Table 1. Decomposition efficiency versus flow rate and mesh type. Needles biased negatively; n-heptane concentration = 33 (55*) ppm

References:

- [1] PEKÁREK, S. – KHUN, J.: *Gas Flow Enhanced Hollow Needle to Plate Electrical Discharge for Decomposition of Volatile Organic Compounds* Czechoslovak Journal of Physics, 2004, pp.784–789.
- [2] PEKÁREK, S. – BÁLEK, R.: *Ozone Generation by Hollow Needle to Plate Electrical Discharge in Ultrasound Field* Journal of Physics D: Applied Physics, 2004, pp.1214–1220.
- [3] PEKÁREK, S. – BÁLEK, R.– POSPÍŠIL, M.: *Effect of Ultrasound Waves on Electrical Characteristics of Hollow Needle to Plate Electrical Discharge in Air or Mixture of Air with VOC* 57 Annual Gaseous Electronic Conference, Bunnatty, Bulletin of the American Physical Society, 2004, pp.21.
- [4] PEKÁREK, S. – NEIRYNCK, D.– LEYS, C.– POSPÍŠIL M. – KRÝSA, J.: *Two Hollow Needles to Mesh Electrical Discharge with TiO₂ Catalyst for VOC Decomposition* Submitted to 17th International Symposium on Plasma Chemistry, Toronto, 2005.

This research has been supported by GA ČR grant No. GA 202/04/0728.

Experimental Study of de-NO_x Processes in Non-Equilibrium Electrical Discharges

S. Pekárek

pekarek@feld.cvut.cz

CTU, Faculty of Electrical Engineering, Department of Physics
Technická 2, 166 27 Prague 6

Nitrogen oxides are formed when fuel is burned in combustion processes. They are toxic and they cause serious health problems. Therefore the development of the NO_x control technologies is an important issue. Non-thermal plasma of electrical discharges gives efficient means for NO decomposition [1,2]. The principle of the non-thermal plasma technologies for NO_x decomposition is to produce plasma in which a majority of energy supplied to the discharge goes into the production of energetic electrons rather than into the gas heating. Even though the electrons are short-lived under atmospheric pressure conditions and rarely collide with the pollutant molecules, they undergo many collisions with the dominant background gas molecules, thus producing radicals through electron impact dissociation and ionization. The radicals in turn reduce and/or oxidize the NO_x molecules.

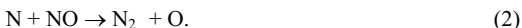
We performed an experimental study of nitric oxide decomposition by DC hollow needle to plate electrical discharge in air [3] and in the N₂ - NO mixtures of a dilute amount of NO [4]. The advantage of application of the hollow needle to plate discharge with the supply of the gas through the needle for NO removal is that all the gas passes through the discharge region and therefore is affected by plasmachemical processes. For the mixture of NO with N₂ only and for the NO concentration only a few hundreds parts per million (ppm), the input electrical energy in the discharge is consumed mainly in two ways:

1. Electron-impact reactions with N₂. The electron impact dissociation of molecular nitrogen N₂ can be described as



The rate coefficient of this reaction is a function of a reduced electric field.

2. Removal of NO, which proceeds mainly via reduction by N radicals. Therefore it is considered that the fastest channel for NO removal is a subsequent reduction of NO by the nitrogen atom N



The rate coefficient of this reaction is $k_2 = 3.1 \times 10^{-11} \text{ cm}^3 \cdot \text{s}^{-1}$. While NO concentration reduces in the gas, the reduction may be caused by other reaction, too. For example, the oxidation by oxygen radicals, produced through the reaction (2) can also take place:



The rate coefficient of this reaction is $k_3 = 9 \times 10^{-32} \text{ cm}^6 \cdot \text{s}^{-1}$.

Following this analysis the removal of NO in the N₂+NO mixture by electrical discharge should be also accompanied by NO₂ formation. To study the NO removal efficiency as well as formation of NO₂ we investigated decomposition of nitric oxide in DC driven atmospheric pressure negative corona discharge [4].

Stainless steel needle (Terumo, Belgium) of the outer diameter 1.2 mm and the inner diameter 0.7 mm was situated axially in the cylindrical metallic discharge chamber. The needle was used as a first electrode. Perpendicular to the needle was situated a second electrode in the form of stainless steel disc. The distance between the tip of the needle and the disc was adjusted to 4 mm. The DC high voltage power supply Technix provided voltage up to 30 kV. A resistor 0.889 166

MΩ ballasted the needle electrode. Stable flow of high-purity nitrogen with a defined quantity of NO was supplied through the needle into the discharge volume. The gas pressure in the discharge chamber was fixed at 1.01×10^5 Pa and controlled by a pressure gauge. Nitrogen (99.9999) (Messer Austria, with certified impurities $H_2O < 0.5$ ppm, $O_2 < 0.5$ ppm, $CO/CO_2 < 0.1$ ppm, $HC < 0.1$ ppm and $Ar < 1$ ppm) was delivered through Bronkhorst *HI-TEC* model mass flow controllers MFC. Quantified traces of NO (20, 100, 200 ppm) were added by the controlled flux of N_2+NO mixture (Pulmonix® forte, Messer Austria, 900 ppm NO in N_2 , with main impurities $H_2O < 3$ ppm, $O_2 < 1$ ppm and $NO_2 < 1$ ppm). To monitor volumetric concentration of nitrogen oxides NO, NO_2 and NO_x in the discharge products we used a GA-60 flue gas analyzer (Madur Electronics) equipped with electrochemical cells (O_2 , CO, SO_2 , NO, NO_2) and a chemiluminescence NO_x analyzer API 200EM (Teledyne Instruments).

The illustrative results showing the NO removal and NO_2 formation for the hollow needle to plate electrical discharge with the needle biased positively and for the flow of the N_2+NO mixture through the needle electrode 2.5 slm are shown in the following table 1. The initial concentration of NO in the mixture was adjusted to 20 ppm. The energy density is defined as a ratio of power delivered to the discharge and a flow of the mixture through the needle.

Energy density [kJ/m^3]	0	1.01	1.9 7	2.89	3.8 3	4.8
NO concentration [ppm]	2 0	18.0 5	14. 7	11.9 3	9.3 3	6.8 2
NO_2 concentration [ppm]	0	0.2	0.8	1.11	1.1 7	1.1 6

Table 1. Concentration of NO and NO_2 for the discharge with needle biased positively.

From the experimental results following conclusions can be taken:

- The NO decomposition in the discharge strongly depends on energy density; with increasing energy density the NO decomposition increases.
- Production of nitrogen dioxide NO_2 versus energy density exhibits a certain maximum.
- Complete NO removal can be more easily obtained for lower initial NO concentrations.
- The ratio of nitric oxide to the sum of nitric oxide and nitrogen dioxide decreases with increasing energy density.

References:

- [1] PENETRANTE, B. – HSIAO, M.: *Comparison of Electrical Discharge Techniques for Nonthermal Plasma Processing of NO in N_2* IEEE Transactions on Plasma Science, 1995, pp.679–687.
- [2] LIN, H. – GAO, X.–LUO, ZY.: *Removal of NO_x from Wet Flue Gas by Corona Discharge* Fuel, 2004, pp.1251–1255.
- [3] PEKÁREK, S. – ROSENKRANZ, J.: *Ozone and Nitrogen Oxides Generation in Gas Flow Enhanced Hollow Needle to plate Discharge in Air*. Ozone Science & Engineering, 2002 pp.221-226.
- [4] PEKÁREK, S. – ŠIMEK, M.: *Nitric Oxides Decomposition by Hollow Needle to Plate Atmospheric Discharge in N_2 – NO mixtures* Submitted to 17 International Symposium on Plasma Chemistry, Toronto 2005.

This research has been supported by GA AV grant No. IAA 1043403.

Section 3

INFORMATICS
&
AUTOMATION ENGINEERING

Implementation of Control in Redundant Parallel Robotic Structures

K. Belda, J. Böhm*, M. Valášek**

belda@utia.cas.cz

CTU, Faculty of Electrical Engineering, Department of Mechanics and Materials,

**Faculty of Mechanical Engineering, Department of Mechanics,
Division of Mechanics of Bodies.

*Institute of Information Theory and Automation, AS CR,
Department of Adaptive Systems
Pod vodárenskou věží 4, 182 08 Praha 8.

Nowadays, the future development of new industrial robots (parts of machine tools and manipulators) requires also improvement and development of their control. In essence, it means a replacement of existing conventional control approaches (e.g. NC systems, PID/PSD control structures) by new approaches, which enable as much as possible to use available information on properties and behavior of given plant.

Conventional approaches provide control of industrial robots only from view of drives as separate units, but they do not solve control from view of whole robotic system. On the other hand, modern control approaches take in to account dynamics and kinematic relations of given machine. In this way, they design energetically useful control actions. These approaches allow increasing of productivity by use of saved energy.

Dynamics and kinematic relations (available information on given robotic plant) can be represented by different mathematical models, often in a form of differential equations. They are obtained according to theory of mechanics (e.g. principle of virtual works, composition of equations of motion by Lagrange's equations, etc.). The equations can be formulated as input-output models or state-space models. For real use, the models are usually transformed to discrete form. Discretization with appropriate sampling period provides naturally computation time for model composition and design of control actions. When the models are nonlinear, then the part of model composition contains also some kind of linearization procedure.

Approaches, using certain mathematical model, are generally called model-based control approaches. There exist a lot of types in control theory. Mostly, they differ by length of prediction to future during computation of control actions. Suitable example of model-based approaches is multi-step Predictive control, applicable in new developed industrial robots.

Basic questions of robot control follow partly from their constructions and partly from technological requirements – expected behavior. In the branch of parallel structures, especially redundantly actuated, fundamental control task is, how to provide optimal cooperation of all drives interconnected by robot arms through movable platform (chuck, gripper).

Predictive control uses mathematical model (description of kinematic relations and dynamics of robot) and quadratic optimality cost function to design of control actions. This approach combines feedback~feedforward parts. The model represents specific prior information, which is used for forming the dominant part of control actions. Attached feedback from measurable robot outputs compensates model inaccuracies and certain bounded disturbance. It composes remaining part of designed actions.

According to marking “predictive”, this control is based on prediction, which is computed by means of mathematical model. Prediction is realized only within certain horizon of prediction. In case of speedily changed systems, the horizon represents only several multiples of sampling period.

Designed actions correspond to current requirements to motion of movable platform. This way, the requirements to input energy are led towards optimal energy consumption. Moreover, among others, Predictive control can be use for trajectory planning of possible motion among points of robot workspace, solution of backlash problem and solution of steady state error in cases of accurate positioning.

In comparison with usual control approaches based on PID/PSD control or other possible high-level model-based controls (Inverse Dynamics Control, Sliding Mode Control), Predictive control offers simple setting of parameters. It generally represents only tuning of two main parameters - horizon of the prediction and input penalization. Their choice is not difficult. Horizon of prediction relates to time constant of controlled system and selected sampling. The magnitude of input penalization (usually normalized so that control error penalization is equaled one), determines stiffness of response of controller and thus even tracking quality of desired trajectory during robot motion. It is selected in comparison to potential of drives.

Presented control approach was successfully tested on two types of constructions based on parallel principle. The constructions represent both horizontal and vertical configurations, which differ by levels of potential energy. It was shown that Predictive control is able to achieve better results than simple realization of PSD controller. For all practical purposes, for industrial use, Predictive control represents promising way to future in spite of more demanding requirements to its preparation (composition of mathematical model; adjustment of predictive algorithm for given real plant – configuration; more precise trajectory planning – smoothing problems).

References:

- [1] BELDA, K. – BÖHM, J. – VALÁŠEK, M.: *State-space Generalized Predictive Control for redundant parallel robots*. Mechanics Based Design of Structures and Machines (31), Marcel Dekker, 2003, pp. 413-432.
- [2] BELDA, K. – BÖHM, J. – VALÁŠEK, M.: *Study of predictive control algorithms for parallel robot structures* Process Control, University of Pardubice, 2004, pp. 1-9.
- [3] BELDA, K. – PÍŠA P., – BÖHM, J. – VALÁŠEK, M.: *Structured model-based control of redundant parallel robot kinematics*. Chemnitz Parallel Kinematics Seminar, Verlag Wissenschaftliche Scripten, 2004, pp. 701-705.
- [4] BELDA, K. – BÖHM, J. – VALÁŠEK, M.: *Digital Control of Over-Actuated Parallel Robots*. Methods and Models in Automation and Robotics, Wydawnictwo Uczelniane Politechniki Szczeciskiej, 2004, pp. 819-824.

This research has been supported by CTU grant No. 0406413.

Control of Distributed Parameters System by MPC Controller

J. Roubal*, V. Havlena**

roubalj@control.felk.cvut.cz

* Department of Control Engineering, Czech Technical University in Prague,
Karlovo náměstí 13, 121 35 Prague 2, Czech Republic

** Honeywell Prague Laboratory, Pod vodárenskou věží 4, 182 08 Prague 8, Czech Republic

There are many industrial processes which have a distributed parameters behaviour. Consequently, these processes cannot be modelled by lumped inputs and lumped outputs models for correct representation. This paper deals with two-dimensional dynamic processes (systems with parameters dependent on two spatial directions) which can be described by lumped inputs and distributed output models.

These distributed parameters models can be mathematically described by partial differential equations [1]. Unlike ordinary differential equations, the partial differential equations contain, in addition, a derivative with respect to the spatial directions. Consequently, the partial differential equations lead to more accurate models but their complexity is larger.

This paper deals with a special type of the partial differential equations which are called parabolic partial differential equations. This type of partial differential equations can describe, for example, a heat transfer process where heat sources (system inputs) operate in a several points and temperature distribution (system output) propagates from these sources to the surrounding.

The dynamic behaviour of the distributed parameters system, which is described by the partial differential equation, can be approximately transformed to a finite-dimensional model, for example, by using the finite difference method [4]. Then the ordinary differential equation model with a large dimension is obtained and can be used for a finite-dimensional controller design.

Unfortunately, for online solving of an optimization problem, e.g. model predictive control approach [2], the large model dimension introduces a problem for the control design. Therefore a model reduction method has to be used, for example reduction by the balanced truncation method.

Variables of every real process have certain limits given by laws of physics. Unlike the classical control law, the model predictive control considers explicitly the future implication of the current control action and this approach enables us to include the constraints of inputs/outputs to the control algorithm [2]. The main idea of the model predictive control is to find the optimal control sequence on the prediction horizon. And then for the feedback control, only the first element of this optimal control sequence is applied as the input control action to the plant and the optimization problem is solved again for the new initial state of the system. This methodology is known as the receding horizon control.

Model predictive control methodology based on lumped inputs and lumped outputs models is described in many publications, for example in [2], but there are many industrial processes which have the distributed parameters behaviour. Therefore my research deals with using the model predictive control approach for distributed parameters systems which can be described by lumped inputs and distributed output models.

This paper presents a predictive controller design for a heat transfer process which is described, for a temperature distribution θ [K], by the following partial differential equation on an open set $\Omega = (0, L_1) \times (0, L_2)$

$$\rho c \frac{d\Theta(x, y, t)}{dt} - \lambda \left(\frac{\partial^2 \Theta(x, y, t)}{\partial x^2} + \frac{\partial^2 \Theta(x, y, t)}{\partial y^2} \right) = f(x, y, t)$$

and the Newton boundary condition on the boundary of the set Ω

$$-\lambda \frac{\partial \Theta(x, y, t)}{\partial n} = \alpha (\Theta(x, y, t) - \Theta_s(x, y, t)),$$

where ρ [kg/m²] is a surface density of a medium, c [Ws/(kg K)] is its thermal capacity, λ [W/K] is a thermal conductivity (independent on the temperature Θ), f [W/m²] represents a surface heat source distribution, α [W/(mK)] is an external heat transfer coefficient and Θ_s [K] is the surrounding temperature.

This description is transformed to the finite dimensional model. The spatial derivatives are replaced by differences [4] and the discrete model in the standard state space notation is obtained

$$\begin{aligned} \mathbf{x}(k+1) &= \mathbf{A}\mathbf{x}(k) + \mathbf{B}\mathbf{u}(k) \\ \mathbf{y}(k) &= \mathbf{C}\mathbf{x}(k) + \mathbf{D}\mathbf{u}(k). \end{aligned}$$

In the equation above, \mathbf{x} is a vector of states, \mathbf{u} is a vector of system inputs, \mathbf{y} is a vector of system outputs and \mathbf{A} , \mathbf{B} , \mathbf{C} , \mathbf{D} are matrices of the system. Because of large dimension of this model, reduction by the balanced truncation method is used and then a predictive controller based on this reduced model is designed.

In [3], range control approach is described for lumped inputs and lumped outputs systems. The main idea of the range control concept is to replace the set point reference by low and high limits. This methodology leads to a very stable and robust control because the manipulated inputs do not compensate the high-frequency component of the noise. My research deals with application of the range control algorithm for the heat transfer process, which can be described by the partial differential equations above.

References:

- [1] LONG, C. A.: *Essential Heat Transfer*, Longman Group, England, 1999, pp. 14–93.
- [2] MACIEJOWSKI, J. M.: *Predictive Control with Constraints*, Prntice Hall, Harlow, England, 2002, pp. č. strany–č. strany.
- [3] HAVLENA, V. – FINDEJS, J.: *Application of Model Predictive control to Advanced Combustion Control*, Control Engineering Practise, 2004, pp. 500–510.
- [4] VITÁSEK, E.: *Numerické metody*, Nakladatelství technické literatury, Praha, 1987, pp. 379–420.

This research has been supported by CTU grant No. CTU0408413.

Design and Analysis of Model Based Predictive Controllers

J. Pekař, V. Havlena*

pekarj@control.felk.cvut.cz

Department of Control Engineering, Faculty of Electrical Engineering, Czech Technical University, Karlovo náměstí 13, 121 35 Prague 2, Czech Republic

* Honeywell Prague Laboratory, Honeywell Int.
Pod vodárenskou věží 4, 182 08 Prague 8, Czech Republic

Model predictive control (MPC) has gained in popularity because it provides a systematic approach to control the industrial processes with constraints on input, output and others variables in control loop. MPC refers to the class of computer control algorithms that use a system model to predict the future responses of a plant. Using this model-based prediction, at each sampling (or control) interval, an MPC algorithm computes an optimal future trajectory of input variables so that behavior of the plant corresponds to our demands as much as possible. The demands are mostly expressed as the cost function which is minimized over an prediction horizon by an MPC algorithm. The output of such an optimization problem is an optimal control sequence over the prediction horizon.

Only the first input in the optimal control sequence is applied to the plant and the entire calculation is repeated at the next sampling interval. This approach is known as receding horizon and enables suppression of incoming disturbances. The implementation of MPC algorithms with receding horizon can be rather computationally demanding because the optimization with constraints has to be solved on-line at each sampling interval. With respect to computational demand, the MPC is often used for slow processes, for example, in chemical and petrochemical industry.

There are two most important advantages of the MPC technology. The first advantage is that the multivariate control problems are handled in a natural and systematic manner. The second advantage, as mentioned above, is the ability to cope with explicit constraints on the controlled and other variables in the control loop. On the other hand, the most obvious weakness of finite horizon MPC was that there was no stability guarantee in early implementations. Next weakness is the need for a good and accurate process model because the model is used for prediction of future system response.

The modification of the standard linear MPC for control the nonlinear model is shown in this contribution. A non-linear PID controller for continuous stirred tank reactor (CSTR) using local model network was presented in [1]. In this contribution we present application of the MPC based on mixture distribution for control of CSTR [2] which is a highly non-linear process. The methodology based on bayesian update of the probability distribution over the set of possible models [3] enables description of a plant by a mixture distribution. The LQ (quadratic optimal state feedback) or LQG (quadratic optimal state feedback with gaussian noise) controller based on a mixture of a set of parallel models with a common state and different parameters only was developed in [4].

In this contribution we present application of model-based predictive controller based on mixture distribution, i.e. a set of parallel models, to CSTR process. This process is highly non-linear. Presented MPC is based on a mixture of linearized models in several operating points parameterized by their probabilities estimated on-line. Provided that the operating point of the process lies within the given set defined by convex envelope of the operating points presented MPC ensures "soft switching" between the individual models. The on-line

estimation of model probabilities is done by a set of Kalman filters in the normalized form. The good performance of algorithm for model probability estimation is very important part of presented MPC algorithm because the resulting MPC is parameterized by them.

It was shown that the model-mixture based MPC presented in this contribution provides a good performance and the switching algorithm provides reliable and fast adaptation. Moreover, the computational complexity is comparable to a linear MPC rather than a typical nonlinear MPC algorithm. The conclusion of the paper is that using above described approach, a good performances and adaptability of MPC controller to different operating point of CSTR can be achieved.

References:

- [1] GAO, R. - O'DYWER, A.- COYLE E.: *A Non-linear PID Controller for CSTR Using Local Model Networks* Proceedings of 4th World Congress on Intelligent Control and Automation, Shanghai, 2002, pp. 3278–3282.
- [2] PEKAŘ, J. - HAVLENA, V. *Control of CSTR Using Model Predictive Controller Based on Mixture Distribution*, In 6th IFAC-Symposium on Nonlinear Control Systems [CD-ROM]. Düsseldorf: VDI/VDE Mess- und Automatisierungstechnik, 2004.
- [3] ŠTECHA, J. - HAVLENA, V. - KRAUS F.: *Decision and Approximation Based Algorithms for Identification with Alternative Models*, Proceedings of 13th IFAC World Congress, San Francisco, 1996 pp. 3a–09.4.
- [4] HAVLENA, V. - ŠTECHA, J.: *LQ/LQG Controller for Parallel Models*, Proceedings of 15th IFAC World Congress, Barcelona, 2002.

This research has been supported by the grant CTU0408313 of the Czech Technical University in Prague.

Colour Rough Textures Modelling

J. Filip, M. Haidl*

filipj@utia.cas.cz

Department of Cybernetics, Faculty of Electrical Engineering, Czech Technical University,
Technická 2, 166 27 Prague 6, Czech Republic

*Institute of Information Theory and Automation, Academy of Sciences of the Czech Rep.,
Pod vodárenskou věží 4, 182 08 Prague 8, Czech Republic

Recent virtual reality systems aim for preserving reflective properties of rough textures as close as possible to an original material during different illumination and view positions. The only way how to reach real visual perception of observed texture is to measure its reflectance properties. These global illumination and view dependent real material properties were called the 4D Bidirectional Reflectance Distribution Function (BRDF). BRDF describes relation between incident light from direction and light reflected by observed material and was approximated by variety of reflectance models applied to computer graphics object rendering.

BRDF is insufficient for textures hence a Bidirectional Texture Function (BTF) was introduced to solve this constraint. BTF describes reflectance of each pixel based on illumination and view position. Hence this function is dependent on illumination and view angles as well as on planar position on observed material surface. The main application of BTF is photo-realistic modeling of real-world surfaces in virtual reality systems which is demanded mainly in fields of computer aided car or interior design. Another interesting BTF application is safety testing of virtually designed interior prototypes in dazzling situations mainly in automotive industry and architecture.

BTF modeling is a new research area, however several BTF measurements and modeling methods have been provided recently. In one of them the BTF has been approximated by biquadratic polynomial luminance in each pixel. Several other solutions were published such as the variants of per-pixel Lafortune model. Alternative approaches to BTF synthesis are based either on intelligent sampling techniques or on adaptive multidimensional statistical models [3,4]. In this contribution we propose two novel BTF models. The first is a fast extension of Lafortune reflectance model [2] and second is probabilistic BTF model based on causal auto-regressive model [4].

Standard Lafortune reflectance model [1] represents reflectance function by means of several reflectance lobes. In the case of the BTF the images corresponding to individual view position were modeled by dedicated Lafortune model. Thus this model is computed in all pixels of images corresponding to actual view position. When the only one-lobe Lafortune model is used the number of stored parametric images is 5 instead of 81 original BTF images for every view position. The model parameters are estimated using Levenberg-Marquardt non-linear fitting algorithm. However, the reflectance function approximation by means of one-lobe reflectance model only is unsatisfactory. The proposed solution is computation of color levels mapping function from an estimated one-lobe model image to original BTF image. This mapping function is computed for every color channel of each BTF image and is represented using polynomial of rank five. So for each image fifteen additional numbers have to be stored, however this number is negligible in comparison with number of Lafortune parameters stored for each pixel. The computation of proposed model [2] is very fast and can be easily implemented in graphical hardware since it requires only several additional linear

operations in comparison with standard Lafortune model. Described model was tested on distinct materials from Bonn University BTF database and results are almost visually indiscernible from original BTF data while the final BTF compression is about 1:20.

In contrast to proposed image-based BTF modeling method [2] we have proposed probabilistic BTF model [4] as well. This model is far more flexible, extremely compressed (few tens of parameters have to be stored only), it may be evaluated directly in procedural form and can be designed to meet certain constraints or properties, so that they can be used to fill an infinite texture space without visible discontinuities [3].

In the case of BTF modeling several additional task have to be solved. As the first step the range-map of original material is estimated. This is performed using photometric stereo which estimates surface range-map from at least three images obtained for different position of illumination source while the camera position is fixed. Such a mutually registered measurements are in BTF available for free. Following step is BTF space segmentation which is done by means of K-means clustering algorithm. As a result is set of cluster representatives which are subsequently spectrally decorrelated using Karhunen-Loeve transformation to obtain set of mono-spectral images. These images are spatially factorized using Gaussian-Laplacian pyramid to obtain separated images corresponding to individual frequency features. These images are analyzed using causal-autoregressive model and finally represented by means of several parameters. During fast synthesis the frequency sub-images are synthesized, the Gaussian-Laplacian pyramid is collapsed to obtain again mono-spectral images which are spectrally correlated using inverse Karhunen-Loeve transformation. During rendering each triangle of rendered 3D object the corresponding synthesized cluster representing image is chosen using cluster index according to actual camera and illumination position and finally combined with a previously estimated range-map in bump/displacement-mapping filter according to light position. This method enables enormous BTF data compression (approx. $1:10^6$) unattainable by any other existing BTF modeling approach while the results of proposed method are exceptionally realistic mainly for materials with irregular patterns as is for example wood, leather, plaster. For materials with regular patterns the regularity is introduced into the model by means of mentioned range-map. This method enable fast rendering implemented in graphical hardware as well and moreover it enables to synthesize BTF of arbitrary size so it can cover large objects in a systems of virtual reality.

References:

- [1] LAFORTUNE E. P., FOO S. CH., TORRANCE K. E., GREENBERG, D. P.: *Non-Linear Approximation of Reflectance Functions*, SIGGRAPH, 1997, pp. 117-126.
- [2] FILIP J., HAINDL M.: *Non-Linear Reflectance Model for Bidirectional Texture Function Synthesis*, In: Proceedings of the 17th IAPR International Conference on Pattern Recognition, Vol 1., 2004, pp. 80-83.
- [3] BENNETT J., KHOTANZAD A.: *Multispectral random filed models for synthesis and analysis of colour images*, IEEE Trans. on Pattern Analysis and Machine Intelligence 20, 1998 pp. 327-332.
- [4] HAINDL M., FILIP J.: *A fast probabilistic Bidirectional Texture Function model*, Image Analysis and Recognition (Lecture Notes in Computer Science 3212), 2004, pp. 298-305.

This work was supported by the EC Project No. IST-2001-34744 RealReflect and by the CTU grant No. CTU0407313.

Architecture Dependent Linear Code Optimizations

Pavel Tvrdík, Ivan Šimeček

tvrdik, xsimecek@fel.cvut.cz

Department of Computer Science, Faculty of Electrical Engineering, Czech Technical University, Technická 2, 166 27 Prague 6, Czech Republic

Every mathematical algorithm for the numerical algebra can be relatively easily rewritten into pseudocode: every mathematic operation in the algorithm is simply transformed into one subroutine from the linear algebra package. This simple algorithm leads to very transparent, error-free codes. But these codes do not respect the inner architecture of the CPU and the memory hierarchy and suffer from low temporal and spatial locality. These drawbacks can be reduced by the applications of SW transformation techniques. These transformations result in better temporal and spatial locality or in more efficient utilization of inner pipelines.

In this paper, we will demonstrate idea of SW transformation on 2 codes of iterative solvers. We will also represent the new code restructuring transformation called *dynamic loop reversal*. This transformation offers a new way to improve the cache utilization.

Linear codes for dense linear algebra consist mainly of loops. A number of SW transformations techniques have been developed in recent years for effective restructuring of these loops [1, 2]. We will demonstrate the idea of SW transformations on 2 basic codes of iterative solvers for huge sparse SLEs:

- The conjugate gradient (CG) method was discovered by Hestenes and Stiefel [3]. The matrix A must be symmetric and positive definite.
- The bi-conjugate gradient (BiCG) method [4] is suitable for symmetric matrix A .

The standard implementations of these algorithms have a serious drawback. If the data cache size is less than the total memory requirements for storing all input, output, and auxiliary arrays, then due to thrashing misses, part or all of these arrays are flushed out of the cache and must be reloaded during the next iteration. This inefficiency can be reduced by application of *loop reversal* and *loop fusion*. The application of loop fusion allows reusing immediately the new computed values of arrays. After the application of loop reversal, the last elements of auxiliary arrays that remain in the cache from the previous loop can be reused.

All results were measured on this HW configuration: Intel Celeron 850 MHz, 256MB RAM, 128 KB L2 cache, 16 KB L1 cache running OS Linux Debian with Intel C compiler version 6.01.

In the measured set (the order of matrix is between $5 \cdot 10^3$ and $2 \cdot 10^4$), the modified CG method achieves speedup about 10% and the modified BiCG method speedup about 45%. Both speedups increase with the order of matrix.

We consider the following standard techniques: *loop unrolling*, *loop blocking*, *loop fusion*, and *loop reversal*. These transformation techniques are well described and common optimizing compilers support them. We describe a new transformation technique, called *dynamic loop reversal* (or alternatively *outer loop controlled loop reversal*), to improve temporal and spatial locality.

Standard “static” loop reversal

In the standard loop reversal, the sense of the passage through the interval of a loop iteration variable is reversed. This rearrangement changes the sequence of memory requirements and reverses data dependencies, and therefore in general, it allows further loop optimizations. The compiler evaluates the data-dependency and estimate the sense of the passage.

Dynamic loop reversal

In nested reversible loops, the loop reversal can be used in another way.

The sense of the passages of the inner loop can be switched by the loop variable of the closest outer loop (the sense of a passage of the inner loop interval is opposite in even and odd iterations of the outer loop). This is why we call it *dynamic loop reversal*.

If the size of the array is less than the cache size, then both codes are equivalent as to the cache utilization. However, if its size exceeds the cache size, then the last elements of arrays are reused within the second **for** loop and vice versa. This leads to even better temporal locality. On the other hand, the saving of the number of cache misses is bounded by the cache size and the explicit *dynamic loop reversal* can confuse the optimizing compiler and avoid further loop optimizations.

The contribution of this paper is twofold.

- (1) We have applied 2 SW transformation techniques on 2 most common linear solvers to increase the cache hit ratio and improve the performance of them. The speedup is equal to the ratio of eliminated cache misses.
- (2) We have proposed a new code restructuring transformation called *dynamic loop reversal*. This transformation brings new possibilities how to optimize the nested loops.

The authors hope, that this work contributes to development of even effecient optimizing compilers.

References:

- [1] K. R. WADLEIGH, I. L. CRAWFORD: *Software optimization for high performance computing*, Hewlett-Packard professional books, 2000.
- [2] M. WOLFE: *High-Performance Compilers for Parallel Computing* Addison-Wesley, Reading, Massachusetts, USA, 1995.
- [3] M. R. HESTENES, E. STIEFEL: *Methods of conjugate gradients for solving linear systems*, J. Nat. Bur. Stand., pp. 409-436, 1952.
- [4] G. MEURANT: *Computer solution of large linear systems*, Elsevier Science B.V., 1999.

This research has been supported by GA AV ČR grant No. IBS 3086102, by IGA CTU FEE grant No. CTU0409313, and by MŠMT under research program #J04/98:212300014.

Software Cache Analyzer

Pavel Tvrđík, Ivan Šimeček

tvrdik, xsimecek@fel.cvut.cz

Department of Computer Science, Faculty of Electrical Engineering, Czech Technical University, Technická 2, 166 27 Prague 6, Czech Republic

Every modern CPU use a complex memory hierarchy, which consists of levels of cache memories. It is really difficult to predict the behavior of this hierarchy for the given program (for details see [1, 2]). The Cache Analyzer (shortly CA) simulates the behavior of a real microprocessor's cache and compute the number of cache misses during a computation. All measurements are done in the "off-line" mode; the CA uses own virtual cache memory for the exact simulation. It also means that another CPU activity doesn't influence the behavior of the CA.

The cache model we consider corresponds to the structure of L1 - L3 caches on vast of modern memory architectures [1]. The i -th level of cache is *s-way set-associative*, consists of *sets* and one set consists of h independent *blocks*. Let *cb*s denotes the cache block size in bytes. We also assume that the whole cache size is used only for data and that the operand read does not cross cache block boundary.

The CA has many important advantages in comparison to the HW CPU cache monitors:

- The CA is supported on every platform, because the CA is implemented as a C library and can be easily included in every program.
- The measurements are not influenced by other processes due to the "off-line" mode of the measurement.
- The CA can measure effects of memory functions not supported by the CPU core (for example "read once" operation) and can serve for the development of more effective cache hierarchies.
- The user can easily change caches configurations for the measurement by the `#define` statement. Parameters for real processors can be easily included from predefined files.
- The user can measure the cache behavior only in an area of interest.
- The measurements with conditions are supported.
- The "off-line mode" guarantees that small quantities of cache misses can be also exactly measured.

But the CA has also potential drawbacks:

- Read operations in the CA are about 200 times slower than HW memory reads because in the CA are all read (or write) operations simulated by software. This drawback is reduced by the fact that the user can measure the cache behavior only in the area of interest.
- The CA requires the additional memory for its own virtual cache memory.
- Only data caches are assumed not TLB neither other parts of memory architecture.
- Only the numbers of cache misses are measured not effects of these misses (memory latencies or stalls).
- Some cache misses cannot be measured (for example these caused by stack operations in CALL-RET sequences).

- For caches which can hold both data and instructions, the effect of loading instructions into the cache is omitted. This drawback is not usually significant because code-sizes of inner loops are much smaller than data-sizes used by these loops.
- The user must have source code in C language and modify it (explicitly include read operations for the CA).

All results were measured on this HW configuration: Intel Celeron 850 MHz, 256MB RAM, 128 KB L2 cache, 16 KB L1 cache running OS Linux with Intel C compiler version 6.01.

For validation of the CA, we have run some test tasks on this computer including subroutines from linear algebra package (for example codes for the sparse matrix-vector multiplication, the Cholesky factorization, the conjugate gradient method etc.) in 2 forms:

- The original code was measured by the HW cache monitor (performance counters in the IA-32 architecture).
- The modified code was measured by the CA.

We also make the analytical estimation of the number of cache misses (for details see [2-4]).

Results from these tests are almost the same. For sure, they can not be exactly the same, because both measurements and the analytical estimation are inexact in different ways, which are discussed above. For simplicity, we can say that differences between these results were smaller than 5%.

We have implemented a simple cache analyzer to study quantitative parameters of the cache behavior during different types of the computation. We have also discussed advantages and drawbacks of this analyzer. The analyzer has been verified on different types of usual tasks. The results were very similar as these obtained from HW cache monitor.

References:

- [1] K. R. WADLEIGH, I. L. CRAWFORD: *Software optimization for high performance computing*, Hewlett-Packard professional books, 2000.
- [2] K. BEYLS, E. D'HOLLANDER: *Exact compile-time calculation of data cache behavior*, Proceedings of PDCS'01, 2001, pp. 617-662.
- [3] X. VERA, J. XUE: *Efficient Compile-Time Analysis of Cache Behaviour for Programs with IF Statements*, International Conference on Algorithms And Architectures for Parallel Processing, Beijing, 2002.
- [4] P. TVRDÍK, I. ŠIMEČEK: *Analytical model for analysis of cache behavior during Cholesky factorization and its variants*, HPSEC, 2004, pp. 617-629.

This research has been supported by GA AV ČR grant No. IBS 3086102, by IGA CTU FEE grant No. CTU0409313, and by MŠMT under research program #J04/98:212300014.

Possibilities of GPU Computing

Ivan Šimeček

`xsimecek@fel.cvut.cz`

Department of Computer Science, Faculty of Electrical Engineering, Czech Technical University, Technická 2, 166 27 Prague 6, Czech Republic

Plenty of numerical algebra libraries have been developed in recent years. These libraries are tuned for the given CPU and its memory architecture, fully utilize its memory hierarchy and inner pipelines. There is a new trend in the high-performance computing: *GPU computing*. This trend is caused by the surprising fact that the most powerful part of modern Intel PCs is not the CPU, but the GPU. Modern graphic cards (shortly GCs) overcome modern CPUs in the memory bandwidth and possibilities of the vector execution. It results in their surprising floating point performance.

First papers about this phenomena were published 5 years ago, when GPUs (more exactly said: their shader units) became programmable. And many papers were published in last two years [1, 2], because the newest GPUs have an ability for the floating-point computation. The main motivation for the GPU computing is that newest Intel CPU, Pentium IV at 4 GHz, has got peak performance about 16 GFlops in comparison to the newest graphic cards that have got peak performance about 200 GFlops, but prices for the newest CPU and the newest GC are comparable!

There are 3 main reasons of speedup of the computation using the GPU (in contrast to the “normal” computation using the CPU unit):

1. The GC has got memory optimized for the maximal bandwidth. This bandwidth is still the same in the whole memory range and is comparable to the in-cache CPU bandwidth. CPU programs must be optimized by experts to achieve the efficient cache utilization.
2. The SIMD extensions of the instruction set (sometimes called *vector instructions*) for the computation are heavily supported. In contrast to the x86 CPUs, the GPUs allow the indirect addressing during the vectorization. There are more inner GPU pipelines in comparison to the CPU architecture.
3. There is no interaction with other processes. On the other hand, nowadays GPUs cannot be shared in the same way as CPU and its resources.

GPUs are designed for the fast computation of complex 3D frames. The ability of the floating-point computation is only the “side-effect” and it implies many disadvantages:

- There are very limited possibilities of GPUs to control the instruction flow. All conditional branches should be evaluated by the CPU, but it slows down a computation and requires the synchronization between the CPU and the GPU. But there is a simple and inexpensive solution for iterative methods: the GPU computes all required operands, sends them to the CPU by AGP bus and the CPU makes only the decision about the convergence.
- Some FPU operations have no support in GPU's instruction set (i.e. EXP operation).
- All computation should be vectorized to maximize the utilization of inner GPU pipelines.
- To achieve the good performance, minimal data transfers between the main memory and the GC are required. The most often way is to transfer all data on the beginning of

the computation to GC's memory and after the computation, to transfer all data in the reversal way. It is not problematic, modern GCs have sufficient amount of the memory (256 MB or more and this size quickly grows), so all required data can be stored in the GC's memory.

- The compilation process is little confusing, 2-staged. Firstly, the C code is analyzed by the company (ATI or nVidia) compiler and the *inter-code* for given GC is generated. Afterward, from the inter-code is generated the final executable code. The reason for this complicated process is that instructions for AGP bus transfers, whose differ among GPUs, must be generated.
- The optimization process is very complicated, only for experts with deep knowledge of the GPU architecture. For example, GPUs differ in the numbers of general purpose registers and the program for GPU must be explicitly modified in that way. There is a lack of GPU profilers.
- Only nowadays newest GPUs (such that GeForce 6800 or ATI X800) support the type *double* for the floating-point computation. Older GPUs support only type *float*.
- There are great possibilities, but the peak performance is almost unreachable. But this is valid same for the CPU and the GPU computing.

All results were measured on this HW configuration: AMD Athlon 1.4 GHz, 256MB RAM, 128 KB L2 cache, 64 KB L1 cache, AGP 4x, Ati Radeon 9800 Pro. We have used this software for the compilation of our programs: BrookGPU, Nvidia CG compiler, Microsoft DirectX SDK, Cygwin utilities, and Microsoft Visual Studio.

We have implemented two basic routines from numerical linear algebra for the GPU:

- Dot product,
- Matrix-vector multiplication.

The GPU implementation of the dot product subroutine is about 1.5 times faster and the matrix-vector multiplication is about 2.5 times faster than the CPU implementation. Both speedups increase with the order of vectors (matrices).

In this paper, we have compared advantages of the CPU and the GPU computing and discussed the main differences. We have demonstrated possibilities of the GPU computing on subroutines from the linear algebra package. The GPU implementation shows great abilities but we can conclude that the effective implementation of the linear algebra package designed for the GPU is a still great challenge.

References:

- [1] I. BUCK, T. FOLEY, D. HORN, J. SUGERMAN, K. FATAHALIAN, M. HOUSTON, P. HANRAHAN: *Brook for gpus: stream computing on graphics hardware*, ACM Trans. Graph., 2004, 23(3):777–786.
- [2] J. KRÜGER, R. WESTERMANN: *Linear algebra operators for gpu implementation of numerical algorithms*, ACM Trans. Graph., 2004, 22(3):908–916.

This research has been supported by GA AV ČR grant No. IBS 3086102, by IGA CTU FEE grant No. CTU0409313, and by MŠMT under research program #J04/98:212300014.

Semi-sparse Cholesky Factorization

Ivan Šimeček

`xsimecek@fel.cvut.cz`

Department of Computer Science, Faculty of Electrical Engineering, Czech Technical University, Technická 2, 166 27 Prague 6, Czech Republic

The Cholesky factorization (shortly *CHF*) is one of basic methods to solve systems of linear equations (shortly SLEs). A task of the CHF is to compute the matrix L , such that $A=LL^T$. The big advantage of this method is that is possible to solve a set of SLEs with the same matrix A , but with different right hand sides.

A matrix A is considered as *dense* if it contains about n^2 nonzero elements and it is *sparse* otherwise. In practice, a matrix is considered sparse if the ratio of nonzero elements drops below 10%.

If a sparse matrix has the nonzero elements occurring only around the main diagonal, it is *banded*. Banded-like matrices with some "peaks" are called *near banded*.

The process of Cholesky factorization of the originally sparse matrix A leads to the matrix L with new nonzero elements, called *fills* (or *fill-in's*). For the minimal number of fills, special process called *symbolic factorization* is needed. Since this process significantly increases the number of required operations, the efficient computation of the CHF for sparse matrices is a still open research problem.

In this paper, we describe a semi-sparse CHF using optimized dense codes, which can effectively compute the factorization of banded or "near banded" matrices with no need of the symbolic factorization.

There are many storage schemes for sparse matrices (for detail see [1, 2]). Two most common are:

- the CSR format

This format is most suitable for really sparse matrices. But for matrices with the large number of fills, this format is ineffective. For further reading see [3].

- the skyline format

For banded or "near banded" matrices, the skyline format is effective. This format is computed in forward to hold nonzero elements generated during the factorization. This implementation leads to semi-sparse code.

Sparse matrices can be factorized iteratively by dense blocks [4]. The algorithm for this is generalized from the recursive form of the CHF. The using of dense blocks reduces the indirect addressing and eliminates global references. But it also increases the amount of required FPU operations, additional memory and it is appropriate only for matrices which have much smaller bandwidth than the order of matrix. There are two main forms:

- Static: Each block (except the last one) has the same size. This is good solution for banded matrices.
- Dynamic: Block sizes can differ. This is good solution for near banded matrices.

In real cases, the bandwidth is not constant (for example, in the finite element method, "peaks" are caused by a discretization of boundary nodes). But the optimal covering of nonzero elements by this "saw-like" shape seems to be NP problem, so some heuristic are needed.

We have also developed the heuristic for solving this problem. This heuristic has relatively large overhead, so the algorithm tests if this complex heuristic pays off (simply by comparison between the average bandwidth and the maximal one). If the average bandwidth is only slightly smaller than maximal one, much simpler algorithm is used (the static version of the factorization is applied).

Since this iterative algorithm for the CHF does not use any global references to matrix, it can be also used for really huge matrices. In this case, blocks are loaded in serial from the disc and then are stored there eliminated. The main memory must hold only elements in two consequent blocks, because this algorithm uses only local references into these two blocks.

All results were measured on this HW configuration: Intel Celeron 850 MHz, 256MB RAM, 128 KB L2 cache, 16 KB L1 cache running OS Linux Debian with Intel C compiler version 6.01.

Our semi-sparse implementation of the CHF for banded matrices achieves the significant performance improvement (the speedup is about 20 % for small values of order of matrix and about 200 % for large values). This speedup is caused by reducing the indirect addressing and increasing the spatial and temporal locality, for larger values it prevents from disc swapping (caused by global references) during the factorization.

References:

- [1] K. R. WADLEIGH, I. L. CRAWFORD: *Software optimization for high performance computing*, Hewlett-Packard professional books, 2000.
- [2] P. TVRDÍK, I. ŠIMEČEK: *Analytical modeling of sparse linear code*, Numerical Analysis and Applications, Rousse, Bulgaria, 2004, pp. 617-629.
- [3] G. KARYPIS, V. KUMAR: *A fast and high quality multilevel scheme for partitioning irregular graphs*, SIAM J. on Scientific Computing, 20:359–392, 1998.
- [4] S. CARR, R. B. LEHOUCQ: *A compiler-blockable algorithm for QR decompositions*, Proceedings of the Eighth SIAM Conference on Parallel Processing for Scientific Computing, San Francisco, CA, 1995.

This research has been supported by GA AV ČR grant No. IBS 3086102, by IGA CTU FEE grant No. CTU0409313, and by MŠMT under research program #J04/98:212300014.

Radiation and Disturbance Caused by PLC Systems

P. Vančata

vancatp@feld.cvut.cz

Department of Telecommunication Engineering, Faculty of Electrical Engineering, Czech Technical University, Technická 2, 166 27 Prague 6, Czech Republic

Systems of Powerline Communications (PLC) providing broadband communication over energy distributions grids are noting another improvements and boom. There was introduced new chipset in 2004 providing transmission rate 200 Mbit/s. When PLC devices will be equipped with this chipset, PLC technology will be forceful rival to ADSL technology. The only problem of PLC technology in comparison with ADSL is lack of standardization.

This contribution will describe project aimed at problematic of standardization and disturbance in connection with PLC systems. The project was divided into two sections – theoretical and practical.

In theoretical part was created technical report containing summary of existing standards that could be use for PLC systems - international (CISPR), European (ETSI) and American (FCC) standards. There are also introduced proposals of new European standards engaged in frequency band used by PLC systems in process: Nutzungsbestimmung 30 (Germany), MPT 1570 (United Kingdom) and NEDAP (Netherlands). Not only producers of PLC systems who often participate on their development but also the opposite side very carefully watch these proposals. On this side could be found operators using different technologies which could be interfered by PLC technology, broadcasting stations and corporations and last but not least clubs of amateur radio broadcasting. The last mentioned most frequently protested against using PLC technology producing quite strong disturbing electromagnetic field jamming their transmission. As an example of broadcasting company dedicating large attention to problems of PLC technology could be mentioned British Broadcasting Corporation (BBC). The BBC held research about impact of radiation from xDSL and PLC systems on AM broadcasting. This research also look on develop proposals of new standards and its results in all cases was negative – these standards will be not able to provide necessary defence for AM broadcasting.

This report also describes new EU-sponsored Powerline project „OPERA“ for „Open PLC European Research Alliance“ as a part of the larger broadband project „Broadband for All“, started on the 1st January 2004. The OPERA project has an estimated time frame of 48 months divided into two phases, each phase will last 24 months. The European Commission’s long-term goal is to further develop the broadband market in Europe and to stimulate the development of complementary and competitive infrastructures, like Powerline systems, as additional pillars beside DSL and cable access. The OPERA project seeks to develop self-sustaining PLC solutions and it is expected that they will spread out further in next 10 years. This long-term vision covers the following aspects of developing: Multiple PLC solutions and applications will converge into an integrated PLC world and roaming agreements between PLC operators will enable PLC services to end-users in a similar way as mobile services are offered now.

Among other objectives connected with OPERA project belong standardization of PLC technology and definition of the business plan and procedures for network maintenance

and service provisioning. The main goal of OPERA project in standardization area is to specify the requirements of the new PLC integrated network and to drive the PLC standardization to achieve the appropriate acceptance and finally penetration of PLC in the mass market. Besides the cost and price reductions such a standard will provide confidence to the operators. The standard should enable multi-vendor plug and play solutions. The approach is to reach an agreement among all interested parties, i.e. PLC technology providers, electric utilities, telecom operators, developers and manufacturers, with support from universities.

Practical part of this project was concentrate on measurement on Ascom PLC system in EMC laboratory of Department of Telecommunication. Is known that modulated PLC data signal (most frequently is used Orthogonal Frequency Division Multiplex or Gaussian Minimum Shift Keying) could disturb other appliances supplied from the same energy grid or other devices placed close to the PLC devices and energy wiring used for transport of PLC data signal. However PLC systems also could be disturbed by noise over the PLC channel. Very strong impairment for PLC systems is any kind of impulsive noise. Source of impulsive noise could be induction motor, light dimmer, television receiver, fluorescent or halogen light and certain switching power supplies producing interference on the 20 MHz band.

Now will be described two examples of realized measurements on Indoor Adapter APA-45i device of Ascom PLC system. Measurements of voltage dips and short interruptions according to CSN EN 61000-4-11 were performed on simulator MACE, product of Seewart Company and was found out that the APA-45i was able to work properly during very short voltage dips (0,5 and 5 periods) for any of tested dip level. In the case of 30% voltage dips was APA-45 able to work properly in whole range of periods (from 0,5 till 50 periods).

The second example was measurements of disturbing applied voltage according to CSN EN 55022. There were RFT Netznachbildung NNB 11 as artificial power grid and RFT SMV 11 as indicator of radiation with quasi-peak detector. Measurements were performed for all possible configurations of output signal levels and disturbing voltage was measured in three series: from alone device APA-45i, from communication between two devices APA-45i and from communication between two devices APA-45i with use of anti-interference filter. The results showed that communication between two devices produces only a little bit higher level of disturbing voltage then one device alone. Levels of disturbing voltage were sometimes exceeding limits of CSN EN 55022 depending on configuration. The last series proved affectivity of anti-interference filter when level of disturbing voltage was always under limits and its average value was about 42 dB μ V lower then without filter.

References:

- [1] P. VANČATA: *Problematic of Powerline Communication Standardization*, Conference Research in Telecommunication Technology (RTT) 2004, 2004, 0115_0095.pdf
- [2] P. VANČATA, I. BAŽANT: *Powerline Communication - Disturbing and Disturbed*, Conference Research in Telecommunication Technology (RTT) 2004, 2004, 0198_0095.pdf
- [3] P. VANČATA: *Evropský projekt na rozvoj technologie Powerline Communication*, Telekomunikace, 7-8/2004, 2004, pp. 13-17.

This research has been supported by FRVŠ G1 (project No. 2069/2004).

Qualitative Aspects of Image Compression Methods in Multimedia Systems

M. Klíma, M. Bernas, L. Husník, P. Páta, K. Roubík

klima@fel.cvut.cz

*Department of Radioelectronics, Faculty of Electrical Engineering, Czech Technical University, Technická 2, 166 27 Prague 6, Czech Republic

The subjective image quality becomes to be an important item in recent multimedia technology. The multimedia systems deal with images of various qualities from different resources and they have to cope with them. Therefore the subjective image quality and its objectivisation is a crucial question. The research project GA ČR No.102/02/0133 “Qualitative Aspects of Image Compression Methods in Multimedia Systems” has been focused on the evaluation of subjective quality of distorted images. The topic is a typical inter-disciplinary problem overlapping selected image processing and biomedical engineering areas. The subjective image quality has a significant impact on the overall QoS (Quality of Service). The QoS is affected by all parts of multimedia chain – sensing, source coding, channel coding, reproduction and retrieving. The subjective quality is given by a perception of observing subject and the technical parameters are of secondary value.

The project has been split into several directions defining the critical issues. The initial problem was targeted to managing a standard subjective image quality evaluation procedure by a group of observers – standardized by ITU-R Rec. BT.500. The evaluation workplace was established and equipped with the professional TV studio monitor and digital tape recorder. The main aim was to create a database of distorted still images and video sequences with evaluated subjective quality according to BT.500. The selection of test images has differed for still pictures and video sequences. In order to avoid an impact of experience with existing image tests such as LENA we have chosen our own set of images (PORTRAIT, SQUARE, GARDEN, POSTERS and FRUIT), the test video sequences have been chosen among recommended EBU sequences (SUSIE, KIEL HARBOUR, COMMERCIAL, FLOWER GARDEN and TITLES). The still picture tests have been processed by either professional codecs (JPEG, JPEG2000, LuraWave) or by our own image codecs (fractals, KLT). The video sequences have processed by a set of widely used videocodecs of MPEG-4 standard (DIVX, XVID, DICAS, 3IVX, D4, VP6, SORENSON SQUEEZE, QUICKTIME,) H.264/AVC standard (VSS), MPEG-2 standard (TSUNAMI) and codecs WMP 9 and REALVIDEO V9. The subjective quality has been evaluated as a function of bitrate reduction or equivalent compression rate. These subjective data have been statistically processed and consequently approximated (polynomial function, logistic function). Generalized dependencies of subjective quality have been drawn for given test picture/sequence and for given codec. The above mentioned codecs have been compared – the comparison criterion 50% of subjective quality. Altogether we have performed almost 10,000 individual quality evaluations. Each observer has been subjected to eye testing by the Snellen optotype in order to eliminate some observers with significant eye malfunction. After that they have been carefully instructed. We have developed our own methodology of subjective tests (based upon the DSCQS type) according to the BT.500 modified for our laboratory conditions. The test video sequences have been created (test + reference, arbitrary order, grey screen separators with identification) with the continuous quality scale from 0 to 100%.

In such a way we have created the distorted still image / video sequence database with relevant subjective quality evaluation. This database has been applied as a reference for testing of various objective image quality metrics. We have verified a set of generally used objective metrics as MSE, PSNR etc. These distortion metrics are well correlated with the subjective perception for low-level distortions. More accurate and complex metrics are based upon the Human Visual System (HVS) models. Based upon the VQEC results some new original modifications have been developed and tested [2].

Apart of testing of professional image compression packages there have been developed original compression approaches oriented to particular application – compression of scientific image information. We have chosen two directions – astronomical images and security images [3].

The audio codec is another very important part of multimedia coding systems. The audio signal coding techniques are very matured and we have tested some selected compression packages. Our attention has been focused to the newest ones applying the psychoacoustic model for coding procedure optimization. The following codecs have been evaluated: FhG, LAME, MP3Pro, AAC, Ogg Vorbis, WMA [4]. Based upon previous experience the method „Double-blind Triple-stimulus with Hidden Reference” has been chosen with the evaluation scale according to the standard ITU-R BS.1284 and the Basic acoustic Quality BAQ has been evaluated. The test tape with 15 different compressions and three different signals has been created. The testing has been introduced by a training part and the test itself has been divided into three 30 minutes sequences.

There have been studied numerous areas of multimedia information quality under this project. Apart of the image compression the overall QoS of multimedia system is affected also by the sensing (cameras) and displaying devices. The additional processing of audiovisual information has also a qualitative impact e.g. virtual studio, special effects etc.

References:

- [1] M. KLÍMA ET AL: *Research Report of GA ČR Project No.: 102/02/0133, FEL - ČVUT 2005, .*
- [2] J. DUŠEK, K. ROUBÍK : *Simulation of Human Visual Perception Properties Using the Human Visual System Model*, Proceedings of SPIE Vol. 5036, 2002, pp. 204-210.
- [3] P. PÁTA, M. KLÍMA: *Efficient Method for Security Image Data Compression*, Proceedings 37th ANNUAL IEEE International Carnahan Conference on Security Technology. Piscataway: IEEE, 2003, pp. 456-459.
- [4] L. HUSNÍK *Methods of Subjective Evaluation of Sound Codecs Proceedings of Workshop Prague: CTU 2003 pp. 482-483*

This work was supported by the Grant Agency of the Czech Republic under Project No. 102/02/0133 "Qualitative Aspects of Image Compression Methods in Multimedia Systems".

The Research of Copper Pairs Characteristics on High Frequency and their Theoretical Limits for Digital Signal Transmission

J. Vodrážka

vodrazka@fel.cvut.cz

CTU FEE, department of telecommunication technology

Technická 2, 166 27 Praha 6

The metallic access networks have been recently using a variety of technical means that enable fast data transmission. The whole family of such systems is called xDSL. This category covers especially the following systems: ADSL (Asymmetric Digital Subscriber Line), VDSL (Very high-speed Digital Subscriber Line), HDSL (High-bit-rate Digital Subscriber Line) and other similar ones. xDSL systems have attracted attention mainly because data for high bit-rate digital services can be transmitted to the end user along the same transmission path (metallic lines) as employed in POTS (Telephone). These systems are used in the so-called "last mile", i.e. in the metallic section of the line (of the order of kilometres) between the central office and the end user.

The article picks up again systematic research of symmetric metallic pairs, especially of their properties concerning high-speed digital signal transmission (1 Mbps and above). The primary importance of these research results is in their relation to the practical usage of xDSL (Digital Subscriber Line) systems, which are widely applied in access networks.

The function of the xDSL system is mainly affected by the line attenuation (line length, wire diameter and type of insulation) and by cross-talk (NEXT, FEXT), which constitute the greatest problem of broadband signals. The cross-talk is the main limiting factor and determinates duplex method of transmission too. The article [1] enlarges on effects of crosstalk for digital transmission, error rate and compares theoretical capacity with practical data rates at VDSL line.

The values of cross-talk differ in dependence on the mutual position of pairs. The strongest couplings exist between pairs of the same quad and between pairs of adjacent quads. The weakest couplings exist between pairs in remote subgroups. The selection of pairs with lower cross-talk couplings in cables is becoming problematic and even insoluble with the increase in broadband digital systems. Moreover, deploying xDSL does not mostly mean adding a system on an available line but extending the existing access line, which has its position in the cable. Allocation of bands for transfer directions downstream and upstream and with it the total width of the band, is dependent on the ADSL variant given by the ITU-T standard [2]. According to the recommendation of the ITU-T G.992.1 today's systems use a frequency band of up to 1.104 MHz. The lower part of the spectrum is of course used for telephone channels and for this reason it counts on the coexistence of ADSL in one conduit with the original analogue telephone connection (ADSL/POTS), which is preserved thanks to separation filters (adapter, splitter). Apart from this, ADSL can also coexist with the basic ISDN-BA connection (ADSL/ISDN).

The variation without an adapter (ADSL splitterless or also ADSL lite) according to recommendation by ITU-T G.992.2 uses a frequency band with half the upper boundary frequency of 552 kHz. Duplex transfer is ensured either by FDD frequency division (Frequency Division Duplex) or with frequency overlap of the upstream and downstream bands with division using an EC coil with suppressed echoes (Echo Cancellation).

The VDSL (Very high speed DSL) line [2], [3], according to the recommendation ITU-T G.993.1, is designed for the final section of the subscriber line, running for between 0.3 km and 1.5 km. Thanks to the expansion in the band to up to 12 MHz, the downstream transmission speed is up to 52 Mbps, and upstream 8 Mbps, with asymmetric transmission speeds.

A symmetric regime with the same transmission speeds in both directions of transmission can also be used. The technical solution is based on ADSL, including co-existence with an analogue telephone or ISDN connection with the help of splitters. VDSL also uses the FDD method only. Schematic development of VDSL consisting of a duplication of the upper boundary of the frequency is a perspective variation for shorter lines with a higher transfer speed.

The determination of duplex method results from different frequency dependence of crosstalk NEXT and FEXT. The results are dependence especially on the line parameters, length of the line and frequency. Other types of xDSL systems use other methods for duplex transmission: the HDSL and SHDSL use hybrid with echo cancellation (EC), the VDSL use frequency division duplex (FDD) and the ADSL use both of one.

On local cables in access networks, systems with different line signals are generally operated. Interaction of systems of different types - Interaction occurs in the frequency band where power spectral densities overlap. Both NEXT and FEXT must be considered in the respective band.

The use of physical xDSL for Ethernet transfer is a very perspective area. The IEEE 802.3ah EMF group bears the marking Ethernet in the First Mile in its name, the task of which was to create a concept and standards for the solution of high-speed access based on an Ethernet interface. EMFC plans count on the fact that at greater distances than can be spanned by VDSL, the SHDSL system will be set up. If higher transfer speed is required, a greater number of pairs can be used, among which the required digital flow will be shared. The concept stated is a reaction to the decrease in interest in analogue telephone connections and the freeing up of pairs in cables connected with this, which can then be used in a multiple manner for high-speed data transfer. Of course while respecting the rules for spectrum management in cables.

References:

- [1] VODRÁŽKA. J.: *Cross-Talk is Determinant of Duplex Method*, In RTT 2004, CTU, Faculty of Electrical Engineering, Department of Telecommunications Engineering, 2004, pp. 0102_0005.
- [2] VODRÁŽKA. J.: *Evolution of ADSL and VDSL Lines*, In RTT 2004, CTU, Faculty of Electrical Engineering, Department of Telecommunications Engineering, 2004, pp. 0101_0005.
- [3] VODRÁŽKA. J.: *Evolution of VDSL Subscriber Lines*, In COFAX-TELEKOMUNIKÁCIE 2004. Bratislava: D&D STUDIO, 2004, pp. 325-326.

This research has been supported by GA ČR grant No. GA 102/01/D116.

Load and Memory Balancing of Parallel Envelope Solver of Large Sparse Linear Systems of Equations

Ondřej Medek a Pavel Tvrđík

xmedeko@fel.cvut.cz, tvrdik@fel.cvut.cz

Department of Computer Science and Engineering, Faculty of Electrical Engineering, Czech Technical University, Karlovo náměstí 13, 121 35 Praha 2, Czech Republic

Many engineering and scientific problems, e. g., those solved by the finite element method (FEM), lead to a large sparse symmetric system of linear equations (SSSLE). If memory capacity or computing performance of a single CPU are not sufficient for solving the SSSLE, then parallelization must be used. We use the SIFEL solver (<http://cml.fsv.cvut.cz/~sifel>) developed at the Czech Technical University, Faculty of Civil Engineering, Department of Structural Mechanics. Among others, it can solve SSSLEs in parallel by the envelope method using the Schur complements. A solution of a problem consists of the 6 following phases:

1. Domain decomposition.
2. Ordering of variables.
3. Assembling of submatrices.
4. Factorization of submatrices (computation of the Schur complements).
5. Solution of the reduced problem.
6. Back substitution in submatrices.

A domain decomposition (Phase 1) of a problem is performed using a graph partitioning. It results in sparse submatrices. An envelope method is used to store these submatrices in the memory and to factorize them. Prior to the solution, the variables of each submatrix are reordered (Phase 2) by the Sloan algorithm to minimize qualities: memory requirements to store the submatrices and the time of the factorization (Phase 4). The submatrices take most of the memory of the solver and their factorization is the most computationally intensive part of the solution.

Our work focuses the first two phases: the domain decomposition and the reordering. They represent as preprocessing in the SIFEL solver. The domain decomposition is performed by the multilevel k -way graph partitioning. As was already observed in [1], a classical domain decomposition decomposes the problem, so that the numbers of variables in the resulting submatrices are roughly equal, but their qualities are disbalanced. Disbalancing of the memory requirements may lead to a crash of the solver on a distributed parallel machine with a limited amount of memory on each processor. The disbalancing of the factorization times increases the execution time of the solver, because the solution of the reduced problem (Phase 5) cannot start before all submatrices are factorized.

To balance the qualities, we have recently developed Quality Balancing (QB) heuristics [2]. The QB heuristics balances estimates of the chosen quality, either memory requirements or the factorization time of submatrices. Since the qualities strongly depend on the ordering of the variables, the QB heuristics incorporates the reordering algorithm into the multilevel k -way graph partitioning schema. The multilevel k -way graph partitioning is based on moving subsets of vertices among the partitions (which correspond to the domains). The QB heuristics after each move recomputes the estimations of qualities of the affected partitions. Prior to the computation of the estimations, the variables in the affected partitions

are reordered. This significantly slows the domain decomposition phase. Therefore the QB heuristics is contributive in the following cases.

1. The decomposition is performed repeatedly. For example, during the solution of nonlinear problems a solver iterates several thousand times using the same decomposition.
2. A SSSLE is solved on a distributed parallel machine with a limited amount of memory per node. Then a submatrix that needs significantly more memory than the other ones, can lead to the crash of the whole solver, whereas a decomposition with balanced memory requirements passes successfully.

The Sloan algorithm was originally designed for serial solvers. During our work with the parallel solver we have developed a new variant, called Boundary Sloan Algorithm (BSA) [3], more suitable for parallel solvers. We have shown on a wide class of benchmarks that the BSA saves in average 15% of memory needed to store the submatrices and 25% of floating point operations (FLOPS) during their factorization.

Finally, we have incorporated the BSA into the QB heuristics. We have shown in [4] that the BSA outperforms the classical Sloan algorithm in terms of a) optimality of balancing, b) minimizing the qualities, and c) running time of the QB heuristics.

References:

- [1] HENDRICSON B.: *Load balancing fictions, falsehoods and fallacies*, Applied Mathematical Modelling 25, 2000, pp. 99-108.
- [2] MEDEK O., TVRDÍK P., KRUIS J.: *Load and Memory Balanced Mesh Partitioning for a Parallel Envelope Method*, EuroPar 2004 Parallel Processing Lecture Notes in Computer Science 3149, Springer, 2004, pp. 734-741.
- [3] MEDEK O., TVRDÍK P.: *Variable Reordering for a Parallel Envelope Method*, Proceedings of the 2004 International Conference on Parallel Processing Workshops, IEEE Computer Society Press, 2004, pp. 254-261.
- [4] MEDEK O., TVRDÍK P.: *Quality Balancing Heuristics with Three Variants of Sloan Algorithm*, Parallel and Distributed Computing And Networks, part of the Twenty-Third IASTED International Multi-Conference on Applied Informatics, 2005, accepted.

This research has been supported by IBS3086102 grant of the Czech Academy of Sciences, by CTU0409113 grant of the Czech Technical University, and by MŠMT under research program \#J04/98:212300014. We would like to thank to Jaroslav KrUIS for providing the SIFEL solver.

Placement and Routing for Dynamic Reconfiguration of FPGAs

Martin Daněk, Jiří Kadlec, Rudolf Matoušek

danek@utia.cas.cz

Institute of Information Theory and Automation of the Academy of Sciences of the Czech Republic, Pod vodárenskou věží 4, 182 08 Praha 8, Czech Republic
Department of Computer Science and Engineering, Faculty of Electrical Engineering, Czech Technical University, Karlovo nám. 13, 121 35 Praha 2, Czech Republic

Introduction: Although runtime dynamic reconfiguration of the FPGA devices has been an issue of the last decade, it has yet to achieve general recognition by the design community. The reasons for this are clear; there exists no straightforward design methodology, and the partitioning and CAD tool support is poor. The text below summarizes general concepts that must be addressed in a new generation of placement and routing algorithms to provide optimal implementation of designs with partial dynamic reconfiguration.

Design issues: Partial dynamic reconfiguration means that the FPGA holds only those parts of user logic that are required at a given time to fulfil the desired function. The parts of logic that are not always required are usually denoted as the *dynamic part*; this logic can be loaded to or unloaded from the FPGA as needed. The part of user logic that must always be present and running is denoted as the *static part*. The static part is handled in the same way as current designs that do not use dynamic reconfiguration, and it requires no special coding style or other treatment.

The dynamic part usually consists of several so-called *dynamic modules* (or d-modules) that are declared as VHDL entities and specified as VHDL instances in the static part. Each instance corresponds to one d-module and is represented by one EDIF file. A dynamic module represents a portion of user logic that can be missing in certain FPGA configurations. On the level of placement and routing this translates to alleviation of the placement and routing constraints, since certain blocks can remain unplaced and nets unrouted without yielding an invalid placement and routing of the design.

A special case of dynamic logic deserves further attention when a design contains several dynamic modules that have the same input and output ports (interface), and that are used exclusively at different design contexts (FPGA configurations). Since such groups of logic can be viewed as a user macro (VHDL instance) with different logic functions at different contexts, we denote them as *supermacros* (or smacros). A supermacro can be viewed as several dynamic modules with inputs connected in parallel and outputs connected through a multiplexer. Each supermacro is specified by one VHDL instance and represented by several EDIF files (i.e. VHDL entities) that have identical input and output ports.

Synthesis issues: Compared to the classical VHDL design the use of dynamic reconfiguration brings new requirements on synthesis of user macros. The designs are usually synthesized as several independent user designs that are packed together during placement and routing, i.e. when all valid FPGA configurations must be assembled to produce valid configuration bitstreams. There are two main synthesis issues: net connectivity, and preservation of macro ports.

Net connectivity is the most critical problem that arises in the last, most complex situation. The problem is that the user assumes that an input in the static part connected to the output in 194

the static part should always remain connected no matter which dynamic modules are present on the FPGA. This is not usually the case, since during reconfiguration current placement and routing tools remove all nets that have at least one port in the dynamic part.

Net connectivity can be analysed according to the following situations: a situation where an output in the static part feeds inputs in the dynamic part, a reverse situation where an output in the dynamic part feeds inputs in the static part, and the last situation being a mix of the former two where an output in the static part feeds both an input in the dynamic part as well as the static part. The problem arising in the first situation is where the actual net branching occurs (i.e. in the static or dynamic interconnect).

The problem with the last situation is that during reconfiguration or in contexts where the output is not present on the FPGA the inputs in the static part are floating, i.e. their value is not defined. This problem must be solved on the synthesis level, for example, by using an interface buffer in the static part that will be enabled only when the corresponding dynamic logic is present.

Macro ports: The problem with user macros is that they are processed in two steps: the first step defines the macro contents and its ports (dynamic logic), the second step connects the macro ports to the top-level design (static logic). A problem occurs when some logic in the macro is optimized away or replaced with a constant value during synthesis, i.e. some ports are completely omitted and some are joined by a common signal net. Since the top-level (i.e. static) design must be synthesized as a separate design, it uses the macro instantiated as a black-box component, which preserves all the interface inputs and outputs. On the other hand, when synthesizing the macro, its interface ports are generated to reflect the actual inputs and outputs used by the macro logic. When integrating together such a macro with the top-level design during mapping, placement and routing, current placement and routing tools find an inconsistency between the static and dynamic part connections and generate an error. This usually does not happen in classical modular designs, since the design flow is the other way round, i.e. the user first defines all macros, gets their post-synthesis interface definitions, and instantiates them as black-box components in the top-level design. There is also no need to unify interfaces of different user macros as is the case with reconfigurable supermacros.

A systematic solution to these problems requires a new approach to logic synthesis and routing. At present, a viable workaround is to preserve all defined entity ports used in user macros, and to transform all connections with mixed inputs and outputs in the static and dynamic part to connections with no direct "static input to static output" connections. This can be easily done by the use of interface buffers generated in a core generator, instantiated as black-boxes in the top-level design as well as in each dynamic module used.

References:

- [1] NASI, K. – DANĚK, M. – KAROUBALIS, T. – POHL, Z.: *Figaro - An Automatic Tool Flow for Designs with Dynamic Reconfiguration*. To appear in: *FPGA2005* The ACM Press 2005
- [2] *The RECONF2 project web page - <http://reconf.org>* RECONF2 2002

This research has been supported by IST-2001-34016 and GA102/04/2137.

Bypass Routing in Survivable Trees

V. Dynda

xdynda@sun.felk.cvut.cz

Department of Computer Science and Engineering, Faculty of Electrical Engineering
Czech Technical University, Karlovo náměstí 13, 121 35, Praha 2, Czech Republic

A *survivable tree* is an overlay tree-topology communication structure capable to deliver messages in a timely manner to all its correct member nodes even in the presence of failures ([1]). It employs a failure recovery scheme supposed to reconnect all the fragments of the failed tree (completeness) and avoid creating cycles in the restored graph (correctness). For this purpose, we have proposed preplanned *bypass ring scheme* [2], [3] based on redundant backup cyclic structures. In this text we outline how these structures, called *bypass rings*, are arranged in the tree and used to route among individual tree fragments in order to deliver messages to all the fragments and thus ensure completeness of the recovery process.

Let $T = (N, L)$ be a tree network, N set of its nodes and L set of overlay edges. Failure in T is a simultaneous failure of nonempty set FC of adjacent nodes from N . Failure of FC causes the tree to be partitioned into fragments T_i ; $i = 1, 2, \dots, \text{card}(A_T(FC))$, where $A_T(FC)$ is a neighbor set of FC in T . The task of the *bypass routing* is to route messages among the fragments, i.e. among $A_T(FC)$ nodes neighboring with FC in a uniform direction and order so that the subsequent steps of the recovery (leader link election and fragment reconnection) can take place. Therefore, at each $A_T(FC)$ node, the bypass routing must find the next $A_T(FC)$ node to send a message to using bypass ring edges and thus create a *bypass cycle* $BC_T(FC)$ – cyclically ordered $A_T(FC)$ nodes surrounding the failure.

The concept of bypass rings is based on *partial order* defined in the overlay tree network. T is partially ordered if for every node $n \in N$ there exists a unique ordering $n_0, n_1, \dots, n_k \in A_T(n)$, $k = \text{deg}_T(n) - 1$ ($\text{deg}_T(n)$ is degree of the node in T) of its tree neighbors according to some attribute (e.g., node identifiers). $\text{seq}_T(n) = n_0, n_1, \dots, n_k$ is called ordered neighbor sequence of n in T . The partial ordering defines direction and arrangement of nodes in the tree; further we suppose the tree to be drawn as a planar graph such that $\text{seq}_T(n)$ of each node follows clockwise direction.

Each bypass ring constituted in tree T , denoted $BR_T(n, d)$, is specified with its center node n and diameter d and it consists of $\text{deg}_T(n)$ bypass edges connecting individual tree branches – potential tree fragments of the center node. The bypass edges are constructed between each two center node branches $B_T(n, n_i)$ and $B_T(n, n_{i+1})$ neighboring in $\text{seq}_T(n)$ such that the initial node of the edge is located on the rightmost path (edge of the branch called *negative ordered ray*) of the left branch in the distance $\lfloor d/2 \rfloor$ from n and its terminal node is located on leftmost path (*positive ordered ray*) of the right branch in the distance $\lceil d/2 \rceil$ from n .

Bypass rings of diameters $1, 2, \dots, d_{\max}$ centered at the same node form a bypass framework $BF_T(n, d_{\max})$ protecting the tree against failure of its center node. To protect the whole tree and to allow for a multiple failure recovery, it is possible to build the framework around every node in the tree. The bypass ring edges connecting branches of every node in the tree allow the bypass routing algorithm to route between branches of a given center node using its rings and use rings of lower diameters centered in particular branches to route through that branches (from the viewpoint of the center node), while preserving the direction.

Supposing that bypass frameworks $BF_T(n, d_{\max})$ are set up around each node $n \in N$, there are d_{\max} bypass edges initiated at each node terminating at nodes in increasing distances (up to d_{\max}) on the positive ordered ray of each of the node's branches, which is an essential

fact for the bypass routing as these edges are used for the branch lookup in searching for the next fragment on $BC_T(FC)$. The routing itself is based on the fact that each faulty cluster is an intersection of the respective tree branches of the nodes neighboring with the cluster, i.e. $\langle FC \rangle_T = \cap B_T(n_i, n_j)$ for all $n_i \in A_T(FC)$, where $n_j \in A_T(n_i)$, $n_j \in FC$.

At each node n_i neighboring with FC , the routing algorithm systematically browses its only tree branch containing the failed nodes using the bypass edges initiated at n_i to find the next node neighboring with FC , node n_{i+1} , which is the next on the bypass cycle. The branch lookup is performed sequentially by checking nodes in increasing distance on the positive ordered ray of the branch (enabled by existence of bypass edges) until the first alive node, n_{i+1} , is not found. The sequence of checked nodes is kept for further use by leader link election.

The same algorithm is used at each of $A_T(FC)$ nodes and together with the partial ordering of the tree it ensures unambiguous ordering of these nodes, i.e. creating the bypass cycle $BC_T(FC)$ around the failure FC and thus allowing further recovery messages to be uniformly exchanged among tree fragments in an effort to restore the tree.

The proof of completeness of the algorithm is based on constructing a rooted vertex-induced subgraph $\langle FC \cup A_T(FC) \rangle$ with an arbitrarily chosen root node $n_r \in A_T(FC)$. The completeness can then be shown by systematical browsing this rooted tree hierarchically according to the partial order which corresponds to the lookup along the positive ordered ray of the respective branch at each $A_T(FC)$ node. However, the bypass routing is not successful in all cases, as d_{max} is a finite number so the constructed bypass frameworks may not be sufficient for recovery of greater failures as the respective bypass edges needed for branch lookup do not exist. It can be shown that the routing is successful only if $dist_T(n_i, n_{i+1}) \leq d_{max}$ for every two $A_T(FC)$ nodes neighboring on $BC_T(FC)$. This follows from the fact that each bypass edge of ring $BR_T(n, d)$ spans $d-1$ tree nodes (by definition) and thus the distance from its initial to its terminal node in T is d . Therefore, the longest bypass edges of rings of diameter d_{max} can be used to route to node (fragment) in distance d_{max} in tree T .

The space complexity of the bypass routing at each node is $O(deg_T(n) * d_{max})$ as each node maintains d_{max} bypass edges for each of its $deg_T(n)$ tree branches. The total work spent by the bypass routing to route a message around FC is $O(card(FC) * avgdeg_T(FC))$, where $avgdeg_T(FC)$ is average degree of nodes in FC .

In this text, we have briefly described the concept of bypass routing in survivable trees, which is based on bypass rings – overlay cyclic backup paths and partial order of the protected tree. We have described the arrangement of the rings and their application in the routing. The routing is complete, supports local failure recovery (involves only failure neighboring nodes) and its feasibility for a given failure depends on d_{max} parameter that can be used to achieve a trade-off between fault-tolerance and complexity of the routing.

References:

- [1] DYNDÁ, V.: *A Concept of Survivable Trees and its Deployment in a Fault-Tolerant Multicast*, Workshop 2004, ČVUT Praha, 2004, pp. 234–235.
- [2] DYNDÁ, V. – RYDLO, P.: *Fault-Tolerant Data Management in a Large-Scale File System*, IEEE ISADS 2002, UDG Guadalajara, Mexico, 2002, pp. 219–235.
- [3] DYNDÁ, V.: *A Simple Scheme for Local Failure Recovery of Multi-directional Multicast Trees*, LNCS 2869, Springer-Verlag, 2003, pp. 66–74.

BR(r) Scheme for Tree Failure Recovery: Applications

V. Dynda

xdynda@sun.felk.cvut.cz

Department of Computer Science and Engineering, Faculty of Electrical Engineering
Czech Technical University, Karlovo náměstí 13, 121 35, Praha 2, Czech Republic

BR(r) scheme for tree failure recovery [1] is a preplanned recovery scheme designed for recovery of *survivable trees* [2] from node failures. The recovery is based on redundant backup cyclic structures, used to reroute the traffic in case of failure and connect the tree fragments. In this paper, we introduce parameterization possibilities of the recovery process that can affect effectiveness of the recovery, optimize the restored tree and even enable operation of the scheme in various classes of applications.

Let assume a protected overlay survivable tree to be modeled as a graph $T = (TM, CE)$, where TM is set of nodes and CE set of core tree edges connecting the nodes. The BR(r) scheme operates in several steps ([3]). First, bypass frameworks – the preplanned cyclic structures needed for routing of recovery messages in case of failure are built and the scheme is *initialized*. When a failure of a set of adjacent nodes $FC \subset TM$ occurs and is detected by nodes neighboring in T , the *designated nodes discovery* (DN discovery) is performed using *bypass routing* mechanism that locates the tree fragments and routes messages cyclically among them through failure neighboring nodes $A_T(FC)$. The DN discovery process identifies one or more *designated nodes* $DN(FC) \subseteq A_T(FC)$ with specific attributes depending on properties of the tree and requirements of the application. These nodes initiate *fragment reconnection* and coordinate the rest of the recovery process. Fragment reconnection is a process of constituting new core tree edges connecting the fragments into a single restored tree and it is based on results of simultaneous *leader link election* (LLE) designed to avoid creating cycles of core edges during the reconnection. The final step of the recovery consists of bypass framework *reconfiguration* according to the changes in the tree topology.

Particularly DN discovery and fragment reconnection step can be adjusted or parameterized specifically for different applications. The application classes are derived from properties of the trees that the scheme is employed to protect. We can distinguish these trees: (A) *undirected trees*, (B) *single-source or rooted directed trees* and (C) *multiple-source trees*. Class A using undirected trees represents the most common type of applications with straightforward operation including some simple overlay multicast systems, loosely-coupled peer-to-peer systems or some on-line games. Class B involves content-distribution systems, divide & conquer computations, multicasting, replication with consistency management based on primary replica or hierarchical data-storing structures. Class C, multiple-source tree, is employed in large-scale file systems and peer-to-peer data sharing systems.

Selection of designated nodes is an important process that differs in each application class since any possible sequence of the new core tree edges connecting the fragments constituted by fragment reconnection always begins at the designated node and it is necessary to keep correctness of the reconnection, i.e. the possible orientation of the edges and mutual logical relationship between fragments from the point of view of tree direction has to be preserved in the restored tree. DN discovery is initiated at each node detecting the failure by sending *DNDISCO* message to other fragments organized in *bypass cycle* $BC(FC)$ by the bypass routing algorithm. The message is transmitted along the cycle until it reaches another discovery initiating node. At each intermediate node, attributes of the node are examined in order to identify the node to be one of the designated nodes.

The examined attributes can be either special-purpose properties specified by the application or tree-related properties. To achieve a correct operation in each type of the tree, the tree-related properties are relevant, particularly the orientation of the core tree edges incident to the node. Just elementary DN discovery is performed in applications of class A, where either each node detecting the failure is the designated node and DN discovery is not performed at all or DN discovery is performed and it identifies each node on $BC(FC)$ to be a designated node, i.e. $DN(FC) = A_T(FC)$.

The situation becomes a bit more complicated in applications of class B as each new core edge created by the fragment reconnection is required to be oriented towards the *common parent node* on $BC(FC)$ (the bypass cycle node closest to the root) so that there is a path from root to each fragment (or vice versa, depending on the particular orientation of the tree). The common parent node, say n_p , is to be found by the DN discovery. Upon receiving the *DNDISCO* message at each node $n_i \in BC(FC)$, a simple test is performed: if the core edge connecting n_i with its only failed neighbor node n_f from FC , $n_f \in FC$, is incident from n_i to n_f , then $n_i = n_p \in DN(FC)$, otherwise $n_i \notin DN(FC)$. In single-source trees, there is always only a single designated node, $card(DN(FC)) = 1$, thus the *DNDISCO* is terminated at n_p . In multiple-source trees, class C, the test is the same, the only difference is that there might be multiple designated nodes on $BC(FC)$, i.e. $card(DN(FC)) \geq 1$.

After the discovery of the designated nodes the LLE process together with the fragment reconnection is launched. The fragment reconnection itself does not depend on the particular class of the application; the fragments are connected with core edges sequentially from each designated node respecting results of LLE. The basic reconnection approach, *LR method*, simply connects fragments on $BC(FC)$ linearly, increasing diameter of the restored tree, while keeping degree of bypass cycle nodes as low as possible. Parameterized *HR-x reconnection method* allows choosing a trade-off as it creates the core edges (n_0, n_i) if $i \equiv 1 \pmod{x}$ or (n_{i-1}, n_i) otherwise, where x is a parameter, $1 \leq x \leq N$, $N = card(A_T(FC))$ is number of fragments, and n_0, n_1, n_2, \dots is numbering of nodes on $BC(FC)$ such that n_0 is a designated node and n_1, n_2, \dots are the subsequent, not yet connected nodes on the bypass cycle up to the leader node determined by LLE. Minimum diameter of the area of the tree recovered using *HR-x* method equals to $\min(2x, N-1)$ and maximum number of new core edges incident to a single $BC(FC)$ node is $\min(\lceil (N-1)/x \rceil + 2, N-1)$. Hence, by choosing an appropriate value of x , it is possible to minimize message delay in the restored tree while meeting bandwidth constraints imposed by the physical network or the application.

We have described variants of designated node discovery and fragment reconnection in $BR(r)$ failure recovery scheme in three elementary classes of applications and shown that they affect the recovery process and its results according to the application requirements.

References:

- [1] DYND, V.: *A Bypass-Ring Scheme for a Fault-Tolerant Multicast*, Acta Polytechnica, vol. 43(2), ČVUT, 2003, pp. 18–24.
- [2] DYND, V.: *A Concept of Survivable Trees and its Deployment in a Fault-Tolerant Multicast*, Workshop 2004, ČVUT Praha, 2004, pp. 234–235.
- [3] DYND, V.: *BR(r) Scheme: A Solution for Survivable Trees*, Workshop 2004, ČVUT Praha, 2004, pp. 236–237.

Fragment Reconnection in Failed Partially Ordered Trees

V. Dynda

`xdynda@sun.felk.cvut.cz`

Department of Computer Science and Engineering, Faculty of Electrical Engineering
Czech Technical University, Karlovo náměstí 13, 121 35, Praha 2, Czech Republic

Partially ordered trees are tree-topology graphs where neighbor vertices of each vertex in the graph are uniquely ordered by some criterion. Overlay tree-topology communication networks (e.g., overlay multicast systems for content distribution) can be modeled as partially ordered trees with the order defined by identification or address of their nodes. When a failure of one or more adjacent nodes occurs in these networks, the tree is partitioned into several fragments. It is a goal of a distributed fault-tolerant scheme to reconnect the fragments into a connected graph keeping an elementary property of correctness – the fragments must be reconnected such that a new graph is a tree, i.e. no cycles are created.

In this text, we outline an efficient method for a distributed fragment reconnection exploiting properties of partially ordered trees and an additional knowledge of arrangement of the failed cluster of tree nodes [1]. The solution is a part of bypass ring scheme [2] designed for tree failure recovery of large-scale peer-to-peer systems [3].

Let suppose a tree graph $T = (V, E)$ with set of nodes V and set of edges E ; *partial order* in T is defined by means of unique nodes identifications $ID(n)$, $n \in V$, such that $seq(n)$ is a sequence of neighbor nodes of n , $A(n)$, ordered by their IDs. When a failure of several adjacent tree nodes $F \subset V$ occurs, the tree is partitioned into N fragments, where $N = card(A(F))$ is a number of tree nodes neighboring in T with F . Let assume further that all these N fragments are organized by a failure recovery scheme into a virtual cycle $C(F) = (A(F), BE)$, where $A(F)$ is set of nodes neighboring with F and BE is set of backup edges (a knowledge) cyclically connecting the nodes according to the partial order.

The objective of the fragment reconnection is to connect the fragments ($A(F)$ nodes) so that no cycle is created, i.e. select a single edge $e \in BE$ to be a *leader* not participating in reconnection; all other backup edges are used to connect the nodes on $C(F)$ in the restore tree. The problem can be transformed to election of a leader node; the leader edge is then the backup edge incident to the elected node. $C(F)$ is the only communication structure for the election. The problem of the edge election in this arrangement is called *circular LLE problem*.

Our solution is based on the famous *Chang-Roberts algorithm* for extrema-finding in circular configuration of processors where each node running for election sends an *ELECTION* message with its identification. On receiving *ELECTION* message, each node compares the received ID with its own ID and if they are equal, it announces itself as a leader. Otherwise it sends *ELECTION* message with the higher of the IDs further along the cycle. The favorable property of Chang-Roberts is a linear message complexity provided that the nodes on the cycle are ordered, which can be profitably exploited in partially ordered trees.

Due to the characteristics of the problem and to ensure required properties of the whole failure recovery, particularly on-line and on-the-fly restoration, the LLE problem is designed to behave differently from the standard leader election so that once a link loses the election, it remains lost until the next failure in the tree and that there is not a state of the algorithm in which there is no leader (i.e., all the fragments might be connected); initially all the BE edges are leaders that are gradually eliminated until a single leader remains. Moreover, the result of the election at each $C(F)$ node should be known as soon as possible.

Provided that only a single failure occurs, i.e. $card(F) = 1$, $F = \{n_j\}$, the LLE is straightforward as $A(F) = seq(n_j)$ and thus $A(F)$ nodes on the cycle $C(F)$ are ordered. Using

ELECTION messages similarly to Chang-Roberts, we can elect the leader within a constant time (provided that all the nodes run for election) using exactly N messages. This is a significant achievement considering the fact that single failures are the most probable in overlay systems.

The LLE problem becomes more complicated when a multiple failure occurs, i.e. when $\text{card}(F) > 1$, as $A(F)$ nodes are not ordered in such a case. The relative order of $C(F)$ nodes is achieved by *hierarchical identifiers* that uniquely identify each node relatively to another node in the tree. Using this construct, it can be shown that leaves of an arbitrary partially ordered rooted tree are ordered ‘per partes’ according to hierarchical identifiers based in their common parent node. Therefore, if there is a common root node $n_r \in F$, $A(F)$ nodes are leaves of the vertex induced subgraph $\langle F \cup A(F) \rangle$ of T and they are ordered in $O(\text{card}(F))$ parts at most. Using $N = \text{card}(A(F))$ *ELECTION* messages in the same way as before, one or more (up to $O(\text{card}(F))$) leaders are elected. These leaders (but one) are thereafter eliminated by a recursive *sweep process* considering hierarchical identifiers based in n_r .

The root node n_r common for $C(F)$ nodes is a faulty node with the minimum identifier. As there is no initial knowledge of the structure and arrangement of the failed cluster F , the node n_r is not known immediately at the beginning of the election. Instead, it is determined together with the respective hierarchical identifiers step by step by the routing algorithm that routes *ELECTION* and *SWEEP* messages between $A(F)$ nodes along the cycle $C(F)$. The routing algorithm systematically checks aliveness of nodes in F and keeps track of it such that a hierarchical identifier of the relevant $A(F)$ nodes based in the faulty node with the minimum known ID can be computed. Finally, the n_r node is learned and only a single leader corresponding to $\text{seq}(n_r)$ remains; other leaders inside tree branches of n_r are swept.

The additional knowledge of the failed cluster structure is exploited to reach $O(N \log_b N)$ average message complexity in a general case in partially ordered trees, where b is the average branching factor in F . Reconnection of fragments caused by a single failure needs only N messages. The same holds true even for fragment reconnection in rooted hierarchically ordered trees (a special case of partially ordered trees, e.g. binary search trees). The time complexity of LLE is $O(N)$.

The LLE algorithm is designed so that the fragment reconnection can be performed simultaneously with the leader election. Once a backup edge connecting two fragments is determined not to be a leader, the fragments are connected together and traffic may go on. We have also developed a more sophisticated method for fragment reconnection ([1]) based on LLE that takes into account also delay and/or bandwidth requirements of the recovered tree.

References:

- [1] DYNDA, V.: *A Bypass-Ring Scheme for a Fault-Tolerant Multicast*, Acta Polytechnica, vol. 43(2), ČVUT, 2003, pp. 18–24.
- [2] DYNDA, V.: *A Simple Scheme for Local Failure Recovery of Multi-directional Multicast Trees*, LNCS 2869, Springer-Verlag, 2003, pp. 66–74.
- [3] DYNDA, V. – RYDLO, P.: *Fault-Tolerant Data Management in the Gaston File System*, Wirtschaftsinformatik 45/3, Friedr. Vieweg & Sohn, 2003, pp. 273–283.

Two-dimensional Pattern Matching

T. Polcar, B. Melichar

polcart@fel.cvut.cz

Department of Computer Science and Engineering, Faculty of Electrical Engineering,
Czech Technical University, Karlovo nám. 13, 121 35 Prague 2, Czech Republic

Two-dimensional pattern matching is a generalization of classical one-dimensional pattern matching into two dimensions. Basically, it is defined as a searching for all occurrences of a rectangular pattern in a rectangular text. As well as in one-dimensional case, this definition of the exact two-dimensional pattern matching can be extended to two-dimensional pattern matching with errors. The most straightforward is the two-dimensional pattern matching with substitutions, which allows substitution (replacement) of at most k symbols.

Let us suppose squared pattern P of size $(m \times m)$, squared text T of size $(n \times n)$, and $\sigma = \min(|A|, m^2)$, where $|A|$ is the size of the alphabet A . The first linear time solution for the exact two-dimensional pattern matching, which requires $O((m^2 + n^2) \log \sigma)$ time, gave Bird [1]. This algorithm is based on the problem linearization and utilizes well known one-dimensional pattern matching techniques (Aho-Corasick and Knuth-Morris-Prat algorithms). Using two-dimensional periodicity, Galil and Park [2] developed an alphabet independent algorithm requiring $O(m^2 + n^2)$ time. The best result in two-dimensional pattern matching with at most k substitutions gave Amir and Landau [3] achieving $O((k + \log \sigma)n^2)$ time using $O(n^2)$ space.

In this paper we present new approach to the two-dimensional pattern matching, which utilizes two-dimensional online tessellation automata. Two-dimensional online tessellation automata were introduced by Inoue and Nakamura [4]. A nondeterministic (deterministic) two-dimensional online tessellation automaton, referred as 2OTA (2DOTA), is a 5-tuple $M = (A, Q, \delta, q_0, F)$, where A is the input alphabet, Q is the finite set of automaton states, $\delta: Q \times Q \times A \rightarrow P(Q)$ ($\delta: Q \times Q \times A \rightarrow Q$) is the transition function ($P(Q)$ is the power set of Q), $q_0 \in Q$ is the initial state, and $F \subset Q$ is the set of final states.

Since 2OTA can be taken as a two-dimensional extension of finite automata, presented method is a generalization of a well known one-dimensional pattern matching algorithm based on finite automata. Thus the algorithm works in three independent phases:

1. create a 2OTA for given pattern and two-dimensional pattern matching problem type,
2. transform this automaton into equivalent 2DOTA,
3. read the input text and report an occurrence of the pattern whenever the automaton reaches a final state.

Since each problem requires special automaton, step 1 is the only step that differs for different two-dimensional pattern matching problems.

The biggest advantage of this approach is the fact that the matching phase (step 3) is always linear. It requires $O(n^2)$ time for the input text of size $(n \times n)$ with very small hidden constant. Moreover, the preprocessing phase does not depend on the size of the input text. On the other hand, the biggest disadvantage is the possibility of the exponential blowup of the number of created states in step 2. It requires $O(|A|2^{m^2})$ time in case of exact two-dimensional pattern matching of the pattern of size $(m \times m)$ and $O(|A|2^{k^2 m^2})$ in case of two-dimensional pattern matching with at most k substitutions. The extra space required by presented

algorithm is given by the size of the created 2DOTA and two lines (or columns) of the input text. So, it requires $O(A|2^{m^2} + n)$ in case of exact two-dimensional pattern matching and $O(A|2^{k^2 m^2} + n)$ in case of two-dimensional pattern matching with at most k substitutions. Therefore, the this two-dimensional pattern matching algorithm is very useful in case that the size of the input text is much greater than the size of the pattern ($m \ll n$), or when the pattern is searched in many input texts because first two steps of the algorithm can be performed only once.

References:

- [1] BIRD, R.S.: *Two dimensional pattern matching* Information Processing Letters 6, 1977, pp. 168–170.
- [2] GALIL, Z. – PARK, K.: *Truly alphabet-independent two-dimensional pattern matching* Proceedings of the 33rd IEEE Annual Symposium on Foundations of Computer Science, 1992, pp. 247–256.
- [3] AMIR, A. – LANDAU, G.: *Fast parallel and serial multidimensional approximate array matching* Theoretical Computer Science 81, 1991, pp. 97–115.
- [4] INOUE, K. – NAKAMURA, A.: *Some properties of two-dimensional on-line tessellation acceptors* Information Sciences 13, 1977, pp. 95–121.

This research has been partially supported by CTU grant no. CTU0409213, by FRVŠ grant no. 2060/04 and by research program MŠMT no. J04/98:212300014.

Rating Information Systems

Karel Hartman

hartman@karnet.fsih.cvut.cz

Department of Management and Economy, Faculty of Mechanical Engineering, Czech Technical University, Horská 3, 128 03 Prague 2, Czech Republic

My contribution connects my work with my previous work when I assessed Information Systems (IS) at the Czech market from dates provided by producers of IS.

This new contribution deals with dates acquired by questionnaires from firms which have got installed some IS.

Because of finding dates I used a questionnaire created in Excel. The reason is an opportunity of an easy interpretation.

These pieces of information are from 12640 clients of all types of organizations. It is 96% of all clients. Number 12640 approaches 100% of all clients.

Contemporary state in the area “All-in-one” IS for the segment of small firms (number of implementation).

- 38% LCS Helios IQ from the concern LCS International
- 15% Altus Vario from the concern ALTUS Development
- 5% Vision32 from the concern Vision Praha
- 5% Microsoft Navision from the concern Microsoft
- 5% Orsoft from the concern ORTEX
- 4% INFORIS Magic Win from the concern INFORIS Softwarehouse
- 28% The rest

Contemporary state in area “All-in-one” IS for the segment of middle firms (number of implementation).

- 15% LCS Helios IQ from the concern LCS International
- 11% Orsoft from the concern ORTEX
- 8% Vision32 from the concern Vision Praha
- 4% Altus Vario from the concern ALTUS Development
- 4% Information System K2 from the concern Q.gir
- 4% Microsoft Navision from the concern Microsoft
- 54% The rest

In my work I concentrated at taking the advantage of standards for the direction of Informational technology (IT).

Nova days companies and organizations have got three standards for the direction of IT, if they do not create an individual standard.

- 1)Standard COBIT(Control Objectives for Information and Related Technology)
- 2)Standard ITIL(Information Technology Infrastructure Library)
- 3)Standard ISO 17799 (Information Technology – Code of Practice for Information Security Management).

These three described standards do not overlap in their target. The strength of the standard COBIT is in instructions for the control of IT and in well defined metrics. ISO 17799 concentrates on the security of IT while ITIL concentrates mainly on process.

Companies which I cooperated with do not use this advantage very much.

100% All answers

5.1% Companies which take the advantage of standards or have got created their own standards for the direction of IT.

Those 5,1% are to be shared :

3.92% Companies take the advantage of standard ISO17799

1.12% Companies take the advantage of standard ITIL

0.56% Companies take the advantage of standard COBIT

0.56% Companies take the advantage of an individual standard

References:

- [1] MOLNÁR,Z *Computer integrated Manufacturing* ČVUT, 1996, pp. 58–78.
- [2] HARTMAN,K: *Rating Information Systems at the Czech market* ČVUT, 2003 4–92.
- [3] HARTMAN,K: *The efficiency of Information Systems* ČVUT, 2000, 8–61

Adaptation of Intelligent Agents in Artificial Life Domain

P. Nahodil, D. Kadleček

nahodil@fel.cvut.cz

CTU, Faculty of Electrical Engineering, Dept. of Cybernetics
Karlovo náměstí 13, 121 35 Praha 2

Artificial Life (ALife) [1], [2] is the part of AI, which tries to model “*the world as it is*” or “*the world as it could be*”. The Mother Nature had billions years to undertake her experiment with living mass and man reached the point when he can imitate her. ALife gets the inspiration from many science disciplines. To name them it is biology, ethology, sociology, psychology, mathematics (grammars) and physics.

The main focus of this work is to design and test *agent architecture enabling adaptive behavior* of agents in Artificial Life (AL) environments [1]. The AL environment is special in the sense that the agent’s environment is very diverse and dynamic. Agent has to exhibit many different behaviors (cannot be specialized). The typical behaviors are foraging, mating, roaming, fighting, predator avoidance etc. The most important properties of agents in AL are adaptation, reactive behavior and survival.

Theoretical apparatus of control engineering, Q-learning and artificial neural networks has been combined with the results of the animal behavior research and ethology to get agents that are capable of behaviors similar to those exhibited by real animals. The resulting architecture extends the previous CZAR agent architecture [2] mainly to address requirements for agent adaptation and prediction:

1. ***The concept of control engineering*** is used to implement physiological state and its dynamics and physical constraints posed by the environment. Moreover it provides solid base for defining a motivational subsystem and cost (penalty) functions used for adaptation and decision-making.
2. ***Classical Q-learning techniques*** are used to map state, action pairs to utilities. Q-learning is able – in contrast to standard reinforcement learning purely based on reward and punishment – deciding on a course of action by considering possible future stages without actually experiencing them.
3. ***Artificial neural networks*** are used to overcome “the complexity and generalization problem”, which is typical in complex environment with large action-state space.
4. ***Several extensions to the classical Q-learning techniques*** are introduced and tested mainly to overcome some of the limitations of reinforcement learning methods based on Q-learning. The standard approximate Q-learning has been enhanced by the concept of the dynamic rebuilding of Q-spaces and parallelization of Q-spaces generation and evaluation. The term Q-space is used because the whole <state, action> space is divided into smaller subspaces that correspond to different behaviors. The concept of dynamic rebuilding of Q-spaces has been introduced to overcome very slow adaptation factor of Q-learning that makes Q-learning ineffective in dynamic environments. The second limitation, that Q-learning algorithms are very focused and thus ineffective when agents exhibit more different behaviors is being solved by doing the Q-spaces generation and evaluation in parallel.

Most of the experiments will be performed in simulations, where several model environments and preconfiguration of agents will be tested in the existing ALS (Artificial Life Simulator) that has been developed to test the predecessor of the agent architecture presented here. A visualization framework has supported the analysis of the experiments. It allows better analysis of huge amount of data [3].

The following *agent behaviors* have been *realized* during tests (each behavior is a separate Q-Space):

- Foraging
- Mating and Reproduction
- Predator Avoidance
- Exploration
- Information Exchange

Important properties of agents with our architecture [4]:

- Agents are capable to learn different independent behaviors. These behaviors can be combined together to form hierarchies. New behaviors can be added on the fly.
- Two behavior types are supported: (i) the automatic ones – more like reflexes and instincts used from ethology (ii) and the more deliberative ones – supports for prediction and complex action sequences.
- Agents adapt their behavior on the fly to reflect changes in the environment – they adapt their behavior motivations and sequences that form the behaviors.

Agents can react both on reactive basis in a complex and changing environment.

References:

- [1] KADLEČEK, D. - NAHODIL, P.: *Adaptive Agents for Artificial Life Domain* In: WSEA TRANSACTION ON SYSTEMS. 2004, vol. 6, no. 3, Athens, 2004, pp. 2427-2432.
- [2] KADLEČEK, D. – NAHODIL, P.: *New Hybrid Architecture in Artificial Life Simulation*. Lecture Notes in AI 2159, Springer Verlag, Berlin, 2001, pp. 143-146.
- [3] NAHODIL, P. - SLAVÍK, P. - KADLEČEK, D. - ŘEHOŘ, D.: *Dynamic Analysis of Agents Behaviour - Combining ALife Visualization and AI* Lecture Notes in AI 3071-Invited paper, Springer Verlag, Berlin, 2004, pp. 346 - 359.
- [4] NAHODIL, P. - KADLEČEK, D.: *Animal-like Control of Intelligent Autonomous Agents* In: Proc. of the 23rd International IASTED Conference MIC2004, ACTA Press, Calgary, 2004, pp. 154 - 159.

This research has been supported by CTU grant No. CTU0407413.

SD Card File System for Atmel FPSLIC

P.Honzík, R.Matoušek*, J.Kadlec**

`peters@utia.cas.cz`

Department of Control Engineering, Faculty of Electrical Engineering, Czech Technical University, Karlovo nám. 13, 121 35 Praha 2, Czech Republic

*Department of Computer Science, Faculty of Electrical Engineering, Czech Technical University, Karlovo nám. 13, 121 35 Praha 2, Czech Republic

**Institute of Information Theory and Automation, Academy of Sciences CR, Pod vodarenskou vezi 4, 182 08 Praha 8, Czech Republic

Atmel AT94K FPSLIC is a VLSI device composed of a built-in field-programmable gate array (FPGA) and a prefabricated AVR microcontroller (micro). The device brings the benefits of both parts: an efficient execution of various logic functions implemented in the FPGA and easy application development in the C language with a short design cycle for the AVR micro. In fact, the AT94K is a micro with any peripheral device you can imagine. There are two interconnect mechanisms: an AVR 8-bit bus with 16 select and interrupt lines, and a 32KB shared AVR program/data memory allowing block data transfers without AVR micro interaction. The AVR can communicate with the outside world by two UART lines. Additional communication interfaces can be implemented in the FPGA. For more information see [4].

The support for the SD memory card file system is built on top of an SD memory card interface that implements low-level read and write operations. It is implemented partially in the FPGA (SPI interface, basic handshake) and partially in the AVR (initialization, read block, write block, error checking). The FPGA part of the SD memory card interface is designed for streaming operations. It has input/output data channels with a simple handshake that is designed for multimedia applications (dictation machine, audio player, etc.). These channels are connected to the AVR memory allowing direct data transfers from/to the card without AVR interaction. A predefined memory block works as a shared area for the file system operations. Read or write functions work with 512-byte data block.

The complete file system library (including FAT12, FAT16, and FAT32) offered by Progressive Resources LLC (see [3]) was too big to fit in the AT94K program memory. The implementation was therefore limited only to FAT16. Still the reduced file system library (including file and directory functions) was too big. A solution was found in a recent project dealing with dynamic reconfiguration (see [1]). The library was decomposed in several subsets: Functions related to the FAT file system was put together with the SD memory card interface functions and placed permanently in the program memory. Non-destructive file functions, destructive functions and directory functions were put in separate software overlays, that are loaded by a simple BIOS-like system on application demand. Each function call is evaluated first; whenever the requested function is not present in the program memory, it is loaded from an external memory storage (flash, SD card, etc.). The programming scheme is kept simple and transparent with the use of standard function calls. More information about the software overlays can be found in [2].

The decomposed file system library can be simply used for any different storage media. It use read/write block operations of the SD card interface. Any other interface that provides the same functions can use this library with only a little effort.

References:

- [1] M.DANĚK, P.HONZÍK, J.KADLEC, R.MATOUŠEK, Z.POHL: *Reconfigurable System-on-a-Programmable-Chip Platform Design & Diagnostics of Electronic Circuits & Sysytem*, Stará Lesná, Slovakia 2004, pp. 21–28.
- [2] P.HONZÍK: *AVR Core Supported Dynamic Reconfiguration* POSTER, 8th International Student Conference on Electrical Engineering, Prague, Czech Republic 2004
- [3] PROGRESSIVE RESOURCES LLC: <http://www.prllc.com> 2004
- [4] ATMEL: <http://www.atmel.com> 2004

We would like to gracefully acknowledge the support for this work provided by Atmel Hellas. This research has been supported by IST-2001-34016 and GA102/04/2137.

Development of an E-learning Course in Fundamentals of the Linux Operation System

P. Soukup

soukup@fsv.cvut.cz

Department of Mapping and Cartography, Faculty of Civil Engineering, Czech Technical University, Technická 2, 166 27 Prague 6, Czech Republic

Distance and online education becomes a favourite supplement of classical teaching methods. There are various forms of use of an accessible technology - starting with partial supplemental materials and finishing with quite independent and complex tutorial courses. Last year, two developing projects with the titles "Innovation of elemental work with computer" and „ Lifelong learning of the CTU employees in information technologies" were carried out at the Czech Technical University (CTU) in Prague. These projects have been managed by the "Centre of education support on the CTU", which has acted as a co-ordinator of the task realized by four various workplaces of the university. Our Department participated in solution of these large projects. In terms of this cooperation we have developed an e-learning course in fundamentals of the Linux operation system. A brief characteristic of the course is mentioned in following text.

The operation system Linux is an efficient, stable and perspective operation system, which finds more and more wide usage [4]. The advantages of Linux compared to other operation systems are in the area of demanding calculations, efficient automation of routine operations and in providing various network services. Within our branch (Geodesy and Cartography) we usually work with extensive sets of geographical data and therefore we introduced an obligatory education in fundamentals of the Linux operation system. Using a command line (necessary for creation scripts and for wider understanding of the system principles) requires deeper study than an intuitive work in a graphic user's environment. The built-in help and available printed publications are usually too detailed and not enough flexible for an operative use. A tutorial course generally accessible via the internet presents a solution of the mentioned problem.

The developed e-learning course in fundamentals of the Linux operation system is based on the technology WWW [2]. Individual web pages of the course follow the valid standard XHTML 1.1. At present the course includes the basic information about operation system Linux and the description of almost all the basic commands. The structure of individual pages of the course is similar. It involves the explanation of the problem supplemented with notes, solved examples and it defines a theme for concrete training. An optional part of the www page is a description of syntax and of main options of particular commands.

Suitable accessories of tutorial courses are the tests, which can check the effectiveness of the study. The program module for testing student's knowledge is a part of the course in fundamentals of the Linux operation system. The module is created in programming system PHP; questions of tests and their configurations are saved in a text file of XML format. Every question has two or more answers. Every answer has its own valuation by number of points. There are three types of test evaluation which differ in a way of calculation the total number of achieved points. Questions and answers may be displayed in various ordering. Questions and answers may be defined as a simple text or as the URL address of web pages. The second mentioned type allows to use within the course all the options and possibilities of web pages.

The program for testing of knowledge is designed quite generally and therefore it can be used also for other purposes [1]. We use this program module? within the tutorial course in a self-testing mode when the test results are not saved anywhere and they serve only as an information for students about the successfulness of their study. For future we may consider a classified option of the program unit, where the results of tests can be registered and become a part of student's classification. Such an option can serve as a necessary feedback for the authors of the course – it may help to identify weaker parts of the course and contribute to its further development.

The e-learning course in fundamentals of the Linux operation system has been developed according to the needs of the relevant study course at our Department. The course is freely available to everyone who is interested in this operation system. The current first version of the course is available on the web address <http://gama.fsv.cvut.cz/~soukup/linux>. We suppose that course will be further developed according to the experience gained from its usage.

The use of the course does not suppose any installation of additional program systems – the whole course is accessible by standard web browsers. At present there is a number of professional software products for creation and administration of tutorial courses (Learning management system - LMS) [3]. The CTU used the WebCT LMS in recent years. This year, the Centre of education support on the CTU has bought a ClassServer LMS by Microsoft. The e-learning course in fundamentals of Linux operation system will be implemented into this LMS environment and it will become a standard component of the CTU tutorial course.

References:

- [1] SOUKUP, P.: *E-learning and Checking of Study Effectiveness by Testing* Proceedings of Conference ICETA 2004: Information and Telecommunications Technologies in Education, Košice, Slovak Republic, ISBN 80-89066-85-2, 2004, pp. 371-375.
- [2] ČÁBELKA, M. – SOUKUP, P.: *Využití internetových technologií při tvorbě výukového kurzu* Proceedings of: 15. Kartografické konference – Geoinformatizácia kartografie, Zvolen, Slovak republic, ISBN 80-89060-04-8, 2003, pp. 49 - 52.
- [3] POULOVÁ, P.: *Komparace vybraných LMS* Proceedings of: Konference Belcom '04: E-learning v České a Slovenské republice: Stav a perspektivy, Praha, ISBN 80-01-02923-9, 2004.
- [4] BRANDEJS, M.: *Linux - praktický průvodce* KONVOJ, s.r.o., Brno, ISBN 80-7302-050-5, 2003.

This article was processed with the support of research intention MSM 210000007 "Complex innovation of technologies at geodesy and cartography".

Telecommunication Network Optimization Algorithms

O.Hudousek

hudouso@feld.cvut.cz

Department of Telecommunication Engineering, Faculty of Electrical Engineering, Czech Technical University, Technická 2, 166 27 Prague 6, Czech Republic

During expansion of existing or deployment of a new telecommunication network, it is important to undertake all actions with respect to economically optimal progress of the operations. Besides pure economic problems, e.g. finding sources to fund the project, it is also necessary to solve problems inherent to the technical realization of the network. Specifically an appropriate architecture and number of network resources have to be chosen. These actions are usually based on corresponding mathematical models of the network and of the carried traffic. Many algorithms have been developed to find optimal solutions of wide variety of the tasks. Nevertheless most of them solve only particular problems in specific types of the networks. This work has been aimed at generalized network optimization problem. In the first phase its computational complexity was examined and subsequently some suitable algorithms solving the task were introduced. A nonhierarchical network was considered being a most general case of the problem. To avoid complexity of some routing protocols only direct, deterministic routing was assumed.

A network optimization problem can formalized as follows: It is given a connected, simple, undirected graph $G=(V,E)$, where V is set of vertices and E set of edges representing potential circuits between nodes of the network. It is also given a matrix of offered traffic A , where each element of the matrix A_{ij} is a vector of parameters describing offered traffic. For each edge e_k a price function $C_k(A_k,D_k)$, where A is vector of parameters describing traffic offered to edge e_k . Vector D_k represents constraints necessary to perform dimensioning of the circuits, e.g. maximal loss allowed. Objective of the problem is to find such paths $P_{i,j}=(i,v_1,v_2,\dots,v_n,j)$, connecting all pairs of nodes i,j , that a criterion function

$$f = \sum_E C_E$$

would be minimized. Offered traffic $A_{i,j}$ contributes to traffic offered to edge e_k by traffic $a_{(i,j)k}$.

Following the formal definition of the problem the computational complexity was examined. Among other results the maximal number of configurations concerning complete graph was derived:

$$NR = \left(\sum_{k=1}^{N-1} \frac{(N-2)!}{(N-k-1)!} \right)^{\frac{N(N-1)}{2}},$$

where NR is number of configurations and N number of vertices.

The stated problem is proved to be NP-complete and thus no algorithm solving it with polynomial time complexity is known. Therefore it is to be expected that the algorithms finding optimal solution will be applicable only for small instances of the problem, none the less they were implemented as results obtained from them could be used to collate efficiency of other class of algorithms. If we trade off finding exact optimal solution for finding nearly optimal solution, it is possible to solve much greater instances of the problem utilizing various approximations (which does not exclude possibility of finding optimal solution).

Described problem belongs to the group of combinatorial optimization problems, for which many general algorithms were already designed. Some of them were examined closer:

- hill climbing algorithm,
- simulated annealing (SA),
- genetic algorithms (GA).

Hill climbing is a local optimization algorithm, which without undertaking additional appropriate measures ends-up search in the local minimum of the criterion function. In this work it was only used to confirm that the criterion function has local extremes. The implementation was instead focused on reminding approaches. Both SA and GA are nondeterministic optimization algorithms and as a result it can not be guaranteed that the result of each execution will be the same. Therefore it is necessary to use analyze results with statistical methods and so was among others implemented evaluation of the Students distribution, which allows determination of the confidential interval. Both algorithms were implemented in their standard form and it is possible to set-up miscellaneous parameters controlling their behavior. To compare their efficiency deterministic branch-and-bound algorithm was also implemented. As a next step, ten task were generated with networks up to ten nodes and subsequently values of algorithms parameters were adjusted so that the difference between optimal and mean solution is smaller than 1%. Details concerning implementation of the optimization algorithms will be published at the Access server [1].

Although the project is aimed at general network optimization, correctness of the implementation had to be proved on real examples. That is why the classical Erlang model of traffic in the telephony network was realized. Network represented by structure of service systems M/M/N/0 according to Kendall's classification. During repeated dimensioning of these systems Erlang first formula plays a key role from the point of view of the execution time requirements. Therefore corresponding evaluation algorithms were studied and their speed was significantly improved [2], [3].

References:

- [1] HUDOUSEK, O.: *Optimalizace nehierarchické telekomunikační sítě*, <http://access.comtel.cz>, vyjde v lednu 2005
- [2] HUDOUSEK, O.: *Evaluation of the Erlang-B formula. RTT 2003 - Proceedings*. FEI, Slovak University of Technology, 2003, p.80-83
- [3] HUDOUSEK, O.: *Precision of Erlang-B Function Evaluation for noninteger number of service lines. Sbornik RTT 2004*, FEL CVUT, 2004

This research has been supported by FRVŠ grant No. 2047/2004.

Design of Self-Testing Circuits Using Parity Codes

P. Kubalík, H. Kubátová

`xkubalik@fel.cvut.cz`, `kubatova@fel.cvut.cz`

Department of Computer Science and Engineering
Czech Technical University
Karlovo nám. 13, 121 35 Prague 2, Czech Republic

This paper describes a design methodology for selection of proper error detecting code for combinational circuits implemented in FPGA. Error detecting codes can be used to satisfy the totally self-checking properties (TSC). The most important criterion is the speed of the fault detection and the safety of the whole circuit with respect to the surrounding environment. Concurrent error detection (CED) techniques are widely used to check the circuit while the original circuit is in normal operation. To increase the reliability of the circuit we assume that the system reconfigures the faulty part.

The regular structure of the FPGA is an advantage for many applications. The time needed to develop a design for FPGA is shorter than for ASIC. FPGAs enable the in-system reprogrammability to correct bugs or update the firmware to implement new standards. The FPGA circuits can be also used in mission critical applications such as aviation, medicine or space missions. The sensitivity of the circuit to the surrounding radiation is increasing due to the evolution of the CMOS technologies. The changes in FPGA memory contents are observable even at the sea level. The impact of particles on digital blocks in the FPGA leads to bit-flips. The process when the high-energy particles impact on the sensitive parts is described as Single Event Upset (SEUs). Some results of SEU effects on the FPGA configuration memory are described in [1].

There are many papers focused on CED in a random logic circuit. The combinational circuits are used as basic elements for testing the method that ensures TSC properties. There are two basic aspects that must be taken into account: fault coverage and area overhead. Fault coverage must be achieved as high as possible for the whole design. The whole design means the original circuit, the parity generator and the checker. Area overhead is a second aspect and must be as small as possible. These two aspects are in contradiction due to the fact that high fault coverage leads to higher area overhead in many cases. For every real design the relationship between the area overhead and the fault coverage must be found. Some results of fault coverage for circuit implemented in FPGAs are described in [2]. Basic methods used for the fault detection in logic circuits are based on a simple duplication and modification of the duplicate circuit described by a multi-level network. This method adds Hamming-like code on primary outputs of the duplicate circuit. This method allows prediction of final area overhead and fault coverage before implementation and simulation. Area overhead in many cases is higher than 100% and fault coverage is up to 99%. The duplicated part can be modified to remove common-mode failures (CMFs). The area overhead plays an important role in popularity of the method used for ensuring the TSC property. Therefore special schemes were designed for circuits with regular structures, for example adders, multipliers or memories. The reason why the CED techniques were not so popular was very high area overhead. These circuits also had a low disposition to temporary faults due to their large transistor size. Nowadays when the deep submicron technology is widely used, CED techniques for circuit with an unknown structure are more and more important.

We have proposed a solution for small combinational circuits. These small parts are combined into a large design. To ensure the parameters of fault coverage and area overhead

we have designed a structure allowing to incorporate these small parts together [3]. The small combinational circuits are modified by the basic method of duplication and simple modification. The checker used for checking every part is situated in the next block where outputs of previous block are used as inputs. Due to this fact the interconnection between two blocks is checked too. In every place with branching signals buffers must be inserted. Buffers are used to keep self-checking properties for every part of the circuit. A fault may be undetected when buffers are not used for some nets. The modification of the duplicate circuit can be done by two basic methods. The first method modifies the circuit described by a multilevel logic leads to a high area overhead for any error checking codes. The Hamming-like codes are strong enough to obtain 100% fault coverage but area overhead is too big due to the number of check bits. The check bits generator, based on this code, uses the generating matrix. The structure of this matrix implies the final area overhead and fault coverage. The fault coverage closely depends on the structure of this matrix. Some experimental results on the fault coverage and the number of parity bits dependence are described in [4]. In many cases, the small area overhead is more important than 100% fault coverage. Due to this fact the single parity code is a minimal solution when only one check bit is generated. The second method is based on a modification of a circuit described by a two level network. This solution leads to a small area overhead while keeping more than 75% fault coverage. This method is not sufficient for arithmetic and logic units due to a high area overhead.

Our future work is devoted to calculation of an area overhead for the structure defined in [5]. We have to discover more precise relations between real FPGA defects and the used fault models. The appropriate decomposition of the designed circuit is under our intensive research.

References:

- [1] M. BELLATO, P. BERNARDI, D. BORTOLATO, A. CANDELORI, M. CESCHIA, A. PACCAGNELLA, M. REBAUDEGO, M. SONZA REORDA, M. VIOLANTE, P. ZAMBOLIN: *Evaluating the effects of SEUs affecting the configuration memory of an SRAM-based FPGA* Design Automation Event for Electronic System in Europe 2004, pp. 584-589.
- [2] C. BOLCHINI, F. SALICE, D. SCIUTO: *Design Self-Checking FPGAs through Error Detection Codes*, 17th IEEE International Symposium on Defect and Fault Tolerance in VLSI Systems (DFT'02), 2002, pp. 60.
- [3] P. KUBALIK, H. KUBATOVA: *High Reliable FPGA Based System Design Methodology*, High Reliable FPGA Based System Design Methodology, In Work in Progress Session of 30th EUROMICRO and DSD 2004. Universitat Linz 2004 pp. 30-31
- [4] P. KUBALIK, H. KUBATOVA *On-line Testing for FPGA* In Proceedings of the Sixth International Scientific Conference Electronic Computers and Informatics ECI2004 2004 pp. 194-199

This research has been in part supported by the GA102/04/2137 grant, CTU0408913 grant and MSM212300014 research program.

Gossiping Algorithms

M. Šoch

soch@sun.felk.cvut.cz

Dept. of Computer Science and Engineering, Faculty of Electrical Engineering, CTU,
Karlovo nám. 13, 121 35 Praha 2, Czech Republic

Collective communication operations frequently occur in parallel computing, and their performance often determines the overall running time of application. One of the fundamental communication problems is gossiping (also called total exchange or all-to-all non-personalized communication). Gossiping is the problem in which every processing unit p wants to send the same packet to every other p . Said differently, initially each of the n processing units contains an amount of data of size h , and finally all processing units know the complete data set of size $n \cdot h$. Gossiping is used in all applications in which the processing units operate autonomously for a while, and then must exchange all gathered data to update their databases. Many aspects of the problem have been investigated for all kinds of interconnection networks [2].

Complexity of gossiping algorithms strongly depends on communication model representing communication subsystem of parallel computer. We know a lot of different communication models. Very common is the telephone communication model. In this model, a processing unit can communicate with only one of its neighbors at a time, but it can both send and receive during this communication. In this paper we assume this communication model. We also assume that in one communication round two communicating processing units can exchange all available data. This is called the unit-cost model, which is considered in most theoretical papers on gossiping.

Design of gossiping algorithms also depends on type of communication network. We know a lot of networks such as hypercubes, meshes, tori, etc. One interesting network is the wrapped butterfly. Hence, we are considering wrapped butterflies, wBF . They form a parametrized class of networks. The k -th network has $k \cdot 2^k$ nodes of degree 4. The nodes are indexed by two-tuples (i, j) , $0 \leq i \leq 2^k - 1$ and $0 \leq j \leq k - 1$. They are connected by straight and cross edges. Straight edges connect nodes $(i, *)$ into i lines. These lines are connected by cross edges. Nodes $(*, j)$ we call rows.

In the unit-cost telephone model we are considering, giving a gossiping schedule of length l , amounts to giving a sequence of l matchings: matching i gives the set of edges that are used in communication round i . In our case we will work with a small set of matchings M_i . To represent a long regular sequence of such matchings, we use the following notation for regular expressions. A term $[x]^k$ means that x is repeated k times. A term $\{xy..j\}^k$ means that the regular expression is starting with x , is of length k , and is composed from x and y which are used alternately. A term $\{..xy\}^k$ means that the regular expression is ending with y , is of length k , and is composed from x and y which are used alternately.

Even more, for gossiping we define two following operations: Going-straight down or up means using only straight connections, moving up or down. Distance x is covered in x rounds. Braiding up or down means using alternating using straight and cross edges, moving up or down. A distance x is covered in 2^x rounds.

For gossiping in wBF_k we use four matchings, covering all edges of wBF_k exactly once. We denote them as follows: M_0 contains all edges between $(i, 2^*j)$ and $(i, 2^*j+1)$, M_1 all edges between $(i, 2^*j-1)$ and $(i, 2^*j)$. Hence, together M_0 and M_1 contain all straight edges. M_2 contains all edges between $(i, 2^*j)$ and $(i+2^l, 2^*j+1)$, and $(i, 2^*j+1)$ and $(i+2^l, 2^*j)$, M_3 all edges

between $(i, 2*j-1)$ and $(i+2^j, 2*j)$, and $(i, 2*j)$ and $(i+2^j, 2*j-1)$. Hence, together M_2 and M_3 contain all cross edges.

Gossiping in wBF_k , $k \geq 4$ and is even, can be done in telephone model in $5*k/2-2$ rounds using $[M_0M_2M_1M_3]^{k/2-1} M_0M_2M_3 \{M_1M_0 \dots\}^{k/2-1}$ that improves result presented in [2].

Wrapped butterfly wBF is vertex symmetric network. It is possible to describe gossiping for any node and due to this symmetricity this description holds for every node. Without loss of generality, we describe gossiping for node $(0,0)$. Gossiping starts by braiding using sequences M_0M_2 and M_1M_3 . Each of these sequences doubles number of informed nodes on every next row. After $2*k-2$ rounds braiding stops. In this moment matching M_3 is used which caused that one complete one row is informed by packet from source node $(0,0)$. More exactly, all nodes at row $(*,k-1)$ are informed. Going-straight operation continues. Packet is distributed by matchings M_1 and M_0 in next $k/2-1$ rounds until all nodes are informed. All together we need $2*k-1+1+k/2-1=5*k/2-1$ rounds.

References:

- [1] BEIER, R. - SIBEYN, J. F.: *Powerful Heuristic for Telephone Gossiping*. Proc. 7th Colloquium on Structural Information and Communication Complexity, Carleton Scientific, 2000, pp. 17-35.
- [2] HROMKOVIČ, J. - KLASING, R. - MONIEN, B. - PEINE, R.: *Dissemination of Information in Interconnection Networks*. Combinatorial Network Theory, Kluwer Academic Publishers, 1996, pp. 125-212.
- [3] SIBEYN, J. F. - ŠOCH, M.: *Optimal Gossiping on CCCs of Even Dimensions*. Submitted to PPL, 2001.
- [4] ŠOCH, M. - TVRDÍK, P.: *Optimal Gossip in Store-and-Forward Noncombining 2-D Tori*. Proc. 3rd International Euro-Par Conference, LNCS 1300, Springer-Verlag, 1997, pp. 234-241.

This research has been supported by MŠMT grant No. MSM 6840770014

The Reliability and Safety Modelling for Safety Critical Application

R. Dobiáš, H. Kubátová

dobiasr@fel.cvut.cz

Department of Computer Science and Engineering, Faculty of Electrical Engineering, Czech Technical University, Karlovo namesti 13, 12135 Prague 2

The reliability and safety analyses, models and characteristics calculations of the safety critical systems are described in this paper. Markov Chain models and Reliability Block diagrams are used for the reliability and safety analyses of the safety critical applications of the common fault-tolerant safety-critical systems.

It is naturally impossible to create a system that tolerates all kinds of faults. Many safety critical systems are designed to tolerate a single fault, which means that a system is fully operational when one of its units fails. Multiple faults can be handled by increased redundancy, but the cost is often higher than the associated gain in dependability. So-called single event upsets (SEU) are often substituted for single faults. A SEU is caused by a high-energy particle and in real world occurs with exponential probability distribution. The consequence is that several fault events can occur close in time (before the damaged system part is repaired) and thus violate the single fault hypothesis. Depending on the failure rate, the probability of such burst of faults can be very small but never zero.

Let us assume a medium-scale safety critical system (e.g. drive-by-wire car). This car can be equipped with a distributed fault tolerant communication subsystem called TTP/C (TTTech, 1999; <http://www.ttagroup.org>). It is based on the single fault assumption and tolerates faults by using active node replication (due to special properties of the architecture, two nodes are sufficient). Since all nodes within the system use the same FT mechanisms, their reliability is essentially the same. If we create reliability model of a single fault tolerant unit (FTU) comprising two TTP/C nodes, we get a basic building block that can be used for easy reliability estimation of larger systems.

The Markov reliability model of a single FTU and its embedding in a higher level (hierarchical) model to compute mission-time related reliability of whole systems is presented. All necessary input parameters are realistic – taken either from measurement by hardware producers or from low-level simulation.

TTP/C protocol has been designed to tolerate any single physical fault in anyone of its constituent parts (a node or bus) without any impact on the operation of a properly configured cluster.

The TTP/C specification doesn't distinguish between permanent and transient node faults. A significant difference between these basic kinds of faults is that transient faults (unlike their permanent counterparts) can come repeatedly in a sequence (possibly attacking the same node or its replica) and the attacked node can regenerate between successive faults. An influence of a sequence of permanent faults can be easily investigated using conventional reliability models when the rate of faults is known.

To evaluate the influence of a sequence of transient faults, a more precise definition of "single fault" is needed. In the following text we will assume single data damaging transient fault that we define as follows:

It will occur at a single time point that is arbitrarily located at the time axis, i.e. the fault can occur at any time with respect to the cluster activity.

The fault can destroy a data item located within a node erasable memory (i.e. CNI, communication controller or host controller local memory). All the nodes can be attacked

with the same probability. The assumed “width” of the fault is one bit. Every bit of the node erasable memory can be attacked with the same probability.

The time distance between any two successive transient faults is large enough to recover from the previous fault (otherwise it is a multiple fault).

This definition includes to some extent also message distortion, because TTP/C stores all messages before sending and after receiving in the CN1 memory. A message can be damaged along with other data while in this memory.

The presented method was used to estimate the reliability of a general TTP/C based system. The results confirm the assumed high reliability of TTP/C system and its general ability to serve as a framework for safety critical automotive control system construction.

On the other side, it is necessary to remember that only a small subset of all possible faults was taken into account. It is obvious that SEUs caused by neutrons are too rare to cause any significant trouble in a heavily replicated system. Future verification work should concentrate on two tasks: first to analyze other possible sources of SEUs (e.g. heavy-ions) and add these sources to this model. This should be not too difficult (only the fault rate increases). The second task is to estimate the reliability of TTP/C based systems in the presence of multiple faults.

The second part of this paper is focused on safety models. The safety is not usually observed reliability parameter by the fault-tolerant systems. The safety is defined as a probability that on the output of the safety-critical system will not be a non-detected error. There are two ways how to increase this probability. The first is way to decrease of failure rate; the second way is to increase the probability that the fault in the system is detected (coverage ratio). It is evident that the safety correlate with the reliability, but it is not possible to mix up these two terms.

The safety models are designed for the demonstration, that the safety-critical system with predicable failure rate of the hardware, with the detection capability and with the safety reaction by the fault meets the requirements for the limitation of the hazard states. There are defined safety integrity levels (SIL) to the intervals of the tolerable hazard rate (THR) in the literature [3].

Each fault in the system hardware should be masked by another hardware fault, which occurs in the redundant part of the system and this situation must be viewed as a hazard situation. The probability of the hazard situation depends on the probability that a fault occurs in the system with another latent fault.

References:

- [1] DOBIÁŠ R., KUBÁTOVÁ H.: *FPGA Based Design of Railway's Interlocking Equipment*, EUROMICRO Symposium on Digital System Design. Piscataway: IEEE, 2004, 467-473
- [2] DOBIÁŠ R., GRILLINGER P., RACEK S.: *Using Markov Models for Evaluation of Single Event Upset in TTP/C Systems*, IFAC Workshop on Programmable Devices and Systems. Gliwice: Silesian Technical University, 2004, 100-104
- [3] STOREY, N.: *Safety-critical computer systems* Prentice Hall ptr, New Jersey, 1996,
- [4] DOBIÁŠ R.: *Stanovení spolehlivosti a bezpečnosti pro systémy odolné a bezpečné proti poruše*, Počítačové architektúry a diagnostika. Bratislava: Ústav informatiky SAV, 2004 16-21

This research has been supported by the GA102/03/0672 grant.

E-learning Course Development to Support Teaching of Programming Tools

M. Fejtová*, P. Smrčka**

fejtovam@k333.felk.cvut.cz

*Department of Cybernetics, Faculty of Electrical Engineering, Czech Technical University, Technická 2, 166 27 Prague 6, Czech Republic

**Institute of Biomedical Engineering, Czech Technical University, Zikova 4, 166 36 Prague 6, Czech Republic

Due to the ever faster development of science and technology, the knowledge acquired during the study before entering the job market is not sufficient for the life-long career. The significance of life-long education is growing. Therefore there are being searched new forms of education that are accessible for broad public and enable individual approach and optimal utilization of precious time of employed people. These requirements can be reached by combination of classical methods with new information and communication technologies (ICT) – approach nowadays called blended e-learning. This approach is suitable for most of the topics relevant for the life-long learning – the only condition of its utilization is computer literacy of its users. Our aim has been to develop simple, illustrative, well-arranged, structured, and easily understandable teaching materials suitable for combined form of study and for self-study that can be efficiently used by all users who want to acquire practical skills for utilization of modern computer and information technologies.

During last decade in advanced countries stress has been laid on versatile satisfaction of one of the basic human rights – right education. However education is not limited to primary education (continuous education of an individual from kindergarten to university level); education must be offered during the whole life – then we speak about life-long learning. Developed systems of life-long learning enable to individuals to enter the process of self-education any time in their career corresponding with changing tasks or perceived needs in their jobs or personal interests. Lifelong learning means expansion of educational process out of schools.

Computers have become common working tools gradually during last decade. We cannot manage without them such operations, as for example launching a space rocket, controlling a NC machine tool or robot, creating magic film illusions of prehistoric animals or action tricks. Till recently we could perceive the presence of computers completely passively. However, that time is over. Nowadays, each of us meets computers daily – at school, library, bank, post office, local authorities or when ordering services of a travel agency. Number of jobs where computer skills are required is growing. We are witnessing revolutionary introduction of computers and information technologies into daily practice. Similarly to Guttenberg typography, this technology brings people unthought-of opportunities and danger at the same time. It opens gate of knowledge and increase of work effectively. However, the same gate may be a cause dividing society to those who can utilize offered advantages and those who cannot. It is obvious that ability to work with computers is becoming new literacy. It is not sufficient to teach pupils and students these skills. Most adults must manage them as well if they want to keep their jobs or to proceed in their career.

The content of the course is transparently structured into several teaching blocks that fully cover area of inevitable computer skills from entire fundamentals (switching on/off the computer, working with the mouse) over advanced document formatting to creation of user-

defined tables and queries. The course is divided into eight basic modules (basic management of PC for absolute laymen, Concepts of Information Technology, Using the Computer and Managing Files, Word Processing, Spreadsheet, Database, Presentation and Information and Communication).

Each module is developed according to the syllabus whose individual points are presented in detail and illustratively in the course. At the beginning of each teaching unit, the given problem is explained in its context. Then detailed description (step by step) of individual acts using both keyboard and mouse follows. The course contains a number of multimedia elements including visual representation of text (individual steps) in the form of video sequences. Since we plan to introduce printed version of the learning course for students, we have completed it with pictorial series that can replace the video sequences. Other multimedia elements are audio comments, clicking maps. Tests with automated evaluation are present as well.

Presented e-learning course is practically applicable to education of fundamentals of computer literacy in presented range. It is well-structured and illustrative. Chosen form introduces knowledge of computer literacy to persons interested in it in clear and attractive form and enables them to verify continuously level of knowledge acquisition. The course is interactive and contains a number of multimedia elements (figures, animations, sound tracks). Prepared modules significantly contribute to easier acquisition of new information, incorporation of this information into context and its successive natural fixation and refreshment. The course is implemented in the MultiPeS e-learning system [1]. Thanks to that the learning pages do not have usual rigorous layout but they have rich content and are user-friendly. Little figure of magician Merlin developed using Microsoft Agent technology cares for user-friendliness in the MultiPeS system. This figure is a guide to students in courses and study materials. It can offer explanation of terms or advice how to proceed in the course.

References:

- [1] M. FEJTOVÁ, J. FEJT, L. LHOTSKÁ: *E-learning System MultiPeS*, EUNITE 2003, Verlag Mainz, Aachen. ISBN 3-86130-194-6. 2003, pp. 377-383.
- [2] M. FEJTOVÁ, J. FEJT, L. SEDLÁČEK, L. LHOTSKÁ: *E-learning Courses in the MultiPeS System*, IADIS Press, Lisboa, 2003, vol. 1,2. ISBN 972-98947-0-1., 2003, pp. 949-952.
- [3] M. FEJTOVÁ, J. FEJT, P. SMRČKA, L. LHOTSKÁ: *E-learningový kurz základů počítačové gramotnosti v systému MultiPeS*, In E-learning v České a Slovenské republice. Praha: ČVUT, díl 1, ISBN 80-01-02923-9., 2004, pp. 184-189.
- [4] P. SMRČKA, M. FEJTOVÁ, J. FEJT, L. LHOTSKÁ: *for Supporting Education of Basics of Computer Literacy*, In Conference Proceedings ICETA 2004. Košice: ELFA. ISBN 80-89066-85-2. 2004 pp. 499-503

This work is based upon work sponsored by the CTU grant No. CTU0417413 "E-learning course development to support teaching of Programming tools" and University Development Foundation grant No. FRV 2015 "Fundamentals of computer literacy".

Simulation of Selected Part of Artificial Life Domain

K. Kohout, P. Nahodil, J. Altmann, F. Duda, L. Foltýn, D. Kadleček, M. Mach, D. Rehoř, J. Svoboda, A. Svrček, O. Fiala
kohoutk@fel.cvut.cz

CTU, Faculty of Electrical Engineering, Dept. of Cybernetics
Karlovo náměstí 13, 121 35 Praha 2

This paper is focused on agents-animates simulation and their environment. Biological systems have inspired the development of a large number of artificial intelligence techniques such as neural networks, genetic and evolutionary programming, robotic and multi-agent systems. Due to the inherent complexity of these systems, a multi-level analysis approach supported with a lot of experiments and simulations is required. Animals, in contrast to the majority of agent applications, in which agents are highly specialized in terms of behavior, deployment environment, learning capabilities etc., incorporate broad set of behaviors and high level of adaptivity, mobility, social capabilities, proactivity, reactivity and are employing various learning methods in one system. They have to provide wide set of behaviors such as predator avoidance, nesting, fighting, eating, exploring, sleeping, reproduction and others.

Motivation for formulation and creation of quite new environment was needed to test our results of research in computer simulation before control and behavior algorithms can be applied to real robots. Simulation or a robotic realization of such systems comes under the Artificial Life domain is dealing with high difficulty problems such as survival in complex unpredictable environment and others [3]. For this purpose few freely available applications were tested. Any of them was designed to be used in such wide manner as was needed. They were focused on one single and simple domain of Artificial Life such as cellular automata, ant colonies, etc. Just few of them provided more complex tools for creation capable, intelligent and self-sufficient creatures (agents). And in addition none of them has complex analytical tools for revising, debugging, comparing and evaluation of simulation and creatures parameters and behavior. Requirements for this simulation environment were as follows. Possibility to simulate various phenomena of Artificial Life domain such as mentioned above. To enable possibility to create much more complicated agents communicating and cooperating with each other. Also easy and flexible export of simulation data for analysis of simulation was required. Enabling modifications to simulation while is still running and also step-by-step tracing even backwards. Provide interesting visualization of agent's world. And also deliver meaningful and beneficial visualization of parameters of simulation. In addition modularity, extensibility and portability were required.

Proposed environment is meant to provide tool for anyone who wants to simulate his Artificial Life phenomena (agents, robots, animates etc.), and do not wants to bother with creation, design and implementation of environment. This referential environment can be used to measure different agent's behaviors created by different users. It also helps the creator to focus more on behavior and not to pay so much attention to simulation environment. It is obvious that one concrete implementation cannot be sufficient for everyone. For this purpose abstract architecture was proposed. This architecture allows designers to benefit from all mentioned above and gives him free hand if something is not exactly the way he wants it. It is a set of propositions and standards definitions and if creator sticks to these recommendations, he will be able to benefit from all of its advantages such as usage of existing external modules.

The proposed abstract architecture consists of several parts. Each one of them is focused to one specific area. It recommends the selected solution in order to maintain interconnectivity and modularity. These parts are as follows. Application engine is main program part. It synchronizes time steps for whole application, contains interfaces to all other parts (modules) of application and also contains and maintains all part of simulation like

agents and environmental layers (see below). Interface between engine and its program surrounding is data representation. Well-defined standard of XML language is supported, but has proved as highly inefficient to transfer along network to other modules of distributed application. For this purpose binary data representation was designed. This binary representation is conversion of XML tree structure to “transfer friendly” and byte effective format.

Environmental layers are the main components of virtual world of agents. They enable to disassemble complex world into simple and easy to implement layers. They can overlap each other and together they will create more complex world composed from few simple layers. The layer is a logically detachable part of world, which is capable to act individually, and which creates the virtual world along with other layers.

All described above is just an algorithm with no human interface. Visualization of designed world can be both attractive and useful tool. For this purpose external visualization module or internal (default) can be used. Internal visualization is meant to debug and observe simulation by creator. External module can be exact opposite while used to present this simulation to wider audience that science community. On-line or off-line tools for analysis parameters flow in time are also supported. Proposed environment is compatible with highly effective 3D visualization tool called VAT and it can be used to observe agents parameters at any time of simulation. Running simulation can also be stopped at any moment and even traced back to certain point and run again to observe if any change of behavior will occur in exactly same situation. Also change of simulation parameters should be available while simulation is running. Agent is any object in simulation either virtually alive (creature, predator) or virtually non-living (trees, food, water, rocks). Sensors and effectors of agent are his interface with virtual world therefore they are part of environment and layers. Besides that agent mind and control are not part of environment and can be also remote.

Here described architecture was implemented and currently is being used in few diploma theses for testing agent control mechanisms and approaches. Effort of creators of this application is to present it as standard for Artificial Life domain specific simulations. Work on this subject follows up with former research of a MRG group on FEE, CTU and it concludes design of new environment for Artificial Life domain simulation. [2] This environment is a basis for other group members to aid them on their diploma and dissertation theses [1] or other experiments. They are used in both the visualization of an environment in which agents live and the visualization of agent parameters over time. This serves better analysis and better behavioral pattern recognition. While designing this architecture special care was applied to modularity of the whole application.

References:

- [1] KOHOUT, K. *Simulace chování animátů a jeho vizualizace* Diplomová práce. Praha: České vysoké učení technické v Praze, fakulta elektrotechnická, katedra kybernetiky 2004.
- [2] KADLEČEK, D. – NAHODIL, P.: *New Hybrid Architecture in Artificial Life Simulation*. In: *Advances in Artificial Life. Lecture Notes in Artificial Intelligence 2159*, Springer Verlag, Berlin, 2001, pp. 143-146.
- [3] NAHODIL, P. - SLAVÍK, P. - KADLEČEK, D. - ŘEHOŘ, D.: *Dynamic Analysis of Agents Behaviour - Combining ALife Visualization and AI* Lecture Notes in AI 3071-Invited paper, Springer Verlag, Berlin, 2004, pp. 346-359.

Image Quality Testing and Comparison for Selected Perspective Image Compression Formats

J. Dušek

xdusek.j

CTU, Faculty of Electrical Engineering, Dept. of Radioelectronics,
Technická 2, 166 27 Praha 6

This work deals with Image quality testing for perspective image compression methods (JPEG 2000, JPEG). For this testing was designed and used two Human Visual System Models (HVS) for image quality evaluation. This work compares results of standard methods and results of HVS models. Standard methods are: subjective and objective methods.

Subjective quality testing is based on many observers that evaluate image quality. These tests have a very strict definition of the observational conditions that are given by unified recommendation of ITU-R. They are time demanding and expensive. Result of this testing is valid just for testing image.

Objective quality testing is given by mathematical approaches that rise from transmission theory, most often by Signal to Noise Ratio or Mean Square Error. Objective image quality evaluation is faster and cheaper than the subjective one. But they have bad correlation with human perception that is given by subjective tests.

The other way how to assess the image quality is usage of a HVS model. Testing with HVS models are faster and cheaper than subjective quality testing and have better correspondence with the human perception than the objective one. Majority of these HVS models requires a tested image and its corresponding matching reference in order to determine the perceptual quality between them. Human vision models can be divided into two groups. The first group comprises one-channel models that computing selected features with the whole entire image. The second ones are multi-channel models based on neuron response of brain cortex that is known as it's selectivity to spatial frequencies and orientation. These models decompose image into many spatial frequency bands and/or orientations. Then, separate thresholds are set for each channel. At the end of the processing the channels are weighted and summarised in order to get a number that represents the overall image quality.

Was selected JPEG, JPEG2000 compression methods and prepared a set of testing images. The used scenes were selected with emphasis on textures, natural scenes, faces and contrasts areas. These images were tested by all listed method and two HVS models.

Subjective results were tested in special laboratory with respecting ITU recommendations. As a testing method was selected Double Stimulus Continuous Quality Scale test that is especially useful for compare a pair of pictures. For objective testing were used MSE and MAE methods. For human visual system testing we implement used two models of HVS. These models respected features of selected method and was tuned by the best results with good correspondence to subjective testing.

Both models that we have design and implement are comparable with other methods and can be used for image quality evaluation. Results of the testing are represented by comparison of used methods especially with HVS testing. Resulting graphs are dependency of the image quality on compression ratio. All results was normalised to range from 0 to 100 so they can be compared. Subjective testing was set as a reference and all other results were compared with

it. Testing by human visual model is easier and less time demanding than with objective testing. In the work testing is presented for one scene and for all scenes that shows range of suitability for image quality testing.

References:

- [1] DUŠEK, J.: *Human Vision Models of Image Quality Evaluation for JPEG2000 Compression Designed in MATLAB* In proc. of conf. Matlab 2004, VŠCHT Prague, 2004, pp. 105-108.
- [2] LAMBRECHT CH. J. VAN DEN B.: *Vision Models and Applications to Image and Video Processing* Kluwer Academic Publisher Netherlands, 2001, p. 229.
- [3] WATSON A. B.: *Digital Images and Human Vision* MIT Press Cambridge, Massachusetts London, England, 1993, p.224.
- [4] OSBERGER W.: *Perceptual Vision Model for Picture Quality Assessment and Compression Applications* Queensland University of Technology, Brisbane Australia, 1999, p. 268.

This research has been supported by CTU0409613 and GAČR No.102/02/0133.

Exploitation of the Open Source Relational Database with Spatial Extension for GIS Needs

V. Honzík, M.Bořík*

vojtech.honzik@fsv.cvut.cz

Department of Mapping and Cartography, Faculty of Civil Engineering, Czech Technical University, Thákurova 7, 166 29 Prague 6, Czech Republic

* Department of Mathematics, Faculty of Civil Engineering, Czech Technical University, Thákurova 7, 166 29 Prague 6, Czech Republic

Current needs on functionality of the Geographic Information Systems frequently call for fully mastering of the automation in inserting the spatial data into project. Those data are nowadays frequently captured by using the GPS technology. It requires the complex technology solution including the data input itself, their verification, transformation to the target coordinate system and primarily the spatial operations on these data. After thoroughful severity examination of all phases of the data import and after considering the architecture of the developing GIS was accepted the use of spatial database. There was only one project found which satisfied both of our demands – licensing policy and functionality. It is PostGIS, system upgrade which gives spatial object support for the RDBMS PostgreSQL. This system upgrade consists from the set of SQL scripts which (when executed on given database) creates necessary data types, metadata tables and functions for their manipulation. PostGIS takes advantage of GEOS library (Geospatial Engine – Open Source).

After then, there is possible not only to store and display spatial data in the spatial database, but also manipulate those using spatial functions and operators in the same way we are used in the area of desktop GIS. The advantage is evident. There are no doubts to the benefits of desktop GIS but there is usually not possible to develop real time data processing system. Using advanced RDBMS there are instruments called triggers which can serve virtually any database operation (such like new entry addition to the database table) by function which provides the processing of particular element to satisfy the consistency of the existing as well as the new data.

The project which is aimed to the visualization of the landscape changes in the area of north Bohemia coal basin urged us in consequential way to find the general solution for spatial data capturing using GPS technology. Because of the data are usually captured in WGS-84 coordinate system, there is necessary to transform them to S-JTSK coordinate system and fill the associated attributes to particular point on the base of spatial relations with existing area features (administrative structure, type of the soil cover, geological data to the given point,...). Data files are unloaded in simple text format and using simple web interface imported to the database. Further spatial data processing in the database is already served by the internal instruments (triggers, internal constraints).

The spatial functions included in PostGIS includes the overlapping functions group (Intersects(), Touches(), Crosses(), Within(), Overlaps(), Contains(), buffer zones creating, creating of the auxiliary information (Area(), Centroid(), Length(), ...) or coordinate transformations (Transform()). There is possible to provide all of the hereinbefore operations using these functions. Presuming optimal query building there is linear dependency of the query performance on the number of processed features. This presumption was tested on the sets of hundreds of thousands point features. The advantages of RDBMS use are evident in the case of really huge data sets (from the tables which exceeds tens thousands features, usually in the orders of hundreds of thousands or millions). In the case of storing the spatial

data into usual file system structures there exist big risk of the loss of gathered data from the reason of the system failure. In regards of transaction mode of data manipulation and common robustness of the data storage in the relational databases (including PostgreSQL) the is not possible to lost considerable amount of data. The maximum loss might be the data which were partially written to the storage place in the time of failure, not more than one transaction block. When using some safe backup schema of the database structures, there is secures pretty good prevention of the data loss.

The spatial data requires very specific method for indexing. In the case of simple attribute columns one can use some simple indexing mechanism (B-Tree) provided by the database. There is not sense to use the same indexing mechanism in the case of spatial data. There is a need to use R-Tree or GiST (Generalized Search Tree) indexes for these data. R-Tree indexes works on the principle of recursive dividing the spatial data area to the regular rectangles. The features are indexed on the base of their envelope to the particular rectangles in the structure. This way is in the opinion of PostGIS developers not supported so good like the GiST method which is preferred. GiST method indexes the features on the base of their topological relations. This indexing needs enormous machine time. On the server with the Athlon processor with the frequency 1200 MHz gave approximately one hour to get the spatial index on the testing table with one million of the line features having average of the 20 vertices. In result, all queries taking the advantage of the spatial indexes are much faster with them. There is always way how to enforce the spatial index use in each query using spatial functions. Reindexing of such a huge table is more simple and faster and is performed transparently when maintaining (vacuuming) the database.

There is possible to say that using the open source spatial relational databases gives indisputable advantages when manipulating huge amounts of spatial data. After examining the situation on the market (comparing the implemented solutions of the ESRI ArcSDE, Oracle Spatial and PostGIS) and considering the cost/performance ratio it seems that selected solution is optimal. One can only wish to have more software tools from commercial as well as from noncommercial sphere available that makes available the direct work with the data stores on the base of PostGIS.

References:

- [1] S. SANTILLI, CH. HODGSON, P. RAMSEY, J. LOUNSBURY, D. BLASBY: *PostGIS Manual*, Refrations Research Inc., Canada, 2004, pp. 7-53.
- [2] B. MOMJIAN: *PostgreSQL Praktický průvodce*, Computer press, 2003 pp. 6-396
- [3] J. TUČEK: *Geografické informační systémy (principy a praxe)*, Computer press, 1998,
- [4] J. KOLÁŘ: *Geografické informační systémy 10*, vydavatelství ČVUT, 1997

This research has been supported by Czech Science Foundation grant registered under the number 205/03/D155 and supported by the research proposal MSM 210000007 Complex innovation of technologies in geodesy and cartography as well.

Two-dimensional Pattern Matching Using Finite Automata

J. Žďárek, B. Melichar

zdarekj@fel.cvut.cz

Department of Computer Science and Engineering
Faculty of Electrical Engineering, Czech Technical University
Karlovo náměstí 13, 121 35 Praha 2, Czech Republic

In our article published in these Proceedings last year we have mentioned some already explored ways and methods of two-dimensional pattern matching performed by finite automata, *e.g.* algorithm of *Bird* and *Baker*. Their algorithm uses mechanisms slightly different from classical finite automata, *i.e.* *Aho* and *Corasick* algorithm for linearisation of the 2D problem, and *Knuth-Morris-Pratt* algorithm for matching 2D occurrences, both can be represented by pattern matching machines (automata using *fail-function*).

Our approach is completely based on finite automata described by classification model [3-4] for 2D pattern matching exact and approximate. The classification criteria are: 1. nature of the pattern (String, seQuence); 2. integrity of the pattern (Full pattern, Subpattern); 3. number of patterns (One, Finite number, Infinite number); 4. way of matching (Exact, approximate using Hamming distance (R), approximate matching using (generalized) Levenshtein distance (D,T), matching using Δ (G), Γ (L) or combined Δ - Γ (H) distance); 5. importance of symbols in a pattern (take Care of all symbols, Don't care of some symbols); 6. number of instances of pattern (One, finite Sequence). Together those criteria describe all known subtypes of 1D pattern matching. Note that we updated the model from [3] in the fourth dimension with distances used in the area of musicology [2], which were not known at the time of publication [3]. The updated classification allows us to describe conveniently new types of automata used for 2D matching.

Now let us describe our new model and general algorithm for reusing of finite automata for 2D pattern matching. As finite automata are able to solve sequential problems, appropriate transformation of multidimensional (nonsequential) problems to sequential ones is needed. The idea of solving multidimensional pattern matching problems using the finite automata is simple: multiple automata should be used passing their results among them, reducing dimension of the problem by one in each step. In the last step classical pattern matching can be used.

A generic algorithm of the two-dimensional pattern matching using the finite automata.

Its input is certain pattern matching problem that specifies the edit distance (if any) and a value k , $1 \leq k \leq mm'-1$, k be the maximum number of allowed errors or $k=0$ for the exact matching. Let pattern array PA be $PA \in A^{m \times m'}$, text array TA be $TA \in A^{n \times n'}$, A be an alphabet. Let PS be the set of all (distinct) columns of PA , treated as individual strings and let us suppose the preprocessing starts vertically, *i.e.* in columns of TA . The output depends on a further specification of searching, *e.g.* reporting all occurrences or first occurrence only, etc.

At first we build a dictionary-matching automaton $M(PS)$ (of type *SFF?CO*), where each final state corresponds to some pattern in PS and eventually to some number of errors found in a particular pattern. Types of errors (if any) are given by a kind of distance considered for 2D matching. Columns of the pattern array are identified by final states of the automaton $M(PS)$. In the second step the automaton $M(PS)$ is applied to each column of TA and a new array, TA' , is generated. Its elements are determined by run of $M(PS)$. In case of the exact matching it suffices to store whether some string from PS ends at a given element. In case of the approximate matching a number of errors for particular strings from PS found in TA must be stored into TA' . Then *string P* over the set of final states of $M(PS)$ is computed. P

represents the exact match of the pattern array PA in further matching: the i^{th} symbol of P is the final state identified with the i^{th} column of PA without considering errors. In the fourth step the string matching automaton M' of type $SFO??O$ is build, searching for P with at most k errors. Counting these errors means to limit the sum of errors found in the second step in each string (column) of PA in a particular 2D occurrence. In the last step the automaton M' locates the representing string P inside the rows of TA' , reporting eventual (1D) occurrences of P in TA' , hence also 2D occurrences of PA in the original TA .

Based on this generic algorithm we developed two specific models and algorithms. Our model of 2D exact pattern matching requires two finite automata: the $M(PS)$ automaton is the $SFFECO$ automaton; the M' automaton is the $SFOECO$ automaton. These automata have neat structure, so they are useful as a model, but they are also nondeterministic. In order to achieve linear time complexity for the 2D exact pattern matching using our method, direct constructions of deterministic finite automata (DFA) should be used. Fortunately, it is possible in this case (cf. [1]): DFA $M(PS)$ can be constructed as *linear dictionary-matching automaton*, DFA M' can be constructed as *linear string-matching automaton*. The 2D exact pattern matching using direct construction of DFA's has linear asymptotic time complexity.

Model for 2D matching using the 2D-Hamming distance (*i.e.* matching with mismatches) employs a NFA $M(PS)$ of type $SFFRCO$ for the approximate matching of set of strings using the Hamming distance. $M(PS)$ consists of $SFORCO$ sub-automata for the approximate pattern matching using the Hamming distance. For counting errors in the preprocessed TA' a SFOLDO automaton is used. These automata are nondeterministic and there is no known method of their direct construction, therefore a simulation is needed, impairing the overall time complexity, that is $O(m \lceil \frac{m}{w} \rceil n^2)$, where m, n denote the length of pattern's and text's side, respectively, and w is the length of the computer word.

Note that these results hold for the finite input alphabet, otherwise they should be multiplied by standard factor $\log(|A|)$, where A is the (unbounded) input alphabet.

References:

- [1] CROCHEMORE, M. – HANCART, C.: *Automata for matching patterns*. In Rozenberg, Salomaa, editors, *Handbook of Formal Languages* Springer-Verlag 1997, pp. 399–462.
- [2] CAMBOUROPOULOS, E., CROCHEMORE, M., ILIOPOULOS, C.S., MOUCHARD, L., PINZON, Y.J.: *Algorithms for computing approximate repetitions in musical sequences*. In Raman, Simpson, editors, *Proceedings of the 10th AWOCA* Perth, WA, Australia 1999 pp. 129–144.
- [3] MELICHAR, B. – HOLUB, J.: *6D classification of pattern matching problems*. In Holub, editor, *Proceedings of the PSCW*. DCSE FEE CTU 1997, pp. 24–32.
- [4] ŽDÁREK, J. – MELICHAR, B.: *Finite Automata and Two-dimensional Pattern Matching* Proceedings of the IS'2004 - Theoretical Computer Science 2004, pp. 185–188.

This research has been supported by: the FRVŠ grant 2060/2004, the Czech Technical University grant CTU0409413 and by the MŠMT research program MŠM 212300014.

Innovation of subject "Communication in Data Networks"

P. Bezpalec

`bezpalec@fel.cvut.cz`

Department of Telecommunication Engineering, Czech Technical University in Prague,
Faculty of Electrical Engineering, Technicka 2, 166 27 Praha 6, Czech Republic

For a graduate in our profession it is important to gain not only theoretical foundation through education, but also an adequate practical proficiency. The main aim of the project was to innovate educational process in subject "Communication in Data Networks" in practical courses as well as in theoretical lectures.

Innovation of practical courses

Main work has been done in innovation of practical courses. Refreshed practical courses syllabus contains seven practical tasks

- Task 1 Universal cabling measurement
- Task 2 Physical level of Ethernet 10 BASE-T
- Task 3 Protocol PPP – basic analysis
- Task 4 Ethernet switch Cisco Catalyst 1900 – connection, configuration and analysis
- Task 5 Router Cisco 2500 – connection, configuration and transmission analysis
- Task 6 VoIP gateway – connection, configuration and analysis
- Task 7 Application level protocols analysis (HTTP, ARP and DHCP)

All input study materials for practical tasks have been innovated and transformed into Internet—ready form and then published to server that belongs to our department (www.comtel.cz → Předměty → 32KD → Materiály pro výuku) and therefore are easily accessible by students.

Innovation of Task 1 – new cables and data distribution box for cabling models demonstration, material and tools to successful task realization (connectors, pliers and punch tools).

Innovation of Task 2 – new test device that accommodate Ethernet (10 BASE-T and 100 BASE-T) parameters to be easier measured, demonstrated and oscilloscope displayed.

Innovation of Task 3 and Task 7 – new device for data communication link analysis equipped by modules for detailed analysis of all data-link and network level protocol (included PPP with authorization PAP or CHAP, DHCP, HTTP, BOOTP, ARP, IP).

Innovation of Task 5 – new specialized cables for connection between two routers (technology V.35 a X.21) and old broken cables repair.

Innovation of Task 6 – new VoIP gateway and control software, yet gateway loaned out.

Innovation of theoretical lectures

New telco knowledge that has been studied has extended a spectrum of lectures. Mainly English written literature has been translated into new lecture base that is in form of MS PowerPoint presentation. This chosen format is able to show new concepts with animated explanation. This is more didactical. An electronic form of new lectures has been placed on Internet (www.comtel.cz → Předměty → 32KD → Materiály pro výuku) and therefore is easily accessible by students.

Conclusion

Main goals of subject innovation are:

- New knowledge implementation.
- Workplace innovation for practical tasks.
- Practical tasks optimization and material, tools and device complementation.
- New study material creation for theoretical lectures.
- All study material is in electronic form of presentation.
- Motivation of IT students to study modern telco technologies.

This research has been supported by FRVS F1 2005/2004.

Implementation Signaling Gateway in Next Generation Network

J. Baloun, V. Lojik

balounj1@fel.cvut.cz

CTU, Faculty of Electrical Engineering, Dept. of Telecommunications

Technická 2, 166 27, Praha 6

With development of Internet happens to intense a data transmit growth, that begins to prevail over telephone traffic in existing telecommunication networks, i.e. telephone services traffic. Current development of telecommunication networks tends to the convergence data and voice services, and therefore to the convergence in the one, integrated and broadband network, that supports all kinds of telecommunication services. It comes to being the network next generation NGN (Next Generation Network). Although the particular conception of this network is not quite clear so far, it is supposed, that its problems will be construct on IP (Internet Protocol) technology.

For the future progress of the multiservice data networks in Next Generation Network is important MPLS technology (Multiprotocol Label Switching), which is used for the IP packets transfer throughout this network. This grant has initially dealt with signaling gateway analysis between MPLS and a mobile network. During the grant solution it arisen change and the analysis concerned with the MPLS and WiMax (wireless metropolitan network) technology. By the reason of time seriousness and complexity the grant solution limits to the signaling analysis of MPLS. Next work will concern with signaling analysis in WiMax technology and consequently in signaling gateway dimensioning design and its mathematical description.

The MPLS technology has arisen mainly by demands on:

- Increasing throughput the routers thanks to the packet switching of the numeral labels with fixed length,
- The packet routing based on the destination address and the next fields in the IP header,
- The hardware usage based on destination address and the next fields in the IP header.

This technology is based on the labelling packets 3rd layer the RM-OSI model principle by marks (labels). Then the packets are transfer through the MPLS network in terms of these labels. The time and processor difficult analyses are wasted in connection with scanning the routing tables, that are realised only in input point. Labels determine the path of packet, but they could specify for example the service type.

Important part of MPLS technology is signaling. The signaling in MPLS technology covers several functions. It is label creation and distribution, LSP (Label Switched Path) creation and LIB (Label Information Base) updating. Label creation may be performed by the three ways: Topology-based, Request-based and Traffic-based. Label creation by topology-based is the method, where the labels are carried altogether with assigned network addresses by means of the routing protocols (BGP, OSPF, ...). Label creation by request-based assigns RSVP packet flow switched path LSP. The last method of label creation is traffic-based. This method assigns label to FEC (Forward Equivalence Class) according to packet header.

The label distribution within MPLS network may be performed by the two ways: Down-Stream Distribution and On-Demand Down-Stream Distribution. In the first case the router with assignment "label – address prefix" informs either neighbour routers in the path

according to routing table with the existing assignments. In the second case, the router that demands data relay requires valid label for the address from neighbour router.

Creation of LSP is performed by the two ways: Independent path selection and Explicit routing. The first method is the switched path LSP created according to valid routing tables by method hop-by-hop. Signaling messages are carried between ingress and egress router MPLS network. In the second method ingress router beforehand defines packets path in the form of partial routers sequence alongside the signaling messages are carried.

Label Information Base (LIB) updating is performed in conservative or liberal mode. With the conservative mode are accepted the only label their assignment comes from neighbouring routers of the network. The liberal mode means the signaling messages accepting from all routers in the network. The demands on label maintenance are growing but the response time is better in the case of the path failure.

The existing routing protocols like BGP and RSVP (after the adaptation RSVP-TE) are used in signaling in MPLS. Special signaling protocols like LDP (Label Distribution Protocol), CR-LDP (Constrained Routing – LDP) and Cisco proprietary TDP (Tag Distribution Protocol) were created.

Technology MPLS starts to be applied in the providers core networks and its main task in the near future is integration with the other technologies, like wireless or mobile networks. Wireless metropolitan technology WiMax enables support ATM (Asynchronous Transfer Mode) and Frame Relay but not MPLS. WiMax supports quality of service (QoS). This concept enables above all the audiovisual and data transmission.

References:

- [1] BLACK, U.: *MPLS and Label Switching Networks* Prentice Hall Series 2001
- [2] MINOLI, D.: *Voice over MPLS, Planning and designing networks* McGraw-Hill TELECOM 2002
- [3] SWEENEY, D.: *WiMax, operator's Manual* Apress 2004
- [4] TECHNOLOGY GUIDE: *Multiprotocol Label Switching (MPLS)* The Applied Technologies Group, 2003, <http://www.techguide.com>

This research has been supported by CTU 0407113.

Network Attached Storage

O. Smíšek

smisek@fd.cvut.cz

CTU, Faculty of Transportation Sciences, Section of Computer Technology and Network Services,

Konviktská 20, 11000 Praha 1

The main task of this project is to increase space for students' work, to enhance opportunities for storing data, to improve connection between Decin's campus and Prague's Faculty of Transportation Sciences. The opportunities of education will be also enhanced – there will be more space to store materials for studying and educational aids on the net. All these tasks are very demanding for file server and for its networking. As shown in [1] Novell NetWare 6 is the Net services software solution that offers secure non-stop access to core network resources. With NetWare 6 students can access files, printers, directories, e-mail and databases across all types of networks, storage platforms and client desktops. NetWare 6 leverages the powerful Novell eDirectory, giving administrators a way to easily manage the network from virtually any Web-enabled, wireless device or traditional desktop computer. NetWare 6 also supports open, Internet standards and includes innovative, browser-based Net services.

NetWare 6 revolutionizes file access and management by incorporating Novell iFolder, a unique Net services solution that enables access to personal files—from anywhere, at anytime—through virtually any Web-enabled device. Moreover, iFolder provides powerful security for your data, ensuring that your files are always protected from prying eyes. Ideal for mobile users, NetWare 6 incorporates NetWare Web Access, interface through which users can access network resources from virtually anywhere in the world. With NetWare Web Access users simply use a standard Web browser to log into CTU's network environment. In fact, NetWare Web Access is conveniently integrated with eDirectory. This means that users can use the same network passwords to enter NetWare Web Access as they use on workstations, KOS, etc.

To further extend of our network's boundaries, NetWare 6 supports various file protocols, including AppleTalk Filing Protocol for Macintosh (AFP), Network File System (NFS) and Common Internet File System (CIFS). NetWare's support for these diverse protocols eliminates the need for client software: communication is accomplished over TCP/IP and native applications are run over the network.

Although a server that just meets the minimum hardware requirements is sure to function, it will by no means be an efficient services provider. In fact, if additional features such as iPrint or NetStorage will be installed, the minimum configuration is not sufficient. The following list defines powerful hardware configuration of new server: Processor Intel Pentium Xeon 3 GHz, 1024 MB RAM, 5x145 GB SCSI 10000 rpm HDD, 2x18 GB SCSI 15000 rpm HDD, gigabit Ethernet network card, SCSI controller supporting raid.

Thanks to this hardware students can use digital materials in better quality in their semestral works. They can use more video files for enhancing their presentations. I choose complete copy of all data and users from old server to new one as a solution of this problem. At the same time I have improved connection between Decin and Prague or more precisely I have built new context called DETAS in novel's tree FD. This means, that all servers in FD tree are in the replica ring. For this copy task I used Novell NetWare Server

Consolidation utility that makes it easy to move files, volumes and directories among NetWare servers. This utility is in high demand because it permits Novell eDirectory attributes to accompany files wherever they are copied.

The timesaving flexibility of the NetWare Server Consolidation utility is particularly useful if we are trying to reorganize our network, consolidate files into a storage area network (SAN) or upgrade to a new version of NetWare. And because it copies files, rather than migrate them, the utility leaves source data intact.

In addition to moving server files and volumes, the NetWare Server Consolidation utility also moves printer agents among Printer Server Managers.

This operation was completed successfully. Of course this software cannot copy user's passwords. Consolidation utility software has created random passwords for all users – eight characters long. This situation has negative impact on network's life, because no one could connect to the server. On the other side this fact caused, that security of the user's passwords has been improved.

After passing this operation the web server Apache, as shown in [2] and NetStorage configuration had to be done.

The experimental tests showed after installation that users created by NetWare Server Consolidation utility have some errors with their home directory configuration and also public rights were not applied correctly. Dealing with this problem represented hours of manual work. At the beginning of running of this system users caused very high network stress on the server so that I had to change 100's mb/s switch to 1000's mb/s one. Next experience showed that NetStorage system is used mainly by part-time students and Apache web server is used mainly by full-time students for their web presentations and personal websites.

This new network attached storage system is at the beginning of its life and at the beginning of its capacity utilization. Next task of this system will be storing lectures video files and helping with data store to all parts of the Faculty of Transportation Sciences.

References:

- [1] PŘICHYŠTAL, O.: *Novel NetWare 6* Computer Press, 2002,
- [2] KABIR, J.: *Apache Server 2* Computer Press 2004,

This research has been supported by CTU0419316.

Ethernet for Real-Time Applications

O. Dolejš

`xdolejs@fel.cvut.cz`

Czech Technical University in Prague, FEE, Department of Control Engineering,
Karlovo nám. 13, 121 35 Prague, Czech Republic

Ethernet was designed for computer networks in 70's without any real-time requirements and it was normalised later as IEEE 802.3 standard. Today, Ethernet is widely spread in office computer communication, which implies high availability and low implementation cost of Ethernet based solution. Therefore Ethernet is very attractive for the automation area due to high performance and wide diagnostics possibilities (using several protocols simultaneously running on the same medium).

Distributed real-time applications have two main requirements for data delivery: time determinism and reliability. Ethernet in general is not deterministic due its media access control (CSMA/CD) and therefore its behaviour under transient overload is not sufficient for any real-time application. On the other hand, if the applications have predictable and bounded number of requests, the behaviour of Ethernet is “nearly” real-time — the probability of the delayed data delivery is very low due to the reasonably low number of accesses compared to the high-bandwidth performance.

Widely used and popular protocol TCP/IP is reliable, but it cannot provide time determinism. The number of retried packets is not predictable and causes the time non-determinism. The UDP/IP protocol is better suited for distributed real-time applications, since it is deterministic (in the sense of packet retransmission). The UDP/IP needs to be combined with an upper layer, which provides packet retransmission suited for control applications due to the UDP/IP's insufficient reliability.

Several communication protocols using Ethernet for automation came up in the last years. Some of them are built on the top of TCP (Modbus TCP, ProfiNet v.1.2), some on the top of UDP (NDDS - Network Data Delivery Service, Modbus UDP) and some are built directly on Ethernet (PowerLink, ProfiNet v.2). NDDS middleware is commercial implementation of RTPS (Real-Time Publish-Subscribe) protocol. ORTE (Open Real-Time Ethernet), our open-source implementation of the RTPS specification, is an alternative to NDDS built on the top of the UDP/IP protocol and tested on Ethernet, freely available at (<http://sourceforge.net/projects/ocera>).

PowerLink, developed by Bernecker&Rainer Company, is a proprietary real-time protocol built directly on the top of the Ethernet link layer. This protocol uses the Time-Division scheme for data delivery, where every node has a time-slot to send its data to avoid the collisions on Ethernet.

The problem of the data delivery probability estimation for NDDS can be partially solved by analytical methods using probability calculation or by experimental results.

In this project the ORTE (Open Real-Time Ethernet) was tested as open-source implementation of RTPS middleware (Real-Time Publish-Subscribe), built upon UDP/IP. To derive the time delay influence of the operating system, we combined the application response time measurement on physic model with the simulation results given by OPNET Modeler.

The special modular program was written for testing ORTE communication. Modularity of the program was used for different configuration varying in number of nodes (PC), application repetition, sent packet length and number of generating packets. This program

conception has allowed very fast reconfiguration of testbed. As was sad before, the same HW configuration was realised in OPNET Modeler, which allows taking advantage of wide HW and SW resources implemented in it.

The establishing the communication between publisher and subscriber was done automatically by simple rules, in each node was generated two publishers and one two subscriber. The application response time was measured as

A special program to start the application remotely was written to ensure the same starting time at all nodes.

The possibility to integrated the ORTE protocol directly into OPNET Modeler was also tried. There was the overwhelming problem during the integration phase due to cooperation OPNET Modeler with external code. ORTE and OPNET code are dependent on time scheduling and this problem wasn't possible to manage with OPNET support.

There was a lot of feedback action to the ORTE developer to solve the ORTE implementation incorrectness.

As a result we have achieved the separation of the processing time in operating system and the communication time (Ethernet). The processing time gives higher jitter to the application response time. The communication time gives no jitter to the application response time due to the switched Ethernet.

Therefore, further development of ORTE will be focused on new implementations in order to obtain deterministic and possibly shorter processing time. The former can be achieved by using real-time operating systems (like RTAI or RT Linux), and the latter by using faster hardware. The faster HW caused shortening of processing ten times, but the variation is still present due to non-real time Linux version, which was used in tests.

The financial subvention from the CTU internal project was used for buying better PC to achieved enormous simulation condition in OPNET Modeler, during tests on Ethernet. And the second financial part of resources was given to attend the international conference .

References:

- [1] KLEINROCK, L., TOBAGI, F.A.: *Packet switching in radio Channels: Part I-Carrier Sense Multiple Access Modes and Their Throughput Delay Characteristic* IEEE Transaction on Communication, 1975, pp. 1400-1416.
- [2] SMOLIK, P., SEBEK, Z., HANZALEK, Z.: *ORTE - Open Source Implementation of Real-Time Publish-Subscribe protocol* Polytechnic Institute of Porto 2003
- [3] DOLEJS, O., HANZALEK, Z.: *Simulation of Ethernet for Real-Time Applications* Cyklus d.o.o., 2003 pp. 1018-1021.
- [4]

This research has been supported by CTU0407913.

Coordinate Systems in PostGIS and Results of the Transformations

M. Bořík*, V. Honzík**

borikm@mat.fsv.cvut.cz

* Department of Mathematics, Faculty of Civil Engineering, Czech Technical University, Thákurova 7, 166 29 Prague 6, Czech Republic

** Department of Mapping and Cartography, Faculty of Civil Engineering, Czech Technical University, Thákurova 7, 166 29 Prague 6, Czech Republic

Coordinate systems in PostGIS and transformation results using freeware **proj** have been demonstrated in this paper. The original program PROJ was developed by Gerald Evenden at the beginning of the eighties in the programming language Fortran for the purposes of the United States Geological Survey, where it served entirely for the calculations in the area of mathematical cartography and in itself was used only as single-purpose utility. The original source code was developed step by step and the next projections were gradually added. In the progress of time was rewritten to the C programming language and today is as a PROJ.4 is distributed under the MIT license as nearly all software created at the government organizations of the United States.

That gives the program practically the public domain status. Program package is maintained by Frank Warmerdam and was revised by him to the form of program library which allows to it the transparent use in various programs working with the spatial data. The original use as a standalone program remained, anyway the usability in the form of program library multiplies its potentials. In the applications with the support of PROJ library is possible to use simultaneously the data from different (supported) coordinate systems and the library supports the necessary transformation calculations to the coordinate system which is used for the work with the data.

All of the computations were performed in the PROJ package programs in the version 4.4.9. For the conversion of the coordinates from planar reference system to the geographic coordinates on the reference sphere is used the program **proj** or program **invproj** for the computations in reverse direction. For the transformations between particular systems is utilized the program **cs2cs** (cs for coordinate system). By reason that the finding and use of the transformation parameters among all of the reference spheres (ellipsoids), in the system PROJ is used one of the reference ellipsoids (ETRF-89) as a transitional and all the transformations are decomposed to two steps – the transformation from the source coordinate system to ETRF-89 and from ETRF-89 to the target coordinate system. However there is no public available authorized transformation parameters between Krassovsky reference ellipsoid (used as reference projection sphere for S-42 coordinate system) and ETRF-89. This article should not only show the features and ways of use of **PostGIS** as a powerful tool for storing and manipulation of the geodata and the remotely network access to them in the frame of expected use by the subjects working with the geodata in the Czech Republic area, but as well the solution of the transformation among particular coordinate systems used in our area using the PROJ library.

Open source projects in the GIS area are monitoring the trends visible in the commercial systems. We can find here mainly desktop oriented systems (QGIS, GRASS) as well as the project aimed to the publication of spatially oriented data in the field of Internet/Intranet (e.g. UMN MapServer). Just like the commercial GIS there is an effort to divide the tools for storing the data and tools for processing them.

The OGC Simple Features Specifications for SQL standard defines the standard object types for GIS, the functions necessary for their manipulation and the set of database tables containing related metadata. From the reason of securing the data and their metadata consistency there are special procedures for the operations of creating or deleting the columns with the spatial objects.

PostGIS defines two tables containing metadata. The **geometry_columns** table with the information for particular tables (only those with the spatial objects) the necessary information about the type of geometry, object dimensions and used coordinate system using the identification number. The identification numbers are stored in the **spatial_ref_sys** table and their values are in accordance with the instruction of European Petroleum Survey Group (EPSG). Along with them are stored the definitions of the individual projections on the base of ESRI prj files and the principal information – the PROJ parameters for manipulation with the coordinate system. The EPSG instruction was selected because of its high elaboration level.

The principles of storing the geodata together with their metadata mentioned in the second paragraph allows to display together data from several coordinate systems. The transformation itself is solved using the functions of PROJ library with the transition over the reference space for which was chosen the reference system ETRS-89 (see [2]).

The PROJ program library solves the transition between different reference spheres using seven element Helmert transformation. This procedure gives acceptable results in the case of modern coordinate systems, but in the case of such heterogenous coordinate systems such like S-JTSK and S-42 gives the results with as much as 5 meter absolute deviation. The alternative method to that one hereinbefore is for instance the evaluation of the increments of the spherical coordinates between two systems using conformal transformation of higher degree with the transformation key which was computed from the set of identical points. This algorithm is used for instance in the cartographic system MATKART.

The precision of the transformation among the coordinate systems S-JTSK, ETRF-89 and S-42 was examined on selected points of DOPNUL campaign [1]. The transformation was divided to four steps. We did the inverse Krovak projection from the JTSK system to Bessel ellipsoid at first, then transformation to ETRF-89 ellipsoid and in consequence to Krassovsky ellipsoid. The last step was the application of the Gauss-Krüger conformal projection from Krassovsky ellipsoid in meridional zones to the S-42 system. PROJ allows the definition of seven parameters of Helmert transformation between both reference ellipsoids and ETRF-89 system, too. The rotation coefficients is necessary to set with plus sign (contrary to [3]).

References:

- [1] KOSTELECKÝ, J.: *Geocentric system and Czech republic trigonometric network*, VÚGTK Zdíby, Proceedings 1996, 41. annual, 1997, pp. 23–30.
- [2] CIMBÁLNÍK, M.– MERVART, L.: *Geodesy I*, ČVUT v Praze, 1997.
- [3] KOLEKTIV AUTORŮ: *Geodetic reference systems in Czech republic*, VÚGTK a VZÚ Prague, 1998.

This research has been supported by GA ČR grant No. GA 205/03/D155.

Location Methods in GSM

Ing. Michal Frýda

fyrdam@feld.cvut.cz

Department of Telecommunication Engineering, Faculty of Electrical Engineering, Czech Technical University, Technická 2, 166 27 Prague 6, Czech Republic

In the Research and Development Centre in Prague we are involved in a project research on the localization methods in GSM networks. There are several proposals on how mobile phones can be positioned. There are also other questions that must be solved before the location-based services will be offered to customers. The most important question is how to provide subscriber's privacy and who should own positioning information. Other issues that must be solved are charging, interoperability between operators and roaming.

The study was based on results published by Neil Chan in "Introduction to Location-Based Services".

Location methods seem to be the important part of future mobile communication. It is a hot topic in the subject of wireless communication. This article tries to give an elementary introduction to location methods. It explains what is location methods, the technology involved, its applications and other noteworthy issues.

Positioning methods, which has been checked can be divided into the following three categories: basic (based on the use of cell identification, or together with timing advance parameter and network measurement report), enhanced (enhanced observed time difference) and advanced (assisted GPS).

The most important thing in location methods is of course the positioning technology, which makes the way to find the location of a mobile station accurately. Due to the unique characteristics of the cellular environment, it is not easy to locate the object precisely. Many advanced methods are used for positioning. The most important are satellite-based technology (A-GPS, Galileo, GLONASS, etc.), network-based technology (Angle of Arrival, Time of Arrival, Time Difference of Arrival, hybrid methods).

The following location methods have been studied. The description of most important attributes is defined below.

The most accurate technology is the GPS (Global Positioning System). GPS is maintained by 24 satellites and few ground stations located around the equator. GPS finds out the location based on the concept of Trilateration, a fundamental geometric principle that allows to find one location when its distance from other known locations is known. GPS is proved to be accurate and useful enough for many years. However, it is not good enough for LBS uses. The main disadvantage is that to use GPS, the mobile station should be in sight of minimum three satellites. This is impossible in indoor or urban areas. Only GPS is not accurate and fast enough for demanding LBS uses.

A-GPS (Assisted GPS) is developed to compensate the weakness of GPS. This is a combination of mobile technology and GPS. It uses local wireless network. The assistance information derived from wireless network is used to substitute the satellite and locate the subscriber. A-GPS is much faster in location acquisition than GPS, more sensitive to signals from GPS satellites and excellent accuracy. The main disadvantage is such approach could be expensive to end-user, because the handsets must be compatible with GPS functionality. New mobile stations are needed.

The location of a mobile station can be determined in accordance with its cell site. Coverage of a whole network is divided into different cells. The covered area is called cell and has its unique cell number called Cell ID. The network coverage in this cell is provided by a base

station. Signals between the mobile system and base station can be used in positioning technology. This kind of the positioning technology uses different methods of triangulation of the signal from serving cells. The basic types of location methods based on network are COO (Cell of Origin). The base station cell area is used as the location of the mobile device. Positioning accuracy depends upon the size of the cell. Accuracy may be 150 meters in urban areas, or 30 kilometers away from the target where base stations are less density of cells. The advantage is the speed of response and no network upgrade is required.

COO is a technology that is widely deployed in wireless networks today. This method is used to meet Phase I requirement of E911 mandate.

D-TOA (Difference in Time of Arrival) is based on different propagation time of a signal from a mobile station to three base stations is used to calculate the location. This system requires a synchronization of the cellular network using GPS or atomic clocks at each base station. It is more accurate than COO, but longer speed of response is required (usually more than 10 seconds).

AOA system (Angle of Arrival) requires a complex of four to twelve antenna array at each of several cells locations. These antenna arrays can work together to determine the angle (relative to the cell site) from which a cellular signal originated. When several cell sites can each determine their angles of arrival, the mobile station location can be estimated from the point of intersection of projected lines drawn out from the cell site at the angle from which the signal originated. The main drawback is the system suffers from distortion of the wavefront of the cellular signal such as multipath. Another problem is that existing cell site antenna are not suitable for angle of arrival.

E-OTD (Enhanced Observed Time Difference) systems operate by placing location receivers or reference beacons, overlaid on the cellular network as a location measurement unit (LMU) at multiple sites geographically dispersed in a wide area. The time differences of arrival of the signal from each base station at the mobile station and the LMU are described in Introduction to Location-Based Service, by Neil Chan, Aug 2003 calculated. The differences in time stamps are then combined to produce intersecting hyperbolic lines from which the location is estimated.

E-OTD schemes offer greater positioning accuracy than cell of origin, between 50 and 125 meters, but have a slower speed of response, typically around five seconds, and require software modified handsets, which means that they cannot be used to provide location specific services to existing customer bases.

Geographic data are required for location methods to function. It provides the data to render structures like road network, buildings and terrains like mountains and rivers. GIS is also used to manage point-of-interest data such as location of gas stations, restaurants, cinema halls, etc. The quality or types of Geographic data needed is dependent in the type of service to be provided to the user. The Geographic data needed should be updated and rich to be able to cater to various demands of LBS.

The main goal of the localization of mobile station is to provide wide range of useful services such as emergency, people tracking applications, information directory service, advertising or location based billing. The results of this project will be used in planned location based services requested by the mobile provider.

This research has not been supported by any grant.

Simulation of Fuzzy Control of Belt Drive Driven by DC Motor

R. Havlíček

`havlicr@fel.cvut.cz`

Department of Mechanic and Material Science, Faculty of Electrical Engineering, Czech
Technical University, Technická 2, 166 27 Prague 6, Czech Republic

Fuzzy regulation is mostly used for driving systems that are difficult to describe mathematically. In case of non-linear systems, it also appears to be more advantageous than classical regulation systems. It is suitable for driving systems completely described mathematically, too. Fuzzy regulation is based on fuzzy set and fuzzy logic theory.

It is necessary to normalize the fuzzy regulator input signals first, i.e. to transform them, so that they would gain values from a normalised universum (a value interval). Then it is necessary to match the normalized data with a degree of membership of one or more fuzzy sets. (The normalised data are a sharp value of input signal.) These procedures are followed by computation of output fuzzy data, using individual rules and selected implication functions. These rules are stored in the knowledge base of the regulator. The output fuzzy data must be defuzzified later, i. e. to find their sharp value and therefore to gain resulting drive signal.

The universum must be covered with fuzzy sets according to these rules: Their sum must cover all the universum; and there must not be any point with a degree of membership equal to zero. Individual degree sets may overlap and their arrangement around all the universum does not have to be even. The number of membership functions determines the maximum number of derivation rules. Usually an odd number of membership functions is chosen, with respect to human perception abilities, i. e. 5 ± 2 . The shape of individual membership function should be as simple as possible, usually made of linear sections. If there are measured data at disposal, it is possible to estimate the membership function shape.

Individual derivation rules give a true picture of a verbal description of an appropriate regulation interference. The rules are in the "if – then" format. The number of the rules used in a fuzzy regulator need not always be a maximum number (The maximum is given by the product of the membership function number of individual input signals).

A belt drive with a moving part was used as a model for the simulation itself. The goal is to control the position of the moving part, which is fastened to the driven wheel of the belt drive through the ball shaft. A DC motor for driving the belt drive and other parts necessary for motor driving were incorporated into the model. Individual parts are modelled with respect to their real characteristics. The whole regulation circuit is a cascade circuit, and fuzzy regulation is used only for the outer loop. The inner loop includes a classical PI regulator. The PI regulator model was implemented by an optimum module method. Of course, other design methods were used too, but for this case the optimum module method was the most suitable one.

The influence of all factors affecting regulation quality were analysed for the fuzzy regulation. These factors for this case include input signals of the fuzzy regulator, the number and coverage of input and output signals, the implication functions used, the shape of membership functions, the total number of rules in the knowledge base of the regulator.

The solution with the regulator with a single input turned up to be unusable. The effect of all the other factors was so small that the resulting regulation quality was not influenced at all or to a tiny extent. This solution is therefore useless for the practice. Adding one more input significantly improved the regulation quality and the effect of the other factors was very easy to identify. The hypothesis, that an even coverage of the universum by membership functions is easy to design, but the result of the regulation process is not completely satisfactory, has proven true. The resulting quality is markedly influenced by neither the number of membership functions nor their shape. On the other hand, with an uneven coverage of the universum and with a suitable membership functions shape, it is possible to gain almost any course of the regulation process. The choice of the implication function and the defuzzification method had a significant effect on the result, but not as significant as the coverage and shape of membership functions. It is essential to note that good results were achieved only in case when the regulator knowledge base did not contain the full number of rules. In case of full rule number usage the regulator did not almost react to the change of the other parameters. Adding a next input to the regulator did not have an effect comparable to the usage of the second input. All the design became much more complicated and individual factors influenced each other to a larger extent; and it was not easy to state the dominance of any of them. Considering the very good results gained while using two input signals of the fuzzy regulator, the influence of more inputs was not further analysed and the usage of three inputs was marked as an ineffective choice.

As stated above, all this research was done only as a computer simulation. The plan is to verify these simulations on a real-life model, which is already being prepared. Considering the fact that the model was made with respect to real characteristics of individual parts, it is assumed that the results will be similar to the simulation results. The drive of the same mechanical system with a different electromotor is also being prepared.

References:

- [1] HAVLÍČEK R.: *Fuzzy řízení mechanických soustav poháněných elektromotory*, Proceedings of IX. International Conference on the Theory of Machines and Mechanisms, Technická univerzita Liberec, 2004, pp. 357–362.
- [2] HAVLÍČEK R.: *Fuzzy řízení řemenového převodu poháněného stejnosměrným elektromotorem*, Sborník 45. mezinárodní konference Kateder částí a mechanismů strojů, VUT Brno, Fakulta strojního inženýrství, Ústav výrobních strojů, systémů a robotiky, 2004, pp. 480–483.

This research has been supported by CTU grant No. CTU0406513

Hardware for Solving Sets of Linear Congruences

J. Hlaváč, R. Lórencz

hlavacj2@fel.cvut.cz, lorencz@fel.cvut.cz

Department of Computer Science and Engineering, Faculty of Electrical Engineering,
Czech Technical University, Karlovo nám. 13, 121 35, Praha 2, Czech Republic

A typical and very frequent task in numerical mathematics is the solution of linear algebraic equations. When solving a set of linear equations (SLE), one often meets the problem of ill-conditioned matrix of the set. For large dense sets of linear equations, which are usually ill-conditioned, the stability of a numerical solution cannot be ensured. Rounding errors during the numerical computations involved in obtaining the solution of the problem cannot be tolerated. Many numerical methods were developed trying, with more or less success, to minimize the influence of the rounding errors on the resulting solution.

Residual number system (RNS) appears to be a suitable number system for implementing certain numerical methods for error-free solving of a SLE. One of such methods is described in [1]. The computational complexity of this method is larger than the complexity of the original task of solving a SLE in the domain of floating-point numbers. Therefore, the mentioned paper describes a design of a parallel architecture of a modular system based on RNS which speeds up the complete calculation.

This modular system consists of a control unit and the so-called Residual Processors (RP) that operate in parallel. The algorithm of solving SLE according to the methods described in [1] using the mentioned modular systems has three basic steps.

1. Conversion of the coefficients of the matrix \mathbf{A} and the elements of the vector \mathbf{b} of a SLE $\mathbf{A}\mathbf{y} = \mathbf{b}$ to systems of sets of linear congruences (SLC) $\mathbf{A}\mathbf{y}_k \equiv \mathbf{b} \pmod{m_k}$, where $k \in [1, r]$ and r is the number of moduli in the utilized RNS.
2. Solving of the r systems of SLC $\mathbf{A}\mathbf{y}_k \equiv \mathbf{b} \pmod{m_k}$ using Gaussian elimination in modular arithmetic modulo m_k . Also, the determinants $d_k = \det \mathbf{A} \pmod{m_k}$ are computed. Then, the solution of SLC $\mathbf{A}\mathbf{y}_k \equiv \mathbf{b} \pmod{m_k}$ is obtained as $\mathbf{z}_k = d_k^{-1} \mathbf{y}_k$.
3. Conversion of the resulting vectors \mathbf{z}_k and the determinants d_k using the mixed radix conversion (MRC) algorithm from the RNS to a single vector \mathbf{z} such that $\mathbf{z}_k = \mathbf{z} \pmod{m_k}$ for $k = 1, 2, \dots, r$. The solution of SLE $\mathbf{A}\mathbf{y} = \mathbf{b}$ is then obtained as $\mathbf{x} = \mathbf{z}/d$.

The first step of the algorithm can be executed in parallel. This means that each RP reads integer elements of the matrix \mathbf{A} and the vector \mathbf{b} of a SLE, and converts them simultaneously into residues modulo m_1, m_2, \dots, m_r . The second step of the algorithm is completely parallel since the solutions of each SLC $\mathbf{A}\mathbf{y}_k \equiv \mathbf{b} \pmod{m_k}$ are independent for every $k = 1, 2, \dots, r$. The RP $_k$ solves the SLC $\mathbf{A}\mathbf{y}_k \equiv \mathbf{b} \pmod{m_k}$. In the third step, cooperation of all RPs is needed to convert the results from RNS to rational numbers using MRC.

For efficient computing of SLE according to the described algorithm using modular systems, the speed of solving the SLC by the RP is crucial. For solving the SLC, four basic arithmetic operations performed in modular arithmetic are used. An important operation in modular arithmetic is the multiplicative modular inverse. Due to its large computational complexity, the problem of efficient computation of the modular multiplicative inverse needs to be solved and a hardware implementation developed. The idea is to use such a designed hardware architecture for modular multiplicative inverse as the basic building block of an arithmetic unit for modular arithmetic, which is an essential part of the vector arithmetic unit inside each RP.

The papers [2,3] detail the design of arithmetic units that are able to perform the four elementary arithmetic operations in modular arithmetic. In the paper [2], the entire

architecture of the arithmetic unit is derived from the architecture that computes the modular inverse using a new left-shift algorithm [4]. The arithmetic unit detailed in paper [3] is derived from the Almost Montgomery Inverse algorithm. Due to the FPGA implementation platform which was used for both arithmetic units, the advantages promised by an efficient implementation of the left-shift algorithm [4] are not utilized. Both designs of the arithmetic units demonstrate the correctness of the utilized design methodology. The papers [2,3] show that the modular inverse algorithms are the most complex ones and therefore it is advantageous to modify the architectures based on these algorithms in a way that allows to perform other operations in modular arithmetic. It is shown that such modifications only marginally worsen the area complexity of the previous circuits that compute modular inverse only.

The knowledge gained from the design of the arithmetic units will serve for their implementation and inclusion in more complex hardware structures. As mentioned above, the goal is to use the designed arithmetic units in vector arithmetic units of the RP for the RNS-based systems for error-free computations. The research performed in this area, a part of which is presented in [2-4], presents a good foundation that fulfils these goals.

References:

- [1] MORHÁČ, M. – LÓRENCZ, R.: *Modular System for Solving Linear Equations Exactly, I. Architecture and Numerical Algorithms*. Computers and Artificial Intelligence, vol. 11, no. 4, 1992, pp. č. 351–361.
- [2] LÓRENCZ, R. – HLAVÁČ, J.: *FPGA Implementation of Arithmetic Unit for Modular Arithmetic*. DDECS – Proceedings of 7th IEEE Workshop on Design and Diagnostics of Electronic Circuits and Systems. Stará Lesná: Institute of Informatics Slovak Academy of Sciences, Bratislava, 2004, pp. 187–190..
- [3] HLAVÁČ, J. – LÓRENCZ, R.: *Modular Arithmetic Unit*. Proceedings of 10th International Conference on Information Systems Analysis and Synthesis. Orlando: IIS – International Institute of Informatics and Systemics, 2004, vol. 2, 2004 pp. 190 – 195.
- [4] LÓRENCZ, R.: *New Algorithm for the Classical Modular Inverse*. Proc. of Workshop on Cryptographic Hardware and Embedded Systems – CHES 2002, August 13-15, 2002, Redwood Shores, California, USA, Springer-Verlag 'LNCS, vol. 2523', 2002, pp 57–70.

Pattern Matching in Compressed Text

J. Lahoda, B. Melichar

lahodaj@fel.cvut.cz

Department of Computer Science and Engineering
Faculty of Electrical Engineering
Czech Technical University
Karlovo náměstí 13
121 35 Prague 2
Czech Republic

The pattern matching in compressed text is relatively new and has undergone huge development in last years. Last year, we have developed an algorithm for pattern matching in text coded by the static binary Huffman coding. We have generalized our approach, in order to provide algorithm capable of performing pattern matching in text coded by certain group of compression methods. The generalized algorithm is able to perform pattern matching in text coded by the (static) finite translation automaton, and so can handle any decompression algorithm that can be represented as a (static) finite translation automaton.

The generalized algorithm works as follows. At the beginning, a pattern matching problem, set of patterns, finite translation automaton representing the decompression algorithm and the coded text are given. Then a pattern matching automaton is constructed for the given pattern matching problem and set of patterns. After that, each state of the pattern matching automaton is replaced by a copy of the translation automaton. The transitions of the pattern matching automaton need to be re-routed. Let us consider transition in the translation automaton from state t_1 to state t_2 for symbol b that translates to string w and a sequence of transitions in the pattern matching automaton for string w from state q_1 to state q_2 . Then, in the newly created automaton create transition from state that corresponds to states t_1 and q_1 into state that corresponds to states t_2 and q_2 for symbol b .

One more problem still exists: as is clear from the above description, by performing one transition in the new automaton, several symbols of the original text may be virtually decoded. As it is not simply possible to recreate this information from the new automaton, we proposed to augment this automaton with two auxiliary tables. The first table ("index" table) contains for each transition how many symbols of the original text were decoded by this transition. This is simply the length of string w . The second table ("match" table) contains offsets of matches that were found by this transition. This table can be constructed by simulating the transitions in the pattern matching automaton for string w .

When the automaton for pattern matching in text coded by the finite translation automaton is constructed, common pattern matching algorithm with some enhancements is employed. The enhancements are quite trivial and are based on the above tables.

The pattern matching using our algorithm runs in time linear to the size of the compressed text (plus preprocessing cost).

We have presented a new algorithm for pattern matching in compressed text. Our algorithm is a generalization of algorithm for pattern matching in text coded by static binary Huffman coding. Our algorithm is based on (deterministic) finite translation automata and is able to handle any compression method, whose decompression algorithm can be expressed as static deterministic finite translation automaton.

In the future, several possible research fields are open. One of them is to handle compressions like adaptive Huffman coding, LZ78, etc. Another is to solve fully compressed pattern matching problems (both text and pattern are compressed).

References:

- [1] LAHODA, J. – MELICHAR, B.: *Pattern Matching in Text Coded By Finite Translation Automaton* Proceedings of the IS'04 - Theoretical Computer Science'04, 2004, pp. 212–214.
- [2] LAHODA, J. – MELICHAR, B.: *Pattern Matching in Huffman Coded Text* Proceedings of the IS'03 - Theoretical Computer Science'03, 2003, pp. 274–279.
- [3] TAKEDA, M.: *Pattern Matching Machine for Text Compressed Using Finite State Model* 1997.
- [4] MELICHAR, B. – HOLUB, J.: *6D Classification of Pattern Matching Problems* Proceedings of the Prague Stringology Club Workshop, 1997, pp. 24–32.

This research has been supported by the Czech Technical University grant CTU0409013 and the Ministry of Education, Youth and Sports of the Czech Republic under research program No. J04/98:212300014 (Research in the area of information technologies and communications) grant No. PG-98488.

Using of VHR and Radar Satellite Data for Environmental Changes Monitoring

L. Halounová, K. Pavelka

pavelka@fsv.cvut.cz

Department of Mapping and Cartography, Faculty of Civil Engineering, Czech Technical University, Thákurova 7, 166 29 Prague 6, Czech Republic

The northern-Bohemia comprises large areas with underground mining and brown coal open-casts. Abandoned open-casts were reclaimed. The reclamation was performed in several possible ways – hydric, forestial and agricultural. Hydric reclamation can be found in the form of new water basins whose main purpose is to fill in land depressions after excavation, to create new part of countryside and to serve as recreational localities. Agricultural reclamation represents changing of previous open mines into agriculturally used areas. Forestial reclamation is a creation of new forests whose good growth and sound stand is a measure of successfulness of the reclamation. The age of reclaimed areas varies from more than 30 years up to still reclaimed areas. The methods used for evaluation of these three types of reclamation from TM satellite data series will be presented

The northern Bohemia is heavily touched by mining activities – on and under the surface. Reclamation activities must follow mine closing and are included in the Czech law as a duty of mining companies. Reclamation can be divided into three phases – technical one, biological one and maintaining one. The technical reclamation comprises surface geotechnical and hydrological corrections and improvements of new surface morphology to be stable and suitable for future non-mining using. Stable slopes, appropriate land consolidation, and/or reliable drainage system, transport network (if necessary) represent the first phase. The second – biological phase is a period formed by reforestation, agricultural using, new grassland creation or water basin fulfilling. The project of these two phases is performed by reclamation experts. The third phase is a maintenance period when reclaimed areas are controlled according to their development compared to their projected developments. This last period ends by handover to previous or new owners. These areas are controlled by reclamation specialists in situ. This project should prove how remote sensing data can be used for evaluation of biological phase and maintenance phase. The area, where reclamations are studied, is situated in the northern Bohemia between Ore Mountains range (forming the frontier Germany – Czech Republic) and the Ohře River. The oldest reclamation is from 1966. Reclamation in certain parts is planned till 2015. The complete area of reclamation is 1416 ha of forest, 920 ha of grassland, 500 ha of agriculture fields and 160 ha of water surfaces. The landscape is relatively flat with a sparse volcano chain. Vegetation indices are values used for characterizing green vegetation quality and extend. NDVI (Normalized differential vegetation index) is the most often used index for evaluation of vegetation state.

NDVI used for TM data is evaluation of tree groups present on areas of individual pixels whose size is 30x 30 meters. NDVI calculated for IKONOS data is NDVI of individual trees (in case of trees older than about 15 years) when pixel size is 4x4 meters. Changes of NDVI were calculated as difference between NDVI of two years. Changes were calculated for the period of 10 years – between 1988 and 1998. The graphs show percentage for reclaimed areas. Reclaimed areas with age above 3 years are areas whose reclamation was older then three years at the year of reclamation end. Reclaimed areas with age under 3 year are areas

whose reclamations were younger than 3 years at the year of reclamation end. Only 5% of reclaimed areas had NDVI (amount of green vegetation) worse after 10 years. Their reclamations were finished in 1970 and 1976. 5 and 3 per cent of reclaimed areas have not shown higher NDVI in their 10 years development. The same situation was in comparison of 4 years changes (1988 – 1992) and 6 years changes (1992 – 1998).

The comparison shown that the period of four years can be used for evaluating reclamation development; tendency showed by this period was the same as that of 6 years and that of 10 years. There more vegetation indices which are studied – RVI, PVI, IPVI, SAVI, TSAVI etc. Their evaluation has not been finished.

RVI is the ratio vegetation index which has been used already for many years. Jordan used and defined it in 1969. It is widely used expressing ratio between two band values where highest values are those with green and sound vegetation. The ratio is to eliminate various albedo effects. The IKONOS data bought for the project is seriously damaged by haze and clouds. The present processing step is oriented to radiometric correction to get data atmospherically corrected. All indices calculated for TM data will be calculated also for the IKONOS corrected data. This calculation will be used for detailed evaluation of tree species of forest reclamation to determine their individual growth quality.

The VHR data (IKONOS) will be used for water and forest reclamation evaluation. Their importance is in their high spatial resolution enabling users to work in high spatial detail – to find small element which are undistinguishable at other data types – lines of detailed water network, landslides/unstable areas and to distinguish detailed classes of general classes – tree types in a forest.

References:

- [1] K.PAVELKA: *An integrated method for vegetation monitoring using remote sensing and ground data*, Hrvatska akademija znanosti, Conference 100 years photogrammetry in Croatia, Proceedings of conference ISBN 953-154-342-9 1998, pp. 367-373
- [2] L.HALOUNOVÁ, K.PAVELKA: *Using of TM data and VHR data for reclaimed areas monitoring using vegetation indices*, ISPRS International Workshop on Processing and Visualisation Using High-resolution Images, the International archives of the photogrammetry, remote sensing and spatial information sciences, Proceedings of workshop, Vol. XXXVI-5/W1, 2004, ISSN 1682-1777, pp. 56-61.
- [3] L.HALOUNOVÁ, K.PAVELKA: *Using of high-resolution satellite data for environmental hazard areas monitoring*, ISPRS International Workshop on Processing and Visualisation Using High-resolution Images, the International archives of the photogrammetry, remote sensing and spatial information sciences, Proceedings of workshop, Vol. XXXVI-5/W1, 2004, pp. 121-128.
- [4] L.HALOUNOVÁ, K.PAVELKA: *Monitoring of Landslide Using Photogrammetry and Remote Sensing*, Brno GIS 98, Proceedings of Conference, ISBN 80-210-1841-0, 1998 pp.235-243

This research has been supported by MŽP grant No. SM/10/70/04.

Update Propagation and Merging in GFS

P. Rydlo, V. Dynda

xrydlo@sun.felk.cvut.cz

Department of Computer Science and Engineering, Faculty of Electrical Engineering
Czech Technical University, Karlovo náměstí 13, 121 35, Praha 2, Czech Republic

GFS is a peer-to-peer file system designed to provide highly available and secure file service in a large-scale environment of the Internet ([1]). It uses massive data replication and efficient update mechanisms in cooperation with cryptography techniques to create a reliable, scalable and secure system. In this paper, we outline the data organization, internal control structures for update propagation and describe update structure and merging.

For performance and availability reasons, each file in GFS is divided into several independently-managed data objects ([2]) allowed to be written or read at any client node (peer) of the system. For each data object, an overlay multi-source multicast scheme is built to organize the data object peers and propagate updates. The scheme consists of two entities: the *administrative organization* representing the logical relationships among peers, managing updates and resolving data consistency issues, and the *multicast tree* representing the physical relationship (i.e., how peers get connected) and providing data delivery services.

The multicast tree of data object d is modeled as an undirected tree graph $R_d = (N_d, E)$, where N_d is set of peers maintaining a replica of the data object and E is set of overlay edges connecting the peers. The multicast tree is a self-adapting dynamical structure reacting and adjusting itself to current network conditions and data object's state to minimize replication costs and balance the overall system overhead in terms of a set of application-specified weighted criteria.

The peers of R_d tree are divided into two disjunctive subsets $N_d = NP_d \cup NA_d$, where NP_d is a set of passive peers that recently either have not generated any data request or have generated only read requests and store the data object primarily for availability reasons or serve as read-only clients and NA_d is set of active peers having generated write requests to the data object. Peer assignment to NP_d and NA_d changes over time according to their activity.

Administrative organization of R_d peers forms a multi-layer hierarchy of clusters recursively defined as follows (where H is the number of layers, $k > 3$ is a constant): Layer 0, denominated L_0 , contains all peers from N_d ; peers in $L_j, j < H-1$ are partitioned into clusters of sizes in $[k, 3k]$, L_{H-1} has only a single cluster of size in $[2, 3k]$; a peer in a cluster at $L_j, j < H$ is selected to be the head of the cluster and becomes a member of layer L_{j+1} if $j < H-1$.

A peer with the highest write request rate in a given administrative area becomes a head of a cluster at L_0 , which consists of its adjacent nodes in R_d . The boundaries of clusters $C_{0,0}, C_{0,1}, \dots, C_{0,r}$ at layer L_0 are determined by behavior of data update propagation in R_d . After a hierarchical consistency agreement at layers $L_i, 0 < i < H$, the data update is disseminated among peers starting at heads of L_0 clusters using the data delivery tree R_d . Each update request creates a parent-child relationship between each two intermediate N_d peers until it reaches a peer that has already received this update. The parent-child relationship dynamically denominates the cluster of each head at L_0 .

In this way, the relation between peers and boundary of clusters alters as network characteristics or the administrative organization changes. From the administrative point of view, R_d tree is set of subtrees (clusters) rooted at the respective cluster heads and connected by boundary nodes. A reliable and secure mechanism for merging of updates at boundary nodes is proposed.

To reliably dispatch and merge updates in the context of GFS means to get all the peers be informed of all updates in the order that is defined by consistency agreement prior disseminating the update.

Each update consists of data to be stored as well as metadata used to preserve data integrity and confidentiality. To achieve reliability of the update mechanism, each update contains modification table T_M , which reflects final state of the given data object this update is being applied on. Following operations and relations are defined on modification tables to determine mutual relation of updates and objects.

- $T_{M1} < T_{M2}$ T_{M1} represents earlier version of data object than T_{M2} . All updates in T_{M1} are contained in T_{M2} in the same order.
- $T_{M1} = T_{M2}$ Versions represented by T_{M1} and T_{M2} are the same. Both tables contain the same entries in the same order.
- $T_{M1} \neq T_{M2}$ Data object versions represented by T_{M1} and T_{M2} are conflicting. Corresponding entries do not match.
- $T_{M1} - T_{M2}$ Subtraction. Represents updates that were applied to data object after updates represented by T_{M2} , i.e. set of updates that are contained in T_{M1} but not in T_{M2} . Order of entries in the result is the same as in T_{M1} .
- $T_{M1} + T_{M2}$ Union. Represents updates contained both in T_{M1} and T_{M2} and updates contained in one table and not in the other. Order of entries is preserved. This operation is applicable only if $T_{M1} < T_{M2}$. or $T_{M2} < T_{M1}$
- $|T_M|$ Cardinality of table T_M (i.e. number of entries in the table).

Level of confidentiality of data objects and updates is achieved by cryptography algorithms employed to encrypt both data and metadata. Sensitive data is encrypted with secret key E_K that is stored in the respective data object in encrypted form as part of metadata. This key is encrypted by public key U_K that is known to group of authorized users thus defining resource access control. Since peer storing the data must be able to perform basic operations on data objects and updates without knowledge of any secret key, modification table T_M is not encrypted.

Finally, integrity of data object is guarded by digital signature S that is calculated from both encrypted and unencrypted data, thus every malicious change is easily detectable [3]. Presence of digital signature provides write control as well, since only user authorized to modify the object should know the key.

References:

- [1] DYND, V. – RYDLO, P.: *P2P Large-Scale File System Architecture*, ECI 2002, TU Kočice, Slovakia, 2002, pp. 152–160.
- [2] DYND, V. – RYDLO, P.: *Fault-Tolerant Data Management in the Gaston Peer-to-Peer File System*, *Wirtschaftsinformatik* 45/3, Friedr. Vieweg & Sohn, 2003, pp. 273–283.
- [3] DYND, V. – RYDLO, P.: *Fault-Tolerant Data Management in a Large-Scale File System*, ISADS 2002, UDG Guadalajara, Mexico, 2002, pp. 219–235.

Objective Quality Evaluation of Compressed Video Sequences

R. Javůrek

`javurer@fel.cvut.cz`

Department of Radioelectronics, Faculty of Electrical Engineering, Czech Technical University, Technická 2, 166 27 Prague 6, Czech Republic

In last several years many compression methods for digital video systems were introduced. It has become very important to devise objective video quality assessment algorithms. The subjective measurement Mean Opinion Score (MOS) is a widely used method on the assessment of image or video quality, but it has several obvious disadvantages. It is very tedious, expensive and impossible to be executed automatically. Instead, an objective image or video quality metric can provide a quality value for a given image or video automatically in a relatively short time. This is very important for real world applications.

All types of objective video quality assessments are based on measurement of differences between the original video and received/degraded video sequence in some way. The easiest objective quality measures are some simple statistics features on the numerical error between the reference and the distorted image. Widely used statistics are Mean Squared Error (MSE) and Peak Signal to Noise Ratio (PSNR). However, MSE and PSNR do not correlate well with subjective quality measures because human of perception distortions and artefacts is unaccounted for.

Subjective quality tests form criteria for objective metrics. Formal test methods for subjective video quality assessment are defined in ITU-R Recommendation BT.500 series (Methodology for the subjective assessment of the quality of television pictures) [1] and ITU-T Recommendation P.910 (Subjective video quality assessment methods for multimedia applications). Recommendations suggest standard viewing conditions, criteria for observer and test scene selection, assessment procedures and analysis methods. Test methods can be divided in two groups: Methods where both reference and test video is presented (Double Stimulus methods) and methods where only test video is presented (Single Stimulus methods).

Systems for objective quality measurement can use measures that correlate with perceptual distortion or can use Human Visual System (HVS) features. Widely used models are Tektronix/Sarnoff, NASA – DVQ Digital Video Quality Model and EPFL – PDM Perceptual Distortion Metric. I have developed two models for quality assessment of MPEG-based codecs. Because we want to run these models real-time and we want to use these models in compression algorithm, simplicity was an important goal. Both models require both reference and degraded sequences.

First model for video quality evaluation uses mathematical measures that correlate with perceptual distortion. These mathematical characteristics were selected by ITS in Colorado [3] from the quality features and parameters suggested by American National Standard Institute, ANSI. The quantitative metric is linear combination of three quality impairment measures. First measurement is a measure of spatial distortion and second and third measurements are both measures of temporal distortion.

Second model for video quality evaluation simulates some stages of human visual system HVS. First steps are decomposition of sequence into different spatial channels and conversion to local contrast LC. Next block is temporal filtering which implements temporal

part of CSF. Then DCT coefficients are converted to just-noticeable difference (jnd). At the next stages sequences are subtracted, mean and maximum distortion is calculated, weighted and pooled to implement masking operation. The result is quality of video sequence.

For quality tests of the models we have used five test sequences from the set of EBU test sequences. We have tested 6 widely used compression methods ((DivX, XviD, Quick Time, Windows Media, MP2 Tsunami and VP6). For each tested compression method we used 5 compression levels at 4096 kbit/s, 2048 kbit/s, 1024 kbit/s, 512 kbit/s and 256 kbit/s and we obtained set of 150 degraded sequences. As a reference values subjective rating of 14 observers were used. Subjective assessment was based on ITU-R Recommendation BT.500. We used Double Stimulus Continuous Quality Scale (DSCQS) method. In this method each trial consists of a pair of stimuli, the reference and the test sequence. The stimuli are each presented twice in trial and with randomly chosen order. The subjects rate each stimulus on a continuous quality scale.

Perceived video quality depend on many factors. Subjective methods described first in this paper are the most precise methods but these methods are expensive and time consuming. Simple pixel-based metrics are very popular because of their simplicity but these metrics are not suitable for digitally compressed images and video.

I have proposed and described two models for objective video quality assessment. Both models and subjective Double Stimulus Continuous Quality Scale (DSCQS) method have been used for quality tests at our department. Obtained data is correlated and it is possible to use proposed objective models, which are faster and cheaper, instead subjective methods for quality tests.

References:

- [1] ITU-R RECOMMENDATION BT.500-11: *Methodology for the subjective assessment of the quality of television pictures* International Telecommunication Union, 2002.
- [2] VQEG: *Final report from the Video Quality Experts Group on the validation of objective models of video quality assessment* VQEG, 2000.
- [3] WEBSTER, A.A. – JONES, C.T. – PINSON, M.H. – WORAN, S.D. – WOLF, S. : *An objective video quality assessment system based on human perception* In SPIE Human Vision, Visual Processing and digital display IV, vol. 1913, 1993, pp. 15–26.
- [4] WINKLER, S.: *A perceptual distortion metric for digital color video* In Proc. SPIE, vol. 3644, 1999, pp. 175–184.

his research has been supported by CTU grant No. CTU 0409913.

Codesign in Celoxica DK3

Michal Kuneš

`xkunes@fel.cvut.cz`

Czech Technical University in Prague, Faculty of Electrical Engineering, Dept. of Computer Science and Engineering, Karlovo nám. 13, 121 35 Praha 2, Czech Republic

The major definitions [3] of HW/SW Codesign essence are:

- the cooperative design of hardware and software components
- the unification of currently separate hardware and software paths
- the movement of functionality between hardware and software
- the meeting of system-level objectives by exploiting the synergism of hardware and software through their concurrent design.

Many developers attempt develop automatic systems and complex methodology for HW/SW Codesign. This target is very complicated, because only the designer knows what he needs and can to done. We developed a simple example for describing the problem of HW/SW Codesign. Example is called AutoCorrelation demo and is based on evaluation of a correlation function.

Correlation is a standard pitch detection algorithm and should be used for data analysis (audio data, cryptographic data).

$$\text{Correlation function: } y_k = \sum_{i=0}^{N-k-1} x_i \cdot x_{i+k} .$$

Example has 2 parts:

First part is **Hardware part**. Hardware part periodically reads the data (max 1024 samples) for analysis (from Audio Input to the memory), evaluates the correlation function and sends the data to the Software part (if the software parts asked for a data).

Software part periodically reads data from Hardware part, calculates X and Y scale factor for drawing outputs and draws data on video output.

AutoCorrelation demo was implemented on Celoxica RC200e Development Board (contains Xilinx XC2V1000 FPGA chip) by using Celoxica DK3, Celoxica DSM communications, Xilinx ISE 6.1 and EDK 6.1. [1], [2] and system clock was 50 MHz.

Software part:

The Microblaze processor core was used for software part.

Hardware part contains:

- 32b, 2 stage-pipelined floating point arithmetic – Adder and Multiplier,
- 4 stage-pipelined, to/from 32b fix point converter - 2x Float2Fixpoint and 1x Fixpoint2Float

Hardware part is Optimized EDIFs based on Celoxica float library ported to DK3 with Peak performance 100Mflops.

- 2x 2048x24b of Block RAM – for inputs data
- 2048x32b of Block RAM - for output data

For communications between hardware and software parts was used Celoxica DSM communications.

Implementation on RC200e

Logic Utilization:

- Slice Flip-Flops – 4827 = 47%
- 4-input Luts – 7465 = 72%

Logic Distribution:

- Slices – 4828 = 94%

HW Part – Behaviour

With system clock on 50MHz and 22,05kHz Audio/800 Samples – 36.3ms (27 blocks/s) the processing of 800 samples needs 6.8ms. It means that the sending window is 29.5ms (800 words needs 0.10 ms - cca. 8M words/s). Drawing of output is from 0.6s to 1.1s.

This example shows that every design has some parts, which needs to be solved separately:

- load data
- data evaluation
- data presentation

In this example was the Codesign made manually but shows what all needs to be done in each design.

References:

- [1] CELOXICA - *Web pages*. [online]. [cit. 1.1.2005] On WWW: <www.celoxica.com>.
- [2] XILINX - *Web pages*. [online]. [cit. 1.1.2005] On WWW: <www.xilinx.com>.
- [3] KUNEŠ M.: *Hardware/Software Codesign*. CTU, Faculty of Electrical Engineering 2004 DC-PSR-2004-11.

This research has been supported by GA 102/04/0737.

Matrix Converter Control

J. Lettl, S. Fligl

lettl@fel.cvut.cz

Czech Technical University in Prague
Faculty of Electrical Engineering
Department of Electric Drives and Traction
Technická 2, 166 27 Praha 6, Czech Republic

The designed concept of the matrix converter control system employed in the hybrid traction drive with electric power splitting is presented. The matrix converter inclusion in the drive is advantageous especially with regard to the reactive component reduction.

Matrix converters [1] provide an all-silicon solution to the problem of converting AC power from one frequency to another, offering almost all the features required of an ideal static frequency changer. They possess many advantages compared to the conventional voltage or current source inverters. A matrix converter does not require energy storage components as a bulky capacitor or an inductance in the DC-link. It enables the bi-directional power flow between the power supply and load. The most of the contemporary modulation strategies are able to provide practically sinusoidal waveforms of the input and output currents with negligible low order harmonics, and to control the input displacement factor.

The matrix converter realised on the base of new progressive semiconductor elements (IGBT's modules) is used to treat the electrically transmitted power part of the hybrid traction drive with electric power splitting. The electrical torque split device consists of a special electric generator with both rotor and stator rotating. The rotor is connected to internal combustion engine and its torque is via air gap electromagnetic forces transmitted to the stator. The torque and the output shaft angular speed constitute the mechanically transmitted power. The remaining part of the internal combustion engine power is transformed into the electric power and represents the input power of the electrical transmission.

Hybrid drives generally can be considered to be an acceptable solution of gas emissions and fuel consumption connected with automobile traffic expansion which constitutes significant ecological problems to deal with. Electric car drives based on electric energy stored in batteries offer solution for vehicles covering short distances only. Nevertheless the internal combustion engine has some specific attributes in contrast to the electric motor. Its high efficiency is accessible in regime of higher output only and it depends on operating point choice given by torque and velocity. A hybrid vehicle equipped both with a fuel tank for internal combustion engine and with an electric battery for electric drive represents one of the possible alternatives.

There are various types of hybrid drives [2]. Promising is propulsion with electric power splitting based on internal combustion engine power splitting into two parts. One part is converted into electric power in a generator, which supplies a traction motor, mechanically connected to vehicle wheels, and the remaining part is transmitted by electromagnetic forces in the air gap to the wheels mechanically without losses in electric machines. The splitting devices can be realized mechanically by a planetary gear or electrically by a special electric generator. In our case the above mentioned special electrical torque split device consisting of the electric generator with both rotor and stator rotating is used.

The special “Host PC – Target PC” digital control system [3], [4] was developed for the realised experimental test bed. The matter consists in the processor throughput. While in case of the digital signal processors it can be as far as 100 MIPS at 16 bit DSP with fixed point, 200 MIPS at 32 bit DSP with fixed point, 20-200 MIPS/MFLOPS at DSP with floating point only, in case of processors for PC it can reach e.g. 9000 MIPS and 2600 MFLOPS.

The basis of the control system consists of two common personal computers. The first one (Host PC) should be equipped with any multitasking operating system and the MatLab programme must be installed on this PC. It serves for compiling of the target real-time applications and for monitoring purposes only, such as downloading and displaying of measured waveforms, commands entry, etc. One serial port of the RS232 standard and one parallel port enabling operation in the ECP mode are inevitable. The second one (Target PC) works in real time and the matrix converter control programme is processed on it only. The most important component of this PC is the Multi I/O PCI card Meilhaus ME-2600i containing A/D and D/A converters and digital inputs and outputs. All the signals are reprocessed and adjusted in interface cards situated in the control rack. Here is also placed the IGBT's switch pulses generating card based on a FPGA device. To make the work easy, the firmware for the Target PC and the monitoring programme for the Host PC were prepared. The firmware consists of the libraries set programmed in the ASSEMBLER and C language enabling faster algorithm implementation and testing. It has the real-time kernel with 50 – 200 microseconds period and contains synchronisation, communication, and I/O card specific routines. The monitoring programme consists of the set of the mutually communicating programmes programmed in the MatLab, JAVA, and C languages. However, from the user sight it seems to be one application only. This software is very important for easy control application developing.

The developed matrix converter control hardware and software makes it possible to achieve greater throughput of the digital control system and its variability. The results obtained on the built-up experimental test bed have proved proper function of the designed conception of the matrix converter control system.

References:

- [1] LETTL, J.: *Steady States of an AC Drive with Unrestricted Frequency Changer*. Acta Technica CSAV, 1984, pp. 350–375.
- [2] ČEŘOVSKÝ, Z. – MINDL, P. – FLÍGL, S. – HANUŠ, P.: *Hybrid Drives and Energy Hybrid Transmission*. Proceedings of TRANSCOM, Žilina, Slovakia, 2001, vol. 6, pp. 21–24.
- [3] LETTL, J. – FLÍGL, S.: *Matrix Converter in Hybrid Drives*. Proceedings of 8th International Conference Problems of Present-day Electrotechnics - PPE 2004, Kiev, Ukraine, 2004, vol. 3, pp. 77–80.
- [4] LETTL, J. – FLÍGL, S.: *Unconventional Application of Matrix Converter System*. Proceedings of 11th Electronic Devices and Systems Conference 2004 – EDS'04, Brno, 2004, pp. 488–492.

This research has been supported by MŠMT grant No. MSM 212300017.

Design Retiming in HDL

L. Kafka, R. Matoušek

kafka11@fel.cvut.cz

Department of Computer Science and Engineering, Czech Technical University, Karlovo náměstí 13, 12135 Praha 2, Czech Republic

Department of Signal Processing, UTIA/CAS, Pod vodárenskou věží 4, 182 08 Praha 8, Czech Republic

This paper deals with an improvement of design timing characteristics by modification at the high abstraction level of the system description. Some synthesis tools such as Synplify Pro provide timing optimizations, called pipelining and retiming. These techniques help the designer unify delay slacks at different inputs, which results in higher system clock frequencies of the produced circuit. Unfortunately these techniques are not available for all devices, for example Atmel FPGAs are not supported. A modification at HDL level is the way how to achieve slight improvement for these devices.

A new technique is based on partitioning of an original design into temporally independent partitions, i.e. that the outputs of any generated partitions are processed only in the following partitions and the outputs of the last partition are connected only to the primary outputs. Flip-flops are inserted between the adjacent partitions; these partitions form the stages of a pipelined design.

The most difficult task is the partitioning process. It should meet following requirements:

- The partitions must be temporally independent. This is essential.
- The delays along the most critical signal paths should be uniformly distributed in the created partitions. A better distribution leads to a higher possible frequency of the partitioned design.
- The interface between adjacent partitions should be as narrow as possible. Fewer flip-flops mean a lower power consumption.

We use the tool VPart (VHDL Partitioner) for design partitioning. This tool was developed in the scope of the European project RECONF2, which deals with design tools and methodology for dynamically reconfigurable devices. The VPart tool splits the VHDL description of an input design into temporally independent partitions which can be used as different contexts in a reconfigurable design. Each of the partitions can be loaded only once in an FPGA to complete one cycle of the original design. Because the partitions are temporally independent, the tool is suitable also for retiming. This tool also generates VHDL descriptions of structures (CUT entities) responsible for a proper connection among partitions.

The VPart partitioning is based mainly on area estimations. We could achieve better results with a tool whose optimization techniques are based on delay estimations.

We have chosen an 18-bit floating point (FP) adder and multiplier for the evaluation of this approach. These macros were generated using Celoxica DK 3.0 suite. The original macros were synthesized using Synplify Pro for reference purposes. The same designs were partitioned by VPart and also synthesized using Synplify Pro. Because the frequency estimations after the synthesis step do not take into account routing delays, we implement

these circuits in FPGAs using Atmel Figaro tool. After place and route the frequency improvement was about 21% for the FP adder and 35% for the FP multiplier.

The proposed approach is applicable to designs where the impact of the additional latency (caused by additional flip-flops) can be eliminated by a specific use of these designs. For example, it can be used for arithmetic units that process a sequence of numbers. Then the additional latency causes the delay of the first result, but it has no impact on the overall performance.

References:

- [1] KIELBIK, R. – MORENO, J. M. – NAPERALSKI, A. – JABLONSKI, G. – SZYMANSKI, T.: *High-Level Partitioning od Digital Systems Based on Dynamically Reconfigurable Devices*, In: Proceedings on FPL Conference, 1993, pp. 271–280.
- [2] KAFKA, L. – KIEBLIK, R. – MATOUŠEK, R. – MORENO, J. M.: *VPart: An Automatic Partitioning Tool for Dynamic Reconfiguration* To appear in: FPGA 2005, The ACM Press, 2005
- [3] *Synplify Pro v7.6 User's Manual* Synplicity, 2004
- [4] *RECONF2 Web Pages* <http://www.reconf.org>

This research has been supported by GACR-102/04/2137 and IST-2001-34016.

Combustion Engine's Running Roughness Measuring and Utilization for Fault Diagnosis

M. Čambál, J. Chyský, M. Novák, I. Uhlíř

Martin.Novak2@fs.cvut.cz

Department of Instrumentation and Control Engineering, Faculty of Mechanical Engineering, Czech Technical University, Technická 4, 166 07 Prague 6, Czech Republic

The presumption for the effective usage of the non-dismantling diagnosis method is that this method is reliable and fast enough for the determination of the type and place where the defect originates. The further requirement is that there is a collection of the typical defects obtainable, which arise most often during the operation. To distinguish and detect precisely and quickly the defect means, that the method has the sufficient differentiation capability. The method, which establishes the defects of the combustion engines by means of the instant angular speed measurement of the crankshaft, complies with this requirement. Therefore the final task for the use in the practice is to create the collection of data knowledge in the sufficient quantity and to store them in the PC memory.

In the laboratory conditions there is a problem, that does not exist the sufficient quantity of the test engines for the forming of the faults collection and therefore the possibilities of the verification of the influence of the single defects are very limited. The way how to proceed is the faults simulation. The simulated fault must be sufficiently expressed but it must not be severe in such a way, that the engine may be damaged.. The range of the simulated defects is therefore rather restricted.

The developed diagnosis method is suitable for the engine with a number of cylinders in the lower level. For this reason the two cylinders and the six cylinders engine was tested and analysed. (ČKD PRAHA 2S110 engine, Liaz 6S130). The defects simulation enclosed the reduction of the output due to the increased mechanical friction losses, due to the untightness of the piston or valve, due to incorrect adjusting of the engine etc. During the tests the courses of the angular acceleration were picked up. They show the changes in the characteristic of the measured course due to the simulated defects mentioned above. To obtain the broader bases of the data it is necessary to carry out the measurement on the other types of the engines with the respect to the number of the cylinders.

Another way how to simulate the defects is the mathematical modelling of the engine. It is then very easy to realize the changes of the input and output parameters. With respect to the complexity of the mathematical methods used and due to the difficulty in getting the required parameters, the work on the model is being carried out. The problem in the final phase of the target is the independent verification of the correctness of the method in question. The standard way is the combustion pressure measurement. It was also followed, but the probes and the software are very expensive and the realisation will continue according to the further situation.

The important property for the method is the reproducibility. That was proved by means of the repeated measurements with the same conditions of the engine. The reproducibility can be used with advantage by the measurement of the good and faulty engine respectively after the repair, which was carried out in the service shop.

The obtained data accuracy from one inductive sensor is influenced mostly by the inaccuracy of teeth manufacturing, because the engine running roughness is in the magnitude of 1 percent of the engine's mean speed. Other influences are vibrations, eccentricity and flywheel magnetization. These influences show themselves as noise in the measured data with

large amplitude and are making the evaluation difficult. The filtration of noise can be achieved by means of moving average filtration, but it is not always easy to find the appropriate filters order with regard to sufficient noise suppression and simultaneously preserve the useful information contained in the measured data. The most common used method, based on time of passage measuring of the marks placed on the flywheel, can not provide more readings during one engine's revolution than is the number of placed marks. It is caused by the transformation of the inductive sensor's signal that is purely analog, to the square wave signal by means of a comparator and by measuring the transformed signal's period with a digital counter. With this transformation, the additional information, contained in the original sensor's signal, from the space between the marks (flywheel teeth) is lost.

We are therefore investigating an alternative method for data measurement and evaluation based on digital signal processors (DSP) utilization and the usage of digital signal processing algorithms currently used in the field of sound and image processing. This way promises the usage of the additional information contained in the spaces between the marks and also the usage of this method for a wide range of engine's revolutions. The easy adaptation of the signal processing algorithms for the present engine's revolutions is advantageous and it is the main reason for DSP utilization.

The described method has been tried out with the data obtained from National Instruments data acquisition card PCI 6024E in the LabView environment and with the digital processing algorithms implemented in Matlab. The card's sampling frequency was set to the maximal value, which is 200 kHz. The results show that this sampling frequency is sufficient for this evaluation method, but it is not sufficient for other methods that have been considered, like the usage of time-frequency analysis.

The obtained results show that the usage of digital signal processing algorithms for engine's running roughness measuring and its utilization for fault diagnosis presents a new way of signal processing and promises the obtainment of more precise results, that the traditional time of passage measuring method. The possibility of higher frequency sampling, longer time interval evaluation and real time processing using DSP's is currently under investigation.

References:

- [1] NOVÁK, M. : *Processing of the signal from inductive sensors for measuring engine's instantaneous angular velocity* In: Proceedings of the 6th International Scientific-Technical Conference on Process Control (Říp 2004). Pardubice, 2004, pp. 246
- [2] ČAMBÁL, M.: *Measurement and Evaluation Optimisation of Running Roughness for Combustion Engine diagnoses* In: Sborník konference KOKA 2003. Liberec: Technická univerzita v Liberci, 2003, pp. 259-262
- [3] ČAMBÁL, M. NOVÁK, L. UHLÍŘ, I. MIFFEK, K.: *Errors Measurement Analysis of Piston Engine Running Roughness* In: Proceedings of Workshop 2003 (online) [CD-ROM]. Prague: CTU 2003

This research has been supported by MŠMT grant No. MSM 212200009.

Algorithm Acceleration in Programmable System on Chip

M. Bečvář, T. Brabec

becvarm@fel.cvut.cz

Department of Computer Science and Engineering,
Faculty of Electrical Engineering, Czech Technical University in Prague,
Karlovo náměstí 13, Praha 2, 121 35

Acceleration is a technique of improving performance of general-purpose processor through employing dedicated hardware units (coprocessors, accelerators) to handle some application specific tasks. Even though the acceleration proved its efficiency in a number of applications (e.g. floating-point coprocessors, graphical accelerators), the issues were encountered that made its benefits doubtful. The main problem was keeping the coprocessor busy most of the time – if the coprocessor is used rarely, investment in its design and maintenance becomes meaningless. This fact and the increasing performance of processors themselves resulted to abandoning the acceleration technique.

However, its idea was revived with the increasing importance of configurable devices, especially FPGAs. Although the performance of the configurable devices is generally lower than of ASICs, it has still proven to be superior over the processors in a field of computation intensive applications (e.g. digital signal processing, image processing, cryptography, etc.). Combination of their performance with a possibility of reconfiguration makes the configurable devices an ideal platform for algorithm acceleration.

Early works tried to accelerate systems based on conventional personal computer. The experiments showed some interesting results. Analysis carried in [1] discovered that most of the performance is lost due to latencies in a peripheral subsystem and due to great overhead of an operating system.

Therefore, the more recent research utilizes so called platform FPGAs that allow complete systems, including a processor core, peripherals and a configurable coprocessor, to be implemented inside a single device. These systems are usually called Configurable System-on-a-Chip (CSoC). A number of publications (e.g. [2]) studying CSoCs reported impressive speedup factors in computation intensive applications.

We have followed these trends and experiment with CSoC in Xilinx Virtex-II and Virtex-II Pro devices. Current generation of EDA tools such as Xilinx EDK (Embedded Development Kit) allows configuring the platform devices with systems based on MicroBlaze or PowerPC604E processor cores. MicroBlaze is a 32-bit RISC processor soft-IP core that can be fully implemented only with programmable resources, while PowerPC is a hard-IP macro immersed into the configurable logic. Both of these processor cores can be attached to IBM CoreConnect bus architecture and thus easily coupled with numerous peripheral IP cores included within EDK. Moreover, it is possible to extend the system by the user-defined components – processor cores, buses, peripherals and dedicated coprocessors.

Three computing kernels (CRC, color-space conversion, DCT) were chosen to illustrate and analyze properties of the selected CSoC architecture. These kernels represent algorithms with different properties and with different acceleration potential. CRC (Cyclic Redundancy Check) is an example of a simple algorithm with extensive bit-level processing and it can thus ideally leverage bit-granular parallelism inherent to configurable logic resources. Color-space conversion (RGB-to-YCrCb) is on the other hand an algorithm that may benefit from spatial advantage of configurable logic over a processor – the logic may implement as many arithmetic units as required by the algorithm to exploit operation-level

parallelism. Finally, DCT (Discrete Cosine Transform) represent a data intensive processing kernel with a moderate amount of control operations. It is an example of algorithm sensitive to a throughput of data-path between memory and data processing unit. More information about these kernels can be found in [3].

All three algorithms were tested with the MicroBlaze based CSoc system. Each algorithm was analyzed in two variants – software-only and accelerated. In the software-only variant, the algorithm was implemented entirely in software and run on the MicroBlaze processor core. The accelerated variant utilized free FPGA resources to implement an algorithm-specific coprocessor to move computation intensive parts of the algorithm into hardware. With the accelerated variant, we experimented with different possibilities how to connect a coprocessor to the MicroBlaze core. In order to make the comparison of the two variants as much objective as possible, a number of software implementations of the individual kernels were examined and the one promoting the best performance was included into the comparison.

The experimental results (see [3] for a complete list) revealed a number of interesting facts. First, we were able to achieve for the selected algorithms performance speedup in factors ranging from two (DCT) to almost twenty (CRC). Even though this validates the original assumption on acceleration potential of configurable SoCs, it may seem that the presented speedups are lower than one would expect. Detailed analysis discovered that even for systems, utilizing low latency SoC buses a data transfer and synchronization overhead poses the most limiting factor. Especially MicroBlaze based system is limited mainly by insufficient support of burst transfers by the processor core. Further experiments showed that the limits could be partially diminished with a proper scheduling of data interactions between unaccelerated (in processor) and accelerated (in coprocessor) portion of the algorithm – e.g. employing such a simple technique as loop unrolling may gain noticeable performance improvements. However, to reach the theoretical upper limit of the performance speedup the architectural changes would be necessary – the coprocessor would need to read source data using burst transfers from a place where are available and write results into a place where the processor would continue in the computation. Proving this hypothesis may be a topic for further research. Nonetheless, based on the mentioned information and supported by our experiments CSoc systems have proven to be a promising architecture for accelerating a class of performance demanding algorithms.

References:

- [1] BEČVÁŘ, M. – SCHMIDT, J.: *Accelariotn of Intel PC - A Quantitative Analysis*, Proceedings of IEEE Workshop of Design and Diagnostics of Electronic Circuits and Systems, 2001, pp. 93–96.
- [2] GOKHALE, M. – FRIGO, J. – MCCABE, J. – THEILER, J. – WOLINSKI, C. – LAVENIER, D.: *Experience with a Hybrid Processor: K-Means Clustering*, Journal of Supercomputing (vol. 26, no. 2), 2003, pp. 131–148.
- [3] BEČVÁŘ, M. – BRABEC, T.: *Implementation of Configurable System on a Chip with MicroBlaze Processor Core*, Proceedings of IFAC Workshop on Programmable Devices and Systems, 2004, pp. 222–227.

Searching for Regularities in Strings using Finite Automata

M.Voráček, B. Melichar

voracem@fel.cvut.cz

Department of Computer Science and Engineering,
Faculty of Electrical Engineering, Czech Technical University,
Karlovo náměstí 13, 121 35 Prague 2, Czech Republic

Generalized and weighted strings are special strings capable of expressing variability and uncertainty of appearance of a symbol in a given position. These types of strings are mainly used in molecular biology as models of the DNA sequence. Characterizing and finding various kinds of periodicities and other regularities in strings are important problems in many areas of science. In molecular biology repetitive elements in chromosomes determine the likelihood of certain diseases, another problems arise during the DNA sequencing process. Examples of regularities are repetitions, borders and covers. In this paper we present a finite state automata approach for finding those types of regularities in weighted and generalized strings.

Firstly we explain some terms used in the following. An *alphabet* is a nonempty finite set of symbols, (e.g. $\{a, c, g, t\}$ is the DNA alphabet). A *generalized string* is a sequence of positions where each position is a set of symbols from a given alphabet (e.g. $\{a, g, t\}\{c, g\}\{t\}\{a, c\}$). A *weighted string* is a finite sequence of positions where each position consists of a set of pairs and each pair consists of symbol and its probability of appearance at the position. The sum of probabilities of all symbols at each position is equal to one (e.g. $\{\{a, 0.5\}, [g, 0.25], [t, 0.25]\}\{[c, 0.5], [g, 0.5]\}\{[t, 1]\}\{[a, 0.75], [c, 0.25]\}$). We see that weighted strings can be seen as an extension of generalized strings by adding weights to the symbols in the sets and on the other hand if we remove weights from a weighted strings we obtain the corresponding generalized string. We say that string $x=x_1x_2\dots x_m$ occurs in generalized string $Y=Y_1Y_2\dots Y_n$ at position p if all symbols of x are elements of corresponding sets of Y ($x_i \in Y_{p+i}$, $1 \leq i \leq m$) and we say that string $x=x_1x_2\dots x_m$ occurs in a weighted string $Z=Z_1Z_2\dots Z_n$ at position p if it occurs at position p in the corresponding generalized string and moreover the sum (*additive probability condition*) or the product (*multiplicative probability condition*) of the symbol probabilities in the corresponding positions are greater than a given constant.

By searching for repetitions we understand searching for factors of a given string that occur at least twice in that string. We are interested in what factors are repeating and what are their positions. More advanced task is searching for borders and covers of a given string. A border of a string is its factor if it is both its suffix and its prefix and a cover of a string is its factor which occurrences cover every position of the string.

We solve the presented problems for case of generalized strings using a special type of finite automaton, which we call *Generalized Suffix Automaton*. We designed *GSA* being inspired by the *Suffix Automaton (SA)*. A Suffix Automaton for a string x is a finite automaton accepting all its suffixes. *SA* is used widely for solving various pattern matching problems including computing regularities in strings. *GSA* is a finite automaton accepting all suffixes of a generalized string.

To obtain (*deterministic*) *GSA* we create first the *nondeterministic GSA (NGSA)* which we consequently determinize. Let us consider a generalized string $Y=Y_1Y_2\dots Y_n$, the *NGSA* for Y can be created in the following way: we create $n + 1$ states numbered $0, 1, \dots, n$. We make state 0 initial and state n final. Next we add transitions from state $i-1$ to state i for every symbol of set Y_i for all sets Y_i of Y . Finally we add epsilon transitions from state 0 to each of states

$1, 2, \dots, n$. The determinization of *NGSA* is performed by the known subset construction and in addition we memorize the set (*d-subset*) of the corresponding states of the *NGSA* for each state of the *GSA*.

Our algorithms for finding regularities in generalized strings are based on the analysis of the states of *GSA* and their *d*-subsets. Every state of *GSA* corresponds to some set of substrings of the string. We can find out this set for a given state by finding all sequences of transitions from the initial state to this state and by the consequent concatenation of labels of the transitions of every found sequence. The elements of the *d*-subset corresponding to the state are the end positions of the found strings and of all their suffixes in that string.

For finding all repetitions in a string we analyze all states having in corresponding *d*-subset two or more elements in the described way. The algorithms for finding borders and covers work with so called *backbone* of *GSA*. A backbone of *GSA* is a part of the automaton where each sequence of transitions from the initial state to any of states corresponds to a prefix of the generalized string. Since border is a prefix and a suffix at the same time, the final states on the backbone of *GSA* correspond to borders and therefore we can find the own borders easily by traversing the backbone from the initial state to all final states similarly as the repetitions are computed. Each cover of a string is also its border and therefore the algorithm for finding covers is an extension of the previous algorithm. We just add a phase when we go through the *d*-subsets of the automaton corresponding to borders and filter out borders which consecutive occurrences contain gaps.

The solutions of presented problems on weighted strings can be divided into two phases: solution of the problem for a generalized string, followed by probability condition verification.

First, we extract the corresponding generalized string from the given weighted string. Then we solve the given problem without considering probability condition for the generalized string and thus obtain a list of results. Finally we create a new list of results from the current list by removing all elements not satisfying probability condition.

The time complexity of the presented algorithms for finding repetitions and covers is $O(n^2)$ and the time complexity of the algorithm for finding borders is $O(n)$ where n is the number of states of *GSA*. The number of states (*space complexity*) of the *GSA* is the open problem. The space complexity of a general finite automaton can be in the worst case exponential. We performed a series of experiments which showed that the size of *GSA* tends not to grow exponentially even in the worst case, both the maximum and the average size of *GSA* seem to be bounded from the top by the quadratic function and from the bottom by the linear function with respect to the size of the input string.

Our future work will be devoted to the development of algorithms solving other problems concerning exact and approximate regularities in generalized strings, such as seeds, periods, etc. based on *GSA*.

References:

- [1] MELICHAR, B. - HOLUB, J. - POLCAR, T.: *Text searching algorithms, Tutorial for Athens course* Manuscript, 2004.
- [2] ILIOPOULOS, C. S. - MOUCHARD, L. - PERDIKURI, K. - TSAKALIDIS, A. K.: *Computing the Repetitions in a Weighted Sequence* Proceedings of the 2003 Prague Stringology Conference (PSC'03), 2003, pp. 91–98.

Quantum Technologies for Trust and Security

M. Dobšíček, J. Kolář, R. Lórencz

dobsicm@fel.cvut.cz

Department of Computer Science and Engineering, Faculty of Electrical Engineering,
Czech Technical University, Technická 2, 166 27 Prague 6, Czech Republic

The objective of this contribution is to give an introduction to fundamental principles and advantages of quantum information processing over the classical ones, especially concerning techniques for protecting privacy of individuals and communities. Technologies for trust and security represent a challenging problem for the digital nowadays. We usually refer to them by a more general term - cryptosystem. The current state of the art is the public-key cryptography which, as other cryptographic primitives, depends directly or indirectly on the assumed computational hardness of such problems in number theory as factoring of integers or computing discrete logarithms.

No practical cipher has been proven computationally secure up to date and according to Shannon's theorem [1], every perfectly secret cipher (i.e. whose ciphertext reveals no information about the message) has to have a secret key of length at least equal to the entropy of the message; hence it is impractical. So called provable computational security only means that an efficient reduction from a standard complexity problem can be given and a cryptosystem is considered to be secure as long as the problem is hard. The Holy Grail of modern cryptography is to base security proofs on information theory (i.e. probability theory) or even better, on some physical laws of the nature instead of complexity theory. Cryptosystems based on the laws of quantum mechanics are always unconditionally secure assuming that we interpret the nature correctly.

The history of quantum information processing goes as far as to well-known pioneer John von Neumann. Quantum computing offers enormous parallelism. The size of computational state space grows exponentially with its physical size, i.e. the number of used quantum bits (qubits). Qubits can be realized by any two-dimensional quantum system. The polarization of photons (vertical/horizontal) or 1/2-spin momentum of particles (up/down) are examples of the ones that are best explored. An isolated quantum system corresponds to a Hilbert space, which is a suitable mathematical framework for describing processes of quantum mechanics. Single qubit with two orthogonal states (denoted by $|0\rangle$ and $|1\rangle$) is told to live in Hilbert space H_2 . While the classical bit can be only in one of the two states 0 or 1, a qubit can take any linear superposition of $|0\rangle$ and $|1\rangle$. A tensor product of n qubits is called an n -qubit quantum register with corresponding Hilbert space H_2^n . If an n -qubit register cannot be written as a tensor product of smaller Hilbert spaces the qubits are told to be entangled. Entanglement is a powerful quantum primitive that allows for even very distant parts of the system to be strongly tied. Its applications vary from speed-up of classical computations (e.g. polynomial time integer-factoring) or quantum key generation to teleportation. Entanglement is the main reason why quantum computers cannot be efficiently simulated by classical ones.

Any quantum evolution can be described by a unitary matrix, thus it is reversible. On the other hand, a measurement is not a unitary event and the original state collapses to one of the base states. Hence any possible information encoded in a superposition is irreversibly lost. This fact together with no cloning theorem (an unknown quantum state cannot be copied -

there is no such unitary transformation) gives us a base for developing quantum cryptography. In 1984, Bennett and Brassard suggested a new protocol [2] for quantum key exchange. Two parties sharing no information can agree on a key that nobody else can figure out. Any eavesdropper on a quantum channel will be easily detected. He neither can make a measurement as it causes irreversible errors in two party's communication, nor make a copy of quantum states for later processing. This is a significant result which cannot be achieved by classical techniques alone. In other words, quantum cryptography offers a way for secure communication for free by quantum mechanics laws themselves.

Apart from secure communication, cryptography also aims at achieving secure computation. Two parties would like to execute a computation modeled by a function $y=f(x_1, x_2)$ without revealing their private inputs. Classically, this can be solved using oblivious transfer or bit commitment schemes. They are both conditional and it is not known yet if they can be based on the same computational assumptions. In quantum world, it has been shown that bit commitment is sufficient to build a quantum oblivious transfer whereas classically this seems impossible. Unfortunately, Mayers in 1996 [3] showed a general attack against all known quantum bit commitment schemes. The result is that quantum bit commitment, at least for now, needs an extra assumption as well as its classical counterpart. Other active research fields in quantum cryptography include techniques for quantum steganography, protocols for message authentication, quantum teleportation and others. A remarkable result is also the possibility of true random number generation. At first, the equally weighted superposition of all base states is created. After a measurement, the collapse to one of the bases is truly random.

Quantum cryptography has already captured the interest of the main world banks. They test the first out-of-the-lab products. However, there is still a lot of research work to be done. Qubits sent over a fiber optic cable cannot travel very far and can work only point-to-point. There is a need for quantum repeaters, which are not available yet. Researchers also try to send qubits through the air - up to satellites and then down to the final destinations. On the other hand, quantum computers are still under a slow development process. The last remarkable success was a 7 qubit system, on which number 15 was factorized in polynomial time using the Shor's algorithm [4]. We do not know yet any technology for building large quantum registers and keeping the system isolated from its environment. But anyway, as miniaturization of computing devices continues, quantum world is our destiny and more progress is expected every day.

References:

- [1] SHANNON, C. E.: *Communication theory of secrecy systems*. Bell System Technical Journal, 1949, vol. 28, pp. 656-715.
- [2] BENNETT, C. H. – BRASSARD, G.: *Quantum cryptography: public key distribution and coin tossing*. IEEE Systems and Signal Processing, 1984, pp. 175-179.
- [3] MAYERS, D.: *Unconditionally secure quantum bit commitment is impossible*. Physical review letters, 1997, vol. 78, pp. 3414-3417.
- [4] SHOR, P. W.: *Polynomial-time algorithms for prime factorization and discrete logarithms on a quantum computer*. SIAM Journal on Computing, 1997, vol. 26/5, pp. 1484-1509.

Searching for Repetitions in the Set of Strings

P. Matyáš

matyap1@fel.cvut.cz

Department of Computer Science and Engineering, FEE, CTU,
Karlovo náměstí 13, 121 35, Praha 2

Searching for repetitions in a text is one of the basic problems in stringology. Repetitions can be searched for in one or in more patterns. We can search for exact or approximate repetitions. The simplest problem to be solved is searching for exact repetitions in one string. Initially, I will define what exactly repetitions are. String $x_2 = a_j a_{j+1} \dots a_{j+m}$ is the exact repetition of string $x_1 = a_i a_{i+1} \dots a_{i+m}$ in text $T = a_1 a_2 \dots a_n$ if $a_i = a_j$, $a_{i+1} = a_{j+1}, \dots$, $a_{i+m} = a_{j+m}$, $i < j$, $0 \leq i, j \leq n$, $1 \leq m < n - \max(i, j) + 1$. The string $x_2 = a_{q,j} a_{q,j+1} \dots a_{q,j+n}$ is the exact repetition of the string $x_1 = a_{q,i} a_{q,i+1} \dots a_{q,i+n}$ in the set of strings $S = \{s_1, s_2, s_3, \dots\}$ if $a_{q,i} = a_{q,j}$, $a_{q,i+1} = a_{q,j+1}, \dots$, $a_{q,i+n} = a_{q,j+n}$ and $i < j$, $s_q \in S$, $0 \leq i, j \leq |s_q|$, $1 \leq n \leq |s_q| - \max(i, j) + 1$. The first real-time algorithm for the exact repetitions searching was published in 1983 by Anatol Olesievitch Slisenko. In the same year, Maxime Crochemore designed an algorithm for searching squares based on factorization of the word. The next interesting algorithm was presented by Roman Kolpakov and Gregory Kucherov in 1990 – it finds maximal repetitions in a word in linear time. This problem can also be solved by the factor automaton. This way is the most interesting for me because I want to generalize it so that it searches for all repetitions in the set of strings.

A factor automaton is a finite automaton which accepts all factors of the string. We can regard factors either as prefixes of suffixes or suffixes of prefixes. This view allows us to construct easily the factor automaton. Initially, we construct the automaton accepting the word T . Let us denote each state of this automaton by the number l , $0 \leq l \leq |T|$. Number k represents the length of the prefix of word T corresponding to this state. Then we insert ε -transitions from the initial state to all the other states and set all the states final states. This automaton is nondeterministic (NFA). Therefore, we determinise it. After the determinisation, we get a DFA in which every state will be labeled by subset of states of the original NFA. These sets shall be called d-subsets. If $D(x) = \{x_1, x_2, \dots, x_k\}$ where $x_1 < x_2 < \dots < x_k$ is any d-subset, we know that the string corresponding to the state labeled by $D(x)$ occurs in the text k -times. Let us denote such string by s_x . We also know that the length of the string s_x is x_1 . The state x_1 in the original NFA corresponds to the first occurrence of the string.

Now it is easy to build the repetitions table. For each d-subset $D(x) = \{x_1, x_2, \dots, x_n\}$ we will write one row in the following way: the columns will contain the d-subset $D(x)$, string s_x corresponding to d-subset $D(x)$, and the states in the original NFA corresponding to all occurrences with their type (e.g. (x_2, G) , (x_3, S)), respectively. Type of occurrence will be denoted by letter F (first occurrence), G (repetition with gap), S (square repetition) or O (repetition with overlapping). How to determine the type of repetition of the occurrence corresponding to the state x_i in the NFA? The repetition corresponding to x_i is a square repetition, if $x_i - x_{i-1} = |s_x|$; it is a repetition with overlapping, if $x_i - x_{i-1} < |s_x|$; and finally, it is a repetition with gap, if $x_i - x_{i-1} > |s_x|$. By finding all the repetitions of s_x , we find all the repetitions of all its suffixes. I considered important to describe the algorithm of searching for repetitions in one string in detail, because it will be the starting point of my future work.

We have two types of sets: finite and infinite. Every finite set can be determined by the enumeration of all its elements. When we want to find all repetitions in the finite set S of strings, we can construct a factor automaton for each of its elements. We label each state by the length of the corresponding prefix and the index of the string from S . Now we can

construct an automaton accepting the union of the languages of these factor automata. We do it by adding a new initial state and the ε -transitions from this new state to the initial states of all factor automata. This automaton is nondeterministic too. After the determinization we can create a table of repetitions in the same way as in the first case. Here, a problem arises: how to determine which of the occurrences is the first one and which are repetitions. If we find more occurrences of a pattern within one string, we are able to distinguish them. If we find two occurrences in two different words separately, we are not able to specify which of them is the first. If we want to distinguish it we must establish an ordering of strings in set S . Now, the first occurrence in this set is the first occurrence in the least string.

Every infinite set of strings can be determined by a regular expression (RE). RE is a string on the set of symbols $A \cup \{\varepsilon, ;, +, *, (,)\}$, which is recursively defined as an empty string ε ; a symbol $a \in A$, and (RE_1) , $(RE_1 \cdot RE_2)$, $(RE_1 + RE_2)$, (RE_1^*) , where RE_1, RE_2 are regular expressions. To be able to denote the language determined by any RE we must define value of it. Value of RE (h) we will define in this way: $h(\varepsilon) = \varepsilon$, $h(a) = a \ \forall a \in A$, $h(RE_1 \cdot RE_2) = h(RE_1) \cdot h(RE_2)$, $h(RE_1 + RE_2) = h(RE_1) \cup h(RE_2)$, $h(RE_1^*) = h(RE_1)^*$. We can see that the results of the operations of concatenation and union (\cdot and $+$) are finite sets, but the result of the operation of iteration ($*$) is infinite.

When we wish to find repetitions in one pattern we start by the construction of a finite automaton accepting this word. When searching for repetitions in the set A of strings represented by any RE we can also start by construction of a FA accepting the language of this RE. Initially, we must construct a syntactical tree of this RE and transfer it to the FA. There are several algorithms how to do it. The most important of them are the Thompson's and the Glushkov's algorithm. The FA built from the RE is nondeterministic in general case. We construct an automaton accepting all the factors of all words from set S by adding ε -transitions from the initial state to all other states. We determinise it. Now is the moment to construct the repetition table. When the RE contains operation of iteration applied to any substring, we are not able to find these repetitions of this substring from transition table of DFA. To find it we must search all cycles in the graph representing transitions of this automaton.

My future work will consist in detailed description of the algorithm for constructing the repetition table, proving of correctness and determining the time and space complexity of it. I would like to generalise it for searching for approximate repetitions in the set of strings.

References:

- [1] NAVARRO, G. – RAFFINOT, M.: *Flexible Pattern Matching in Strings* Cambridge University Press, 2002, 99 - 144
- [2] MELICHAR, B. – HOLUB, J. – POLCAR, T. *Text Searching Algorithms* FEE, CTU Prague, 2004,
- [3] MELICHAR, B. *Repetitions in Text and Finite Automata* Proceedings of FASTAR Days 2004, edited by Loek Cleophas and Bruce W. Watson 2004.

Multiple Path Interference and Its Impact on system Design

Jaroslav Burcik

burcik@fel.cvut.cz

Department of Telecommunications, Faculty of Electrical Engineering, Czech Technical University, Technická 2, 166 27 Prague 6, Czech Republic

Until 1990, the main causes of signal degradation in transmission were fiber nonlinearity and amplified spontaneous emission (ASE) from optical amplifiers. More recently a third type of system degradation, involving the unwanted beating of the signal with a number of weak interferers, has become increasingly important.

These interferers can result from imperfect extinction of the drop signal in optical cross-connect, add-drop multiplexers, connectors and double-Rayleigh scattering in the transmission span. Multiple Path Interference (MPI) has become increasingly relevant with optical amplifiers based on distributed Raman amplification [1]. The classic example is that of two partial reflectors, spaced by some distance along a fiber link. If an amplifier is placed between the reflectors, the double-pass gain may be enough to offset the weak reflections, increasing the MPI. Problem is, that in case MPI, additional (unwanted) optical paths, with losses orders of magnitude greater than the main path, lead to interfering signals at the receiver, and have a significant impact on system performance. The signal beats with delayed replicas of itself at the detector and induces inband crosstalk.

MPI has been defined as coherent or incoherent MPI based on the product of the source laser linewidth ($\Delta\nu$) a time delay ($\Delta\tau$) of the reflections that causes it. Specifically, coherent MPI is defined by $\Delta\nu \cdot \Delta\tau < 1$, and incoherent MPI by $\Delta\nu \cdot \Delta\tau \geq 1$. Using these definitions, for a standard telecommunications grade DFB laser linewidth of 10 MHz, any reflections occurring within 10m or so can be categorized as coherent MPI and any reflections greater than 10m as incoherent MPI. MPI caused by Double-Rayleigh Backscattering (DRB) due Raman amplification is typically generated over kilometers of fiber length. Hence most MPI generated from backscattering events in practical WDM systems can be thought to be of the incoherent type.

The most widely used class of optical receivers employed today uses optically preamplified direct detection in order to reduce the impact of electronics noise to insignificance. Thus higher receiver sensitivities can be obtained than those achieved in practice for PIN or APD receiver. In optically preamplified receiver the dominating noise sources originate from beating between the signal and ASE as well as from beating of ASE itself [4]. Therefore this class of receivers is frequently termed beat noise limited. In optical communication system using discrete inline optical amplifiers, ASE is added at each amplifier. If distributed amplification is employed, ASE is generated continuously along the transmission path. Because ASE is present in both propagation directions, originally counter propagating ASE that is Rayleigh backscattered and amplified together with the signal can also be observed at the receiver. In the presence of MPI, the beating of the signal and MPI can give rise to appreciable levels of MPI-induced beat noise, which additionally impairs detection [2].

The quantity of ultimate interest when assessing the performance of optical receivers and their sensitivity, is best specified in terms of required OSNR, that is, an OSNR value at the optical receiver input that guarantees a certain bit error ratio (BER) at the output of sampling and

decision device. It has been shown [3] that $BER = 0.5 \operatorname{erfc}(Q/\sqrt{2})$, where $\operatorname{erfc}[x]$ denotes complementary error function and Q is Q-factor. Q factor for system limited by both ASE and MPI can be accurately approximated by a function involving the sum of the inverse OSNRs. For OSNR penalty due MPI we can express

$$OSNR_{PEN} = -10 \log \left(1 - \frac{1}{TF_Q} \cdot \frac{Q_{REF}^2}{OSNR_{MPI}} \cdot \frac{1+r}{(1-\sqrt{r})^2} \right) \quad [\text{dB}]$$

Where TF_Q mean Q-based MPI tolerance factor
 r mean inverse extinction ratio of optical signal

$$\text{MPI tolerance factor } TF_Q \text{ we can express } TF_Q = \frac{Patt_{Sig}^2}{Patt_{Sig-MPI}^2}$$

Where $Patt_{Sig}$ is peak signal attenuation factor due filtering
 $Patt_{MPI}$ attenuation factor for variance of beating between signal and MPI due filtering.

The overall receiver performance depends on a weighted sum of inverse OSNRs due ASE and MPI. Receiver degradations due to MPI were specified in terms of OSNR penalties. A large amount of ASE mitigates the impact of MPI, whereas a poor signal extinction ratio dramatically reduces a system's robustness to MPI and high peak-to-average optical power ratio after demultiplexer helps to reduce the impact of MPI. This statement which implies that RZ using short pulses is more robust toward MPI than high duty cycle RZ or even NRZ. Practically amount of tolerable MPI power is typically some 20 dB below the signal power, independent of data rate.

References:

- [1] FLUDGER, C. R. S. – MEARS, R. J.: *Electrical Measurements of Multipath Interference in Distributed Raman Amplifiers* Journal of lightwave technology, 2001, vol.19, No.4.
- [2] ZHENG, W. – SANDERSAI, H.P.: *Measurement and System Impact of Multipath Interference From Dispersion Compensating Modules* IEEE Transaction on Instrumentation and Measurement, 2004, vol. 53.
- [3] ISLAM, M. N.: *Raman Amplifiers for telecommunications* Springer-Verlag, 2004, ISBN 0-387-40656-5.
- [4] BURČÍK, J. – SRNEC, J.: *Non-linear effects restrictions in long-haul 10G Ethernet optical transmissions* 9th OptoElectronics and Communications Conference OECC/COIN2004, Yokohama, Japan, 2004, ISBN 4-89114-044-5.

This work was funded by the Czech Science Foundation (GA ČR) within grant No. GA102/04/0773

Control Design Using Bypass for Sliding Mode Applied to Time Delay Systems

J. Fišer*, P. Zítek**

Jaromir.Fiser@fs.cvut.cz

* Centre for Applied Cybernetics (cAk), Czech Technical University, Technická 4, 166 27 Praha 6, Czech Republic

** Department of Instrumentation and Control Engineering, Faculty of Mechanical Engineering, Czech Technical University, Technická 4, 166 27 Praha 6, Czech Republic

Originally, the standard Sliding Mode Control (SMC) has been introduced by [2]. Later on, the SMC of time delay systems has been developed by applying equivalent control method. Usually, the SMC of time delay systems is designed by Lyapunov-like functional application. The SMC with standard switching surface applied to time delay systems, referred to as anisochronic, has been presented recently in [3]. The developed SMC scheme uses the so-called anisochronic state feedback working on sliding mode principle. In order to avoid chattering phenomenon, the second-order SMC has been applied to time delay systems. However, time delay distributions in system description resulted in control algorithm infeasible (anticipative) relations, which are to be recovered by the prediction of measured state vector. The unified approach to state vector prediction of time delay systems is based on Smith predictor, and time delay compensation is then based on system spectrum decomposition. Finally, a special attention is to be paid to the implementation of distributed delays in designed control algorithm, because not included hidden samples in the sampler and zero-order holder can bring about numerical instability of approximated system with distributed delays.

Unlike the previous results the presented SMC scheme for time delay systems consists in another approach to time delay compensation, which is based on functional extension of IMC (Internal Model Control) [4]. Advantageously, the IMC is generally more robust than Smith predictor based control, therefore the IMC is combined with the SMC for time delay systems in this contribution. In fact, the original Smith predictor based control scheme is proposed to be transformed into IMC-like scheme, when applying a so-called bypass for sliding mode presented in [1].

Summarizing the statements above, the presented paper is a contribution to SMC design achieved by the help of the IMC, when the controlled time delay systems are described as retarded time delay systems with complex character of control variable. Moreover, the system is meant complex in mathematical manner. The reason why the complex based SMC design for time delay systems is developed, is that it allows to cope with perturbations of time delay systems. Finally, an example of the SMC design is added.

The model of the plant is supposed to be described by the transfer function corresponding to I/O relation, where the numerator and the denominator are quasipolynomials. Hence, there are infinite number of poles and zeroes of the model describing time delay systems. At the same time, the time delay systems are of retarded type.

In practice, the SMC is implemented as a composition of two variables as follows

$$u = u_n + u_s \quad (1)$$

where u_n is nominal (continuous) control and u_s is sliding (discontinuous) control. Mostly, the nominal control is substituted by an equivalent control u_{eq} , originally introduced by [2]. The standard SMC is then being designed as discontinuous based function

$$u(t) = \begin{cases} u(y)^+, & m(y) > 0, \\ u(y)^-, & m(y) < 0, \end{cases} \forall t \quad (2)$$

where $S = \{y \in \mathbb{R} : m(y) = 0\}$ is desired switching curve.

First, the nominal control synthesis is applied and then that the sliding mode control synthesis is obtained. The former results in designing a continuous controller, the latter in designing the equivalent control u_{eq} and a fixed gain of discontinuous control function. Moreover, the SMC design suggests the equivalent control u_{eq} to be in coincidence with the nominal control u_n , which considerably simplifies the SMC scheme. Next, control error including perturbations are not amplified, because of omitting a boundary layer of the sliding variable m . To the end, the bypass for sliding mode is achieved by a model of desired output trajectory introducing anisochronic output feedback.

The nominal control synthesis is designed to be based on dynamics inversion. Due to apparent structure similarity of the SMC scheme, consisting of the bypass and Smith predictor, to IMC-like scheme with actuator nonlinearity, the IMC based design of the continuous controller is suggested. Then, the case of $u_s = 0$ is considered, because of $m = 0$, i.e. ideal tracking the desired output trajectory. In other words, there is ideally not any model/plant mismatch.

The synthesis of the discontinuous control is exclusively focused on determining the fixed gain, because of previously achieved nominal control u_n . Finally, the complex control variable is introduced to determine the fixed gain, and hence to robustly reject perturbations.

References:

- [1] JUNGER, I. B., STEIL, J. J.: *Static Sliding-Motion Phenomena in Dynamical Systems*. IEEE Transactions on Automatic Control, Vol. 48, No. 4, 2003, pp. 680–686.
- [2] UTKIN, V.: *Variable Structure Systems with Sliding Modes: A Survey*. IEEE Transactions on Automatic Control, Vol. AC-22, No. 2, 1977, pp. 212–222.
- [3] ZÍTEK, P., FIŠER, J., VYHLÍDAL, T.: *Sliding Mode Control of Time Delay Systems*. 1st IFAC Symposium on System Structure and Control (SSSC'01), 2001, 27–29 August, Prague, Czech Republic.
- [4] ZÍTEK, P., HLAVA, J.: *Anisochronic Internal Model Control of Time Delay Systems*. Control Engineering Practice, Vol. 9, No. 5, 2001, pp. 501–516.

This work was supported by the Ministry of Education of the Czech Republic under Project LN00B096.

Throughput Modelling of Symmetrical Digital Subscriber Lines

P. Jareš

`jaresp@fel.cvut.cz`

Department of Telecommunications Engineering, Faculty of Electrical Engineering,
Czech Technical University,
Technická 2, 166 27 Praha 6, Czech Republic

Abstract

Testing of new transmission technologies, before the implementation of real operator's network, it is nowadays necessary need. We have to find out the influence of new technology on spectral compatibility of access network, own options of new technologies and its credit (transmission performance) for the operator. The paper describes the method of noise generation for performance testing.

Testing workplace for throughput modelling

There are two tests before the new transmission technology implementation into the access network. The first is test for throughput modelling and the second is for spectral compatibility. Both kinds of test are performed in laboratory conditions. The reason is obvious. During the testing of new transmission system directly in operator's access network there could be other transmissions technology influence of paying customers. Therefore we have to create situation and condition of real access network in laboratory. Network development, which would substitute the access network and would be for the test purposes only, is very difficult in economy way and in these days of efficient computers and mathematic models absurd. So we can create programmes and models, which save the money, work and time, but which are highly precise and liable in results and conclusions.

International Standardization Organization appoints in the frame of recommendation for individual transmission technologies, not only the transmit characteristics for reach of spectral compatibility, but also referential conditions for performance testing.

Disturbance generators in spectral domain

Noise caused by crosstalk from near symmetric pairs mainly influences the function of xDSL systems. For xDSL systems, where the method of Echo Cancellation is used for duplex transmission creation, is dominant crosstalk NEXT (Near End Crosstalk). This mainly regards to the systems with symmetrical transmission rate as HDSL and SHDSL are. Asymmetrical systems, ADSL and VDSL use mainly the method of Frequency Division Multiplex for duplex transmission creation. Therefore there is influence on theirs activity especially the FEXT (Far End Crosstalk). We might gain the result mask PSD of disturbance signal by two ways:

- The simplified way is to use defined PSD profile models of disturbance from ITU-T.
- The precise way is in superposition of PSD transmit masks of individual transmission technologies and modelling of PSD result mask disturbing crosstalk.

Program for disturbance generation

Disturbance generator for the xDSL transmission technologies is created in the MatLab v6.5 background of The MathWorks, Inc. The program is solved modularly. That means, that the main program body needs for individual tasks subordinated modules that execute their specific functions and calculations. When the calculations are done, these are given back to the main program body. The main sense was to create structure, which would be easy to modify and in which would be possible to add whole new modules of new transmission technologies. And this depends on the actual standardization state. The programs have intuitive graphic interface created in GUIDE component for easy initial parameters settings and result display.

Disturbance generation for xDSL lines

Disturbance generation program is universal for all xDSL systems and it is based on recommendation for individual transmission technologies and common recommendation ITU-T G.996.1. Program is designed for solving the spectral compatibility problems and for determination of crosstalk disturbance between individual transmission technologies before they are applied in operator's access network. Therefore this program do not use model profiles (defined by ITU-T or ETSI), but the program allows to combine types and amounts of individual transmission technologies. Instead of defined model profiles, the program uses PSD transmission masks directly of each technology. The user can calculate the disturbance from following transmission technologies: HDSL, SHDSL, ISDN-BRA, ISDN-PRI, ADSL over POTS, ADSL over ISDN-BRA. System ADSL might be FDM or EC.

Programs determines PSD transmission mask for each given transmission system. From the PSD mask and from the amount of transmission systems we have to calculate frequency and length dependency of resulting crosstalk. From the calculated disturbance PSD mask we can obtain waveform with the use of inverse Fourier transformation. We will obtain the resulting waveform by counting of time process of each technology. The resulting waveform will be transferred to the tested loop through the coupling circuit.

References:

- [1] JAREŠ, P.: *Throughput modelling of ADSL and SHDSL* RTT Praha, 2004, s. 0145_0041. ISBN 80-01-03063-6.
- [2] JAREŠ, P.: *Test workplace for throughput modeling of xDSL* RTT Praha, 2004, s. 0144_0041. ISBN 80-01-03063-6.

This research has been supported by CTU grand No. CTU0407213.

File Integrity Checking in GFS

P. Rydlo

xrydlo@sun.felk.cvut.cz

Department of Computer Science and Engineering, Faculty of Electrical Engineering
Czech Technical University, Karlovo náměstí 13, 121 35, Praha 2, Czech Republic

In Global File System (GFS) that is based on peer-to-peer technology, confidentiality and integrity of data plays one of the most important roles. Since the system employs massive data replication, many vulnerable and possibly malicious peers are involved. In this paper we focus on data integrity, internal structures and mechanisms that build a reliable yet performance sufficient system.

As performance and availability is key feature of the system, each file in GFS is divided into several independently managed data objects (as in [1]) allowed to be stored at any cooperating peer of the GFS. Due to distributed nature of the system efficient and robust integrity mechanism has to be developed, moreover, anonymity of P2P environment stresses requirements to data confidentiality that - if provided - can enrich possible area of system deployment.

File integrity in the scope of GFS consists of integrity schema applied on data objects holding file data as well as of mechanisms that guarantee the schema. Important aspect of the schema is its resistance against intended attacks or just “disaster attacks”.

We use cryptography hash functions as a primary mean to provide integrity checking. This mechanism is powerful enough for areas where trustful peers are expected and involved. Suitable functions are such as SHA-1, MD5 (due to recent weakness discovery, MD5 algorithm should be carefully reviewed) etc. Using selected hash function, integrity schema is as follows (also known as *full file hash*). All data that form data object O are hashed by the selected function H and resulting code $h=H(O)$ is appended to the object. Integrity checking mechanism is then straightforward: upon receiving the object O , its hash value h' is calculated using the same function H ($h' = H(O)$) and values are compared. For the verified file holds that calculated hash value and value read are equal ($h' = h$).

Performance penalties however are significant, since the whole object has to be read by the entity that performs the check even if it needs only part of the object (e.g. it is interested only in its i -th change [2]). *Hash tree* schema based on Merkle Hash Trees [4] removes this disadvantage and is supposed to behave well on large objects as well. The basic idea is to hash pieces of the object (segments) independently and combine and hash resulting hashes in the tree fashion till resulting “root” hash is calculated, which behaves similarly as the hash from full file hash approach. Since data object is internally composed of original data area and area of changes [3], these could form required segments that are to be hashed independently. Using this approach need for storage space increases, since all hashes and subhashes created during hash tree construction need to be stored as well. We argue that this penalty is worth increasing overall performance (not only we reduce amount of data transmitted, but we also reduce calculation required to create comparison hash value). Verifying a single change in data object means to verify its hash against root hash. This calculation can be performed without knowledge of all other pieces that form the object, since only specific subhashes from the tree are involved in this check.

Since root hash considered so far hasn't been stored at trusted peer, its protection in general purpose P2P system is highly desirable. Two basic approaches can be applied here: keyed hash functions and digital signatures. Keyed hash functions are suitable only for

systems where no need for check at peers is required, since this schema is dependent on knowledge of a secret key that is involved in calculation of the hash value and that must not be revealed to the outer world. The latter schema is intended for systems where check at nodes is required or is necessary for correct functionality. Digital signature S guards the whole object O and also the root hash. The signature is calculated using signature key S_K that is held by users that are authorized to perform write operations. Verification is performed using public key U_K that is known to the world and is held by all peers storing the object and is also held by all users of the object. Integrity check of data object segment is then straightforward. Entity verifying the segment simply calculates its hash value, combines it with all necessary subhashes till it calculates its root hash. The real root hash is verified (it is “decrypted” by public key U_K and signatures are compared) and compared to calculated hash. Integrity of the segment is verified when both hash values are equal.

The schema using digital signature is the strongest way to check integrity of the file, however suffers from certain performance degradation since operations with private key S_K are slower then operations that use symmetrical cryptography algorithms. This degradation, however, is independent of object or segment size.

As been outlined earlier, this schema not only can be used for file integrity checking purposes but can also be used for resource access control, where possession of the signature key S_K implies user’s authorization to modify the object.

References:

- [1] DYNDÁ, V. – RYDLO, P.: *P2P Large-Scale File System Architecture*. ECI 2002, TU Košice, Slovakia, 2002, pp. 152–160.
- [2] DYNDÁ, V. – RYDLO, P.: *Fault-Tolerant Data Management in the Gaston Peer-to-Peer File System*. *Wirtschaftsinformatik* 45/3, Friedr. Vieweg & Sohn, 2003, pp. 273–283.
- [3] DYNDÁ, V. – RYDLO, P.: *Fault-Tolerant Data Management in a Large-Scale File System* ISADS 2002, UDG Guadalajara, Mexico, 2002, pp. 219–235.
- [4] MERKLE, R.: *Secrecy, authentication, and public key systems* Dept. of Electrical Engineering, Stanford University, 1979.

Transmission Parameters Analysis of the Low Voltage Power Lines

Tomáš Hubený, Jiří Vodrážka

hubenyt@fel.cvut.cz, vodrazka@fel.cvut.cz

Faculty of Electrical Engineering – Department of Telecommunication Engineering
Czech Technical University in Prague
Technická 2, Prague, Dejvice

It is known, the transfer line is the most expensive part of the wires telecommunication systems. Hence it is the idea of power line grids application for other purposes. Reason of communication and power signals combination is evident. With worldwide coverage of 95 percents the power line grid is the biggest grid in all over the world. The power line grids were already used for non-power signal transfer at the beginning of the twentieth century, but only for simple applications, such as centralized telecontrol, service phone signals etc. The final ten years of the last century brought requirement for the power line broad-band high speed transfers. It took place, although these lines have unfavorable properties – for example it can be affected by incursive electromagnetic field, surrounding these lines. Thanks to mass expansion of the Internet, it is possible to use power line grid for that informative technology, too. Many world companies have started developing transfer systems, enabling communication by means of electric distributive grid. New systems have been arising. These systems are marked by following abbreviation: PLC (Power Line Communication), PL (Power Line), PLCS (Power Line Communication Systems), DPL (Digital Power Line) or PDSL (Power Digital Subscriber Line). Other possibility, included in power line communication, is application of home networking. It means that different electrical devices form a local network. This network can be configured or controlled by remote control. These principles has been starting according to progress in computer equipment. In the low voltage power line grids, we can chance upon the following telecommunication broadband services: access to the Internet or intranet, video-streaming, LAN in the building, LAN in the flat.

Power line system provides permanent internet connectivity. Nevertheless power line grid represents shared transfer medium, therefore final bit rate (or transmission speed) decreases in proportion to number of power line users. By reason of network sharing there is a necessity of data security. Noise of power line system is a problematic field. Power line data transmission can disturb a radio communication or power line system can be disturbed simultaneously. It affects service reliability. Power line signal is attenuated towards users – see [1]. This attenuation together with receiver sensitivity mean physical limit of transmission distance. Further there is a danger of reverbations. These reverbations can be caused by reflections from non-correct terminated points. Nowadays, there exist 2 different possibilities of power line systems. The first one is the narrow band variant that is suitable for places where the low noise level is assumed but it provides transmission rate of hundred kbps only. As to modulation, there is often used FSK (Frequency Shift Keying) or QPSK (Quadrature Phase Shift Keying). The second one is the broadband alternative that offers transmission rate of tens Mbps. Because of attenuation it is inevitable to use the processes such as a broadband modulation in spread spectrum, quick synchronization and adaptive error correction. The solution is possible by using OFDM modulation (Orthogonal Frequency Division Multiplex). This solution is suitable for errors cancellation. These errors are made by interference of direct and reflected signals. The power line transfer is realized in a short data frames, because it is possible to transfer only a small data quantity until the errors appear. Power line technology is an unreliable network infrastructure, therefore it is necessary to use FEC

(Forward Error Correction) at data link layer. As to medium access control, power line system uses the method of token passing. This method is known from Token Ring local area network. Method that is used in Ethernet networks (CSMA/CD - Carrier Sense Multiple Access with Collision Detection) is not suitable in case of power line communication, because in power line grids it is difficult to recognize the signal in the noise. For token passing among network nodes, there is used the three-way handshake method. According to this procedure, there is no possibility of token loss.

The pilot workplace has been realized at department of telecommunication engineering. This workplace represented cascade model of distributive low voltage grid. The model contained distribution box, electricity meters, circuit breakers, power wires and electrical outlets. The attenuation and the characteristic impedance have been measured at this workplace. Further there have been measured the attenuation of wire pairs and cross-talk between pairs of power lines in L-PE-N system. A network analyzer Rohde & Schwarz ZVRE has been using for that measurements. As to kinds of measured power wires, there have been measured cables of the following types: CYKYLO 3Cx1.5, CYKYLO 3Cx2.5, CYKY 3Cx1.5, CYKY 3Cx2.5 and CYKY 5Cx2.5. The length of these cables was 100 meters. According to measured values there have been performed the approximation of the specific attenuation by means of modified eleven parameters model of Deutsche Telekom company – see [2]. For assignment of the specific attenuation, there have been made a computer simulation. This application is open to public and placed on web server of department of telecommunication engineering – see [3]. Software allows simulation of the primary and secondary wire parameters according to wire diameter, thickness and material of insulation, wire temperature etc. Knowledge of the primary and secondary parameters is important for assessment of maximum transfer speed or more precisely throughput of an information channel – see [4]. There has been made software in MatLab environment for simulation of transmission parameters of cascade according to non-terminated cable branches as well as influence of electricity meters and circuit breakers.

The results will be published in the first half of the year 2005.

References:

- [1] HUBENÝ, T.: *Jevy ovlivňující útlum symetrických kabelových vedení*, Access Server [online], Prague: CTU, Faculty of Electrical Engineering, Department of Telecommunications Engineering, 2004, <http://access.comtel.cz/view.php?cisloclanku=2004120201>
- [2] HUBENÝ, T. - VODRÁŽKA, J.: *Phenomena Determining the Attenuation of the Symmetric Cable Wires*, In Proceedings of International Conferency RTT 2004, 2004, [CD ROM]
- [3] HUBENÝ, T.: *Simulace symetrických vedení Matlab Web Server* [online], Prague: CTU, Faculty of Electrical Engineering, Department of Telecommunications Engineering, 2004, <http://matlab.feld.cvut.cz/view.php?cisloclanku=2004101801>
- [4] HUBENÝ, T. – VODRÁŽKA, J.: *Modelling the Primary and Secondary Parameters of Telecommunication Lines*, In Proceedings of International Conferency COFAX - TELEKOMUNIKÁCIE 2004, Bratislava: D&D STUDIO 2004, pp. 287 - 288

This research has been supported by FRV grant 2066/G1.

High Precision Computing through Interval Arithmetic Paradigm

T. Brabec, R. Lórencz

brabect1@fel.cvut.cz

Department of Computer Science and Engineering,
Faculty of Electrical Engineering, Czech Technical University in Prague,
Karlovo náměstí 13, Praha 2, 121 35

Computers became an indispensable part of scientific research. The more difficult problems are being solved, the more confidence in computers the researchers have. Still, every researcher needs to be cautious and always has to worry about the correctness of results obtained from machine-based computations. To demonstrate this skepticism, let's paraphrase from [1] a well-known example that illustrates how inaccurate scientific computations may be. Consider a real-valued function defined by the equation $f(a,b) = 333.75b^6 + a^2(11a^2b^2 - b^6 - 121b^4 - 2) + 5.5b^8 + a/(2b)$. For the parameters with values $a = 77617.0$ and $b = 33096.0$, calculating the value of function using up to 121 bits of precision yields an incorrect result. The correct result is actually $f(a,b) = -0.82739605994682135 \pm 5 \cdot 10^{-17}$ [1]. This extreme example is an illustration of a numerical error called catastrophic cancellation, which is a combination of cancellation with accumulated round-off errors. Round-off error is a difference between the actual value of a real number and its machine-representable image. This error is a result of using a finite set of floating-point numbers to represent infinite set of real/rational numbers. Cancellation occurs in a situation when two nearby quantities are being subtracted – since their most significant digits are matching, they will cancel each other. When the operands are subjects of even low round-off errors, their subtraction may cancel most of the meaningful digits and left most likely only inaccurate digits. Such cancellation significantly magnifies the round-off error and is thus called catastrophic.

Unfortunately, the presented numerical errors are inherent properties of floating-point arithmetic and can never be completely diminished. Though there exist methods that try to minimize these errors. Variable precision (or multi-precision) arithmetic is one such method. It attempts to minimize round-off error through an increase of bits representing a floating-point number. One may generally say that the more bits for a floating-point number, the more precise results may floating-point arithmetic produce. Nonetheless, the above example clearly illustrates that up to some (usually unknown) limit the increase of floating-point number bit-length cannot guarantee correct results. Completely different approach is presented by methods forming a category called exact arithmetic. Examples of these methods include arithmetic systems based on continued fractions expansions and infinite sequences of linear maps. They are characterized by inconvenient number formats (e.g. rational number format with fixed/floating slash) and computation to arbitrary precision. Drawbacks of the exact methods are considerably less effective numerical algorithms than compared with standard or variable precision floating-point arithmetic. Somewhere in between variable precision and exact arithmetic are so called self-validating numerical methods. Their self-validity corresponds to a property that together with a computed result value they provide information on its correctness. Interval arithmetic is one example of such methods.

The interval arithmetic has been proposed as an extension of the floating-point arithmetic. It provides an efficient approach to automatic monitoring of round-off errors and their magnification through cancellation during machine computations. It may further trace errors that occur due to approximation and non-exact inputs. The basic idea of this paradigm comes out from a definition of the interval, a continuum of real numbers defined by its

endpoints. The interval is a basic element for every arithmetic operation and it is used to represent bounds, within which the result of the operation is guaranteed to lie. A pair of floating-point numbers defining the interval endpoints determines these bounds. The distance between these endpoints indicates the actual accuracy of the result of interval arithmetic operations – the more distant the endpoint values, the less accurate the result.

The fact that the interval arithmetic utilizes the floating-point arithmetic ensures considerably faster algorithms than possible with the exact methods. On the other hand the erroneous character of the floating-point arithmetic naturally affects the precision of computed results. However, thanks to directed outward rounding (i.e. rounding the lower endpoint downward and the higher endpoint upward) it is possible to ensure interval inclusion of the correct, real-valued result. Ideally, every computation starts with exact numbers in a form of a degenerate interval $[x, x]$. With every arithmetic operation, the result is a subject to round-off errors and the interval bounds start to diverge and their distance increases. Consider the following relation: $[x_1, x_2] + [y_1, y_2] = [z_1, z_2]$, where x_1, x_2, y_1, y_2 are non-negative, $x_1 \leq x_2$, $y_1 \leq y_2$, and $z_1 = rndd(x_1+y_1) \leq rndu(x_2+y_2) = z_2$ ($rndd$ and $rndu$ mean round downward and upward, respectively). Due to round-off error it is likely to happen that $z_1 < z_2$, even if $x_1 = x_2$ and $y_1 = y_2$. Therefore, naive application of the interval arithmetic may quickly lead to very large intervals [2]. These provide no useful information except for the indication of a completely wrong result. Fortunately, methods have been developed that perform computations resulting into narrow intervals. These include techniques such as iterative refinement, a priori and a posteriori enclosure methods, etc. (see [2] for more details). Other ways to improve sharpness of the interval computations are published in [3]. Another possibility for high precision computing offers a combination of the interval paradigm with the variable precision or exact arithmetic.

The basics of the interval arithmetic were originally published forty years ago, in the work of R. E. Moore [4]. Since then, it has been developing as a specialized branch of a numerical analysis and its principles have been greatly extended. During that time, the interval analysis helped to develop entirely new algorithms and was used to solve fundamental problems that appear to have no other solution [1]. Examples of problems, to which interval arithmetic was successfully applied, include solving systems of linear and nonlinear equations, global optimization, etc. Nonetheless, despite its achievements and increasing number of advocates the interval arithmetic stands outside the mainstream of scientific computing. Therefore, it may be an interesting field for further research.

References:

- [1] WALSTER, G. W.: *Interval Arithmetic: The New Floating-Point Arithmetic Paradigm*, Manuscript, 1997.
- [2] SCHULTE, M. J.: *A Variable-Precision, Interval Arithmetic Processor*, PhD Thesis, University of Texas at Austin, 1996.
- [3] WALSTER, G. W., HANSEN, E. R.: *Interval Algebra, Composite Functions and Dependence in Compilers*, Manuscript, 1998.
- [4] MOOR, R. E.: *Interval Analysis*, Prentice Hall, 1966.

GF(p) Montgomery Multiplication for Cryptosystems on FPGA

J. Buček, R. Lórencz

bucekj@fel.cvut.cz, lorencz@fel.cvut.cz

Department of Computer Science and Engineering, Faculty of Electrical Engineering, Czech Technical University, Karlovo náměstí 13, 121 35 Praha 2, Czech Republic

Cryptographic systems are often based on operations in modular arithmetic. Examples thereof are RSA, Diffie-Hellman, ElGamal and elliptic curve cryptosystems. The cryptographic algorithms used to implement the security properties are often based on modular exponentiation which is achieved by repeated modular multiplication, where the most time consuming operation is modular multiplication. Montgomery multiplication is widely used for this purpose since its hardware implementation can be significantly faster than the conventional modular multiplication.

As opposed to the conventional modular multiplication, the Montgomery's algorithm does not use division by the modulus N , rather it uses division by 2^i , which is faster, since it is done merely by shifting (i is an integer). The reduction step is performed depending on the least significant digit of the intermediate result, rather than on the most significant one, as in the case of a conventional multiplication. This causes another speedup, since the critical path does not necessarily go through the full carry chain of the adder. When multiplying short words, the speed advantage of the Montgomery multiplication may not turn into real speedup. In cryptographic applications however, we often multiply very long operands, up to 2048 bits and beyond. In order to achieve high speed for long operands we have to use special techniques like pipelining and redundant encoding.

The underlying technology is often an Application Specific Integrated Circuit (ASIC) or a reconfigurable architecture such as a Field Programmable Gate Array (FPGA). Other technology includes general purpose processors, DSPs or embedded microcontrollers. There are many hardware implementations of Montgomery multiplication ranging from simple sequential architectures implementing the binary variant of the algorithm to complex unified GF(p) and GF(2ⁿ) pipelined and high-radix architectures.

We have presented a modified pipelined architecture [1,4] on which we have studied the influence of word size and pipeline depth on the resulting area and speed. The architecture consists of a computing pipeline of p processing elements. Each processing element (PE) computes w bits of the intermediate result. Each PE consists of 2 partial product generators, 2 adders and a shift and alignment layer, which includes registers. The latency of a single PE is 1 clock cycle. The PEs are separated by registers, therefore the latency of one pipeline stage is 2 clock cycles. We have adapted the architecture to the FPGA by utilizing the native fast binary adders, thus eliminating the need to use the carry-save encoding. We have shown that the architecture is scalable in pipeline depth as well as in word size. When increasing the word size however, the column size of the used FPGA limits the length of one binary adder. If the adder is longer than the column size, the carry chain breaks at the column boundary and the fast carry path is interrupted with a slow general-purpose routing path. Therefore the maximum operating frequency drops significantly when the word size exceeds the column size.

Another studied architecture [2,3] is sequential (not pipelined) and uses carry-save encoding of the operands. We have modified the carry-save encoding in order to control the redundancy of the used code. Conventional carry-save encoding has a redundancy of 100 %, i.e. each digit consists of a sum bit and a carry bit. We have modified the encoding so that the

carry bit is saved only for each word of w bits. The redundancy is $(100\%)/w$, i.e. w times smaller. We have implemented the Montgomery modular multiplication in FPGA using modified carry-save encoding. By utilizing the dedicated carry logic in the FPGA, we have been able to save circuit area. The results show a decrease in occupied area for word size $w > 1$. The clock frequency also decreases, however, we can find a minimum time-area product for $w > 1$ while saving more than 20 % area.

References:

- [1] BUČEK, J.: *Montgomery Multiplication on FPGA*, 8th International Student Conference on Electrical Engineering POSTER 2004, CVUT FEL Praha, 2004, pp. IC5 1–5.
- [2] BUČEK, J. – LÓRENCZ, R.: *Montgomery Multiplication on FPGA with Modified Carry-Save Encoding*, International Conference on Signals and Electronic Systems, ICSES'04, 2004, pp. 313–315.
- [3] MCIVOR, C. – MCLOONE, M. – MCCANNY, J. – DALY, A. – MARNANE, W.: *Fast Montgomery Modular Multiplication and RSA Cryptographic Processor Architectures*, 37th Asilomar Conference on Signals, Systems, and Computers, Nov 2003.
- [4] SAVAŞ, E. – TENCA, A.F. – KOÇ, Ç.K.: *A Scalable and Unified Multiplier Architecture for Finite Fields $GF(p)$ and $GF(2^m)$* , Proc. Second Int'l Workshop Cryptographic Hardware and Embedded Systems – CHES 2000, Aug. 2000.

Building Automation in the Education of Control Systems

P. Burget, V. Vozár, B. Kirchmann

burgetpa@control.felk.cvut.cz

Czech Technical University in Prague

Faculty of Electrical Engineering, Department of Control Engineering

Karlovo náměstí 13, 121 35 Prague 2, Czech Republic

The aim of this project has been to design and implement a model of an administration building equipped with modern control and automatic processes in chosen areas of building automation, such as lighting, heating, ventilation, security systems, control of particular electrical appliances, etc., by Lonworks technology. The model states are required to be observable and controllable not only by means of selected physical appliances at the model itself, but also via intranet/internet. The model is to become an aid for educational purposes as well as for the purposes of further presentation.

Lonworks technology is a type of a control electronic network with random access to the medium with collision detection (CSMA/CD) and LonTalk communication protocol. There is no physical layer defined in LonTalk network protocol definition, thus we are allowed to choose the topology and the transmission medium. The choice is a matter of the system requirements (transmission rate, the way the gadgets are interconnected) and the properties of the environment (disturbance, gadgets accessibility) in which the system is implemented. Due to its flexibility, open topology with communication interface FT-10 (twisted pair as the medium, see [1] for more detail) was chosen for our model. The gadgets (nodes) interconnected by this technology create distributed (decentralized) control system. There are network variables defined for each system node. Communication of all nodes as well as the implementation of individual processes is programmed by virtual interconnection of particular network variables.

To make the control of lighting more convenient there is the DALI (Digital Addressable Lighting Interface) technology used in particular parts of the model. This technology is master-slave type. It enables the light level of each slave element to be smoothly adjusted from 0 up to 100%, moreover, it provides you with the possibility to allocate individual slave elements into different groups and thus produce various light scenes. One can further define for each slave element minimum and maximum light intensity, and the intensity in case the communication with the master element fails.

The building model itself with dimensions 2600x750x1600mm consists of three main rooms (boardroom, office n.1, office n. 2) operated and controlled by Lonworks technology (Echelon - USA) into which some other system of building automation such as Wago control system with systems of light control DALI and wireless system EnOcean (boardroom), DESIGO RX by Siemens (office n.1) and WizPLC (SW PLC, office n.2) have been connected. For presentation purposes, the possibility to split up the model and handle separately the smaller part with the boardroom, so that all the manipulation is easier, has been left.

To control the boardroom, Wago system series 750 consisting of programmable logic controller with the interface for Lonworks technology and input/output modules, DALI master element and EnOcean master element, were chosen. There are four main processes to be controlled in the boardroom - the light and temperature regulation, the predefined light

scenes invoking and the operating of three motors that control the movement of the door, the blinds and the screen.

The office n.1 has been supported by DESIGO RX system (SIEMENS). Such systems are modular and are supposed to be used mainly in office precinct. There are the light regulation (done by analogue stabilizers), the temperature regulation and the control of motors (door and window movement, external blind) implemented in this office. The room is thermally insulated so that thermal losses of the other rooms can be compared. There is a radiator used for heating.

To provide the control of the second office the SW PLC with gadgets on LON bus was chosen. This PLC runs on server that is located in the model of the building and to which a 15" LCD display with touch-panel is connected. Such a display allows us to visualize the states and processes and gives us the possibility to operate individual rooms. Again, the light regulation (converter DALI/LON), the temperature regulation and the control of motors have been solved in the similar manners as in the office n.1. In addition to a common radiator, the office n.2 is equipped with floor heating.

As a consequence of the preceding paragraphs, it can be seen that different control and communication structures were used to demonstrate the variety of means used in commercial building automation applications. The students can compare the traditional centralized approach based on DESIGO RX and direct analog control of lighting and heating, and on the contrary the completely decentralized approach based on intelligent LonWorks devices controlled with a SoftPLC. As a combination of both approaches can be seen the boardroom installation, which uses direct connection of sensors and actuators as well as distributed LonWorks communication. Moreover, wireless communication based on modern elements is shown.

The building model represents the modern solution of Building Automation allowing a significant decrease of energy losses in a building and an increase of its safety level. The variety of technologies used in the model will certainly be useful for great number of future students, who will be given a chance to familiarize with them.

References:

- [1] LOY, D. – DIETRICH, D. – SCHWEINZER, H.-J.: *Open Control Networks LonWorks/EIA 709 Technology* Kluwer Academic Publishers, 2001.
- [2] CARLSON, R. A. – GIANDOMENICO, R.: *Understanding Building Automation Systems* R.S. Means Company, Inc., 1991.

This research has been supported by project FRVŠ 2004/2007.

Data mining and visualization tools

Lenka Nováková

`novakova@labe.felk.cvut.cz`

Department of Cybernetics, Faculty of Electrical Engineering, Czech Technical University
Technická 2, 166 27 Prague 6, Czech Republic

Data mining is an interdisciplinary discipline involving database technology and data warehouses, statistics, machine learning, pattern recognition, soft computing and visualization. The aim of data mining is to identify hypothesis about dependencies in the analyzed real data, which are interesting and valid. Data mining exhibits some aspects of an art – it is an art to choose an interesting task to be solved as well as to identify the best set of attributes to be considered. All over it there has been designed a methodology, which identifies the basic steps of the DM process and their dependencies. This is the CRISP methodology. Its first step is dedicated to understanding the data. The treated data can be described using great number of attributes and it has to be decided which of these attributes are relevant for the task to be solved and which are not. We need information about individual attributes and relations between attributes. After this, we can clean data, transform data and make data ready for some modeling method.

Visualization of the data is important part of data mining, because the graph or picture is for human easier to analyze and understand than long list of numbers or strings. It is important tool for communication between data mining expert on one side and data domain expert (for example physician).

Visualization can help us to understand data, prepare data or test hypotheses. There exists a strict limit of graph dimension, because the world around us has only three dimensions and human understands only this 3D world. But for data mining we need more than 3 dimensions, because the data has normally more than 3 attributes. It means if we want to visualize multidimensional data, we must transform the data to only two or three dimensions [2].

SumatraTT 2.0 is a user-friendly modular system for data preprocessing, aimed at both data mining and data warehousing (Extraction, Transformation and Load process, ETL), which is developed at our department [3].

It consists of the graphical core providing a platform for defining the transformation and a set of modules solving various tasks of data preprocessing. Some modules cover generic tasks and there are also groups of very specialized modules targeted to specific problems. The graphical interface helps the user to quickly build the intended transformation without any programming, as the set of available modules is sufficient for most applications. In rare cases when the task goes beyond the scope of prepared subtasks /modules, it can require simple scripting.

In SumatraTT, the most preferred approach to data processing is streaming {one record is loaded, fully processed and saved. In this way huge data can be processed. Exception to this rule are modules requiring all data available and thus appropriate for smaller datasets (for example dynamic graphs). As a compromise solution, we are using the concept of an internal database. It means that data is first stored temporarily to the internal database, which is further processed by means of SQL.

SumatraTT is an open system with GNU Public License built on open technologies (including popular GPL projects JFreeChart, BeanShell scripting, or McCoI database). Using such libraries brings fast development. Moreover, the libraries are growing independently on

development of SumatraTT. This way, the whole system is being actually developed by a number of developers. The openness together with modularity (especially independence between modules) enables creating a wide scope of modules, from which it is possible to choose appropriate ones best fitting particular needs. Thus, modules of insufficient quality can be easily omitted, while the best ones become a part of the official release.

Data visualization levels in SumatraTT:

First Touch Review - Any data mining application commences by a report about the studied data from the point of view of each used attribute: the structure, distribution, and frequency of values has to be analyzed separately for each attribute. Such a report is generated by the First-Touch Review, which informs about elementary statistical characteristics of individual attributes and includes corresponding graphs and histograms. It serves as a quick overview over the analyzed data and provides the user with input he/she will need to make the decisions concerning design of further processing, visualization or choice of attributes which could be completely omitted (due to constant values, excessively erroneous values, etc.).

Static - The static visualization depicts relations between pairs of attributes and the corresponding output is generated without user's intervention (or with a very simple setup). Let us recall as typical examples of static visualizations e.g. tabular list of values, graphs (e.g. 2D/3D bars or pie graphs, histograms, etc.

Interactive - Through interactive visualization the user can reach more profound understanding of the role of the individual attributes and explore some dependencies between them by asking various questions. The data miner can e.g. click on a point in one of the 2D graphs and the system answers by a number of items in the source data, which fall into this point. This goal is not achievable by static visualization; hence an interactive environment is required.

Advanced - To understand the results of the last set of advanced visualization techniques special knowledge is required. The user has to know what the particular type of the graph is able to depict and how the resulting image should be interpreted. Modules for RadViz visualization or Parallel coordinates are typical representatives of this set.

Interactive visualization and advance visualization levels have been complemented by new visualization modules (e.g. RadViz [4]). The resulting system will support and simplify work in any data mining project.

References:

- [1] PYLE D.: *Data Preparation For Data Mining* Morgan Kaufmann, 1999.
- [2] FAYYAD, U. - GRINSTEIN, G.G. - WIERSE A.: *Information Visualization in Data Mining and Knowledge Discovery* Morgan Kaufmann, 1999.
- [3] *SumatraTT* WWW homepage, <http://krizik.felk.cvut.cz/Sumatra>
- [4] KLEMA, J. - FLEK, O. - KOUT, J. - NOVAKOVA, L.: Intelligent Diagnosis and Learning in Centrifugal Pumps. In *Emerging Solutions for Future Manufacturing Systems*. New York: Springer, 2004, s. 513-522.

This research has been supported by CTU grant No. CTU0407513.

Analysis of GPS Flight Data

S. Kroupa*, D. Pachner *, Z.Pech*

xkroupa@control.cvut.cz, pachner@control.felk.cvut.cz,
pech@control.felk.cvut.cz

*Department of Control Engineering, Faculty of Electrical Engineering, Czech Technical University, Technická 2, 166 27 Prague 6, Czech Republic

This paper is focused on the flight data analysis gathered from the GPS receivers. The main goal was the inclusion of this analysis in the educational course pursued by the existing course 'Flight management systems'. The new laboratory tasks were designed. The goal of this project was also to improve our algorithms for data validation for aircraft industry of sports flying (paragliding, hang gliding, ultralight flying, soaring flying), which represents a fast developing area with high potential and growth, keeping the technological know how up to date. Due to the cost and weight limits there is a need for low cost flight instruments and minimization of redundancy of the systems.

For to reach the goals of this project we have set several task to be done. From this point we have decided to provide following steps in our research:

a) To create new a web server to manage all gathered resources (articles, program utilities for data analysis, Matlab toolboxes) to cover the range of this research field. This part is also currently used in courses 'Flight Management Systems I & II'. Commercial and free resource software was analyzed for communication, navigation tasks (OziExplorer, SeeYou, MapSource, GPSmapper, GPSTrackMaker). In our laboratory, students should familiarize with all available resources and geographical databases of terrain elevation data (dted - NMEA) and Matlab toolboxes such as MapToolbox, GPS Toolbox, Extended Kalman Toolbox for to provide flight data analysis and maps creation. This learning material should be used to support the courses 'Avionics systems I, II' and 'Flight Navigation' too. The inclusion of terrain profile in flight displays is a new area of strong effort in avionics systems development. The artificial flight displays of a new generation should have a terrain profile built in to avoid a ground collision.

b) To create a mathematical aircraft model and provide data analysis using developed algorithms – detection of failures of flight data sensors. The results were presented in [1],[2]. The algorithm was continuously improved. In order to handle huge sets of data a new identification toolbox for Matlab was created. This new tool enables several features: the system (aircraft) identification based on several data analyzing procedures – user friendly graphical user interface for data validation and manipulation, finding maximum likelihood linearizing transformation, ARX model identification, model order reduction and graphical verification of data fitting. One feature of our data analysis tool allows to introduce artificial sensor failures to test the fault detection algorithm behavior.

c) To prove the simulation results on real flight data. Several flight data measurements were taken in order to find the aircraft dynamics for various flight regimes and the dynamics of the aircraft was identified. The flight envelope was analyzed. The obtained model was used for sensor data verification. The obtained results (the identification toolbox and fault detection

algorithm) were implemented as a new laboratory task for the course Flight Management system. We have decided to include also the data from inertial navigation in order to identify fast modes of the system. This task is currently solved in cooperation with Department of Measurement, CTU-FEL, which designed an inertial measurement unit and now the precision of measurements is being improved.

d) New textbooks were bought for educational purposes 'Dynamics of Flight: Stability and Control' (B. Etkin) and 'Aircraft Control Systems: Practical Issues in Design and Implementation' (R. Pratt).

e) A map GPS receiver was bought for laboratory experiments. The students should have a possibility to carry out experiments of their own and perform real-time data analysis, familiarize themselves with available tools and resources (introduction to the GPS maps problematic and creating own maps for GPS devices).

f) The results of realized experiments are supposed to be used in the fault tolerant helicopter autopilot project.

g) A model of a glider wing was created. The lift performance of non-rigid body wing lift characteristic was experimentally validated (lift force dependency on the angle of attack, chord wing deflection). The new area of application is spreading for military and rescue applications of glider autopilot design for precise landing systems.

To summarize, the goals of this project were accomplished, new laboratory task were created and new research results were presented.

References:

- [1] KROUPA, Š. - PACHNER, D.: *The Aircraft A310 Flight Data Fault Detection using ARX-based Wiener Hammerstein model* CVUT, In proceedings: 8th International Student Conference on Electrical Engineering, Prague, 2004, CD-ROM.
- [2] KROUPA, Š. - PACHNER, D *Validation and fault detection of flight data measurement* Vojenská letecká akadémia, Košice, In proceedings: Nové trendy v rozvoji letectva, ISBN 80-7166-050-7 2004, 32-38.

This work was funded by the Czech Technical University CTU within the framework of the program IGS (Grant CTU0418413). The authors appreciate very much the support..

Some Internal Structures of the Execution Engine

M. Dráb, L. Kalvoda, S. Vratislav, M. Dlouhá

drab@kepler.fjfi.cvut.cz

Department of Solid State Engineering, Faculty of Nuclear Science and Physical Engineering, Czech Technical University, Trojanova 13, 120 00 Prague 2, Czech Republic

In the past year the development and implementation of the Execution Engine Virtual Processing Unit [1, 2] continued. VPU EE is the core part of project INDECS, which aims towards creating a flexible software system, that would drive a physical experimental device, especially a neutron diffractometer, collect the measured data, and analyze them.

The EE has more sources of instructions [1, 2]. Each source together with its resources (registers, memory blocks ...) forms a so called virtual context. When EE is executing instructions, it has to decide from which virtual context to execute the next instruction. The mechanism chosen here is a variant of priority based cooperative multitasking.

As opposed to the task switching on the hardware CPU, there is no big overhead when switching virtual contexts on the EE. So we can allow making the decision of which virtual context to execute before each instruction execution, instead of running each task in some time intervals and using rather complex scheduling algorithms. This offers us a very nice, simple, and effective way to implement some mechanisms related to task switching, such as interrupts and events.

Each virtual context is assigned an integer number called the virtual priority. Virtual priority of each virtual context determines the source of the next executed instruction. Selected will be that running virtual context, which has the highest virtual priority. If there are more running virtual contexts with the same (highest) priority, then they shall be handled one by one using a round-robin principle. To support that, the EE runs its internal 64-bit Instruction Execution Clock Counter (IECC), which increments by 1 upon execution of each virtual instruction, and its value is then stored in the Last Instruction Execution (LIE) register within the virtual context that was the source of the last executed instruction. Then when the EE has to decide which virtual context to select as an instruction source among those with the same (highest) priority, it selects the one that has the value in the LIE register in the greatest backwards distance from the current value in the IECC register. Note, that it is not necessarily the lowest value among the LIE registers, because we want to achieve the correct functionality even in the very unlikely event of overflowing of the IECC register. (Probability of overflowing is quite remote, as it would take over a thousand years of running at the unlikely instruction execution rate of 5 GHz to achieve overflowing of the IECC.)

EE is not designed to run just some totally independent processes, like most CPUs are. Instead, it is supposed to run processes that would cooperate together in order to achieve the given common task. It is up to the programmer to make the virtual processes behaving correctly among themselves. EE is not supposed to be a protective barrier between different processes. It should rather be an effective tool helping the programmer to perform a specific task. By choosing this approach we can again omit the rather complex interprocess protection and security mechanism. To achieve the overall security of the system it is only necessary to keep the whole EE system shielded against unwilling external intrusions and each programmer that writes code for the EE has to keep in mind that the code must behave properly.

As mentioned above, the selected scheduling mechanism makes the implementation of interrupt and event (sometimes also referred to as exception, and it differs from interrupt in the way that it is risen by an external, possibly hardware, source, while interrupts originate

from the internal, usually software, source) mechanisms very simple. Because of the way virtual processes are executed here, there is no need to take any special care about interrupting them, as they are in fact rescheduled after execution of every virtual instruction. So that the interrupt or event handling in a way that is common to most CPUs can be done just by creating some separate virtual process with sufficiently high virtual priority, put it to sleep and awaken it by the appropriate interrupt or event. This way, however, not only separate virtual processes with the proposed high priority can be awakened, but any virtual process can.

The mechanism works in the following way. Put the identifier of the selected virtual context you want to wake up in one of the Global Handler (GH) registers. Set the appropriate bit (of the same order as it the number of the chosen GH register) of the i -th Global Event Mask (GEM i) register to a 1, where i is the number of the event. Then when the event occurs, all virtual contexts that are attached to it by the above described mechanism are awakened. This means that there can be more than just one virtual process awakened by one single event.

With a little addition of three more register sets the barrier synchronization mechanism of more virtual processes is also implemented. These sets are the Global Barrier Comparator Overflow (GBCO) registers, Global Barrier Counter (GBCN) registers, and the Global Barrier Event (GBE) registers. After each barrier instruction in each of the virtual processes that are about to be synchronized, the specified GBCN register increases by one and the virtual context falls asleep. When that GBCN register reaches the value of the adequate GBCN register, the event specified in the appropriate GBE register is arisen. Before all this happens, an appropriate mask must be set in the related GEM register and appropriate GH registers must be preset as well.

This was just a brief overview of some mechanisms related to the scheduling of the EE VPU. Further development of project INDECS is expected in the following year with hope to achieve final usable system that could drive our neutron diffractometer KSN-2 experimental device.

References:

- [1] DRÁB, M.: *Project INDECS: The Design of a Superior System of Data Collection and Analysis (Diploma Thesis)* Faculty of Nuclear Science and Physical Engineering, Czech Technical University, Prague, CZ, May 2003.
- [2] DRÁB, M. – KALVODA, L. – VRATISLAV, S. – DLOUHÁ, M.: *Execution Engine: The Virtual Processing Unit for Driving Physical Experimental Systems*, Proceedings of Workshop 2004, Part A, Special Issue, Volume 8, Czech Technical University in Prague, March 2004, pp. 306–č. 307.

This research has been supported by GA 202/03/0981 and MSM 210000021.

Investigation of Cellular Automata for Diagnostic Purposes

Jan Schmidt

`schmidt@fel.cvut.cz`

Dept. of Computer Science and Engineering, FEE ČTU, Karlovo náměstí 13, Praha 2, 121 35

Cellular automata (CA) are an attractive source of test vectors for built-in self-test (BIST) in digital circuits [1,2]. The circuit under test is considered to be combinational, therefore ordering of the test vector and surplus vectors do not matter. The quality of a test vector generator is judged by its area and test duration. Various methods are used to improve the quality, e.g. by combining the generator with a test vector storage or by decoding the output by synthesized circuits. The task of optimum generator synthesis has an enormous solution space. Therefore, all known methods limit the solution space artificially. To simplify the synthesis further, heuristic functions and auxiliary criteria are employed to guide the synthesis. In this category, one of the best-known ideas is to observe the Hamming weight (the number of binary ones) of generator outputs and to compare it against the given test vectors. Either the Hamming weight of each output (*local weights*) or the Hamming weight of all output at a time (*global weight*) can be used as the similarity criterion.

In this application, cellular automata are area-efficient and produce reasonable quality output [1], yet they are difficult to control. With a given CA structure (usually a 1-dimensional ring and a 3-neighbourhood), only two parameters remain to adapt the CA generator to the test vectors: the CA transient function ('rule' in CA terminology) and the initial state (seed). Moreover, little is known about the relationship between these parameters and output characteristics such as Hamming weight.

Real-life BIST generators have hundreds or thousands of outputs and produce thousands to tens of thousands vectors. A CA implementing such a generator has a state space, which is impossible to be explored exhaustively, and uses only a very small portion of that space. To select the above mentioned CA parameters means in fact to select a 'good spot' in the state space, and to find a rule which is simple enough and permits for such good spots in the state space.

The presented work is an initial study in controlling CA for diagnostic purposes. The main idea is to work with CA so small that the entire state space can be investigated. The obvious advantage is that relevant phenomena can be conveniently observed in e.g. Hamming weight plots or state diagram charts. The drawback is that the applicability of the results on real-life devices is not guaranteed and has to be proven. This does not, however, prevent us to use such a study to direct further research.

The software and hardware used for the investigation was able to generate, store and analyze state spaces of CA with width of up to 29 bits. We investigated

- additive CA, such as Rule 90 or Rule 60, also used in [1];
- non-additive CA lying on 'the edge of chaos' [3], also known as Class IV, such as Rule 110;
- heterogenous CA composed mainly of the elements listed above.

We focused on CA of prime width, also in accordance with [1]. An additive CA can be seen as a device multiplying its state by a fixed polynomial (which usually has to be irreducible), or as an interaction between symmetries (automorphisms) of the CA ring and the 292

automorphisms of the CA transient function. The latter approach shows that translation symmetries of the ring cause portions of the state space to fold.

First of all, transients and attractors of the selected CA were investigated for Hamming weights. We found that the weight lies almost completely in a range between approximately $1/3$ and $2/3$ of the CA width. Average weight of separate attractors varied by 10 – 20%. Some attractors (primarily rule 110) show cyclic Hamming weight, with period equal to the CA width or even a fraction of it where the width is not prime. Rule 60 CA exhibited behavior derived in [3] for rule 90: states with odd weight are initial only and cannot occur in evolution.

The transients behaved differently. Although they are rather short in our 'toy' CAs, they exhibited weights similar to that mentioned in [1], where the relative weight of 0.1 has been maintained for many steps.

To control local weights, we tried to 'inject' CA sites with higher Langton's lambda [2] into an otherwise homogenous ring. The heterogeneous rings behaved in an acceptable manner, the attractors being smaller and less similar, provided that the 'injected' sites were not too numerous and not too close.

From these observations, we conclude the following directions for our future research. The investigation of CA symmetries seems to be both desirable from the diagnostic point of view and promising from the theoretical viewpoint. Also, to find unreachable (initial) states for more rules is of interest. Mixing rules in a CA seems to be a brute force approach; to develop a feasible method out of it, much more shall be known about what rules to mix and how to keep the CA behavior sufficiently complex.

References:

- [1] NOVÁK, O: *Pseudorandom, Weighted Random and Pseudoexhaustive Test Patterns Generated in Universal Cellular automata*. In: Lecture Notes in Computer Science 1667, Springer, 1999 pp. 303–320.
- [2] CHAUDHURI, P.P. ET AL *Additive Cellular Automata Theory and Applications Volume I*. IEEE Computer Society Press, 1997, 240 p.
- [3] WOLFRAM, S. – MARTIN, O. – ODYZKO, A. M.: *Algebraic Properties of Cellular Automata* . In: Communications in Mathematical Physics, Springer, 1984 pp. 219–258.

This research has been supported by MSM 212300014.

Inovation of subject Switching systems I

David Jandera, Petr Koloros

janderd@fel.cvut.cz

Department of Telecommunications, Faculty of Electrical Engineering, Czech Technical University, Technická 2, 166 27 Prague 6, Czech Republic

The Subject Switching Systems I is mandatory subject for students in branch Telecommunication technology. This subject has on our department a long tradition and belong to pillar of telecommunication branch. According to very fast changes in our branch and setting up new technologies was very important adapt subject to this changes and give students new experiences and practical knowledge. Mainly the practical part of this subject needed innovation, because previously the exercises was only on theoretical base. In sequence was necessary to adjust succession contents of lectures and practical exercises.

The point of our project was to implement practical experiences to learning program of switching systems. In first step was prepared new program of lecture classes and in sequence with this to prepare new practical exercises. Switching technology is the topic of subjects Switching systems I, Switching systems II, and marginally in Telecommunication systems.

It was very important to innovate subject of Telecommunications systems, because it's designated for all students in Bachelor branch Electronics and Communication technology. Because students have very little knowledge about telecommunications, it is important to prepare easy demonstration exercises which can help the students to acquire the basic knowledge and make telecommunications more attractive for them. The different task is to prepare learning program for subject Switching systems I,II. These two subject should get the students complex knowledge about switching technology, compare all generations and give them good knowledge of newest technology and principals of signalization, voice traffic handling, tariffication and projecting large telecommunication networks. Student should get complete knowledge to continue in following subjects which is more oriented to network planning and implementing of new technologies based on IN, NGN etc.

Owing to this innovation the subject go though a radical change, which prove in content of lecture part and mainly in exercises, which was completely projected with respect of new learning possibilities. Exercises are based on possibilities of new reconstructed laboratory of Switching systems. This innovation is helpful not only for this subject, because the technological background is used up in other subject taught on our department.

New laboratory exercises give students practical part of taught topic. They have good opportunity to experiment with this technology and find out new experiences. This idea gives students opportunity of individual work and thank to their interest get broad view, critical and real thinking, which is very important solving real problems in practice.

Our Laboratory of switching systems has a very good technological background, thanks to modern telecommunication technology and measuring tools. We can provide our students background for measuring and configure all four generations of switching systems.

- Main task was to design working places with consideration for future expansion and advancement. Project placement of individual devices and measuring workplaces.

- Build up network of PbX technology, project numbering plan and connect of them (Ericsson MD110) to public telecommunication network. We realize to connect our technology to data transmission technology and cables to measure transmission parameters. We want to use highest number of signalization interfaces to show students interoperability between systems of different generations.

- Result of our work is complete realization of workplaces for student work in groups, made cycle of laboratory exercises for independent work and optimisation of seminars for maximal pedagogical effect.

Prepared cycle of laboratory exercises

1. *Analog signalizations* - measuring of physical representation of signals on connection between two PbX and connection to public network.
2. *Digital signalization CAS* - measuring signalization on boundary between two PbX with E1 interface and CAS signalization
3. *Digital signalization CCS* - measuring signalization on boundary between two PbX with E1 interface and CCS-Qsig
4. *Synchronization in digital network* -determination of synchronization state on boundary PbXes with ISDN BRI interface and evaluation of connection quality.
5. *Transmission of analog signal through digital systems* – determination of parameters for different types of connection (one Exchange, between two systems, in large network)
6. *Management of PbX system* – configuration and service PbX systems (Ericsson, TTC, Siemens, Goldstar)
7. *Tarrification* – work with tariffication system Calom, verifying voice data traffic realized through actual branches, type of call and price for call

Innovated exercises was implemented in learning program for students in bachelor studying plan. Last semester pass of first cycle of laboratory exercises. Students accept this innovation very positive and help us make some improvements for better demonstration and understanding new practical knowledges. We want to follow up next semester with preparation similar exercises in SSY II which will be more oriented on projecting telecommunication networks and specialized for amplify knowledges about SS7 and VoIP principals

References:

[1] JOHN G. VAN BOSSE, *Signaling in Telecommunication Networks*, Wiley-Interscience, 15 January, 1997, ISBN: 0471573779

[2] TRAVIS RUSSEL, *Signaling system #7-Fourth edition*, Mc Graff Hill 2002, ISBN: 0-07-138772-2

This research has been supported by FRVS grant No. F1-2016/2004

Applications of Genetic Algorithms

J. Kubalík, P. Pošík, L. Lhotská, J. Kléma

kubalik@labe.felk.cvut.cz, lhotska@fel.cvut.cz

CTU, Faculty of Electrical Engineering, Dept. of Cybernetics
Technická 2, 166 27 Praha 6

Genetic algorithms (GAs) are probabilistic search techniques, which operate on a population of chromosomes. Each chromosome represents a potential solution to the given problem. In a standard GA, binary strings of 1s and 0s represent the chromosomes. Each chromosome is assigned a fitness value expressing its quality with respect to the given objective function. Such a population of chromosomes is evolved by means of reproduction and recombination operators in order to breed the optimal solution's chromosome. The evolution runs until some termination-condition is fulfilled, usually the number of genetic operations to be performed is specified. The best chromosome encountered so far is then considered as the found solution. The use of the population is apparently advantageous since it provides more information to properly bias the search. On the other hand the bigger is the used population the more computations are carried out. Note that every generation all newly created or somehow modified chromosomes must be evaluated. This becomes an important issue when the evaluation procedure is not trivial. So when applying the GA to such a real problem one should find a trade-off between the quality of the solution to be found and the amount of computation to be spent. Genetic algorithms have good potential for solving problems such as scheduling and resource allocation. They have started to be used in combination with other AI techniques in so-called hybrid systems.

In our research we have focused on several problems arising from practical applications. Let us describe briefly three of them, namely planning of rescue operations, identification of economically unstable licenced subjects, and setup of parameters of an instance-based system. The aim of the search and rescue operations (mainly in urban environments) is activity coordination and planning for a rescue squad in case of emergencies or catastrophes in order to search for injured persons and to review of all specified places [1]. The main task – searching for survived persons or objects with an unknown position – is called the exploration problem: plan a tour for each squad member so that every point in the environment can be visible by at least one member. This problem can be solved in two steps. Locations for sensing are found in the first step, followed by finding an optimal strategy how to connect these sites by m squad members. Such a problem can be restated as the Multiple Travelling Salesmen Problem (MTSP): given N cities and A agents, find an optimal tour for each agent so that every city is visited exactly once. A typical criterion to be optimized is the overall time spent by the squad during the task execution. The ability to solve the MTSP in a fast and optimal way therefore plays an important role in the rescue scenario. In this work, there has been selected the natural path representation for encoding the agents tours in the form of the linear string. This means that the tour is represented by a sequence of integer numbers, where each number represents the name of the city and the order of numbers is the order of cities in the tour. The edge recombination crossover operator is used. GA with the steady-state evolutionary model is used. This means that it operates on a single population. The whole population is randomly initialized first. Then the population is modified through the steps – selection of parents, cross the parents over, and applying the mutation, single tour optimization and longest tour shortening to the offsprings – until the stopping criterion is fulfilled. The currently worst individual of the population is replaced by the newly generated solution in each generation cycle.

The main goal of the second task is to develop a tool for automatic identification of the companies that could cancel the supply due to economic problems without detailed examination of each company. In order to achieve the goal two approaches have been chosen [2]. The first one is based on development of an aggregate evaluation criterion for assessing the firms. The solved problem can be restated as a knowledge mining task, where given the existing database of firms, records one wants to extract the knowledge of what is a good and what is a bad firm (measured in terms of economic stability). If each record is assigned an indicator that expresses its stability then the task belongs to the class of supervised learning. Once a model acquiring the knowledge contained in the presented training database is built it can be used for classification of new records with unknown economic stability. In this work we use artificial neural networks and multivariate decision trees for modeling the knowledge. The multivariate decision trees are generated by genetic programming.

The third task is an application of the novel modification of genetic algorithms called a *genetic algorithm with limited convergence* (GALCO) to the hard parameter tuning problem. The GALCO algorithm is based on the idea that the population is explicitly prevented from becoming too homogenous by simply imposing limits on its convergence. This is achieved by special replacement strategy equipped with a new recombination operator. The algorithm was used in the system iBARET (Instance-BAsed REasoning Tool) [3]. This system takes a traditional instance-based learning approach and enhances it from several points of view. This article focuses on techniques of feature weighting combined with different methods of the model evaluation. It discusses and compares GALCO modification with respect to the traditional tuning approaches on the real world problem of the prediction of the heart operation results. The proposed algorithm was experimentally tested on a real-world problem and its performance was compared to that of a standard incremental GA and a simple sequential algorithm. The results are in agreement with our intuition that the algorithm should be able to deliver a reasonably good solution in a shorter time than the other two tested algorithms. Another important observation is that the performance of the algorithm is much less sensitive to the used population size than the standard GA. This allows using rather small populations without losing an explorative power of the algorithm whilst ensuring that the population will not prematurely converge.

References:

- [1] KUBALÍK, J. - KLÉMA, J. - KULICH, M.: *Application of Soft Computing Techniques to Rescue Operation Planning* ICAISC 2004, Springer Verlag, 2004 pp. 897-902
- [2] KUBALÍK, J. - JIŘINA, M. - STARÝ, O. - LHOTSKÁ, L. - SUCHÝ, J.: *Application of Soft Computing Techniques to Classification of Licensed Subjects* IFIP International Conference on Information Technology for Balanced Automation Systems in Manufacturing and Services, Springer, 2004, pp. 481-488.
- [3] KLÉMA, J. - KUBALÍK, J. - PALOUŠ, J.: *Optimized Model Tuning in Medical Systems* IEEE CBMS 2002, IEEE Computer Society, 2002, pp. 59-64.

This research has been supported by GAČR grant No.102/02/0132.

Fundamentals of Computer Literacy

M. Fejtová, J. Fejt L. Lhotská

fejtvam@k333.felk.cvut.cz, lhotska@fel.cvut.cz

CTU, Faculty of Electrical Engineering, Dept. of Cybernetics
Technická 2, 166 27 Praha 6

The European Union is a major patron of the learning economy. E-learning is the core business of the learning economy; it was one of the issues in the first call in the 6th Framework Programme as well. Information is extracted, packaged, delivered, marketed and audited. It is globally disseminated, untouched by human hands. E-learning is a modern form of distant education that utilizes the most up-to-date information technologies in the form of electronic distributed education. Its main advantages are versatile flexibility and saving. Multimedia course combines text explanation with animations, video sequences, audio recordings, graphics, schemas and testing objects. The aim of e-learning is not to replace classical education in all areas. However it is a suitable supplement even for such areas where classical style is due to the direct contact between students and teachers regarded for irreplaceable. E-learning brings a number of communication tools from e-mail to videoconferences that enable teachers to contact individually each student. Based on the information from the electronic course, the teacher has precise information what the student's score in certain parts is, how much time he/she spends in certain parts of the course, how he/she responds questions. Thanks to the communication tools the teacher can communicate with a certain student more intensively than in classical lessons.

Based on the above-mentioned aspects, we have decided at the Department of Cybernetics to develop an e-learning system **MultiPeS (Multimedia Pedagogical System)** that could help us continuously increase quality of teaching and include the latest research results. It is designed as an open modular system, which enables its simple further extension. Information about individual lectures and lessons are saved in standard XML format that significantly simplifies possibility of cooperation with other systems. Based on the developed project, the MultiPeS system enables to generate on its output a course in both HTML and XML formats. XML format enables to use fully the structure and depth of all information included in the course. For example, it is very easy to search information by its type or keywords. Another great advantage of the XML format is that textual content of the course is separated from the graphical presentation, which makes all modifications and text structure maintenance easier and significantly supports export to various format types. Further advantage of the system is its simple and intuitive control.

At present, each of us meets computers daily – at school, library, bank, post office, at local authorities or when ordering services of a travel agency. Number of jobs where computer skills are required is growing. However, this technology brings people unthought-of opportunities and danger at the same time. It opens gate of knowledge and increase of work efficiency. However, the same gate may be a cause dividing society to those who can utilize offered advantages and those who cannot. It is obvious that ability to work with computers is becoming new literacy. It is not sufficient to teach pupils and students these skills. Most adults must manage them as well if they want to keep their jobs or to proceed in their career.

The aim of our work has been to develop a specialized e-learning course in the MultiPeS e-learning system (Multimedia Pedagogical System) whose content would fully cover problems of learning the fundamental work with computer and common program tools. It introduces knowledge of computer literacy to persons interested in it in a clear and attractive form and

enables them to verify continuously level of knowledge acquisition. The course is interactive and contains a number of multimedia elements (figures, animations, sound tracks). Prepared modules significantly contribute to easier acquisition of new information, incorporation of this information into context and its successive natural fixation and refreshment. The course is divided into eight basic modules. Great emphasis is laid on the fact that the content must be presented to students interactively and illustratively.

Module 0 – Basic Management of PC for Absolute Laymen - opens up students entire fundamentals of work with a computer using instructive videos with a sound track commenting the activities. Module 1 – Concepts of Information Technology (IT) - requires the student to have an understanding of some of the main concepts of IT at a general level. The student is required to understand the make-up of a personal computer in terms of hardware and software and to understand some of the concepts of IT such as data storage and memory. The student shall be aware of some of the important security and legal issues associated with using computers. Module 2 – Using the Computer and Managing Files - requires the student to demonstrate knowledge and competence in using the common functions of a personal computer and its operating system. The student shall be able to adjust main settings, use the built-in help features and deal with a non-responding application. Module 3 – Word Processing - requires the student to demonstrate the ability to use a word processing application on a computer. The student shall be able to accomplish everyday tasks associated with creating, formatting and finishing small sized word processing documents ready for distribution. Module 4 – Spreadsheet - requires the student to understand the concept of spreadsheets and to demonstrate the ability to use a spreadsheet application on a computer. The student shall understand and be able to accomplish tasks associated with developing, formatting, modifying and using a spreadsheet of limited scope ready for distribution. Module 5 – Database - requires the student to understand some of the main concepts of databases and demonstrate the ability to use a database on a computer. The student shall be able to create and modify tables, queries, forms and reports, and prepare outputs ready for distribution. Module 6 – Presentation - requires the student to demonstrate competence in using presentation tools on a computer. The student shall be able to accomplish tasks such as creating, formatting, modifying and preparing presentations using different slide layouts for display and printed distribution. Module 7 – Information and Communication - is divided in two sections. The first section, Information, requires the student to understand some of the concepts and terms associated with using the Internet, and to appreciate some of the security considerations. In the second section, Communication, the student is required to understand some of the concepts of electronic mail (e-mail), together with having an appreciation of some of the security considerations associated with using e-mail.

References:

- [1] FEJTOVÁ, M. – FEJT, J. - SEDLÁČEK, L. - LHOTSKÁ, L.: *MultiPeS e-learning system* MIPRO 2004 - Computers in Education, 2004, pp. 60-65.

This research has been supported by FRVS grant No. 2015/2004.

Image Attributes for Comparison Process

M. Čadík

cadikm@sgi.felk.cvut.cz

Department of Computer Science and Engineering, Faculty of Electrical Engineering, Czech Technical University in Prague, Karlovo náměstí 13, 121 35 Prague 2, Czech Republic

The problem of reproduction of high dynamic range (HDR) images on the devices with restricted (low) dynamic range (LDR) is well established in the field of computer graphics. There exist various approaches (see an overview by Devlin et al. [1]) to this issue which span typically several research areas including computer graphics, image processing, physiology, neurology, psychology, etc. These approaches assume thorough knowledge of both the objective and subjective attributes of an image. The problem is that the attributes are not defined at all or are defined very vaguely or ambiguously. Moreover, some of the attributes have very strong bindings to the others; however these bindings are not clear.

In this contribution, we present a summary of image attributes that are used extensively in the tone mapping methods and relations and bindings between them. This overview is not just useful to get in to the tone mapping field, or when implementing a tone mapping operator, but it is very desirable for two reasons: it is necessary to have all image attributes precisely defined when conducting a comparison of tone mapping operators (which is very desirable), and it is useful when designing an automatic comparison or image quality metric [2], as well.

Viewing the transformed HDR image should produce a subjective experience that corresponds well with viewing the real scene. This means that the reproduced image should look as natural as possible. Therefore, the *naturalness* is the goal of tone mapping methods. However, if we want to have our result natural, we must define the naturalness of an image in some sense. Unfortunately, the naturalness is definitely very subjective quantity. We propose that the naturalness connects other image attributes together, namely the *brightness*, *contrast*, *colour reproduction*, *detail reproduction*, *visibility preservation*, *visual acuity*, *glare*, and *artifacts*. It implies that the naturalness can be replaced by the composition of the other attributes. If we are able to measure the other attributes, we are able to assess the naturalness by the weighted sum of the other attributes.

Brightness is a quantity that measures the subjective sensation produced by a particular luminance (brightness is the *perceived luminance* [3]). A linear scale for brightness expressed in brils was proposed, where one *bril* is equivalent to the brightness induced by a 1 second exposure to a 5° white target of $1/(\pi \times 10^2)$ cd/m². The subjective brightness, B, grows as a power function of luminance: $B=k(L-L_0)^\alpha$, where k is a constant, L₀ is the threshold luminance, and α is an exponent between 0.333 and 0.49, depending on the level of adaptation. Although the expression above gives a convenient relationship between luminance and brightness for simple targets, the overall brightness of an image is more complex. Thanks to the light adaptation of the human visual system (HVS), people are quite insensitive to absolute levels of illumination. The perceived dimension of brightness is due largely to the *contrast* of one region with a surrounding region [4]. When two small adjacent paths of the retina are stimulated by light, each patch not only responds to the light but also *inhibits* the response of its neighbor. By providing a dark surround to any patch, we reduce the inhibition it receives, and its response to the same amount of light is increased - this phenomenon is called *simultaneous contrast* and it depends strongly on the *semantics* of the scene.

There exist two commonly used definitions for measuring the *contrast*, the Michelson's and the Weber's definition. The *Michelson definition* is as follows: $C=(L_{\max}-$

$L_{\min}) / (L_{\max} + L_{\min})$, where L_{\max} and L_{\min} are the maximum and minimum luminance values, respectively. The Michelson's definition is usually used when measuring the contrast of periodic patterns. The Weber's contrast is used to measure the *local contrast* of a single target against a uniform background. The *Weber definition* is as follows: $C = \Delta L / L$, where ΔL is the difference of the target luminance from the background luminance. Another definition of contrast that is suitable for *complex images* was proposed. *Local band-limited contrast* assigns a contrast value to every point in the image as a function of the spatial frequency band. For each frequency band, the contrast is defined as the ratio of the bandpass-filtered image at that frequency to the low-pass image filtered to an octave below the same frequency. The contrast at the band is represented as a 2D array: $c(x,y) = a(x,y) / l(x,y)$, where $a(x,y)$ is the bandpass-filtered image, $l(x,y)$ is the local luminance mean image, and $l(x,y) > 0$.

Owing to scattering of the light in the human cornea, lens, and retina, and due to diffraction in the cell structures on the outer radial areas of the lens, the *bloom* (veiling luminance) and *flare lines* (ciliary corona) are seen around very bright objects. The diffraction effects of circular optical grating formed by the radial fibers at the periphery of the crystalline lens cause the *lenticular halo*. All these real-world phenomena are commonly referred to as *glare effects*. Since the dynamic range of traditional output devices is not sufficient to evoke such phenomena, we must simulate the human response artificially to improve the *naturalness* of an image. Several works on the simulation of glare effects have been published and some tone mapping operators have included the glare simulation as well. It has been verified that the simulation of glare can substantially increase the apparent *brightness* of light sources in digital images.

As a consequence of tone mapping transformation, *artifacts* may evolve in the output image. The artifacts are degrading the quality and are also reducing the *naturalness* of the output image. Simple local tone mapping operators typically exhibit halo artifacts. *Halo artifacts* are caused by contrast reversals. This often happens for small bright features or sharp high-contrast edges, where a bright feature cause strong attenuation of the neighbouring pixels and surround the feature or high-contrast edge with a noticeable dark band or halo.

In this contribution, we have presented an overview of image attributes for comparison of tone mapping operators. This overview is useful when designing an automatic comparison metric or image quality metric, as well. We have defined the attributes, and relations and bindings between them. Since many affected image attributes are purely subjective, we will perform thorough subjective testing to verify the proposed features.

References:

- [1] DEVLIN, K. – CHALMERS, A. – WILKIE, A. – PURGATHOFER, W.: *Tone Reproduction and Physically Based Spectral Rendering*, The Eurographics Association, 2002, pp. 101–123.
- [2] ČADÍK, M. – SLAVÍK, P.: *Evaluation of Two Principal Approaches to Objective Image Quality Assessment*, IEEE Computer Society Press, 2004, pp. 513–518.
- [3] ADELSON, E.: *Lightness Perception and Lightness Illusions*, The Cognitive Neurosciences, 2000, pp. 339–351.
- [4] PALMER, S.: *Vision Science – Photons to Phenomenology*, The MIT Press, 2002.

This research has been supported by the Czech Technical University in Prague, grant No. CTU0408813.

Kernel-Level Communication Library for Linux

M. Kačer, D. Langr

xkacer@fel.cvut.cz

Department of Computer Science and Engineering, Faculty of Electrical Engineering,
Czech Technical University, Karlovo náměstí 13, 121 35 Prague 2, Czech Republic

Linux is an example of an open-source operating system kernel. It means the source code of the kernel is public and anyone can read and modify it. This is very useful, because some tasks require modifications and/or enhancements to the OS kernel. Without the modifications, such tasks either cannot be solved at all, or would be very inefficient or complicated.

An example of such task is a process migration module, which needs to access memory space of processes, their internal data structures, etc [1]. This module also needs to communicate between OS kernels running on different computers. It turned out that such a communication is not an easy task on the OS kernel level.

To support communication between Linux kernels, we have developed a universal kernel-level communication library called KKC, which stands for *Kernel to Kernel Communication*. The library can be used by other kernel modules that need to communicate with other computers on a network. Such modules are called *customer modules* in this text.

The KKC library has following features:

- Simple API. Inside the kernel, it is relatively difficult to utilize standard network sockets. The library provides simple interface, easy to use in customer modules.
- Architecture independency. The library is not limited to TCP/IP protocols family. Customer modules can use the library to access various network architectures (e.g., fast switching networks, such as Myrinet) in a uniform and transparent way.
- Buffering. The library supports combining of primitive data values, such as integer numbers, into data buffers, which are then sent in a single network operation. On the receiving side, the library is able to break the buffer back into individual values.
- Modular design. The library has a form of a Linux kernel module. Separate modules are used to provide support for particular network architectures. New modules can easily be added when a new architecture needs to be supported. The modules are loaded automatically by the KKC library using a Linux kernel module loader (*kmod*).
- Connection oriented. The KKC library provides mechanisms to create a *connection* between two Linux kernels and to send and receive data through it. If underlying network architecture does not support connections, the library must simulate them.

To describe the KKC library, we need to briefly mention two kernel services provided by a standard Linux kernel. A Linux kernel module loader *kmod* can be used to automatically load modules into the kernel when some functionality is needed. A *sysctl* service allows to pass arbitrary values from user space programs to kernel utilities using virtual "files" of a special filesystem.

Before using the communication library, a module called *kkc* must be loaded into the kernel. This module provides general function which hide architecture dependent code. It also contains functions to initialize the library and to release its resources when the module is to be removed from the kernel.

When a customer module needs to make a connection, it calls a general *kkc_connect* function and passes a destination address to it. To ensure architecture independency, the address is a plain string value consisting of two parts:

- name of the network architecture and
- architecture-dependent address of the destination computer.

For example, if the TCP/IP protocols are used, the address may be "tcp:192.168.1.1:987".

The *kkc_connect* function splits the address into two parts and checks whether a module for the specific network architecture is present in the kernel. If not, it is automatically loaded using the Linux *kmod* service. The second part of the address is then passed to an architecture-dependent function provided by that module.

The destination address is usually provided by an end user, not a customer module. This means the customer module just reads it from either a configuration file or using the *sysctl* system. The address is then passed to the KKC library unchanged, allowing the user to specify any network architecture transparently to the customer module. This makes the customer module totally unaware of the underlying network architecture and it also allows to have several connections, each of them using different network.

On the other side of the connection, a *kkc_listen* function is called, which is basically analogous to a combination of TCP/IP *bind* and *listen* functions. Similarly to *kkc_connect*, the *kkc_listen* also takes a string argument specifying a port or a network interface to listen at. Again, the argument is composed of two parts: the identification of network architecture and an architecture-dependent part.

The *kkc_listen* function also ensures that a module for the particular network architecture is loaded and then calls an architecture-dependent function provided by that module. After the call, incoming connection can be accepted by a *kkc_accept* function.

Once a connection is established, *kkc_send* and *kkc_receive* functions are used to send and receive data through it.

If a customer module needs to send a large number of values, it can use a *kkc_buf_alloc* function to create a buffer. Then, the individual values are stored into the buffer, which grows automatically, as needed. Finally, the whole buffer is sent through a network connection. Buffering improves the efficiency of the communication and it also makes the usage of the library more comfortable in some situations.

The KKC library is a universal library that hides particular network architecture and allows customer kernel modules to communicate with other computers in a uniform and transparent way. At the first sight, the API of the library is very similar to the BSD socket interface, which allows customer modules programmers to easily understand the semantics of all functions.

References:

- [1] LANGR, D. : *Návrh a implementace základů systému Clondike*. Diplomová práce FEL ČVUT, 2004.
- [2] BOVET, D.P. – CESATI, M.: *Understanding the Linux Kernel, 2nd Edition*. O'Reilly & Associates, Inc., 2002.

This research has been supported by MŠMT grant No. MSM6840770014.

Timeout-Based Protocol for Monitoring Workstation Clusters

M. Kačer

`xkacer@fel.cvut.cz`

Department of Computer Science and Engineering, Faculty of Electrical Engineering,
Czech Technical University, Karlovo náměstí 13, 121 35 Prague 2, Czech Republic

Clusters of Linux workstations are a relatively cheap computing platform. Beside high-performance, there is also a need for high-availability of such clusters. This basically means there is no single point of failure. If a node fails or becomes unavailable due to a network error, other nodes take over the node's function. To cope with failures, we first need to detect them. For this purpose, nodes of a cluster must monitor each other. We have proposed a monitoring protocol, which allows detecting failures of nodes and communication links.

In [1], a timeout-based failure detector is proposed and its correctness proven. Although our proposal works on similar principles, there are two important differences: our solution can be used for more than three nodes and it is also more resistant to packet loss and/or delay of the communication network.

Communication States

Each node in a cluster can be in one of four communication states. Each node remembers not only its own state, but also the states of all other nodes. This information may eventually be inconsistent among the nodes. The states are:

- **ALIVE:** The node is functional and sees at least half of the other nodes also in the ALIVE state. This "majority" condition ensures that there cannot be two disconnected groups of ALIVE nodes.
- **DEAD:** The node is not operational or its status is unknown.
- **CANDID:** The node is ready to be ALIVE. This state is used before entering the ALIVE state for some time to confirm that the node is seen by all other ALIVE nodes. It is also used when the node is operational but the majority condition is not satisfied.
- **FAIL:** Permanent or repeating failure detected. This is identical to the DEAD state but a human administrator action is required to recover from it. This state is used to prevent the node from trying to switch to the ALIVE state again and negatively affecting function of other nodes.

Heart-Beats

To achieve reliable monitoring, each node periodically broadcasts heart-beats to all other nodes. A heart-beat contains following information:

- sender identification,
- heart-beat serial number, and
- an array containing following information for every node in the system:
 - node state,
 - time elapsed from the last heart-beat received from that node, and
 - the serial number of the last heart-beat received from that node.

When no heart-beat is received from any node for some specific time (called an *inactivity timeout*), the node is marked as DEAD.

Communication Failures

The underlying communication medium is considered unreliable. The monitoring protocol can cope with the following types of malfunction:

- **Heart-beat loss.** Because the inactivity timeout is several times larger than the period of heart-beats, the loss of one or two heart-beats does not cause any troubles. Only if a significant number of consecutive heart-beats are lost, the sending node is marked as DEAD, this information is then distributed among all nodes.
- **Out-of-order heart-beats.** If the order of heart-beats is accidentally changed by the communication layer (for example, if one of the heart-beats is delayed significantly), the receiving side detects it using heart-beat sequence numbers. Heart-beats older than the newest heart-beat already received are ignored.
- **Delayed communication.** Whenever a heart-beat sent from a node N is received by a node M , it contains (among others) the serial number of the last heart-beat received from M by N . The M node can use this information to check the round-trip time. If the time is too large, the heart-beat is ignored. If the communication is delayed permanently, one of the nodes will eventually mark the other as DEAD.

Conditions

The monitoring algorithm will function properly, if two important requirements are satisfied: sufficient process responsiveness and limited time drift.

Process responsiveness. The nodes must be fast enough to react quickly to any events, such as to incoming heart-beats. Moreover, the monitoring process must be scheduled by the operating system often enough to generate heart-beats and perform other actions.

If this condition is violated (for example, the CPU load on the node is too high), there could be serious implications because the time measurements would be very inaccurate. Again, this situation is eventually detected and the corresponding node is marked as DEAD. As pointed out in [1], there are ways to assure that no process performs any "dangerous" instruction before the detection occurs.

Limited time drift. Since the solution is based on timeouts, it is required that the system time on all nodes runs fluently. There are no explicit requirements on the accuracy of the absolute time; just the system clock drift must be limited.

The above requirement is very weak and is satisfied in virtually any real-life setup. The only problem can arise if the system time is changed (e.g., by an administrator) suddenly. In this case, the heart-beats will be ignored for some time and the particular node will be marked as DEAD eventually.

A pilot implementation of the proposed monitoring protocol was created and tested. It proved the protocol is simple, robust and can detect node failures quickly and reliably.

References:

- [1] FETZER, C.: *Perfect Failure Detection In Timed Asynchronous Systems*. In IEEE Transactions on Computers, ISSN 0018-9340, Feb 2003, pp. 99–112.

This research has been supported by MŠMT grant No. MSM6840770014.

Authentication Protocol Resistant To Online Dictionary Attacks

T. Vanek

vanekt1@fel.cvut.cz

Department of Telecommunication Engineering, Faculty of Electrical Engineering,
Czech Technical University, Technická 2, 166 27 Prague 6, Czech Republic

Nowadays, the most wide spread method of authentication is through the use of passwords. Passwords are very suitable for users, easy to implement and so are very popular. There are more secure authentication schemes which are using security tokens, smartcards etc. but none of them is wide spread. The password based authentication, although very convenient, has some lacks due to the nature of this system. People have tendency to choose short and simple passwords that they can remember and such these passwords belong to a very small domain. Thus, they are susceptible to dictionary attacks. There are several instances of such attacks on various systems throughout the world. Password based systems mainly suffer from off-line and on-line dictionary attacks.

Off-line dictionary attack requires adversary who monitors communication on the communication channel to record data for a successful protocol execution. The adversary then goes off-line and tests passwords against the recorded protocol execution data without contacting the server at all. In on-line dictionary attack, the adversary tries the possible passwords by logging in on-line. Off-line dictionary attacks can be prevented by using public key cryptography suggested in the literature many times. In the case of on-line dictionary attacks, there are only few possibilities how to prevent them. Most of them are difficult to implement or its implementation is not very effective.

Password based systems are vulnerable to on-line dictionary attacks. Countermeasures adopted to prevent the on-line dictionary attacks are very expensive and not very effective. Among majors methods' preventing on-line attacks belongs:

- Delayed response
- Locking of user accounts
- CAPTCHA

Delayed Response

Server using this method of protection will not allow more than one user request per defined time interval. This may prevent an attacker from checking sufficiently many passwords in a reasonable time. It's very effective for local machines but is ineffective in a network environment. The attacker can try many login attempts in parallel and elude the timing measure using the fact that user logins are typically handled by servers that can handle many login sessions in parallel. A system which enables logins over a network and has many accounts also suffers from such attacks because an attacker is usually interested in breaking any account in the system, rather than targeting a specific account.

Locking of user accounts

After defined number of unsuccessful attempt to login, server locks account of the particular user for sometime e.g. 5 minutes. This is helpful in preventing dictionary attack by limiting the number of wrong guesses in a given time, but there are problems with this system in large networks. If account locking is used then the system will become susceptible to denial of service (DoS) attack and similarly to the distributed DoS (DDoS).

CAPTCHA

CAPTCHA is an acronym for Completely Automated Public Turing Test to Tell Computers and Humans Apart. This method uses some challenge which is sent to the user while attempting to login. This challenge is proven to be easy for humans to respond but rather difficult for computers (because on-line attacker is a programmed computer) to answer. Usually it's a picture of distorted or numbers and characters. This scheme was an effective countermeasure against on-line dictionary attacks. But, due to recent developments in Artificial Intelligence there are programs which can quickly and correctly interpret and answer these challenges. Due to these developments, even CAPTCHA is not considered to be a secure technique to prevent on-line dictionary attacks.

In [3] Goyal describes based on one way hash functions which seems effective and easy to implement. This method reduces the risk of success on-line dictionary attack due to computations made on client side. Client has to compute a response on challenge sent by server. The computation of this response is designed to be time consuming operation.

Their protocol uses only fast one way hash functions. The user and the server are required to perform a few hash calculations for logging in. The system is deliberately made time consuming and computationally intensive for the client. This ensures that client is not able to make a large number of authentication requests per second. System is extremely efficient for the server. This method may solve the problem of on-line dictionary attacks.

References:

- [1] LAMPORT L.: *Password Authentication with Insecure Communication* Communications of the ACM, 24, 1981 pp. 770-772
- [2] GOYAL V., KUMAR V., SINGH M. *A Protocol to Counter Online Dictionary Attacks* IAS'05, 2004,
- [3] PINKAS B., SANDER T. *Securing passwords against dictionary attacks* Proceedings of the 9th ACM conference on Computer and Communications Security 2002 pp. 348-356

Internet Textbook SARI and Remote Scale Models

J. Fuka, M. Kutil

fuka@fel.cvut.cz

Department of Control Engineering, Faculty of Electrical Engineering, Czech Technical University, Technická 2, 166 27 Prague 6, Czech Republic

Distance forms of learning are more and more popular mainly with expanding potentials for connection to the Internet. Especially for technical branches there is necessary to prepare their laboratory experiments using remote control through the Internet. Laboratories of Automatic Control Theory of the Department of Control Engineering FEE CTU in Prague [2] are well equipped with standard scale models (Ball and Beam, Couple Tanks, Servos, Helicopter, Thermal system etc). These models are primary controlled by local PC with AD/DA cards using Matlab[®] and Simulink[®] and they are inconvenient for remote control. In cooperation with our students we developed two new systems to fulfill Internet specific requirements - the Levitation and the Lathe. Remote control of these models was built in to the Internet textbook SARI [3].

The Internet textbook SARI was created like a support for basic courses of theory of automatic control "Systems and Models" and "Systems and Control" with a goal to enhanced teaching methods [1]. The Internet textbook (still mainly in Czech language) is available at <http://dce.felk.cvut.cz/sari> and is based on CSS, PHP and SQL technology. This version includes complete publishing system with an integrated discussion forum, control-engineering dictionary, and references on libraries, where the recommended books are available. Online computing of teaching simulation programs is available by implementing Matlab Web Server[®]. The most important part of the design of the Internet textbook is intelligible and fast navigation in the texts and other components like utilities for Matlab. The main tool is the menu on the left side of the page. It's possible to access every page by few clicks, using this tree menu, which is composed to be the most effective by searching for the required page. The second useful part is an m-file downloading page. The user can see dependencies on the other m-files or examples of use. The page offers downloading single file or generates complete pack needed for running. Automatic syntax hi-lighting is also available. This is apt for fast searching inside the m-file.

Web interface with a lot of capabilities was designed for the administration of the textbook. The web interface was chosen to make alternating of the pages most simple, to allow the administration also for not advanced webmasters. The system shows detailed access statistics for each page. Accounts for people creating the pages are divided into groups. This enables them to make different actions like alternating page contents, menu structure or the base system. The root manages these accounts, which shouldn't be unique. The editing of pages is possible in two ways. Profound changes of the textbook can be made by direct HTML or PHP editing, though it places high demands on the users' skills. The minor changes can be achieved via the built-in WYSIWYG editor, which is useful for standard pages but has limited abilities. The page should have set it's description, list of keywords, group allowed to deleting and editing it's content or setting the visibility attribute.

Last but not least topic which is going to improve quality of education is remote control of the physical model experiments. These models are identified and controlled in practical lessons of control engineering. Next two sections depict new scale models.

Primary part of the "Levitation" model [4] is vertically orientated two meters long transparent plastic tube. A flow of the air from a ventilator levitates a body placed inside.

Position of the body is mainly continuously measured by a laser sensor, which is placed above the tube. Auxiliary sensors measure pressure in the tube, speed of the ventilator, power voltage of the ventilator, and discrete position of the body by reflex sensors. Power voltage of the ventilator, which is implicating the amount of airflow inside the tube, can be set either manually from control panel or via remote control.

Web camera view of the model is available. The model is controlled either by a programmable logical controller PLC-5 or a personal computer equipped with special measuring card. There were designed two types of visualization accessible through the Internet. The first visualization uses the programmable controller, the second one a personal computer. You can visit both pages using SARI textbook or the address <http://vznaseni.felk.cvut.cz>. The web pages issued by processor of programmable controller are only for process monitoring. Web server that runs on the personal computer enables full control. Measured data are stored to database and subsequently are used for generating visualization on web pages as table, graph or xml files. There is a multi-user system for model access and user authentication. The advantage of using database is a personalized connection to the model for each user. Local control is standard one.

The second one model is multiple axis servo model – the “Lathe”. In practice, it is a model of the lathe, which can only copy surface of the finished workpiece. The position of the slide head is read from two incremental rotary sensors, the distance from the surface is measured by tactile inductive drift meter and rotating speed of spindle by tachodynamo. Motion in axis is driven by 24V DC motor. The slide head movements are directed manually, or by ControlLogix programmable controller equipped with special motion module, or by personal computer. We have designed new control electronic switch with remote changeover. ControlLogix system offers new Ethernet web server module, which also allows full remote access. The process is again monitor by a web camera.

Our new models were ready for teaching in the last semester. We have got a positive acceptance from students which have worked with these models.

References:

- [1] JOHN, J. - FUKA, J.: *Innovation of Basic Subjects in Automatic Control* In: Proceedings of 2nd International Conference on Automatic Control [CD-ROM]. Barcelona: CIMNE, 2002, pp. 232 - 235.
- [2] FUKA, J.: *Laboratories of Automatic Control Theory of the Department of Control Engineering FEE CTU in Prague* Automatizace, 2003, pp. 497 – 500.
- [3] FUKA, J. - KUTIL, M. - VANĚK, F.: *SARI - Internet Textbook for Basic Control Education* In: Proceedings of Process Control '03 [CD-ROM]. Bratislava: Slovak University of Technology, 2003 pp. 106 - 1/4.
- [4] KUTIL, M. – FUKA, J.: *Control of model using Internet* In Proceedings of the 6th International Scientific-Technical Conference on Process Control (CD-ROM). Pardubice: University of Pardubice, 2004, pp. 223 - e-version 6 pp.

This research has been supported by the Czech Ministry of Education within the framework of the programs FRVŠ (Grant 2025/2004).

Gloom of Modern Econometrics and Impacts of Prescott's Nobel Prize 2004 Work

Jiří Trinkewitz

xtrinkew@control.felk.cvut.cz

Faculty of Electrical Engineering, Czech Technical University,
Charles Square 13, 121 35, Prague, Czech Republic

Keynesian models were in mid-1970s criticized on methodological grounds. Robert Lucas's research in mid-1970s showed that the relationships between macroeconomic variables are likely to be influenced by economic policy itself. F.Kydland and E.Prescott's received Prize in Economic Sciences in Memory of Alfred Nobel, 11 October 2004 [2] for their contribution to dynamic macroeconomics. The fact that there is only one generally valid equation used in presented model, which has been driven from Capital by Karl Marx, foreshadows that there is very few robust foundations in modern econometrics up to this day. To enable a comparison our NAIP framework is being presented. But let us pay attention, such broader frameworks as this used now in dynamic models has shaky base. If other Mr. Lucas comes modern econometrics could fall like a house of cards.

Prescot's framework consists of two state variables [2]: z_t – technology shock (or change) and k_t – capital stock. z_t follows AR process $z_{t+1} = \rho z_t + \varepsilon_{t+1}$. $k_{t+1} = k_t(1-\delta) + r(z_t, k_t, l_t) \cdot k_t + w(z_t, k_t, l_t) \cdot l_t - h_c(z_t, k_t)$, where $l_t = h_l(z_t, k_t)$. This equation describes that added value is all production, which is not consumed as wage. (Taxes are assumed to be paid only from wages). Compare it with this NAIRU framework [1][3][4]: First equation is expectation augmented Phillips curve $\pi = \pi_c + c_1 \cdot (u - u_N) + c_2(\mathbf{d}) \cdot \mathbf{x} + e_1$, $c_1 < 0$, filled up with external shocks, next equation describes unemployment gap. $g_U = c_3(\mathbf{d}) \cdot g_U + c_4(\mathbf{d}) \cdot \Delta i + c_5(\mathbf{d}) \cdot \mathbf{x} + e_2$, it is AR process influenced by oil price and interest rate. Unobservable status variable of natural rate of unemployment is then AR process like this: $u_N(t+1) = u_N(t) + e_4$ and unemployment rate is then $u = u_N + g_U + e_3$. Finally suppose dummy expectations like this: $\pi_c(t) = \pi(t-1)$.

Let us compare these two models. Prescott's status variables are well specified from control theory's point of view. These variables represent values, which slightly changes according to shocks and inputs. Moreover the product logically depends on technology level and capital stock. Additional capital or better technology activate extra product.

In opposite NAIRU state variables do not behave like primary states but more likely as responses or combination of basic states. It is impossible to prove whether they have character of state variable or they completely have not. It is not common that peoples building econometric models have so good feeling like F.Kydland and E.Prescott. Many models use empirically established laws and it does not matter how do status variables look like.

Algorithms needed to solve dynamic econometric models are already developed. It is possible to compute these tasks both analytical and numerical way. Way how to do it is well described in previous works. [1][4]

Nowadays is our effort focussed on creation of cookbook describing, how to create purged models. Information gathered from output does not fully describe structure of system. There exist infinity of mathematically equivalent models, but only one is the pure one which most closely describes reality. Only such model allows us to make deep analysis of system behaviours and it will make results more credible for future research..

References:

- [1] ŠTECHA, J. – TRINKEWITZ, J. – VAŠÍČEK, O. ET AL.: *Alternative Models of Adaptive and Near-Rational Expectations-Classification by Bootstrap Filter Modeling and Control of Economic Systems*. Klagenfurt : University of Klagenfurt, 2001, p. 200-201.
- [2] *The Royal Swedish Academy of Sciences, The Prize in Economic Sciences 2004, Advanced Information (pdf)*: [online].Stockholm, 2004 - [cit. 5.1.2005], available on: <http://www.kva.se/KVA_Root/files/newspics/DOC_20041011123429_28842881920_ecoadv04.pdf>
- [3] KICHIAN M.: *Measuring Potential Output within a State-Space Framework* Working paper 99-9 Bank of Canada, Ottawa , 1999.
- [4] TRINKEWITZ, J.: *Makroekonomické modely a jejich hodnocení užitím paralelních simulací*. tri.wz.cz, 2003, available on: <<http://tri.wz.cz/minimum7final.doc>>

This research has been supported by CTU0284086.

Efficient Number Representation for Floating-point Operations

P. Štukjunger, M. Bečvář

stukjup@fel.cvut.cz

Department of Computer Science and Engineering,
Faculty of Electrical Engineering, Czech Technical University in Prague,
Karlovo náměstí 13, Praha 2, 121 35

Thanks to continuously growing level of integration of contemporary VLSI integrated circuits, floating-point units are more and more frequently implemented in hardware. The IEEE 754 standard [1] is generally accepted and used standard for floating-point number representation in almost all systems using floating-point operations.

General structures of basic operations (i.e. addition, subtraction, multiplication and division) for such units are well known [2-3]. Basic floating-point computation algorithms are straightforward. The situation gets more complicated when the floating-point arithmetic unit should comply with IEEE 754 standard. Exceptional cases, namely denormals and special values, have to be taken into account. Denormals, the feature introduced in IEEE 754 to implement so-called gradual underflow, are numbers whose significand is not normalized. Since most of the floating-point implementation structures count on the fact that input operands are normalized, introducing denormals leads to plenty of problems. The task of solving these problems is not difficult, but area and delay consuming. Quite often, designers deal with these problems simply by not allowing denormals in their designs. Second exceptional case, the special values, is not as big issue as denormals, but still requires some extra area.

In [4], a new internal floating-point numbers representation is introduced, which copes with the exceptional cases just mentioned. It means that all arithmetic units work with numbers in the internal representation. If input operands or result are required to be in IEEE 754 standard representation, a translation unit has to be used. To describe the internal representation, first IEEE 754 standard requirements are discussed, and based on them the description of the new representation is given.

The IEEE 754 standard defines single and double precisions with 32 and 64 bits respectively. It also defines single and double extended precisions with at least 43 and 79 bits respectively. The following text focuses on single precision only, however the conclusions can be generalized for all the other representations defined by the standard. The single precision representation consists of 32 bits: one sign bit, exponent (8 bits) and magnitude (23 bits). Depending on operation to be performed: for exponent, fixed-point added-subtractor is needed and for magnitude, fixed-point added-subtractor, multiplier or divider is needed. Furthermore, there must be additional logic that deals with denormals and special values.

In the internal representation, denormals are avoided by increasing number of bits of exponent. This way, any denormal of IEEE 754 standard can be represented as a normalized number in the internal representation. Increasing number of exponent bits doubles the range of numbers, which can be represented, and therefore gives enough space for representing all numbers which are considered denormals in IEEE 754 standard as a normalized numbers in the internal representation (for example in single precision, standard 8-bit exponent gives the range -128 to 127, not considering that some values are dedicated for special use, however, using 9-bit exponent in the internal representation offers range -256 to 255, which covers all the denormal values of the standard representation) The result of an operation in the internal representation, which would be a denormal, is considered as underflow. Eight extra flag bits

are included in the internal representation to represent special values. In this way, no conversion circuits are needed to detect these special values in contrast to IEEE 754 standard representation, which requires unpacking and packing before and after the operation respectively, because it encodes these values as dedicated values of significand and exponent.

Compared to the requirements of unit working in IEEE 754 standard representation, the internal representation [4] requires only one additional bit of fixed-point adder-subtractor for exponent. There is no need for additional logic that deals with denormals, neither a circuit that packs/unpacks special values. This results in smaller area consumption and shorter execution times. The benefits of the internal representation are not great, when it is used to implement a single floating-point operation, because two conversion units (IEEE to internal and internal to IEEE representation) are required. However, using the internal representation in more complex arithmetic unit, which would use a set of several floating-point operations, will show advantages of the representation.

References:

- [1] ANSI AND IEEE: *ANSI/IEEE Standard Std. 754-1985* New York, 1985.
- [2] ERCEGOVAC, M. – LANG, T.: *Digital Arithmetic*, Morgan Kaufmann Publishers, San Francisco, 2003.
- [3] LIGON III, W. B. – MCMILLAN, S. – MONN, G. – SCHOONOVER, K. – STIVERS, F. – UNDERWOOD, K. D.: *A Re-evaluation of the Practicality of Floating-point Operations on FPGAs*, IEEE Symposium on FPGAs for Custom Computing Machines 1998.
- [4] STUKJUNGER, P.: *Arithmetic in FPGA*, Diploma thesis, 2004.

Verification of CAN Bus Behaviour in Real-Time Systems

J. Krákora

krakorj@felk.cvut.cz

Czech Technical University in Prague, Faculty of Electrical Engineering,
Department of Control Engineering
Karlovo náměstí 13, Prague 2, 121 35, Czech Republic

This project dealt with a verification approach of a real time distributed system. Let us assume such system consisting of application processes (designed by application developer) running under Real-Time Operating System (RTOS e.g. OSEK) while using several processors interconnected via standard broadcast communication based on the Controller Area Network (CAN). The crucial problem is to verify both time properties (e.g. message response time, schedulability of periodic processes, response time) and logic properties (e.g. deadlock, mutual exclusion, priority based access) of the applications incorporating two kinds of shared resources - the processor and the bus. Classical approaches deal separately either with the processor sharing (studied for example by RMS) or with the bus sharing (e.g. CAN message latency studied by Tindell [1]).

Task schedulability on single-processor and multiprocessor systems is a widely studied subject. For example Rate Monotonic Scheduling (RMS) can be used to guarantee schedulability, when the application consisting of periodic processes is running on a single-processor with priority based pre-emptive kernel and the processes have their respective deadlines at the end of the period. RMS assigns fixed priorities to the processes according to their request rate (inverse to their period deadline), therefore the highest priority is assigned to the processes with highest frequency. Schedulability of such processes can be verified using Utilization bound theorem or Completion time theorem.

An important part of this project was to improve the CAN arbitration model composed of several timed automata: a bus automaton and a transmitter automaton per each message ID. Concrete CAN model, based on discrete event system is presented in [2]. The model consists of an arbitration automaton and a transceiver automaton per each message transmitted in the system. The Interface between the transceiver and the upper layer model (tasks) is provided by synchronization channels. Verification of the CAN model was compared to the results achieved by Tindell and Burns.

The next part of the project dealt with an integration of the CAN model with the model of the RTOS developed in [3]. The approach assumes a fine grain model treating the task internal structure, OS kernel, communication layer and the controlled environment. The task model consists of several blocks of code called computations, calls of OS services, selected variables, code branching and loops (affected by values of selected variables). The OS kernel model formalizes operating system services functionality. The controlled environment model, specifying arrival times of events, releasing the tasks and the messages, plays the key role in the system verification. An comprehensive analysis of this model behavior (automatically done by model checking tool UPPAAL) considers task and messages response times corresponding to a realistic phasing, realistic tasks and messages arrival times, realistic blocking and realistic execution time in a relation to the modeled code branching. Therefore the verification result is as precise as the model is.

Finally, the qualities of the project RTOS and communication bus modeling approach were proved on a real test bed. The test bed configuration consists of PC104 device and a several Motorola HC12 boards. The PC104 was configured as follows: CAN PCI card running RTLinux with OCERA LinCAN driver. The Motorola HC12 board includes MsCAN driver. The measurement on the test bed showed that our approach was correct.

The results of the project were presented at the FISITA 2004 - World Automotive Congress in Barcelona, at the 11th IFAC Symposium on Information Control Problems in Manufacturing and at the IEEE International Workshop on Factory Communication Systems in Vienna [4].

The list of the project results is as follows:

- Improved timed automata model of CAN was developed.
- The model was included to the RTOS model.
- A distributed RT system model was realized by the model and its properties were verified by temporal logic.
- Properties of such approach were validated at a test bed consisting of PC104 and three Motorola HC12 boards and compared to the timed automata results.
- The results were presented at several conferences (IFAC, IEEE).

References:

- [1] K. TINDELL AND A. BURNS: *Guaranteed message latencies for distributed safety critical hard real-time networks* . 1994 .
- [2] J. KRÁKORA AND Z. HANZÁLEK: *Timed automata approach to CAN verification* In 11th IFAC Symposium on Information Control Problems in Manufacturing - INCOM 2004 , 2004, CDROM.
- [3] L. WASZNIOWSKI, AND Z. HANZÁLEK: *Analysis of real-time operating system based applications* FORMATS 2003, 2003, pp. č. strany–č. strany.
- [4] J. KRÁKORA, L. WASZNIOWSKI, P. PÍŠA AND Z. HANZÁLEK: *Timed Automata Approach to Real Time Distributed System Verification* In Proceedings of 2004 IEEE International Workshop on Factory Communication Systems, 2004, pp. 407–410.

This research has been supported by CTU grant No. CTU0408113

Laboratory Model "Bathyscaph"

M. Hofreiter

hofreite@fsid.cvut.cz

Institute of Instrumentation and Control Technology, Faculty of Mechanical Engineering,
Czech Technical University in Prague, Technická 4, 166 07 Prague 6, Czech Republic

Automatic control is one of today's most significant areas of science and technology. This can be attributed to the fact that automation is linked to the development of almost every form of technology. By its very nature, automatic control is a multidisciplinary subject; therefore, the common course "Automatic Control" is required for all third-year students in the Faculty of Mechanical Engineering (CTU in Prague), see [2]. It is also important for students to have practical skills and abilities which are usually only gained through experience. This can only be possible by the hands-on use of equipment. Practical training as a component of the course is given at the Laboratory of Automatic Control, which is one of the laboratories of the Institute of Instrumentation and Control Technology (IICT), see [3], [4].

Laboratory models allow the practicing of fundamentals of logic, analog and digital control. In order to increase interest in control engineering, the old laboratory equipment is gradually being removed and replaced by new equipment. The laboratory equipment and software must be user friendly, flexible and reliable. New apparatuses are manufactured at IICT with the aid of students but the design, development, manufacture and testing of appropriate experimental physical models are always a long-term matter. Therefore a scientific-research consortium was formed to join their potentials and to develop experimental equipment for education purposes in the field of automatic control. The members of the research consortium are teachers and research workers from four Czech universities and the Czech Academy of Sciences. Each member of the proposed consortium already has broad experience with designing physical experimental models. The principal task of each member is to design, develop and construct a physical experimental model that reflects the physical reality of some process as well as its static and dynamic characteristics. IICT, as a member of the consortium, has decided to construct a new laboratory model called "Bathyscaph".

The laboratory model "Bathyscaph" is an original laboratory model that demonstrates the motion of a hollow cylinder (bathyscaph) within a water tank [1]. The average density of the bathyscaph (including the enclosed air) is almost the same as the density of water. When the pressure above the surface of the water is changed, the volume of the air within the bathyscaph will also change. This means that the average density of the bathyscaph will be changed by a density slightly above or below that of water allowing the bathyscaph to move up or down. The motion of the bathyscaph depends upon this pressure. The position of the bathyscaph is measured by an ultrasonic sensor. The pressure above the water surface is adjusted with the aid of an air pump and an outlet valve. The pressure above the water surface may also be changed by the second outlet valve simulating a disturbance. Both the outlet valves are governed by servomotors, which are controlled by computer. The basic aim of the control is to maintain the bathyscaph in a desired position. The laboratory model is also equipped with a sensor for measuring the pressure above the water surface and thus utilizes advanced control strategies such as cascade control etc.

An extensive range of experiments can be carried out with this apparatus:

Real-Time digital processing

PID controller design for ball position stabilization and trajectory tracking

LQ/LQG controller design based on state and I/O model

Fuzzy controller design

Adaptive controller design

Nonlinear controller design

System modelling and identification is another application where the laboratory model may be used.

The laboratory equipment uses a MATLAB/SIMULINK environment for system analysis, control algorithm design and simulation. Furthermore the Real-Time Toolbox (Humusoft s.r.o.) for using MATLAB in real time, data acquisition, signal processing and on-line control.

This piece of educational equipment is both lightweight and compact, thus it is easily portable. In the year 2005 the next four laboratory models will be manufactured at IICT for the other members of the consortium.

References:

- [1] M. HOFREITER, F. ZÁMEK: *Consortial Approach to Development of Experimental Models*, Research report CTU-FME, Praha 2003, pp. 24, (in Czech)
- [2] P. ZÍTEC, M. HOFREITER, J. HLAVA: *Automatic Control*, CTU, Praha 2004, pp.148, (in Czech)
- [3] M. HOFREITER, D. BAUEROVÁ, J. HLAVA, F. KRÁL, M. MARTINÁSKOVÁ, M. MATUŠŮ: *Examples and Exercises from Automatic Control*, CTU , Praha 2004, pp. 142, (in Czech)
- [4] [HTTP://WWW.FSID.CVUT.CZ/CZ/U210/AR/INDEX.HTM](http://www.fsid.cvut.cz/cz/u210/ar/index.htm)

This research has been supported by GA ČR grant No. 102/03/0625

Modelling and Control of Linear Combustion Engine

P. Němeček, O. Vysoký

Nemecep1@fel.cvut.cz

Department of Control engineering, Faculty of Electrical Engineering
Czech Technical University, Karlovo náměstí 13, Prague 2, 121 35, Czech Republic

A Linear Combustion Engine (LCE) is a special type of combustion engine representing a new approach concerning the conversion of the chemical energy of hydrocarbon fuel into electrical energy. Unlike conventional engines, this type of engine does not use a crankshaft, and generates electric energy directly by a linear movement of pistons.

The LCE moving part consists only of two rod-connected pistons, which move from one side to another. The reduced amount of moving parts and strict linear movement of pistons significantly increase the durability of the LCE, simplify the lubrication of pistons and increase efficiency. During operation, the pistons are accelerated by a combustion mixture and move from one side to the opposite side. The released energy is partially used to compress the fuel mixture in the opposite cylinder. This action is repeated periodically. The difference between the energy released by the combustion mixture and the energy consumed by mixture compression and mechanical losses is drained from the system as electric energy by a linear motor-generator which is also used as a starter during the start of LCE. Finally, the motor-generator also allows the prevention of the LCE from stopping when a misfire occurs.

Because the motion of a moving part is not constrained by a crankshaft, the controller must provide precise control of a moving part's position in order to avoid collision between the piston and the cylinder head. The controller must also detect possible misfires and intervene appropriately. This presents a key problem related to the feasibility of the LCE. The control features should also maximize the electric energy drained from the LCE.

The main drawbacks of a conventional two-stroke engine (e.g., high emissions of pollutants and irregularity at low speed) could be partially eliminated by the use of a precise fuel mixture system (e.g., air assisted fuel injection).

A number of papers, which examine a combined linear alternator and combustion engine system, have been published; however, most of these works concern the coupling of a linear alternator and Stirling engine [3]. A configuration with two opposed cylinders and two-stroke cycle is described [2] and [1], but these works are focused mainly on simulation, but control is not considered. Another configuration with one piston and spring is discussed in [4]. This configuration also allows the use of a four-stroke cycle, but in this case external electric energy is needed for steady operation.

Our real LCE model employs two 50ccm cylinders with direct fuel injectors. These DiTech technology injectors use the air assisted fuel injection method, which allows proper mixture preparation and consequently low emissions. The linear motor-generator has power 1 kW and is driven through a 3-phase IGBT bridge.

In our case a powerful Motorola PowerPC based system produced and supplied by DSPACE Company is used for control of the LCE. The modern, high-level design methods utilize Real Time Workshop, Matlab and Simulink for precise real-time control. Main advantage of this high level approach is a short implementation time of control algorithms in comparison to "C" or assembly language based development. Control algorithms, which are tested on the Simulink model, can be also used directly for the real model control.

Currently we consider only the control of the linear motor-generator and the combustion engine operates only in one mode at the constant speed. Therefore the parameters like spark position, fuel-air mixture ratio etc. are set to the constant values, which are based on the experimental system identification. Motor-generator control provides keeping of the pistons in some limits and thereby the steady operation of whole LCE prototype.

Two control loops are used to control the movement of the linear motor-generator. The outer loop provides tracking of the desired trajectory. The output value of this regulator is a desired force, which should be generated by the linear motor-generator. This force is dependent on the actual currents through the motor-generator coils, therefore another regulation loop is necessary to provide the appropriate current control (motor-generator is supplied by the voltage from the PWM modulator).

Although the prototype at this time is very crude, it enables experiments, which are very important for further research. Currently a steady operation of the LCE was achieved, which demonstrates a feasibility of the LCE project. Previous work also indicated problems of the current LCE design. The main problem is in electric motor-generator, because its parameters are not sufficient for draining of energy from the combustion engine. Therefore only poor fuel mixtures can be used (braking force of the motor-generator is not high enough) and it has a negative effect on efficiency of the LCE. The key problem is also the design of the control algorithm, which maximizes drained electric energy and concurrently provides a steady operation of the LCE (also in case of a misfire).

Generally the linear combustion engine seems to be a perspective device concerning the conversion of the chemical energy of hydrocarbon fuel into the electrical energy. With some essential improvements in the current design it can offer advantages over the traditionally used rotary system.

References:

- [1] CAWTHORNE, W.R.: *Optimization of a Brushless Permanent Magnet Linear Alternator for Use With a Linear Internal Combustion Engine. PhD Thesis*, West Virginia University, 1999,
- [2] CLARK, N.N. – FAMOURI, P.: *Modeling and development of a linear engine* In 1998 Spring Technical Conference of the ASME Internal Combustion Engine Division, 1998, vol. 30-2.
- [3] HOLLIDAY, J.C. – HOWELL, S.G. – RICHTER, M.: *Free-Piston Linear Alternator Solar Stirling Engine Concept* Proceedings of the 21st Intersociety Energy Conversion Engineering Conference, 1986, 468-473.
- [4] ZHANG, X.: *Modeling and simulation of a hybrid engine. Master's thesis* University of Regina, 1997

This research has been supported by CTU grant No. CTU CTU0408213.

Iterative Detection and Turbo-coding Methods in Spatial Diversity MIMO System

Jan Včelák and Milan Kníže

vcelakj@fel.cvut.cz

CTU, Faculty of Electrical Engineering, Department of Radioelectronics K13137
Technická 2, Prague 6, 166 27

Diversity techniques, like space, time or frequency diversity, are well known methods to improve reliability of the wireless transmission systems and system resistance against distortions. Among diversity techniques, the space diversity is the most promising one, because it does not require additional bandwidth, and does not introduce additional delays in signal transmission. The space diversity is based on the fact, that two signals detached in space exhibit the independent fading in radio channel. The real break through in system reliability and system performance was made by introducing the diversity at the transmitter and receiver side. Telatar [1] shows high system capacity improvements achieved by usage of multiple receive as well as transmit antennas Multiple-input multiple-output (MIMO) channel.

The proposed work deal with design and analysis of advanced detection algorithms, that exploit as much as possible such information theoretic bounds. The detector in our sense is digital part of the receiver, which serve as data estimator and channel nuisance parameter synchronizer. Advanced receiver represent for the adaptive, near-optimal receiver with lowest possible complexity. From recent research is obvious, that such detector must be based on iterative principle [2]. Iterative principle is method for joint parameters and data estimation, where the global structure of the receiver are reached by the network of subsystems, which interchanged marginal soft information on estimated parameters. Principle itself can be seen as a complexity reduction method, because its complexity grows linearly with the number of subsystems over an optimal processing. So we have focused on implementation problems connected with iterative processing.

An iterative detector consists of a network of blocks, which correspond to soft inverses to individual coders in the transmitter or channel. Some of these blocks perform the Soft-in Soft-out (SISO) algorithm usually realized by Forward-Backward algorithm (FBA). The complexity of a SISO algorithm grows exponentially with the constraint length of the code or length of channel memory. Therefore we exploited a suitable approximations to conventional SISO algorithm, which would not significantly affect the global receiver performance. We applied the state reduction techniques such as hard and soft decision feedback of currently available decisions and reduction the number of survivors. This situation is more complicated than in conventional hard decision decoder, because the local modifications influences all members in the network. Then we analyzed the influence of complexity reduction on convergence rate and error performance. The outputs are intended to be used for finding suitable methods with good trade-off between those characteristics.

The most elementary approach to estimate channel state information (CSI) is independent estimator which passing estimates to the detector. The advantage of such iterative network is that the synchronizer can re-estimate the parameters based on improved marginal soft informations at each iteration, where these soft informations exploit global structure of the system [3]. Second approach evaluates an exact expressions of the joint soft metric and

related to adaptive SISO block for both data and nuisance parameter [4]. However, implementation complexity of joint decoding and CSI estimation is always huge. The most of approximations of joint adaptive processing are based on various trellis pruning techniques such as well known per-survivor processing. Such method exploits hard decision about the most probable sequences as a training symbols for temporal parameter estimation and apply these estimates to joint metric evaluation. From recent research it seemed to be obvious, that for slowly changing parameters wins parametrized iterative networks with independent estimators. The general theoretical framework was enough developed in [4]. Our aim was to explore the fundamental problems, limiting the performance of the decoding network. We have developed a few representatives of real decoding networks and explored their performance depending on initial CSI choice. Next we discussed the possibilities how to force the network to iterate to correct estimate and rise a convergence rate.

Finally, the serially concatenated codes and corresponding iterative receivers for space-time diversity systems were constructed and analyzed. We found the recursive space-time inner code convenient, because it offer us extra spatial diversity gain in addition to interleaving gain comes from MIMO flat fading channel. Moreover we constructed an iterative equalizer for MIMO frequency selective channel. The next generation mobile system developers appealingly call for proper space-time diversity receiver techniques and our analytical and simulation results seriously contribute on the way to real system implementation.

References:

- [1] TELATAR, E.: *Capacity of Multi-antenna Gaussian Channel* AT&T-Bell Labs Internal Tech. Report, June 1995
- [2] CHUGG, K. – ANASTASOPOULOS, A. – CHEN, X: *Iterative Detection, Adaptability, Complexity Reduction and Applications* Kluwer Academic Publishers, 2001,
- [3] SÝKORA, J.: *Iterative Decoding Networks with Iteratively Data Eliminating SDD and EM Based Channel State Estimator* PIMRC, 2004
- [4] ANASTASOPOULOS, A., CHUGG, K.: *Adaptive Soft-Output Algorithms for Iterative Detection with Parametric Uncertainty* IEEE Trans. on Comm, Oct. 2001, pp. 1638–1649.

This research has been supported by CTU0410213.

Inovation of "Coupled Drives" Laboratory Model

Ing. F.Vaněk, Ing. J.Fuka

vanek@control.felk.cvut.cz

Departement of Control Engineering, Faculty of Electrical Engineering, Czech Technical University,
Technická 2, 166 27 Prague 6, Czech Republic

Department of control engineering provide education in the field of basic and advanced modeling and control of dynamic systems. During laboratory lessons, students use models of dynamic systems in the Laboratory of automatic control. In the case measurement and control of astatic systems, it is suitable just the model of coupled drives.

Construction of new coupled drives model can be divided into 7 part:

- mechanic construction
- drives
- power electronic
- manual control and indicators
- rotation and position measurement
- circuit for control of system dynamic
- PC interface

Mechanic construction

For the mechanic construction, cost-effective and flexible part from Item international company was selected. The basic chassis is built using 30mm profile (Profile 6 - standard). For the most of side panel, semi-transparent acrylat glass (plexi, Perspex 30% from AXOM s.r.o.) is used. The door is full transparent. The alluminium belt pulley is used (diameter 34mm). The length of toothed belt is 1050mm.

Drives

Based on a analysis, the Maxon DC-drives (Re-max series) was selected. Drives are attached to belt pulleys due to planetary gearheads GP22 (conversion ratio 4,4:1).

Power electronic

Based on a analysis a number of commercial power circuit (output power, dimension, price,...), it was decided, that the power electronic (power amplifier) is better not to buy as a full-block. The power electronic was built with IC TD340 (Linear technology, circuit for full H-bridge control). As a switching element, the power HEX-FET transistors IRF530 (International rectifier, 14A) was used.

Because TD340 need non-standard input signals (1,2V – 3.6V, rotation direction), voltage converter from +/-10V is added. This converter permits the precision calibration of power amplifier too.

The power supply is compound from two parts. The 1st is standard ATX PC-power supply (power 12V for drives, 5V), 2nd part is basic +/-15V DC power supply (operational amplifiers,...) with 7815/7915 IC. The ATX power supply was partially changed, modified ATX-power supply does not need starting impulse (PC starting button).

Manual control and indicators

For the model testing and measurement, the manual control block is needed. Two potentiometers was connected to circuit. The manual or external (PC) control can be switched by means of toggle switch on face-panel.

Rotation and position measurement

For the measurement of rotatin speed of belt pulley, the IRC sensors from Maxon is used.

Circuit for control of system dynamic

This circuit is not necessary for model operation. The model enables to change dynamic parameters of motors. This mean it is able to modify model parameters for different groups of students. The time constant of motor could by set in the range of 7ms (mechanical time constant) till 5s.

PC-interface

Coupled drives model is connected into PC through i/o card MF614 (Humusoft). This card work with:

- 2 IRC channels
- 2 analog input
- 2 analog output

The model of coupled drives enables to students to verify basic algorithm of dynamic system modeling, learn about disruptive effect of the real world to the basic law of control in real conditions. This new model is usable in many of our school subject. Contrary to commercially produced model, our model is not only cost-effective, but is usable in the wide range of situations.

Regrettably, schemas, block diagrams and photos are not allowed :-((

This research has been supported by čislo grant CTU04-18513 .

Robust Control and Reference Tracking for Nonlinear Uncertain Systems

B. Reháč, S. Čelíkovský

rehakb@control.felk.cvut.cz

ĚVUT FEL, Katedra řídicí techniky, Karlovo nám. 13., Praha 2

As already indicated, to solve the system of equations ($\text{\ref{Systemrovnic}}$) we aim to use methods for direct solution of this partial differential equation. Since we cannot find the exact solution in general we need to apply a numerical method. Since the system ($\text{\ref{Systemrovnic}}$) consists of two equations where one equation is differential and the second one is algebraic (and there are two unknown functions x , u) our computation consists of two steps - first we choose the control $u(v)$ and we solve the partial differential equation. Then we adjust the control u so that an error (defined below) is minimized. Then we repeat this procedure until a sufficiently precise approximation of the solution of the system is found.

A crucial point for solving the nonlinear output-tracking problem is to find the solution $x(v)$ of the system of equations called the regulator equation.

It is possible if and only if there exists a solution $x(v), u(v)$ of the system of the regulator equations. The manifold $(x(v), v)$ is the output zeroing manifold if $x(v)$ is the solution of the regulator equation. Then there exists a function c and a matrix L such that the control attains the form

$$u=L(x-x(v))+c(v).$$

As already indicated, to solve the system of regulator equations we aim to use methods for direct solution of this partial differential equation. Since we cannot find the exact solution in general we need to apply a numerical method. Since the system consists of two equations where one equation is differential and the second one is algebraic (and there are two unknown functions x , u) our computation consists of two steps - first we choose the control $u(v)$ and we solve the partial differential equation. Then we adjust the control u so that an error (defined below) is minimized. Then we repeat this procedure until a sufficiently precise approximation of the solution of the system is found.

The way how the system was obtained does not yield any boundary conditions since validity of this equations for each v is assumed. The only condition posed on the function x is $x(0)=0$. Nevertheless we cannot numerically solve the system on the whole space. Rather we have to restrict the solution on a bounded domain while we assume that all possible trajectories of the

exosystem lie in this domain. Further we are forced to introduce appropriate boundary conditions for the system. We propose to use the Dirichlet boundary conditions.

The values for the control u_0 are chosen so that a properly defined error functional is minimized. The adjusting procedure of the function u_0 is as follows. The values of this function at the points $V=(1/2i, 1/2j)$ with $i, j=-4, -3, -2, -1, 0, 1, 2, 3, 4$ such that V is in the domain introduced above. The values in other points of the domain are obtained by the spline interpolation. Hence adjusting the values at the points V lying outside the domain has a good sense as long as these values influence the solution on the domain through the interpolation. A modified direct search is applied for adjusting the design parameters.

This method was applied to an example from the references. However the limited space does not allow to describe the results in detail.

References:

- [1] HUANG, J.: *Asymptotic tracking of a nonminimum phase nonlinear system with nonhyperbolic zero dynamics* IEEE Trans. on AC, 2000, pp. 542-546.
- [2] HUANG, J.: *Output regulation of nonzero systems with nonlinear zero dynamics* IEEE Trans. on AC, 2003, pp. č. 1497-1500.
- [3] ISIDORI, A.: *Nonlinear Systems* Springer Verlag, , 1996,
- [4] ROOS, H.-G., STYNES, M., TOBISKA, L.: *Numerical methods for singularly perturbed differential equations. Convection-diffusion and flow problems* Springer Verlag, 1996

This research has been supported by the CTU grant No. 11-84151.

Multi-modal Modeling by Sketching

R. Ženka, P. Slavík

zenkar1@fel.cvut.cz

Department of Computer Science and Engineering, Faculty of Electrical Engineering,
Czech Technical University, Technická 2, 166 27 Prague 6, Czech Republic

The research of creating 3D models by means of computer graphics has inspired development of many very powerful modeling packages (Maya, 3D Studio Max, Lightwave). These packages allow experienced users to create very detailed and complicated 3D scenes. The power of the modeling tools unfortunately goes hand in hand with considerable complexity of the user interface, which renders the most sophisticated modeling packages unusable for a common, untrained user. The classical WIMP user interface is no longer useful, which leads to development of alternative means of user interaction, often referred to as Post-WIMP interfaces.

Sketch-based interfaces are recently being researched in order to simplify the modeling process. Modeling by sketching trades the precision and detail of common modeling techniques for the simplicity of user interface. A sketch-based interface resembles a blank piece of paper onto which the user sketches images. The sketches are being recognized and translated into 3D shapes in more or less intuitive manner. This approach allows even the users without any technical background to create simple 3D models by drawing them. Some of these interfaces [1] are even simple enough to be used by children after few minutes of explanation.

The main limiting factor of sketch-based modeling is the ambiguity of sketched input. Since each sketch can have multiple interpretations, the modeling system has to resolve these ambiguities. The modeling software either constrains the class of possible objects the user can create (for instance the software can be used only for modeling objects with sharp edges) or it constrains the way the user is allowed to sketch (for instance by prescribing specific gestures for drawing particular objects). In both cases, the software imposes certain limits to the actions of the user that stem from the ambiguous input.

In our work we disambiguate the user input by a multi-modal user interface [2] that performs concurrent speech and sketch recognition. As the users sketch, they describe the emerging design verbally. The modeling resembles explaining the design to another person. The software is capable of recognizing a set of keywords and phrases that serve as hints concerning the nature of the sketched object. This way the user has higher freedom while drawing and the sketch recognition is more robust.

It has been shown that “informal interfaces”, such as sketch-based ones, are better for rapid creating of concepts [3]. The imprecision of the input can actually be a benefit, since it frees the user from the urge to create precise and detailed model at times, when the precision is not required and achieving it would be even counter-productive. However, since the models entered by sketching are imprecise, they have to be rendered in a way, which does not emphasize the lack of precision.

Common rendering techniques are not suitable for displaying the models created by sketching. These techniques strive to present the model in high detail, which lets even small errors show. Instead we used methods of non-photorealistic rendering (NPR) that are able to present the model in sketchy manner that matches the quality of user input. The sketchiness of the rendering can be introduced by special modifications to the rendering pipeline and can be

implemented in hardware [4] using common graphics accelerators. Although the use of a special rendering technique might seem unnecessary in the context of creating a modeling tool, it turns out that proper rendering can lead to higher user satisfaction and even faster modeling.

As a test of our approach, we developed an application that lets the user place various pre-defined objects from a database into the 3D scene by sketching the rough shape of the object and speaking its name. Such application can be used for instance for rapid office furnishing, where there is only a limited set of furniture that can be placed into the scene. We use geometrical constraints for positioning the objects in 3D, for instance in the case of an office the objects have to stand on the ground or be placed atop other objects.

We allow simple rendering of non-photorealistic panoramic images of the created scenes, that can be easily shared on the web with users that are not familiar with VRML or other 3D formats. Moreover, by using the panoramic images the model can be delivered in non-photorealistic format, which would otherwise require specialized software. The panoramas can even be used for simple annotation (either on a computer or after being printed out), which enables collaboration between users in a very simple manner.

We have proven the multi-modal interface to be useful for creating of simple 3D scenes. The sketches allow the user to place the objects directly at the desired location in the scene, while the spoken input raises the robustness of the sketch recognition dramatically. The interface also allows recording of the entire process of creation including the speech. The recording can be replayed, or used as automatic annotation of the model. It is possible to replay the spoken words that were uttered during creation of various model parts simply by clicking them. This way the user can store a lot of additional information without a need to type it explicitly.

We used a TabletPC platform for the implementation. This platform was very natural to use for our project, since TabletPCs provide necessary hardware and software libraries that allow them serve as “smart paper” that can be directly sketched on. We take advantage of the built-in libraries for sketch capturing and handling as well as of Microsoft Speech API for speech recognition. Since we rely on TabletPC-specific library for sketch rendering, small modification is necessary to run the software on a common PC equipped with a tablet.

References:

- [1] T. IGARASHI, S. MATSUOKA, H. TANAKA: *Teddy: a sketching interface for 3D freeform design* Proc. of the 26th annual conference on Computer graphics and interactive techniques , 1995, pp. 409–416.
- [2] S. OVIATT, A. DE ANGELI, K. KUHN: *Integration and synchronization of input modes during multimodal human-computer interaction* Proc. of the workshop "Referring Phenomena in a Multimedia Context and their Computational Treatment", ACL/EACL'97, 1997, pp. 1–13.
- [3] B. P. BAILEY, J.KONSTAN: *Are informal tools better?: comparing DEMAIS, pencil and paper, and authorware for early multimedia design* Proc. of the conference on Human factors in computing systems 2003 pp. 313–320
- [4] M. MCGUIRE, J. HUGHES: *Hardware-determined feature edges* Proc. of the 3rd international symposium on Non-photorealistic animation and rendering 2004 pp. 35–147

This research has been supported by Microsoft Research and by CTU grant 13089D/04/A .

Sensitivity Analysis of Inverse Kinematics Problem Solved by Extended Jacobian Inversion Method

M. Šoch, R. Lórencz

sochm@fel.cvut.cz, lorencz@fel.cvut.cz

Department of Computer Science, Faculty of Electrical Engineering, Czech Technical University, Karlovo nám. 13, 121 35 Prague 2, Czech Republic

There are two main approaches when animating articulated structures, e.g. human bodies, etc. Forward kinematics and Inverse kinematics [1]. Inverse kinematics is more natural method for use in field of animating articulated structures. This is due to the fact that the end-effector (end point of the structure) is the only part being taken into the account. The rest of the structure is controlled by the system itself. There is no influence from the side of animator to control inner parts of the structure.

Several techniques have been developed to solve Inverse kinematics – Jacobian inversion, Jacobian transposition, CCD (Cyclic Coordinate Descent) and others [1], [2].

We have focused on Jacobian inversion method due to its mathematical simplicity and purity. The system is described by set of non-linear equations. It is possible to simplify it into one vector equation

$$\overset{p}{k} = \overset{p}{f}(\overset{p}{q}), \quad (1)$$

where $\overset{p}{q}$ is the status vector of the system (angles between neighboring segments) and $\overset{p}{k}$ is position of the end-effector. But (1) describes Forward kinematics however. For Inverse kinematics it is necessary to have inverse form of (1). It usually leads to more than one solution. Hence the differentiating is applied to obtain equation for solving Inverse kinematics

$$d\overset{p}{q} = \mathbf{J}^{-1}(\overset{p}{q}) \cdot d\overset{p}{k}, \quad (2)$$

where $J_{ij}(\overset{p}{q}) = \frac{\partial f_i(\overset{p}{q})}{\partial q_j}$ is matrix called Jacobian ($\mathbf{J}^{-1}(\overset{p}{q})$ is inversion matrix related to $\mathbf{J}(\overset{p}{q})$).

The major problem of (2) is finding inversion of $\mathbf{J}(\overset{p}{q})$ which is usually non-square matrix. Some Generalized inversion method can be used in this case, for instance inversion based on Singular Value Decomposition. But there are problems with numerical stability. Next, there is still no control of inner parts of the structure however. Thus we decided to extend the Jacobian. First, to omit using of generalized inversion and next to be able to control all the structure [4].

Problems and Potential Solution

We have received one major problem with proposed solution. We were unable of exact control of the structure. We were not capable to solve this problem analytically thus we decided to use Sensitivity analysis [3] to determine the dependencies in the whole system. Sensitivity analysis helps to determine changes of the system regarding the changes of the system parameters.

In case of Inverse kinematics independent parameters are represented by position vector $\overset{p}{k}$ and observed parameters are represented by status vector $\overset{p}{q}$. Sensitivity function is defined as

$$\mathbf{S} = \left. \frac{\partial \overset{p}{g}_i(\overset{p}{k})}{\partial \overset{p}{k}} \right|_{\overset{p}{k}_0} \quad \text{or} \quad S_{ij} = \left. \frac{\partial g_i(\overset{p}{k})}{\partial x_j} \right|_{\overset{p}{k}_0}. \quad (3)$$

The function $\overset{P}{g}(\overset{K}{x})$ in (3) is inverse function to function $\overset{P}{f}(\overset{P}{q})$ in (1). Find this inverse function is impossible in case of vector $\overset{K}{x}$ describing just position of end-effector. However function $\overset{P}{g}(\overset{K}{x})$ can be found according to construction of vector $\overset{K}{x}$ as described in [4]. The structure is treated by $N-1$ independent pairs and main link – origin to end-effector. Each pair consists of two neighboring segments.

When finding function $\overset{P}{g}(\overset{K}{x}) = \overset{P}{f}^{-1}(\overset{P}{x})$ it is appropriate to start from the first pair. It implies at most two solutions according to $\overset{P}{l}_{01}$. Using the third segment l_2 and the second pair $\overset{P}{l}_{12}$ there will be still at most two solutions for three segments now. The preceding algorithm is applied to all the structure and at the end there will be still at most two solutions. In the case that there are still two solutions the final decision will be given by main link – origin to end-effector. With the algorithm stated above it is possible to find analytical expression of status vector $\overset{P}{q} = \overset{P}{f}(\overset{K}{x})$ for $N \geq 3$.

Knowing the analytical form of $\overset{P}{q} = \overset{P}{f}(\overset{K}{x})$ then the sensitivity function can be also expressed analytically and computed easily for each parameter of vector $\overset{K}{x} = [\overset{P}{l}_1, \overset{P}{l}_{01}, \overset{P}{l}_{12}, \overset{P}{K}, \overset{P}{l}_{N-2, N-1}]$ where each parameter $\overset{P}{l}_{ij}$ represent paired parameter consisting of two components $\overset{P}{l}_{ij} = [x_{ij}, y_{ij}]$.

Having the knowledge of the sensitivity of the system to the particular parameters it is possible to control all the structure and reach desired movement of all parts instead of controlling only end-effector. Controlling of inner parts includes also imposing constraints to the joints for example based on physical principles, etc.

References:

- [1] WATT, A. – WATT, M.: *Advanced animation and rendering techniques*. Addison-Wesley, 1992.
- [2] PAUL, R. P.: *Robot manipulators: Mathematics, programming and control*. MIT press, Cambridge, MA, 1981.
- [3] FRANK, P.M.: *Introduction to System Sensitivity Theory*. Academic Press, 1975.
- [4] ŠOCH, M. – LÓRENCZ, R.: *Solving Inverse Kinematics – Jacobian Inversion Method in a Plane*. In Proceedings of 11th International Workshop on Systems, Signals, Image Processing and Ambient multimedia, Poznań: PTETiS, 2004, pp. 95-97.

Course on Dynamics of Multidisciplinary and Controlled Systems in a Virtual Lab

Heřman Mann

mann@vc.cvut.cz

Computing and Information Centre, Czech Technical University,
Zikova 4, 166 35 Prague 6, Czech Republic

The course aiming at motivating young people to engineering study, and at improving engineering training using innovative didactic and technological approaches has been developed. The resulting web-based training modules are supported across the Internet by tools like a robust simulation engine, publishing and monitoring system, and an environment for virtual experiments. The international consortium participating in the development consisted of the Czech Technical University in Prague (Coordinator), Ruhr-Universität, Bochum, Fraunhofer Institute for Integrated Circuits, Dresden, Tallaght Institute of Technology, Dublin, University of Sussex, Brighton. The course is freely available at <http://virtual.cvut.cz/dynlab/course/>

The emphasis and style of the course differs from most of the existing courses on engineering dynamics and control by

- exposing learners to a novel systematic and efficient methodology for realistic modeling of multidisciplinary system dynamics applicable to electrical, magnetic, thermal, fluid, acoustic and mechanical dynamic effects in a unified way
- introducing learners to the methodology through simple, yet practical, examples to stimulate their interest in engineering before exposing them to rigor math
- giving learners a 'better feel' for the topic by problem graphical visualization and interactive virtual experiments
- allowing different target groups to select individual paths through the course tailor-made to their actual needs and respecting their background
- allowing both for self-study and remote tutoring combined with investigative and collaborative modes of learning
- integrating computers into the course curriculum consistently and giving learners a hands-on opportunity to acquire the necessary skills
- exploiting the computers not only for equation solving, but also for their formulation minimizing thus the learners' distraction from their study objectives
- giving learners the opportunity to benefit from the 'organizational learning', i.e. from utilizing knowledge recorded during previous problem solving both in academia and industry

The main target groups of the course are

- distance-education students at different levels of vocational study and training
- students wishing to complement the traditional face-to-face courses
- practicing engineers in the context of their continuing education or lifelong learning
- teachers intending to innovate the courses on dynamics and control they teach

Learning modes in the course:

Learning objective	Prerequisites	Course assignment	
		Given	Task
stirring up interest in dynamics	high-school math and physics	3D virtual model of a real system	to modify system parameters and excitation to observe changes in its dynamic behavior
introduction to dynamic modeling	high-school math and physics	configuration of a real system	to set up the corresponding multipole diagram and to simulate its behavior
more advanced dynamic modeling	fundamentals of system dynamics	configuration of a real system	to set up the multipole diagram from custom-made submodels and to simulate its behaviour
formulation of system equations	introduction to dynamic modeling	configuration of a real system	to form corresponding equations and to solve them, to set up the multipole diagram, and to compare the solution with simulation results
introduction to control design	formulation of system equations	model of a plant & control objectives	to reduce the model, to design control, and to verify it using the plant unreduced model
introduction to system design	introduction to control design	system specification	to design system configuration and to optimize its parameters

References:

- [1] MANN, H. – ŠEVČENKO, M. : *Course on dynamics of multidisciplinary controlled systems in a virtual lab*. Proc. 6th IFAC Symposium on Advances in Control Education, Oulu, 2003, pp. 161-166.
- [2] MANN, H. – ŠEVČENKO, M. : *Multipole diagrams for efficient design of mechatronic systems*. Proc. Int. Conf. on Mechatronics, Loughborough University, 2003, pp. 41-46.
- [3] MANN, H. – ŠEVČENKO, M. : *Simulation and Virtual Lab Experiments across the Internet*. Int. Conf. on Engineering Education, Valencia, 2003.
- [4] MANN, H. – ŠEVČENKO, M. : *Innovative didactic concepts and tools for system dynamics and control*. Int. Conf. on Engineering Education, Valencia, 2003.
- [5] MANN, H. et al: *eMerge – An European education network for dissemination of online laboratory experiments*. Int. Conf. on Engineering Education, Valencia, 2003, Poster.
- [6] MANN, H. – ŠEVČENKO, M. : *Internet-based design, learning and collaboration environment for Mechatronics*. Proc. Int. Workshop on Research and Education in Mechatronics, University of Applied Sciences, Bochum, 2003, pp. 189-196.
- [7] MANN, H. – ŠEVČENKO, M. : *Internet-based collaboration and learning environment for efficient simulation or control design*. ASME Int. Mechanical Engineering Congress and R&D Expo, Washington, 2003.
- [8] MANN, H.: *Unified engineering dynamics on the Web*. Proc. CALIE04 – Computer Aided Learning in Engineering Education. Grenoble, 2004, pp. 63-74.
- [9] MANN, H.: *Efficient Modeling and Simulation of Multidisciplinary Systems across the Internet*. CACSD 2004 - IEEE International Symposium on Computer Aided Control Systems Design, Taipei, Taiwan, 2004, Tutorial.
- [10] MANN, H.: *Web-based course on dynamics of multidisciplinary controlled Systems*. Proc. MechRob – Mechatronics & Robotics, Aachen, 2004.

This research has been supported by grants: Leonardo da Vinci CZ/02/B/F/PP/134001, Socrates Minerva 100671-CP-1-2002-1-FR-MINERVA, and FRVŠ 2115/2004.

Graphical User Interface for Robust Control

Petr Urban

urbanp1@control.felk.cvut.cz

Department of Control Engineering
Czech Technical University in Prague
Charles square 13
121 35 Prague, Czech Republic

Robust control theory has certain tools for design of robust controller intended for control of systems with uncertain parameters. Design of static output feedback simultaneous stabilization of scalar plants with uncertain parameters is interesting problem. In these cases when it goes about only one parameter, the results are available now in [2], [3], [4]. For instance, it is possible to compute the stability interval, i.e. an interval of values of the uncertain parameter (gain of the static output feedback) for which the system is stable.

In the case of more than one uncertain parameter, the situation is a lot more difficult from the theoretical point of view. Nonetheless, in a two or three-parameter case it is possible to take advantage of some graphical routines available in common CACSD packages and the possible result is the (2D) or (3D) picture. More n-dimensional picture isn't good from practical aspect, i.e. comprehensive, visual orientation.

In case of control loop analysis can finding parameters represents i.e. uncertain parameters of closed loop characteristic polynomial $p(s,q,r) = a_0(q,r) + a_1(q,r)s + \dots + a_i(q,r)s^i$, $i = 1, \dots, N$, denote the closed loop characteristic polynomial of degree N where $a_i(q,r)s^i$ are scalar multivariate polynomials with uncertain parameters q, r . Our objective is to find a region for parameters q, r for which the closed loop characteristic polynomial is stable. This is the first problem that we have solved in the first part of this work. The next problem can be problem when we would like to find parameters of PI, PD and PID (or in discrete-time case PS, PD and PSD) controllers. This was the main solution of our work. At this point when it goes about design of control loop (controller) can finding parameters q, r represents i.e. individual gain of classical dynamic controllers - PI, PD, PID (PS, PD, PSD) consequently K_i, K_d, K_p or K, T_i, T_d . The question is: "How we can find these parameters for which will be the control loop stable?".

This can be solved in continuous-time case using the Hermite polynomial stability criterion and using the Schur-Cohn-Fujiwara polynomial stability criterion: Hermite stability criterion say, that the polynomial $p(s)$ is stable if and only if the symmetric Hermite matrix H defined in [1] is positive definite and Schur-Cohn-Fujiwara stability criterion say, that the polynomial $a(z)$ is stable if and only if the symmetric Schur-Cohn matrix S defined in [1] is positive definite.

In the first step we must compute the closed-loop characteristic polynomial for designed controller. In the next step we compute the Hermite (or Schur-Cohn) stability matrix for obtained closed-loop polynomial (it depend on the degree of the polynomial). After this we substitute the coefficients of the closed-loop polynomial to the stability matrix and compute the determinant of the stability matrix and its subdeterminants. From this procedure we obtain matrices in which "1" represents that for this value is the determinant (or subdeterminant) positive and "0" represents that for this value is the determinant (or subdeterminant) negative. Now we use these matrices to draw areas of parameters. For this we have used standard Matlab routines, see Matlab. We obtain 2-dimensional pictures. Last

operation is drawing the boundary curves. These curves we obtain from decomposition of the stability matrix determinant. Result from this procedure is the set of controllers that are stabilizing the plant.

Second part of our work consists from building graphical user interface for this solution. Input of our interface is the plant which is set with external description - transfer function (the face is the same like in Polynomial Toolbox). Plant can be in continuous-time case using operator "s" or "p" and in discrete-time case using parameter "z". Output of our interface is the area of uncertain parameters of designed controller for which is the closed-loop stable (all controllers which stabilize the plant). For continuous-time plant it is possible to find all continuous-time PI, PD and PID controllers and for discrete-time plant all PS, PD and PSD controllers. The GUI-Graphical User Interface is designed and created using Matlab Graphical User Interface Builder see [3] and Polynomial Toolbox see [4]. User can choose from nine types of controllers, six types of continuous-time controllers and three types of discrete-time controllers.

The graphical user interface allows user to communicate with Matlab: import plant data from Matlab Workspace and export designed controller data to Matlab Workspace. They have been created tools for viewing roots of the closed-loop polynomial and for computing the sensitivity and complementary sensitivity functions and its bode diagrams. Also is possible to export all computed and used data to file (*.m or *.txt). Single part of the graphical user interface is the stand-alone application. This application has been compiled using Matlab Compiler and it allows to run this graphical user interface in every computer where the user have not the Matlab. To run this application on random computer demands install the MATLAB Component Runtime library utility in executable file MCRInstaller.exe. This library is available in every Matlab installation and must be distributed with this version of our graphical user interface.

At this time there are some extensions for this problem solution: the first is implementation of optimization criteria; next is possibility to modify the stability area using some transformation; last possible extension is extension to more uncertain parameters, but there are problems with drawing the stability area (in 3-dimensional pictures it is always possible, but when parameters are four or more then it is not good possible to draw this areas) we must draw cuts.

References:

- [1] BARNETT, S.: *Polynomial and Linear Control Systems* Marcel Dekker, Inc. 1983 pp. č. strany-č. strany.
- [2] KUČERA, V. – HENRION, D. - ŠEBEK, M.: *An algorithm for static output feedback simultaneous stabilization of scalar plants* Proceedings of the World Congress on Automatic Control, IFAC, Barcelona, Spain, July 2002
- [3] THE MATHWORKS *Creating Graphical User Interface* The Mathworks, Inc. <http://www.mathworks.com/access/helpdesk/help/techdoc/creating_guis/creating_guis.s.html> July 2002
- [4] POLYX, LDT.: *Polynomial Toolbox 3.0 (prelease)* Polyx, Ltd. <<http://www.polyx.com>> 2004

This research has been supported by CTU 0408713.

Data Source Aggregation in Semantic Web

M. Švihla, I. Jelínek

svihlml@fel.cvut.cz

Department of Computer Science and Engineering,
Faculty of Electrical Engineering, Czech Technical University,
Karlovo náměstí 13, 121 35 Praha 2, Czech republic

The semantic web is an extension of the current web, in which information is given well-defined, computer understandable meaning. This concept enables an automatic processing of web resources by search engines, software agents or computer applications. This is possible due to metadata that describes various web resources in the way the computers can 'understand' the meaning of an information. Basic technologies of the semantic web are RDF, the language capable express knowledges, and ontologies, formal descriptions of terms, relations and rules used in the metadata. Since the fundamental standards for the semantic web are already finished [3], the research in this area is focused on extending of the current web by semantic web concepts.

One long-term vision of the semantic web is making the web a global universal medium of a data exchange. The current web data formats such as HTML or PDF are not able to represent information in a transparent way. Even if two web resources describe one particular object, the information cannot be merged automatically. The human user can read these two pages and merge information in his brain, but this cannot be done by machines to create one knowledge of those two. However, this would be possible if the information were described also by semantic web metadata. Then the information can be automatically aggregated, stored and processed.

We discuss a problem of a web resources aggregation in this paper. There are usually various information sources dedicated to one knowledge domain on the web. For example, information about movies and cinemas in specific area can be published on information portals, online magazines, blogs, wikis or web databases. These resources are usually presented in traditional web formats. The information aggregation can be then divided into the two main problems. The first task is to create semantic web metadata that extend the current resources. The second problem is how these metadata can be aggregated and processed in order to create a complex information service for human users.

Our previous work [1] was focused on the former issue. We designed and implemented tool that can semantically enrich dynamic web pages generated from a relational database. The system was designed to be simple and flexible, so it can be easy to make it part of an existing web application. If various web sites from one knowledge domain adopted this system and made agreement on one ontology, they would be able to publish RDF metadata that has the same vocabulary. That means those metadata would create a transparent and public information representation, which can be used by any interested part on the web.

Of course these knowledges can be also aggregated and merged in order to create one centralized knowledge base over the particular information domain. This issue is our current interest. We are designing the semantic web portal [2] that would be able to harvest, merge, process and publish information in one particular knowledge domain. The first step of this process is a search for interesting pieces of information on the web. Then RDF metadata are downloaded by some robot, preprocessed and stored in a knowledge base. This knowledge base can contain information about one object that come from different web resources, but this data are merged so they are compact knowledges. Content of this knowledge base can be

again published as RDF metadata, or it can be datasource for web portal that serves various advanced features for human users, e.g. semantic search.

Our work covers both parts of the information workflow on the semantic web - the generating and the processing of metadata. This complex research serves many challenges. Until now we have designed and implemented the system that can generate RDF metadata to extend dynamic web pages. Currently we are designing the model of aggregation system and we plan its implementation in the near future.

The complex system would enable data exchange in one particular knowledge domain, which is a step to more global vision of semantic web as a universal and transparent data medium.

References:

- [1] SVIHLA, M. – JELINEK, J.: *Two Layer Mapping from Database to RDF*, Proceedings of Electronic Computers and Informatics (ECI) 2004, Kosice, Slovakia, 2004.
- [2] LARA, R.: *An Evaluation of Semantic Web Portals*, IADIS International Conference on Applied Computing 2004, Spain, 2004.
- [3] W3C: *The Semantic Web Activity*, <http://www.w3.org/2001/sw/>, 2005.

This work is part of the semantic web research in Webing research group at Department of Computer Science and Engineering at FEE CTU Prague.

TEMCON - Transmission Electron Microscope Control

Ing. Zdeněk Hurák, PhD., Ing. Martin Hromčík

`z.hurak@c-a-k.cz`

Department of Control Engineering and Center for Applied Cybernetics, Faculty of Electrical Engineering, Czech Technical University, Karlovo náměstí 13/E, 12135, Praha 2.

Motivation for the project

The objective of the TEMCON (Transmission Electron Microscope CONtrol) project was to initiate a new interdisciplinary applied research direction at Czech Technical University in Prague. This new highly attractive research area lies at the intersection of automatic control, electronics and physics. The motivation for this was bringing advanced know-how from the field of automatic control to the application domain of electron microscopy.

The proposers of the project have succeeded in developing a good contact with a Czech hi-tech company developing and producing innovative low-voltage transmission electron microscopes – Delong Instruments, Inc., Brno <<http://www.dicomps.com/>>.

Objectives of the project

1. equip the laboratory with necessary devices
2. in discussions with the industrial partner, determine the concrete technical problems of common interest
3. formulate two doctoral projects and get students for it
4. prepare materials for a big joint project (either with GACR or MPO CR) from which the doctoral students could be payed and a laboratory laser interferometer could be bought.

Outputs from the first phase of the project

1. A mini-laboratory was set up at the corner of a room of the rather theoretical Division of Automatic Control CAK:
 - PC equipped with DAQ cards,
 - development HW-SW kits for 8-bit RISC microcontroller AVR and 32-bit digital signal processor TI C2000,
 - high-precision voltage source, function generator, digital oscilloscope, multimeter,
 - precise electric drill, professional toolset for electricians, gripper,
 - license of a software package Eagle for designing electrical circuits that allows use in projects,
 - specialized integrated circuits for driving piezos,
 - practical books on electronics and piezoelectrics,
 - membership in IEEE Ultrasonics, Ferroelectrics, and Frequency Control Society.
2. Prototype of a 3D piezoelectric nanopositioning stage based on stick-slip phenomenon was designed by the industrial partner and provided for free to the researchers at CAK to design control system for it. As an outcome of numerous technical discussions, the industrial partner equipped the stage with a 2D capacitive position sensor.
3. With the real positioning stage in the laboratory, several technical tasks were identified for the immediate future, mainly done in two doctoral projects that are beginning in march 2005:

- perform basic experimental identification of the positioning stage with a laser interferometer. From the rough model determine requirements on the driving and measuring electrical circuits, design and implement driving circuits for the 3D piezoelectric stick-slip actuator. In essence, it is a very fast high-voltage amplifier (up to 250V) for a capacitive load,
 - design and implement electronics for 2D capacitive sensor based on changing cross section of a moving flat electrode and a quadruple of fixed flat electrodes,
 - develop a mathematical model of the stage and verify with a more advanced experimental identification,
 - compute various controllers (PID, LQG, H_2 , H_∞ , l_1) for positioning in x-y plane and verify using simulation and laboratory experiments
4. long term technical tasks were discussed with the industrial partner
- with the automatic positioning in the horizontal x-y plane, plug also the vertical z-axis into the positioning feedback. However, the measured variable used here for the feedback will not be obtained from a position sensor but from the image processing unit. Therefore, the problems of determining defocusation in run-time will be studied. It is at this moment, that colleagues from Center for Machine Perception at CTU will be invited to participate.

The expected practical outcome of this joint research is a fully automatic electron microscope that moves the observed object to a desired position in horizontal plane fast and precisely and always keeps the image focused without assistance of the operator.

This research has been supported by CTU grant No. CTU0414913.

Section 4

**ELECTRICAL ENGINEERING
&
INSTRUMENTATION**

Calibration Procedure at Shanghai Satellite Laser Ranging Observatory

**P. Bendová, K. Hamal, I. Procházka, J. Blažej,
Yang Fumin*, Huang Peicheng*, Zhang Zhongping***

hamal@troja.fjfi.cvut.cz

Department of Physical Electronics, Faculty of Nuclear Sciences and Physical Engineering,
Czech Technical University, Břehová 7, 115 19 Prague 1, Czech Republic

* Shanghai Observatory, Chinese Academy of Sciences,
80 Nandan Road, Shanghai 200030, People Republic of China

The goal of the project is the Satellite Laser Ranging (SLR) with the operational range of 500 to 40 000 km. The applications of the results are in geophysics, space geodesy, ecology, climatology and other Earth sciences. The recent SLR systems achieve a single shot precision of several millimeters; the accuracy is on one centimeter level. The principal error contributor for the accuracy is the atmosphere and its refractive index. To determine the refractive index and its influence on the laser ranging accuracy, the two wavelengths approach has been proposed. The satellites will be ranged simultaneously on two different laser wavelengths, the analysis of the measured propagation time difference will enable to improve existing models of the refraction index profile.

The laser ranging experiment has been carried out at the satellite laser station in Shanghai, China in 2002-2004. The Shanghai Observatory has modified the tracking telescope and the laser transmitter. The Nd:YAG laser with the second harmonics generator and the Raman generator delivers several mJ of energy at the wavelengths 0.46, 0.532 and 0.68 μm in the pulses 25-35 picoseconds long. The experiments optimizing the Raman conversion have been carried out in the CTU Prague labs. The conversion efficiency, output energy and the far filed beam profile have been investigated and optimized for the SLR purposes [1]. The first satellite laser ranging results on two wavelengths have been completed in October 2003 [2], [3]. The results confirmed the concept of the system and the proper operation of its components.

Simultaneously, the new system calibration schemes, set-ups and procedures have been developed at CTU in Prague. These calibration procedures must ensure the system calibration stability and reproducibility on a picosecond level to enable the determination of the refraction index on the basis of the two wavelength SLR measurements. The calibration procedures are based on the Portable Calibration Standard device. To meet the current and the future requirements on the calibration standard, the existing device has been upgraded for the high repetition rate. The version PET2K has been completed in 2004. The new feature is the increase of the maximum repetition rate of laser ranging from the original value of 100 Hz up to 2 000 Hz. This upgrade required both entire hardware reconstruction and the control software package re-configuration, as well. The extensive software package for data acquisition, noise reduction data analysis, editing and fitting has been significantly reconstructed, debugged and tested on the simulated and real satellite laser ranging data.

The millimeter precision satellite laser ranging is based on the echo signal detector consisting of the solid state photon counter developed at the CTU in Prague. This unique solid state detector is capable to detect optical signals containing 1 – 1000 photons with the time resolution 5 – 20 picoseconds. The detector contains a built in compensation circuit, which eliminates the dependence of the detection delay within the dynamical range 1:1000. The new

technique for determination of the number of photon involved in the detection has been developed, tested and implemented. This technique is based on a measurement of the avalanche pulse risetime variations in the range 10-30 picoseconds. The new electronic circuits have been developed, tested and incorporated into the Portable Calibration Standard PET2k [4]. The possibility to determine the echo signal strength will improve the system stability and data productivity.

The SLR station timing system configuration has been tested for the Chinese tracking network. The timing based on a Stanford Research counter SR620, Hewlett Packard HP5370B counter, Riga event timer A031-ET and Shanghai Observatory LTT timer have been compared the PET2k. The timing resolution, linearity, temporal and temperature stability have been tested in a series of indoor and field tests at the facilities in Prague and Shanghai Observatory respectively. The performance of the PET timing system is superb in all the tested parameters, however, the system costs are not acceptable for the Chinese tracking network. The event timer A031-ET made by Riga University proved to be an acceptable compromise, its linearity, stability are comparable to the PET2k, the timing resolution is 12-15 ps in comparison to 3 ps of the PET2k. The A031-ET system would enable laser ranging with precision 4-5 mm rms while keeping the costs at acceptable level. The development stage of the LTT timing system constructed by the Shanghai Observatory has been found an attractive candidate for the near future projects. Once the timing linearity will be mapped and compensated, it will provide resolution 20-30 ps with multistop capability in a space qualified package.

The output of the project is the upgrade of the Satellite Laser Ranging Observatory of the Shanghai Observatory to the two wavelengths mode for the sub-centimeter ranging precision and accuracy.

References:

- [1] HAMAL, K. – PROCHÁZKA, I. – BLAŽEJ, J. – YANG FUMIN – JINGFU HU: *Multi-frequency Laser for Millimeter Satellite Ranging*, CTU Workshop 2003, CTU Prague, 2003, pp. 235-236.
- [2] ZHONGPING, Z. – FUMIN, Y. – HU, J. – WANZHEN, C. – JUPING, C. – RENDONG, L.: *Two-Wavelength Satellite Laser Ranging Experiment at Shanghai Observatory*, 14th International Laser Ranging Workshop, San Fernando, Spain, June 7-11, 2004, published in Boletín ROA No. 4/2004, Real Instituto Observatorio de la Armada, en San Fernando, ISSN 1131-5040, edited by J.M.Davila, 2004, [online] <http://www.roa.es/14workshop-laser/#Presentations>.
- [3] YANG FUMIN – JINGFU HU: *Multi-color Satellite Laser Ranging at Shanghai Observatory*, report Shanghai Observatory #35403, 2003.
- [4] PROCHÁZKA, I. – HAMAL, K.: *Signal Strength Monitor for C-SPAD Receiver*, 14th International Laser Ranging Workshop, San Fernando, Spain, June 7-11, 2004, published in Boletín ROA No. 4/2004, Real Instituto Observatorio de la Armada, en San Fernando, ISSN 1131-5040, edited by J.M.Davila, 2004, [online] <http://www.roa.es/14workshop-laser/#Presentations>.

This research has been supported by ME705.

Solid State Detector for Space Applications

I. Procházka, K. Hamal, J. Blažej

blazej@troja.fjfi.cvut.cz

Department of Physical Electronics, Faculty of Nuclear Sciences and Physical Engineering,
Czech Technical University, Břehová 7, 115 19 Prague 1, Czech Republic

We are reporting on the achievements of the project “Solid state photon counter for space applications”, which has been supported by the grant GACR 102/02/0122 in the period 2002-2004. The goal of the project is the development of the solid state photon counting detector for the space projects: time scales synchronization using laser light and in the laser altimeter for planetary exploration. The main goal was the development of detector version capable to operate in extreme temperature range, high radiation flux, and low dark count rate. Integral part of the detector is the active quenching and gating circuit, which will be tailored for the prepared projects, as well.

The photon counter is operating on the principle of the avalanche photodiode pulse biased above its break voltage. Its main features are: high timing resolution, high quantum efficiency and wavelength range in comparison to the photomultiplier. This photon counter has been adopted for satellite laser ranging, it is in use at numerous satellite laser ranging stations in Austria, United Kingdom, Germany, China, Japan, Australia, and France. The photon counter developed in our labs has several unique characteristics attractive for its space applications: small size and low mass, low sensitivity to cosmic radiation, low bias voltage, capability to operate in an extreme temperature range, operation without any analog signal processing. The deep space application of the photon counter has been proposed in 1990 for the Soviet/Russian projects Mars. The detector was a part of the compact laser altimeter onboard a balloon probe dedicated to Mars’s atmosphere studies. The research and development has been co-ordinate by the Space Research Institute, Moscow. In late nineties, our detector has been used as an echo signal detector in the Lidar for atmospheric studies on board of the NASA Mars Polar Lander 98.

In the last three years, the photon counting detector has been optimized for several space born applications [1]. We have acquired experimental data on atmospheric fluctuations measurements and their influence on laser ranging precision. The laser ranging chain based on solid state photon counting detector has been used. Three independent path configurations have been studied: 4.3-kilometer horizontal path, slant path at elevation 10–80 degrees and slant path from ground to space. The laser ranging has been performed using the satellite laser ranging system in Graz, Austria. The system precision is 6 picoseconds (single shot RMS) and the measurement repetition rate is 2 kHz. That enables us to monitor fast fluctuations with period of the order of milliseconds. The atmospheric seeing conditions have been measured simultaneously. We have identified and measured contribution of the atmospheric fluctuations to the ranging precision and time spectrum of these fluctuations for the first time [2].

For the laser ranging purposes, the new technique has been developed, which enables to determine the number of photons involved in a detection process. The technique is based on a fact, that the avalanche build up time reflects the number of photons triggering the avalanche. The software simulator of the avalanche buildup model has been developed and tuned along with the experimental technique [3]. For the proposed project of optical transponder for space navigation, the version of photon counting detector has been developed and optimized. The detector is capable of both gated and not gated operation with relatively high count rates. As a

part of an optical transponder it will enable to range on an interplanetary scale with decimeter accuracy [4]. The new application of our detector in space is the photon counting detector for the space segment of the T2L2 joint project of the Europe and China. The Time Transfer by Laser Light T2L2 project is dedicated for time scales synchronization by means of picosecond laser pulses. Study carried out in the OCA labs, Grasse, France, demonstrated, that our detector is the fastest detector available for this project. It permits to time tag the events with the precision 3-5 picoseconds. Early 2004 the radiation lifetime tests verified the excellent long term stability of the detector under high cosmic radiation dose. In contrast to the competitive photon counting detectors, our structure should be able to operate for more than 10 years in space condition without additional shielding. The detector chips and the active quenching and gating circuits have been tests together with the partner group in Shanghai, China.

The European Space Agency ESA prepares, among others, the Laser Altimeter for Planetary Exploration (LAPE). It will be a compact laser altimeter based on a photon counting principle. It should be capable to range the planet Mercury surface from the altitude 400-1400 km with one meter resolution. We have built a laboratory sample of the Technology Demonstrator of this altimeter, which is based on a diode pumped microlaser and a solid state photon counting detector. We have demonstrated the algorithms to extract the useful signal from the background noise and the decimeter ranging accuracy.

The project did enable future elaboration of the solid state photon counting technique at the University and permitted participation of the laboratory in a top-class international space project.

References:

- [1] PROCHÁZKA, I.: *Solid state photon counting for planetary altimetry, atmospheric Lidar and deep space navigation*, published in Tools and Technologies for Future Planetary Exploration, ESA Publication Division EPD, Special Publication SP-543, ISBN 92-9092-854-9, 2004, p. 27.
- [2] PROCHÁZKA, I. – HAMAL, K. – KRÁL, L.: *Atmospheric fluctuation induced laser ranging jitter*, the 11th International Symposium on Remote Sensing, Conference on Laser Radar Techniques, Canary Islands, Spain, SPIE 5575, September, 2004, p. 23.
- [3] BLAŽEJ, J. – PROCHÁZKA, I. – HAMAL, K.: *Avalanche photodiode based photon counter number resolving* the 10th International Symposium on Remote Sensing, Conference on Laser Radar Techniques, Barcelona, Spain, September 8-9, published in SPIE 5240-27, 2003 p. 101.
- [4] PROCHÁZKA, I. – HAMAL, K. – BLAŽEJ, J. – SOPKO, B.: *SPAD Detector Package for Space Born Applications* the 13th International Workshop on Laser Ranging, Washington DC, Nov. 7-11, 2002, [online] http://cddisa.gsfc.nasa.gov/lw13/lw_proceedings.html

This research has been supported by GA102/02/0122.

Improvement of Laboratory of Microprocessor Applications

J. Novák

`jnovak@fel.cvut.cz`

Department of Measurement, Faculty of Electrical Engineering, Czech Technical University, Technická 2, 166 27 Prague 6, Czech Republic

Nearly in all today electronic devices the microprocessors play an important role. It begins with simple detection of pressing the pushbuttons, cooperation on data acquisition or control process, continues with complex DSP algorithms and ends with status presentation and communication with the higher-level system. Each of these applications is relatively specific and requires special knowledge in both the hardware and software fields. The aim of the education in the Laboratory of Microprocessor Applications (below only Laboratory) is to focus on the use of theoretical knowledge and to acquaint students with practical limits of its implementation.

The education in the Laboratory is provided in several subjects, each of them is focused on particular area – basic microprocessor application in instrumentation, signal processing in instrumentation, advanced instrumentation applications and finally the application for data communications. Passing these subjects, student are able to design and develop standard instruments, intelligent sensors and actuators for fieldbus networks and similar devices, used in today control, measurement and data acquisition systems. Their new skills are later proved in solving the diploma thesis, which often includes the practical implementation of the developed approach.

Two years ago the status of laboratory equipment was unsatisfactory. Ten workplaces were equipped with diskless computers connected to LAN with local file server and an Internet access. All the laboratory instrumentation consisted of two analog/digital and three analog oscilloscopes, 1 old logic analyzer, 1 multimeter, 1 function generator and number of power supply sources (three level, regulated). Development tools available were focused on microprocessor family I8051 – a basic kit with 80C52 processor, EPROM with serial monitor and RAM for program download, and an enhanced kit with 80C537 processor, EPROM with serial monitor, RAM, LED display and 4 pushbuttons. The processor bus and additional ports are available to connect with solder less breadboard for further hardware development. For implementation of DSP algorithms several kits with Analog Devices' DSPs were available. The status of the software was poor as well. Three operating systems were available, MS DOS, Windows 3.11 and Windows 98, all from the network resources. For I8051 family the assembler and C compiler were available, as well as serial debugger, the same for DSPs. Basic software for CPLD design and programming was also available, as well as the MATLAB/Simulink environment for simulations. Nevertheless, the student projects solved in the laboratory included rather sophisticated instruments like digital oscilloscope, communication over GPIB bus or intelligent sensor for the CAN bus.

Above described situation together with fact, that students have been interested in subjects being taught in Laboratory, we decided to considerably improve the quality and number of instruments and development kits in laboratory, as well as the quality and sorts of available software equipment.

In the year 2003 the first phase of project started. We bought 4 combined DSO scopes/logic analyzers and 6 DPO scopes with high bandwidth and sampling rate to support

the high-speed digital design. We also bought 5 single channel arbitrary generators with software support for easy design of required test signals. The diskless workstations were extended with hard discs and operating system was installed locally. The number of development kits was increased so that each working group of students had its own within the whole semester. The OrCAD system was installed for all laboratory workplaces to allow schematic and PCB design for student projects. The same was done for the MaxPlus2 development environment that supports CPLD and FPGA design in VHDL. The communication environment was extended with PCI CAN cards with appropriate software, which can be used for tasks solving the implementation of CAN bus nodes.

In the year 2004 the project continued with the second phase. We purchased the TLA5203 logic analyzer with option for synchronization with the oscilloscope, 2 dual-channel arbitrary generators, 5 programmable power supplies and set of universal programmers. We also purchased 5 development kits with ARM7 TDMI core based processors and the JTAG debugger for ARM with the trace memory support. These kits are intended to replace the 80C537 kits in projects that require more powerful processor. LabWindows CVI was installed on laboratory workplaces to support the GPIB programming. The GPIB is implemented using USB ↔ GPIB converter. Available software was also extended with programming environment for universal programmers and development tools for ARM7 based kits.

The specialized kits were developed for rapid implementation of CAN, Measurement Bus, IEEE488 and USB communication interfaces, which are used in student projects. Also available is the newly developed FPGA kit, which features the local microprocessor, analog input and output (codec) for implementation of DSP algorithms, LED display and pushbuttons, PS/2 port, VGA output and 24 general purpose I/O pins. The basic library of IPs implements function modules for the peripherals mentioned above.

The Laboratory is now fully equipped for projects focused on hardware and software implementation of modern measurement instruments and intelligent sensors, including data communication in industrial distributed systems. It is used either in regular laboratory education, either for bachelor, diploma and doctoral thesis projects. For students it is accessible 10 hours per day, often including Saturdays and Sundays.

References:

- [1] P. KOCOUREK, J. NOVÁK: *Distributed System Set for Laboratory Education*, IMEKO TC-4 9th International Symposium on Measurement of Electrical Quantities, 1997, pp. 205-208.
- [2] P. KOCOUREK, J. NOVÁK: *Teaching of FPGA Applications in Instrumentation*, IMEKO TC-4 International Symposium on Electrical Measurement and Instrumentation, Proceedings Vol. 2, 2002, pp. 543-546.
- [3] J. NOVÁK, P. KOCOUREK: *FPGA Breadboard for the Rapid Hardware Development*, Proceedings of CTU Workshop, Vol. A, 2002, pp. 448-449.

This work has been supported by the FRVŠ project FRV 2001 A 2004.

The Application of Platinum Silicide in Power Semiconductor Devices

D. Kolesnikov, J. Vobecký

kolesd1@feld.cvut.cz

Dept. of Microelectronics, Faculty of Electrical Engineering, Czech Technical University
Technická 2, 166 27 Prague 6, Czech Republic

Novel device technologies are closely linked to the use of new materials. A good example is the replacement of the conventional aluminum interconnects in microprocessors by copper ones. This example is also followed in the field of power devices, where copper-based technology was recently successfully used to decrease the overall resistance of power MOSFETs in the ON-State regime [1].

The aim of this project is to find potential benefits of the copper-based contact technology in the field of high-power devices, like that of silicon diodes with maximal ON-State current exceeding 100A. For this purpose, the electrical parameters of diodes with new contact stacks were designed, characterized and compared with those of the traditional aluminum-based technology [2 - 4].

For experiment, the Al-Ti-Ni-Ag, Ti-Ni-Ag, PtSi, PtSi-Al, PtSi-AlCuSi, PtSi-TiW-AlCuSi, PtSi-TiW-Ni-Cu stacks were chosen as anode contact of the 2.5kV/100A high-power P-i-N diode. The starting material is 130 Ω .cm n-type float zone silicon cut in the <111> plane. The diode has 16 mm in diameter and about 370 μ m of thickness.

The Pt, AlCuSi, TiW, Cu and Ni contact layers were deposited in *r.f.* plasma deposition system from corresponding targets in ON-Semiconductor, Rožnov pod Radhoštěm and TTS, Prague. The thicknesses of deposited layers and the conditions of thermal processing were varied in order to find optimal electrical parameters. A special care was dedicated to the processing of PtSi layer that was found to have a dominant impact on the quality of contacts. The sintering of sputtered Pt anode layer (50, 100, 200 nm thick) was used to form the PtSi layer. The sintering was performed at optimal temperature of 450°C and sintering time was varied from 40 to 100 min. The diodes without PtSi buffer layer were processed as well. The aluminum cathode layer was evaporated and sintered in the standard way. The diodes with new contact stacks were compared with the reference one provided with two 10 μ m thick aluminum anode and cathode contact layers.

To characterize the contact structures the forward I-V curves of diodes were measured in four point arrangement at constant temperatures +30 - +125 °C under a constant contact loading of 300 ± 1 kg. Application of a pulse measurement principle ($t_{ON} = 150 \mu$ s, $f = 4$ Hz) was used to minimize the self heating effect. Forward voltage drop, differential resistance, serial resistance, crossing point current and their temperature dependencies were evaluated from the measured I-V curves.

The diode with PtSi anode contact with the smallest sputtered Pt thickness (50 nm) has been found to possess the lowest values of both forward voltage drop and differential resistance as well. Unfortunately, the mechanical stability of such contact is poor. At the same time, this contact cannot be used for soldering. This motivated us to add strain buffer layers made from aluminum (TiW-Al) and copper (TiW-Ni-Cu) including diffusion barriers based on TiW and TiW-Ni. The introduction of these layers led to the increase of the diode voltage

drop and series resistance, but the mechanical reliability of diode in press pack increased due to higher metal thickness.

Further evaluation has showed that in spite of two extra barriers between silicon and top metal, the diode with copper contacts possesses lower voltage drop and series resistance than that of aluminum contact owing to low barrier-metal resistances and nearly equal electrical conductivity of sputtered copper. Moreover, for the copper contact, the application of thin PtSi layer between silicon and TiW-Ni barrier layer was found absolutely necessary to achieve lower overall contact resistance compared to that of Al contacts and reproducible parameters at the same time. The best contact resistance was obtained for the contacts with the lowest thickness of copper. However, the contact systems of some high-power devices require also very good mechanical ruggedness for which a thicker strain buffer layer is needed to eliminate the roughness of lapped surface in order to meet the mechanical demands of press-pack housing. The lapping is beneficial for getting rid of the defects originating from high-temperature processing and cannot be avoided. To cope with this problem, additional etching step was added after diffusion of doping elements and a special set of samples was prepared to evaluate this provision. The effect of etching the lapped surface was found to have negligible effect on the electrical parameters, but the mechanical stability was improved on the level of thick aluminum layers even with thinner copper layers. As there was found a reserve in the quality of interface between the PtSi and buffer layer, further optimization of copper deposition conditions is necessary to fully utilize the beneficial features of this element.

Beside the effort to minimize the voltage drop, the thermal behavior was studied, namely the magnitude of current at which appears the crossing of cold and hot forward I-V curves. So far, the existence of this effect was attributed to bulk phenomena, namely the struggle between the increasing injection of anode p-n junction (decreasing barrier height) and decreasing carrier mobility with growing temperature, and the influence of contact was not taken into account. However, the measurements have shown that there is a significant influence of contact technology on the magnitude of the crossing point current. The evaluation enabled us to conclude that the negative temperature coefficient of thinner contacts (caused by the dominating thermal dependence of barrier height) can be compensated in thicker contacts by the positive temperature coefficient of metal electrical conductivity.

References:

- [1] J. COOK, M. AZAM, P. LEUNG, M. GRUPPEN: *Performance of vertical power devices with contact-level copper metallization*, Thin Solid Films, 1999, pp. 14–21.
- [2] D. KOLESNIKOV, J. VOBECKÝ: *The Analysis of Ohmic Contacts for High-Power Devices*, 7th International Seminar on Power Semiconductors, Prague, 2004, pp. 33–38.
- [3] D. KOLESNIKOV, J. VOBECKÝ: *Copper Versus Aluminum Contacts for Silicon Devices*, The Fifth International Conference on Advanced Semiconductor Devices and Microsystems, Smolenice Castle, Slovakia, 2004, pp. 175–178.
- [4] D. KOLESNIKOV, J. VOBECKÝ: *Advanced Contact Stacks for High-Power Devices*, 2nd Ukrainian Scientific Conference on Physics of Semiconductors, Yuriy Fedkovich Chernivtsi National University, Ukraine, 2004, pp. 92–93.

This research has been supported by číslo CTU0407613.

Ultrathin MOVPE Grown InAs Layers in GaAs Characterized by Photomodulated Reflectance Spectroscopy

P. Hazdra, J. Voves, E. Hulicius*, J. Pangrác*

hazdra@fel.cvut.cz

Department of Microelectronics, Faculty of Electrical Engineering, Czech Technical University in Prague, Technická 2, 166 27 Prague 6, Czech Republic

*Institute of Physics, Academy of Sciences

Cukrovarnická 10, 162 53 Prague 6, Czech Republic

Ultrathin (subnanometer) InAs layers in GaAs matrix reveal extremely high optical recombination efficiency which persists even at elevated temperatures. Embedding them into the AlGaAs/GaAs waveguide as a laser active region gives an opportunity to produce highly efficient and reliable near infrared lasers. We showed that lasers with different ultrathin InAs structures in AlGaAs/GaAs waveguide prepared by Metal-Organic Vapor Phase Epitaxy (MOVPE) can lasing at different wavelengths from 890 to 1100 nm with low threshold current density (up to 0.12 kA/cm²) and high quantum efficiency (up to 35 %) [1,2].

Control of the growth and further optimization of these ultrathin InAs layer structures necessitates application of adequate diagnostic techniques capable to characterize them quickly and accurately. Optical characterization methods offer fast, non-destructive and contactless option. The most popular technique, photoluminescence (PL), works best at low temperatures and yields mainly ground-state interband transitions. In-plane photocurrent (PC) measurement under different polarizations allows to separate optical transitions to light hole (lh) and heavy hole (hh) states [2]. Photomodulated reflectance (PR) spectroscopy [3] uses laser pump source to periodically perturb sample dielectric function. The alternating component of the sample reflectance, which is subsequently measured, exhibits sharp derivative-like spectral features in the region of interband transitions. As a result, PR provides equivalent energy resolution to that of PL at low temperatures and probes wider range of critical points, highlighting the ground-state and also many high-order interband optical transitions from which band structure can be deduced. For this reason, we focused in this stage of the project on development of the PR setup for characterization of MOVPE grown InAs δ -layer structures forming subnanometer single-quantum wells (SQW), double-quantum wells (DQW) and multi-quantum wells (MQW) in GaAs. Results of PR measurement were compared with PL and PC data and observed optical transitions were interpreted by simulation of electronic states in quantum wells using 1D Schrödinger numerical solver.

Ultrathin InAs structures in GaAs matrix were grown in an AIXTRON 200 MOVPE reactor on (100) oriented GaAs substrate using TMGa, TMIn and AsH₃ as precursors. Low growth temperature (500°C) in combination with low growth rate (below 0.1 nm/s) was used to ensure high layer quality. High V/III ratio (180) was used to limit quantum dot and other 3D objects formation. Different structures were grown to calibrate the growth and optimize optical properties: single InAs δ -layers (SQW) with variable thickness W_L , two coupled 0.45 nm InAs layers (DQW) separated by GaAs spacer with thickness S_L , and various types of MQW with different number of ultrathin layers, W_L , and S_L . Structures were covered by 42 nm thick GaAs cap.

Photomodulated reflectance was measured at room temperature using the standard set-up consisting of the tuneable monochromatic probe light source provided by a tungsten-halogen lamp and the JY640 0.64 m focal length single grating monochromator. The modulation light source made by an unfocussed 5 mW red HeNe laser mechanically chopped at 626 Hz. The reflected probe beam was measured by a cooled Ge detector protected from any scattered laserlight by a high pass filter. The weak electrical signal was recorded using standard lock-in technique. The photoluminescence and photocurrent experiment was performed using in principle the same apparatus. The Q-switched DPSS laser working at 532 nm was used as the excitation source for PL measurement and some spectra were recorded at 10 K using the Oxford Instruments CC1104 cryocooler.

All measured PR spectra showed strong resonances corresponding to the optical transitions in InAs/GaAs SQWs, DQWs, MQWs. The transition energies were obtained from fitting the PR data with the first derivatives of the Gaussian line shape. The strongest resonances arising at lowest energy were attributed to E1H1 transitions which were fundamental in all investigated structures and they were also detected by PL. Besides the E1H1 transitions, PR spectra showed E1L1 transitions – the lowest energy transitions for light holes, which were also resolved in some of the PC spectra, and series of transitions between excited states, e.g. E2H2, E2H1, etc. Some of these transitions, e.g. E1H2, are forbidden, but the built-in electric field in the structure makes them possible to be observed in PR measurement. The existence of built-in electric field was confirmed both by the presence of Franz-Keldysh oscillations in spectra above the GaAs resonance and the shift of the PC absorption edge for samples grown on the tellurium doped substrate. Identified transition energies were subsequently compared with simulation of the electronic states in particular InAs/GaAs structures. In this way, their electronic band structure and structural properties (layer thicknesses and compositions) were elucidated [4]. Results show that the room temperature photoreflectance measurement provides more detailed information compared to PL and PC spectroscopy. Received data can be readily used for control and optimization of the MOVPE growth of ultrathin InAs layers in GaAs.

References:

- [1] J. OSWALD, E. HULICIUS, J. PANGRÁC, K. MELICHAR, T. ŠIMEČEK, O. PETŘÍČEK, K. KULDOVÁ, P. HAZDRA, J. VOVES: *Lasers with δ -InAs layer in GaAs*, Material Science and Engineering B 88(2-3), 2002, pp. 312-316.
- [2] P. HAZDRA, J. VOVES, J. OSWALD, E. HULICIUS, J. PANGRÁC, T. ŠIMEČEK : *InAs δ -layer structures in GaAs grown by MOVPE and characterised by luminescence and photocurrent spectroscopy*, Journal of Crystal Growth, Vol. 248C, 2003, pp. 328-332.
- [3] J. MISIEWICZ, G. SEK, R. KUDRAWIEC, AND P. SITAREK *Photomodulated reflectance and transmittance: optical characterisation of novel semiconductor materials and device structures*, Thin Solid Films 450, 2004, pp. 14–22.
- [4] P. HAZDRA, J. VOVES, E. HULICIUS, J. PANGRÁC: *Optical characterization of MOVPE grown delta-InAs layers in GaAs*, physica status solidi (c), 2005, in print.

This research has been supported by the grant No. IAA1010318 of the Grant Agency of the Academy of Sciences of the Czech Republic and the Research Programme of the Czech Ministry of Education MSM6840770014.

Education of the Digital Signal Processing in Telecommunication Engineering

P. Zahradník

zahradni@fel.cvut.cz

Department of Telecommunication Engineering, Faculty of Electrical Engineering, Czech Technical University, Technická 2, 166 27 Prague 6, Czech Republic

The paper deals with the education of the subject “Digital Signal Processing in Telecommunication Engineering” at the Czech Technical University in Prague. The education of the digital signal processing was substantially updated. New syllabus of the subject is presented.

The practical training in the digital signal processing in the telecommunication engineering at the Czech Technical University in Prague was traditionally based mainly on Matlab experiments in the past. Only few seminars were devoted to the old Digital Signal Processor (DSP) TMS320C50. In order to cope with the advanced of the DSP technology, the syllabus of the subject was substantially changed. The practical training is based on the Very Long Instruction Word (VLIW) DSPs, both with the floating point (320C6711) and fix point (320C6416) arithmetic in form of commercial DSP Starter Kits (DSK) [1]. In order to make the training more efficient, special in house made daughter cards were designed and realized. The best students can design and realize their own special purpose hardware using our universal daughter cards.

Old Syllabus of the Lectures

- Analog and digital signals, conversion
- Integral transforms
- Implementation of transformation procedures
- Design of digital IIR filter
- Design of digital FIR filter
- Decimation and interpolation filters
- Noise properties, stability of digital filters
- Architectures of the digital signal processors
- Adaptive filtering
- Digitizing of speech
- Parametric coding
- Digitizing of broadcast related signals
- Digitizing of images and video signals

New Syllabus of the Lectures

- Analog and digital signals, conversion
- Integral transforms
- Implementation of transformation procedures
- Design of digital IIR filter
- Design of digital FIR filter
- Decimation and interpolation filters
- Digital Signal Processors, introduction, VLIW architecture
- Noise properties, stability of digital filters

DPS TMS320C6x, instruction set, architecture
Design of systems with DSP
Adaptive algorithms in telecommunication
Digitizing of speech, parametric coding
Digitizing of broadcast related signals, images and video signals
Digital image processing, compression

Old Syllabus of the Seminars

Program tools for the analysis and synthesis of discrete systems
Matlab basics
Integral transforms (DFT, FFT, DCT)
Analysis and synthesis of a digital IIR filters
Analysis and synthesis of a digital FIR filters
Decimation and interpolation filters, signal resampling
Development tools for the realization of digital systems using digital signal processors
Instruction sets of digital signal processors
Design and simulation of discrete systems
Realization of discrete system
Speech compression
Test
Evaluation of the properties of the discrete system

New Syllabus of the Seminars

Program tools for the analysis and synthesis of discrete systems
Matlab basics
Integral transforms, decimation, interpolation, resampling
Analysis and synthesis of digital IIR and FIR filters
DSP VLIW TMS320C6x
Development tools for DSP, Code composer studio, DSK 320C6711
Implementation of convolution and correlation on DSK TMS320C6711
Implementation of echo on DSK TMS320C6711
Implementation of FFT, DFT, DCT on DSK TMS320C6711.
Implementation of DTMF coding and decoding on DSK TMS320C6711
Implementation of echo cancelling on DSK TMS320C6711
Implementation of motion detection on DSK TMS320C6416
Implementation of image filtering on DSK TMS320C6416
Presentation of semester projects

References:

[1] WWW.TI.COM

This work has been supported by MŠMT grant No. FRVŠ F1-2023.

Digital Audio Signal Processing

F. Kadlec, L. Husník, Z. Bureš

kadlec@fel.cvut.cz

Department of Radioelectronics, Faculty of Electrical Engineering,
Czech Technical University, Technická 2, 166 27 Prague 6, Czech Republic

The project consisted of three main parts, entitled Digital Audio Signal Processing with Respect to Their Perception, Measurement and Analysis of Audio Systems Using MLS and Swept Signals, and finally Processing of Low Level Audio Signals Recorded in Noisy Environment.

In the first part of the project, multiple measuring signals were designed and generated in order to determine the quality loss induced by perceptual audio compression systems, e.g. MPEG or ATTRAC [1-4]. These consisted of combinations of sine waves and filtered random noise. Masking thresholds of human auditory system were taken into account, the levels of individual spectral components were carefully chosen. The effect of more or less severe reduction of bit rate of the measuring signals was explored, with emphasis on changes of resulting spectral shape. Distortions introduced by tandem coding were examined, using selected combinations of bit rates in the compression stages. Real low-level signals were also subject to digital processing, including spectral shaping of the error signal and dithering. Implementations of the former procedure took advantage of two different ways of noise shaping, one using a psychoacoustic filter in the feedback loop, the other using multiple feedback of the delayed output signal. Concerning the latter method, an adequate dither with desired properties was designed and applied. According to valid recommendations, subjective listening tests were performed to judge the quality of the processed signals, both compressed and noise-shaped. All the test signals were recorded on a CD and reproduced using professional electro-acoustic system in a listening room. At first, selected listeners were trained to be able to detect undesirable audio artifacts caused by compression. The most common distortions (i.e. aliasing, pre-echo, birdies, speech reverberation, collapse of the stereo image) were presented using numerous tutorial sound samples. Also, the reasons and mechanisms of generation of the coding artifacts were briefly discussed. The trained listeners subsequently participated in the listening tests. A suitable set of testing signals was prepared, containing excerpts from orchestral and organ music, drums, vocals, as well as from male speech and recitation. The effect of the bit rate reduction and noise shaping was assessed. Both from the spectral analysis and subjective listening tests, the bit rate of 128 kbps appears to be the threshold beyond which the distortions of the compressed signals are not apparent to majority of listeners. The listening tests also proved that the implemented noise shaping systems meet the initial requirements and can help to improve perception of digitally processed signals. The first noise shaping algorithm is especially suitable for use in combination with high sample rate, the second one can be advantageously utilized during the quantization process or word length truncation.

In the second part we started from the fact, that transfer functions of acoustical and electroacoustical systems may be established by classical methods using harmonic signals, or by impulse methods. Nevertheless, recent development in digital signal processing makes feasible the use of pseudorandom Maximum-Length Sequences signals. MLS signals are used to excite tested acoustical, electroacoustical or combined systems. The system response is recorded and digitally processed. The result describes the impulse response of the system

under test with its frequency response. These methods have good immunity against external noise ingress. Our work describes testing of combined systems, consisting of electroacoustic transducers and acoustical systems.

Digital signal processing makes it possible to use another efficient method, based on a sweeping frequency signal, for measurement of transfer properties of systems. The method is based on excitation of system by a logarithmically swept harmonic signal within the whole bandwidth of interest, together with recording of system's response to this signal. A so-called "inversion filter" can be derived from the driving signal. The filter is a signal having a reciprocal level of the driving signal's frequency spectrum. By convolution of a system's response with this inversion filter we can obtain an impulse response of the system under test. This method also enables analysis of non-linear distortion of tested electroacoustic systems. Our research deals with optimum design of driving signal, numeric calculation of system's impulse response, non-linear component analysis and immunity of this method against ambient noise of the location in which this measurement takes place. In our work we concentrated on confirmation of the feasibility and accuracy of analysis of created non-linear distortion. The modeling confirmed theoretical conclusions. Results obtained on system models confirmed theoretical assumptions [5].

In the third part of our project, processing of low level acoustic signals recorded in noisy environment was examined. First, signals produced by small species were recorded (here we used spiders of the Palpimanidae family), which were treated using MATLAB program package. The improvement of the signal-to-noise ratio was achieved, thus preparing the method for recording signals in natural environment of small animals [6,7].

References:

- [1] KADLEC, F.: *Optimization of Generated Audio Test Signals*. In: Proceedings of Forum Acusticum, 3th European Congress on Acoustics, Sevilla, Spain, 16-20 Sept., 2002, 6 p.
- [2] KADLEC, F.: *Psychoacoustic Processing of Test Signals*. In: The 146th Meeting of the Acoustical Society of America, 2003, Austin, Texas, Abstract.
- [3] DOBEŠ, J.: *An Accuracy Comparison of the Digital Filter Poles-Zeros Analysis with MATLAB and CIA Algorithms*. Radioengineering, Vol. 12, 2003, No. 4, pp. 1-5.
- [4] KADLEC, F.: *Signal processing from psychoacoustic point of view*. In: Proceedings of 18th International Congress on Acoustics ICA 2004, Kyoto, Japan, April 2004, 6 p.
- [5] KADLEC, F.- PORUBA, P.: *Measurement and analysis of acoustical and electro acoustical systems using swept signals*. In: Proceedings of Internoise 2004, The 33rd International Congress and Exposition on Noise Control Engineering, Prague, August 22-25, 2004, 6 p.
- [6] HUSNÍK, L. – PEKÁR, S.: *Snímání a analýza zvuků vydávaných pavouky rodu Palpimanus (Araneae: Palpimanidae)*. Akustické listy, Čs. akustická společnost, 2002, č. 4, s. 20-23.
- [7] KADLEC, F. - HUSNÍK, L. - PEKÁR, S.: *Zpracování slabých akustických signálů malých živočichů zaznamenaných v neoptimálních podmínkách*. In: MATLAB 2004, Kongresové centrum ČVUT, Praha, 4. 11. 2004, s. 208–213.

This research has been supported by GAČR 102/02/0156 "Digital Audio Signal Processing".

Radiation Defect Profiles Created by High Energy Protons and Alphas: Simulation of Their Influence on Silicon Power Diodes

V. Komarnitsky, P. Hazdra

komarv1@fel.cvut.cz

Department of Microelectronics, Faculty of Electrical Engineering,
Czech Technical University, Technická 2, 166 27 Prague 6, Czech Republic

New generation of silicon power devices is faced with increasing tasks regarding their switching speed performance. Advanced method of carrier lifetime control have to be used to speed-up device turn-off without substantial deterioration of ON-state losses. For this reason, traditional techniques of lifetime killing, like diffusion of noble metals, were replaced by irradiation with high energy particles. Irradiation with protons and alphas in combination with electron irradiation allows creation of nearly arbitrary carrier lifetime profile [1] and very good controllability and reproducibility of lifetime killing process. In this project, we focused on detailed characterization of radiation defects and their profiles resulting from proton and alpha-particle irradiation in the MeV range. Profile parameters and defect introduction rates were further used for simulation of irradiated structures using modern Technology Computer Aided Design (TCAD) tool to predict the effect of irradiation on device performance.

Radiation defects produced by high energy ions were investigated in the low-doped (phosphorous concentration below 10^{14} cm^{-3}) <100>-oriented FZ silicon substrate forming the n-base of 1.7kV/100A power planar p^+nn^+ chip diodes for power modules from ABB Switzerland Ltd., Semiconductors. The diodes were irradiated with 1.8, 2.8 and 3.6 MeV protons ($^1\text{H}^+$) and 3.6, 8, 12 and 14.5 MeV alphas ($^4\text{He}^{2+}$) using the 5 MeV tandem accelerator in FZ Rossendorf. The irradiation with low fluences ranging from 7×10^9 to $2 \times 10^{10} \text{ cm}^{-2}$ ($^1\text{H}^+$) and 1.4×10^9 to 1×10^{10} ($^4\text{He}^{2+}$) were used for defect characterization. Higher fluences of alphas (up to $5 \times 10^{11} \text{ cm}^{-2}$) were used to modify static and dynamic parameters of investigated diodes.

To fully characterize radiation defects, the following methods were used: the capacitance deep level transient spectroscopy (C-DLTS), I-V profiling, the high voltage current transient spectroscopy (HV-CTS), and C-V measurement.

C-DLTS spectra of proton irradiated samples revealed six electron traps and two holes traps while only three electron trap levels and one hole trap were detected in samples irradiated with helium [2]. The most prominent recombination levels were attributed to the acceptor level of vacancy-oxygen pair VO^{-0} at $E_c-0.167 \text{ eV}$ and the single acceptor level of divacancy V_2^{-0} at $E_c-0.436 \text{ eV}$. While the VO pair set the lifetime at high injection levels, the single acceptor level of divacancy is responsible for the carrier recombination at low injection levels and charge generation in depletion regime.

Profiles of dominant recombination levels measured by HV-CTS and C-DLTS were compared with primary vacancy distributions obtained from simulation using the Monte Carlo code SRIM2000. Results show that divacancy profiles, consisting of a sharp defect peak with a tail extending to the irradiated surface, follow in principle the simulated distributions. The peak depth R_D and its straggle ΔR_D were estimated both for helium and hydrogen irradiation. As we summarized in [3], SRIM simulation exhibited a good agreement with experiment concerning the divacancy peak depth while the measured straggle showed noticeable broadening. For protons and alphas the difference was in the range of 0.6-0.7 μm and 0.7-1.4

μm respectively. The introduction rates of particular defects, which were defined as a fraction of total number of produced defects to total amount of primary vacancies, were established for different ion energies. An example of data received from HVCTS measurement is shown in Table 1 where profile parameters of vacancy-related defects in silicon irradiated with 12 MeV alphas and 2.8 MeV protons are compared.

Table 1. Profile parameters and introduction rates for defects in silicon irradiated with 12 MeV alphas (left) and 2.8 MeV protons (right)

12 MeV He				2.8 MeV H			
Defect	$R_D/\Delta R_D$ [μm]	Introduction rate $\times 10^2$		Defect	$R_D/\Delta R_D$ [μm]	Introduction rate $\times 10^2$	
		Peak	Tail			Peak	Tail
VO^{-0}	91.6 / 1.88	2.9	2.4	VO^{-0}	84.7/2.45	1.6	1.3
V_2^{-0}	92.7 / 2.11	1.1	1.7	V_2^{-0}	84.5/2.98	0.90	1.1
Vacancy	91.9 / 0.98 (simulation)			Vacancy	81.7 / 2.14 (simulation)		

Simulation of unirradiated and irradiated diodes was performed using device simulator ATLAS from Silvaco Inc. The simulator possesses a model of thermal recombination/generation with full trap dynamics and arbitrary distribution of defect levels. Two dominant recombination levels, the acceptor level of vacancy-oxygen pair VO^{-0} and the single acceptor level of divacancy V_2^{-0} were used to simulate the effect of irradiation. The defects were characterized by their profiles, capture cross sections and bandgap positions [4]. To receive realistic magnitudes of defect capture cross sections, we have to extract them from room temperature I-V and Open Voltage Circuit Decay (OCVD) data since the magnitudes measured by DLTS are valid only at cryogenic temperatures. Simulated static and dynamic characteristics of irradiated devices showed a good agreement with experimental ones.

References:

- [1] P. HAZDRA, J. VOBECKÝ, H. DORSCHNER, K. BRAND: *Axial Lifetime Control in Silicon Power Diodes by Irradiation with Protons, Alphas, Low- And High-Energy Electrons*, Microelectronics Journal 35 (3) 2004, pp. 249-257.
- [2] P. HAZDRA, V. KOMARNITSKY, *Accurate Identification of Radiation Defect Profiles in Silicon after Irradiation with Protons and Alpha-Particles in the MeV Range*, Solid State Phenomena 95-96, 2004, pp. 387-392.
- [3] P. HAZDRA, V. KOMARNICKIJ, *Effect of proton and alpha irradiation on advanced silicon power devices: defect profiles and stability*, Proceedings of ASDAM'04, 2004, pp. 223-226.
- [4] V. KOMARNITSKY, P. HAZDRA, *Identification of Radiation Defect Profiles for Accurate Simulation of Power Devices Irradiated with Protons, Alphas and Low-Energy Electrons* Proceedings of ISPS'04, Prague 2004, pp. 177-182.

This research has been supported by the European Community - Access to Research Infrastructure Action of the Improving Human Potential Program project HPRI-1999-00039, the grant No. GAAV 102/03/0456 of the Grant Agency of the Czech Republic, and the MŠMT grant No. MSM 6840770014.

Optimal Control of Active Magnetic Bearing

L. Synek

synek1@fel.cvut.cz

Department of Electric Drives and Traction, Faculty of Electrical Engineering,
Czech Technical University, Technická 2, 166 27 Prague 6, Czech Republic

This paper proposes a method to estimate the position of suspended body that hovers due to the electromagnetic force. The position information of the suspended body can be extracted from the coil currents, which contain the high frequency components due to the injected high frequency voltage without any additional hardware. The most popular configuration applied is the "classical" one of gap sensor, current control, current-amplifier and magnetic coil. The novel method realizes stable and well damped levitation without any sensor hardware at the rotor. This is achieved by using the coil voltage of the magnetic bearing as system input (voltage instead of current amplifiers) and the current as system output. It is demonstrated that the resulting system is observable and controllable in the sense of control theory, allowing a magnetic bearing to be stabilized with a simple linear controller using current measurements alone. The problem is cast as a nonlinear regulation problem and an internal model-based regulator able to offset the noise in spite of the presence of unknown parameters affecting the model of the system is designed. The controller is designed using nested saturation functions and is able to provide a global region of attraction. The control of coil currents and the position of suspended body are performed with the digital controller using DSP.

Active magnetic bearings require some form of control, based on feedback of the position of the suspended object, to overcome open-loop instability and to achieve targeted system performance by modifying the bearing dynamics.

In many potential applications of magnetic bearings, the number of wires which must pass between the bearing controller and the components in the rotating machine needs to be minimized. Such a requirement may arise either from economic or reliability considerations. An exaggerated example of this is provided by the application of magnetic bearings to heart pumps where wires must either pass through the chest cavity (transcutaneous) or be inductively coupled to an external transmission/reception device. In either case, minimizing the wire count is a paramount design concern.

The wires feeding the electromagnets can, to some extent, be minimized by interconnection of the magnets. A more substantial reduction in wire count can be achieved by eliminating the discrete position sensing device and, instead, determining the position of the suspended object from information available in the electromagnet signals. Elimination of the discrete sensing device has such additional benefits as lowering the cost of the system and removing the potential failure of the sensing element, thus improving the reliability of the overall system. Other potential advantages include elimination of sensor-actuator noise and reduction in noise infiltration because the bearing switching signal is now information rather than noise (as it is when a discrete sensor is used). Magnetic bearings which estimate the position from the information available in the electromagnet signals are referred to as "self-sensing".

Previously, there have been two mainstream approaches for developing self-sensing magnetic bearings. One approach is to use a Luenberger observer designed from a linearized state-space representation of voltage-controlled magnetic bearings. Due to the nonlinearities

involved with the physics of the bearing, this approach has limited applicability. The other approach considers the air gap as a parameter of the system rather than a state. Previous attempts using parameter estimation were hampered by force feed-through (the infiltration of force information into the position estimates).

My idea is a nonlinear parameter estimation technique by which the position of a rotor supported in magnetic bearings may be deduced from the bearing current waveform. The bearing currents are presumed to be developed by a bi-state switching amplifier which produces a substantial high frequency switching ripple. The amplitude of this ripple is a function of power supply voltage, switching duty cycle, and bearing inductance. Inductance is predominantly a function of the bearing air gap or, equivalently, the rotor position, while the duty cycle is fundamentally dependent upon the developed bearing force. Ideally, the estimator should exactly extract rotor position information while perfectly rejecting bearing force information.

Before summarizing previous research on self-sensing magnetic bearings, it seems necessary to point out the fundamental drawback to any self-sensing approach. Capacity and thermal considerations usually lead to an actuator structure with magnetic paths whose reluctance substantially exceeds that of the air gaps at high frequencies (20 kHz or more). In contrast, high sensitivity and good rejection of magnetic nonlinearities are achieved in variable reluctance sensors by ensuring that the iron reluctance is on par with or substantially less than that of the air gaps. Thus, the overall sensing performance of a self-sensing magnetic bearing can be expected to be inferior to that of a discrete variable reluctance sensor when evaluated solely in terms of sensitivity, bandwidth, and linearity. In deciding whether such an approach is appropriate to a given application, the system-level advantages of self-sensing bearings must be weighed against expected performance shortcomings.

When the bearing is a perfect inductor, the aforementioned functional relationships are easily established and the gap dependence is monotonic. Since voltage and duty cycle are both easily measured, the relationships can be inverted with a non-linear parameter estimator to extract the rotor position. The estimator embeds a model of the bearing inductance parameterized by the air gap. This simulation is subject to the same switching voltage as the actual magnetic bearing coils. A feedback loop compares the simulated current waveform with the actual current and adjusts the gap length parameter until the two waveforms match.

One of the objectives of my dissertation research is to develop a mechanism that estimates the gap position by processing the current switching waveform. Other objectives are to identify no idealities that are normally neglected in modeling the magnetic bearing and to investigate the effects of these no idealities on the performance of the estimator.

References:

- [1] PAVELKA, J. – SYNEK, L.: *Design and Realization of Active Magnetic Combined Bearing* Workshop, 2003 pp. 790–791.

Control of Platinum Profiles in Silicon by Radiation Enhanced Diffusion

P. Hazdra, J. Vobecký

hazdra@fel.cvut.cz

Department of Microelectronics, Faculty of Electrical Engineering, Czech Technical University in Prague, Technická 2, 16627 Prague 6, Czech Republic

Modern silicon power electronics necessitates introduction of different profiles of defects acting as effective centers for recombination of excess charge carriers. Radiation defects produced by irradiation with high-energy protons, alphas and electrons are being now widely used for this purpose [1]. The advantage of irradiation technology is a high controllability, but electrical parameters of radiation defects are far from optimum. On the contrary, platinum atoms at substitutional position in silicon lattice (Pt_s) are ideal recombination centers, but the creation of an arbitrary platinum profile is difficult. The application of radiation damage to guide the in-diffusion of platinum atoms is one possibility to get an arbitrary profile of ideal recombination centers.

Recent investigation [2] showed that the high-energy implantation of helium atoms produces radiation damage which is optimum to guide the in-diffusion of platinum without negative side effects. We successfully used this technique in power diodes to shape concentration profiles of platinum diffusing from the thin platinum silicide (PtSi) surface layer [3], however, the controllability of the amount of introduced Pt_s was low. Therefore, we decided to replace the PtSi layer by platinum implantation to control the amount of in-diffused Pt_s . At the top of it, we examined various single and multiple energy helium implantations to shape platinum profiles at different depths of silicon substrate.

Radiation enhanced diffusion of platinum was studied on the low-doped $\langle 100 \rangle$ -oriented float zone n -type silicon substrate forming the n -base of the planar p^+nn^+ diodes. The diodes were first implanted with 1 MeV platinum ions in the dose range from 5×10^{11} to 5×10^{12} cm^{-2} to create a homogeneous and finite source for platinum in-diffusion. Excluding the reference samples, the diodes were subsequently subjected to single and multiple energy implantations of helium ions with energies of 7, 9, 11 and 13 MeV and a dose of 10^{12} cm^{-2} . Two processes were used for the platinum in-diffusion. The standard process A consisted from 20 minutes furnace annealing at 725°C in vacuum. Two step annealing process B used an additional anneal at 675°C for 20 minutes prior the implantation of helium ions. The aim was to decrease the amount of defects produced by platinum implantation without noticeable redistribution of platinum atoms. Electrically active defects were then characterized by capacitance deep level transient spectroscopy (C-DLTS) and high-voltage current transient spectroscopy (HV-CTS).

Results C-DLTS and HV-CTS measurements [4] show that the diode without helium co-implantation exhibits nearly flat distribution of Pt_s , whereas in helium co-implanted diodes, the substitutional platinum almost perfectly decorates the simulated distribution of primary damage (vacancies). Detailed analysis of measured profiles shows that platinum accumulates at the peaks of the radiation damage given by helium implantation. Regardless on the helium energy, measured peaks of platinum concentration exhibit a constant broadening (about $5\mu\text{m}$) compared to the simulated distribution of primary damage. Accumulation of Pt_s in the region between the peak and the implanted surface (the tail region) is higher (approx. $20\times$) than might be expected from the simulated distribution of the primary

damage. This applies for all profiles measured on samples implanted with different doses of platinum and different energies of helium ions. In contrast with simulated distribution of primary damage, all Pt_s profiles show a significant extension behind the end-of-range of helium ions. Since the platinum labels vacancy-like defects, this extension can confirm the presence of these defects in this region as it was recently shown for silicon irradiated with high energy alphas.

Although, the shape of the platinum profile is qualitatively given by the distribution of radiation damage, the total amount of in-diffused platinum measured for helium implantations with different energies is constant (approximately 0.04% of the platinum dose) and does not scale with the number of introduced radiation defects. This confirms that, compared to the guided in-diffusion from the surface PtSi layer [3], platinum implantation produces a limited and controllable source for platinum in-diffusion. The low amount of in-diffused Pt_s is caused by defects produced by platinum implantation which serve as sinks for platinum interstitials. To confirm this assumption and to increase the amount of in-diffused platinum, we partially removed this damage by annealing which preceded the helium implantation (process B). Results show that the removal of the damage produced by platinum implantation significantly increases the amount of in-diffused platinum. For both treatments, the amount of in-diffused platinum is, up to a certain limit, linearly dependent on the dose of platinum implantation.

We also examined capability of the technique to shape an arbitrary profile of platinum substitutionals in different depths of the target. For this purpose we created a complex profile of radiation damage by multiple energy co-implantation of helium (7, 9, 11 and 13 MeV with equal doses of $1 \times 10^{12} \text{ cm}^{-2}$). Also in this case, the resulting Pt_s profile was fully given by the distribution of radiation defects produced by easy controllable helium co-implantation. Profile measurement disclosed that the shape of the distribution follows well the principles established for the single energy helium co-implantation (the Pt_s concentration ratio between the peak/tail region equal to 2) [4]. All this brings the possibility to produce an arbitrary profile of ideal recombination centre closer to reality.

References:

- [1] HAZDRA, P. – VOBECKÝ, J. – BRAND, K.: *Optimum Lifetime Structuring in Silicon Power Diodes by Means of Various Irradiation Techniques*, Nuclear Instruments and Methods in Physics Research B 186(1-4), 2002, pp. 414–418.
- [2] SCHMIDT D.C., SVENSSON B.G., GODEYS., NTSOENZOK E., BARBOT J.F., BLANCHARD C.: *The Influence of Diffusion Temperature and Ion Dose on Proximity Gettering of Platinum in Silicon Implanted with Alpha Particles at Low Doses*, Appl. Phys. Lett. Vol. 74, 1999, pp. 3329–3331.
- [3] VOBECKÝ J., HAZDRA P.: *High-power P-i-N Diode With the Local lifetime Control Based on the Proximity Gettering of Platinum*, IEEE Electron Device Letters Vol. 23, 2002, pp. 392–394.
- [4] HAZDRA, P. – VOBECKÝ, J.: *Radiation Enhanced Diffusion of Implanted Platinum in Silicon Guided by Helium Co-Implantation for Arbitrary Control of Platinum Profile*, Nuclear Instruments and Methods in Physics Research B, 2005, in print.

This research has been supported by the grant No. GA 102/03/0456 of the Grant Agency of the Czech Republic and the Research Programme of the Czech Ministry of Education MSM6840770017.

Transfer Functions of Elementary Transducers as Filters of Digital Signal in Acoustic Systems with Direct D/A Conversion

L. Husník

husnik@fel.cvut.cz

Department of Radioelectronics, Faculty of Electrical Engineering
Czech Technical University, Technická 2, 166 27 Prague 6, Czech Republic

Topics related to problems regarding systems with the direct digital-to-analog conversion, which are called by many “digital loudspeakers” have been appearing in the scientific literature in the past twenty years although their number has not been great. Their main characteristics is the absence of a conventional digital-to-analog (D/A) converter processing an electric signal and having an electric signal as an output when driven by the digital signal. The D/A conversion is performed either by adding mechanical forces acting on the voice coil system or by adding acoustic pressures radiated by individual parts of the system representing three-state bit signals. Undesired products of such conversion can be removed by using acoustic filters.

Such transducers can be embodied in several ways The first one is the system sometimes called multiple voice coil system, in which the conversion is performed by adding forces caused by voice coils with numbers of turns which are weighted according to the bit weight, the second possibility is a system with the number of membranes corresponding to the number of bits, each respective membrane having the area proportional to the bit weight of signal used as the source signal. The last possibility is using a field of transducers, which are connected into groups with the same excitation signal. Each group has the number of transducers proportional to the weight of the bit signal.

Digital loudspeakers bear in their design inherent problems, among others - those related to spatial distribution of elements and problems of elementary transducers, which should theoretically have ideally flat frequency response so that the reconstituted acoustic field would be undistorted, but of course, in reality this cannot be achieved. The former problem was examined in the previous papers [1], [2], [3], the latter problem is examined in the present work.

Because of their transfer function, transducers act as filters, in most cases due to their fabrication as band pass filters, some may work well even at low frequencies. This fact results from their physical nature, transducers with magnetic field have their transfer functions in the form of a band pass filter with cut off frequencies depending on the mass and compliance of the system. Transducers with electric field are capable of transmitting frequencies theoretically from zero, but real embodiments show some drop in sensitivity at low frequencies due to leakage.

In both cases break point frequencies are given by dimensions of transducers, especially membranes, their material constants, and tension forces. In this part of work we concentrated on modeling various types of frequency responses and their influence on bit signals radiated by individual transducers of transducer field. Comparison of the original signal and the signal filtered by the transducer is made using statistics.

At this stage transfer functions were modeled by modifications of the cosine function, which provides their realistic first estimate. Input signals were two-state digital signals, the waveforms of which were chosen arbitrarily. Main parameters to be changed in this analysis are the frequency of the transfer function maximum (frequency shift), the width of the transfer

function (T), and the side slopes of the transfer function (power). In this way we can achieve a wide range of types of transducer functions, which can be fitted to transfer functions of real transducers. Narrower types of the transfer functions model those of piezoelectric transducers with one main resonant frequency, which can be mechanically attenuated and thus frequency band broadened.

As a result, waveforms of digital signals which were filtered by modeled transfer functions of various types have been calculated and presented in forms of figures in which the original signal, the filter/transducer transfer function and the resulting filtered signal can be seen. Data are processed statistically by cross-correlation function stating the resemblance of the input and resulting signals. Theoretical substantiation of the fact, that transducers constituting a digital loudspeaker do not have to have an ideally flat impulse response, can be derived by writing mathematical description of both analog reproduction with the D/A conversion performed on the electrical side of the system and digital reproduction, where D/A conversion is performed either on acoustic or mechanical side of the system. The only difference being the placement of weighted summation (which is in fact the nature of the D/A conversion), which can be mathematically done on any place as convenient.

The future work will comprise further analysis of combination of both mentioned problems, i.e. influence of the path delay and the transfer functions of transducer constituting the digital loudspeaker.

References:

- [1] HUSNÍK, L.: *Digital Loudspeaker* CTU Reports, Proceedings of Workshop 2004, Vol. 8, 2004, pp. 386–387.
- [2] HUSNÍK, L.: *Audio Going Digital – Present State and History of Digital Transducers* Proceedings of X Symposium New Trends in Audio and Video, Wrocław, 2004, pp. 47–52.
- [3] HUSNÍK, L.: *Analýza vlivu rozložení bitů v poli měničů reproduktoru s přímou digitálně analogovou přeměnou* Akustické listy, 3, Vol. 9, 2003, pp. 14–16.
- [4] HUSNÍK, L.: *Influence of Transducer Transfer Function on the Signal Radiated by a Digital Loudspeaker* Proceedings of Digital Technologies 2004, Žilina, 2004, pp. 91–96.

This research has been supported by the Research Programme MSM-212300016.

8th International Student Conference on Electrical Engineering POSTER 2004

L. Husník, L. Lhotská, T. Bílek, Z. Škvor

husnik@fel.cvut.cz

CTU, Faculty of Electrical Engineering
Technická 2, 166 27 Prague 6

Student's research activity should be integral part of the whole pedagogical process at all universities. Its main aim is to support independent creative work of students and stimulate practical application of theoretical knowledge acquired during their study. We take for necessary and very useful to organize regularly student scientific conferences, namely because of comparison of contributions to solution of a certain research problem at different domestic and foreign institutions, establishing personal contact among young researchers, development of personal skills, and development of habits of research work and its presentation.

Students' scientific conferences POSTER organized by the Faculty of Electrical Engineering of the Czech Technical University in Prague began in 1995 as an internal meeting of students from all CTU faculties interested in the field of electrical engineering. In 1997, after two-year's experience, we decided to open this event to students from other Czech and foreign universities and invite both undergraduate and postgraduate students from neighbouring countries. Seven following successful successors in 1998, 1999, 2000, 2001, 2002 and 2003 confirmed that this was a right choice.

The 8th international student conference on electrical engineering POSTER 2004 showed on further growing interest in this conference which was manifested by another 10 % increase of submitted contributions. The program committee selected for presentation 220 contributions of both undergraduate and postgraduate students from another record-breaking number of 270 submitted abstracts. Criteria of acceptance were namely based on the scientific quality and originality of students' contribution. Majority of contributions came from FEE CTU (131), 44 from other Czech universities and 33 from foreign countries (Germany, Poland, France, Hungary, Italy, Estonia). The contributions were presented as posters in seven parallel sections:

<i>Communications</i>	<i>33 posters</i>
<i>Electronics and Instrumentation</i>	<i>41 posters</i>
<i>History of Science and Technology</i>	<i>8 posters</i>
<i>Informatics and Cybernetics</i>	<i>61 posters</i>
<i>Management</i>	<i>12 posters</i>
<i>Natural Sciences</i>	<i>24 posters</i>
<i>Power Engineering</i>	<i>29 posters</i>

The History and Science and Technology Section is a new section which has as its aim to raise public interest in the history of technical sciences.

Proceedings of the conference [1] were published in the form of the CD-ROM, which was distributed to all conference participants. The paper size was limited to 6 pages in the set format and by 1MB of the submitted file in the .pdf format.

POSTER 2004 was sponsored by the CTU Grant Agency, FEE CTU Prague, various companies (Schneider Electric, Siemens, Orange and Green, CertiCon, Vápenka Vitošov and T-Mobile) and scientific societies (the Czechoslovak section of IEEE, its Joint MTT/AP/ED Chapter), which provided organizers with numerous prizes (mobile phones, printers, digital cameras, journal subscriptions and cash prizes).

Members of evaluating committees chose winners and further rewarded contributions in individual sections. A total of 39 posters were awarded, 26 from FEE CTU Prague, 6 from other Czech universities and 7 from abroad. Winners in respective categories are listed below:

C18 – Milan Kníže: Linear Diversity Precoders Designed for Block-Fading Delay Limited MIMO Channel

EI 35 – Jan Včelák: Navigation System with AMR Sensors and Accelerometers

HS4 – Tomáš Martan: Investigation into History of Solitons

IC27 – Jan Koutník: Temporal Mapping in Categorizing and Learning Module

PE3 – Christian P. Dick: Improved Implementation Technique for Sensorless Control of Switched Reluctance Motor Drives

M6 – Martin Hrivňák – Energy Conceptions

NS10 – Markus Huelsbusch, Nikolaj Blanik, Thomas Kirschkamp: Perfusion Studies of the Eyeground Using Contrast Agents

Six domestic student presentations, one in each section, received the IEEE Prize awarded by the committee of the Czechoslovakia section of IEEE.

To conclude we can state that the 8th International Student Conference POSTER 2004 was very successful. This fact is substantiated by yet another record-breaking number of participants and increased quality of presented posters. The program committee decided to continue in organizing this conference in the year 2005. The 9th POSTER 2005 is scheduled for May 26 2005, the first call of papers is already in circulation.

References:

- [1] HUSNÍK, L. – LHOTSKÁ, L. (EDS.) : POSTER 2004. *Proceedings of the Conference (CD Rom) CTU FEE Prague, 2004.*
- [2] HUSNÍK, L.: 8. mezinárodní studentská konference POSTER 2004 na FEL ČVUT Pražská technika Nr. 3,4, 2004, pp36-36.

This research has been supported by CTU grant No. 0418113.

3D Prediction of Electromagnetic Wave Propagation for Wideband Systems Working in MM Band

S. Zvánovec

xzvanove@feld.cvut.cz

Department of Electromagnetic Field, Faculty of Electrical Engineering,
Czech Technical University, Technická 2, 166 27 Prague 6, Czech Republic

Introduction

The very tight competition in the telecommunication market leads network operators and service providers to seek new effective and efficient ways of data transmitting and system deployment. The moving into new, previously unused high frequencies (tens of GHz), promises higher frequency bands to be allocated to each service and consequently higher bit rates offered to customers.

The millimeter-wave spectrum offers enormous application potential and has chance to become the next frontier for terrestrial wireless communications. The employment of frequencies above about 30 GHz (e.g. for Local Multipoint Distributions Systems –LMDS) has also great challenges from electromagnetic wave propagation point of view. It would be emphasized that propagation in the millimeter-wave frequency bands are in several aspects different from those at the lower frequency bands used by cellular (GSM) and wireless LAN systems. It includes for e.g. the attenuation due to rain, which is the main factor limiting the range of high-reliability microwave links above 30 GHz, or other differences like diffraction, influence of foliage etc. Propagation model is the fundamental tool for designing and analyzing the fixed broadband wireless systems.

Realization

The diffraction on dielectric wedge (building corner) in millimeter frequency band has been investigated both theoretically and experimentally to provide knowledge support for ray tracing/launching calculations of LMDS interference issues in urban areas. The main motivation was to find balance between a reasonably reliable results and necessary demands on the calculation complexity and input data accuracy. A measurement system was developed at the Department of Electromagnetic Field. This system consists of a transmitter, receiver and two antennas: an open waveguide was used as a transmitting antenna, the receiving antenna was of a horn type.

Measurements of diffraction were performed in anechoic chamber. Used frequencies were 18 GHz and 38 GHz. Two types of diffracted material were utilized. The first: the perfectly conducting wedge with wedge angle of 90 degrees, which was made of a metal reflection foil and an aluminum plate. And the second: the dielectric wedge formed by two breeze-blocks standing next to each other.

The basic signal propagation planning and analyzing tool has been developed to study time-space characteristics of LMDS. The main goal is an investigation of LMDS (or similar systems of new generation working above 30 GHz) system performance against various propagation phenomena (e.g. variations of precipitation, diffraction). The main software module of the tool enables several forms of input. The subscriber positions can be generated

randomly according to a chosen statistical distribution. Heights of subscriber stations above ground can be chosen either as constant values or as Rayleigh distributed values with adequate factor. Input rain rate distributions in space can be chosen from known statistics or the actual radar data for given region are considered.

The signal propagation simulations for LMDS system presently enable to generate: coverage of investigated area by selected number of hubs, potential interferers (since the subscribers in MWS utilize narrow beam antenna only limited number of subscribers can be affected by interference from another than nearest base station), received signal level, attenuation through rain, availability of service in area influenced by time variable rainfall. When a time series of rain rate distribution in space is entered various system characteristics can be simulated in space and time: coverage, interference, site diversity improvements etc.

Results

The results coming from realization of the project has been published at international conference VTC 2004 in Los Angeles [1], symposium URSI in Australia [2] and at conferences Radioelektronika in Bratislava [3] and Poster 2004 in Prague [4].

References:

- [1] S. ZVÁNOVEC, P. PECHAČ: *Site Diversity Time-Space Simulations for LMDS*, In Proceedings of the 2004 60th Vehicular Technology Conference [CD-ROM], 2004
- [2] S. ZVÁNOVEC, P. PECHAČ, M. MAZÁNEK: *Space-time simulations of point-to-multipoint radio systems performance during rain events using radar data*, URSI Commission F Triennium Open Symposium, Australia, 2004, pp. 208-212
- [3] S. ZVÁNOVEC, P. PECHAČ: *MSignal Propagation Simulation Tool for LMDS*, Radioelektronika 2004 - Conference Proceedings. Bratislava: Slovak University of Technology, Slovak Republic, 2004, pp. 205-208.
- [4] S. ZVÁNOVEC: *Time-space modeling of MWS systems working in millimeter wavebands*, POSTER 2004 [CD-ROM]. Prague: CTU, Faculty of Electrical Engineering, 2004.

This work has been supported by the grant CTU 0407013 "3D prediction of electromagnetic wave propagation for wideband systems working in mm band" .

Communications over DC Power Lines

M. Purkert, M. Trnka

trnkam3@fel.cvut.cz

Department of Measurement, Faculty of Electrical Engineering, Czech Technical University, Technická 2, 166 27 Prague 6, Czech Republic

Using power lines for communication purposes is not a new idea. Power Lines Communications (PLC) represent a potential simplicity for communications among different devices, because it does not need additional wires for connecting devices network together. Nowadays PLC are expected to be used in homes and offices for sharing or providing connection to the Internet and for home automation. The main interest of our work is to study possibility for using PLC in industrial environment for real-time data exchange with special focus on automotive industry, where we would like to implement our principle to replace a comfort communication based on CAN bus by any communication using power lines.

The first thing to be considered is power lines channel properties. Power lines compared to designed communication media are a very hostile environment that has to be studied from various points of view when communication is to be established. Important properties are a transfer function, network impedance and distortion on power line network. Because of short distances in a car, transfer function is characterized by periodic notches caused by reflections at the non terminated ends of lines. This is a property of network that could not be avoided and communication has to take this feature into account. Structure of power network in a car has a star topology with lead battery plugged in the center of it. This leads to low impedance, fewer than 10 ohms, at frequency band from DC up to about 4 MHz. Distortion on mentioned power lines network in band above 4 MHz is a subject of further study.

The principle used for our developing communication is created with respect to power lines channel characteristics and expected utilization as an industrial fieldbus system. It means we tried to find a modulation scheme that is robust enough that does not need channel equalization and is easy to detect as well to keep modem complexity at lowest possible level. For this reason we selected a Binary Frequency Shift Keying with lots of orthogonal carrier frequencies used to transmit the same information. In time domain two symbols are generated using Inverse Discrete Fourier Transform to represent binary values. The first symbol has a pseudorandom code (any sequence of +1 and -1) assigned at even frequencies in intended frequency range, while zeros are used elsewhere. The other has a pseudorandom code assigned at odd frequencies in intended frequency range with zeros elsewhere. As a consequence these two symbols are formed by a sequence of samples that have two identical halves of the same module, but odd frequencies assigned symbol has a second half 180 deg. phase shifted against the first one. Detection of communication based on these two symbols is a simple constant time correlation at half symbol period with low pass filter attached at the output of the correlator. Thanks to symbols properties output of the low pass filter produces base band PAM signal that is processed by common techniques for PAM signal detection and reception. Because the information carried by these two symbols does not depend on phase shifts at different frequencies and symbols occupy wide spectra we expect that this communication will be robust enough to successfully beat bad channel properties at the cost of bandwidth wasting.

This principle has been simulated using Matlab/Simulink environment before self implementation. Simulation model took AWGN frequency selective channel into account. Simulation results showed a good modulation's properties face to face SNR up to 10 dB and more than one half in-band spectra suppressed. Simulation itself did not bring rounding noise into account so we expected worse properties on real system.

Introduced communication has been realized using demonstration system based on FPGA. The main goal of the project was creating a universal hardware whereon communication principle can be tested and improved. At this time we have two development boards to evolve the communication at the physical level. Our communication occupies frequency band in a range approximately 4 MHz to 16 MHz. Two symbols, that represents logic high and logic low levels, consist of 256 samples each and was generated using IFFT in MatLab. In the FPGA these symbols are stored in a memory block. The main drawback of storing those symbols in memory is constant speed at the physical level that is compensated by easy implementation. Communication's physical layer data rate is 195 kbps. Digital Signal Processing operates at 50 MHz sampling frequency.

To analyze bit error rates boards are equipped with Universal Serial Bus interface to connect to a Personal Computer. Massive bit error rate study has not been performed yet, but after a few tests on subject car it seems that physical layer is as robust as expected and communication is stable even during transient states caused by switch of high power appliances such as front side lights. Achieved bit error ratio was around 10^{-5} . Final application will use LDPC for forward bit error correction.

During our future work we plan to focus on optimization of current system. Determine boundary limits of used communication principle in terms of communication channel properties, resolution of analog to digital converter and rounding in signal processing path. Next, we would like to optimize existing system and find balanced compromise between reliability and complexity of detection method. Two additional boards will be created to develop a suitable Medium Access Control for this communication based on Carrier Sense Multiple Access with Collision Avoidance, Token ring or Master Slave principle. We will perform massive channel properties study to adopt communication straight to it that might lead to simplification of devices which affects price of whole system.

References:

- [1] TRNKA, M.: Doctoral thesis FEE CTU Department of Measurement, 2005

This research has been supported by research program LN00B073 sponsored by the Ministry of Education of the Czech Republic.

Scientific Facility for Space Research

Model of Electromagnetic Vibration Damping

J.Masarik-M.Plihal-J.Zdenek

zdenek@fel.cvut.cz

CTU - Czech Technical University in Prague
Faculty of Electrical Engineering
Department of Electric Drives and Traction
Technicka 2, 16627 Praha 6, Czech Republic

Quality of many industrial materials processed by melting with following crystallization or solidification is negatively influenced by Earth's gravitation. Some alloys cannot be produced on Earth at all. Basic material experiments have been carried out in space stations in the Earth's orbit in micro-gravity environment during several last years and next are under preparation. Samples of selected materials are processed in equipment called crystallizer, which is a mechatronic computerized facility consisting of multi-zone tubular furnace, electrical vibration-less very low-speed drives for precise positioning of processed samples and manipulating of in-sample measurement facility, furnace heaters, power converters, furnace temperature measurement and control electronics, gravitation measurement unit, crew Interface Computer (CIC), telemetry channels and other auxiliary units. Some material experiments last relatively long time, one day or more and processing is fully automatic based on computer program prepared on the Earth by physicists. Processed samples are transported to the Earth to be analyzed.

Facility basic requirement is vibrationless behavior during all time material is processed. Scientific facility for material high temperature processing have been in operation in the orbital station MIR during ESA EUROMIR missions several years ago. Facility have been equipped with vibrationless electrical drives. Microgravity measurements proved very good behavior of that drives, no vibration noise was measured from this source. But another problem aroused; astronaut motions inside station and their contacts with the parts of station induce spurious vibrations and influence resulting quality of processed samples of material. Newly prepared facility have to be equipped with damped platform on which the working part of furnace will be placed. The paper presents some basic principles and first results of design of electromagnetic damping platform model for new facility.

Model is based on following assumptions:

- translation only considered (no rotation)
- moving object has rigid body (no deformation by external force)

Model input data used to complete mathematical model are as follows:

- space station mass $m_s = 470$ t, (mass of completely assembled space station ISS)
- astronaut mass $m_k = 80$ kg.

It is necessary to know maximal value of astronaut body acceleration to complete model. On The Earth man vertical jump upward maximal acceleration value is approx. 4 m/s and time of takeoff is approx. $t = 0,3$ (if constant acceleration is supposed). Max acceleration value used in model is 20 m/s^2 . (nearly zero gravity environment in the space station)

Space station crew motion model:

To simulate motion of crew, generator of pseudo random values is used (with limitation of output value and zero mean value). From point of view of long time period (e.g. one day) crew is supposed to be on same place (in the morning and in the evening) inside limited space of the space station

Damping method model:

Mono mass model is supposed based on active damping model used in automobile techniques.

Forced damping oscillation formula is:

$$\ddot{a} = \frac{F - F_R}{m} - 2\gamma \dot{a} - \frac{k}{m} a$$

- **F** - external force exciting motion of system [N]
- **F_R** - regulation action
- **a** - deflection [m] and its derivations (speed, acceleration)
- **γ** - damping coefficient [1/s]
- **k** - oscillator rigidity [N/m]
- **m** - damped facility mass (estimated approx. 80 kg)

With the above stated parameters space station acceleration can be calculated. Acceleration is induced by motion of one astronaut when he takes off from the wall of space station If acceleration of crew member is $\mathbf{a} = 20 \text{ ms}^{-2}$, calculated space station acceleration is $\mathbf{a}_s = 0,378 * 10^{-3} \text{ ms}^{-2}$. This values are in compliance with the data measured in space station MIR during several scientific missions. Based on the presented, model simulation of dependence of acceleration, speed and path (deflection) of the system on the exciting force and on the mode of damping (passive vs. active) has been calculated.

References:

- [1] NAHLE,R.-ROESTEL,R.-SCHMIDT,K.-WITTMANN,K.: *TITUS a New Facility for Materials Sciences Experiments in Space* 46th Int.Astronautical. Congress. Oslo, 1995
- [2] BARTA,C.-JR.-BARTA,C.SEN.-BERNAS,M.-NAHLE,R.-ROESTEL,R.: *Advanced TITUS Facility Tool for the Crystal Growth and Solidification on Board the International Space Station* Proc.of ICCG-13 Kyoto, 2001
- [3] ZDENEK,K.-KOUCKY,L.-MNUK,P.: *Network Node for Temperature Control of Scientific Equipment for High Temperature Material Processing in Space Station*. Proc.of IFAC ws. PDS2003 Ostrava 2003, pp.291-294.
- [4] ZDENEK,J.-KOUCKY,L.-MNUK,P.: *Node for Drive Control of Scientific Equipment for High Temperature Material Processing in Space Station* Proc.of EDPE2003,High Tatras, 2003, pp.201-206

A New Concept of PTP Vector Network Analyzer

V. Závodný, K. Hoffmann, Z. Skvor

zavodnv@fel.cvut.cz

Department of Electromagnetic Field, Faculty of Electrical Engineering,

Czech Technical University,

Technická 2, 166 27 Prague 6, Czech Republic

Six-port vector network analyzers (VNA) are well known for decades, [1]. Similar concept using only a scalar network analyzer and a PTP was designed in [2], where only a basic principle was designed and experimentally verified using a PTP with properties far from optimum. No recommendations for the structure of the PTP were given. Some suggestions for an optimum three state PTP can be found in [3], yet the states of the PTP are unpractical for a realization and are suitable only in a narrow frequency bandwidth. The main demand in the PTP design is to realize optimum states valid on the whole Smith chart in wide frequency band. These demands can be hardly satisfied with any minimum 3-states PTP. The solution is a new concept of the PTP vector network analyzer based on redundant multi-state PTP. It releases the demands on PTP so that they must be satisfied only in a part of Smith chart. The concept can be summarized into three key steps.

- over-determination of measured data using more than three minimum states of the PTP
- approximate determination of measured reflection coefficient in Smith chart using proper three PTP states
- state the measured reflection coefficient more precisely applying the best PTP states determined in given frequency in corresponding part of Smith chart by proper test criteria

The purpose of this paper is to present proper criteria for the PTP state selection and a new circuit solution for individual states of the 7-state PTP.

Theory

A typical arrangement of the new PTP vector network analyzer with seven switched PTP states. An unknown reflection coefficient Γ_{DUT} is modified by s-parameters of the PTP and measured by a scalar analyzer (SA) as certain Γ_m . The relation can be modified to quadratic plane equation where A_x, B_x, \dots, G_x are real constants. These seven real constants completely define the quadratic plane at one frequency above the complex plane Γ_{DUT} . The constants can be found by calibration [3]. The vertical line with diamonds corresponds to the Γ_{DUT} position. This line intersects the quadratic planes in points on certain circle counter lines. A common intersection of these circles transformed into the plane of Smith chart determines Γ_{DUT} position. At least 3-state PTP must be used for a unique determination of measured Γ_{DUT} , see [1]. In real measurements some noise error signal superimposed on measured power must be considered. This noise will produced error at the Γ_{DUT} space determination. A multi-state PTP makes possible to choose the best states for a certain area in the Smith chart. Four test criteria were developed for the selection.

Gradient criterion: The criterion discovers areas in the quadratic plane where even a small noise error in measured reflected Γ_m , will produce a significant error at Γ_{DUT} determination.

Angle criterion: This criterion determines the circle cross angle for the whole x-y plane. Angles between 30-90 degrees are acceptable producing low errors in Γ_{DUT} determination process.

Vector product criterion: It is a more complex criterion. For two quadratic planes we can explain two gradient vectors in each point of the x-y plane. The module of the vector product of the gradient vectors displayed at the x-y plane gives information including both gradient and angle results.

Noise error criterion: A noise error signal superimposed on measured reflection coefficient moves the positions of circle counter lines which determine the Γ_{DUT} position. It results in the error area with four border cross points. If the geometric distance between the Γ_{DUT} position and the most outlying point is computed and displayed at x-y plane, the measurement noise dependency can be obtained.

7-State PTP: The novel 7-state PTP consists of switched elementary two ports composed from thru connection and serial and parallel RC, RL and R combinations connected to 50 Ω microstrip line. It was designed for the frequency band 240-1600 MHz. The structure and the values of components of this PTP were optimized using the new test criteria. Corresponding quadratic planes are shown in Fig.4. The elements were chosen so that the individual quadratic planes were sufficiently different in the whole frequency band.

Experimental results: The above declared test criteria were tested on two PTP. The first one 6-state PTP based on FET transistors mounted at 7mm coaxial structure and designed for the frequency bandwidth 7-14 GHz was used for experiments in [1]. This first sample of a PTP was not optimized with respect to minimization of measurement uncertainties.

The second one was the new 7-state PTP.

The tests were carried out by the following way. The complex plane of a reflection coefficient was scanned with the step of 0.1. In each point on the frequency of interest all combinations of quadratic plane pairs were tested and the best and the second best results were chosen to be displayed. 7-state to 3-state optimum PTP reduction was carried out by this way.

References:

- [1] G. F. ENGEN *THE SIX-PORT REFLECTOMETER: AN ALTERNATIVE NETWORK ANALYZER* IEEE TRANS. MICROWAVE THEORY TECH., DEC. 1977, PP. 1075-1083
- [2] HOFFMANN, K. – ŠKVOR, Z.: *A NOVEL VECTOR NETWORK ANALYZER* IEEE TRANS. MICROWAVE THEORY TECH., 1998, VOL. MTT-46, PP. 2520-2523
- [3] KLUSÁČEK, V.: *Vektorové měření pomocí skalárního analyzátoru*. PhD. Thesis in Czech, CTU Prague, Faculty of Electrical Engineering, August 2001,
- [4] ,

This research has been supported by CTU0406913.

The Utilization of an In-System Programmable Analog Circuit for Education

M. Havlan, P. Kosek, O. Hudousek

havlan@fel.cvut.cz

CTU, Faculty of Electrical Engineering,
Department of Telecommunication Engineering
Technická 2, CZ-166 27 PRAHA 6

During the lessons of subjects Construction of Telecommunication Systems and Construction of Transmission Systems at the Department of Telecommunications Engineering, good experiences with students education using developer kits were gained. Kits with programmable gate arrays (internally called FPGA_PCI_ISA_BOARD) developed at the department, are being used. These boards, with either ISA or PCI bus, contain among others FPGA circuit Xilinx XC2S150, which features universality of digital functions realization. Other kits are also used, with circuits for particular telecommunication application. A board with ISA bus only (internally called E1_ISA_BOARD), contains Dallas Semiconductor circuit DS21554 SCT - E1 Single Chip Transceiver. It is integrated E1 interface controller (also called E1 Framer) and E1 LIU – Line Interface Unit. This board also contains DS2172 circuit (produced by the same company), which is designed as a BERT – Bit Error Rate Tester. More details about these developer kits may be found in references [1].

Based upon good results with students education using the described developer kits, which covered purely digital applications area, an idea came up to familiarize students with possibilities of relatively new integrated circuits, which interconnect “two worlds – digital and analog”. Functions realized with these circuits are purely analog or analog-digital mixed (filtration, subtraction, multiplying, comparing, power elements control, time delay, PLL realization, frequency division, A/D and D/A conversion, ...), but its control is digital. These circuits are called “in system programmable analog integrated circuits”. Details about the market supply are in the references [1].

Circuits with similar function are offered by Zetex company (<http://www.zetex.com/>) but much more sophisticated integrated circuits (ICs) offers Lattice company under labels ispPAC, ispPAC Power Manager and as a hot news offers frequency generator circuits labeled as ispCLOCK, see web page of Lattice company [4].

While choosing the proper circuits for practical project for laboratory education, theoretical background of students (who are to take the above mentioned subjects) had to be taken into account. Practical realization of the project and its didactic point of view, limited by the given time during one theoretical lesson and practical part – three lessons in the labs and available measurement equipment, also had to be taken into account. Groundwork for theoretical part presented during the theoretical lesson is released in the reference [3].

In the end, circuits from Lattice company were chosen for their features, price and usability in the lessons and are used for one practical project realization.

The purpose of this subject is to practically familiarize students with programmable analog components. For this intention has been chosen frequency band pass filter realization for ADSL modem, ATU-R transmit side, which serves to limit the output signal frequency spectrum in a way to meet the spectral mask requirements according to ITU-T G.992.1 recommendation. This filter consists of cascaded High Pass and Low Pass filters, realized using ICs ispPAC10 and ispPAC80.

Before realization of the project, it is necessary, that students get familiar with the functions of oscilloscope ETC M221, generator ETC M321 (PC measuring boards, see [1]),

and program environment of ETC Wobbler, see <http://www.etc.sk/ftp/documents/wobbler/1.00/wobbsvk.pdf>, which are being used during the lessons.

During realization of this project, five workplaces with developer kits ICs ispPAC10 and ispPAC80 were created, because one workplace is to be used for max. three students (that is given by the total capacity of one practical class, which is 15 students). Further, it was necessary to design and make units for matching symmetrical interfaces to existing measurement equipment: arbitrary waveform generator ETC M321 and oscilloscope ETC M221. These equipment (PC boards) have asymmetrical interfaces only. The matching units for interconnection of symmetrical interfaces of telecommunication equipment and asymmetrical interfaces of measurement devices were designed and made at the Department of Telecommunications Engineering and are versatile designed from the point of view of impedance value at symmetrical interfaces so they would be usable for all standard used impedances at symmetrical interfaces in telecommunications.

During the project realization students design, program, simulate and measure the characteristics of each block of the frequency band pass filter of the ADSL modem transmit side according to the particular project assignment.

Particular project assignments, other details and links will be released in the end of February 2005 on the website www.comtel.cz in the subject Construction of Telecommunication Systems section. First practical lessons of this subject will start in the summer term of the school year 2004/2005.

References:

- [1] HAVLAN, M. - ŠEDIVÝ, M. - HUDOUSEK, O. - BURČÍK, J. - KOSEK, P.: *Konstrukce telekomunikačních zařízení. Cvičení. 1. vyd.*, Vydavatelství ČVUT Praha: 2004 pp. 164-176. ISBN 80-01-03035-0.
- [2] HAVLAN, M. - KOSEK, P. - HUDOUSEK, O.: *Implementation of Analog Interface by Programmable Analog ICs*. In RTT 2004 [CD-ROM]. Prague: CTU, Faculty of Electrical Engineering, Department of Telecommunications Engineering, 2004, pp. 0229_0122. ISBN 80-01-03063-6.
- [3] HAVLAN, M. - ŠEDIVÝ, M.: *Konstrukce telekomunikačních zařízení. Přednášky. 1. vyd.*, Vydavatelství ČVUT Praha: February 2005 (In the Press), pp. 224 - 232.
- [4] [HTTP://WWW.LATTICESEMI.COM/](http://WWW.LATTICESEMI.COM/)

This research has been supported by FRV 2009 F1/2004.

3-D Components in Microwave Planar Structures

V. Sokol*

sokolv@fel.cvut.cz

*Dept. of Electromagnetic Field, Faculty of Electrical Eng., Czech Technical University, Technická 2, 166 27 Prague 6, Czech Republic

Abstract - Rapid growth in wireless communication systems has led to a requirement for smaller, higher performance and lower cost RF and microwave circuits and systems. Recently, standard planar constructions have been replaced by a multilayer arrangement using modern materials and new 3-D components. However, such stacking in multilayer structures push both active and passive circuit components into closer proximity and the design problem becomes very complex indeed. Fortunately, the design problem can be solved using electromagnetic field simulator as a very efficient CAD tool. The aim of this paper is to demonstrate advantages of 3-D structures and outline methodology of its modeling as well.

The short wavelength radiation sources used for materials removal emit at both low (synchrotron radiation sources) and high peak power (sources based on hot dense plasmas). With low-peak-power sources, materials are removed by photon-induced desorption of material components from the irradiated sample surface. Each x-ray photon carries enough energy to break any chemical bond. This energy is also usually higher than the cohesive energy of any crystal. Therefore the photons absorbed in the near-surface region may also create small fragments of the sample material, which are emitted into the vacuum. It is necessary to underline that, in the case of low-peak-intensity irradiation, material is removed from the surface and a very thin near-surface layer only. Quite a different situation is expected when a high-peak-power source delivers a single high-energy pulse onto the sample. The sample is exposed to a high local dose of radiation (given by the energy content of the pulse and the absorption length of the radiation in the irradiated material) in a short period of time (given by the pulse duration) – thus a very high dose rate. This means that a large number of events which cause radiation-induced structural decomposition (i.e. polymer chain scissions, etc.) occur almost simultaneously in a relatively thick layer of irradiated material. Since a significant part of the radiation energy absorbed in the material is thermalized, sudden overheating of the layer, which is also chemically altered by the radiation, must be taken into account. On the whole, the overheated fragmented region of the sample represents a new phase, which tends to blow off into the vacuum.

In this contribution we present the results of a study of the ablation of PMMA, PTFE, and Si irradiated by intense soft x-ray radiation emitted from laser-produced plasmas. The high - temperature plasma was created by focusing a 1315-nm laser beam from the PALS, iodine laser system (Institute of Physics, ASCR, Prague) on the surface of a metallic target placed in a vacuum chamber. A gas fill in the interaction chamber was used to reduce charged particle emission from the plasma before arriving at the sample surface. By varying the operational parameters of the plasma sources, we covered a wide range of photon energies, pulse energies, and pulse durations of the short-wavelength radiation pulses with which the chosen samples were irradiated.

It has been demonstrated that the operating conditions of this sources can be optimized to provide enough soft x-ray radiation, emitted in sufficiently short pulses, to ablate PTFE, PMMA and Si. Polymer layers with a thickness of several hundred nanometers were ablated

by a single shot, under optimum irradiation conditions. Silicon, an example of an inorganic, covalently bound crystalline material, is much more resistant to x-ray ablation than organic polymers. PTFE sample was ablated to level of depth from 0.1 μm up to 0.6 μm , PMMA up to 0.8 μm and Si up to 0.2 μm through a nickel mesh by intense XUV radiation emitted from laser produced plasma, driven by the laser pulse focusing on the molybdenum-target surface.

This finding, plus the hydrodynamic-like structures which were observed in irradiated areas of the polymer samples, supports a model of x-ray ablation based on the assumption of radiation-induced scissions of the polymer chains, resulting in formation of a fluid-like phase. Removal of macroscopic amounts of the material is then realized by expansion, ejection, and vaporization of this phase (overheated by the dissipated fraction of absorbed radiation) into vacuum. Reduction of the soft x-ray fluence by increasing the plasma-sample distance and locating the target at the laser beam focus, results in a dramatic decrease of ablation efficiency. The localization of samples at different distances from the x-ray source made it possible to investigate the x-ray dose and dose rate effects on ablation processes under constant spectral properties of the x-ray source. Comparing this result of ablation depth profiles we can measure the space dependence of X ray intensity with respect to the assumed r^{-2} decrease in the intensity far away from the plasma.

References:

- [1] L. JUHA: *Materials ablation with soft x-rays*, Čs. čas. fyz. 50, 2000, pp. 110-118.
- [2] J. JUHA, J. KRÁSA, A. PRĀG, A. CEJNAROVÁ, D. CHVOSTOVÁ, J. KRAVÁRIK, P. KUBEŠ, YU. L. BAKSHAEV, A. S. CHERNENKO, V. D. KOROLEV, V. I. TUMANOV, M. I. IVANOV, M. SCHOLZ, L. RYČ, K. TOMASZEWSKI, R. VISKUP, F. P. BOODY, J. KODYMOVÁ: *Ablation of PMMA, PTFE and Si by single pulse of soft X-Rays emitted from hot dense plasmas*, High-Power Laser Ablation IV, Claude R. Phipps, Editor, Proceedings of SPIE Vol. 4760, 2002, pp. 1098-1105.
- [3] J. JUHA, A. PRĀG, J. KRÁSA, A. CEJNAROVÁ, B. KRÁLIKOVÁ, J. SKÁLA, D. CHVOSTOVÁ, V. VORLÍČEK, J. KRZYWINSKI, A. ANDREJCZUK, M. JUREK, D. KLINGER, R. SOBIERAJSKI, H. FIEDOROWICZ, A. BARTNIK, L. PÍNA, J. KRAVÁRIK, P. KUBEŠ, YU. L. BAKSHAEV, A. S. CHERNENKO, V. D. KOROLEV, M. I. IVANOV, M. SCHOLZ, L. RYČ, K. TOMASZEWSKI, R. VISKUP, F. P. BOODY: *Ablation of Organic Polymers and Elemental Solids Induced by Intense XUV Radiation*, X-Ray Lasers 2002, 8th International Conference on X-Ray Lasers, American Institute of Physics, 2002, pp. 504-509.

This work has been conducted at the Department of Electromagnetic Field of Czech Technical University in Prague and supported by internal grant of CTU No.: 0406813.

Objective Image Quality Evaluation Using Artificial Neural Network

K. Fliegel

fliegek@fel.cvut.cz

Department of Radioelectronics, Faculty of Electrical Engineering,
Czech Technical University, Technická 2, 166 27 Prague 6, Czech Republic

This paper deals with the enhanced approach to the objective quality assessment of video signals in the multimedia systems. Objective image and video quality evaluation plays very important role in the systems for signal recording and transmission. Higher precision of the image quality evaluation helps to optimize both recording and transmission system in order to minimize the bitrate needed to achieve as high image quality as possible. This paper presents the brief overview of the subjective and objective image quality evaluation methods and shows the proposal of the system for the video quality assessment using Artificial Neural Network (ANN).

There are two main methods for image quality assessment: subjective and objective. Subjective methods (evaluation by the group of human observers) offer the most precise results, but these methods are time consuming, costly and they cannot be easily automated. Methodology for the subjective image quality assessment has quite strict requirements for the viewing conditions. These conditions are described in the ITU-R BT.500 recommendation [4]. We have conducted number of subjective tests using slightly modified methodology in our laboratory. This laboratory is equipped with the reference source of the video signal - digital video tape recorder (DVCam format) - and professional calibrated CRT display. Realized subjective tests were performed with both video signal and static images. Source images and sequences were distorted by several compression algorithms or noisy communication channel. We chose Double Stimulus Continuous Quality Scale test that is especially useful to compare a pair of pictures or video sequences. A series of testing images and videos were prepared with various compression ratios and compression methods. The types of the scenes were selected in order to emphasize textures, natural scenes, faces and contrast areas. Besides these natural scenes video sequences typical for the security technology were also used. The image compression in the field of security technology has to be treated and evaluated as a distorting process affecting a final performance of imaging system. The most critical point can be described as a preservation of relevant image features important for a particular application such as identification, classification etc. Most of video coders are optimized for the maximum subjective quality (natural scene) but the security systems have different requirements and priorities e.g. a correct identification of relevant object (face, fingerprint, car plate). The visual impression in these systems is of a secondary importance.

Among the objective quality evaluation methods belong methods using mathematical characteristics [1] and methods utilizing model of the Human Visual System (HVS). There is no universally usable objective characteristic that allows describing the whole variety of distortions incurred by today imaging systems. The objective image quality evaluation is a very complex problem and relates to the human visual perception. There are several approaches generally used. In the field of image processing it is usually Mean Square Error (MSE) or Peak Signal to Noise Ratio (PSNR) that can be easily evaluated when both distorted

and original (source) images are available. There are numerous attempts to objectivize the evaluation of the subjective image quality. Among many possibilities the HVS (Human Visual System) modeling seems to be most promising. We are working on several modified models suitable for the field of multimedia and security technology.

Systems that measure the quality of an image or image sequence usually consist of a component to compute the values of particular measures, and a component that combines the values into a quality score. Combination of the measures can be done by simple mathematical formula or some more advanced approach can be used. One of the methods to combine the particular measurements is to use an Artificial Neural Network (ANN) [2, 3]. The main aim of this approach is to automatically derive a score that is the same as, or at least correlated with the Mean Opinion Score (MOS) obtained from the subjective votes of many observers. Features that can be used as an input to the ANN for video quality evaluation can be divided into six main groups: 1) Pixel difference-based measures, 2) Correlation-based measures, 3) Edge-based measures, 4) Spectral distance-based measures, 5) Context-based measures and 6) HVS-based measures. Twenty six measures belonging to the one of the groups are described in [1]. Among features comprising spatial distortion information belong simplest PSNR and MSE, which are the most widely used quality metrics but these are insufficient to precisely measure the objective quality of the sequence.

Preliminary experiments with the model using neural network were conducted. Results are promising, but larger training and testing sets are needed for the future development of this technique. This is very time consuming process because of many subjective tests. The main future effort in this research will be devoted to the selection of the most suitable features-measures as inputs to the combining ANN. After this step combining ANN will be trained and tested with sufficient sets of subjective votes. Obtained results of the new video quality assessment approach will be compared to the results from older methods and after statistical evaluation the gain of the new approach over older methods will be verified. Video quality assessment system using ANN without reference (non-distorted) sequence can also be implemented. In this - no reference - approach the important coding parameters of the particular source coder should be used as inputs of the combining ANN. Systems without reference are suitable only for the particular coder or distortion type but this method is not appropriate for the general video quality assessment.

References:

- [1] AVCIBAS, I. - SANKUR, B. - SAYOOD, K.: *Statistical evaluation of image quality measures*, Journal of Electronic Imaging, vol. 11, no. 2, SPIE-Int. Soc. Opt. Eng, April 2002, pp. 206-223.
- [2] MORRIS, T. - ANGUS, K. - BUTT, R. - CHILTON, A. - DETTMAN, P. - MCCOY, S.: *CQA-subjective video codec quality analyser*, BMVC99, Proceedings of the 10th British Machine Vision Conference, vol. 1, Nottingham, UK, Univ. Nottingham, 1999, pp. 123-132.
- [3] HU, Y. H. - HWANG, J.-N.: *Handbook of neural network signal processing*, The electrical engineering and applied signal processing series, CRC Press, 2002, ISBN 0-8493-2359-2.
- [4] ITU-R, *REC. BT.500-10*, 2000.

This research has been supported by GA CR grant No. 102/05/2054.

SYNTFIL – Synthesis of Electric Filters in Maple software

J. Hospodka

hospodka@feld.cvut.cz

Czech Technical University, Faculty of Electrical Engineering,
Department of Circuit Theory (K13131)
Technická 2, 166 27 Prague 6, Czech Republic
Tel: +420 224 352 066, Fax: +420 233 339 805

A system for analog filter design is presented in this contribution. The system consists of a special library of functions SYNTFIL (SYNTesis of FILTers) [1] for Maple™ software. The library contains functions for solving particular tasks in the complete design procedure of electric filters. The library includes:

- Set of functions for solving approximation tasks: normalization and computation of Butterworth, Chebyshev, Cauer (types A, B and C) and Inverse Chebyshev (types A and B) approximations, i.e. computation of gain and characteristic function.
- Set of functions for LC filter synthesis according to calculated gain and characteristic functions: computation of chain matrix from gain and characteristic function for a chosen filter termination, realization of LC ladder filter from chain matrix transformation of LC ladder structure of normalized lowpass filter (NLP) to lowpass (LP), highpass (HP), bandpass (BP) or band-rejection (BS).
- Set of functions for cascade design of active RC (ARC) filters: NLP pole-zero frequency transformation, biquadratic functions forming (pole-zero pairing), determination of biquad cascading order, calculation of gain distribution and realization of particular biquads.
- Functions for resulting filter structures analysis including of Q-factors of inductors for LC ladders and DC open-loop gain and unity-gain frequency of operational amplifiers for ARC filters.

Specification of all filter types (lowpass, highpass, bandpass and band-rejection filter characteristic) is transformed first to normalized lowpass filter characteristic. It is solved by LP2NLP, HP2NLP, BP2NLP (or BP22NLP) and BS2LP functions of the SYNTFIL library. Magnitude approximation is solved for normalized lowpass filters by above mentioned methods, i.e. Butterworth, Chebyshev, Cauer [3] and Inverse Chebyshev approximation.

Power transfer ratio, characteristic function and zeros of transfer function (poles of power transfer ratio) as a result of approximation task, are next used for calculation of a filter chain matrix. Elements of LC ladders structure of normalized lowpass filter can be calculated ("dropped") from the chain matrix by function `DropNLP`. Resulting scheme of filter required type including real element values is reached by applying inverse frequency transformation to normalized lowpass filter structure. Namely by `ElemLP`, `ElemHP`, `ElemBP` (or `ElemBP2`) and `ElemBS` function for lowpass, highpass, bandpass and band-rejection respectively.

Active synthesis of filters in the SYNTFIL library is based on cascade synthesis [2]. Transfer function poles and zeros of normalized lowpass filter are obtained from approximation task. They are consequently transformed to ω_o, Q and eventually ω_c parameters of partial biquadratic transfer functions so-called biquads of resulting filter type. The pole-zero pairing is solved within transformation functions (NLP2LP, NLP2HP, NLP2BP and NLP2BS). The functions return sequence of the particular section parameters so that the order

of cascaded sections is optimal. ARCBLOCK function distributes total gain to particular sections – biquads. This function calculates the gain constant so that dynamic of whole filter is balanced. It means that maxima of magnitudes after each section in cascade filter structure have the same level. These functions are usually called by means of ARCSYNT function for circuit synthesis for biquads synthesis by active circuits.

Analysis of all resulting filter structures (including LC ladder filters and cascade structures of ARC filters) can be made by MAKEH function.

The library can be used in original environment of Maple, for which it was designed. It is possible to use the library directly in MATLAB® using Extended Symbolic Math Toolbox [4]. MATLAB users can also derive benefit from the library by this way. Maple command outputs are interpreted in MATLAB as a string format. They should be converted first for direct processing in MATLAB environment. The interface tool (m-files) is now being prepared to provide this conversion.

The SYNTFIL library of function for system Maple includes all necessary tools for complex design of analog electrical filters. The library is drawn up in the view of teaching filter design at our university. The presented system supports students to work in an interactive way during the whole design process. The particular results can be mathematically treated and/or verified what is necessary for high-quality teaching software. This system is well structured and transparent but on the other hand it demands familiarity with MAPLE software. It was the reason for the creation of new WWW interface which enables simple filter design using the SYNTFIL library without the necessity of any special software installation [1].

References:

- [1] HOSPODKA, J. – BIČÁK, J.: *Syntfil – Synthesis of Electric Filters* Proceedings of Maple Summer Workshop MWS 2004, Waterloo ON, Canada 2004
- [2] HOSPODKA, J.: *Cascade Realization of Electrical Filters Using Syntfil Package* Proceedings of the Digital Communications '03 EDIS-vydavatelstvo ŽU, ISBN 80-8070-165-2, 2003, pp. 25–29.
- [3] BIČÁK, J.: *Cauer Approximation and Elliptic Integrals in Program Maple* Proceedings of the Polish-Hungarian-Czech Workshop on Circuit Theory, Signal Processing, and Applications, Prague CTU, ISBN 80-01-02825-9, 2003, pp. č. 1–6.
- [4] BIČÁK, J. – HOSPODKA, J.: *Using Syntfil Package in MATLAB for Analog Filter Design* Proceedings of the Digital Communications '03 EDIS-vydavatelstvo ŽU, ISBN 80-8070-334-5, 2004, pp. 1–4.

This research has been supported by CTU grant No. CTU0414413.

Maple is a trademark of Waterloo Maple Inc.

MATLAB is a registered trademark of The MathWorks, Inc.

All other trademarks are property of their respective owners.

Measuring Optical Losses of the Planar Waveguides Fabricated by Ion Exchange of Ag^+ -- Na^+ and Li^+ -- Na^+ .

K. Bušek, J. Schröfel

busekk@feld.cvut.cz

Department of Microelectronics, Faculty of Electrical Engineering, Czech Technical University, Technická 3, 166 28 Prague, Czech Republic

J. Spirkova, P. Tresnakova-Nebolova

Institute of Chemical Technology Prague, Technická 5, 166 28 Prague, Czech Republic

Optical losses they are some from fundamental parameter optical planar waveguides usable for base planar laser structure. In planar optical waveguides with value optical losses move in terms of till tenths dB/cm. Basic requirements they are what minimal optical losses optical waveguides in the area working wave length. Optical losses was measured on samples by using method sensing scattered optical radiation from waveguide layer by the help of CCD camera. Advantage this method is contactless measuring optical losses.

For measuring optical losses was used method scan scattered optical radiation in waveguide layer by the help of CCD camera. This method was realized in the workplace ČVUT - FEL (in optical laboratory). Measuring optical losses was realized on planar optical waveguides fabricated by the ion exchange of $\text{Ag}^+ \leftrightarrow \text{Na}^+$ and $\text{Li}^+ \leftrightarrow \text{Na}^+$ in mats of several type glass namely on figure in original state and further on samples after mechanical surfacing (polished surface). Every sample was measured in more point (five till ten) depending on length sample, scatter optical radiation at the end sample. Accurate shift CCD camera (in upright and horizontal direction) was secured currency by the help of stand with micro-shift. Measuring was effected for every sample number of time. Most error (till 20%) with there probably boots inaccurate setting focus distance object-lens CCD camera from surface metering waveguides. For more accurately setting it is necessary on-calibrate near of each of sample distance focalization on calibration mark on surface waveguide. Size calibration mark depends on parameter scanning CCD camera. In our case was using camera with CDD microchip with resolution 1288x1288 pixels on surface 0,5 cm² in 256 colours gray. Method measuring optical losses by the help of CCD camera measuring only stray losses from surface waveguide layer. From repeated metering set of samples was findings, that surface waveguide layer and type disturbances on surface waveguide layer markedly affection optical losses in these waveguides. If are deep defects on surface waveguide, then they are metering optical losses hight affection these defects. At point defects happen to strong de-excitation optical radiation from waveguide layer. After polished surface of samples get near majority metering samples to increasing optical losses. Possible causes increasing optical losses in samples 607, 610, 628, 740, 565, 571, 589 is more. One of themselves it can be rise by other disturbances at burnished finish waveguide. To decrease optical losses till about one dB/cm get near samples 608, 686 and 702. All these samples shell they substrate GIL 49. All metering saples with polishet surface see.

Measuring optical losses separate modes in planar optical waveguides fabricated by the ion exchange of $\text{Ag}^+ \leftrightarrow \text{Na}^+$. From measured values it was possible deduced, that in measured waveguides had higher quidee modes major optical losses than lower quidee mode. In some cases was difference measured optical losses successive following quidee mode

approaches below errors using measuring method.

We reported about metering optical losses of the planar ion exchanged waveguides in glass by the help of CCD camera. Metering optical losses was effected on planar optical waveguides fabricated by the ion exchange of $\text{Ag}^+ \leftrightarrow \text{Na}^+$ and $\text{Li}^+ \leftrightarrow \text{Na}^+$. Relative Error using measured method with move about 20%. Quality of the optically surfaces markedly affection optical losses in measuring waveguides. Limits usability method measuring optical losses scan scattered radiation by the help of CCD camera with in our case move about 0,5 dB/cm. With longer time ion exchanges with magnify dept waveguide layer and in waveguide is more guided wave, and grown optical losses in these waveguides. Used method for metering optical losses with show advantageous to fast and contactless metering. Disadvantage is quantity factor (shieling undesirable radiation, critical focus CCD camera), which affect measurement error.

References:

- [1] S. IRAJ. NAJAFI: *Introduction to Glass Integrated Optics*, House Inc., 1992.
- [2] PAVLÍNA TŘEŠŇÁKOVÁ-NEBOLOVÁ: *Thesis - The planar ion exchanged waveguides in glass containing ion coppers, silver and erbium*, Prague institute of inorganic Chemical Technology, 2003.
- [3] K. BUŠEK: *Thesis - Research dielectric planar waveguide for laser applications* ČVUT - FEE Prague, 2004.

Measuring System for Verification of Contactless Measurement Methods that Use CCD Cameras

T. Radil*, J. Fischer*, R. Dvořák**, J. Kučera*

radilt1@feld.cvut.cz

* Department of Measurement, Faculty of Electrical Engineering, Czech Technical University
Technická 2, 166 27 Prague 6, Czech Republic

Department of Manufacturing Technology, Faculty of Mechanical Engineering, Czech
Technical University, Technická 4, 166 27 Prague 6, Czech Republic

The aim of this project was to design and build an automated measuring system that would enable detailed examination of contactless measurement methods developed in our lab. The research program of our lab focuses on contactless optical measurement methods of e.g. dimension, position or velocity measurement. The research covers both conventional measurement methods and novel methods such as the so-called shadow projection methods [1].

Since various measurement methods have often very different and even contradictory claims to the measurement set-up, the designed measuring system is modular. The measuring system consists of following parts:

- Mechanical set-up
- Measuring camera
- Illuminator
- Software

The mechanical set-up has to secure fixed distances between individual parts of the measuring system. The MayTec aluminium profile system was chosen for this purpose. This profile system enables to easily reconfigure the measuring system in order to meet the demands of the particular measurement method.

In some cases the measurement method requires to adjust precisely the position of one part of the set-up with respect to others (e.g. adjusting the position of the measured object during position measurement). For these purposes the mechanical set-up is equipped with a linear positioning table. The positioning table has a span of 20 cm. An incremental sensor with position resolution of 1 μm is used to indicate the actual position of the positioning table.

From the beginning the project intended to use both standard CCD cameras and measuring cameras designed in our lab. Standard CCD cameras with CCIR output are used mainly for conventional measurement methods while the cameras designed in our lab (such as the camera with CMOS area sensor [2] or the CCD line-scan camera ULC84 [3]) are used mainly for novel measurement methods. In the scope of this project no new camera was designed. However three sensor modules for the line-scan camera ULC84 were developed. These modules are designed for the linear CCD sensors Toshiba TCD1205D and TCD1304AP and for the linear CCD sensor Sony ILX553A. These sensors were chosen because they have high resolution (small pixel width) but still they have big pixel area which secures sufficient output signal level even in case of low illumination.

The type and parameters of the illuminator are crucial for the performance of the contactless optical measurement methods. For example the so-called shadow projection methods [1] require an illuminator built using multiple point light sources while conventional

measurement methods sometimes use large area diffusion back-light illuminators. In order to meet demands of various measurement methods the designed measuring system is equipped with several illuminators. Two illuminators with point light sources were built – the first contains laser diodes SLD6505A, the second was built using miniature LEDs Osram LGU260-EO. The back light illuminator with illuminated area of 24.5×15 cm can be used during conventional measurements to back illuminate the measured test in order to increase its contrast. Two modules with laser diodes and optional collimation lenses (type ALA12-3-650; optical output power 3 mW, $\lambda = 650$ nm) can be used both for conventional and novel methods of measurement.

The whole measuring system is controlled by the OpticLab software we developed using the LabWindows/CVI development environment. OpticLab is able to acquire and process data from standard CCD cameras connected to the PC via frame grabber and from the CCD line-scan camera ULC84. Support for more measuring cameras designed in our lab will be added in the near future. OpticLab can also control the illuminators (as required by e.g. the so-called shadow projection methods [1]) and up to three independent positioning tables. This enables to perform a fully automated measurement that consists of several hundreds measurement steps.

The designed measuring system helps us to test measurement methods that were developed in our lab. The measuring system was already used in research – e.g. for dimension measurement using CMOS area sensor [2]. Parts of the system are used by students in our lab during their work on semester projects and diploma thesis. The measuring system will also be used during the laboratory exercises of the subject “Optoelectrical Sensors and Videometry”.

References:

- [1] FISCHER, J. – HAASZ, V. – RADIL, T.: *Simple Device for Small Dimension Measurement Using CCD Sensor* IMEKO TC4 12th International Symposium: Electrical Measurement and Instrumentation, Zagreb, 2002, pp. 433–437.
- [2] FISCHER, J. – RADIL, T. – ŠEDIVÝ, J.: *The Triangulation Method of Contact-less Dimension Measurement Using an Area CMOS Imaging Sensor* IMEKO TC4 13th International Symposium on Measurements for Research and Industry Applications, Athens, 2004, pp. 625–630.
- [3] FISCHER, J. – RADIL, T.: *DSP Based Measuring Line-Scan CCD* IDAACS'2003 Ternopil Academy of National Economy, Lviv, 2003, pp. 345–348.

This research has been supported by grant No. FRV 2064 G1.

Analysis and Filtering of Ultrasonic signal

V. Matz, M. Kreidl, R. Šmíd

matzv@fel.cvut.cz

*Department of Measurement, Faculty of Electrical Engineering, Czech Technical University, Technická 2, 166 27 Prague 6, Czech Republic

Ultrasonic non-destructive testing is used for detecting of flaws in materials. Ultrasound uses the transmission of high-frequency sound waves into a material to detect a discontinuity or to locate changes in material properties. Measured ultrasonic signal characterizes structure of materials. Measured signal consider back-wall echo, echo from flaw named fault echo and other echoes which are caused by noise or by scattering of signal from grains including in material. These echoes falsification back-wall and fault echo. The noise has to be cancelled by using methods for filtering of ultrasonic signal [1]. There are several sources of noise that can hide a fault. A common source of noise is electronic circuitry, which is used for processing the ultrasonic signal, and scattering at the inhomogeneities in the structure of a grainy material. The amplitude of the fault echoes can be smaller than the amplitude of the noise, and the noise can totally masks echoes characterizing faults. This case is undesirable, because we cannot correctly identify flaws in the material. The most frequent usage of ultrasonic testing is for weld inspection. In welds there is big probability of cracking. For this determination we have to use a method for reducing the ultrasonic signal noise.

This paper describes method for reducing ultrasonic signal noise. For measure of ultrasonic signals we used the material with coarse grain structure, which is used for constructing airplane engines. The most common application in signal processing is used discrete wavelet transform. The discrete wavelet transform [2] can be used as an efficient filtering method for families of signals that have a few nonzero wavelet coefficients for a given wavelet family. This is fulfilled for most ultrasonic signals. The standard filtering (also called de-noising) procedure affects the signal in both frequency and amplitude, and involves three steps. The basic version of the procedure consists of:

- a) decomposition of the signal using discrete wavelet transform into N levels using bandpass filtering and decimation to obtain the approximation and detailed coefficients,
- b) thresholding of detailed coefficients,
- c) reconstruction of the signal from detailed and approximation coefficients using the inverse transform (IDWT).

For decomposition of the signal it is very important to choose a suitable mother wavelet. The shape of the mother wavelet has to be very similar to the ultrasonic echo. The best results were obtained with the discrete Meyer wavelet. In the proposed procedure, local thresholding of detailed coefficients was used [2]. We computed the threshold at each level of decomposition from the detailed coefficients (Dc), and this value was used for thresholding in the same level. For thresholding we propose new threshold value based on standard deviation:

$$\text{Threshold} = k \cdot \sqrt{\frac{1}{N-1} \cdot \sum_{i=1}^N (Dc_i - \overline{Dc})^2}, \quad (1)$$

where N is the length of signal.

In our study we used noisy signal measured on coarse-grain structure material and we changed amplitude of fault echo from 10 to 1020 % of the effective noise value. A value of 1020 % of effective noise value corresponds to 100 % of back-wall echo. The noise reduction for a signal without fault echo is 18.56 dB. For signals with a simulated fault echo the noise 384

reduction ratio was from 17.65 dB to 19.72 dB. We also investigated improvements in sensitivity of fault detection. Our method allows identification of faults with relative amplitude higher than 132.6 % of the effective noise value.

In other work we used similar methods as discrete wavelet transform named wavelet packets [3]. The wavelet packets method is a generalization of wavelet decomposition that offers a larger range of possibilities for signal analysis. In wavelet analysis, a signal is split into an approximation and detail coefficients. The approximation is then itself split into a second-level approximation and detail, and the process is repeated. In wavelet packets analysis, the detail coefficients as well as the approximation coefficients can be split. In case of wavelet packets global thresholding in Matlab is used, but for better results of filtering we used local thresholding. In this case we compared both methods discrete wavelet transforms filtering and wavelet packets filtering. We created simulated ultrasonic signal. A noise with normally random distribution was added to the ultrasonic signal and the level of noise was changed from value 1 to 90 % of maximum amplitude of back wall echo. Up to value 10 % of noise of maximum amplitude of back wall echo, discrete wavelet transform has better results. In the opposite from value of 12.5 % of noise of maximum amplitude of back wall echo wavelet packets bring better results. Better overall results bring wavelet packets method. For higher level of noise (12.5 % of back-wall echo) filtering by wavelet packets has better results then discrete wavelet transform filtering. The highest difference between signal to noise ratio is for value 90 % of back-wall echo. For the following work we use for filtering of ultrasonic signal method based on wavelet packets.

References:

- [1] ŠMÍD, R. - MATZ, V. - KREIDL, M.: *Ultrasonic Signal Filtering*. In Defektoskopie 2003. Praha: Česká společnost pro nedestruktivní testování, 2003, vs. 259-262. ISBN 80-214-2475-3.
- [2] MATZ, V. - KREIDL, M. - ŠMÍD, R.: *Signal-to-Noise Ratio Improvement Based on the Discrete Wavelet Transform in Ultrasonic Defectoscopy*. Acta Polytechnica, 2004, vol. 44, no. 4, s. 61-66. ISSN 1210-2709.
- [3] MATZ, V. - KREIDL, M. - ŠMÍD, R.: *Comparison of Methods Based on Discrete Wavelet Transform Used for Filtering of Ultrasonic Signal*. In Defektoskopie 2004. Praha: Česká společnost pro nedestruktivní testování, 2004, s. 115-120. ISBN 80-214-2749-3.

This research has been supported by MŠMT grant No. MSM210000015.

Design of the Electronic Evaluation Circuits for the Pressure Sensors

A. Bouřa, M. Husák, P. Kulha, M. Seidenglanz

bouraa@feld.cvut.cz

Department of Microelectronics, Faculty of Electrical Engineering, Czech Technical University, Technická 2, 166 27 Prague 6, Czech Republic

One of the most important parts of the design the sensor system is to provide the signal from the sensor to the output. In modern systems, to provide to the output means to include the measured signal to the framework of the signals from the other sensors. There are several ways how to do it. Generally, to include the signal in the framework means to connect the sensors to some kind of a bus and continuously to operate with their signals. This bus can be represented by the wires or it can be virtual i.e. that the sensors are wireless. In cases where it is difficult or impossible to guide the cables (e.g. moving or rotary part of some machine) the wireless solution is essential.

Other important part of the design is the temperature compensation and the compensation of the power supply drift. Modern smart sensors need to be as much as possible compact and easy to handle. So this compensation must be internal and designed for a wide range of possible values.

The power consumption needs to be reduced to the minimum to manage a long operating time of the wireless device. Low power supply by one single lithium cell is handy.

Modern systems used to be digital hence the signal from the sensor also has to be in the digital form.

My work has several parts. First, I summarize the principles of the measuring the pressure with the special accent on the possibility of representing the measured pressure by the electric signal. I embrace the principles from the oldest techniques to techniques based on the MEMS technologies.

Then I discuss the circuits for the temperature compensations of the sensor, amplifiers, analog to digital converters and radiofrequency transmitter which are suitable for the integrated wireless pressure sensor. First part of my work is ended by description of the sensor MPX4115A, microcontroller MC68HC908RK2 and PLL tuned UHF transmitter MC33493/D which can be used in commercial applications (produced by Motorola).

Main purpose of my work is the design of an analog to digital converter, suitable for the cooperation with the pressure sensor MPX4115A and with some kind of transmitter.

My concept of the solution of this problem is an analog to digital converter called V/F converter, which is able to transfigure its internal structure to a shift register and consequently drive a modulation of the transmitter. V/F converter is based on an oscillator where the frequency of the oscillations depends on the input voltage (VCO – Voltage Controlled Oscillator). Counting the impulses from this oscillator for some time we obtain a digital number which is proportional to the input voltage from the pressure sensor.

In my design, after counting the counter changes its internal structure to the shift register and the counted number is sent to the bus or directly to the transmitter.

This concept enables construction of very simple and effective temperature and power supply swing compensation. This compensation is based on the symmetry of the circuit. The counter of the impulses from the VCO is controlled by another counter clocked by VCO of the same construction as the first VCO driven by voltage from the sensor. While

the first VCO changes its frequency proportionally to the input voltage from the pressure sensor the second oscillator is driven by the constant voltage and its frequency change only due to drift of the temperature and drift of the power supply. Counted number, which represents the measured pressure, depends directly proportionally on the frequency of the first VCO and inversely proportionally on the frequency of the second one. If we consider that the oscillators are of the same structure and that they are linear, the counted number is independent on the temperature and the power supply swing.

Device was designed and tested in program WinSpice using CMOS technology in order to manage minimal power consumption. Several simulations were made in order to prove the supposition of the temperature and power compensations. Results of these simulations are discussed.

Design considers with the possibility of remaking it for the simulation in CADENCE. My structure can be useful as a particular part in some bigger project.

References:

- [1] FRADEN, J.: *Handbook of modern sensors Physics, Design, and Applications*, American Institute of Physics, 1997
- [2] JOHNS, D. – Ken, M.: *Analog integrated circuits design*, University of Toronto, 1996
- [3] HAASZ, V. – Sedláček, M.: *Elektrická měření přístroje a metody*, Vydavatelství ČVUT, 2000
- [4] KRÍŠŤAN, L. – VACHALA, V.: *Příručka pro navrhování elektronických obvodů*, SNTL – Nakladatelství technické literatury, 1982

Bistable laser diode with a multiple-divided contact stripe

V. Jeřábek

jerabek@fel.cvut.cz

Department of Microelectronics, Faculty of Electrical Engineering, Czech Technical University, Technická 2, 166 27 Prague 6, Czech Republic

A new field which arose throughout the past few years is the field of integrated optoelectronics. Within this field of hybrid or even monolithic structures of optics, optoelectronic and electronic components are becoming useful for the transmission of information in the increase of speed up to several gigabits per second.

In the integrated optoelectronics field, there are also some rather new optoelectronic components originating. One of these is the bistable semiconductor laser diode (BLD) that makes use of the physical principle of saturated optical absorption. The general optical bistability belongs to a physical phenomenon, which was first assumed by Szöke in the year 1969 and only after, the words were experimentally observed. It was five years later, when Lasher thought about bistability especially through the semiconductor laser diode (LD). Optical bistability by LD belongs amongst the nonlinear dynamic optical phenomenon, originating in LD radiation, the essence of which is Q switching. This physical mechanism is based on nonlinear dependence of the absorption coefficient in the absorbing region of the divided active layer of the semiconductor LD and appears in LD radiation by providing the origin of self pulsations or optical bistability [1]. Few years ago, several papers took place, which described the origin of bistability on LD with a multiple heterostructure that was purposefully modified by dividing the stripe contact for achieving the bistable mode. The papers differed according to the physical mechanism bistability, technology and also according to the method of mask divided stripe contact [3].

As far as ternary BLD structures are concerned, the works used universally demanding technological creations in order to prevent the current spreading under the contact and to achieve a very low threshold current. With these structures, the continual bistable regime was achieved in room temperature. From the BLD created at the quaternary structures, the bistable mode was achieved by an easier technological order by using the multiply divided stripe contact. The component was working in the progressive bistable mode only under mild cooling. The important characteristic expressing the bistable BLD properties is the W-A characteristic. Its analytic expression is possible to be deduced by statically solving a set of three so called rate equations. The W-A characteristic was theoretically and also experimentally determined by a line of authorities [1], [4]. Under certain simplifying preconditions, it is possible to derive from the analytic expression, also basic conditions of bistability arising and also the conditions necessary for the origin of self pulsations in LD radiation.

This article deals with theoretical results and experiments, which led to the demonstration of optical bistability on the specially modified LD created on the double heterostructure GaAlA/GaAs with saturable absorption section. The used BLD structure made it possible for the bistability to arise only in the current impulse mode. To prove the bistability, the time method for bistability impulse verification (BIV) by LD, eventually BLD was proposed. With the use of the BIV method, basic parameters of the hysteresis loop of the W-A characteristic samples of realized BLD were determined. Also the mathematic model of the W-A characteristic was derived, used for the simulation of the characteristic for the

realized BLD. The achieved characteristics were optimized in accordance to the measured results. Element values of the electrical equivalent circuit of the BLD for small changes of signal were calculated for selected operating points of the simulated W-A characteristics.

The BLD was realized by using the ternary GaAs/GaAlAs structure with a double hetero junction and a multiple-divided contact stripe. The manner of masking was selected according to [2], the contact isle distance was increased from 10 to 20 μm . The axis length of the contact isles is 30 μm and the width is 10 μm . To verify bistability, two synchronized impulse power generators were used, whose impulses were lead to the measured sample, fixed in the measuring head. Current from the first generator set the BLD operating point, the second generator generated the setting and resetting impulse. Waveforms were monitored on the sampling oscilloscope and recorded on the plotter. The waveforms made it possible to determine the BLD impulse W-A characteristic and read the basic parameters of the hysteresis loop.

The dependency of bistability on the temperature is monitored by measuring the BLD W-A characteristic. The method uses the W-A characteristic integral impulse measuring device, which makes it possible to change the filling coefficient of exciting current impulses and to monitor the dependency of the integrated optical power on the amplitude of exciting current impulses and records this dependency on a plotter. The BLD element was placed into a cryostat and the impact of the temperature on the parameters of the W-A characteristic hysteresis loop was monitored for various temperatures. The range of temperatures where bistability occurred was from - 10 to + 22°C.

For verifying the theory of the measured results, the mathematical model of the W-A characteristic was derived by a static solution of the system of rate equations [4], respecting the dependency of the lifetime of carriers to their concentration in the active BLD layer. Physical constants were determined from the measuring of the cut-off frequency of the modulation characteristic of BLD below the threshold and from frequency measuring of foton-electron resonance of samples above the threshold. Values of physical constants were optimized throughout the simulation process. For selected points of operation on the W-A characteristic, the equivalent electrical small signal BLD circuit was calculated for small signal changes. Based on the knowledge of equivalent electrical small signal circuit, the stability of the semiconductor LD radiation can be analyzed, or an electronic modulation circuit can also be designed, to reach the required radiant response of the semiconductor LD respectively BLD.

References:

- [1] CH. HARDER, K. LAU, A. YARIV: *Bistability and pulsations in semiconductor lasers with inhomogenous current injection*, J. Quantum Electronics, QE 18, 1982 pp. 1351-1356.
- [2] H. KAWAGUCHI, G. IWANE: *Bistable operation in semiconductor lasers with inhomogenous excitation* Electron.Letters, Volume 17, 1991 pp. 167-173.
- [3] S. I. PEGG, M. J. ADAMS AND K. POGUNTKE: *Simultaneous absorptive and dispersive all-optical switching of a multi-section bistable laser diode*, Optics Communications, Volume 174, Issues 1-4, 2000, pp. 191-194.
- [4] V.JEŘÁBEK: *Characteristics of the bistable laser diode with a multiple-divided contact strip*, Slaboproudý obzor, Volume 50, 1998, pp.9-16

Overview of the Experimental GNSS Software Receiver Design Issues

P. Puričer, J. Špaček, P. Kovář, L. Seidl

puricep@fel.cvut.cz

Department of Radioelectronics, Faculty of Electrical Engineering, Czech Technical University, Technická 2, 166 27 Prague 6, Czech Republic

Introduction

Modern approach to signal processing in radio systems moves more and more to digital signal processing. High performance analog to digital and digital to analog converters together with high computational power of programmable devices and digital signal processors enable to digitally realize both basic blocks and whole signal processing stages in present systems like radio receivers and radio transmitters. It is possible to process signal bandwidth of hundreds of MHz without loss of dynamic range.

The concept of radio receiver, whose main parts of signal processing chain are realized digitally by programmable digital circuits, is usually called Software Defined Radio (SDR) or simply Software Radio.

Experimental GNSS software receiver

The experimental GNSS receiver [1-3] based on software radio architecture has been developed at the Czech Technical University for the processing of present and future global navigation satellite systems. For the biggest possible versatility, the modular concept was chosen. The receiver consists of three units: two-channel RF unit that covers frequency band 1 – 2 GHz, a DSP unit based on FPGA device, and a high power computer unit. In the first version of receiver the DSP unit was based on FPGA Virtex-II platform realized as a PCI interface card for PC workstation running Windows 2000 operating system.

The main difficulties with the first version of GNSS receiver were represented by problems with real time handling of the GNSS correlators and communication with the DSP card via PCI bus. The discussed problems are fully solved in the latest version, which is based on the Virtex-II Pro platform. The new FPGA platform enables single chip integration of all digital processing parts, i.e. correlators and computer for tracking and navigation task resolving. For achieving higher reliability of the whole system, the true real time multitasking operating system MicroC/OS-II is chosen instead of Windows 2000.

Virtex-II Pro FPGA chip includes two PowerPC processors operating at 300 MHz with 128 Kbytes internal and 8 Mbytes shared external memory and peripherals connected on shared peripheral bus OPB, like UART, timer, interrupt controller and array of ten to fifty GPS/GLONASS correlators.

Signal processing design and implementation in GNSS software receiver

Generally, the SDR concept can be realized by two ways. The first approach uses description of signal processing algorithms completely in some of programming languages and its implementation in processor or DSP device. The second approach enables to share signal processing between structures of programmable logic (e.g. FPGA) and algorithms running in processor. The signal processing is then represented by combination of code describing configuration of programmable logic and code running in processor. Simple but numerically

demanding operations e.g. signal filtration, modulation, demodulation, and coding are realized by programmable structures in FPGA device. The other operations that are less computationally demanding but very complex are then executed by convenient processors or DSP devices. These operations include data processing in link and network layers and system interface and control, programmed by assembler or higher programming languages. The FPGA devices, e.g. Xilinx Virtex-II Pro with several PowerPC cores embedded in the device, profit from embedded processor power and its direct connection to blocks formed by FPGA structures without loss of structures available for use in the design. The concept of embedded hardware processor in FPGA device was chosen for experimental GNSS receiver described in this paper.

The software design flow combines both FPGA configuration and software for processor. For seamless integration of both parts, it can be used some kind of various CAD Integrated design environments (IDE) provided by FPGA devices manufacturers. For the design of experimental GNSS receiver from this paper the combination of IDE Xilinx Platform Studio by Xilinx was used.

DSP software design flow begins by the system modeling and evaluation in Matlab Simulink using Xilinx Blockset. Then the Simulink system is compiled using Xilinx System Generator for DSP to the VHDL language.

Simulink models do not support some special subsystems like bi-directional busses and other special circuits. These auxiliary blocks are described directly in VHDL language and they are added to the project. The VHDL code is processed in the standard software ISE 5.1 tools by Xilinx. Before the implementation of the program to the FPGA the correct function of the DSP can be simulated using VHDL simulation tools. Final target code is then implemented inside the FPGA and tested in the real hardware.

Conclusion

SDR concept is prospective approach to signal processing in radio systems, including navigation systems. The advantage of software oriented approach resides in easy configuration and modification of signal processing algorithms.

References:

- [1] F. VEJRAŽKA, P. KOVÁŘ, L. SEIDL, P. KAČMAŘÍK: *Experimental Software Receiver of Signal of Satellite Navigation Systems* In: Proceedings of the 11th IAIN World Congress on Smart Navigation - Systems and Services, Deutsche Gesellschaft für Ordnung und Navigation (DGON), Berlin 2003.
- [2] . VEJRAŽKA, P. KOVÁŘ, L. SEIDL, P. KAČMAŘÍK: *Experimental GPS Software Receiver for Indoor Navigation*. In: Proceedings of 2003 International Symposium on GPS/GNSS, Tokyo University of Marine Science and Technology, Tokyo, 2003, pp. 3–8.
- [3] P. KAČMAŘÍK, P. KOVÁŘ, L. SEIDL, M. VIČAN, P. PURIČER, J. ŠPAČEK, F. VEJRAŽKA: *Software Solution of GNSS Receiver*. In: Proceedings of Workshop 2004, ČVUT, Praha, 2004, pp. 440–č. 441.

This research has been supported by grant of the Ministry of Transport of the Czech Republic "Participation of the Czech Republic in Galileo Project" CE802210112.

Advanced Methods of Description of Imaging Systems

J. Hozman

hozman@fel.cvut.cz

Institute for Biomedical Engineering, Czech Technical University,
Sítňá 3105, 272 01 Kladno, Czech Republic

Recently the imaging technology plays very important role in the field of biomedical technology. In many imaging systems, the imaging with semiconductor devices is replacing the conventional photography. Image sensors based on CCD and CMOS technology are more suitable than the conventional photography. Because there is preferred the evaluation of image quality, some relevant dependencies concerning to the geometrical structure (2D sampling structure) of the image sensor, especially in the case of large area image sensors are very important. Based on long term experience the MTF (Modulation Transfer Function) has been used as one of the common image quality parameter – in more cases in the image quality evaluation based on the two-dimensional MTF.

In a standard imaging approach an imaging system is described by the Point Spread Function (PSF) or the Modulation Transfer Function (MTF). There can be defined the response of imaging system to the point light source (2D Dirac impulse) as the impulse response or PSF. The PSF is frequently used to characterize, e.g. the optical blur. The relationship between the image and original is given by the convolution of the original with PSF [1]. In the frequency domain the convolution (a linear system is supposed) becomes a product. The Fourier transform of the PSF is known as the Optical Transfer Function (OTF). The OTF is generally complex and thus it has a module and argument. The module OTF is called the MTF or Contrast Transfer Function (CTF). The argument is called the Phase Transfer Function (PTF). In our case is supposed imaging systems without aberrations. It implies, that $PTF=0$. There can be also defined so called “contrast” that helps to describe the contrast transfer efficiency by MTF with respect to spatial frequencies with appropriate brightness. All parts of the imaging systems, i.e. atmosphere, objective, image sensor, image processing, image display and finally the observer's eye can be described by the MTF. The MTF of the whole imaging system is than given by the product of all particular MTFs. But the main task was to evaluate the sensor MTF.

There are very useful relationships among the PSF, OTF and MTF via Fourier transform [1]. We have used the analogy between optical imaging systems and electro-optical imaging systems. Because the CCD and CMOS sensors are so called intensity sensors, it means that they cannot sense phase information, and thus we can consider the pixel shape and pixel sensitivity profile as PSF. Then we can use the same mathematical operations as above described.

There are several approaches how to obtain the OTF (MTF) including 2D case [2]. From the point of view of the image sensor we have used the following methods:

- Image sensor OTF computation based on the definition of the pixel shape and sampling grid [1-3],
- Computation of the MTF based on the contrast modulation evaluation [1-3],
- Computation of the MTF based on the deconvolution [2],
- MTF measurement based on the random patterns or LSF (ESF) [4].

From the point of the image sensor there is very important to describe the process of spatial image sampling. Based on the theory of sampling, we can state that the real sampling model of the image sensor is represented by the convolution of an input image and a finite sampling aperture with different distribution over the sampling aperture area multiplied by sampling functions (sampling grid) [2]. There is also included to our consideration the effect of fill factor [2].

From the theoretical point of view we have computed the detector MTF for the set of different pixel shapes (rectangular shaped detector, L-shaped detector, rhombus shaped detector, hexagonal shaped detector, octagonal shaped detector and circular shaped detector) [3]. The uniform pixel sensitivity distribution was used within the all sections. The linear spatial invariant systems were used. MTF of the linear spatial variant system has been partially solved, e.g. for the case of the log-polar arrangement of the sensor or for the retina like sensors utilizing the retina structures from animals. Nevertheless the systematic solution will be performed in the future.

From the point of view of the requirements of the system modeling we have used GUI application called Image Sensor MOdeling Toolbox (ISMOT) [3]. This application enables modeling of the following tasks:

- Optical subsystem properties (f , D , distance, λ),
- Spatial frequency settings,
- Detector shape and sampling grid,
- CCD sensor specific properties (diffusion, CTE),
- GUI chart properties (selected MTFs, overall MTF of selected subsystems).

We have tested the different geometrical structures of an area image sensor, based on finding of optimal MTF, e.g. to have Nyquist spatial frequency as high as possible and minimum and small peaks beyond the Nyquist spatial frequency, that represent aliasing. Currently, most of the CCD or CMOS detector arrays utilize a rectangular geometry. However, other detecting and sampling structures may offer an improved performance, like rhombus [3]. If the sampling geometry is rhombus, there is possibility to obtain 100% fill factor as well. There was tested a sensitivity distribution also. We have used LSF (Line Spread Function) profile as a suitable tool. An ideal sensitivity distribution is Dirac impulse from that follows $MTF=100\%$. The Gauss distribution sensitivity seems to be an optimal case. References:

- [1] S. VITEK, J. HOZMAN: *Image Quality Influenced by Image Sensor Parameters*, Proceedings of SPIE Vol. 5036, SPIE Press, 2002, pp. 14-19.
- [2] J. HOZMAN, K. FLIEGEL, S. VÍTEK, P. PÁTA: *The Effect of Image Sensor Configurations on Image Quality*, Proceedings IWSSIP'03 - Recent Trends in Multimedia Information Processing, Sdělovací technika, 2003, pp. 272-275.
- [3] J. HOZMAN, K. FLIEGEL: *Optimal Sampling Structure of Image Sensors from the Point of View of Image Quality*, Proceedings of the 11th International Workshop on Signals, Systems, and Image Processing – IWSSIP'04, 2004, pp. 371-374.
- [4] S. VÍTEK, J. HOZMAN, P. PÁTA: *Analyse of Transfer Function of Image Sensors*, Proceedings of the INTEGRAL Universe, European Space Agency, 2004, pp. 801-804.

This research has been supported by CTU grant No. CTU0409813.

Sensors and Microsystems with Thin-Film Piezoresistive Layers for Measurement of Mechanical Values at High Temperatures

P. Kulha*, M. Husák*, Z. Výborný, F. Vaněk*****

kulhap@fel.cvut.cz

*Department of Microelectronics, Faculty of Electrical Engineering, Czech Technical University, Technická 2, 166 27 Prague 6, Czech Republic

**Institute of Physics, AS CR, Cukrovarnická 10, 162 53 Prague 6, Czech Republic

***Institute of Thermomechanics, AS CR, Dolejškova 5, 182 00 Praha 8, Czech Republic

We present properties of piezoresistive sensor with thin-film piezoresistive layers. In this paper is described methodology of measurement and modeling of these sensors with the aim to use that structure as a sensor of mechanical quantities [1,2]. Static parameters and temperature range of their usability have been measured on realized samples. We compare sensors based on implanted strain gauges and sputtered thin-film strain gauges as well. The basic function of the semiconductor strain gauge is based on transforming the changes of dimension in certain direction to change its electric resistance [2]. Deformation of measured object causes the change of strain gauge dimension. It allows measuring of plenty nonelectrical quantities such deformation, bending, force, acceleration etc.

There were designed a new topologies of testing thin-film piezoresistive structures in the first stage. The experimental work followed, the material constants (gauge factor etc.) was obtained and used in MEMS simulator CoventorWare. The designed topologies were simulated and verified. There are several testing structures, from single resistors through half-bridges to full Wheatstone bridges and complex structures with several half-bridges.

The software package CoventorWare was used for design of mechanical and thermal characteristics of the structure. The tools enable design, modelling and successive modification of designed MEMS structures. For successful simulation, it is necessary to input all material constants correctly. There have been realised Mechanical, Piezoresistive and Thermal simulations [1,3].

Mechanical simulation calculates bend of the cantilever and value of mechanical strain on the surface of the cantilever caused by this bend.

Piezoresistive simulation calculates magnitude of voltage on meander at constant current in dependence on cantilever deformation caused by effective force.

Thermal simulation, results of this simulation are data on mechanical strain arising in connection of cantilever with base due to different thermal expansion of material of base and Si.

There have been measured a number of parameters of realised samples in dependence on mechanical strain and temperature and reverse voltage and junction capacity as well. From the measured values there have been calculated further parameters like values of piezoresistive coefficients, coefficients of deformation sensitivity, deviations from linearity, hysteresis and temperature coefficients of resistance.

The main goals of this work were: to establish measurement system which is controlled via personal computer via GPIB bus. This allows automatic measurement and data acquisition and processing. The next goal was design and characterisation of sensors with thin-film sputtered layers. Measured and calculated characteristics piezoresistive samples exhibit very good linearity, low hysteresis at load but unfortunately the gauge factor is relatively low. The future work will focus on increasing of gauge factor and sensitivity of our piezoresistive layers and design of sensors based on materials suitable for high temperatures e.g. diamond or silicon carbide [4].

References:

- [1] J.W. GARGNER *Microsensors, MEMS, and Smart Devices* Wiley 2000
- [2] M. ELWENSPOEK, R. WIEGERINK *Mechanical Microsensors* Springer 2002,
- [3] L. CAO, S.C. MANTELL *Simulation and fabrication of piezoresistive membrane type MEMS strain sensors, Journal Sensors and Actuators A: Physical* Vol./Iss. : 80 / 3 2002, pp. 273-279
- [4] E. BENNICI, M. COCUZZA, F. GIORGIS, P. MANDRACCI, C.F. PIRRI, S. PORRO, C. RICCIARDI, D. BICH, V. GUGLIELMETTI, P. SCHINA, A. TARONI, D. CRESCINI *Silicon carbide for application in MEMS technology and sensors* Proceedings of the II National Meeting on Silicon Carbide 2002

This research has been supported by CTU grant No. CTU0407713

Quantum Devices Transport Simulation

T. Třebický, J. Voves

trebict@feld.cvut.cz

Department of Microelectronics, Faculty of Electrical Engineering, Czech Technical University, Technická 2, 166 27 Prague 6, Czech Republic

Simulation is very important phase in development of semiconductor structures. Main purpose of the procedure of simulation is in testing the functionality of given structure and to determine its significant characteristics. With more sophisticated simulators in terms of the best physical model we can even predict the properties of these structures. It might put aside the manufacturing of non functional devices, so its place in a stage of development is well-earned.

There exist a lot of possible physical models that lead to the same quantitative results. All these models have in common the Schrödinger equation and can be classified as either dynamic (coherent) or kinetic. Most uses of the Schrödinger equation for quantum system simulation are based on a scaled single-particle wavefunction as the state function, since the exact many-particle wavefunction becomes unmanageably complex with more than just a few carriers. Two features of quantum electronic devices have not been accurately treated with the Schrödinger equation approach: absorbing boundary conditions (*e.g.*, ohmic contacts) in a transient simulation, and inelastic scattering. We can see this as a crucial problem and focus to find other way that will lead to better results without systematic limitations. Kinetic models such as density matrix, Green function or Wigner function are the way. They employ statistical state function, rather than the exact many-quanta wavefunction as with the Schrödinger function (SE) or one wavefunction per energy as with the transfer matrix method (TMM). Quantum statistical mechanics does not attempt to retain all information about the evolutions and interactions of perhaps millions of distinct quanta, but rather deals with continuous distributions of particles and interactions. A statistical state function is thus a natural and efficient way to model particles in many-body systems. A statistical approach should also be quite accurate - the myriad single-particle wavefunctions intermingle so completely that they can not be distinguished anyway. The statistical state function is usually formed by assuming total particle independence (the one-particle approximation).

If we speak of accuracy, we also have to mention the computational speed of simulations. In other words we talk about efficiency of model's algorithm. We can say that SE and TMM uses one of the lowest computational-requirement algorithms. In contrast the Green function approach has relatively bad computation efficiency. Remaining two models, the density matrix and Wigner function takes a middle position in this comparison.

Let's focus on the TMM which popularity is mainly due to its simplicity (in both theory and programming), and which is currently the only implemented solution of our quantum device simulator. The TMM represents one possible way to surmount the absorbing boundary problem of the Schrödinger equation - solving the equation in steady-state. The TMM is based on the assumptions that particles enter and leave the system as continuous beams with amplitudes given by the fixed boundary conditions, that a particle beam entering at a given energy is perfectly phase-coherent, and that particle beams at different energies do not interact. The result is a state function for each particle beam which is simply a scaled, steady-state, single-particle wavefunction. However, because it is based directly on the Schrödinger equation, the TMM also can not handle irreversibility (inelastic scattering). Further, because continuous particle beams are assumed throughout the system, transient simulations are almost impossible to implement using the TMM.

Another aspect of every computer simulation resides in representation of numbers on different platforms. Our case is based on x86 where is very difficult to combine required accuracy and absolute time of simulation because of the calculation of extremely low or high exponential numbers. Only possible solution is to choose between different levels of arithmetic's precision.

Actually we are interested in simulation of resonant tunneling diodes even though the simulator is capable of dealing with arbitrary quantum device structure. Particular process of computing characteristic properties consists of several stages. First of all we have to transform the current structure to a suitable grid using a proper procedure, in our case piecewise-constant node-bounded potential profile. Next step consists of two closely tied parts. We have to count so called transmission amplitude T of an incident wavefunction for all significant energies throughout the whole structure (grid respectively). Each result of T has to be properly add to arrive at total current flow through the device. In every point of the grid for all computed energies the wavefunction coefficients has to be stored because of the future calculation of the carrier density profile.

Important property of every quantum device simulator is self-consistency. It is a smooth cross-over between Schrödinger equation and Poisson equation to get the authentic potential profile in according to accumulation of carriers. This solution enables us to clearly observe the current-voltage characteristic's hysteresis. Another enhancement consists in a simple but significant modification of the TMM which rests on the use of node-centered grid regions, where grid interfaces are half-way between nodes rather than at the nodes of the grid. We might even add in a piece-wise linear interpolation or use a finite element analysis to obtain even more creditable potential profile.

In despite of the limitations of the TMM stated above the objective results of simulation are close to being real.

References:

- [1] BIEGEL, B. A.: *Quantum Electronic Device Simulation* A Dissertation 1997, pp. 48-49
- [2] DAVIES, J. H.: *The Physics of Low-Dimensional Semiconductors* ISBN 0-521-48148(48491), pp. 145-177

Inovation of Control Systems Education

P. Burget, J.Pšenička, J. Bayer, B. Kirchmann

burgetpa@control.felk.cvut.cz

Czech Technical University in Prague

Faculty of Electrical Engineering, Department of Control Engineering

Karlovo nám. 13, 121 35 Praha 2

The main goal of this work is to design and realize a mechanical model controlled by synchronous motors. We show their synchronization and cooperation. Controlling of each motor is provided by servo drive (Acopos) that is controlled by PLC via communication Ethernet PowerLink [3]. Originally, we intended to use application profile ProfiDrive v3.0, which is based on Profibus DP-V2. However, finally we decided to base the model on a real-time Ethernet protocol, namely Ethernet Powerlink. Several of the main reasons are the increasing popularity and usability of real-time Ethernet communication and proven functionality of one of such protocols, i.e. Ethernet Powerlink.

Positional control [1]

Part of many automation tasks is to control one or more axes, not only in the areas of CNC applications. In real world, this problem is often tightly interconnected with general control of the machine or technology, thus providing space for applications and/or products, integrating both the general control and multi-axes synchronization.

Requirements for such tasks are obvious – on one hand it is comfortable to work with PLC with all its advantages (arbitrary control algorithms, extensive memory, great communication and visualization possibilities), on the other hand the servo drives [2] (usually and preferably digital ones) must be precise enough, offering high dynamics and accuracy for the whole process.

Unfortunately this solution usually has a disadvantage – the necessity to solve the own application tasks (it means the general and position control tasks), and the transfer of the information and commands from one part to another ones, i.e. the communication between the PLC and the servo drives. Using standard analog or digital signals for the transmission, only limited features of the servo drives can be exploited, although such data transfer can be fast and simple. A better solution is to use communications possibilities of the servo drives and PLC, e.g. CAN, Profibus DP-V2 or Ethernet PowerLink.

As mentioned above, we decided to use Ethernet PowerLink, which is a modern protocol for the data transfer in real time, allowing synchronization of the individual nodes, mutual communication among the drives without master intervention, etc. Ethernet PowerLink has a constant cycle time with the minimum jitter of synchronization ticks. For this reason it is suitable for control of multi-axis mechanisms.

Position control itself can may be realized by special control commands called ncActions[1] and/or by defined CAM profiles. The **positioning procedure via ncActions** is programmed in an application task in the master PLC using a data-structure representation of the controlled axis. The structure's individual members describe the characteristics of the axis (input/output signals, parameters of the regulator, limit values, set target values for the movements, e.g. speed, position and acceleration, actual values etc.) The ncActions operate above the NC structure, issuing commands for parameterization and control (e.g. initialization parameters, switch on/off the regulator, start/stop movement etc.). The NC manager of the PLC then performs the communication with the operating system of the servo drive using

Ethernet PowerLink, and handles the following jobs during cyclic operation: transfer parameter data (e.g. control parameter, encoder parameter, motor data etc.), process data (e.g. temperature values, current dynamic power, etc.) and commands to the servo amplifier, read status data (warnings and errors) from servo amplifier and make entries in the NC structure.

The operating system of the servo drive obtains: set value generator (calculates an optimal set value sequence from the application parameters without exceeding the specified maximum values), actual value evaluation (evaluation of the encoder data, line currents and temperature values) and control logic.

The **control via CAM profiles** is realized by defined trajectories of the position, speed and acceleration. The defined CAM profile is depends on the behavior of the master axis, which represents the course of time. The CAM profile does not handle parameters of regulator and others parameters of the servo drive. To set the parameters ncActions must be used. The graphic editor is used to define necessary trajectories. We must define master – slave dependence of axes and can define technology functions, e.g. electronic gearbox, switch CAM, position CAM, CNC systems and etc.

Controlled model

There are two linear belt modules (from the Bosch Rexroth company) mounted on a steel construction. Every module is driven by a synchronous servo motor. The next servo motor is fixed at each module. At this motor a holder of the ball is mounted. As a result, one pair of servo motors executes movements up or down and second pair of motors executes movement to the side.

The individual motors contain encoder (resolver) to scan the actual position and speed. Motors handling vertical movement contain an electric brake. All motors are controlled by the servo drives [2]. Separate movement of all motors is realized by the pulse width modulation (PWM) of the supply voltage of each motor with the basic frequency 20 kHz. This frequency is sufficient to the exact realization of the calculated actions. The control algorithm is processed in the PLC, which realizes the transfer of the commands to the servo drive and exchanges all controls and status data via Ethernet PowerLink with the communication cycle of 400ms.

The model is programmed to execute two functions. First of them is the “Catapult” which consist of kicking up (drop) the ball in the vertical direction and follow-up catching this ball. This part was programmed by “ncActions”. Second function is the “Juggler” which throwing the ball between the both holders from one side to second and was programmed using “CAM profiles”. The touch screen, which is integrated in the PLC, is used to control the model and to visualize the actual data.

References:

- [1] B+R INDUSTRIE-ELEKTRONIK: *Stnacpint_e.pdf* Aut, 2004 pp. 154–242.
- [2] B+R INDUSTRIE-ELEKTRONIK: *MAACP2-E.pdf* Aut, 2003, pp. 31–97.
- [3] B+R INDUSTRIE-ELEKTRONIK: *PowerLinkWP_0005_eng.pdf* Aut, 2002
- [4] VALENTINE, R.: *Motor Control Electronics Handbook*, McGraw-Hill Handbooks, 1998.

This research has been supported by project CTU0418313.

Modelling of Special Types of Acoustic Receivers

P. Honzík, M. Lukeš, D. Kovář

honzikp@fel.cvut.cz

Department of Radioelectronics, Faculty of Electrical Engineering, Czech Technical University, Technická 2, 166 27 Prague 6, Czech Republic

In recent years the acoustic receivers are becoming specialized, their fabrication is more complicated and more expensive. As a result the importance of the modelling of these systems is rising. This contribution deals with miniature silicon condenser microphones with different shapes of moving and back electrodes and microphone with direct analog-to-digital conversion. The model is based on electro-acoustic analogy [1] and the study leads to the equivalent lumped element circuit.

First, the properties of thin plates of different shapes used as moving electrodes were studied. The displacement of the plates was found by solving the wave equation, which is the differential equation of the fourth order. From the displacement the mechanical impedance is derived [2]. We assumed an equivalent circuit of the moving plate in the form of the second Foster's reactance two-pole network. The comparison of the impedance of this network and the mechanical impedance of the moving plate gives the expressions for the mechanical masses and mechanical compliances. Using this method the equivalent lumped element circuits of rectangular and circular plates clamped at the centre and at the edges have been found. The analytical results have been verified by the numerical analysis using the Finite Elements Method.

The thinner the air-gap between moving and back electrode is, the more sensitive the microphone gets, but due to the air viscosity the movement of the moving electrode is more damped. In order to suppress this damping the back electrode can be perforated, but there is another way more suitable for micromachining fabrication, which is a non-planar back electrode. The electrostatic transducer with rectangular moving electrode and non-planar non-perforated back electrode as a miniature silicon microphone has been studied [3]. The equations describing the electroacoustic transduction by the transducer coefficient, the transducer capacitance, generalized displacement and negative stiffness have been derived and these coefficients have been expressed. We consider the moving electrode being the rectangular diaphragm and vibrating under the first resonance frequency. Then the equivalent circuit of the diaphragm can be simplified to the serial combination of one mechanical mass and one mechanical compliance. The equivalent circuit of the air-gap is the two-port network having the output connected to the peripheral cavity, which is modelled by its compliance. The two-port network modelling the air-gap consists of a compliance, a mass and a resistance. The expression of the compliance and the mass comes from the solution of wave equation for velocity potential which is derived from the continuity equation. The resistance caused by the air viscosity can be derived supposing an incompressible viscous fluid in the air-gap. The equation of motion for this fluid is the Navier-Stokes equation. By solving this equation we find the velocity and the volume velocity in the air-gap and its relation to the acoustic pressure in the air-gap. The ratio of the pressure and the volume velocity is simply the acoustic impedance, at low frequencies we take into account only the resistance caused by the viscous losses. This resistance models the damping of the moving electrode.

Another type of special acoustic receiver is the microphone with direct analog-to-digital conversion. We have focused on the electrostatic transducer with the new concept of detecting and driving electrodes [4]. This transducer consists of the diaphragm positioned between the detecting electrode and several driving electrodes. The displacement of the

diaphragm caused by the acoustic pressure is detected by the detecting electrode as in the case of classical condenser microphone. Then the driving electrodes working as the actuators compensate this displacement. Every driving electrode corresponds to one bit, the digital information is which driving electrodes have to be activated to compensate the diaphragm displacement. The diaphragm displacement compensating effect is weighted by the significance of the bit for each driving electrode. In the case of our transducer this weighting is realized by the different area of the driving electrodes. The non-piston like vibrating mode of the circular diaphragm was taken into account. The electrostatic transducer with circular diaphragm, planar or non-planar detecting electrode and several prototypes of driving electrodes for 4, 5 and 6 bits direct analog-to-digital converting microphone have been realized. Subsequent work will focus on the electronic parts of the microphone.

In this work the using of electro-acoustic analogy for modelling of some special types of acoustic receivers has been presented. The equivalent lumped element circuit of thin plates of different shapes used as moving electrodes was found, the theory of electrostatic transducer with rectangular moving electrode and non-planar non-perforated back electrode as a miniature silicon microphone has been studied and the experimental electrostatic transducer used as the microphone with direct analog-to-digital conversion was described.

References:

- [1] ŠKVOR, Z.: *Akustika a elektroakustika* Praha: Academia, 2001.
- [2] LUKEŠ, M.: *Mechanical Impedance of Thin Rectangular and Circular Plates* Proceedings of Inter-Noise 2004 [CD-ROM]. Prague: Czech Acoustic Society, 2004, pp. 750.
- [3] HONZÍK, P.: *Miniature Silicon Microphone with Non-Planar Back Plate* 8th International Student Conference on Electrical Engineering, POSTER 2004, May 20 2004, Prague [CD-ROM]. Praha: CVUT FEL Praha, 2004, pp. EI10.
- [4] KOVÁŘ, D.: *Thin Circular Diaphragm as a Part of a Direct Converting Digital Transducer* Proceedings of Inter-Noise 2004 [CD-ROM]. Prague: Czech Acoustic Society, 2004, pp. 789.

This research has been supported by CTU grant No. CTU0409713.

LC Network for Generation of Solitons

T. Martan

`martant@feld.cvut.cz`

Department of Electromagnetic Field, Faculty of Electrical Engineering, Czech Technical University, Technická 2, 166 27 Prague 6

Institute of Radio Engineering and Electronics, Academy of Sciences of the Czech Republic, Chaberská 57, 182 51, Prague 8.

Introduction

This paper deals with construction of LC network and with measurement of voltage Korteweg-de Vreis (KdV) solitons, which were generated on this nonlinear LC network.

The voltage KdV solitons are analogy of optical solitons, which can be generated e.g. in standard single-mode optical fibers or in special optical fibers, such as in high nonlinear microstructure optical fibers or in fiber tapers. KdV solitons were generated on newly constructed LC network from different input voltage profiles. Nonlinear LC network was constructed for stable solitons generation and for observation of phenomena, which nascent during solitons propagation.

Construction of the LC Network

Non-linear LC network consists of cascade of LC sections. Each non-linear LC section contains inductor and voltage variable capacitor (Varicap). Inductors with constant inductance $L = 28 \mu\text{H}$ ($\pm 2 \mu\text{H}$, measured on frequency $f = 1 \text{ MHz}$) were made by copper wire winding on toroidal core (T 10, $\mu_r = 230$). The Varicaps KB 109G were used in all non-linear LC sections, too. The capacity of the Varicaps was changed by a reverse voltage. The Varicap capacity was changed from $C_v = 30 \text{ pF}$ up to $C_v = 6 \text{ pF}$ for reverse voltage from $U_v = 3 \text{ V}$ up to $U_v = 25 \text{ V}$.

Measurement and Simulation

Constant voltage supply, analytical function generator and two-channel oscilloscope were used for measurement.

Constant voltage supply was used for Varicaps operating point set-up. An analytical function generator was used for generating of input voltage profiles. The two-channel oscilloscope and a personal computer were used for representation of recorded waveform.

One of two probes of oscilloscope was situated at the input of non-linear LC network. Second oscilloscope probe was situated at n-unit of four-terminal network for observation of transformation of input voltage profile. PC was used also for mathematical modeling of soliton properties and for comparing measured soliton shape and calculated soliton shape.

Stable solitons were propagating through nonlinear LC network after input voltage profile transformation. Time (distance) of transformation was depended on frequency and

amplitude of periodic input voltage and on reverse voltage of Varicaps. Time (distance) of transformation was not depended on shape of input voltage profile.

Conclusions

Stable soliton pulses were generated from different input voltage profiles on constructed nonlinear LC network. Input voltage profile was changed after very short time and during profile transformation of input voltage was measured stable solitons propagating on LC network without change of shape, amplitude, and velocity.

Stable soliton pulses were molded from all input voltage profiles (sinusoidal, rectangular and triangular). A few series of measurement was obtained by the two-channel oscilloscope. Each of series of measurement corresponded with one of input periodic course of voltage. Transformation of input periodic voltage profile and consequential formation of solitons were registered. These series of measurement was obtained by magnitude setting of reverse voltage of varicaps, by different magnitude setting of amplitude of input periodic voltage profile and different frequencies. Solitons was generated consequently from all input voltage profile (sinusoidal, rectangular and triangular) and in these all cases reached an agreement with theoretical behaviour of solution of Korteweg-de Vries (KdV) equation.

By measurement was demonstrated nonlinear behaviour of KdV solitons during solitons propagation. Solitons with different amplitude was formed on LC network for observation of velocity dependence of amplitude of soliton pulse. Soliton pulses are described by hyperbolic secans, which is solution of KdV equation. By measurement was verified mathematical model of propagation of soliton pulses with different amplitudes. A soliton of high amplitude travels faster than anyone of low amplitude. Measurement demonstrated other properties of solitons. Solitons saved their identities (shapes, velocities, and directions of propagation) after collisions. During the overlap time interval their joint amplitude changes non-linearly.

References:

- [1] MARTAN, T. - NOVOTNÝ, K. *Nelineární článkové vedení pro demonstraci mřížkových solitonů*, Sborník vzdělávacích a vědeckovýzkumných činností a nabídek, IEEE Czechoslovakia Section, Prague, 2004.
- [2] MARTAN, T.: *Measurement of Nonlinear Interaction of Voltage KdV Solitons*, Poster 2003, CTU, Faculty of Electrical Engineering, 2003, s. EI21, Prague, 2003.
- [3] MARTAN, T.: *Nelineární článkové vedení pro buzení solitonových pulsů, (diploma thesis)* Czech technical University in Prague, Dept. of Electromagnetic Field, Prague, 2001.
- [4] HASEGAWA, A. – KODAMA, Y.: *Solitons in Optical Communications*, Oxford University press, 1995.

This research has been supported by CTU grant No. CTU0406713.

Verification of CAN Bus Behaviour in Real-Time Systems

J. Krákora

krakorj@felk.cvut.cz

Czech Technical University in Prague, Faculty of Electrical Engineering,
Department of Control Engineering
Karlovo náměstí 13, Prague 2, 121 35, Czech Republic

This project dealt with a verification approach of a real time distributed system. Let us assume such system consisting of application processes (designed by application developer) running under Real-Time Operating System (RTOS e.g. OSEK) while using several processors interconnected via standard broadcast communication based on the Controller Area Network (CAN). The crucial problem is to verify both time properties (e.g. message response time, schedulability of periodic processes, response time) and logic properties (e.g. deadlock, mutual exclusion, priority based access) of the applications incorporating two kinds of shared resources - the processor and the bus. Classical approaches deal separately either with the processor sharing (studied for example by RMS) or with the bus sharing (e.g. CAN message latency studied by Tindell [1]).

Task schedulability on single-processor and multiprocessor systems is a widely studied subject. For example Rate Monotonic Scheduling (RMS) can be used to guarantee schedulability, when the application consisting of periodic processes is running on a single-processor with priority based pre-emptive kernel and the processes have their respective deadlines at the end of the period. RMS assigns fixed priorities to the processes according to their request rate (inverse to their period deadline), therefore the highest priority is assigned to the processes with highest frequency. Schedulability of such processes can be verified using Utilization bound theorem or Completion time theorem.

An important part of this project was to improve the CAN arbitration model composed of several timed automata: a bus automaton and a transmitter automaton per each message ID. Concrete CAN model, based on discrete event system is presented in [2]. The model consists of an arbitration automaton and a transceiver automaton per each message transmitted in the system. The Interface between the transceiver and the upper layer model (tasks) is provided by synchronization channels. Verification of the CAN model was compared to the results achieved by Tindell and Burns.

The next part of the project dealt with an integration of the CAN model with the model of the RTOS developed in [3]. The approach assumes a fine grain model treating the task internal structure, OS kernel, communication layer and the controlled environment. The task model consists of several blocks of code called computations, calls of OS services, selected variables, code branching and loops (affected by values of selected variables). The OS kernel model formalizes operating system services functionality. The controlled environment model, specifying arrival times of events, releasing the tasks or the messages, plays the key role in the system verification. An comprehensive analysis of this model behavior (automatically done by model checking tool UPPAAL) considers task and messages response times corresponding to a realistic phasing, realistic tasks and messages arrival times, realistic blocking and realistic execution time in a relation to the modeled code branching. Therefore the verification result is as precise as the model is.

Finally, the qualities of the project RTOS and communication bus modeling approach were proved on a real test bed. The test bed configuration consists of PC104 device and a several Motorola HC12 boards. The PC104 was configured as follows: CAN PCI card running RTLinux with OCERA LinCAN driver. The Motorola HC12 board includes MsCAN driver. The measurement on the test bed showed that our approach was correct.

The results of the project were presented at the FISITA 2004 - World Automotive Congress in Barcelona, at the 11th IFAC Symposium on Information Control Problems in Manufacturing and at the IEEE International Workshop on Factory Communication Systems in Vienna [4].

The list of the project results is as follows:

- Improved timed automata model of CAN was developed.
- The model was included to the RTOS model.
- A distributed RT system model was realized by the model and its properties were verified by temporal logic.
- Properties of such approach were validated at a test bed consisting of PC104 and three Motorola HC12 boards and compared to the timed automata results.
- The results were presented at several conferences (IFAC, IEEE).

References:

- [1] K. TINDELL AND A. BURNS: *Guaranteed message latencies for distributed safety critical hard real-time networks* . 1994 .
- [2] J. KRÁKORA AND Z. HANZÁLEK: *Timed automata approach to CAN verification* In 11th IFAC Symposium on Information Control Problems in Manufacturing - INCOM 2004 , 2004, CDROM.
- [3] L. WASZNIOWSKI, AND Z. HANZÁLEK: *Analysis of real-time operating system based applications* FORMATS 2003, 2003, pp. č. strany–č. strany.
- [4] J. KRÁKORA, L. WASZNIOWSKI, P. PÍŠA AND Z. HANZÁLEK: *Timed Automata Approach to Real Time Distributed System Verification* In Proceedings of 2004 IEEE International Workshop on Factory Communication Systems, 2004, pp. 407–410.

This research has been supported by CTU grant No. CTU0408113

Signal Acquisition and Tracking Methods in GNSS

L. Seidl, P. Kovář, P. Puričar, J. Špaček, M. Vičan, P. Kačmařík, F. Vejražka

Seidl@feld.cvut.cz

Czech Technical University, Faculty of Electrical Engineering, Department of
Radioelectronics
Technická 2, 166 27, Praha 6, Czech Republic

Global Navigation Satellite Systems (GNSS) represent a commonly used positioning, navigation and localization systems. GPS system is the most widespread Global Navigation Satellite System, it is the only one fully applicable global satellite position determination system on the world at present. The GPS can be perceived as a model for other following systems – Russian GLONASS and Galileo. The new European GNSS system Galileo is planned to be usable in 2008 and will bring an extension of the current GPS satellite segment to the 54-60 satellites. The integrated GNSS system GPS+Galileo will be more reliable due to better signal coverage and the safety and integrity improvement.

The GNSS position determination is based on the satellite-to-user distance measurement. GNSS satellites transmit the specially designed signal with spread spectrum modulation. The signal propagation delay is measured to obtain the distance information. Because the satellite orbital parameters are known, position and velocity of users receiver equipment is computed consecutively.

Development of the new European GNSS system Galileo, modernization of the GPS, and implementation of augmented systems WAAS and EGNOS require new approach to investigation of the signal processing in the receiver. Due to this challenge the Experimental GNSS Receiver based on Software Defined Radio (SDR) Architecture has been developed at the Czech Technical University in Prague. The receiver is determined for research and development of new GNSS signal processing algorithms including massive parallel processing for indoor navigation and for the study of new forms of the GNSS signals transmitted during the early phase of the Galileo mission.

The Experimental GNSS Receiver consists of two units: the Radio Frequency Unit (RFU) and the Digital Signal Processing Unit (DSP). The RFU contains two independent equivalent channels; each channel can operate at any frequency in the frequency band from 1 to 2 GHz. The bandwidth of each channel is adjustable up to 36 MHz. The output immediate-frequency wide-band signal (122-158 MHz) is sampled by 8-bit A/D converter with very low jitter and samples are passed to the DSP unit.

The DSP unit is based on the on the FPGA Virtex-II Pro. This solution presents integration of very powerful gate array with two or more processor cores PowerPC (PPC 405E) on 300 MHz and other support circuits such as set of multipliers for parallel algorithm realization or 200 to 600 kilobytes of in-chip memory. The concentration of these circuits in one chip device allows compact solution of complicated DSP unit. The used FPGA platform enables single chip integration of all digital processing parts of the GNSS receiver, i.e. correlators and signal filtering, signal tracking tasks and finally position-velocity-time (PVT) resolving, system integrity monitoring, navigation and other related tasks. The FPGA is fully programmable and one iteration of design procedure takes several tens of minutes only. Therefore, many variants of DSP algorithm solution can be verified and tested with real signal in suitable time duration.

The described DSP unit version is a successor of previous one based on the FPGA Virtex-II without internal PowerPC cores. This DSP unit was used for several early experiments in our laboratory and for weak parts inquiry of the receiver design.

The GNSS uses spread spectrum modulated signals. This modulation technique complicates detection of weak signals without adequately precise priori estimations of code delay and Doppler frequency shift. These parameters are unknown at the beginning of the signal search process. However, the parameter space has to be searched in both code-delay domain (with size M) and Doppler frequency domain (with size N). Since the sequential searching in two-dimensional space $M \cdot N$ is very slow, optimized parallel or quasi-parallel algorithms are investigated. Parallel search in code-delay domain requires using of massive parallel correlator structures and brings considerable requirements to hardware complexity and capacity. Parallel search in Doppler frequency domain can be realized effectively by FFT.

The GNSS signal synchronization in tracking phase is kept by two feedback loops – code-delay lock loop (DLL) and carrier-phase lock loop (PLL). Design of DLL in case of Galileo or modernized GPS signal is complicated due to used BOC signal modulation. Correlation function of BOC signal contains multiple local peaks. These side peaks phenomenon causes ambiguity in code-delay tracking and will be studied and investigated in the future. Using standard GPS correlation techniques for BOC signal tracking is not suitable because of ambiguity risk. Special correlators and code-delay discriminators design will be provided and tested in both forms – by software simulation on numeric signal model and by real signal testing with Experimental GNSS Receiver hardware.

The weak GNSS signal acquisition and BOC modulated signal tracking are the actual problems, which will be investigated in projects of new Galileo and modernized GPS receiver design and verifications of these receivers. We presume that developed Experimental GNSS Receiver is usable to be suitable platform for testing and development.

References:

- [1] KOVÁŘ, P. - VEJRAŽKA, F. - SEIDL, L. - KAČMAŘÍK, P.: *Reception of Signals of GLONASS System by Experimental GNSS Receiver*. In 11th Saint Petersburg International Conference on Integrated Navigation Systems. Moscow: Russian Academy of Sciences, 2004, pp. 210-212.
- [2] KOVÁŘ, P. - VEJRAŽKA, F. - ŠPAČEK, J.: *Availability of the EGNOS System for a Land Mobile User*. In Proceedings of the 2004 International Symposium on GPS/GNSS, GNSS-2004. Sydney: University of New South Wales, 2004, pp. 1-2.
- [3] SEIDL, L. - KOVÁŘ, P. - VIČAN, M. - KAČMAŘÍK, P. - VEJRAŽKA, F.: *GPS Signal Search Algorithm for Difficult Environment*. In Conference Proceedings of Radioelektronika 2004. Bratislava: Slovak University of Technology, 2004, vol. 1, pp. 140-143.
- [4] PURIČER, P. - KOVÁŘ, P. - ŠPAČEK, J. - VEJRAŽKA, F. - SEIDL, L. - ET AL.: *Signal Processing in Experimental GNSS Software Receiver*. In Proceedings of the 2nd ESA Workshop on Satellite Navigation User Equipment Technologies '2004. Noordwijk: ESA Publications Division, 2004, pp. 366-372.

This research has been supported by MD 802/210/112.

Modeling of IR Image Sensors

Stanislav Vítek

viteks@feld.cvut.cz

Department of Radioelectronics, Faculty of Electrical Engineering,
Czech Technical University,
Technická 2, 166 27 Prague 6, Czech Republic

The finding of the optimal model of the real imaging system (including the image sensors) is constantly actual theme in an area of obtaining, processing, reproduction (visualization) and archiving of any imaging data. All imaging data, in analogue and in digital representation, are distorted by the effects of sensing device (optical part and the active sensing unit – imaging sensor), by the effect of compressions (we can treat the compression algorithm as any other imaging system) and at the end by the effect of recording device. For the high-quality reproduction and potentially machine processing of the image data is necessary work down impact of imaging system and try to obtain better issues.

Specific part of this problem is special imaging systems used for scientific purposes, for example for example for obtaining of the imaging data in medicine and astronomy. Especially in astronomy is evident progress in technology for obtaining of imaging data in invisible parts of spectra – near infrared band (IR) and RTG band. The imaging sensors used for those purposes are based on another physical principles than the sensors used for visible part of spectra. In this part of research is necessary to determine criteria of image quality (objective and subjective) and find the model of imaging system which will be respect parameters required to determine this model.

In a standard imaging approach we describe an imaging system by the PSF or the MTF. We can define the response of the imaging system to a point light source (2D Dirac impulse) as the impulse response or the Point Spread Function (PSF). The PSF is frequently used to characterize e.g. the optical blur. The relationship of the imaged object and the original is given by the convolution of the original object with PSF. All parts of the imaging systems, i.e. atmosphere, objective, image sensor, image processing (including image compression methods as well), image display and finally the observer's eye can be described by MTF. The MTF of the whole imaging system based on the above-mentioned equations is than given by the product of all particular MTF.

There are a few approaches how to obtain the Modulation Transfer Function of image sensor. At first it is approach based on restoration methods, including deconvolution. Within these methods we use only image data and computational workstation. At second we can use specialized measuring system, e.g. interferometer that enabled to obtain 2D MTF. But this method is exacting in cost. At third there in our approach required to perform a set of 1D MTF (in a lot of angles) computational based on the contrast evaluation within the sinusoidal test pattern projection onto the imaging system. Then we can perform 3D interpolation to obtain a complete 2D MTF. This last approach was also implemented in Matlab and was used within the obtaining results.

In an area of the imaging sensor we are interesting of many parameters and only part of them has real impact to consequential image and quality of this image. Interesting

parameters for simulation purposes are fill factor, sampling distances, dimensions of pixels and area sensitivity of pixels. We can consider a few possible arrangement of sampling aperture: rectangular pixels, L-shaped pixels and symmetrical octagonal pixels.

For the modeling of all imaging systems is very usable the Matlab environment which is a full featured, flexible and low cost allowance of traditional measurement methods. The next task for the referenced work will be method for the obtaining of the better quality of imaging data – super-resolution.

References:

- [1] VITEK, S., VEJDELEK, J., PATA, P., BECVAR, M., CASTRO-TIRADO, A.J.: *The System for Autofocusing of wide-field cameras*, The 5-th Integral workshop 2004, pp. 797-799.
- [2] VITEK, S., PATA, P., HOZMAN, J.: *Analyse of transfer function of image sensors*, The 5-th Integral workshop, 2004, pp. 801-804.
- [3] HOLST, G.C.: *CCD arrays, Cameras and Displays*, SPIE press, Bellingham, 1998
- [4] YADID-PECHT, O.: *The Geometrical Modulation Transfer Fuction (MTF) - for different pixel active area shapes*, Optical Engineering 34, 2000, pp. 859–865.

This research has been supported by CTU grant No. CTU0410313.

Bistable Laser Diode with a Multiple-divided Contact Stripe

V. Jeřábek

jerabek@fel.cvut.cz

Department of Microelectronics, Faculty of Electrical Engineering, Czech Technical University, Technická 2, 166 27 Prague 6, Czech Republic

A new field which arose throughout the past few years is the field of integrated optoelectronics. Within this field of hybrid or even monolithic structures of optics, optoelectronic and electronic components are becoming useful for the transmission of information in the increase of speed up to several gigabits per second.

In the integrated optoelectronics field, there are also some rather new optoelectronic components originating. One of these is the bistable semiconductor laser diode (BLD) that makes use of the physical principle of saturated optical absorption. The general optical bistability belongs to a physical phenomenon, which was first assumed by Szöke in the year 1969 and only after, the words were experimentally observed. It was five years later, when Lasher thought about bistability especially through the semiconductor laser diode (LD). Optical bistability by LD belongs amongst the nonlinear dynamic optical phenomenon, originating in LD radiation, the essence of which is Q switching. This physical mechanism is based on nonlinear dependence of the absorption coefficient in the absorbing region of the divided active layer of the semiconductor LD and appears in LD radiation by providing the origin of self pulsations or optical bistability [1]. Few years ago, several papers took place, which described the origin of bistability on LD with a multiple heterostructure that was purposefully modified by dividing the stripe contact for achieving the bistable mode. The papers differed according to the physical mechanism bistability, technology and also according to the method of mask divided stripe contact [3].

As far as ternary BLD structures are concerned, the works used universally demanding technological creations in order to prevent the current spreading under the contact and to achieve a very low threshold current. With these structures, the continual bistable regime was achieved in room temperature. From the BLD created at the quaternary structures, the bistable mode was achieved by an easier technological order by using the multiply divided stripe contact. The component was working in the progressive bistable mode only under mild cooling. The important characteristic expressing the bistable BLD properties is the W-A characteristic. Its analytic expression is possible to be deduced by statically solving a set of three so called rate equations. The W-A characteristic was theoretically and also experimentally determined by a line of authorities [1], [4]. Under certain simplifying preconditions, it is possible to derive from the analytic expression, also basic conditions of bistability arising and also the conditions necessary for the origin of self pulsations in LD radiation.

This article deals with theoretical results and experiments, which led to the demonstration of optical bistability on the specially modified LD created on the double heterostructure GaAlAs/GaAs with saturable absorption section. The used BLD structure made it possible for the bistability to arise only in the current impulse mode. To prove the bistability, the time method for bistability impulse verification (BIV) by LD, eventually BLD was proposed. With the use of the BIV method, basic parameters of the hysteresis loop of the W-A characteristic samples of realized BLD were determined. Also the mathematic model of

the W-A characteristic was derived, used for the simulation of the characteristic for the realized BLD. The achieved characteristics were optimized in accordance to the measured results. Element values of the electrical equivalent circuit of the BLD for small changes of signal were calculated for selected operating points of the simulated W-A characteristics. The BLD was realized by using the ternary GaAs/GaAlAs structure with a double hetero junction and a multiple-divided contact stripe. The manner of masking was selected according to [2], the contact isle distance was increased from 10 to 20 μm . The axis length of the contact isles is 30 μm and the width is 10 μm . To verify bistability, two synchronized impulse power generators were used, whose impulses were lead to the measured sample, fixed in the measuring head. Current from the first generator set the BLD operating point, the second generator generated the setting and resetting impulse. Waveforms were monitored on the sampling oscilloscope and recorded on the plotter. The waveforms made it possible to determine the BLD impulse W-A characteristic and read the basic parameters of the hysteresis loop.

The dependency of bistability on the temperature is monitored by measuring the BLD W-A characteristic. The method uses the W-A characteristic integral impulse measuring device, which makes it possible to change the filling coefficient of exciting current impulses and to monitor the dependency of the integrated optical power on the amplitude of exciting current impulses and records this dependency on a plotter. The BLD element was placed into a cryostat and the impact of the temperature on the parameters of the W-A characteristic hysteresis loop was monitored for various temperatures. The range of temperatures where bistability occurred was from - 10 to + 22°C.

For verifying the theory of the measured results, the mathematical model of the W-A characteristic was derived by a static solution of the system of rate equations [4], respecting the dependency of the lifetime of carriers to their concentration in the active BLD layer. Physical constants were determined from the measuring of the cut-off frequency of the modulation characteristic of BLD below the threshold and from frequency measuring of foton-electron resonance of samples above the threshold. Values of physical constants were optimized throughout the simulation process. For selected points of operation on the W-A characteristic, the equivalent electrical small signal BLD circuit was calculated for small signal changes. Based on the knowledge of equivalent electrical small signal circuit, the stability of the semiconductor LD radiation can be analyzed, or an electronic modulation circuit can also be designed, to reach the required radiant response of the semiconductor LD respectfullyBLD.

References:

- [1] CH. HARDER, K. LAU, A. YARIV: *Bistability and pulsations in semiconductor lasers with inhomogenous current injection*, J. Quantum Electronics, QE 18, 1982 pp. 1351-1356.
- [2] H. KAWAGUCHI, G. IWANE: *Bistable operation in semiconductor lasers with inhomogenous excitation* Electron.Letters, Volume 17, 1991 pp. 167-173.
- [3] S. I. PEGG, M. J. ADAMS AND K. POGUNTKE: *Simultaneous absorptive and dispersive all-optical switching of a multi-section bistable laser diode*, Optics Communications, Volume 174, Issues 1-4, 2000, pp. 191-194.
- [4] V.JEŘÁBEK: *Characteristics of the bistable laser diode with a multiple-divided contact strip*, Slaboproudý obzor, Volume 50, 1998, pp.9-16

Educational Microcontroller at The Faculty of Transportation Sciences CTU in Prague

M.Leso*, V. Fábera**

leso@fd.cvut.cz, fabera@fd.cvut.cz

*Department of Control and Telematics, Faculty of Transportation Sciences,
Czech Technical University, Konviktská 20, 110 00 Praha 1, Czech Republic

**Department of Informatics and Telecommunications, Faculty of Transportation Sciences,
Czech Technical University, Konviktská 20, 110 00 Praha 1, Czech Republic

At the Faculty of Transportation Science was teaching course "Introduction to Computer Hardware" since 2000/2001. New course "One-chip microcontrollers" since 2005/2006 has been taught as continuation and amplification into one-chip microcontrollers. The course is in the category of optional subject and they are recommended for students who study "Automatization in Transportation and Telecommunications" specialization. The subject covers problems of One-chip microcontrollers and logical circuits, their architecture and design, programming etc.. For practical testing and developing with microcontrollers is very useful for students if they have an opportunity to work in laboratory, to connect some circuits and verify their functionality. For this purpose we accommodate the laboratory with some educational electronic modules.

As a general architecture we had choose AVR 8-bit architecture developed by Atmel inc. This architecture is new, modern, simply and powerful. Is very ideal for first contact with microcontroller and sufficient powerful for more application. In the concrete ATmega16 microcontroller was select. ATmega16 include in-circuit debugging across JTAG interface. For in-circuit debugging we buy JTAG debugger from MCU firm. This is the cheapest solution form in-circuit debugging compatible with AVRStudio.

For basic programming and using of microcontroller is used STK 500 developing board. For additional application we developed two extended boards connectable to STK500 across connectors.

- LCD display 16*2 characters and 9 buttons keyboards
- Traffic cross-road with 18LED's and 8Button's for simulating traffic cross-road controller

Interfaces of both extended boards are based on Xilinx CPLD, that serves make variety of connection interfaces between all peripheral and microcontrollers.

For programming of ATmega microcontrollers is usable free assembler compiler in AVRStudio development system from Atmel. For C programming is usable free GNU compiler AVRGCC. AVRStudio serves as simulator and in-circuit debugger for AVR microcontrollers is freeware.

Next the logic systems is added from Digilent inc. of this systems:

- PegasusXC2 evaluation board with Xilinx Spartan2 FPGA and some peripheral – Buttons,LEDs,7-segments display, etc.
- CERES evaluation board with Xilinx Coolrunner CPLD and some peripheral

This FPGA and CPLD boards are connectable to STK500 board across one interface.

Finally, new microcontrollers, logic systems and testing boards are added to educational laboratory. Students will be able to do some experiments with microcontrollers and logical circuits.

This research has been supported CTU 0419216.

Navigation System with Magnetometers and Accelerometers

J. Včelák*, P. Kašpar

vcelakj1@feld.cvut.cz

Department of Measurement, Faculty of Electrical Engineering, Czech Technical University in Prague, Technická 2, 166 27 Prague 6, Czech Republic

Navigation systems are used in many applications. One of the most important and original are military application where high accuracy and reliability is necessary. New civil applications appear in last few years for navigation systems. Electronic navigation systems and compasses are currently used in cars, ships, submarines, GPS locators, mobile phones or watches, security systems underground drilling systems. To the group of electronic navigation systems belong also magnetic navigation systems, strap-down systems satellite navigation systems like GPS or GLONASS, star tracking systems, radio beacon navigation, ultra-low frequency navigation for submarines and others. We are concerning in the group of navigation systems that determine actual azimuth from measuring of Earth's magnetic field vector. In case of low cost low power electronic compasses the components of Earth's magnetic field vector are usually measured by AMR. In more precise systems fluxgates are used. Low cost systems are suitable for battery powered devices and the dimensions could be also very small. The main disadvantage of these systems is, that the magnetic field vector (the direction and total value) is influenced by ferromagnetic object near by the system. When the accurate measurement of azimuth is necessary we have to measure actual roll and pitch of the device especially in case of planes, yachts, ships or submarines. Most electronic compasses without tilt sensing are able to measure accurate azimuth only when they are perfectly adjusted in horizontal plane. But in case of planes, yachts, ships or submarines it is not possible to assure perfectly horizontal plane of measurement. It is very suitable to have information about actual roll and pitch to calculate real azimuth in every position of the electronic compass.

After we have considered all these facts we decided to develop low cost, low power navigation system with AMR (anisotropic magneto-resistance) sensors. Developed navigation system provides accurate information about actual azimuth, roll and pitch in every position. Our developed navigation system uses AMR sensor for magnetic field measurement and accelerometers are used to measure actual roll and pitch.

Sensors part consists of three-axis accelerometer and three-axis AMR magnetometer. The sensor part is designed for universal using of several AMR magnetometers from different suppliers (sensors Honeywell HMC100X, HMC102X and Philips KMZ 5X can be used). Both triplets of sensors create in ideal case orthogonal coordinate systems. We use three non-magnetic MEMS accelerometers to calculate actual roll and pitch of the device. The AMR magnetic sensors are placed as far as possible from driving electronics in order to minimize magnetic interference.

The AMR sensors and accelerometers provide analog output value. This output value is digitalized by six Δ - Σ A/D converters. All six Δ - Σ A/D converters are triggered by same clock signal in order to define sample take-off time. These low power (0.6mW) A/D converters are equipped with differential inputs, programmable gain amplifier and serial interface. Digitalized values are sent to microprocessor using serial interface. AMR sensors

are powered by three adjustable current sources. Current supply provides higher temperature stability than voltage supply.

The set and reset pulses (flipping AMR sensors) are periodically generated by flipping circuit. The influence of cross-axis effect is then reduced by two readings of their output values (one after set flipping pulse and the other after reset flipping pulse).

Digital part consists Dev16 kit for 16-bit Fujitsu MB90F543 microprocessor. This microprocessor is equipped with RAM and FLASH memory and directly provides filtration of data and calculation of actual azimuth, roll and pitch. Calculated data are directly displayed on a character display and parameters of measurement could be set up using connected AT keyboard. Measured data are also sent to the PC (if it is connected) for further processing. Whole system is battery powered and is able to work stand alone (without PC) for more than 24 hours without charging.

Output values of roll and pitch are calculated from measured values of G_x , G_y , G_z and azimuth is calculated from measured vector of magnetic field H_x, H_y, H_z corrected with regard to actual roll and pitch. The correction for actual pitch and roll is done by mathematical rotation of H sensors triplet as it would be in horizontal plane. The advantage of this design with magnetometers and accelerometers is that the calculated azimuth is not influenced by actual roll or pitch in ideal case.

As the placing of sensors is not ideal (the sensors in triplets are not perpendicular to each other and the axes of triplets don't align together) the calibration of deviation angles is necessary. We have developed non-magnetic calibration device to calibrate these deviation angles. The calibration of three deviation angles for both sensor triplets is done by simple roll rotation of the sensor part in homogenous magnetic field. The compensation of the deviation angles is done by numeric backward rotation of the sensor coordinate system

After the compensation of deviations the accuracy of azimuth determination is better than $\pm 0.8^\circ$ in whole range and the general accuracy of roll and pitch determination is better than 0.1° (range of azimuth measurement 360° , pitch $\pm 40^\circ$ and roll $\pm 180^\circ$). The residual error is caused by the cross-axis effect and also by the inaccurate determination of deviation angles.

References:

- [1] HONEYWELL: *Application note AN205A: Cross-axis effect for AMR Magnetic sensors*, <http://www.ssec.honeywell.com/magnetic/datasheets/an215.pdf>
- [2] M.J. CARUSO: *Applications of Magnetoresistive Sensors in Navigation Systems* Honeywell, www.ssec.honeywell.com

This work was funded by the Internal Grant CTU No.CTU0410413: Navigation systems with AMR Sensors and Accelerometers

Peripheral Circuits for the Silicon MEMS Microphones

M. Seidenglanz, M. Husák, P. Kulha, A. Bouřa

seidenm@fel.cvut.cz

Department of Microelectronics, Faculty of Electrical Engineering,
Czech Technical University, Technická 2, 166 27 Prague 6, Czech Republic

A new generation of small high-performance microphones based on silicon micromachining has been focused on the need to monolithically integrate the sensor structure with an electronic circuit to maximize the performance. Compared to conventional microphones those devices have potential advantages of small size, high reliability and reduced parasitic capacitance. Furthermore signal processing circuits can be integrated on one chip with a microphone's structure. Capacitive microphones may be subdivided into two branches: condenser and electrets microphones. The condenser microphone requires an external bias voltage for operation, but this is not the case for the electrets microphone since it has an internal built-in bias.

My work is aim at design of front-end and biasing peripheral circuits for MEMS (Micro – electro – mechanical systems) integrated silicon capacitive microphones. Design of the high input impedance, low-noise and wide-band preamplifier suitable for these microphones is solve in both versions from discrete components and microelectronic IC.

The condenser microphone from standpoint of his electrical connectors is possible to replace by an equivalent electrical circuit, which consists from a signal voltage generator u_s and a capacitor C_s in series. Toward effective transmission of a low signal voltage is then necessary to following preamplifier has a high value of input resistance with minimal noise. The most important function of preamplifier is impedance match of output impedance of transducer that is with respect to his capacitive character too high-level, especially within the low frequency range. To amplify of low-level signal mostly happen as far as in the following amplification stages.

Preamplifier from discrete components is identified to testing and measurement already realized MEMS transducer. Requirement of high-level input impedance and high voltage gain challenge to using of noninverting operational amplifier. In case of using only one amplification stage with required gain occurs too large limitation of the frequency bandwidth. In case of using several amplification stage in cascade again growth the noise. One of the feasible solutions is composite amplifier using dual low-noise amplifier OPA2111 with JFET input transistors. This preamplifier was designed and realized as a system for testing and measuring of standalone transducers.

The integration of front-end circuits on common chip together with transducer is advantageous from many standpoints. Among most important is increasing sensitivity with decrease noise by suppressing of parasitic parameters. Most frequently used is CMOS technology, sometimes BiCMOS and others. The simplest solution is to use MOSFET transistor connected as a source follower. Better performance can be achieved using Operational Transconductance Amplifiers (OTA). At present, our work is focus on simulation of this preamplifier in SPICE type simulator and on design of the layout of IC chips in CMOS technology.

The capacitive microphones need for their operation a biasing voltage that may have a value of tens Volts or more. An application of silicon capacitive microphone with an integrated DC-DC voltage converter for biasing the device can be interesting in low-power applications.

Charge pumps are circuits that can pump charge up-ward to produce voltages higher than the regular supply voltage. Using only capacitors, which takes less area than inductors in an integrated circuit, allows charge pump circuits to be fully integrated. Charge pumps suitable for the integration are often proposed on principle of Dickson's pump. Dickson's charge pump contains n MOSFET transistor (where n means number of stages) that function as a diodes, so that the charges can be pushed only in one direction. These transistors are switched by two out-of-phase clock signals. Efficiency of these charge pump isn't as high as efficiency of other DC-DC converters, but power consumption of bias circuits is negligible low.

References:

- [1] MIR, S. - RUFER, L. - THORAUD, B.-Z. - SIMO, M.: *CMOS Front-End for Capacitive Micromachined Ultrasonic Transducers* TIMA Laboratory, Grenoble
- [2] PEDERSON, M. - OLTHUIS, W. - BERGVELD, P.: *High-Performance Condenser Microphone with Fully Integrated CMOS Amplifier and DC-DC Voltage Converter* Journal of Microelectromechanical systems
- [3] SILVA-MARTINEZ, J. - SALCEDO-SUNER, J.: *A CMOS Preamplifier for Electret Microphones* IEEE, 1995
- [4] AMENDOLA, G. - BLANCHARD, Y. - EXERTIER, A. - SPIRKOVITCH, S. - ALQUIE, G.: *A CMOS, self-biased charge amplifier* IEEE, 1999

Section 5

MATERIALS ENGINEERING

Inverse Analysis of Coupled Water and Salt Transport in Porous Materials Using a Diffusion-Advection Model

R. Černý, Z. Pavlík

cernyr@fsv.cvut.cz

CTU, Faculty of Civil Engineering, Dept. Structural Mechanics
Thákurova 7, 166 29 Praha 6

The mathematical analysis of experimentally determined salt profiles depends on the assumed mode of salt transport in the material. If purely diffusion transport is assumed, common methods for solving the inverse problems for parabolic equations can be used. The simplest method makes the assumption that the diffusion coefficient is constant, the domain under solution is semi-infinite, and the boundary condition on the remaining side of a one-dimensional arrangement is Dirichlet-type. Then diffusion coefficient can be identified using the simple analytical solution of the parabolic problem with error function (e.g. [1]).

The dependence of the diffusion coefficient on salt concentration can be found if some more sophisticated methods for the analysis of measured salt profiles are used. One of the methods that can be potentially used to determine concentration dependent chloride diffusion coefficients in an analogous way as with simple moisture diffusion or simple heat conduction is a classical Boltzmann-Matano analysis (see [2], [3]).

Another step towards a more realistic description of the salt transport in porous building materials is the assumption of coupled water and salt transport and the application of the diffusion-advection equation

$$\frac{\partial(wC_f)}{\partial t} = \text{div}(wD \text{ grad}C_f) - \text{div}(C_f \mathbf{v}) - \frac{\partial C_b}{\partial t}, \quad (1)$$

where w is the volumetric water content [m^3/m^3], C_f the concentration of free ions in water [kg/m^3], C_b the concentration of bonded ions in the whole porous body [kg/m^3], D the ion diffusivity [m^2/s] and \mathbf{v} the Darcy's velocity of the liquid phase [m/s], together with the water mass balance equation

$$\frac{\partial w}{\partial t} = \text{div}(\kappa \text{ grad}w), \quad (2)$$

where κ is the moisture diffusivity [m^2/s].

Assuming the Darcy's velocity in the diffusion form,

$$\mathbf{v} = -\kappa \text{ grad} w, \quad (3)$$

we arrive at a system of two parabolic equations with two unknown variables w , C_f , and two principal material parameters, D , κ .

In the case of a 1-D transport, this system of two parabolic equations can be subjected to an inverse analysis in a similar way as for one parabolic equation, provided the initial and boundary conditions are simple enough, and the material parameters D , κ can be identified as functions of water content and salt concentration.

The simplest possibility of such an inverse analysis is an extension of the Boltzmann-Matano treatment under the same assumptions of constant initial conditions and Dirichlet boundary conditions on both ends of the specimen for both moisture content and salt concentration where one of the Dirichlet boundary conditions is equal to the initial condition.

The Boltzmann transformation then leads to the system of equations

$$2 \frac{d}{d\eta} \left(C_f \kappa \frac{dw}{d\eta} \right) + 2 \frac{d}{d\eta} \left(Dw \frac{dC_f}{d\eta} \right) + \eta \frac{d(wC_f)}{d\eta} + \eta \frac{dC_b}{dC_f} \frac{dC_f}{d\eta} = 0 \quad (4)$$

$$2 \frac{d}{d\eta} \left(\kappa \frac{dw}{d\eta} \right) + \eta \frac{dw}{d\eta} = 0 \quad (5)$$

Performing the second transformation providing that in the known time $t = t_0$, $w(x, t_0)$, $C_f(x, t_0)$, $C_b(x, t_0)$ are known,

$$z = \eta \cdot \sqrt{t_0}, \quad (6)$$

we have

$$2 \frac{d}{dz} \left(C_f \kappa \frac{dw}{dz} \right) + 2 \frac{d}{dz} \left(Dw \frac{dC_f}{dz} \right) + \frac{z}{t_0} \cdot \frac{d(wC_f)}{dz} + \frac{z}{t_0} \cdot \frac{dC_b}{dC_f} \cdot \frac{dC_f}{dz} = 0 \quad (7)$$

$$2 \frac{d}{dz} \left(\kappa(z) \frac{dw}{dz} \right) + \frac{z}{t_0} \frac{dw}{dz} = 0 \quad (8)$$

From Eq. (8) we can determine

$$\kappa(z_0) = \frac{1}{2t_0 \left(\frac{dw}{dz} \right)_{z_0}} \int_{z_0}^{\infty} z \frac{dw}{dz} dz \quad (9)$$

where $\kappa(z_0) = \kappa(w_0, C_{f0})$, $w_0 = w(z_0, t_0)$, $C_{f0} = C_f(z_0, t_0)$,

and finally using (8) and (9) we arrive at

$$D(z_0) = - \frac{C_f(z_0) \kappa(z_0) \left(\frac{dw}{dz} \right)_{z_0}}{w(z_0) \cdot \left(\frac{dC_f}{dz} \right)_{z_0}} + \frac{1}{2t_0 \cdot w(z_0) \cdot \left(\frac{dC_f}{dz} \right)_{z_0}} \int_{z_0}^{\infty} z \left(\frac{d(wC_f)}{dz} + \frac{dC_b}{dC_f} \frac{dC_f}{dz} \right) dz \quad (10)$$

where $D(z_0) = D(w_0, C_{f0})$.

References:

- [1] CARSLAW, H.S., JAEGER, J.C.: *Conduction of Heat in Solids*. Clarendon Press, Oxford, 1959.
- [2] MATANO, C: *On the relation between the diffusion coefficient and concentration of solid metals*. Jap. J. Phys., Vol. 8 1933, pp. 109-115.
- [3] ČERNÝ R., ROVNANÍKOVÁ, P.: *Transport Processes in Concrete*. Spon Press, London, 2002.

This research has been supported by EC within the 6th Framework Programme, under contract No. SSP1 – CT- 2003-501571.

Basic Hygric and Thermal Properties of Two Self-Compacting Concrete Mixtures

E. Mňahončáková, M. Jiříčková*, R. Černý*

cernyr@fsv.cvut.cz

Department of Physics, Faculty of Civil Engineering, Czech Technical University, Thákurova 7, 166 29 Prague 6, Czech Republic

*Department of Structural Mechanics, Faculty of Civil Engineering, Czech Technical University, Thákurova 7, 166 29 Prague 6, Czech Republic

Concrete mixtures were prepared according to Okamura and Ozawa [1]. Their composition is given in Table 1. The basic properties of the SCC mixtures are shown in Table 2. The S1 mixture containing calcareous filler achieved lower porosity and thus higher bulk density and matrix density compared to the S2 mixture containing fly ash.

Table 1 The composition of concrete mixtures

Component	Unit	S1	S2
cement	kg/m ³	379	394
water	kg/m ³	177	155
limestone	kg/m ³	253	-
fly ash	kg/m ³	-	263
w/c	-	0.46	0.39
superplasticizers	% mass	2.4	2.0
sand 0/2	kg/m ³	746	746
aggregate 2/16	kg/m ³	746	746
amount of air (calculated)	dm ³ /m ³	40	30

Table 2 Basic properties of studied SCC

SCC	ψ_0 [%]	ρ [kg m ⁻³]	ρ_{mat} [kg m ⁻³]
S1	11.1	2260	2542
S2	13.3	2161	2492

Table 3 Water

transport properties of studied SCC

vapor

SCC	97/50%			5/48%		
	δ [s]	D [m ² s ⁻¹]	μ [-]	δ [s]	D [m ² s ⁻¹]	μ [-]
S1	1.56E-11	2.13E-06	10.8	8.618E-12	1.17E-06	19.5
S2	2.63E-11	3.58E-06	6.5	8.613E-12	1.17E-06	19.5

The water vapor transport parameters of the studied SCC mixtures are shown in Table 3. The measured data revealed a basic information that the values of water vapor diffusion

coefficient corresponding to the lower values of relative humidity (5-48%) were always lower than those for higher relative humidity values (97-50%). Comparing the data measured for the particular mixtures S1 and S2, we can see that the values of water vapor diffusion coefficient of S1 were in the range of higher relative humidity about 40% lower than for S2. This is in a general agreement with the open porosity data in Table 2. However, in the range of lower relative humidity were the water vapor diffusion coefficients basically the same for both materials. This may indicate higher amount of smaller pores in the material S2.

Table 4 Water transport properties of studied SCC

SCC	A [kg m ⁻²]	w _{sat} [kg m ⁻³]	κ [m ² s ⁻¹]
S1	0.0086	110	6.72E-09
S2	0.0052	132	1.57E-09

The results of measuring liquid water transport parameters in Table 4 show that the material S2 with higher porosity transported liquid water in much slower way than the material S1. Its water absorption coefficient was 65% higher and the moisture diffusivity more than four times higher compared to S1. These findings indicate that the material S2 had significantly lower amount of bigger (capillary) pores in the 1-10 μm range (where the transport of liquid water is fastest) than the material S1. This is also in a good agreement with the dry cup data for water vapor diffusion coefficients in Table 3 that indicated higher amount of smaller pores in the material S2.

Table 5 Thermal properties of studied SCC

SCC	λ (W/mK)	C (J/m ³ K)	a (m ² /s)
S1	3.50	1.84	1.90
S2	2.61	1.77	1.47

The thermal parameters data in Table 5 show that the material S1 had higher thermal conductivity than S2. This is in a qualitative agreement with the open porosity data in Table 2. The volumetric heat capacity of S1 was slightly higher than of S2. The thermal diffusivity of S1 was higher compared to S2 which corresponds to the fact that the difference in thermal conductivity between the two studied materials was higher than the difference in the volumetric heat capacity.

References:

- [1] OKAMURA H., OZAWA K.: *Design for Self-Compacting Concrete*. Concrete Library of JSCE, No. 25, June 1995.

This research has been supported by the MŠMT project PL-52

Experimental Setup for Monitoring Coupled Water and Salt Transport in Building Materials

M. Jiříčková, Z. Pavlík, R. Černý

cernyr@fsv.cvut.cz

CTU, Faculty of Civil Engineering, Dept. Structural Mechanics
Thákurova 7, 166 29 Praha 6

The most frequently used methods for the determination of salt diffusion coefficients in building materials use the experimental set-up designed for concrete in the so-called „Rapid Chloride Permeability Test“ (sometimes called as “Migration Test”), which was developed at the beginning of the 1980s in USA (see [1]). The experiment uses two cells separated by a plate specimen of the measured material. In measuring chloride diffusion, cell 1 normally contains a NaCl solution, and cell 2 is filled with a NaOH solution of the same molar concentration as that of the chloride source solution. Two mesh electrodes are fitted, one on each side of the concrete specimen in such a way that the electric field is applied primarily across the test specimen.

Another possibility for determining the salt diffusion coefficient is to use a mathematical analysis of measured salt profiles. A typical experiment for the determination of the salt profile in a concrete specimen was described in [2] for chloride penetration. Concrete samples cured in wet conditions were exposed to a chloride solution from one side in a one-dimensional transport arrangement. After a specified time, slices 3-4 mm thick were cut in the near-surface layer for chloride analysis. The total chloride content was extracted from the specimens using a boiling nitric acid solution for 30 minutes. The free chloride content was determined after a contact time of 3 minutes between water and concrete. Chloride concentrations were measured by potentiometry using a titrated silver nitrate solution.

In this paper, we propose an improved experimental setup for monitoring coupled water and salt transport in building materials. During a single experiment in the conditions of one-sided salt-in-water solution uptake, both salt diffusion coefficient in dependence on concentration and moisture diffusivity in dependence on moisture content are determined. The organization of the experiments is the same as in common water sorption experiments. The samples are exposed by their 40 x 40 mm face to a salt solution with the known concentration. Duration of the experiment is chosen to be different for several (typically 3-5) different groups of samples. After this time, the samples are cut into typically 8-16 pieces and in each piece water content and salt concentration are measured. Moisture content is determined by the gravimetric method using weighing the moist and dried specimens. In the determination of salt concentration, the particular samples are after drying first ground by a vibration mill so that grains smaller than 0.063 mm are obtained. Then, 10 g of the ground sample is subjected to a chemical analysis so that the total amount of salt in the specimen is determined. Finally, the experimental salt concentration profiles and moisture profiles are subjected to an inverse analysis.

The solution of the inverse problem can be done in several ways. The first possibility is using the diffusion model for both water and salt transport without the cross effects. In such case, the result of the inverse analysis is the identification of apparent water and salt transport parameters instead of the basic parameters of the coupled water and salt transport defined exactly in the sense of irreversible thermodynamics. The main difference between the apparent parameters and the thermodynamically “pure” parameters of the coupled water and salt transport is that the apparent parameters do not express “pure” effects but combined

effects. So, the apparent salt diffusion coefficients include not only the free salt diffusion in the porous space but also the effect of salt bonding on the pore walls and the effect of salt transport due to the water movement. The notion of apparent moisture diffusivity then means that it is related not to the water itself but to the salt-in-water solution, i.e. the whole liquid phase. The second, more accurate possibility is using the diffusion-advection model (see e.g. [3]). The parameters expressing the diffusion and advection in the process of salt transport in a way of rigorous thermodynamics of irreversible processes can only be obtained after determination of the effect of bound salts on the total salt concentration measured in the proposed experiment. For this, it is necessary to determine the ion binding isotherm. Then, the amount of bound salts can be expressed in terms of the free chloride concentration and the ion binding isotherm as a conversion parameter, and the inverse analysis of the diffusion-advection equation can be done in a similar way as for the diffusion model.

It should be noted that common methods of solution of the inverse problem of water and/or salt transport are not based on an exact mathematical solution. The solution is rather a physical one. In addition, the input parameters of the inverse problem are given in the form of point-wise defined functions. This requires data approximation including smoothing of the originally measured data sets that may introduce significant errors to the analysis. Therefore, the verification of results obtained by the solution of the inverse problem at least in the physical or technical sense is necessary. The easiest way to do that is the substitution of the calculated moisture diffusivity and/or salt diffusion coefficient into the original diffusion or diffusion-advection equation and numerical solution of the problem. If the inverse analysis was precise enough, the measured and calculated water and/or concentration fields should coincide within a certain error range. However, this is not always the case and some optimization of the calculation procedure is necessary. The simplest way how to do such an optimization procedure is using the error and trial method. First, we choose a smoothing factor of the data approximation function. Then, we perform the backward analysis, i.e., the solution of the inverse problem. The result is used afterwards as the input parameter in a forward analysis. Finally, the agreement between the calculated water and/or concentration fields and the original measured data is evaluated using a common least-square procedure. If the least-square difference between the measured and calculated data falls within given limits, the process of optimization is stopped. Otherwise, another value of the smoothing factor is chosen and the whole procedure is repeated until a good closeness-of fit is achieved.

References:

- [1] WHITING, D.: *Determination of the Chloride Permeability of Concrete*. Report No. FHWA/RD-81/119. Portland Cement Association, NTIS DB No. 82140724, 1981.
- [2] BAROGHEL-BOUNY V, CHAUSSADENT T, RAHARINAIVO A.: *Experimental investigations on binding of chloride and combined effects of moisture and chloride in cementitious materials*. Proceedings of the RILEM International Workshop Chloride Penetration into Concrete, St-Remy-les-Chevreuse, pp. 290-301, 1997.
- [3] ČERNÝ R., ROVNANÍKOVÁ, P.: *Transport Processes in Concrete*. Spon Press, London, 2002.

This research has been supported by the MŠMT KONTAKT project PL-51.

Basic System of Experimental Methods for Testing and Quality Evaluation of New Building Materials

R. Černý, Z. Pavlík

cernyr@fsv.cvut.cz

CTU, Faculty of Civil Engineering, Dept. Structural Mechanics
Thákurova 7, 166 29 Praha 6

In the project “Testing and quality evaluation of new materials by a combination of techniques used in civil engineering and geophysics” (see [1], [2] for details) the Czech research team is concentrated first on laboratory techniques for determination of basic field variables of heat and moisture transport (moisture content, relative humidity, temperature, capillary pressure) and hygric and thermal transport and storage parameters (moisture diffusivity, water vapor diffusion coefficient, sorption isotherms, water retention curves, thermal conductivity, specific heat capacity). In the subsequent phase, implementation of the laboratory techniques in semi-scale conditions and in situ is the main task. The laboratory methods are analyzed and adjusted with the primary aim to transfer them into the large-scale conditions. In the verification of techniques for monitoring heat and moisture transport, the newly developed semi-scale system of climatic chambers NONSTAT is used, utilizing relatively complicated and expensive measuring equipment, whose application is not assumed for common measurements but for special aimed experiments looking for critical problems. For instance, in the case of a concrete envelope such problem can present the area close to the surface exposed to the aggressive environment or close to the thermal insulation layer. Therefore, moisture, temperature, relative humidity and capillary pressure fields are monitored in the material element. Data for temperature and relative humidity corresponding to the reference year for Prague are used in the system of climatic chambers to simulate external conditions. This experiment is so close to the reality of the building site that the experience can be directly transferred to the conditions in situ.

In the first phase of the project solution the laboratory techniques for determination of basic field variables of heat and moisture transport (moisture content, relative humidity, temperature, capillary pressure) and hygric and thermal transport and storage parameters (moisture diffusivity, water vapor diffusion coefficient, sorption isotherms, water retention curves, thermal conductivity, specific heat capacity) were analyzed and examples of their application were given. On the basis of this analysis, the basic system of experimental methods suitable for testing and quality evaluation of new materials both in laboratory conditions and in situ was designed.

Among the methods for determination of moisture content in laboratory conditions, the capacitance method (see e.g. [3]) can be chosen for the inclusion in the system as a basic method. The time-domain reflectometry (TDR) method can be considered as an alternative for measurements in more complicated conditions for moisture measurements. For the measurements of relative humidity in both laboratory and field conditions, we have chosen capacitance sensors designed by Ahlborn. For the measurements of temperature, the resistance thermometers built in the capacitance probe for relative humidity measurements designed by Ahlborn were used. For the measurements of capillary pressure, we have chosen the mini-tensiometer for laboratory measurements designed by Plagge.

For the determination of apparent moisture diffusivity, given by a characteristic value that does not depend on the moisture content, the water sorptivity experiment was chosen. In the determination of moisture dependent moisture diffusivity from the moisture profiles, we have to choose between two experimental setups. In the first experiment, specimen is fixed in horizontal position in order to eliminate the effect of gravity on moisture transport, and in the second experiment specimen is fixed in vertical position. For the determination of moisture diffusivity coefficient from the moisture profiles we have chosen the Matano method as the basic method (see e.g. [3]). For measuring water vapor diffusion permeability we have chosen the standard cup method where the measurement is carried out in steady state under isothermal conditions. For the measurements of the adsorption isotherms we suggest the desiccator method. For the determination of moisture retention curves we suggest the pressure plate device. For the determination of thermal conductivity and specific heat capacity we propose the application of the commercial device ISOMET 2104, which belongs to the simplest and most convenient for a practical use.

In the first phase of verification of the designed system in laboratory and semi-scale conditions, the research work was concentrated on the laboratory methods for determination of moisture diffusivity, water vapor diffusion coefficient, sorption isotherms, thermal conductivity and specific heat capacity. In the semi-scale test, moisture content, relative humidity and temperature were monitored. The basic tested material was high-quality concrete C90/105 containing microsilica. This concrete has a potential of application for technically demanding structures including those in marine environment. For the sake of comparison, the same mixture of concrete C60/75 was prepared without microsilica. The building envelope studied in the semi-scale test consisted from the interior to the exterior of high-quality concrete wall 200 mm thick, material KAM developed by Sakret, Ltd., on cement glue principle for sticking the thermal insulation boards in a thickness of 10 mm, thermal insulating boards INROCK by Rockwool, SA, on the basis of hydrophilic mineral wool with dual density in a thickness of 80 mm. The exterior plaster on the basis of KAM material was reinforced by a plastic net.

The results of the first phase of the verification procedure showed that the designed system is very promising and may have good perspectives for the application in the practice. This is to be confirmed in the second phase of the verification tests.

References:

- [1] ČERNÝ, R. ET AL.: *Testing and Quality Evaluation of New Materials by a Combination of Techniques Used in Civil Engineering and Geophysics*. Progress Report, CTU Prague, 2003.
- [2] ČERNÝ, R. ET AL.: *Testing and Quality Evaluation of New Materials by a Combination of Techniques Used in Civil Engineering and Geophysics*. Progress Report, CTU Prague, 2004.
- [3] ČERNÝ R., ROVNANÍKOVÁ, P.: *Transport Processes in Concrete*. Spon Press, London, 2002.

This research has been supported by the Ministry of Education of Czech Republic, under grant No. ME 682.

Thermal and Hygric Characteristics of Composite Materials on the Basis of Alkali-Activated Slag

L.Friedlová, R. Černý

friedlova@email.cz

Czech Technical University, Faculty of Civil Engineering, Department of Structural Mechanics, Thákurova 7, 166 29 Praha 6, Czech Republic

Portland or blended cement as traditional binder in concrete is the most universal binder to date although it has a number of disadvantages, such as high energetic demand for its production, low resistance against aggressive substances and instability at high temperatures.

At the end of 20th century there appeared a trend of low-energy binders based on the utilization of secondary raw materials. In this respect, slag is one of the possibilities how to expand the range of concrete and mortars by other materials that meet the requirements to binders and in many aspects have better properties than classical Portland cement. Granulated blast furnace slag is used as a component of blended cements. However, in this case its hydraulic properties are not fully utilized because at grinding together with clinker and gypsum, a part of grains remains unreacted due to its difficult grindability.

Alkali activation of granulated blast furnace slag makes possible a more effective and more economic utilization of its hydraulic properties. For the alkali activation, any aluminosilicate material with pozzolanic, hydraulic or potentially hydraulic properties can be used. The most appropriate and most studied option is alkali activation of granulated blast furnace slag and kaolinite [1]. Granulated blast furnace slag is characterized by the ratio of the glassy and the crystalline phase, and by its chemical and mineralogical composition. While slags of acidic character crystallize with difficulties, basic slags crystallize relatively easily. The crystalline phases with calcium hydroxide have a very low reactivity but the amorphous phases react easily in the presence of basic compounds. Therefore, for the binder production rapidly cooled slag of amorphous character is used. Higher basicity of slags characterized by the modulus of basicity, is for the alkali activation very important and is given by so-called modulus of basicity M_z .

At the activation of slags in highly basic environment, it is not necessary to maintain strict requirements concerning the amount of glassy phase and the chemical composition, as for instance in blended cements. For the slag activation, Bédidor applied already in 1737 [2] lime that reacts in the same way as calcium hydroxide formed by cement hydration. However, the application of silicates, carbonates or hydroxides of alkali metals [3] appears more appropriate for slag activation.

Among the hygric properties of concrete based on the alkali-activated slag, only water permeability was previously measured [4]. As for other transport parameters, air permeability in concrete based on alkali-activated slag was measured by the Figg test, and chloride diffusion in concretes and pastes based on alkali-activated slag and on its blend with cement was studied. Thermal properties of concrete based on alkali-activated slag were not found in commonly used databases.

As it follows from the above survey, properties of materials on the basis of alkali-activated slag were studied only relatively seldom to date. When some parameters were measured, then it were mostly mechanical properties. Hygric properties such as moisture diffusivity or water vapor permeability depending on the moisture content were not yet seriously measured even in normal conditions (on the basis of water permeability and air

permeability it is possible to get some estimates but serious data not at all), for the thermal parameters the situation is very similar. The effect of high temperatures on hygric and thermal properties was not studied at all.

Alkali-activated materials have many benefits. These are above all high strength materials, corrosion resistive materials, partially resistive to high temperatures. Therefore, a determination of a complete set of mechanical, thermal and hygric properties of materials based on alkali-activated slag both in normal conditions and after high temperature exposure is very urgent. Performing this task, a significant extension of knowledge of these parameters will be achieved, which will make possible a serious analysis of their reaction to high temperature exposure.

In this paper, a slag-based material alkali-activated using water-glass solution with a composition given in Table 1 was analyzed. First results of the measurements of basic thermal and hygric properties of this material are shown in Table 2.

Table 1 Composition of the alkali activated slag material

Sand aggregates [g]			Slag [g]	Alkali-activation silicate admixture [g]	Water [ml]
PG1	PG2	PG3			
1350	1350	1350	450	90	190

Table 2 Basic thermal and hygric properties of alkali-activated composite material

Thermal conductivity [Wm ⁻¹ K ⁻¹]	Volumetric heat capacity [10 ⁶ Jm ⁻³ K ⁻¹]	Thermal diffusivity [10 ⁻⁶ m ² s ⁻¹]	Moisture diffusivity [m ² s ⁻¹]
1.59 ± 2.4%	1.73 ± 2.6%	0.92 ± 0.7%	1.84 E-07 ± 21.5%

References:

- [1] DAVIDOVITS, J., DAVIDOVITS, R. AND JAMES, C *Geopolymere*, Saint-Quentin 1999,
- [2] MATOUŠKOVÁ, A., *Od tradičního vápenictví na území Českého krasu ke vzniku moderní továrny na výrobu portlandského cementu v Králově Dvoře v roce 1911*. Vydala Královodvorská cementárna a.s, Králův Dvůr, 1995.
- [3] SHI, C., DAY, R.L., *Some Factors Affecting Early Hydration of Alkali-Slag Cements*. Cement and Concrete Research, 1996, Vol. 26, No. 3, pp. 439-447.
- [4] SHI, C., *Strength, Pore Structure and Permeability of Alkali-Activated Slag Mortars* Cement and Concrete Research, 1996, Vol. 26, 1789-1799.

This research has been supported by GA ČR grant No.103/04/0139.

Effect of Admixtures on the Properties of FGD Gypsum

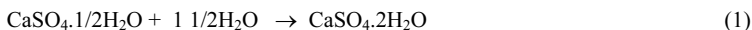
P. Tesárek, R. Černý

tesarek@fsv.cvut.cz

Czech Technical University, Faculty of Civil Engineering, Department of Structural Mechanics, Thákurova 7, 166 29 Praha 6, Czech Republic

Determination of a complete set of mechanical, thermal and hygric properties of practically any type of non-modified and modified gypsum is a very actual problem. Complete sets of these parameters are not available and without their knowledge it is impossible to perform any serious hygrothermal analysis of building elements based on these materials.

The solid structure of calcined gypsum is created by reverse hydration from the flue waste gas desulfurization (FGD) gypsum $\text{CaSO}_4 \cdot 1/2\text{H}_2\text{O}$ when gypsum $\text{CaSO}_4 \cdot 2\text{H}_2\text{O}$ is formed according to the equation:



This compound is relatively soluble in water; its solubility is 256 mg in 100 g of water at 20°C. The resistance of hardened gypsum against water is generally a serious problem. For the utilization of gypsum elements in the exterior, it is necessary to modify it so that it would exhibit more suitable properties and longer service life.

We have done the classification of the FGD gypsum from the electric power station Počerady according to the Czech standard ČSN 72 2301. This classification consists in determination of grinding fineness using the 0.2 mm sieve residue, initial and final setting times using the Vicat device and compressive strength for the time of two hours after mixing. According to our results the FGD gypsum can be classified as G-13 B III [1]. During the development process of the various types of modified gypsum it is always necessary to assess the quality of their parameters in some way. A set of reference measurements on common gypsum samples was carried out for the sake of future comparisons with the data obtained for modified gypsum [2][3].

The first investigations of modified gypsum were aimed at the effect of plasticizers and hydrophobization on its basic properties. The water/gypsum ratio, type of admixture, and the concentration of the admixture of the measured materials are shown in Table 1.

Materials	Water/gypsum ratio	Admixtures	Designation	Concentration
S0	0.627	none	none	none
S1	0.5	a plasticizer	PERAMIN SMF 20	0.5 % by mass
S2	0.5	a plasticizer	MELAMIN F4000	0.2 % by mass
S3	0.627	a hydroph. admixture	IMESTA IBS 47	0.5 % by mass
S4	0.627	a hydroph. admixture	ZONYL 9027	5.0 % solution

Table 1 Composition of measured materials

The measurements of mechanical, hygric and thermal properties of gypsum modified by using plasticizers have shown that both plasticizers basically can be used in further modifications. The main goal, which was the improvement of mechanical properties, was achieved for both plasticizers. However, it should be noted that the effect of PERAMIN SMF 20 in a concentration of 0.5% of the mass of the solid phase was more pronounced compared to the second used plasticizer MELAMIN F 4000 in a concentration of 0.2% of mass of the solid phase. The water and water vapour transport properties of both modified materials were either the same or lower than for the reference material, the more favourable properties were achieved again with PERAMIN SMF 20. On the other hand, the thermal conductivity of both modified FGD gypsum materials increased which is not a positive factor but quite a logical result taking into consideration the effect of any plasticizer in general [4].

The measurements of basic properties of gypsum modified by hydrophobization admixtures have shown that only the hydrophobization admixture ZONYL 9027 can be used in further applications. This admixture decreased the apparent moisture diffusivity of FGD gypsum by about two orders of magnitude, which is a very good result. The modified material exhibited liquid water properties somewhere on the level of common cement based materials. Also, the hygroscopic behaviour of the material was reduced, and the material exhibited best thermal properties among the studied gypsum materials. On the other hand, the hygric properties of the material with the hydrophobization admixture IMESTA IBS 47 (concentration 0.5% by mass) were improved in the hygroscopic range only. The liquid water transport in this material remained practically the same fast as in the reference gypsum material. This is not an acceptable result because any fast liquid water transport can lead to a fast increase in water content in the material and consequently to the worsening of mechanical properties.

Next stages of the development of modified gypsum will be aimed at the combinations of different admixtures and the comparison with obtained data.

References:

- [1] P. TESÁREK, R. ČERNÝ, J. DRCHALOVÁ, J. KOLÍSKO, *Mechanical, thermal and hygric properties of hardened flue gas desulfurization gypsum - Part II*, Stavební obzor Vol.13, No. 8, 2004 pp. 242-245.
- [2] P. TESÁREK, R. ČERNÝ, J. DRCHALOVÁ, P. ROVNANÍKOVÁ, *Thermal and hygric properties of gypsum: Reference measurements*.s Thermophysics 2003, Bratislava 2003, pp.52-57.
- [3] P. TESÁREK, R. ČERNÝ, J. DRCHALOVÁ, P. ROVNANÍKOVÁ, J. KOLÍSKO, *Mechanical, thermal and hygric properties of hardened flue gas desulfurization gypsum - Part I*, Stavební obzor, Vol. 13, No. 5, 2004, pp.138-142
- [4] P. TESÁREK, L. FRIEDLOVÁ, J. KOLÍSKO, P. ROVNANÍKOVÁ, R. ČERNÝ, *Mechanical, thermal and hygric properties of modified gypsum: the effect of plasticizers*, Roczniki inzynierii budowlanej, 2004, pp.25-30.

This research has been supported by GA ČR grant No. 103/03/0006.

Lime Plasters with Pozzolanic Admixtures: a Perspective Material for Building Renovation

V. Tydlitát, P. Tesárek, R. Černý

tydlitat@fsv.cvut.cz

Czech Technical University, Faculty of Civil Engineering, Department of Structural Mechanics, Thákurova 7, 166 29 Praha 6, Czech Republic

There is a generally accepted view in the cultural heritage community that materials used for renovation of historical buildings should be similar to the original materials and their composition should be similar to that used in the time of origin of a particular building. This is the reason, why experts do not accept using Portland cement in plasters for renovation of historical buildings.

Historically used binders are materials based on lime and admixtures with pozzolanic properties. We tried to prove in our development the use of metakaoline, grinded brick and grinded enamel glass as pozzolana admixtures in lime-pozzolana plaster mixtures. These materials form first a solid structure of CSH compounds and hydrated calcium aluminates, later calcium carbonates.

For renovation of historic buildings there were proposed three new lime plasters with pozzolanic admixtures [1–3]. Proposed plasters do not contain new binders as Portland cement. Plasters contain lime (CL 90 Czech-Moravien Cement Mokrá), pozzolanic admixture and sand (with continuous granulometry 0 to 4 mm) in relation 1:1:3. The amount of water was between 1.2 and 1.5 multiple of the amount of lime. Pozzolana admixtures used were metakaoline (manufactured in U.K. and in Bohemia), grinded brick ceramics from brick-fields in Hodonín and in Dolní Jirčany and grinded enamel glass from Mefrit plc., ČR. The second step in developing new plasters was the addition of zinc stearate as a hydrophobic admixture in the amount of 0.4% by mass [4].

The hydrophobization of the three studied lime-pozzolana plasters by the use of zinc stearate resulted in the following changes of their basic, mechanical and hygric properties. The open porosity of the hydrophobized plasters decreased significantly and their bulk density increased compared to plasters without zinc stearate. The compressive strength and the bending strength of the lime/metakaoline plaster decreased only moderately after hydrophobization but for the lime/grinded brick plaster and for the lime/grinded enamel glass plaster the strengths were down to three times lower. The water vapor sorption of lime/metakaolin plaster decreased about four times after hydrophobization but the corresponding decrease for the remaining two lime-pozzolana plasters was only 30-40%. The liquid water transport properties of all three studied plasters decreased significantly after the hydrophobization. For the apparent moisture diffusivity it was the decrease in the range of one to two orders of magnitude.

Selected basic, mechanical, hygric and thermal properties of hydrophobized lime plasters with pozzolanic admixtures are compared in Table 1 with properties of the lime plaster (lime:sand:water 1:3:1) without zinc stearate.

Plasters	Bulk density	Open porosity	Bending strength (28 days)	Pressure strength (28 days)	Apparent moisture diffusivity	Water vapor diffusion resistance factor	Dry thermal conductivity
	[kgm ⁻³]	[m ³ m ⁻³]	[MPa]	[MPa]	[m ² s ⁻¹]	[-]	[Wm ⁻¹ K ⁻¹]
Lime plaster	1658	0.34	0,32	1.11	6.86E-07	15.0	0.73
With metakaoline Božičany	1437	0.37	1.36	2.88	1.19E-08	15.6	0.46
With grinded brick	1870	0.14	0.65	1.26	1.06E-08	13.9	0.77
With grinded enamel glass	1840	0.14	0.56	0.70	9.00E-09	12.0	0.73

Table 1 Basic properties of the lime plaster and hydrophobized lime-pozzolana plasters with 0.4 % of zinc stearate.

It can be concluded that among the lime-pozzolana plasters studied in this research the most favorable properties exhibited the lime-metakaolin plaster. The hydrophobization of this plaster has led to a significant decrease of liquid water transport properties and water vapor sorption while the mechanical properties preserved their high values. This makes very good prerequisites for its application in the renovation of historical buildings instead of the common lime plasters.

Better properties than lime plaster showed all pozzolana plasters. For use in Czech Republic we can recommend pozzolana plaster with metakaoline from Sedlecký kaolin a.s. Božičany and plaster with grinded brick.

References:

- [1] V. TYDLITÁT, A. KUNCA, J. DRCHALOVÁ, M. JIŘIČKOVÁ, R. ČERNÝ: *Mechanical, Hygric and Thermal Properties of Lime Plasters with Pozzolanitic Admixtures*. Stavební obzor, Vol. 13, No. 2, 2004, pp. 38-44.
- [2] R. ČERNÝ, J. DRCHALOVÁ, A. KUNCA, V. TYDLITÁT, P. ROVNANÍKOVÁ.: *Thermal and Hygric Properties of Lime Plasters with Pozzolanitic Admixtures for Historical Buildings*, Research in Building Physics, Lisse: A. A. Balkema Publisher 2003, pp. 27-33.
- [3] V. TYDLITÁT, P. ROVNANÍKOVÁ, R. ČERNÝ, P. TESÁREK, A. KUNCA: *Selected Properties of Hydrophobized Lime Plasters with Pozzolanitic Admixtures*. Mezinárodní slovenský a český kalorimetrický seminář 2004, 2004, pp. 75-78.
- [4] P. TESÁREK, V. TYDLITÁT, P. ROVNANÍKOVÁ, R. ČERNÝ: *Effect of Hydrophobization on The Properties of Lime Plasters with Pozzolanitic Admixtures*. Roczники Inżynierii Budowlanej, Vol.10, No. 4, 2004, pp. 45-52

This research has been supported by GA ČR grant No. 103/02/1081.

Tensile properties of neutron irradiated reactor pressure vessel steel

Petr Haušild*, Miloš Kytka**, Miroslav Karlík*, Pavel Pešek**

Petr.Hausild@fjfi.cvut.cz

*Department of Materials, Faculty of Nuclear Sciences and Physical Engineering, Czech Technical University, Trojanova 13, 120 00 Praha 2, Czech Republic

**Integrity and Technical Engineering Division, Nuclear Research Institute, Husinec - Řež 130, 250 68 Řež, Czech Republic

The mechanical properties of pressure vessel steels are a decisive factor in the complex safety assessments of nuclear power plants. There has been extensive research on fracture behaviour of these types of steel and the mechanical properties can be improved by thermal treatment leading to a bainitic microstructure. The steel chosen for this study was the 15Ch2MFA (15Cr2MoV) tempered bainitic steels used for fabrication of pressure vessels of VVER 440-type nuclear reactors [1]. The forged plate of 190 mm thickness was subjected to the thermal treatment consisting of normalizing at 1010°C/12 hours followed by cooling in air, and tempering at 730°C/14 hours followed by cooling in furnace. The resulting microstructure corresponds to the tempered bainite.

The standard tensile specimens were taken at a depth position at one quarter of the plate thickness from the surface (1/4t position) in the T (transverse) and orientation. The specimens were enclosed and neutron irradiated in the same capsules as standard surveillance specimens. The chains contained the set of activation monitors (including fast as well as thermal neutrons) and also fission monitors. Each capsule contained two rings of copper wire to evaluate the azimuthal fluence. The capsules were irradiated in emptied surveillance channels in the nuclear reactor of VVER 440-type. The mean irradiation temperature was estimated after evaluation of the melting temperature monitors to 275°C. Tensile tests were carried out on the INSTRON 1342/8500+ hydraulic testing machine at constant crosshead speed of 0.5 mm.min⁻¹.

The results of tensile test of neutron irradiated and non-irradiated specimens are listed in Table 1. After irradiation, the yield stress and the tensile strength are increased. The elongation after irradiation is firstly decreased (12.5% after neutron fluence, $\Phi_n=3.3 \cdot 10^{23}$ n.m⁻² comparing to 17.8% at the non-irradiated state) but with increasing neutron fluence slightly increases (14.5% after neutron fluence, $\Phi_n=9.5 \cdot 10^{23}$ n.m⁻²).

Φ_n [n.m ⁻²] ($E > 1$ MeV)	Yield stress [MPa]	Tensile strength [MPa]	A [%]
0	560	670	17.8
3.3×10^{23}	665	745	12.5
7.1×10^{23}	700	770	13.2
9.5×10^{23}	710	785	14.5

Tab. 1 Results of tensile tests of 15Ch2MFA steel before and after neutron irradiation (average value from 2 tests).

The influence of irradiation on hardening can be seen from the fit of the stress-strain

curve by a Ramberg-Osgood relationship [2]:

$$\varepsilon = \frac{\sigma}{E} + 0.002 \left(\frac{\sigma}{\sigma_{0.2}} \right)^n \quad (1)$$

where E is Young modulus, $\sigma_{0.2}$ is an equivalent yield stress, and n a parameter defining the sharpness of the knee of the stress strain-curve.

Hardening exponent n is increased from 12 in non-irradiated state to 24 after neutron irradiation but remains unchanged after further irradiation dose (up to neutron fluence, $\Phi_i = 9.5 \cdot 10^{23} \text{ n.m}^{-2}$). Lower hardening rate after irradiation is probably induced by an easier glide after the first dislocation glide through the nanoscale defects generated by neutron damage [3].

The change in hardening can also probably explain a slight increase of elongation after irradiation. In non-irradiated steels hardening capacity tends to decrease as yield strength increases [4]. In irradiated steel, higher yield stress retards the localisation of plastic deformation (necking) and consequently the elongation is slightly increased with increasing neutron fluence.

References:

- [1] KOUTSKÝ, J. – KOČÍK, J.: *Radiation Damage of Structural Materials, Materials Science Monographs, Vol. 79*, Elsevier Science Publ., Amsterdam, 1994.
- [2] RAMBERG, W. – OSGOOD, W.: *Description of Stress Strain Curves by Three Parameters. Technical Note No. 902*, National Advisory Committee for Aeronautics, Washington DC, 1943.
- [3] ODETTE, G.R. – LUCAS, G.E.: *Embrittlement of Nuclear Reactor Pressure Vessels, JOM 53(7)*, 2001, pp. 18-22.
- [4] KNOTT, J.F.: *Micro-mechanisms of fracture and the fracture toughness of engineering alloys*, in D. M. R. Taplin (Ed.): *Fracture 1977, ICF4, Vol. 1*, 1977, pp. 61-92.

This research has been supported by the Grant Agency of the Czech Republic in the frame of the project No. 106/04/0066.

Influence of neutron fluence on ductile crack growth in reactor pressure vessel steel

Petr Hausild*, Miloš Kytka, Miroslav Karlík*, Pavel Pešek****

`Petr.Hausild@fjfi.cvut.cz`

*Department of Materials, Faculty of Nuclear Sciences and Physical Engineering, Czech Technical University, Trojanova 13, 120 00 Praha 2, Czech Republic

**Integrity and Technical Engineering Division, Nuclear Research Institute, Husinec - Řež 130, 250 68 Řež, Czech Republic

Instrumented Charpy impact test is widely employed for determining the Ductile-to-Brittle Transition Temperature (DBTT) and for characterization of neutron induced embrittlement of nuclear reactor pressure vessel steels. Resistance to brittle fracture is one of decisive factors in the complex safety assessments of nuclear power plants. However, the final (brittle) fracture is frequently preceded by ductile tearing in the DBTT range. Ductile crack growth preceding the unstable cleavage fracture changes significantly the stress-strain field ahead of the notch root or the crack tip (stress, strain and constraint, see e.g. Refs. [1,2]). Premature ductile crack growth can, therefore, lead to a sudden increase of the stress ahead of the notch root and it can, consequently, lead to the cleavage initiation.

Although there has been an extensive research on the micromechanisms of ductile fracture, only a little has been published about the influence of irradiation on ductile crack growth. In previous research of fractured impact and/or static loaded Charpy specimens from A508 Cl.3 reactor pressure vessel steel [1,3], the ductile area situated next to the notch root (after extracting of shear fracture near the lateral faces) was found to be closely correlated with the CVN impact energy even for the areas of surface less than 1 mm² (corresponding values of impact energy were lower than 20 J). In the temperature range from -60 °C to 0 °C (DBTT range) and strain rates of 10⁻³ s⁻¹ (quasi-static loaded specimens) and 10³ s⁻¹ (impact loaded specimens), the micromechanisms and kinetics of ductile crack growth were found to be the same, independent on temperature and strain rate.

In the paper presented, the influence of neutron irradiation on ductile crack initiation and growth is studied on fracture surfaces of impact loaded Charpy specimens broken in the DBTT range. The steel chosen for this study was the 15Ch2MFA (15Cr2MoV) tempered bainitic steels used for fabrication of pressure vessels of VVER 440-type nuclear reactors [4]. The Charpy V-notch (CVN) specimens were taken at a depth position at one quarter of the plate thickness from the surface (1/4r position) in the T-S (long transverse-short transverse) orientation. The specimens were enclosed and neutron irradiated (in the same capsules as standard surveillance specimens) in emptied surveillance channels in the nuclear reactor of VVER 440-type. The mean irradiation temperature was estimated after evaluation of the melting temperature monitors to 275 °C.

Charpy tests were carried out on an instrumented impact pendulum device Tinius-Olsen 74 (sampling frequency was 1 MHz) with nominal impact energy 358.5 J and nominal impact velocity 5.1 m.s⁻¹ at various temperatures ranging from -190 °C to +240 °C. Measurement of ductile crack length (situated next to the notch root) was carried out on the photographs acquired by a standard CCD camera. The final fracture in CVN specimens occurred in DBTT range by cleavage. The cleavage facets reflect the light more than the ductile dimples, which makes possible to distinguish the ductile dimpled zones on the fracture surface. The ductile crack length was measured as the mean value of crack extensions at nine

equally spaced points centred about the specimen centreline (ASTM E1820-99). For non-irradiated specimens, the methodology was confirmed by measurement of ductile crack length in a Scanning Electron Microscope (SEM) Jeol JSM 840.

Neutron-irradiation caused a shift of DBTT of about 65°C after neutron fluence, $\Phi_n \sim 10^{24} \text{ n.m}^{-2}$. Neutron-irradiation caused a slight decrease of the upper shelf energy from about 110 J in non-irradiated state to about 95 J after neutron fluence $\Phi_n \sim 10^{24} \text{ n.m}^{-2}$. The influence of irradiation can be seen on instrumented test record. With increasing neutron fluence the maximum reaction force increases. Conversely, the fracture displacement, d_F (striker displacement at brittle fracture initiation) and the force at the crack arrest, F_A decrease.

Measured ductile crack lengths, Δa exhibit a quasi-linear dependence of ductile crack length on the fracture energy; practically the same curves are obtained for neutron irradiated and non-irradiated specimens. There is no significant acceleration in ductile crack initiation or growth with increasing neutron fluence. Measured shear band widths exhibit a quasi-linear dependence of the shear band width on the fracture energy and/or fracture displacement. The slope of the dependence of the shear band width on fracture energy (and/or fracture displacement) increases with increasing neutron fluence. The increasing amount of shear fracture on fracture surface could explain the decrease of upper shelf energy. In non-irradiated specimens broken completely in a ductile manner, the amount of shear fracture was about 20%. In specimens irradiated by neutron fluence $\Phi_n \sim 10^{24} \text{ n.m}^{-2}$, the amount of shear fracture increased to about 30%. This corresponds well to observed decrease of upper shelf energy of about 15 J.

Presented results indicate that the micromechanisms and kinetics of ductile crack growth are therefore the same, independent on neutron fluence (up to given neutron fluences) and the DBTT shift is primary caused by higher stresses developed at the notch root of irradiated specimens due to the matrix hardening and not due to the faster ductile crack initiation or growth.

References:

- [1] HAUŠILD, P. – NEDBAL, I. – BERDIN, C. – PRIOUL, C.: *The Influence of Ductile Tearing on Fracture Energy in the Ductile-to-Brittle Transition Temperature Range*, Materials Science and Engineering A335, 2002, pp. 164-174.
- [2] ROSSOLL, A. – BERDIN, C. – PRIOUL, C.: *Determination of the fracture toughness of a low alloy steel by the instrumented Charpy impact test*, International Journal of Fracture 115, 2002, pp. 205-226.
- [3] HAUŠILD, P. – NEDBAL, I.: *Vliv teploty a rychlosti deformace na tvárný lom reaktorové oceli A508*, Kovové Materiály 41(4), 2003, pp. 81-86.
- [4] KOUTSKÝ, J. – KOČÍK, J.: *Radiation Damage of Structural Materials*, Materials Science Monographs, Vol. 79, Elsevier Science Publ., Amsterdam, 1994.

This research has been supported by the Grant Agency of the Czech Republic in the frame of the project No. 106/04/0066.

Innovation of Computer Graphics Stream at the CTU FEE

I. Jelinek

jelinek@fel.cvut.cz

Department of Computer Science and Engineering, Faculty of Electrical Engineering,

Czech Technical University, Technická 2, 166 27 Prague 6, Czech Republic

The main aim of the project “Innovation of Computer Graphics Stream at the CTU FEE” was to improve of software instrumentation of the Laboratory of Computer Graphics at the Department of Computer Science and Engineering by the top products of computer graphics software. There were chosen 9 sections of computer graphics applications for innovation:

- Bitmap graphics editors
- Vector graphic editors
- DTP systems
- 2D animations systems
- 3D animations systems
- Authoring systems for web
- Authoring systems for CD ROM
- Developing systems web
- Video signal processing systems
-

A market research of possible computer graphics products in every section of the computer graphics application was undertaken. Then the criteria for selection of one product every application were established. The results of a selection procedure are presented in the following table.

Bitmap graphics editors	Adobe PhotoShop 7.0
Vector graphic editors	Corel Draw Graphics Suite 11 CZ (*)
DTP systems	Adobe InDesign 2.0 CZ
2D animations systems	Macromedia Flash MX 2004 (*)
3D animations systems	Autodesk 3DS MAX5.1, MAYA
Authoring systems for web	Macromedia DRAMWeaver MX (*)
Authoring systems for CD ROM	Macromedia Director MX Win
CAD systems	Autodesk Inventor Prof (*)
Video signal processing systems	Adobe Premiere 6.0

(*) bought from the grant and new installed

All the delivered products were immediately installed and used in the undergraduate course “Computer Graphics Applications”. In the frame of students’ projects of this course there were prepared the tutorials for students training for every application of Computer Graphics.

The instrumentation of the Laboratory of Computer Graphics at the Department of Computer Science and Engineering was qualitatively improved. This equipment is for the disposal not only for the students of the department also for all the students of the faculty.

This research has been supported by FRVŠ grant No. FRV 2013 F1.

Study and Development of CrN layers prepared by the Multiplex IBAD/CVD Technology

D. Tischler, S. Semenko, O. Pacherová, J. Gurovič

Daniel.Tischler@fs.cvut.cz

Czech Technical University, Faculty of Mechanical Engineering, Technická 4, Prague 6, Zip Code 166 07, Czech Republic.

Surface modification technologies can be divided into two groups. In the first group there are technologies, by which the surface layer of an original material is directly modified. Examples of these technologies are diffusion technologies, e.g. nitridation and ion implantation. In the second group there are technologies, by which the deposited layer with desired properties is created on the surface of original material... [1] Examples of these technologies are PVD (Physical vapour deposition), MOCVD (Metal organic chemical vapour deposition) and IBAD (Ion beam assisted deposition). Each technology has some advantages but also some disadvantages. It is beneficial to combine various technologies, especially from different groups, to make use of their advantages and limit their disadvantages. This paper deals with combination of IBAD and MOCVD, which be called **multiplex IBAD/MOCVD technology**.

IBAD process can work under relatively low temperatures, it is very well controllable and it also possible to control component ratio during deposition, so the desired concentration of component profile in the coating can be determined. The important advantage of IBAD is the very high adhesion of coatings. The high adhesion of coatings is given by consequence of ion beam mixing at the interface between coating and substrate. On the other side the high energy facilities can reach only relatively low ion current and therefore also low process productivity, what is the disadvantage of high energy IBAD method. MOCVD is a specialized area of CVD which utilizes metallo-organic compounds as precursors usually in combination with hybrids or other reactants. Metalorganic chemical vapour deposition (MOCVD) is an attractive process for the deposition of thin film dielectrics and other coatings, because it works under relatively low growth temperatures, high growth rates, and conformal coverage of substrates and lithographed high aspect ratio features. In such a chemical process for thin film deposition, the composition and structure of the film are determined by the chemical precursors used and the conditions (e.g. temperature and pressure) employed for film deposition. Thus, the properties of a MOCVD-grown film (electrical, optical, magnetic, and mechanical) are determined by a variety of physical and chemical processes involved in it's growth. In MOCVD process there are not particles with energies as high as the IBAD process and therefore adhesion problems often take place. This is disadvantage of the MOCVD process. But the advantage of MOCVD method is high process productivity in comparison with high energy IBAD process, because of higher coating thickness rate.

The CrN coatings were prepared on flat steel substrates AISI 616 (diameter 20×4). The side indented for coating deposition was mechanically polished with SiC paper and then diamond paste down to a final grade of $0,05 \mu\text{m}$. Substrates were cleaned ultrasonically in ethanol bath. The substrate surfaces were bombard by nitrogen ions accelerated to energy of 90 keV in ion implantater. During this ion bombardment the sputter cleaning proceeds and, in the case of some materials, the hardening of substrate surface area took place because of nitrogen ion implantation. This hardening is beneficial to avoid the breaking through hard deposited layer on a softer substrate. Prior to the growth coating CrN of technology MOCVD, the substrates were heated in H_2 atmosphere at 400°C in the MOCVD reactor for 10 min in order

to remove the native oxide from substrate surfaces. The growth temperature was 330°C, except for the initial CrN nucleation layer which was grown on AISI 316 substrate. Depositions of the chromium nitride thin films were carried out in a horizontal, hot-wall; low-pressure MOCVD reactor built in Department of Physics. It comprises a fused silica reactor tube of 90 mm (inner) diameter and 100 cm length, evacuated by a two-stage rotary vane pump (250 l/min). The precursor, Bis(benzene) chromium is a crystalline compound that sublimates. It is taken in the form of a fine powder placed in a silica boat which, in turn, is kept in a stainless steel vaporizer, whose temperature may be controlled to within 1 °C. The vapours of the precursors are carried into the reaction chamber by high purity argon, whose flow is regulated by an electronic mass flow controller. After the above process (900 nm thick) the samples were load into IBAD process. The sample has been load into chamber of IBAD process. Nitrogen ion beam etching at 90 keV/ 2 mA was employed to clean and activate the coating of substrate. After the ion bombardment, adhesion were improve by bombardment by ions with such energies to enable ions to reach coating (MOCVD) -coating (IBAD) interface. A dynamic recoil mixing was then used to prepare the interface, which combined the bombard with simultaneous sputtering of chromium (-10 kV/ 0,033 A). Then, because of collision cascades induced by bombardment, intensive ion beam mixing proceeds at the interface what is very beneficial for increasing of adhesion of coating on the thin film of MOCVD. During the CrN deposition, the same sputtering parameters were used, while the ion beam bombardment was kept at 90 keV/ 2 mA. The processing pressure was about 2×10^{-5} Pa. The deposition time was 4 h and the temperature was held below 180 °C. The thickness of the CrN coating (IBAD) was about 0,7 µm and its surface roughness was about the same as that of the substrate (0,05 µm). The microhardness of the coatings were investigated by means of equipment Leitz. The microhardness of prepared coatings was measured by Vickers method. The load on the indenter was applied in the range of (50 – 300) mN in five steps (50,100,150,200,300).The microhardness of the CrN coatings was HV_{0,005} 630 MPa which was measured by a Leitz Microhardness Tester. Dimensions of indentation figures were measured optically by microscope Leitz with camera connected to PC. The total thickness of coatings were about 1,5 µm. Example of the microhardness measurement of the multiplex IBAD/MOCVD CrN coatings together with dependence of the Vickers microhardness (HV) on the load in above mentioned range. The analogical of microhardness of shown to dependence of the substrate itself is, too. The microhardness value in case of substrate with coating is much higher than that in case of substrate only. It can be seen that microhardness values for the lowest load in the case of substrate with coating is about 2,3 times higher than that in the case of substrate only and what next values are approximately conformable. If we apply the load of 50 to 1000 mN to the sample surface gives hardness of 300 to 650 HV what leads to the indentation depth values of order of units of micrometers and the thickness of the coating is about 1500 nm.

References:

- [1] CERNY, F.- SMOLIK, J - GUROVIC, J.- GORODINSKIY, V.: *Multiplex IBAD/PACVD Technology* Surface modification technologies XIV, Ohio 2001, pp. č. 522 - 525

This research has been supported by CTU grant No. CTU021084046.

Study and prepared Cr(N) layers as anticorrosive protection.

T. Horaždovský, D. Tischler, S. Semenko, S. Vacková, J. Gurovič and V. Chmelík.

Daniel.Tischler@fs.cvut.cz

Czech Technical University, Faculty of Mechanical Engineering, Technická 4, Prague 6, Zip Code 166 07, Czech Republic.

CrN coating is usually used for surface protection of cutting tools, die blocks, pressing moulds etc. Wear resistance and other mechanical properties are very important at the applications, but also high temperature stability and corrosion resistance are very significant. Corrosion properties are usually examined by high temperature oxidation tests but sometimes are used low temperature tests in aqueous electrolytes are applied. Tests in electrolytes are fast and simple, but in principle their results give evidence about porosity and not about high temperature corrosion resistance.

There are not too many papers concerning anticorrosion properties of CrN_x IBAD, are so limited our literature overview was extended to all types of nitrides. Mitterer et al. [1] have used the nitride coatings to surface protection of steel mould for aluminium casting. The coatings were formed by titanium and aluminum nitrides, which were deposited by magnetron like PACVD (Plasma Assisted Chemical Vapour Deposition) methods. These coatings have shown high resistance against corrosion fatigue and oxidation during laboratory tests. Field test has given remarkable increasing of the mould life-time. Scharf with Barnard [2] have deposited IBAD nitride coatings, but from our point of view these coatings were too thin (around 5 nm). Wang et al. [3] have studied oxidation behavior of CrN coatings, which were deposited on AISI 304 steel. Samples have been tested at temperature 300 – 800 °C for 60 minutes. In the deposited state, the coating contains besides CrN a small amount β-Cr₂N phase. Over 600 °C the CrN phase turns to change to β-Cr₂N and transformation is finished at 800 °C. Oxidation of the nitrides was observed at temperature above 500 °C and size of the oxide and nitride grains increases with temperature. As regards the temperature stability of nitride coatings there are similar conclusions in paper [4]. It has studied the influence of deposition parameters on CrN magnetron coatings and general corrosion resistance he has tested by electrochemical method in desecrated 1 M H₂SO₄ at room temperature. It is very interesting that the hardest coatings (1790 HV) have shown maximum portion of Cr₂N phase. According to the substoichiometric Cr₂N coatings have microhardness up to 2100 HV. Their bad adhesion he has explain by high level of internal stresses. He has found out the crystals of metal chromium in addition to CrN and Cr₂N. In the coatings have had very good adhesion and corrosion resistance.

The coatings were deposited on samples (of diameter 20 mm and thickness 4 mm) made from high-nickel INCO 738 alloy and stainless AISI 316 steel. Substrate surface was before coating deposition mechanically grinded and polished. Before own deposition process the samples were ultrasonically degreased in acetone. Process conditions: First 0,1 μm thick chromium layer was deposited by electron beam evaporation followed simultaneous chromium evaporation (flow density $1.8 \times 10^{17} \text{ m}^{-2} \cdot \text{s}^{-1}$) and nitrogen ions bombardment (flow density $3.9 \times 10^{17} \text{ m}^{-2} \cdot \text{s}^{-1}$). Nitrogen ions energy was 91,6 keV. Total thickness (nominal) of coating was about 2 μm. Corrosion tests: Corrosion tests were taken in air at temperatures 700

and 800 °C for total time 500 h. The tests were interrupted after 50, 100, 200 and 500 h. Corrosion kinetics was evaluated by gravimetric measuring of weight gains during each test interruption. Each point in the diagrams represents the arithmetical average from weighing of 10 samples.

The dynamic microhardness (DHV) of coatings was measured by nanoindenter at 2 g (IBAD coatings). Thicknesses of coatings were measured by calotest method (i.e. coatings were grinded through by rotating sphere and the thicknesses were measured on grinded surface by light microscope). Adhesion of coatings were measured by scratch tester (with cone tip) at trust force varying in range 0 – 80 N. Chemical composition of coatings in as deposited state was measured by electron probe microanalyzator (with wave dispersion of emitted X-rays) at electron beam energy 10, 15 and 20 keV.

Given results of scratch test are to some extent distorted by fact, that test tip very easy deforms austenitic substrate. The deformation causes supplementary stress and peeling of coating. The thicker magnetron coating is failed also by de-cohesion inside the coating. This phenomenon is inherence of high level of internal stresses. Results of chemical analysis show, that all studied coatings contain large amount of non-reacted pure chromium in addition to chromium nitride.

Corrosion resistance of CrN_x coatings is better than resistance of substrate. It means that atomic mixing which is on the coating – substrate interface has negligible influence on protection ability of the coating. In addition to it IBAD coatings oxidize at 900 °C very quickly and arising oxide layer has no protection ability. By contrast the magnetron coating has at 900 °C good protection ability and fast oxidation comes only at 1000 °C. Moreover oxide layer arising from magnetron coatings slows down the corrosion rate of substrate in comparison with non-coated one. The processing gas residua occluded in magnetron coatings can caused its breaking and peeling during high temperature exposure. Therefore it is suitable to degasify the coatings by vacuum annealing for a few hours at temperature 600 °C .

References:

- [1] MITTERER, C. – HOLLER, F.- USTEL, F.- HEIM, D.: Surface and Coatings Technology 125 2000 č. 233.
- [2] SCHARF, T. – BARNARD, J.: Journal of Information Storage and Processing Systems 2000 č. 185.
- [3] WANG, C.C.: Journal of the Electrochemical Society 150 2003 pp. č. 199–č. 204.
- [4] HEAU, C.: Surface and Coatings Technology 121 , 1999 pp. č. 200 – č. 205.

This research has been supported by 1184173

The Variations of Thermal Conductivity and Porosity of Cementitious Composites Due to the Thermal Load

J. Toman, E. Mňahončáková, P. Rovnaníková*, R. Černý**

cernyr@fsv.cvut.cz

Department of Physics, Faculty of Civil Engineering, Czech Technical University, Thákurova 7, 166 29 Prague 6, Czech Republic

*Institute of Chemistry, Faculty of Civil Engineering, Brno University of Technology, Žižkova 17, 662 37 Brno, Czech Republic

**Department of Structural Mechanics, Faculty of Civil Engineering, Czech Technical University, Thákurova 7, 166 29 Prague 6, Czech Republic

Cementitious composites contain a significant amount of pores of different size that can be filled either by air or water. Therefore, both the total pore volume and the distribution of pores can affect their thermal conductivity in a very significant way. In this paper, the effect of the amount and the size of the pores on the thermal conductivity is studied for two carbon fiber reinforced cement composites. The changes in their porosity are induced by the thermal load, tensile load and their combinations.

The measurements were done on two different types of carbon fiber reinforced cement composites (CFRC) produced in the laboratories of VUSH Brno that will be denoted as UC II, UC III in what follows. Portland cement CEM I 52.5 Mokr was used for UC II, high alumina cement Alcoa CA-14M for UC III. Carbon fiber was PAN for UC II, pitch based for UC III, both with 10 mm length. Water in the amount corresponding to the w/c ratio of 0.9 was added to the mixture for UC II, 0.73 for UC III.

In the experimental measurements, eleven various specimen pre-treatment conditions were tested:

- Reference specimen not exposed to any load.
- Specimen exposed to a gradual temperature increase up to 600, 800 and 1000°C during two hours, then left for another 2 hours at the final temperature and slowly cooled.
- Specimen exposed to tensile load up to breaking.
- Specimen exposed first to tensile load up to breaking, then to a gradual temperature increase up to 600, 800 and 1000°C during two hours, after that left for another 2 hours at the final temperature and slowly cooled.
- Specimen exposed to a gradual temperature increase up to 600, 800 and 1000°C during two hours, then left for another 2 hours at the final temperature, slowly cooled and finally exposed to tensile load up to breaking.

The thermal conductivity was measured using the commercial device ISOMET 2104 (Applied Precision, Ltd., SK). It is equipped with various types of optional probes, where surface probes are suitable for hard materials. The measurement is based on analysis of the temperature response of the analyzed material to heat flow impulses.

The thermal load up to 1000°C, tensile load up to breaking and their combinations were found to have very different effects on the thermal conductivity of the two investigated types of CFRC. Generally it can be concluded that the effect of thermal load was much more remarkable than that of tensile load. The thermal decomposition processes also dominated the changes of thermal conductivity for all the analyzed combinations of thermal and tensile load.

The effect of high alumina cement on the thermal conductivity of samples subjected to elevated temperatures was not found to be so distinct as it might be anticipated from the expected stabilization of the aluminat structure after the conversion occurring at relatively low temperatures. After the pre-heating procedures, the thermal conductivity of the CFRC material UC III containing high alumina cement was very similar to the properties of the material UC II containing common Portland cement. The reason for this could be the autoclaving of UC II applied at its production.

In looking for the correlation of thermal conductivity of thermally pre-treated UC II samples with the porosity measurements we realized that compared to the reference specimen, the porosity of UC II for the 600⁰C pre-heating decreased by 8%, for 800⁰C it increased by 22% and for 1000⁰C by 44%. The changes in the pore distribution were more remarkable. For the 600⁰C pre-heating the most distinct peak of the incremental volume curve of UC II at 20 nm decreased to about one half and the amount of bigger pores increased in practically the whole range. The 800⁰C pre-heating then led to an almost complete reversal of the pore distribution curve. The 20 nm peak completely disappeared and a new peak at about 3 μm became dominant. The pre-heating to 1000⁰C resulted in a remarkable increase of the amount of bigger pores in a relatively wide range of 200 nm to 10 μm. The relatively low effect of the pre-heating of the material UC II to 600⁰C on its pore structure indicates that the decomposition of Ca(OH)₂ supposed to take place in Portland cement based composites at about 460-480 °C [1] was of much lower importance in our particular case which was probably due to the autoclaving procedure applied in the specimen production.

The remarkable decrease in thermal conductivity of UC III after the 600⁰C pre-heating was clearly a consequence of a significant increase of porosity after heating. The global pore characteristics show that the samples of UC III preheated to 600⁰C exhibited an about 20% increase in porosity compared to the reference specimens. Comparison of the respective pore distribution curves shows for the 600⁰C preheated UC III samples a shift of the most distinct peak from 1 μm to 1.5 μm and its increase by about 25%. This peak remained at the same position also for the specimens pre-heated to 800⁰C and 1000⁰C which is in a good accordance with the thermal conductivity measurements.

It seems surprising that the very significant difference in the pore distribution curves of the samples pre-heated to 600⁰C and 800⁰C resulted in only relatively small difference in thermal conductivity. However, the overall character of the correlation of changes in thermal conductivity with the changes in the porosity and in the pore distribution looks similar as in the case of the above analyzed differences between the room temperature values of thermal conductivity and porosity of UC II and UC III. It can be summarized that for the measurements throughout this paper, the higher porosity has led in all cases to lower thermal conductivity but the presence of bigger pores resulted in an increase of thermal conductivity, probably due to the appearance of thermal bridges.

References:

- [1] Z.P. BAŽANT, M.F. KAPLAN: *Concrete at High Temperatures: Material Properties and Mathematical Models*, Longman, Harlow, 1996.

This research has been supported by the MŠMT KONTAKT project SK-2.

Yield Strength of Low Carbon Cast Steels

K.Macek, J.Cejp, Ganwarich Pluphrach

karel.macek@fs.cvut.cz

CTU, Faculty of Mechanical Engineering, Dept. of Materials Eng.
Karlovo n. 13, 121 35 Praha 2

Demands for weldable, tough steel with improved yield strength lead to microalloying of low carbon steel with aluminium, vanadium, titanium and niobium singly or by combining these chemical elements. Unlike to famous wrought high strength low alloyed (HSLA) steels, the cast steels can not be strengthened by means of plastic deformation during thermomechanical treatment. Hence, the improved yield strength can be attained only by carefully controlled heat treatment, which should not be too complicated. Normalizing and/or solution annealing come under consideration.

Yield strength of every polycrystalline metallic material obeys extended Hall-Petch relationship

$$R_y = R_0 + \Delta R_a + \Delta R_g + \Delta R_p + \Delta R_t \quad (1)$$

where R_0 is friction stress and ΔR_t are contributions owing to alloying, grain-size refinement, precipitation and phase transformation, respectively. The friction stress R_0 is usually taken as 40 MPa for low carbon low alloyed steels, alloying contribution ΔR_a is related only to solid solution strengthening and is linearly proportional to the concentration of chemical element $k_a \cdot (\text{wt.\%X})$ [1]. Grain size contribution $\Delta R_g = k_g \cdot d^{-1/2}$, where d is the grain diameter. Precipitation contribution ΔR_p is proportional to precipitation potential (M), $\Delta R_p = k_p \cdot (M)$, when (M) is the content of precipitate forming metallic element in austenite [2]. Generally, it is considered that M is able to create dispersed precipitates of carbide MC, nitride MN or carbonitride M(C,N). The precipitation potential (M) is derived from solubility product, which e.g. for aluminium nitride has form [3]

$$\log [(Al).(N)] = 1,95 - \frac{7400}{T} \quad (2)$$

Last term in relation (1) represent matrix phase transformation strengthening. According to [1] this contribution can be neglected, if the phase transformation product is pearlite, however in case of bainite or acicular ferrite that may be present in microstructure, we suggest following expression

$$\Delta R_t = f_B \cdot (150 + 15 \cdot l^{-1/2}) \quad (3)$$

where f_B is volume fraction of microstructural component and l [mm] is lath size, taken as mean linear intercept. When relation (3) is used, the rule of mixtures should be applied also on contribution ΔR_g reflecting above all the polygonal ferrite grain size.

The objective of this paper is verify the validity of above described model for prediction of yield strength on low carbon steel 19Mn5 singly microalloyed (killed) with aluminium in two kinds of heat treatment – normalizing (N) or solution annealing (SA).

Pilot-plant heat had following chemical composition (in wt.%) : 0,19 % C–1,16 % Mn–0,25 % Si–0,023 % P–0,009 % S–0,12 % Cr–0,20 % Ni–0,08 % Mo–<0,01 % V–<0,01 % Ti–<0,01 % Nb–0,34 % Cu–0,040 % Al–0,008 % N. The heat was casted into plates with dimensions 30x250x350 mm which were normalized 900 °C, 3 h, air cool or solution annealed 1100 °C, 10 h, air cool.

Tensile tests were conducted at room temperature on device INSTRON 5582 (100 kN) in accordance with standard ČSN EN 100002-1. We obtained following average (3 specimen) mechanical properties :

steel 19Mn5N – $R_{p0,2} = 378$ MPa, $R_m = 629$ MPa, $A = 24$ %, $Z = 33$ %
 steel 19Mn5SA – $R_{p0,2} = 350$ MPa, $R_m = 585$ MPa, $A = 18$ %, $Z = 35$ %

Quantitative light microscopy gave these characteristics :

steel 19Mn5N – polygonal ferrite and pearlite : vol. fraction 76,7 %, grain size 18 μm
 acicular ferrite : vol. fraction 23,3 %, lath size 5 μm
 steel 19Mn5SA – polygonal ferrite and pearlite : vol. fraction 79,6, grain size 33 μm
 acicular ferrite : vol. fraction 20,4 %, lath size 10 μm

Predicted yield strength computed from eq. (1) with all the contributions and experimental yield strength $R_{p,0,2}$ are summarized in next table (values in MPa) :

Steel	R_0	ΔR_a	ΔR_g	ΔR_p	ΔR_t	R_y	$R_{p0,2}$
19Mn5N	40	95,5	114,5	39	84	373	378
19Mn5SA	40	95,5	87,5	60	61	344	350

Notes : values of k_a were taken from [1], precipit. potential (Al) was computed from eq. (2) and k_p was estimated as 1500.

In conclusion is to be emphasized that the model based on Hall-Petch relationship works fairly well, but chosen conditions of solution annealing decreased the yield strength of steel 19Mn5. New relation for contribution caused by transformation strengthening (3) was suggested.

References:

- [1] PICKERING,F.B.: *Physical Metallurgy and the Design of Steels*. London, Applied Science 1978, pp. 62- 72.
- [2] LIN,H.R. – HENDRICKSON,A.A.: *Metalurg. Trans. Vol. 19A, 1988, pp. 1471-1480.*
- [3] STRID, J. – EASTERLING,K.E.: *Acta Metalurgica, Vol.33, 1985, pp.2057-2074.*

This research has been supported by GA ĆR grant No. 106/03/0473

Research of Technology Used for Fabrication of Active and Passive Waveguides on Semiconductor Base

V. Prajzler, I. Hüttel*, J. Špírková*, J. Oswald**,
V. Peřina***, J. Haméček*, V. Machovič*, Z. Burián

Vasek.Prajzler@email.cz

Department of Microelectronics, Faculty of Electrical Engineering,
Czech Technical University,
Technická 2, 166 27 Prague 6, Czech Republic

* Institute of Chemical Technology,
Technická 5, 166 28, Prague 6, Czech Republic

** Institute of Physics, Academy of Sciences,
Cukrovarnická 10, Prague 6, Czech Republic

*** Institute of Nuclear Physics, Academy of Sciences,
Řež near Prague, Czech Republic

Gallium nitride (GaN) and related nitride compounds semiconductor materials have attracted considerable attention because of their possibility to be used in optoelectronics devices such as blue/green light emitting diodes and laser diodes. GaN is a wide band gap semiconductor crystallising in the wurtzite structure with a direct gap of 3.50 eV at 300 K [1]. GaN is usually fabricated by MOCVD (Metal Organic Chemical Vapor Deposition), but many research group produced GaN by using MBE (Molecular Beam Epitaxy) or HVPE (Hydride Vapor Phase Epitaxy). GaN layers can be deposited on various substrates, such as silicon carbide (6H-SiC), sapphire (Al_2O_3), lithium gallium oxide (LiGaO_2), and silicon (Si(111)).

The rare earth (RE) doped optical materials are of significant current interest for applications as solid state laser, optical amplifiers and full color display. The most interesting RE ion is erbium [2], because erbium doped semiconductor can be used as light source emitting at 1.54 μm , which is of great interest for optical fiber communication system. It was previously shown in [3] that the thermal quenching in Er-doped semiconductors decreased the bandgap. Therefore wide bandgap such as GaN are suitable hosts for the RE elements.

This paper will give an overview of our development of the RE doped GaN layers fabricated by magnetron sputtering. The GaN samples were deposited by using the *Balzers Pfeiffer PLS 160* system from gallium oxide target (purity 99.99%, Sigma-Aldrich) on silicon, silica on silicon or Corning glass substrates. Typical growth parameters were: deposition temperature 300 K, deposition time 60 - 240 min, nitrogen-argon ratio 3:7, total gas pressure 3.4 Pa, power 50 Watts. For erbium and ytterbium doping into the gallium nitride films the pellets of $\text{Er}_2\text{O}_3\text{:Yb}_2\text{O}_3$ (99.9% purity, Sigma-Aldrich) or Er:Yb powder were put on the top of Ga_2O_3 target.

The structure of the deposited GaN thin films was studied by the XRD (X-ray diffraction). Fabricated samples had amorphous texture with poorly developed crystals. The composition of the deposited layers was determined by means of nuclear analytical methods. The Ga:N ratio and content of oxygen (O) was obtained by the Rutherford Back-Scattering

(RBS) measurement using 2.4 MeV protons. The content of the incorporated erbium and ytterbium was determined by RBS using both the 2.4 MeV protons and 2.2 MeV alpha particles. The amount of the incorporated erbium differed depending on the area of the target covered by the $\text{Er}_2\text{O}_3\text{:Yb}_2\text{O}_3$ pellets or Er:Yb powder as well as on the erosion area represented by the part of the surface covered by the RE source.

The transmission spectra of the samples in the spectral region from 300 nm to 600 nm at room temperature were taken as well. For that the tungsten lamp and monochromator MDR 23 were used as light source and the light transmitted through the samples was detected by the pyro-detector. Transmission spectra of the samples fabricated by magnetron sputtering onto the Corning glass (to ensure that the light will be transmitted through the whole structure) were compared with the GaN fabricated by the MOCVD deposited onto sapphire substrate. The absorption edge at the GaN samples fabricated by magnetron sputtering was not so steep as the GaN samples fabricated by MOCVD. The reason is the GaN on the sapphire substrate had monocrystalline structure.

The Ar laser ILA-120 at $\lambda_{\text{ex}} = 488 \text{ nm}$ with $E_{\text{ex}} = 100 \text{ mW}$ and semiconductor laser P4300 at $\lambda_{\text{ex}} = 980 \text{ nm}$ with $E_{\text{ex}} = 500 \text{ mW}$ were applied for photoluminescence measurement. We observed PL emission peak at 1 530 nm at room temperature due to excitation into the $^4\text{I}_{15/2} \rightarrow ^4\text{I}_{7/2}$ and due to $^4\text{I}_{11/2} \rightarrow ^4\text{I}_{15/2}$ transition. The strongest photoluminescence we observed at the Er:GaN sample fabricated by sputtering with two Er_2O_3 pellets (5 mm diameter) laying on the top of the Ga_2O_3 target. For more details of the fabrication process and RE doped GaN properties see [4].

The magnetron sputtering was used to fabricate RE doped GaN layers fabricated by magnetron sputtering on various substrate using a gaseous mixture of nitrogen and argon as precursors. The doping of the GaN films with RE occurred simultaneously with the sputtering process when placing the metal RE pellets or RE powder onto the Ga_2O_3 target. The amount of the incorporated erbium increased with increasing weight of the RE pellets or RE powder. We observed photoluminescence emission at 1 550 nm due to the $^4\text{I}_{13/2} \rightarrow ^4\text{I}_{15/2}$ transition under excitation at 488 nm and 980 nm.

References:

- [1] S.M. WIDSTRAND, K.O. MAGNUSSON, M.I. LARSSON, L.S.O. JOHANSSON, J.B. GUSTAFSSON, E. MOONS, H.W. YEOM, H. MIKI, M. OSHIMA: *Preparation of Stoichiometric GaN(0001) - 1×1 Studied with Spectromicroscopy*, Surface Science, 572: (2-3), 2004, pp. 409-417.
- [2] A.POLMAN: *Erbium implanted thin film photonic materials*, Journal of Applied Physics, 82: (1), 1997, pp.1-39.
- [3] P.N. FAVENNEC, H. LCHARIDON, M. SALVI, D. MOUTONNET, Y. LEGUILLOU: *Luminescence of Erbium Implanted in Various Semiconductors - IV-Materials, III-V-Materials and II-VI Materials*, Electronics Letters 25: (11), 1989, pp. 718-719.
- [4] V. PRAJZLER, J. SCHRÖFEL, I. HÜTTEL, J. ŠPIRKOVÁ, V. MACHOVIČ, V. PEŘINA: *Er:GaN Thin Films Fabricated by Magnetron Sputtering*, The 2nd International Conference on Technological Advances of Thin Films & Surface Coatings, Incorporating Nanotechnology Business Forum - CD Proceedings Singapore, 2004, 34-OTF-A315.

This research has been supported by GA ČR grant No. 104/03/0385 and No. GA 104/03/0387 and the CTU grant No. CTU0407813.

Polymer Optical Planar Waveguides Containing Erbium Ions

V. Prajzler, M. Prajer *, I. Hüttel*,
J. Špirková*, J. Ondráčková*, J. Oswald**

Vasek.Prajzler@email.cz

Department of Microelectronics, Faculty of Electrical Engineering,
Czech Technical University,
Technická 2, 166 27 Prague 6, Czech Republic

* Institute of Chemical Technology,*
Technická 5, 166 28, Prague 6, Czech Republic

** Institute of Physics, Academy of Sciences,
Cukrovarnická 10, Prague 6, Czech Republic

We report about fabrication and properties of the erbium ions containing Poly(1-vinylpyrrolidone-co-vinyl acetate) (PEO), Polymethylmethacrylate (PMMA) and Polystyrene (PS) planar optical waveguides fabricated by spin coating.

Semiconductor materials and dielectric materials such as lithium niobate are relative expensive and the processes used to fabricate optical devices are very complicated. Polymer-based optical layers offer a low-cost alternative for inorganic optical waveguides. Optical polymers can be transparent, with low absorption loss below 0.1 dB/cm at the key communication wavelengths of 1 300 and 1 550 nm [1] and the fabrication process is not complex. Rare earth (RE) doped optical materials can be used for fabrication of solid state lasers and optical amplifiers. The most interesting RE ions is Erbium (Er^{3+}), because Er^{3+} doped optical materials can be used for fabrication of optical amplifiers operating at 1 550 nm due to the $\text{Er}^{3+} {}^4\text{I}_{13/2} \rightarrow {}^4\text{I}_{15/2}$ optical transition [2].

The polymer optical waveguides were theoretically designed by using mathematical modification of the dispersion equation. We determined the number of guided modes and critical thickness of the waveguides. After that the polymer layers were fabricated by spin coating on silicon and silica-on silica substrates. The drawing of the spin-coating set-up and designed optical waveguides were previously described in [3].

For the coating the polystyrene Sigma-Aldrich, M_w 20 000, $\rho = 1.05 \text{ g/cm}^3$, $T_g = 104 \text{ }^\circ\text{C}$ was dissolved in toluene (Penta, $\rho = 0.8675 \text{ g/cm}^3$) obtaining thus solutions with different PS concentrations. The fabrication procedure was as follows: a drop of the PS solution was trickled down onto the substrate from a pipette, then the substrate was let to spin round, the PS drop covered the substrate surface and partially evaporated out. Rare earth ions can not be directly dissolved in the polymer precursors. To introduce the erbium ions into the polymer matrix, we synthesised the chelate complex 8-hydroxychinoline that was then mixed with strongly diluted solutions of several polymers as, e.g. Poly(1-vinylpyrrolidone-co-vinyl acetate) (PEO), Polymethylmethacrylate (PMMA) or Polystyrene (PS). The mixture of the polymer and the chelate was then deposited onto substrate wafers by spin coating [4]. The best samples were obtained when dropping 2 ml of the PS solution on the spin coater, waiting for 5 s to let the drop to spill on the substrate and then to spin dry (2 000 - 4 000 rev/min). The deposited layers were then let to dry for 30 minutes at 80 $^\circ\text{C}$. For example, using 6% PS solution and 2 500 rev/min gave 6 μm thick PS optical layers.

Properties of the fabricated layers were analyzed by various methods. Refractive indices of the samples were determined using refractometer at wavelength range from 300 to 800 nm and by prism coupling method at 632.8 nm. Optical losses were evaluated by scanning the light scattered from the waveguides by the CCD camera. The absorption spectra were taken at wavelength range from 300 to 600 nm. Photoluminescence properties of the samples were measured using Ar laser at 488 nm.

All the samples deposited onto the silica-on-silicon substrate had waveguiding properties. The number of propagating modes varied from 1 to 12 depending on the thickness of the deposited layers. For the PS waveguides the value of the refractive index was 1.52 at 632.8 nm. The measured thickness of the waveguide corresponds well with calculated values. Observed differences between calculated and experimental depths of the waveguides, which are rather small (less than 10%), are due to low values of the refractive indices inserted into the used dispersion equation. For more details see [3]. Optical losses of the best samples without erbium were found to be below 0.2 dB/cm. Doping with Er^{3+} makes the optical losses to increase, probably because clusters of erbium scattered the propagating light. We observed photoluminescence emission at 1550 nm due to ${}^4\text{I}_{13/2} \rightarrow {}^4\text{I}_{15/2}$ under excitation at 488 nm.

References:

- [1] L. ELDADA: *Organic Photonic Materials and Devices IV*, Proceedings of SPIE Vol. 4642 OPTOELECTRONICS 2002.
- [2] L.H. SLOOFF: *Rare-Earth Doped Polymer Waveguides and Light Emitting Diodes*, PhD thesis 2000 ISBN: 90-393-2537-5.
- [3] M. PRAJER, V. PRAJZLER: *Polymer Optical Planar Waveguide*, 8th International Student Conference on Electrical Engineering, POSTER 2004, NS19.
- [4] R. MICHALEK *Handbook of Thin Films Process Technology*, IOP Publishing Bristol and Philadelphia 1995.

This research has been supported by GA ĀR grant No. 104/03/0385.

Measurement of Optical Losses in Gallium Nitride Layers

V. Prajzler, M. Skalský*, I. Hüttel**, J. Špírková**,
J. Stejskal**, V. Drahoš, Z. Burian

Vasek.Prajzler@email.cz

Department of Microelectronics, Faculty of Electrical Engineering,
Czech Technical University,
Technická 2, 166 27 Prague 6, Czech Republic

* Institute of Radio Engineering and Electronics,
Academy of Sciences of the Czech Republic,
Chaberska 57, 18251 Prague 8, Czech Republic

** Institute of Chemical Technology,
Technická 5, 166 28, Prague 6, Czech Republic

Optical losses and refractive indices are two of the most important parameters which characterize the quality of optical waveguides. We would like to present simple measurement method that allows us to determine nondestructively the propagation losses and method for refractive index measurement in optical planar waveguides. This loss measurement technique involves the measurement of transmitted and scattering light intensity as a function of propagation distance along the waveguide. For determination of refractive indices we used two-prism mode spectroscopy.

Principle of the scattered light measurement method, which we use to characterize the gallium nitride (GaN) layer fabricated by MOCVD (Metal Organic Chemical Vapor Deposition) on sapphire substrates [1], is based on the distribution of light scattered by imperfections in the optical planar waveguides. The vertically polarized (TE) laser beam which goes through a system of mirrors, a half-wave plate and a linear polarizer is guided into the optical planar waveguide by an optical prism. The optical coupler prism and the measured planar waveguide are mounted on a rotation stage. This allows us to select the individual guided mode for the measurement of optical losses. This guided mode passing through the optical planar waveguide and the optical light beam are dispersed at in homogeneities in the optical waveguides, so that the scattered light is generated. The light streak from the top of the optical planar waveguides is detected by a CCD video camera which is connected with an AD converter and a computer. The CCD camera is situated above the optical planar waveguide and it is focused on a region of interest on the surface of the waveguide core. The intensity of the scattered optical light must be set between level 0 and 255 points. Then the image of the scattered light can be taken and stored. This two-dimensional image is reduced to one-dimension one by summing the pixels intensities in each column separately. Then we obtained the one dimension light intensity which is a function of distance. The obtained profile of the scattered light is 5 mm long and it is divided into 1288 columns. The number of the columns depends on the maximum resolution of the chip used in the CCD video camera. In our case maximum resolution in the CCD chip was 1028 x 1288 pixels by 256 gray-levels. For a uniform loss along the waveguide length this measurement method is independent of which section of the optical waveguide is imaged. The scattered light decreases exponentially along the length of the optical planar waveguides. The attenuation coefficient is obtained by fitting the measured light intensity to decreasing exponential function. The attenuation coefficient is then recalculated and expressed in dB/cm units.

The scattered light measurement method can be used for measuring optical losses in planar waveguides. This technique has the advantage of being nondestructive, rapid, accurate, readily automated. It requires no special sample preparation and it is independent on the light coupling efficiency to the waveguide. This measurement method can evaluate optical losses in range from less than 1 dB/cm to more than 100 dB/cm. More details about this method are given in [2].

We demonstrate this measurement method for measuring optical losses in GaN planar waveguides. Optical losses were measured at the wavelength 632.8 nm and 781 nm. For optical coupling we used the Bi₁₂GeO₂₀ prism ($n=2.54350$, $\lambda=632.8$ nm; $n=2.494756$, $\lambda=781$ nm).

The smallest obtained value of optical attenuation was less than 3.5 dB/cm at 632.8 nm and 3 dB/cm at 781 nm (TE mode).

Waveguides properties of the planar waveguides were determined by measuring the effective indices by two-prism mode spectroscopy at 632.8 nm and 781 nm. We used the same prism for optical coupling as well as for optical losses measurement. The measured data were evaluated by using the inverse WKB method [3].

We observed 7 modes for TE polarization. Basic effective refractive index was $N_0=2.349278$ at $\lambda=632.8$ nm. However, we can not determine basic mode for TM polarization. The main reason is the small difference between the refractive index of GaN layers and the coupling prism. The thickness of the GaN layers was calculated from propagation constant of the TE and TM modes and it was 2.071 μm (TE mode) and 2.041 μm (TM mode). The difference is only 40 nm, which corresponds to 1.5 % of total thickness. We think that the reason for this difference is small inhomogeneous refractive index on the boundary between the substrate and the GaN layers. We observed 6 TE modes at $\lambda=781$ nm and the thickness corresponds to 2.022 μm . The thickness calculated for both TE and TM modes differed by 1 %, which is due to inhomogeneous thickness of the GaN sample. The refractive index were $n_o=2.35375$ (TE mode) and $n_c=2.39267$ (TM mode) at $\lambda=632.8$ nm. The refractive index (at $\lambda=781$ nm) were $n_o=2.33740$ (TE mode) and $n_c=2.37519$ (TM mode).

References:

- [1] H. MORKOC, S. STRITE, G.B. GAO, M.E. LIN, B. SVERDLOV, M. BURNS: *Large-Band-GaP SiC, III-V Nitride, and II-VI ZnSe-Based Semiconductor-Device Technologies*, Journal of Applied Physics 76: (3), 1994, pp. 1363-1398.
- [2] B.M. FOLEY, P. MELMAN: *Novel loss measurement technique for optical waveguides by imaging of scattered light*, Electronics Letters, 28: (6), 1992, pp. 584-585.
- [3] J.M. WHITE, P.F. HEIDRICH: *Optical Waveguide Refractive Index Profiles Determined from Measurement of Mode Indices: a Simple Analysis*, 15: (1), Applied Optics 1976, pp.151.
- [4] M.SKALSKÝ, J. JANATA, J. ČTYROKÝ, J. STEJSKAL. I. HUTTEL *Optical Properties of GaN Layers on Sapphire Substrate*, Optical Communications 2001, TECH-MARKET 2001, pp.81-85.

This research has been supported by GA ĀR grant No. 104/03/0385 and No. GA 104/03/0387.

Textural Fractography of Fatigue Failures under Variable Cycle Loading - Direct Solution

H. Lauschmann, J. Šumbera, F. Šiška, I. Nedbal

lausch@kmat.fjfi.cvut.cz

Department of Materials, Faculty of Nuclear Sciences and Physical Engineering, Czech Technical University, Trojanova 13, Praha 2, 120 00

The main task of the **quantitative fractography of fatigue failures** consists in relating the morphology of crack surface with crack growth rate (CGR). Typically, we investigate a set of images (obtained by scanning electron microscope, SEM) of fracture surfaces, with assigned values of CGR. The aim is an algorithm for estimation of the CGR directly from the image. Then we are able to estimate CGR for fracture surfaces from practical service, and to reconstitute the history of the failure.

Textural fractography of fatigue failures [1] is a new method, which has been developed since 1990 in the Dept. of Materials, FNSPE. SEM images of fracture surfaces are analyzed as image textures. Many methods may be used: decomposition of the image (Fourier, wavelet, ...), random field models (Gibbs, Markov, ...), extracting textural elements and modeling them by means of stochastic geometry, etc. Images are individually characterized by a set of textural parameters - a feature vector $f = [f_1, \dots, f_k]$.

The relation between the feature vector and CGR is expressed standardly in the **multilinear form** $\log(v) = \sum c_j f_j + c_{k+1}$, where index $j = 1, \dots, k$, denotes image features. The set of constants $c = [c_1, \dots, c_{k+1}]$ can be simply estimated by the least squares method. By means of testing statistical significance of the contribution of single image features f_j that ones not predicating CGR are excluded.

Up to now, routine fractographic reconstitution of fatigue crack growth was limited to cases of **constant cycle loading**. However, the cyclic loading in practice is usually **variable**. Morphologies of fracture surfaces are complicated and deeply dependent on loading regime. The time reconstitution of fractures was possible only individually in certain cases, and its reliability was limited. A general, unifying approach for these cases was highly desirable.

The conventional presumption, valid only for constant cycle loading, is: "Crack surface morphology is unambiguously related to the (conventional) CGR." Let us generalize the presumption as follows: "We will suppose the possibility to define the **reference crack growth rate (RCGR)**, which is unambiguously related to **selected features** of fracture surface morphology". The concept of RCGR implies a more general definition of time (in conventional approach time is defined as the number of loading cycles N).

A method how RCGR can be estimated from a cycle-by-cycle crack growth model was published by Lauschmann et al. during 2004 [2,3].

For a cyclic loading with variable, sufficiently stationary parameters, we may suppose that **the ratio between RCGR and conventional CGR can be approximately expressed by a constant B linked only to the given type of loading** (particularly, for constant cycle loading $B = 1$). Projecting this presumption into the system of equations mentioned above results in a more general regression formula with the absolute element c_{k+1} special for the given type of loading. The difference $c_{k+1, \text{constant cycle}} - c_{k+1, \text{variable cycle}}$ is just equal to constant $\log(B)$. This makes possible to estimate B for different types of loading [4].

The method was tested on a set of three CT-specimens from aluminium alloy AlCu4Mg1, loaded by different loading processes: constant cycle, constant cycle with a regulary overloading (called "Z+1"), and a random block. Crack growth was measured and recorded. Crack surfaces were documented by SEM images in magnification 200 x, which were

assigned values of the mean CGR pertinent to the center of the image. Images were normalized and two decomposition methods were applied to estimate the feature vectors: The two-dimensional Fourier transformation and the wavelet transformation.

Both methods gave almost the same values of B ($B_{Z+1} = 1.69$, $B_{\text{random}} = 4.9$). Moreover, for random loading the result is very close to that obtained by physical model [2,3]. When RCGR is estimated as CGR multiplied by B , a very tight relation (close to equality) of crack rates measured and estimated from single images is reached.

By imaging only image features which remained in the final model [4], we can see the elements of fracture surface morphology which are common for all fracture surfaces without any respect to the type of loading.

We may conclude: **For the reference crack growth rate, some common morphologic features are present in all fracture surfaces**, without any influence of different loading conditions. On the contrary, the conventional crack growth rate has no morphologic correlate common for all fracture surfaces.

Results reached are highly valuable for the practical application. The concept of reference crack growth rate opens way to **routine fractographic reconstitution of fatigue crack growth under variable cycle loading**. The direct solution is limited to experimental fractographic techniques and does not require the knowledge of the loading sequence. It enables to estimate directly from images of fracture surface an important characteristic B , which characterizes the loading process.

Recent methodological progress described above significantly improves possibilities of the quantitative fractography of fatigue failures.

References:

- [1] H. LAUSCHMANN H., M. TŮMA, O. RÁČEK, I. NEDBAL: *Textural fractography*. Image Analysis and Stereology, Special issue Vol.21, 2002, pp.S49-S59
- [2] H. LAUSCHMANN, F. ŠIŠKA, I. NEDBAL: *Textural fractography of fatigue failures under variable cycle loading*. In: Workshop 2004, Part A. CTU Prague 2004, pp.542-543.
- [3] H. LAUSCHMANN, F. ŠIŠKA, I. NEDBAL: *Textural fractography of fatigue failures under variable cycle loading*. In: Materials structure and micromechanics of fracture, Brno June 23-25, 2004. To be published in Trans Tech. Publ. 2005.
- [4] H. LAUSCHMANN, J. ŠUMBERA, F. ŠIŠKA, I. NEDBAL: *Fractography of fatigue fractures: Common features in different image textures*. Accepted for: 9. European Congress on Stereology and Image Analysis, Zakopane, May 10-13, 2005.

This research has been supported by the Ministry of Education of the Czech Republic, research project No. Cez:J04/98:210000021, "Diagnostics of Materials".

Elastic Properties of NiTi and CuAlNi Shape Memory Alloys in the Vicinity of Martensitic Transformation

P. Sedlák **, H. Seiner* **, M.Landa**, V. Novák***, P. Šittner***

sedlak@troja.fjfi.cvut.cz

*CTU Faculty of Nuclear Sciences and Physical Engineering, Trojanova 13, 120 00 Prague 2, Czech Republic

**Institute of Thermomechanics, Czech Academy of Sciences, Dolejskova 5, 182 00 Prague 8, Czech Republic

***Institute of Physics, Czech Academy of Sciences, Na Slovance, 182 00 Prague 8, Czech Republic

Cu-based shape memory alloys (SMA) are known to show thermoelastic martensitic transformations (MT) into various martensitic phases: β'_1 (18R), γ'_1 (2H), α'_1 (6R). These MTs are first order phase transformations driven by the external stress or temperature. When these transformations proceed, the interacting phases are separated by mobile phase interfaces. Mobile twinning like interfaces exist also within the martensitic phases. Although knowledge of the elastic constants of the individual phases is essential to describe reliably the mechanical behavior of Cu SMAs, only very limited experimental data are available namely concerning the low temperature / high stress martensite phases.

Elastic properties of the cubic high temperature phase are relatively well known, including their temperature dependence. Particularly, variation of the austenite elastic constants in the vicinity of the phase transition has been thoroughly investigated and related with the soft mode of the [110](1-10) TA2 phonons [2,3]. On the other hand, there are only few references in the literature concerning the elastic properties of the lower symmetry martensite phases in SMAs. This is mainly because of the experimental difficulties related to the preparation of multiple sufficiently large single crystals of low symmetry martensite phases needed for the ultrasonic experimental methods used to evaluate the elastic constants.

In this contribution the elastic constants of cubic austenite and orthorhombic 2H martensite phases existing in Cu-Al-Ni shape memory alloy were determined taking advantage of easy twinning deformation in the martensite state. Multiple parallelepiped shaped samples were prepared to carry out acoustic measurements on the 2H martensite phase and the elastic constants were evaluated using a dedicated newly developed optimization method which is based on inversion of ultrasound wave velocities measured in redundant number of general crystal directions. This method allows to minimize the uncertainty in evaluated elastic constants stemming from the experimental error in determination of the single crystal orientation. It is believed, that, for low symmetry materials such as 2H martensite phase in CuAlNi, which require multiple velocity measurements to evaluate complete set of elastic constants, the optimization approach is more precise and less laborious compared to standard direct determination method.

It follows from the comparison of the elastic properties of the austenite and 2H martensite phase that: i) although the elastic properties change significantly with the martensitic transformation, the elastic anisotropy of the austenite is inherited by the martensite phase in the first approximation, ii) the martensite crystal is softer for most of the crystal directions, but becomes elastically harder particularly in crystal directions, where the parent austenite

phase was softest. This causes the martensite phase to be slightly less anisotropic in spite of its lower symmetry.

The softest elastic modulus in the martensitic structure corresponds to the qT_2 wave propagating along a directions close to the $(110)_M$, $(100)_M$ and $(001)_M$. These modes are inherited from two of the C' and one of the C_S of austenite. The existence of such elastic modes in martensite appears to be a common feature among Cu-based alloys which transform to different martensitic structures.

In the case of polycrystals, obviously much depends on the crystallographic texture not only in the parent austenite phase but also in the stress induced martensite phase. Since texture in the stress induced martensite phase evolves dynamically and depends on the applied stress state, the Young modulus of the SMA polycrystal containing stress induced martensite phase would be curiously different in tension and compression and might even depend on the deformation history.

The evaluation of thermo-mechanical properties of NiTi wires intended for stent applications was carried out by combination of tensile tests at constant temperature with in-situ ultrasonic measurements (wave speed, attenuation) and electrical resistivity measurements. It was found that the mechanical and electric resistance results were mainly sensitive to R-B19' stress induced martensitic transformation, but the ultrasonic wave speed and attenuation varied most significantly when the R-phase reorientation or distortion took place.

References:

- [1] SEDLÁK, P. – SEINER, H. – LANDA, M. – NOVÁK, V. – ŠITTNER, P. – MAÑOSA, LL.: *Elastic Constants of 2H Martensite in CuAlNi Single Crystal* Engineering Mechanics, Vol.11, 2004, pp. 1–6.
- [2] LANDA, M. – NOVÁK, V. – SEDLÁK, P. – ŠITTNER, P.: *Ultrasonics Characterization of Cu-Al-Ni Single Crystals Lattice Stability in the Vicinity of the Phase Transition* Ultrasonics, Vol.42, 2004, pp. 519–526.
- [3] ČERNOCH, T. – LANDA, M. – NOVÁK, V. – SEDLÁK, P. – ŠITTNER, P.: *Acoustic Characterization of the Elastic Properties of Austenite Phase and Martensitic Transformations in CuAlNi Shape Memory Alloys* Journal of Alloys and Compounds, Vol.378, 2004, pp. 140–144.

This research has been supported by CTU grant No.CTU0410814.

Influence of High Temperature Degradation on Fatigue Crack Growth in Cr-Mo Tube Steels

J. Kunz*, J. Siegl*, P. Kopřiva*, J. Kudrman**

jiri.kunz@fjfi.cvut.cz

*Department of Materials, Faculty of Nuclear Sciences and Physical Engineering,
Czech Technical University in Prague, Trojanova 13, 120 00 Prague 2, Czech Republic

**UJP PRAHA a.s., Nad Kaminkou 1345, 156 10 Prague 5 - Zbraslav, Czech Republic

In chemical and power engineering, tube systems are exposed to complex mechanical loading, high temperature, corrosion environment, etc. Long-time influence and interaction of severe conditions can result in the degradation of crucial properties of structural materials.

Experimental research, the results of which are summarized in the contribution presented, was aimed to the study of fatigue properties of three chrome-molybdenum steels: P91, ČSN 15 313 and N10 (21CrVMoW12). CT-specimens of thickness $B = 8$ mm and width $W = 50$ mm used in the experimental program were cut out from thick-walled tubes. Generally, materials of the tubes were tested in two different stages – original (without degradation), and degraded:

- 1) steel P91
 - a) original state (specimens were cut out from a new tube),
 - b) service degradation was simulated by annealing at $T = 625^\circ\text{C}$ for 5000 hours,
- 2) steel ČSN 15 313
 - a) original state (specimens were cut out from a new tube),
 - b) service degradation was simulated by annealing at $T = 650^\circ\text{C}$ for 500 or 1000 hours,
- 3) steel N10
 - a) quasi-original state was obtained by means of two-stage regeneration of material degraded in service: normalization annealing at $T = 1100^\circ\text{C}$ for 2 hours, and tempering at $T = 720^\circ\text{C}$ for 4 hours,
 - b) degraded in service – specimens were cut out from the tube after 165 000 hours of industry service at temperature $T = 350^\circ\text{C}$ and pressure $p = 32.5$ MPa.

Besides the material state, also orientation and location of specimens in the tube wall were under study, but the influence of these factors on fatigue crack growth was negligible.

During high-cycle fatigue tests, an influence stress ratio R characterizing the mean stress (i.e., static part of time variable loading) was studied. For the fatigue crack length measuring, two simultaneous methods were applied: direct optical monitoring of the crack on the specimen surface, and drop potential method. Macroscopic crack growth rate $v = da/dN$ determined by means of secant method was presented as a function of stress intensity factor range ΔK . The data $(\Delta K_i, v_i)$, $i = 1, 2, \dots, n$ were fitted by regression function in the form of [1]

$$v = C \cdot (\Delta K^m - \Delta K_{th}^m),$$

where C , m , and ΔK_{th} are parameters determined by means of least squares method [2]. Regression parameter ΔK_{th} represents a rough estimation of threshold value of stress intensity factor range. In consequence of material degradation, the results obtained indicate an increase of exponent m but also simultaneous decrease of constant C , thus both relation $v = v(\Delta K)$ and estimated threshold values ΔK_{th} are almost identical for original and degraded states of all three steels: $\Delta K_{th}(R=0.05) = (12.9 \div 13.8)$ MPa.m^{1/2}, and $\Delta K_{th}(R=0.3) = (11.9 \div 12.7)$ MPa.m^{1/2}.

Higher stress ratio R results in less crack closure and thus in higher fatigue crack growth rate. This influence can be eliminated by application of effective value of stress intensity factor range ΔK_{eff} instead of nominal value ΔK . Effective value can be calculated by means of relationship $\Delta K_{eff} = U(R) \cdot \Delta K$, where $U(R) \leq 1$. Form and parameters of the function $U(R)$ depend on the material and testing (service) conditions. For the Cr-Mo steels under study, use of the relation $U(R) = 0.75 + 0.25 \cdot R$ [3] was suitable – crack growth rates for both $R = 0.05$ and $R = 0.3$ were able to unify into one data set correlated by ΔK_{eff} . Data $(\Delta K_{eff,i}, v_i)$, $i = 1, 2, \dots, n$ were fitted by regression function in the modified form

$$v = C \cdot (\Delta K_{eff}^m - \Delta K_{eff,th}^m).$$

Both v vs. ΔK , and v vs. ΔK_{eff} relations represent the significant characteristic fatigue properties of the studied Cr-Mo steels under given conditions.

Stress ratio R has substantial influence also on the threshold value of stress intensity factor range ΔK_{th} – increase of R results in decrease of ΔK_{th} . The indicated dependence can be analytically expressed by means of empirical relationship [4]

$$\Delta K_{th}(R) = \Delta K_{th,0} (1 - R)^\gamma,$$

where $\Delta K_{th,0}$ means the threshold value at $R = 0$ and exponent γ ($0 \leq \gamma \leq 1$) quantifies a sensitivity of ΔK_{th} on R for given material and environment. Parameters $\Delta K_{th,0}$ and γ were estimated for the three Cr-Mo steels under study on the base of experimentally determined ΔK_{th} at $R = 0.05$ and $R = 0.3$. The results indicated that values of $\Delta K_{th,0}$ are practically independent of steel type and its state ($\Delta K_{th,0} = (13 \div 14)$ MPa.m^{1/2}), but exponent γ is varying: the most sensitive on stress ratio is steel P91 in degraded state ($\gamma = 0.446$), the least value $\gamma = 0.150$ corresponds to steel 15 313 in all states. Relations $\Delta K_{th} = \Delta K_{th}(R)$ established by this way allow a rough estimation of ΔK_{th} at whichever values of stress ratio $R \geq 0$.

Results of fractographic analysis of fractures of fatigued specimens are corresponding to the results of fatigue tests: there is no substantial influence of all factors under study (including steel type and material state) on character of fracture. In all cases, striation formation has prevailed as a dominant micromechanism controlling the fatigue crack growth. In addition to this, some other minority mechanisms took a part in the failure process: intergranular decohesion (in the range of lower ΔK values), decohesion or failure of sulphide inclusions, and transgranular ductile fracture. Percentage fracture areas corresponding to the mentioned individual mechanisms slightly differ in individual cases, but this fact is negligible from practical point of view.

References:

- [1] KLESNIL, M. – LUKÁŠ, P.: *Únava kovových materiálů při mechanickém namáhání*. Praha, Academia 1976, 222 p.
- [2] KOPŘIVA, P. – KUNZ, J.: *Statistical Processing of Experimental Data on Fatigue Crack Growth*. In: Proc. CTU Seminar 94. Part C. CTU Prague 1994, pp.129-130.
- [3] MADDOX, S.J. – CURNEY, T.R. – MUMMEY, A.M. – BOOTH, G.S.: *An Investigation of the Influence of Applied Stress Ratio on Fatigue Crack Propagation in Structural Steels (Research Report 72/1978)*. Cambridge, Welding Institute 1978.
- [4] KLESNIL, M. – LUKÁŠ, P.: *The Effect of Stress Cycle Asymmetry on Fatigue Crack Growth*. Mater. Sci. Engng, 9, 1972, pp. 231-239.

This research has been supported by projects FD-K2/22 and CEZ:J04-98:210000021.

Basic Methodology for the Assessment of Production Technology of Cement Composites with Non-Metallic Fiber Reinforcement

J. Němečková, R. Černý, P. Pačevět, L. Kopecký, J. Němeček

`jitka.nemeckova@fsv.cvut.cz`

Department of Structural Mechanics, Faculty of Civil Engineering, Czech Technical University, Thákurova 7, 166 29 Praha 6, Czech Republic

The assessment of production technology of cement composites with non-metallic fiber reinforcement was based on the evaluation of various mechanical, hygric and thermal properties. The methodology included the following four basic testing methods:

- a) methods for assessment of thermal and hygric parameters at normal temperatures,
- b) methods for assessment of thermal properties at high temperatures,
- c) methods for assessment of mechanical properties,
- d) methods for study of changes of the internal structure and composition,
- e) methods for assessment of micromechanical properties.

Results of the methods mentioned above are aimed to closely characterize conditions to which the materials are exposed in building structures. Methods must be suitable for investigating the materials not only at their virgin state at normal temperatures but also after the exposition to different static, dynamic and cyclic mechanical loading and to high temperatures.

Methods for assessment of thermal and hygric parameters at normal temperatures are based on the following parameters. Thermal conductivity, thermal diffusivity and specific heat capacity are measured with the aid of ISOMET 2104. The measurement with this apparatus is based on the analysis of time development of thermal response on thermal flux impulses into the material. Water vapor diffusion coefficient is measured by the method without thermal gradient that is based on the one-dimensional diffusion of water vapor through the specimen. Moisture absorption coefficient and average coefficient of moisture conductivity are based on the monitoring of the time dependence of the sample moistening. Further parameters belonging to this group of methods are moisture dependent moisture diffusivity, moisture expansion coefficient and thermal expansion coefficient [1].

Methods for assessment of thermal properties at high temperatures are based on the following parameters [2]. High temperature thermal diffusivity is measured by the method of non-stationary one-sided sample heating. This method lies in the measurement of temperature dependence on time and location in a sample exposed to high temperature. High temperature specific heat capacity is based on the measurement of thermal energy increment of the system. Basic idea of this non-adiabatic method consists in a precise correction of thermal losses. High temperature thermal conductivity is assessed with indirect method from the two above coefficients and bulk density. High temperature coefficient of thermal expansion is based on the principle of comparative measurement of two specimens. One sample is made of the measured material whilst the other is a material with known thermal expansion.

Methods for assessment of mechanical properties use standard test such as direct tension test with the whole force-displacement diagram recording, three-point bending test and dynamic tension tests. These properties are measured with the MTS Alliance TR 30 that is an electromechanical machine with the capacity of 30 kN in tension. It is equipped with a special device for three-point bending and with several gauges for force and displacement measurement. Dynamic testing is designed as a fatigue test of notched specimens loaded by 1 000 to 10 000 cycles in 60-70% of the tension capacity [3].

Methods for study of changes of the internal structure and composition utilize the electron microscopy. Environmental scanning electron microscope Phillips XL30 is capable of standard topological analysis of nonconductive specimens in high and low vacuum. It is equipped with the EDX (element X-ray) analysis for composition assessment of the sample. Further, the microscope is capable of orientation imaging analysis for determination of microstructural and crystallographic orientation.

Micromechanical methods are used to support basic macroscopic findings [4]. These methods are time consuming and therefore used for verification of the aforementioned ones. Selected specimens are tested for micromechanical properties such as elastic modulus and hardness in the order of several microns. Measurements are carried out with Nanotest nanoindenter. This apparatus produces very small imprints of the diamond tip into the material. The force-displacement diagram is measured and evaluated for given properties at this microscale.

All the methodologies described above will be used for the development of the new technology for production of cement composites with non-metallic fiber reinforcement intended for heavy industries and operations at high temperatures. The criterion for successful development of the new technology will be the comparison with the recent technology.

References:

- [1] J. DRCHALOVÁ, R. ČERNÝ: *Non-Steady-State Methods for Determining the Moisture Diffusivity of Porous Materials*, Int. Comm. in Heat and Mass Transfer, 1998, pp. 109-116.
- [2] R. ČERNÝ, J. TOMAN: *Determination of Temperature- and Moisture-Dependent Thermal Conductivity by Solving the Inverse Problem of Heat Conduction*, Proc. of International Symposium on Moisture Problems in Building Walls, V.P. de Freitas, V. Abrantes (eds.), 1995, pp. 299-308.
- [3] P. PADEVĚT: *Vývoj vlastností betonu se zvýšením jeho teploty*, Proceedings of 2nd International Conference on New Trends in Statics and Dynamics of Buildings, 2003.
- [4] J. NĚMEČEK, Z. BITNAR, *Micromechanical Properties of Cement Pastes at Elevated Temperatures*, Proceedings of the 2004 International Conference on Computational & Experimental Engineering & Sciences, 2004.

This research has been supported by the Ministry of Industry and Trade of Czech Republic, under grant No. FT – TA/019.

Detection Possibility of Microstructure of Steel by Eddy Current

J. Hořejší*, J. Pitter**, P. Tichý**, L. Vokurka***, J. Cejp*

horejsi@atg.cz

*CTU, Faculty of Mechanical Engineering, Dept. of Materials Eng.
Karlovo nám. 13, 121 35 Praha 2

**ATG, Beranových 65, 199 02 Praha-Letňany

***TU Liberec, Faculty of Mechanical Engineering, Dept. Material
Halkova 6, 461 17 Liberec

At the last time it was discovered series of studies concerning of using eddy-current (ET) to monitoring microstructure and its changes. Study [1] described methodics of detection structural changes – first of all precipitation of secondary phase – in forming austenitic stainless steels. Amount of deformation martensite in identical type of material investigate De Backer et al. [2] and ferrite R. Becker et al. [3]. Philosophy of detection of content nonmetallic inclusions (too in austenitic matrix) including preparations of standard specimens described Pudov and Sobolev [4]. Another founded works deal with detection of microstructure effects (like martensite creation, carbides precipitation, plastic deformation etc.) on unalloyed or low-alloyed steels, let us say in aluminium alloys. To all mentioned applications was common multifrequency measuring of electric conductivity and total response including influence of permeability and conductivity.

Microstructure changes of steels and alloys were studied on carbon steels. Transformations at annealing of quenched microstructure were observation. For multifrequency measuring was using common through probes. ET measuring has been supply by metallographic analysis by the help of the light microscope. Analysis results showed very good sensitivity of ET on microstructure changes of the carbon steels at the heat treatment.

For experiments were using specimens of steel 12 040 and 12 060 shaped roller with diameter 11,2 mm and length 67 mm. Specimens were heated according to figure 1 (also included labelling of single specimens).

Figure 1. Heat treatment and single specimens labelling

heat treatment	specimen label	
	12 040	12 060
non treated (supplied condition)	40	60
soft annealing 680 – 720 °C	41	61
normalization 840 – 870 °C	42	62
normalization 950 °C	43	63
quenching 850 - 880 °C	44	64
quenching 950 – 960 °C	45	65
quenching 850 °C + tempering 400 °C	46	66
quenching 850 °C + tempering 500 °C	47	67
quenching 850 °C + tempering 600 °C	48	68
quenching 850 °C + tempering 670 °C	49	69

Microstructure of single annealed specimens was ferritic-pearlitic in various proportions according to the conditions of annealing. Hardened if you like treated specimens were microstructure that changed from martensite-bainite up to sorbite, which again depend on the conditions of heat treatment. ET measurement has been effected on structurescope IBG Eddyliner P with the pair of through probes, which one serves as measuring and second as compensative. As a compensative were used specimens in supplied condition (spec.40 let us say 60). Measurement has been executed with eight operating frequencies of range 25Hz-25kHz.

Measured responses of eddy-current resulting that for identification of microstructure is for both steels optimum frequency 630Hz. At other used frequencies is difference among measured response lower or even inconsiderable. With used comparative specimens (steel in supplied condition) it is possible well distinguish quenched specimens from treated let us say from annealed and single annealed with each other. There isn't yet too obvious resolution inside the group of the treated specimens. Innovation would be possible to achieve by using of another specimen like comparative. In the present time it is prepared continuation of the experiments.

Example demonstrate, that eddy currents it is possible use for monitoring microstructure changes off metal material. Concrete using method depends on character analyze material and microstructure effect, which we want to observe. Inseparable section of the analyses is the well made metallographic classification of reference sample.

References:

- [1] V. A. SANDOVSKII ET AL.: *Russian Journal of Non-destructive Testing*, 38 (2002), No.12, pp. 919-926.
- [2] F. DE BACKER ET AL.: *Proceedings of 2nd International Conference on NDE in Relation to Structural Integrity for Nuclear and Pressurized Components*, EPRI, 2000.
- [3] V. I. PUDOV, A. S. SOBOLEV.: *Russian Journal of Non-destructive Testing*, 39 (2003), No.1, pp. 18-22.
- [4] J. BOWLER.: *publikace na serveru*: Center for Non-destructive Evaluation of Iowa State University, 2002, www.cnde.iastate.edu.

This research has been supported by CEZ 210000021.

Properties of PVD Coatings for Cutting

Tools

A.Winklerová, J.Miřejovský, J.Cejp

alzbeta.winklerova@centrum.cz

CTU, Faculty of Mechanical Engineering, Dept. of Materials Eng.
Karlovo n. 13, 121 35 Praha 2

The mechanical and tribological behavior of cutting tools with thin coatings, prepared for commercial purposes were studied. All samples were prepared on plates from sintered WC. Except chemical composition, total thickness and morphology the adhesion, universal and plastic hardness ($F_{\max}=30$ mN), Young's modulus E , wear rate steel in humid air during ball – on – disc – test at 20°C and 500°C under normal load $F_N=5$ N, has been evaluated [1,2].

The hardness measurement was based on indentation characteristics of relation between the load of indenter head L [gf] and the depth of indenter penetration h [μm]. The values of universal hardness H_{un} , plastic hardness H_p and Young's modulus were obtained using the load 0 – 80 N. Scratch tests were conducted and showed that critical load L_c is higher for monolayer TiN coatings, indicated TiN adhesion better to substrate than the multilayer TiAlCN coatings.

Plastic and brittle behaviors are related with hardness and Young's modulus. Nanocomposite TiAlN/Si₃N₄ coatings exhibited high values hardness and Young's modulus, behavior of this coating was brittle. Plastic behaviors are related with structure of coating and it occurred monolayer film and monolayer gradient film.

Friction tests against 100 C6 steel and Si₄N₃ were conducted using a ball – on – disk tribometer. Coating with addition of Al content greatly affects the hardness and oxidation resistance. The formation of a dense Al₂O₃ layer protects (Ti,Al)N even at high temperature. It is extensively used for cutting with high speed. Friction behavior of coating (Ti,Al)N exhibited wear rate K at 20°C same as for temperature 500°C.

Multilayer TiN with content Al and C has a low friction behavior due to the formation of a graphite transfer layer on the wear track. The low friction behavior decreases the wear rate of the Al₂O₃.

Very important role of morphology and tool coating roughness has been observed in case of critical normal load F_C measured during scratch – test. The hard and tough coatings prepared by arc technology exhibit lower critical load F_C than magnetron sputtered coating with nearly the same hardness and Young's modulus values. The technology of preparation and total coating thickness influenced also the final radius of the cutting edge.

The presence of macroparticles in multilayer is considered as a drawback for the type of applications these coatings are designed for. Their incorporation alters significantly the surface morphology and roughness, changing the real contact area and thus the friction coefficient.

Additionally, the pinholes created by their debonding have a deleterious effect on erosion and corrosion resistance of the coating by exposing the multilayer structure to the element.

References:

- [1] WESRGARD,R. – B.BROMARK,M: *Mechanical and tribological charkterization of DC magnetron sputtered TaN films*. Surface and coatings technology, 97 pp.779-784.
- [2] MIŘEJOVSKÝ,J: *Příprava vícevrstvých povlaků metodou PVD*, DP ČVUT FS,ÚMI, 2002

This research has been supported by CEZ 212200008.

Continuous Casting Technologies for Production of Aluminium Alloy Sheets for Transportation Applications

M. Karlík, M. Slámová*, Z. Juříček, K. Sejk***
Y. Birol****, M. Dündar*******

karlik@kmat.fjfi.cvut.cz

CTU, Faculty of Nuclear Sciences and Physical Engineering, Dept. of Materials
Trojanova 13, 120 00 Praha 2,

* Research Institute for Metals Ltd., Panenské Břežany, 250 70 Odolena Voda

** Aluminium Works Břidličná, Bruntálská 8, 793 51 Břidličná

*** Aeronautical Research and Test Institute, Beranových 130, 199 05 Prague - Letňany,
Czech Republic

**** Tübitak, Marmara Research Center, 41470 Gebze, Kocaeli, Turkey

***** ASSAN Aluminium Works, 81700 Tuzla - Istanbul, Turkey

This paper summarizes results of research and development works carried out in the Department of Materials of the Czech Technical University in Prague in the frame of the European project EUREKA E!2530 CONTCASTALTRANS "Continuous casting technologies for production of aluminium alloy sheets for transportation applications".

The partner countries of this project were Turkey and Czech Republic. The main participant in the project was the Turkish producer of aluminium alloy sheets ASSAN Aluminium Works (ASSAN). On the Turkish side there was a second partner – the research institute Marmara Research Center, Gebze, Kocaeli. Research efforts on the Czech side were coordinated by the Research Institute for Metals Panenské Břežany, other participants were AL INVEST Břidličná, a.s. (AIB), producer of aluminium alloy sheets, the Department of Metal Physics of Charles University in Prague, Aeronautical Research and Test Institute, Plc., Prague-Letňany and Department of Materials of the Czech Technical University in Prague.

The research works were organized mainly at the national level, with exchange of samples of materials and also of some experience during the visits of the Czech participants in Turkey and the Turkish partners in Czech Republic. Several common research papers were published at international conferences and congresses.

A primary goal in today's automotive industry is weight reduction resulting in fuel economy improvement and emission reductions. Aluminium alloys, having one-third density of steel and a superior strength-to-weight ratio could provide up to 50 % weight reductions when used in automotive sheet applications. However, to perform the same function, Al alloy sheets produced by conventional direct-chill (DC) casting and hot rolling route cost usually four or five times more than steel sheet. Therefore, production of low-cost/high-quality Al-Mg (AA5xxx) sheets by twin-roll casting (TRC) can help to increase the employment of wrought aluminium alloys in automotive applications.

In the project, the structure and properties of TRC materials were compared with the DC cast and hot-rolled sheets, taken as reference materials. Research and development works were then carried out solely on TRC sheets from AA 5754 (AlMg3), AA 5052 (AlMg2.5), AA 5182 (AlMg4.5Mn0.4), AA 5049 (AlMg2Mn0.8) and AA 6016 (AlSi1.2Mg0.4) alloys, fabricated by both aluminium sheet producers. AL INVEST Břidličná, a.s. (AIB) uses Pechiney twin-roll casters producing strips 8.4 mm thick, while ASSAN Aluminium uses 466

Fata-Hunter casters, usually casting at thickness less than 6 mm. The Fata-Hunter casters allow casting also at significantly lower thicknesses and some experimental works were performed using strips cast at 3 mm at higher speed than the conventional ones.

The first results of research and development efforts have shown that mechanical properties, formability and corrosion resistance of Al-Mg twin-roll cast alloys are equivalent or superior when compared with DC cast and hot-rolled materials [1]. The materials prepared by both different technologies exhibited different microstructures. Second-phase particles were coarser and less numerous in DC cast sheets. The grain size in TRC sheets is of the same magnitude or finer than in DC-cast sheets. AA5052 samples had anisotropic grains, whereas AA5182 samples have almost isotropic grains. Texture evaluations indicated that DC-cast samples differ from TRC samples by the presence of a strong cube texture component and of relatively strong retained rolling texture. TRC samples exhibit a weak retained rolling texture or an unusual texture with orientations very different from the known ideal textures. The differences in the crystallographic texture of TRC- and DC-cast samples are due to the differences in iron content in solid solution resulting from the different solidification rates of both casting methods [2].

Forming limit diagrams of selected final gauge sheets were measured and also simulated using finite element modeling method. The results of modeling yielded complementary information about the formability of the materials [3].

Solid solution decomposition of an Al-Mg-Si alloy (AA6016) was investigated by means of microhardness, tensile test, electrical conductivity, differential scanning calorimetry and transmission electron microscopy. The aim of the study was to improve the paint-bake response of a twin-roll cast sheet by employing artificial aging between the solution treatment and the paint-bake cycle. During pre-ageing at 180°C, stable GP1 zones form first and suppress the natural ageing after the pre-ageing treatment. Clusters and small GP1 zones are reverted and stable β'' nuclei are formed. During the paint-bake cycle these nuclei grow readily to become coherent β'' particles. Consequently, the yield strength considerably increases. A pre-ageing treatment for 2-10 minutes at 180°C is optimum for the twin-roll cast 6016 sheet to offer a sufficient bake-hardening response without impairing the stampability and the shape accuracy during manufacturing of the body panel at the automotive plant [4].

References:

- [1] KARLÍK, M. - SLÁMOVÁ, M. - JANEČEK, M. - HOMOLA, P.: *Microstructure evolution of twin-roll cast Al-Mg alloys during downstream processing*, Kovové materiály - Metallic Materials 40, 2002, pp 330-340.
- [2] SLÁMOVÁ, M. - KARLÍK, M. - ROBAUT, F. - SLÁMA, P. - VÉRON, M: *Differences in microstructure and texture of Al-Mg sheets produced by twin-roll continuous casting and by direct-chill casting*, Materials Characterization 49, 2003 pp. 231-240.
- [3] ŠKROB, J.: *Finite element modeling of Al-Mg thin sheet formability tests*, Diploma Thesis, [Report V-KMAT-581/04], CTU Prague, Dept. of Materials, 2004, 104 p.
- [4] BIROL, Y. - KARLÍK, M: *Bake hardening response of a twin-roll cast Al-Mg-Si alloy*, Materials Science and Technology, 2005, (in press).

This research has been supported by the Ministry of Education, Youth and Sports of the Czech Republic in the frame of the European programme EUREKA (project E! 2530 CONTCASTALTRANS).

Solution of Heat and Moisture Transport in a System with Interior Thermal Insulation Using the Computer Code TRANSMAT

J. Maděra, M. Pánek, R. Černý

madera@fsv.cvut.cz

Department of Structural Mechanics, Faculty of Civil Engineering, Czech Technical University, Thákurova 7, 166 29 Prague 6, Czech Republic

The application of interior thermal insulation systems on building envelopes is not a natural solution but sometimes there is no other option available. A typical example is a historical building, where the facade has to be kept in its original appearance mostly, and the exterior insulation systems are excluded for that reason. In that case the development of such an insulation system would allow to prevent moisture damages and to upgrade the thermal properties of the envelope as the only reasonable option.

In this computational analysis, we have chosen interior thermal insulation system consisting of internal plaster, insulation material and water vapor retarder. In the internal side there was light plaster with the thickness of 10 mm. We have chosen two different materials as thermal insulation, with the thickness of 100 mm. Insulation I was hydrophilic material with low value of hygroscopic moisture, Insulation II hydrophobic material with low value of water vapor resistance factor. The thickness of water vapor retarder was 10 mm. We assumed no air gap between the water vapor retarder and the old structure. We considered glue or mastic as the water vapor retarder, which was applied directly on the old structure. As old bearing structure we have chosen a brick wall with the thickness of 450 mm. On the external side there was lime plaster with the thickness of 20 mm.

The physical properties of basic materials were partially obtained from material database, which was created in the form of an internet application. The physical properties of insulation materials are given in Table 1.

Table 1. Material parameters of insulation materials

	ρ [kg/m ³]	c [J/kgK]	κ [m ² /s]	μ [-]	λ_{dry} [W/mK]	λ_{hyg} [W/mK]	λ_{sat} [W/mK]	θ_{sat} [Vol %]	θ_{hyg} [Vol %]
I	150	840	$1 \cdot 10^{-7} \cdot e^{0,0485 \cdot \theta}$	2	0,04	0,048	1,1	95	0,16
II	280	840	$5 \cdot 10^{-13} \cdot e^{0,1486 \cdot \theta}$	3	0,055	0,066	1,2	31	0,73

General aim was to analyze the hygrothermal performance of the designed insulation systems with different insulation materials and to find the best water vapor resistance factor and moisture diffusivity for the water vapor retarder.

For the calculations we employed the computer simulation tool TRANSMAT 4.3 which was developed in the Department of Structural Mechanics, Faculty of Civil Engineering, Czech Technical University in Prague in order to support the investigation of the coupled heat and moisture transport in porous building materials. The modelling of transient transport processes leads into a system of non-linear partial differential equations. The construction of the code is based on the application of the general finite element computer simulation tool SIFEL (Simple Finite Elements) developed in the Department of Structural

Mechanics, FCE CTU. The moisture and heat balance equations were formulated according to Künzl [1]. For the interior insulation systems this is a crucial factor because liquid moisture is almost always the basic cause of defects and failures.

The proper initial and boundary conditions of the model are crucial factor affecting the reliability of the calculations. Therefore, the calculations should be done for exactly the same situation as it will be done in the practical reconstruction on building site. First, the boundary conditions for the external side should be as accurate as possible. This can be achieved by using the meteorological data for the locality as close as possible to the real object. Second, the initial conditions should be realistic. To this point, the calculations should be done first for the construction without the interior insulation system. Third, the calculations with the interior insulation system should be started exactly in the same time of year when the real reconstruction will begin.

In our calculations, we chose the 1st of May as the starting point, when we assumed the application of the insulation system on the load-bearing structure was done. For the insulation systems, there were taken initial values of field variables corresponding to the values inside (temperature equal to 21°C and relative humidity equal to 60%). The systems with interior thermal insulations were exposed from inside to the above constant conditions and from outside to climatic conditions corresponding to the reference year for Prague (temperature, relative humidity, vertical rain, wind speed, wind direction, short wave radiation, long wave radiation).

We have chosen two critical profiles in the evaluation of performance of the envelope, A-A', B-B', where the profile A-A' was between water vapor retarder and insulation material, profile B-B' was between old structure and water vapor retarder. In these profiles we had calculated the dependence of the relative humidity and temperature on the time.

For the Insulation I we found the optimal value of water vapor resistance factor equal to 5 and the value of moisture diffusivity equal to $1.10^{-10} e^{0.0923.0} \text{ m}^2/\text{s}$. The maximum values of relative humidity were then about 80 %, which is very far from the condensation limit. The Insulation II exhibited much worse hygrothermal performance. We found the optimal value of water vapor resistance factor equal to 5 and the value of moisture diffusivity equal to $1.10^{-10} e^{0.0923.0} \text{ m}^2/\text{s}$. The maximum values of relative humidity were then about 94 %, which is very close to the condensation limit. However, any other variant did not improve this problem.

References:

- [1] KUENZEL H.M.: *Simultaneous Heat and Moisture Transport in Building Components*, PhD Thesis. IRB Verlag, Stuttgart, 1995.

This research has been supported by CTU grant No. CTU0413011

TRANSMAT – a Computer Simulation Tool for Modeling Coupled Heat and Moisture Transport in Building Materials

Jiří Maděra, Robert Černý

madera@fsv.cvut.cz

Department of Structural Mechanics, Faculty of Civil Engineering, Czech Technical University, Thákurova 7, 166 29 Prague 6, Czech Republic

The computer simulation tool TRANSMAT 4.3 was developed in the Department of Structural Mechanics, Faculty of Civil Engineering, Czech Technical University in Prague in order to support the investigation of the coupled heat and moisture transport in porous building materials. The simulation of the thermal and hygric behaviour of constructive building details is possible for 1D, 2D problems. The modelling of transient transport processes leads into a system of non-linear partial differential equations. The construction of the code is based on the application of the general finite element computer simulation tool SIFEL (Simple Finite Elements) developed in the Department of Structural Mechanics, FCE CTU. The basic variables characterizing the hygro-thermal state of building constructions (temperature, moisture content, relative humidity) can be obtained as functions of space and time. A particular advantage of the numerical simulation program is the possibility of investigation of variants concerning different constructions, different materials and different climatic loads. Constructive details of buildings and building materials can be optimized using the numerical simulation, and the reliability of constructions for different given indoor and outdoor climates can be judged.

The moisture and heat balance equations were formulated according to Künzle [1]:

$$\frac{d\rho_v}{d\varphi} \frac{\partial\varphi}{\partial t} = \text{div}[D_\varphi \text{grad}\varphi + \delta_p \text{grad}(\varphi p_s)], \quad (1)$$

$$\frac{dH}{dT} \frac{\partial T}{\partial t} = \text{div}(\lambda \text{grad}T) + L_v \text{div}[\delta_p \text{grad}(\varphi p_s)], \quad (2)$$

where ρ_v is the partial moisture density, φ the relative humidity, δ_p the water vapor permeability, p_s the partial pressure of saturated water vapor in the air, H the enthalpy density, L_v the latent heat of evaporation of water, λ the thermal conductivity and T is the temperature. The liquid water transport coefficient is defined as

$$D_\varphi = D_w \frac{d\rho_v}{d\varphi} \quad (3)$$

The computer simulation tool TRANSMAT 4.3 consists of several parts for data input, initialisation and output, numerical calculation and data representation. The user interface program TRANSMAT 4.3 has been developed for PC - Windows 2000/XP in order to facilitate the input data handling. Using TRANSMAT 4.3, the input files can be edited for SIFEL, and the user has access to the data bases of materials, climatic data and construction details. In order to enable changes in the input files, the information about projects is stored in a user-friendly format.

The time required for simulations depends strongly on several factors: the discretization, the material properties, the initial conditions, the climatic or constant boundary conditions and the output properties.

The transport coefficients and the storage coefficients of the system of partial differential equations for coupled heat and moisture transport are dependent on the material properties and the variables of state. The material properties are described by material functions (analytical functions with parameters and/or interpolation and approximation of measured data). The available material specifications are contained in the material database, which was created in the form of an internet application.

The conditions of simulation problems are defined by “Conditions” part. Available conditions types are initial and boundary conditions. The initial conditions to be specified are temperature and relative humidity. The boundary conditions we can use: „Dirichlet conditions“, „Newton conditions“, „Neumann conditions“ and special boundary conditions. The special boundary conditions are climatic conditions describing time dependent loads corresponding to boundary conditions or field conditions. The evolution with time of the climatic conditions can be expressed by numerical values initialized from climatic data files. The numerical data initialized from climatic data files may be a set of measured data on a reference object, a test reference year (TRY) or another arbitrary climatic data. The climatic data files should contain a header block with an information about the climatic condition, its input/output unit, the given time format and its usage. The climatic data for a common application are assumed in the form of the test reference year for Prague provided by the Czech Hydrometeorological Institute. The first given time point is January 1th at 01:00:00. Therefore, the climatic value of January 1th at 00:00:00 is automatically set from the last value of December 31th at 24:00:00. The values during the first hour of the year are calculated by interpolation between December 31th at 24:00:00 and January 1th at 01:00:00.

SIFEL allows to define various output file formats, for example GID, Open_DX and classical data outputs. The formats of SIFEL output files depend on their data presentation type and their specific settings according to the output data records contained in the input file. SIFEL distinguishes three data presentation types:

- 2D-Presentations, a single time dependent variable
- 3D-Presentations, a variable dependent on time and one spatial coordinate (x or y)
- 4D-Presentations, a variable dependent on time and two spatial coordinates (x and

y).

For the graphical representation of simulation results in TRANSMAT, the TransGraph code can be used. TransGraph is an external program, which can present 2D and 3D graphs. The usage of other external programs is also possible as the output files are easily readable.

References:

- [1] KUENZEL H.M.: *Simultaneous Heat and Moisture Transport in Building Components, PhD Thesis*. IRB Verlag, Stuttgart, 1995.

This research has been supported by GA ČR grant No. GA 201/04/1503.

Water and Water Vapor Transport Properties of Hydrophilic Mineral Wool

P. Michálek, M. Jiříčková, Z. Pavlík, R. Černý

pavlikz@fsv.cvut.cz

Department of Structural Mechanics, Faculty of Civil Engineering, Czech Technical University, Thákurova 7, 166 29 Prague 6, Czech Republic

Mineral wool based materials are frequently used in various technical applications. Probably the most widespread target of mineral wool products is their application in building industry in the form of thermal insulation boards. However, they can also be utilized for acoustic insulation, fire protection, cement reinforcement, pipe insulation and as synthetic soils for plant growing.

Many mineral wool products are provided with hydrophobic substances because the presence of water in the material is undesirable for the majority of applications. The main argument for hydrophobization is the fact that water in mineral wool increases its thermal conductivity several times, which leads to the loss of thermal insulation properties. However, in some cases the hydrophobization can result in problems for a structure, particularly if mineral wool materials are improperly used. The capacity of mineral wool for absorbing hygroscopic moisture is very low and its water vapor diffusion permeability very high. This combination of properties may lead to water condensation in the material, for instance if mineral wool boards would be used as interior thermal insulation. In such case the hydrophobization would lead to water accumulation in lower parts of the boards and subsequent damage of the structure.

Hydrophilic additives are used only seldom in mineral wool products. Practically the only notable application of hydrophilic mineral wool is in the form of synthetic soils for plant growing where water saturation of the material is necessary for its proper function. However, the capability of a fibrous material with hydrophilic substances to transport rapidly liquid water makes very good prerequisites for a variety of other applications such as interior thermal insulation, desalination of old buildings, drying out of flooded buildings where such favorable hygric properties could be conveniently employed.

Among the material properties of mineral wool based materials, thermal properties appear to be of particular importance for their practical applications. Therefore, practically every catalogue list of any material producer contains thermal conductivity, sometimes also specific heat capacity but this is only one characteristic value mostly.

Moisture transport and storage properties of mineral wool products are in the scientific literature not so frequent as thermal properties. Basic information can be obtained easily. In every catalogue list, there is given water vapor diffusion resistance factor, which is very similar for most mineral wool boards. However, obtaining more data is very difficult. The apparent reason is that for common hydrophobized mineral wool materials additional hygric properties are not very interesting for practical purposes. Liquid water transport cannot be realized in such a material and water retention is excluded.

The thermal and hygric properties of hydrophilic materials on mineral wool basis were not published yet in the relevant sources. The apparent reason is their very rare application in technical practice. However, for these types of materials the lack of knowledge of these

parameters has much worse consequences than for common mineral wool products. Particularly critical is the knowledge of moisture transport and storage parameters in the overhygroscopic range. Without these parameters no serious hygrothermal analysis of any building structures involving these materials can be done. Therefore, the determination of thermal and hygric properties of hydrophilic materials on mineral wool basis appears to be an actual problem.

In this paper, complete sets of moisture transport and storage parameters of two new hydrophilic mineral wool materials having a potential to be utilized in building structures are determined. For the sake of comparison, the same measurements are also performed for two hydrophobic mineral wool products and two mineral wool materials without any specific admixtures. The materials analyzed in this paper were produced specifically for testing purposes by Rockwool CZ, SA.

Several modifications of the cup method were employed in the measurements of water vapor diffusion resistance factor [1], namely the dry cup method, wet cup method and dry-wet cup method. The apparent moisture diffusivity was determined on the basis of a common water sorption experiment [2]. Sorption isotherms were measured by the classical desiccator method. The water retention curves were determined by the pressure plate method [3].

The measurements of hygric properties of two new hydrophilic mineral wools in this paper revealed very good perspectives for this type of material. While their water vapor transport and storage properties remained on the same very good level characteristic for common mineral wool materials their liquid water transport and water storage parameters were significantly improved compared to the hydrophobic mineral wool materials and mineral wools without any specific admixtures. The new hydrophilic mineral wool materials can transport liquid water in a similar way as ceramic brick possessing a high capillary activity, their liquid water storage properties are somewhere between ceramic brick and autoclaved aerated concrete.

References:

- [1] K. K. HANSEN, H. B. LUND: *Cup method for determination of water vapour transmission properties of building materials, sources of uncertainty in the method*, Proceedings of the 2nd Symposium Building Physics in the Nordic Countries, J.V. Thue (ed.). (Trondheim: Tapir), 1990, pp. 291-298.
- [2] M. K. KUMARAN: *Moisture diffusivity of building materials from water absorption measurements*, IEA Annex 24 Report T3-CA-94/01, Ottawa, 1994.
- [3] M. JIŘIČKOVÁ, R. ČERNÝ, P. ROVNANÍKOVÁ: *Measurement of moisture storage parameters of building materials*, Acta Polytechnica, Vol. 43, 2003, pp. 39-43.

This research has been supported by GA ČR grant No. GA 106/04/0138.

A Comparison of Hygric Properties of Three Different Insulation Materials

Z. Pavlík, M. Jiříčková, P. Tesárek, M. Gazdo, R. Černý

pavlikz@fsv.cvut.cz

Department of Structural Mechanics, Faculty of Civil Engineering, Czech Technical University, Thákurova 7, 166 29 Prague 6, Czech Republic

The amount of energy required to the heating of buildings depends on the thermal performance of the particular building envelopes. It is commonly assessed primarily using the thermal properties of the applied materials. Therefore, thermal insulation materials are the major contributors and obvious practical and logical first steps towards achieving energy efficiency especially in envelope-load dominated buildings located in areas with harsh climatic conditions. In addition to the operating temperature affecting the thermal properties of thermal insulation materials [1], the material moisture content is another major factor influencing the thermal conductivity of insulation materials. The higher material moisture content causes the higher thermal conductivity. In buildings, insulation materials used in walls and roofs normally exhibit higher moisture content when compared to test conditions. The ambient air humidity and indoor conditions, as well as the envelope system moisture characteristics, play an important role in determining the moisture status of the insulation material. When the external conditions are not favorable, condensation can occur within the insulation material, what in consequences causes a total disturbance of its thermal insulation function. Studies on the impact of moisture content on insulation thermal performance concluded that the effectiveness of insulating materials at higher moisture content is reduced in proportion to the moisture content level. Higher thermal conductivity is obtained due to the increased energy transfer by conduction and, under certain conditions, by the evaporation-condensation process, in which moisture moves from warm to cold regions.

In reference to facts given above, not only the thermal parameters of thermal insulation materials have to be determined, but also the assesment of hygric properties should be done in order to make a proper design of thermal insulation systems.

The objective of this paper is to present a comparison of hygric properties of three different thermal insulation materials, namely expanded polystyrene, hydrophilic mineral wool with different densities and calcium silicate, which should indicate the proper area of the application of the studied materials in building envelopes structures. In the laboratory experiments, the expanded self-extinguishing polystyrene produced by MUREXIN-AUSTROTHERM Ltd., Slovakia, two hydrophilic mineral wool materials denoted as INROCK hard and INROCK soft, developed by Rockwool Inc., and calcium silicate based material produced by Calsitherm, Germany, were tested.

In the experimental work, the entire assessment of hygric properties, describing the transport and storage of both liquid water and water vapor, was carried out in the conditions of air-conditioned laboratory (relative humidity $30 \pm 5\%$, temperature $25 \pm 2^\circ\text{C}$). The apparent moisture diffusivity was determined by a common sorption experiment. The monitored water flux into the specimen during the suction process and previously determined vacuum saturation moisture content were then employed to the determination of apparent moisture diffusivity. The moisture diffusivity coefficient in dependence on moisture content

was determined from moisture profiles measured by the capacitance method applying the methods of inverse analysis. In the hygroscopic moisture range, where the transport of water vapor is the dominant mode of moisture transfer, the moisture storage function is called the sorption isotherm. It expresses the dependence of moisture content in the material on relative humidity. During the experiments, the specimens of studied materials were placed into the desiccators with six different salt solutions corresponding to specific relative humidities and the steady-state value of mass was determined. In the overhygroscopic moisture range, where liquid water transport is the dominant mode of moisture transfer, the moisture storage function is called the water retention curve. It expresses the dependence of moisture content on capillary pressure. The experiments were made using pressure plate apparatus. To describe the water vapor transport, the measurements of water vapor permeability, water vapor diffusion coefficient and water vapor resistance factor were done using the cup method based on the Czech standard ČSN 72 7031. Details of the employed methods are described in [2] in more detail.

The measurements of hygric properties of the tested materials revealed high differences between the studied insulation materials. Systematically, the highest values of moisture diffusivity were observed for calcium silicate and hydrophilic mineral wool materials, whereas in the measurement on expanded polystyrene no moisture flux was observed. Also the water vapor transport was much higher for the calcium silicate material and hydrophilic mineral wools in comparison with expanded polystyrene. Concerning the storage properties, the absorption of water vapor in matrix of expanded polystyrene was almost negligible, whereas the highest values were obtained for calcium silicate material. The water retention curves for mineral wools and polystyrene were almost identical, for calcium silicate were obtained values typically six time higher. From the measured results it is evident that expanded polystyrene should be applied on the exterior side of building envelopes because of its relatively high liquid water resistance. On the other side, this type of material is impracticable for interior thermal insulation systems without application of a proper water vapor retarder layer by reasons of danger of water condensation. In this type of insulation systems, the calcium silicate and mineral wool materials will find use, as their relatively high liquid water transport parameters enable the transport of condensed water from the insulation layer. Certain limitations of the application of calcium silicate material we can see in its relatively high solubility in water, which in the conditions of higher moisture content may negatively affect its thermal insulation function.

References:

- [1] I. M. BUDAIWI, A. A. ABDU, M. S. AL-HOMUD: *Variations of thermal conductivity of insulation materials under different operating temperatures: impact of envelope induced cooling load*, Journal of Architectural Engineering, 8(4), 2002, pp. 125-132.
- [2] M. JIŘIČKOVÁ: *Application of TDR microprobes, minitensiometry and minihygrometry to the determination of moisture transport and moisture storage parameters of building materials*, Ph.D. thesis, CTU Prague, Faculty of Civil Engineering, 2003.

This research has been supported by GA ČR grant No. GA 106/04/0138.

Experimental Assessment of Thermal Properties of Thermal Insulation Materials as a Basis for Their Proper Technical Utilization

Z. Pavlík, M. Jiříčková, P. Tesárek, M. Gazdo, R. Černý

pavlikz@fsv.cvut.cz

Department of Structural Mechanics, Faculty of Civil Engineering, Czech Technical University, Thákurova 7, 166 29 Prague 6, Czech Republic

A continuous increase of requirements on the thermal function of building structures which was started about thirty years ago is driven in particular by the fact that the buildings are large consumers of energy. Especially in regions with unfavourable climate, a substantial share of energy goes to heat and cool buildings. This heating and air-conditioning cost can be reduced to a certain degree through many means. Particularly notable among them is the proper design of a building envelope, its components and the use of proper building materials.

The application of proper type of thermal insulation in buildings does not only contribute to the reduction of the required air-conditioning system size but also to reduction of the annual energy cost. Additionally, it helps in extending the periods of thermal comfort without reliance on mechanical air-conditioning particularly during inter-seasons periods.

The properties of different types of thermal insulation materials are given by their performance characteristic as are e.g. bulk density, thermal conductivity, fire resistance, water absorption, resistance to direct sunlight, maximum service temperature, durability (if compression reduces value of thermal resistance), sound absorption, price, eventually potential health risks [1]. The proper type of thermal insulation is then chosen regarding to the intended practical application.

The objective of this paper is to present basic physical and thermal properties of four different types of thermal insulation materials on the basis of expanded polystyrene, hydrophilic mineral wool with different densities and calcium silicate. The complex knowledge of the presented material parameters is necessary in relation to their proper technical utilization and application in building structures. However, the producers of thermal insulation materials afford only basic overview of material parameters, mostly without the description of the methods and conditions of their determination, what can cause in consequence hard failures of the realized building structures.

In the experimental work, expanded self-extinguishing polystyrene produced by MUREXIN-AUSTROTHERM Ltd., Slovakia, is chosen as ordinarily used material for exterior thermal insulation of building envelopes. Materials on the hydrophilic mineral wool basis denoted MU and INROCK are newly developed products by Rockwool Inc. designed in cooperation with our laboratory in the frame of EU project INSUMAT for a utilization in interior contact thermal insulation systems [2]. Capillary active calcium silicate based material was produced by Calsitherm, Germany, and is used as interior thermal insulation material and fire resistance thermal protection [3].

Among the basic physical properties, the bulk density, matrix density, saturation moisture content and total open porosity were measured using vacuum saturation experiment and Archimedes weight concept [4].

The measurements of thermal conductivity, thermal diffusivity and specific heat capacity were performed on samples freely left in laboratory conditions (relative humidity $30 \pm 5\%$, temperature $25 \pm 2^\circ\text{C}$). For the measurement of thermal properties, the commercial device ISOMET 2104 developed by Applied Precision, Ltd. operating on impulse technique was used. The particular measurements were performed by surface probe with the measuring range of thermal conductivity of $0.03 - 0.3 \text{ W/mK}$ and the measuring error of 5%.

The measured results revealed very good thermal insulation properties of all tested materials. From the studied materials, the expanded polystyrene and mineral wool based materials had the thermal conductivity coefficient markedly lower in comparison with calcium silicate. The sorptivity test provided an information on the resistivity of insulation materials against the infiltration of liquid water. The obtained results showed that expanded polystyrene had the highest resistivity to transport of liquid moisture. Therefore it should find use especially in exterior thermal insulation systems exposed to an impact of unfavourable climatic conditions. On the other hand, the materials on the basis of hydrophilic mineral wool and calcium silicate are proper for an application in interior contact insulation systems as a possible transport of liquid moisture can be realized easily, either along the fibers provided by hydrophilic admixtures in mineral wool materials or directly through the porous structure of calcium silicate.

It should be noted that the obtained results are not yet complete at the moment. In the future work it will be necessary to supplement presented results by measurements of other, particularly hygric material parameters and to include an influence of temperature, moisture content and relative humidity of the material on the measured material parameters. Using the completely determined material parameters, it will be possible to correctly assess the hygric and thermal performance of the studied materials, e.g. utilizing advanced computational simulations techniques solving the problem of coupled heat and moisture transport in building materials themselves or in their multi-layered systems.

References:

- [1] M. S. AL-HOMOUD: *Performance characteristics and practical applications of common building thermal insulation materials*, Building and Environment 40, 2005, pp. 351-364.
- [2] Z. PAVLÍK, J. PAVLÍK, R. ČERNÝ: *Experimental analysis of an interior thermal insulation system on the mineral wool basis*, Proceedings of 11. Bauklimatisches Symposium in Dresden, Vol. 2, 2002, pp. 634-642.
- [3] P. HAUPL, K. JURK, H. PETZOLD: *Inside thermal insulation for historical facades*, Proceedings of the 2nd International Conference on Building Physics, A. A. Balkema Publishers, Leuven, 2003, pp. 463-470.
- [4] M. JIŘIČKOVÁ: *Application of TDR microprobes, minitensiometry and minihygroscopy to the determination of moisture transport and moisture storage parameters of building materials*, Ph.D. thesis, CTU Prague, Faculty of Civil Engineering, 2003.

This research has been supported by GA ČR grant No. GA 106/04/0138.

Thermal and Hygric Properties of Ceramic Brick: Reference Data Measurements for Application in Modeling Coupled Moisture and Heat Transport

Z. Pavlík, M. Jiříčková, P. Tesárek, P. Rybár, R. Černý

pavlikz@fsv.cvut.cz

Department of Structural Mechanics, Faculty of Civil Engineering, Czech Technical University, Thákurova 7, 166 29 Prague 6, Czech Republic

Utilization of advanced computer codes solving the problem of coupled moisture and heat transport is a recognized technique in the assessment of the hygrothermal function of porous building materials themselves or their multi-layered systems. Application of computational analysis makes it possible to study an investigated structure in wider time intervals what is very important for predicting the durability and the service life of studied structures. On the other hand, this treatment assumes a complete determination of thermal and hygric material parameters that should be done very precisely and rigorously because a combination of particular errors from material parameters measurements can lead to high inaccuracies in a computer analysis.

Although most of building materials are applied in building structures for many years, determination of their thermal, hygric and other physical properties was not in the center of interests of building designers and engineers until now. Presently, when the requirements on buildings structures are increasing, the question of the entire knowledge of material properties applied in buildings structures is getting to be actual.

In this paper, a complete set of physical, thermal and hygric material parameters of ceramic brick is collected to support computational modeling of coupled moisture and heat transport in brick structures. The hygrothermal properties of different kinds of ceramic bricks are considered as relatively comfortable in general. However, some differences in their properties should be expected given especially by the fact, that the raw material for their production can be varied as well as the manufacturing technology. Therefore, for particular ceramic bricks, the measurements of material parameters have to be done. In this paper, ceramic brick produced by brickworks Nebužely, Czech Republic, is tested.

For the studied material, the measurements of bulk density, matrix density, vacuum saturation moisture content, total open porosity, thermal conductivity, specific heat capacity, apparent moisture diffusivity, water absorption coefficient, moisture diffusivity in dependence on moisture content, water vapor diffusion coefficient and water vapor resistance factor were performed.

In the determination of basic physical properties, the samples of tested materials were first completely dried at the temperature of 100°C to obtain the dry mass. The dried samples were then placed into the desiccator, which was fully filled by distilled water and evacuated for 24 hours. On the basis of measured Archimedes weight of saturated samples, the calculation of remaining above given physical parameters was performed [1].

Determination of the apparent value of moisture diffusivity was done on the basis of a common water suction experiment, where the inflow of water into the sample was continuously monitored. From the shape of the suction curve, the water absorption coefficient

was assessed and the apparent value of moisture diffusivity was calculated from the known vacuum saturation moisture content [2]. Since the apparent value of moisture diffusivity is only constant value insufficient for computational modeling, determination of moisture diffusivity in dependence on moisture content was done on the basis of inverse analysis of moisture profiles measured by the capacitance method. For the inverse analysis, the Matano method was applied on the basis of the previous experience with the solution of the inverse problem of liquid moisture transport [3].

To characterize the water vapor transport through the brick material, the assessment of water vapor diffusion coefficient and water vapor resistance factor was done employing the cup method according to the Czech standard ČSN 72 7031, with different values of applied relative humidity.

The measurements of thermal properties were done using the commercial device ISOMET 2104 with the surface sensor having the measuring range of thermal conductivity 0.5–2.0 W/mK and the measuring range of specific heat capacity $1.5 \cdot 10^6$ – $4.0 \cdot 10^6$ J/m³K. The measurement is based on the analysis of temperature response of the tested materials on thermal flux impulses emitted from the sensor. Because of a strong dependence of thermal material properties on moisture content and temperature, the measurements of thermal conductivity and specific heat capacity were done on completely dried samples, samples left freely in laboratory at constant relative humidity 50% and on capillary saturated samples. At first, the measurements were performed at constant laboratory temperature of $21 \pm 2^\circ\text{C}$. Then, the temperature dependent thermal properties were determined in the temperature range of -10°C to $+30^\circ\text{C}$. During this experiment, the sample together with the sensor was placed into the climatic chamber, where the temperature changes were simulated and the changes of thermal properties were continuously monitored. The time necessary to achieve the temperature equilibration of the measured material was estimated in advance by calculations.

The results presented in this work will be introduced into the material database of the newly designed computer code TRANSMAT 4.3, solving the problem of coupled moisture and heat transport in porous building materials. The measured results give also general information about the hygrothermal performance of the studied material, particularly in comparison with other previously tested materials.

References:

- [1] M. JIŘIČKOVÁ: *Application of TDR microprobes, minitensiometry and minihygroscopy to the determination of moisture transport and moisture storage parameters of building materials*, Ph.D. thesis, CTU Prague, Faculty of Civil Engineering, 2003.
- [2] M. K. KUMARAN: *Moisture diffusivity of building materials from water absorption measurements*, IEA Annex 24 Report T3-CA-94/01, Ottawa, 1994.
- [3] DRCHALOVÁ J., PAVLÍK Z., ČERNÝ R.: *A Comparison of various techniques for determination of moisture diffusivity from moisture profiles*, Proceeding of the 6th Symposium of Building Physics in the Nordic Countries, Trondheim, vol. 1, 2002, p. 135-142.

This research has been supported by GA ČR grant No. GA 201/04/1503.

Inverse Modeling of Water and Salt Transport in Building Materials: The Choice of a Proper Model.

Z. Pavlík, R. Černý

pavlikz@fsv.cvut.cz

Department of Structural Mechanics, Faculty of Civil Engineering, Czech Technical University, Thákurova 7, 166 29 Prague 6, Czech Republic

Modeling salt transport in building materials is an effective tool in service life assessment because it makes it possible to predict the salt profiles in a building element. However, modeling just the salt transport may not be sufficient, because the transportable salts are always dissolved in water. Therefore, combined water and salt transport should be used in mathematical models of degradation processes.

In this paper, a computational inverse analysis of coupled water and chloride transport in cement mortar is done in order to identify the water and salt transport parameters that are necessary as input data for the models of coupled water and salt transport. On the basis of obtained results, the choice of a proper model for description of coupled water and salt transport is discussed.

In the computational inverse analysis of the coupled water and chloride transport in cement mortar, we assumed, for simplicity, a simple diffusion model of either water or salt transport without any cross effects. Therefore, the result of our analysis was the identification of apparent water and salt transport parameters instead of the basic parameters of the coupled water and salt transport, defined exactly in the sense of irreversible thermodynamics.

The main difference between the apparent parameters and the thermodynamically “pure” parameters of the coupled water and salt transport is that the apparent parameters do not express “pure” effects, but combined effects. So, the apparent chloride diffusion coefficients include not only the free chloride diffusion in the porous space but also the effect of chlorides bonding on the pore walls and the effect of chloride transport due to the water movement. The notion of apparent moisture diffusivity then means that it is related not to the water itself, but to the chloride-in-water solution, i.e. the whole liquid phase.

Under these simplifying assumptions, we have formally obtained the same parabolic differential equations and the same boundary and initial conditions for both water transport and chloride transport. Therefore, the calculation of concentration-dependent diffusion coefficients from the measured chloride concentration profiles could be done using basically the same inverse methods as those for the determination of moisture-dependent moisture diffusivity or temperature-dependent thermal conductivity. In the solution of the inverse problem to the parabolic differential equations, we assumed that the water or concentration field $C(x,t)$ was known from the experimental measurements as well as the initial and boundary conditions of the experiment. Solving an inverse problem in this particular case meant the determination of the $D(C)$ function using the above data. On the basis of the previous experience with the solution of inverse problems of moisture diffusion and heat conduction [1], we employed for determination of the $D(C)$ function in this paper the Matano method.

The calculated results show that systematically, both apparent chloride diffusion coefficient and apparent moisture diffusivity calculated using the profiles corresponding to 24

hours exposure to the chloride solution are higher than those determined from the 168 hours profiles. This result gives an evidence of the time dependence of both apparent chloride diffusion coefficients and apparent moisture diffusivities. On the other hand, this feature was not observed for the penetration of distilled water where the difference in calculated moisture diffusivity was somewhere on the edge of the error range of the method. From known water and concentration fields $C(x,t)$ determined previously in laboratory experiments, there is obvious, that the water penetrates into the specimen much faster than chlorides. However, the measured chloride concentrations close to the surface after already 24 hours of penetration were higher than the concentration in the penetrating solution. This reveals that a part of chloride ions is apparently bound on the pore walls of the matrix and is immobilized so that it cannot further take part in transport processes in the solution. As a consequence, the calculated apparent transport parameters are lowered. This effect can be described in more advanced phenomenological models by using ion binding isotherm as a storage parameter of salt transport [2].

On the other hand, the water molecules cannot be adsorbed on the pore walls in such extent as in usual situation when chloride ions are not present because a part of potential van der Waals bonds on the walls is blocked by the chloride ions. Therefore, water molecules are transported by faster capillary forces in higher extent than usually and the apparent transport coefficients are higher. However, this effect leads after some time to partial separation of water molecules and the chloride ions in the solution, the solution on the penetration front becomes more dilute and water molecules on the front can again be adsorbed on the pore walls easier, similarly as in the case when no chlorides are dissociated in the solution. As a consequence, the transport coefficients of water in the porous medium are lower than in the initial phase and the higher viscosity of the chloride solution compared to the distilled water begins to play a significant role for the transport rate. The apparent chloride transport coefficients also become lower because they do not include such high extent of ions fixed on the pore walls and the ion transport in the solution begins to prevail.

In this paper, an attempt towards better understanding of mechanisms driving the coupled water and chloride transport in cement mortar was done using simple evaluation methods based on the diffusion model of both water and salt transport. Although this type of models is not the only one that can be used for modeling water transport in cement based materials, and maybe even not the most appropriate one particularly for more complicated transport problems [2], their simplicity makes it possible to analyze fundamental phenomena, which in more complex models could be more or less hidden, in a very straightforward way.

References:

- [1] J. DRCHALOVÁ, R. ČERNÝ: *Non steady-state methods for determining the moisture diffusivity of porous materials*, Int. Comm. Heat and Mass Transfer, Vol. 25, 1998, pp. 109-116.
- [2] R. ČERNÝ, P. ROVNANÍKOVÁ: *Transport Processes in Concrete*, Spon Press, London, 2002.

This research has been supported by GA ČR grant No. GA 103/04/P085.

Experimental Setup for Measuring Moisture Profiles in Building Materials Using Time-Domain Reflectometry

Z. Pavlík, M. Jiříčková, R. Černý

pavlikz@fsv.cvut.cz

Department of Structural Mechanics, Faculty of Civil Engineering, Czech Technical University, Thákurova 7, 166 29 Prague 6, Czech Republic

In this paper, we present the time domain reflectometry technique for moisture measurement as a relatively new method for building materials with a good potential for the application in both laboratory and in situ conditions. The time domain reflectometry (TDR) method was commonly used for the measurement of moisture content in soil science until now. Therefore, the measuring technology and the measuring procedure have to be adjusted for an application in the investigation of porous building materials.

The time-domain reflectometry (TDR) technique presents a specific methodology among the microwave impulse techniques. A device based on the TDR principle launches electromagnetic waves and then measures the amplitudes of the reflected waves together with the time intervals between launching the waves and detecting the reflections. The fundamental element in any TDR equipment used for the determination of moisture content in porous materials is a metallic cable tester. In the experimental work in this paper, we used the cable tester LOM/RS/6/mps Easy Test, Poland, which is based on the TDR technology with \sin^2 -like needle pulse having rise-time of about 200 ps. It is a computer aided instrument [1], originally designed for measurements of soil moisture. The built-in computer serves for controlling TDR needle-pulse circuitry action, recording TDR voltage-versus time traces, and calculating the pulse propagation time along particular TDR probe rods and the dielectric constant of measured material.

A variety of TDR probes of different shapes and types have been designed so far. For instance, Topp et al. [2] used a coaxial cell in a direct (but much larger) extension of the coaxial cable. Nissen and Moldrup [3] described a three-rod coaxial probe, where the shield of the coaxial cable was replaced by two metal rods of the same length as the conductor.

In this paper, we used a two-rod miniprobe LP/ms (Easy Test) for the determination of instantaneous moisture profiles that was designed by Malicki et al. [4]. This probe is designed for monitoring changes in water and salt distribution in the material. The sensor is made of two 53 mm long parallel stainless steel rods, having 0.8 mm in diameter and separated by 5 mm. The sphere of influence was determined with the help of a simple experiment. The probe was fixed in the beaker and during the measurement, there was added water step by step. From the measured data (dielectric constant in dependence on water level) there was found out that the sphere of influence creates the cylinder having diameter about 7 mm and height about 60 mm, circumference around the rods of sensor. The accuracy of moisture content reading is $\pm 2\%$ of displayed water content.

The measuring technology can be divided into three basic steps; probe calibration, sample arrangement and probes placing, data evaluation and calculation of moisture content.

The probe calibration has to be done for every probe on the basis of known dielectric constants of water and benzene. The applicability of TDR method for measurements of moisture content in building materials was tested performing the vertical suction experiment

on dry samples of cellular concrete produced by Ytong, Germany. The sample size was 70x50x330 mm. At first, samples were water and water vapor insulated with Epoxy resin on four lateral sides to ensure the one-dimensional transport. Then, sixteen LP/m probes were installed into each sample into the holes bored before. The probes were fixed and water and water vapor insulated with the technical plasticine. The moisture transport was continuously monitored, and the experiment was stopped before the water suction has reached the end of the measured sample. The experiment was performed in air-conditioned laboratory at $23 \pm 1^\circ\text{C}$ and $30 \pm 2\%$ of relative humidity.

The determination of moisture content in the material from the measured dielectric constant was done using conversion function proposed by Malicki et. al. [4] where the bulk density of a studied material has to be known from the previous vacuum saturation test.

Preliminary experiments performed with the samples of cellular concrete have clearly shown a good perspective of the TDR method for measuring moisture content in porous building materials. Contrary to the other currently used methods for determination of moisture content, the application of TDR method does not require calibration by the gravimetric method for every material. The TDR probe calibration can be done in advance all once for every single probe. Another advantage of the TDR method is that it is well applicable for the materials with higher salinity, where an application of other widespread methods such as the resistance method or the capacitance method is impossible due to their significant loss of accuracy. It should also be noted that the TDR method has a high potential not only in laboratory measurements, and its field version makes possible long term monitoring of moisture content in situ, directly on building site.

References:

- [1] M. A. MALICKI, W. M. SKIERUCHA: *A manually controlled TDR soil moisture meter operating with 300 ps rise-time needle pulse*, Irrigation Science, Vol. 10, 1989, pp. 153-163.
- [2] G. C. TOPP, J. L. DAVIS, A. P. ANNAN: *Electromagnetic determination of soil water content: Measurements in coaxial transmission lines*, Water Resources Research, Vol. 16, 1980, pp. 574-582.
- [3] H. H. NISSEN, P. MOLDRUP: *Theoretical background for the TDR methodology*, SP Report No. 11. Danish Institute of Plant and Soil Science, Lyngby, 1995, pp. 9-23.
- [4] M. A. MALICKI, R. PLAGGE, M. RENGER, R. T. WALCZAK: *Application of time-domain reflectometry (TDR) soil moisture miniprobe for the determination of unsaturated soil water characteristics from undisturbed soil cores*, Irrigation Science, Vol. 13, 1994, pp. 65-72.

This work was funded by the Czech Ministry of Education grant No. MŠMT PL-44.

Application of Fractal Geometry in Textural Fractography of Fatigue Failures

Z. Sekerešová, H. Lauschmann

lausch@kmat.fjfi.cvut.cz

Department of Materials, Faculty of Nuclear Sciences and Physical Engineering, Czech Technical University, Trojanova 13, Praha 2, 120 00

Among other methods within textural fractography, also fractal geometry was used to describe the textures in images of fatigue crack surfaces.

The standard application of fractal geometry [4] consists in *box counting method* [3]. It is based on continuous covering of the followed image or space objects with a network of boxes of side r , while the magnitude of the box side is changed in each step. The number of boxes $N(r)$, necessary for the coverage of the object perimeter, is detected. The relation between the number of boxes and the magnitude of the box side determines the value of the fractal dimension D in the relationship $D = \log(N(r)) / \log(1/r)$. Fundamental prerequisite of the fractal geometry is self-similarity - the value D is constant in all steps, and may be estimated as the slope of a line. The magnitude r stands here for the unit of length of the object under study. $N(r)$ represents measured length, while $1/r$ is factor of scaling.

The fractographic application of fractal geometry consists in relating fractal dimension characterizing images of fracture surfaces, with fatigue crack growth rate.

The first experimental basis for the development of textural fractography methods were the fracture surfaces of three specimens from an extensive research programme aimed at fatigue characteristics of austenitic stainless steels AISI 304L used in nuclear power plants. The CT specimen had proportions $60 \times 62.5 \times 5$ mm.

Specimens were loaded by a constant cycle loading in tension with $P_{\min} = 1450$ N, $P_{\max} = 4850$ N, frequency $0.5 \div 10$ Hz, at temperature 20°C in a corrosive aggressive aqueous solution (B-water). The status of crack growth was regularly recorded during the loading in the form of couples [number of cycles N , crack length a]. Crack length was measured by a microscope on specimen surface and simultaneously estimated from the measurement by potential method.

Fatigue crack surfaces were documented using SEM with magnification 200 x. Real image area was 0.6×0.45 mm. Images were located in the middle of the crack surface. The shift of the neighbouring images 0.4 mm forms continuous strip with small overlap of the images. The direction of crack growth in images is from the bottom up. Images were digitalized with resolution 1600×1200 pixels at 256 brightness levels (8 bit). For every specimen the acquisition was about 45 pictures.

The estimation of fractal characteristics was provided in two ways.

1. Normalized greyscale pictures were replaced by a fibre process [1], which provided images of fibrous idealizations of elongated light objects in resolution 1600×1200 pixels in binary map (logical field). A 2D box-counting method was applied at fibres [2].

2. The second method consisted in processing of the normalized greyscale pictures with the box-counting method in 3D [2]. Here grey scale forms the third dimension, giving cubes $r \times r \times r$. The principle is the same as in the first case: step by step overlaying the picture, with changing measure r . The dimension $r_{\min} = 20$ pixels of the smallest cube was chosen so that it would be possible to recognize a small textural element within. Then the equidistant sequence $r_{\min} + \Delta r, r_{\min} + 2\Delta r, \dots, 320$ with $\Delta r = 15$ pixels, was followed.

Application was computationally realized in environment of MATLAB [2].

Within the first method, the presumption of the linearity of the dependence of $\log N(r)$ on $\log 1/r$ was not fulfilled. That means, binary representations of fibres were not self-similar. Therefore, fractal dimensions could be estimated only as rough approximations. On the basis of the results, it was possible to speculate about a linear dependence between logarithm of crack growth rate and fractal dimension. Unfortunately, the scatter of single values was too large. However, from the fractographic standpoint, the results show undoubtedly that fractal dimension of fracture morphology increases with crack growth rate.

Problems with an insufficient self-similarity were smaller (but also present) at box-counting 3D method. Nevertheless, it seems to be the right way in the development of applications using fractal geometry. Acceptable tight linear or quadratic dependences of crack growth rate on fractal dimension were obtained for each particular specimen. Within the future development of this method, the ratio between length and brightness units will be optimized.

The results of the first applications of fractal geometry in fractography of fatigue failures showed, first of all, to a fundamental problem: the morphology of fatigue fracture surfaces is far from the main presumption of self-similarity. There are many ways how it could be overcome, for example:

1. Within the theory of fractal geometry: to follow the concept of self-affinity or the concept of multifractals.

2. Within fractography of fatigue failures: to extend the frame of analysis to a large range of magnifications. Then the same locality of fracture surface could be analyzed in many scales and its detailed structure could be investigated.

3. To use the estimated values $\log(N(r))$ directly as image features without fitting them by a line, or to fit them by a more general dependence with parameters serving as final image features.

The fractal analysis of images of fatigue fracture surfaces is a promising research direction within textural fractography of fatigue failures.

References:

- [1] LAUSCHMANN H., TŮMA M, RÁČEK O, NEDBAL I: *Textural fractography*. Image Analysis and Stereology, Special issue Vol.21, 2002, pp.S49-S59
- [2] SEKEREŠOVÁ Z.: *Application of fractal geometry in textural fractography of fatigue fractures*. [Research project - in Czech.] CTU Prague, FNSPE, Dept. of Materials 2004, 52 p.
- [3] FALCONER K.: *Techniques in fractal geometry*. Chichester: Wiley-Academy, 1997, 256p.
- [4] MANDEBROTT B.B.: *Fractal Geometry of nature*. New York: Freeman, 1982, 469 p.

This research has been supported by the Ministry of Education of the Czech Republic, research project No. Cez.:J04/98:21000021, "Diagnostics of Materials".

Computational Simulation of Hygrothermal Performance of Building Envelopes on Modified FGD Gypsum Basis

P. Tesárek, J. Maděra, M. Pánek, R. Černý

`tesarek@fsv.cvut.cz`

Czech Technical University, Faculty of Civil Engineering, Department of Structural Mechanics, Thákurova 7, 166 29 Praha 6, Czech Republic

The computer simulation of temperature and relative humidity fields in building envelope systems based on modified gypsum was performed with the primary aim to assess their hygrothermal performance. The computational analysis of the hygrothermal performance of the studied multi-layered building envelope was done using computer program DELPHIN 4.4 (TU Dresden). Contrary to other software packages for modeling heat and moisture transport working with temperature and relative humidity only, DELPHIN 4.4 also includes capillary pressure as one of the basic state variables, which makes it possible to determine the transport of liquid moisture with much better precision and reliability [1].

In our calculations, we chose the 1st of January as the starting point, when we assumed the construction of building envelopes on modified gypsum basis provided by an exterior thermal insulation system to be done. For the insulation systems, there were taken initial values of field variables corresponding to the values of temperature of 21°C and relative humidity of 70 %. The systems with exterior thermal insulation were exposed from inside to constant conditions (temperature equal to 20°C and relative humidity equal to 50,60 and 70 %) and from outside to the climatic conditions corresponding to the reference year for Prague. Initial conditions for gypsum were different (50-90% relative humidity).

We have solved three variations of FDG gypsum wall, namely from the raw material and from two different types of modified (hydrophobized) gypsum, with the thickness of 300 mm. On the external side there was thermal insulation with a thickness of 100 mm on mineral wool basis (Rockwool) and lime plaster. The physical properties of modified and non-modified gypsum materials were measured in our laboratory [2] [3]. The physical properties of mineral wool and lime plaster were partially obtained from the material database in the computer code DELPHIN 4.4 and partially measured in our laboratory.

The modification of FGD gypsum for the utilization of gypsum elements in the exterior is necessary primarily due to the unfavorable water transport properties of basic gypsum. So, the primary aim is to achieve more suitable properties and longer service life. Possibilities of such modifications are basically two. The first one is using a hydrophobization admixture in the course of sample production. The second one is impregnation of specimen surfaces. In our investigation we used the first option.

Hydrophobization admixtures used for our investigation were common commercially available materials. The first modification contained the admixture IMESTA IBS 47 produced by Imesta Inc., Dubá u České Lípy, CZ. Concentration of this admixture was 0.5% by mass. The second one contained the admixture ZONYL 9027 (a fluorochemical solution that provides a durable, subsurface, transparent, protective barrier against oil and water on porous surfaces) produced by Du Pont, USA. This admixture was used as a 5 % solution in water. Basic properties, which were used for our simulations, are shown in Table 1.

Materials	Bulk density	Open porosity	Apparent moisture diffusivity	Water vapor diffusion res. factor
	[kgm ⁻³]	[m ³ m ⁻³]	[m ² s ⁻¹]	[-]
raw material	1019	0.60	2.6E-7	14.3
gypsum with IMESTA IBS 47	942	0.63	1.47E-7	15.0
gypsum with ZONYL 9027	941	0.66	7.32E-9	15.0

Table1 Basic properties of applied materials.

Computational analyses show that after one or one and a half year, for the initial conditions of 90 % relative humidity in the gypsum wall, there are in the gypsum wall basically the same conditions as in the interior. In general, the time to achieve this situation is strongly dependent on the initial conditions in gypsum (temperature and relative humidity), where relative humidity has a very significant effect. This conclusion is very interesting for future development of technology and future production of elements on FGD gypsum basis because the freshly produced gypsum specimens have very high value of relative humidity and drying is very slow in laboratory conditions (temperature 25°C and relative humidity 50%).

The effect of hydrophobization admixtures, particularly of ZONYL 9027, was found to be very distinct. They reduced significantly the daily and yearly variations of relative humidity in the gypsum element. This is a very positive feature because it leads to a reduction of hygric stresses in the structure. For multi-layered building envelopes this seems to be particularly important.

References:

- [1] J. GRUNEWALD: DELPHIN 4.1 - Documentation, Theoretical Fundamentals. TU Dresden, Dresden 2000.
- [2] P. TESÁREK, R. ČERNÝ, J. DRCHALOVÁ, P. ROVNANÍKOVÁ: Thermal and hygric properties of gypsum: Reference Measurements Thermophysics 2003, 2003 pp.52-57
- [3] P. TESÁREK, R. ČERNÝ, J. DRCHALOVÁ, P. ROVNANÍKOVÁ, J. KOLÍSKO: Mechanical, thermal and hygric properties of hardened flue gas desulfurization gypsum - Part I, Stavební obzor Vol. 13, No.5, 2004, .pp.138-142.

This research has been supported by GA ČR grant No. 103/03/0006.

Measurement of Basic Material Parameters of High Performance Concrete Using SORPTOMATIC 1990

D. Stoklasová, M. Jiříčková, R. Černý

d i t a . s t o k l a s o v a @ f s v . c v u t . c z

Department of Structural Mechanics, Faculty of Civil Engineering, Czech Technical University, Thákurova 7, 166 29 Praha 6, Czech Republic

Most of solid and powder materials both natural (stones, soils, minerals, etc.) and manufactory produced (cements, ceramics, composites, etc.) contain a certain internal volume, which is distributed in the form of pores, cavities, and cracks of different sizes and shapes to form a porous system of solid matrix. The total sum of these volumes is called porosity which is a basic material property strongly affecting important physical properties such as mechanical strength, durability or adsorption properties of solid materials. The knowledge of pore structure makes prediction of material behaviour under different environmental conditions possible. Two main pore types can be distinguished, namely closed and open. Closed pores are completely isolated from the external surface and not able to be accessed by external fluids. These influence material parameters like density, mechanical or thermal properties. On the other hand open pores are connected to the external surface, are accessible to fluids. They can be basically divided into dead-end or interconnected pores.

The complete characterisation of material parameters can be measured using a combination of different techniques, namely mercury porosimetry, for pore size and particle size distribution, bulk and matrix density, total porosity and pore area distribution measurement, gas adsorption, for specific surface, pores distribution and pores total volume determination, and helium pycnometry, the only one for real density measurement. The choice of a particular technique usage depends also on the material pore size.

SORPTOMATIC 1990 is fully automatic analytical instrument based on a static volumetric principle to characterise solid samples, which can be used for gas adsorption/desorption and chemical adsorption measurement [1]. By using inert gases such as nitrogen, it is possible to determine the basic properties of a large scale of solids and powders, in the case of very low specific surfaces (non porous materials) krypton can be used, while for some ultramicroporous solids (zeolites) argon physisorption is applicable. Chemisorption technique provides information on the quality, activity and selectivity of a wide range of catalysts, using reactive gases, for example hydrogen, carbon monoxide or ammonia.

If a gas or vapour comes in contact with an adsorbent (material surface), adsorbed material molecules are distributed between gaseous and adsorbent phases. Surface atoms do not entirely exchange their valence electrons with those nearby and thus form free electrons, which enable liquid or gaseous molecules coming into contact with solid surface to combine with it by relatively weak interaction called Van der Waals bonding. At constant temperature the quantity adsorbed depends on pressure and adsorbent. It is known that the isothermal adsorption increases with pressure and decreases with temperature.

The specific surface area represents the outer surface for non-porous solids, while for porous solids it is considered as an outer surface similar to that of non-porous solid plus an inside surface remarkably superior to the outer one, which is formed by the surface total pores. In order to calculate the adsorbent surface area it is necessary to determine the gas volume relative to the monomolecular layer and to know the value of the gas adsorbed molecular section area.

The SORPTOMATIC 1990 consists of two main parts: control and analytical sections. The brain of instrument is a powerful microprocessor controlling and monitoring all phases

during both the analysis and the sample pre-treatment. If the PC is connected with the instrument the system status, actual experimental conditions and the adsorption in a real time can be monitored. Common coolants for the analyses are liquid nitrogen or argon, different ovens are available to perform analyses from room temperature up to 450°C.

The main aim of this paper was to determine the basic material parameters of a high performance concrete. The basic tested material was high performance concrete C90/105 containing microsilica and denoted as BI in what follows. For the sake of comparison, the same mixture of concrete C60/75 (denoted as BII) was prepared without microsilica. In order to analyze the effect of aggregates, two other mixtures based on BI and BII were prepared. The first one denoted as BBI, BBII was cement mortar without the 8-16 mm aggregate fraction. The second one was cement paste denoted as PI, PII.

The samples were prepared in the form of standard prisms sizes 40x40x160 mm. After twenty eight day hardening period they were cut and milled into powder or crushed into small particles. After that they were drying in an oven to achieve a constant so called zero weight. The samples were analyzed using nitrogen gas. The results show the influence of silica fume suspension addition and a great effect of aggregate granularity.

References:

- [1] THERMO FINNIGEN *Sorptomatic 1990, Instruction Manual* Thermo Finnigen Italia S.p.A. 2002.

This research has been supported by GA ĀR grant No. GA 103/03/1350.

Microstructure of Fe-3wt.%Si Monocrystal close to the Fracture Surface

M. Karlík, P. Haušild, M. Landa*

karlik@kmat.fjfi.cvut.cz

CTU, Faculty of Nuclear Sciences and Physical Engineering, Department of Materials
Trojanova 13, 120 00 Praha 2,

* Institute of Thermomechanics, Academy of Sciences of the Czech Republic,
Dolejškova 5, 182 00 Praha 8, Czech Republic

Although known for more than a century, the ductile-to-brittle transition (DBT) of ferritic steels with decreasing temperature remains a fundamental issue in engineering, metallurgy and material science. Almost all structural ferritic steels show this transition: Above the DBT temperature the ferritic steels are characterised by a ductile dimple fracture accompanied by high energy absorption. Below the DBT temperature, the fracture mechanism is transgranular cleavage and only little energy is absorbed. When the specimens are tested in the ductile-to-brittle transition region, cleavage crack initiation is frequently preceded by ductile crack growth and the values of energy to fracture exhibit a large scatter. The understanding of the ductile to brittle transition depends mainly on the determination of a reliable cleavage criterion, well established on physical basis.

The resistance against brittle fracture plays an essential role in the safety assessments of important engineering structures made of steel (rails, bridges, pressure vessels, nuclear power plants). Since brittle fracture can lead to a catastrophic failure of the structure components, the fracture behaviour of ferritic steels has been extensively studied [1-3] and models relating the fracture toughness of the steel to its yield and fracture stresses through characteristic distances in the microstructure or using a statistical local approach have been proposed. However, the above-mentioned models cannot explain either the sharp upturn of the DBT curve or the increase of energy scatter in the ductile-to-brittle transition. Almost all these models expect a single mechanism of cleavage initiation. Our recent results showed that this condition is not necessarily fulfilled in larger temperature ranges in which more cleavage initiation mechanisms can coexist. A more detailed understanding of the physical mechanisms of cleavage is then necessary to predict the behaviour of the steel during operation.

Deeper knowledge of relationships between mechanical characteristics and micromechanisms of initiation and propagation of fracture in structural steels, especially at lower temperatures and at temperatures in the transition region, play therefore a very important role as well in chemical composition and microstructural design, as in a rational estimation of service safety of engineering structures. The purpose of the research effort is to carry out a physical-metallurgy analysis characterising an influence of microstructural, geometrical and loading parameters on initiation and propagation of cracking in structural steels. Besides steels, cleavage initiation mechanisms are analysed on Fe2-3wt.%Si considered as a model material for studying the cleavage fracture of bcc metals.

In the present work, the ductile to brittle transition (DBT) in α -iron was studied on four oriented single crystals of a Fe-3wt%Si alloy using acoustic emission, scanning and transmission electron microscopy. The experimental results are compared to the molecular dynamic simulations. Single-edge notched specimens 95 mm \times 10 mm \times 2 mm were loaded in tension at room temperature. The crosshead speed was changed in the range from 0.1 to 5.0 mm/min, the crack propagated in the (001) plane and in the [-110] direction. The tension fracture tests confirmed a strong dependence of the character of fracture on loading rate. The results indicate that the DBT temperature for loading rates 1-5 mm/min lies in the region of room temperature. Under the lowest loading rate, a plastic zone was formed at the notch tip - scanning electron microscopy showed a wavy relief of the non-crystallographic slip in this region. Faster loading lead to brittle fracture. Fractographic analysis of one of the samples broken at 1 mm/min loading showed flat cleavage facets and tongues formed by the interaction of the crack with deformation twins. Besides the tongues, the fracture surface of the second sample ruptured at the same loading rate exhibited signs of plastic deformation. In the first sample, transmission electron microscopy in the vicinity of the fracture surface confirmed deformation twinning and a very low dislocation density. In the second sample, the deformation twinning was assisted by slip of dislocations.

Molecular dynamics simulations with an empirical Y-potential for α -iron confirmed that crack growth has a more brittle character under high loading rates. Under a slower loading rate, the crack growth is more difficult since it is impeded by emission of the shielding dislocations from the crack tip in the $\langle 111 \rangle \{112\}$ slip system. New simulations with a semi-empirical N-body potential have been performed for the loading rate equivalent to crosshead speed of 1mm/min. The simulations show that the running crack can produce twins in the $\langle 111 \rangle \{112\}$ slip systems. It later causes new rupture along the twin-twin interfaces, which creates jogs (tongues) on fracture surfaces.

References:

- [1] RITCHIE R.O. - KNOTT J.F. - RICE J.R.: *On the relationship between critical tensile stress and fracture toughness in mild steel*, J. Mech. Phys. Solids 21, 1973, p. 395.
- [2] CURRY D.A.: *Cleavage micromechanisms of crack extensions in steels*, Metal Science 14, 1980, p. 319.
- [3] HAHN G.T.: *The influence of microstructure on brittle fracture toughness*, Metallurgical Transactions 15A, 1984, p. 947.
- [4] LANDA M. - MACHOVÁ A. - PŘEVOROVSKÝ Z. - ČERV J. - ADÁMEK J.: *Crack growth in single crystals of α -iron (3wt.% Si)*, Czechoslovak Journal of Physics 48, 1998, p. 1589.

This research has been supported by the Czech Science Foundation grant (project "Physical aspects of the transition behaviour of ferritic steels", GA CR 106/04/066).

Fracture of Fe₃Al-Zr intermetallic alloy at elevated temperatures

Jakub Prah^{*}, Petr Hausild^{*}, Miroslav Karlík^{*}, Jean-François Crenn^{**}

Petr.Hausild@fjfi.cvut.cz

^{*}Department of Materials, Faculty of Nuclear Sciences and Physical Engineering, Czech Technical University, Trojanova 13, 120 00 Praha 2, Czech Republic

^{**}Université de Bretagne-Sud, Laboratoire de Génie Mécanique et Matériaux, Rue de Saint-Maudé, BP92116, 56321 Lorient, France

Alloys based on Fe₃Al and FeAl rank to the most studied intermetallics particularly because of their low price, low density, good wear resistance, relative easy fabrication and high corrosion resistance in oxidizing and sulfidizing environments. However, there have been also two main disadvantages limiting their use – low ductility at ambient temperature and low strength at elevated temperatures [1]. The first one was characterized as an extrinsic effect caused by water vapour from surrounding atmosphere (hydrogen embrittlement) [2]. Many alloying elements were used to improve the properties of Fe₃Al alloys (Cr, Si, Ce, B, Zr, Y, Nb, W, etc.). Some are beneficial for increasing tensile strength (Mo, Nb), some increase room temperature (RT) ductility by hindering the embrittlement (Cr), some help to increase fatigue crack growth resistance (Zr, C) [3]. The aim of this paper is to investigate the tensile and fatigue properties of Fe-31.5Al-3.5Cr-0.25Zr-0.2C (at.%) alloy at room and elevated temperatures in order to verify the effect of Zr and C on fatigue behaviour of Fe-31.5Al-3.5Cr (at.%) alloy.

The mentioned alloy was prepared by vacuum induction melting and casting. The ingot was hot rolled at 1100°C to a plate 7 mm thick and subsequently quenched into mineral oil. After machining by milling, all the test specimens were annealed in air at 700°C for 2 hours to relieve internal stresses and then quenched into mineral oil. The material microstructure was recovered, with elongated grains having up to 1 mm in the direction of rolling and up to 300 μm in the transverse direction. Static tensile tests were carried out at temperatures 20 (RT), 200, 300, 400, 500, and 600 °C respectively on INSTRON 1195 testing machine equipped with a resistance-heated furnace. At each temperature, two cylindrical buttonhead specimens having 3 mm in diameter and 22 mm gauge length were tested at the constant crosshead speed of 2 mm/min (initial strain rate $1.6 \times 10^{-3} \text{ s}^{-1}$). Fatigue crack growth experiments were performed on compact tension (CT) specimens of thickness $B=5$ mm and width $W=40$ mm. The notch was prepared by electro-discharge cutting using a wire 0.2 mm in diameter. The initial crack length a_o was 6.5 mm. The fatigue crack propagated perpendicularly to the rolling direction. The specimens were loaded in tension at 20°C, 300°C and 500°C on a computer-controlled servohydraulic loading machine INOVA ZUZ 50 equipped with a resistance-heated furnace. The frequency of loading was 10 Hz, the stress ratio R was 0.042 and the maximum load was 4.8 kN.

The basic mechanical characteristics, 0.2% proof stress ($R_p0.2$), ultimate tensile strength (R_m) and tensile elongation (A), were measured at six different temperatures. Considering the range from 20°C to 540°C (D0₃ region), $R_p0.2$ and R_m had their minimum at 200°C, while the maximum values were reached at 300°C (R_m) and 500°C ($R_p0.2$), respectively. The values of $R_p0.2$ and R_m measured at 20°C and 500°C were comparable and the values of $R_p0.2$ and R_m at 600°C (B2 region) were practically identical. Tensile elongation at elevated temperatures was 3 ÷ 4 times higher than tensile elongation at room temperature.

In D0₃ region the elongation slightly increased with temperature, except for 400°C, where the value dropped down to 10%. At 600°C, in B2 region, the elongation was substantially higher than at 500°C (D0₃ region). Described temperature dependencies are in good agreement with the dependencies from Ref. [4] (experiments on Fe-28Al-3.6Cr-0.1Ce-0.16C (at.%) alloy). The only difference consists in evolution of elongation with temperature. While in Ref. [4] the elongation after reaching its maximum value (11.5%) drops approximately to the same value as at RT (~2.5%) at 300°C, in the present study the elongation was higher (17.2%) at 500°C than of RT and 300°C values. Fracture surfaces of broken tensile specimens changed from transgranular cleavage facets at RT to entirely ductile dimpled fracture at 600°C.

For evaluating of fatigue crack growth resistance, $v\text{-}\Delta K$ curves were plotted for each test temperature. The significant increase of slope (about 4 times) was observed comparing the curves corresponding to 20°C and 300°C. The shift to higher crack growth rates of almost 2 magnitudes with almost no change of slope was found when comparing $v\text{-}\Delta K$ curve corresponding to 500°C to the curve for 300°C. Both these changes were observed as well in Ref. [4]. The only difference is in the upper estimate of threshold value of ΔK , which was higher in Ref. [4]. This is probably a consequence of alloying by zirconium.

There were no important changes in character of morphology of fatigue fracture surface with increasing test temperature or with increasing stress intensity factor. The main fracture micromechanism was transgranular cleavage. Besides the transgranular cleavage, transgranular quasi-cleavage facets, ductile fatigue striations and brittle striations were also found on fatigue fracture surfaces. In the region of final fracture, there is a significant increase of signs of plastic deformation with increasing temperature. Similarly as on static fracture surfaces of broken tensile specimens it is possible to see a continuous change of fracture mechanisms from transgranular cleavage at 20°C to ductile dimpled fracture at 500°C.

References:

- [1] MCKAMEY, C.G. – DEVAN, J.H. – TORTORELLI, P.F. – SIKKA, V.K.: *A Review of Recent Development in Fe3Al-based Alloys*, J. Mater. Res. 6(8), 1991, pp. 1779-1805.
- [2] ALVEN, D.A. – STOLOFF, N.S.: *Fatigue Crack Growth of Fe3Al,Cr Alloys*, Scripta Mater. 34, 1996, pp. 1937-1942.
- [3] ALVEN, D.A. – STOLOFF, N.S.: *The Influence of Composition on the Environmental Embrittlement of Fe3Al Alloys*, Mater. Sci. Eng. A239–240, 1997, pp. 362-368.
- [4] HAUŠILD, P. – KARLÍK, M. – NEDBAL, I. – PRAHL, J.: *Fatigue Crack Propagation in an Fe3Al-based Alloy Tested at Elevated Temperatures*, Kovové Materiály 42(3), 2004, pp. 156-164.

This research has been supported by the Grant Agency of the Czech Republic in the frame of the project No. 106/02/0687.

Neutron Diffraction Texture Investigations of Zircaloy-4 Tubes

M. Dlouhá*, S. Vratislav*, L. Kalvoda*, A. Chichev*

dlouha@troja.fjfi.cvut.cz

*Department of Solid State Engin., Faculty of Nucl. Sciences and Physical Engin., Czech Technical University, Trojanova 13, Prague 2, 120 00, Czech Republic

To understand better the behaviour and the tube properties it is very important to examine in detail the dependence of the tube mechanical properties on its structure and texture formed in shaping/created in forming and thermal processing. The presented article contributes to the study of these problems developing both the results of [1], which deals with the anisotropy analysis of zirconium alloy tube mechanical properties and the knowledge of [2], where the development of Zirconium tube textures in the course of their plastic deformation is discussed.

The most widespread method of examining textures of shaped/formed materials has been X-ray diffraction. However, its usage is limited only to a thin surface layer of the sample. To gain information on volume textures it is then necessary to use specially treated samples. For this reason it is advantageous to make use of heat neutron diffraction method which provides the image of the average texture in the whole sample volume. Absorptive and scattering characteristics of heat neutrons (namely high penetrative ability of neutrons into most metals), as well as a large cross section of neutron beams used in experiments (as large as 10cm^3) allow to arrange the experiment in the way that makes it possible to irradiate the whole volume of the sample. The knowledge of the mean texture in the sample volume is very important in observing the deformation processes prior to initiation of the tube integrity/compactness damage.

Owing to the fact that neutron diffraction can provide a complete image of the mean texture in the volume of massive samples, it is suitable for non-destructive observations of volume kinetics of processes, which form the type and clearness/sharpness of textures. Together with the three-dimensional oriented distribution function which has been widely used in texture analysis, neutron diffraction is an important source of experimental information for the study of anisotropy of other physical properties of industrial materials such as elasticity, plasticity, magnetic anisotropy, corrosion resistance, and the like. This article presents the results of texture investigations of Zircaloy-4 tubes. Neutron diffraction and inversion pole figures were used to characterize the texture of samples. The main interest is given to the analysis of texture changes under different tensile test conditions including tensile force direction, annealing temperature and tensile test temperature. Four different specimens of different orientation to the tube axis were tested. The examined tension specimens were sampled from tubes made of Zircaloy-4 alloy (SANDVIK). The properties of the measured samples were then formed by thermal and mechanical processing characterized by the annealing temperature, the tensile test temperature, and the tensile force direction.

Neutronographic experiments were made using the KSN-2 diffractometer in the neutron diffraction laboratory of the Faculty of Nuclear Sciences and Physical Engineering. The apparatus worked at a regime for measuring powder diffraction diagrams. For measuring inversion pole figures the KSN-2 was equipped with TG-1 texture goniometer [3]. The measured samples were composed of five sheets of flat tension specimens examined in an open-end tensile test first. The tested area of the specimen was limited by a suitable deflection

of the monochromatic neutron beam. Thus the diffracted intensity was strengthened only by the part of the tension specimen lying less than 6 mm far from the failure point (it was measured along the longitudinal tube axis). The wavelength of the monochromatic neutron beam was 0.1031 nm, the KSN-2 resolution for the given monochromator parameters (Zn (002) monocrystal) and collimation system reached a level of $\Delta d/d = 0.009$ (d – interplanar parameter).

The apparatus parameters mentioned above made it possible for zirconium to measure intensities of 13 diffraction lines: from reflection (100) to (114). The needed values of integral intensities and their standard deviations were found by profile analysis of neutronograms.

By means of the procedure mentioned above, inversion pole figures have been calculated from integral intensities in both coordinate systems N , T , L and P , Q , R . Pole densities and texture indices have been calculated using the INVPOL program and f_i texture parameters using the NETINV program [4]. The experimental conditions have been chosen in order that the obtained texture characteristics error would not exceed a level of 10%.

The above mentioned texture changes of tested specimens caused by different conditions in the tensile test can be summarized as follows:

- The perpendicular orientation of crystallite basal planes towards the tube radius has been remarkably preferred for all the four specimens and is not affected by changing the tensile test conditions. The tensile force directed along the L tube axis does not cause any change in the preferred orientation.
- The tensile force in the R direction at an angle of 22° to the reference direction T in the L - T plane leads to a considerable texture change which results especially in substantial decrease in the level of p_{002} pole density for the L direction, the crystallites being turned around the crystallographic hexagonal axis c . The planes of a $(hk0)$ type, (e.g., (100), (210), or (110)) do not show any considerable preference of their pole orientations for being parallel to the L direction.
- The temperature increase in the tensile test from the room temperature to 310°C is reflected in decreasing the overall texture clearness/sharpness, its previous character being maintained. The average decrease in pole density values resulting from the temperature increase reaches roughly 25%.

References:

- [1] J.CEJP, B.CECH: *Materials ablation with soft x-rays*, Acta Polytechnika 4, 1988 pp.5-8.
- [2] E.TENCKHOFF: *Zirconium in Nuclear Application*, ASTM SST, Philadelphia, Editor, Proceedings of SPIE Vol. 4760, 1974, pp. 179-181.
- [3] M.DLOUHÁ, J.JEŘÁBEK, S.VRATISLAV: *Goniometr pro měření přímých pólových obrazců metodou neutronové difrakce*, Jaderná Energie, 29, 1983, pp.316-318.
- [4] M.DLOUHÁ, S.VRATISLAV: Vyzk.zpráva FJFI, KIPL, 1998, pp.1-15.

This research has been supported by GA ČR grant 202/03/0981 and by MŠMT grant MSM 210000021.

Image Analysis of Cement Paste

K. Forstová, J. Němeček

katerina.forstova@fsv.cvut.cz, jiri.nemecek@fsv.cvut.cz

Department of Structural Mechanics, Faculty of Civil Engineering, Czech Technical University in Prague, Thákurova 7, 166 29 Prague 6, Czech Republic

Image analysis method for porosity estimation of various material has been investigated. Results of such measurements are reported for a cement paste of water/cement ratio 0.5 and for porcelain and ceramic. In addition, the same specimens were analyzed using conventional porosimetry. The aim of this study was to develop a method for investigating and establishing pore size distribution measurement in cement paste using backscatter electron (BSE) and image analyses. Newly presented method has disadvantages in specimen preparation, image thresholding and limited resolution. Compared to the conventional porosimetry, image analysis performs better in the matter of pore shapes, upper pore size limit, and in statistical distribution of pores within specimen.

Hardened cement paste is a porous material. Porosity is one of the important phases of the microstructure of cement paste. Since it has great influence on strength and other properties in this material, the pore structure should be monitored. There exist at least three types of pores: the smallest gel pores embedded within C-S-H gel (typical size up to 10 nm), capillary pores of size up to 10 μm and above this limit the air pores, in the well-rounded shape. Reasonable resolution limit of environmental scanning electron microscope (ESEM) images for cement paste has been found around 1 μm . From this restriction it can be concluded that resolution below this value provides no information about pore shapes, therefore only upper range of capillary pores can be analyzed and characterized.

Techniques for studying the microstructure of cement paste can be divided into three categories. The first gives information about the average volume fraction occupied by one or more phases or by pores. Examples of such bulk techniques include thermo gravimetric analysis and quantitative X-ray diffraction. The second category provides information on the distribution of sizes of a component (i.e. porosity). Such techniques include: mercury intrusion porosimetry and low temperature calorimetry. In the third category, there are microscopical techniques. These provide a vast range of information on the microstructure in visual form including that obtained by techniques in the two previous categories.

A wide range of optical and electron microscopical techniques have been used in this study. For an automatic analysis, a technique must produce images which represent well the bulk microstructure. Different phases and porosity should be clearly identified and distinguished. These requirements preclude the secondary electron imaging of surfaces, but it has been found that backscattered electron images are well suited for this purpose. Contrast in BSE images is produced by variations in atomic number within the specimen, the resulting image displays in gray scale the shape and possible phase of microstructure surface. Typical image contains black color which represents empty pores, white color of mainly unhydrated clinker minerals. Gray levels can be assigned to hydration products (C-S-H gel, calcium hydroxide, ettringite etc.) but there has not been found a way how to distinguish these phases according to the gray level. Successful outcome that lies within accepted limits is strongly dependent on thresholding level, i.e. separation of pores from the rest of phases.

The objective of specimen preparation for microscopic analysis is to provide a polished surface. The microstructural characterization described above has been carried out on a backscattered electron microscope type XL30 ESEM-TMP (produced by FEI PHILIPS). Contrast and brightness of microscope is set in such a way that image provides sharp edges with good differentiation between voids and bulk.

This study carries out investigation of three specimens – a cement paste (w/c ratio 0.5), a porcelain and a ceramics. The reason of using porcelain and ceramics was to have some more homogeneous, reference material. The pores are better recognized and have more regular shape then the pores in ordinary cement paste. Forty images were captured from each specimen using ESEM microscope at different magnifications. For the processing of images, the software named LUCIA (produced by Laboratory Imaging) was used. LUCIA enables image segmentation and is capable of images conversion. This software allows measuring in automatic or interactive mode. Automatic measurement mode works on the binary images only. Interactive measurement mode enable to access length, area, angle and colorimetry measurements with the option to annotate the picture with the measured values. At first, the properties in interest should be chosen, i.e. area of pores. Segmentation is a process through which the image is partitioned into meaningful regions based only on the intensity of the pixels. Segmentation by the thresholding is the simplest approach. A contrast color is used for coloring of pores. Gray limits must be defined in automatic thresholding. The low threshold level was always set to zero since the black color corresponds to pore. The high threshold level is very sensitive for results. Parametric study of high threshold level vs. resulting porosity has been carried out. There has been found ascending relationship between these two values, which means that steeper increase occurs at higher threshold level. The reasonable high threshold level should be determined by calibration with another technique, such as porosimetry. This was done using mercury porosimetry from which the calibrated value of high threshold level was found.

Carlo Erba Porosimeter 2000 was used for conventional porosity measurement. It is an automatic instrument used for the determination of pore size and pore volume distribution in the range of 3,7 to 7500 nm pore radius. Pore volume is measured by a capacitance system, used in Mercury Intrusion Porosimetry (MIP). This technique is used for the measurement of pore size distribution, and has an advantage in such way that it is able to span the measurement of pore sizes ranging from a few nanometers to several hundred micrometers. Since a specimen has the distribution of pore sizes ranging from sub-nanometer to many millimeters, MIP forms an important tool in the characterisation of pore size distribution and total volume of porosity.

Quantitative microstructural analysis of pores requires proper sample preparation and adequate microscope images. The results of porosity are dependent on high threshold level value. For good results it is necessary to specify reasonable high threshold level. This value is calibrated with another experimental method. Based on the parametric study made on 40 images of cement paste with w/c = 0.5 it was found that described image analysis is capable of assesment of pore volume. The results are highly dependent on high thresholding value that has to be calibrated using a separate experimental technique. Image analysis is suitable for gray images rather than black-white images. Disadvantage of this method is that only a part of pore volume can be identified. The main advantage of image analysis is the identification of pore shapes.

References:

- [1] *From materials science to construction materials engineering - Pore structure and materials properties, Proceedings of the First International RILEM Congress, ed. J. C. Maso*, Chapman and Hall Ltd 1987
- [2] *Microstructure of Cement-Based Systems/ Bonding and interfaces in cementitious materials, Proceedings from symposium in Boston Materials Research Society 1994*
- [3] SOROUSIAN, P. - ELZAFRANEY, M. - NOSSONI, A. *Specimen preparation and image processing and analysis techniques for automated qualification of concrete microcracks and voids* Cement and Concrete Research 2003

This research has been supported by GAČR 103/05/0896 and MSM 684 0770003

Improvement of Application Properties of Gypsum

A.Vimmrová, L. Svoboda

vimmrova@fsv.cvut.cz

Department of Building Materials, Faculty of Civil Engineering, Czech Technical University, Thákurova 7, 166 29 Praha 6, Czech Republic

Gypsum is very old material but in the recent time its importance is growing with the increasing amount of gypsum from flue gas desulphurisation (FDG). The application properties of natural and FDG gypsum are possible to improve by adding of appropriate ingredients. Some possibilities how to improve the consistency, workability and the strength of the gypsum binder were tested. Also the best formulation of the foamed gypsum products (with better value of bulk density and thermal conductivity) was tested. These additives were tested: plasticizers, dispersions and several types of fibres. As foaming agents for preparing of foamed gypsum was used chalk or sodium bicarbonate with some acid components. All the tested additives are available in powder form. The powder form was chosen because it enables to formulate dry gypsum mixtures ready for preparing of gypsum products on the construction site.

First the reduction of water amount in the gypsum mixture by the plasticizers was tested. As plasticizers were chosen Melment F10G, (which is determined particularly for gypsum), Stachement NN, Stachesil and superplasticizer Melflux PP 100F. The flow tests on the slurry of normal consistency (according ČSN 72 2301) were accomplished with the batch recommended by the manufacturers. The results of the tests are shown in the table 1. The biggest influence has the superplasticizer, there is no difference between special gypsum plasticizer and universal one. The plasticizer with higher batching (Stachesil) considerably reduces the flow of the slurry.

Table 1: Diameter of gypsum slurry after flow test in cm

Amount [%] Plasticizer	0 *	0,1	0,2	0,5	0,75	1	1,5	2	2,5	5	10	15
Melment F10G	18,0			27,0		26,5	31,0	31,0	30,7			
Stachement NN				25,3		27,6	28,9	29,6	28,0			
Stachesil										14,0	15,0	12,0
Melflux PP 100F		21,5	27,0	31,0	32,5	34,2						

* mixture of normal consistency

The most efficient additive, Melflux PP 100F was tested in two-phase optimization experiment together with dispersion Vinnapas RI 551 Z. The influence of the combination of dispersion and plasticizer on bending strength and compressive strength was tested. Test pieces in the size 40x40x160 mm were prepared from the gypsum mixture of normal consistency with amount of the dispersion: 0, 1%, 2% from weight of gypsum and with the plasticizer in amounts 0, 0,5 % and 1 %. The results are shown in table 2.

Tab. 2: Bending and compressive strength

Dispersion Plasticizer	Bending strength R_y [Mpa]			Compressive strength R_t [Mpa]		
	0 %	1 %	2 %	0 %	1 %	2 %
0 %	3,10	3,70	3,73	6,11	6,44	6,83
0,5 %	3,47	3,31	3,42	6,63	5,89	6,12
1 %	1,14	1,56	1,44	3,13	3,89	3,30

The higher amount of plasticizer considerably reduces both the bending and the compressive strength. This happens also in the case, that the amount of water is reduced. The addition of dispersion has some improving influence on the strength, but in combination with plasticizer the dispersion is not able to compensate the loss of the strength caused by the plasticizer.

Further the influence of different types of fibres on the strength of the gypsum mixture was tested. The polypropylene, glass and paper fibres were tested. The results of the tests were not so good as was to be expected.

The last part of the experiments was aimed at finding the best suitable composition of the gypsum foamed by the carbon dioxide, originated from chemical reaction between salt of carbonic acid and some stronger acid component. This type of reaction was chosen because all components can exist in powder form and therefore is possible to prefabricate dry mixture for preparing of the foamed gypsum on the construction site.

A wide scale of solid acid components was tested together with chalk (CaCO_3) or sodium bicarbonate (NaHCO_3). The best suitable acid components seem to be tartaric acid and aluminum sulphate. Mixtures with the chalk and one of these components can achieve lightweight products (with bulk density less than 500 kg/m^3) with reasonable strength.

References:

- [1] SCHULZE, W. – TISCHER, W. – ETTTEL, W. – LACH, V.: *Necementové malty a betony* SNTL, 1990 .
- [2] KARNI, J. – KARNI, E.: *Gypsum in construction: origin and properties* Materials and Structures 28, 1995, pp. 92-100.
- [3] COLAK, A.: *Density and strength characteristic of foamed gypsum* Cement & Concrete Composites 22, 2000, pp. 193-200.
- [4] GUSTAW, K. – ROSZCZYNIALSKI, W.: *Gipsy porowate* Cement, wapno, gyps 7, 1977, pp. 181-184.

This research has been supported by CTU0400811.

Strain Energy Density and Crack Rate along the Curved Fatigue Crack Front

T. Denk, V. Oliva, A. Materna

denk@kmat.fjfi.cvut.cz

Department of Materials, Faculty of Nuclear Sciences and Physical Engineering,
Czech Technical University, Trojanova 13, 120 00 Prague 2, Czech Republic

For many years, it is known that loading which varies in time leads to a specific type failure – fatigue. It has been studied intensively right from the beginning. Experiments with real objects and real loading parameters are unacceptably expensive and time consuming. Therefore, many sophisticated methods for studying fatigue have been developed to describe this process and allow for simplification of the experiments while maintaining credibility of the results. These methods include for example a fractographic analysis of fracture surfaces, linear and nonlinear fracture mechanics, or elastic-plastic models based on finite element method (FEM).

Generally, two-dimensional approach has been preferred. Only past few years, mostly due to the progress in computers, it is possible to study the three-dimensional nature of the fatigue crack growth process. In most cases, 3D models are natural extension of 2D ones. On the other hand, 3D model enables us to simulate effects that are present in reality but the 2D model cannot include, such as crack front curvature or shear lips.

This paper will focus on strain energy density along the curved crack front and some of the aspects of energetic models for local crack rate prediction. The presented results are obtained from FEM simulations in MSC Marc. The geometry of the models, material and loading parameters used in the models comply with real experiments performed in VZLU Inc. [1]. In the experiments, CCP specimens (the thickness $B=6\text{mm}$, the width $2W=58\text{mm}$, the length $2L=180\text{mm}$) made of aluminum alloy 2024-T42 were used. The detailed description of the simulations can be found in [2], it can be briefly summarized as follows.

Two test specimens, P2 and P6, with significantly different loading, were chosen for the simulations. The loading parameters ($\Delta S = 31.3\text{MPa}$ and $R = 0.5$ for P2, $\Delta S = 45\text{MPa}$ and $R = 0$ for P6) caused that the formation of the shear lips in the marginal part of the crack fronts began at significantly different crack lengths ($a=11.975\text{mm}$ for P2, $a=6.525\text{mm}$ for P6). For the first pair of simulations, the fatigue crack lengths corresponded exactly to these lengths mentioned above (standard crack). To be able to study the process of energy accumulation as the crack grows, another two simulations were performed for each of the test specimens. These simulations were completely same except for the crack length which was by 2 mm shorter or by 2 mm longer (shorter crack, and longer crack). The shapes of the curved crack fronts were determined from fractographic observation. In order to prevent a distortion of results due to large plastic zone after the first loading cycle and to induce a steady state conditions, the crack growth was simulated with the path $380\mu\text{m}$ long. A rigid surface was inserted into the crack plane (instead of the opposite part of the specimen) to simulate the contact of crack faces during the crack closure. The model assumed small deformations. The finite element mesh was intensively refined in the vicinity of the crack front, where the smallest eight-noded hexagonal elements ($2\times 2\times 2\mu\text{m}$) were situated.

There are many approaches to calculate crack rate. In this paper, the Sih's method [3], which is one of the first 2D energy-based fatigue crack rate prediction methods, is used. If it is extended for 3D and modified for FEM simulations, it can be briefly formulated as follows. Let us consider a material element P perpendicularly before the crack front point F. Let the distance between F and P be Δr . The mean strain energy density at point P in the present

inactive cycle is λ_m , and the increment of λ ($[\lambda]=\text{mJ}/\text{mm}^3$) during this cycle is $\Delta\lambda$. Assuming that λ_m roughly represents the critical accumulated energy and that the energy increments during the following real cycles are roughly constant and equal to $\Delta\lambda$, then the local crack rate at point F can be estimated as

$$v = \frac{\Delta r \cdot \Delta \lambda}{\lambda_c - \lambda_m} \quad (1)$$

Usually, critical strain energy density λ_c is assumed to be a material constant. If this was true, the method would represent a relatively simple and efficient tool for crack rate prediction. The value of λ_c can be measured in low cycle fatigue tests, and for the material 2024-T42 it is $\lambda_c = 970 \text{ mJ}/\text{mm}^3$ [4]. However, the calculated crack rate (for the standard crack) was not in agreement with the experiment and predicted unrealistically high crack rate in the marginal part of the crack front. Therefore, it was decided to reverse the relation (1), and knowing the crack rate, the value of λ_c along the crack front has been calculated. From the middle, where $\lambda_c = 500 \text{ mJ}/\text{mm}^3$, to the margin, it is growing slowly. Approaching the margin, the increase of λ_c is steeper and steeper. On the free surface, it reaches up to $\lambda_c = 4000 \text{ mJ}/\text{mm}^3$.

The change in λ_c with the depth under the free surface could be interpreted as a consequence of growing deformation constraint which can be characterized, for example, by the local value of stress triaxiality h (σ_m/σ_{eff}). Nevertheless, results for specimen P6 show that not even function $\lambda_c = \lambda_c(h)$ is “unchanging” for the given material.

The same procedure has been also applied on the models with shorter and longer crack. The results are qualitatively the same, λ_c changes along the crack front with slow increase in the middle and steep increase in the marginal part. The difference is in a magnitude. The values for the shorter crack in P6 are higher than for the standard crack, the greatest difference is in the marginal part. Similarly, the values for the standard crack are higher than for the longer crack, but the difference is not so significant. It seems that as the crack grows, the λ_c decreases and for very long cracks, it reaches some lower bound limiting curve. This has been supported by the results from the model of specimen P2. The cracks are longer, compared to P6, and they exhibit the same dependence on the depth below free surface. But there is no significant change in λ_c with the crack length.

It seems that not only the magnitude of the accumulated energy is relevant, but generally also the way in which the accumulation takes place.

References:

- [1] BALÁŠOVÁ, M. - BERÁNKOVÁ, I. - PÁNEK, M.: *Fatigue Crack Growth Characteristics in MT Specimens 6mm Wide Made of 2024-T42 Aluminium Alloy. [Research report Z-3669/98.] [in Czech] VZLÚ, Praha - Letňany, 1998, pp.1-43.*
- [2] DENK, T.: *Three-dimensional Fatigue Crack Growth Simulation. [in Czech] ČVUT-FJFI-KMAT, Praha 2003, pp. 1-88.*
- [3] SIH, G. C. – MOYER, E. T. JR.: *Path Dependent Nature of Fatigue Crack Growth. Engng. Fract. Mech. 17 vol. 3 1983 p. 269-280.*
- [4] OLIVA, V. - KUNEŠ, I.: *Modelling of Inherent Barriers against Fatigue Crack Growth. [in Czech] ČVUT-FJFI-KMAT, Praha 1990 str. 5 - 80.*

This research has been supported by MŠMT grant No. MSM 210000021.

FEM Simulation of Plastic Zone in Front of the Fatigue Crack with Shear Lips

A. Materna, V. Oliva, T. Denk

Ales.Materna@fjfi.cvut.cz

CTU, Faculty of Nuclear Sciences and Physical Engineering, Dept. of Materials,
Trojanova 13, 120 00 Praha 2

The authors have recently studied deformation mechanics around the propagating through-thickness planar fatigue crack with straight ([1]) and realistically curved front ([2]). The primary motivation of such FEM computations was an extension of usual two-dimensional fracture mechanics concepts for cracks under loading mode I to three dimensions. A quantitative understanding of three-dimensional effects could improve the methodology for the fatigue crack growth rate prediction in more complicated crack configurations (e.g., surface cracks and through-thickness cracks in parts with complex cross-sectional area). Some attention has also been paid to direct evaluation of the crack growth rate from parameters of the stress and strain field around the crack front. Such approaches based mostly on HRR estimation of the energy dissipated ahead of the crack front have recently appeared more frequently (e.g., [3], [4]).

In this paper, numerical simulation of the cyclic stress-strain field in front of the fatigue crack with shear lips is discussed. The model curved crack front shape is chosen to closely correspond to the crack front obtained experimentally. The model presented represents a new approximation of the real fatigue crack.

3D nonlinear finite element model was created using software MSC.Marc. Contrary to previous simulations with planar cracks, the modelled crack geometry has no symmetry condition in plane of flat growth. Therefore, one quarter of the CCP specimen had to be modelled, and symmetrical constraints were added to simulate the rest of the body.

Because of 3D shape of the crack front, the finite element mesh construction was complicated. The resulting mesh consists of three connected parts A, B, and C. 8-noded hexahedral elements in A were created by expansion of quadrilateral elements along the curved front. The element size varies – the smallest elements $2 \times 2 \times 2 \mu\text{m}$ are situated at the front under the free surface, where large stress and strain gradients were expected. The element size increases towards the centre of the thickness and away from the crack front. The number of elements along the slant and flat part of the front is 11 and 9, respectively. Four-noded tetrahedral elements in the transition part B were produced by automatic generator. The rest of body C is covered by a regular mesh consisting of 8-noded hexahedral elements. Each boundary element from A and C is connected to two boundary elements from B.

The material behaviour was considered as elastic-plastic with kinematic hardening. Small strain formulation was used.

In order to prevent the crack surfaces from penetrating, contact algorithm had to be used. The relative motion of crack surfaces is tracked, and when contact occurs, direct constraints are placed on the motion using boundary conditions – both kinematic constraints on transformed degrees of freedom and nodal forces. Crack advance is realized by the change of contact algorithm parameters: relative motion between unfractured (future) crack surfaces

is not permitted. A prescribed front jump is modelled by enabling relative motion between elements adjacent to the crack plane ahead of the crack front during the so-called active cycles. An “idle” model cycle without crack propagation is inserted between two active cycles. It is reasonable to suppose that the crack front deformation mechanics in the idle cycle will be close to that in the real cycle with very small crack extension. The total prescribed crack extension during 44 applied model load cycles was 0.45 mm. In the simulation presented, no friction of crack surfaces was involved.

Numerical simulation in the shear lips area indicates that the experimentally observed plane of propagation is not given by the maximum tangential stress condition and it is slightly inclined also to the plane of maximum shear stress.

The plastic zone size in crack plane has been determined according to the condition of nonzero equivalent plastic strains. The extensive zone detected along the whole slant crack front is not localized only into the thin surface layer, as in the case of planar crack with curved front ([2]).

The plastic zone size corresponds to the distribution of plastic strain energy density dissipated ahead of the crack front. Both dissipated energy and critical energy to fracture are several times higher for the shear mode than for the tensile mode.

A quantitative characterization of plasticity induced crack closure is essential for an assessment of effective values of stress intensity factors. At this moment, the results achieved provide only a basic qualitative view: no plasticity-induced closure appears in the mid-thickness, whereas the closure is very intensive in the surface layer.

References:

- [1] OLIVA, V. – MATERNA, A.– MICHLÍK, P.: *Three-Dimensional FEM Model of the Fatigue Crack Growth in a Thick CT Specimen*. In: Proceedings of the 3rd International Conference on Materials Structure & Micromechanics of Fracture, Brno University of Technology, 2001, pp. 368–378.
- [2] OLIVA, V. – MATERNA, A. – DENK, T.: *FEM Model of Planar Fatigue Crack with Curved Crack Front*. In: Fractography 2003, IMR SAS Košice, 2003, pp. 26–33.
- [3] SKELTON, R.P. – VILHELMSSEN, T.– WEBSTER, G.A.: *Energy Criteria and Cumulative Damage during Fatigue Crack Growth*. Int. J. Fatigue, 20, 1998, pp. 641–649.
- [4] PANDEY, K.N. – CHAND, S.: *An Energy Based Fatigue Crack Growth Model*. Int. J. Fatigue, 25, 2003, pp. 771–778.

This research has been supported by MŠMT grant No. MSM 210000021.

Project ITER: FEM Simulation of Mechanical Tests of a Primary First Wall Panel Attachment System

V. Oliva, T. Denk, A. Materna

Vladislav.Oliva@fjfi.cvut.cz

CTU, Faculty of Nuclear Sciences and Physical Engineering, Dept. of Materials,
Trojanova 13, 120 00 Praha 2

ITER is an international project to develop fusion energy as the way to a clean and sustainable energy source [1]. The current design is a cost effective tokamak, whose programmatic objective is to provide an integrated demonstration of the scientific and technological feasibility of fusion energy. The blanket-shield system is the innermost part of the ITER reactor, directly exposed to the plasma. Its basic function is to provide the main thermal and nuclear shielding to the vessel and external reactor components.

The Blanket-shield concept is a modular configuration mechanically attached onto the vessel. Three types of modules are required: the baffle modules, the limiter modules and the primary first wall (PFW) modules. The latter consist of a water-cooled austenitic stainless steel shield block and separable PFW panels, mechanically attached onto the shield block. The PFW panels use a copper alloy as a heat sink material bonded to a stainless steel backing plate and beryllium as a protection material to cope with the plasma/wall interactions. The PFW modules are designed to sustain a peak heat flux of 0.5 MW/m^2 , a maximum neutron wall load of 0.8 MW/m^2 and an average neutron fluence of at least 0.3 MWa/m^2 .

A mechanical test programme has been proposed to check the fatigue behaviour and the strength limit of the PFW panel attachment system under loads simulating the mechanical loads occurring during off-normal plasma operations such as disruptions, vertical displacement events or halo currents [2].

For this test programme, the attachment of the ITER PFW panels onto the shield block is considered through the direct rear access bolting. This option consists of PFW panels with one central 5-mm thick poloidal key located at the rear side of the panels. The mechanical function of this key is to bear poloidal and toroidal forces as well as radial moments. It allows also electrical contact of the panel to shield only at a central location minimising therefore the electro-magnetic loads. The panels are attached by means of one row of 10 studs located on the key to minimise the current density going through the studs during electro-magnetic loads.

Test programme includes the performance of five types of tests:

Test No. 1 on blind hole thread - The objective is to check the behaviour of the PFW panel blind hole thread. In particular, the effect of the operation temperature of $200 \text{ }^\circ\text{C}$ on the pre-load of the stud will be investigated as well as the possible relaxation of the stainless steel thread under the required pre-load and temperature. The strength limit of the blind hole thread shall also be assessed.

Test No. 2 on poloidal moment - The objective is to study the fatigue behaviour of the attachment system under cyclic poloidal moments at different pre-tension forces.

Test No. 3 on radial moment - The objective is to study the fatigue behaviour of the attachment system under cyclic radial moments at different pre-tension forces.

Test No. 4 on radial pulling force - The objective is to study the fatigue behaviour of the attachment system under cyclic radial pulling pressure at different pre-tension forces.

Test No. 5 on poloidal force - The objective is to study the fatigue behaviour of the attachment system, in particular of the contact pressure areas, under a poloidal force at different pre-tension forces.

Three participants from the Czech Republic are involved in performing of described mechanical test programme: Design of both the PFW test panel and supporting plate mock-up, which represents shield block, and all FEM computations are realized in the Department of Materials, FNSPE, CTU in Prague. The stainless steel test objects will be fabricated in Vitkovice Steel, a.s. and all mechanical tests will be performed in Skoda Research Ltd.

Originally, the thickness of the supporting plate mock-ups was supposed to be 300 mm. Due to forging limitations in Vitkovice Steel, only 100 mm thick plates could be fabricated. Therefore, some preliminary FEM computations were performed to quantify the change in stiffness of whole attachment system.

Fully 3D mesh consists of approximately 5000 finite elements. Contact between PFW test panel and supporting plate mock-up were considered. The pre-load on the studs for assembling the panel to the support structure is realized by the pre-tension forces and consequent “gluing” of bolt head to the surrounding material. External loadings of the PFW test panels were prescribed according to specifications of Test No. 2 – 4.

The stiffness of the attachment system was judged by the gaps between the panel and the supporting plate, mainly in area of the key. According to results from all simulations, the increase of stiffness by additional bolting the middle of the 100 mm thick supporting plate bottom to the ground is sufficient and, in that case, constrained 100 mm thick plate is a good and cheaper representation of the 300 mm thick plate behaviour.

References:

- [1] <http://www.iter.org/>
- [2] LORENZETTO, P. at al.: *Mechanical Testing of a PFW Panel Attachment System*. Rep. No. EFDA/04-1137, CSU EFDA Garching, 2004, 30 p.

This research has been supported by MŠMT grant No. OK 453.

Structure Changes of Concrete Due to Gamma Radiation

V. Sopko, L. Samek

vit.sopko@fs.cvut.cz

Department of Physics, Faculty of Mechanical Engineering, Czech Technical University,
Technická 4, 166 27, Prague 6, Czech Republic

This project is focused on concrete structure, which are used as a radiation shielding. Many projects are recently dealing with storage of waste radioactive fuel. Many different kinds of material may achieve the desired reduction of radiation if a sufficient thickness is used. Excessive thickness can cause space shortage and also economical difficulties. On the other hand, different types of materials are available such as lead but its durability for high temperatures is not suitable. Water is good shielding material but to keep the tanks at good conditions seems unrealizable and risk from hydrogen created during radiolysis due to gamma radiation also. So concrete is considered to be an excellent and versatile shielding material and is widely used for the shielding of nuclear power plants, particle accelerators, research reactors, laboratory hot cells and other facilities.

It is proposed that main part of shielding should be made from concrete. This concrete applied in radiation shielding should resist for any influence from outside and inside with lowest physical mechanical or chemical changes for a long period. Recent experience with concrete durability show its suitability for intermediate storage shielding.

As known, the radiation neutron and photon flow are mainly problem of shielding. Neutron flow is attenuated by hydrogen atoms, which are part of the concrete shielding as water in cement paste and aggregates such as serpentine. The cement hydrates and so contains different types of water. Water in the concrete can therefore be present in three states: as chemically bonded water in hydrates, water in the gel pores, and water in the capillary pores. The water in each of these states is held with different degrees of firmness: the water in the capillary pores is considered to be free whilst the water in the hydrated compounds is chemically bound water. It is hard to predict the distribution of the water between the states mentioned above, and for convenience the water in concrete is divided into evaporable and non-evaporable water. Non-evaporable water, also referred to as fixed water, is regarded as the water held by the cement paste after drying to constant weight at 105°C. This water consists mainly of chemically bound water in the cement-hydrates is about 24 per cent by weight of the hydrated cement.

On the other hand, gamma radiation is causing problems because of water radiolysis. Measurements of concrete samples irradiated by gamma radiation are showing changes in mechanical properties. The decreasing of strength is not negligible. The changes are induced by gamma radiation and are on chemical basis. Not only radiolysis is the main problem of these changes but also thermal stresses. Above all the radiolysis also changes structure of voids. The voids contain water with soluble compounds and gamma radiation produced radicals, which attack concrete structure. Amount of meso, makro and micro pores decreases about on one third for dose of half megagrey.

Operating temperatures in a nuclear reactor are high, and heat from this source may also be transferred to the concrete radiation shielding. The effect of heat on the water content of concrete is necessary to consider. Elevated temperatures accelerate the diffusion of water in concrete, and for temperatures in range between 40 and 105°C affects evaporable water content. At temperatures exceeding 105°C the amount of non-evaporable water in the concrete decreases.

Yuan [2] also reported that at elevated temperatures and relative vapour pressures exceeding 0,25 the equilibrium moisture content of concrete increased with increasing w/c ratio. Experimental results in Japan also indicated that the ratio of the weight of non-evaporable water to the weight of cement in a cement paste increased as the initial effective w/c ratio increased. It may be suggested from these results that one way of increasing the water content of hardened concrete is to increase the initial w/c ratio. This must, however, be considered in the context of the effects on other concrete properties especially strength.

References:

- [1] KAPLAN, M. F.: *Concrete Radiation Shielding - Nuclear Physics Concrete and Construction*. Logman Scientific & Technical 1989.
- [2] YUAN, R. L.: *The Effect of Temperature on the Drying of Concrete*. Ibid., 1972, pp. 901–1017.
- [3] KARASUDA, S.–HOSHINO, I.: *Dry density of Concrete at Elevated Temperature*. Amer. Concr. Inst. Special Publication SP34, 1972, pp. 931.
- [4] SOPKO, V.–TRTÍK, K.–VODÁK, F.: *Influence of Gamma Radiation on Concrete Strength*. Acta Polytechnica 2004 pp. 57–58

This research has been supported by MŠMT grant No. MSM J04/98:210000018.

The 3D Reconstruction of Fracture Morphology by Means of a Metallographic Microscope

M. Ponec, I. Karovičová, H. Lauschmann

lausch@kmat.fjfi.cvut.cz

Department of Materials, Faculty of Nuclear Sciences and Physical Engineering, Czech Technical University, Trojanova 13, Praha 2, 120 00

The standard imaging technique in fractography is the **scanning electron microscopy** (SEM). It provides large depth-of-focus and high contrast images at a large variability in magnification. However, the relation between the third dimension of fracture surface (depth of the fracture morphology) and the image brightness is complicated, and the real morphology cannot be reconstituted from the image. Although many tasks were solved by using SEM, the real 3D reconstruction of the fracture shape brings much richer fractographic information.

From a 3D model, it is possible to evaluate quantitative fractographic parameters such as surface roughness, profile and height of fatigue striations, the extent of plastic deformation, etc. 3D reconstructions of corresponding regions of both surfaces of a crack enable us to perform volume measurements and to determine critical tip opening displacement (CTOD). A height map can be expressed as a grayscale image, the brightness of which represents the height, and visually interpreted. The fractal dimension and many other characteristics of the fracture surface in 3D can be estimated [1].

The 3D reconstruction of a fracture surface can be obtained by several techniques:

Using **SEM** requires creation of stereo images (stereo pairs). Two images of the same region are taken with a slightly different tilt of the specimen. From these images, an automatic image analysis system generates digital elevation models (DEM) consisting of about 10^4 to 10^5 sampling points [1]. The main problem of the automatic elevations of the DEM is the identification of corresponding points in both images, representing the same point on the specimen (homologue points). The solution procedure is generally called matching. The three-dimensional surface point is represented by a small area in the image - the so-called window. The window of a point to be searched for in the second image is shifted within a certain area, and at each position a correlation measure is calculated. The maximum value of the correlation measure matrix defines the homologue point in the second image. The algorithm is hierarchical; at the first level the image is divided into a small number of rectangles for which initial parallax values are found. At the following levels, these rectangles are subdivided and the procedure is repeated. The height in the DEM is subsequently calculated from the x-parallel axis between two corresponding points, thereby generating a complete 3D reconstruction of the fracture surface.

As for the **laser scanning confocal microscopy** (LSCM), in addition to good resolution and a broad magnification range, confocal imaging can be performed at room temperature and pressure, and does not require a conductive specimen surface. With the confocal microscopy, three-dimensional images are formed by acquiring series of images of the same object at consecutive focal planes. This is achieved by a series of diaphragms that focuses light supplied by a laser onto the sample. The reflected and fluorescent light passes through a point detector which discards rays that are reflected or fluoresced by planes which are not in focus. A three-dimensional representation can be assembled using automated image analysis to reconstruct the shape of the fracture surface from the series of images [3].

Both methods (SEM, LSCM) are connected with expensive equipment. Therefore, we investigate to solve the task by means of a **metallographic microscope** - a modification of an ordinary optical microscope. Its main disadvantage is a small depth-of-focus. In contrast to

LSCM, images of non-planar surfaces contain not only actually focused objects, but also "blurred" contributions of objects from all depths of the surface. Therefore, the reconstruction of specimen surface from a series of equidistantly focused images is much more complicated.

The concept of obtaining depth information by processing a large amount of image data acquired with a small depth of field requires a particular knowledge of the **image formation model**. Contrary to systems for the macroscopic objects, a sequence of image frames of the microscopic object is acquired by moving the object itself (on a translational stage) rather than by changing camera parameters. During the acquisition of the images all camera parameters must remain stationary. In each image frame, objects in the scene will be blurred depending on their distance from the focused plane [4].

Two kinds of information are recovered during the 3D reconstruction. One is the geometric information about the shape of an observed object. The other is textural information of the object's surface.

For an accurate reconstruction of 3D shape and focused image a precise estimation of the **point spread function** of the optical system is crucial. A very complex model based on the electromagnetic wave theory is required because of the aberrations of the optical system. Also the absence of relatively reliable depth maps of testing samples, produced by another method, makes the estimation of the reconstruction error difficult.

The traditional image focus analysis methods are based on **focus measure**. As a typical focus measure, the presence of details is used, expressed for example by the gray level variance, spectral density of high frequencies, etc. It is estimated at each pixel in a small neighborhood around the pixel [2], throughout the sequence of all images. At each pixel, the image frame which has the maximum focus measure among the images in the sequence is found by a search procedure. The gray level of the pixel in this image frame gives the gray level of the focused image for that pixel. The depth is proportional to the index of this image frame.

Further development of a new approach taking advantage of all the data from the sequence of equidistantly focused images for improved reconstruction accuracy is in progress.

References:

- [1] M. TANAKA, Y. KIMURA, L. CHOUANINE, J. TAGUCHI, R. KATO: *Quantitative Analysis of Three-dimensional Fatigue Fracture Surface Reconstructed by Stereo Matching Method*. ISIJ International, 43, NO.9, 2003, pp.1453-1460.
- [2] M. TUMA: *The spacial reconstruction of a fracture surface morphology based on imaging by a metallographic microscope*. [Master thesis.] FNSPE CTU Prague, Dept. of Materials, 2000, 53 p.
- [3] K.E. KURTIS, N. H. EL-ASHKAR, C. L. COLLINS, N. N. NAIK: *Examining Cement-based Materiale by Laser Scanning Confocal Microscopy*. Cement & Concrete Composites 25, 2003, pp.695-701.
- [4] K.S. NAYAR, Y. NAKAGAWA: *Shape from Focus*. IEEE Transactions on Pattern Analysis and Machine Intelligence, Vol. 16, No. 8, 1994, pp. 824-831.

This research has been supported by the Ministry of Education of the Czech Republic, research project No. Cez:J04/98:210000021, "Diagnostics of Materials".

Texture Analysis of poly(Vinyl Chloride) Foils

L. Kalvoda, M. Dlouhá, P. Sedlák, S. Vratislav

ladislav.kalvoda@tiscali.cz

Department of Solid State Engineering, Faculty of Nuclear Science and Physical Engineering, Czech Technical University, Trojanova 13, 120 00 Prague 2

Poly(vinyl chloride) (PVC), together with polyethylene and polypropylene, is one of the most widely produced technical polymers today. It is used in a broad range of applications, for instance in automotive industries, fabrication of electrical accessories, civil engineering, and medicine. Thus, the material properties of the resulting products and their relation to the composition of the raw material, fabrication procedure, and resulting microstructure are becoming increasingly important, and are subjected to the extensive research.

Despite of a common long-lasting effort in investigation of PVC microstructure, serious questions remain still opened concerning the micro-arrangement and orientation of polymer chains, as related to the applied deformation and thermal treatment. The reason lies undoubtedly in the high complexity of the PVC material itself. To achieve deeper understanding of its morphology, it has to be considered at three levels at least: molecular level, level of nano- and micro-aggregates, and, finally, at level of macro-particles. Similarly complex is also the type of PVC chain packing, varying from a purely amorphous state to a crystalline one. The later usually amounts about 10% (wt.), but influences strongly on properties and processibility of PVC. Experimental data collected so far have supported the supposition that there are two types of crystalline domains which can be populated under usual PVC processing conditions (180° C, presence of plasticizer in the mixture) stimulating a PVC gel phase formation: fringed micelles with polymer chains oriented along a main stretching direction (SD) possessing a well developed three dimensional order ("c-orientation" of PVC chains), and lamellar platelets with the crystalline axes a along the SD ordered over long distance in one or two dimensions only ("a-orientation"). It is commonly accepted that the crystallites with the a-orientation are grown from the amorphous phase during the gel stretching process rather than coming in existence by re-orientation of the c-oriented crystallites. The low percentage of syndiotactic sequences typically present in a commercial PVC further stimulates the elastic gel formation. The contingent gel phase can be oriented during the subsequent processing performed at lower temperatures (usually ca. 70 – 100°C). Thus, existence of the two types of crystalline domains can be expected in volume of the drawn sheets produced from a standard commercial material.

The presented research has been focused on further elucidation of PVC microstructural order, mainly using advantages of neutron radiation. The wide angle neutron diffraction (WAND) data were complemented by optical birefringence (OB) measurements providing information about an average orientation of all polymer chains. More detailed overview of the obtained results have been published elsewhere [1]. Very recently, we have also recorded wide angle X-ray diffraction (WAXD) patterns, and compared them with the WAND results. Evaluation of the later experiments is still in progress and will be reported later.

The PVC sheets used in our investigations were stretched uniaxially (at constant width), equally biaxially, and unequally biaxially. The planar strain ratio (ϵ_d) was in the range 2.0 ÷ 4.84. Small samples of the foils (oblong shape, 10 x 20 mm) with different deformation ratios 2.0 x 1.0, 2.0 x 1.4, 2.4 x 1.4, 1.7 x 1.7, and 2.2 x 2.2 were at first examined by OB

measurements. The three samples possessing a superior optical anisotropy (2.4 x 1.4, 1.7 x 1.7, and 2.2 x 2.2) were selected for the subsequent WAND and WAXD measurements. Texture of crystalline domains was analyzed in relation to the following principal directions: SD, the transversal direction (TD), and the sheet normal direction (ND).

The setup for in-plane OB measurements consisted of He-Ne laser, polarizing optics, light intensity detection system, and goniometer with the sample holder. For every sample, two parameters were obtained: $c\Gamma$ characterizing a level of the in-plane anisotropy, and α_0 providing an angular declination of the optical indicatrix from SD in plane of the tested sample. WAND experiments were performed on the neutron spectrometer KSN-2 installed at the horizontal channel HK-2 of the experimental nuclear reactor LVR-15 situated in Institute of Nuclear Research in Řež. The diffraction patterns (neutron wavelength $\lambda = 0.1362$ nm) were scanned in the 2θ -range $5^\circ - 40^\circ$. Stacks of the sample foils with the total thickness 2 – 3 mm were used in place of specimens, and examined both in symmetrical transmission and symmetrical reflection position. WAXD diffraction patterns (CoK α radiation, Bragg-Brentano geometry) were collected in the 2θ -range $5^\circ - 40^\circ$.

Non-zero in-plane optical anisotropy was observed for the samples with $\varepsilon_A \geq 2.8$. It was ascending with the ε_A -value, irrespective of the type of sample stretching. It is known that the anisotropy can be correlated with the type of in-plane polymer chains orientation: a higher value corresponds to a larger fraction of in-plane aligned polymer chains. The average direction of chains (characterized by the α_0 -value) was observed to be increasingly declined from the SD with the ε_A rising up. The maximal deviation was obtained for the 2.2 x 2.2 sheet: $\alpha_0 = 25^\circ$. The result is compatible with the idea of the drawing-induced genesis of the a-oriented phase, but it is rather contradictory to the planar uniformity expected for equally biaxially stretched foils. Thus, further research is necessary to elucidate the effect in detail.

The obtained WAND patterns did not allow for determination of standard inverted pole figures (IPFs). Therefore, “cumulative” IPFs were calculated, the integration running over two distinct 2θ -regions expected to contain (010), (200), (110), and (201), (111), (211) PVC reflections, respectively. The obtained IPFs were compatible with the dominant orientation of polymer chains in the stretching plane of the sheets for all investigated samples, in agreement with our previously reported results [2]. The tendency was more pronounced for the equally biaxially stretched samples. An unusually strong and sharp (200) reflection ($d = 0.522$ nm) was observed in diffraction patterns of the equally biaxially stretched samples, recorded in the symmetrical reflection position, and in the transmission setting with the TD oriented along the scattering vector. The remarkably low half-width of the (200) reflection suggested that the coherence length of corresponding crystalline domains has to exceed 50 - 100 nm along the scattering direction. The lamellar platelets might be considered in this regard. Preliminary measurements also showed that the (200) pole angular distribution is very narrow in the SD-ND plane, providing evidence about a high orientation uniformity of the diffracting structure. The measurements of complete (200) pole figures are recently in progress.

References:

- [1] KALVODA, L. – DLOUHÁ, M. – VRATISLAV, S. – LUKÁŠ, R. – GILBERT, M. *Texture analysis of poly(vinyl chloride) foils*, Solid State Phenomena, 2005, in press.
- [2] KALVODA, L. – DLOUHÁ, M. – VRATISLAV, S. *Neutronographic texture analysis of polymer foils*, Proceedings of CTU Workshop, 2004, pp.562 – 563.

This research has been kindly supported by grants GA 202/03/0981 and MSM210000021.

Novel Sensors of Alkali Metal Ions Based on Optical Fibers

R. Klepáček, L. Kalvoda

rudolf.klepacek@seznam.cz

Department of Solid State Engineering, Faculty of Nuclear Science and Physical Engineering, Czech Technical University, Trojanova 13, 120 00 Prague 2

Detection of various chemical substances in variety of environs belongs to the contemporary priorities. It starts with sensing of noxious agents in drinking water, and ends with analysis of human blood. Together with the broad range of detection targets, there is also plenty of sensing methods and physical principles applied in praxis. One of the sensing groups, promising from the point of its applicability and fabrication expenses, is constituted of the sensors (chemical, physical, biological, biochemical) based on utilization of optical fibers. Chemical fiber optic sensors of alkali ions in water environ have also been in focus of the presented research.

In fiber optic chemical sensors, it is the optical fiber that mediates the conversion of a monitored chemical concentration onto the output information. Light propagates through the fiber and creates an electromagnetic field with the intensity highest in the fiber core and exponentially decaying into the fiber coat. The so-called evanescent field, influenced by the coat material, facilitates the desired contact between the transmitted light beam and the surrounding environ.

Very often, principal of fiber optic sensors is based on measuring radiation intensity transmitted through the system and integrated over a selected wavelength window (λ_1, λ_2). The target analyte permeates into the coat matrix causing fiducial changes of some (spectrally-dependent) material property, such as fluorescence, light absorption, refractive index, or turbidity. So, one of the crucial parts of a sensor design has to be devoted to creation of a coat, permeable enough for the target analyte, and accommodating a suitable reagent showing a desired reaction with the later. In our system under development, we decided to use spectral variations of optical absorption as the 'sensing' quantity. Such sensor operation then depends on spectral changes of specific absorbency of the fiber coat (A) in presence of the target analyte (M): $A(\lambda) + M \rightarrow A'(\lambda)$. Described on a molecular level, the chosen reagent moieties chemically react with the target analyte causing changes of the evanescent field absorption in the fiber coat, and hereby modifying also the light flux in the core. The spectral distribution of the guided light intensity is evaluated and compared with a calibration curve relating the later with the analyte concentration data. Thus, the target analyte concentration in the investigated environ can be determined.

The above described scheme was adopted as the core of our system intended for detection of alkali metal ions ($M^+ = Na^+, K^+, Ca^{2+}, Mg^{2+}$) in water environs. A tetra(ethyl acetate) calix[4]arene kindly supplied by Dr. P. Lhoták from ICT Prague was chosen in place of an ion-selective reagent (ionophore) forming chemical complexes with the alkali ions. For the later showing negligible absorption in the VIS/NIR spectral range, the system design had to be further eked out with a lipophilic chromophore. The later reacts on variations of the proton concentration inside the sensing fiber coat (caused by the $M^+ \leftrightarrow H^+$ exchange occurring on the coating/water interface) by a distinct change of optical absorbency in VIS range. Application of such combination of an ionophore with a lipophilic chromophore in an optical sensing system was once before suggested in [1, 2].

The first step in testing the proposed scheme was focused on evaluation of the chemical reaction of the chosen ionophore with the target alkali ions, especially on its

selectivity and pH-dependence (detailed overview is given in [3]). The fiber coating containing the ionophore was simulated by a lipophilic organic solution of the ionophore (a liquid membrane). An extraction rate of the target ions from an aqueous to the organic phase (hexane was chosen in our case) was quantified by specific electrical conductivity measurements (a standard Pt-probe attached to the conductometer Radelkis OK104), and pH measurements (a standard combined glass/AgCl electrode) of the water solution. The solutions were filled in an inert plastic cell, bottom of which formed a movable piston allowing changes of the water/hexane interface level. The cell was kept under nitrogen atmosphere to prevent an undesirable dissolution of aerial carbide dioxide in the aqueous phase.

The obtained results can be summarized as follows. Two groups of solutions, hydroxides and chlorides, were used in the tests. In case of the hydroxide solutions, an expected decrease of the electrical conductivity (due to the alkali ion's extraction into the organic phase) was accompanied by a decrease of the pH-value, and traces of ethanol were detected in the resulting aqueous solutions. It led us to the conclusion that a basic hydrolysis of the ionophore side groups is taking place, reaction scheme of which could be very likely such as: $-COOEt + OH^- + M^+ \rightarrow -COOM + EtOH$. Stability constant (K) (defined as a product of the concentrations of the species entering the reaction divided by the concentration of the reaction product) of the later reaction was calculated from the conductivity data for all the alkali ions under examination: $K_{Na^+} = 7.3 \times 10^{-7}$, $K_{K^+} = 6.5 \times 10^{-8}$, $K_{Ca^{2+}} = 1.6 \times 10^{-5}$, $K_{Mg^{2+}}$: no measurable reaction. Thus, the highest selectivity towards the target ion ($\sim 1/K$) was obtained for the potassium ions.

No measurable change of the specific conductivity was observed in case of the chloride solutions. On the other hand, pH of all the solutions was growing during the contact with the ionophore solution, reaching a level of saturation after several hours. An acidic hydrolysis process, summarized as: $-COOEt + H^+ + OH^- + Cl^- \rightarrow -COOH + EtCl + OH^-$ might be compatible with the observed behavior.

In future, our effort will be focused on selection, preparation and tests of ionophores or chromo-ionophores with a higher chemical stability, showing a well-defined, selective complex formation in both the slightly acidic and basic water environs. The promising candidate groups includes other calix[n]arene derivatives, crown ethers, and calix[4]arencrowns.

References:

- [1] O'NEIL, S. – CONWAY, S. – TWELLMAYER, J. – EGAN, O. - NOLAN, K. – DIAMOND, D., *Ion selective optode membranes*, Analytica Chimica Acta 398, 1999, pp. 1-11.
- [2] MORF, W.E. – SEILER, K. – RUSTERHOLTZ, B. – SIMON, W., *Design of calcium-selective optode membrane based on neutral ionophores*, Anal. Chem. 62, 1990, pp. 738–742.
- [3] KLEPÁČEK, R., *Spektroskopická studie ovlivnění interakcí vybraných kovových ionů s vhodnými reagenty a polymerickými membránami v roztocích*, Diploma theses, FNSPE CTU Prague, 2004.

Quantitative Texture Analysis of Grain-Oriented Steel Sheets

Stanislav Vratislav*, Maja Dlouhá*, Ladislav Kalvoda* and A. Grišin*

stanislav.vratislav@fjfi.cvut.cz

*Faculty of Nuclear Sciences and Physical Engineering, CTU in Prague, Brehova 7, 115 19 Prague 1, Czech Republic

In a number of countries the neutron diffraction method is used on a large scale in solid-state physics and metallurgy research. In many others the construction of research reactors is making such research possible. Less well known is the possibility of applying neutron diffraction to structure studies in polycrystalline materials. At present rapid advances in technology are making such investigations more and more useful. It is rather obvious that the properties of polycrystalline materials depend on their structure. The grain orientation distribution – texture – gives important information about this structure and influences the properties of materials. For example, texture influences both the behavior of polycrystalline materials during thermal or mechanical treatment and the anisotropy of various physical properties in technical materials. Consequently, there are several areas in physics and metallurgy, of which nuclear technology (investigations of fuel elements and fuel tubes) is an important example, where texture studies should be performed.

Our laboratory developed and tested experimental and calculation techniques for quantitative texture analysis based on the ODF (orientation distribution function) combined with the diffraction of thermal neutrons. The texture experiments were carried out on the KSN-2 diffractometer using the TG-1 texture goniometer [1]. The monochromatic wavelength was 0.1023 nm and single-crystal Zn(002) was used like monochromator. The experimental data were measured by means of the TG-1 goniometer in transmission or reflection arrangement and pole figures were determined. The measured data are corrected for absorption, irradiated volume, and they are normalised. The experimental data processed in this manner are used to calculate the coefficients of expansion to express the measured direct pole figures using spherical functions. The determined pole figures are used to calculate the coefficients of expansion $C_l^{\mu\nu}$ for expanding the ODF function into a number of generalised spherical functions. The ODF leaves the program package in the form of sections through the Euler space either for φ_1 or $\varphi_2 = \text{const}$ (in 5° steps) and ODF's can also be depicted graphically in the individual sections. All texture characteristics can be obtained from these TODFND-codes [1,2,3]: pole figures, inverse pole figures, ODF ($f(g)$) values in the 5° steps), parameters of the ideal orientations (HKL) $\langle uvw \rangle$, texture index J , volume fraction coefficient f , fiber texture distribution. The distribution of crystal orientation, or texture, in polycrystalline materials is calculated and displayed by a wide variety of graphic formats for comparison with published results.

Silicon steel belongs among the most important soft magnetic materials in use today. Applications vary in quantities from the few ounces used in small relays or pulse transformers to tons used in generators, motors, and transformers. Continued growth in electrical power generation has required development of better steels to decrease wasteful dissipation of energy in electrical apparatus and to minimise the physical dimensions of the increasingly powerful equipment now demanded. During the last ten years a lot of research has been carried out world wide to gain a better insight the magnetic behaviour of electrical steels (silicon steel sheets containing 3% of silicon) used in rotating electrical machines and transformers. One of the main task in this field of research is directed to investigate the

relation between microstructural properties and the final magnetic properties. It means, that actual research field concerns the study of the relation between the macroscopic electromagnetic behaviour and the microstructural properties, like grain size and texture.

We have examined over 25 specimens, which were prepared by the Sheet Rolling plant. The complete quantitative texture analysis was performed on the mentioned different silicon steel samples [4] and the dependence of the final texture (texture form, level of the $f(g)$ values) on the different processing stages (the I. and II. cold rolling) was obtained. As the list of our results is very large the selected texture characteristics of only four specimens (with the processing stages listen in Tab.1 are given. Pole figures were measured for (110), (200) and (211) reflections of Fe-3%Si steel sheets and the ODF function was determined. Results are given in Tab. 1.

Table 1: Characteristic parameters of the investigated Fe-3%Si samples

Sample	T_{IV} [°C]	T_{IIV} [°C]	$f(g)$ (011)<100>	J	f [%]	Z_p [W/kg]	B [T]
1	20	20	48.2	3 9	36.5	1.450	1.73 9
2	200	20	34.2	2 3	29.2	1.570	1.70 3
3	20	200	21.5	1 6	27.4	1.760	1.66 3
4	200	200	13.3	1 4	24.1	1.830	1.64 6

Remarks: T_{IV} [°C] – temperature of the I. cold rolling, T_{IIV} [°C] – temperature of the II. cold rolling, $f(g)$ – ODF's values; (HKL) <uvw> – ideal orientation, J - texture index, f [%] – volume fraction, Z_p [W/kg] – power losses; B [T] – magnetization

It appears, that the best texture form and $f(g)$ values were obtained at $T_{IV} = T_{IIV} = 20$ °C, i.e. for sample 1 (power losses Z_p are lowest and B is highest). In this treatment we have determined very sharp and narrow form of the $f(g)$ peak values. If the temperatures are going up to 200 °C, the texture values are going down and the texture peak half-width is more wider. These conclusion are confirmed simultaneously by the distribution of the power losses in the rolling plane.

Neutron diffraction is a very powerful and suitable tool for microstructure and texture characterisation of these oriented silicon steel sheets and generally grain-oriented materials.

References:

- [1] S. VRATISLAV, M. DLOUHÁ, J. JEŘÁBEK: *Jaderná energie*, 29, 1983, pp. č. 316-321.
- [2] M. DLOUHÁ, S. VRATISLAV, M. MERTA: *In: Proc. of the CTU WORKSHOP* vol. 3, Prague, 1993, pp. č. 207-208.
- [3] S. VRATISLAV, M. DLOUHÁ: *In: Proc. of the Int. Conf. Mathematical Methods of Texture Analysis* Dubna, Russia, 1995, pp. 49-50.
- [4] S. VRATISLAV, M. DLOUHÁ, L. KALVODA: *Neutron Diffraction Texture Analysis of Oriented Sheets* LETAM-ISGMP, Université de Metz, Ile du Saulcy, F-57045 Metz Cedex 01, 2004, pp. 209-210.

This research has been supported by MŠMT grant No. MSM210000021 and by GA ČR grant No. GA 202/03/0981.

Chemisorbed Zeolitic Catalysts Studied by Powder Neutron Diffraction and ^{13}C MAS NMR

S. Vratislav*, M. Dlouhá*, A. Chichev*, A. Balagurov**, V. Bosáček***

stanislav.vratislav@fjfi.cvut.cz

*Department of Solid State Engineering, Faculty of Nuclear Sciences and Physical Engineering, Czech Technical University, Břehová 7, 115 19 Prague 1, Czech Republic

**Joint Institute of Nuclear Research, Dubna, Russia

***J. Heyrovský Institute of Physical Chemistry, 182 23 Prague 8, Czech Republic

Zeolites and related microporous materials have common and diverse applications. They are used as catalysts to produce gasoline and pharmaceuticals. For medical and industrial purposes, they are employed to separate N_2 , O_2 and other gases. Formulated in household detergents, they remove the calcium ions that make water „hard“. Zeolites also sequester radioactive ions for environmental remediation. Many new applications, in areas such as batteries and fuel cells, are being investigated. Knowledge of structures has been quite important for developing new materials, as well as for tailoring properties of existing materials. Neutron powder diffraction is very valuable for this work, since single crystals are rarely available and because understanding the sitting of light atoms is paramount.

Experimental results [1] as well as theoretical investigations [2] showed that chemical properties of protons are controlled by actual basicity of the lattice oxygen atoms and by the character of bonds where protons are attached. Experimental support was obtained also from the results of diffraction methods, where namely neutron diffraction provided direct evidence on the location of protons in faujasites with various H^+/Na^+ ratio [2]. The aim of our study was to estimate the location of chemisorbed species in the lattice and to elucidate the role and participation of various lattice oxygen types in chemisorption of methyl cations. We have made an attempt to estimate regular distribution of cations and chemisorbed species over the lattice and to locate chemisorbed CH_3^+ ions at different oxygen atoms.

The investigations of the zeolitic catalysts in the Laboratory of neutron diffraction FNSPE CTU led to determinate the structural parameters of the basic faujasite framework together with the location of chemisorbed species and the distribution of sodium cations after chemisorption. Suitable crystalline powders of NaY, NaX and NaLSX with high content of sodium cations and with low content of defects and decationation were used in this study. Neutron powder diffraction patterns were collected at temperature of 298 and 7 K on the KSN-2 diffractometer, which is placed at the LVR-15 research reactor in Řež near Prague. This device was equipped with close circuit liquid helium cryostat - type CP-62-ST/5 (Cryophysics SA). The wavelength of 0.1362 nm was used and the resolution $\delta d/d=0.00075$ was achieved (d is the interplanar spacing). The complete structural parameters were determined by Rietveld analysis of powder neutron diffraction data using the GSAS software package including the Fourier maps. The reaction of methyl iodide with sodium cations was used for the preparation of anchored methyl groups in the structure of zeolites. ^{13}C MAS NMR spectra were measured on a BRUKER DSX200 spectrometer. Experimental evidence of the created chemisorbed methyl groups after reaction of methyl iodide with Na^+ cations of the zeolite was obtained from ^{13}C MAS NMR spectra as described earlier [1]. This method allowed to control the conversion of methyl iodide to surface methoxy species on a quantitative level.

Our results obtained by powder neutron diffraction and ^{13}C MAS NMR can be summarized in this way:

-Chemisorbed methylum ions are located in the Y type faujasites structure at the lattice oxygen O_I as bridging-type methoxy group characterized by the ^{13}C MAS NMR signal at 56.5 ppm. For the sodium ions, the S_I sites in the hexagonal prism and the S_{I'} sites in the sodalite cage are both partially occupied with occupation factors of ca. 0.14 and 0.57 respectively, whereas the S_{II} site in the supercage is full. The T(Al, Si) positions and oxygen positions O(1)-O(4) are fully occupied. An agreement factors on integrated intensities $R_{\text{wp}} = 6.92\%$ and $R_p = 5.14\%$ were obtained. The space group is Fd3m with a lattice parameter $a = 2.4851(7)$ nm [3].

-Methylum ions are located in X faujasite at O₄ and O₁ lattice oxygen atoms only in α -supercavity. Although the location at two different sites corresponds well with two observed ^{13}C MAS NMR signals at 54 and 58 ppm of surface bridging methoxyls, the existence of the signal at 58 ppm cannot be explained unequivocally. Rietveld analysis of the neutron diffraction data of NaX samples led to the complete set of the structural parameters for both the origin NaX sample and that with chemisorbed methyl species [3,4]. The structural analysis was treated in frame of Fd3 space group with $a = 2.4976(7)$ nm, $R_{\text{wp}} = 0.0516$, $R_p = 0.0468$ (origin NaX sample) and with $a = 2.4895(6)$ nm, $R_{\text{wp}} = 0.0523$, $R_w = 0.0487$ (chemisorbed NaX sample). For chemisorbed NaX sample we have determined the occupation numbers of cations and the location of CD₃ groups with the center in the position 96g (0.387, 0.387, 0.119). The occupation numbers of Na cations in chemisorbed NaX were decreased for S_{I'} and S_{I''} and increased for S_{III} in comparison with the initial NaX. S_{II} is practically fully occupied in both cases. We observed serious changes in the structural arrangement of the Na⁺ cations after chemisorption (not only in occupation factors but sometimes also in coordinates).

-Parameters of NaLSX given in [4] were refined in both recently discussed space groups, as in Fd3 space group as in Fddd (orthorhombic) group but without any significant difference. Cations are distributed over six possible sites in the frame of Fd3 space group. For NaLSX we observed in addition another effect resulting from the influence of chemisorbed species on the geometry. This effect was associated with some distortion of cubooctahedra caused probably by chemisorbed species together with associated cation displacement.

References:

- [1] Z. JIRÁK, S. VRATISLAV, V. BOSÁČEK: J.Phys. Chem. Solids 41, 1980, pp. 1098-95.
- [2] W.J. MORTIER, J.SAUER, J.A. LERCHER, H. NOLLER: J.Phys. Chem. 88, 1984, pp. 905-910.
- [3] S. VRATISLAV, M. DLOUHÁ, V. BOSÁČEK: Physica B 276-278, 2000, pp. 29-31
- [4] S. VRATISLAV, M. DLOUHÁ, V. BOSÁČEK: Applied Physics A 74, 2002, pp. 1320-21

This research has been supported by GA ČR grant No. GA 202/03/0981 and by MŠMT grant No. MSM210000021.

Hygric and Thermal Properties of a Cracked High Performance Concrete

E. Mňahončáková*, M. Jiříčková**, R. Černý**

mňahoncakovaeva@fsv.cvut.cz

*Department of Physics, Faculty of Civil Engineering, Czech Technical University, Thákurova 7, 166 29 Praha 6, Czech Republic

**Department of Structural Mechanics, Faculty of Civil Engineering, Czech Technical University, Thákurova 7, 166 29 Praha 6, Czech Republic

Nowadays, concrete belongs to the most extensively used materials in construction industry. Requirements on increasing load or on reduction of the construction thickness become highly actual. In particular, extension of concrete durability lies in focus of interest. Principal aim of this paper is to analyze basic hygric and thermal properties of cracked high-performance concrete. The obtained data can be applied as input parameters for computer simulations aimed to the prediction of concrete service life.

The high performance concrete of two basic compositions C90/105 and C60/75, marked as BI and BII, respectively, was chosen as a basic tested material. The first one, BI, was composed of cement CEM I 52.5 R, silica fume suspension, aggregate of 0-16 mm granulity, accelerant Lentan VZ33, larry Woerment FM794, and water of given proportion. The second one, BII, had the same composition as BI except for the silica fume suspension. To analyse the effect of aggregates on heat and moisture transport parameters, the cement pastes marked as PI and PII, and concretes without the aggregates of 8-16 mm granulity marked as BBI and BBII, were also studied. The measured samples were loaded by temperature of 600°C to get cracked concrete samples. Temperature loading was provided using the furnace BVD 100/KY. At first specimens were heated with temperature increase rate of 10°C/min until the final temperature was achieved. Then, it followed the loading period of 120 minutes and then the samples were slowly cooled down.

The experiments for measuring hygric and thermal parameters were carried out at 25±2°C in laboratory conditions (relative humidity about 30-35%); another set of measurements was done with the various values of relative humidity. The sample sizes depended on the laboratory test type. The initial state for all the measurements was dry material.

Hygrothermal behaviour of building materials is described by thermal and hygric properties. Among the thermal properties, the most important are thermal conductivity λ [$W m^{-1} K^{-1}$], thermal diffusivity a [$m^2 s^{-1}$], and specific heat capacity c [$J kg^{-1} K^{-1}$]. They were measured by the commercial device ISOMET 2104 (Applied Precision). The measuring method is based on an analysis of the temperature response of the analyzed material to heat flow impulses. The dimension of the specimens for determination of thermal parameters was 71 x 71 x 50 mm.

One of the common hygric material properties is water vapour diffusion resistance factor μ [-], basically measured according to the standard ČSN 72 7031 [1]. In the measurements was employed the standard cup method (dry and wet). In the first one the sealed cup containing silica gel (5% relative humidity) was placed in a controlled climatic chamber with 50% relative humidity and weighed periodically. In the second one the cup containing water was placed in an environment with the temperature about 25°C and relative humidity about 50%. The measurements were done in a period of two weeks. The steady state

values of mass gain or mass loss determined by linear regression for the last five readings were used for the determination of water vapor transfer properties.

The simplest way, how to describe liquid water transport through a porous material, can be by way of water suction experiment. The water sorptivity was measured using a standard experimental setup. The specimen was water and vapor-proof insulated on four edges and the face side was immersed 1-2 mm in the water, constant water level in tank was achieved by a Mariott's bottle with two capillary tubes. One of them, inside diameter 2 mm, was ducked under the water level, second one, inside diameter 5 mm, was above water level. The automatic balance allowed recording the increase of mass. The known water flux into the specimen during the suction process can be employed to the determination of apparent moisture diffusivity [2]. The water absorption coefficient, A , is calculated from the linear part of the dependence of the increase of tested sample's mass [$kg\ m^{-2}$] on the square root of time [$s^{1/2}$]. Then moisture diffusivity κ [m^2/s] can be calculated from the vacuum saturation moisture content and water absorption coefficient according a simple equation [3].

The results of measurements of both thermal and hygric properties of cracked high performance concrete in Table 1 show the effect of aggregate presence and aggregate size but the influence of silica fume suspension was not found to be very significant.

Table 1 Basic thermal and hygric properties of cracked high-performance concrete

Type of cracked concrete	μ		κ [$m^2\ s^{-1}$]	λ [$W\ m^{-1}\ K^{-1}$]
	[-]			
	97-25%	5-97%		
BI	15.82	15.35	9.174E-08	1.133
BII	10.40	13.24	1.137E-07	1.433
BBI	13.78	12.25	2.472E-07	1.593
BBII	11.03	10.63	1.970E-07	1.350
PI	10.24	7.24	5.458E-07	0.510
PII	17.45	10.81	1.995E-07	0.414

References:

- [1] ČSN 72 7031: *Měření součinitele difúze vodní páry stavebních materiálů metodou bez teplotního spádu*. ÚNM Praha, 1974, pp. 1-7.
- [2] DRCHALOVÁ, J., ČERNÝ, R.: *Moisture Diffusivity of High Performance Concrete*. Acta Polytechnica, 39(1999), pp. 39-45.
- [3] KUMARAN, M. K.: *Report on Measurements to Determine Moisture Diffusivity of Eastern White Pine*. IEA Annex XXIV Report T3-CA-92/04, 1994.

This research has been supported by the GA ČR project No.103/03/1350.

Microstructure and Mechanical Properties of the Accumulative Roll Bonded AA 8006 Alloy

P. Homola, M. Karlík a M. Slámová*

Miroslav.Karlik@fjfi.cvut.cz

Czech Technical University, Faculty of Nuclear Sciences and Physical Engineering,
Department of Materials, Trojanova 13, 120 00 Praha 2

* Research Institute for Metals, Panenské Břežany 50, 250 70 Odolena Voda

Accumulative Roll Bonding (ARB) enables the production of large amounts of ultra-fine grained (UFG) sheets with improved strength and is thus a promising method for industrial applications. The process involves repetitions of surface processing, stacking, rolling to 50% reduction, and cutting. The rolling bonds the sheets and after 6 to 8 cycles, UFG materials with high strength and good ductility are produced.

ARB has been successfully used to prepare UFG sheets from different ingot cast aluminium alloys [1]. Alloys issued from continuous twin-roll casting (TRC) exhibit finer second phase dispersion and smaller grains than ingot cast alloys [2]. They are thus regarded as good starting materials for ARB and they are expected to have thermally stable UFG structures. TRC AlFeMn sheets were successfully AR-bonded up to the 5th cycle at 200 °C and up to the 6th cycle at higher temperatures (250, 300, 350 °C). The effect of rolling temperature on the quality of roll bonding, grain refinement, and hardness was studied.

Twin-roll cast homogenised and cold rolled sheets of 2.0 mm thickness of a commercial aluminium alloy AA8006 (supplied by Al INVEST Břidličná, a.s., Czech Republic) were used in the experiments. Its chemical composition is in the following table (wt.%):

<i>Fe</i>	<i>Mn</i>	<i>Si</i>	<i>Cu</i>	<i>Mg</i>	<i>Zn</i>	<i>Ti</i>	<i>Al</i>
1.51	0.40	0.16	0.006	0.003	0.012	0.014	Balance

Recrystallized material was prepared by annealing for 0.5h at 450 °C. ARB processing consisted in the repetition of 5 steps: 1) surface degreasing in tetrachlorethylene and wire-brushing with 0.3 mm steel wire brush; 2) stacking of two pieces of 300 x 50 x 2 mm; 3) pieces joining by Al wires; 4) heating in an electrical furnace to 200, 250, 300 and 350 °C; 5) bonding by rolling without lubricant to 50% reduction in thickness. Roll diameter of 340 mm and peripheral speed of 0.7 m/min were applied in all cases. In order to prevent the propagation of edge cracks, specimen edges were trimmed and smoothed down after each cycle.

The initial and deformed microstructure was examined using light microscopy (LM) and transmission electron microscopy (TEM). LM observations were carried out in the plane normal to the long transverse direction (TD-plane) on samples oxidised in Barker's solution by electrolytic etching. TEM foils 3 mm in diameter were prepared in the rolling plane by twin-jet polishing (-30°C, 30 V) using 6% solution of HClO₄ in methanol.

Vickers hardness HV10 measurements on sheet surface and tensile tests were used for evaluating the strength of processed materials. Tensile test specimens were machined in direction (TD) perpendicular to the rolling direction. The gauge length and gauge width were 20 mm and 8 mm, respectively. The crosshead speed was 1 mm/min.

After initial failures to achieve good roll bonding, five successful ARB cycles were performed at 200 °C. The results of those experiments are reported in [3] and are compared with the results of ARB processing at higher temperatures. The input sheets used for ARB were recrystallized with grain size of 20 µm in the rolling direction (RD) and 15 µm in ND.

LM examinations indicate that the samples processed at 200 °C exhibit deformed grain structure typical for heavily cold rolled aluminium sheets. TEM examinations after the first ARB cycle reveal subgrains of size from 0.5 to 1.5 µm. During subsequent cycles, low-angle boundaries convert to high-angle boundaries. Dislocation density in subgrains or grains remains almost unchanged throughout all cycles and is indicative for a recovered substructure. In the samples with 2nd and 5th cycles, 150 µm wide areas with much finer grains (0.1 to 0.3 µm in diameter) are observed. X-ray energy dispersion analysis does not show any difference in matrix composition in these areas; neither fine-dispersed particles that could pin grain boundaries are observed. Tsuji et al. [4] suggest that these extremely refined grains are formed as result of the intensive friction and shear deformation involved in surface brushing. In contrast to the specimens ARB processed at 200 °C, coarser grains form in specimens processed at 350 °C. TEM examinations confirm that the average grain size refines in the 1st cycle down to 1.3 µm and it remains almost unchanged by further processing. Both LM and TEM indicate that local subgrain coarsening and recrystallization occur during the heating to 350 °C. These processes cause the low hardening achieved by ARB processing at 350 °C. However, areas of grain size as small as 500 nm are also locally observed. The situation is similar also during processing at 250 °C and 300 °C, where deformation recovery is also observed and is more pronounced at larger strains.

ARB at 200 °C results in hardness increase from 28 to 58 (after two cycles), i.e. by a factor of 2.2. HV10 rises a little during subsequent cycles up to 61.4. Better roll bonding is obtained when the sheets are processed at 250, 300 and 350 °C, but smaller increase in hardness is achieved. When the alloy is processed at 350°C, HV10 increases from 30 to 49 and no increase is observed during subsequent cycles. Processing at lower temperatures (250 and 300 °C) leads to a small improvement in the strengthening introduced by ARB. The maximum relative increase in hardness in samples processed at $T \geq 250$ °C is not higher than 1.7 times the initial value. Therefore, ARB induced strengthening is not stable at temperatures above 250 °C. The behaviour of tensile strength is similar to that of hardness.

References:

- [1] TSUJI, N. – KAMIKAWA, N. – KIM, H.W. – MINAMINO, Y.: *Fabrication of bulk nanostructured materials by ARB (Accumulative Roll Bonding) process*, in "Ultrafine Grained Materials III" TMS, 2004, pp. 219–226.
- [2] SLÁMOVÁ, M.: *Annealing response of AA8006 and AA8011 thin strips - effect of pre-treatment and strain level*, Aluminium 77, 2001, pp. 801–808.
- [3] KARLÍK, M. – HOMOLA, P. – SLÁMOVÁ, M.: *Accumulative roll-bonding: First experience with a twin-roll cast AA8006 alloy*, J. of Alloys and Compounds 378, 2004, pp. 322–325.
- [4] TSUJI, N. – HUANG, X. – NAKASHIMA, H.: *Microstructure of metals and alloys deformed to ultrahigh strains*, in Proc. of the 25th Risø International Symposium on Material Science: Evolution of Deformation Microstructure in 3D, 2004, pp. 147–170.

This research has been supported by the Czech Science Foundation (GA CR 106/03/0790).

Pozzolanic Admixtures in Lime Plasters - Mechanical Stress Caused by Temperature and Moisture Changes

A. Kunca, V. Tydlitát, R. Černý, P. Rovnaníková*

kunca@fsv.cvut.cz

CTU, Faculty of Civil Engineering, Dept. of Structural Mechanics

Thákurova 7, 166 29 Praha 6

*Technical University of Brno, Faculty of Civil Engineering, Institute of Chemistry,
Žižkova 17, 662 37 Brno

The renovation of historical buildings leads to use of the original materials, that were used hundreds years ago. The similarity between new plasters and old plasters is also needed to preserve cultural heritage. In these plasters it is not acceptable to use Portland cement and all the binders applied at renovation should be similar to those used in the past. Lime plasters are materials for exterior use that were applied on the old buildings.

Plasters are exposed to the external conditions such as temperature changes, wind, rain etc. They are supposed to resist to big volume changes. For the historical buildings were used binders with pozzolanic properties. Pozzolanic admixtures improve the mechanical strength and resistance to the temperature changes and to the frost action. The pozzolanic admixtures caused the development of a solid structure in plasters such as CSH gels and calcium aluminates.

In this research we applied three pozzolanic admixtures: metakaoline (Metastar 501 UK), grinded brick pottery (Cihelny Hodonín), grinded enamel glass (Mefrit a.s. Mělník). Three lime plasters were produced. The plasters composition was lime (CL 90 Czech-Moravian Cement Mokrá), sand with continuous granulometry, water and pozzolanic admixtures in 1:3:1.2:1 proportion. A comparison was done with reference lime plaster as well.

The mechanical strength of studied plasters was two or three times higher in comparison with the lime plaster, only lime plaster with grinded enamel glass had the mechanical strength of the same magnitude. Thermal properties were changed only for lime plaster with metakaoline. This had two times lower thermal conductivity.

The biggest problem of the new plasters was the change of the thermal and hygric expansion coefficients. The coefficient of thermal expansion was for the lime plaster with metakaoline lower, which is a positive feature, but for the other plasters it was higher than for the reference lime plaster. The coefficients of hygric expansion were in comparison with reference lime plaster two times higher that could potentially lead to cracking. Therefore, numerical simulation and calculation of the hygric and thermal changes of the lime plasters was applied to predict possible cracking and to avoid the destruction of the lime plaster.

The simulation of the thermal and hygric behaviour of lime plasters was made by the use of Delphin program that is developed at the TU Dresden. The simulation enabled to observe the yearly development of the capillary condensed water, thermal flows, the highest and the lowest temperature in the construction. The construction was from outside: 30 mm of the analyzed lime plaster, 450 mm brick, 30 mm Calsitherm inside insulation, 15 mm lime cement plaster. The simulation has shown the history of the plaster in two-year simulation. The effects of higher temperatures on the southwest side and of the dominant direction of the wind and rainwater on the northwest side of the construction was considered in the simulation and in the calculation.

The differences between the temperature on the inner and outer side of the plasters, and also the temperature differences in the whole construction during the year were 522

calculated. The differences in the water content during the whole simulation were studied as well.

Plasters	Thermal expansion coefficient	Max. relative thermal deformation during the year	Hygric expansion coefficient	Max. relative hygric deformation during the year	Mechanical stress from the deformation	Plaster strength after 28 days	Crack- ing
	α_t	ε_t	α_w	ε_w	σ	F	
	[K ⁻¹]	[mm/mm]	[w. % ⁻¹]	[mm/mm]	[MPa]	[MPa]	
Lime plaster	0.0000116	0.00064	0.0000334	0.00058	0.53	1.11	no
With metakaoline	0.0000062	0.00035	0.0000607	0.00152	1.15	2.36	no
With grinded brick pottery	0.0000108	0.00060	0.0000720	0.00127	2.09	4.06	no
With grinded enamel glass	0.0000146	0.00082	0.0000755	0.00125	1.35	1.12	yes

Table 1 Cracking evaluation in the lime plaster and lime plasters with pozzolana admixtures

The results show the maximal relative thermal and hygric deformation during the year. From these values were calculated the maximal mechanical stresses, which were compared with the mechanical strength of the plasters.

Lime plasters as an exterior and interior finishing surface are exposed to the thermal and hygric stress. The numerical durability analysis consisting in determination of cracking resistance of lime plasters with pozzolanic admixtures exposed to thermal and hygric volume changes revealed that lime plaster, lime plaster with metakaoline and lime plaster with grinded brick met well our requirements. In the lime plaster with grinded enamel glass the appearance of cracks was found as very probable. In a further simulation process the hydrophobized lime plasters will be observed. The hydrophobization causes lower water absorption and lower hygric changes. So, better mechanical behaviour can be expected also for the lime plaster with grinded enamel glass. At the moment, from the point of the cracking resistance we can recommend all the studied lime plasters except for the lime plaster with grinded enamel glass for the further use on historical buildings.

References:

- [1] R. ČERNÝ, J. DRCHALOVÁ, A. KUNCA, V. TYDLITÁT, P. ROVNANÍKOVÁ.: *Thermal and Hygric Properties of Lime Plasters with Pozzolonic Admixtures for Historical Buildings*. Research in Building Physics, Lisse: A. A. Balkema Publisher, 2003, pp. 27-33.
- [2] KUNCA, A.; TYDLITÁT, V.; DRCHALOVÁ, J.; ČERNÝ, R.; ROVNANÍKOVÁ, P.: *Mixture Development for Renewal Plasters of Historical Buildings and Determination of Basic Properties*. CTU Reports Proceeding of Workshop 2004 Part A Special issue March 2004 Volume 8 Prague: CTU 2004, pp. 534-535.

This research has been supported by GA CR grant No. 103/02/1081.

Influence of Materials on Wear of Blade

Impellers

D. Čuprová*, I. Fořt**, J. Cejp*, T. Jirout**, F. Rieger**

dita.cuprova@post.cz

*CTU, Faculty of Mechanical Engineering, Dept. of Materials Eng.
Karlovo n. 13, 121 35 Praha 2

**CTU, Faculty of Mechanical Engineering, Dept. of Process Eng.
Technická 4, 166 29 Praha 6

In all areas of particulate technology where solid particles are handled structures in contact with the particles will exhibit erosion wear. In some applications this wear may be so severe as to limit the life of a component or plant, while in others it may be negligible [1].

The erosion process of a pitched blade impeller in a solid-liquid suspension was recently studied [2,3,4], and a simplified two parameter model of the process was proposed and experimentally verified. The erosion wear of the impeller blade caused by particles of higher hardness can be described by an analytical approximation in exponential form of the profile of the leading edge of the worn blade

$$H(R) = 1 - C \exp[k(1 - R)], \quad (1)$$

where the dimensionless transversal coordinate along the width of the blade is

$$H(R) = \frac{y}{h} \quad (2)$$

where the dimensionless longitudinal (radial) coordinate along the radius of the blade is

$$R = \frac{2r}{D}. \quad (3)$$

Parameters h and D characterize the width and diameter of impeller, respectively.

The value of the parameters of Eq. (1) – the wear rate constant k and the geometric parameter of the blade C – were calculated by the least square method from the experimentally found profile of the worn blade. While the wear rate constant exhibits a monotonous dependence on the pitch angle, only, the geometric parameter is dependent both on the pitch angle and in linear form on the impeller speed as well as on time.

This study attempts to extend our knowledge about the mechanism of erosion wear of the blades of pitched blade impellers in a solid-liquid suspension to determine the influence of the blade material (hardness) on both parameters of Eq. (1). Four blade pitched blade impeller (pitch angle $\alpha = 30^\circ$), pumping downwards was investigated in a pilot plant fully baffled agitated vessel (vessel diameter $T = 300$ mm, four baffles of width $b = 30$ mm, impeller diameter $D = 100$ mm, impeller off bottom clearance $H_2 = 100$ mm) with water suspension of corundum (volumetric concentration $c_V = 5\%$, average size of particles $d_p = 0.257$ mm, density $\rho_S = 3\,900$ kg/m³). The impeller speed was held at the level of complete homogeneity of solid suspension under turbulent regime of flow of agitated batch. The shape of four worn blades was scanned in a time series and all obtained blade profiles were correlated according to the exponential form of Eq. (1). Metallic blades were made from various materials of different hardness :

aluminium Al 99,8 (HV 34), Al 99,5 (HV 40), brass Cu Zn37 (HV 74), brass Cu Zn40Pb2 (HV 134), construction steel C10E (HV 112), stainless steel X5CrNi18-10 (HV 194).

Results of experiments cover dependences of both parameters of Eq. (1) on time and hardness. The geometric parameter of blade C was changed between 0.025 (X5CrNi18-10) and 0.25 (Al 99,8) and value of wear rate constant k was detected from 5,01 (CuZn40Pb2) to 5,7 (Al 99,5) during time 80 hours.

Dependence of relative mass erosion wear on time and Vickers hardness was similar and decreased with increasing Vickers hardness of tested metals.

References:

- [1] HUTCHINGS,I.: *Wear by Particule*. Chem.Eng.Sci., 1987, vol.42,No.4, pp.869-878.
- [2] FOŘT,I.,AMBROS,F.,MEDEK,J.: *Study of Wear and Tear of Axial Flow Impellers*. Proceedings of the Fluid Mixing VI Conference (Editor: H. Benkreira), Bradford (UK) 1999, p. 59-68.
- [3] FOŘT,I.,AMBROS,F.,MEDEK,J.: *Study of Wear of Pitched Blade Impellers*. *Acta Polytechnica*, 2000, Vol. 40, No. 5-6, pp. 5-10.
- [4] FOŘT,I.,AMBROS,F.,MEDEK,J.: *Erosion Wear of Axial Flow Impellers in a Solid-liquid Suspension*. *Acta Polytechnica*, 2001, Vol. 41, No. 1, pp. 23-28.

This research has been supported by CEZ 212200008.

Residual Stress Analysis of Steel Surfaces after Progressive Methods of Machining

N. Ganev, I. Kraus

Ganev@troja.fjfi.cvut.cz

Department of Solid State Engineering, Faculty of Nuclear Sciences and Physical Engineering, Czech Technical University in Prague, Trojanova 13, 120 00 Prague 2, Czech Republic

The sign and magnitude of residual stresses and generally all diffraction characteristics of treated surfaces always depend on the type of material and on the parameters of applied technology of their machining. The character of stresses on the workpiece surface and beneath it affects its functionality. Compressive stresses increase fatigue limit and improve wear resistance, whereas tensile stresses decrease fatigue strength and make destruction of frictional surfaces easy.

At present, the most generally recognized residual stress classification is based on the volume magnitude in which the stresses are of constant value and direction (i.e. they are homogeneous). The classification takes into account the extent of the acting stress [1 – 3].

Macroscopic (first order) residual stresses are approximately homogeneous in a macroscopic volume (in many crystallites) of the material. Its linear dimensions are at least of the order of millimeters. The volume can be of the shape of an extensive layer of minute thickness. Macroscopic stresses cause an angular shift of diffraction lines, which disappears after the investigated body under loading has been appropriately cut, or stress relaxed.

Microscopic (second order) residual stresses are approximately homogeneous in volumes of a dimension comparable to the grain size. The force and moment equilibrium is supposed even in a great number of crystallites. Homogeneous microscopic stresses can result in a symmetrical broadening of diffraction lines. Consequently profiles of individual diffraction lines contain an important information about defects of crystalline lattice (real structure of polycrystalline materials), e.g. about crystallite size and lattice microstrains (local variations of the lattice parameter).

The research is being carried out on two sets of steel specimens: (a) tool steel (Czech grade 19 436 – 2.0 % C, 12.0 % Cr, 0.4 % Mn). The samples was prepared from material in quenched (K) and as-received (NK) state; (b) low-alloy steel (Czech grade 14 220 – 0.15 % C, 1.0 % Cr, 1.4 % Mn). Material was in the as-received state. The squared samples $15 \times 15 \times 7 \text{ mm}^3$ was cut from bars.

The analysed samples was prepared by using two methods of unconventional machining and grinding: (a) **Electro-discharge machining** (fine cut) was realised with an AGIEETRON IMPAKT device and both graphite and copper electrodes. Working conditions were automatically optimised on the base of the required roughness of the cut surfaces; (b) **Electro chemical grinding** was performed using a WENAT device with NaNO_3 electrolyte and a diamond wheel; (c) **Ground samples** were prepared with cooling on a horizontal spindle surface grinding machine *BPH 20*.

Besides the ferritic (α -Fe) and austenitic (γ -Fe) phases a minority fraction of Cr_7C_3 (PDF No 11-550, 5-720, 6-0683) was observed in the surface layers of 19436 samples. The ratio of the two Fe crystalline phases was estimated using the standardless method designed by J. Fiala [6] assuming that the content of Cr_7C_3 is negligible.

The values of the microstrains and the crystallite size were obtained from the broadening of single lines by the method of Voigt function [4, 5]. The microstresses were

calculated from the microstrains by using the Hook law to allow a direct comparison with the macroscopic stresses.

CONCLUSIONS

1. Biaxial state of residual macroscopic stresses found on the electro discharge cut surfaces is nearly isotropic, i.e. $\sigma_L \approx \sigma_T$.
2. Considerably higher tensile stresses in the surface layers of the samples cut with a graphite electrode correspond to a higher heat loading in this case of machining conditions. Only compressive residual macroscopic stresses were obtained on the electro chemically treated surfaces. It is a result of the predominant mechanical interaction of the diamond wheel with the treated material. The state of residual stresses is slightly anisotropic and $|\sigma_L| > |\sigma_T|$. The ground samples have an appreciably anisotropic state of compressive residual stresses where $|\sigma_L| \gg |\sigma_T|$.
4. The quenched samples 19436 treated by EDM have more great microstresses than the samples treated by ECM and by grinding. On the contrary, the as received samples 19436 and the samples 14220 treated by EDM have microstresses approximately equal to zero.
5. The method EDM Cu leads to narrower diffraction lines than the method EDM G. The particle size in the case of EDM G is smaller than after EDM Cu.
6. The treatments ECM and grinding lead to the similar diffraction broadening, but its reasons are different.

References:

- [1] KRAUS, I., GANEV, N.: *Technické aplikace difrakční analýzy*, Nakladatelství ČVUT v Praze, Praha 2004.
- [2] ČERNÁNSKÝ, M.: in *Defect and Microstructure Analysis by Diffraction*. Eds. R. L. Snyder, J. Fiala and H. J. Bunge, Oxford University Press, Oxford 1999 pp. 613 – 651.
- [3] KRAUS, I., GANEV, N.: in *Industrial Application of X-Ray Diffraction*. Eds. F. H. Chung and D. K. Smith, Marcel Dekker, New York 1999, pp. 793 – 811.
- [4] de KEIJSER, TH. H., LANGFORD J. I., MITTEMEIJER E. J., VOGELS, A. B. P.: *J. Appl. Cryst.*, **15** (1982) 308 – 314.
- [5] NANDI, R. K., KUO H. K., SCHLOSBERG W., WISSLER G., COHEN, J.B. AND CRIST, B. JR.: *J. Appl. Cryst.* **7** (1984), 22 – 26.
- [6] FIALA, J: *Kovové Mater.*, **5** (1967), 559 – 562.

The research was supported by the Grant Agency of the Czech Republic (Grant No 106/03/1039) and by MŠMT grant No. MSM 210000021."

Grain Size of Ferrite in Low Carbon Microalloyed Cast Steels

Ganwarich Pluphrach
pganwarich@yahoo.com

CTU, Faculty of Mechanical Engineering, Dept. of Materials Eng.
Karlovo n.13, 121 35 Praha 2

Low carbon cast steels are nowadays usually microalloyed with small additions of alloying elements that retard austenite recrystallization and pin austenite grain boundary movement by the formation of small carbide and/or nitride precipitates. These elements include vanadium, niobium, and titanium. The microalloyed steels are produced for a variety of offshore platform, centrifugal cast pipe, support, frame, housing, coupler, ingot mold, bucket, universal joint, arms associated with bloom furnace, boiler vessel and cast steel tube application with yield strength varying from 400-600 MPa. The microalloyed steels are alloys of iron and with less than 0.18% carbon and with manganese, silicon and other elements in small quantities. The latter elements are present for their desirable effects. [1]

Microalloying elements can affect the constitution, characteristics and behavior of microalloyed steels in many ways. Some of the major effects of these elements are, solid solution and precipitation strengthening, grain refinement of austenite and ferrite and possibly transformation temperature control. [1]

The ferrite grain size of a microalloyed steel can have a major effect on mechanical and physical properties. The Hall-Petch equation illustrates the relation that exists between grain size and yield stress;

$$\sigma_y = \sigma_0 + kd^{-1/2} \quad (1)$$

It has been shown that for microalloyed steels, the also fracture stress is related to ferrite grain size by a -0.5 exponent. [3]

Ferrite grain size can be measured by several different methods. One of the earliest methods of evaluating of microalloyed steels was developed by Spektor. [4] Metallographic techniques for measuring grain size were originally based on point counting or linear intersection lengths (chords). [2]

Ferrite grain size determination of metallographic microalloyed steels in as-cast state (non heat – treatment) specimens should be done in a magnification suited to the size of the grains so that small grains may not be lost. The degree of magnification will be limited by the fact that the picture must include a sufficient number of grains. [4]

Spektor considers the penetration of a polydispersed system of spheres by a straight line or secant. There are many spheres of diameter d_j , the centers of which are distributed in space with statistical uniformity. The distance from the center of the sphere to the intersecting chord is

$$x(i, j) = \sqrt{\left(\frac{d_j}{2}\right)^2 - \left(\frac{l_i}{2}\right)^2} \quad (2)$$

where l_i is the length of the chord. The number chords per unit length of the secant having lengths between l_i and d_j is calculated next. There are $N_V(j)$ centers of spheres per unit volume of the structure, the number of chords per unit length of the secant will be

$$N_L(i, j) = \pi x^2(i, j)N_V(j) = \frac{\pi}{4}(d_j^2 - l_i^2)N_V(j) \quad (3)$$

It is sufficient to represent the distribution of particle sizes as a discontinuous function with a limited number of class intervals. The working formula is obtained. [4]

$$N_V(j) = \frac{4}{\pi\Delta^2} \left[\frac{n_L(j)}{2j-1} - \frac{n_L(j+1)}{2j+1} \right] \quad (4)$$

In following table, there are gathered selected results of my investigations on six samples.

Table 1 Size distribution and yield stress of ferrite grains of microalloyed steels in as-cast state

1	2	3	4	5	6	7	8
Items	Steels	Range of Chord lengths, μm	Number of chords per mm., $n_L(j)$	Diameter of grains d_j , mm	Number of grains per mm ³ , $N_V(j)$	Evaluate mean grain size, \bar{d} , μm	$\sigma_y = \sigma_0 + kd^{1/2}$, Mpa
1	17Mn6	0 - 260	183	0.026-0.260	1.013×10^5	39.9	140.1
2	16MnV6	0 - 150	688	0.015-0.150	13.4114×10^5	22.6	173.0
3	19MnNb6	0 - 170	542	0.017-0.170	7.3575×10^5	26.3	163.3
4	22MnVNb6	0 - 130	625	0.013-0.130	14.0886×10^5	20.2	180.7
5	17MnTi6	0 - 160	671	0.016-0.160	13.3789×10^5	22.1	174.5
6	18MnVTi6	0 - 140	876	0.014-0.140	22.6714×10^5	19.2	184.3

Notes: values of σ_0 is usually taken as 40 MPa and k as $20 \text{ MPa} \cdot \text{m}^{-1/2}$ (constant value).

The evaluation mean ferrite grain size (\bar{d}) of microalloyed steels in as-cast state were 22.6, 26.3, 20.2, 22.1 and 19.2 μm that showed a secondary structure response. Vanadium is known to promote precipitation strengthening and made smaller mean grain size than steels without it. The mean grain size of ferrite in steel 17Mn6 is largest than other steels because it is not microalloyed. The microalloyed steel 19MnNb6 with niobium added is very difficult to dissolve in its austenite phase. This steel is without heat-treatment so that it has largest austenite-ferrite grain size and lowest yield stress than other microalloyed steels.

Metallographic analysis of the secondary ferrite grain size of microalloyed steels in as-cast state after Spektor's method is carried out. Qualitatively, a good correlation was found between mean grain size and yield stress.

References:

- [1] VOIGT, R.C.- SVOBODA, J.M.: Development and Application of HSLA Cast Steels. Eight International Conference on Offshore Mechanics and Arctic Engineering. The Hague, March 19-23, 1989, pp.353-359
- [2] International Standard (ISO 643): Steels – Micrographic determination of the apparent grain size. 2nd ed., 2003
- [3] HELZ, D.W. – RYPIEN, D.V.: Quantitative Metallographic and Ultrasonic Grain Size Measurement in Iron Alloys. Conf. Proc. of Quantitative Microscopy and Image Analysis. ASM International Materials Park Ohio 44073-0002, 1994
- [4] DEHOFF, R.T. – RHINES, F.N.: Quantitative Microscopy. McGraw-Hill, New York, 1968.

This research has been supported by GA ĀR grant No.106/03/0473.

Study and Preparation of CrN, CrCN and Cr(x)C(y) Layers as a Protection against Corrosion.

Testing of Mechanical Properties.

L. Berka*, N.V. Murafa*, D. Tischler**

***berka@fsv.cvut.cz**

*Department of Building Structures-Laboratory of Microscopy, Faculty of Civil Engineering, Czech Technical University, Thákurova 7, 166 29 Prague 6, Czech Republic

**Department of Physics, Faculty of Mechanical Engineering, Czech Technical University, Technická 4, 166 07 Prague 6, Czech Republic

Hardness testing is a method frequently used for evaluation of the resistance of body surfaces to the influence of contact loading. The Vickers hardness test is applied for this purpose in a case when the material is sufficiently ductile and no cracks occur in the corners of the indents. Testing of the surface hardness of such materials as glass and ceramics, on the basis of the Vickers testing method, must take into account the energy that is spent on cracks extension. The paper [1] describes a method evaluating a resistance of a material against microcracks formation on its surface. To evaluate the conditions for crack extension it is necessary to test a specimen under external loading. The suggested procedure involves a bent strip. As bending stresses are known, from them and from the differences in cracks length, along and across the strip, the resistance of the material surface to against the crack propagation is determined. This technique was still verified for different kind of brittle materials [2][3].

A study of the mechanical properties of evaporated Cr₂N layers is conducted as from the point of view of their hardness so from the point of view of their toughness, using the PAAR-MHT 10V Microhardness Tester. This instrument consists of a sensor with a Vickers type diamond tip and a control unit. This permits programming of the chosen maximum load in the range of 0.5 – 400gr, the rate of a growth of the load and the dwell time of the maximum load. The sensor is screwed into the head of a Zeiss Amplival optical microscope, the objective of which has usually a magnification of 40 times. A JAI digital camera, with 768 x 572 pixels resolution, is used to record the indent images, where the length of of the imprints diagonals is measured using Tescan Atlas software.

A problem studied today is a characterisation of the mechanical properties of thin Cr₂N layers, used to a protection of metal parts against corrosion. The layers are deposited on a bed of the monocrystalline Si plate and of the high strength steel - CZ Standard (ČSN) 17346, by PACVD technology. The Cr₂N thin layers, are created at the same conditions, which leads to a semicrystalline material structure. The standard quantity of Vickers hardness of all specimens was then determined and compared with that of a pure Si plate oversurface, which was used for a bed of the evaporated layers .

The method evaluating the resistance of a materials surface to the growth of microcracks length is derived from techniques used for fracture toughness testing . The difference between macro and micro toughness testing depends on whether the stress state, that causes crack propagation, is present in the material before or after the moment when the crack initiates. The device used for Vickers hardness test was therefore extended by a bending device. A surface crack toughness of strip specimens with Si and high strength steel bed was then tested [4].

The specimen with the Cr_2N layer on the Si plate bed has the strip form with the size of 8x30mm and with the layer thickness of 1,5 μm . The strip specimen is then glued by supercement to the stiff arms having the 10 mm span between them. The prepared specimen is loaded according to scheme of three point bending, in a special device, which is put into the microhardness tester.

The specimen with the Cr_2N layer on the high strength steel bed has the strip form with the size of 8x110mm. The thickness of the bed plate is 1mm, the layer thickness is 1,5 μm . The strip specimen is then glued by supercement to the stiff arms, with the 10 mm span between them. The whole specimen is bent in the newly worked three point bending device, which is put into the microhardness tester.

The Vickers indents are done into the specimens surface, in the place of central supporting point, so that they don't change the whole stress state. The indents done were at four magnitudes of the load, i.e. 20,30,40,50 [g] and for two levels of bending loads. The microscopic images of indents are digitally recorded and the length of diagonal cracks was measured. A magnitudes of the quantities, characterizing a resistance of materials surface with Cr_2N anticorrosion layer against microcracks spreading, are calculated.

References:

- [1] BERKA, L. MURAFKA, N.: *On the Estimation of the Toughness of Surface Microcracks*, Kluwer Publ.-International Journal of Fracture 2004, Vol.128, pp. 115-120.
- [2] BERKA, L. MURAFKA, N.: *Analysis of Stresses and Deformation at an Evaluation of microhardness and Surface Toughness*, Experimental Stress Analysis 2004, 42nd International Conference, Czech Society for Mechanics, Plzeň Kašperské hory, Czech Republic, 2004, pp. 23-26.
- [3] BERKA, L. MURAFKA, N.: *On a Testing of mechanical Properties of material surfaces*, Materials Structure and Micromechanics of Fracture, 4th International Conference, CSNMT Brno, Czech Republic, 2004, p.74.
- [4] MURAFKA, N. BERKA, L.: *On an Evaluation of the Surface Microcracks Toughness of Glasses and of Ceramics*, Junior Euromat 2004, European Conference, FEMS-DGM Frankfurt Lausanne, Switzerland.

This research has been supported by CTU grant No. 0417311. The authors appreciate the support of CTU Grant Agency for their research work.

Consortium for R&D of Tribological Coatings

R.Novák, T.Kubart, D.Nováková*, T.Polcar*, T.Vítů

Rudolf.Novak@fs.cvut.cz

Institute of Physics, Faculty of mechanical Engineering, Czech Technical University,
Technická 4, 166 07 Praha 6, Czech republic
Department of Applied mathematics, Faculty of Transportation Sciences, Czech technical
University, Na Florenci 25, 110 00 Praha 1, Czech Republic

Introduction

Consortium for research and development of nanostructural coatings for improvement of tribological properties of machine elements is successor of the project „Centre of research and application of the coatings increasing the life-time and reliability of machine elements“ which has been solved at the Institute of Physics FME in the years 2000 – 2002 and which was supported by MPO in the frame of the program „Centers“. This “Consortium” project has been supported by Ministry of Industry and Trade again. Its aim is the development of nanostructural coatings with new tribological properties including the development of the PVD deposition technology on the surface of selected machine elements and initiation of the coatings production at the collaborating companies. These coatings contribute to the decreasing of energy consumption due to lower friction and to the increasing of the machine elements life-time. They also enable the design and production of new types of environmentally acceptable machine parts, e.g. gear boxes with low consumption of lubricants or sliding bearing working without oil-based lubricants. The research is aimed to the application of newest information of the basic research in the branch of nanostructural coatings. It is especially considered that all parts of the life-cycle of the coated machine elements are in agreement with the environmental demands.

Consortium and scope of its activity

Consortium consists of three members: CTU Prague, HVM Plasma Ltd. and Ecochem Inc. (late ČKD Technical Laboratories, Inc.) and its activity has been specialized in several fields of research and development : research of the composition of wear resistant or self-lubricated coatings, research and development of PVD technology for these types of coating deposition, characterization of tribological properties and optimum choice of coatings composition for specific application in industry scale.

Coatings research

Investigation of hard and wear resistant coatings was aimed to the study of the temperature dependent parameters of TiN, CoCr and CoCrN coatings. All investigated coatings were sputtered by means of a system of unbalanced magnetrons with pulsed d.c. supply. The most important deposition parameters (e.g. total and partial pressures of Ar+N₂ mixture, sample bias) were registered. The adhesion was measured with a scratch tester, for coating structure and internal stress evaluation the XRD and for coatings hardness the Hanemann microhardness were used. The temperature dependence of tribological parameters was determined by means of a high temperature tribometer in the temperature range RT – 800 °C. Apart from the major variables of normal load, contact area, sliding speed and testing time also the temperature was controlled and monitored during all tests. Analysis on wear test tracks was performed using the ball crater method. Optical measurement and image analysis of a ball crater produced over the wear track helped to reveal the failure mechanism, to

determine the presence of brittle interfaces or lack of adhesion. The analysis of determined temperature dependences could estimate the part of frictionally generated defects and of thermally activated processes on the wear rate or on the total coating failure.

Self-lubricated coatings could strongly decrease friction coefficient and working temperature of the surfaces of machine elements. Most frequently used coating is MoS₂, but this coating performance in humid air and water vapour deteriorates its tribological properties. Therefore the comparative measurements of tribological characteristics of MoS₂ and MoSe₂ were carried out. The investigated coatings were sputtered by means of unbalanced magnetron and the deposition conditions varied in argon pressure, substrate temperature and bias. The tribological measurements were provided in the same way as in the case of hard coatings. The results showed that the temperature dependence of friction coefficient and wear rate were nearly the same for both materials. But only negligible dependence of tribological properties of MoSe₂ on air humidity in comparison with MoS₂ proved that molybdenum diselenide was a very promising material for self-lubricating coatings.

Coatings applications in industry

Selected results of coatings applications realized in the year 2004:

- important increasing of the life-time of elements used in high pressure hydraulic systems with DLC coatings,
- prolonging of the life time of injection moulds and increasing of the surface quality of the mouldings with the DLC and other coatings,
- DLC coatings on highly stressed elements of spinning systems enabled construction of the new generation of textile machines,
- hard coatings on knives and blades used in glass industry increased multiple prolonging of their life-times.

References:

- [1] POLCAR, T.- KUBART, T.- NOVÁK, R.- KOPECKÝ, L.- ŠIROKÝ, P.: *Comparison of Tribological behaviour of TiN, TiCN and CrN at Elevated Temperatures* Surface and Coatings technology, 2004 (in print)
- [2] KUBART, T.- POLCAR, T.- KOPECKÝ, L.- NOVÁK, R.- NOVÁKOVÁ, D.: *Temperature Dependence of Tribological Properties of MoS₂ and MoSe₂ Coatings* Surface and Coatings Technology 2004 (in print)
- [3] NOVÁK, R.- KUBART, T.- POLCAR, T.: *Temperature Dependence of Tribological Properties of Hard and Self-lubricating Coatings* sborník konf. PRAGOTRIB, Czech Tribological Society Vydavatel, 2004
- [4] POLCAR, T.- KUBART, T.- NOVÁK, R.- NOVÁKOVÁ, D., ŠIROKÝ, P.: *Tribological Characteristics of CrCN Coatings at Elevated Temperatures* Book of abstracts 10th Joint Vacuum Conference, Portoroz, Slovenija, 2004, pp. 85

This research has been supported by grantof the Ministry of Industry and Trade No. FD-K3/104.

Microscopic Analysis of Hardness of a Material Surfaces and Evaporated Layers

N.V.Murafa*, L.Berka*, O.Bláhová**, I.Štěpánek**

N.Murafa@seznam.cz

*Department of Building Structures, Faculty of Civil Engineering, Czech Technical University, Thákurova 7, 166 29 Prague 6, Czech Republic

**Department of Materials Science and Technology, Faculty of Mechanical Engineering, University of West Bohemia, Veleslavínova 11, 301 14 Plzen, Czech Republic

Hardness testing with the use of Vickers, Knopp or Berkovich indent tip methods was frequently employed in the past for estimating the resistance of material surfaces to damage caused by a contact load. Indent techniques are applied today to characterise material properties in a more general sense. The indent process therefore needs to be analysed. Two reviews from this field have been presented recently. In these papers, the interest is focused on application of indent methods for an estimation of the properties of hard materials and ceramics, and on the analysis of strain fields and residual stresses generated by Vicker's indentation in brittle materials.

When indent methods are applied for characterising materials, it is necessary to take into account that bulk material properties and quantities, such as modulus of elasticity, yield stress and critical stress intensity factor, are defined at a homogeneous stress state of the material macrovolume. A decomposition of the indent object, which is strongly local and non-homogeneous, into the individual damage components, is the main problem in estimating the hardness quantity. The hardness quantity derived on this basis is always conventional. The surface properties can be classified exactly by a combination of the indent method and external loading, which is chosen in such a way as to cause a state of homogeneous stress on the specimen surface, which is superposed with the stress state caused by the indent [1]. This technique was verified by estimating material surface resistance to cracking initiated by an indent.

The Vickers test is reliable method for measuring the hardness of materials. Vickers hardness is a measure of the hardness of a material, calculated from the size of an impression produced under load by a pyramid-shaped diamond indenter. The indenter employed in the Vickers test is a square-based pyramid whose opposite sides meet at the apex at an angle of 136°. The diamond tip is pressed into the surface of the material at loads ranging up to approximately 20kg and 400gr (in our case) and the size of the impression (usually no more than 0.05 mm) is measured with the aid of a calibrated microscope. The Vickers number H_v is calculated using the standard formula [1] [3].

The testing of surface mechanical properties with using the Vickers method, must take into account crack formation in the indent corners. A quantitative estimation, based on the Vickers testing method, must take into account the energy spent on crack spreading. The area marked around the indent by the crack tips is deformed by the indent elastically, and it is from here, that this energy is released. The mean intensity of the indent force over this area thus characterizes a surface property of a material, similar to its hardness, which can be named toughness T_v . The Vicker's toughness is calculated therefore from the formula similar H_v [1] [4].

To evaluate the conditions for crack propagation, it is necessary to test the specimen under loading. The suggested procedure involves a bent strip. The Vickers indents are carried out in such a way that the edges of the indent pyramid are oriented parallel and orthogonally to the strip length. When the indent is now made, the bending stresses cause cracks that are orthogonal to the strip length to be bigger. As bending stresses are known, from them and from the difference in the crack lengths along and across the strip, the resistance to the propagation of cracks in the material surface can be determined [2].

In our research we were especially interested in mechanical properties of brittle materials and layers.

- The monocrystalline Si plates without and with thin Cr₂N layers which are deposited on a bed plate by PVD and CVD technologies. Specimens have the strip form, the size of which is of 6x40x0,5 mm.
- The thermally sprayed coatings WC-Co, WC-Co-Cr, Cr₃C₂-NiCr, NiCrBSi, 316L, WC, S49 were deposited on a bed from the carbon steel of Czech Standard (ČSN) 12 050. The specimens were provided by Škoda Research institute Plzeň. The specimens have the strip form and are of the size of 8x110x3 mm.
- The glass bars with the size of 11x150x8 mm.

The microscopic images of indents are digitally recorded and the length of diagonal cracks was measured using Atlas TESCAN software. A magnitudes of the quantities, characterizing the resistance of materials surface with anticorrosion layer against microcracks spreading, are calculated.

References:

- [1] BERKA, L. MURAFKA, N.: *On the Estimation of the Toughness of Surface Microcracks*, Kluwer Publ.-International Journal of Fracture, 2004, Vol.128, pp. 115-120.
- [2] BERKA, L. MURAFKA, N.: *Analysis of Stresses and Deformation at an Evaluation of microhardness and Surface Toughness*, Experimental Stress Analysis 2004, 42nd International Conference, Czech Society for Mechanics, Plzeň, Kašperské hory, Czech Republic, 2004, pp. 23-26.
- [3] BERKA, L. MURAFKA, N.: *On a Testing of mechanical Properties of material surfaces*, Materials Structure and Micromechanics of Fracture, 4th International Conference, CSNMT, Brno, Czech Republic, 2004, p.74.
- [4] MURAFKA, N. BERKA, L.: *On an Evaluation of the Surface Microcracks Toughness of Glasses and of Ceramics*, Junior Euromat 2004, European Conference, FEMS-DGM Frankfurt, Lausanne, Switzerland, 2004.

This research has been supported by CTU0400911. The authors appreciate the support given by the CTU Grant Agency.

A Few Comments on Life Time of Automobile Components

J. Zýka

zyka@kmat.fjfi.cvut.cz

CTU, Faculty of Nuclear Sciences and Physical Engineering, Department of materials,
Trojanova 13, 120 00 Praha 2

Automobile industry has within Czech Republic old tradition. This is one of the reason why other automobile manufacturer and their suppliers are coming to our country to establish their production factories. Transfer of production is often accompanied by transfer of development and by the need of solving problems in production and in the quality of products. In both cases, there could arrive a need of using methods or means, which the manufacturer does not have in command. This could be a possibility to establish a cooperation with academic sphere, especially with technical universities.

In this article we describe particular case of cooperation with some automobile components manufacturer. The analyzed object was a spring, which has been broken under cyclic loading before estimated time of the test. The aim of the analysis was to find out cause of the fracture (defects etc.).

The analyzed spring was not complete, because some small pieces had not been found after the failure. Nevertheless we had enough of material to conduct the analysis. The spring is manufactured of thin narrow tape made of stainless steel. Then it is formed by cold bending and by cutting.

It was the place where cross-section of the spring was reduced by cutting, where three fractures arose. Firstly we observed the spring's surface optically with the magnitude 20x. The surface was gleaming without any visible defects. The fracture surfaces were partially mechanically corrupted. On one of them we could distinguish several steps of the fissure propagation and the final phase of the fracture.

Further step of our investigation was a detailed fractographic analysis of the fracture surfaces by the means of scanning electron microscope. Conducting the analysis, we had to cope with corrupted stage of the surfaces. The corruption was caused probably by the pressure phase of the loading cycle. However we found on each fracture surface striations, evidence of fatigue. On the least corrupted fracture surface we could find an initiation of the fracture, direction of propagation of the fracture and the final phase of the fracture. The fracture originated on two adjacent surface defects (fissures) on the edge of the spring surface and the cutting. These fissures were about 10 μ m long and 1 μ m wide. We found more fissures of this kind on the surface; on the edge, near the fracture initiation, alongside the fracture and also on the fracture surface. Similar situation was observed in the case of other fracture were the initiation of the fracture was small fissure on the outer edge of the spring.

Consequently, we tried to look for the surface fissures on the whole surface of the spring. We found areas with fissures of the same type as described. But these were much longer (tens of microns). Once, we found an area of netting of the fissures. This was on the spring's part that was not loaded. So we could assume that fissures originated before the loading, hence we suppose they are caused by the production process.

This analysis was completed by surface analysis of other two springs, which were not broken. One of the springs was tested, the other was in the stage just after manufacturing. On both

springs we found fissures and fissure like defects with local surface deformation. Amount and dimensions was much lesser on the not loaded spring.

The last step of our investigation was metallographic analysis of the spring's structure. We measured grains' dimensions (length –hundred of microns, thickness – microns). Depth of surface fissures was approximately 5 μ m.

Final results of the analysis of the spring's fracture are as follows. Fracture propagation mechanism was fatigue. Fracture initiated on the surface fissures on the edges of the spring. Typical dimensions of the fissures are: width - 1 μ m, length – tens of microns, depth – 5 μ m. These fissures were found also at other places on the spring's surface far from the initiation sites. The fissures helped also in the propagation of the fracture.

Further we found appearance of the fissures on other springs. There we found also local deformation of the surface, which could serve as a starting point for fissure initiation.

Exact origin of the described surface defects is not yet known. We suppose that critical points are depletion of plasticity of the steel band by rolling, e.g. by too high reduction, and not sufficient lubrication of rolling cylinders. Chemical and electrochemical effects (cleaning process) can also support creation of the defects. It will be necessary to analyze surface of the steel band after each step of production for exact determination of the process step which is responsible for the creation of the defects.

At recent stage of analysis we recommend for prevention of premature failures to use material with better state of the surface (without fissures and defects, with higher plasticity) or take existence of the defects into the account and change the dimensions of the spring and/or the parameters of loading cycles.

References:

- [1] ZÝKA, J.: *Analýza povrchu pružin* (in czech), Technical report T288, UJP PRAHA a.s 2004, 12p.

Electro-Osmotic Flow in Building Materials III

L. Balík, L. Svoboda*

balik@klok.cvut.cz

CTU, Klokner Institute
Šolínova 7, 166 08 Prague 6

*CTU, Faculty of civil Engineering, Dept. of building Materials
Thákurova 7, 166 29 Prague 6

During the rehabilitation of historical buildings attacked by moisture, the continuously increasing emphasis is put on the non-destructive approach of the methods used. The method based on the existence of the electro-kinetics phenomenon (e.g. electro-osmosis) belongs to the advisable methods in this field. Next advantage of this method is possible to see in easier installation of system in case of substructures, which brings savings in consequence and the possibility of constant control of function.

This thesis starts from the results of doctoral thesis of authors and it enlarges the knowledge of electroosmosis upon the effect of applied voltage.

The aim of the work was to notice the influence of applied voltage on transport of salt brine through the structure of tested samples. The major criteria in view were:

- The volume of transported solution from the solid phase to the particulate material (bulk phase).
- The passed charge through samples.
- The determination of the mean value of current.
- The calculation of linear regression of the curve of humidity in tested samples.

The samples were constructed in order to constitute the condition in situ, so it's represented conversion between solid and bulk phases. The solid phase was formed by the clay brick sample of cylinder shape. The bulk phase was created by cohesionless dust of the clay brick base.

The samples were wetted and insulated uniformly within the possibility. The salt concentration of embedded dilution corresponded with the rise degree scale values of salinity of wall (in accordance with ČSN P 73 0610). The apparatus EMIS 03 and EMIS 04 [4] was applied as the electrical source and multi-channel interface.

The tests passed on three samples configurations. The voltage of 5 V was applied to configuration 1, 10 V to configuration 2 and 20 V to configuration 3. The time of voltage application was comparable for all samples. The results of measurement brought the next knowledge:

- The configuration of samples and their material base create favorable conditions for electro-osmotic flow, where the gradient of humidity grows in the direction of cathode.
- The values of linear regression are comparable in the solid and bulk phase in the case of 5 V applications. The larger value of linear regression of bulk phases were observed in the cases of 10 and 20 V applications.
- In the case of 5 V application was transported 3, 6 g solution from solid to bulk phase during 115 days period. This volume represents approximately 5 % of the inserted solution into solid phase before voltage application. The current

density, with use of the mean value of current, was $0,23 \text{ A/m}^2$. The value of charge, which passed through the sample, was 4122 C.

- In the case of 10 V application was transported 8,05g solution from solid to bulk phase during 112 days period. This volume represents approximately 12% of inserted solution into solid phase before voltage application. The current density, with use of the mean value of current, was $0,37 \text{ A/m}^2$. The value of charge, which passed through the sample, was 6005 C.
- In the case of 20 V application was transported 21,18g solution from solid to bulk phase during 112 days period. This volume represents 21% of inserted solution into solid phase before voltage application. The current density, with use of the mean value of current, was $0,42 \text{ A/m}^2$. The value of charge, which passed through the sample, was 9065 C.

After approximately 115 day period the volume of solution removed from solid to bulk phase was positively correlated with the voltage value. The quadruplicated increasing of voltage caused quadruplicated volume of transported solution during development twofold current density. The quadruplicated increasing of voltage caused twofold increase of the passed charge.

Results of the analysis showed that the efficiency a process of electro-osmotic flow and so the employment of the electro osmosis for dewatering of walls is affected by the value of applied voltage and by the current density. The inserted voltage is directly affected by the electric source. Its value is limited by the health safety and the guarantee period. The current density is not influenced only the applied voltage, but also the electrochemical conditions of the internal environment. The study of the properties of this environment and its influent on electric conductivity can contribute to the accurate design electro-osmotic application in holding the voltage value.

References:

- [1] BALÍK, L.: *Využití elektroosmózy k dodatečnému vysušování zdiva*. Ph.D. Thesis. Praha ČVUT, 2004, 242 p.
- [2] BALÍK, L. – SVOBODA, L.: *Studium podmínek pro efektivní použití elektroosmotického vysoušení* In: *Construmat 2002* ČVUT Praha, 2002, pp. 8-9.
- [3] BALÍK, L. – SVOBODA, L.: *Porovnání pískovce a opuky z hlediska účinnosti elektroosmotického působení na transport elektrolytu obsaženého ve struktuře těchto materiálů*. In: *Construmat 2003* Štúrovo, 2003 pp. 11-13.
- [4] BALÍK, L. – SVOBODA, L.: *Electro-Osmotic Flow in Building Materials II*. In: *Proceedings of Workshop 2004 Part A*. Prague Czech Technical University in Prague, 2004, pp. 594-595.

This research has been supported by CTU grant No.CTU 0416631.

Changes of Material Characteristics of Concrete under the Freeze-Thaw Loading

T. Doležel, P. Konvalinka

tomas.dolezel@fsv.cvut.cz

Department of Structural Mechanics, Faculty of Civil Engineering,
Czech Technical University,
Thákurova 7, 166 29 Prague 6, Czech Republic

This paper presents the damage of concrete and its dependence on different strength grades of plain concrete under the action of load and freeze-thaw cycles and analyzes changes of material characteristics of concrete in compression. The loss of compressive strength of concrete specimens subjected to loading was determined. Experimental results show that material characteristics of concrete specimens are strongly influenced by the damage process of freeze-thaw cycles, which is of great importance to durability of concrete under the comprehensive conditions.

The fact that cyclic changes of temperature loading have an influence on quality and durability of concrete structures is very well known. Many researchers dealt with the effect of such a loading on material characteristics of concrete in compression, especially on modulus of elasticity of concrete in compression. In this article, the material characteristics (cylinder compressive strength) for two different strength grades of concrete (C25/30 and C45/55) are demonstrated.

All compression tests have been carried out using the GROND DSM 2500 apparatus at the Department of Structural Mechanics of the Czech Technical University (CTU) in Prague.

The apparatus consists of a stiff loading frame having the capacity of 2 500 kN. The elevation of the loading platen is 100 mm. The loading frame is provided with a hydraulic servomechanism, which has been used when loading a specimen in order to measure softening under the deformation control. A constant strain rate of 1×10^{-5} m/s has been used.

The axial strains were measured by tensiometers. The strain gauges were located on the two opposite sides of the specimen and symmetrically in the quarters of the round loading platens of the loading apparatus.

As strain gauges located on the specimen the INOVA PXA 50 strain gauges were used having the measuring base equal to 100 mm. As strain gauges located in the quarters of the cylindrical steel loading platens of testing apparatus the SANDNER EXA strain gauges were used with the measuring base equal to 25 mm.

The separate readings of the two strain gauges on the specimen as well as of four strain gauges on the loading platens were recorded for information on the uniformity of deformations of a specimen during the test. The measurements had to be corrected for the deformations of the loading platens and for extra deformations due to the setting of the loading platen against the specimen. This setting is due to non-flatness of the specimen surface, non-parallelism of loading platen surface and specimen surface and internal setting of the loading platens. The corrections have been made by the software, by which the measured data have been evaluated.

Special attention was paid to the flatness and parallelism of the loading surfaces. This is necessary for uniform loading. The top surface of all specimens was finished using the concrete paste. The direction of casting was simply done by the shape of steel rigid form and was perpendicular to the direction of loading. Significant differences in the test results can be found for loading parallel and perpendicular to the direction of casting.

Special care was taken when manufacturing the specimens. Steel rigid moulds were used for manufacturing of all the cylinder (150x300mm) specimens. Specimens were compacted on a vibration table for 30 seconds, kept in the moulds for two days under wet cloths to prevent drying out, and after demoulding they were placed in a fresh water basin until the age of 28 days and kept in sealed plastic bags with some water added afterwards. Before freeze-thaw loading, the specimens were taken out from the plastic bags and exhibited to open air. Material components of both grades of concrete have the maximum aggregate size 16 mm, no admixtures, and w/c ratio equal to 0.41.

The age of concrete at time instant of testing varied from four to five months. At that age, standard compression tests on not loaded cylinders resulted in average compressive strengths of 49,6MPa for concrete C25/30 and 65,3MPa for concrete C45/50.

The specimens were placed into the freezer with temperature of -20°C and afterwards into the water basin with temperature of +20°C. The measured temperatures inside the specimen during the full cycle changed from -12°C to +12°C.

Three groups of specimens were tested. Each group consists of three cylinders, the first group with no freeze-thaw loading, the second group loaded with 25 cycles of freeze-thaw loading and the third group loaded with 50 cycles of freeze-thaw loading.

From results of the cylinder compression tests can be seen that the ability of concrete C45/55 to resist the damage of freeze-thaw loading is much higher than for concrete C25/30. The reduction of cylinder compressive strength after 50 cycles of freeze-thaw loading is 10% for C45/55, and 41% for C25/30.

Almost no differences were found for 25 and 50 cycles of cyclic loading for concrete C45/55. Much different ability to resist the damage of freeze-thaw loading was found for concrete C25/30. The reduction of peak stress value was 25% for 25 cycles, and 40% for 50 cycles of loading.

This study has investigated the material characteristics of two different strength grades of plain concrete subjected to cyclic changes of freeze-thaw loading, and proposed the relationships between the number of freeze-thaw cycles and cylinder compressive strength. Based on this study, the following conclusions have been made:

- compressive strength of concrete C45/55 subjected to freeze-thaw loading attains 90% of the initial strength value after 50 cycles of loading
- obviously larger is the damage of concrete C25/30, the compressive strength subjected to freeze-thaw loading attains only 59% of the initial strength value after 50 cycles of loading.

References:

- [1] T. DOLEŽEL, D. JANDEKOVÁ, P. KONVALINKA: *Vliv cyklů zmrazování a rozmrazování na materiálové charakteristiky betonu*. Stavební obzor 5/2004, 2004, pp. 143-145.
- [2] T. DOLEŽEL: *Material characteristics of concrete loaded by freeze-thaw loading* Sborník konference Experimental Methods and Measurement Techniques in Monitoring and Supervising Engineering Structures and Their Numerical Analysis, 2004, pp. 15-18.

This research has been supported by MŠMT grant No. FRVŠ G1 1943/2004.

Fracture Behaviour of Functionally Graded Materials

J. Bensch, J. Siegl

jan.bensch@fjfi.cvut.cz

CTU, Faculty of Nuclear Sciences and Physical Engineering, Dept. of Materials
Trojanova 13, 120 00 Praha 2

Functionally graded materials (FGMs) provide a solution to many advanced applications where two or more materials with distinct properties are required to be put together. The most often used definition says that FGM is a material characterised by a gradual change of microstructure and/or composition in its volume, which is designed and manufactured in order to achieve different functional requirements at different locations of the part [1]. Basically, there are two main types of FGM, i.e., continuously graded materials and the so called multi-layer-composites. The first type shows continuously changing properties, while the second one, composed of a number of homogenous sublayeres, shows step-vice changing properties.

Replacing the sharp interface by a gradual transition of properties and characteristics from one side of the body to the other, reduces the mismatch in properties, such as mechanical and thermal properties, to minimum. This could be beneficial in the view of the following arguments mentioned in the literature (see, e.g., [2]): (i) thermal stresses can be reduced; (ii) thermal stresses at critical locations can be reduced; (iii) stress jumps at the interface can be avoided; (iv) the driving force for crack extension can be reduced; (v) the tendency for delamination of brittle coating on a ductile substrate can be avoided; and (vi) the strength of the interfacial bond, which may be characterised by the interfacial fracture toughness, can be increased.

Although not all these arguments are in many cases convincing, at present FGMs are used due to their benefits all over the world. The ceramic-metal FGM systems exploit the heat, oxidation, corrosion, and wear resistance typical of ceramics, and the strength and toughness typical of metals [3]. So, they can be used as thermal barrier coatings (FGM TBC) in power generation and propulsion applications, such as gas turbines, diesel and jet engines. Other applications are, for example, hard protective surface layers on cutting tools, parts of pumps, aircraft engine lines, etc., or ballistic applications. Combinations of various materials are used in biomedicine to produce biocompatible implants with mechanical characteristics close to live tissues, e.g., bones, etc. Other kinds of FGMs are applied to piezoelectric actuators to provide devices of higher strain, life-time, and reliability. Despite the wide range of application possibilities, the characteristics and structures of only a few FGM systems are known well enough. The reason consists in the general complex structure and inhomogeneity of the FGMs, as well as in the huge spectrum of processing methods and their parameters causing, that materials produced in different labs show distinct variability in properties.

The above spectrum of fabrication processes includes two dominant methods, which are the powder metallurgy and the thermal spraying (most often plasma spraying), and some minority methods as the combustion synthesis, high temperature in-situ synthesis, and chemical (CVD) and physical vapour deposition (PVD). The fabrication process of FGM is one of the most important areas in FGM research [4]. The aim is to optimise the processes in order to get materials of required properties in the desired quality of acceptable price. It is important to notice, that high costs and fabrication problems still remain the most limiting factors of FGMs applications.

The experimental part of the research will be performed in close cooperation with the Institute of Plasma Physics of the Academy of Sciences of the Czech Republic. This institute

has at its disposal, above all, the water stabilized plasma (WSP[®]) torch, which is a unique apparatus usable for producing self-standing bodies made of FGM. The IPP has also other testing facilities, such as the arrangement for performing three- or four-point bending tests, wear tests or X-ray diffraction analysis (XRD), at the IPP. The work has to be started by testing the methodology on some FGM specimens, which are already prepared, just to justify their usability for FGMs, which has not been tested and is known from the literature only. After that, the specimens of the desired composition will be prepared.

Preparation of three types of multilayered FGMs is now expected. The first one is composed of brown alumina ($\text{Al}_2\text{O}_3 + 3\% \text{TiO}_2$) and olivine ($\text{SiO}_2 + \text{Fe}_2\text{O}_3 + \text{MgO}$). Alumina is widely used for its high hardness and good thermal resistance in industrial applications; the addition of small amount of titanium oxide then leads to lowering the melting temperature and makes easy the sintering of individual particles. Olivine is sometimes used as a thin interlayer to improve ceramic coating adhesion on steel substrates, because of its advantageous value of thermal expansion coefficient. The second FGM system will consist of alumina and zirconia ($\text{Al}_2\text{O}_3 / \text{ZrO}_2$); the third one will be a multi-layered composite composed of $\text{Al}_2\text{O}_3 / \text{Ni} / \text{Ni} / \text{Al}_2\text{O}_3$ layers. In the next part of the research, the methods for fabrication of continuously graded FGMs by WSP[®] will be developed.

For testing the above FGM systems the following methods and approaches will be employed:

- The phase analysis will be accomplished by means of XRD, also nucleation, if present, of new phases during post-processing or thermomechanical loading will be observed;
- The XRD analysis will be used also for measuring the existing residual stresses in the material;
- Mechanical characteristics will be determined by bending tests, using of the indentation methods comes also into consideration;
- Fatigue properties of FGM coatings and their influence on fatigue life will be studied on "SF-Test" material tester;
- Microscopic studies of structural characteristics will be done by light as well as scanning electron microscopy and by local electron microanalysis.

All results will be compared with those of homogeneous materials of similar composition or systems with sharp interface which were obtained during the previous research.

References:

- [1] SURESH, S. – MORTENSEN, A.: *Fundamentals of Functionally Graded Materials*. IOM Communications, London, 1998, 165 p.
- [2] BAHR, H.-A. – BALKE, H. – FETT, T. – HOFINGER, I. – KIRCHHOFF, G. – MUNZ, D. – NEUBRAND, A. – SEMENOV, A.S. – WEISS, H.-J. – YANG, Y.Y.: *Cracks in Functionally Graded Materials*. Materials Science and Engineering, A362, 2003, pp. 2-16.
- [3] RANGARAJ, S. – KOKINI, K.: *Estimating the Fracture Resistance of Functionally Graded Thermal Barrier Coatings from Thermal Shock Tests*. Surface and Coatings Technology, 173, 2003, pp. 201-212.
- [4] SAMPATH, S. – HERMAN, H. – SHIMODA, N. – SAITO, T.: *Thermal Spray Processing of FGMs*. MRS Bulletin, 20(1), 1995, 27-31.

This research will be supported by GA ĆR grant No. GA 106/05/0483.

Heat Treatment of Wind Power Station Shafts

K. Dalíková*, Z. Nový**, D. Kešner**

klara.dalikova@fjfi.cvut.cz

*Department of Materials, Faculty of Nuclear Sciences and Physical Engineering, Czech Technical University, Trojanova 13, 120 00 Prague 2, Czech Republic

**Comtes FHT Ltd., Lobežská E-981, 326 00 Pilsen, Czech Republic

The flanged shafts of wind power stations are made from heat-treated steels 34CrNiMo6 and 42CrMo4. These materials are selected for big forged pieces especially because of their high hardenability. At present time wind power station shafts are treated in ŠKODA KOVÁRNÝ Pilsen, Ltd. Heat treatment is composed of marquenching with subsequent tempering. By this technological process – quenching and tempering – is obtained fine-grained structure with uniform distribution of fine carbides. This structure leads to improvement of the mechanical properties. The main parameter of the quench and tempered sizable shaft is the achieved hardened depth below surface. Importance of the hardening depth level consists not only in stiffness of the whole shaft but also in its fatigue characteristics.

The experimental program was aimed at finding such a heat treatment which would lead to the most effective full hardening of the flange shaft. Marquenching process was sought that would provide hardened structure in greatest possible depth combined with crack-free state of material.

The technology of flanged shaft production starts with roughing an ingot into a stepped roll workpiece. After reheating to initial forging temperature of 1050 °C the flange with required dimensions is forged on an upsetting plate. Then the forged piece is air-cooled to 600 °C at the most. Subsequently the piece is placed in the furnace heated at 550 °C where temperature is gradually raised to 850 °C. After achieving hardening temperature in the whole volume of the forged piece, marquenching follows. It includes a short transport in ambient air and subsequent submersion in water. Here the forged piece is left until the material cools to temperature close to M_s . Then it is withdrawn and submerged in oil. Cooling in oil is finished after the temperature of about 120 – 160 °C is achieved. The piece is then placed in the furnace heated to 200 °C and the furnace temperature is stepped up to tempering temperature of 630 °C. After soaking the piece is air-cooled.

For this purpose a computational model of marquenching was created by means of DEFORM 2D programme. This numerical simulation modelled the real processes of the heat treatment. The experimental specimens were treated by a thermal-deformation simulator according to the computed cooling curves for marquenching. Then the specimens were submitted to metallographic analyses by light microscopy and to hardness and microhardness measurements. Material for testing from the real treated flanged shaft was obtained. These specimens were also submitted to metallographic analysis and the results were compared with the mentioned experiments. On the basis of the realized experiments and obtained results the possibility of marquenching in water was assessed.

The aim of numerical simulation of processing of flanged shafts from 34CrNiMo6 and 42CrMo4 steels was to monitor the distribution of the temperature field during the process of marquenching, i.e. cooling in air, water and oil. The program DEFORM 2D was chosen for this computer simulation. Thereby were obtained specific temperatures throughout the processing time and in given computational nodes of the flanged shaft. Six measurement points near the end of the shaft in different depths below the surface were chosen after the 544

computation. In these points were graphically registered the courses of temperature during the whole process of the heat treatment. The obtained cooling curves were mapped on CCT diagrams of the steels. Subsequently the heat treatment optimization was performed: the calculation of marquenching process modifications. Numerical simulation of extended delay in water from previous 22 to 28 minutes was performed and the influence on the microstructure was monitored.

Results obtained from numerical model were the basis for physical simulation on the experimental specimens of the heat treatment with the aid of the SMITWELD TTU 2002 thermomechanical simulator.

The interpretation of acquired results is greatly complicated by the carbon segregation, or, as the case may be, alloying elements, which manifests by great structural heterogeneity. The experimental study of the developing microstructures was only conducted after the first phase of the heat treatment – marquenching. The final mechanical properties of the flanged shafts are achieved through the second part of the heat treatment process – tempering.

The structural analyses show that the fraction of the hardening structures in the depth of 100 mm below the surface is high, i.e. substantially higher than 50 %, in both methods of the treatment. Nevertheless, it occurs that the relative toughness values in thus treated shafts are insufficient. This can be caused by unfavourable morphology of the hardening structure. Results of the performed experiments suggest that the most suitable hardened structure is probably a fine mixture of martensite and lower bainite. However, upper bainite dominates in larger depths of the hardened layer.

The computer simulation enables to determine the distribution of the temperature course within the part, which could not be measured in practice. The results of the calculation and subsequent materials analysis show that the extended delay in water does not have marked influence on the 42CrMo4 material with respect to the resulting hardened depth. Conversely, the proposed water cooling delay extension of the material 34CrNiMo6 appears as a benefit. The results of the numerical simulation suggest other possibilities of optimization of power station shafts treatment – namely by selection of a suitable forming process and subsequent heat treatment.

References:

- [1] DALÍKOVÁ, K.: *Heat Treatment of Wind Power Station Shafts* Graduation theses, KMM ZČU, Pilsen, 2003.
- [2] FIŠER, P. – JÍRA, T.: *Modifications of the Technology of Flanged Shafts Heat Treatment* Research report of the company COMTES FHT, Ltd., 2002.
- [3] FIŠER, P. – JÍRA, T.: *Distribution of the Upsetting Operation of the Flanged Shaft Head* Research report of the company COMTES FHT, Ltd., 1999.
- [4] PATEROVÁ, H.: *Influence of Cooling Rate from Austenization Temperature to the Structure of Steel 34CrNiMo6* Graduation theses, KMM ZČU, Pilsen, 1999.

X-ray diffraction analysis of Zr-based alloys oxidized in steam at 1000 °C

G.Gosmanová, I.Kraus, N.Ganev, V.Vrtílková*

gosmanov@troja.fjfi.cvut.cz

CTU, Faculty of Nuclear and Physical Engineering, Dept. of Solid State Engineering,
Trojanova 13, 120 00 Praha 2

*ŠKODA-UJP Praha, Inc., Nad Kamínkou 1345, 156 10 Praha – Zbraslav, Czech Republic

Zirconium alloys are currently used as cladding materials of the fuel elements of water-cooled reactors. However their high-temperature behavior (under conditions being typical for LOCA) is still the object of extensive research.

The aim of this contribution is to present the results of X-ray diffraction analysis of two Zr-based alloys oxidized at 1000 °C. The crystallographic cell unit characteristics were evaluated by analysis of three selected diffraction lines of the metal substrate after oxidation. The same characteristics were examined for unoxidized standards of the both alloys.

The cladding tubes of Zr1Nb (Russia) and Zircaloy-4 (Zry-4 Sandvik) alloys were exposed for different time in a water steam environment at 1000 °C. Then the part of tubes was slowly cooled up to 700 °C and quenched in water. The rest part was quenched in water immediately after oxidation. This paper deals with the former case, the latter will be the object of follow-up research.

Specimens of dimensions $4 \times 15 \times 0.5$ mm³ were prepared by longitudinal cutting, grinding and etching the outer surface of tubes. The metal sections of oxidized tubes were the object of X-ray investigation. The peripheral parts of flat surface (approx. of 1 mm wide) were shaded off by slides, thus the X-ray measurements were carried out on the inner parts of tubes oxidized.

A ω - goniometer SIEMENS with Cr K α radiation was used to measure diffraction patterns. Three diffraction lines (112), (204) and (004) of α -Zr were recorded for the 2θ range of measurement ($110^\circ \div 128^\circ$). A fitting procedure had to be used to obtain the accurate values of the peak positions and consequently interplanar d_{hkl} spacings. The lattice constants **a**, **c** and unit cell volume **V** have been calculated for hexagonal α -Zr matrix of oxidized specimens.

The same procedure was applied on the standard samples of both the alloys under investigation.

The relative changes of unit cell volumes can be calculated from the results obtained for oxidized and as-received specimens. The results of calculation are given in Tables 1 and 2. As it was seen from diffraction diagrams, the strong textures occur in the metal substrate of both the alloys after oxidation. Texture varies with the exposure time especially for Zry-4 alloy. This fact can affect the accuracy of evaluation of appropriate values. Therefore the three equations instead of (necessary) two were used for calculation the lattice constants in order to check the obtained results.

It follows from the tables that the lattice space of both the alloys was changed after oxidation but in different mode, both quantitative and qualitative. Primarily there is a significant difference between the values of relative increase of unit cell volumes of the both alloys. At short time (10 and 30 min) exposures this values for Zr1Nb alloy are almost 10 times greater than for Zry-4. Furthermore, whereas the unit cell volume **V** of Zr1Nb alloy increases nearly steadily with each exposure, **V** of Zry-4 alloy stagnates up to 120 min exposure.

Table 1

Lattice constants, unit cell volumes and their relative changes of Zr1Nb specimens oxidized in steam at 1000 °C with various exposures

specimen	exposure,(min)	a (nm)	c (nm)	V (nm ³)	relative change, %
Zr1Nb ST	X	0,3232	0,5149	0,046578	X
NM 009	3	0,3233	0,5165	0,04674	0,4
NM 010	15	0,3234	0,5164	0,04678	0,4
NM 011	30	0,3238	0,5163	0,04687	0,6
NM 012	60	0,3238	0,5175	0,04698	0,8
NM 014	120	0,3247	0,5176	0,04726	1,5
NM 013	195	0,3246	0,5191	0,04736	1,7

Table 2

Lattice constants, unit cell volumes and their relative changes of Zircaloy-4 specimens oxidized in steam at 1000 °C with various exposures

specimen	exposure,(min)	a (nm)	c (nm)	V (nm ³)	relative change, %
Zry-4 ST	X	0,3231	0,5151	0,046580	X
SM 009	3	0,3230	0,5154	0,04657	0,0
SM 010	15	0,3231	0,5155	0,04660	0,04
SM 011	30	0,3232	0,5155	0,04660	0,03
SM 012	60	0,3231	0,5152	0,04658	0,02
SM 014	120	0,3233	0,5159	0,04670	0,3
SM 013	195	0,3238	0,5163	0,04686	0,5

The large difference between the crystallographic unit cell volumes of the both alloys can be probably related to hydrogen uptake. This assumption corresponds with the data presented in [1], where the values of hydrogen content and relative hydrogen uptake for the same alloys oxidized at the same conditions were in the same relation as mentioned above for V. Thus the value of crystallographic unit cell volume would be appeared as a sensitive indicator for such a type of processes.

References:

- [1] BÖHMERT, J. - DIETRICH, M. - LINEK, J.: *Comparative studies on high-temperature corrosion of ZrNb1 and Zircaloy-4* Nuclear Engineering and Design, vol. 147, Elsevier Science Publishers, 1993, pp.53-62.

This research has been supported by MSM 210000021.



CTU

REPORTS

Proceedings of
WORKSHOP 2005
Part B

CZECH
TECHNICAL
UNIVERSITY
IN PRAGUE

SPECIAL ISSUE

March 2005
Volume 9

These are the Proceedings of the Thirteenth Annual university-wide seminar WORKSHOP 2005 which took place at the Czech Technical University in Prague from 21st to 25th March, 2005.

The aim of the seminar is to present and discuss the latest results obtained by researchers especially at the Czech Technical University in Prague and at collaborating institutions.

The organizing committee has selected a total of 514 contributions divided into 15 different areas of interest:

• **Part A:**

- mathematics
- physics
- informatics and automation engineering
- electrical engineering and instrumentation
- materials engineering

• **Part B:**

- mechanics and thermodynamics
- mechanical engineering
- production systems, technology and technological processes automatisaton
- energetics and power engineering
- nuclear engineering
- chemistry
- biomedical engineering
- civil engineering
- architecture, town planning, geodesy and cartography
- transportation, logistics, economy and management

Organizing committee:

Chairman: Bohuslav Říha

Members (in alphabetical order):

Karel Andrejsek, Tomáš Brandejský, Vítězslava Drtinová, Jiří Houkal, Libor Husník, Zbyněk Kabelík, Květa Lejčková, Milan Němec, Markéta Růžičková, Ondřej Rypar, Bohuslav Říha, Jana Schneiderová, Ida Skopalová, Pavel Smrčka, Jan Šístek, Eva Šmídová, Jaroslav Zeman

Prague, March 2005

ISBN 80-01-03201-9

This book was prepared from the input files supplied by the authors. No additional English style corrections of the included articles were made by the compositor.

Published by the Czech Technical University in Prague. Printed by CTU Publishing House.

Dynamics of Heat Systems with Heat Pump and Various Degree of Accumulation.....	610
<i>S. Nesvadbová, R. Nový, K. Brož</i>	
Intensification of Pulse-Jet Cleaning of Industrial Filters.....	612
<i>P. Vybíral</i>	
Development and Verification of the Methodology of Welded Joints Testing Considering Multiaxial Loading	614
<i>M. Růžička, R. Pěnička, M. Hejman</i>	
Application for Teaching the Influence of Control Driven Units in Mechatronic Systems	616
<i>J. Vondřích, R. Havlíček, K. Belda</i>	
Panel Radiators	618
<i>R. Vavříčka, J. Bašta</i>	
Experimental Equipment for Checking Sources of Aerodynamic Sound.....	620
<i>M. Kučera, L. Mareš, J. Votlučka</i>	
Environmental Engineering of Buildings	622
<i>R. Nový, F. Drkal, K. Brož, J. Hemerka, K. Hemzal, J. Bašta</i>	
The Influence of Random Multiaxial Nonproportional Stress on the Fatigue Life of Machine Parts	624
<i>M. Růžička, J. Papuga, M. Balda, J. Svoboda</i>	
The Optimization of Aeration Equipment.....	626
<i>J. Andreovský, J. Melichar, J. Novotný, M. Brich</i>	
Design Tool for Modern Buildings Control Strategy.....	628
<i>J. Becvar, F. Drkal</i>	
Experimental Solution of Air Flow in a Ventilation Knot of the Road Tunnel.....	630
<i>V. Zbořil, K. Hemzal, M. Trubačová, J. Schwarzer</i>	
The Heat Transfer Coefficient Measurement of Solar Energy Collector Glazing Cover	632
<i>B. Šourek</i>	

8. SECTION PRODUCTION SYSTEMS, TECHNOLOGY, TECHNOLOGICAL, PROCESSES AUTOMATION

Simulation in Modern Manufacturing Design	636
<i>T. Růžička</i>	
Research of Laser Micro-Milling Technology and the Examples of Industry Utilization....	638
<i>Z. Hovorková</i>	
5-AXIS MILLING	640
<i>M. Vrabec, P. Hampl, J. Kafka</i>	
Implementation of GPS System into Education in Subject of Department of Manufacturing Technology.....	642
<i>P. Hampl, J. Podaný</i>	

Best of Breed.....	644
<i>K. Hartman</i>	
Models of Automated Production Systems.....	646
<i>M. Draessler, J. Žáček</i>	
Innovation of Courses in Quality Control.....	648
<i>V. Chmelík</i>	
Methodology Objective Evaluation of the Quality of Soldered Joints.....	650
<i>K. Dušek, J. Urbánek</i>	
Modeling of Process Dynamics in Glass Industry.....	652
<i>P. Havel</i>	

9. ENERGETICS AND POWER ENGINEERING

Solid State Synchronized Switcher.....	656
<i>P. Mindl, Z. Čeřovský</i>	
Position Sensors for High Speed Motors with Magnetic Bearings.....	658
<i>J. Pavelka, B. Syrovatka, D. Vydra</i>	
Optimal Control of Active Magnetic Bearing.....	660
<i>L. Synek</i>	
Hole Drilling Method for Stress Identification of Materials and Structures.....	662
<i>K. Vitek, K. Doubrava, T. Mareš, M. Španiel</i>	
Optimization of The Hole Drilling Method Principle Conditions for Stress Identification.....	664
<i>K. Vitek</i>	

10. NUCLEAR ENGINEERING

Pigment Identification with X-Ray Fluorescence Analysis.....	670
<i>T. Trojek, T. Čechák, M. Musilek, D. Králová</i>	
Radioactive Aerosol Capture in the Containment of a Nuclear Power Plant.....	672
<i>T. Trojek</i>	
Prompt Evaluation of the Air Kerma Rate in Environmental Radiation Fields Monitoring.....	674
<i>J. Klusoň, L. Thinová, T. Čechák</i>	
MOX Utilization: Evaluation of Impacts on Radioactive Waste Inventory.....	676
<i>A. Zib, L. Novotná, P. Šebela, K. Matějka</i>	

Nuclear Reactor Physics – e-Learning on Internet	678
<i>J. Zeman, M. Kubešová, J. Rataj</i>	
Nuclear Facilities, Nuclear Safety and Radiation Protection.....	680
<i>K. Matějka, J. Zeman</i>	
Operational Reactor Physics – Multimedia CD-ROM	682
<i>L. Sklenka, M. Šedlbauer</i>	
Prospects and Acceptance of Nuclear Power Engineering in Czech Republic.....	684
<i>D. Kobylka, J. Zeman, K. Matějka</i>	
Importance of the Source Term Description in the Safety Assessment of Spent Fuel Disposal	686
<i>D. Vopálka</i>	
Studies of PbWO ₄ Crystals Behavior for Electromagnetic Calorimeters on High Energy Electron and Pion Beams	688
<i>J. Blaha, J. Fay, M. Finger, M. Finger, S. Gascon-Shotkin, B. Ille, M. Slunečka</i>	
Effective Dose Calculation Using Radon Daughters and Aerosol Particles Measurement in Bozkov Dolomite Cave.....	690
<i>L. Thinova, Z. Berka, E. Brandejsova, V. Zdímal, D. Milka</i>	
Spectrometry Characteristic of Photon-Fields and Atmospheric Radionuclide Deposits Monitoring in One Part of Southern Bohemia.....	692
<i>J. Kluson, L. Thinova, T. Cechak, T. Trojek</i>	
The Alpha Ray of Radon Daughters in Water and in Air Used the Detection Unit “YAPMARE” with Scintillation Detector YAP: Ce Measurement.....	694
<i>L. Thinova, A. Kunka, P. Malý, F. Notaristefani, K. Blazek, T. Trojek, L. Moucka</i>	
Development of Independent Power Protection System for VR-1 Training Reactor	696
<i>M. Kropík, M. Juříčková, K. Matějka</i>	
Testing of the Upgraded Control System of the VR-1 Training Reactor.....	698
<i>M. Juříčková, V. Cháb</i>	
Control System Experience.....	700
<i>V. Cháb, M. Kropík</i>	
Determination of Energy Neutron Spectrum at Reactor VR-1 Sparrow	702
<i>K. Katovský, A. Kolros, P. Paluska</i>	
Integration of Czech Nuclear Engineering Education into European Educational System..	704
<i>L. Sklenka, K. Matějka, J. Rataj, K. Katovský</i>	
Processing and Analysis of Results from Experimental Measurements with Subcritical Blanket BLAŽKA and External Neutron Source NG2 at Cyclotron in Nuclear Physics Institute, Academy of Sciences of the Czech Republic	706
<i>J. Rataj</i>	
Participation of DNR FNSPE CTU in the Project of the Nuclear Transmutation System SFINX - Irradiation Experiment with the Module B417 at the Training Reactor VR-1	708
<i>J. Rataj, K. Matějka, A. Kolros</i>	

Delimitation of Fullerit Use Potential for Radiation Detector Manufacturing	710
<i>V. Linhart, E. Belas, J. Sodomka, B. Sopko</i>	
Use of TL in-vivo Dosimetry for Determination of Radiation Burden of Patients due to X-ray Examinations	712
<i>L. Novák, L. Musílek</i>	
Determination of Neutron Spectrum in REGATA Irradiation Channels of IBR-2 Reactor.....	714
<i>A. Kolros, K. Katovský, S. Pavlov</i>	
Correction of Neutron Detection System Dead Time	716
<i>A. Kolros</i>	
Determination of Hafnium in Zircon by INAA on Training Reactor VR-1 Sparrow	718
<i>R. Štaubr, A. Kolros, M. Vobecký</i>	
Innovation and Development of Basic Practical Exercises from Radiation Detection and Dosimetry	720
<i>T. Čechák, J. Gerndt</i>	
Getting More Accurate Estimation of ²²² Rn - Dose Obtained from Integral Measurement Using Continuale Shape of Volume Activity Analysis in Residential Area.....	722
<i>A. Ridžiková, A. Froňka, L. Moučka</i>	

11. CHEMISTRY

Fate of Heavy Metals in Urban Freshwater Ecosystems	726
<i>D. Komínková, J. Nábělková</i>	
Radiation Removal of Lead from Aqueous Solutions in Presence of Solid Promoters.....	728
<i>M. Pospíšil, V. Čuba, B. Drtinová, J. Dolanský</i>	
Seasonal Variations in the Disinfection By-Products Precursor Profile of a Surface Water in Flaje Catchment.....	730
<i>A. Grünwald, K. Slavičková, M. Slaviček, B. Šťastný, R. Veselý</i>	
Removal of Natural Organic Matters from Water.....	732
<i>A. Grünwald, K. Slavičková, M. Slaviček, B. Šťastný, K. Vlčková</i>	
The Assessment of Mean Molecular Weight of Aldrich Humic Acid.....	734
<i>K. Štamberg, P. Beneš</i>	
Use of the Free-Liquid Electrophoresis for the Analysis of Thorium Complexation with Humic Acid at Low pH Values	736
<i>P. Beneš</i>	
The Modeling of Spectral and Photochemical Properties of Diimine Transition Metal Carbonyl Complexes.	738
<i>J. Šebera, S. Zdlíš, A. Vlček</i>	

Applicability Limitations of Hummel-Dreyer Method for Radionuclides-Humic Acids Equilibria Studies: Complexation of Cobalt (II), Europium (III) and Thorium (IV) with Aldrich Humic Acid	740
<i>J. Dolanský, B. Drtinová, M. Cabalka, D. Vopálka, P. Beneš</i>	
Prospects of Study of the Radiation Corrosion in the Water/Carbon Steel Systems	742
<i>S. Neufuss, V. Čuba, A. Vokál, M. Pospíšil, R. Silber</i>	
Sorbents of Toxic Metals and Radionuclides Based on Immobilized Humic Acid and Chitosan.....	744
<i>G. Mizerová, J. Mížera, V. Machovič, L. Borecká</i>	
Utilization of Ionizing Radiation for Removal of Co (II) From Aqueous Solutions	746
<i>P. Kovařík, M. Pospíšil, V. Čuba</i>	
Determination Methods of Selected Chemical Parametres of Water – Steel System Exposed to Ionizing Radiation.....	748
<i>M. Buňata, V. Múčka, V. Čuba, R. Silber</i>	
Decontamination of Soils by Electrochemical Means	750
<i>M. Němec, J. John</i>	
Electron Beam Wastewater Treatment Up-Flow Irradiation Device	752
<i>R. Silber, V. Múčka, M. Pospíšil, V. Čuba</i>	
Comparison of Sorption Properties of Malonamide-Based Solid Extractants with the Behaviour of their Active Components in Liquid-Liquid Extraction	754
<i>J. Šuláková, J. John, F. Šebesta</i>	
Elimination of Interfering Activities from Solid Phase Extractants in Radiochemical Neutron Activation Analysis of Biological and Environmental Samples.....	756
<i>M. Lučaníková, J. Kučera, F. Šebesta, J. John</i>	
Implantation of Nitrogen Ions into the Nickel Oxide Catalyst	758
<i>V. Múčka, F. Černý, B. Sopko, V. Čuba, D. Tischler, M. Buňata, D. Kobliha</i>	

12. BIOMEDICAL ENGINEERING

Biomechanics of Treatment of Children Axial Skeleton Deformities	762
<i>J. Čulík</i>	
Modelling of Influence of Tracheal Gas Insufflation on Artificial Lung Ventilation.....	764
<i>V. Kopelet, K. Vališová, K. Roubík</i>	
Optical Ultrasound Probe Localization for 3D Imaging in Medicine.....	766
<i>Z. Szabó</i>	
A Wavelet Approach to Biomedical Shape Description	768
<i>R. Šmíd</i>	
Kinematics of Human Masticatory Movements in Dependence on Bolus Pattern.....	770
<i>T. Goldmann, L. Himmlová</i>	

Efficient Compensation of the Light Attenuation with Depth in Confocal Microscopy	772
<i>M. Čapek, L. Kubínová</i>	
Modular Measuring Chain “ADVANCED PDA” Designated for Support of the Medical and Biomedical Engineering Research	774
<i>K. Hána, R. Fiala, J. Kašpar, P. Smrčka</i>	
Mobile Device for Diagnostic Measuring of Galvanic Cells in Oral Cavity.....	776
<i>K. Hána, J. Procházková, P. Smrčka, H. Kučerová, J. Kašpar, M. Míkovský</i>	
Realistic Simulation in Joint Replacement of Human Joints.....	778
<i>L. Franta, J. Pražák</i>	
Development of Algorithm for Analog Data Acquisition by the PDA in the Real-Time	780
<i>K. Hána</i>	
Measuring and Processing of EEG Signal in the High Noise Environment.....	782
<i>J. Kašpar, P. Smrčka, K. Hána, J. Mužik</i>	
The Design of Architectures for Multiagents Systems for Health Service.....	784
<i>P. Novák, M. Fejtová</i>	
Ultrasonic Immersion Measurement of CFRP Composites Elastic Coefficients – Preliminary Study for Cortical Bone Elastic Properties Assignment	786
<i>T. Goldmann, M. Landa, H. Seiner</i>	
Combination of Laser Fabricated ZrO ₂ and HA Layers for Coating of Tooth Implants.....	788
<i>P. Mašínová, M. Jelínek, T. Kocourek, K. Jurek, V. Studnička, W. Mróz, T. Dostálová, K. Smetana</i>	
ATR BIOLAB - System for Achilles Tendon Reflex Measurement	790
<i>P. Kneppo, M. Týšler, V. Rosík, J. Ždiňák, J. Švehlíková</i>	
Evaluation of the Mechanical Loading Change Influence on the Hip Joint Osteoarthritis Development.....	792
<i>Z. Horák, M. Stupka, J. Martiník, J. Vrána</i>	
Non-linear Analysis of the Heart Rate Variability – a New Cybernetic Gate Into Central Nervous System	794
<i>P. Smrčka, K. Hána, J. Kašpar</i>	
E-learning Course Development to Support Teaching of Programming Tools	796
<i>M. Fejtová, J. Fejt, P. Smrčka</i>	
Unsteady Fluid Flow with Focus on Hemodynamics	798
<i>J. Matěcha, H. Netřebská, J. Adamec</i>	
Using the PIV Method for Blood Flow Investigation.....	800
<i>J. Matěcha, K. Vališová, J. Adamec</i>	
Experimental Line to the Self-excited Oscillation of the Thin-walled Elastic Tubes.....	802
<i>H. Chlup, F. Maršík, S. Konvičková</i>	
System for Evaluation of Microwave Applicators.....	804
<i>J. Herza, T. Martan</i>	

Physical Model of the Bloodstream Systemic Resistance of Human.....	806
<i>H. Chlup, S. Komvičková</i>	
Methods and Technical Tools for an Analysis of Sudden Cardiovascular Death in the Horse	808
<i>J. Holčík, K. Hána, P. Kozelek, M. Kohut, R. Fiala</i>	
Calculation of the Knee Muscle Forces During Squatting.....	810
<i>M. Vilímek, M. Sochor</i>	
Is the Knowledge of the Real Activation Signal Necessary in the Muscle Forces Calculation?.....	812
<i>M. Vilímek, M. Sochor</i>	
An Artificial Neural Network in Prediction of Elbow Actuators Forces.....	814
<i>J. Vejpustková, M. Vilímek, M. Sochor</i>	
The Sensitivity of the Muscular Parameters to the Muscle Force Prediction.....	816
<i>J. Vejpustková, M. Vilímek, M. Sochor</i>	
Corticothalamic Model of Human Brain	818
<i>R. Novák, K. Hána</i>	
Intelligent Systems in Medicine.....	820
<i>L. Lhotská, J. Macek, J. Rieger, V. Chudáček</i>	
Driver's Vigilance Identification by Means of RBF Neural Network – Influence of Artefacts.....	822
<i>M. Mráz, K. Hána, M. Šnorek</i>	
Method and Technological Tool for Early Non-Invasive Diagnostics of Bronchogenical Carcinoma by Means of Temperature Measuring in Air Passages	824
<i>J. Holčík, K. Hána, P. Smrčka, J. Kašpar</i>	
Wear Resistance Evaluation of Implants with DLC Coat.....	826
<i>R. Sedláček, J. Rosenkrancová</i>	
Laser Beam Interaction with Material during the Production of Stents	828
<i>P. Císařovský, J. Dunovský</i>	
Our Experiences with Tensile Tests of Arterial Layers.....	830
<i>L. Horný, H. Chlup, R. Sedlacek, S. Konvickova</i>	
New Approach to Evaluate Risk of Aneurysmatic Rupture.....	832
<i>L. Horný, J. Vtípil</i>	
Determination of Mechanical Properties of Human Coronary Artery.....	834
<i>J. Benes, L. Horný, S. Konvickova, H. Chlup</i>	
Modelling of the Human Respiratory System	836
<i>M. Rozanek, K. Roubik</i>	

13. CIVIL ENGINEERING

Limit States and Design of Materially Non-Homogenous Structures	840
<i>J. Studnička, J. Macháček, J. Dolejš, A. Kuklíková</i>	
Iron Release from Corroded Iron Pipes in Drinking Water Distribution System	842
<i>A. Grünwald, K. Slavičková, M. Slaviček, B. Šťastný</i>	
The Effect of Residence Time on the Biological Stability of Water in a Distribution System.....	844
<i>A. Grünwald, N. Strnadová, B. Šťastný, K. Slavičková, M. Slaviček</i>	
Application of Cooled Ceiling.....	846
<i>V. Zmrhal</i>	
Rotational Restraint Of Purlins – Effect Of Primary Loading.....	848
<i>T. Vraný</i>	
Climatic Effects on Composite Steel and Concrete Bridges	850
<i>J. Římal, V. Jelínek, J. Chod, K. Maleček, A. Kovářová, V. Sopko, J. Zaoralová, H. Horká, S. Kasíková, L. Samek</i>	
Prospects of Renewable Materials and Resources in Construction Industry.....	852
<i>M. Hezl, P. Svoboda</i>	
Modelling of Impacts of Land Use and Technical Measures to Storage Capacity of the Basin	854
<i>K. Uhlířová</i>	
Low Temperature Bituminous Binders and Their Impact on Selected Rheological Properties of Asphalt Mixes.....	856
<i>J. Valentin</i>	
Measurement of Temperature in Concrete Bridges	858
<i>O. Tomaschko, V. Hrdoušek</i>	
Modelling of Chlorine Decay in a Part of South Bohemian Drinking Water Distribution System	860
<i>K. Slavičková, A. Grünwald, M. Slaviček, B. Šťastný, K. Štrausová</i>	
Laboratory test of Reinforcing Grids in Compacted Asphalt Mixes	862
<i>P. Mondschein</i>	
Soil Erosion Assessment in Larger Watersheds Using GIS Tools	864
<i>J. Krása, T. Dostál, K. Vrána</i>	
Solving Gap in the Prefabricated Bearing Wall	866
<i>K. Sládek</i>	
Ensuring of a Pit, Underpinning of Existing Structures – on-Line Course	868
<i>Z. Jeřichová, M. Dubnová, R. Míkula</i>	
Application of Artificial Neural Network to Control the Coagulant Dosing in Water Treatment Plant.....	870
<i>A. Grünwald, P. Fošumpaur</i>	

Optimization of a Turbine Intake Structure	872
<i>P. Fošumpaur, F. Čihák</i>	
Adaptive Control of Water Resources in Climate Change Conditions	874
<i>P. Fošumpaur, F. Klouček</i>	
A Neural Network Approach for the Optimisation of Water Treatment Plant Management	876
<i>A. Grünwald, P. Fošumpaur</i>	
Fatigue of Composite Steel and Concrete Structures	878
<i>J. Mareček, J. Studnička</i>	
Using SAR Interferometry for Detecting Landslides and Subsidence in the Coal Basin in Northern Bohemia.....	880
<i>J. Kianička, I. Čapková</i>	
Application Of Ums and Sisim Numerical Models for Classification of Brownfields in the Czech Republic.	882
<i>J. Hajaš, V. Kuráž</i>	
Connection of HDM 4 System with Current Statistic and Diagnostic Systems	884
<i>O. Ryneš</i>	
Improvement of Concrete Surface Layer by Epoxide Coatings	886
<i>L. Svoboda</i>	
Risk Engineering and Reliability of Technical Systems	888
<i>M. Holický, J. Marková, B. Novotný, M. Sýkora</i>	
The Measuring of Hygric and Thermal Properties of Clay Plasters	890
<i>R. Vějmelka, E. Mňahončáková, J. Toman, J. Drchalová</i>	
Verification of Laser Scanning Systems Possibilities	892
<i>T. Křemen</i>	
Using of 3D Scanners in Geodesy and Historical Monuments Care	894
<i>K. Pavelka, J. Pazdera, J. Záleská</i>	
Semi-rigid Joint of Timber Frame.....	896
<i>R. Vyhálek</i>	
Ecological Fly Ash-Sludge Composites.....	898
<i>E. Pospíšilová</i>	
Soil Erosion and Surface Runoff Problems Assessment with GIS Tools Application.....	900
<i>K. Vrána, T. Dostál, M. Dočkal, H. Nováková, P. Koudelka, V. David, J. Krása, J. Koláčková, M. Bečvář</i>	
Experimental Background for the Load Capacity Analysis of the Nature Stone Masonry	902
<i>M. Vokáč, P. Bouška</i>	
Determination of Principles for Design of Small Watercourses Rehabilitation	904
<i>P. Koudelka, T. Mrázková, K. Vrána</i>	

Functional Qualification and Optimization of Building Structures	906
<i>J. Witzany, J. Šejnoha, J. Procházka, J. Studnička, J. Jettmar, F. Lehovc, V. Vorel, H. Krejčířiková, J. Jarušková</i>	
On Flexible Pavement Design	908
<i>F. Luxemburk, B. Novotný</i>	
Method of Optimal Alternative Selected Technological Method Realization of Underground Buildings from Technological-Economy Perspective	910
<i>K. Štrobl</i>	
Mankind and Their Environment.....	912
<i>J. Šafránková, W. Drozenová</i>	
Numerical Simulation of Fibre Concrete Members.....	914
<i>A. Kohoutková, V. Křístek, I. Broukalová</i>	
Testing of Behaviour of Fibre in Structure of Concrete	916
<i>O. Vlasák, K. Trtik</i>	
Reliability of Timber Members and Joints.....	918
<i>P. Kuklík, A. Kuklíková</i>	
Environmental Impact of Buildings – Life Cycle Assessment	920
<i>M. Vonka</i>	
Structured Approach to Estimation of Surface Runoff from Small Watersheds.....	922
<i>V. David</i>	
Determination of Crack Width of Fibreconcrete Elements.....	924
<i>P. Machula, A. Kohoutková, I. Broukalová</i>	
Determination of Material Characteristic of Fibreconcrete from Laboratory Tested Beams Behavior for Structural Analysis by Inverse Analysis.....	926
<i>I. Broukalová, A. Kohoutková</i>	
Serviceability Limit State of Prestressed Concrete Bridges	928
<i>V. Křístek, A. Kohoutková, J. Vitek</i>	
Estimation of the Soil Hydraulic Properties in Headwater Territory.....	930
<i>M. Dohnal, J. Dušek, T. Vogel, M. Šanda</i>	
Competitive Corrugated Sheeting Through Connection Fire Resistance	932
<i>P. Studecká</i>	
Monitoring of Dynamic Behavior Changes of Two Types of Structures.....	934
<i>T. Plachý, M. Polák</i>	
Stochastic Response and Stability of Imperfect Structures with Random Additive and Parametric Excitation	936
<i>J. Náprstek, A. Kohoutková, V. Křístek</i>	
Effect of Cladding on Stability Parameters of Framed Steel Structure	938
<i>V. Hapl, T. Vraný</i>	
Sustainable Development and Concrete Structures	940
<i>B. Teplý, A. Kohoutková, P. Hájek, V. Křístek</i>	

Mapping of Recultivated Areas Using Remote Sensing.....	942
<i>P. Junek</i>	
Research into Non-Force Effects and Aggressive Environment Affecting the Ageing of Historical Structures with Special Emphasis on Charles Bridge in Prague.....	944
<i>J. Witzany, M. Gregerová, P. Pospíšil, A. Materna, T. Klečka, J. Kolisko, Š. Šílarová, E. Burgetová, T. Čejka, J. Pašek, R. Wasserbauer, R. Zigler, P. Cikrle</i>	
Completing and Analysing of Experimental Geodetic Network for Movements Monitoring of Historical Structures	946
<i>T. Jiříkovský</i>	
Object Analysis of Mathematical Model of Geodetic Networks Adjustment.....	948
<i>J. Pytel</i>	
Fire Resistance of Timber Construction	950
<i>P. Hejduk, P. Kuklík</i>	
Quazi-Random Numbers Generation Using Simulated Annealing	952
<i>M. Lepš, Z. Vítangerová</i>	
Progressive Composite Steel-Concrete Element – Stage 2.....	954
<i>J. Moták</i>	
Influence of Climate Change over Water Management Systems.....	956
<i>L. Satrapa</i>	
Approach to Risk Evaluation for Water Management Systems.....	958
<i>L. Satrapa</i>	
Local Buckling of Flange under Fire	960
<i>J. Charvát, F. Wald</i>	
Comparison of Two Conceptually Different Pesticide Leaching Models in Vadose Zone.....	962
<i>J. Dušek, T. Vogel, M. Dohnal, M. Šanda</i>	
Analysis of Clayey Soils Parameters Using Isotropic Consolidation Triaxial Tests	964
<i>T. Janda</i>	
Modelling of Hydraulic Jump in Closed Conduit.....	966
<i>P. Fatka, J. Pollert, Z. Koniček</i>	
Masonry Arch Bridges	968
<i>T. Dvorský, V. Kukaň, P. Řeřicha</i>	
Accuracy Evaluation of Wire Strain Gages for Dynamic Measurements of Engineering Structures	970
<i>M. Černý</i>	
Standardization of the Validation Criteria's for the Dynamic Landscape Development and the Landscape Management	972
<i>A. Vokurka</i>	
Experimental Research of Structural Materials and Technologies	974
<i>F. Luxemburk, B. Novotný, P. Bouška, P. Mondschein</i>	

Uncertainty in Open Channel Analyses under Extreme Flow Conditions.....	976
<i>P. Sklenář, M. Salaj</i>	
Testing of RC Beams Strengthened by CFRP in Bending.....	978
<i>M. Černý</i>	
Thermal-Moisture Problems of External Skins of Civic Building-Distribution-Effect of Moisture and Temperature on Biodeterioration.....	980
<i>P. Bednářová, D. Bedlovičová</i>	
The Automatic Classification of B&W Aerial Photos	982
<i>L. Halounová</i>	

14. ARCHITECTURE, TOWN PLANNING, GEODESY AND CARTOGRAPHY

Optimum Laser Systems in Industrial Metrology (part 6).....	986
<i>M. Kašpar, R. Blažek, P. Hánek, J. Pospíšil, M. Štroner, L. Linková</i>	
Development of the Laserscanner, Testing of the Influence of the Materials and the Configuration.....	988
<i>J. Pospíšil, M. Štroner, B. Koska, T. Křemen, M. Kašpar</i>	
Rainfall Simulator Aided Research of Soil Erosion Using Field Data	990
<i>J. Koláčková, T. Dostál</i>	
Generalization and Intergation of Geodata	992
<i>J. Zaoralová</i>	
Railway Heritage in the Czech Republic	994
<i>T. Šenberger, M. Zlámaný</i>	
Testing Possibilities of Using a Standard Digital Camera at Laser and Optic Rotating Scanner. Investigating Method to Evaluate Accuracy of 3D Scanning Systems.....	996
<i>B. Koska</i>	
Information System Dikat-P	998
<i>J. Zaoralová</i>	
Exhibitions adn Presentations in the Atrium of the Faculty of Civil Engineering and Architecture	1000
<i>K. Kroftová , V. Šlapeta</i>	
Buildings in Decline in the Textile Industry – Possible New Uses	1002
<i>M. Koiš</i>	
Bohemian and Moravian Breweries.....	1004
<i>Š. Jiroušková, L. Doležal, T. Kužel</i>	
The Electronic Interactive Textbook/Publication “Technical and Industrial Buildings in Prague”	1006
<i>B. Fagner, Š. Jiroušková, L. Popelová, V. Valchářová, P. Vorlík, M. Zlámaný</i>	

Research of Historical and Contemporary Architecture – 6th Phase (Year 2004).....	1008
<i>P. Urlich, M. Ebel, B. Fanta, E. Fantová, B. Filsaková, M. Hauserová, K. Kibic, P. Kalina, M. Rykl, O. Ševčík, J. Škabrada, P. Škranc, P. Vlček, P. Vorlík</i>	
Model Methods of Design, Model and Presentation Techniques in Architecture	1010
<i>M. Fischer, R. Hanus, J. Pospíšil, D. Smitka, T. Šenberger</i>	
Brownfields and Their Consequences.....	1012
<i>Z. Kramářová</i>	
Brownfields and Industrial Heritage – the Tools for the Revival of Towns and Landscapes.	1014
<i>T. Šenberger, F. Štědrý</i>	
Formation of Planners in the Next Decade – Trends and Strategy	1016
<i>I. Horký, A. Mansfeldová</i>	

15. TRANSPORTATION, LOGISTICS, ECONOMY AND MANAGEMENT

Reliability Aspects in Contemporary Management.....	1020
<i>R. Flegl</i>	
Decision Making for Production.....	1022
<i>M. Kavan</i>	
Effectivity of Research	1024
<i>H.Nassereddine, M.Ayoubi</i>	
Defining and Assessing E-learning	1026
<i>D. Tvrđiková</i>	
The Risk Modified Strategy Modeling	1028
<i>P. Dlask, V. Beran</i>	
Simulation and Value at Risk	1030
<i>V. Beran, P. Dlask</i>	
The Investigation of the Unexacting Restructuring of Basic Internal Relations in Small and Medium Enterprises.....	1032
<i>G. Tomek, V. Vávrová</i>	
The Effect of Transport Infrastructure on Regional Development	1034
<i>F. Lehovec</i>	
Upgrading the Communication Skills and Managerial Abilities of PhD Students of the Czech Technical University in Prague.....	1036
<i>B. Duchoň, V. Soyková</i>	
The Question of Effectiveness Evaluation of R&S Activities	1038
<i>M. Soukup, M. Rejha, H. Nassereddine</i>	
Computer Based Training of Air Transport Pilots at CTU	1040
<i>P. Hvězda, B. Stavovčík, T. Mikl</i>	

The Analysis of Traffic Networks and Attended Region Interaction	1042
<i>L. Týfa, M. Vachtl</i>	
Public Orders in the Praxis – Software	1044
<i>R. Heralová, J. Franěk</i>	
Analysing and Measuring Quality in Services.....	1046
<i>B. Košetická, J. Kožíšek</i>	
Input-Output Models as the Tool of Target Costing Method.....	1048
<i>L. Zeman, K. Macík</i>	
Size Effect in the Risk Theory	1050
<i>P. Erben</i>	
Problems of the Traffic Safety Evaluation Objectivity	1052
<i>P. Slabý, M. Hála, P. Karličý</i>	
Application of Balanced Scorecard in Siska Printing Works	1054
<i>J. Beneš, M.Volf</i>	
Utilization of Picocell Nets for Transmission Information in Transportation	1056
<i>J. Bláha, Z. Bělinová, J. Kazda</i>	
Human Factor in Production Management	1058
<i>J. Lastivková, Z. Molnár</i>	
Two Special Transformations of Linear Programs Used to Decision Making under Incomplete Information about Scenarios Probabilities.....	1060
<i>L. Vaniš</i>	
The Role of Foreign Direct Investment in Restructuring of Manufacturing Industry	1062
<i>H. Pačesová</i>	
Recruitment Process.....	1064
<i>T. Šulcová</i>	
The Aerodynamic Characteristics of Helicopter Main Rotor	1066
<i>R. Pohl, J. Šesták</i>	
The Sociological Research on the CTU Students Opinions	1068
<i>J. Šafránková</i>	
Interactive Model of Feasibility Study	1070
<i>J. Frková</i>	
Integration of Utility Characteristics of Engineering Products for Determination of Their Market Prices	1072
<i>J. Trkal</i>	
Problematic of Reconstruction of Diesel Locomotives on Compressed Natural Gas Operation	1074
<i>B. Drápal, C. Novotný</i>	
Two Models Supporting Cost Decision-Making	1076
<i>M. Zralý, M. Plachý, O. Šmíd</i>	

Barriers to IT Outsourcing in Czech Manufacturing Enterprises	1078
<i>J. Zahradník</i>	
Opportunities and Threats of the Czech Industry Connected with Progress of the Electricity Prices.....	1080
<i>Z. Jobánek</i>	
Problematics of Digital Toll in Czech Republic	1082
<i>J. Svoboda, P. Mačat</i>	
System Dynamics Models in Teaching Process.....	1084
<i>D. Vytlačil</i>	
New Technical Specifications TP 170 for Road Pavements Design.....	1086
<i>L. Věbr</i>	
The Problems of Concrete Road Pavements.....	1088
<i>L. Věbr</i>	
Innovation of a Specialized Workplace for AIP Systems Training in Road Pavement Engineering	1090
<i>L. Věbr</i>	
Using Modern Methods for Urban Roads Design	1092
<i>L. Věbr</i>	
Profiling of Approaches to Project Management.....	1094
<i>L. Michalík, M. Prajer</i>	
Optimalization of Flight Plannig Process at General Aviation Operator.....	1096
<i>T. Mikl, J. Chmelík, M. Kameník, P. Hvězda</i>	
Management and Economics of Post and Delivery Services.....	1098
<i>O. Hölzl, P. Stejskal</i>	
Personal Vehicle Occupancy in Relation to the Season, the Day of Week and the Hour of Day.....	1100
<i>Z. Čarská</i>	
System for Monitoring of Hazardous Goods Transport.....	1102
<i>M. Svítek</i>	
ITS Architecture of the Czech Republic	1104
<i>M. Svítek</i>	

Section 6

MECHANICS
&
THERMODYNAMICS

A Construction of a Heat Transfer Research Facility

M. Knob, J. Adamec, P.Šafařík

`martin.knob@fs.cvut.cz`

ČVUT v Praze, Strojní fakulta, Technická 4, 166 07 Praha 6

Heat transfer is still one of the most challenging problems in almost all branches of engineering. The specific needs of particular engineering branches make huge differences between the approaches and methodologies used in the research, ranging from heat and mass transfer in civil engineering (i.e. the calculation of both the heat losses and the humidity condensation), through cooling of the electronic equipment in electrical engineering, to various applications in mechanical engineering (e.g. drying of paper, or construction of heat exchangers). In each of the above mentioned application, different approach to the research is used, since different outcomes are expected.

In mechanical engineering, one of the most frequent topics is the increasing of the energy sources efficiency. This can be done using either the heat recuperation (like in modern stationary gas turbines), or the cogeneration (e.g. in a combined cycle power plants). Regardless of the above mentioned ways of increasing the use value, increasing the highest temperature, reached in the thermal cycle, always leads to the improvement of the efficiency, and can be, therefore, combined with the above mentioned methods of efficiency raise.

In future, gas turbines are expected to play a key role in power supply policy, namely their utilization as a local low output source of both the electric and the thermal energy is expected, whether oil or hydrogen is used as the fuel. In order to reach the maximum efficiency of such a gas turbine, the maximum temperature in the cycle should be as high as possible. Recently, the temperatures in the combustion chamber and in the first turbine- stage are very close to the melting point of their material. Therefore, an intensive cooling of them is absolutely necessary.

A standard way of combustion chamber cooling is the film cooling, which is a powerful technique, ensuring its compactness and sufficiently long life- time.

Because of the centrifugal force, the first turbine stage is exposed to extreme mechanical stresses, the effect of which is raised by the high temperature, needed for the high efficiency of the turbine. These two factors give raise to a strong need to cool the blades down.

Recently, two basic ways of cooling the blades are subject to research. The first is utilization of the above mentioned film- cooling, the disadvantage of which is a severe decrease of the aerodynamic performance of the blade, caused by the mixing of the cold air injected into the expanding exhaust gases. The second way is internal cooling of the blade, which can lead to the suppression of the cold air injected through the bleeding holes during the film cooling.

Recently ([1]), the rib induced secondary flow was discovered as the most powerful way of heat transfer enhancement in the internal blade- cooling and therefore the rib- roughened channels are considered the best solution. Although since [1] was published, plenty of reports have been written, severe lack of basic hydro dynamical data still persists. The researchers focus their attention on various rib arrangements and report the Nusselt number distributions together with the pressure drop data. So far, no researcher has focused on the physical processes accompanying secondary flow.

The aim of this research is the description of the secondary flow phenomenon through simplification. In order to obtain reliable data, an aerodynamic research facility was constructed. The facility enables, due to its module construction, the research in both the internal and the external aerodynamics.

The research in internal aerodynamics is limited to channels of rectangular cross- sections with aspect ratio 2:3. This limit is caused by the construction of the original aerodynamic contraction, needed to obtain a uniform velocity profile, free of any disturbances or turbulent fluctuations. This part of the facility can be used for any rib arrangement and, also, for theoretical research of secondary flow, induced by different ways, than by rib- roughening. One of these ways can be an injection of an additional fluid by suitably arranged bleeding holes ([2]). If the bleeding holes will be arranged in a contra running directions with a transverse distance, the injected fluid will have a moment of momentum, which will be redistributed in the flow by the shear stress. The redistributed moment of momentum introduces swirl into the main flow- the secondary flow is created ([3]).

The above mentioned way of inducing the secondary flow brings many advantages for basic research of this phenomenon, e.g. the secondary flow is induced with no influence of recirculation zones downstream of possible ribs.

The research in external aerodynamics can be focused namely on the research of impinging jets, both the planar and the axisymmetric.

The research of plane impinging jet can be connected to the research of the secondary flow by the idea, that the flow structure in a channel with secondary flow is similar to the impingement of plane jet into a rectangular cavity ([4]).

References:

- [1] KIML, R. – MOCHIZUKI, S. – MURATA, A.: *Heat Transfer Mechanism in a Rectangular Passage with V- and H- Shaped Ribs*, Journal of Flow Visualisation and Image Processing, vol. 8 2001 pp. 51–68.
- [2] NAKABE, K. – SUZUKI, K – INAOKA, K. – HIGASHIO, A. – ACTON, J.S. – CHEN, W.: *Generation of Longitudinal Vortices in Internal Flows with an Inclined Impinging Jet and Enhancement of Target Plate Heat Transfer* International Journal of Heat and Fluid Flow 1998 pp. 573–č. 581.
- [3] KNOB, M. – SLÁDEK, A. – ADAMEC, J.: *Ideový návrh tepelného výměníku* Rajcecké Teplice 2004, pp. 169–174.
- [4] KNOB, M. – ŠAFARÍK, P. – ADAMEC, J.: *The Effect of the Side Walls on the Heat Transfer Characteristics of a Two- Diemensional Impinging Slot Jet* Proceedings of Colloquium Fluid Dynamics 2004 pp. 67–70.

This research has been supported by CTU grant CTU0404912.

Multimedia Support for Teaching Mechanics

J. Vondřich, R. Havlíček, K. Belda

vondrich@fel.cvut.cz

Department of Mechanics and Materials Science, Faculty of Electrical Engineering, Czech Technical University, Technická 2, 166 27 Prague 6, Czech Republic

It has been demonstrated in numerous papers [1-4] that numerical solutions of mechanical, hydro-mechanical, electromechanical and other system are an inherent part of the Bachelors, Masters and PhD studies at CTU in Prague in the Faculty of Electrical Engineering, in the courses of Mechanics, Dynamics of Mechanical Systems and Dynamics of Processes. The paper presents the modelling and simulation of those systems with one and more degrees of freedom, their numerical solution with Matlab and Simulink and applications for teaching mechanics via the web (<http://volt.feld.cvut.cz/vyuka/DMS/index.htm>). Different numerically solved models; mechanical, hydro-mechanical, electromechanical systems with driven motors, load moments and control units, with Matlab and Simulink, are presented on the web and applied in Mechanics courses.

First the two video programs on the web pages demonstrate the building of models of machinery, the determination of the number of degrees of freedom and methods of compilation of the equations of motions. These methods are explained in several models with one degree of freedom. The commands of Matlab are explained on the web. These commands of Matlab are explained on easy examples. The numerical solution for models of mechanical, hydro-mechanical and electromechanical systems are explained in 20 models of systems with one and more degree of freedom (<http://volt.feld.cvut.cz/vyuka/DMS/index.htm>):

- 1) A model of machinery with an unbalanced rotor location on an elastic frame. The model has one degree of freedom. Vibration on the body of machinery is solved numerically.
- 2) A model of machinery with an unbalanced rotor location on two elastic frames. The model has two degrees of freedom. Vibration on both bodies of machinery is solved numerically.
- 3) A model of a two mass torsion system with elastic coupling. The model has two degrees of freedom. Vibration on both masses is solved numerically.
- 4) A model of machinery with direct current driving motor, gear, elastic coupling and load moment. The driving moment M_h of the direct current motor is $M_h = M_0 - B\omega$, where M_0 ...starting torque, B ...constant, ω ...angular velocity of the motor. The model has two degrees of freedom. The loading moment has different courses: a) transient curve, b) square wave pulse, c) periodic square wave pulse, d) load changed with square of velocity – e.g. ventilator fan, compressor, centrifugal pump, etc. Vibration on both masses is solved numerically.
- 5) The some machinery such as the machinery in example 4, is driven by an asynchronous motor. The driving moment with a static non-linear characteristic of asynchronous motor (Kloss's moment characteristic) is $M_m = 2s_z s M_0 / (s_z^2 + s^2)$, where $s = 1 - \omega / \omega_{SYN}$ is a slip in respect to a synchronous angle velocity ω_{SYN} , and s_z is a parameter, which give the slip value, for which the moment M_0 is the

maximum. For value $s_z=0.25$ the maximum of moment is given by $\omega_M = (1 - s_z)\omega_{SYN} = 0.75\omega_{SYN}$. The system has two degrees of freedom.

- 6) A model machinery with a driven asynchronous motor, gear, rack, elastic coupling and loading force acting on a rack. The system has two degrees of freedom.
- 7) A model of a planer manipulator acting only in plane x,y , with two motors with constant driving moment. The model has two degrees of freedom.
- 8) A Model of a hydro-mechanical system with two interconnecting tanks. The system has two degrees of freedom.
- 9) A model of a quadruple mass torsion system with an elastic shaft, driving with the moment $M_n(\varphi_n) = 1,209 M_0 \cos(\varphi_n - n \frac{\pi}{3})$. The model has four degrees of freedom.
- 10) A model of a gear driven by an asynchronous motor and loading with two loading moments. The system has four degrees of freedom.
- 11) A model of a manipulator moving in the axes x,y,z and driven with two direct-current motors. The system has three degrees of freedom.
- 12) Vibration of a body hung-up on two springs (6-1). The system has one degree of freedom.
- 13) The determination of the deflection pointer of a measuring apparatus (6-2).
- 14) The movement of a mechanical system with two degrees of freedom (6-6).
- 15) The starting of a motor with ventilator (4.2-1).
- 16) The starting and braking of a rotor driven by shunt motor (4.3-2)
- 17) The model of lifting mechanism driven by motor (4.3-3).
- 18) The model of a feed cam (4.3-4).
- 19) The movement of a double pendulum (4.3-7).
- 20) The movement of a liquid column (7.3-2).

Examples No.12-20 are solution analytic in the textbook CTU, Faculty of Electrical Engineering S. Jirků: *Mechanika a termodynamika – cvičení*, 1992. The students have the possibility to compare numerical and analytic solutions. Also, instruction for compiled these examples are for other models of mechanical and hydro-mechanical systems and their numerical solution with Matlab and Simulink.

References:

- [1] S. JIRKŮ, J. VONDRŮCH: *Analysis of Manufacturing with Asynchronous Motor*, Proceedings of 12th FAIM Dresden, 2002, pp. 141-143 and 12 pages on the CD ROM.
- [2] J. VONDRŮCH, E.THÖNDEL: *Application of Matlab in Engineering Education*, Society for Modelling and Simulation, Proceedings of WMC'03, Orlando 2003, pp. 105-109.
- [3] J. VONDRŮCH: *Application of Modelling in Engineering Education*, IASTED, Proceedings of 4th MSO2004, Kauai, 2004, pp. 342-348.
- [4] J. VONDRŮCH, S. JIRKŮ: *Application of Modelling of Machine Systems and Simulations of their Operating Behaviour*, IASTED, Proceedings 9th MIC, Innsbruck 2000 pp. 615-619

This research has been supported by the Czech Ministry of Education grant No. 2027 .

Influence of the Oscillatory Flow Parameters on Flow Separation

K. Vališová, M. Knob, J. Adamec

katerina.valisova@fs.cvut.cz

Department of Fluid Dynamics and Power Engineering
Division of Fluid Mechanics and Thermodynamics
Faculty of Mechanical Engineering
Czech Technical University
Technická 4, 166 07 Prague 6, Czech Republic

The research of flow separation is aimed at clarifying more minutely the formerly obtained knowledge from the field of the flow in model of the airways ([2], [3]), where was shown that when flow separation occurs (e.g. in branching, behind the rib etc.) the longitudinal mass transport enhances significantly.

The flow in airways is from the viewpoint of fluid mechanics very specific, because it is oscillatory flow to the “death end” during which is the net mass transport equal zero. However, the exchange of the breathing gases is possible.

Recently in medicine is expanding usage of artificial breathing HFV (High Frequency Ventilation) which uses because of reduction of pressure high breathing frequencies and small tidal volumes – very often even smaller than the death space (the area of airways, where the gases cannot be exchanged). It is well-known from practice, that the gas exchange is even for so small tidal volumes efficient, although the mechanism, how that efficient exchange can occur and the influence of breathing condition (especially the Reynolds and Womersley number), has not been yet fully clarified.

It was shown experimentally – by comparing the flow in bifurcation, in the duct with ribs and in the smooth duct – that the decisive part of axial mass transport is caused by formation and extinction of flow separation zones, where the fluid is during a part of oscillating cycle captured till the change of the flow direction. In smooth duct, where no flow separation occurs, is axial mass transport minimal.

The research of this phenomena and especially the extent of flow separation zone with dependence on flow parameters can be very useful for application in medicine, for detail clarifying of mass transport during HFV and its further clinical expansion.

The research of mass transport during oscillatory flow (breathing) due to flow separation was so far done on simplified model of lungs, which helped to approach to real condition but on the other hand considering the complexity of flow and influences of other phenomena (the bent of the flow, Taylor dispersion, complex velocity profiles) it was not possible to assess the part of each mechanism on mass transport.

To avoid another mechanism of mass transport, which occur in branching, this research is aimed at flow in direct channel, where the flow separation is caused by a rib.

The problem is solved numerically and simultaneously the experimental device is built, where the numerical results can be verified.

For the simplifying the problem is the flow considered as two-dimensional, the width of cross-section of experimental channel is several times longer than its high (200 x 40 mm). The rib is placed on the bottom along all width of the channel. Its dimensions are 5 x 5 mm. Because of conservation of value of non-dimensional parameters water is used as working fluid and for that case is also solved numerical model.

The experimental device is constructed to allow the measurement of velocity profiles by means of optical method PIV (Particle Image Velocimetry). Oscillator consists of piston and motion screw driven by stepping motor. It enables to change frequency of the oscillation and also the stroke of the piston and so the change of tidal volume. Designed experimental setup allows also the modification of the velocity during each cycle.

For numerical simulation was used software Fluent 6.1. The problem was solved like two-dimensional.

The stationary case was solved for varying Reynolds number covering the field of normal breathing and artificial high frequency ventilation and the length of flow separation zone depending on Reynolds number was evaluated.

Further the non-stationary computation for higher Womersley number was done. As it follows from numerical simulations, for two – dimensional case remains in vicinity of the rib structure of six permanently formed and vanished vortices. Although the mass transport was not modeled, it is clear, that vortices significantly contribute to mixing the fluid and so to the mass transport during oscillatory flow.

References:

- [1] GROTBORG, J.B.: *Pulmonary Flow and Transport Phenomena*, Annual Reviews Inc, 1994, pp. 529 – 572.
- [2] MOCHIZUKI, S., TOGASHI, Y., MURATA, A.: *Visualisation of Axial Mass Transport of Reciprocating Flow inside Branching Tube System*, Proceedings of the 3rd Pacific Symposium on Flow Visualization and Image Processing, 2001.
- [3] VALIŠOVÁ, K., MOCHIZUKI, S., ADAMEC, J.: *Experimentální studie proudění v modelu dýchacích cest*, Proceedings of Students' Work in the Year 2002/2003, Ú12107.1, 2003, pp. 119 – 129.
- [4] FRESCONI, F. E., WEXLER, A. S., PRASAD, A. K.: *Expiration Flow in a Symmetric Bifurcation*, Experiments in Fluids, 2003, pp. 493 – 501.

This research has been supported by CTU grant No. CTU0405412.

Numerical homogenization of perforated plates

A. Somolová, J. Zeman

zemanj@cml.fsv.cvut.cz

Department of Structural Mechanics, Faculty of Civil Engineering, Czech Technical University in Prague, Thákurova 7, 166 29, Prague 6, Czech Republic

Perforated plates, i.e. plates “weakened” with a large number of holes of various shapes, are generally recognized as attractive structural members. This is mainly due to the fact that these structures offer substantial weight reduction while keeping the load-bearing capacity of a member relatively unchanged even for a high degree of perforation. In addition, the shape and degree of perforation can be optimized and adjusted for specific needs, which makes these structures even more attractive. Therefore, ability to accurately predict overall behavior of these structures is definitely of practical importance.

A particular example of such a study is provided by the work of Máca and Fajman summarized in [1]. In this contribution, authors performed a detailed computational study of the critical load of perforated webs made of acrylic glass for a variety of shapes of the openings and degree of overall perforation. In addition to detailed numerical simulations, comparison to extensive experimental data had also been presented to demonstrate high accuracy of the predicted values. Nevertheless, the applicability of the presented methodology is rather limited owing to the fact that authors in [1] simulated the response of the complete structure, i.e. a plate with all geometrical details. Such a direct simulation is feasible only for restricted sizes of structural members (such as the members subjected to experimental analysis); for realistic structures it presents obstacles both in terms of computational demands and mesh generation.

When analyzing structures, where the typical size of an opening is much smaller than the typical size of a structure, it appears to be advantageous to rely on homogenization methods. In this framework, the complicated perforated structure is replaced with an equivalent homogeneous one with properties based on the perforation pattern. The overall analysis then naturally splits into two scales: the *microscale* level, which defines behavior of the equivalent homogeneous structure, and the *macroscale* level linked to the overall behavior of the structure under the imposed load. There exist a vast body of literature related to homogenization problems; the recent book by Lewiński and Telega [2] summarizes state of the art in application of these methods to plate and shell structures. In particular, the theory presented in [2, Chapters 2 and 3] suggests that the appropriate model of the structure on the macroscale level is the classical Kirchhoff thin plate theory, regardless of geometry of the perforation and the thickness of the plate. These facts are taken into account in the microscale problem, which is substantially different for thin (Kirchhoff) and thick (Mindlin) plate models.

In particular problem of determination of the critical load of a perforated compressed web, the microscale problem is set once the geometry of the periodic unit cell is specified by the perforation pattern. The macroscale problem then reduces to the determination of the critical load for a homogeneous (but generally anisotropic) unidirectional compressed plate. This is a classical problem of plate theory for which the analytical solution can be easily found in the literature; see, e.g. [2].

The interaction between the macro- and micro-scale is ensured using kinematics on the macroscale level. Since the appropriate macroscale model is the Kirchhoff plate, the only macroscopic kinematical information available is a curvature tensor on the macroscale; see

also [3] for similar analysis in an one-dimensional setting. In order to specify the microscale problem, this information must be supplemented with appropriate periodic boundary conditions. If the microscale unit cell problem is set within the Kirchhoff framework, it suffices to prescribe these conditions for the rotation fields in the unit cell only. However, if the Mindlin model is adopted for the microscale, additional conditions for the deflection field need to be included to complete the microscale problem. In the next step, the unit cell problem is solved and used to determine the average moment intensities, which then directly lead to the definition of the effective properties; see again [2] for more detailed discussion.

Once the microscale unit cell problem is set, an appropriate numerical method needs to be invoked for its solution. In this contribution, the Finite Element method-based commercial software **ADINA** [4] was used to obtain the results. For the Kirchhoff-based unit cell, the three-node DKT finite element was used, while the four-node MITC element was employed for the Mindlin unit cell problem; see [4] for additional details and relevant references. The concept of control points was used to describe the average curvature tensor on the microscale; the periodic boundary conditions were imposed using constraint equations implemented in the **ADINA** code. The average moments can then be easily obtained from reactions found at the control points.

Using the introduced methodology, the critical loads for the structures analyzed in [1] were determined and compared to the experimental values. For all cases, it was consistently found that the results obtained using the Mindlin model on the microscale level were in much better agreement with experimental data than for the model based on the Kirchhoff assumptions. This is probably caused by additional influence of shear, which is taken into account in the Mindlin model. Moreover, in most cases the accuracy of the results was approximately 5-10%, which is acceptable from the point of view of practical requirements.

Nevertheless, the accuracy of the predicted critical load was for certain shape of openings substantially lower than those reported in [1]. This can be attributed to the simplifying assumptions adopted in the homogenization-based analysis, namely the perfect periodicity of the perforation pattern, the periodicity of curvature fields and the assumed cylindrical shape of the bending. A more detailed analysis of these factors will be a subject of the future research. On the other hand, the presented methodology is rather general, allows for substantial reduction of computational time and can be used for more general problems including geometrically non-linear effects.

References:

- [1] MÁČA, J. - FAJMAN, P.: *Numerical analysis of perforated webs*, Numerical analysis of perforated webs, 3(5), 1996, pp. 331-335.
- [2] LEWIŃSKI, T. - TELEGA, J.J.: *Plates, laminates and shells : Asymptotic analysis*, Series on Advances in Mathematics for Applied Sciences, Vol. 52, 1999, World Scientific, Singapore, New Jersey, London, Hong Kong.
- [3] SOMOLOVÁ, A. - ZEMAN, J.: *Homogenizace prizmatické konzoly [Homogenization of a cantilever beam]*, Stavební obzor, 13(9), 2004, pp. 282-287 (in czech).
- [4] ADINA R&D : *ADINA Theory and Modeling Guide. Volume I: ADINA*, 2003, see also web page <http://www.adina.com>.

This research has been supported by GAČR grant No. 103/04/P254.

Global optimization of “black-box” functions using stochastic optimization methods

J. Skoček, A. Kučerová, M. Lepš

honzaskocek@seznam.cz

Department of Structural Mechanics, Faculty of Civil Engineering, Czech Technical University in Prague, Thákurova 7, 166 29, Prague 6, Czech Republic

The goal of the work presented in this paper is the minimization of function calls necessary for locating the global extreme of an investigated function. The investigated function is supposed to be a “black-box” function, which means that we do not have any knowledge about functions properties such as its differentiability or continuity. Therefore, classical deterministic methods cannot be used in this case and stochastic global optimization algorithms seem to be preferable. In addition, an attention is paid to minimization of the number of function calls as the “black-box” function is assumed to be the most expensive part of the solving process.

The algorithm introduced in this contribution is the combination of a neural network and a genetic algorithm. The principle of the algorithm is to approximate the investigated function by a neural network, to locate the global extreme for this approximation by genetic algorithm and subsequently to improve the approximation in next cycles.

The type of the used neural network is the Radial Basis Function Network (RBFN) [1,2], that approximates black-box function by the sum of base functions values and neural weights for each neuron. The value of a base function is influenced by its “distance” from neuron’s center vector to vector of variables, for which we want to know the approximate function value. The neural weights are derived from the condition of equality between the values of black-box function and its RBFN approximation. This condition is represented by a system of N linear equations, where N stands for the number of neurons.

The global maximum of this approximation is found by GRAdient-based Atavistic Differential Evolution (GRADE) algorithm [4]. Now, it is possible to improve the ability of RBFN to approximate the black-box function by adding new neurons into the neural network. Adding the right neural centers is the most important step of each cycle of solution process. It determines the efficiency of the whole algorithm. In our case, three points are added in each cycle. The first one is the maximum found by GRADE algorithm, the second one is a randomly created point inside the definition domain. The last added point is acquired by different methods. In particular, three methods of generating new points were tested:

- a new point is located in the (hyper)cube with the center localized in the maximum found by GRADE and side length derived from the number of optima found in this (hyper)cube in previous cycles.
- The second method adds a new point with respect to the standard deviation, computed for values of maxima found in previous cycles. The randomly created vector is multiplied by the standard deviation and added to the current maximum found by the GRADE algorithm.
- The last method counts difference between maxima found by genetic algorithm in last two steps and adds this difference to the better one of them. This method is called gradient method of adding new point.

The results of numerical experiments shows that the gradient method is the most effective, both from the point of view of the number of function calls necessary for locating

the global maximum and from the point of view of standard deviation of number of function calls. Therefore, the gradient method was used for all subsequent tests.

The introduced algorithm was tested in solving the twenty-function test set [3] and one real-world problem of optimal control of structures undergoing large displacements [4].

- The set of twenty functions includes various functions with the dimensions up to twenty. This set was solved by many other algorithms, such as differential evolution, binary genetic algorithm, extended binary genetic algorithm and Simplified Atavistic Differential Evolution (SADE). The comparison shows that presented algorithm is able to solve effectively functions with specific properties. Namely, the dimension of the problem solved should not be too high and the function should not have many peaks with steep slopes. For functions with high dimensions and steep slopes it is necessary to have a large number of approximating neurons. As a result, the system of linear equations for determination of neural weights is too large and the algorithm becomes ineffective. But in all other cases, when optimized functions fulfill the specified properties, comparison shows very strong decrease of function calls necessary for locating the global extreme.
- The problem of optimal control of structures undergoing large displacements [4] was also solved by SADE and GRADE. In this case, the number of function calls decreased approximately four times, which is quite promising for the solution of more complex optimization problems from this area.

To conclude, the algorithm presented in this paper allows us to achieve a very strong reduction of function calls necessary for locating the global maximum of black-box functions. On the other hand, robustness of the algorithm decreased as the algorithm is not able to solve all types of functions. The more detailed investigation of this behavior of the algorithm will be a subject of the future research.

References:

- [1] NAKAYAMA, H. - INOUE, K. - YOSHIMORI, Y.: *Approximate optimization using computational intelligence and its application to reinforcement of cable-stayed bridges*, ECCOMAS 2004, Book of Abstracts II, 2004, pp. 437.
- [2] KARAKASIS, M. K. - GIANNAKOGLU, K. C.: *On the use of surrogate evaluation models in multi-objective evolutionary algorithms*, ECCOMAS 2004, Book of Abstracts II, 2004, pp. 446.
- [3] HRSTKA, O. - KUČEROVÁ, A. *Improvements of real coded genetic algorithms based on differential operators preventing the premature convergence*, Advances in Engineering Software, 35(3-4), 2004, pp. 237-246.
- [4] IBRAHIMBEGOVIC, A. - KNOPF-LENOIR, C. - KUČEROVÁ, A. - VILLON, P. *Optimal design and optimal control of structures undergoing finite rotations and elastic deformations*, International Journal for Numerical Methods in Engineering, 61(14), 2004, pp. 2428-2460.

This research has been supported by GAČR grant No. 106/03/0180.

Thermal Gains from Computers and Monitors

M. Duška

duška@fsid.cvut.cz

Department of Environmental Engineering, Faculty of Mechanical Engineering, Czech Technical University, Technická 2, 166 27 Prague 6, Czech Republic

Internal thermal gains from the office equipment represents a major portion of cooling load of air condition systems in office buildings nowadays. The increase of internal gains is associated with wide using of personal computers and information systems. There are a lot of problems connected with thermal gains from office equipment. Just some of them have been already solved with the previous research. One problem is determination of real total heat gain from equipments. This was usually estimated based on the nameplate power consumption ratings. Total heat gain was measured in previous research as power input. It was found that actual total heat gain ranged from 7% to 32% of nameplate power consumption. This presented result illustrates the dramatic difference that exists between nameplate rating consumption and actual measured consumption. Air-conditioning systems designed based on nameplate data would result in extra first costs and in operating costs for the whole life of building. Another problem is diversity factor of equipment. Diversity is influenced by occupants, their work and by the types of equipment they use. For detailed system design using advanced methods (like computer simulations) there is a dynamic profile of the office equipment need. Absence of this data led to this research project. The goal of the project is to determine mathematical model of real thermal gains from PCs and monitors. As thermal gains from PCs and monitors depend on people using it, it was necessary to perform field measurement of computer's and monitor's power input in real office building.

The measurement was performed in Škoda AUTO office building from August to December 2004. Each of almost 200 PCs and monitors was measured during one-week period and its usage was evaluated. The special datalogger based on principle of pulse wattmeter was developed and constructed for the purpose of the measurement. Measurement device consisted of one memory module DM8 and eight pulse sensors of power input HMP64-ISP1 connected by data cable. Each pulse sensor was installed to wall socket and electrical appliance was plugged in. As pulse sensors of power input measure specific amount of energy, it sends pulse to memory module. Memory module saves pulses from sensors in given time interval. Module is capable to store about 8400 records from each of the eight input slots. The three minute interval was used in pervious studies as sufficient time to set maximal thermal gain. Time interval set to three minutes enabled more than 14 days of continuous measurement in our case. The memory module was connected to computer and measured data were saved in CSV format for later processing. To shorten the total time of experiment two separate sets of dataloggers with pulse sensors were used simultaneously. Equipment was measured in one-week period or in two-week periods at most. Installation and dismantlement of measuring equipment took less than one hour. It is not probable that this procedure led to loss of accuracy of mathematical model.

The measured data had to be filtrated before processing due to the power failures in measured building during the experiment. The measurement of workstation, which was not used in one day at all, was not included to later processing. Approximately 30% of the measured data were excluded. From filtrated data of three-minute intervals were average hour

consumptions calculated for each measurement. It is supposed that equipments of the same mark and type have the same maximum power consumption. Therefore PCs were separated to five groups of the same brand and type and monitors to four groups. The average three-minute maximal consumption (taken as the maximum consumption value from three-minute intervals) and average hour time behaviour were created for each group. The average group hour consumptions were compared to group maximum consumption to obtain non-dimensional parameter dependent on time. Then were calculated mean proportional hour data separately for PCs and for monitors. It has been calculate as average of proportional hour data of equipment's group. Results are presented in appending table. Results of this research project will be used to detailed system design using advanced methods (like computer simulations).

		Time behaviour proportional thermal gains of equipment													
		PC							Monitor						
Time [h]		Mo	Tu	We	Th	Fr	Sa	Su	Mo	Tu	We	Th	Fr	Sa	Su
	0	13%	22%	22%	20%	16%	12%	12%	6%	7%	8%	5%	6%	6%	6%
	1	13%	22%	21%	20%	16%	12%	12%	6%	7%	7%	5%	6%	6%	6%
	2	13%	22%	21%	20%	16%	12%	12%	6%	7%	6%	5%	6%	6%	6%
	3	13%	22%	21%	20%	16%	12%	12%	6%	7%	6%	5%	6%	6%	6%
	4	13%	22%	21%	20%	16%	12%	12%	6%	7%	6%	5%	6%	6%	6%
	5	13%	22%	21%	20%	16%	12%	12%	6%	7%	6%	5%	6%	6%	6%
	6	16%	25%	23%	22%	19%	12%	12%	16%	17%	13%	12%	14%	6%	6%
	7	42%	43%	47%	40%	40%	12%	12%	54%	51%	52%	46%	46%	6%	6%
	8	58%	62%	63%	61%	58%	12%	12%	75%	76%	71%	74%	68%	6%	6%
	9	66%	68%	70%	66%	59%	12%	12%	84%	82%	77%	73%	67%	6%	6%
	10	69%	70%	71%	70%	60%	12%	12%	82%	80%	73%	74%	66%	6%	6%
	11	70%	72%	74%	68%	57%	12%	12%	78%	81%	78%	75%	68%	6%	6%
	12	73%	72%	74%	68%	60%	12%	12%	83%	81%	81%	77%	70%	6%	6%
	13	70%	70%	70%	70%	59%	12%	12%	82%	77%	83%	74%	67%	6%	6%
	14	65%	66%	63%	61%	51%	12%	12%	71%	61%	75%	66%	60%	6%	6%
	15	49%	50%	50%	42%	34%	12%	12%	54%	41%	50%	41%	38%	6%	6%
	16	33%	37%	39%	31%	15%	12%	12%	27%	28%	23%	23%	13%	6%	6%
	17	26%	29%	25%	26%	15%	12%	12%	19%	19%	16%	17%	9%	6%	6%
	18	24%	23%	21%	21%	14%	12%	12%	14%	10%	8%	11%	9%	6%	6%
	19	23%	20%	20%	19%	14%	12%	12%	10%	8%	8%	6%	7%	6%	6%
	20	22%	20%	20%	19%	12%	12%	12%	8%	7%	6%	5%	6%	6%	6%
	21	22%	21%	20%	19%	12%	12%	12%	7%	8%	6%	5%	6%	6%	6%
	22	22%	21%	20%	19%	12%	12%	12%	7%	9%	6%	5%	6%	6%	6%
23	22%	20%	20%	19%	12%	12%	12%	7%	7%	6%	5%	6%	6%	6%	

References:

- [1] M. DUŠKA, F. DRKAL, M. LAIN: *Tepelné zisky z vnitřních vybavení administrativních budov*, Klimatizace a větrání 2004. Praha: Společnost pro techniku prostředí, 2004, pp. 7-15.
- [2] M. DUŠKA, F. DRKAL, M. LAIN: *Tepelné zisky z vnitřních vybavení administrativních budov*, Vytápění, větrání, instalace, Vol. 5 2004, pp.7-11

This research has been supported by FRVŠ grant No. FRVŠš 1977.

PIV Measurement Teaching Based on Student Laboratory Work at Faculty of Mechanical Engineering

J. Novotný, J. Matěcha, J. Nožička

markvart@seznam.cz

Department of Fluid Dynamics and Power Engineering, Division of Fluid Dynamics and Thermomechanics, Faculty of Mechanical Engineering, Czech Technical University in Prague, Technická 2, 166 27 Prague 6, Czech Republic

The object of this project was implementation of PIV measurement and method based on PIV system like stereo PIV, PLIF (Planar Laser Induced Fluorescence) and IPI (Interferometric Particle Imaging) on student laboratory work at Faculty of Mechanical Engineering Department of Fluid Dynamics and Thermodynamics. Objective our project was design and constructs four student laboratory works:

1. Measurement two dimensional flow field whit low Reynolds number by standard PIV technique
2. Measurement velocity profile in tube by stereo PIV system -laminar and turbulent flow field
3. Measurement concentration and temperature by PLIF-Planar Laser Induced Florescence
4. Measurement two phase flow by IPI- Interferometric Particle Imaging

The next and most important objective our project was design and construct Low-cost PIV. Low-cost PIV system which we designed is consisting from CCD Camera LU175M whit resolution 1024 x 1280 pixel and continual Laser 50 mJ, whit 532 nm wave length. Using this CCD camera is very advantageous that is why there is possible to change frame rate repetition from 15 fps at 1280x1024 to 60fps at 640x480. The next advantage is possibility to change time of exposure. This camera is connected to the PC using standard high speed USB 2.0 (480Mbits/sec) connector and therefore is possible to us this CCD camera whit all PC whit system Microsoft XP. This Low-cost PIV system was used for measurement two dimensional flow field whit low Reynolds number. The results of this measurement (images whit seeding particle) is possible to analyze by standard commercial software FlowManager by Dantec dynamics or using one's own PIV software.

For measurement of two phase flow by IPI the experiment in moist wet steam will be designed. The aim of the experiment was to measure velocity of the growth of condensing nucleus in the wet steam dependent on velocity of condensation. For the experiments in wet steam the experimental setup was designed and constructed, generating superheated steam at lowered pressure and temperature of 50°C. Low pressure and temperature of hot vapour was chosen in order to minimize the risk of the accident at the wall's disruption. The size of condensing nucleus was measured by the method of Interferometric Particle Imaging IPI. The IPI method is a technique for determining the particle size of transparent and spherical particles based on calculating the fringes captured on a CCD array. The number of fringes depends on the particle size and on the optical configuration. The experimental setup used is identical with the setup for measuring flow by the stereo PIV method. The only difference is in using special camera mount comprising transparent mirror and enabling focusing both cameras to one point. The results of the development are measured growth of condensing nucleus and the histograms of sizes of all measured particles depending on time and condensation velocity.

For measurement velocity profile in tube by stereo PIV system the experimental setup was designed and constructed. For this experiment the test section for reduce the noise because of reflection and refractive index was designed and constructed. Using this special test section we were able to measure to wall in boundary layer. Results of these experiments were turbulent and laminar velocity profile.

For measurement concentration and temperature by PLIF the experiment for measured temperature boundary layer on vertical wall was designed and constructed. Using special camera mount there were able to observe one measurement test section by two cameras. One CCD camera was used for two dimensional measurement of velocity boundary layer and second CCD camera was used for measurement temperature boundary layer. Diameter of test section was 20mm x 20mm and thickness temperature boundary layer was about 2 mm. Because of very small test section and thickness of boundary layer there was necessary to design one's own PLIF software. Using this software we was to able measured this temperature boundary layer in small test section.

The methodology of measurement for all student laboratory works was booking and would by used for teaching in laboratory of Division of Fluid Dynamics and Thermodynamics.

References:

- [1] KOTOUČ, M.; NOVOTNÝ, J.: *Nizkorozpočtové PIV* In: Colloquium fluid dynamics 2004 Institute of Thermomechanics AS CR, 2004, pp. 87-90. ISBN 80-85918-89-7.
- [2] ČÍŽEK, J.; NOVOTNÝ, J.; ADAMEC, J.: *Měření volné konvekce metodou PIV/PLIF* In: Colloquium fluid dynamics 2004 Institute of Thermomechanics AS CR, 2004, pp. 17-20. ISBN 80-85918-89-7.
- [3] NOVOTNÝ, J.; NOVÁKOVÁ, L.; NOŽIČKA, J.; ADAMEC, J.: *Measurement of Two Phase Flow* In: 4th International Conference on Advanced Engineering Design [CD-ROM] Glasgow, 2004, ISBN 80-86059-41-3.
- [4] NOVOTNÝ, J.; NOVÁKOVÁ, L.; NOŽIČKA, J.: *Zefektivnění IPI algoritmu* In: Aplikácia experimentálných a numerických metód v mechanike tekutín, Žilinská univerzita v Žilíně, 2004, pp. 301-304 ISBN 80-8070-234-9.

This research has been supported by CTU CTU0417912 .

Number of Modes in Calculation of Seismic Response of Structures

K. Pohl*, J. Máca **

karel.pohl@fsv.cvut.cz

*Department of Structural Mechanics, Faculty of Civil Engineering, Czech Technical University, Thákurova 7, 166 29 Prague 6, Czech Republic

**Department of Structural Mechanics, Faculty of Civil Engineering, Czech Technical University, Thákurova 7, 166 29 Prague 6, Czech Republic

The objective of this paper describe the number of mode shapes in the dynamic response of structures. New technical standard EUROCODE 8 is being prepared in Europe in these days. It concerns the influence of earthquake to structures. This standard expects that common structures will be calculated with so called response spectrum. When using this method it is very important to choose carefully the number of considered mode shapes. Suggested standard implements quite simple criterion for determination of number of considered oscillation shapes which is based on so called equivalent modal mass. This criterion was not yet tested in details.

The method of calculation the seismic response of building structures according to EUROCODE 8 is based on simplified assumptions. This simplification is based on transformation of dynamic load given by seismic action to the equivalent static load by method of multi-modal analysis (e.g. combination of mode shapes). Conversion of dynamic task to static solution is fundamental for design practice where the solution of tasks with time variable load exceed the possibilities usual in engineering practice. Next remarkable simplification of calculation the response of structure is an assumption of linear material behavior. Inaccuracy flown from this simplification grows with choice of material which show apparent non-linear behavior (e.g. reinforced-concrete structures). In order to take into account the dissipation capabilities of the construction in the calculation, linear analysis will be made, based on design response spectrum that is smaller than an elastic spectrum. This reduction can be achieved by implementation of ductility factor q (in EC8 called behavior factor). All of these significantly simplifying suppositions lead (according to the type of a construction) to inaccuracy in assignment of resultant construction response. A comparison of thus assigned structure's response calculation with a calculation based on detailed analysis of the construction can lead to a modification of the minimal number of oscillation shapes criterion considered in the calculation, as assumed in the EUROCODE 8.

A verification of the minimal number of mode shapes criterion for a determination of structural response under seismic load was done for an atypical structure of a high-rise building. It was a constructionally complicated building sensitive to dynamic load. The second structure considered was a steel truss tower. In these problems was used a 3-D spatial model with a linear material behavior. Both structures were calculated by a method of mode superposition (multi-modal response analysis). It was proven that the criterion of minimal number of mode shapes is strongly overestimated mainly for steel tower structures. Also for the high-rise building structure it was proven that the response definition was from more than 80% based on the first oscillation shape relevant for given direction. For intermediate directions is the situation more complicated, but these directions are not crucial according to the size of structure's response. In implementation of assumption of knowing the exact definition of structure's response there is a possibility to proclaim above mentioned calculation

as conservative and reduce the requirement for minimal number of oscillation shapes, if it would be proven that the reduction for specified type of structure is sufficiently secure.

For detailed analysis of reinforced-concrete frame structures a non-linear analysis was used. The primary algorithms was based on requirement of definition of dynamic structural response, natural frequencies and mode shapes etc. This calculation is now being implemented to the SIFEL program which is being developed at the Department of Structural Mechanics, Faculty of Civil Engineering, Czech Technical University in Prague. On a simple reinforced-concrete structure was used a non-linear structural analysis was done. Within this calculation we can observe, apart of redistribution of internal stresses, also change of natural frequencies. The natural frequency has an essential influence on a defining the value of seismic action. We are able to track the natural frequency (softening of structural system) we can track also the influence of this change on the size of the seismic action. By this change is understood an increase of structural resistance to seismic action, therefore the linear dependence between increase of effective value of maximum acceleration a_g and seismic shake F_k does not apply. With non-linear analysis it will occur a significant increase of structural movement, but the influence to reallocation of internal intensity is not crucial and it is actually beneficial for solidity of construction system. Reduction of natural frequency, which conversely can be crucial, can cause even a reduction of the size of internal intense in the construction and thus contribute to an impair of requirement of minimal oscillation shape number in calculation of structure's response to a seismic load. For appraisal of structure resistance these internal intense are crucial.

The criterion of number of mode shapes considered in the calculation of structural response to a seismic action as presumed by EUROCODE 8 norm appears not to be satisfactory. In the project was proven that the final response of structure is remarkably based on the first mode shape. If we take into account the non-linear structure behavior and the reduction of seismic action influenced by it's softening, we can strengthen the influence of the first oscillation shape given by the linear calculation to the overall structural response. It is necessary to execute a detailed analysis of all types of structures because the influence of non-linear behavior is not possible to generalize for all types of structures. The project will be next focused on comparison of results obtained by multi-modal response spectrum analysis and direct integration of equations of motion. New adjustments of the minimal mode shape number criterion considered for calculation of specified type of structure will be suggested, in order to receive more effective calculation of linear structural response, which appears to be most appropriate for common use in engineer practice.

References:

- [1] K. POHL: *The Response of Structure of High Rise to Seismic Loading at Use ČSN 73 0036 And ČSN P ENV 1998-1-1*, Staticko-konstrukčné a stavebno-fyzikálne problémy stavebných konštrukcií, Košice: Technická Univerzita , 2004, pp. 301-306.
- [2] K. POHL: *The Non-linear Response of Structure to Seismic Loading*, Staticko-konstrukčné a stavebno-fyzikálne problémy stavebných konštrukcií, Košice: Technická Univerzita , 2004, pp. 295-300.

This work was funded by CTU grant No. CTU0401311 .

Wind Tunnel Testing of Blade Cascade and Airfoils in 2D Flow Conditions

Milan Matějka, Lukáš Popelka, Natálie Součková

`milan.matejka@fs.cvut.cz`

Department of Fluid Dynamics and Thermodynamics U207.1

Faculty of Mechanical Engineering

Czech Technical University

Technická 4, 166 07 Prague 6, Czech Republic

Nowadays, the experimental research of shear layer and transition to turbulence is still on one of the first places of scientific interest. This study of influences of inlet flow parameters is new direction at world research.

Our project was directed to the airfoils and blade cascade at the condition of low Reynolds number flow. These points at issue are one of the research lines solved at department 12107 – new wind tunnel of 1200 x 400 mm cross-section was built in our laboratory under contribution of CTU grant.

It has been shown, that not only turbulence intensity, but also dissipation length parameter play an important role in transition process. An aim of current research is to prove the impact on integral aerodynamic coefficients (such as drag and lift) on streamline bodies. To enable such measurement, the flow in wind tunnel should be significantly modified. In front of examined airfoil or blade cascade is now placed turbulence generator.

Two grids are used - the first one is coarse and it is placed just downstream the inlet contraction of the tunnel. The second one, fine, is placed in front of the measurement area. Both are designed as replaceable part of the aerodynamic tunnel for future possibilities to change it. Thanks to this is a well defined inlet flow comes to the leading edge of airfoil or blade cascade. Chord used on models is 400 mm, which with standard operational conditions yields test Reynolds number up to 300 000. Locking device for total and static pressure are placed in front of test section. The same variables can be evaluated by traversing in the wake behind the body.

Measurement procedure is adequate to proven practice used in best wind tunnels worldwide – lift can be evaluated from pressure distribution over model surface. Drag is calculated by means of momentum balance in wake behind airfoil. Required velocities are measured by Particle Image Velocimetry, which is a laser supported optical method. Our team proved higher accuracy than with the standard pressure rake. Use of large transparent panels facilitates usage of the method and required calibration. The use of hot-wire anemometry for same purpose will be examined as well.

As an initial experiment, the visualization of flow field of Wortmann FX66-17AII-182 airfoil with air brake has been carried out. PIV method has been used; this measurement has been also utilised as a test case of the whole system. Investigated area has been divided into several sub-regions which have been evaluated separately. Such procedure enabled better resolution of velocity gradients. The function of air brake under various angles of attack of base airfoil has been studied.

Different air brake geometry was applied at NACA 23012 airfoil – noticeable wake has been visualised.

An importance of proper flap function is pronounced both at sport and transport airplanes. MS(1)-0313 is widely used in this category, hence a model with simple flap has been prepared and wind tunnel tested.

All presented measurements have been aimed at possibilities of lift and drag control. A study of entirely new topic of active flow control has been started which expanded initial topic of the grant. The concept of active flow control on blade cascade has been created by means of synthetic jets. The manufacture of simple airfoil test case has been started as well.

Airfoil design and optimization for sailplane application is another important topic and final results have been gained for club class. Wind tunnel testing has continued by the study of the boundary layer separation on typical club class airfoil.

Design features of the airfoil using numerical solutions and measurement were presented [1]. General application of numerical method in feasibility studies of experimental research is written [2]. Methodology of PIV measurement and limits of evaluation of turbulence properties was studied [3]. Interaction of synthetic jet with free shear layer and its usage for boundary layer thickness control was introduced [4].

The new wind tunnel and its valuable equipment opens further field of aerodynamic research in the laboratory of the department U207.1 aiming at compressor aerodynamics, blade cascades, airplane aerodynamics and airfoil .

References:

- [1] POPELKA, L. – MATĚJKA, M. - NOŽIČKA, J.: *CLUB CLASS SAILPLAIN AIRFOIL Design* Advanced Engineering Design in Glasgow, 2004, D1.02.
- [2] MATĚJKA, J. – POPELKA, L.: *THE ROLE OF CFD SIMULATIONS IN PRELIMINARY STAGE OF EXPERIMENTAL RESEARCH* Topical Problems of Fluid Mechanics 2004, Praha: Ústav termomechaniky AV ČR 2004, pp. č. 97–č. 98.
- [3] MATĚJKA, M. – KNOB, M.: *PIV MEASUREMENT OF A PLANE WAKE BEHIND A PRISM* Fluid Mechanics and Thermodynamics 2004, pp. č. 99–č. 104.
- [4] MATĚJKA, M. – URUBA, V.: *INTERAKCE VOLNÉ SMYKOVÉ VRSTVY SE SYNTETIZOVANÝM PAPRSKEM* Colloquium Fluid Dynamics 2004, Praha: Ústav termomechaniky AV ČR, 2004, pp. č. 123–č. 126.

This research has been supported by CTU0405212.

Methodology Development for Optimization Tasks in Aerodynamics

A. Sládek

a.les.sladek@fs.cvut.cz

Department of Fluid Dynamics and Power Engineering,
Faculty of Mechanical Engineering, Czech Technical University in Prague,
Technická 4, 16607 Prague 6, Czech Republic

Optimization methods became an efficient tool in practical and research problems many years ago, but the application of optimization methods in fluid dynamics is still difficult. The most limiting factor of the usage of optimization methods in fluid dynamics is an enormous consumption of the time needed to obtain the objective function from the results of numerical simulation. Thereafter very sensitive choice of the optimisation method is needed for efficient solution of each optimization task in aerodynamics. Presented work deals with the development of methodology for the problems of fluid dynamics and is primarily focused on direct search methods.

An appropriate choice of the optimization method in aerodynamic task is always complex problem. One has to consider that the solution of optimization problem is closely connected with numerical solution. The enormous time consumption of numerical simulation in fluid dynamics is not the only problem to be dealt with. Mesh adaptive techniques which are needed to correct solution of the system of equations (Euler or Navier-Stokes equations) with finite volume or finite difference schemes always superpose some noise function on the objective function, which can be naturally nonlinear, nonsmooth or discontinuous. Objective function with low-amplitude, high frequency oscillations is challenging for all optimization methods. For such optimization problems, two main usable groups of optimization methods will be described in the following two paragraphs.

The first group of methods contains stochastic methods, evolutionary algorithms (genetic algorithms, differential evolution, swarm optimization, etc.) or simulated annealing. All these advanced methods are generally very good for solving global optimization problems but they are not very efficient for optimization tasks with low dimensionality due to comparatively high number of objective function evaluations. Recently, an effort to lower the number of function calls with assistance of so called "metamodels" [1]. The metamodel approximate real objective function with algebraic expression of objective function gained from trained neural network or another type of artificial intelligence algorithms (self-organizing maps, Kohonen structures). On such metamodel part of the calculation is done.

The second group of methods contains direct search methods as a part of deterministic methods (gradient methods are hard to use in problems of fluid dynamics due to noisy character of objective function). Direct search methods are best known as unconstrained optimization techniques that do not explicitly use derivatives. Direct search methods were formally proposed and widely applied in the 1960s but fell out of favor with the mathematical optimization community by the early 1970s because they lacked coherent mathematical analysis. In the past fifteen years, these methods have seen a revival due, in part, to the appearance of mathematical analysis, as well as to interest in parallel and distributed computing [2].

For testing the efficiency of direct search methods, the basic set of testing functions [4] was applied, namely Spherical function, Elliptical function and general Roosenbrock test function. Results obtained on these smooth functions up to \mathbf{R}^{10} dimensions were published and discussed in [3] and some conclusions for practical use of direct search methods were derived.

As a good choice from the set of tested direct search methods we can recommend the Roosenbrock method and the Hook-Jeevse method, which are generally more efficient than the Nelder-Mead simplex algorithm or the Polytop method for the functions with low amplitude noise. The Nelder-Mead simplex algorithm or Polytop method seems to be a good choice for the problems with up to 10 dimensions and for the functions with medium amplitude of noise on objective function. Moreover, these methods with applied rough step, are good for the first estimate of the starting point of the following optimization process. All direct search methods should be used up to 20 dimensions of search space, for problems with more than 20 dimensions we can strictly recommend use of evolutionary algorithms or other sophisticated methods described at the beginning of the article. For the functions where the amplitudes of noise are relatively high to the ratio of mean value change in objective function all the direct search methods fail and some more sophisticated method must be applied on optimization process.

For further progress, coupling of direct search methods or evolutionary algorithms with neural networks should be investigated. Such optimization approach seems to have a great potential for industrial applications with hundreds of design parameters.

References:

- [1] GIANNAKOGLU, K. C. – PAPADIMITRIOU, D. I. – KAMPOLIS, I. C.: *Coupling Evolutionary Algorithms, Surrogate Models and Adjoint Methods in Inverse Design and Optimization Problems* In: Optimization Methods & Tools for Multicriteria /Multidisciplinary Design - Applications to Aeronautics and Turbomachinery, von Karman Institut Lecture Series 2004-07, Brussel 2004 pp. 65–93.
- [2] KOLDA, T. G. – LEWIS, R.M. – TORCZON, V.: *Optimisation by Direct Search: New Perspectives on Some Classical and Modern Methods* In: Society for Industrial and Applied Mathematics Review, Vol. 45, No. 3, 2003, pp. 358–482.
- [3] SLÁDEK, A.: *Přímé metody optimalizace v úlohách mechaniky tekutin* In: Colloquium FLUID DYNAMICS 2004. Praha: AV ČR, Ústav termomechaniky 2004 pp. 165–168.
- [4] SLÁDEK, A. – HYHLÍK, T. – ŠAFAŘÍK, P.: *Optimization Methods for Hydrodynamics Tasks* In: XXIIIrd International Scientific Conference of Departments of Fluid Mechanics and Thermodynamics. Zvolen: TU Zvolen, 2004, pp. 232–236.

This research has been supported by CTU0405312

Optimization of the Air Coanda Ejector

R. Kunčar

kuncar@fsid.cvut.cz

CTU, Faculty of Mechanical Engineering, Dept. of Fluid Dynamic and Power Engineering,
Division of Compressors, Refrigerating and Hydraulic Machines, Technická 4,
166 07 Praha 6

Air ejectors are spread at the area of distribution at different stuffs, aeronautics and air conditioning. These devices are usually designed in respect to their purpose. Efficiency of the ejector influences its utilization like substitution conventional appliances.

This article is devoted to improve sufficiency and describe the behaviours of these air machines. Therefore new measuring circuit was installed to validate and inquire more precise values. The measuring devices were chosen due to special literature and previous measuring experience. This device is mostly used for transport of gas, liquid or steam. Its theoretical efficiency is based on the design of the entry canals, mixture chamber, diffuser and applied transport matter. Inlet canals should admit of reaching required velocities and satisfy aerodynamic principles. Pressure difference implicates interaction and interposition between driving and driven gas in subsequent mixture chamber so that driving air warfts driven air by mixture and energy transfer. The rest of the transfered kinetic energy is enacted inside the diffuser. The diffuser is joined on the measuring track. The measuring spot was created in space of envolved velocity profile and constant static pressure to ensure true measuring data. It is usually in distance 5 times throat diameter behind diffuser. The measuring line contains digital flowmeter, which is located at the end. It works on principle of Carman's fluxes. At the end of the trackline there is also adjustable throttle. This choking element simulates different pressure conditions at the outletline. The driving air is produced by screw compressor Atmos SE 80 with maximum flow volume 75 m³/h. Admission line of driving air is equipped with pressure and temperature probe. The ejector sucks driven air outright from laboratory room close to the barometric conditions. At the measuring track there was installed Coanda ejector with adjustable width of the slot to elicit optimal gap from measured values. Characteristic diameter of the ejector throat was 51 mm. The air ejector achieved maximum efficiency at 0.2 mm width of the slot. The measuring track contains throttle to simulate frictional losses in following ducting. We verified decreasing amount of transported air by risen value of the outlet pressure. The pressure growth 20 Pa (pressure behind diffuser) causes flow volume drop about 10 %. As a result of high decreasing energy it is important to consider the loss which arise from line length and high velocity. It determinates scale of using even though if pipe enlarges its size. The admission line of the ejector provides change of compressed air flow due to air relief branch with installed rotameter. Thus it enables comparison at particular working conditions at the suction part by the same level of pressure. Values of the driving compressed air were in range 1 up to 3 bars at the ejector entry, values of the compressed air in compressor were about 0.5 up to 1 bar higher than at the ejector. Real valuations of supply air are usually about 7 bars in ordinary compressed air distribution. It satisfies as compressed air source with supposed reinforcement 15 by given conditions. This reinforcement is stated as rate of the driven and the driving mass flow.

In some practical cases ejector equipment is applied without diffuser and is directly lined up on subsequent conduit. Function of the diffuser is partly substituted that conduit however high speed of the air flow provokes crucial losses in consequence unstable fluctuant flow air.

Practice also offers single ejector applications, it is made for exhaustion of gaseous matters either they are rising or they are dissipating heat by manifold actions. Ejector reaches value of reinforcement up to 30 at this settlement. The reinforcement value helps us to compare chosen device to another at some parts like channels, walls or shapes. It represents the operation of whole apparatus.

On the other side we can start from mathematical equations for the mixture chamber, but it do not have to lead to goal. The validity of these equations is usually limited.

Mathematical model for fundamental mixing effect is formularized by dynamics and energy equations

$$\bar{u} \frac{\partial \bar{u}}{\partial x} = -\frac{1}{\rho} \frac{d \bar{p}}{dx} + \frac{\bar{u}}{2\Psi} \frac{\partial}{\partial \Psi} \left[\frac{\mu v^2 \rho \bar{u}}{2\Psi} \frac{\partial \bar{u}}{\partial \Psi} - \overline{(\rho v) \mu} \right]$$

$$\bar{u} C_p \frac{\partial \bar{T}}{\partial x} = \frac{\bar{u}}{\rho} \frac{d \bar{p}}{dx} + \frac{\bar{u}}{2\Psi} \frac{\partial}{\partial \Psi} \frac{k_l y^2 \rho \bar{u}}{2\Psi} \frac{\partial \bar{T}}{\partial \Psi} - C_p \overline{(\rho v) T''} \bar{u} + \frac{\phi}{\rho}$$

that is generally unsolvable in this form.

These turbine engines generally achieve smaller operation than classic conventional devices. On the other side turbojet machines substitute them and offer low investing costs, minimal process cost and portability. They have advantage for special and irregular running.

References:

- [1] HIBŠ, M: *Podzvukové difuzory*, SNTL, 1985, pp. č. 25-36
- [2] HIBŠ, M: *Proudové přístroje*, SNTL, 1959, pp. č. 51-73

This research has been supported by CTU grant No. CTU0405012.

Section 7

MECHANICAL ENGINEERING

Aerodynamic Sound by Low Mach Numbers

M. Kučera, R. Nový

miroslav.kucera@fs.cvut.cz

Department of Environmental Engineering, Czech Technical University in Prague,
Technická 4, 166 07, Prague 6, Czech Republic

Air conditioning equipment ensures thermal comfort in important public buildings such as hospitals, theatres, concert halls, TV and broadcasting studios. In all these cases the indoor spaces are very demanding with respect to holding the level of noise within the required limits.

Air conditioning pipe manifolds in the above buildings are terminated by inlets and outlets, which serve for the uniform supply of air. This is usually achieved by airflow control in the individual branches by throttling (dynamic pressure losses). Outlets together with control elements (predominantly butterfly dampers) are in addition to the above sources of aerodynamic noise. Designers are above all faced by problems related with the noise of outlets and control elements, which are either integrated into terminal elements or located very near to them. Usually there is not enough space to reduce the noise by means of sound dampers. The aim of the present paper, which is the result of an implemented research project, is to consider possibilities of the reduction of aerodynamic noise already in the control elements themselves.

Butterfly dampers are both from the viewpoint of their production costs and price cheap products. However they have insufficient highly non-linear working characteristics, from which it is apparent, that at a small slewing angle θ ($^\circ$) the dampers offer nearly no resistance to the flowing air. Only at greater slewing angles the dynamic pressure loss coefficient ξ (-) grows substantially, however as already mentioned, the course of the control is non-linear.

The aerodynamic noise is generated by a control butterfly damper with a specific section area of 0.1 m^2 and can be characterized by the sound power level A_{LWA} (dB) in dependence on the airflow rate V (m^3/h). A detailed analysis of the generation of noise in a butterfly damper shows that the critical part, where a prevailing portion of the sound power is generated, is the constricted part of the flow field. The flow velocity of air in this place grows considerably. In view of a commonly known fact, that the generation of aerodynamic noise is proportional to the 6th power of the airflow velocity, approaches have been sought to achieve the required reduction of pressure in a duct at lower airflow velocities.

From the experiments performed a regressive equation can be set determining the dependence of the level of the sound power A on the airflow velocity w_c . As follows from the presented results the dependence concerned can be expressed by an increase of the level of the sound power A by approx. 21 dB at a duplication of the airflow velocity in the constricted part of the control element.

If a conventional orifice plate or perforated sheet is used in the duct as a resistance element, then the airflow rate will be set to a constant value. The aerodynamic noise generated for the flow of air through a single hole into free space is generally known.

If the outlet hole is arranged as a set of small holes, practical results show that the generation of sound power can be reduced. Dependence sound power level on air flow was found out for sheet with perforation 33 % and 66 % in the duct with diameter $\Phi=0,355 \text{ m}$ ($0,1 \text{ m}^2$). From the analysis of the results of measurement is evident that for example the sound

power level is equal to 28 dB for perforation 33 % and 16 dB for perforation 66 % both causes with air flow $1000 \text{ m}^3/\text{h}$.

If the design of the damper is combined with a perforated sheet, in the first approximation a hypothesis could be applied, that in a series arrangement the resistances are summed up.

The effect was studied of the system "Butterfly damper + perforated sheet", in which the throttling elements were series arranged. On the basis of the performed experiments the behaviour of a newly created control element with an assumed pressure loss of 50 Pa.

The results of the experiments indicate a possible linearization of the working characteristic by series arrangement of the damper and the perforated sheet.

The required reduction of the supply pressure was achieved in two stages. At a constant value of the total reduction of pressure the fraction of the pressure loss in the damper is given by a change of the setting of the angle θ to a lower value. This automatically leads to a reduced generation of noise in the damper, since the airflow velocity w_c in the narrowest profile drops significantly.

One way how to change the working characteristic of a throttling element and simultaneously reduce the noise it generates, is to arrange more butterfly dampers in series. Experiments were carried out with two identical dampers. Here the noise of one butterfly damper was compared with that of two series arranged dampers with an identical pressure gradient. Theoretical analysis could offer a noise reduction by up to 6 dB. Experiments have proved a reduction of noise by approx. 4 dB. One explanation of this phenomenon is at hand. The sound power corrected by filter A involves the effect of the shape of the spectrum. It has been proved that the spectrum of the generated aerodynamic noise is displaced on the frequency axis in dependence on the homothetic Strouhal number Sh , which induces a correction of the sound power A .

From the analysis of the results of experiment, which mapping dependence the sound power level on total pressure loss, is follow the reduction of pressure difference can be done as series arrangement of throttling elements. Series arrangement of throttling elements has been resulted in decrease velocity of air in the constricted part of throttling element. This effect causes decrease of sound power level emitting in the duct. Within the scope of this grant experimental work proceeds with an aim to obtain an overview of other combinations of throttling elements appropriate for air conditioning equipment.

References:

- [1] KUČERA, M. – NOVÝ, R.: *Reduction of Noise Generated by Damper* In: The Eleventh Internation Congress on Sound and Vibration. St. Petersburg" The International Institute of Acoustic and Vibration 2004, pp. 3097 - 3104.
- [2] NOVÝ, R.: *Noise and Vibration* CTU in Prague 1995, 389 pages.
- [3] FRY, A.: *Noise Control in Building Services* Pergamon Press Oxford, 1988, 441 pages.
- [4] EYNOLDS, D. D. – BLEDSOE, J. M.: *Algoritmus for HVAC acoustics* Ashrae, 1991, 441 pages.

This research has been supported by FRVŠ grant No. 1982/G1.

Panel radiators

R. Vavříčka, J. Bašta

Roman.Vavricka@fs.cvut.cz

Department of Environment, Czech Technical University in Prague, Faculty of Mechanical Engineering, Technická 4, 166 07 Prague 6 - Dejvice, Czech Republic

The radiator is important part of heating systems. Project of radiator for example type, location, technique of working, have direct impact to thermal comfort of heated space. Is important, in order to the project of radiator took thermal comfort of occupant into account to the full along with economy requirements.

With the panel radiators it was determined during the measurement under standard conditions that the nominal heat output by the radiators called „short“ is constant both for single-side top and for diagonal top connections. This information is not valid for called „long ($L \geq 4 \cdot H$)“ panel radiators.

This phenomenon is read different. Germany technical literature is inclined to explain it as of ejector effect. By long radiator with single-side top connection the ejector effect means that induction cold water come up first heating flue connected with top distribution box. Consequently the mean surface temperature of radiator is cutting down along with decrease of heat output. This information was published in article of Abel, Bott and Schlapmann in 1993 [L4].

In other literature [L1, L2, L3] interprets this phenomenon as significant decrease in dynamic pressure in top connection box wit respect to its length. Due to the pressure loss of the radiator, which in the form of friction and local resistance increases with length of the radiator, predominant part of flow is immediately returned to bottom collecting box and to the outflow from the radiator. In the second half of the radiator unordered (chaotic) flow occurs and velocity moves in the order of 10^{-9} [m/s] here. Take place such small velocity conditions determinate convection heat transfer coefficient inside the water, but at the same time more marked cooling water by flow trough complete radiator. The water stayed in radiator for a long time and the temperature gradient (temperature of medium minus room temperature). Temperature gradient in radiator is more highly than nominal temperature gradient. Insufficient warming-through of radiator by inlet hot water is the cause decrease mean surface temperature thereby decrease heat output by radiator with single-side top connection.

This problem we are solved by mathematic simulation and experimental verification temperature fields by surface temperature mapping. We carried out mathematical simulation on two types of panel radiators. The first type was „short“ model. This model corresponded to panel radiator KORADO Radik Klasik type 10 – 500 x 500 (the first number is the type of panels, the second number is the radiator of height, the third number is the radiator of length) with single-side top connection and diagonal top connection by nominal and double flow. The second type called „long“ model corresponded to panel radiator KORADO Radik Klasik type 10 – 500 x 2000 with single-side top connection and diagonal top connection by nominal and double flow. In experiment the surface temperature is mapping with the assistance of contactless thermometer (radiant heat pyrometer) Testo Quickstep 860-T2. The panel radiator type 10 – 500 x 500 and type 10 – 500 x 2000 was measured always single side-top and diagonal top connection.

By radiator type 10 – 500 x 500 with single-side top connection the temperature fields obtained by mathematic simulation is compared with experiment both causes showed creation the colder area in the right bottom corner of radiator. The colder area is caused by decrease of water current velocity in this part of radiator. The mean temperature of radiator, which is the

70 °C for both causes, corresponded to 75 % radiator heights by experiment and this temperature is distribution for all its length. On the contrary by the mathematic simulation the mean temperature is transferred lower and its course of temperature have more diagonal character. By the same type of radiator, but diagonal top connection, the mean temperature is transferred under 75 % radiator heights. By the mathematic simulation the mean temperature corresponded to 60 % radiator heights and by the experiment it is 65 % radiator heights. The colder area, which by the mathematic simulation is in the middle of bottom part of radiator, is moved moderately to right by experiment.

Type 10 – 500 x 2000 with the single side-top connection. The mathematic simulation demonstrated reduces of flow in the second half of radiator with ensuing minimal heat transfer. However by the experiment the colder area is in the bottom part of radiator. This area covered almost all length of radiator and reaches about the 20 % radiator heights. Both figures of temperature fields are not so much different for diagonal top connection of long radiator. In the distance about 80 to 100 mm from inlet of hot water to the radiator is predominant part of flow ripped to the bottom collection box and conducted back to the heating system. But by the mathematic simulation is seen, that flow of water is continuously separated for all length of radiator. Due to pressure distribution in the radiator occur to deceleration of flow in its half-length thereby bigger cooling water. Difference in temperature distribution by experiment and mathematic simulation have the same cause as by single side-top connection.

From the analysis of the results of mathematic simulation and experimentally obtained temperature fields is reason of decrease of heat output by single side-top connection of radiator decrease of dynamic pressure in the top connection box. From the confrontation the experiment and mathematic simulation, the diagonal top connection is better, because near concordance is evident as short as long radiator. The causes of difference between temperature fields by single side-top connection are caused first of all inlet hot water to the radiator trough distance ring. This cause will be part of next research. Advantage diagonal top connection of long panel radiator with ratio $L/H \geq 4$ is possibility reached higher surface temperature of radiator thereby better utilization of heat surface. On the basis of acquired results we can recommend even more and change the condition of distinguishing „long” and “short” radiator with respect to the connection. As „long” radiators for which the above-mentioned recommendation of the connection is valid we consider panel radiators, which fulfill the condition ($L \geq 3H$).

References:

- [1] VAVŘIČKA, R.: *The pictures of flow inside water by radiator* Dissertation - Czech Technical University – Department Environment, 2002, 73 pages.
- [2] VAVŘIČKA, R., BAŠTA, J.: *Computer simulation of long panel radiators* Building and environmental simulations 2004, 2004, pp. 107–111.
- [3] VAVŘIČKA, R., BAŠTA, J., SCHWARZER, J.: *Problems with connections of long panel radiators* Modelling and Simulation for Environmental Engineering, Praha: CTU Publishing House 2004, pp. 109–113.
- [4] ABEL, H., - BOTT, H., - SCHLAPMANN, - D.: *Raumheizkörper* Heizungstechnik, v.13, no. 4, 1990, pp.928-935.

This research has been supported by VZ MŠMT č.:XXXXXXXXXX.

Evaluation of Indoor Air Temperature and Operative Temperature in Air-Conditioned Room

Lubomír Hrgaš, František Drkal

Lubomir.Hargas@fs.cvut.cz

Department of Environmental Engineering, Faculty of Mechanical Engineering, Czech Technical University, Technická 2, 166 27 Prague 6, Czech Republic

The paper deals with the evaluation of operative / globe temperature and indoor air temperature by computer simulation method (ESP-r) and their comparing with measured temperatures in real air-conditioned room. Difference between operative / globe temperature and indoor air temperature is given by mean radiant temperature in the room which is affected with indoor and outdoor radiant sources.

Room in which was measurement carried out is located on the top floor of Faculty of Mechanical Engineering, CTU in Prague building on Department of Environmental Engineering. The room is mostly used as meeting room during working days approximately from 8:00 to 17:00. Meeting room is 7,3 m long, 4,6 m wide and 3,1 m high. Construction of the building is formed by iron-concrete skeleton. Sole outer wall is oriented on the South-east. Windows in the room are from steely frame with clear glass with $U = 2,4 \text{ W}/(\text{m}^2 \cdot \text{K})$. Area of windows is approximately 60 % of the wall surface. Two from three windows is possible to cover with black draperies. Internal walls are built-up by wooden cupboards with books. Ceiling and remaining parts are painted with white colour. Meeting room is equipped with ceiling air-conditioning unit Mitsubishi with cooling load 3,7 kW and heating load 4,0 kW.

Measurement of physical parameters of internal environ and selected surfaces in the room has been carried out in period from 12.5.2004 to 11.6.2004. This period was divided to three parts. In each period has been defined specific conditions: 12.5. – 24.5. - measurement with draperies and without air-conditioning, 12.5. – 24.5. - measurement without draperies and without air-conditioning, 2.6. – 11.6. - measurement without draperies and with active air-conditioning (thermostat has been set to 23 °C). This physical parameters has been measured: indoor air temperature t_i (°C), globe temperature t_g (°C), surface temperature t_p (°C) and outdoor air temperature t_e (°C). Indoor air temperature t_i (°C) in the room was measured with shaded thermometer in two points, at the window and near internal wall at height of 1,7 m from the floor. This dimension according to CSN ISO 7726 standard is representing height of head of stand-up person. Equal conditions was used for notice globe temperature t_g (°C) with globe thermometer (diameter at 100 mm). Surface temperature t_p (°C) has been scanned with four thermometers on selected superficies (window, floor, cabinet, ceiling). Thermometers were fit with isolation against radiation of surrounding walls. There was also recorded the temperature of shaded thermometer and globe temperature in the space between the roof and the ceiling above the meeting room as well as outdoor air temperature t_e (°C). Measured parameters were recorded on measuring central outfitted with additional card with A/D converter. The central was installed at beside room in order to its operation untouched measurement in the meeting room with additional heat gain. The sensors which were used for measurement of temperature are in a matter of fact semiconductor thermometers. For communication with measuring card and for recording of measured data (interval of record was 15 minutes) was used Eflab program. Velocity of air flow in the room was recorded with programmable central Almemo 3290 (Ahlborn) by resist sensor (heating string). As the air velocity was not higher than 0,2 m/s it was possible in the next steps to evaluate operative temperature as arithmetical average of air temperature in room and mean radiant temperature.

Calculation model of the meeting room was created with ESP-r simulation program. Meeting room was simulated as two-zone model. The first zone was the room. The second zone was formed with space between the roof and the ceiling above the meeting room. For calculation of operative temperature in random point in the room and in random position of the person is needed to use MRT (mean radiant temperature) sensor. Sensor has block shape with this dimensions 0,3 x 0,3 x 1,1 m (w x t x h) and it is placed 0,7 m from the floor. This dimension represents the stand-up person. For simulation were not applied data for reference climatic year in Prague but own database of climatic entries. This database was measured and recorded in solar laboratory at Department of environmental engineering.

From measurement in the real room come out that indoor air temperatures and mean radiant temperatures are very similar. If these temperatures are identical also the operative temperature is equal to them because it is their average value. If these temperatures are identical also the operative temperature is equal to them because it is their average value. This can be truth only when the airflow velocity in the room is not higher than 0,2 m/s as well as in our case. At simulation with ESP-r was distinction between indoor air temperature and mean radiant temperature little bit higher but did not overdraw value of 2 K. Values of temperatures received with measurement and simulation shows relatively good equality. This can be truth only when measurement was overshoot under setting conditions and it was not obstructed by outer effects. For instance the air-conditioning was active when it should be turn off. After its turn off the temperature was relatively quick returned to required values so it had not long-time effect to measurement process.

References:

- [1] ČSN EN ISO 7726; *Tepelné prostředí - Přístroje a metody měření fyzikálních veličin*, Federální úřad pro normalizaci a měření, 1993.
- [2] PČSN EN ISO 7730; *Mírné tepelné prostředí - Stanovení ukazatelů PMV a PPD popis podmínek tepelné pohody*, Český normalizační institut, 1997.
- [3] VLÁDNÍ NAŘÍZENÍ Č. 523/2002 SB. *Podmínky ochrany zdraví zaměstnanců při práci*, částka 180, Sbírka zákonů ČR, 2002.
- [4] NOVÝ, R.; A KOL.: *Technika prostředí*, 2000.

This research has been supported by FRVS 1978/G1.

High pressure casting technology - methodology

A. Herman, B. Bednář, L. Maroušek, B. Stunová

Ales.Herman@fs.cvut.cz

CTU, Faculty of Mechanical Engineering, Department of Manufacturing Technology,
Technická 4, 166 07 Prague 6

The die casting process is a true metal casting process, since metals are melted and then solidified within molds having cavities shaped to the design of the required parts. In the casting processes that utilize sand or plaster for molds, the mold is destroyed by the molten metal heat or when extracting the casting from the mold. In the die casting process, the hardened steel molds can withstand the casting heat and are constructed with movable sections which allow easy removal of the solidified casting. Therefore, these molds are reusable and can be used for producing thousands, or even millions, of castings. These permanent molds, called "dies", are reusable and are subjected to high levels of force or pressure and include complex mechanisms.

The die casting process actually has three sub-processes. These are: permanent mold casting (gravity die casting), low-pressure die casting, and high-pressure die casting. In North America, the term die casting is used to mean high-pressure die casting, although the technology embraces all three sub-processes. The three processes differ mainly in the amount of pressure, which is used to force the molten metal into the die. All three use reusable dies as molds. In permanent mold casting, the molten metal is poured into the mold and flows only at the force of gravity. The low-pressure process utilizes pressures up to 1.5 MPa to force the molten metal into the die. The high-pressure die casting process subjects the molten metal in the die to pressures between 7.0 and 140 MPa. As the pressure is increased, there is a corresponding reduction in the time required for the molten metal to fill the die.

An increase in the molten metal injection pressure requires the machine to apply a corresponding increase in force to hold the die halves together. The internal metal hydraulic pressure can be very high; consequently, die casting machines clamp the dies closed with a great amount of force (more than 25 MN (3 000 t) of force). To apply such high pressure, the molten metal is ladled into a cylindrical chamber and a hydraulically driven plunger pushes the metal into the die. The machines are made to automatically cycle through their sequence of motions. The cycle consists of die close, apply clamping force to the die, ladle molten metal, inject molten metal into the die, wait for the metal to solidify in the die, open the die, and eject the casting from the die. The die absorbs the solidification heat from the casting, and the heat must be processed through the die, away from the cavity area before the next casting is made. The design and control of the heat flow through the die is one of the most critical and challenging aspects of the process.

Die casting is a manufacturing process that is just one step within an industrial system that processes raw materials into consumer goods. The raw materials are from either metal bearing ores or metal scrap. The zinc or magnesium die casting alloys originate directly from the ore. The alloys are refined into ingot of high purity by mining and/or smelting companies and sold as "primary" metals. The larger die casting companies purchase the "pure" ingot and add the other constituents to make the proper alloy. Most of the smaller die casting companies purchase the metal pre-alloyed from either the smelter or an independent alloyer that specializes in buying the pure metals and producing the die casting alloys. Most aluminum and copper base die casting alloys are secondary alloys that are refined from scrap metals. The scrap may be collected from other manufacturing operations, such as the offal from sheet stamping or the shavings from machining operations. Much of this scrap comes from items

that have outlived their usefulness and are being disposed. The secondary smelting companies purchase the scrap, then sort and refine it into the die casting alloys. Some metal(s) may be added during the process to make the alloy composition correct. The smelter casts the alloys into ingots, which are purchased by the die casting companies.

When cast, each casting contains extra metal in the form of sprues (biscuits), runners, overflows and flash that must be removed. The extra material is usually cut from the casting with a trimming die in a power press. These trimmings are utilized as scrap by the die casting companies.

In some instances, the die casting company sells the castings in their "as trimmed" condition to companies that manufacture products that include the castings. Other die casting companies will perform additional machining and metal finishing operations (i.e. polishing, buffing, electroplating, painting and machining) to the casting before shipping it to the customer. In these instances, the purchaser of the die casting simply assembles the finished part into the final product. The die casting operation often is located in the factory that produces a final product, such as home appliance manufacturers, automobile companies, and hardware producers.

Die casting is a highly specialized segment of the manufacturing industry. Among the industries affected by die casting are: machine tool, tool and die, utility, construction, banking, marketing, transportation and communications. Some supporting industries have evolved specialty factions that concentrate on servicing the die casting industry, such as the machine tool, tool and die, process lubricants and industrial furnace industries.

Many companies are independent and specialized only in producing die castings. These companies obtain their business through competitive bidding on a job-by-job basis. These "custom" die casters range in size from those having three or four small die casting machines to multi-plant corporations with many large die casting machine.

Some die casting companies have developed proprietary product lines that dominate their productive capacity. These may have once been custom die casting companies, or may have been established to make a product and are involved in die casting because it is the best way to produce their product. When die casting facilities are maintained within a company to support some other activity, the die casting operation is considered a "captive" operation.

The automobile, small engine, outboard marine products and builder's hardware industries have large captive die casting facilities (many machines with big clamping capacity up to 32 MN - 3 000 t). Similarly, most manufacturers of fractional horsepower electric induction motors have captive die casting facilities. Many other metal working companies also have die casting facilities which may consist of a single small die casting machine with a much larger manufacturing facility, while companies may also devote a substantial portion of their manufacturing effort to die casting. Since a die casting operation requires specialized engineering and highly trained personal for the supportive maintenance equipment, it is usually most economical to have at least 12 medium-sized machines. Smaller groupings of die casting equipment will not justify the proper supporting staff and facilities. The economics are quite different if the die casting operation is limited to machines with less than 1.0 MN (100 t) clamping capacity. The economic unit size may then be as small as three or four machines.

References:

- [1] *Die Casting Handbook*, NADCA, 2001,

This research has been supported by project FRV 1972/F1.

Dynamics of Heat Systems with Heat Pump and Various Degree of Accumulation

S. Nesvadbová, R. Nový, K. Brož

snesvadbova@seznam.cz

Department of Environmental Engineering, Faculty of Mechanical Engineering, Czech Technical University, Technická 4, 166 07 Prague 6, Czech Republic

Dynamics was investigated in a test room with middle ability of heat accumulation, which was not affected by outside climatic conditions directly. This slab-on-ground test room is placed in ground floor of Department of Environmental Engineering laboratory. Heat loss is created by external air supply to the test room. Heat pump was used for this experiment and heats this laboratory and offices contiguous to this laboratory. Heat pump source is ground with dry earth bore filled with non-freezing mixture. This heat pump is heat source for heating system with plate heaters. This heating system consists of 11 plate heaters with temperature gradient 50/40 °C, circulating pump and expansion tank. There is plate heater placed in the test room that covers its heat loss. Heater in the test room is projected on heat loss value 419 W. Total heat loss of all heated rooms is 6,6 kW in this case. Heat pump equipments are storage tank and heating coil too. The volume of tank storage is 0,5 m³. Heating coil could be use as added heat source if increased heat supply is required. This occasion can come at drop of external temperature value below 0 °C.

Measurements were carried out in two measuring places. The first one is the test room and the second one is a room with heat pump. In this experiment were measured values necessary for evaluation and appreciation of dynamic behaviour of plate heater with heat pump heat source.

All dynamic experiments were measured under two working states. In the first working state heat is supplied only by the heater to the test room and the other heaters are closed by thermostatic valves. In the second one heat is supplied to the whole heating system but dynamic changes are measured only in the test room. Dynamic measurements were made at common heating operation, at start of heater by switch-on heat pump from cool state of all system or after heat pump switch-off. For next dynamic measurement were used storage tank. Circulating pump is in function after heat pump switch-off and storage tank supplies heat to heated space. Further change was made this way: heat pump was started but circulating pump was turned off until heat pump switch-off, that is heat pump operates as long as storage tank is not fully charged. Then circulating pump is released and heating system starts extracting heat from storage tank. Before this experiment heating system and heat pump are let to cool down totally. Further measurements were realized at simultaneous operation of heat pump and heating coil namely either at current start this both device or heating coil is attached to heat pump during heat pump operation. Behaviour of this combined heat device is measured within common operation too in order to characters appreciation for heat purposes.

Heater dynamics is criticized according to heater heat inertia. Heat inertia depends on water content in heating system mainly. Heat inertia is influenced by heater material less. Plate heaters have the smallest water content hence they are characterized by the lowest heat inertia value. Plate heaters reach fastest thermal comfort after switch-on of heat source in heated space. After heat source switch-off, air temperature drops in heated space quickly too.

In the case, that heat was supplied only to the test room, heater was characterized by twice lower value of approach heat inertia than in the case of supply of heat to all heated spaces for all measured dynamical changes. The lowest value of approach inertia was reached

at simultaneous start of heat pump and heating coil. The higher value of approach inertia was obtained at instantaneous heat delivered to the heating system. This was realized by circulating pump switch-on after storage tank full charge and heat pump switch-off. Heater had the slowest response at common switch-on of heat pump from cool state. Heater in the test room did not reach its rated power even at working state of whole heating system. The obtained measured approach inertia results are compared with values presented in [2].

In the case of heat source switch-off, without usage of tank storage accumulated heat, medium (water) temperatures in the heating system pipes dropped very quickly at both working states. Consequently, air temperatures went down in the test room as well. Heater was able to heat the test room during 5,5 hours as much as its 50 % rated power by using of tank storage accumulated heat. In the case of whole heating system operation, this period of heat supply from storage tank to the test room was eleven times shorter. This period took 30 min.

Modifications of external climatic conditions have negligible impact on the heat pump performance because heat pump heat source is earth bore, whose temperature is usually stationary throughout heat period. Therefore heat pump has almost constant value of coefficient of performance (COP). External temperature decline influences increase of heat loss value of heated space. It is suitable to use additional heat source to heat pump – heating coil in winter season. Current operation of heat pump with heating coil reduces heat pump energy consumption by one third and ensures more balanced heat pump operation and shutdown periods. Heater reached its rated power in all examined cases of operation of heat pump with heating coil. Heat pump operation period was five times shorter at working state of the test room heating only than at heat pump common operation in the case of whole heating system heating. Heater rated power was even exceeded in the case of the test room heating only for example at heat pump switch-on or heat pump common operation or at heat pump with heating coil operation. Heat loss in the test room was covered from the tank storage mainly at this working state because heat supply was much smaller than at working state of whole heating system and heat pump was for most of day switched off.

Measurement results show that usage of tank storage is very suitable and useful for heating system with plate heaters because heat pump need not switch and shut off so often. In the period, when heat pump is switched off temperature fall in heated space is covered by heat accumulated in the tank storage. Heat is accumulated in the tank storage during heat pump operation so that heat that is not consumed in the heating system is saved to the tank storage. This tank storage was charged from totally cool state until its full recharge for the duration of 70 min at no heat supply to the heating system.

References:

- [1] NESVADBOVÁ, S.: *Studie dynamiky systému tepelné čerpadlo - otopná soustava*, Diploma work - ČVUT, 2003, pp.1-100.
- [2] BAŠTA, J.: *Otopné plochy*, ČVUT, 2001, pp. 73-114.
- [3] BROŽ, K.: *Vytápění*, ČVUT, 1998, pp. 35-89.
- [4] BROŽ, K.– ŠOUREK, B.: *Alternativní zdroje energie*, ČVUT, 2003, pp. 66-97.

This research has been supported by CTU grant No. CTU0405512 and by FRVŠ grant No. FRVŠ 1985/G1.

Intensification of Pulse-Jet Cleaning of Industrial Filters

P. Vybírál

vybiral5@post.cz

Department of Environmental Engineering, Faculty of Mechanical Engineering, Czech Technical University, Technická 4, 166 07 Praha 6

Currently a pulse-jet cleaning is practically dominant way of the effective separating of suspended particles from flue gases. Most industrial filters with the pulse-jet cleaning are fabric bag filters, known as the pulse-jet fabric filters.

The area of pulse-jet cleaning of industrial filters has been studied in the Department of Environmental Engineering of the Czech Technical University since 1996 and different partial targets have been studied. At the beginning problems of geometry optimization of the elements of pulse-jet cleaning were investigated [1]. This contribution is focused on the investigation of the influence of volumes of both inlet (dirty) and outlet (clean) part of the filter to the pulse-jet cleaning efficiency.

The main important criteria were defined [1], by reason of evaluation of tested alternatives. These criteria are established on the background research, expressing the basic features of the pulse pressure time signal in the bag and have decisive influence on pulse-jet cleaning. According to the criteria the evaluation system was determined [1]. This system consists of 6 evaluation factors, that come from the measured pressure time dependence $\Delta p(\tau)$ at three distances from the mixing nozzle outlet.

For solving problems of the pulse-jet cleaning an experimental filter unit with a single filter bag [1] was built in the laboratory of the Department of Environmental Engineering in 1996 and 1997. The filter was constructed from real filter parts and it is equipped with a filter bag of diameter 127 mm (5'') and length 2730 mm. The filter is equipped with instrumentation for measuring all parameters necessary for describing the time dependence of pulse-jet cleaning.

In the beginning experiments of investigation the influence of volumes both the inlet (dirty) and outlet (clean) part of the filter to the pulse-jet cleaning efficiency 6 different alternatives of filter volumes were tested (3 alternatives of the inlet volume and 2 alternatives of the outlet volume) [2],[3]. Results showed, that volumes of the inlet and outlet filter parts have a significant influence to the pulse-jet cleaning efficiency. The best evaluated was the alternative with the highest filter volume on the inlet as well as on the outlet of the filter. This conclusion is unfortunately in contradiction with the practice of filter designers, who aim at minimizing the filter volume per filtering area.

For the proper research of this problem the reconstruction of the experimental filter was made [4]. Reconstructed inlet part of the filter has the additional volumes situated symmetrically in four directions. The total volume of 12 additional inlet chambers is 684 l, so summarized with the original inlet volume (316 l), the maximal inlet volume of the filter is 1000 l. The volume of one additional chamber can be reduced either about one third on 38 l or about two third on 19 l by means of a barrier. Thanks to this possibility 4 alternatives of inlet volumes are offered. The new outlet additional chamber has volume of 90 l, that can be again reduced either about one third on 60 l or about two third on 30 l. The maximal outlet volume is 150 l (the original outlet volume is 60 l). 4 alternatives of outlet volumes together with 4 alternatives of inlet volumes originate totally 16 alternatives of arrangement of the experimental filter. Values of specific volumes (inlet and outlet volume per one cleaned filter bag) of the experimental filter cover and exceed range of specific volumes of real filters.

Conditions of the experiments were slightly modified compared with the previous experiments. Thus new results [4] cannot be directly compared with results of the previous period. By this reason the original ranges of measured values and the point evaluation (established already in the period of the geometry optimization of the elements of pulse-jet cleaning) were changed according to new measured values. Therefore these experiments represent the individual part, that is focused on detailed investigation of the influence of filter volumes to the pulse-jet cleaning efficiency.

The best evaluated is the alternative with the highest filter volume both on the inlet and the outlet of the filter. The size of the outlet volume as well as the inlet volume has a positive influence to the point evaluation of the tested alternative. In case of higher filter volumes a gradient of change of the point evaluation is lower than in area of lower filter volumes. The developed point evaluation system can be considered as a measure of the pulse-jet cleaning efficiency of bag filters. The higher point evaluation of the alternative, the higher efficiency of the pulse-jet cleaning is. The pulse-jet cleaning efficiency is nearly connected with a pressurized air consumption and a filter pressure drop and thus directly influences operating costs.

The used pressure measuring system scanned the difference between a static pressure inside the filter bag and a static pressure outside the filter bag as the differential pressure. In the final period of experiments the pressure measuring system was changed. Components of the differential pressure (a pressure inside and a pressure outside the filter bag against the atmospheric pressure) were scanned by means of a new measuring system.

Four alternatives with the minimum and the maximum inlet and outlet filter volume were investigated by means of the new measuring system. An under-pressure in the outlet filter part is strongly influenced by the outlet volume – the lower outlet volume, the higher the under-pressure. Pressures along the filter bag (in the inlet filter part) depend mainly on the inlet volume – the lower inlet volume, the higher the overpressure. If the volume of the outlet filter chamber is small, the mass of an induced gas by the pulse-jet cleaning elements is reduced and the effective differential pressure decreases. A limitation of the inlet part of the filter decreases the effective differential pressure, because the counter-pressure outside the filter bag is increased.

References:

- [1] DOUBEK, P.: *Pulse-Jet Cleaning of Industrial Filters*, PhD Thesis CTU Prague, 2001
- [2] HEMERKA, J. - VYBÍRAL, P. - ADÁMEK, V.: *Improvement of Pulse-Jet Cleaning of Industrial Filters*, European Aerosol Conference 2003 - Catania, WIP Press, Southampton, 2003 p.495-504
- [3] ADÁMEK, V.: *Improvement of Function of Pulse-Jet Cleaning of Industrial Filters*, Diploma Work CTU Prague, 2000
- [4] HEMERKA, J. – VYBÍRAL, P. - KOVÁŘÍK, K.: *Volume of Industrial Filter and Function of Pulse-Jet Cleaning Vytápění - větrání - instalace*, odb. časopis Společnosti pro techniku prostředí, accepted for publication in 2005

This research has been supported by CTU0405612, by FRVŠ grant No. FRVŠ 1989 and by MŠMT grant No. MSM 210000011.

Development and Verification of the Methodology of Welded Joints Testing Considering Multiaxial Loading

M. Růžička*, R. Pěnička*, M. Hejman**

milan.ruzicka@fs.cvut.cz

*Department of Mechanics, Faculty of Mechanical Engineering, Czech Technical University, Technická 4, 166 07 Prague 6, Czech Republic

**SKODA Research Institute, Tylova 57, 316 00 Plzeň, Czech Republic

During the development of the parts of machines or constructions it is necessary to consider a damage caused by the fatigue of material. Generally it is possible to find many types of welds and structural welded nodes. There is a problem of the absence of basic fatigue data and their accuracy already in the stage of their design so that the qualified fatigue life assessment could be carried out [1]. Welded joints for infinite life can be designed in accordance with the classical processes of uniaxial fatigue life assessment. There is rather complicated stressing on the structures in the welds and their neighbourhood. Its influence will appear only during laboratory fatigue life testing of the given structural joints. The common goal of the grant was to find a methodology of testing and calculations of thin walled welded profiles which would enable to implement a qualified fatigue life assessment before testing itself. Such a virtual testing allows to optimize the given structural joint already in the stage of the design.

The next goal of the project was the investigation of the principles of the fatigue damage of the chosen typical structural welded nodes used in the skeleton frame of the vehicles (mainly trolleybuses and buses) under uniaxial and multiaxial loading and the proposal of the fatigue life assessment methodology. For this purpose the project has been solved both theoretically and experimentally. The aim of the experimental part has been ensuring the reliable data about the formation of fatigue defect and its propagation measured under the defined conditions exposed to different proportional and nonproportional combination of loading. The results served as a base for the theoretical part. Except own experimental results the experimental results available in the literature [2] has been used.

Tests were performed for the sinusoidal loading in tension, bending, torsion and combination in bending and torsion. Basic tests on elementary tests specimens served for obtaining complete collection of fatigue data for the different types of technological and structural notches. The S-N fatigue curves for five types of flat specimens in tension or in bending were investigated. They present the technological and structural notches effect of the weld. Next three S-N curves were investigated for proportional and nonproportional loading in bending and torsion on the two types of welded thin – wall profile joints (40x40x2 mm and 60x40x3 mm) [4]. Material of the hole specimens was structural steel 11 373.1 - S235 JRG2. The strain-life curve of this steel was too experimentally investigated to describe the basic fatigue parameters for elasto-plastic (low cycle) fatigue life [3].

During the tests the point of the expected origin of fatigue damage has been monitored in detail and the level of the stress in the base of the weld has been measured by the strain gauges. The SPATE (conventional measurement VZLÚ Prague) method was tested too. Most these simple and combined loading tests were performed on the electro hydraulic test machines of the Dynamic Testing Laboratory of the SKODA Research Institute. Plzeň. Auxiliary static tests to the calculations of the determination of necessary material parameters have been realized together with FME CTU in Prague.

At the same time as experiments an analysis and comparison of the methods of fatigue life assessment has been carried out by means of the NSA (nominal) LESA (local elastic) and LPSA (local plastic stress approach) with the modification for welded joints. The finite elements method (FEM) for stress calculation was widely used to apply of NSA according the Eurocode 3 Standard as well as the local methods. Different FEM models of flat and tubular welded joints were calculated by ANSYS, ABAQUS and COSMOS-M software. Calculated stress distribution was compared with the experimental stress analysis. A new structural stress approach as the uniaxial fatigue life prediction method was proposed. Also the other uniaxial local approaches (for example SWT and Landgraf parameter) as well as notch approaches were checked [2]. Last but not least the multiaxial criteria were verified. For this analysis our own computer program MAXA [2] (MultiAXial Analysis) was used and modified. Though the calculation results were ambiguous, best results for proportional and nonproportional loading gave the method according to Kenmeugne at all.

Direct application of attained outcomes will be in the optimization of complicated welded structures of the public transport vehicles frames, where is possible to modify the calculation for other types of structural nodes. This way can significantly reduce the cost of the structure design and its complicated and expensive experimental verification. Further importance of the project is in the creation of the software for the prediction of the fatigue life of welded joints exposed to the combined loading. At the same time created database of experimental results with detailed description of parameters and test conditions is an important source of information for both applied research and pedagogical purposes.

References:

- [1] RŮŽIČKA, M. - PĚNIČKA, R. - HEJMAN, M. - KEPKA, M.: *Fatigue Strength of Thin-Walled Welded Tubes*. In: GESA- Symposium 2003. Sicherheit und Wirtschaftlichkeit durch Messtechnik, Monitoring und Beanspruchungsanalyse. 12-13. 6. 2003. VDI-Berichte 1757, pp. 517-524, ISBN 3-18-091757-1. VDI Verlag GmBh, Düsseldorf, SRN 2003.
- [2] RŮŽIČKA, M.- PAPUGA, J.- HEJMAN, M.-PĚNIČKA, R.: *Expert System for Assessing the Fatigue Resistance of Thin-Wall Profile Weld*. In: Computational Mechanics, WCCM VI in conjunction with APCOM'04, Sept. 5-10, 2004, Beijing, China, Tsinghua University Press & Springer-Verlag 2004, CD ROM, ISBN 7-89494-512-9, pp. 1-10
- [3] RŮŽIČKA, M.- PAPUGA, J.- ŠPANIEL, M. - HEJMAN, M.: *Fatigue life calculation methods of thin-wall welded joints profiles*. In: Computational Mechanics 2004, ZČU Plzeň, 2004, pp.453-460
- [4] HEJMAN, M. - SMOLA M. - RŮŽIČKA, M.- PĚNIČKA, J.: *Eperimental Results of the welded joints tests*. In: Computational Mechanics 2004, ZČU Plzeň, 2004, pp.131-136

This research has been supported by GA ČR grant No. GA 101/02/0141.

Application for Teaching the Influence of Control Driven Units in Mechatronic Systems

J. Vondřich, R. Havlíček, K. Belda

vondrich@fel.cvut.cz

Fakulta elektrotechnická, Katedra mechaniky a materiálů, Technická 2, 166 27 Praha 6

The paper presents the solution of a model of a mechatronic system with a moment characteristic of an asynchronous or a direct current motor. The system is compiled with a driving motor, gearbox, mechanisms, kinematics bonds, control units and a driven machine. The equations of motion of the system are in most cases systems of non-linear algebraic-differential equations. The reason for non-linear equations is the non-linearity of kinematical bonds, passive resistances, dampers or elastic elements. Their analytic solution is limited to a few exceptional incidents. For the solution of non-linear systems it is necessary the use numerical methods in connection with computer systems. Compared to other possible software products Matlab appeared to be the most successful for teaching.

The part of the Bachelors and Masters studies at the Faculty of Electrical Engineering of the Czech Technical University includes courses in Mechanics and especially in the field of Electrical Power Engineering and Control Engineering. The courses proceed on a basis, which the students have received in physics in their first two years of studies. These courses widen their technical and practical knowledge. The students get to know methods of vector and analytic static systems, kinematics planar mechanisms and especially dynamic systems with one and more degrees of freedom. For the compilation equation of motion, the Newton's second law or the Lagrangian equations of second order are being used. The computational system Matlab-Simulink uses a numerical solution in order to solve the mathematical model, i.e. the system of non-linear differential equations of the second order. The modeling, numerical solution and dynamical simulation of operating behavior of system make it possible to design the parameters of this system.

Mostly an asynchronous or a direct current motor drives the system. The driving moment with a static non-linear characteristic of an asynchronous motor (Kloss's moment characteristic) is

$$M_m = 2s_Z s M_0 / (s_Z^2 + s^2), \quad (1)$$

where $s = 1 - \omega / \omega_{SYN}$ is a slip in respect to a synchronous angle velocity ω_{SYN} , and s_Z is a parameter, which determines the slip value, for which the moment M_0 is the maximum. For value $s_Z = 0.25$ the maximum of moment is by $\omega_M = (1 - s_Z) \omega_{SYN} = 0.75 \omega_{SYN}$.

The driving moment M_h of a direct current motor is

$$M_h = M_0 - B\omega, \quad (2)$$

where M_0 ...starting torque, B ...constant, ω ...angular velocity of the motor. The equations (1) and (2) are solved with the computer system Simulink. A reduced model can substitute the mechatronic system, which is mostly a two mass torsion system with reduced

moments of inertia I_1, I_2 and two degrees of freedom. The mathematical model of this reduced model is represented by the equations of motion based on Newton's second law:

$$I_1 \ddot{\varphi}_1 + b(\dot{\varphi}_1 - i\dot{\varphi}_2) + k(\varphi_1 - i\varphi_2) + b_c(\dot{\varphi}_1 - i\dot{\varphi}_2) + k_c(\varphi_1 - i\varphi_2) + d_c(\varphi_1 - i\varphi_2)^3 = M_h, \quad (3)$$

$$I_2 \ddot{\varphi}_2 - b(\dot{\varphi}_1 - i\dot{\varphi}_2)i - k(\varphi_1 - i\varphi_2)i - b_c(\dot{\varphi}_1 - i\dot{\varphi}_2)i - k_c(\varphi_1 - i\varphi_2)i - d_c(\varphi_1 - i\varphi_2)^3 i = -M_z, \quad (4)$$

$$\text{where } k = G \pi d^4 / 32 l,$$

G	- modulus of rigidity of shaft,	l	- length of shaft,
M_h	- driving moment of motor,	i	- resulting gear ratio,
d	- diameter of shaft,	k	- spring constant of shaft,
M_z	- moment of load of driven machine,	b	- damping constant of shaft,
I_1, I_2	- reduced moment of inertia of masses of driven and driving elements,		

k_c, b_c, d_c - parameters descriptive of non-linear course of elastic moment in coupling.

Equations (3) and (4) are solved with Matlab-Simulink. With the simulation of different courses of moments of load M_z and different courses of the driving moments for the asynchronous a direct-current motor it is possible to determine the time dependences for example of $\varphi_1, \varphi_2, \dot{\varphi}_1, \dot{\varphi}_2$ and the designs of a control unit for the moment of load. The numerical solution with SW Matlab – Simulink of this system will be compared with the results of experimental measuring on two mass torsion laboratory model [1-3] driven and braking with servomotors M406I-070-01-70 (VUES Brno), sensing unit ECN 1313 (Heidenhain) and transducer Servostar 603 (Danahar Motion). The knowledge of the dynamic characteristic of mechatronic systems is important for the designing of the whole system as well as for the regulation and control of different processes. The modeling and dynamic simulation of operating duty of system make the realization of operating behavior for this system possible for students. Different numerically solved systems with driven motors, load moments, and control units, with Matlab and Simulink, are presented on the web and applied in courses of Mechanics, Dynamic of processes and Dynamic of mechanical systems.

References:

- [1] J. VONDŘICH: *Application of Modeling and Simulation in Engineering Education* IASTED, Proceedings of the Fourth IASTED Conference on MSO, Kauai, 2004, pp. 342–348.
- [2] S. JIRKŮ, J. VONDŘICH: *Analysis of Manufacturing System with Asynchronous Motor* Proceedings of FAIM Dresden, 2002, pp. 141-143 and 12 pages on the CD ROM.
- [3] J. VONDŘICH, E. THÖNDEL: *Application of Matlab in Engineering Education*, SCS, Proceedings of the Conference MSO, Orlando, 2003, pp. 105–109.

This research has been supported by CTU grant No. CTU0418213.

Panel Radiators

R. Vavříčka, J. Bašta

Roman.Vavricka@fs.cvut.cz

Department of Environment, Czech Technical University in Prague, Faculty of Mechanical Engineering, Technická 4, 166 07 Prague 6 - Dejvice, Czech Republic

The radiator is important part of heating systems. Project of radiator for example type, location, technique of working, have direct impact to thermal comfort of heated space. Is important, in order to the project of radiator took thermal comfort of occupant into account to the full along with economy requirements.

With the panel radiators it was determined during the measurement under standard conditions that the nominal heat output by the radiators called „short“ is constant both for single-side top and for diagonal top connections. This information is not valid for called „long ($L \geq 4 \cdot H$)“ panel radiators.

This phenomenon is read different. Germany technical literature is inclined to explain it as of ejector effect. By long radiator with single-side top connection the ejector effect means that induction cold water come up first heating flue connected with top distribution box. Consequently the mean surface temperature of radiator is cutting down along with decrease of heat output. This information was published in article of Abel, Bott and Schlapmann in 1993 [L4].

In other literature [L1, L2, L3] interprets this phenomenon as significant decrease in dynamic pressure in top connection box wit respect to its length. Due to the pressure loss of the radiator, which in the form of friction and local resistance increases with length of the radiator, predominant part of flow is immediately returned to bottom collecting box and to the outflow from the radiator. In the second half of the radiator unordered (chaotic) flow occurs and velocity moves in the order of 10^{-9} [m/s] here. Take place such small velocity conditions determinate convection heat transfer coefficient inside the water, but at the same time more marked cooling water by flow trough complete radiator. The water stayed in radiator for a long time and the temperature gradient (temperature of medium minus room temperature). Temperature gradient in radiator is more highly than nominal temperature gradient. Insufficient warming-through of radiator by inlet hot water is the cause decrease mean surface temperature thereby decrease heat output by radiator with single-side top connection.

This problem we are solved by mathematic simulation and experimental verification temperature fields by surface temperature mapping. We carried out mathematical simulation on two types of panel radiators. The first type was „short“ model. This model corresponded to panel radiator KORADO Radik Klasik type 10 – 500 x 500 (the first number is the type of panels, the second number is the radiator of height, the third number is the radiator of length) with single-side top connection and diagonal top connection by nominal and double flow. The second type called „long“ model corresponded to panel radiator KORADO Radik Klasik type 10 – 500 x 2000 with single-side top connection and diagonal top connection by nominal and double flow. In experiment the surface temperature is mapping with the assistance of contactless thermometer (radiant heat pyrometer) Testo Quickstep 860-T2. The panel radiator type 10 – 500 x 500 and type 10 – 500 x 2000 was measured always single side-top and diagonal top connection.

By radiator type 10 – 500 x 500 with single-side top connection the temperature fields obtained by mathematic simulation is compared with experiment both causes showed creation the colder area in the right bottom corner of radiator. The colder area is caused by decrease of water current velocity in this part of radiator. The mean temperature of radiator, which is the

70 °C for both causes, corresponded to 75 % radiator heights by experiment and this temperature is distribution for all its length. On the contrary by the mathematic simulation the mean temperature is transferred lower and its course of temperature have more diagonal character. By the same type of radiator, but diagonal top connection, the mean temperature is transferred under 75 % radiator heights. By the mathematic simulation the mean temperature corresponded to 60 % radiator heights and by the experiment it is 65 % radiator heights. The colder area, which by the mathematic simulation is in the middle of bottom part of radiator, is moved moderately to right by experiment.

Type 10 – 500 x 2000 with the single side-top connection. The mathematic simulation demonstrated reduces of flow in the second half of radiator with ensuing minimal heat transfer. However by the experiment the colder area is in the bottom part of radiator. This area covered almost all length of radiator and reaches about the 20 % radiator heights. Both figures of temperature fields are not so much different for diagonal top connection of long radiator. In the distance about 80 to 100 mm from inlet of hot water to the radiator is predominant part of flow ripped to the bottom collection box and conducted back to the heating system. But by the mathematic simulation is seen, that flow of water is continuously separated for all length of radiator. Due to pressure distribution in the radiator occur to deceleration of flow in its half-length thereby bigger cooling water. Difference in temperature distribution by experiment and mathematic simulation have the same cause as by single side-top connection.

From the analysis of the results of mathematic simulation and experimentally obtained temperature fields is reason of decrease of heat output by single side-top connection of radiator decrease of dynamic pressure in the top connection box. From the confrontation the experiment and mathematic simulation, the diagonal top connection is better, because near concordance is evident as short as long radiator. The causes of difference between temperature fields by single side-top connection are caused first of all inlet hot water to the radiator trough distance ring. This cause will be part of next research. Advantage diagonal top connection of long panel radiator with ratio $L/H \geq 4$ is possibility reached higher surface temperature of radiator thereby better utilization of heat surface. On the basis of acquired results we can recommend even more and change the condition of distinguishing „long” and “short” radiator with respect to the connection. As „long” radiators for which the above-mentioned recommendation of the connection is valid we consider panel radiators, which fulfill the condition ($L \geq 3H$).

References:

- [1] VAVŘIČKA, R.: *The pictures of flow inside water by radiator* Dissertation - Czech Technical University – Department Environment, 2002, 73 pages.
- [2] VAVŘIČKA, R., BAŠTA, J.: *Computer simulation of long panel radiators* Building and environmental simulations 2004, 2004, pp. 107–111.
- [3] VAVŘIČKA, R., BAŠTA, J., SCHWARZER, J.: *Problems with connections of long panel radiators* Modelling and Simulation for Environmental Engineering, Praha: CTU Publishing House 2004, pp. 109–113.
- [4] ABEL, H., - BOTT, H., - SCHLAPMANN, - D.: *Raumheizkörper* Heizungstechnik, v.13, no. 4, 1990, pp.928-935.

This research has been supported by MŠMT grant No. MSM 34-11101.

Experimental Equipment for Checking Sources of Aerodynamic Sound

M. Kučera, L. Mareš, J. Votlučka

miroslav.kucera@fs.cvut.cz

Department of Environmental Engineering, Czech Technical University in Prague,
Technická 4, 166 07, Prague 6, Czech Republic

The aim of the project was the design of an experimental stand for the measurement of the sound power of selected items of HVAC equipment, particularly those designed for comfortable HVAC equipment. Consequently it was necessary to comply with requirements for low background noise, i.e. noise of the HVAC equipment as a whole. Due to the fact that an such experimental stand has been already established in the noise laboratory (free-field room) of the Department of Environmental Engineering, which, however does not meet the required values of background noise, another appropriate system was investigated. The existing system uses a ventilator for the achievement of the required air flow. This system, working in a continuous mode of operation, has a significant drawback from the viewpoint of background noise.

The source of air in the newly designed system is a pressure vessel (property of the Department of Environmental Engineering) with an approximate volume of 5.9 m^3 situated in the yard between the laboratory halls. The above method of the achievement of the required air flow is based on the expansion of air supplied from the pressure vessel. Consequently such operation is not continuous – in the first stage the vessel is filled by a compressor with air up to the required pressure and only afterwards controlled expansion occurs. The advantage of the above system is that a significant source of aerodynamic noise – the ventilator – can be omitted.

Besides the above pressure vessel use was also made of an existing DN 100 ductwork. A ball valve which serves for the closing of the supply duct to the aerodynamic tunnel was mounted at the outlet of the pressure vessel. Beyond the valve the duct leads from the outer space (yard) perpendicularly into the corridor of the laboratory halls and further runs under the ceiling into the workshop of the Department of Environmental Engineering, where it is connected to the aerodynamic tunnel.

The aerodynamic tunnel runs longitudinally through the workshop of the Department of Environmental Engineering and its end opens into the free-field room. The tunnel is mounted in four suspensions anchored into the ceiling of the workshop. The tunnel comprises two sections of high-pressure MOPVC PN 12.5 ducts with a 315 mm outer diameter and a 8.5 mm wall thickness. The total length of the tunnel is about 12m. Flexible sound dampers (FLEXO) are mounted inside the MOPVC ducts.

Individual parts of the tunnel are secured against shifting by means of special flanges and also normal modified flanges. The sound dampers inside the MOPVC ducts are joined by flanges.

Compressed air is supplied by a GX5C single-stage screw compressor with an output of 10 l/s. The compressor is housed in a soundproof case together with a 200 l receiver.

Compressed air is supplied from the compressor to the pressure vessel via a 1" duct and designed in such a way to enable the use of the compressor for current work in the workshop.

One of the main problems of the design was to ensure the required control of the expansion of air from the pressure vessel. At first throttling of air by a single orifice situated in the removable segment of the ductwork in the workshop was considered (exchange of the

orifice for various air flow requirements was assumed). This system, however, can be hardly considered as a source of "quiet air" since air flows through one orifice at sonic velocity (up till the moment the pressure ratio drops beyond the critical limit). During the outlet of the fluid aerodynamic noise is radiated. The total sound power irradiated depends on the 8th power of the air flow rate at high values of the Mach number ($Ma > 0.8$). For lower values of the Mach number the value of the power of the air flow rate decreases which leads to a reduction of the aerodynamic noise. From fluid thermodynamics it follows that if low values of the Mach number are to be achieved, the air flow must be subsonic. In order to be able to achieve subsonic air flow, the pressure ratio must drop below the critical limit.

From the above it is apparent that the designed system requires not only air flow control but also reduction of the air flow rate. The above has led to considerations to use a system of orifices still situated in the removable segment of the ductwork in the workshop. Later, however, it appeared that a more appropriate solution would be a cascade of "sieves" (punched-plate screens) situated inside the pressure vessel. This concept appeared to be advantageous mainly from the viewpoint of the layout but also from the viewpoint of vibrations since this system is situated farther from the place of measurement.

The use of a cascade of "sieves" causes a reduction of the pressure ratio in the individual stages and consequently leads to a reduction of the air flow rate. For a given cascade the initial air flow is preset and during expansion continuously decreases. For a different initial air flow another set of punched-plate screens (further "sieves") designed for the given air flow must be used in order to achieve the required pressure at the inlet of the aerodynamic tunnel.

As it has been mentioned earlier, the equipment for air flow control is situated inside the pressure vessel. The pressure vessel has only one main "entry port" in its lower part and four smaller ports in the upper part. Inside the pressure vessel from each of the ports in the upper part a DN 150 duct leads vertically to approximately $\frac{1}{2}$ of the height of the pressure vessel. Two of these ports are sealed with flanges outside the pressure vessel and the two remaining ports serve for the discharge and supply of air into the pressure vessel. The air flow reductor is suspended on the vertical discharge duct, which supplies air to the aerodynamic tunnel.

The application of the principle of pressure differences made it possible to gradually reduce the air flow rate in the cascade and thus to reduce the noise of the aerodynamic tunnel as a whole and also to enable an easier and more rapid control of the entire system.

References:

- [1] NOVÝ, R.: *Noise and Vibration* CTU in Prague, 1995, 389 pages.
- [2] VOTLUČKA, J.: *Aerodynamic Sound Sources Dissertation* Czech Technical University - Department Environment, 2005, 51 pages.
- [3] REYNOLDS, D. D. – BLEDSOE, J. M.: *Algorithmus for HVAC acoustics* Ashrae, 1991, 441 pages.
- [4] HARRIS, C. M.: *Handbook of Noise Control* McGraw-Hill Book Company New York, 1979, 930 pages.

This research has been supported by MŠMT grant No. MSM 34-11101.

Environmental Engineering of Buildings

R. Nový, F. Drkal, K. Brož, J. Hemerka, K. Hemzal, J. Bašta

Richard.Novy@fs.cvut.cz

Department of Environmental Engineering, Faculty of Mechanical Engineering, Czech Technical University in Prague, Technická 4, 166 04 Prague 6, Czech Republic

In this contribution we present the result of following topics which were successfully solved in 2004:

In the area of **Air Pollution Control** were analysed different methods of classified sampling of emissions and for the next application was recommended a classification with a cyclone separator. In the laboratory of the Department was built a new testing line and experimental tests of the cyclone separator with $\phi D = 78$ mm were realised. From the results of experiments follows, that the cyclone separator $\phi D = 78$ mm can be used as a “PM10 classifier” only at a low flow rate under $3 \text{ m}^3/\text{hour}$. In the 2004 was realised an exacting reconstruction of the laboratory testing filter for investigation the pulse-jet cleaning of industrial filters and extensive experiments of investigation of inlet and outlet filter volume influence to the efficiency of pulse-jet cleaning were then carried out. Results of experiments turned out that both inlet and outlet filter volumes play an important positive role for the pulse-jet cleaning efficiency, expressed at experiments by means of a point evaluation system. Our important conclusion is unfortunately in contradiction with the practice of filter designers, who aim at the minimising the filter volume per filtering area.

In the area of **Noise Control** was made an analysis of the behaviour of selected variants of the connection of thermostatic valves to an experimental heating system. The aim was to monitor the behaviour of elements comprising the system and to suggest the most appropriate alternative of the design of heating systems with regard to the suppression of undesirable noise. In conclusion results are presented of experiments which led to recommendations on an optimization of the design of heating systems with regard to the suppression of noise.

The flow of air through ducts is mainly controlled by throttling (except for the control of the performance of fans, where variation speed is used). All throttling elements are sources of aerodynamic noise. The most common throttling elements in air conditioning systems are butterfly (single-blade) or multiblade dampers. The main object of the present paper is an analysis of the working characteristic of a butterfly damper in a pipe with a circular section in terms of noise generation. Also possible improvements are sought of the working characteristics of dampers by a substantial reduction of the aerodynamic noise. Finally a successful solution is presented based on the cascade expansion of air in a duct achieving a reduction of noise by approx. 6 dB.

The control of the performance of **Heating Radiators** is performed by regulating the flow of heating water. By fitting a thermostatic valve at the entry to a heating radiator the process of regulation of the flow of water (closing of valve) is accompanied by an increase of local losses, occurrence of cavitations and subsequent production of noise and its transfer to the heating radiator. The radiator due to its large surface area is an ideal medium for the transmission of noise into dwelling spaces.

The advancement for **Renewable Energy Sources Utilisation** - The reconstruction of testing stand for solar collectors power characteristics, Facade solar collectors – computer simulation of its performance, Long-term testing evaluation of glass collector cover or of windows soiling, Optical behaviour under different slopes, Starting testing of combined heat

accumulator (for heating and soft water) and for different renewable energy sources applications (heat pump, solar system, boiler burning wood), The measuring of heat transfer coefficient at outer surface of solar collector glass cover, Multivalent renewable energy source in Herbertov – continuous monitoring and performance data evaluation, Passive and active glass Fresnel lens research and results application at bio-technological system in the town of Nove Hradý, Mathematical modelling of two types of hybrid solar collectors, heating and photovoltaic - air and water simultaneously as the heat transfer media, The development of vacuum tube solar collector with heat pipes – the prototype, Mathematical modelling and computer simulation of the dynamic performance of heating systems with renewable energy sources.

In the area of **Ventilation and air-conditioning** are presented following results:

Important role in sustaining or improving the quality of environment in Prague down town city has operation ventilation of road tunnel Mrazovka. The use of research work results on the design of ventilation system (made under support of Research Project), contribute to safety and economical operation ventilation (with 2 MW power input of installed fan motors). Physical modelling results of individual parts the fire ventilation system secures the safety evacuation of tunnel users by stratification of smoke under the ceiling.

The research was aimed at the development and application of analytical methods, experiments, computer modelling and simulations in the design and performance assessment of ventilation and air-conditioning systems. The most important projects performed within the framework of the Research Plan were focused on:

Theoretical and experimental analysis of indoor air flow (construction of a climate room, CFD simulations, laboratory measurements of temperature and concentration patterns in ventilated rooms);

Development of energy models for buildings and HVAC systems (using the ESP-r software);

Cooling ceilings (computer-based simulation and analysis of thermal comfort, energy performance, measurement of temperature patterns and indoor comfort parameters);

Application of information technologies in control of HVAC systems;

Radiant heating system combined with displacement ventilation (computer simulation, field experiments).

References:

- [1] MATUŠKA, T. - ŠOUREK, B.: *Fasade Solar Collectors* In: EuroSun 2004. Munich, Germany, 2004, pp. 460–469, ISBN 3-9809656-0-0,.
- [2] NOVÝ, R.- KUČERA, M.: *Reduction of Noise Generated by Damper* In: 11. International Congress on Sound and Vibration, St. Petersburg, 2004, pp. 3097–3104, ISBN 5-7325-0816-3.
- [3] LAIN, M.-DRKAL, F.-HENSEN, J.- ZMRHAL, V.: *Low Energy Cooling Techniques for Retrofitted Office Buildings in Central Europe* In: Ventilation and Retrofitting, Brussels: AIVC INIVE EEIG, 2004, pp. 79–84, ISBN 2-9600355-6-9.
- [4] BROŽ, K.: *Elektrina za sluneční energie s využitím akumulace do křemičitého písku* In: Vytápění, větrání, instalace, 2004 pp. 164-166, ISSN 1210-1389.

This research has been supported by MŠMT grant No. MSM 210000011.

The Influence of Random Multiaxial Nonproportional Stress on the Fatigue Life of Machine Parts

M. Růžička*, J. Papuga*, M. Balda**, J. Svoboda**

`milan.ruzicka@fs.cvut.cz`

* Dept. of Mechanics, Faculty of Mechanical Engineering, CTU in Prague, Technická 4,
166 07 Prague 6, Czech Republic

** CDM, IT AS CR, Veleslavínova 11, 301 14 Pízen, Czech Republic

Rapid development of computers and computer aided design opens relatively new way of fatigue damage computation. Real stress or strain tensors obtained from FE-analysis can be used as a direct input to the locally based methods. Such improvement in detailed description of local load states on engineering components gives interesting possibility how to further improve prediction capabilities in fatigue damage computation – above all in the case of complicated shapes of constructions or complicated loading.

The locally based methods are still in development. Although there is some public acceptance of methods processing the complicated local load state to the reduced uniaxial value (so-called uniaxial methods), any extension towards the more precise multiaxial solution (processing complete local stress or strain state, see [2]) is still doubtful.

The aim of the project described here was to build a PragTic software for a fatigue damage calculation, that would be able to read FE-model and calculation data, collect the data about planned damage calculation and run it. Accent was also laid on the requirement of future extensibility, fast work with huge bundles of data and simple way of use.

Since the load histories and FE-analysis data can be very lengthy, the main part of solution was interested in the question how to increase speed of calculation and efficiently use the memory of computer. The final solution uses splitting of data into separated binary files, where each file consists of a number of components with the same dimension. Binary files are used in order to accelerate access to the desired data. Whenever needed, a whole bunch of entities is uploaded from the file saved on the hard disc to the memory - not only the desired entity is read. The accompanying cached data are usable in much shorter time and thus reduce the time which would be used for any access to the hard disc.

Separation into equally dimensioned data blocks is preserved in the memory. These “data-vectors” are basic entities for any operation. Some higher system had to be build in order to take care of these data-vectors. This managing utility is called the data-base in PragTic project. It cares for opening and closing of files, read of data to the memory and their save to the files and also provides description of them to the user. It also identifies dependencies, i.e. cases where some data-vector is necessary for description of another one. Such solution is used in cases where the final entity has some parts of unequal lengths (e.g. element table of incidencies in the description of elements).

The software code is written in the C/C++ language. Advantages of C++ Builder were used in the development, thus the PragTic is Windows-oriented. Nowadays the user interface is sufficiently built to record all necessary inputs for fatigue damage calculation. It allows to import and edit all parts of input data.

In order to enable great variety in forms of imported FE-data, the import is performed in semi-automated way. User designates the heading line of the record, where the description of data is saved in the most of FE-software. A tentative upload is done, in order to test the file and data. Afterwards the user can inspect the result and changed or omit some parts of imported data. When finished, he starts the real import.

As regards the now implemented calculation methods, these are (for further details see [2]):

- Uniaxial: by Smith, Watson & Topper; Morrow strain based; Morrow energetic; Bergmann; Erdogan & Roberts; Heitmann; Pospisil; Feltner;
- Multiaxial: by Socie; Findley; McDiarmid; Kenmeugne et al.; Papadopoulos; Wang & Brown.

The load history decomposition implements following methods: rain-flow counting method and several its clones (concerning which component of stress/strain state is counted), method presented by Wang & Brown in 1996, longest chord method and minimum circumscribed method. In case of shear load path decomposition, two methods for separation of cycles are implemented – separation by load path crossings and by local extremes of von Mises stress.

The main obstacle in nowadays computations by PragTic is absence of some criteria for elastic-plastic accommodation of multiaxial load states. Accommodation is implemented only in its uniaxial variants – by Neuber and by Glinka. This deficiency limits PragTic's use of multiaxial methods to the high-cycle fatigue region, where the degree of plastization is neglectable.

In order to get appropriate data for computation, a set of 30 experimental tests was performed. Testing specimens machined from CSN 41 1523.1 were subjected to random loading in non-proportional tension and torsion. For further information see [1].

Due to lack of a proper method for the elastic-plastic accommodation in multiaxial states, the prediction comparison of these specimens was performed on uniaxial methods only. All gathered experimental data show too great influence of plasticity. Among uniaxial methods the best solution was obtained from Morrow's energetic method, which gives lowest scatter of results in contrast to experiment. Nevertheless it leads to the most unconservative results among uniaxial methods and vice-versa for other methods. As a whole, the results of methods tend to be unconservative and relatively highly scattered. Such results could be expected due to nature of uniaxial methods.

To complete and enlarge the testing of methods to multiaxial solution, another comparison of prediction capabilities was made on high-cycle experimental data of the same steel under proportional and non-proportional combination of harmonic tension and torsion (see [3], [4]). Here the best solution was obtained from the integral criterion by Kenmeugne et al. The prediction accuracy is much better here ([3], [4]).

References:

- [1] BALDA, M. - SVOBODA, J. - FRÖHLICH, V.: *Using hypotheses for calculating fatigue lives of parts exposed to combined random loads. In: Engineering Mechanics 2003 IT AS CR 2003*, pp. 16-17.
- [2] PAPUGA, J. - RŮŽIČKA, M. - BALDA, M.: *Metody multiaxiální analýzy únavové životnosti. In: Sborník příspěvků semináře Únava a lomová mechanika 2002 - Metodické a aplikační problémy* Skoda Vyzkum, 2004, pp. 1-26.
- [3] RŮŽIČKA, M. - PAPUGA, J. - BALDA, M. - SVOBODA, J.: *Data Processing Line for Multiaxial Fatigue Computation and Its Experimental Verification. In: AED 2004 [CD-ROM]* Orgit, 2004, pp 1-10.
- [4] PAPUGA, J. - RŮŽIČKA, M. - BALDA, M. - SVOBODA, J.: *Several high-cycle fatigue multiaxial criteria compared with experimental results. In: Danubia-Adria 2004* Croatian Society of Mechanics 2004 pp. 286-287.

This research has been supported by GA ČR grant No. GA 101/02/0043.

The Optimization of Aeration Equipment

J. Andreovský*, J. Melichar*, J. Novotný**, M. Brich*

andreovs@student.fsoid.cvut.cz

*Department of Fluid Dynamics and Power Engineering, Division of Compressors, Refrigerating and Hydraulic Machines, Faculty of Mechanical Engineering, Czech Technical University, Technická 4, 166 07 Prague 6, Czech Republic

**Department of Fluid Dynamics and Power Engineering, Division of Fluid Dynamics and Thermodynamics, Faculty of Mechanical Engineering, Czech Technical University, Technická 4, 166 07 Prague 6, Czech Republic

The mechanical surface aerator of pneu – hydraulic type is an alternative solution to known aerate systems. The aeration equipment draws the air in term of hydrodynamic effect of propeller, submerged under the surface of liquid, more to principle of function is on [1] [2]. Axial impeller and aeration equipment have to provide desired parameters.

Comparative parameters were chosen the same as with similar equipment of this type. The main chosen comparative parameters were these:

Suction air flow	Q_g	$[m^3 \cdot h^{-1}]$
Power consumption of electric motor in gas – liquid	P_g	$[W]$
Power consumption of electric motor in ungasged liquid	P	$[W]$
Depth of submerged propeller	h	$[cm]$
Revolution of aeration equipment	n	$[s^{-1}]$
Specific power consumption in gas – liquid	P_g/Q_g	$[W \cdot h \cdot m^{-3}]$

Experimental results were reached using laboratory aeration equipment. The laboratory equipment had nominal power consumption 1,1 kW and its nominal speed was 2900 rpm. The laboratory aeration equipment was used with two different propellers. Both three blade propellers were $D = 80$ mm in diameter, $d_{he} = 20$ mm in external diameter of hub and $d_{hi} = 14,5$ mm in internal diameter of hub. Length of hub was 120 mm. Both propellers of the aeration equipment were tested in chosen positions according to the amount of dissolved oxygen. Shape of the propeller with high comparative parameters, that was simultaneously able to provide high amount of dissolved oxygen, was chosen as the basic shape for next phase of optimization. The experiment was carried out in block vessel, which was 4 m long, 1 m deep and 1 m wide.

Following results were reached using the aeration equipment with nominal power consumption 5,5 kW at speed of 2925 rpm. This aeration equipment was used with three propellers. Propellers were $D = 120$ mm in diameter, $d_{he} = 50$ mm in external diameter of hub and $d_{hi} = 23$ mm in internal diameter of hub. Length of hub was 95 mm. The development and production of propellers has been done by modern junction method altogether with classic technologies. The shape of blades was generated in 3D Cad system. The graphical design of blades is subsequently transformed into real shape using Rapid Prototyping technology. FMD (Fused deposition modeling) technology for making the blades was also used. The blades were cast from brass and then cut. The final product is mandrel controlled. The blades are soldered (with use of silver) to hub of the propeller.

Propellers of laboratory aeration equipment were compared in chosen position. The influence of number of the blades in this case was found accordingly to comparative parameters and amount of dissolved oxygen. The experiment was carried out in block vessel, which was 10,4 m long, 1,31 m deep and 1,55 m wide. For the measurement suction air flow was developed a torus input jet. The jet provides the input resistance lesser than conventional flow meter.

For following design of propeller and its velocity rate determination, the flow pattern was found. The flow pattern of aeration equipment (1,1 kW) was observed using PIV method and was found in co-operation with Division of Fluid Dynamics and Thermodynamics (CTU) [3]. Aeration equipment was installed in measuring line of Department of Hydrotechnics (CTU). Measurement was realized in 2D using just one CCD camera. Plastic debris or air bubbles were used as particle seeding and experimental equipment was operated in the same block vessel as mentioned above. Research of flow pattern was carried out in a gas-free liquid (non – aeration steady) under given conditions. The dependence of the liquid flow rate on depth submersion has been found. The next determination of 3D flow patterns for propellers with 120 mm diameter should be used with five hole probe. The five hole probe was standardized on air accordingly to its intended use.

The characteristic parameters of conventional air pump (air flow rate, power consumption and others) were used as foundation for partial economical judgment.

References:

- [1] J. MELICHAR, J. ANDREOVSKÝ, J. NOVOTNÝ: *Experimentální zjištění parametrů aeračního zařízení* Zborník prednášok konferencie STU 2004, Bratislava SK, 2004, pp. s7. 32-42, ISBN 80-227-2105-0.
- [2] J. MELICHAR, J. ANDREOVSKÝ: *The effect of design changes on the parametres of an aerator* Workshop 2004, sborník referátů CTU Reports, Praha Vol. B, 2004, pp. 670-671.
- [3] J. NOVOTNÝ, J. NOŽIČKA: *Název Sborník přednášek konference Hydrosphere 2004 Optimalizace návrhu a provozu stokových sítí a ČOV 2004, Břeclav CZ, 2004, pp.s. 227-228, ISBN 80-86020-41-4.*
- [4] J. MELICHAR: *Optimalizace oběžného kola provzdušňovacího zařízení kapalin* Journal of Hydrology and Hydromechanics, Vol. 51, No.2., 2003, pp. 150-157, ISSN 0042-790X.

This research has been supported by číslo FIS 1084048 ČVUT CTU0404812 and by VZ J04/98:212200009.

Design tool for modern buildings control strategy

J. BECVAR, F. DRKAL

becvar@volny.cz

Czech Technical University in Prague, Faculty of Mechanical Engineering, Department of Environmental Engineering, Technicka 4, 166 07 Prague 6

This paper deals with building and HVAC system design in modern building and control strategies of these systems in order to save energy. During designing of buildings and systems working in a buildings the designers not take in to account these systems as a one unit but design and optimize each system separately. Each device (for example air conditioning) can be on high technical level but when these devices do not cooperate with others (for example shading device) the result is not optimal and goes to energy losses.

In older building the different devices were designed step by step but also in this case the designer can take in to account the older installed devices and optimized them together with a new devices as one unit. In modern buildings it is already known which devices will be installed (for example air conditioning, slab cooling, shading device ...) and it is necessary to take in to account each device.

In this project model environment based on a computer simulation was created in which is possible to simulate the dynamic behavior of building and the systems working in the building. In this environment we can simulate the building and the devices in this building and we can apply and compare different solutions.

As a case study is shown a meeting room in the 8-th floor at Department of Environmental Engineering in the building of Czech Technical University in Prague – Faculty of mechanical Engineering. This building consists of massive metal – concrete construction and the envelope is largely from glass. Building is largely heated by slab heating system “Crytall “ (a water pipe circle embedded in heavy thermal mass construction).

When this system was designed it was expected that this system will be used also for cooling in summer days, but it was never used and the system is used only for heating. In this room is installed local cooling unit, but in this building there are many rooms where is no cooling device. So in the summer day the occupants suffer from very bad condition. On this room it is shown how can different devices (cooling unit, slab cooling, shading devices, night ventilation) cooperate in order to save the energy. The devices which running costs are cheaper should be running first and only when it is beyond of this device to hold the thermal comfort in acceptable level the other devices should start. A numbers of models of meeting room with air heating, slab heating, shading, night ventilation system, air cooling system, slab cooling system and their combination in computer environment ESP-r (environmental simulation program – research) was created. In order to get environment identical with Prague conditions the complete climate database from CHMU (Czech Hydrometeorology Department) was both. Because the year 2003 was extremely warm it was both the year 2003. The climate data from CHMU were in the form which was not possible to load in ESP-r climate database maintenance so the data obtain from CHMU first must have been put in the unix form. ESP-r climate database uses this climate data: Global radiation, Diffuse radiation, Temperature, Outside relative humidity, Wind speed, Wind direction for 365 days in a year and 24 hours in a day. Because the data from CHMU for radiation contains only global radiation the diffuse radiation must have been calculated with using Erbs model.

Each model of the room and device contains geometric data, construction and material data with all physical properties, complex climate data, control law, and operations as number of people, internal gains etc. For the result analyses were used the inside dry bulb temperature,

thermal comfort (PMV- Predicted Mean Vote and PPD – Percentage of People Dissatisfied), energy delivered, hours above value (26°C). On each model runs the simulation from 1.1.2003 until 31.12.2003. The results analyses were made in hottest week (10.8.-17.8.) and in coldest week (6.1.-13.1.2003). In coldest week the energy delivered by heating (air system) in to room is 211 kWhrs and by slab heating 447 kWhrs. The energy demand for heating at slab heating system is higher then by air heating system. This is caused by accumulation of high thermal mass of the concrete slab. But we can see that the thermal comfort is much better then at heating by the air. It is caused by different way of heat transfer. The heat transfer is by radiation and does not caused the drafts.

In the summer when no device is running the temperature in the room in the hottest day rise to 45 °C. When the shading device is running (blinds) the temperature in the room rise to 40°C these conditions still represents great discomfort. When the shading device and night ventilation are running the thermal condition are much better. The maximum temperature in the room rise to 32°C.

When air cooling unit is running the maximum temperature is 30°C and the energy delivered is –124 kWhrs and PPD is 50 %. When the slab cooling system is running the maximum temperature is 30°C, energy delivered is 256 kWhrs and PPD is 30 %.

When air cooling unit and shading device are running the maximum temperature is 29°C, energy delivered is –86 kWhrs and PPD is 35 %. When slab cooling system and shading device are running the maximum temperature is 27°C, energy delivered is –184 kWhrs and PPD is 20 %. When the air cooling unit, shading device and night ventilation are running the maximum temperature is 28°C, energy delivered is –28 kWhrs and PPD is 20 %. When the slab cooling system, shading device and night ventilation are running the maximum temperature is 26°C, energy delivered –83 kWhrs and PPD is 10 %.

From the results is obvious that when the shading device, night ventilation and cooling systems cooperate properly, we can save about 70 % of energy. From the results we can also see that thermal comfort is better at slab cooling system because this system does not caused the cold drafts and the heat transfer at this system is mostly by radiation.

At the slab cooling system is energy delivered in to the room higher but total energy consumption of this system is lower because this system is low-energy cooling system and is based on water loop circle (pipe embeded in a concrete slab) and as a cooling source can be used for example river etc. The other advantage is that high thermal mass of the concrete slab work as a accumulator. In the night when is the electricity cheaper is “charged by cool” and during the day can provide acceptable thermal conditions for a few hours.

References:

- [1] LIDDAMENT, M.W.: *Technical synthesis report:Low energy cooling systems* AIVC, 2001, 32 pp.
- [2] ANON, J.: *Review of low energy cooling technologies* CANMET, 1995, 90 pp.
- [3] ROEL, H.: *Detailed design tool for low energy cooling technologies* BRE Ltd, 2000, 200 pp.
- [4] WINCKELMANN, F.C. – FEUSTEL, H.E.: *Development of a model to simulate the performance of hydronic radiant cooling ceilings* ASHRAE, 1995 pp. 730–743.

This research has been supported by grant: G1 1976/2004

Experimental Solution of Air Flow in a Ventilation Knot of the Road Tunnel

V. Zbořil, K. Hemzal, M. Trubačová, J. Schwarzer

viktor.zboril@fs.cvut.cz

Department of Environmental Engineering, Faculty of Mechanical Engineering,
Czech Technical University in Prague,
Technická 4, 166 27 Prague 6, Czech Republic

The project deals with ventilation of the road tunnel called “Blanka” which is a part of future City Ring in Prague.

Ventilation of tunnel tubes is problematic because of high concentration of polluted air in long unventilated sections. Polluted air needs to be drained at once and at the same moment fresh air must be supplied. Flow rates which are needed for long tunnels are high and air-exhausting devices are financially demanding and energy consuming. That is why conditions need to be optimized as much as possible, for example by suitable proposal of exhaust inlets.

Aim of the project:

- Experimental verification of the right function of proposed solution, appreciation of rate of interaction between exhaust and supply part of a ventilation knot, proposal of shape and placement of exhaust inlets which are placed in the ceiling, proposal of shape of the exhaust flue, proposal of shape of guiding blades in the exhaust flue.
- Control of results, which were achieved by measuring, by CFD simulation.

Input boundary conditions:

- project documentation of the future tunnel “Blanka”
- preliminary proposal of solution of balance of ventilated tunnel tube

Experimental verification was carried out on 1:40 model. The model was built following the project documentation of a real tunnel. Construction details which did not have any influence on the overall air flow were vanished.

Exhaust inlets were proposed in two alternatives. The first one was built on method of constant pressure maintenance in exhaust flue; inlets were getting wider in the direction of exhausting. The second one used constant profile of inlets along the whole length of exhausting part. The inlets were rectangular in both cases.

Air got sucked in by exhaust inlets into exhaust flue and lead into machine room and further outside. There were guiding blades in the turn-off of the exhaust flue. Their aim was to decrease pressure loss. Connection of fans was proposed in a way, that the first one simulated air-motion inducted by moving cars and jet fans in the tunnel. The second one simulated exhaust and supply machine room of the system. Both circuits were considered to be closed.

As a result of the measurement, we found out large non-uniformity in exhaustion of the inlets with variable profile. Exhaustion effect in this case was 85,6%. Exhaustion of the inlets with constant profile was more balanced, nevertheless, exhaustion effect was only 76%. Interaction

between supply inlet and exhaustion area was minimal. Pressure loss in the turn-off of the exhaust flue verifies observance of requirements put on proposed guiding blades.

We see the alternative of inlets with variable profile as preferential, the decisive characteristics being exhaustive effect (with regard to exhaust of pollutants). Non-uniformity of exhaustion is less important.

For full control of correctness of the experiment we performed computer simulation of the preferred alternative. The CFD model was made in a preprocessor called GAMBIT and meshed with more than 1 500 000 cells. Software package FLUENT was used for computational fluid dynamics simulations. The k- ϵ RNG turbulence model was used for solution. Boundary conditions corresponded with the experiment.

The results of both the experiment and the computer simulation correspond well. They confirm that the approach towards the project was correct.

References:

- [1] TRUBAČOVÁ, M.: *Větrání automobilového tunelu* Diplomová práce Ú12116 FS CTU Prague, 2005, pp. 45–67.

This research has been supported by FRVS grant No. 1990/G1.

The Heat transfer Coefficient Measurement of Solar Energy Collector Glazing Cover

B. Šourek

sourek@fsid.cvut.cz

ČVUT v Praze, Fakulta strojní, Ústav techniky prostředí, Technická 4, Praha 6

The goal set out for this research project was to describe precisely and define the procedures to be used to determine the heat transfer coefficient on the solar radiation collectors' outer glazing. This heat transfer coefficient is influencing significantly the collector performance characteristics in their final form.

Once accomplished, this project should have given three major results:

- Completion of the test measuring line to be used to determine the solar radiation collector operational characteristics via the thrust fans installed to control air flow around the solar radiation collectors;
- Newly arisen instrumentation able to measure the heat transfer coefficient on the solar radiation collector outer glazing;
- Mathematical model supporting the interpretation of the experimentation results – the value of the heat transfer coefficient expressed as function of the wind velocity and direction, sloping and orientation of the surface being cooled down.

It is very problematic to determine the convective heat transfer from the solar collector glazing outer surface outdoor. A vast number of formulas derived from the experiments that simulate more or less aptly the solar collector boundary conditions can be found in the scientific bibliography. The collector mechanical dimensions, its inclination, air flow thrust angle, turbulence intensity or a portion of an unobstructed current, all of this will find its reflection in the resulting value of the heat transfer coefficient.

The measuring line used to measure the heat transfer coefficient on the glazing outer side is based on the knowledge attained from the abstracts from the articles published in the specialized bibliography.

The measuring line itself consists of the insulated glazing with a heating foil installed on its bottom (internal) side. Knowing the input power delivered into the foil under the given thermal conditions, one can determine the heat transfer coefficient on the glazing outer side. Beside, the foil will also be installed on the real solar radiation collector and the results will be compared. But this measurement has not yet been realized because of the delayed beginning of the measurement as a whole. The measurement on the real solar radiation collector is supposed to be commenced in the first quarter of 2005.

The measurement itself is mainly being carried out during the nighttime hours in order to avoid the solar radiation influences.

Eight temperature sensors, wired to the measuring system central control panel are measuring the surface temperature of the glazing. The panel has the TEDIA MU measuring modules able to process various types of inputs. Other quantities being measured within the research project are the ambient temperature, wind velocity and direction. These measurements form a standard part of the measuring system central control panel, being carried out round the clock. The TEDIA MU 1211, are used to measure the voltage and current values indispensable for the heating foil input power monitoring.

Due to the troubles in purchasing the heating foil as a vital component for the measuring, the measuring system has been commissioned as late as in early December. Since then, only a few measurements have been taken during a cloudless sky, as the clouds might have affected the results (contribution of a long-term radiation against the sky).

It was even enough to base the measurement analyzing procedure giving as its result the heat transfer coefficient on the outer glazing on these partial results only. Currently, the heat transfer coefficient is being analyzed in its dependence on the ambient temperature, wind velocity and direction.

But the measurements have demonstrated a disadvantageous measuring line location on the platform of the Environment Technology Institute's solar laboratory. On its one side, the platform is overshadowed by the extension building. Thus, a pocket has arisen on the northeastern side, affecting the frequency of the related wind directions. But due the limitations on the measuring platform size, no better place could be found. At one of this internal grant outputs, there is a request for the GAČR grant called "Thermal Characteristics & dynamic Responses of the Integrated Active and Passive Solar Elements in the Facades and Roof Structures". As on of its parts, this grant will comprise the construction of a flexible measurement point on the secluded Štípoň Station, where the measurement will take place on the flat surface of the building without any protrusions and other influencing construction works.

This grant ought mainly to show that the heat transfer coefficient on the outer glazing can be measured in this way. Only the partial measurement results have shown the measuring line in full compliance with the given requirements and that the necessary heat transfer coefficient curves can be obtained from the corresponding results.

References:

This research has been supported by CTU 0413612.

Section 8

**PRODUCTION SYSTEMS,
TECHNOLOGY, TECHNOLOGICAL
PROCESSES AUTOMATION**

Simulation in Modern Manufacturing Design

T. Růžička

Ruzicka@fs.cvut.cz

Department of Manufacturing Technology, Faculty of Mechanical Engineering, Czech Technical University, Technická 4, 166 07, Prague 6, Czech Republic

This article introduces results of input analysis for doctoral thesis. Thesis topic is Theory of Modelling Manufacturing Systems and Processes with Using Simulation Programs. It explains the meaning and the essence of simulation and introduces thesis aims.

In the last decade the business environment has been changed by dramatic events. After opening of the world market, a national competition has transformed into a world competition. Sharp development of communication, increase of computer power and break of duty barriers lead manufacturing companies to reach the best quality of products and services. The key issues for business success are quickly made decisions, their accuracy and correct implementation. Multinational companies play the most important role in the current Czech industry. They brought capital, modern methods and tools that ensure quality and successful production. Cooperation with these companies has been a very good occasion for Czech small and medium size enterprises (SMEs). They can become direct suppliers and through multinational companies deliver their products to the entire world. Wide range of Czech SMEs have taken these occasions and they also changed their position in the supply chain. They moved from dependence on multinational company to the indispensable position.

Design manufacturing systems and processes is the first stage in building success. Only correct decisions “What to produce?” and “How to produce?” can be developed and ensured by other activities as accounting, financial management, human resource management, strategy and business planning etc. Just these two questions are objects of Design manufacturing. Three main rules for correct design are as follows:

- A designer should be able to analyse past
- A designer should be able to control present
- A designer should be able to predict future

It is necessary to actively use these rules, furthermore quickly and with high accuracy. For the realization of the first two rules, it is necessary to correctly implement information system in the company. Obviously, there is a very limited offer of powerful tools for prediction of future in the market. Nevertheless, development of cheap and powerful hardware and software enables the usage of simulation. Simulation has range of definitions, but in the context of manufacturing design it can be defined as “Technique of building a computer model of a real or proposed system so that the behaviour of the system under specific conditions may be studied“. There are many types of simulation. Main division is into two groups – Discrete and Continuous Simulation. Continuous Simulation is usually used for modelling mechanism (robotic etc.). Design manufacture uses usually Discrete Event Simulation, which is represented by a series of events. There are three main approaches:

- Comparison – used for analysis of previously made decisions and their impacts, comparison of results help chose a good decision

- Prediction – used for prediction of changes in behaviour of system in a particular point in time in the future
- Investigation – in the specific situations it is important to study behaviour itself rather than performance parameters, it is interesting to see how the simulation behaves and reacts to normal and abnormal stimuli

Simulation is used in situations, where it is impractical to experiment with real system, because it is dangerous or expensive, etc. We can also experiment with a new system that has not been built yet. Simulation is a powerful tool for designers. It can be used in design stage (alternative design) or in operation stage (alternative operation policies).

Software, which uses simulation technique, has been developed since the end 1980s. For the first time, simulation was used in 1960 in the British steel industry. Nowadays, the most widespread tools are Witness (developed since 1988), ProModel (developed since 1990) and Arena (developed since 1994). All these tools are very large and sophisticated systems, that can solve wide range of problems. They can work in 2-D and 3-D environment. Their drawbacks are the need for advanced ability users and high costs of investment. In the fact, these tools are applicable and feasible for only large world enterprises, for example Boeing. Majority of companies would use simulation only as an external service for solving several problems. Therefore they can't fully implement and utilise all its advantages.

These tools aren't often appropriate for SMEs. It is fact that now some producers attempt to offer their tools and systems also to SMEs, but it won't probably spread, because their philosophy isn't in accordance with philosophy of SMEs. They strive for easy organizational structure, where the next level is not desirable. In the same way large software usually requests high experience and moreover is often moved off main information flow. Then these tools become inefficient.

The main aim of my thesis is to find compromise between the real needs of Czech SMEs, their possibilities and simulation software. Partial aims are:

- Incorporate simulation in design manufacture so that the next new organizational level won't arise and volume of work will not increase
- Set up level differentiation of the model to practical value, moreover to eliminate unessential details and highlight important elements
- Identify important indicators, which will be available for managers in every time
- Connect actual state of manufacturing system and usage of the model
- Implement solution in real production for adequate costs

It is clear that only active company that improves its activities and implement continuous improvement process, reach the success. However, the crucial aspect is to develop both product and design manufacturing together.

References:

- [1] RŮŽIČKA, T.: *Simulace - zbraň konkurenceschopnosti* MM Průmyslové spektrum, 2004, č.11.

Research of Laser Micro-Milling Technology and the Examples of Industry Utilization

Z. Hovorková

Z.Hovorkova@rcmt.cvut.cz

Research Center of Manufacturing Technology, Faculty of Mechanical Engineering, Czech Technical University, Horská 3, 128 00 Prague 2, Czech Republic

Research in the field of laser micro-milling technology, using laser beam as a cutting tool, was oriented first of all on the estimate of the following characteristics:

- optimum laser working characteristics for different materials,
- number of laser-beam passes, needed for micro-milling into the desired depth,
- quality of the machined surface,
- wall chamfers of the machined cavity,
- size accuracy of machined surface, residual stresses,
- changes of the micro-hardness of the work material at the place of the laser-beam influence,
- size of heat affected zone.

Experiments were performed on different kinds of materials - constructional chromium steel to heat treatment, tool carbon steel and high-speed cutting steel, brass, electrolytic copper, titanium, duralumin, aluminum, zinc, carbon, iron and bronze. The speed of laser-beam movement was changed within the range of 20, 25, 30, 50, 60, 80 and 100 mm.s⁻¹. The number of laser-beam passes was changed in these experiments too.

Here are presented the experimental results:

- Between the depth and the numbers of laser-beam passes there is a linear dependence. The depth of cavity grows linear with the growing numbers of laser-beam passes. The equations of achievement depth of stock removal on the numbers of laser-beam passes and responsibility values R^2 for different speed of laser-beam movement were obtained from measured values. Mentioned equations make possible to determine the working conditions for achievement of desired depth of cavity for laser micro-milling before the full machining.
- The quality of the machined surface was valued according to the parameters R_a and R_y . Roughnesses of the surface R_a and R_y increase with the growing numbers of laser-beam passes. The best quality of the machined surface was reached at copper working, contrariwise the worst quality of the machined surface was found out at high-speed cutting steel.
- The chamfer angle of the cavity wall increases with the growing speed of laser-beam movement. The largest chamfers were found out in steel 14 100 and the smallest in brass. Bigger chamfers are placed vertically to the direction of laser-beam movement and smaller are in the direction of laser-beam movement.
- Size accuracy of machined surface is approximately in the range from 0,05 to 0,5 mm.
- The residual stresses were measured by two methods, namely the method of the gradual eating away of the material and the method of the diffraction of the X-ray. By the method of the gradual eating away of the material it was established that the residual stresses have the character of tensile stresses. In dependence on the numbers of laser-beam passes the measured values were in the range from 9 to 80 MPa. By the method of diffraction of the X-ray the tension stresses were established at the high-speed cutting steel 19 852 at the depth of 3 μ m from the work piece surface. Regarding the low values

of the measured residual stresses and with regard to previously acquired pieces of knowledge from the running of machined forms it is possible to state that residual stresses have no influence on the working life of the form. On the contrary, secondary hardening and also the rising of the micro-hardness was achieved.

- From the distribution of the dependence of the micro-hardness on the distance from the work piece surface it follows that the depth of the influenced thickness depends especially on the number of laser-beam passes. At tested materials it moved from 0,0018 mm (at steel 19 857) to 0,022 mm (at steel 19 312). With the increasing numbers of laser-beam passes the depth of the influenced thickness grows too. On the machined surfaces no micro-cracks were established.

This technology is suitable especially for production of forms for plastic die-casting, printing blocks, laser micro-milling into different depths, punches, EDM electrodes and tools for the ultrasonic machining.

Laser micro-milling technology has a lot of advantages, such as big flexibility. It is enough to compile a program for a computer. By micro-milling it is possible to machine even the heat-treated, hard and hard-machining materials. This technology is more accurate and quicker than technologies used so far (e.g. engraving). It is possible to produce even very small and complicated shapes of business LOGO in 2D and 3D, e.g. marking using the type height less than 1 mm.

In case of integration of laser into machine-tool it is possible to produce form, punch or electrode by combination of the conventional way of machining with laser technologies on one clamping of the work piece, by which the production accuracy increases. In the production of punches it is necessary to take into consideration that the marks on punch have to be produced inclined along 30°. If it is not done when punching it results very quickly in deformation of marks.

In the Research Center of Manufacturing Technology the detailed research of laser micro-milling technology is carried out. It is centred on database creation enabling the assessment of optimum working conditions for different materials. The program for simulation of laser technology processes is being developed as well. Our tendency is to apply the results of our research immediately into industrial practice.

References:

- [1] ŘASA, J. – HOVORKOVÁ, Z.: *Machines and Technologies for Unconventional Tooling Methods*. Machine Tools on EMO Milano 2004, Prague, February 2003, p.43-48, ISBN 80-903421-0-8.
- [2] ŘASA, J. – HOVORKOVÁ, Z. - JINDROVÁ, R.: *Research Results of Laser Micro-Milling Technology, Industrial Applications*. MATAR PRAGUE 2004, Machine Tools, Automation and Robotics in Mechanical Engineering, Proceedings of Plenary Session of all Section, Prague, September 2004, p. 63-70, ISBN 80-903421-2-4.
- [3] ŘASA, J. – HOVORKOVÁ, Z.: *Laser in Moulding and Former Productions*. Optimization of Panel Production, Prague, October 2003, p.56-65, ISBN 80-239-1768-4.
- [4] CHRYSOLOURIS, G.: *Laser Machining: Theory and Practice*. Springer-Verlag New York Inc., 1991, ISBN 3-540-97498-9.

This research has been supported by MŠMT grant No. MSM LN00B128.

5-AXIS MILLING

M. Vrabec, P. Hampl, J. Kafka*

vrabec@fsid.cvut.cz

Department of Manufacturing Technology, Faculty of Mechanical Engineering, Czech Technical University, Technická 4, 166 07 Prague 6, Czech Republic

* Donátova 2 / 620, 150 00 Prague 5, Czech Republic

Key words: 5-axis milling, surface residual stresses

Five Axis machining has been used in aerospace applications for many years but it is only recently that the tool making industry has shown similar interest. The main advantage of 5 Axis machining is the ability to save time by machining complex shapes in a single set-up. Additional benefit comes from allowing the use of shorter cutters that permit more accurate machining. 5 Axis machining allows the user to create continuous 5 Axis tool paths across complex surface. The tool paths are fully gouge checked and support a wide range of machining strategies and all tool types. A wide range of machining strategies can be used to machine models that would previously require multiple set ups. Tool paths are created by defining side angle, lead and lean for the tool.

Aim of research: A contribution to improvement knowledge influence of 5-axis milling (lean for the tool in face of material, method of chip removal) on dimensional and geometrical accuracy and operational ability of machine parts.

Specimens investigated:

- 15th samples of prismatic shape 15x10x70 mm.
- Cutting surface of aluminium 6995 – T6 (Al-Mg-Si) after thermal treatment and tracer controlled milling (at setting different cutting conditions, slant tool in face of material, and parallel and up cut milling). Cutting tool was spherical-end milling cutter Ø 8 mm, from high-speed steel, ZPS Zlín 511415, Sp 60NC,HSS Co5

For the analysis of surface quality were used two methods.

- Surface roughness measurement was performed by means of apparatus TALYSURF 6.
- Measurements of residual stresses were performed with method of electrolytic etching and processed with computer. Stresses were measured circa in the middle of the cutting surface.
-

Results of measurements

Is evident, that tensile values of residual stresses isn't as great as is pertinent finish allowance and then surface properties will depend on used finishing operation. For surface finishing is possible 5-axis milling with copying cutter regard as perspective. Get past this way cutting dynamically stressed surface.

References:

- [1] PKUKLÍK, O., JANDEČKA, K., ČESÁNEK, J.: *Analýza obrábění tvarových ploch při vyklonění nástroje* Strojírenská technologie Plzeň , KTO ZČU 2004,

This research has been supported by CTU 0418012.

Implementation of GPS System into Education in Subject of Department of Manufacturing Technology

P. Hampl, J. Podaný

petr.hampl@fs.cvut.cz

Department of Manufacturing Technology, Faculty of Mechanical Engineering, Czech Technical University, Technická 4, 166 07 Prague 6, Czech Republic

The GPS system (Geometrical Product Specifications) unifies technical standard documents on basis of a GPS matrix. The GPS matrix covers main demands of mechanical engineering in particular branches and creates a basis of a line communication supporting product output.

All phases (construction, technology, metrology and quality management) of production are included in this description. The EU directions about declaration of conformity contain set conditions for products. In order to comply with these conditions the manufacturers must keep the requisite identification of articles. The identification is provided by design documentation, which helps with determination of conformity declaration according to a module principle. Of course, the design documentations has to be created in agreement with the GPS principles.

Until the present time any educational course showing the GPS system has not been taught at the Faculty of Mechanical Engineering of CTU in Prague. On that account an effective innovation of specialized technical courses is being proceeded in the curricula at Department of Manufacturing Technology. The changes are actual both for the branch of study Production Engineering and for the other fields of study. This raise the educational standards on generally reputable level and students obtain large experience with problems of global view on production.

This project was aimed at a complex description of the GPS system (Geometrical product specifications) and its sequence on an industrial process with utilization of innovative educational programmes in the chosen technical courses. The innovation consists in a practical training and its possible implementation into topics of technical lectures. The stress laid especially on the introduction and development of the GPS system in conditions of the industrial manufacture, and on using the modern technical facilities (digital measuring instruments, scoring instruments), that are in equipment of laboratories at the Department of Manufacturing Technology.

The goal is a systematic adoption of experience from the application development of the GPS system into education. This means qualitative improvement and modernization in teaching of technical courses at the Department of Manufacturing Technology, of CTU in Prague. Next objective of the new educational methods was the active wiring of all students into practical training and to extend the scope with solving their diploma or doctoral thesis. The overall effort was the better readiness of graduated students of the Faculty of Mechanical Engineering for practice, which requires increasing demands on active knowledge of the GPS systems.

In the first phase the higher expertness and experience of the GPS systems (Geometrical product specifications) was obtained thanks to studying the scientific literature, EU standards and participation in technical seminars and sessions. Above mentioned expertness and experience was systematically implemented especially into these courses: Mechanical Engineering Metrology, Quality Control and Complex Inspection of Production

Quality. This innovation can be used for new conception of lectures and at the same time for solving diploma thesis and doctoral thesis.

In second phase the acquired experience was evaluated and then implemented into the modern educational conception of the GPS systems in all forms of studies at the Faculty of Mechanical Engineering of CTU in Prague.

References:

- [1] HUMIENNY, Z.: *Geometrical Product Specifications: course for technical universities* Warsaw University of Technology, 2001, 3.1–7.7.
- [2] GRIFFITH, GARY K.: *Measuring and gaging geometrical tolerances* Prentice Hall and Technology, 1994, pp. 201–299.

This research has been supported by FRVS grant No. 1971/F1.

Best of breed

Karel Hartman

hartman@karnet.fsih.cvut.cz

Department of Management and Economy, Faculty of Mechanical Engineering, Czech Technical University, Horská 3, 128 03 Prague 2, Czech Republic

Characterization of progressive systems and the next part deals with pros and cones of systems.

Name	Exact description of systems
Prevent of a defect	System, which occupies the elimination of mistakes, caused by people during the working process. The target of the system is to create such a workplace where it is possible to reveal a human error and a subsequent bug immediately at the place of their origin and to prevent the fault on its way to a next operation.
KANBAN	A Japanese expression for the commission which subsequent the process (operation) order needed in number of parts from the process preceded. Today the comprehend this system as planned at pull.
JIDOKA	A Japanese expression for an „autonomous workplace” where the operator is freed from passive supervision over machines and it is allowed to him to utilize time meaningfully.
Zero injuries	The Company plan concentrates on the prevention in the area of safety work and on the protection of health during the work in which all the staff participate. The target is to eliminate injuries and harms at work..
Fast changes	The Company plan concentrates on doing away with wasting and loss of time by exchanging tools. The reduction of these unproductive times is a requirement for reaching the synchronous production and reduction of working up and stock.
5 S	5S - abbreviation for five basic principles by the respect is of which it is permanently secured clean and effectively organized workplace in which every item has got its own place.
MOST	(Maynard Operations Sequence Technique) The system of measuring work by beforehand appointed times at scope of which the norms of the consumption of time are unwound from a detailed motion analysis of given activity and the cards give objective time.

TPM	The system of the maintenance in which there are all activities connected with maintenance of machines and apparatus done by all the profession groups. The target of TPM is to maximal utilize machines and apparatus.
Dynamic development of the process	The system which always allows all the workers of a concern to actively participate in suggestions and realizations of measuring and whose target is to be an effective process.
Team organization	The form and organization of work founded at upper stage of cooperation among workers who aim their activity at the reach of selected targets.
Motivation system	System of objective remuneration of individuals and teams which based on reaching of individual qualifications and evaluation of reaching of team performance.
“Elasticity“	Possibility of IS to adapt to the needs of the company. The possibility to connect all the systems to fill in the targets given by BSC.
BSC	Total strategy of the company which is split into wickedly selected strategy. This strategy has got all-company character and all departments have to cooperate.
KAIZEN	Japanese philosophy of the management based on permanent small improvements for which all the workers of the company are responsible. The most important things are control and innovation.
Just-in-Time	Supplement of material directly to a fixed production place in exact sequence with piece assembled. Effort to reduce stock at minimal level.
6 SIGMA	Reaching the level six sigma means that the firm is reaching the top level in the area of quality an effective. The customers are satisfied. The target costs are getting lower and the sale and profit are getting higher.

References:

- [1] MOLNÁR,Z *Computer integrated Manufacturing* ČVUT, 1996, pp. 58–78.
- [2] HARTMAN,K: *Rating Information Systems at the Czech market* ČVUT, 2003 4–92.
- [3] HARTMAN,K: *The efficiency of Information Systems* ČVUT, 2000, 8–61

Models of Automated Production Systems

M. Draessler, J. Žáček

draessm@fel.cvut.cz

Department of Industrial Technology, Faculty of Electrical Engineering, Czech Technical University, Technická 2, 166 27 Prague 6, Czech Republic

The main aim of this project was to enhance the exercises of automation on the department of industrial technology at the CTU FEE by means of small functional models of automated production systems and robots. We have decided to buy and improve some training models. This paper deals with the improvements of communication and control interface for these models in order to satisfy various claims posed by various forms of exercises at our department. The models are also suitable for purposes of some diploma and semester works.

The mentioned models are made by German company FischerTechnik and are assembled from several types of plastic building blocks, which provide high variability of model solution. FischerTechnik offers lack of small and simple toy models for children based on electrical or pneumatic drives, with the possibility of computer control by their software. FischerTechnik also offers few ready-made so called „training models“, which replace the real systems for training purposes. The prime aim was to buy the models in this configuration:

3-D robot with interface and expansion module, **production line with two machining centers** and conveyor belts with interface and expansion module, **punching machine and conveyor belt** with interface, **control software LLWin**.

The 3D robot was finally replaced by four „industry robots“ all for the same price as the 3D robot. The ready-made models are equipped with FischerTechnik interface for serial communication with control computer via RS232 by default. Only the „industry robots“ don't have these interfaces, but we decided not to purchase them, because of some difficulties mentioned below.

The need of cheaper and for education more suitable variant of interface lead to design and development of our own control and communication interface.

Purchased and completed models together with developed adaptable software equipment should be in next semesters incorporated to exercises of four courses lectured at the department. Some of them deal with the computer control via the serial bus and some deal with the control using Programmable Logic Controllers.

Except of the courses, we assume, that the models will be used within some degree, bachelor or semester works. Currently, two degree works are being worked up using these models. The first of them deals with the control by PLC, the second provides visualization and control of the model with PLC by Czech SCADA system Control Web.

Every model is equipped with a number of 9 or 24 volt DC drive (in our case, the cheaper 9 Volt variant was used) and up to eight switches. The switches are used for positioning, as the limit switches on one hand and as an incremental sensor (with cam shaft) of position on the other hand. Besides these switch sensors, some models use optical sensors.

Original interface can control up to four DC drives and watch up to 8 switches and 2 analog inputs. Interface has its own communication protocol and is controlled by the software LLWin. Also an expansion module (further digital I/O) can be added.

The supplied software LLWin allows to program the models using the flowcharts, which are drawn in LLWin editor. This software is also suitable rather for introduction to problematics. For control of complex system consisting of more models is more suitable any

of the SCADA systems with appropriate driver for bus communication, own program written in standard programming language (Pascal, C/C++, Basic), or PLC ladder program.

There are some disadvantages of the standard solution of interface.

- 1) The communication interface is point-to-point serial interface RS232, so we can't use one control computer for control of complex system consisting of tens of models.
- 2) The interface cannot be individually addressed, so we cannot simply transform the RS232 signal levels to some bus standard (e.g. RS485).
- 3) Neither the expansion module can be used for control of more models, because only one expansion module can be connected to the interface. In addition the expansion box can not be used when we want to control the models as separate units (e.g. in exercises where one student or a small group of students controls one model)
- 4) The firmware in the controller and the communication protocol are not very transparent and may not be overwritten, so programming the model with own software and original interface would be a problem.
- 5) The interface doesn't allow the use of PLC control, because the power part and control part of the interface are coupled together and the logical signals are quite unreachable, so there is no possibility to connect the PLC.
- 6) The cost of standard interface is excessively high.

It is suitable to design and develop such an interface, which would be able to eliminate the mentioned disadvantages of the standard interfaces. These standard interfaces are planned to be used in the basic courses of automation (13AVS) for introduction to problematics.

Each interface consists of two parts, the power part and the control part, which can be separated. The power part can be connected directly to PLC or to control part by the ribbon cable. When control part is connected, the model may be controlled via the RS485 bus.

Outputs of power driver part are realized by two bridge drivers L298 for driving of 4 DC servodrives. The driver is controlled by two signals, one enabling the driver and one for choosing the direction of motion. At every input there is simple amplifier for optical sensor (or microswitch) and optoisolation, so that the inputs can be connected directly to 24V inputs of PLC.

The control part is equipped with 8bit AVR microcontroller ATmega16, which acts as communication interface and as the controller for the power driver part.. The unit is connected by two-wire communication bus to control computer via the RS485 bus. In this configuration it is possible to control all the models on one bus by one computer.

The model may be controlled by appropriate software. In case of a SCADA system, we need a software driver for interfacing the models with the system kernel. The other possibility is to create own control software in any of standard programming languages.

Currently both the SCADA and the own software control is possible, but in the simplest form usable in the exercises. Further development is assumed by some students' works.

References:

This work was supported by the FRVŠ grant No. FRVS 2038/2004.

Innovation of courses in quality control

V. Chmelík

vaclav.chmelik@fs.cvut.cz

Department of Manufacturing Technology, CTU in Prague, Faculty of Mechanical Engineering, Technická 4, 166 07 Prague 6, Czech Republic

Quality has become an increasingly important concept, especially in the field of production, if not so much in areas like the mining of primary commodities. Tough, rigorous competition on the world market requires that quality must be on the required level.

The new approach to quality is integrated. It is not merely some annex to production, but forms an integral part of control, project planning, production preparation, and then of the utilization of products or services by the customer. It is a way of thinking, a course of action, or even a philosophy of life.

Hence, all graduates of the mechanical engineering faculty must have at least a basic understanding of quality and methods of quality assurance. Graduates of technical aspects of mechanical engineering need much greater knowledge. Quality assurance rests on mastering the processes and improving them on an ongoing basis. It is important to have a correct understanding of methods and information, and of reliability, availability and appropriate processing of data.

The greatest asset provided by project grant is a good supply of modern publications and textbooks. These materials, including software, cover the whole spectrum of modern methods of quality control. The books include the latest works of leading authors and the latest editions of standard works. These materials not only contribute considerably to the modernisation of courses in quality control, but are also a major facility for students and experts from industry working on projects, dissertations and solutions to technical problems occurring in the workplace.

The newly-acquired software equipment will have a significant impact on the quality of courses that can be offered. Last year we used MS Excel for processing data. The new Minitab 14 computer laboratory equipment enables illustrations to be introduced into all exercises, and it will now be possible for students to process their own data. The exercises will be more interesting, and there will be more time for working on methods of interpretation. In addition, the equipment will be accessible for all students of technology for processing all experimentally-measured data, primarily in their diploma and dissertation projects.

The individual licences for Minitab 14 and Design Expert will be utilized mainly in lectures and colloquia, in a combination of notebook plus projector, and in some diploma projects on applications, e.g., of non-normal distributions, for planning extensive experiments.

The acquired software will in general raise the standard and effectiveness of experimental work, and will enable better planning and interpretation of experiments carried out by students of the department.

Titles of exercises in courses where Minitab 14 software will be used (underlined):

Quality Control:

1. Statistical analysis of a file.
2. Gauge calibration (R&R method).
3. Statistical control: design of control charts from measured values.
4. Analysis of control chart analysis with various courses of characters.

5. Pareto analysis.
6. Statistical acceptance.
7. Credit

Complex Inspection of Production Quality:

1. Detailed statistical analysis of a large file.
2. Work under a normal distribution curve.
3. Comparison of hypergeometrical, binomical and Poisson distribution.
4. Statistical control: design of control charts from alternative characters.
5. Analysis of control charts and specific types of statistical control.
6. Statistical acceptance: design of OC curve and AOQL curve of nonconformities.
7. Credit

A one semester LifeLong Learning course has been prepared:

Importance and Scope of DOE Methods (Experimental Design)

A diploma project is now being completed on the Influence of Scanning, Feed and Process of Manufacturing on Surface Quality in the Production of Molds. *Design Expert* was used for planning and interpretation of the results.

Other courses being worked on are:

A New Approach to Quality Costs,

A Comparison of Individual Methods of DOE.

Both courses are supported by books and software acquired from the grant.

This research has been supported by FRVS No. 1973/F1.

Methodology Objective Evaluation of the Quality of Soldered Joints

K. Dušek, J. Urbánek

dusekk1@fel.cvut.cz, urbanek@fel.cvut.cz

CTU, Fac. of Electrical Engineering, Dept. of Electrotechnology, Technická 2, 166 27
Praha6

Soldered joints have influence on general quality of electronic assembly equipment (electronic assembly equipment on PCB – print circuit board). The decision about acceptability or non-acceptability of the specific soldered joint is provided according to strictly given criteria. The criteria for a visual control are also given. The visual control can be done manually (for example by magnifying glass or microscope) or automatically (for example by cameras or laser etc.).

Mechanical tests are mainly used for resistance evaluation of components, parts and whole products against mechanical stress, which is applied on objects during function, transport and storage. Mechanical stress is caused by external forces that have been applied on the object. In practice, low mechanical resistance of products is one of the most frequent problems. That's why investigation of mechanical stability and resistance is very important.

The first step of the experiment was the creation of the test samples. In the second step images were created by a microscope and digital camera. Each image is made several times with a different focus depth. The last step is the creation of a sharp image via software. The sharp image is created from the sequence of images with the different focus depth. For the creation of the sharp images and for image evaluation we used LUCIA IMAGE software with EDF (extended focus depth) module.

For analyzed samples we used PCBs (printed circuit board) with the same properties. On PCBs we applied lead solder paste (Sn62Pb36Ag2) and lead free solder paste (Sn96Ag2). Some of the samples were set up by SMD resistors (1206, 0 Ω). All the samples were put into a continuous furnace with the temperature profile. Both solders – lead (Sn62Pb36Ag2) and lead free (Sn96Ag2) were reflowed. Then we evaluated common properties of the soldered joints such as: wetting wetting angle, cone length.

The next step was application of the mechanical stresses on the test samples. There we have used image analysis for evaluation proportions of cracks.

Before and after mechanical stress on the samples we have measured electrical resistance of the soldered SMD resistors by tetra-point method. Then we compared values of electrical resistance of lead and lead free soldered SMD resistors.

Using the image analysis of the soldered joints it is possible to compare or evaluate suitable properties, for example: wetting angle, solder cone length, surface structure of lead and lead free solders. With image analysis we can compare properties of the soldered joints before as well as after different types of stresses.

Mechanical stress applied on the samples could cause the occurrence of cracks on the surface of the soldered joints. Proportions and frequency of cracks depend on the stress and type of mechanical tests. Proportions and frequency of cracks is possible evaluation by the image analysis.

Mechanical stress also changes electrical properties of the soldered joints, such as electrical resistance. Electrical resistance of the soldered joints increases with the strange of mechanical stres.

The value of the electrical resistance of the lead free (Sn96Ag2) soldered connection is higher than the value of the electrical resistance of lead (Sn62Pb36Ag2) soldered connection. Nevertheless the influence of mechanical stress on the value of the electrical resistance is more perceptible at the lead solder. Too strong mechanical stress can also cause disconnection of the electrical conductive way.

Moreover, we can also evaluate conductive adhesives in the same way.

References:

- [1] MACH P., SKOČIL V., URBÁNEK J.: *Montáž v elektrotechnice* ČVUT, Praha , 2001 pp.180-240.
- [2] ORTH T.: *Vliv pulzního mechanického namáhání na vlastosti spojů realizovaných elektricky vodivými lepidly* Bakalářská práce, 2003
- [3] HWANG J. S.: *Lead-free technology Electrochemical publications* Environment-friendly electronics 2001 pp. č. strany–č. strany.

This research has been supported b: FRV 2040 G1

Modeling of Process Dynamics in Glass Industry

P. Havel

havelp@fel.cvut.cz

Department of Control Engineering, Faculty of Electrical Engineering,
Czech Technical University, Technická 2, 166 27 Prague 6, Czech Republic

Performance of controllers applied in glass production depends a lot on models used for the control design and verification. Hence, main objective of the research was to create a suitable model and simulate the process for the purposes of controller design. Several approaches to modeling such systems have been tried before. First of all, simulation can be done using CFD mathematical modeling. It is computationally very slow and therefore is more suitable for feeders or furnace design rather than iterative design and testing of control algorithms. Recently, some research has been done in order to derive reduced (low-order) linear models from existing CFD models, i.e. models based on first principles. Another frequently used method is black-box model identification. Simple first-order transfer function plus dead time (FOPDT) linear models are the most common ones.

A different approach to the problem was carried out in this project. The main aim was to find a nonlinear model that is not necessarily so accurate but still can show the significant effects of control actions and major relations among variables in the system and can capture the nonlinear nature of the process. A simulation model was developed and tested for a feeder used for fiber drawing consisting of five zones. For a successful production it is crucial to deliver glass to all the bushings at temperatures, which are measured by thermocouples, within quite a narrow band. Heat losses are compensated by controlled gas burners above the glass layer in the feeder.

Process Modeling

First, the feeder was divided into finite lumps and then a bond-graph modeling method was applied since bond graphs are particularly suitable for large-scale mixed systems containing a lot of components, subsystems and interconnections among them. A glass furnace with forehearth and many feeders is an example of such a complex system.

The bond-graph model of the feeder consists of two mutually interacting parts – hydraulic and thermal. The hydraulic model of each zone contains three so-called hydraulic resistors. Their resistances determine the glass flow in the upper (or lower) layer between the neighboring zones and influence the top-down flow between the layers. The hydraulic resistances are assumed to be proportional to the glass dynamic viscosity and since the dynamic viscosity is nonlinearly dependent on temperature we get strong nonlinear dependence between temperature and hydraulic resistance and this makes the entire feeder model nonlinear as well. A bond graph of the thermal model is much more complex; it involves convective, conductive and radiant heat flows between the zones and between the atmosphere and glass layer.

Estimation of parameters

The result of bond-graph approach based on physical laws driving the process is a simplified nonlinear low-order model with significant dead-times available in the form of a computer simulation scheme. The model is a multiple-input-multiple-output system with 8 inputs and 5 outputs. Most of its parameters have straightforward physical meaning and were

determined from a prior knowledge about the system (dimensions etc.). However, eight of the parameters could not be found that easily and needed to be tuned by the optimization algorithm. As possible ranges of these parameters are known identification from data acquired from the real process leads to a constrained optimization problem. If data fitting based on least-squares criterion is used and the employed model of the system is nonlinear, a non-convex optimization problem with multiple local minima often results. In consequence, a global optimization technique has to be applied.

Within this project three selected global optimization algorithms were tested for parameter estimation – local gradient-based search, simulated annealing and DIRECT algorithm. For our case, multiple local search outperformed the other two algorithms. Moreover, the local search always gave us, at least, after several trials an upper bound for the objective function. Increasing the number of evaluations might give better results with the other algorithms, however, in practical applications the computation time is a major issue.

Simulation results

Results of simulations showed a good match with the original data from the real system. Model with the optimized parameters was also validated on completely different segments of the historical records than used for parameter estimation. Nevertheless, the results are still satisfactory and confirm correctness of the chosen physical model structure.

To improve performance of current PID-based control system of the feeder it was suggested that the atmosphere above the glass layer would be separated by refractory partitions. Then each feeder zone would have its own valve that control the flow rate of gas-air mixture through burners and the atmosphere temperatures above the glass layer can be set more or less independently. A multivariable linear-quadratic (LQ) controller was then designed and tested on the nonlinear model in order to show how the feeder partitions and advanced control can help to stabilize glass temperatures above the bushings. All the undesired disturbing changes in glass temperatures were significantly rejected.

Conclusions

To sum up, a novel approach to modeling systems in glass industry for the purpose of control design and validation was developed and verified for the case of a real industrial glass feeder. Despite the high level of simplification and abstraction of the real process the proposed model proved to be satisfactory in showing major effects and correlation among variables in the process. Also, simulation speed was several times higher than a real time. Moreover, validity of the nonlinear model is not limited to a narrow range around the operating point as it is with linear black-box models.

References:

This research has been supported by CTU grant No. CTU 0408013.

Section 9

ENERGETICS
&
POWER ENGINEERING

Solid State Synchronized Switcher

P. Mindl, Z.Čeřovský

mindl@fel.cvut.cz

Department of Electric Drives and Traction, Faculty of Electrical Engineering, Czech Technical University, Technická 2, 166 27 Prague 6, Czech Republic

Switching on and off in electric circuits is connected with transient phenomena. Current or voltage surges usually occur and influence negatively the switch itself, switched appliance and electric network. To minimize this influence is a very serious problem. To use electro mechanic contactor is impossible do to on-time scatter of different contactors. Important improvement brought the replacement of the mechanic switch by an electronic solid-state thyristor switch with special inner control circuits. Such a solution enables to implement the switch-on time with respect to the phase of AC voltage according to the impedance angle of the switched load. In the case of single phase load the transient current depends on the switch-on time. Would the RL load be switched on the voltage with delay angle $\alpha = \arctg \omega L/R$ after the voltage passes zero the over current value will be zero. That means that inductance L with negligible resistance R should be switched on the sinusoidal voltage with delay angle 90 degrees. Such rule is easily to realise on one phase loads. When the load has three phases a good compromise should be taken.

The paper deals with the problem what compromise in the switching of induction three phase machines by means of electronic switch would be simple and good one.

For the mathematical model the space vector theory was used. [1] [2]. Space vector of three phase currents is given by the equation

$$i_s = \frac{2}{3}(i_a + \bar{a}i_b + \bar{a}^2i_c) \quad \text{where} \quad \bar{a} = e^{j\frac{2\pi}{3}} = -\frac{1}{2} + j\frac{\sqrt{3}}{2} \quad \text{is the complex unit.}$$

Similar equations hold for three phase voltages u_a , u_b , u_c and for three phase magnetic linkages Ψ_a , Ψ_b , Ψ_c . Mathematical model of the induction machine is described with 5 following equations written in p.u. (proportional unites) system, time is in sec:

S denotes stator, R denotes rotor, 1 denotes α component, 2 denotes β component, ω denotes angular velocity and M denotes torque

$$\frac{d\psi_{S1}}{dt} = \omega_N \left\{ U_{ef} \sqrt{2} \cos[\omega_N(t + t_0)] - \frac{R_S}{\sigma L_S} \psi_{S1} + \frac{L_m}{L_r} \frac{R_S}{\sigma L_S} \psi_{R1} \right\} \quad (1)$$

$$\frac{d\psi_{S2}}{dt} = \omega_N \left\{ U_{ef} \sqrt{2} \sin[\omega_N(t + t_0)] - \frac{R_S}{\sigma L_S} \psi_{S2} + \frac{L_m}{L_r} \frac{R_S}{\sigma L_S} \psi_{R2} \right\} \quad (2)$$

$$\frac{d\psi_{R1}}{dt} = \omega_N \left\{ \frac{L_m}{L_S} \frac{R_R}{\sigma L_R} \psi_{S1} - \frac{R_R}{\sigma L_R} \psi_{R1} - p\omega \psi_{R2} \right\} \quad (3)$$

$$\frac{d\psi_{R2}}{dt} = \omega_N \left\{ \frac{L_m}{L_S} \frac{R_R}{\sigma L_R} \psi_{S2} - \frac{R_R}{\sigma L_R} \psi_{R2} + p\omega \psi_{R1} \right\} \quad (4)$$

$$\frac{d\omega}{dt} = \omega_N \left\{ \frac{L_m}{2\sigma L_S L_R \theta} (\psi_{R1} \psi_{S2} - \psi_{R2} \psi_{S1}) - \frac{M_{mech}}{\theta_R} \right\} \quad (5)$$

Let us study the influence of sequential switching of terminals of the electric machine. We switch first two terminals to build magnetic flux in the machine and after a while we switch the third phase on. For this purpose the mathematical model is derived for two-phase connection of the machine to the mains.

The switching on begins with switching terminals “b” and “c” on the mains voltage. Terminal “a” is not connected at this moment. After a short time third terminal “a” will be connected on mains. There are two parameters that can be changed. The first parameter is the moment of two terminals (b,c) connection, the second parameter is the duration of this connection after which is motor connected completely on mains.

To minimize transient currents in accordance to theoretical results, three-phase synchronized switcher, was built. Switcher consists of three AC anti-parallel thyristors channels controlled by opto-coupler elements and control electronics. The control circuits, enabling such sequential switching consists of three blocks. The first block is synchronized impulse generator, producing square wave pulse, which front end is synchronized by mains voltage L1 and is delayed with respect to instant of voltage zero. Other two blocks enable generate second, time delayed impulse and its amplification for third switching channel. Obtained experimental results verified very good theoretical prepositions.

References:

- [1] KOVÁCS, K.P.-RÁCZ, I.: *Transiente Vorgänge in Wechselstrommaschinen* Budapest, 1959
- [2] ČEŘOVKÝ, Z.: *Contribution to the calculation of induction motor transients after switching directly to the network* Electrical Journal 27 - CAS 1976 pp.52–70
- [3] MINDL, P.: *Solid State Switching in LV Network* Journal Elektro No 6 FCC 1998, pp. 3–7

This research has been supported by MSM 212300017.

Position Sensors for High Speed Motors with Magnetic Bearings

J. Pavelka*, B. Syrovatka**, D. Vydra*

pavelka@fel.cvut.cz

*Department of Electric Drives and Traction, Faculty of Electrical Engineering, Czech Technical University, Technická 2, 166 27 Prague 6, Czech Republic

**Department of Radioelectronics, Faculty of Electrical Engineering, Czech Technical University, Technická 2, 166 27 Prague 6, Czech Republic

Any rotating machine must be provided with bearings. Some special applications have special requirements on the bearing function as for vacuum and clean-room technique, ultra-high-speed applications and drives with vibration dumping control. One of possible solutions is to use magnetic bearings. Generally radial and axial stabilizations are based on actual information about rotor displacement. Position sensors are necessary part of stabilization system for each active magnetic bearing. Control algorithm depends on the principle of magnetic bearing. Sensors must be very fast and they must have preferably linear output dependence on the rotor position. Planned rotor speed of our application is higher as 100.000 rpm. The following types of sensors were considered.

A. Hall sensors

Use of Hall sensor was very promising at the research beginning. Many experiments were made with sensors KSY14. The time delay of Hall sensor output signal is for high speed application too long. Another disadvantage is output signal dependence on the magnetic field in the air gap.

B. Tuned inductive sensors

Experiments with inductive high frequency sensors were carried out. The detection principle is based on the measuring of the voltage in one of two coils connected in half-bridge. Sensor worked with resonance frequency 423 kHz. All experimental results were correct and applicable till the stator wasn't powered by PWM voltage. Voltage higher harmonics produce disturbed magnetic field influencing sensor signals negatively. Design of the filter does not succeed without any acceptable time delay.

C. Capacity sensors

Capacity sensor was also tested. Its advantage is in the measuring principle. Electric field is not influenced by magnetic field in the motor air gap. Sensor is formed by two electrodes. One electrode is located between coils, conductive board under the motor is the second one. Rotor displacement changes geometric configuration and consequently changes capacity impedance. The disadvantage is given by the dependence of dielectric characteristic on temperature and humidity.

D. Optical and ultrasonic sensors

The advantage of both sensor types is in the measuring principle. Optical and ultrasonic measuring signals are not influenced by magnetic field. Optical sensors can be used only in applications where the sensor pollution is eliminated. Ultrasonic sensors were investigated, but they are too big and expensive. Further application of those sensors isn't possible because of the described disadvantages.

E. Eddy current sensors

Eddy Current Sensors (ECS) are advantageous for precision, non-contact displacement sensing where the range of the target (rotor) displacement x is relatively small ($x = 0.5 - 3.0\text{mm}$). They are useful especially everywhere the magnetic bearing (MB) environment is polluted (dirty, humid, dusty) or where the sensing through the non-conductive or non-magnetic intervening materials is required.

ECS formed by the coils L_A , L_B are arranged in the measuring – control system almost exclusively as a balanced differential bridge where each sensor coil works usually in resonance regime tuned to resonance with the condensers C_A , C_B . Sensor coils driven by the AC RF current from the exciting generator induces eddy current in nearby metallic rotor creating a weakly coupled air-core transformer. Any radial movement of the rotor changes the coupling which causes the imbalance of the bridge resulting in the difference between output signals from both of the R,L,C bridge branches. Magnitude of this differential signal V_{dif} is proportional to the displacement x . This signal serves (after analog filtering and amplification, respectively moreover DSP processing) as corrective feedback signal which drives electronic power blocks of MB in order to secure effective levitation (balance) of MB rotor. Possibly the used DSP enables mainly further efficient signal filtering (digitally), because the environment of sensors coils is highly “polluted” by the electromagnetic smog generated by the MB power driving coils. DSP serves also for another purposes of course – e.g. for linearization of the characteristic $V_{dif} = f(x)$, synchronous demodulation etc.

ECS systems are being developed and tested.

References:

- [1] GEMPP, T. - SCHÖB, R.: *Design of Bearingless Canned Motor Pump*, Kanazawa Japan, August 1996, pp. 333-338.
- [2] PAVELKA, J. - KOMÁREK, P. - VYDRA, D.: *High Speed Motors with Active Magnetic Bearings* 11th International EPE-PEMC Conference 2004, Riga, Latvia 2004 CD-ROM Proceedings paper A51249.
- [3] LARSONNEUR, R. - BÜHLER, P.: *New Radial Sensor for Active Magnetic Bearings* Ninth ISMB 2004 Conference, Lexington, Kentucky 2004 CD-ROM Proceedings paper 86

This research has been supported by grant GA ČR 101/03/0448.

Optimal Control of Active Magnetic Bearing

L. Synek

synek1@fel.cvut.cz

Department of Electric Drives and Traction, Faculty of Electrical Engineering,
Czech Technical University, Technická 2, 166 27 Prague 6, Czech Republic

This paper proposes a method to estimate the position of suspended body that hovers due to the electromagnetic force. The position information of the suspended body can be extracted from the coil currents, which contain the high frequency components due to the injected high frequency voltage without any additional hardware. The most popular configuration applied is the "classical" one of gap sensor, current control, current-amplifier and magnetic coil. The novel method realizes stable and well damped levitation without any sensor hardware at the rotor. This is achieved by using the coil voltage of the magnetic bearing as system input (voltage instead of current amplifiers) and the current as system output. It is demonstrated that the resulting system is observable and controllable in the sense of control theory, allowing a magnetic bearing to be stabilized with a simple linear controller using current measurements alone. The problem is cast as a nonlinear regulation problem and an internal model-based regulator able to offset the noise in spite of the presence of unknown parameters affecting the model of the system is designed. The controller is designed using nested saturation functions and is able to provide a global region of attraction. The control of coil currents and the position of suspended body are performed with the digital controller using DSP.

Active magnetic bearings require some form of control, based on feedback of the position of the suspended object, to overcome open-loop instability and to achieve targeted system performance by modifying the bearing dynamics.

In many potential applications of magnetic bearings, the number of wires which must pass between the bearing controller and the components in the rotating machine needs to be minimized. Such a requirement may arise either from economic or reliability considerations. An exaggerated example of this is provided by the application of magnetic bearings to heart pumps where wires must either pass through the chest cavity (transcutaneous) or be inductively coupled to an external transmission/reception device. In either case, minimizing the wire count is a paramount design concern.

The wires feeding the electromagnets can, to some extent, be minimized by interconnection of the magnets. A more substantial reduction in wire count can be achieved by eliminating the discrete position sensing device and, instead, determining the position of the suspended object from information available in the electromagnet signals. Elimination of the discrete sensing device has such additional benefits as lowering the cost of the system and removing the potential failure of the sensing element, thus improving the reliability of the overall system. Other potential advantages include elimination of sensor-actuator noise and reduction in noise infiltration because the bearing switching signal is now information rather than noise (as it is when a discrete sensor is used). Magnetic bearings which estimate the position from the information available in the electromagnet signals are referred to as "self-sensing".

Previously, there have been two mainstream approaches for developing self-sensing magnetic bearings. One approach is to use a Luenberger observer designed from a linearized state-space representation of voltage-controlled magnetic bearings. Due to the nonlinearities

involved with the physics of the bearing, this approach has limited applicability. The other approach considers the air gap as a parameter of the system rather than a state. Previous attempts using parameter estimation were hampered by force feed-through (the infiltration of force information into the position estimates).

My idea is a nonlinear parameter estimation technique by which the position of a rotor supported in magnetic bearings may be deduced from the bearing current waveform. The bearing currents are presumed to be developed by a bi-state switching amplifier which produces a substantial high frequency switching ripple. The amplitude of this ripple is a function of power supply voltage, switching duty cycle, and bearing inductance. Inductance is predominantly a function of the bearing air gap or, equivalently, the rotor position, while the duty cycle is fundamentally dependent upon the developed bearing force. Ideally, the estimator should exactly extract rotor position information while perfectly rejecting bearing force information.

Before summarizing previous research on self-sensing magnetic bearings, it seems necessary to point out the fundamental drawback to any self-sensing approach. Capacity and thermal considerations usually lead to an actuator structure with magnetic paths whose reluctance substantially exceeds that of the air gaps at high frequencies (20 kHz or more). In contrast, high sensitivity and good rejection of magnetic nonlinearities are achieved in variable reluctance sensors by ensuring that the iron reluctance is on par with or substantially less than that of the air gaps. Thus, the overall sensing performance of a self-sensing magnetic bearing can be expected to be inferior to that of a discrete variable reluctance sensor when evaluated solely in terms of sensitivity, bandwidth, and linearity. In deciding whether such an approach is appropriate to a given application, the system-level advantages of self-sensing bearings must be weighed against expected performance shortcomings.

When the bearing is a perfect inductor, the aforementioned functional relationships are easily established and the gap dependence is monotonic. Since voltage and duty cycle are both easily measured, the relationships can be inverted with a non-linear parameter estimator to extract the rotor position. The estimator embeds a model of the bearing inductance parameterized by the air gap. This simulation is subject to the same switching voltage as the actual magnetic bearing coils. A feedback loop compares the simulated current waveform with the actual current and adjusts the gap length parameter until the two waveforms match.

One of the objectives of my dissertation research is to develop a mechanism that estimates the gap position by processing the current switching waveform. Other objectives are to identify no idealities that are normally neglected in modeling the magnetic bearing and to investigate the effects of these no idealities on the performance of the estimator.

References:

- [1] PAVELKA, J. – SYNEK, L.: *Design and Realization of Active Magnetic Combined Bearing* Workshop, 2003 pp. 790–791.

Hole Drilling Method for Stress Identification of Materials and Structures

K. Vítek, K. Doubrava, T. Mareš, M. Španiel

vitek@fsid.cvut.cz

Department of Mechanics, Faculty of Mechanical Engineering, CTU in Prague,

Technická 4, 166 07 Prague 6, Czech Republic

Knowledge of the stress state in materials and structures belongs to basic parameters and, particularly from the limit analysis point of view, the assessment of stress distribution in the structure surface layers appears to be decisive. In this paper, a formulation of an experimental method, based on strain gauges application and enabling assessment of the stress state in materials (obeying Hooke's Law) and structures, is presented. The methodology presented in this paper is based on the drilling principle, which was developed already in the last century, formulating the drilling method to be applied for the residual stress identification based on prof. G. Kirch's analysis of a modified plate theory with ideally circular hole. A new theory, introduced in this paper, is based on numerical simulations of the drilling process and is applicable for the stress identification in both ideal holes, which is standardized for residual stress [E837-01,e1 *Standard Test Method for Determining Residual Stresses by the Hole-Drilling Strain-Gauge Method*], and drilled holes when considering their imperfections both with static and dynamic problems of the experimental stress analysis. We are engaged in mutual relations of the aspects of the formulated mathematic model of the new method with the aspects of its verification by physical experiments, since the two methods mingle.

The principle of the experimental drilling method to be applied for the stress distribution assessment is based on a strain gauge rosette application (see the scheme) on the surface of investigated structure. Subsequent drilling of a hole of radius R_0 in the middle of the rosette causes a change of the structure shape and thus released deformation on the surface in the hole vicinity is measured with this rosette. The strains measured in this way are calibrated for individual types of rosettes in dependence on the principal stress introduced parallel with the free surface. The theory of the stress assessment, based on the superposition method, determines directions of the principal stresses σ_x , σ_y , and their distribution along the hole depth, in the planes parallel with the structure surface plane. The principal stress zero component σ_z is perpendicular to the surface in the investigated points on the drilled hole which corresponds to reality in small depths when the surface is unloaded. In this theory of the uniaxial stress assessment, we formulate distribution of strains in the drilled hole vicinity, by means of a finite number of Fourier series members:

$$\varepsilon(\alpha, \sigma) = \sum_{i=1}^n [C_i \cdot \cos(i \cdot \alpha) + D_i \cdot \sin(i \cdot \alpha)].$$

At the location of the strain gauge rosette in dependence on the principal stress σ and angle α about this principal stress. After normalizing the formula by σ , the ideal strain gauge signal $\delta(\alpha)$ is:

$$\delta(\alpha) = \varepsilon(\alpha, \sigma) / \sigma = \left\{ \sum_{i=1}^n [C_i \cdot \cos(i \cdot \alpha) + D_i \cdot \sin(i \cdot \alpha)] \right\} / \sigma$$

$$\delta(\alpha) = \sum_{i=1}^n [C_i / \sigma \cdot \cos(i \cdot \alpha) + D_i / \sigma \cdot \sin(i \cdot \alpha)]$$

$$\delta(\alpha) = \sum_{i=1}^n [c_i \cdot \cos(i \cdot \alpha) + d_i \cdot \sin(i \cdot \alpha)]$$

Utilizing these normalized constants, the strain gauge rosette signals ε_i , ε_j , ε_k , corresponding to 2D stress state σ_x , σ_y , can be expressed by the superposition method. From this system of linearly independent equations, stress parameters (usually principal stresses σ_x , σ_y and angle α of their position), corresponding to the hole depth of an ideal hole, can be clearly assessed (here $\alpha_{i,j}$ means an angle between the i -th strain gauge ε_i and the j -th principal stress direction σ_j):

$$\varepsilon_i = \sigma_x \cdot \delta(\alpha_{i,x}) + \sigma_y \cdot \delta(\alpha_{i,y})$$

$$\varepsilon_j = \sigma_x \cdot \delta(\alpha_{j,x}) + \sigma_y \cdot \delta(\alpha_{j,y})$$

$$\varepsilon_{ki} = \sigma_x \cdot \delta(\alpha_{k,x}) + \sigma_y \cdot \delta(\alpha_{k,y})$$

Numerical modelling appears to be fundamental in developing the drilling process methodologies. In numerical models, individual influences can be separated and thus, by means of goal-directed calculations, a database of constants of applied goniometric series can be created for all the spectrum of imperfections. At physical experiments, imperfections with respect to ideally drilled hole are necessary be identified and, on their basis, a computing model, based on the corresponding constants, matching a specified real hole, be classified.

References:

- [1] [1]VÍTEK, K.- DOUBRAVA, K.- HOLÝ, S.- MAREŠ, T.: *Hole-Drilling Method Test Using Bending Specimen*, 40th International conference Experimental Stress Analysis, EAN-2002, Prague 2002, pp.267 - 272. ISBN 80-01-02547-0.

This research was supported by the grant of: GAČR_106/05/2036.

Optimization of The Hole Drilling Method Principle Conditions for Stress Identification

K. Vítek

vitek@fsid.cvut.cz

Department of Mechanics, Faculty of Mechanical Engineering, CTU in Prague,

Technická 4, 166 07 Prague 6, Czech Republic

Frequent cases of stress state assessment can be encountered with in operation where, due to the experimental analysis, the production process would be necessary either modified or interrupt. Further we are focused on materials and products after their production stages have been performed, when it deals with the residual stress caused by the production technologies themselves and when a plastic flow could deform the structures as a consequence of extreme loading. In all the cases, a common strain gauge application is problematic and the drilling principle is more suitable. In the case of static or quasi – static loading, the calibration process can be utilized to assessing stress profile in dependence on the depth of drilled semi-destructive hole. With dynamic loading, the stress distribution along the hole depth is not possible to assess since both the hole drilling and the stress changes depend on time. Practical meaning of the drilling method is concerned of structure surface layers up to the depth of about a few millimetres. As soon as the investigated object is non-comparably more sizeable than the drilled hole dimensions it is possible to suppose small gradients of the stress components to be in this mm-depth and a choice of the drill hole depth influences the sensitivity of these experiments – the deeper we drill the greater is the gauge response (to depth about hole diameter). Therefore the individual influences projected to the experiment results are possible to define only in the case of their external separation. Such a small hole made in the investigated object is possible maintain at many cases or it can be tooled out by a way suitable for surface defects elimination.

At next can be concluded, that only two relatively simple experimental measurements of two displacements on the bar specimen are sufficient for identification of basic material constants - Young's modulus E and Poisson's ratio μ - by the here presented method. The knowledge of this both material constants is required for precise application of the drilling hole method for stress identification [Standard Test Method E837-01,e1].

Any classic tensile experiment can introduce significant uncertainty, regarding the boundary condition definition, into the elastic constants' definition. Moreover, necessity to measure small strains by strain-gages arises. Thus the identification of material properties by the help of tensile experiments is time demanding and quite high-priced. In contrast, a simply shaped bar body, variously loaded, can be manufactured easily and prepared fast for the experimental use. It can be modeled quickly in the frame of any relevant computational system. The possibility to measure experimentally displacements on such simple bar construction is attractive, together with the fact that the strain sensitivity can be adjusted by means of proper choice of bar's dimensions. The sensitivity of a measuring instrumentation is then adapted. The measuring instrumentation should be purely mechanical and no extra investments into strain-gages are necessary.

The bending diagram of dependency of displacement \mathbf{v} on the force \mathbf{F} , which is obtained from the linear regression analysis in the form: $\mathbf{v} = \mathbf{a} * \mathbf{F}$ in the validity range of the Hooke's law. Generally, the slope of regression line $\mathbf{a}(\mathbf{E}, \mu)$ is a function of Young's modulus \mathbf{E} , Poisson's ratio μ and of constant dimensions of expected bar specimen. When the specimen is shaped as a circle with mean radius \mathbf{R} and with a constant rectangular cross-section (height in radial direction \mathbf{h} and width \mathbf{b}), by the FE-analysis concerning the Poisson's ratio μ and displacement $\mathbf{v}(\mathbf{E}, \mu)$ for the chosen unit force \mathbf{F} is adapted by polynomial regression thus, the displacement \mathbf{v} is a weak function of μ and dominant function of \mathbf{E} .

The elastic modulus' identification can be done, when the inverse proportion of $\mathbf{v}(\mathbf{E}, \mu)$ displacement to elastic modulus \mathbf{E} is documented (prepared via power function regression on calculated variants). Since the slope \mathbf{a} of the regression line on experimental data corresponds to displacement \mathbf{v} for given unit force \mathbf{F} , the elasticity modulus \mathbf{E} can be determined as an intersection of the regression line from the experiment and of the regression hyperbole set from calculations, i.e. from the equality: $\mathbf{v} = \mathbf{a} * \mathbf{F} = \mathbf{a} * \mathbf{1} = \mathbf{c} * \mathbf{E}^{-1}$. The elasticity modulus is then given in accordance with the previous equation from the ratio: $\mathbf{E} = \mathbf{c}/\mathbf{a}$.

The determination of Poisson's ratio is based on the hypothesis of "simple functional dependency of bar's displacement under a dominant combination of torsion and bending on Poisson's ratio μ ". The circle is loaded by a force perpendicular to the bar's plane and the displacement \mathbf{u} in the direction of \mathbf{F} is measured, leading to the linear regression line $\mathbf{u}(\mathbf{F}) = \mathbf{p} * \mathbf{F}$. The calculations of the displacement $\mathbf{u}(\mu)$ are performed with the use of unit loading force \mathbf{F} and constant elasticity modulus \mathbf{E} . They are characterized by a regression line, which is a strongly linear function of μ in the form: $\mathbf{u}(\mu, \mathbf{E}) = \mathbf{g} * \mu + \mathbf{h}$. The constant \mathbf{h} is a function of elasticity modulus \mathbf{E} only, which is already set from the previous analysis of the first displacement \mathbf{v} .

Thus the \mathbf{h} constant can be determined from the calculation of displacement $\mathbf{u}(\mu, \mathbf{E})$ of the bar's model loaded by unit force \mathbf{F} and with material constants in the form: $\mathbf{E} =$ previous analysis, $\mu = 0$. Thanks to the second suitable combination of constants ($\mathbf{E} =$ previous analysis, $\mu = 1$) the constant \mathbf{g} of the regression line stems from calculated deformation \mathbf{u} as: $\mathbf{g} = \mathbf{u} - \mathbf{h}$. The Poisson's ratio can be found as an intersection of the linear regression of experimental data and of the linear regression of calculations: $\mathbf{u}(\mu, \mathbf{E}) = (\mathbf{g} * \mu + \mathbf{h}) * \mathbf{F} = \mathbf{p} * \mathbf{F}$. This leads to: $\mu = (\mathbf{p} - \mathbf{h})/\mathbf{g}$.

References:

- [1] VÍTEK, K.- DOUBRAVA, K.- HOLÝ, S.- MAREŠ, T.: *Hole-Drilling Method Test Using Bending Specimen*, 40th International conference Experimental Stress Analysis, EAN-2002, Prague 2002, pp.267 - 272, ISBN 80-01-02547-0.
- [2] VÍTEK, K.: *Identification of Elasticity Constant using the Etalon Bar Method*, 40th International conference Experimental Stress Analysis, EAN-2002, Prague 2002, pp.261 - 266, ISBN 80-01-02547-0

This research was supported by the grant of: GAČR_106/05/2036.

Section 10

NUCLEAR ENGINEERING

Radioactive Aerosol Capture in the Containment of a Nuclear Power Plant

T. Trojek

trojek@fjfi.cvut.cz

Department of Dosimetry and Application of Ionizing Radiation, Faculty of Nuclear Sciences and Physical Engineering, Czech Technical University, Břehová 7, 115 19 Prague 1, Czech Republic

A containment of a nuclear power plant represents a concrete cover that should prevent the escape of radionuclides into environment. In the case of serious nuclear accident, vapor and radioactive materials escape to the containment building. This mixture starts to flow outwards through different leakages due to pressure difference between containment and environment. The amount of escaped radioactive materials depends on containment conditions and the properties of leakages and radionuclides. This work deals with radioactive aerosols passing through a narrow rectangular or circular crack. The main task is to predict the ratio of retained and escaped radioactive particle for various aerosol and crack dimensions.

Calculation of gas, vapor and aerosol flow through a narrow crack is derived from theory described in [1]. Mixture properties (velocity, pressure, temperature, etc.) are changing along the crack and can be determined by solution of system of conservation equations. General modeling of this mixture represents a complicated task that cannot be easily solved [2]. For this reason, some simplifications were done to make it possible the solving of the most frequently incident cases. In order to simplify the general transport equation, steady state system is considered, i.e. all terms with time derivatives are neglected in transport equations. The crack is considered to be a long non-curved hole of rectangular or cylindrical shape. Dimensions of the crack are expressed by its length and hydraulic diameter. Since the length and hydraulic diameter are the most important parameters that influence transport of air, properties of walls of the crack are also substantial in some cases. For example, high difference in air and wall temperature affects dramatically the flow of air due to high energy transfer between air and walls that is directly proportional to the temperature difference. Information on pressure (partial pressure of dry air and partial pressure of vapor) and temperature of air in the point of enter to the crack are required. Temperature, velocity, and partial pressures of dry air and vapor are changing only along the crack in the direction of flow, i.e. the mixture is averaged over the cross section of the crack. Their magnitudes are considered constant facing to wall (vertical direction to the direction of the flow) and dry air and vapor are assumed to be homogeneously mixed. Other air parameters (air viscosity, specific heat, vapor diffusion coefficient, etc.) are derived from previous quantities. Pressure difference or air pressure in environment is a last parameter required for calculation.

The objective of the calculation is to assign variation of temperature, velocity, and partial pressures of air, aerosol diameter, and aerosol density from enter to exit of the crack. These magnitudes depend on position in the crack. They are determined by solving a system of equations. This system comprises equations for energy and momentum balance, dry air mass balance, vapor mass balance, aerosol mass balance, and aerosol grow equation. These six differential equations demand six initial conditions, i.e. air temperature, dry air pressure, vapor pressure, aerosol density, aerosol diameter close to enter to the crack, and pressure of the mixture at the end of the crack. Mixture pressure at the end of the crack is assumed to be

equal to air pressure in environment. Used model takes into account all processes and interactions that can significantly influence the result. The dry air mass balance equation is simple, because the flow of dry air is constant from beginning to the end of the crack. Since the flux is equal to a product of velocity and density, any change of velocity in the crack causes contrary change of density. Similar behavior occurs in the case of vapor flow if vapor condensation is not applied. If air humidity is higher than equilibrium humidity at temperature of wall, vapor starts to condensate on it. On the contrary, condensed water can evaporate from wall surfaces to air. Both these effects may significantly change the flow conditions due to high energy, which is released and used up during condensation and evaporation respectively. Momentum balance and energy balance equation are more complex, because they comprise effects caused by air contraction and expansion, energy transfer between air and walls of crack, and so on.

The system of six differential equations was numerically solved with a Runge-Kutte algorithm. For the purpose of numerical calculation, crack is divided to many parts characterizing air and wall properties over cross section of the crack in its certain section. The equations, transformed to the form required for numerical solving, enable to assign temperature, velocity, dry air and vapor pressure, and aerosol particle density in a specific part of the crack.

Calculation results show the influence of aerosol diameter, crack wall temperature, mixture pressure, and hydraulic diameter on deposition rate in a crack for aerosol diameter from 0.1 to 10 μm [3], [4]. Three deposition mechanisms were taken into account, i.e. gravitational settling, diffusiophoresis, and thermophoresis. Gravitational settling asserts oneself predominantly for aerosol particle with a diameter higher than 1 μm . If the temperatures of a mixture and crack walls differ, the lateral temperature gradient appears and thermophoresis contributes to aerosol settling. Diffusiophoresis can dramatically change the flow, but it appears only in the case of vapor condensation or water evaporation on crack walls.

References:

- [1] M. M. R. WILLIAMS: *A Model for the Transport of Vapours, Gas and Aerosol Droplets through Tubes and Crack*, Progress in Nuclear Energy, 1996, pp. 316-416.
- [2] R. I. NIGMATULIN: *Dynamics of multiphase media*, Volume I, Hemisphere Pub Co., 1991
- [3] T. TROJEK, T. ČECHÁK, L. MOUČKA, A. FRONČKA: *Modeling of Air Flow through a Narrow Crack*, Book of Abstracts 4th European Conference on Protection against Radon at Home and at Work, 2004, ISBN 80-01-03009-1
- [4] T. TROJEK, T. ČECHÁK: *Transport a zadržení aerosolů v netěsnostech kontejnmentu jaderné elektrárny*, Výzkumná zpráva JFPI ČVUT, 2003, 36 s.

Pigment Identification with X-Ray Fluorescence Analysis

T. Trojek, T. Čechák, M. Musílek, D. Králová*

trojek@fjfi.cvut.cz

Department of Dosimetry and Application of Ionizing Radiation, Faculty of Nuclear Sciences and Physical Engineering, Czech Technical University, Břehová 7, 115 19 Prague 1, Czech Republic

* National Library of the Czech Republic, Central Depository Hostivař, Sodomkova 2/1146, 102 00 Prague 10, Czech Republic

Energy dispersive X-ray fluorescence (EDXRF) is a nondestructive and noninvasive analytical technique allowing quantitative multi-elemental analysis of the surface of investigated sample. Its principle consists in excitation and detection of characteristic radiation created in a sample by incident X-ray photons that are emitted from a suitable source. Portable EDXRF apparatuses enable in-situ measurements, therefore it an excellent tool in research on various objects of art [1], [2], [3]. Recent studies at DDAIR (Department of Dosimetry and Application of Ionizing Radiation) are focused especially on identification of old pigments that were used on decoration of wall paintings and manuscripts. EDXRF provides, together with the others analytical techniques, important information required for restoration and study of paintings or manuscript illuminations.

Two different apparatuses are used for pigment identification at DDAIR. The first one applies annular radionuclide source (^{55}Fe , ^{238}Pu , or ^{241}Am sources with activities in the order of hundreds of MBq) for excitation of characteristic radiation. The ORTEC Si(Li) detector with an effective diameter of 6 mm and a thickness of 5 mm (FWHM = 170 eV for the line 5.9 keV of ^{55}Fe) is used for detection of characteristic radiation and spectra recording. Due to relative big thickness, photons up 60 keV are detected with good efficiency. This detector is cooled by liquid nitrogen in a small transportable Dewar vessel with a volume of 5 l for in situ measurements. The CANBERRA 35+ multichannel analyzer serves for laboratory measurement and the ORTEC DART for measurements in situ. Lead collimator ensures detection of characteristic radiation only from desired area of a measured object. The diameter of investigated area depends on collimator diameter and is approximately equal to 1 cm.

The second apparatus was constructed at DDAIR in order to measure smaller areas. In comparison with the first one, radionuclide source is replaced with a miniature X-ray tube with molybdenum anode that produces much more intensive X-ray beam than common radionuclide sources. This X-ray tube (TF 3001 Oxford Instruments) works at a voltage of 30 keV and a maximum current of 100 μA . The X-ray beam is focused to measured object by means of an aluminum collimator. The incident angle is 45 degrees and the beam spot has a diameter of approximately 1 mm. Characteristic radiation is detected by Amptek Si-PiN detector connected to MCA8000A multichannel analyzer. The Si-PiN detector is cooled by electric current, and therefore does not require Dewar vessel with liquid nitrogen. Its detection efficiency is worse due to small dimensions of sensitive detection volume. Two light emitting diodes were added for the purpose of targeting of measured point. Whole apparatus is place in a box, made of lead glass, to reduce the intensity of ionizing radiation in the laboratory.

Acquired spectra are evaluated with QXAS-AXIL computer code that enables peak searching and net peak area determination. This software provide also quantitative analysis (based on fundamental parameter method or method of empirical coefficient), but that is 670

usually not essential in the case of pigment identification.

Pigment in wall painting or manuscripts can be recognized usually only from the presence of various chemical elements. Quantitative analysis is complicated because of badly defined layers of paints. The EDXRF performed with the apparatus with radionuclide source was successfully applied to pigment identification in wall paintings, e.g. in Karlštejn and Žirovnice castles. Žirovnice is a Gothic castle from 13th century in S.E. Bohemia. After a fire in 1964 the castle was restored and valuable Gothic frescoes from the rebuilding in 2nd half of 15th century were brought to light. The measurements, carried out in three rooms (the Chapel, the anteroom, and the “Green Chamber”, identified various characteristic paints, e.g. azurite, malachite, and minium. The second apparatus was utilized in analysis of illumination of old manuscripts. Its ability to target a small area showed itself as the main advantage in the case of measurements of fine paints. For example, Českobudějovický gradual, dating back to the 15th century contains several illuminated parchment. We were able to recognize pigments even if they were located very close to themselves [4].

Qualitative EDXRF analysis can provide valuable information on pigment composition and thus contribute to understanding the history of works of art and help the conservators use the most convenient method of restoring. The following research is focused on multilayer pigment identification.

References:

- [1] T. ČECHÁK, J. GERNDT, I. KOPECKÁ, L. MUSÍLEK: *X-ray fluorescence in research on Czech cultural monuments*, Nuclear Instruments and Methods in Physics Research B 213, 2004, pp. 735-740.
- [2] T. ČECHÁK, L. MUSÍLEK, I. KOPECKÁ, J. GERNDT, T. TROJEK: *Application of X-Ray Fluorescence in Art*, European Conference on X-Ray Spectrometry. Cagliari: Kassiopea Group S.r.l., Vol. 1, 2004.
- [3] A. DENKER, J. OPITZ-COUTUREAU: *Paintings - high energy proton detect pigments and paint-layers*, Nuclear Instruments and Methods in Physics Research B 213, 2004, pp. 677-682.
- [4] T. TROJEK: *Rentgenfluorescenční analýza inkoustů a pigmentů*, Technical Report, FJFI ČVUT, 2004

Pigment Identification with X-Ray Fluorescence Analysis

T. Trojek, T. Čechák, M. Musílek, D. Králová*

trojek@fjfi.cvut.cz

Department of Dosimetry and Application of Ionizing Radiation, Faculty of Nuclear Sciences and Physical Engineering, Czech Technical University, Břehová 7, 115 19 Prague 1, Czech Republic

* National Library of the Czech Republic, Central Depository Hostivař, Sodomkova 2/1146, 102 00 Prague 10, Czech Republic

Energy dispersive X-ray fluorescence (EDXRF) is a nondestructive and noninvasive analytical technique allowing quantitative multi-elemental analysis of the surface of investigated sample. Its principle consists in excitation and detection of characteristic radiation created in a sample by incident X-ray photons that are emitted from a suitable source. Portable EDXRF apparatuses enable in-situ measurements, therefore it an excellent tool in research on various objects of art [1], [2], [3]. Recent studies at DDAIR (Department of Dosimetry and Application of Ionizing Radiation) are focused especially on identification of old pigments that were used on decoration of wall paintings and manuscripts. EDXRF provides, together with the others analytical techniques, important information required for restoration and study of paintings or manuscript illuminations.

Two different apparatuses are used for pigment identification at DDAIR. The first one applies annular radionuclide source (^{55}Fe , ^{238}Pu , or ^{241}Am sources with activities in the order of hundreds of MBq) for excitation of characteristic radiation. The ORTEC Si(Li) detector with an effective diameter of 6 mm and a thickness of 5 mm (FWHM = 170 eV for the line 5.9 keV of ^{55}Fe) is used for detection of characteristic radiation and spectra recording. Due to relative big thickness, photons up 60 keV are detected with good efficiency. This detector is cooled by liquid nitrogen in a small transportable Dewar vessel with a volume of 5 l for in situ measurements. The CANBERRA 35+ multichannel analyzer serves for laboratory measurement and the ORTEC DART for measurements in situ. Lead collimator ensures detection of characteristic radiation only from desired area of a measured object. The diameter of investigated area depends on collimator diameter and is approximately equal to 1 cm.

The second apparatus was constructed at DDAIR in order to measure smaller areas. In comparison with the first one, radionuclide source is replaced with a miniature X-ray tube with molybdenum anode that produces much more intensive X-ray beam than common radionuclide sources. This X-ray tube (TF 3001 Oxford Instruments) works at a voltage of 30 keV and a maximum current of 100 μA . The X-ray beam is focused to measured object by means of an aluminum collimator. The incident angle is 45 degrees and the beam spot has a diameter of approximately 1 mm. Characteristic radiation is detected by Amptek Si-PiN detector connected to MCA8000A multichannel analyzer. The Si-PiN detector is cooled by electric current, and therefore does not require Dewar vessel with liquid nitrogen. Its detection efficiency is worse due to small dimensions of sensitive detection volume. Two light emitting diodes were added for the purpose of targeting of measured point. Whole apparatus is place in a box, made of lead glass, to reduce the intensity of ionizing radiation in the laboratory.

Acquired spectra are evaluated with QXAS-AXIL computer code that enables peak searching and net peak area determination. This software provide also quantitative analysis (based on fundamental parameter method or method of empirical coefficient), but that is

usually not essential in the case of pigment identification.

Pigment in wall painting or manuscripts can be recognized usually only from the presence of various chemical elements. Quantitative analysis is complicated because of badly defined layers of paints. The EDXRF performed with the apparatus with radionuclide source was successfully applied to pigment identification in wall paintings, e.g. in Karlštejn and Žirovnice castles. Žirovnice is a Gothic castle from 13th century in S.E. Bohemia. After a fire in 1964 the castle was restored and valuable Gothic frescoes from the rebuilding in 2nd half of 15th century were brought to light. The measurements, carried out in three rooms (the Chapel, the anteroom, and the “Green Chamber”, identified various characteristic paints, e.g. azurite, malachite, and minium. The second apparatus was utilized in analysis of illumination of old manuscripts. Its ability to target a small area showed itself as the main advantage in the case of measurements of fine paints. For example, Českobudějovický gradual, dating back to the 15th century contains several illuminated parchment. We were able to recognize pigments even if they were located very close to themselves [4].

Qualitative EDXRF analysis can provide valuable information on pigment composition and thus contribute to understanding the history of works of art and help the conservators used the most convenient method of restoring. The following research is focused on multilayer pigment identification.

References:

- [1] T. ČECHÁK, J. GERNDT, I. KOPECKÁ, L. MUSÍLEK: *X-ray fluorescence in research on Czech cultural monuments*, Nuclear Instruments and Methods in Physics Research B 213, 2004, pp. 735-740.
- [2] T. ČECHÁK, L. MUSÍLEK, I. KOPECKÁ, J. GERNDT, T. TROJEK: *Application of X-Ray Fluorescence in Art*, European Conference on X-Ray Spectrometry. Cagliari: Kassiopea Group S.r.l., Vol. 1, 2004,
- [3] A. DENKER, J. OPITZ-COUTUREAU: *Paintings - high energy proton detect pigments and paint-layers*, Nuclear Instruments and Methods in Physics Research B 213, 2004, pp. 677-682.
- [4] T. TROJEK: *Rentgenfluorescenční analýza inkoustů a pigmentů*, Technical Report, FJFI ČVUT, 2004

Prompt Evaluation of the Air Kerma Rate in Environmental Radiation Fields Monitoring

J. Klusoň, L. Thinová, T. Čechák

kluson@fjfi.cvut.cz

Department of Dosimetry and Application of Ionizing Radiation, Faculty of Nuclear Sciences and Physical Engineering, Břehová 7, 115 19 Prague 1, Czech Republic

Monitoring of the radiation fields in the environment and determination of the origin (fields can be generated not only by natural radionuclides but also by man-made contaminants) and characteristics of these fields is important part of radiation protection tasks. Gamma fields in the in-situ environmental monitoring are usually characterized by some suitable dosimetric quantity (recommended is air kerma rate) measured in some reference conditions (typical standard is measurement in the reference point 1 meter above ground, if possible on the free plain terrain). Taking into account variability and fluctuations of the natural background, measured integral value of the air kerma rate is generally not sufficient to detect and/or identify low level contamination and spectrometry measurements are necessary in such cases.

The method for the in-situ scintillation gamma spectrometry data processing and analysis was developed for these purposes. Method is based on the deconvolution technique using detection systems response matrices, calculated by Monte Carlo simulation. Result of the experimental spectra processing is energy distribution of air kerma rate that enable to identify the radiation sources and their contributions in the measured field. Next advantage (in addition to the qualitative new spectral information mentioned above) is that developed method does need neither calibration nor corrections for the energy dependence (both included in the calculated response matrix). Method and its application is described in [1], some examples of the typical applications for gamma fields in-situ environmental monitoring are in [2, 3].

Discussed spectrometry method is based on the off-line data processing (usually iterative deconvolution procedure) and need relatively good statistics (i.e. quite long data acquisition) for the good (without random noise) results of data processing/analysis. Relatively long period of the data acquisition and off-line processing can be disadvantage in some cases (e.g. rapid scanning, accidental monitoring, etc.). For this reason the prompt method using dependence between air kerma rate and count rate was developed and tested for $\varnothing 3'' \times 3''$ NaI(Tl) detection system and natural background fields. Verification of such method was based on the number of spectrometry measurements sets available from many in-situ environmental monitoring applications (radiological assessment of the Semipalatinsk nuclear weapons test site, study of the radiological impacts of the uranium industry and uranium ore processing, monitoring of the environmental impact of the spent fuel temporary storage operation, running project of monitoring of the environmental impact of the NPP Temelin operation in its neighborhood, etc. – see examples in [2, 3]). Results of the several hundreds in-situ gamma spectrometry measurements (for several detectors and range of different conditions) were analyzed and statistically evaluated and used for the calibration of the proposed prompt method [4]. Linear fit of experimental data was used to analyze dependence of air kerma rate on the used detection system count rate and deviations of individual measurements from the fit were evaluated statistically. It was proved that air kerma rate can be derived from the count rate with error up to 10% (on $\pm 2\sigma$ significance level, with assumption of the detector given size, given character of the field, i.e. character of the natural background and practically no discrimination, i.e. measurement cover whole energy interval

~0 – 3 MeV). Calibration function depends only on the type, shape and size of the used detector. On the other hand it was shown, that calculated dependence is not valid for gamma fields originated from other than natural sources - e.g. fields with high energy components (from reactors and accelerators), fields of specific sources (e.g. point sources as ^{137}Cs , ^{60}Co , beams from such sources, etc.).

In the context with these issues, the problems of the detectors internal activity, response to the cosmic radiation and detectors responses directional dependence were studied and analyzed.

References:

- [1] KLUSOŇ, J.: *Environmental Monitoring and In Situ Gamma Spectrometry* Radiation Physics and Chemistry, vol. 61, No 1, ISSN 0969-806X, 2001, pp. č. 209–216.
- [2] THINOVÁ, L. – KLUSOŇ, J. – ČECHÁK, T. – TROJEK, T.: *Spectrometry Characteristics of Photon-Fields and Atmospheric Radionuclide Deposit Monitoring in One Part of Southern Bohemia* In: Program & Abstracts 6th International Conference on High Levels of Natural Radiation and Radon Areas. Osaka: Kinki University, National Institute of Radiological Sciences, Vol. 1, 2004, pp. č. 121.
- [3] THINOVÁ, L.. – KLUSOŇ, J. – TROJEK, T. – ČECHÁK, T.: *Biomonitoring atmosférické depozice radionuklidů a stanovení spektrometrických a dozimetrických charakteristik fotonových polí v okolí JE Temelín v letech 2000 - 2003* In: Sborník příspěvků 18. Konference: Radionuklidy a ionizující záření ve vodním hospodářství, Praha ČSSI, díl 1, ISBN 80-02-01666-1, 2004, pp. č. 126–131.
- [4] KLUSOŇ, J. – THINOVÁ, L. – ČECHÁK, T.: *Možnosti rychlého stanovení příkonu kermy ve vzduchu* Sborník rozšířených abstraktů XXVI. Dny Radiační ochrany, Praha - ČVUT, Fakulta jaderná a fyzikálně inženýrská, KDAIZ, díl 1., ISBN 80-01-03076-8, 2004, pp. č. 142–145.

MOX Utilization: Evaluation of Impacts on Radioactive Waste Inventory

A. Zíb, L. Novotná, P. Šebela, K. Matějka

zib@troja.fjfi.cvut.cz

Department of Nuclear Reactors, Faculty of Nuclear Sciences and Physical Engineering,
Czech Technical University, V Holešovičkách 2, 180 00 Prague 8, Czech Republic

The solution to the problem of the spent nuclear fuel disposal is one of the key conditions for the further development of the nuclear power industry in the Czech Republic. An one through cycle with final depository can be one possible solution (currently preferred), another one can be a closed cycle.

No fully closed cycle technology is currently available anywhere in the world. What is used commercially in several countries (France, The U.K., Japan, Russia etc.) is the burning of MOX fuel manufactured by the reprocessing of spent uranium fuel assemblies (i.e. partial closing of the cycle).

Due to the fact that Temelin NPP is licensed for the usage of MOX fuel, it is reasonable to assess a possibility of MOX fuel loading to its core and the possible impact on the inventory of the nuclear waste – namely in comparison with the currently employed uranium one-through cycle. Such comparison was carried out in the publication [1], the content and key findings of which are briefly summarized in the following text.

The main goal of the publication was the comparison of one-through uranium cycles to eventual cycles using MOX fuel from the point of view of the radioactive waste inventory and its main forms generated by the cycles. That is why nine main scenarios were formulated – three one-through cycle scenarios (for the Temelin NPP service life of 40, 50 and 60 years), three MOX cycle scenarios with single reprocessing (MOX is produced only by the reprocessing of spent uranium fuel, service life of NPP is 40, 50 and 60 years) and three MOX cycle scenarios with double reprocessing (both spent uranium and MOX fuels are reprocessed).

For every scenario formulated, the nuclear waste inventory and its forms were evaluated. The special focus was given to cycles characterized by the longest studied NPP service life (i.e. 60 years) due to the fact these cycles vary one from another the most. The key findings from the analysis carried out are as follows:

- The weight of uranium cycles waste is less than 6% compared to one for MOX cycles (depleted uranium is considered to be waste). Moreover, there is just a single form of waste – spent fuel assemblies (if not disassembled) – for uranium cycles contrary to multiple forms for MOX cycles (spent fuel assemblies, construction materials, depleted uranium from reprocessing and HWL – glass containing actinides and fission products from reprocessing).
- Only if depleted uranium from reprocessing can be further recycled or utilized beneficially (i.e. it is not waste and it can be excluded from waste weight), MOX cycles produce less waste by 25-30% in comparison with uranium ones.
- There are two significant forms of waste (measured by weight) for MOX cycles: depleted uranium from reprocessing (30-40% of waste weight) and not-reprocessed spent fuel assemblies (25-30%).

- Spent products mass is almost identical for all nine types of cycles.

Mass of actinides (uranium excluded) is higher for uranium cycles than for MOX cycles. Difference is app. 15-30%.

References:

- [1] ZÍB A. A KOL.: *Modelové ocenění dopadů použití paliva MOX na inventář RAO* výzkumná zpráva, ČVUT, FJFI – KJR, Praha 2004,
- [2] MATĚJKA K. A KOL.: *Ocenění dopadů použití MOX paliva na ukládání VJP* výzkumná zpráva, ČVUT, FJFI – KJR, Praha, 2001,
- [3] ZÍB, A.: *Vyhořelé jaderné palivo v České republice*, disertační práce, ČVUT, FJFI, Praha, 2001
- [4] NOVOTNÁ L.: *Modelové výpočty palivových cyklů s palivem typu MOX* diplomová práce, ČVUT, FJFI – KJR, Praha, 2002

Nuclear Reactor Physics - e-Learning on Internet

J. Zeman, M. Kubešová, J. Rataj

jaroslav.zeman@fjfi.cvut.cz

Department of Nuclear Reactors, Faculty of Nuclear Sciences and Physical Engineering,
Czech Technical University in Prague, V Holešovičkách 2, 180 00 Prague 8, Czech Republic

The main purpose of this project is to integrate new teaching/learning methods and new scientific findings into the „Reactor Physics 1“ course offered at the Department of Nuclear Reactors of the Faculty of Nuclear Sciences and Physical Engineering of Czech Technical University in Prague.

The final product of our project is an electronic teaching/learning program on a CD-ROM. The program consists of 2 parts:

1. Web page „Reactor physics 1“ (in Czech „Reaktorová fyzika 1“), created in the programming language HTML,
2. Presentation of lectures in „Reactor Physics 1“ created in the programme MS PowerPoint.

The first part covers both reactor physics based on the diffusion theory and the fundamentals in reactor physics based on the transport theory. The second part covers reactor physics based on the diffusion theory only.

Both parts have been created based on lectures and textbooks for „Reactor Physics 1“ course . A collection of tables, diagrams and pictures accompany each lecture.

The web page of this subject is available for students on the web server of Faculty of Nuclear Sciences and Physical Engineering. The e-address:

http://www.fjfi.cvut.cz/reaktorova_fyzika1/.

The presentation of lectures created in the programm MS PowerPoint and can be found on:

http://www.fjfi.cvut.cz/reaktorova_fyzika1/prezentace/.

The e-lectures can be browsed on a CD-ROM or accessed directly on the Internet. It is possible to download and save them into a personal computer and print or update them and use them as an in-class support or consult them where no internet connection is available.

The web page and the e-lectures encompass the program in “Reactor Physics 1” for the students of the Faculty of Nuclear Sciences and Physical Engineering in the specializations of „Nuclear Reactor Theory and Engineering“, „Nuclear Energy and the Environment“ and „Nuclear Facilities“.

The web page has the same structure as the lecturenotes in „Reactor Physics 1“. New color pictures and diagrams were added, some of them are animated. In the main menu, there are links to individual chapters and in each chapter, there are links to subchapters. The main menu makes a reference to the contents in which it is possible to choose and access any sub-chapter of your choice.

The presentation of lectures in “Reactor Physics 1” consists of 8 chapters:

- Nuclear reactors
- Neutron reactions
- Fission chain reaction
- Neutron diffusion
- Slowing down neutrons
- Bare homogeneous thermal reactor
- Reflected homogeneous thermal reactor
- Physical principles of the ADS systems

The visual presentation includes 429 photos in total, covering the topics of our e-programme. The programme is by no means a substitute for students’ participation in lectures, nor does it contain all the information required at the examination on the subject. It is a supplementary material facilitating both preparation for practicals and in-class orientation during the lecture. Students needn’t take all the notes or search for source information.

This teaching/training material for the students of the Faculty of Nuclear Sciences and Physical Engineering of Czech Technical University in Prague has filled a gap in teaching tools, since no such open-access, summarising material has been developed before for the branch of nuclear engineering.

References:

- [1] J. ZEMAN: *Reactor Physics I*, Lecturenotes of the University, CTU in Prague, 2003 (in Czech).
- [2] A. M. WEINBERG, E.P. WIGNER: *The Physical Theory of Neutron Chain Reactors*, The University of Chicago Press, 1958.
- [3] A. F. HENRY: *Nuclear-Reactor Anylysis*, The MIT Press, Cambridge, Massachusetts and London, England, 1975.

This work has been supported by the grant of the Universities Development Fund of the Czech Republic (FRVŠ ČR) No. 2084/2004.

Nuclear Facilities, Nuclear Safety and Radiation Protection

K. Matějka, J. Zeman

karel.matejka@fjfi.cvut.cz

Department of Nuclear Reactors, Faculty of Nuclear Sciences and Physical Engineering,
Czech Technical University, V Holešovičkách 2, 180 00 Prague 8, Czech Republic

This paper is focused on the main results of research plan MSM 210000020 in year 2004 in which 7 workplaces of CTU were involved. The main investigator was the Department of Nuclear Reactors of the Faculty of Nuclear Sciences and Physical Engineering of Czech Technical University in Prague CTU (FNSPE CTU). The research was a follow-up of the investigation conducted in previous years and it covers the areas listed below:

Department of Nuclear Reactors – FNSPE CTU

Nuclear facilities and nuclear safety – research was continued in the fields of: nuclear safety analyses, monitoring the trends of european requirements on newly built nuclear power plants and nuclear facilities and installations, training eligible staff specialists and an innovation project for the VR-1 control equipment.

- Application of computational codes MCNP 4C and MCNPX version 2.1.5 and data library ENDF B/6 for the calculation of neutron physical core parameters of research pool reactors and verification of computational parameters at VR-1 training reactor experiments for the core configurations realised in 2004 year.
- Quality control in the development of highly reliable software and work on quality assurance of programmable arrays (PLA). It deals with circuits assuring hardware functions for nuclear safety control.
- Innovation of the VR-1 reactor control and safety system.

Department of Dosimetry and Application of Ionizing Radiation – FNSPE CTU

- Development of computational programmes for modelling gas behavior, aerosols and vapor and their transport in case of serious incidents in a NPP. Application of the Monte-Carlo method for a more precise calculation of the detector response.

Department of Nuclear Chemistry - FNSPE CTU

- Topic of migration of radioactive contaminants in the environment:
Study of methods and ways of incorporation of both equilibrium surface complexation models and experimentally verified kinetic interaction models into dynamic transport models. Such modifications of the dynamic model is especially important for the simulation of migration of various types of radioactive contaminants in the near- and far-field of radioactive waste disposals.
- Topic of liquid radioactive wastes:
New findings about the composite sorbents containing extraction agents will be used for the development of new procedures in separation of radionuclides from model or real liquid radioactive wastes.

Department of Materials – FNSPE CTU

- New findings about the failure processes in chosen types of steel used in nuclear power engineering. These findings will be applicable at all stages of nuclear power installation structural design. A database of failure mechanisms is a basis for the future evaluation of residual life and contributes to the enhancement of safety and reliability of structural parts where failure may occur. In our particular case, fatigue failure was studied in austenitic and bainitic steels and corrosive properties were studied in zirconium alloys.

Department of Solid State Engineering – FNSPE CTU

- Research was carried out in the context of a long-term program in “Neutronographic structural analysis of materials and development of methods based on neutron wave properties”. Program files for collection and processing data from powder neutron and X-ray diffraction were created. The work concentrated on:
 - Control of neutronographic experiments in the field of quantitative texture analysis by means of the orientation distribution function (ODF) for the description of crystallite orientation,
 - Creating and testing computer codes for recording and processing experimental data measured by linear position-sensitive detectors and for the designation of direct pole figures.

Department of Electric Power Engineering – Faculty of Electrical Engineering of CTU

- Establishment of testing centers for testing the electrodiagnostic expert system currently in operation. Testing and verification of an expert system for electrodiagnostics of insulation systems in power engineering installations. Gradual acquisition of new findings.
- Protections and a control system testing new approaches were implemented on a physical model of the block. Also methods of a more precise estimation of the reactor power in the real time were developed.

Department of Physics – Faculty of Civil Engineering of CTU

- Study of mechanic and structural changes in concrete used in a NPP under the thermal shock and radiation. The results will serve as a base for controlled aging of concrete structures in a NPP.

References:

- [1] M. KROPÍK, V. CHÁB, M. JUŘIČKOVÁ: *Požadavky na systém nezávislé výkonové ochrany školního jaderného reaktoru VR-1*, Výzkumná zpráva, Katedra jaderných reaktorů JFI ČVUT v Praze, 2004. 15 s.
- [2] J. KLUSOŇ, T. ČECHÁK: *Calculation of the radionuclides concentrations from in-situ spectrometry data measured by semiconductor spectrometer*, in the Proceedings of the IRPA Regional Congress on Radiation Protection in Neighbouring Countries of Central Europe 2003, Bratislava, Slovakia, 2003.
- [3] D. VOPÁLKA, A. VOKÁL: *A New Code for Modelling the Near Field Diffusion Releases from the Final Disposal of Nuclear Waste*, Czechoslovak Journal of Physics, vol. 53, Suppl. A, p. A127-A133, 2003.

This research has been supported by MSM 210000020.

Operational Reactor Physics - Multimedia CD-ROM

E. Sklenka, M. Šedlbauer

sklenka@troja.fjfi.cvut.cz

Department of Nuclear Reactors, Faculty of Nuclear Sciences and Physical Engineering,
Czech Technical University, V Holešovičkách 2, 180 00 Prague 8, Czech Republic

Understanding of a processes and phenomena in the core of nuclear reactor are essential basis for safe operation of each reactor. Behavior of the nuclear fuel in the core and after unloading from reactor is very important not only for nuclear safety, but also for environmental impact and economy of the operation. One of the lectures, which are conducts at the Department of Nuclear Reactors and deal with nuclear fuel behavior in the reactor, is Operational reactor physics.

Textbook Operational reactor physics, which was published at Czech Technical University Press at 2001, is one of the key sources for the lecture at the Department of Nuclear Reactors. Printing version of textbooks are quickly obsolete mainly on the subjects focused for applied physics and not allowed use multimedia sources of information as video-shoots, animations, interactive mock-up calculations, etc.

Multimedia CD-ROM "Operational reactor physics", which was developed at the Department of Nuclear Reactors, is new source with both "classical" printing and "new" multimedia information. CD-ROM is appointed not only for students from Faculty of Nuclear Sciences and Physical Engineering, but also for all students from power engineering department from other Czech universities.

Multimedia CD-ROM Operational reactor physics is produced as a comprehensive set of texts, pictures, photos, mock-up calculations and video-shoots which are joints to one unit by standard web tools as Html and CSS 2.0 styles. Anyone who wants use CD-ROM does not need any special software. CD-ROM consists of five educational modules:

Modulus THEORETICAL BASIS - consists of four main theoretical parts, which is necessary basis for study of operational reactor physics:

- Long-term kinetics - study of the isotopic changes of the fuel in the nuclear power reactors,
- Medium-term kinetics - study of the Samarium and Xenon poisoning and oscillations influence to the standard and abnormal operation of the nuclear power reactors,
- Linear reactivity model - study of the reactivity behavior during fuel cycle, use of the linear reactivity model in PWRs
- Cast-down operation - study of the reactivity coefficients and cast-down operation at the end of fuel cycle.

Modulus MATLAB MOCK-UP consists of basic mock-up calculations in the MatLab environment for both long-term and medium-term kinetics.

Modulus FUEL CYCLE consists of the descriptions of the nuclear fuel, fuel cycle, fuel management and fuel loadings and patterns used in the PWRs (both Russian and Western

types) and BWRs & CANDU Reactors with deep focus on the both Czech NPPs in Dukovany and Temelín.

Modulus SPENT FUEL consists of two parts:

- Study of the inventory & physical behaviors of the spent nuclear fuel after unloading from the NPP Core,
- Descriptions of the different types of the wet and dry interim storages for spent fuel storing with deep focus to the CASTOR transport and storage casks.

Modulus VIDEO-SHOOTS consists of different video-shoots which support information from fuel cycle and spent fuel modules.

Multimedia CD-ROM "Operational Reactor Physics" brings new potential in the modern aspect of educational process at the Department of Nuclear Reactors and it will be useful tool for anyone who wants to find up-to-date information on operational reactor physics.

References:

- [1] Ľ. SKLENKA: *Provozní reaktorová fyzika - Multimediální CD-ROM* Research report, ČVUT FJFI Praha, 2004
- [2] Ľ. SKLENKA: *Provozní reaktorová fyzika* ECTU textbook, 2001 410 p. ISBN 80-01-02283-8 (in Czech)
- [3] G. M. BALLARD (ED.): *nuclear Safety - After Three Mile Island & Chernobyl* Clsevier Applied Science, London and New York, 1988, 480 p. ISBN 1-85166-235-9
- [4] P. OTČENÁŠEK *Nestacionární stavy jaderných reaktorů* CTU textbook, 1982, (in Czech)

This research has been supported by MŠMT grant No. MSM 2083/2004.

Prospects and Acceptance of Nuclear Power Engineering in Czech Republic

D. Kobyłka, J. Zeman, K. Matějka

kobyłka@troja.fjfi.cvut.cz

Department of Nuclear Reactors, Faculty of Nuclear Sciences and Physical Engineering,
Czech Technical University, V Holešovičkách 2, 180 00 Prague 8, Czech Republic

There are two significant nuclear power plants in the Czech Republic (NPP Dukovany, NPP Temelin) with 6 reactor units of total electric power 3722 MW. Furthermore there are a few of training and research reactors, with low or zero power, and great number of little radiation sources, above all in the health service and industry. Certainly the number of the nuclear facilities will be increased. Also the new “National energy concept of Czech republic” will propagate this situation. Opposite this reality, the knowledge about this field of human activity (the nuclear physics, the nuclear industry, the radiation utilization, etc.) is not widespread abroad citizens of the Czech republic.

With a view to change this situation, the Department of Nuclear Reactors (DNR), in cooperation of the Department of Dosimetry and Application of Ionizing Radiation (DDAIR) and the Department of Nuclear Chemistry (DNC), all departments from Faculty of Nuclear Sciences and Physical Engineering (FNSPE), prepared a new general course aimed at the nuclear power engineering and its impact on the environment and the society. The course was named „Prospects and Acceptance of Nuclear Power Engineering in Czech Republic“. It is addressed to civil servants (employees of: ministries, regional, district and municipal authorities, etc.) who have only basic knowledge of nuclear field. The course graduation will bring the qualification of the civil servants for accountable and objective assessments about nuclear facilities.

The course consists of 130 lessons, every lesson take 45 minutes. The 84 lessons of this amount take the lectures, and the 19 lessons of training and consultations. Finally, excursions to several nuclear facilities take the 27 lessons (without traffic time). The lessons are organized in the 19 thematic lectures, each take 3 or 6 lessons with the one lesson of discussion. Consequently the course will take in two consecutive semesters.

The following course curriculum was prepared on the DNR:

1. Introduction to power engineering and nuclear power engineering, short history (6+1 lessons)
2. Introduction to nuclear physics (3+1)
3. Nuclear reactors overview (6+1)
4. Nuclear fuel cycle and its development (6+1)
5. Design and operation of nuclear power plants (6+1)
6. World development of nuclear power engineering (3 +1)
7. Fusion systems (3+1)
8. Spent fuel management: transport, medium-term storage (6+1)
9. Transmutation systems (3+1)
10. Radioactive waste and spent fuel repositories (3+1)
11. Radionuclides migration in environment (6+1)
12. Nuclear safety (6+1)
13. Radiation protection (6+1)
14. Emergency preparedness (3+1)
15. Legislation (6+1)
16. Lifetime of nuclear installations (3+1)

17. Impact of nuclear power engineering on environment (3+1)
18. Social aspects of nuclear power utilization (3+1)
19. Summary of „Prospects and Acceptance of Nuclear Power Engineering in Czech Republic“, discussions (3+1)
20. Excursions:
 - a. Training reactor VR-1 of the Nuclear reactors department, FNSPE (3 lessons)
 - b. Reactor LVR-15 and LR-0 of the Nuclear Research Institute plc, Rez near Prague (5 lessons)
 - c. Cyclotron of the Nuclear Physics Institute and the Fluorine Chemistry Department, NRI plc, Rez near Prague (5 lessons)
 - d. TOKAMAK of the Institute of Plasma Physics, AS CR (3 lessons)
 - e. Nuclear Power plant Dukovany (3 lessons)
 - f. Nuclear Power plant Temelín and water power plant (e.g. Štěchovice, Orlik) (5 lessons)
 - g. Coal power plant or heating power station (3 lessons).

Various lecturers from 9 institutions (DNR–FNSPE, DDAIR–FNSPE, DNC–FNSPE, NRI plc Rez near Prague, Institute of Plasma Physics - AS CR, Radioactive Waste Repository Authority, State Office for Nuclear Safety, NPP Temelin, Czech Power Company) will lecture the individual subject lessons. The abstracts of the individual lectures are prepared at the present time.

In the year 2004, about 65 government boards were addressed during the investigation of interest. We can mention for example: Ministry of Transport, Ministry of Industry and Trade, Ministry of the Interior, Ministry of the Environment of the Czech Republic, Office of the Czech Republic Government, State Environmental Fund of the Czech Republic, State Energy Inspection, National Security Authority Regulations, Energy Regulatory Office, Regional authorities, etc.

About 30 persons showing interest from 9 government boards were entered. The 15 peoples from various government boards were chosen for the first running of the course, which will start at the summer semester of the year 2005.

References:

This research has been supported by Development & Transformation Fund of Ministry of Education, Youth and Sports No. 74/2004.

Importance of the Source Term Description in the Safety Assessment of Spent Fuel Disposal

D. Vopálka

vopalka@fjfi.cvut.cz

Department of Nuclear Chemistry, Faculty of Nuclear Sciences and Physical Engineering,
Czech Technical University in Prague, Břehová 7, 115 19 Prague 1, Czech Republic

Deep geological storage was chosen as a concept for disposal of spent nuclear fuel in many countries. The canisters with spent nuclear fuel produced during the operation of nuclear reactors are planned to be disposed of in an underground repository. Canisters will be surrounded by compacted bentonite that will retard the migration of safety-relevant radionuclides into the host rock.

The construction of underground repository should be preceded by the thoroughly safety analysis prescribed by nuclear safety authorities, which would have to appreciate the safety requirements and criteria proposed. This complex system of judgments, called performance assessment (PA), consisted of numerous steps in various fields of knowledge and experience, includes also mathematical modelling of migration of all dangerous radionuclides from canisters with spent fuel possibly damaged in the future into the environment. The path of radionuclides that should be modelled used to be divided into two main areas: (i) near-field region represented by engineered barriers (canister, compacted bentonite) and (ii) far-field region formed by rock in which would be the repository situated (natural barrier).

The canister itself with assemblies of spent fuel represents for the modelling in the near-field region so called source term. As it is assumed that the transport through the bentonite layer will be controlled by diffusion, the model of canister that should contain at least the inventory of radionuclides, and model of canister corrosion and model of leaching of studied radionuclides from the fuel matrix and contaminated structural parts, forms the initial boundary condition for the solution of diffusion equation in the near-field region. For complex modelling performed by special environmental codes based on the description of radionuclide migration in the far-field region the source term used to be represented by all the man-made area, which includes also near-field region. In both approaches the source term is a complex system, behaviour of which is described by a set of models, functions, variables and parameters.

The own code, MIVCYL, which enables the modelling of radionuclide transport from the canister through the bentonite layer in the cylindrical geometry, was prepared in our laboratory [1]. The code solves the diffusion equation in the cylindrical configuration for various types of initial and boundary conditions. The advantage of this code is (i) its ability to take into account an arbitrary shape of non-linear equilibrium function describing the interaction between radionuclides diluted in the seepage water and the sorbing surface of bentonite and (ii) stability of it for broad ranges of initial and boundary conditions. The code was successfully verified with codes PAGODA [1] and GoldSim [2] that are commercially delivered by organization working in the PA-field. The sub-model of the code MIVCYL, which describes the source term, includes radioactive decay and ingrowth of nuclides in the canister, the set of subroutines describing degradation models of fuel matrix in the canister and leaching of studied nuclides, solubility limitation of the concentrations of the latter, and ideal mixing in the free volume of the canister.

The influence of source term model parameters on the release rates of studied radionuclides from the near-field region was studied by numerical experiments [1-2]. It was stated that the extent of their influence depends also on the type of the studied nuclide. The migration of solubility limited nuclides is influenced by physical parameters of the system (void volume of the container, porosity of the bentonite layer) more significantly than that of nuclides, concentration of which in the void volume is not controlled by solubility, or the model of leaching in the water present in the void volume in the canister is very important mainly for nuclides that does not sorb on the bentonite surface. From our results, it could be recommended to bind the leaching of all nuclides with the degradation of fuel matrix controlled preferentially by leaching of uranium that depends on solubility limitation and retardation of it in the bentonite layer. Using this approach the modelled release rates of most of the dangerous nuclides would be lesser than previously reported (e.g., [3]), which would describe the reality more properly.

Our approach includes nor the history of canister degradation nor the influence of corrosion products on the sorption of radionuclides that affects the retardation of them. The models of these processes are not at hand as the conceptual description of them is under development as yet. The implementation of these models into the source term model will not be simple but it seems to be necessary for the acquirement of a more realistic safety assessment of the repository.

References:

- [1] VOPÁLKA, D. – VOKÁL, A.: *A New Code for Modelling the Near Field Diffusion Releases from the Final Disposal of Nuclear Waste*. Czechoslovak Journal of Physics, Vol. 53, Suppl. A, 2003, pp. A127–A133.
- [2] LUKIN, D. – VOPÁLKA, D. – VOKÁL, A.: *Transportní model pole blízkých interakcí. Citlivostní analýza a hodnocení vlivu vstupních parametrů na zdrojový člen HÚ*. Report ÚJV-12137 CH, ÚJV Řež a.s., 2004, 36 p.
- [3] VIENO, T. – NORDMAN, H.: *Interim Report on Safety Assessment of Spent Fuel Disposal TILA-96*. Report POSIVA-96-17, 1996, 176 p.

This research has been supported by MŠMT grant No. MSM 21000020 and by MPO grant No. 1H-PK/25.

Studies of PbWO₄ Crystals Behavior for Electromagnetic Calorimeters on High Energy Electron and Pion Beams

Jan Blaha, Jean Fay*, Miroslav Finger**, Michael Finger***, Suzanne Gascon-Shotkin*,
Bernard Ille*, Miroslav Slunečka**

jan.blaha@fjfi.cvut.cz

Czech Technical University in Prague, Faculty of Nuclear Sciences and Physical Engineering,
Břehová 7, 115 19 Praha 1, Czech Republic

*Institut de Physique Nucleaire de Lyon, IN2P3/CNRS and Universite Claude Bernard Lyon I,
4, rue Enrico Fermi, 692 22 Villeurbanne cedex, France

**Charles University, Faculty of Mathematics and Physics, V Holešovičkách 2, 180 00 Praha
8, Czech Republic

***Laboratory of Nuclear Problems, Joint Institute for Nuclear Research, 141980 Dubna,
Russia

The electromagnetic calorimeter (ECAL), currently under construction for the CMS experiment at the Large Hadron Collider (LHC) at the European Organization for Nuclear Research (CERN), has been designed to very precise energy and position measurements of electrons and photons produced in proton-proton collision at 14 TeV center-of-mass energy. The calorimeter consists of 61200 lead tungstate (PbWO₄) crystals read out by avalanche photodiodes (APDs) in the central barrel region and 14648 crystals read out by vacuum phototriodes (VPT) in the endcap regions. All the components of the calorimeter will be operating in a challenging environment: a magnetic field of 4 T, a time of 25 ns between bunch crossings, and a radiation dose of ~1-2 kGy/year for LHC operation at maximum luminosity [1].

The calorimeter barrel will be built from 36 supermodules. Each supermodule consists of 1700 crystals with APDs and associated electronics, monitoring systems and services. Lead tungstate crystals are a homogeneous detection medium with a short radiation length X_0 of 0.89 cm and a small Molière radius of 2.19 cm, which allows the construction of a compact and a fine granularity calorimeter. The time constant of the scintillation mechanism is well adapted to the 25 ns LHC bunch crossing rate, and radiation hardness has been achieved by appropriate doping and growth methods. On the other hand, the relatively low light yield necessitates the usage of a phototodetector with intrinsic gain. In addition, the sensitivity of both the crystal and photo-detector responses to temperature fluctuation requires a precise control of the temperature stability. All components of the calorimeter have been tested during the manufacturing process in regional centers as well as on CERN beams before final construction.

During the past few years functional properties of individual parts of the electromagnetic calorimeter were tested on beams of various high energy particles (electrons, muons and pions). Results of the analysis of the test experiments have served to elaborate on the general engineering-technical solutions of the electromagnetic calorimeter construction and optimize its spectrometric and operating properties. Hence the first fully equipped supermodule SM10 with final technical solutions was prepared and tested on electron, muon and pion beams in Autumn 2004. The supermodule was installed on a remotely controlled calibration table which allowed the crystals to receive the particles from the beam as if they come from the vertex. Auxiliary equipment such as scintillating fiber hodoscopes were installed as well. During 6 weeks of the beam test period the stability of the whole system

(voltage, temperature, dark current, laser monitoring) was monitored, particularly the function of on-detector electronics.

Most of the time the crystals were tested with electrons. The main priority of the test of SM10 was an intercalibration that was done with 120 GeV electrons (for all the active channels ~ 1225) and for 10 % of channels with 50 GeV. A detailed scan in eta geometry (85 crystal centers and 84 boundaries) with 50, 120, 180, 250 GeV electrons; high statistic position scan across module boundaries; energy scan/uniform coverage (four 3x3 crystal arrays); muons (150 GeV) and pions energy scan (50, 120, 180, 250 GeV); and test with cosmic rays was also performed. Test beam measurements on the supermodule thus could serve the following main objectives: intercalibrations, test on data acquisition and online software, the moving table, the understanding of the laser monitoring system, stability checks of the laser and the cooling systems, and the preparation for offline analysis. In addition, measurements of the crystal behavior under radiation, and comparison of the crystals' response to laser light and beam particles; comparison of the crystal light yield as obtained from the laboratory measurements and from the beam data. The offline data analysis and processing is currently being worked on and the preliminary results should be found in [2].

The beam test measurements with the first supermodule have given very encouraging indications and valuable results that the ambitious design goals could be met. The mechanics and the photodetectors are already ready or under production. The electronics have achieved their specified performance. The individual components of the calorimeter are working as expected.

References:

- [1] THE CMS COLLABORATION: *CMS Electromagnetic Calorimeter Project - Technical Design Report* CERN/LHCC 97-33 (1997), CERN, Geneva, Switzerland 1997
- [2] THE CMS COLLABORATION: *CMS Week, 6-10 December 2004*
<http://agenda.cern.ch/fullAgenda.php?ida=a045408> 2004

This research has been supported by the Czech Technical University in Prague within the grants IGS CVUT 10 84-113, Ministry of Education, Youth and Sports of the Czech Republic the grant FRVS 2086/2004 and the program Barrande 2004-011-1.

Effective Dose Calculation Using Radon Daughters and Aerosol Particles Measurement in Bozkov Dolomite Cave

Thinova, L.*, Berka, Z.*, Brandejsova, E.*, Zdimal, V.***, Milka, D.***

thinova@fjfi.cvut.cz

*CTU, Faculty of Nuclear Sciences and Physical Engineering, Brehova 7, Prague 1, Czech Republic

**Institute of Chemical Process Fundamentals, AS CR, Rozvojova 2, Prague 6, Czech Republic

***Bozkov Dolomite Cave Direction, 512 13 Bozkov, Czech Republic

Abstract

Conservative methodology for estimation of a potential dose in caves employs solid state alpha track detectors. Obtained data are converted into annual effective doses in agreement with the ICRP recommendations (using the “caves factor”). The more precisely determined value would have a significant impact on the radon remedies or on restricting the time guides spent in the underground. To define the calculation of the effective dose in caves, the following measurements were carried out: continual radon measurement (differences in ERC between working hours and night-time and daily and seasonal radon concentration variations); regular radon and daughters measurement through the sampling procedure to specify proportion of radon daughters; regular indoor air flow measurement to study the location of radon supply and its transfer among individual parts of the cave; natural radioactive elements content evaluation in sub soils and in water inside/outside to study radon sources in the cave; aerosol particle-size spectrum measurement for determination of free fraction (cave-apartment comparison); guides/visitors behaviour monitoring to record time spent in cave and to assign it to the continuously monitored levels of Rn concentration; results summarizing and comparison with “official” values.

Introduction

Carst caves fall among regions with exceptionally high radon concentrations, (despite the very low uranium content in limestone) that are caused by minimal airflow and negligible air exchange. The conversion factor (which plays the fundamental part for dose calculation) is dependent on aerosol particle size spectrum resolution and on distribution of radon daughters among the attached and unattached fraction [1]. With the aim to particularize the calculation of the effective dose in caves, the following measurements were carried out: continual radon measurements (differences in ERC between working hours and night-time and daily and seasonal radon concentration variations descry); regular radon and daughters measurements using a sampling procedure to specify proportion of radon daughters; regular indoor air flow measurements to study the location of radon supply and its transfer among individual areas of the cave; natural radioactive elements content evaluation in sub soils and in water inside/outside to study radon sources in the cave; 5-day aerosol particle-size spectrum measurements for determination of free fraction and for comparison of aerosol spectra in apartment and cave; guides/visitors behavior monitoring to record time spent in cave and to

assign in to the continuously monitored levels of Rn concentration. All obtained data were used for the effective dose calculation.

Effective dose calculation

The entire effective dose a person receives from the radon daughters was calculated as the sum of all effective doses obtained from individual sizes of aerosols (including the unattached fraction) using the following assumptions: in caves, only ^{222}Rn and its daughters occur; the mutual ratio of radon daughters and equilibrium factor is constant; the spectrum of aerosols is constant [2].

Conclusions

Occurrence of aerosols particles with diameter 1-10 μm is caused by visitors or personnel presence. Concentration of aerosols with diameter approximately 100-200 nm seems to be stable, larger-size aerosols are produced by visitors only. Small aerosols are produced by an intensive work or movement. Time spent inside by guides must be related to the actual radon concentration at given time. Personal dosimeters are advised. Using the factors described above, the effective dose was recalculated without any significant simplification as in case of SONS's methodology (no direct aerosol measurement had been carried out). The resulting values are fully comparable with the "official" values. Therefore, we have established that the methodology commonly used for dose estimation is correct. So far, we are unable to determine the ratio of attached and unattached portion that could significantly influence the calculations.

All results should be used as input parameters for dose-in-lungs model LUDEP calculation.

References:

- [1] ICRP: *Protection against Radon-222 at Home and at Work*. ICRP Publication 65, Pergamon Press, Oxford, UK, 1993.
- [2] W. C. HIHDS: *Aerosol Technology, Properties, Behavior, and Measurement of Aerosol Particles*. Second edition. John Witney & Sons, New York, 1998.

The presentation of this research at the conference in Japan has been supported by CTU grant No. CTU0416314.

Spectrometry Characteristic of Photon-fields and Atmospheric Radionuclide Deposits Monitoring in One Part of Southern Bohemia

J. Kluson*, L. Thinova*, T. Cechak*, T. Trojek*

thinova@fjfi.cvut.cz

*CTU, Faculty of Nuclear Sciences and Physical Engineering, Brehova 7, Prague 1, Czech Republic

Abstract

The (bio)monitoring in the neighborhood of Nuclear Power Plant Temelin (NPP) started in year 2000 – one year before the initial power plant operation. Biomonitoring is continuing fifth year where in the years 2000, 2002 and 2004 the spectrometry characteristic of photo-fields measurement was included. The area of interest contained 29 sampled locations along eight radial profiles intersecting the area up to distance from 2 to 20 km around NPP. Laboratory as well as in situ gamma spectrometric method enables to determine presence of natural and manmade radionuclides with very good limits of detection. In situ gamma spectrometry consist of determination air kerma rate from direct measurement (special energy compensated plastic scintillation detector) and air kerma rate calculation from photon spectra measurement (scintillation detector NaI(Tl) diameter 3" by 3"). The laboratory gamma spectrometric measurement (geometry of Marinelli containers) is used for determination of radionuclides in the samples of pine bark, Shreber's moss, forest humus, edible mushrooms and forest berries. The trend analysis of measurements results serve for completing of the main task of this project: to describe the influence of NPP Temelin on the radiation increase in its neighborhood. Only ^{137}Cs of manmade radionuclides has been identified.

Introduction

Atmospheric radionuclide deposit monitoring in the environment is often conducted using bioindicators. For the past fifth years, FNSPE CTU in Prague took part in monitoring the influence of NPP Temelin on the environment within 20-km radius of the plant. Using ecological principles, the changes in environment quality are indicated by biological indicator changes. We chosen forest humus, surface of pine bark, Shreber's moss, edible mushrooms, and forest berries.

The year 2000 was designated as reference year before the start of the NPP operation, and 2001 was the year of the initial operation. Research will continue in the following years. The biomonitoring for year 2000, 2002, and 2004 also included assessment of the dosimetry and spectrometry characteristic of the photon-fields.

Monitored area

Monitored area contains 29 sampled locations along eight radial profiles intersecting the area of interest (the measuring points are located 2-5-10-20 km from NPP, distance of 20 km is a comparison area). The pine bark and moss were sampled at the selected sites twice yearly, at spring and fall, forest humus once during spring months, mushrooms and berries once in growing seasons. The top 3 mm of tree bark were taken in reference height of 1m along the circumference of the trunk. To prevent contamination by soil the moss samples were cut by scissors. Forest humus was sampled with respect to resolution of surface layers, according to

the degree of hummification. In total, 203 samples in 2000, 222 samples in 2001, 223 samples in 2002 and 251 samples in 2003 were collected.

In situ gamma spectrometry is conducted at selected 15 points in order to sufficiently cover the area of interest.

Materials and methods

In the gamma spectrometry laboratory, the samples were, after drying (for example on case of mushrooms the weight loss was 90%) enclosed in Marinelli containers (0.5 l), surrounding during the measurements coaxial HPGe detector. Processing of measured spectra in the range up to 3 MeV provided mass related activity (Bq/kg) of naturally radioactive elements (^{40}K , ^{226}Ra , and ^{232}Th) and contaminant ^{137}Cs (resulting from nuclear weapon tests in the fifties of last century and from Chernobyl accident fallout) use program SP DEMOS. The resulting data were used for the trend analysis. Two model situations had to be studied: *Firstly*, one accident or several ones, occurring in a short term, would lead to relative extensive radionuclide escape. *Secondly*, a small amount of radionuclides is continuously escaping and depositing during the regular operation.

Two methods of the gamma fields in situ measurements of the dosimetric characteristics were selected (all measurements were conducted in altitude 1 meter):

1. Determination of air kerma rate by direct measurement
2. Air kerma rate calculation from photon spectra measurement by use of portable spectrometer with scintillation detector NaI(Tl) diameter 3" by 3" in the energy range up to 3 MeV

Conclusions

The measured spectra represent characteristic spectra of natural background. In the calculated energy distribution of air kerma rate is not possible to identify (with the exception of the above mentioned ^{137}Cs) any significant contribution of any man-made radionuclide. Based on the so-far obtained results of monitoring, as well as of the trend analysis, it can be stated that it was confirmed that JETE operation does not have any impact on the level of natural background in the measured reference points.

References:

- [1] L. THINOVÁ, T. ČECHÁK, J. KLUSOŇ, T. TROJEK: *Bio-monitoring of the radionuclide atmospheric deposits in the neighbourhood of the NPP Temelin*. Research Report, CTU. 2000, 2002
- [2] J. FRÁNA: *SP Demos*. ÚJF Řež. Spectra analysis programme.
- [3] K. KUPKA: *Statistické řízení jakosti*. Trilobite Statistical Software. Pardubice 2001. ISBN 80-238-1818-X
- [4] M. MELOUN, J. MILITKÝ: *Statistické zpracování experimentálních dat*. Ars Magna. Praha 1998. ISBN 80-7219-003-2

The presentation of this research at the conference in Japan has been supported byCTU grant No. CTU0416314

The Alpha Ray of Radon Daughters in Water and in Air Used the Detection Unit "YAPMARE" with Scintillation Detector YAP:Ce Measurement

L. Thinova*, A. Kunka**, P. Maly**, F. de Notaristefani ***, K. Blazek**, T. Trojek*,
L. Moucka ****

thinova@fjfi.cvut.cz

* CTU, Faculty of Nuclear Sciences and Physical Engineering, Brehova 7, Prague 1, Czech Republic

** Crytur Ltd., Palackého 175, Turnov, Czech Republic

*** INFN Sezione di Roma, Rome, Italy

**** National Radiation Protection Institute, Bartoskova 25, Prague, Czech Republic

Abstract

With focus on the detection of the Rn concentration in water in extreme conditions, the detection unit YAPMARE was developed by company CRYTUR Ltd. The main part of the detection unit is a detection probe based on the Ø25x100mm YAP:Ce detector (chemical formula is $YAlO_3$ doped Ce). The measured water covers approximately 95% of the crystal surface (the detection volume is 12 ml). Measurements of ^{222}Rn and ^{220}Rn standards for determination of individual peaks in spectra were conducted, including observation of the ^{222}Rn (and its daughters) behavior. For YAPMARE calibration the fresh water from drilled-well from Lounovice area (biotitic granodiorite - adamellite) was taken. The calibration was carried out with the assistance of radon in water monitor RADIM 4. Results of the Lounovice water measurement: detection limit about 50 Bq/l, calibration coefficient 1,1.10-3 imp/s be 1Bq/l. The results of the fresh water and air samples measurements have demonstrated the main *advantages* (spectrometric results of the measurement, possibility for water or air samples evaluation) and *disadvantages* (large size of scintillation crystal increases gamma ray background, calibration for each water with particular composition, detector cleaning using HCl acid). A thin plate YAP:Ce version was tested for alpha particle detection.

Introduction

With a focus on earthquake forecasting by detection of the Rn concentration in water, the detection unit YAPMARE was developed by the company CRYTUR Ltd. The main part of the detection unit is a detection probe based on the Ø25x100mm YAP:Ce detector, made of monocrystalline YAP:Ce (chemical formula is $YAlO_3$ doped Ce) grown by the Czochralski method in Crytur Ltd. The detection unit was described in [1, 2]. Between October 2003 and May 2004 the following tests were carried out: (i) gamma and alpha energy calibration using radionuclide etalons; (ii) identification of spectrum peaks using "air" ^{222}Rn and ^{220}Rn standards; (iii) a long-time monitoring for stability and background elimination; (iv) completion of water sampling methodology; (v) measurement of high radon activity water from Jachymov mines; (vi) measurements of fresh and standard Rn water; and (vii) the detection- unit calibration using RADIM 4 (a monitor for water radon samples). On the basis of those results was started a study of YAP:Ce crystal sorption characteristic.

Materials and methods

For radon activity measurement, fresh water from drilled-well (Rn concentration of water samples were 700 - 900 Bq/l) in Lounovice area (adamellite) was taken. Completely filled special bottle 0,5 l was carefully closed and bottles were kept in refrigerator for restriction of evaporation. For each following measurement was always used a new bottle. The detection unit was used in the stationary regime. The measurement of radon in water activity was started after establishment of equilibrium between radon daughters (3 h). The time measurement interval was 2 hours. After each measurement the detection unit was cleaned with HCl acid for 20 minutes, rinsed with water and after that background and energy stability was checked. Calibration of detection unit YAPMARE was carried out with the assistance of radon in water monitor RADIM 4

Results and conclusions

The test measurements indicated the influence of the gamma ray background, which can be minimized in the laboratory e.g. ten times with use of Pb shielding with 25mm thickness. The results of the first water and air samples measurement have demonstrated the main advantages (linear dependence towards gamma ray and alpha ray, spectrometric results of the measurement, possibility for water or air samples evaluation) and disadvantages (large size of scintillation crystal increases gamma ray background in area ^{214}Po , alpha calibration is necessary to be repeated again for measurements of a new type of water, thoron influence in high active fresh water samples, necessity of detector cleaning by HCl acid). A thin plate YAP:Ce version was tested for alpha particle detection.

Results of the Lounovice water (ph 6,7) measurement: detection limit about 50 Bq/l, calibration coefficient $1,1 \cdot 10^{-3}$ imp/s be 1Bq/l. The calibration coefficient and detection limit are dependent on the chemical composition of water. As a result of unit leakage, a deficit of Rn activity occurs during long-run measurements, an effect that must be prevented when implementing flow-through measurement method.

References:

- [1] A. KUNKA, P. MALY, K. BLAZEK, F. DE NOTARISTEFANI, B. SOPKO.: *New YAP:Ce scintillation detection for determination of ^{222}Rn in water*. Radiation Measurements, 2004, Vol. 38/4-6 pp. 829-832.
- [2] A. KUNKA, P. MALY, K. BLAZEK, F. DE NOTARISTEFANI, B. SOPKO.: *Measurement of Rn and other gamma and alpha radionuclides in water with the help of a new detection unit based on scintillation single crystal YAP:Ce* To be published in Elsevier Science "Nuclear Instruments and Measurements, 2005.

The presentation of this research at the conference in Japan has been supported by CTU grant No. CTU0416314

Development of Independent Power Protection System for VR-1 Training Reactor

M. Kropík, M. Juříčková, K. Matějka

kropik@troja.fjfi.cvut.cz

Department of Nuclear Reactors, Faculty of Nuclear Sciences and Physical Engineering,
Czech Technical University, V Holešovičkách 2, CZ 180 00 Prague 8, Czech Republic

This contribution deals with the VR-1 training reactor independent power protection upgrade. The VR-1 training reactor has been operated since 1990 by the Department of Nuclear Reactors FNSPE CTU in Prague. The reactor was designed and constructed by the Škoda Company in co-operation with the Faculty. The VR-1 reactor is a pool-type light-water reactor based on enriched uranium (36%). Its thermal power is up to 5kW. The moderator of neutrons is light demineralised water that is also used as a reflector, a biological shielding and a coolant. Heat is removed from the core with natural convection. The VR-1 reactor is utilised particularly for training of university students and nuclear power plant staff. Research at the VR-1 reactor is mainly aimed at the preparation and testing of new educational methodologies, investigation of reactor lattice parameters, reactor dynamics study, research in the field of control equipment, neutron detector calibration, etc.

The reactor I&C seems to be obsolete now, and its upgrade is being carried out. The upgrade is being done gradually during holidays in order not to disturb the reactor utilisation during teaching and training. The first stage was the human-machine interface and the control room upgrade in 2001. During the second stage of the upgrade, the control rod drivers and the safety circuits were replaced. The third stage, the control system upgrade was carried out in 2003. The fourth stage, the independent power protection system upgrade described in this contribution is being upgraded now. All upgrades are being carried out in cooperation with Škoda Nuclear Machinery Company.

The independent power protection system is component of the reactor safety (protection) system. There are strict requirements on quality and reliability of nuclear facility safety systems. The independent power protection system is a computer based system, so there is necessary to fulfil quality requirements on both hardware and software.

The independent power protection system is redundant and consists of four individual channels. Each channel evaluates the reactor power and the velocity of power changes and compares them with safety limits. If the safety limits are exceeded, the channel disconnects its safety relay. The relays of all channels are connected to the reactor safety circuits. The safety circuits evaluate the states of individual channel relays in the logic 'two out of three'. If the logic condition is met, the safety circuits break the control rods power supply. The rods fall down into the reactor active core and stop the fission reaction.

At the start of the channel development, the general channel requirements, the hardware and software requirements [1] were prepared.

The input of the independent power protection channel is the neutron boron chamber located under the reactor vessel. Because of the chamber sensitivity and a significant distance from the reactor active core, the chamber signal is evaluated in the pulse regime only. The chamber

signal is amplified and processed with a discriminator. Pulses from the discriminator are counted in the digital portion of the channel.

The digital portion of the independent power protection channel is multiprocessor-based. The channel structure supports division of channel functions to individual microcomputers. There are two microcomputers to calculate the reactor power and the velocity of power changes, to compare them with the safety limits and to control the safety relay. These microcomputers are the most significant for nuclear safety. The microcomputers work parallel and their outputs are checked by a supervisory microcomputer. This microcomputer compares data from the calculation microcomputers, and if they are different (problem indication), the supervisory microcomputer disconnects the channel safety relay. The next microcomputer is a communication one. The communication microcomputer guarantees the communication between the independent power protection channel and the reactor control system. The communication is serial with fibre optic lines.

The channel provides test functions. It is possible to connect the channel input instead of the neutron chamber with test pulses and to test the channel response. Moreover, the discrimination can be changed, and its influence is evaluated. Next, discrimination level and chamber high voltage power supply are evaluated by A/D converters and checked. If a problem is found, the channel safety relay is disconnected.

The software for the channel was developed with respect to [2]. The software development was based on the software requirements [1]. The next phase of the software development was the software design. The software modules, algorithms and data structures were proposed. Furthermore, the software design was coded in the C language regarding [3]. The software was then integrated with the hardware and is now carefully tested during non-active and active tests. Configuration management, verification and validation accompanied the independent power protection system software development [4].

The developed independent power protection system is being tested now and is installed during the summer holiday 2005. The system substantially improves nuclear safety, availability and utilisation of the VR-1 reactor. The reactor I&C upgrade continues with the operational power measurement system upgrade in 2006. The complete reactor I&C upgrade brings the reactor I&C to top conditions and enables a prolongation of their functionality and maintainability for at least 10 next years

References:

- [1] KROPÍK, M. - CHÁB, V. - JUŘÍČKOVÁ, M.: *Independent Power Protection System General, Hardware and Software Requirements* DNR FNSPE CTU, 2004
- [2] *Software for Computers in the Safety Systems of Nuclear Power Plants IEC-880* Geneva, 1986
- [3] HECHT, H. - HECHT, M. - GRAFF, S.: *Review Guidelines on Software Languages for Use in NPP Safety Systems* U.S. Nuclear Regulatory Commission, 1996
- [4] KROPÍK, M. - JUŘÍČKOVÁ, M. - CHÁB, V.: *Quality Assurance, Verification & Validation and Configuration Management Plans* DNR FNSPE CTU, 2004

This research has been supported by the MŠMT grants MSM 210000020 and FRVŠ 2076/2004.

Testing of the Upgraded Control System of the VR-1 Training Reactor

M. Juříčková, V. Cháb

jurickov@troja.fjfi.cvut.cz

CTU Faculty of Nuclear Sciences and Physical Engineering, Department of Nuclear Reactors, V Holešovičkách 2, CZ 180 00 Prague 8, Czech Republic

The VR-1 training reactor has been operated since 1990 by the Department of Nuclear Reactors, at the Faculty of Nuclear Sciences and Physical Engineering of Czech Technical University in Prague. The reactor was designed and built by the Škoda Company in co-operation with the Faculty. The reactor control and safety system (I&C) was developed in the mid- 80s. The original system is digital, it utilizes 8-bit microcomputers with software written in the assembly language. The technical design of the control and safety system is now quite obsolete. There are also problems with maintenance, and since its development, the quality demands (e.g. the IAEA, IEC, and IEEE recommendations and standards) were significantly evolved. Therefore, it was decided to upgrade the present control and safety system with the aim to apply the latest available techniques and technology.

The principal upgrade of the control and safety system started in 2001. The first stage was the human-machine interface upgrade. During the second stage of the upgrade in 2002, the control rod drives and the safety circuits were replaced. The third stage – the control system upgrade – was carried out in 2003. The next upgrade stage is the independent power protection (IPP) channels upgrade in 2005. During the last stage, the operational power measurement (OPM) channels will be upgraded probably in 2006.

The upgraded control system is based on a high quality industrial PC mounted in a 19" crate and Simatic PLCs for dedicated functions. The operating system of the PC is the Microsoft Windows XP with the real time support RTX of the VentureCom Company. The software for the control system was developed according to requirements in MS Visual C. A large amount of work has been devoted to the software requirements to specify all dependencies, modes and permitted actions, safety measures, etc. The control system receives data from the operational power measuring and independent power protection channels and compares them with safety limits, and it also controls the safety circuits. Furthermore, it calculates the average values of the important variables (power, power change rate), and sends data and system status to the human-machine interface. Next, it receives commands and button inputs from the operator's desk and carries them out according to the reactor operation mode. Finally, it serves as an automatic power regulating system.

The upgraded control system was thoroughly tested. First, the non-active tests were carried out. During these tests, the core of the reactor was subcritical; HPIB and VXI controlled instruments generated the input signals that provide alternative pulses and current as from neutron chambers to simulate various operational and emergency conditions. The instruments control and tests evaluation were implemented using the Agilent VEE development system. The second stage was the active testing. The behaviour of the whole I&C was investigated under the standard as well as non-standard operating conditions.

First, the non-active tests started with the whole system behaviour checking. The reactor start-up and operation were carried out with simulated input signals and deep subcritical core of the nuclear reactor.

Next, basic safety functions of the control system were tested. The reactor operation conditions were simulated in such a way to provide exceeding of the reactor power and the power change rate safety limits. During these tests, the control system used more rigorous

safety limits in comparison with the reactor protection system to check the safety function of the control system only. Various reactor power courses were prepared for the control software of testing facility to simulate emergency situations mentioned above.

The new control system provides also advanced safety features in comparison to the old one. There is built in a check for the reactivity excess during the reactor start-up when condition for the transition to standard operation is met, and safety, experimental or control rods are not in proper positions (typically too low with high reactivity excess). Conditions for these types of safety function initiation were simulated, and proper response was checked during standard operation, dynamic experiments and basic critical experiment modes.

Further safety function of the control system deals with deviations among individual neutron flux (reactor power) measuring channels. If such deviation is too large, it indicates some problem in those channels. When the power deviation of channel X exceeds 50% of the reactor power (arithmetic mean of all 3 channels) during the reactor start-up or 25% during the standard reactor mode, the operational power measuring channel X is changed from the status "Measure" to the status "Failure". If only 2 channels are in the status "Measure", the power deviation is calculated as the difference between these 2 channels related to the lower one. All tests were carried out on different levels of the initial reactor power during the start-up and on the initial power of 10000 counts per second during the standard operational mode.

Faults and errors discovered during the non-active testing were fixed, and new tests were carried out to approve these amendments.

After the successful non-active checking, the active test of the control system were carried out. During these tests, the reactor core was put into the standard configuration. Again, all safety features of the control system, transitions among reactor modes and submodes were tested. All control functions, commands and validity of their execution were verified. The automatic power regulator was also tested.

The tests described in this article contributed to the successful upgrade of the VR-1 training reactor control system. The tests approved the compliance of the new control system with requirements set on it. The new control system substantially improves the reactor safety, operational comfort and facilitates the work of the reactor staff.

References:

- [1] KROPÍK, M. -CHÁB, V.: *Control System Software Requirements* DNR FNSPE CTU in Prague, 2003
- [2] KROPÍK, M. - MATĚJKA, K. - JUŘÍČKOVÁ, M. - CHUDÝ, R.: *Safety System Validation* Enlarged Halden Programme Group Meeting, Loen, Norway, 1999
- [3] KROPÍK, M. - MATĚJKA, K. - CHÁB, V.: *Upgrade of Training Reactor VR 1 Control System* Enlarged Halden Programme Group Meeting, Sandefjord, Norway, 2004
- [4] SKLENKA, Ľ. - MATĚJKA, K. - KROPÍK, M. *Improving of Safe Operation and New Open Policy at VR 1 Reactor* International Conference on Research Reactor Utilization, Safety, Decommissioning, Fuel and Waste Management, IAEA Vienna, 2003

This research has been supported by the MŠMT grants MSM 210000020 and FRVŠ 2511/2003.

Control System Experience

V. Cháb, M. Kropík

chab@troja.fjfi.cvut.cz

Department of Nuclear Reactors, Faculty of Nuclear Sciences and Physical Engineering
Czech Technical University, V Holešovičkách 2, CZ 180 00 Prague 8, Czech Republic

This article deals with experience of the VR-1 training reactor new control system operation. The VR-1 training reactor has been operated since 1990. The reactor was designed and built by the Škoda Company in co-operation with the Faculty. The reactor utilizes a digital control and safety system (I&C) that was developed in the mid- 80s. Even if the present control and safety system fully covers the demands that are put on it, its technical design is obsolete to a certain extent at the present time. Also some new internationally respected demands to ensure the quality and the qualification (e.g. the IAEA, IEC, and IEEE recommendations and standards) were not or could not be considered. Therefore, it was decided to upgrade the present control and safety system with the aim to apply the latest available techniques and technology observing the above mentioned recommendations and standards.

Because of the typically annual financial planning and the frequent utilization of the VR-1 training reactor during the academic terms, it was decided to carry out the upgrade of the control and safety system gradually, in stages during holidays so as not to affect the training at the reactor. The first stage of the I&C upgrade was the human-machine interface and the control room upgrade in 2001. During the second stage of the upgrade in 2002, the control rod drives and the safety circuits were replaced [1].

The third stage, the VR-1 training reactor control system upgrade [2] was accomplished in the summer and autumn 2003, some amendments and succeeding tests were carried out in winter 2004. The general contractor of the project was Škoda Nuclear Machinery Company Plzeň, the hardware and software subcontractor was the dataPartner Company České Budějovice. Necessary changes in the human-machine interface induced by the control system upgrade were done by the ZAT Company Příbram. The Department of Nuclear Reactor prepared the software requirements, solved specific electronics and software tasks and carried out the tests of the upgraded control system and associated systems.

The upgraded control system is based on a high quality industrial PC mounted in a 19" crate that cooperates with Simatic S7-200 PLCs utilized for dedicated functions. The operating system of the PC is the Microsoft Windows XP with the real time support RTX of the VentureCom Company. The computer is equipped with 8 RS232 lines for communication with the reactor power measuring and power protection channels (the reactor protection system), with the RS485 (Profibus) line for communication with the Simatic control rod and I/O PLCs and with the Ethernet line for data transfer to the human-machine interface.

The complete control system was thoroughly tested. The detailed description of the control system tests can be found in [3].

The new control system provides better comfort of reactor operation and nuclear safety. New commands were added in comparison to the old control system to simplify the reactor operator work; e.g. the experimental rod position setting, operational status and setting information, reactor mode change. New batch commands were introduced into the control system. The system offers batch commands consisting of up to 200 individual commands to accomplish intended reactor power courses, etc. There is possible to store produced batches

on the computer hard disc for a future utilization. The batches are very useful for training of students.

Safety functions of the control system were significantly improved during the upgrade. The control system can initiate the safety action because of the reactor power, velocity of power changes and deviation among individual measuring channels safety limits exceeding. Next, the deviation between given and real reactor power is evaluated, and the exceeding of the safety limit also causes the reactor scram. The reactivity excess during the reactor start-up is checked, and if the reactor power reaches the proper value for the transition into the standard operation mode with low position of control rods, the safety function (rod fall) is initiated.

The absorber rod diagnostics was improved. If the rod falls from its top position, the rod fall time is measured and stored for the rod reliability evaluation. Furthermore, new control system abilities for the rod tests were introduced. During the rod test, the velocity of the rod movement is measured and stored; then the rod falls down from the top position and the fall time is measured. These tests contribute to better checking and maintenance of control rods.

One and half year experience revealed some problems in the new control system despite of thorough testing. Some of these problems were because of software requirements [4] uncertainties that specify all dependencies, modes and permitted actions, safety measures, etc. If the "Rod Drop" command was done (e.g. during the measuring of the control rod calibration), the control system blocked safety signal of minimal reactor power but the warning signal was active. Operator could not move the control rod up because the system generated warning signal, which blocks rod up motion. The control system requirements were corrected. Moreover, some ideas were gathered how to implement some improvements. Also, some minor mistakes in the programmer's work localized by experienced operators were fixed by the software manufacturer.

The operational experience with the new control system is positive. The new control system is more user friendly than the old one, provides better comfort of the reactor operation and nuclear safety.

References:

- [1] KROPÍK, M. – MATĚJKA, K.: *Upgrade of the VR-1 Training Reactor I&C* Enlarged Halden Programme Group Meeting Storefjell, Norway, 2002 .
- [2] KROPÍK, M. - MATĚJKA, K. - CHÁB, V.: *Upgrade of Training Reactor VR 1 Control System* Enlarged Halden Programme Group Meeting, Sandefjord, Norway, 2004
- [3] JUŘÍČKOVÁ, M. -CHÁB, V.: *Testing of the Upgraded Control System of the VR-1 Training Reactor* CTU Workshop, 2005
- [4] KROPÍK, M. - CHÁB, V.: *Control System Software Requirements* DNR FNSPE CTU, 2003

This research has been supported by the MŠMT grants MSM 210000020 and FRVŠ 2511/2003.

Determination of Energy Neutron Spectrum at Reactor VR-1 Sparrow

K. Katovský, A. Kolros, P. Paluska

k.katovsky@sh.cvut.cz

Department of Nuclear Reactors, Faculty of Nuclear Sciences and Physical Engineering, Czech Technical University in Prague, V Holešovičkách 2, 180 00 Prague, Czech Republic

Energy neutron spectrum in the reactor core is a very important property, which is essential for complete understanding of experimental investigations performed in the core. VR-1 reactor's spectrum had already been basically studied - introductory experimental [1] and theoretical [2] research had been done. Objectives of our investigation were in coupling, comparing and improving of both methods, it means extension of experimental measurement and more precise theoretical prediction of energy neutron spectrum. The bottom of the pneumatic transfer system's pipeline was chosen for this study, because this geometrical point was very important due to frequent use of the pneumatic transfer system for experimental studies (e.g. material and activation analysis).

Theoretical prediction of the spectrum was calculated by Monte Carlo code MCNP version 4C [3]. This code is world-widely used and very well validated. Default ENDF/B-6 based libraries were used. Energy distribution of neutrons was calculated in 15, 83, 106, 246 and 620 energy groups structure. The 15 groups library was chosen due to its use in the past and the 620 groups library due to correspondence with energy structure used by SAND-II code [4], which was appear in experimental data analysis. Processing and visualization of MCNP output spectrum were improved too.

Experimental determination of energy distribution of neutrons was performed by activation analysis method i.e. thin foils from various highly pure materials with variable activation cross-sections and reaction thresholds were irradiated inside the core and then analyzed using γ -spectroscopy methods. Two new experiments were carried out. Measured data were joined with a third one-year-old experiment [1] using measurement of Au foil activity. The same Au foil was irradiated in all three experiments, so results should be normalized in according to saturated activities values [6]. Reaction rates obtained by such normalization can be afterwards processed together. Activation foils kit was irradiated in the same geometrical point that was used for calculation. After irradiation the γ -spectra of irradiated foils were measured by HPGe detector. In general, 11 foils (i.e. Au, Mo, W, Sc, Fe, Ni, NaCl, V, In, Mg, Al) were irradiated, measured and analyzed. During this project, methodology of HPGe detector efficiency has been significantly improved. Until now, simple power function of energy was used to fit efficiency curve. For this data analysis efficiency function ε was used in exponential form: $\varepsilon = \exp\{S_n[\ln(E)]\}$, where S_n is a polynomial function of logarithmic argument of energy [7]. Measured γ -spectra were analyzed using standard procedure; areas of the γ -peaks have been fitted by Deimos code [5], reaction rates were calculated by VYNAKT code (developed during this investigation in Department of Nuclear Reactors FNSPE CTU in Prague). Reaction rates were used as input parameters for SAND-II code, which applied iterative method for neutron spectra unfolding. Results of MCNP-4C (theoretical calculation) and SAND-II (processed experimental data) were compared. It was the first step of experimental methodology validation and it brought a lot of interesting ideas and suggestions for future work.

One of future major plans is improvement of high-energy parts of energy neutron spectrum measurement. It mainly needs measurement of (n,p) , (n,n') , $(n,2n)$, (n,α) reactions, which usually have high energy of reaction's threshold but small reaction cross-section. These measurements need extension of irradiation time (preferably at increased power of reactor) and long-time γ -measurements. Next step should be increase of HPGe detectors efficiency by reducing of distance between measured foil and HPGe detector. Such a reduction needs improve of efficiency calibration by using surface calibration sources, and consideration of coincidence summing of γ -quanta. Also data analysis should be improved. Main problem is incompleteness of SAND-II data library. All this methodology is in preparation and new experiments are planned for the year 2005.

References:

- [1] PALUSKA, P.: *Měření neutronového spektra v aktivní zóně reaktoru VR-1*, KJR FJFI ČVUT v Praze, 2003, Výzkumný úkol.
- [2] RATAJ, J. – KOLROS, A. – MATĚJKA, K.: *Dílčí podklady pro řešení projektu Blanka*, KJR FJFI ČVUT v Praze, 2004.
- [3] BRIESMEISTER, J. F. ET AL.: *MCNP4C: Monte Carlo N-Particle Transport Code System*, Los Alamos National Laboratory, LA-13709-M, 2000.
- [4] MAREK, M.: *Implementace programu SAND II na počítače PC*, ÚJV Řež u Prahy, 1991, ÚJV 9451.
- [5] FRANA, J.: *Deimos code*, J.Radioanal.Nucl.Chem., 2003, 257, 583-589.
- [6] BARTEJSOVÁ, E.: *Spektrum neutronů v aktivní zóně reaktoru VR-1 Vrabec*, KJR FJFI ČVUT v Praze, 2004, Výzkumný úkol.
- [7] ADAM, J. ET AL.: *Program Package and Supplements to Activation Analysis for Calculations of Nuclear Reactions Cross-Sections*, JINR Dubna, 2000, P10-2000-28.

This research has been supported by the Czech Ministry of Education - Universities Development Fund (FRVŠ ČR); grant No.2090/2004 - Validation of Experimental Measurement of Energy Neutron Spectrum on Reactor VR-1.

Integration of Czech Nuclear Engineering Education into European Educational System

E. Sklenka, K. Matějka, J. Rataj, K. Katovský

`sklenka@troja.fjfi.cvut.cz`

Department of Nuclear Reactors, Faculty of Nuclear Sciences and Physical Engineering, Czech Technical University in Prague, V Holešovičkách 2, 180 00 Prague, Czech Republic

In according to present European and worldwide activities, Department of Nuclear Reactors initialize an idea of CENEN – “Czech Nuclear Education Network”, national institution which aims its effort to nuclear education in Czech Republic. Association is based on principles of ENEN – “European Nuclear Education Network Association” founded as part of 5th European Framework Programme [1]. The main objective of the CENEN (as well as ENEN in European level) is the preservation and further development of a higher nuclear education and expertise. This idea should be realized through the co-operation between Czech Universities involved in education and research in the nuclear engineering field. Future plan is enlargement of co-operation to research centers, nuclear industry and regulatory body. CENEN will promote and further developed the collaboration in nuclear engineering education of academicians, engineers and researches; ensure the quality of nuclear engineering education and training.

Essential aim of CENEN is increase attractiveness for nuclear engineering studies; open studies for wider number of students and incorporate Czech nuclear education into European education network. Future objectives should be also definition of Czech Master of Science Degree in Nuclear Engineering (as part of European M.Sc. Standard), promotion of exchange of students and teachers participating in the frame of CENEN network, and establishment of mutual lectures and training courses. Activity in founding national education network is also motivated by successful work of BNEN – “Belgian Nuclear Higher Education Network” [2]. BNEN Association is based on national co-operation and experiences with collaboration are great. Five Belgian universities in co-operation with SCK-CEN research center organize common courses and lectures, which are provided by individual BNEN partners for all students.

First activities of CENEN will be based on experiences with present projects in which Department of Nuclear Reactors participate. Czech Technical University in Prague represents the Czech Republic in ENEN and WNU (World Nuclear University) and collaborates in NEPTUNO (Nuclear Platform of Training and University Organization) project in the scope of 6th European Framework Programme. Department of Nuclear Reactors has also experiences with projects Erasmus, Erasmus-Mundus and Eugen-Wigner Course [3], which attend in 2003 and 2004 students from many European countries, and it takes place in Prague, Vienna, Bratislava and Budapest. Next course is planned in the year 2005. Organization of national meetings, seminars and workshops should be also initial activity of the CENEN.

Department of Nuclear Reactor CTU in Prague organized the preliminary CENEN seminar on November 2004. Seminar was called “Integration of the Czech higher education into European and world’s educational structures”. All representatives of Czech universities, which engage in nuclear engineering education, were invited to participation in seminar. All attendee agree with CENEN establishment. Representatives of departments and institutes of Czech Technical University in Prague, The University of West Bohemia in Pilsen, Brno

University of Technology, and VŠB-Technical University Of Ostrava are highly interested in this activity and they will be founding members of the CENEN. In seminar first version of future statutes [4] were created and discussed. Statutes and foundation charter of the CENEN will be signed in first quarter of the year 2005. Participants of the seminar come to agreement that official web pages of the CENEN will be set up. Internet presentation will include foundation charter, statutes, aims and objectives of the CENEN. Each member of the association will be presented here, with annotation of all lectures and trainings courses regarding nuclear engineering education provided by the institution.

References:

- [1] MOONS, F. ET AL: *ENEN Association Statutes* Atomic Energy Commission - CEA, France, 2002 .
- [2] VAN CAMP, B. ET AL: *Agreement concerning an interuniversity programme in Nuclear Engineering organised within the Framework of the Belgian Nuclear Higher Education Network (BNEN)* BNEN, Belgium 2002 .
- [3] MATĚJKA, K. ET AL: *Reactor Physics Course at VR-1 Reactor - Textbook for Eugen Wigner Training Course on Reactor Physics Experiments* CTU Prague, 2004, 58 p.
- [4] SKLENKA, L. ET AL: *CENEN - Czech Technical Education Network Association Statutes (Preliminary version)* Department of Nuclear Reactors CTU Prague, 2004.

This research has been supported by Development & Transformation Fund of the Ministry of Education, Youth and Sports No. 55/2004.

Processing and Analysis of Results from Experimental Measurements with Subcritical Blanket BLAŽKA and External Neutron Source NG2 at Cyclotron in Nuclear Physics Institute, Academy of Sciences of the Czech Republic

J. Rataj

rataj@troja.fjfi.cvut.cz

Department of Nuclear Reactors, Faculty of Nuclear Sciences and Physical Engineering,
Czech Technical University,
V Holešovičkách 2, 180 00 Prague 8, Czech Republic

Faculty of Nuclear Sciences and Physical Engineering, Department of Nuclear Reactors (FNSPE DNR), solves problems associated with a dynamics behaviour of subcritical reactor with external neutron source and provides wide information for study of transmutation technology. FNSPE DNR closely co-operates with Nuclear Physics Institute (NPI), Academy of Sciences of the Czech Republic in study of this issue. In a close collaboration of the NPI Řež and at the FSNPE DNR, the high-power external neutron source at the NPI Fast Neutron Facility (FNF) and the module of the fluoride-salt subcritical blanket Blažka at the FSNPE DNR were developed. Both, the basic characteristics of these facilities and the forthcoming research program are outlined. Experimental research program concerns the neutronics of AD (Accelerator Driven) system which employs a subcritical blanket Blažka and an external fast-neutron source NG2.

DNR, FSNPE prepared design and fabrication of subcritical blanket named Blažka. Blanket consists especially of these materials:

- Graphite
- NaF in powdered state
- Fuel elements EK-10.

Fuel elements EK-10 are grouped beside oneself in square lattice (fuel elements constitute nine square fields in total – 3x3). Blanket contains 232 fuel elements EK-10 in total (approximately 1856 g ^{235}U). Powdered NaF is put in polyethylene covers. These covers protect fuel elements from chemically aggressive NaF. All fuel elements (EK-10) are polyethylene covers with NaF. Graphite blocks fill leftover area in lattice. These all materials were stacked up in aluminium cover. In the centre of the blanket is removable graphite block, which can be changed for another materials or some equipment (for example external neutron source). Blanket contains three measurement channels, which can be used for different detectors installations inside the blanket.

Design and manufacture of NG2 target station, which includes the high-power heavy water target and a beam line from the negative-ion extractor, have been completed in year 2001. NG2 facility comprises high-performance target station for gaseous, liquid and solid target (heat load to 1 kW) and ion-optical lines. These ion-optical lines ensure transport of accelerated ions from negative-ion extractor (at NPI cyclotron U-120M) on target. Trial installation of target station to NPI cyclotron was carried out in year 2002. A lot of measurements were performed with NG2 target station during years 2002 and 2003. Experiments were focused on measurement of basic neutron characteristics (spatial and spectral neutron distribution from target) for various targets. We intend to use at first Be target (reaction $\text{Be}(d, xn)$) and later D_2O target (streaming D_2O target, reaction $\text{D}_2\text{O}(p, xn)$)

for experiment with subcritical blanket Blazka and external neutron source at NPI Řež. Theoretical model of NG2 target station is made by MCNPX code for various targets (Be, D₂O and Li).

Following works were made in year 2000 – 2004:

- Basic critical experiment with core B4 at training reactor VR-1, one component of this core was subcritical blanket Blazka (DNR, FSNPE),
- Experiments with the subcritical blanket Blazka and AmBe external neutron source (DNR, FSNPE),
- Computational verification of the above mentioned experiments by MCNP and MCNPX computational codes (DNR, FSNPE) by MCNP and MCNPX computational codes (DNR, FSNPE)
- Basic neutron measurements with the NG2 target station (NPI, Řež),
- Computational verification of neutron distribution from the NG2 target station (NPI, Rez and DNR, FSNPE),
- Testing of the measurement system (Mc-256) with the chamber SNM-13 at NG2 target station (NPI, Rez and DNR, FSNPE),

All experimental data from the above mentioned experiments were compared with calculated data. For all calculations was used code MCNPX (version 2.5.d). Experimental and calculation data were processed and analysed by code Tecplot 10. All results were processed in graphs and tables.

References:

- [1] RATAJ, J.: *Experimental study of neutronic parameters of developed modules of ADS blanket at the reactor VR-1* diploma theses, DNR FSNPE CTU Prague, 2001.
- [2] BEM, P. – DOBEŠ, J. – KROHA, V. – ŠTURSA, J. – MATĚJKA, K. – RATAJ, J.: *Research program for the cyclotron driven fluoride-salt subcritical assembly at NPI Accelerator Applications/Accelerator Driven Transmutation Technology and Applications '01*, Reno, Nevada 2001.
- [3] RATAJ, J.: *Příprava experimentu s podkritickým souborem BLAŽKA a vnějším neutronovým zdrojem NG2 na cyklotronu v ÚJF AV ČR* 3rd Nicolas's Young Generation Informal Meeting, VUT Brno, 2003.
- [4] RATAJ, J.: *Experimental Study of Subcritical Blanket Blažka with External Neutron Source NG2 at Nuclear Physics Institute, Řež* International Youth Nuclear Congress, Toronto, Canada, 2004.

This research has been supported by CTU grant No CTU0411614.

Participation of DNR FNSPE CTU in the Project of the Nuclear Transmutation System SFINX - Irradiation Experiment with the Module B417 at the Training Reactor VR-1

J. Rataj, K. Matějka, A. Kolros

`rataj@troja.fjfi.cvut.cz`

Department of Nuclear Reactors, Faculty of Nuclear Sciences and Physical Engineering,
Czech Technical University,
V Holešovičkách 2, 180 00 Prague 8, Czech Republic

Department of Nuclear Reactors (DNR), Faculty of Nuclear Sciences and Physical Engineering (FNSPE) has been studying transmutation technology for many years. In the year 1996 department became a member of TRANSMUTATION consortium of the Czech Republic. Other consortium members are:

- Nuclear Research Institute (NRI) Řež,
- Nuclear Physics Institute (NPI), Academy of Sciences of Czech Republic Řež,
- ŠKODA Nuclear Machinery in Plzeň.

This consortium is focused mostly on transmutations with liquid fuel on fluoride base (project SFINX). Since 1997 the main application research works at Department of Nuclear Reactors, FNSPE were focused on thorough preparation of behavioral modeling attestation of subcritical system with external source, which is a part of the national TRANSMUTATION project (project SFINX).

Under this research DNR closely co-operates with NRI Řež. In a close collaboration of the NRI Řež and at the DNR, FNSPE the irradiation experiment with module B417 in core B6 at the training reactor VR-1 were prepared and realized. Experiment with module B417 was intended to gain information on neutronic and physical characteristics of graphite and NaF, which are components of this module and will be probably a part of future TRANSMUTOR.

Module B417 consists of:

- aluminium cover (138x138x850 mm),
- graphite,
- main irradiation channel (aluminium cylinder \varnothing 48x3 mm),
- backward channel (aluminium cylinder \varnothing 35x3 mm),
- balance channel (aluminium cylinder \varnothing 35x3 mm).

Main balance channel and backward channel are placed in the graphite and main irradiation channel is placed in a void. Height of channels correspond to the length of the active part of the IRT-3M fuel element. Main irradiation channel and backward channel were completely filled by solid NaF in the shape of small cylinders. Balance channel was filled by NaF cylinders only in one-third of its height. In the centre of the NaF cylinders were made gaps for installations of activation wires. All channels are placed in aluminium covers. Aluminium cover can be hermetically sealed by thick top with quick stopper and so the top can be quickly removed.

Irradiation experiment with the module B417 took place at the training reactor VR-1 in June 2004. In the first step were put Cu wires into module B417 (in NaF cylinders, in

aluminium covers and in graphite) and then was module placed into the position F5,4 – G5,4 of the core B6. Core B6 contained:

- module B417,
- seven 6-tube fuel assemblies,
- seven 4-tube fuel assemblies,
- eight graphite two-blocks.

The critical state with the B4 core configuration was attained on June 1, 2004 at 10:00. Positions of control rods were: scram rods - up, first experimental rod - up, second experimental rod - 550, fine control rod - 362 and coarse control rod - 520 mm. The power of the reactor was 2E8. At this power modul B417 was irradiated half an hour.

Irradiated wires were analysed and we determined the thermal neutron flux density distribution in several positions in the module B417 (in the vertical direction of module). Experimental results were compared with calculated results.

References:

- [1] RATAJ, J. – KOLROS, A.– MATĚJKA, K: *Dílčí podklady pro řešení projektu BLANKA* KJR, FJFI, ČVUT, Praha, 2004
- [2] RATAJ, J. – MATĚJKA, K.: *Zpráva o průběhu ZKE se zónou B6* KJR, FJFI, ČVUT, Praha, 2003,
- [3] RATAJ, J. – MATĚJKA, K.: *Program ZKE se zónou B6* KJR, FJFI, ČVUT, Praha, 2003,

This research has been supported by MTI grant FT-TA/055

Delimitation of Fullerit Use Potential for Radiation Detector Manufacturing

V. Linhart, E. Belas*, J. Sodomka, B. Sopko*****

Vladimir.Linhart@utef.cvut.cz

Institute of Experimental and Applied Physics, Czech Technical University, Horská 3a/22,
128 00 Prague 2 - Albertov, Czech Republic

* Institute of Physics, Charles University, Ke Karlovu 5, 121 16 Prague 2, Czech Republic

** Department of Mechanics and Materials, Faculty of Transportation Sciences, Czech
Technical University, Na Florenci 25, 110 00 Prague 1, Czech Republic

*** Department of Physics, Faculty of Mechanical Engineering, Czech Technical University,
Technická 2, 166 27 Prague 6, Czech Republic

Research of a new type of semiconductor detector of ionization radiation is presented. This work describes the basic principles of semiconductor detectors and summarizes the current application of such devices. Fundamental information about fullerene-like materials, the potential reasons for the use of fullerit and our first results are given.

The basic principle of detection of ionization radiation by semiconductor detectors is based on collecting the charge resulting from ionization. This collection is possible only in the case, when the detector material is able to conduct the charge carriers (electrons and also holes). However, this detector material must have such a little amount of native charge carriers so that the ionized charge can be measured. The collection is enabled by an electric field created between electrodes situated on the crystal surface. The electrodes have three roles. First, to provide the collection field. Second, namely in the case of Schottky and P-N junction, to reduce the current streaming through the detector bulk. And third, to provide a connection with the electronics, which reads the collected charge. Consequently, the requirement for contact and material homogeneity, as well as for the little amount of native carriers, is crucial for the suitable performance of semiconductor detectors.

Silicon and germanium are semiconductors the most frequently used materials in radiation detector manufacture. Both materials can be produced with good homogeneity and with 100% charge collection efficiency. Other semiconductors, such as InP, GaAs, CdTe, CZT, etc, are continuously investigated, however without significant definite results.

Silicon surface barrier detectors are appropriate for detection of heavy charged particles (e.g. protons, alpha-particles, etc). With a thin film of a neutron sensitive material on their front side these devices can serve as neutron detector. Silicon lithium-drifted detectors are suitable for the precise X-ray and low-energy gamma spectroscopy. However, the use of these SiLi-detectors requires cooling down to liquid nitrogen temperatures.

High Purity Germanium (HPGe) detectors are suitable for precise gamma spectroscopy. Their disadvantage is, as for SiLi-detectors, the need for cooling to liquid nitrogen temperatures. Therefore, composed semiconductors (InP, GaAs, etc) are being developed as detectors which can be operated at room temperatures. However, these materials exhibit many defects, namely anti-site defects, causing very short life time of holes. This reality degrades their spectroscopic resolution. This problem can be solved by the discovery of a new material.

The fullerene is a macromolecule consisting of 60 or 70 carbon atoms arranged to form a sphere. The term fullerene is used in this work to denote the molecules which are

composed of 60 atoms of carbon. Fullerene molecules crystallize in the face centered cubic lattice. This crystal is called fullerit. The bonds between the molecules are mediated only by Van der Waals forces. Therefore, the fullerit is soft and brittle. The fullerit exhibits a low sublimation temperature which can be exploited to obtain millimeter-size single crystals by the vapor growth technique. Moreover, the fullerit is a semiconductor with a band-gap of 1.5 eV [1] which is greater than the band-gap of other semiconductors such as Si (1.124 eV), InP (1.344 eV), and GaAs (1.429 eV) [2,3].

The large band-gap of fullerit brings about a negligible amount of native carriers into the conduction band, and therefore, fullerit detectors would be able to operate under room temperature. Furthermore, a fullerit consists of identical molecules – fullerenes. This fact renders anti-site defects impossible, and consequently, an improved spectroscopic resolution is expected. Detector manufacturing from the fullerenes which are stuffed by atoms or molecules sensitive to indirect ionization radiation would permit production of detectors which are sensitive to any arbitrary radiation. If these ideas prove correct, the fullerit, as a new detection material from nanotechnology, would open new incalculable frontiers. The main aim of our project is to learn how to prepare macro-crystals out of fullerit, to verify if these crystals are suitable as radiation detector, to find out a way of metallization, and to prepare an application project submitted to an external grant agency.

Acquiring a fullerit macro-crystal is the first result of our project. The crystal was produced by the vapor growth technique by the following way: The fullerit pieces, no greater than 500 μm , were placed into a quartz tube with vacuum of 4×10^{-4} Pa. Before sealing the tube, the fullerit pieces were heated up in order that fullerit impurities are desorbed. After sealing, the 20 cm long tube was inserted into a horizontal furnace. One end of the tube, containing the fullerit pieces, was kept at 700°C. In the opposite end of the tube the macro-crystal of the fullerene was grown, the temperature kept at 660°C for several days. The macro-crystal produced has diameter 1 cm and length also about 1 cm.

Further evaluation of results is underway.

References:

- [1] DRESSELHAUS, M.S.; DRESSELHAUS, G.; EKLUND, P.C.: *Science of Fullerenes and Carbon Nanotubes*, University of Kentucky, 1995, ISBN 0-12-221820-5.
- [2] DARGYS, A.; KUNDROTAS, J.: *Handbook on Physical Properties of Ge, Si, GaAs, and InP*, Science and Encyclopedia Publisher, 1994, ISBN 5-420-01088-7.
- [3] DUBECKÝ, F.; ZAŤKO, B.; NEČAS, V.; SEKÁČOVÁ, M.; FORNARI, R.; GOMBIA, E.; BOHÁČEK, P.; KREMPASKÝ, M.; PELFER, P.G.: *Recent improvements in detection performance of radiation detector based on bulk semi-insulating InP*, Nuclear Instruments and Methods in Physics Research, 2002, Vol. A 487, pp. 27-32.

This research has been supported by CTU grant No. CTU0416951.

Use of TL in-vivo Dosimetry for Determination of Radiation Burden of Patients due to X-ray Examinations

L. Novák* **, L. Musílek*

leos.novak@suro.cz

*Department of Dosimetry and Application of Ionising Radiation, Faculty of Nuclear Sciences and Physical Engineering, Czech Technical University, Břehová 7, 115 19 Prague 1, Czech Republic

**National Radiation Protection Institute, Šrobárova 48, 100 00 Prague 10, Czech Republic

Diagnostic procedures using X-rays are the most common application of radiation in medicine. The amount of radiation received by the population during X-ray examinations can be expressed in terms of a collective dose. To quantify the collective dose, typical effective doses per X-ray procedures must be known. The effective doses for X-ray examinations range between several microsieverts and several millisieverts. Effective dose is a weighted-organ dose quantity and therefore can not be measured directly. To obtain a value of effective dose, it is essential to know absorbed doses in all radiosensitive organs. There are two approaches available to determine the organ doses for particular X-ray examination. The first approach is to use a simplified mathematical model of a human body and a Monte Carlo simulation of radiation transport through this mathematical phantom. The second approach is to use an anthropomorphic phantom loaded with appropriate detectors and irradiate it in the same way as a patient undergoing an X-ray examination. Thermoluminescent dosimeters (TLDs) as the detectors are most suitable for this purpose. This method can verify the Monte Carlo model and also allows assessing of organ and effective doses for very complex and difficult X-ray procedures such as interventional examinations, for which the computational models are not yet available. In this study organ and effective doses for four types of routine X-ray examinations were evaluated using the direct method with an anthropomorphic phantom and TLDs. The results were compared with two most widely used computational programs.

Before the phantom measurements, whole TLD system was optimized. Main problems in dosimetry in diagnostic radiology are very low doses applied to patients and also wide range of energies in the X-ray emission spectrum. Moreover, photon energies in a spectrum range usually between 20 kV – 120 kV; TL detectors show strong energy dependence in this energy range. To avoid too high uncertainty due to energy dependence and to detect doses in a microgray range, LiF:Mg,Cu,P as a TL material was chosen, because of its tissue equivalence and therefore very low energy dependence, and its very high sensitivity. This material has also excellent fading properties, its light sensitivity is negligible and annealing procedure is very simple. As a reader, manual TL system Harshaw 4500 with corresponding software Winrems was used to measure and evaluate the signal from TL dosimeters.

Before each irradiation-readout cycle an oven-annealing was performed. The TLDs were annealed at 240°C for 10 minutes and then they were rapidly cooled down to room temperature. After the first oven annealing, an individual background and individual sensitivity correction coefficients were assessed for each of the TLD. When corrected, readout values show differences $\pm 5\%$ (2 SD). After these initial experiments, energy and angular dependence of the TLDs were determined. If calibrated in the corresponding energy range (similar voltage and half-value layer), the energy dependence doesn't exceed $\pm 2\%$. Angular dependence doesn't exceed 5% if the orientation of a TLD in a measurement field matches the orientation in a calibration field. There were no need for fading correction during the experiments, because measurement and calibration dosimeters were annealed, irradiated and readout together in the same time. Calibration of the TLDs was performed against PTW

DIADOS electrometer and corresponding semiconductor detector with combined uncertainty 5% (2SD). Combined uncertainty of a dose assessment with TLDs is less than 10%.

To obtain absorbed doses to radiosensitive organs an anthropomorphic RANDO phantom loaded with 100 TLDs was used for each type of examination. The RANDO phantom consists of a bone, lung and soft tissue equivalent material and simulates a torso of a reference man. It is sectioned into 35 slices 2,5 cm thick. Holes of 5 mm in diameter are drilled in a 3 x 3 cm array in each slice. Correlation between a position of the radiosensitive organs in a human body and the holes in the slices of the phantom was made according to anatomical atlas of CT slices [1]. Exposures of the phantom were performed using a Chirana MP-15 X-ray unit. Standard X-ray examination of a chest (low and high voltage technique), head, and abdomen were simulated. Calibration of the TLDs in terms of air kerma was made at the same unit. In the energy range of radiation used in diagnostic radiology, air kerma and absorbed dose in air can be considered equal. To convert the dose in air to dose in tissue or dose to bone and bone marrow, dose in air was multiplied by a factor 1,06 or 1,1 respectively [2, 3].

The organ doses measured inside the phantom and corresponding effective doses were compared with doses obtained from two Monte Carlo based programs PCXMC and NRPB [3, 4]. Effective doses computed by the programs for lung examinations were 0,04 mSv for low voltage technique and 0,03 mSv for high voltage technique. TLD measurements indicated 0,06 mSv and 0,05 mSv respectively. For the head examination, effective doses were 0,06 mSv for PCXMC program, 0,03 mSv for NRPB program, and 0,07 mSv for TLD measurement. For the abdomen examination effective doses were 0,89 mSv for PCXMC program, 0,68 mSv for NRPB program, and 1,22 mSv for TLD measurement. The results from TLD measurements were systematically higher than the results from the computational models. The reason is an insufficient coverage of large organs (skin, bones) with TLDs. Because of a small number of TLDs, the dosimeters were placed only into organ parts with maximum dose. Quite good agreement was achieved in head examination, where coverage of the head region of the phantom with TLDs was satisfactory. The second reason for the discrepancies is a difference in an organ position in mathematical and anthropomorphic phantoms and a setting of X-ray field at the phantoms. To achieve a better agreement between the results, it is essential to perform the measurements with a greater number of TLDs and also compare the results also with other sources of available data.

References:

- [1] FLECKENSTEIN, P., TRANUM-JENSEN, J.: *Anatomy in diagnostic imaging* Blackwell Publishing, 2001, pp. 262–350.
- [2] TOIVONEN, M., ASCHAN, C., RANNIKKO, S., KARILA, K., SAVOLAINEN, S.: *Organ dose determinations of X-ray examinations using TL detectors for verification of computed doses* Radiat. Prot. Dos., Vol. 66, Nos. 1-4, 1996 pp. 289–294.
- [3] TAPIOVAARA, M., LAKKISTO, M., SERVOMAA, A.: *A PC-based Monte Carlo program for calculating patient doses in medical x-ray examinations* STUK-A139 1997
- [4] HART, D., JONES, D.G., WALL, B.F.: *Normalised Organ Doses for Medical X-Ray Examinations Calculated Using Monte Carlo Techniques* NRPB-SR262 1994

This research has been supported by CTU grant No. CTU0411414.

Determination of Neutron Spectrum in REGATA Irradiation Channels of IBR-2 Reactor

A. Kolros, K. Katovský, S. S. Pavlov*

kolros@troja.fjfi.cvut.cz

CTU, Faculty of Nuclear Sciences and Physical Engineering, Dept. of Nuclear Reactors
V Holešovičkách 2, 180 00 Prague 8, Czech Republic

*Joint Institute for Nuclear Research, Frank Laboratory of Neutron Physics, Department of
Neutron Activation Analysis, 141980 Dubna, RUSSIA

Instrumental neutron activation analysis (INAA) is a method used for the determination of elements in biomonitoring of the atmospheric deposition at the IBR-2 reactor in JINR Dubna. The comparative method is commonly used for the analysis of the deposits there. The principle of this method is simple, the accuracy depends on the preparation of suitable standards. The practical realization of the analysis can be difficult for multielement samples or in case of the epithermal INAA. The knowledge of a neutron spectrum can help in this situation or can raise the accuracy of the analysis. It is useful for quality assurance.

The IBR-2 is an experimental fast reactor working in a pulsed mode and reaching high density neutron flux in the core. Plutonium oxide is used as fuel. Liquid sodium is used as a moderator, wolfram as a reflector and light water as a coolant is. The cooling is forced. The thermal steady power is 2 MW, the thermal power in the pulse is 1500 MW. The width of the thermal neutron pulse is 320 μ s, the pulse frequency is 5 Hz. Maximal thermal neutron flux is $1 \times 10^{13} \text{ n.cm}^{-2} \cdot \text{s}^{-1}$, maximal fast neutron flux is $1.5 \times 10^{14} \text{ n.cm}^{-2} \cdot \text{s}^{-1}$.

REGATA is an experimental system used for INAA at the IBR-2 reactor. Regata contains four channels for the irradiation of samples, pneumatic transport system and gamaspectrometric systems for the measurement of activated samples. The neutron spectrum was evaluated only in channels CH1 and CH2. These channels are connected with a pneumatic transport system and they are cooled by air. The neutron flux inside the channels is lower than stated for the reactor. Maximal thermal neutron flux is $4.5 \times 10^{11} \text{ n.cm}^{-2} \cdot \text{s}^{-1}$, maximal epithermal neutron flux is $8 \times 10^{10} \text{ n.cm}^{-2} \cdot \text{s}^{-1}$, maximal fast neutron flux is $3 \times 10^{11} \text{ n.cm}^{-2} \cdot \text{s}^{-1}$. The temperature inside the channels is about 50 °C. The original covering of the channel CH1 was made a cadmium layer of thickness 1.5 mm in 1982.

A program SAND II was used for the calculation of neutron energy spectra. This program was developed by OAK RIDGE National Laboratory, Tennessee, USA. An iterative perturbation method was used to obtain a 'best fit' neutron flux spectrum for a given input set of infinitely dilute foil activities. The calculation procedure consists of a selection of known flux spectra forms to serve as an initial approximation to the solution, and subsequent iteration to a form acceptable as an appropriate solution. The solution is specified either as a time-integrated flux (fluence) for a pulsed environment or as a flux for a steady-state neutron environment. The SAND-II Data Library, distributed with a package, contains 40 types of foils and 3 covers. The simplifield version of SAND-II with 99 groups was used in this application [3]. The input neutron spectrum was taken from [1], [2].

Experimental determination of neutron energy distribution was performed by the activation analysis method. Two sets of foils, i.e. In, Cu, Mn, Au, Ni, Ti, Fe, Mg, Al, In+Cd, Cu+Cd, Mn+Cd, Au+Cd were prepared for the measurement. A set of 13 foils was irradiated in each channel. Each foil was inserted into an inner capsule of a polyethylene transport container and irradiated. The working regime for irradiation, decay and accumulation of gamma spectra of each foil was optimised. It depended on the weight and cross section of foil, half-life of decay and gamma emission of daughter nucleus, detection efficiency of gamma detector, etc.

The program VYNAKT was used for the calculation of irradiated foil activity, namely their reaction rate. This program was developed by FNSPE, the Department of Nuclear Reactors, in 2004. The input parameters are the time parameters of foils irradiation and foils measurement, reactor power, weight the foil, reaction type, material composition, foil thickness, etc. The data for the VYNAKT were extracted from the Reus-Westmeier Catalog [4], which is a compilation and evaluation of gamma-ray and other data related to the decay of all nuclides known from paper and electronic sources. Gamma energy and intensity of daughter nuclei are directly sought in the table.

A simple cadmium ratio of selected elements was calculated for both channels. The results obtained are 0.784 for reaction $^{55}\text{Mn}(n,g)$, 0.836 for $^{115}\text{In}(n,g)$, 0.857 for $^{197}\text{Au}(n,g)$, 0.629 for $^{63}\text{Cu}(n,g)$. Although the channel CH1 has its own cadmium covering, the values of cadmium ratio are lower than 1. It indicates the depletion of cadmium covering. The results obtained for channel CH2 without the covering are 0.203 for reaction $^{55}\text{Mn}(n,g)$, 0.350 for $^{115}\text{In}(n,g)$, 0.545 for $^{197}\text{Au}(n,g)$, 0.267 for $^{63}\text{Cu}(n,g)$. The ratio of CH2 is lower than the ratio of CH1. These results corresponded to our expectation.

The selected reactions (i.e. $^{46}\text{Ti}(n,p)$, $^{47}\text{Ti}(n,p)$, $^{48}\text{Ti}(n,p)$, $^{54}\text{Fe}(n,p)$, $^{56}\text{Fe}(n,p)$, $^{58}\text{Fe}(n,g)$, $^{58}\text{Ni}(n,p)$, $^{60}\text{Ni}(n,p)$, $^{197}\text{Au}(n,g)$, $^{27}\text{Al}(n,a)$, $^{24}\text{Mg}(n,p)$, $^{55}\text{Mn}(n,\gamma)$, $^{115}\text{In}(n,\gamma)$, $^{115}\text{In}(n,n')$, $^{115}\text{In}(n,2n)$, $^{197}\text{Au}(n,\gamma)$, $^{58}\text{Ni}(n,2n)$, $^{58}\text{Ni}(n,p)$, $^{60}\text{Ni}(n,p)$, $^{63}\text{Cu}(n,\gamma)$) were chosen for analysis by SAND-II program. The first precalculation indicated similar behaviour of neutron spectrum in irradiated channels as stated in [1], [2].

References:

- [1] FRONTASYEVA, M.V. - PAVLOV, S.S.: *Analytical Investigations at the IBR-2 reactor in Dubna* JINR E14-2000-177 2000 pp. č. 35-43.
- [2] PERESEDOROV, V.F. - ROGOV, A.D.: *Modelirovanie i analiz energeticeskich spektrov nejtronov dlja oblucatelnych kanalov reaktora IBR-2* Kratkije soobscenija OIJI No. 1 [75]-96, Dubna 1996, pp. č. 69-74.
- [3] MAREK, M.: *Implementace programu SANDII na počítače PC ÚJV 9451 R,D, ÚJV Řež u Prahy*, 1991
- [4] REUS, U. - WESTMEIER, W.: *Catalog of Gamma-Rays from radioactive Decay* Vol. 29, Springer Verlag, 2000

This research has been supported by MŠMT grant No. MSM 210000019.

Correction of Neutron Detection System

Dead Time

A. Kolros

kolros@troja.fjfi.cvut.cz

CTU, Faculty of Nuclear Sciences and Physical Engineering, Dept. of Nuclear Reactors
V Holešovičkách 2, 180 00 Prague 8, Czech Republic

The topics of neutron detection and detectors are related to the nuclear reactor specification of neutron field parameters (flux density, fluence, spectrum). Neutron gas detectors are mainly used in experiments. They allow us to obtain immediate information about the neutron field inside the reactor.

Generally, gas detectors take advantage of the fact that, when the ionizing particle passes through the detector contents, the gas filling is ionized. But neutrons are indirectly ionizing particles. The detection of neutrons comes from the fact that when neutrons pass through a suitable material, secondary charged particles are formed as a result of ionization. Therefore, the walls of the detector are covered with the B10 isotope or with the fission materials uranium, thorium, plutonium or else the detectors are filled with special gas, for example BF₃, ³He, ¹H.

The ionization chamber, proportional detector or corona detector are commonly used. If the response of the detector is proportional to the energy of impinged particles, we can say that the detector has spectrometric properties. The detector can be connected in the pulse or current mode. In the pulse mode, the number of pulses is proportional to the number of impinged particles. The reactor core is not only the source of neutrons, but also of gamma radiation. The sensitivity of neutron detectors is small, but not insignificant for gamma radiation. Due to this fact, by using the amplitude discrimination the neutron response can be distinguished from the detector noise and from the accompanying radiation which has small ionization compared to α particles or fission fragments. The setting of the gamma and neutron discrimination threshold is a delicate operation. In the current mode, the current response is measured. The size of it is proportional to the charge formed by ionization during a time unit. The current mode is advantageous at high rates of impinged particles when the individual pulses are overlapped. A compensated ionization chamber or a fission chamber combined with the Campbell method is used for discrimination of undesirable gamma.

Dead Time of the Detectors

The influence of dead time comes into effect with non-linearity of the detector response in dependence on the rate of impinged particles. Dead time of the detector is defined as a time interval τ that follows after each recorded pulse at the detector output and during which the detector is not able to respond to a next stimulus on the input. Two types of dead time are known. If within the time interval τ a new stimulus appears, which is not recorded on the output but leads to prolongation of dead time, it is called dead time of cumulative type. If the new stimulus does not affect the duration of dead time, it is dead time of non-cumulative type. The values of dead time are from one to tens μ s. Generally, dead time of detectors depends on dimensions, geometry, voltage, detector type, the rate and the kind of impinged particles

To measure detector dead time, a number of methods are used. The two-source method, the maximum rate method, the method based on statistical fluctuations of the measured rate, the method of the source with short half-life, the method of electronically forced dead time.

Dead Time of Detection Systems

Dead time is not only a matter of the detector. The measuring chain contains an amplifier, a discriminator, a high voltage supply, a single or a multichannel analyzer, a counter etc. Each of these parts is characterized by its own type and value of dead time. Resulting dead time of detection system is their combination. The way of hardware and software discrimination set-up plays an important role in dead time. Now, in practice it is better to determine the correlation coefficient rather than dead time. The dependence between the true interaction rate and the recorded count rate can be expressed by the correlation coefficient. This method is commonly used at the VR-1 reactor.

The fact that the system working in the current mode has not its own dead time is an advantage for determination of detection system dead time. The response of both detection systems is measured together. The VR-1 reactor can change the power within the range of 0.1 W - 5 kW. The response of the pulse system is directly compared with the compensation ionization chamber connected in the current mode, in which the negative influence of dead time is eliminated. If the reactor power is increased step by step we get a set of response values of the measured detector and the ionization chamber. It can be very well expressed by a 3rd degree polynomial. Due to the fact that for a low rate the influence of dead time is insignificant, the start rate must be lower than 500 s⁻¹.

Since for the low initial rate the correction needn't be done, it is possible to claim that the true rate is equal to the recorded rate. For each step it is possible calculate a true rate and correlation coefficient. This is a method of dead time calibration for the whole detection system. It can be applied to any other measurement. If we use the same set up of detection system, then we always get the right results. Its another advantage is that the range of measurement is wider. This method is not suitable for the systems containing Wilkinson A/D converter.

References:

- [1] KOLROS, A.: *Korekce mrtvé doby detekčního systému* Sborník rozšířených abstraktů, XXVI. Dny radiční ochrany. ČVUT v Praze, 2004, pp. 172-175. ISBN 80-01-03076-8.
- [2] MATĚJKA, K. - KOLROS, A. - KROPÍK, M. - SKLENKA, L.: *Reactor Physics Course at VR 1 Reactor* 1. ed. Praha: ČVUT, Fakulta jaderná a fyzikálně inženýrská, Katedra jaderných reaktorů, 2004, ISBN 80-01-03097-0
- [3] KNOLL, G.F.: *Radiation Detection and Measurement* John Wiley & Sons, Inc, New York, 2000 ISBN 0-471-07338-5

This research has been supported by MŠMT grant No. MSM 210000019.

Determination of Hafnium in Zircon by INAA on training reactor VR-1 Sparrow

R. Štaubr, A. Kolros, M. Vobecký*

kolros@troja.fjfi.cvut.cz

CTU, Faculty of Nuclear Sciences and Physical Engineering, Dept. of Nuclear Reactors
V Holešovičkách 2, 180 00 Prague 8, Czech Republic

*Academy of Sciences of the Czech Republic, Institute of Analytical Chemistry,
Videňská 1083, 142 20 Prague 4, Czech Republic

Zirconium, as an element is a metal, which is used in nuclear engineering as sheet of fuel elements. Hafnium is an undesirable admixture. The aim of this study was to determine the concentration of Hafnium in the mineral Zircon from different geological deposits. The name Zircon comes from the Arabic „zargun“, which is a derivative from a Persian „zar“ = gold and „gun“ = color. Zircon has been known since antiquity, but its first modern description was made by Werner (1783).

We obtained Zircons from mineralogical museum at Faculty of Natural Sciences at Charles University in Prague. Zircons from six places around the world were analysed in our laboratory. The sample called R1 is from the location Třebivlice-Posedice in the Czech Republic. Other samples, called „RR2-RR17“, are from the location around the world such as Mias Ural (RR2,RR3,RR4), Siam (RR5,RR6,RR7), Madagascar (RR8,RR9,RR10), Naéki-Japan (RR11,RR12,RR13,RR14) and Ceylon (RR15, RR16,RR17). For the determination of Hafnium in Zircons a short-term instrumental neutron activation analysis was used.

Facility and equipment

The activation was carried out in the core of the training nuclear reactor VR-1 Sparrow at Faculty of Nuclear Sciences and Physical Engineering of CTU in Prag. VR-1 is a small reactor and can operate at maximum power 5 kW ($2,5 \times 10^9$ n.cm⁻².s⁻¹). VR-1 Sparrow is a pool-type reactor with a 36 % enriched ²³⁵U metal fuel in Al-cladding. Maximum continuous operation time of VR-1 is 4 hours. The core is equipped with a number of irradiation positions. For a short term activation of examined samples, a vertical channel inside the core equipped with pneumatic irradiation system was used. The transfer time of a sample from the reactor core to the laboratory is approximately 3,5 s. The laboratory is equipped with high resolution gamma ray spectrometric system with a HPGe detector (FWHM 1,8 keV, rel. efficiency 25 %). Gamma-ray spectrum analysis and quantification were done using the software packages currently used at the laboratory (Canberra AccuSpecB, ND ASAP).

Measurement

Short-term irradiation mode of instrumental neutron activation analysis based on analytical response of gamma line 214,3 keV of short-lived radionuclide ^{179m}Hf (18,67s) was applied for determination of Hafnium in the mineral Zircon ZrSiO₄. Cross section σ_{capture} for the reaction ¹⁷⁸Hf(n, γ)^{179m}Hf is 52 barns. The optimal working regime was: irradiation in a neutron flux 1×10^9 n.cm⁻².s⁻¹ during 50 s, decay time 20 s, and accumulation of gamma-ray spectrum of induced radioactivity during 40 s. The elemental abundance of Hafnium was determined using the comparator mode (the net peak area of ^{178m}Hf in a sample is compared with the same net peak area of hafnium standard).

The sensitivity of non-destructive determination of Hafnium concentrations depends on the background level of the accumulated spectrum of the gamma emitted from the activation products of the other elemental components in the analysed sample, e.g. ^{28}Al , $^{165\text{m}}\text{Dy}$, $^{46\text{m}}\text{Sc}$, ^{239}U , ^{27}Mg , ^{56}Mn .

The level of gamma radiation was checked by external device and the dose rate of gamma on the surface of the most active sample was $70 \mu\text{Gy/h}$. Because the reactor core is small, the impact on reactivity was checked and a change of reactivity was lower than $+0,02 \beta_{\text{ef}}$.

Samples and standards

Cylindrical capsules of ultrapure high-pressure polyethylene (dia 1,6 cm, height 5,5cm) were used for the analysis. Samples of weight 0,1 - 2 g were sealed in pre-cleaned polyethylene bags. The Hafnium standard series were prepared in the form of solutions from pure stoichiometric Hafnium dioxide HfO_2 (specpure, Johnson-Matthey). Ten standards of different contents of Hafnium from 1 mg up to 24 mg were used for the analysis.

Results

Samples and standards were irradiated one by one (not together) at a constant neutron flux. For the detected peak area, dead time correction was made. Error in time of irradiation was < 2 s. Statistical error of net peak area is always $< 1\%$ (because of the criterium > 10000 counts in net peak area) except samples (RR16, RR17, RR18), were it is $< 2\%$. The results are underlined. First is the name of the sample, second its weight, third concentration of Hf [%] and fourth is the detection limit [$\mu\text{g/g}$]. (R1, 1966, 0.32, 14.66), (RR2, 1017.1, 0.57, 21.01), (RR3, 1063, 0.55, 20.98), (RR4, 575.6, 0.65, 27.57), (RR5, 568.3, 0.51, 25.18), (RR6, 729.1, 0.48, 21.54), (RR7, 517.8, 0.48, 32.30), (RR8, 560.7, 1.58, 50.62), (RR9, 878.2, 1.79, 46.69), (RR10, 832.5, 0.72, 37.04), (RR11, 638.6, 3.16, 69.71), (RR12, 690.9, 3.69, 76.33), (RR13, 175.6, 2.90, 132.71), (RR14, 102.6, 4.40, 151.11), (RR15, 349.5, 0.28, 30.19), (RR16, 235.6, 0.18, 50.49), (RR17, 92.9, 0.37, 61.68).

Conclusion

The results of the determination of Hafnium in Zircons by short-term INAA at VR-1 show, that Hafnium can be easily determined. Moreover, this application is to representative for short-term INAA, that will be included into a practice for students.

References:

- [1] KOLROS, A. – VOBECKÝ, M.: *Aplikace krátkodobé INAA na reaktoru nulového výkonu VR-1 VRABEC* Souhrn přednášek semináře Radioanalytické metody - IAA 02, 5. září 2002 Praha, Spektroskopická společnost J. M. Marci a Česká společnost chemická, rok, pp. č. strany–č. strany.
- [2] ŘANDA, Z.: *Nondestructive Neutron Activation Analysys of Mineral MATerials III* CAEC NIC Zbraslav, Prague, 1979.

This research has been supported by MŠMT grant No. MSM 210000019.

Innovation and Development of Basic Practical Exercises from Radiation Detection and Dosimetry

T. Čechák, J. Gerndt

cechak@fjfi.cvut.cz

Department of Dosimetry and Application of Ionising Radiation of FNSPE CTU, Břehová 7,
115 19 Prague 1.

Practical knowledge of properties of nuclear radiation and basic nuclear measuring techniques, application of nuclear radiation in analytical and solid state measurements and dosimetric measurements are the part of the Basic Practical Training and Advanced Practical Training in Detection and Dosimetry of Ionizing Radiation on the Department of Dosimetry and Application of Ionizing Radiation at the Faculty of Nuclear Science and Physical Engineering, CTU in Prague.

The training is practically oriented with a special emphasis on practical work with typical modules in nuclear spectroscopy instruments. The programme of the training includes practical exercises carried out individually, by the trainees under permanent supervision of the experienced staff members of the department. Good training facilities available and properly designed programme of the training should update knowledge, improve background and develop practical skills of the trainees in different areas of modern nuclear electronics.

There are primarily two laboratory courses at the Department of Dosimetry and Application of Ionizing Radiation. These labs are obligatory for all students of Nuclear Engineering and for students of newly opened branch of study Radiology in Medicine, too. In addition to students of our own university we welcome in our laboratories in special courses some students from other Czech and European universities, for example in ATHENS program- Advanced Technology Higher Education Network, Socrates. In the framework of this program the Course on Application of Ionizing Radiation is organised by our department for the foreign students mostly from France and Spain.

The programme of the training includes the following topics [1]:

- Principles of radiation detection, namely for α , β , X and γ rays.
- Characteristics of spectrometry systems based on gas filled, scintillation and semiconductor detectors.
- Dosimetry, personal dosimetry and radiation protection.
- Basics of application of X-rays in diagnostics of crystalline materials.

Because previous measuring instruments CAMAC in these laboratories was out of date, we asked grant to purchase new modern instruments, and to change and partially expand our laboratory workplaces.

List of required and already obtained instruments follows [2]:

Radon source RF 2000,
ORTEC Model TRUMP – PCI – 8 k (Multichannel Analyzer),
ORTEC Model 418A Universal Coincidence,
ISO-DEBYEFLEX 3003 – 60 kV X-Ray Equipment in table casing,
X-ray tubes: 9.365.70.13.08 c -DX-Cu 10x1-S 2000 W short anode,

9.365.76.13.08 c -DX-Co 10x1-S 1800 W short anode

3 pieces of each of following ORTEC instruments:

Mini Bin and Power Supply Model 4006,
2-kV Bias Voltage Supply Model 478,
5-kV Detector Bias Supply Model 659,
Amplifier and Timing SCA Model 590A,
Timer and Counter ORTEC Model 871,

Summary price of all is 1,585 kCZK and was paid from grant Nr. 2075Aa FRVS CR and 366 kCZK (VAT + transportation costs) from own department budget.

The new equipment made us possible to modernize the old experimental exercises and build new exercises e.g. radon measuring in environment, in preparation for example are $\beta - \gamma$ coincidence activity measuring and Bonner's sphere neutron spectrometer.

The course will introduce now the students to the experimental background, concerning the dosimetry, application of ionizing radiation and radionuclides in industry, medicine, etc. Depending on the mode of application, information is in most cases obtained through effects interaction ionizing radiation with matter. Detection and evaluation of radiation spectra can give the desired information about these effects.

The experiments give our students the chance to develop professional ability, both in performing a substantial experiment and in relating experiment to theory. Most students find these experiments more demanding and more satisfying than the short experiments of the Basic practical exercises. The experiments are described briefly in the Practical instructions on the www pages [3] under pass phrases 16ZPRA, 16PDDZ.

References:

- [1] KNOLL, G. F.: *Radiation Detection and Measurement*, John Wiley & Sons, New York, 1979
- [2] <http://www.ortec-online.com>
- [3] <http://www.fjfi.cvut.cz/DesktopDefault.aspx?ModuleId=569>

This research has been supported by grant Nr. 2075Aa of FRVS CR

Getting More Accurate Estimation of ^{222}Rn - Dose Obtained from Integral Measurement Using Continuale Shape of Volume Activity Analysis in Residential Area

A. Ridzиковá *, A. Froňka **, L. Moučka **

ridzikova@hotmail.com

* CTU, Faculty of Nuclear Sciences and Physical Engineering, Department of Dosimetry and Application of Ionizing Radiation, Czech Republic

** National Radiation Protection Institute, Prague, Czech Republic

Abstract

UNSCEAR reported that the effective doses due to inhalation of radon ^{222}Rn and its daughter nuclei account on average for about half of all natural sources of radiation. The dose absorbed in lungs tissue cannot be measured directly, but can be estimated. In the European countries and in the legislation of Czech Republic, for the estimation of effective dose the recommendation of ICRP 65 is used, which comes from epidemiological studies at Uranium mines [1]. In the annual report of the ICRP 65 for protection against Radon for general public at home are recommended conversion coefficient for the annual exposure to radon concentration and radon to exposure to effective dose. It is adequate use an equilibrium factor 0,4 and an occupancy of 7000 hours per year indoor home in the and the relationship between the annual exposure. radon concentration. In the present investigation, we will study the dose relevant factors in order to get a more accurate estimation of ^{222}Rn .

In our study, we have tried to establish, based on the analysis of 12 weekly continual measurements and 4 integral measurements in different seasons, which uncertainties enter into this estimation. We have decided to use the values from a bedroom, in average, the most from the whole yearly effective dose indoor take a person before sleeping (around 8 hours per day), when occurred intensively in bedroom. It is adequate to use an equilibrium factor 0,4 and an occupancy of 7000 hours per year for conversion coefficients recommended in the annual report ICRP. We have tried to estimate individual occupancy for each room based on analysis of 116 examined persons. The values of average occupancy in the bedroom is 2850 hours/year (approximately 2 weeks people use to spend outdoors), in the kitchen is 800 hours/year and in the living room 1400 hours/year. The total occupancy is 28 % lower than recommended. This accepted model does not included difference in age, gender, morphometry and physiological parameters of the respiratory tract, which can influence the dose. We have found, that for the more accurate estimate it is not sufficient to know only the weekly averaged value of concentration measured in one term, but also it is important to know the value of f and to estimate the real individual time of stay, when we do accept this approach for the dose estimation.

References:

- [1] ICRP PUBLICATION 65: *Protection Against Radon -222 at Home and Work*. Annals of the ICRP, Pergamon Press, Oxford, 1993

CTU0411514

Section 11

CHEMISTRY

Fate of Heavy Metals in Urban Freshwater Ecosystems

D. Komínková*, J. Nábělková*,

kominkova@lermo.cz

*CTU, Faculty of Civil Engineering, Laboratory of Ecological Risks in Urban Drainage,
Thákurova 7, 166 29, Prague

During the last few decades, anthropogenic activities have had negative consequences for the natural environment. This unfavorable impact also has been seen in aquatic ecosystems. Human activity has resulted in the increase of harmful substances which enter into aquatic ecosystems as wastewater. Heavy metals (HM) belong to the group of extraneous substances, which destroy the balance of water ecosystems and belong to the group of the most dangerous substances entering aquatic ecosystems. HM issues, their mobility in aquatic ecosystems and their toxicological impact on organisms is still not very well understood, especially in an environment where frequent and fast changes of conditions occur. This type of the environment is present especially in small urban streams, where the urban drainage significantly changes the flow, physical and chemical conditions of water (pH, conductivity, hardness, redox potential, concentration of nutrients and pollutants, etc.). These changes can lead to a remobilisation of pollutants from sediment back to water. Substances become easily bioavailable for aquatic organisms and through the food chain enter higher trophic levels. This paper is focused on the study of HM remobilisation possibilities and changes of distribution coefficients leading to remobilization as a result of changing conditions in stream caused by urban drainage. The paper also reports consequent changes of bioaccumulation coefficient for different species of benthos community, which seems to be the best indicator of aquatic community quality in small urban streams.

The study stream, the Botic creek, is the largest tributary of the Vltava River in Prague, capital of the Czech Republic. The stream is in study section impacted by two CSOs and one SSO. The quality of wastewater from the overflows is influenced by industry. Industrial plants participate especially in Cu and Zn contamination. The SSO contributes to stream pollution by high concentration of Pb.

The impact of most common changes in urban streams, as changes of pH, hardness, HM concentrations in medium, was studied in laboratory conditions as well as in field.

Laboratory experimentation is carried out by batch adsorption test based on EPA methodology (Page, 1999) and is focused on Cu, Zn and Pb, elements which are most dangerous in study environment. Preliminary results show different behavior of tested metals during experimentation. Divergence was observed already in equilibrium time (5 days for Cu, 10 days for Zn). An experimentation under conditions of highly risky metal concentrations in liquid phase (dosed concentrations 1mg/l- 30 mg/l, which can occur in stream in case of an ecological accident) has showed that however most of metal is bound from water to sediment during test, concentrations in water still remain in risky levels, higher then ecologically acceptable limits. It can be caused by limited amount of sediment sample taking for experiment, in which all adsorption positions have been occupied. Moreover, a small amount of other metals was released from solid phase to water during testing; Cu shows higher ability of expulsion than Zn. HM in solid phase after testing were analysed by a sequential extraction procedure according to Tessier. Differences between Cu and Zn binding behavior are evident.

Whereas Cu prefers binding into organic matter, Zn binds mainly in residual and carbonates fractions.

Differences in binding behavior of elements are very important for the biological availability of metals in aquatic ecosystem. This is especially important as several sediment-feeding macrobenthic organisms in polluted waters develop a large biomass and become thereby a major nutrient source for many organisms in higher trophical levels.

Conclusion

The fate of heavy metals in urban streams depends on changes caused by urban drainage. Frequent changes caused by entering wastewater into stream can evoke remobilization of HM from sediment, in some cases high concentration of one metal can expulse other metal from sediment and use free binding capacity instead of the originally present element (Cu show this ability very strong). Different binding behavior of HM is crucial for their bioavailability and consequently for there bioaccumulation to body tissue of aquatic organisms.

References:

- [1] PAGE, S.D. A KOL. *Understanding Variation in Partition Coefficient, K_d, Values*. US EPA, Office of Air and Radiation. EPA 402-R-99-004A. 2004

This research has been supported by GA 203/03/P044.

Radiation Removal of Lead from Aqueous Solutions in Presence of Solid Promoters

M. Pospíšil, V. Čuba*, B. Drtinová, J. Dolanský

milan.pospisil@fjfi.cvut.cz

CTU, Faculty of Nuclear Sciences and Physical Engineering, Břehová 7, 115 19 Prague 1, Czech Republic

*CTU, Centre for Radiochemistry and Radiation Chemistry, Břehová 7, 115 19 Prague 1, Czech Republic

The most heavy metals present predominantly in industrial wastewater in different concentration are usually toxic substances and even at trace level belong to the most dangerous contaminants for the human organism. Therefore, seeking for some effective and economically convenient methods of their removal from aqueous solutions seems to be one of the most actual tasks. Conventional chemical methods used for this purpose are not only complicated

(multistage processes) but also expensive and their efficiency is not often sufficient. As it has been shown in some papers, the radiation can be successfully used for the reduction of metal ions to insoluble, easily separable metallic form [1,2] or to the lower -less toxic oxidation state [3]. Because the metals or metal ions reduced to lower oxidation states by reducing products of water radiolysis (hydrated electrons and H atoms) may be reoxidized to the initial forms by hydroxyl radicals, the suitable scavenger of these radicals must be introduced to the system. From our earlier study dealing with removal of lead from aqueous solutions [2] and determination of optimum conditions of this process it follows that Na(K) formate appears to be more effective scavenger of OH radicals when compared with aliphatic alcohols which are also usually used for this purpose. Moreover, many other factors such as pH, initial concentration of salt, type and dose of applied radiation as well as the presence of different promoters may substantially affect not only kinetics and mechanism of elemental reactions but also the efficiency of the whole radiation process including the precipitation of metals.

This contribution presents the results of our preliminary experiments focused on the removal of lead from aqueous solutions containing some selected solid promoters and investigation of their influence on the radiation process under study. In the first series of experiments the typical sorbents namely zeolite in Na cycle, bentonite and active carbon differing in their specific surface areas were applied. The contact time with solution was 24 h. The non- deaerated or nitrogen bubbled solutions of lead nitrate with initial concentration of 100 mg /L containing 10^{-2} mol/L HCOONa with or without addition of different amount (0,125 – 0,5 mg/ ml) of sorbent were irradiated in sealed thin – glass ampoules by accelerated electrons of an average energy of 4,5 MeV from a high- frequency linear accelerator (dose rate of 0,5 kGy/s) at the doses ranging from 0,5 to 15 kGy. The irradiation of the samples with solid was performed under intensive stirring. The Fricke dosimeter was used for the dose estimation. After treatment the centrifugation (21 400 g) was used for the separation of the product – finely dispersed metallic particles precipitated from the solution and their portions adsorbed on the surface of solid in the case of irradiated heterogeneous starting systems. The changes in lead concentration were determined by means of atomic absorption spectroscopy with flame atomization with the error of ± 5 %. In addition to the above mentioned sorbents in the second series of experiments the promoters based on different oxides such as SiO₂, TiO₂, γ - Al₂O₃, CuO, NiO and Cu₂O with unified concentration of 0, 25 mg/ml under otherwise identical conditions were applied.

It was found that the amount of adsorbed ions increases in the sequence bentonite, active carbon, zeolite and this quantity appears to be independent of the magnitude of specific surface areas. In the same sequence increases the positive effect of promoter (compared with homogeneous system without addition of solid phase) expressed as radiation chemical yield $G(-Pb^{2+})$ or by degree of reduction achieved at given dose. In accordance with reductive mechanism of the process under study its efficiency may be substantially increased when the oxygen dissolved in solution is removed by preliminary bubbling with nitrogen. With increasing dose of irradiation the influence of both positive effects (presence of sorbent and deaeration) decreases.

Radiation adsorption removal of lead conducted with oxide promoters under identical conditions showed the best results with CuO, TiO₂ and Cu₂O oxides whereas the effect of SiO₂, NiO and γ - Al₂O₃ oxides was almost negligible. Very weak correlation between the amount of adsorbed ions and magnitude of positive effect has been found. Both these quantities appear to be significantly affected by the concentration of scavenger – HCOONa. The cuprous oxide probably directly acts in the mechanism of reaction so that 50 % reduction of Pb²⁺ ions may be attained without addition of scavenger.

References:

- [1] FUJITA, N. – MATSUURA, CH. - HIROISHI, D. - SAIGO, K.: *Radiation-induced Precipitation of Nickel Ion in Aqueous Solution Saturated with Hydrogen Gas*. Rad. Phys. Chem. 53, 1998, pp.603 - 609 .
- [2] POSPÍŠIL, M. - MÚČKA, V. - ČUBA, V. - SILBER, R. - HEJNOVÁ, P. - DOLANSKÝ, J.: *Removal of Selected Heavy Metals (Lead and Cadmium) from Aqueous Solutions Using Ionizing Radiation*. Proc. Sixth Internat. Symposium and Exhibition on Environmental Contamination in Central and Eastern Europe and the Commonwealth of Independent States, September 1 - 4 , 2003, Prague, Czech Republic, Abstracts p. 112.
- [3] PONOMAREV, A. V. - BLUDENKO, A. V. - MAKAROV, I. E. - PIKAEV, A. K. - KIM, D. K. - KIM, Y. - HAN, B.: *Combined Electron-beam and Adsorption Purification of Water from Mercury and Chromium Using Materials of Vegetable Origin as Sorbents*. Rad. Phys. Chem. 49, 1997, pp. 473- 476.

This research has been supported by GACR grant No. 104/04/P071.

Seasonal Variations in the Disinfection By-Products Precursor Profile of a Surface Water in Flaje Catchment

A. Grünwald, K. Slavíčková, M. Slavíček, B. Šťastný, R. Veselý

grunwald@fsv.cvut.cz

Department of Sanitary and Ecological Engineering, Faculty of Civil Engineering, Czech Technical University, Thákurova 7, 166, 29 Prague 6, Czech Republic

Natural organic matter (NOM) present in natural waters is a complex heterogeneous mixture composed of humic acids, fulvic acids, low molecular weight organic acids, carbohydrates, proteins and other compounds classes [1]. The understanding of dissolved organic matter properties, as a function of size is a crucial factor to determine NOM treatability.

NOM is considered to be the primary organic precursor to disinfection by-products (DBP) formation and it is present in nearly all natural waters. Today, the majority of DBP control strategies (e.g. enhanced coagulation, carbon adsorption and membrane filtration) focus on the removal of NOM from water prior to disinfectant/oxidant addition. In general, total organic carbon (TOC) removal is used as a criterion for effectiveness.

Extensive research has been conducted to understand NOM composition. Much of this research has relied on the fractionation of natural waters into operationally defined discrete fractions based on adsorption chromatography employing synthetic resins. However, questions have been raised about such isolation and fractionation techniques because NOM is cycled through large changes in pH (2 to 10), which may chemically alter its structure. Fractions isolated by adsorption chromatography have been characterized using a range of proximate and sophisticated spectroscopic techniques including pyrolysis GC/MS, C-NMR and IR/FTIR [2]. However, this kind of analysis may not be generally applicable because it is time consuming, expensive, and requires considerable operator expertise. NOM can also be characterized by nonspecific parameters e.g. DOC and UV₂₅₄ absorbance.

NOM found in water consists of both hydrophobic and hydrophilic components where the largest fraction is generally hydrophobic acids, which makes up approximately 50% of the dissolved organic carbon (DOC). These can be described as the aquatic acids (aliphatic carboxylic acids of 5 – 9 carbons), one- and two-ring aromatic carboxylic acids, one- and two-ring phenols and humic substances comprising of humic and fulvic acids. The hydrophilic fraction can contain polyfunctional organic acids and aliphatic acids of five or fewer carbons.

The humic substances are generally regarded as the main cause of natural colour and THM and HAA formation potential (PTHM, PHAAF). For example it has been reported that the hydrophobic fraction produced THM 51 $\mu\text{g}\cdot\text{mg}^{-1}$ DOC when compared to 21 $\mu\text{g}\cdot\text{mg}^{-1}$ DOC for the hydrophilic acid fraction [3].

Disinfection by-products (DBPs) are comprised of several organic compounds that are formed by reactions in water between chemical oxidants, NOM and bromide. Trihalomethanes (THMs) and haloacetic acids (HAAs) are the two major classes of DBPs commonly found in waters disinfected with chlorine. The presence of such DBPs in drinking water is undesirable because they are suspected to be toxic, carcinogenic, and mutagenic to humans if ingested over extended periods of time [4].

A sampling programme has been undertaken to investigate the nature and fate of natural organic matter (NOM) in the water from Rašeliník, Flájský Brook, Mackovský Brook and Radní Brook. Water samples were collected also from the reservoir Fláje inlet and after coagulation and filtration on the Meziboří Water Treatment Plant. Samples were taken each

month during the period 2002 – 2004. Changes in the dissolved organic carbon (DOC), COD, UV absorbance at 254 nm, specific UV absorbance SUVA, trihalomethane formation potential PTHM and halogenderivates of acetic acid formation potential PHAA were measured in all samples.

Based on the interpretation of results we conclude that the NOM was not the same for the different source waters. The results showed that there was an increase in the amount of THM and HAA precursors in autumn compared with winter, summer and spring. This corresponded with an increase in the NOM amount in all water sources.

References:

- [1] NYSTROM M., RUOHOMAKI K., KAIPIA L.: *Humic acid as a fouling agent in filtration*. Desalination 106, 1996, pp. 79 – 87.
- [2] KITIS M., KARANFIL T., KILDUFF J.E., WIGTON A.: *The reactivity of natural organic matter to disinfection by-products formation and its relation to specific ultraviolet absorbance*. Water Sci and Technol. 43, 2, 2001, pp. 9 – 16.
- [3] KRASNER S.W., CROUÉ J.P., BUFFLE J., PERDUE E.M.: *Three approaches for characterizing NOM*. J. Am. Water Works Assoc. 88, 6, 1996, pp. 66 - 79.
- [4] MINNEAR R.A., AMY G.L.: *Disinfection By-products in Water Treatment: The Chemistry of Their Formation and Control*. Lewis Publ. , 1996, pp. č. 21-24.

This work has been supported by grant GA ČR No. 103/02/0243, Project with the TU Dresden No 790111440, NAZV QD 1004 and MŠMT grant MSM J04/98:211100002.

Removal of Natural Organic Matters from Water

A. Grünwald, K. Slavičková, M. Slaviček, B. Šťastný, K. Vlčková

grunwald@fsv.cvut.cz

Departement of Sanitary and Ecological Engineering, Faculty of Civil Engineering, Czech Technical University, Thákurova 7, 166 29 Prague 6, Czech Republic

Natural organic matters (NOM) is a complex of organic compounds that occurs universally mainly in surface waters. The dominant fraction of aquatic NOM is comprised of humic substances, which are responsible for 40 – 80% of the dissolved organic carbon (DOC) in many surface waters. Yeah and Huang [1] have proposed that the organic in natural water are fractionated into humic acid, fulvic acid, hydrophilic acid a neutral fraction. The major functional groups present in humic acid are carboxylic acids, phenol acids, alcoholic hydroxyl groups, keto groups and quinonoid groups.

The range of NOM in water varies from water to water and seasonally. This consequently leads to variations in the reactivity of NOM with chemical disinfectants such as chlorine.

NOM affects potable water quality in many aspects. The following reasons explain why humic compounds must be removed from raw water:

- The yellow color of humic compounds is incompatible with the requirement that drinking water is colorless
- Humic compounds have a potential for bacterial regrowth
- When disinfectants are used in water treatment processes, they lead to the formation of toxic disinfection by-products like THM, HAA and other
- Humic compounds can form complexes with heavy metals present in water, as a consequence, they reach the consumer since they cannot be precipitated in the water treatment plant
- Humic compounds lower the efficiency of treatment processes.

NOM have several characteristics that influence on how they may be removed from water. First of all humic substances are large organic molecules that carry a negative charge. This gives them colloidal characteristics making them removable from water by coagulation and subsequent flock separation. The negative charge characteristic is also utilized when separating humic compounds from water by ion exchange.

Among the proposed methods for the control of disinfections by-products, advanced oxidation processes (AOP) deserve more study for potential applications in drinking water treatment. AOP. AOP can effectively mineralize many organic compounds and have become attractive for the control of organic compounds in water and also for the control of disinfections by-products precursors.

The UV/H₂O₂ process is an example of a homogenous AOP. Generally, the effectiveness of homogenous light – driven oxidation processes is associated with very reactive species, such as hydroxyl radicals which are generated in the reaction mixture by the direct photolysis of H₂O₂ under UV radiation [2].

Fenton reagents have also been used for degradation of NOM in water [3]. Reactions were pH sensitive, and acidic conditions were necessary for iron solubility.

This study was conducted to determine the effect of hydrogen peroxide, Fenton reagent, and permanganate and son chemical process on degradation of NOM in surface water in Fláje catchments. Specific work included the investigation of the effect of those process parameters

on the DOC removal, including the humic matter concentration, chemical dosage (H_2O_2 , Fenton reagent, KMnO_4) and reaction time. The role of granular activated carbon (GAC) and synthetic anionic exchange resin on the adsorption of NOM from surface water was investigated as well.

The optimum KMnO_4 dose was found to be $2,0 \text{ mg.l}^{-1}$ for the oxidation of NOM in this study. Under optimum conditions process achieved greater than 90% removal of DOC and UV_{254} absorbance.

References:

- [1] YEAH H.H., HUANG W.J.: *The efate of dissolved organics in water purification processes treating polluted raw water*. Water Sci. Tech. 27, 1993, 71 - 80.
- [2] WANG G.S., HSIEH S.T., HONG CH.S.: *Destruction of Humic Acid in Water by UV Light-Catalyzed Oxidation with Hydrogen Peroxide*. Water Res. 34, 2000, 15, 3882 - 3887.
- [3] LINDSEY M.E., TARR M.A.: *Quantitation of hydroxyl radical during Fenton oxidation following a single addition of iron and peroxide*. Chemosphere 41, 2000, 409 – 417.

This work has been supported by grant GA ĀR No. 103/02/0243, Project with the TU Dresden No 790111440, NAZV QD 1004 and MŠMT grant MSMJ04/98:211100002.

The Assessment of Mean Molecular Weight of Aldrich Humic Acid

K. Štamberg, P. Beneš

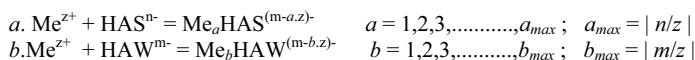
karel.stamberg@fjfi.cvut.cz

Department of Nuclear Chemistry, Faculty of Nuclear Science and Physical Engineering,
Czech Technical University, Břehová 7, 11519 Prague 1, Czech Republic

Many data and informations exist in the literature which support of macromolecular and polydisperse character of humic substances (HS). Depending on the type and origin of HS, on the way of their isolation and pretreatment or purification, their molecular weight was reported to lie in the range approx. from 10^2 to 10^5 dalton [1]. Using new techniques such AFFFF (Asymetrical Flow Field-Flow Fractionation, for size distribution) or TOF-SIMS (Time-of-Flight Secondary Ion Mass Spectrometry, for mass distribution) quite different results were obtained indicating that the mean molecular weight of HS can be much smaller, somewhere between 10^2 and 10^3 dalton. Earlier data were explained as due to an aggregation of individual molecules of HS [2].

With the aim to contribute to the knowledge of molecular weights of humic acids and the associated effects of metal complexation, we have used the MMWM (Mean Molecular Weight Model) model [3] and the experimental results of Eu - humic acid complexation study by dialysis and ion exchange methods [4] for assesment of mean molecular weight of Aldrich humic acid (*MHA*). The approach employed consisted in two steps: (1) the calculation of the abundance of Eu humate, %*EuHA*, as a function of *MHA* for pH 4 and 6 using MMWM model, (2) the comparison of the calculated results with experimental data expressed as %*EuHA* for pH 4 and 6 and deduction of the value of *MHA*.

In the case of MMWM, it is assumed that the complexation takes place at $\text{pH} < 8 - 8.5$, i.e., only with dissociated carboxylic groups of HA, namely with so called strong carboxylic groups (HAS^{n-} , more acidic) and so called weak carboxylic groups (HAW^{m-} , less acidic); this classification is based on the evaluation of titration curve of Aldrich HA [3]. In accordance with the results of electrophoretic measurements [3], the complexation reactions can be written:



If both the reactions occur simultaneously (probably above pH 4), then



$(\text{HAS}^{n-} + \text{HAW}^{m-})^{p-}$ denotes one mole of HA^{p-} with total charge $p- = n- + m-$ where $n-$ is contributed by dissociated carboxylic groups of type HAS and $m-$ by dissociated carboxylic groups of type HAW. Similarly, the sum $(\text{Me}_a\text{HAS}^{(n-a.z)-} + \text{Me}_b\text{HAW}^{(m-b.z)-})^{(p-a.z-b.z)-}$ denotes one mole of HA whose carboxylic groups HAS + HAW are occupied by cations $(a+b).\text{Me}^{z+}$. Polyanionic molecule HA^{p-} represents central ion in the complex formation, in contrast to the classical concept of complex formation where this role is played by a cation. The maximum values of stoichiometric coefficients, a_{\max} and b_{\max} , should correspond to the zero charge of the complex for given pH.

In the first step above mentioned, the abundances of individual species, i.e., Eu^{3+} , $\text{Eu}_a\text{HAS}^{(n-a,3)-}$, $\text{Eu}_b\text{HAW}^{(m-b,3)-}$, $(\text{Eu}_a\text{HAS}^{(n-a,3)-} + \text{Eu}_b\text{HAW}^{(m-b,3)-})^{(p-a,3-b,3)-} \equiv \text{EuHA}$, for different values of mean molecular weight of HA (*MHA*) were calculated as a function of pH. In the course of iteration calculations, it was also looked for the values of stoichiometric coefficients and for the values of corresponding stability constants. In addition, the charges of HA molecules for pH 4 and 6 as a function of *MHA* were computed.

In the second step, the mean molecular weight was assessed by comparison of the abundance of Eu humate, %*EuHA*, calculated by the MMWM model for pH 4 and 6 as a function of *MHA*, with experimental data obtained by dialysis and ion exchange [4] as %*EuHA* for the same values of pH, i.e., for pH 4 (%*EuHA* amounted to 35 %) and pH 6 (%*EuHA* amounted to 84.5 %). The comparison points to the values between approx. 0.6 kDa for pH 4 and 1.6 kDa for pH 6. This interval is in relatively good agreement with the measurements using the AFFFF and TOF-SIMS techniques [2] ($M_n = 0.445$ kDa; $M_w = 0.626$ kDa, size range = 0.150 – 3 kDa, where M_n is number-average molecular weight and M_w is weight-average molecular weight); simultaneously, the influence of pH on the slight aggregation of HA in the presence of Eu(III) can be deduced.

Linear dependences, calculated by means of MMWM model, exist between charge ($p\{-\}$) of HA molecules and *MHA*; naturally, the charge depends on pH. In the case of low values of the charge, i.e. if valency of the metal $z\{+\} > p\{-\}$, the formation of the larger entities type of Me_pHA_z can be expected.

References:

- [1] HAYES, M. B. (ED.): *Humic Substances II* John Wiley and Sons Ltd., 1989, pp. 449.
- [2] WOLF, M. - SZYM CZAK, W. - CHANEL, V. - BUCKAU, G.: *Molecular Size and Mass Distribution of Humic Substances Measured by AFFFF and TOF-SIMS* Second Technical Progress Report, FZKA 6969, Karlsruhe, 2004, pp. 95.
- [3] ŠTAMBERG, K. - BENEŠ, P. - MIZERA, J. - DOLANSKÝ, J. - VOPÁLKA, D. - CHALUPSKÁ, K.: *Modelling of Metal-Humate Complexation Based on the Mean Molecular Weight and Charge of Humic Substances: Application to Eu(III) Humate Complexation Using Ion Exchange* J.Radioanal.Nucl.Chem., Vol. 256, No. 2, 2003, pp. 329.
- [4] BENEŠ, P. - ŠTAMBERG, K. - MIZERA, J. - PROCHÁZKOVÁ, Š.: *Comparison of Dialysis, Electrophoresis, Ion Exchange and Ultrafiltration as Methods for Analysis of Complexation of Europium with Humic Acid* Second Technical Progress Report, FZKA 6969, Karlsruhe, 2004, pp. 265.

This research has been supported by MŠMT grant No. MSM 210000019.

Use of the Free-Liquid Electrophoresis for the Analysis of Thorium Complexation with Humic Acid at Low pH Values

P. Beněš

Petr.Benes@fjfi.cvut.cz

Department of Nuclear Chemistry, Faculty of Nuclear Science and Physical Engineering,
Czech Technical University, Břehová 7, 115 19 Praha 1, Czech Republic

Complexation with humic substances can significantly affect speciation, toxicity and migration of metals and radionuclides in the environment, therefore it has been extensively studied. In this paper, free-liquid electrophoresis [1] was used for the study of thorium complexation with Aldrich humic acid (HA) with the aim to test applicability of the method under difficult conditions (low thorium concentration, hydrolysis and large adsorption losses) and to obtain missing data on the complexation at low pH values.

Electrophoretic mobility u of thorium labelled with ^{234}Th was measured in aqueous solutions of 0.01M ($\text{HClO}_4 + \text{NaClO}_4$) as a function of pH (2-4), concentration of thorium ($[\text{Th}] \leq 10^{-7} - 10^{-5} \text{ M}$) and concentration of HA (0 – 10 mg/L). It was found that in the absence of HA the mobility ${}_+u$ towards cathode decreased with pH and decreasing $[\text{Th}]$. This was due to hydrolysis of Th^{4+} and formation of thorium pseudocolloids by adsorption of thorium ($[\text{Th}] \leq 10^{-6} \text{ M}$) on colloidal impurities ever present in solutions. The mobility towards anode ${}_ -u$ was negligible except for that of carrier-free ^{234}Th . Addition of HA caused decrease in ${}_+u$ and increase in ${}_ -u$ due to formation of negatively charged or neutral complexes ThHA.

Abundance of ThHA ($\%ThHA$) was calculated from the decrease of ${}_+u$ assuming that only mononuclear cationic forms of thorium (Th^{4+} and hydroxocomplexes) and neutral or negatively charged ThHA complexes were present. Therefore, cathodic mobility of 10^{-5} M Th in the absence of humic acid was used to represent mobility of the cationic forms. At lower concentration of thorium pseudocolloids exist and at higher concentration polynuclear hydroxocomplexes and colloidal hydroxide can be formed. Accuracy of determination of $\%ThHA$ depends on the value of $\%ThHA$ and on the adsorption of thorium prior to electrophoresis on the mixing vessel and during electrophoresis on the electrophoretic cell.

If $\%ThHA$ is close to 100%, the large adsorption can exert only minor effect on its value, which can be lowered due to a shift of equilibrium between ThHA complexes and cationic thorium species in favour of the latter, caused by the adsorption. Such effect was probably responsible for the lower values of $\%ThHA$ found in this work for 10^{-7} M Th . The accuracy of $\%ThHA$ values lower than about 90% is generally worse, mainly due to possible kinetic lability of ThHA complex, which can result in an apparent increase of calculated $\%ThHA$. For this and other reasons, $\%ThHA$ values lower than 90% found should be considered as maximum possible values for the given conditions.

The values of $\%ThHA$ obtained (see Table 1) indicated nearly complete binding of Th to ThHA complexes upon addition of 10 mg/L HA except for 10^{-5} M Th at pH 2 and 3, where significant effect of saturation of HA capacity for Th was found. Similar effect was observed with 10^{-7} M Th and 0.1 mg/L HA. In these two cases, however, the binding of thorium by HA exceeded capacity of dissociated carboxyl groups of HA thus pointing to at least partial displacement of H^+ ions from non-dissociated carboxyl groups.

Table 1 %ThHA as a function of pH and initial concentration of Th and HA

[Th] mol/L	[HA] mg/L	pH 2	pH 3	pH 4
10^{-7}	0.1	53.8 ± 10.0	90.3 ± 4.2	92.4 ± 1.9
10^{-7}	1.0	90.8 ± 1.8	95.2 ± 1.7	92.5 ± 3.2
10^{-7}	10	92.2 ± 0.8	89.3 ± 1.9	92.6 ± 2.5
10^{-6}	10	99.4 ± 0.6	97.4 ± 1.2	97.2 ± 2.4
10^{-5}	10	54.6 ± 2.5	89.4 ± 1.1	97.3 ± 1.2

The values of %ThHA obtained were used for calculation of the mean negative electrophoretic mobilities of ThHA complexes μ_{ThHA} from the corresponding values of μ of thorium found in the presence of humic acid. The calculated values of μ_{ThHA} can be considered as minimum possible values. They mostly increase with pH and decrease with [Th]/[HA] ratio (see Table 2). Surprisingly, complete charge neutralization of humic acid (and thus zero or positive mobility) was not found even in cases, when ThHA complexes were formed from a large excess of positively charged thorium ions over dissociated carboxyl groups of humic acid. This is important for the calculation of stability constants of ThHA complexes when the charge neutralization is often assumed.

Table 2 - μ_{ThHA} , in $10^{-4} \text{ cm}^2 \text{ s}^{-1} \text{ V}^{-1}$, as a function of pH and initial concentration of thorium and humic acid

[Th] mol/L	[HA] mg/L	pH 2	pH 3	pH 4
10^{-7}	0.1	0.74 ± 0.12	1.39 ± 0.11	2.21 ± 0.14
10^{-7}	1.0	1.31 ± 0.15	2.36 ± 0.27	2.52 ± 0.10
10^{-7}	10	1.43 ± 0.04	2.53 ± 0.10	2.25 ± 0.25
10^{-6}	10	1.26 ± 0.27	1.83 ± 0.07	2.72 ± 0.20
10^{-5}	10	0.87 ± 0.26	0.55 ± 0.08	0.69 ± 0.34

References:

- [1] BENEŠ, P. – MAJER, V.: *Trace Chemistry of Aqueous Solutions* Academia/Elsevier, 1980, pp. 41–44.

This research has been supported by the EC Commission under contract No. FIKW-CT-2001-00128 and by the grant No. MSM 210000019 of the Czech Ministry of Education.

The Modeling of Spectral and Photochemical Properties of Diimine Transition Metal Carbonyl Complexes.

J. Šebera*[^], S. Zálíš*^{*}, and A. Vlček, Jr.*^{^^}

sebera@jh-inst.cas.cz

* J. Heyrovský Institute of Physical Chemistry, Academy of Sciences of the Czech Republic, Dolejškova 3, CZ-182 23 Prague, Czech Republic

[^] Czech Technical University, Faculty of Nuclear Sciences and Physical Engineering, Department of Nuclear Chemistry, Břehová 7, Prague 1, Czech Republic, 115 19

^{^^} Department of Chemistry, Queen Mary, University of London, Mile End Road, London E1 4NS, United Kingdom

The flexibility of the coordination sphere of mixed valence carbonyl complexes enables to tune spectral and photochemical properties. The variety of excited states is illustrated on Ru, Re and W mixed ligand carbonyl complexes. The lowest excited states of $[\text{W}(\text{CO})_4\text{L}]$ and $[\text{W}(\text{CO})_5\text{L}']$ ($\text{L}=\text{N},\text{N}'$ -di-methyl-1,4-diazabutadiene, ethylenediamine, 2,2'-bipyridine, phenantroline; $\text{L}'=\text{pyridine}$, 4-CN-pyridine, piperidine) complexes were found to be either $\text{W} \rightarrow \pi^*(\text{L})$ or $\text{W} \rightarrow \pi^*(\text{CO})$ in character, depending on the type of the hetero-ligand. Within *trans*(X,X)- $[\text{Ru}(\text{X})_2(\text{CO})_2(\text{L})]$ ($X = \text{Cl}, \text{Br}, \text{I}$) and *fac*- $[\text{Re}(\text{X})(\text{CO})_3(\text{L})]$ ($X = \text{NCS}, \text{halide}$) complexes the lowest electronic transitions are identified as mixed $\text{X} \rightarrow \text{L}/\text{M} \rightarrow \text{L}$ ligand to ligand and metal to ligand charge transfer (XLCT/MLCT). In order to characterize how the particular lowest excited state reflects the coordination sphere variation, a combined experimental and theoretical study was performed. The interpretation and modeling of experimentally measured UV-VIS, emission, picosecond time-resolved IR and resonance Raman (rR) spectra is based on DFT calculations.

The ground-state electronic structures were calculated by density functional theory (DFT) method. The spectral transitions and charge density redistributions in the course of excitations were calculated by the time-dependent DFT (TD-DFT) method. Lowest excited states of the closed-shell complexes were optimized at TD-DFT level or unrestricted Kohn – Sham calculations on the lowest-lying triplet state. The electrostatic solvent influence on spectra was modeled using the polarizable - continuum model (PCM) or conductor - like screening model (COSMO). The interpretation of ground and excited state IR spectra was based on the vibration analysis at optimized structures. The calculations assigned the lowest lying transitions within all system studied, simulated ground and excited-state IR spectra correspond closely to the experimental spectra measured by ps-time-resolved IR spectroscopy.

Table 1. Wavenumbers (cm^{-1}) of ground- and excited state vibrations of $[\text{Re}(\text{NCS})(\text{CO})_3(\text{N},\text{N})]$ measured and calculated in a MeCN solution. Calculation: Turbomole, PBE0, COSMO calculated values scaled by a factor of 0.9445 to achieve a best correspondence between calculated and experimental values for the ground-state.

$[\text{Re}(\text{NCS})(\text{CO})_3(\text{R-DAB})]^a$				$[\text{Re}(\text{NCS})(\text{CO})_3(\text{bpy})]$			
GS		ES		GS		ES	
Calc.	Exp.	Calc.	Exp.	Calc.	Exp.	Calc.	Exp.
1919, A'(2)	1922	1956(CO)	1944	1911, A'(2)	1918	1952(CO)	1952
1927, A''	1922	1994(CO; A'')	1986	1914, A''	1918	2010(NCS+CO)	2002
2027, A'(1)	2027	2014(NCS+CO)	2045	2023, A'(1)	2026	2038(NCS+CO)	2041
2101(NCS)	2099	2036(NCS+CO)	2059 ^b	2104(NCS)	2097	2082(CO; A'')	2072

^a Measured for R = iPr, calculated for R = Me

^b Poorly resolved band, wavenumber determined by Gaussian fitting.

Table 1 shows the good correspondence between calculated and experimental vibration ground and excited state frequencies for $[\text{Re}(\text{NCS})(\text{CO})_3(\text{L})]$ complexes. It can be concluded that TD-DFT calculations well reproduce the electronic absorption spectra, ground- and excited-state provided that the solvent is included into the calculations and the excited state structure is optimized at the TD-DFT level.

References:

- [1] ZÁLIŠ S., FARRELL I. R. AND VLČEK A., JR.,: *The Involvement of Metal-to-CO Charge Transfer and Ligand-Field Excited States in the Spectroscopy and Photochemistry of Mixed-Ligand Metal Carbonyls. A Theoretical and Spectroscopic Study of $[\text{W}(\text{CO})_4(1,2\text{-Ethylenediamine})]$ and $[\text{W}(\text{CO})_4(\text{N},\text{N}'\text{-Bis-alkyl-1,4-diazabutadiene})]$* J. Am. Chem. Soc., Vol. 125, 2003, pp. 4580-4592.

This research has been supported by the Grant Agency of the Academy of Sciences of the Czech Republic (grant No. 1ET400400413).

Applicability Limitations of Hummel-Dreyer Method for Radionuclides-Humic Acids Equilibria Studies: Complexation of Cobalt(II), Europium(III) and Thorium(IV) with Aldrich Humic Acid

J.Dolanský, B.Drtínová, M.Cabalka, D.Vopálka, P.Beneš

dolansky@fjfi.cvut.cz

Department of Nuclear Chemistry, Faculty of Nuclear Sciences and Physical Engineering, Czech Technical University, Břehová 7, 115 19 Praha 1

One of the methods for studying metal-ligand complexation equilibria, Hummel–Dreyer method [1], has an unique advantage over the conventional static equilibrium methods in that metal ion concentration can be kept at a desired and predetermined value during the experiment so that metal complex and ligand are in dynamic equilibrium with “free” metal throughout the process of their separation. In gel chromatography, one advantage often cited says that separation is in an ideal case governed only by the size of molecules separated (size exclusion mechanism) and therefore the equilibrium is believed to be unperturbed by interactions with solid phase of the gel. Macromolecules should elute at void volume of column, low molecular weight species at total liquid volume.

This work summarizes our results on critical examination of an application of a gel chromatographic variant of Hummel – Dreyer method for studying of di- tri- and tetravalent metals complexation with humic acid, in continuation of our previous results presented on CTU WORKSHOPS [2,3]. In search of an efficient separation, four different columns were tested: Sephadex column G-15, Ultrahydrogel 120, Glycidyl-methacrylate column GMB 200, and TSK-GEL column G3000SWXL. Aldrich Humic Acid (AHA) was used as standard humic acid, europium, cobalt and thorium were chosen as models for important radionuclides present in nuclear waste. Mobile phase contained known concentrations of metals studied and pH and metal buffering medium (citrate for Co and Eu and carbonate for Th). Samples with a constant amount of AHA and various total metal content (internal standards) were injected, fractions collected and amount of Co and Eu in fractions determined by AAS/OES. In other series of experiments $^{152,154}\text{Eu}$ and ^{234}Th were used as radioactive tracers and activity of individual fractions was measured.

Conditions for the correct use of the method were evaluated, mainly for effective separation and equilibrium preservation. Results cast doubt upon the main advantage of the method – size exclusion mechanism of separation and equilibrium unperturbed by interaction of sample with gel. On all chromatographic columns studied elution volumes of low molecular weight metal species do not correspond to their molecular size. From the comparison of elution volumes with speciation calculations by program PHREEQC [3,4] it is concluded that the efficiency of the separation depends on the charge and concentration of low molecular weight forms (citrate and carbonate complexes prevail) because ionic exclusion takes place. In the case of Co and Eu choice of gel, buffer, pH, ionic strength and metal concentration enables finding of suitable conditions for the separation but drastically reduces the range of applicability of the method and enhances the uncertainty of interaction constants. The best separation was achieved at pH 5, $I = 0.01 - 0.1$ (NaClO_4), 0.001 mol/l citrate buffer and $5 \times 10^{-5} \text{ mol/l}$ total concentration of Eu or Co. In the case of Th suitable separation conditions were not found in any of columns tested. Another „non size-exclusion effect“ which take place is sorption of humic acid and metals on gel. A thorough estimation of uncertainty of $^{\text{K}}$ (CoAHA) determination revealed [4] that to the high standard relative

combined uncertainty (26%) mostly contributes the uncertainty of values of stability constants of Co-citrate complexes and the uncertainty of AHA concentration in sample (because of relatively high sorption of AHA on column, from 8 to 25%). In the case of thorium, 10 – 29% decrease of sample activity after passing through column was observed, evidently due to sorption and/or isotopic exchange.

Taking into account uncertainty of determination, the values of interaction constants obtained [3,4] are in fairly good agreement with results published by other authors and with results of our measurements [4] performed on the same samples of AHA by ion exchange and ultrafiltration methods. To achieve sufficient precision, readily measurable amount of metal-humic acid complex (MAHA) must be formed, corresponding to analytical method sensitivity. This way the sensitivity of analytical method also limits the range of applicable experimental conditions. The chromatographic method leads to sample dilution and larger concentrations of metal and AHA are necessary. Also solubility of AHA (and consequently the amount of AHA in sample) is limited and strongly pH dependent. Due to low sensitivity, AAS/OES determination of Eu in fractions is applicable only to larger (SEPHADEX, low pressure) columns. The problems may be overcome by use of radioactive tracers.

From our results, the following conclusions can be derived. The gel chromatographic variant of Hummel–Dreyer method gives results comparable (in terms of interaction constants) to other more frequently used methods, but some precautions must be taken. The effective separation of MAHA from low molecular weight metal species is a must. In search of separation conditions, speciation calculations proved to be a very useful tool. So called „non size-exclusion effects“ must be diminished and their contribution to the combined uncertainty of interaction constants values thoroughly calculated. Many experimentalist neglect the sorption of reaction components on gel, but sorption may constitute a very important factor, mainly in the case of metals of higher valency. One doubt remains concerning the accuracy of the method. The complexation reaction must reach equilibrium before the MAHA peak leaves the column. Fulfillment of this requirement is difficult to check, therefore the method may yield data only on the first rapid stage of complexation. It is evident that more kinetic data are necessary.

References:

- [1] HUMMEL, J.P. - DREYER, W.J.: *Measurement of Protein -Binding Phenomena by Gel Filtration*, Biochim. Biophys. Acta 63, 1962, pp. 530-532.
- [2] DRTINOVÁ, B. – DOLANSKÝ, J.: *High - Performance Gel Chromatography with Post - Column Reaction for the Determination of Europium in the Presence of Humic Acid*, CTU Reports, Volume 5, 2001, pp. 740-741.
- [3] CABALKA, M. – DRTINOVÁ, B - DOLANSKÝ, J. - VOPÁLKA, D.: *Study of Cobalt and Europium Interaction with Humic Acid by Gel Chromatography*, CTU Reports, Volume 7, 2003, pp. 858-859.
- [4] CABALKA, M.: *Metoda gelové chromatografie při studiu interakce kovů s huminovými látkami*, ČVUT, Fakulta jaderná a fyzikálně inženýrská, Katedra jaderné chemie, Disertační práce, 2004.

This research has been supported by MŠMT grant No. MSM 210000020.

Prospects of Study of the Radiation Corrosion in the Water/Carbon Steel Systems

S. Neufuss*, V. Čuba**, A. Vokál**, M. Pospíšil*, R. Silber*

neufuss@fjfi.cvut.cz

* CTU, Faculty of Nuclear Sciences and Physical Engineering, Department of Nuclear Chemistry, Břehová 7, 115 19 Prague 1

** CTU, Centre for Radiochemistry and Radiation Chemistry, Břehová 7, 115 19 Praha 1,

The study of corrosion in water/carbon steel systems has important impact on evaluating which materials are suitable for construction of containers for storage of spent nuclear fuel in deep repository. Containers present the most important barrier preventing leakage of spent nuclear fuel to the environment. It is supposed that spent nuclear fuel containers will be mainly constructed from carbon steel. It is necessary to consider the possibility of groundwater leaching into the container due to random defects or human mistakes. Oxygen dissolved in natural water will be consumed in reactions with organic compounds of soil. Thus, water reaching deep repository should be deoxygenated. Oxygen is main corrosive agent present in water. Nevertheless, even in deoxygenated water occur corrosion effects, especially when reinforced by some outer influence and specific environment. This is the case of deep repository environment. Ionizing radiation emitted by radionuclides present in spent nuclear fuel will cause radiolysis of water. It can certainly affect redox-potential of water. Highly reactive intermediate products of water radiolysis (radical and ion products $\cdot\text{OH}$, e_{aq}^- , $\text{H}\cdot$ and molecular products H_2O_2 , H_2) may cause corrosion effects despite the lack of oxygen. Some of these species are much stronger oxidizing agents than oxygen. Therefore, the study of radiation corrosion of carbon steel/deoxygenated water systems is important for safety precautions of deep repository.

The paper deals with some possibilities of experimental simulation of conditions in deep repository in the case of groundwater leaching into the spent nuclear fuel container. Proposed experiments consist of several steps:

- Preparation of deoxygenated water
- Chemical pre-treatment of steel samples
- Construction of corrosion cells
- Irradiation of samples
- Evaluation of effects of dose, dose rate and type of applied ionizing radiation
- Determination of corrosion products

Deoxygenated water was prepared in special box with overpressure of inert atmosphere. Large volume of distilled water was bubbled with nitrogen. Argon seems to be an ideal medium for these purposes, but nitrogen seems to have sufficient effect as well. The time of bubbling is dependent on volume of distilled water and gas pressure.

Steel tablets (size 3×1 cm, thickness 1mm) were treated in 1% solution of a hydrochloric acid to remove rust, oxygen and other contaminants from their surface. Tablets were treated for 1 hour. All operations were performed in the box under inner atmosphere.

Corrosion cells consist of glass ampoules with inserted steel tablet. Ampoules were completely filled with water. Corrosion cells were carefully closed so that oxygen diffusion during irradiation was kept at minimum level.

Prepared samples in corrosion cells were irradiated using radionuclide gamma-source ^{60}Co . Applied doses varied from 1 to 10 kGy. Progress of radiation corrosion in deoxygenated water was compared with corrosion progress in non-treated water so that effect of oxygen could be discerned. Thus, degree of corrosion caused by deoxygenated water radiolysis products was obtained.

It is possible to apply several physico-chemical methods for quantitative and qualitative analysis of the corrosion products (mainly Fe^{2+} and Fe^{3+}). Atomic absorption spectrometry may be utilized for determination of total ferric and ferrous ions concentration in solution. For analysis of steel tablet surface, roentgen micro-structural analysis can be employed, provided the layer of corrosion products on the surface of steel has sufficient thickness. UV/VIS spectrophotometry may be used for distinguishing between Fe^{2+} and Fe^{3+} ions.

Preliminary obtained results show that significant differences between radiation corrosion progress in deoxygenated and non-treated water exist. Even in deoxygenated water was observed significant concentration of corrosion products. The differences are probably caused by oxygen present in non-treated water. Based on preliminary results, detailed and more thorough study of corrosion effects in deoxygenated water/carbon steel system is necessary.

References:

- [1] NEUFUSS, S.: *Vliv záření na chování radionuklidů v okolí kontejnerů s vyhořelým palivem v hlubinném úložišti* rešeršní práce, 2004, 21 stran.
- [2] BRUNO, J.- CERA, E.- GRIVÉ, M.: *Experimental determination and chemical modelling of radiolytic processes at the spent fuel/water interface*, SKB TR-99-26, 1999, 7 stran.

Sorbents of Toxic Metals and Radionuclides Based on Immobilized Humic Acid and Chitosan

G. Mizerová, J. Mizera*, V. Machovič**, L. Borecká**

mizerova@fjfi.cvut.cz

Department of Nuclear Chemistry, Faculty of Nuclear Sciences and Physical Engineering,
Czech Technical University, Břehová 7, 115 19 Praha 1, Czech Republic

*Nuclear Physics Institute, Academy of Sciences of the Czech Republic,
250 68 Řež u Prahy, Czech Republic

**Institute of Rock Structure and Mechanics, Academy of Sciences of the Czech Republic,
V Holesovičkách 41, 182 09 Praha 8, Czech Republic

Low-rank coal, particularly postsedimentary oxidized coal (oxihumulite or leonardite) represents a potential low-cost sorbent of toxic metals and radionuclides for use in waste water treatment, groundwater remediation, and construction of active geochemical barriers. The sorption ability of coal is given primarily by oxygen functional groups (mainly carboxylic and phenolic) contained in humic substances (HS), natural polyelectrolytes immobilized in situ in coal matrix. Partial solubility, i.e. leaching of HS from coal, and insufficient mechanical stability of coal particles in neutral and alkaline solutions deteriorate their sorption ability especially at utilization for dynamic column operations. Chitosan (poly[(1⁻4)-β-D-glucosamine]) is a polysaccharide derived from chitin, a major component of the shells of crustacean organisms (crabs, shrimps), insects, and some fungi mycelia, the second most abundant biopolymer next to cellulose. Chitosan is produced from chitin by deacetylation with alkali. Among number of applications in various fields, chitosan has been considered to be a promising sorbent for removing heavy metals and radionuclides from polluted waters, and also as a prospective material in removal of HS from water by coagulation forming an insoluble complex. This research has been aimed to investigation of sorption properties of sorbents made by blending coal and chitosan.

Sorption of Cs, Co and Eu on coal in mixture with chitosan was studied as function of pH (~ 3 - 6). Coal samples - oxihumulite and its parent lignite (from the same seam) - originated from from the Sokolov Basin, Czech Republic. Samples were sieved to 0.3 - 0.5 mm, lignite was oxidized on air at 140°C for 200 hours to increase degree of oxygen functionalities. All samples were protonized by 1M HCl. Aldrich humic acid (purified, protonized, HA) was used as a reference sample. Chitosan (Fluka, highly viscous) was used as received.

Acidobasic properties of coal samples, chitosan and HA were studied by potentiometric titration. Titration curves reflected deprotonation of coal carboxyl and protonation of chitosan amino groups. A strong buffering action of chitosan at the neutral region was observed. Kinetics of HA adsorption on chitosan was studied by spectrophotometric determination of HA concentration (from absorbance at λ=254 nm) in solution of HA (20 mg/L) with chitosan added (1 g/L) at pH ~ 6.5. About 22 % HA was sorbed within the first hour, the sorption maximum of 37 % was reached after less than 10 hours. The chitosan covered with HA obtained under these conditions, dried, was characterized by the FTIR spectrum. The band at 1740 cm⁻¹ was assigned to C=O, 1636 cm⁻¹ to aromatic C=C, 1577 cm⁻¹ to COO⁻, 1463 and 1377 cm⁻¹ to aliphatic CH₃, CH₂ of HA. Chitosan showed C-O bonds at 1155, 1073, 1033 cm⁻¹, the amide I band of parent chitin at 1655 cm⁻¹ and the deformation N-H bands were merged in the aromatic C=C bonds of HA.

Batch sorption experiments using radiotracer method with ^{134}Cs , ^{60}Co , and ^{152}Eu were carried out under following conditions: $V=10$ mL, 100 mg of coal, 0 - 10 - 50 mg of chitosan, ionic strength $I = 0.1$, Cs, Co and Eu concentration of 2.9×10^{-5} , 2.7×10^{-5} , 1.9×10^{-6} mol L^{-1} respectively. After pH adjustment and 24 h shaking, centrifugation was applied to separate phases. Activities in solution were measured by γ -spectrometry.

Distribution coefficients K_d increasing in the order $\text{Cs} < \text{Co} < \text{Eu}$ reflected increasing charge of a cation and its increasing ability of complexation with HS. In acidic media, K_d s increased with pH due to dissociation of the carboxylic binding sites of HS. In neutral media, K_d s of Eu (for oxihumulite also Co) decreased with pH due to formation of soluble HS complexes.

An improved sorption efficiency of the coal sorbents at neutral pH was obtained in mixture with chitosan, namely for oxihumulite at sorption of Eu and Co. Addition of chitosan prevents deterioration of the sorption ability probably via removing the HS complexes from solution by formation of an insoluble complex $-\text{NH}_3^+ \dots -\text{OOC}-\text{R}$. Buffering capacity (acidobasic) of chitosan may have a positive effect as well.

References:

- [1] MASNEROVÁ, G. - MIZERA, J. - MACHOVIČ, V. - BORECKÁ, L.: *Oxidized Low-Rank Coals – In Situ Immobilized Humic Substances*. PRAGUE 2003, 6th International Symposium and Exhibition on Environmental Contamination in Central and Eastern Europe and the Commonwealth of Independent States, Florida State University and CTU, 2003, p.215
- [2] MASNEROVÁ, G. - MIZERA, J. - MACHOVIČ, V. - BORECKÁ, L.: *Oxidized Low-Rank Coals – In Situ Immobilized Humic Substances*. CTU Reports Vol.8 - Proceedings of Workshop 2004, Part B, 2004, pp. 782-783.
- [3] MASNEROVÁ, G. - MIZERA, J. - MACHOVIČ, V. - BORECKÁ, L.: *Sorbents of Toxic Metals Based on Low Rank Coal and Chitosan*. 56. sjezd chemických společností, Ostrava 6.-9.9.2004, 2004.

This research has been supported by CTU grant No. CTU0411114 and the grant A3111306 of the ASCR Grant Agency.

Utilization of Ionizing Radiation for Removal of Co(II) From Aqueous Solutions

Petr Kovařík*, Milan Pospíšil*, Václav Čuba**

Petr.Kovarik@fjfi.cvut.cz

*FJFI CTU, Department of Nuclear Chemistry, Břehová 7, Praha 1, 115 19

** Centre for Radiochemistry and Radiation Chemistry, Břehová 7, Praha 1, 115 19

Heavy metals contaminating predominantly industrial wastewater are potentially threatening for human health. Cobalt contaminates the environment from natural sources and the burning of coal or oil or the production of cobalt alloys. The general population is exposed to low concentrations of cobalt in air, water, and food. Cobalt has both beneficial and harmful effect on health. It is part of vitamin B12, which is essential for good health. At high levels of concentration, it may harm the lungs (respiratory sensitization, asthma), skin (allergic dermatitis) and heart. Presented paper deals with radiation reduction of cobalt ions from aqueous solutions using electron beam irradiation.

The principle of radiation reduction of heavy metals from aqueous solutions was described in many papers [1]. The system (water solution of specific metal) after irradiation contains particles of both oxidative (OH radicals are the most important), and reductive character. These particles originate from water radiolysis. It is necessary to decrease the concentration of OH radicals in solution due to possible reoxidation of reduced metal. For this purpose the scavengers of OH radicals are used. These scavengers may be aliphatic alcohols or organics species (potassium formate). After irradiation the reduced metal can be in less toxic soluble valence state ($\text{Cr}^{6+} \rightarrow \text{Cr}^{3+}$), and/or in form of insoluble solid ($\text{Co}^{2+} \rightarrow \text{Co}^0$). Reduced metal can be subsequently separated using filtration or centrifugation.

Performed experiments were aimed at study of water solutions of Co^{2+} (in form of nitrate). Solutions of different initial concentrations ranging from 10 mg/l to 200 mg/l of Co^{2+} were irradiated in sealed thin – glass ampoules by accelerated electrons from a high frequency linear accelerator (dose rates of 0.5 and 1 kGy s^{-1}). Doses ranging from 0.5 to 70 kGy were applied. After irradiation, the centrifugation (25 min; 5000 rpm) was used to separate the possible precipitate. After centrifugation, the atomic absorption spectroscopy with flame atomization was used to determine the concentration of Co^{2+} in solution.

The preliminary experiments show that cobalt can be reduced using the accelerated electrons irradiation. However, in comparison with lead reduction [2], it is necessary to apply higher doses of radiation to obtain desired effect. It was found out that without addition of substances scavenging OH radicals, degree of radiation reduction is virtually negligible due to mutual recombination of oxidizing and reducing products of water radiolysis. As the most convenient scavenger of OH radicals the potassium formate was used. Its standard concentration was $1 \cdot 10^{-2} \text{ mol dm}^{-3}$. Distilled water was used and the pH of irradiated solutions was not adjusted. The 90 % reduction was observed at the dose of 70 kGy if the initial concentration was 100 mg/l and concentration of potassium formate was $1 \cdot 10^{-2} \text{ mol dm}^{-3}$. The 99% reduction was found at the dose of 70 kGy if the initial concentration of Co^{2+} was 200 mg/l and the concentration of potassium formate was $1 \cdot 10^{-1} \text{ mol dm}^{-3}$. Obtained results show that the irradiation can decompose potassium formate at doses of 40 kGy and higher. Product of potassium formate decomposition may further contribute to reduction of Co^{2+} . When ethanol was used as OH radicals scavenger (concentration 1% Vol.) instead of potassium formate, higher doses of radiation are necessary for Co^{2+} reduction to desired degree.

References:

- [1] CHAYCHIAN, M. – AL-SHEIKHLY, M.– SILVERMAN, J., ET AL.: *The mechanism of removal of heavy metals from water by ionizing radiation* Radiat. Phys. Chem., 1998, Vol. 53, pp. 145 – 150.
- [2] POSPÍŠIL, M. - MŮČKA, V. - HEJNOVÁ, P. - SILBER, R. - DOLANSKÝ, J.: *Utilization of Ionizing Radiation for Removal of Some Toxic Heavy Metals from Aqueous Solutions* Proceedings of Workshop 2003 (online) [CD-ROM]. Prague: CTU, 2003, Vol. B, pp. 852 – 853.

This research has been supported by GAČR 104/04/P071.

Determination Methods of Selected Chemical Parametres of Water - Steel System Exposed to Ionizing Radiation

M. Buřata, V. Můčka, V. Čuba*, R. Silber

bunata@fjfi.cvut.cz

Department of Nuclear Chemistry, Faculty of Physical Engineering and Nuclear Science, Czech Technical University, Břehová 7, 115 19 Prague 1

*The Centre for Radiochemistry and Radiation Chemistry, Czech Technical University, Břehová 7, 115 19 Prague 1

There are two main sources of spent nuclear fuel Czech Republic, Dukovany and Temelin nuclear power plants. In the next sixty years, the state government is planning construction of a deep repository, where spent nuclear fuel would be stored in special containers at a depth of hundreds of meters underground. Safety system consists of several engineering barriers - dry container, a corrosion resistant envelope and a bentonite barrier. This complex system inhibits leakage of the radionuclides into the environment, so that no exceeding of the allowed contamination limits should occur. It is necessary to ensure a dry environment inside the container and to prevent possible corrosion of material. However, it is impossible to totally eliminate the possibility of container water contamination. Some material defects or human operator failure could occur, although the probability of this event is very low (about 10^{-3}). Due to presence of water, the corrosion of the container may occur. Moreover, ionizing radiation emitted by the radionuclides increases electrochemical potential (Eh) and changes the pH of the medium due to water radiolysis.

Processes running in the aforementioned system can be studied by determining some selected parameters, like the amount of solid corrosion products, the concentration of ferric and ferrous ions in the water solution, pH or Eh. Therefore, selection and verification of appropriate analytic methods is needed. These methods should be fast and simple to perform. In addition, the methods should be selective (e.g. differentiation between $\text{Fe}^{2+}/\text{Fe}^{3+}$ ions or between corrosive products), sufficiently responsive and applicable in a wide range of the studied values.

Two groups of the laboratory samples were used for the experiments. The first group consisted of the samples prepared from pure chemicals (e.g. solutions of ferric or ferrous salts). The second group consists of model samples. The model sample is steel tablet put into the glass ampoules filled with water under anoxic conditions. Samples were irradiated with various doses of gamma radiation. ^{60}Co radionuclide source was used for irradiation.

The concentration of the iron ions in the solution can be determined by UV/VIS spectrophotometry and atomic absorption spectrometry. Due to iron complexing reaction, the UV/VIS method allows the determination of ferric and ferrous ions in the same sample. By reaction with phenantrolin, ferrous ions create red complex ferrioin, which absorbs visible light of wavelength about 500 nm. Ferric ions absorbs in UV – range (about 300 nm). The actual experimental data showed that the detection limit of the iron determination was about 10^{-4} g.l^{-1} .

Atomic absorption spectrometry (AAS) is one of the most sensitive methods for determination of many metals. The lowest determination limit of iron is declared 10^{-7} g.l^{-1} . The instrumental equipment allows fast and reliable performance of measurement. Its only disadvantage is the impossibility of the separate determination of the different iron ions in the same sample. Using AAS, it is possible to determine just the total concentration of iron in

solution. This problem can be solved by a very fast separation of one form, followed by the determination of two parallel samples. This separation can be performed by the reaction of ferric ions with the cupferon complexing agent that results in the precipitation of iron complex. After ultrafiltration or centrifugation, the solution contains only the ferrous ions. In the case of the determination of more concentrate samples, the separation is better replaced by use of UV/VIS spectrophotometry, especially if the condition of the higher ferric-ions concentration applies. Both UV/VIS spectrophotometry and AAS were studied on the laboratory samples.

The main solid corrosive products are the ferric oxide Fe_2O_3 and the ferrous-ferric oxide Fe_3O_4 . These substances form mainly on the surface of steel. It is possible to determine them either directly on the steel tablet or separately after its complete displacement from the surface. An appropriate method for its determination is an X-ray microstructural analysis, provided the layer of corrosive products has sufficient thickness. Like AAS or UV/VIS spectrophotometry, X-ray microstructural analysis was studied on both groups of laboratory samples.

Activation analysis is a very effective, but difficult method. An irradiation of the steel tablet by thermal neutrons results in many nuclear reactions, one of which is $^{58}\text{Fe} (n,\gamma) ^{59}\text{Fe}$ (2.5 yrs) reaction. The ^{59}Fe isotope is well-specifiable by gamma-spectrometry. By an activity measurement of this isotope, information about an iron distribution in the system can be acquired (including adsorption on glass). However, this method has some disadvantages. It is necessary to use a neutron source emitting intensive neutron flow, or to irradiate the sample for a long time. Use of stronger neutron source (e.g. nuclear reactor) results in problems with open radionuclide transportation. Because of this, application of this method for purposes of presented study is in theoretical phase.

Four methods are applicable for the study of steel–water system exposed to ionizing radiation. By combination of these methods, it is possible to obtain the data required for studying the processes running in system. Combination of UV/VIS spectrophotometry and the atomic absorption spectrometry can determine the concentration of the ferric and ferrous ions in the water solution, the x-ray microstructural analysis is usable for the determination of solid corrosive products. The determination process can be carried out with the neutron activation analysis, whose results can give the information about distribution of iron in whole system.

References:

- [1] BRUNO, J. - CERA, E.- EKLUND, U-B. - ERIKSEN, T. - GRIVE, M. - SPAHIU, K.: *Experimental determination and chemical modelling of radiolytic processes at the spent fuel/water interface* SKB Report, TR-99-26, 1999, 7 pages
- [2] SHARLAND, S.M. - NEWTON, C.J.: *The long-term prediction of corrosion of stainless steel nuclear waste canisters* Mat. Res. Soc. Symp. Proc. Vol. 127, Berlin 1989, pp 123 - 129

Decontamination of Soils by Electrochemical Means

M. Němec*, J. John**

mojmir.nemec@fjfi.cvut.cz

*Department of Nuclear Chemistry, Faculty of Nuclear Sciences and Physical Engineering, Czech Technical University, Břehová 7, 115 19 Prague 1, Czech Republic

**Centre for Radichemistry nad Radiation Chemistry, Czech Technical University, Břehová 7, 115 19 Prague 1, Czech Republic

The operation or malfunctions of nuclear facilities and development or testing of nuclear weapons caused environmental contamination by fission nuclides at many places all over the world. Remediation and/or decontamination procedures are necessary for the restoration of the environment. The treatment processes for the contaminated soils can be divided into two categories. The first one is "in situ" decontamination and it is used mainly for remediation of large areas. The second category groups techniques for treatment of soil, that has been removed from its original location, in special treatment devices [1]. These techniques are used namely for high active soils from localized contaminations, such as those from the Jaslovské Bohunice nuclear power plant (NPP), where some leaks from liquid waste tanks occurred in 1977 and fission products, mainly ^{137}Cs , contaminated the neighbouring soil. Several decontamination procedures were described for treatment of such soils - classic leaching, soil fractionation, biological methods (e.g. phytoextraction), thermochemical, and electrochemical (electrokinetic or electrolytic) methods [1].

At the Czech Technical University in Prague, soil decontamination techniques have been studied for several years [2-4]. The leaching procedures (batch or "sorption" leaching) did not allow to achieve more than 30% caesium desorption from the soil [2]. Caesium thermodesorption was demonstrated not to be very efficient either; quantitative caesium separation could be achieved only from solutions resulting from fusion of the soil with special fluxes [2,3]. The most promising results were achieved by electrolytic decontamination.

In this method soil is electrolyzed very close to the anode in an acid electrolyte. The released caesium migrates to the cathode and it is available for the consequent separation. In preliminary experiments [4], more than 97% of caesium was released from soils contaminated long time ago. The aim of this study was to perform optimisation of the parameters of this method.

Electrochemical decontamination is a complex process, which is influenced by many parameters. For the process optimisation, some of them should be kept stationary, which is often not possible. This fact causes many difficulties in the determination of the influence of individual parameters and, of course, mechanism of the process. The main parameters of the process are: electric current and voltage, electrolyte composition and concentration, temperature, and, naturally, also type of the soil and caesium bonds inside it. The first part of the optimisation consisted of design and construction of a new electrolytic device, which allows continuous measurement, and recording and storing of the obtained electric data. Because the process runs at the constant electric current, corresponding voltage is measured by multimeter connected to the computer with a meter software. Released radiocaesium is separated in a column with inorganic ion exchanger based on potassium-nickel ferrocyanide. The electrolyte from the cathodic compartment is periodically pumped to the column located inside a NaI(Tl) scintillation detector, where the caesium cations are sorbed. After the equilibrium between ^{137}Cs and its daughter $^{137\text{m}}\text{Ba}$ (which is actually measured) is established,

the activity and the related yield of decontamination could be measured. The activity data are also stored in the computer.

In the experiment, it has been demonstrated that the new electrochemical cell allows better and faster decontamination and easier and more precise study of the process. The soil from the Jaslovské Bohunice NPP contaminated sites was electrolyzed in the ammonium phosphate and phosphoric acid mixed solution. The whole process took 22 hours in approximately 2 hour steps, a constant current of 1.5 A was applied. After this time more than 99% of the radiocaesium was separated from the soil, the total energy consumption was about 186 Wh/g. In the previous tests, maximum decontamination reached 97% after 38 hours of electrolysis at comparable conditions, the total energy consumption was 280 Wh/g. In agreement with the literature data, the process efficiency was found to strongly depend on the operating temperature, but this influence has not been tested in detail, yet.

Future experiments will test behaviour of the system at different currents (0.5, 1 A), different electrolytes (chlorides, nitrates, sulphates and others) and their concentration. All the processes will be tested at the same temperature, which requires partially different design of the electrolytic cell, the influence of the temperature will be determined separately.

The results obtained as yet demonstrate the efficiency, simplicity and speed of the proposed method. It is possible to release even very strongly bound caesium ions from the soil contaminated long time ago. However, further experiments and detailed testing will be necessary to scale the method up to industrial application.

References:

- [1] Anon.: *Technologies for Remediation of Radioactively Contaminated Sites*, IAEA TECDOC Series No. 1086, ISSN 1011-4289, IAEA Vienna, 1999.
- [2] M. NĚMEC, J. JOHN, J. REZBÁRIK, M. PRAŽSKÁ, P. SKŘEHOT: *Remediation of Soils Contaminated by 137Cs* In: Abstracts of the 10th International Conference SIS'03, Separation of Ionic Solutes 2003 (6.-11.September 2003), Podbanské, Comenius University, Bratislava, Slovakia 2003, p. 47-48.
- [3] P. SKŘEHOT, M. NĚMEC, J. JOHN: *Thermochemical Methods of Soil Decontamination* In: Proc. Prague 2003 - Sixth International Symposium and Exhibition on Environmental Contamination in Central and Eastern Europe and the Commonwealth of Independent States, Prague 2003 CD-ROM Edition, FSU, Tallahassee, FL, USA, , 2003, Paper No. 407 (6 pp.)
- [4] M. NĚMEC, J. JOHN, J. REZBÁRIK, M. PRAŽSKÁ: *Electrochemical Decontamination of Soils Debated by 137Cs* In: Proc. Prague 2003, Sixth International Symposium & Exhibition on Environmental Contamination in Central & Eastern Europe and the Commonwealth of Independent States, Prague 2003 CD-ROM Edition, FSU, Tallahassee, FL, USA, 2003, Paper No. 413 (5 pp.).

This research has been supported by CTU grant No. CTU 0411214.

Electron Beam Wastewater Treatment Up-flow Irradiation Device

R.Silber, V.Můčka, M.Pospíšil, V.Čuba*

Rostislav.Silber@fjfi.cvut.cz

CTU, Faculty of Nuclear Sciences and Physical Engineering, Dept of Nuclear Chemistry, Břehová 7, 115 19 Praha 1, *CTU, Centre for Radiochemistry and Radiation Chemistry, Břehová 7, 115 19 Praha 1

Removal of organic chlorinated compounds from wastewater and contaminated ground or drinking water is one of the most actual problems of water treatment technologies. Conventional treatment methods are not sufficiently efficient and radiation treatment represents promising alternative. Water radiolysis results in production of free radicals which interact with target molecules of pollutants. However, it is necessary to optimize radiation treatment technology for full – scale application, especially due to process efficiency and cost effectiveness.

Based on previous results (1,2), new experiments in the large volume pilot plant were performed. This pilot plant has been developed and constructed using experience with similar device used for radiation degradation of PCBs in alkaline 2-propanol (3).

The pilot plant was set-up to treat wastewater and other liquids. It enables to process liquids at a flow rate ranging from 0,2 to 2 m³ per hour with average dose 3 - 30 kGy per one throw-flow at maximum power of accelerator depending on flow rate or 0,3 to 3 kGy per one throw-flow at maximum flow rate depending on power of accelerator. Two vessels with capacity of 75 litres were used for storage and homogenisation of contaminated media and for storage of the irradiated liquid. Glass pump was used for homogenisation and for pumping of liquid through the irradiation device, specifically constructed for this purpose. The system allowed to collect samples of liquid medium before and after irradiation.

Irradiation may be carried out in two ways. One is the circulation arrangement, the other is one-way flow arrangement. In the first case liquid medium circulates within homogenisation vessel and the irradiation cell. Estimation of applied doses is based on time of circulation and power output of e-beam accelerator. During one-way flow arrangement medium flows under irradiation device between homogenisation and collection vessels and dose estimation is based on the flow rate and the power output of e-beam accelerator.

The linear pulse electron beam accelerator LINAC-4-1200 (TESLA V.T. Mikroel) was used as the source of electrons with mean energy 4,5 MeV. The current of the electrons can be regulated from 20 to 350 microamperes. Electron beam is scanned on area of 60 cm length and 2,5 cm width at frequency 50 Hz. Thickness of irradiated stream is 0,8 cm. Absorbed dose is evaluated using calorimetric system or acetate dosimetry.

Synthetic samples of contaminated drinking water and groundwater have been prepared by dilution of saturated C₂Cl₄, CHCl₃ and C₂H₂Cl₄ water solutions in distilled water (concentration range 10⁻⁴ – 10⁻³ mol.l⁻¹). Synthetic ground water has been prepared by the dissolution of nitrate, hydrogencarbonate and sulphate ions (10⁻³ mol.l⁻¹). Experiments were performed in the presence of oxygen in irradiated samples.

The efficiency of radiation treatment was verified using gas chromatographic analysis. CHROMPACK analyser (model CP 9002, ECD, DATA-APEX integrator) was

utilized. Amount of chloride ions generated by radiation degradation of chlorinated pollutants was determined electrochemically using selective chloride electrode.

In the circulation arrangement the dependence of pollutant degradation degree on dose was found. Obtained dose values were consequently used in the one-way flow-through arrangement. The maximum flow rate and maximum power of accelerator were used, one-way flow dose was 3 kGy.

Obtained data provide informations on scale-up effect of wastewater treatment for a commercial scale plant design and for economic feasibility studies concerning radiation treatment of wastewater.

References:

- [1] MÚČKA, V.-POLÁKOVÁ, D.-POSPÍŠIL, M.-SILBER, R.: *Dechlorination of chloroform in aqueous solution influenced by nitrate and hydrocarbonate ions* Radiat.Phys.Chem. 68, 2003, pp. 787–791.
- [2] MÚČKA, V.-LÍZALOVÁ, B.-POSPÍŠIL, M.-SILBER, R.-POLÁKOVÁ, D.-BARTONÍČEK, B.: *Radiation dechlorination of PCE in aqueous solution under various condition* Radiat.Phys.Chem. 67, 2003, pp. 539-544.
- [3] MÚČKA, V.-SILBER, R.-POSPÍŠIL, M.: *Electron beam degradation of PCE and large volume flow-trough equipment for radiation degradation of halogenated liquid organic compounds* Radiat.Phys.Chem. 55 1999 pp. 93-97.

This research has been supported by GA CR 104/02/1442.

Comparison of Sorption Properties of Malonamide-based Solid Extractants with the Behaviour of their Active Components in Liquid-Liquid Extraction

J. Šuláková*,**, Jan John*,**, F. Šebesta**

sulakova@fjfi.cvut.cz

*Centre for Radiochemistry and Radiation Chemistry, Czech Technical University in Prague, Břehová 7, 115 19 Prague 1, Czech Republic

**Department of Nuclear Chemistry, Faculty of Nuclear Sciences and Physical Engineering, Czech Technical University in Prague, Břehová 7, 115 19 Prague 1, Czech Republic

The nuclear wastes, produced by the reprocessing of spent nuclear fuel contain Long-Lived Radionuclides (LLR), essentially belonging to the family of the actinide elements (An), which induce important radiotoxicity for the long-term. These wastes are usually vitrified and supposed to be disposed off into deep geological repositories. Elimination of LLR from the vitrified wastes constitutes the Partitioning and Transmutation (P&T) strategy. (P&T) concerns the P – Partitioning of the actinides, which are contained in the nuclear wastes and the T – Transmutation of these actinides into short-lived or stable nuclides by nuclear means.

DIAMEX process, with malonamide compounds as extractants, is a tentatively tolerable process for chemical separation of minor actinides and lanthanides from high level liquid nuclear wastes issuing the reprocessing of spent nuclear fuels. For similar type of applications, novel composite solid extractants (SEX) / extraction chromatographic systems, with dimethyldibutyltetradecylmalonamide (DMDBDTMA–PAN) or dimethyldioctylhexyl oxyethylmalonamide (DMDOHEMA–PAN) as extractants and modified polyacrylonitrile (PAN) binding matrix, have been developed at the Czech Technical University in Prague [1]. The main advantage of the new SEX-based procedures is combination of the selectivity typical for liquid-liquid extraction with the simplicity of column arrangement.

A detailed study of sorption properties of the DMDBDTMA–PAN and DMDOHEMA–PAN solid extractants was performed. In the first phase, dependences of Eu, Am, Pu, and U weight distribution coefficients on all the DMDBDTMA–PAN and DMDOHEMA–PAN materials (prepared from solution of PAN in DMSO or from its solution in cc HNO₃) on nitric acid concentration have been determined. The experimental data have been correlated with the published data [2-4] on behaviour of DMDBDTMA and DMDOHEMA in liquid-liquid extraction.

It has been found that, in the nitric acid concentration range 2–8 mol/l, the behaviour of the solid extractants closely follows the behaviour of DMDBDTMA or DMDOHEMA in liquid-liquid extraction – for all the nuclides a sharp peak was observed on the dependence of D_g on nitric acid concentration at the HNO₃ concentration 6 mol/l. At this peak, the values of the distribution coefficients are $D_g(\text{Eu}) \approx D_g(\text{Am}) \sim 35$ ml/g, $D_g(\text{Pu}) \sim 17\,000$ ml/g, and $D_g(\text{U}) \sim 5\,000$ ml/g for DMDBDTMA–PAN material, and $D_g(\text{Eu}) \sim 50$ ml/g, $D_g(\text{Am}) \sim 100$ ml/g, $D_g(\text{Pu}) \sim 15\,000$ ml/g and $D_g(\text{U}) \sim 4\,700$ ml/g for DMDOHEMA–PAN material. All these values are significantly higher than the values that can be calculated from the published values of D using theoretical equation

$$D_g = D \cdot \frac{w_{org}}{\rho_{org}}$$

where w_{org} is the mass fraction of the extractant or its solution in the solid extractant and ρ_{org} is the density of the extractant or its solution. This fact is another argument in favour of the application of solid extractants with polyacrylonitrile binding matrix.

A comparison of the performance of the solid extractants prepared from solution of PAN in DMSO or from its solution in cc HNO_3 revealed that the behaviour of materials prepared by these two different procedures is almost identical in all the nitric acid concentration range for all the nuclides studied. The only exception to this rule was the behaviour of plutonium on the DMBTDMA–PAN absorbers, where the D_g values in the nitric acid concentration range 0.05–2 mol/l are significantly higher for the DMBTDMA–PAN(HNO_3) material than for the DMBTDMA–PAN(DMSO) one.

When comparing the performance of the DMBTDMA–PAN materials with the DMDOHEMA–PAN one, the following differences can be seen in the nitric acid concentration range 2–8 mol/l:

- for Eu and Am, the D_g values are generally higher for the DMDOHEMA–PAN material;
- while no Am / Eu separation is observed with the DMBTDMA–PAN material, Am / Eu separation factor $SF_{Am/Eu} \sim 2$ is achieved with DMDOHEMA–PAN;
- for DMBTDMA–PAN, the U and Pu D_g values are at first almost identical, with increasing nitric acid concentration no peak is observed for plutonium (contrary to uranium). For DMDOHEMA–PAN, the curves are almost parallel and $D_g(\text{Pu})$ are about 2.5 times higher than $D_g(\text{U})$.

When correlating the behaviour of the solid extractants with that of DMBTDMA or DMDOHEMA proper in liquid-liquid extraction at low nitric acid concentrations a rather unexpected finding was done. At nitric acid concentrations below 1 mol/l, the D_g values of all the nuclides sharply increase. Contrary to this, a steady decrease of D values with nitric acid concentration was reported even in this nitric acid concentration region for the liquid-liquid extraction system. Currently, the reason for this difference is unclear, more research will be needed to explain this effect.

References:

- [1] ŠEBESTA, F.: *Composite Absorbers Consisting of Inorganic Ion-Exchangers and Polyacrylonitrile Binding Matrix. I. Methods of Modification of Properties of Inorganic Ion-Exchangers for Application in Column Packed Beds*, J. Radioanal. Nucl. Chem., 220(1), 1997, pp. 77–78.
- [2] MADIC, C. – HUDSON, M.J.: *High-Level Liquid Waste Partitioning by Means of Completely Incinerable Extractants*, Report EUR 18038, 1998.
- [3] CHOPPIN, G.R. – KHANKHASAYEV, M.K. – PLENDL, H.S.: *Chemical Separation in Nuclear Waste Management. The state of the art and look to the future*, Florida State University, USA, 2002, p. 40.
- [4] NIGOND, L. – MUSIKAS, C. – CUIILLERDIER, C.: *Extraction by N,N,N',N'-tetraalkyl-2-alkylpropane-1,3 diamides. II. U(VI) and Pu(IV)*, Solvent Extraction and Ion Exchange, 12(2), 1994, pp. 297–323.

This research has been supported by European Commission Grant FI6W-CT-2003-508 854.

Elimination of Interfering Activities from Solid Phase Extractants in Radiochemical Neutron Activation Analysis of Biological and Environmental Samples

M. Lučaníková, J. Kučera*, F. Šebesta, J. John**

lucanikova@fjfi.cvut.cz

Department of Nuclear Chemistry, Faculty of Nuclear Sciences and Physical Engineering, Czech Technical University in Prague, Břehová 7, 115 19 Prague 1, Czech Republic

*Department of Nuclear Spectroscopy, Nuclear Physics Institute, Academy of Sciences of the Czech Republic, 250 68 Řež near Prague, Czech Republic

**Centre for Radiochemistry and Radiation Chemistry, Czech Technical University in Prague, Břehová 7, 115 19 Prague 1, Czech Republic

One of the crucial problems in determination of the majority of essential and toxic trace elements, such as As, Cd, Cr, Cu, Hg, I, Mo, Sb, Se, Si, V, etc. in biological and environmental materials by neutron activation analysis (NAA) is that overwhelming activities of namely ^{24}Na , ^{42}K and ^{82}Br are formed on neutron activation, which cause a high background in γ -ray spectrometry. Therefore, the interfering activities of ^{24}Na , ^{42}K and ^{82}Br are to be eliminated to enable determination of the above trace elements. Usually, the most efficient way of their elimination is radiochemical neutron activation analysis (RNAA). However, a relatively high retention of ^{24}Na , ^{42}K , ^{82}Br was found in the development of new RNAA procedures using composite materials – extraction agents embedded in the modified polyacrylonitrile matrix (solid phase extractants – SPE). The retention of ^{24}Na , ^{82}Br and ^{42}K in the polyacrylonitrile (PAN) matrix from real biological samples was 5.34 %, 1.53 % and 0.16 %, respectively, and it was therefore necessary to find a procedure for elimination of these activities, especially of ^{24}Na and ^{82}Br .

It was found that radio-sodium can be selectively and quantitatively ($> 99.9\%$) removed from solutions of dilute minerals acids resulting from decomposition of irradiated biological and environmental samples using a pre-treatment column filled with specifically tailored composite material prepared by incorporation of crystalline polyantimonic acid into the PAN matrix. This inorganic ion exchanger has an extremely high distribution coefficient for sodium ions in acid solutions ($D_g > 10^4$) and exhibits suitable capacity and hydrodynamic properties in column experiments when embedded into the inert PAN matrix. The breakthrough capacity for sodium ion was $5.58 \cdot 10^{-1} \text{ mmol} \cdot \text{g}^{-1}$ in $4\text{M H}_2\text{SO}_4$ at a flow rate of $0.3 \text{ mL} \cdot \text{min}^{-1}$. Thus, the proposed procedure of ^{24}Na elimination proved to be very simple and effective.

Elimination of radio-bromine appeared to be a more complex task, because of its occurrence as elemental bromine (Br_2) and ionic species (Br^- and BrO_3^-) after sample decomposition in a mixture of mineral acid. As it is known, BrO_3^- ion is a strong oxidant in acid medium and reacts with Br^- ion according to the reaction



Speciation of bromine was studied after sample decomposition in a mixture of $\text{HNO}_3 + \text{H}_2\text{SO}_4 + \text{HClO}_4$ at the final temperature of $\sim 250^\circ\text{C}$. The BrO_3^- ions were determined by iodometric titration, while the Br^- ions were determined by manganometric titration.

Since, the bromine concentrations are at the $\mu\text{g} \cdot \text{g}^{-1}$ or lower level in biological samples, the determination of bromine forms using common analytical techniques is not

feasible. Therefore, inactive Br^- and/or BrO_3^- species (in amounts of 400 mg of Br) were added to the biological samples before decomposition in model experiments. The residual concentrations of both ionic bromine species in solutions resulting from mineralisation of the samples were below 1 %, which was due to their conversion to volatile elementary bromine formed according to the aforementioned reaction. This was obvious also from discolouring of the originally yellow colour of the solution. The BrO_3^- species were observed in the analysed solutions even in the case they were not added to the sample, apparently due to oxidation of elementary bromine or Br^- ions directly to BrO_3^- ions.

The main attention was paid to finding the most effective way of elimination of the undesired retention of radio-bromine on the PAN-based SPE in column experiments. For this purpose, different compositions of the feed solutions and different elution modes were tested. The retention of various forms of bromine was investigated with appropriate tracers prepared by irradiation of Br^- and BrO_3^- salts by neutron activation in VVR-15 nuclear reactor of the Nuclear Research Institute Řež, plc. for 2 hours in quartz sealed vials, at a thermal neutron fluence rate of $2\text{--}3 \cdot 10^{13} \text{ cm}^{-2} \cdot \text{s}^{-1}$. For column experiments, a glass column with a 1 cm diameter and a 5 cm bed height was used; it was filled with 0.2 g of SPE. 5 mL fractions of the feed solutions containing the radiotracers of $^{82}\text{Br}^-$ and/or $^{82}\text{BrO}_3^-$ and inactive carriers of Br^- and/or BrO_3^- in concentrations of $0.1 \text{ mol} \cdot \text{L}^{-1}$ were passed through the column at a flow rate of 0.3 mL min^{-1} . Then the activity of ^{82}Br in 5 mL fractions of the effluents or in the SPE material were counted in 30 mL polyethylene vials using a coaxial HPGe detector with a relative efficiency of 53 % and FWHM resolution of 1.8 keV. Significantly higher retention (by factor of 3) was observed for BrO_3^- species in comparison with Br^- species. The lowest radio-bromine retention ($\sim 11 \%$) was obtained when the feed solution contained $0.1 \text{ mol} \cdot \text{L}^{-1}$ concentration of KBr. Bromine elimination could be further improved by washing the SPE after sorption with a solution of 1M H_2SO_4 containing either 0.1M KBr or 0.1M KBrO_3 or a mixture of 0.1M KBr and 0.1M KBrO_3 . Of these procedures, the best elimination of radio-bromine was obtained by washing of SPE with the solution of 1M H_2SO_4 containing 0.1M KBr [1]. In this way, the majority of radio-bromine species were eluted, resulting in decontamination factor of the order $1.1 \cdot 10^3$. This favourably high decontamination factor appeared to be important not only for reducing the background in gamma-ray spectrometry in RNAA, but it also prevented deterioration of extraction properties of SPE due to oxidation of the extraction agents with elementary bromine and/or bromate species.

This proposed procedure for elimination of radio-bromine also helped to suppress the retention of radio-potassium on SPE by the action of potassium ions in both the feed and washing solutions.

References:

- [1] LUČAŇÍKOVÁ, J. – KUČERA, J. – JOHN, J.– ŠEBESTA, F.: *Eliminácie záchytu bromu na pevnom extraktante s polyakrylonitrilovou maticou*, Chem. Listy, 2004, 754.

This research has been supported by GA ČR grant No. GA 203/04/0943.

Implantation of Nitrogen Ions into the Nickel Oxide Catalyst

V. Můčka*, F. Černý**, B. Sopko**, V. Čuba*,***, D. Tischler**, M. Buňata*, D. Koblíha*

viliam.mucka@fjfi.cvut.cz

* Faculty of Nuclear Sciences and Physical Engineering, Břehová 7, 115 19 Praha 1, Czech Republic

** Faculty of Mechanical Engineering, Technická 4, 166 07 Praha 6, Czech Republic

*** Centre for Radio- and Radiation Chemistry, Břehová 7, 115 19 Praha 1, Czech Republic

Most of reactions utilized in industry are created by heterogeneous catalytic reactions in which various catalysts (precious metals, oxides or sulfides of transition metals, silica, zeolites, etc.) are used. Their properties determine, in such a way, the economic convenience of the processes. Hence, optimizations of the catalysts are needed. The irradiation of the catalysts prior to their use represents an alternative possibility how to optimize their catalytic properties [1]. A special method, used for this purpose, seems to be the implantation of various ions into the surface of the solid phase. This method enables to affect the optical, semiconducting [2], scintillation [3] or catalytic properties of the solids.

The objective of this study was to investigate the influence of implantation of nitrogen ions into the surface of nickel oxide on its catalytic activity. On that score, the commercial nickel oxide (Merck, analytical grade), with a particle size higher than 0.1 mm, was introduced into the stainless steel cage with the mesh size of 0.1 mm. The whole cage was incorporated into the chamber of implantation equipment. The N_2^+ - and N^+ -ions (in the ratio 3:1, the energy of 90 keV and the whole ion current of 1.5 mA) were implanted into the nickel oxide under the vacuum of 3×10^{-3} Pa during a rotation of the cage (30 rotations per 1 minute) for the time period of 2 h. The implanted sample (about of 0.2 g) was introduced into the chemical reactor containing of 20 mL of 1.2 M dm^{-3} hydrogen peroxide aqueous solution. The kinetic of the hydrogen peroxide decomposition at four different temperatures ranging from 25 to 40 °C was investigated by means of measuring of the rates of oxygen evolution at every temperature and constant pressure. The untreated nickel oxide was tested, of course, under the same conditions. Both rate constant and the apparent activation energy was used for description of kinetic of hydrogen peroxide decomposition (estimated with average errors of ± 4 and ± 5 %, respectively). Specific surface areas of both non-treated and implanted samples were measured by low-temperature adsorption of nitrogen. The obtained results give evidence that the decomposition of hydrogen peroxide proceeds, under the given conditions, as a pseudo first-order process on both non-treated and treated samples. The average values of the rate constants, apparent activation energies as well as of relative changes in these quantities, obtained from six independent measurements, are given in the following Table.

Table

Rate constants k_m [$L g^{-1} min^{-1}$] at different temperatures T [$^{\circ}C$], apparent activation energies E_a [$kJ mol^{-1}$] prior (A) and after (B) implantation and their relative changes Δ [%]

Sample	A	B	AB
T	$k_m \times 10^2$		Δ
25	3.4	4.5	30.6
30	4.8	6.1	27.8
35	7.4	9.1	22.5
40	12.7	14.8	16.6
E_a	67.8	61.9	8.7

An increase in the rate constants due to the implantation is obvious from the Table. The increase falls sharply from the values of 30 % up to the 16 % with increasing temperature of the reaction. In contrast to it, no changes were found in the apparent activation energies of the reaction in the range of insecurity of the measurements. No changes were observed as well in the surface area values. Based on the results obtained in this paper it may be assumed that the surface concentrations of the catalytic sites increase after the implantation. The rise seems not to be accompanied by any changes in the efficiency of the catalytic sites. May be that some charge defects create on the surface of the implanted oxide and they disappear at higher temperature of the test reaction. Nevertheless, the created sites seem to be relatively stable at room temperature in air because no changes in the catalytic activity of the treated samples were observed during the storage of the implanted samples in air at room temperature for the time period of five days.

Systematic studies will be performed in this field in future. The attention will be focused first of all on the dependence of implantation effect on the dose of ion-irradiation, the energies of the implanted ions and, last but not least, on the qualitative character of the solids as well as of the implanted ions.

References:

- [1] MÚČKA, V.: *Vliv ionizujícího záření na katalyzátory heterogenních katalytických reakcí*. Pokroky chemie Academia, Praha, 1986, pp. 83.
- [2] BORANY, J. – HEERA, V. - HELM, M. - JAEGER, H. U. - MOELLER, W. (EDS.): *Annual Report* Forschungszentrum Rossendorf, Institute of Ion Beam Physics and Materials, 2003, pp. 127.
- [3] PEJCHAL, J. – BOHACEK, P. - NIKL, M. - MUCKA, V. - POSPISIL, M. - KOBAYASHI, M. - USUKI, Y.: *Radiation Damage of Doubly Doped PbWO₄:(Mo, A3+) scintillator* Radiation Measurements, vol. 38, 2004, 385–388.

Section 12

BIOMEDICAL ENGINEERING

Biomechanics of Treatment of Children Axial Skeleton Deformities

J. Čulík

culik@ubmi.cvut.cz

Institute of Biomedical Engineering, Sítná 3105, 272 01 Kladno, Czech rep.

The non skeletal children spine scoliosis (deformation of chest curve) is usual treated by corrective braces. The brace pushes on child trunk and has a force effect on spine. If the brace is used for a long time the pathologic spine curve it corrected. The brace is worked individually for each patient at this manner: the first is made a plaster negative and then a positive form of child trunk. The orthotic according to his and orthopaedist experience deeps the plaster positive form at the place where the brace has to push on the child trunk. The plastic brace is then made according to this plaster form. The brace after its application pushes at the places, where the form has been deepened (the small shoe principle). The paper shows the computer aid system of brace form design and treatment course prognosis.

The brace has a force effect on patient body surface and the result is stress state in the spine and a spine deformation which corrected a pathologic form of spinal curve. The behaviour between brace force and spine deformation and stress state is calculated with help the finite element method. It was supposed that the vertebrae bodies have no deformations and soft tissue is elastic. The potential energy was calculated only for the inter-vertebrae discs and ligaments and for the pressed soft tissue region of the trunk. The inertia moment has to be determined for inter-vertebrae disc and ligament cross-sections. The cross-section is divided to triangles and the third parts of areas for each triangle are concentrated to its side centres. Because it is no deformation between vertebrae centre and inter-vertebrae disc boulder, the central spine line is at this part straight. The finite element method is applied as 3D problem for the frontal and sagittal plane and torsion effect.

The parameters of node deformation are the 3 displacements and the 3 rotation at vertebrae centres. The finite element is the spine part between the neighbouring vertebrae centres. The element stiffness matrix is derived for inter-vertebrae disc and ligaments only and then it is recalculated for vertebrae centres because the deformation at vertebra part has a lineal course. The influence of trunk soft tissue is considered as an elastic ground. A brace form brings the trunk surface displacements. The potential energy of system is calculated for inter-vertebrae discs and ligaments (vertebrae are stiff and have no deformation) and for compressed trunk soft tissue part. The brace pushes at a child trunk at the place, where the plaster positive form has been deepened; it means that the trunk surface (surface of soft tissue) has at these places the non-zero prescribed displacements. The system is loaded by trunk surface displacement which is given by brace form.

The pathologic spinal curve is measured on the X-ray. The bought ends of spinal curve are connected by line and the places and values of spinal curve extremes are measured. The spinal curve is approximated between extremes by cubic polynomials (the polynomial is given by value and zero derivations at bought sides) and by quadratic polynomial at the start and finish parts (the polynomial is given by zero value at boulder side and non-zero value and zero derivation at inner part). The X-ray of spine can be made for patient with a brace and then the brace effect can be observed.

The two algorithms were implemented on computer:

1st algorithm - The input values are trunk surface displacements given by brace form (the thick of the layer which was deepened from plaster positive form of child trunk) and pathologic spinal curve measured from X-ray. The results are displacements and rotations at vertebrae centres (spine deformation - correction of pathologic spine state) and the spine stress state. The results are calculated with help the finite element method. The algorithm is used if the brace is made and its influence on spinal curve is checked.

2nd algorithm - The input values are X-rays without and with brace. The difference between the spinal curves without and with brace effect is spine deformation (spinal curve correction). The stiffness matrix of the finite element method is the same as at the 1st algorithm but the given values are spine deformation and result values are trunk surface displacement (brace form). The algorithm is used if the brace is made, we have the X-ray patient with brace and the brace influence is checked. The aim of treatment is ideal spinal curve, it is optimal if the spinal curve with brace is near this ideal curve. If the ideal spinal curve is set for spinal curve with brace to the 2nd algorithm the ideal brace form is obtained.

The remodelling of spine curvature depends on the spinal stress state, time of brace application and type of spinal defect according to King and Moe. The orthopaedist measures the lumbar and thoracic angles, the angles between tangents at points of spinal curve where it change its curvature. The second aim of the program is computer prognosis of treatment course. The program algorithm considers that the lumbar and thoracic angles correction is neceptual constant in time. The spinal correction is given by exponential function

$$\alpha(t) = \alpha_0 k^t$$

The spinal curves are divided according to King to five types. Parameter k can be determined statistical for King's curve type or precisely if the X-ray of the patient spine is made in time t_1 and the angle value $\alpha(t_1)$ is known, then the parameter k can be determined. If the further values of lumbar or thoracic angles are known the treatment course (angle α) can be approximated by the other function.

The results from algorithms of treatment prognosis were verified with treatment course of real patients and the values of parameters were judged for variable types of spinal curves and stress state intensities.

References:

- [1] ČULÍK, J. – MAŘÍK, I.: *Spine Stress State Under Brace Effect and Scoliosis Treatment Computer Simulation*. Journal of Musculoskeletal & Neuronal Interaction, vol. 4, n. 2, June 2004, International Society of Musculoskeletal and Neuronal Interaction 2004, pp. 214 - 215.
- [2] ČULÍK, J. – MAŘÍK, I.: *Computer Solving of Spine Deformation*. Proceeding Engineering Mechanics 2004, Czech Academy of Sciency, Technical University of Brno 2004, pp. 65 - 66.
- [3] ČULÍK, J. – MAŘÍK, I. - ČERNÝ, P. - ZUBINA, P.: *PC Simulation of Scolioses Treatment by Bracing*. Journal of Musculoskeletal & Neuronal Interaction, vol 2, n. 4, June 2002 2002, pp. 388 - 389.

Modelling of Influence of Tracheal Gas Insufflation on Artificial Lung Ventilation

V. Kopelent * **, K. Vališová***, K. Roubík**

kopelev@fel.cvut.cz

* Department of Radioelectronics, Faculty of Electrical Engineering, CTU in Prague, Technická 2, 166 27, Prague 6, CR

** Institute of Biomedical Engineering, CTU in Prague, Sítná 3105, 272 02 36 Kladno 2, CR

*** Department of Fluid Mechanics, Faculty of Civil Engineering, CTU in Prague, Technická 3, 166 27, Prague 6, CR

The great break is occurring in the medicine in last years. The goal of each intervention is to be safe for a patient and it must be maximal effective. Therefore many interventions are going to be improved. These changes could not miss artificial lung ventilation.

One example can be introduction of the high frequency ventilation (HFV) into the clinical practice. HFV does not follow physiological ventilation parameters as the conventional ventilation (CV). Tidal volume and breathing frequency belong between physiological ventilation parameters. HFV uses tidal volumes, which are the same or less than dead space in the respiratory system and the breathing frequency is one hundred times greater than volumes used in CV.

Protective ventilatory methods are gradually introduced into the clinical practice. Therefore it is necessary to design model of the respiratory system for finding optimal ventilation strategy. The mathematical modelling is one method, which can get some answers on many questions about the artificial lung ventilation. Present models can not be used, because they are based on conventional mechanisms of a gas transport, but unconventional methods are based on different principles. It was written before.

This work is based on Jongh's model [1]. The Jongh's model simplifies the lung structure. The lungs are substituted by using a divergent tube with non-linear growing diameter. Model parameters follow real anatomical structure of the lungs [2]. Jongh's model does not respect some physical laws and therefore had to be modified. One law which is not respected was the tidal volume which is whole delivered to the end of the respiratory system. This is not possible in the real world. Tracheal gas insufflation is implemented into repaired model as a source of the ventilatory mixture. The model outputs are compared with another model and also with an animal experiment. The other modelling approach is based on electro-acoustic analogy. This approach does not allow description of gases concentrations during artificial ventilation, but permits simulation of pressure amplitude and the tidal volume distribution in the lung structure. The model based on Jongh's model has a good agreement with an animal experiment and with the model based on the electro acoustic analogy. This model is the first, which permitted simulation of the behaviour of the respiratory system during conventional and unconventional ventilation regime.

The described model still contains a lot of simplifications. For that reason it must be known contribution of each gas transport mechanism to remove these simplifications. Therefore was designed a unique mechanical model which allows simulation of a patient breathing. The model is consisted of a mechanism, which is powered by stepping motor. This motor substitutes a work of the breathing. Four pistons are fixed in the mechanism and they are filled by a contrast liquid. The lung structure is substituted by a glass model. The glass model contains the first three lung generations, which are made in ratio proportionally the real lung structure. The glass model is placed into a water reservoir, because visual representation

in the air is very complicated. Therefore all breathing parameters are recalculated for visual representation at water using a Womersley and a Reynolds number. The fresh ventilatory mixture is modelled as water marked by ink. The breathing frequency was set accordingly to air Womersley number. The water reservoir is illuminated from the bottom. A camera is perpendicularly situated to the upper part.

The glass model is captured by a camera for whole time of the simulation. It is very big benefit, that captured data (simulation results) for different simulation can be very easily compared with each other. This property was used for a comparison of a gas flow in the glass model and in a straight pipe. The straight pipe has the same mechanical parameters as the zero generation of the glass model (the trachea). Two cases of model simulation will be described in the following part of the text.

The first case is a simulation, where the glass model is placed into the reservoir. Marked water by ink is presented in the system before an entrance to the model. Marked water was delivered to the end of the glass model after two breathing cycles. The way through the glass model is 33 centimetres long from the glass model entrance. The second case of this experiment is a simulation made on a straight pipe with the same mechanical parameters as the generation zero in the glass model. There are set the same ventilatory parameters as for the first simulation. Marked water did not get to the end of the pipe. Marked water reached only 22 centimetres from the entrance of the pipe. The distance 22 centimetres was reached at the end of the inspiration phase. The tidal volume at the end of expiration was situated at the pipe beginning. This result is very different from the first case, where the tidal volume moved to the next lung generation, deeply into the lung structure.

It is evident that bifurcations play very significant role in a gas transport in the respiration system. This effect can not be caused by a change of cross-sectional area of the glass model, because the cross-sectional area grows with a higher generation. If the cross-sectional area is decreased with higher generation, the distance reached by tidal volume will be higher. It means that the gas gets deeply into the lung structure. The cross-sectional area grows in the real lung structure and this shows that the whirls presented at the bifurcations play a very significant role in the gas transport.

Therefore it is necessary to involve modelling whirl's effect into design of the model of the gas transport. This effect can not be described in a one-dimension; therefore it is needed to make at least a two-dimensional model. The presented work showed a reason of the whirls presented at the bifurcations. There is a very big motivation, because the final model will be widely used in the clinical practice. Some doctors could suggest optimal ventilatory parameters for every patient. The model will get some results, which can explain a transport of the ventilatory mixture. These data are impossible to get by measuring on a human being.

References:

- [1] JONGH, DE F.H.C.: *Ventilation modelling of the human lung*. Delft, Delft university of technology, 1995, pp. 197. ISBN 90-5623-014-X.
- [2] BURRI P.H. ET AL.: *Ultra structure and Morphometry of the Human lung*. Ann. Thorac. Surg., 2000, pp. 31-49.

This research has been supported by CTU grant No. CTU0410013.

Optical Ultrasound Probe Localization for 3D Imaging in Medicine

Z. Szabó*

szabo@ubmi.cvut.cz

* Institute for Biomedical Engineering, Czech Technical University, nám. Sítná 3105
272 01 Kladno 2, Czech Republic

Over the past few decades numerous efforts have focused on the development of various types of three-dimensional (3D) ultrasound imaging techniques. Only in the last few years has technology progressed sufficiently to make clinically useful systems, due to the enormous computing demands needed to produce such images. In general, current free-hand systems are based on commercially available transducer arrays whose position is monitored by a position-sensing device, so during the acquisition, 2D images and position data are stored in a computer for subsequent reconstruction of 3D volume.

This paper is dealing with multi-camera system, where the probe localization is performed based on different views from the cameras, which are following it (or some corresponding marks). Designing such a system for position and orientation determination of the ultrasound probe should take into account an optimal number of cameras, the specifications of the environment and the progress of examination, too. It should be an alternative solution to magnetic systems with higher length accuracy, eliminating its disadvantages as e.g. sensitivity on electric conducting materials around.

Position-Sensing Techniques

We may select among five basic position-sensing techniques based on the (i) acoustic ranging, (ii) mechanical articulated arm, (iii) a magnetic field sensor, (iv) image correlation techniques and (v) an optical tracker. Acoustic sensors receive signals which are emitted by ultrasonic emitters and determine location via time-of-flight. Mechanical sensors determine the position based upon measurements of joint angles and kinematics of the device. Magnetic sensors measure electrical currents induced in three orthogonal coils when the receiver is moved within a magnetic field. Image correlation methods measure image-to-image correlation loss to estimate the position. Last, optical tracker systems track the position of one or more markers and use geometric triangulation to determine the location of these markers.

The optical tracking system provides reliable and accurate position determination for medical application in the case, when there is always a free line of sight between the markers and cameras. Additionally, the optical tracker does not involve any magnetic field for determination of position data and consequently does not permit any deformation of these data in the presence of metallic structures that is unavoidable in a surgical environment.

Optical tracking systems

Optical tracking systems are already widely used in different kind of applications e.g., robotic, monitoring, virtual and augmented reality where the orientation and the position of a real physical object is required. Their principle is based on the analysis of 2-dimensional projections of image features received by CCD cameras. The camera system for 3D ultrasound localizes the tip of the ultrasound probe by tracking the motion of markers that are mounted on the body of the device.

A known mathematical model can be used for cameras calibration in order to calculating intrinsic (focal length, location of the image center, effective pixel size, radial distortion coefficient of the lens) and extrinsic (rotation matrix, translation vector) camera

parameters [1]. During the tracking, the markers are automatically matched and triangulated within the images.

Optical system resolution

The resolution of the optical system is defined as the smallest change that can be detected by a sensor (in our case, by a CCD sensor inside the camera). For more complicated systems consisting from more than one camera we can derive the final resolution stepwise beginning with the resolution in one dimension.

One camera (one CCD sensor) having P sensing elements and viewing range α in both directions, can cause error due to these limitations and the distance l as follows:

$$e = \sqrt{2} \cdot l \cdot \operatorname{tg}\left(\frac{\alpha}{2P}\right),$$

where α is defining the range of camera view in horizontal direction.

In the case of two cameras suppose the next simplifications: the cameras are equally far from the investigated point; they are not turned around their optical axes, and the angle between them (between their optical axes) is γ , then the maximum possible error due to the finite number of sensing elements is:

$$e = \frac{1}{2} \sqrt{y_1^2 + y_2^2 - 2y_1y_2 \cos(180 - (\gamma + \delta_1 + \delta_2)) + x_1^2},$$

where δ_1 and δ_2 are angles defining axes differing from the optical axes. The investigated point is lying on the intersection of these axes. y_1 , y_2 and x_1 define a 3D space in the distance l_1 and l_2 from the cameras, where the movement of the point in 3D scene will not take effect on the cameras.

Several simplifications were used in our consideration, which should be emphasized on the end. Commercially available CCD cameras in contrast with the analysis above have generally different number of sensing elements in vertical and horizontal directions and their resolution will slightly differ. The final resolution of the system also depends on their position and the presented results are valid on the case when the cameras are not turned around their optical axes. Also there is a possibility to specify more precisely the investigated point position from the brightness of several nearest pixels on the image by some kind of approximation algorithms.

References:

- [1] SONKA, M., HLAVAC V., BOYLE R.: *Image Processing, Analysis, and Machine Vision* PWS Publishing 1999 pp. 448-486.
- [2] NELSON T.R., DOWNEY D.B., PRETORIUS D.H., FENSTER A.: *Three-Dimensional Ultrasound* Lippincott Williams & Wilkins 1999
- [3] RIBO, M.: *State of the Art Report on Optical Tracking* Internet site address: http://www.vrvis.at/TR/2001/TR_VRVis_2001_025_Full.pdf 2001
- [4] PRATIKAKIS I., BARILLOT CH., DARNAULT P.: *Towards Free-Hand 3-D Ultrasound* Internet address: <ftp.inria.fr/INRIA/publication/publi-pdf/RR/RR-4399.pdf> 2001

This research has been supported by the grants GA CR no. 102/03/D030 and GACR No. 102/02/0890.

A Wavelet Approach to Biomedical Shape Description

R. Šmíd

smid@fel.cvut.cz

Department of Measurement, Faculty of Electrical Engineering, Czech Technical University, Technická 2, 166 27 Prague 6, Czech Republic

The aim of the project “Characterization of morphological reactions of organ cultures by means of wavelet transform based correlation and cepstral analysis” was to develop and evaluate the new methods for videometric evaluation of changes in morphology and growth parameters of dorsal root ganglia used for neurotoxicity in-vitro testing.

Neurotoxicity seems to be one of the most important toxicological problems. The nervous system consists of a huge number of highly specialized cells connected in a complex manner. Cells in the central nervous system (CNS) are protected to a certain extent by the blood - brain barrier. Peripheral nervous system, however, being more directly exposed to the neurotoxic agents, is more vulnerable.

The changes of morphological characteristics and growth parameters of neurites growing out from cultured dorsal root ganglia can be used for evaluation of the reaction of ganglia to toxic agents. The method originated from Department of Teratology, Institute of Experimental Medicine ASCR, was introduced as a promising new toxicity test that can be used as an alternative to tests carried out on laboratory animals.

The described project was focused on multiscale methods for planar shape description based on wavelet transform. For comparison the radial length distribution was used as a benchmark method. The research covered methods of continuous and discrete wavelet transform, wavelet packets and wavelet correlation.

The continuous wavelet transform based method uses maxima lines of scalogram for representation of planar shape. The Euclidean distance between the end-points of maxima lines from two evaluated representations is related to similarity of two shapes. A weighting of scale axis of scalogram can be used for differentiation between local and global shape features, between details and overall shape. The main disadvantage of the method is computational inefficiency due to redundant nature of signal decomposition. A solution of the mentioned problem can be non-redundant signal decomposition based on orthogonal dyadic scheme used in discrete wavelet transform or wavelet packets.

The planar shape description method based on discrete wavelet transform uses the detail and approximation coefficients resulting from dyadic decomposition of the complex signal representing the parameterized contour. The distance between appropriate coefficients of signal decompositions related to two evaluated shapes serves as a measure of similarity. The weighting of the blocks at certain levels tune the sensitivity to local and global shape features. The method is also usable for shape averaging through inverse wavelet transform of mean coefficients.

Wavelet packet analysis provides more efficient tool for signal decomposition and representation than discrete wavelet transform due to the full decomposition of every detail and approximation of the analyzed signal. Planar shape described as a complex signal can be represented using complex wavelet packets. This multiscale approach gives more adaptability in the selection of signal representation over discrete and continuous wavelet methods. The parameterized contour expressed as a signal in complex plane is decomposed to wavelet packets by normal scheme that consists from low-pass and hi-pass filtering and downsampling. The wavelet packet method corresponds algorithmically to standard sub-band coding schemes and is numerically as fast as the FFT algorithm. From the standard used

wavelet families the Meyer wavelet exhibits desired symmetry and smoothness in the points of maximal curvature of analyzed shape.

The raw output from wavelet packets decomposition is a full binary tree which contains redundant information; the optimal set of wavelet packets must be selected as a proper graph in this tree. Obtained non-redundant set of coefficients represents the shape descriptor. The level of decomposition for a packet is measure of scale or locality of the shape features. The descriptors set is composed from packets at different scales; thus it is possible to reduce the descriptor to important scales only.

In the feature selection process we use a variant of linear discriminant analysis. The objective of this processing stage is to perform dimensionality reduction while preserving as much of the class discriminatory information as possible. The result of the procedure is a set of wavelet packets coefficients determined by discrimination tree for non-redundant and complete description of shape.

Symmetries and periodic components in the ganglia shapes were studied using wavelet autocorrelation. This method is based on circular autocorrelation applied on the coefficients of continuous wavelet transform for a fixed scale. Thresholded maxima in the autocorrelation scale-space carry the information about scale and period of the periodic shape components.

The result of the described project is a set of methods for videometric evaluation of morphological changes in organ cultures suitable for experimental *in-vitro* neurotoxicity testing.

References:

- [1] ŠMÍD, R. - ĎAĎO, S.: *Wavelet Correlation for Biomedical Shape Evaluation* Measurement Science Review, No.3, 2003, pp. 67–70.
- [2] ŠMÍD, R. : *Planar Shape Description using Wavelet Packets for Biomedical Applications* in IEEE International Symposium on Signal Processing and Information Technology, Darmstadt, 2003.
- [3] ŠMÍD, R. - ĎAĎO, S.: *Wavelet Correlation for Biomedical Shape Evaluation* Measurement 2003 - Proceedings of the 4th International Conference on Measurement. Bratislava, 2003, pp. 256–259.
- [4] ĎAĎO, S. - ŠMÍD, R. – HOLUB, J.: *Zkoumání morfologických reakcí spinálních ganglií metodami 3D mikroskopie*, Konference Nové směry v spracovani signalov. Tatranské Zruby: Vojenská Akadémia v Liptovskom Mikuláši, 2004, pp. 149–152.

This research has been supported by the Czech Ministry of Education within the framework of the project "Transdisciplinary Research in Biomedical Engineering".

Kinematics of Human Masticatory Movements in dependence on bolus pattern

T. Goldmann, L. Himmlová*

goldmann@biomed.fsic.cvut.cz

Faculty of Mechanical Engineering, Department of Mechanics, Laboratory of Biomechanics of Man, Technická 4, 166 07, Praha 6, Czech Republic

*Institute of Dental Research, Vinohradská 48, 120 21, Praha 2, Czech Republic

Masticatory movements during function are technically a typical example of kinematically and mechanically indeterminate system. Jaw movements are realized by a large count of masticatory muscles. While these muscles are activated heterogeneously [1] each muscle is able to influence more than one degree of freedom [2]. All muscles act together and generate a resultant force and torque (six degrees of freedom) with respect to the lower jaw [4]. The distribution of forces and torques necessary to perform any movement over the different parts is not established. Consequently, the system is mechanically redundant.

Two segments, the mandible and the skull, are able to move with respect to each other. Two temporomandibular joints guide these movements. Mandibular condyle articulates incongruently with the articular fossa of the temporal bone in each joint. The articular capsule is slack. Due to this construction both joints allow for movements with six degrees of freedom (rotation – depression and elevation, side to side movements – lateropulsion and translation – propulsion and retropulsion). If the joint surfaces are assumed to be undeformable and maintain contact all the time, the mandible is still able to move with four degrees of freedom. Jaw movements in particular anatomical directions can be defined by the three dimensional path of point, that is rigidly connected with lower jaw. Movement of this point can be scanned and its path can be reconstructed by motion analysis technique.

The aim of this experiment was detection of path of lower jaw movement during mastication, duration of processing of one bite depending on its character (hard and soft aliment) and peak amplitude of this motion. The knowledge of lower jaw movement in population is very important for dominant anatomical direction assessment during adduction and for bite force direction specification.

The method of motion analysis for recording of three-dimensional mandible movements was used in this study. Specially developed and individualized sensor was rigidly attached to lower jaw of each patient. Additional black paper skin markers were put on patient face, particularly above eyebrows, on nose dorsum and above upper lip. These markers were made for definition of local coordinated system, where the motion of sensor was observed. The x, y, z coordinates represent mandibular movement in mesio-distal (lateropulsion, mediopulsion), cranio-caudal (abduction, adduction) and vestibulo-oral direction (propulsion retropulsion) respectively. The origin of local (non-stationary) coordinated system was placed on nose dorsum marker. Kinematical transformation relations between primary (stationary) coordinated system and local (non-stationary) coordinated system were determined by means of kinematical transformations matrix technique. Each subject of experimental research was asked to masticate one bite of hard and soft nutrition (nuts, pastry).

The motion of markers and sensor was mark-scanned by three digital video camera recorders. The shutter was used for the synchronization. Recorders calibration was achieved by specially constructed calibrating cage. Video records, 3D motion reconstruction by direct linear transformation and results processing was performed by APAS system. Results and

kinematical transformations between coordinated systems were evaluated by the MATLAB system.

Marginal movements (maximal opening, dextro- and sinistropulsion) were performed by each patient at the beginning of each measurement. Then patient inserted into his mouth one bite of soft aliment and started to masticate. The same process was repeated with hard aliment. All 32 patients participating in this trial had natural dentition. Duration of hard (t1) and soft (t2) bolus masticating and peak amplitude of masticating movement (in percent) in x, y and z axis related to peak amplitude of marginal movements (Amp 1 – hard aliment, Amp 2 – soft aliment) were evaluated for each patient. All measured quantities were averaged; median, maximal, minimal and standard deviation values were set and they are shown in table.

Logical presumptions that bite character affects processing duration were statistically significant, because count of patients with longer duration of soft bite processing was approximately one third of researched set of patients. This conduces to finding, that the mastication is highly individual process influenced not only by anatomical conditions, but also by specific manner acquired during life.

Understanding of mastication development and knowledge of some physiological relationships is very important for principal anatomical direction assignment during adduction and for statement of resultant direction of loading within mastication. These results can be used for ideal reconstruction of defected dentition from mastication point of view, planning treatment of some masticatory apparatus disorders and/or treatment procedure validation. Results can also affect design and usage of materials for dental implants, their position in jaws and shape of occlusal surface of bridgeworks and dentures.

Values measured in this pilot study suggest, that masticatory movements are very individual and that their relationships should be more precisely examined.

References:

- [1] BLANKSMA, N.G. - VAN EIJDEN, T.M.G.J. - VAN RUIJVEN, L.J. - WEIJS, W.A.: *Electromyographic heterogeneity in the human temporalis and masseter muscles during dynamics tasks guided by visual feedback*, Journal of Dental Research 76, 1997, pp. 542 – 551.
- [2] VAN DER HELM, F.C.T. - VEENBAAS, R.: *Modelling the mechanical effect of muscles with large attachment sites: application to the shoulder mechanism*, Journal of Biomechanics 24, 1991, pp. č. 1151-1163.
- [3] KOOLSTRA, J.H. - VAN EIJDEN, T.M.G.J.: *Three-dimensional dynamical capabilities of the human masticatory muscles*, Journal of Biomechanics 32, 1999, pp. č. 145-152
- [4] MERICSKE-STERN R. - ASSAL P. - BUERGIN W.: *Simultaneous force measurements in 3 dimensions on oral endosseous implants in vitro and in vivo*, Clinical Oral Implants Research 7, 1996, pp. 378-386.

This research has been supported by Grant Agency Min. of Health, grant No. 00002377901 and by MSMT grant No. MSM 6840770012.

Efficient Compensation of the Light Attenuation with Depth in Confocal Microscopy

M. Čapek* **, L. Kubínová**

capek@ubmi.cvut.cz

*Institute for Biomedical Engineering, Czech Technical University, Zikova 4,
166 36 Prague 6, Czech Republic

**Institute of Physiology, Academy of Sciences of the Czech Republic, Vídeňská 1083,
142 20 Prague 4, Czech Republic

A confocal laser scanning microscope (CLSM) gives possibility to scan images from a biological specimen in different depths and obtain a stack of precisely registered fluorescent images within the specimen.

Fluorescent image intensities from a CLSM suffer from several distortions. Particularly, images captured from deep layers of the specimen are often darker than images from the top most layers due to absorption and scattering of both excitation and fluorescent light. These effects cause problems in subsequent analysis of biological objects. Therefore, methods for compensation of the light attenuation with depth must be used.

Several papers have depicted some solutions of this problem until now [1-3]. Generally, methods described there are based on the post-processing of data. We have chosen another, potentially more efficient approach, which lies in software optimization of the microscope hardware during scanning. Our second method is based on the post-processing too by using a simple optimization of image intensities in the image stack.

In our experiments we have used a Leica SP2 AOBS CLSM that is controlled by a personal computer equipped by the proprietary Leica Confocal Software. This software contains a Macro Developer giving the user a possibility to develop macros in Visual Basic language to tune the CLSM hardware.

Two important parameters that can be tuned during scanning are "PMT Gain" and "Offset". Offset represents a value of a signal intensity corresponding to a background, i.e. intensities below the offset are set to zero and intensities above are depicted. PMT Gain, i.e. a gain of photomultiplier tubes, describes amplification of the signal during scanning. In order to preserve fast scanning of the specimen we have chosen to optimize PMT Gain only.

We have developed a macro called SCOM (Series Capture Optimization Macro) in the above described environment. In the beginning the macro tests the specimen according to level of intensities in the predefined number of evenly spaced layers of the specimen. This is done in order to speed up the macro by avoiding the repeated scanning of all images of the specimen, since the scanning of an image is a relatively slow process. As a measure of the intensity level we have chosen an average value of pixel intensity values of a layer (AVPI). Only intensities higher than a predefined threshold are considered. The main advantage of this measure is its independency on pixel positions, since images from different layers of the specimen do not correspond. To get the same value of AVPI in all tested layers, the value of PMT Gain is optimized by "n-step search". This optimization strategy uses decreasing steps to achieve the global minimum of difference of AVPI of two layers. Having values of PMT Gain of tested layers, the values of PMT Gain of all layers are piecewise linearly interpolated

and the resulting stack of images is captured. If small or irregular objects are present in the specimen, it is possible to apply the macro only on a selected region of interest.

The important advantage of the described method consists in preserving the information content of images within the whole specimen. Information degradation due to the attenuation is lowered. On the contrary, the level of background noise grows by increasing PMT Gain in deep layers. This could be solved by 2-parameter optimization taking into account both PMT Gain and Offset. However, this approach would significantly slow down the scanning of the specimen, which is not desirable.

A similar approach we have applied in the post-processing method. However, there is no necessity of tested layers, since the post-processing of images by a personal computer is much faster than the scanning of images by a CLSM. The method optimizes AVPI of all images of the stack directly by adding or subtracting a value to image pixels. At the end of the procedure the whole stack is intensity equalized. The method has been implemented within a modular Ellipse software system (ViDiTo Company, Slovakia; <http://www.ellipse.sk>) for the visualization and processing of 2D/3D biological data sets. This post-processing method is computationally fast, simple, and at the same time yielding good visualization results.

To conclude, we have developed two methods for compensation of the light attenuation with depth for the use in confocal microscopy. The first method is based on tuning the hardware and is very efficient, since the information degradation of data is lowered already during the scanning. But it is relatively slow. The second method is based on the post-processing and it does not enhance information content of data, but it improves visualization of data and is fast.

References:

- [1] A. LILJEBORG, M. CZADER, A. PORWIT: *A method to compensate for light attenuation with depth in three-dimensional DNA image cytometry using a confocal scanning laser microscope*. Journal of Microscopy, Vol. 177, Pt 2, February 1995, pp. 108-114.
- [2] F. MARGADANT, T. LEEMANN, P. NIEDERER: *A precise light attenuation correction for confocal scanning microscopy with $O(n^4/3)$ computing time and $O(n)$ memory requirements for n voxels*. Journal of Microscopy, Vol. 182, Pt 2, May 1996, pp. 121-132.
- [4] C. KERVRANN, D. LEGLAND, L. PARDINI: *Robust incremental compensation of the light attenuation with depth in 3D fluorescence microscopy*. Journal of Microscopy, Vol. 215, Pt 1, June 2004, pp. 297-314.

The study was supported by the Academy of Sciences of the Czech Republic (Grants KJB6011309, AVOZ 5011922), by the Ministry of Education of the Slovak Republic together with the Ministry of Education, Youth and Sport of the Czech Republic (KONTAKT grant No.139), and by the Ministry of Development (G.S.R.T.) of the Hellenic Republic together with the Ministry of Education, Youth and Sport of the Czech Republic (KONTAKT grant No. ME688 and RC_3_19).

Modular Measuring Chain "ADVANCED PDA" Designated for Support of the Medical and Biomedical Engineering Research

K. Hána, R. Fiala, J. Kašpar, P. Smrčka

hana@ubmi.cvut.cz

Institute of Biomedical Engineering, Czech Technical University, Zikova 4, 166 36 Prague 6,
Czech Republic

About the project

The „ADVANCED PDA“ project was developed at the Institute of Biomedical Engineering CVUT in Prague. Its basic function is the scanning of biological and technical signals. This system was originally designed for technical support of our own research projects (telemetry, monitoring and storage of biomedical signals). Due to satisfactory results, experiences and significance of this topic, „ADVANCED PDA“ project has overwhelmed the needs of our institute and it was decided to make it available for public in form of customer modular system.

The system is able to acquire signals via input sensors at **several levels**:

Biological signals:

EKG, EEG, skin resistance, body temperature, blood pressure, actigraphy, myography, spirometry.

Physical and technical quantities:

Temperature, pressure, acceleration, pH, flow rate, electrical current and voltage, illumination, GPS positioning, angle.

Measurement, processing and visual representation

Measured signals are digitalized and processed by the central control unit, then passed on by selectable communication interface (metallic connection (RS232, USB), wireless interface (BlueTooth, WiFi, GSM, GPRS-ethernet) for displaying, archiving and further evaluation in given imaging unit (classical PC, notebook (OS WIN/Linux), PDA platform (PocketPC 2003)).

Modularity

The most advantageous feature of the system is its modularity. The whole chain is composed from preassembled modules via internal interfaces which represents very fast, effective and inexpensive solution. By simple software or hardware adjustments we can measure other quantities than those included by default modules.

Software

Most components are available from our own development incl. all software tools. Selection of the appropriate connection interface ensures the maximum users comfort and opens the gate into modern world of communication.

Accomplished applications:

- Viligant Car
- Equine ECG
- Scuba Diving Monitor
- Pulmonary Thermometer
- Applications in Civil Engineering
- Stimuli Sensing Unit

Modular measuring chain ADVANCED PDA is ready to be strong and affordable tool for all potential partners in research and industrial area, see <http://www.ubmi.cvut.cz/pda>.

References:

- [1] BITTNER, R. - SMRCKA, P. - VYSOKY, P. - HANA, K. - POUSEK, L. - SCHREIB, P.: *Detecting of Fatigue States of a Car Driver* Springer-Verlag, 2000, 260-273.
- [2] HANA, K.: *The Implementation of EEG and Peripheral Biofeedback Processing in the Real-Time UWB* in Pilsen, 2000, 65-67.
- [3] SMRCKA, P. - HANA, K.: *Changes in Multifractal Behaviour of Heart Rate Variability under Extremal Conditions* CTU in Prague, 2001, 868-869.
- [4] TREFNY, Z. - HERCZEGH, S. - HANA, K. - TOMAN, V. - DAVID, E.: *From Ballistocardiography to Quantitative Seismocardiography-Measurement of Systolic Force and Time-Frequency Relationships in Cardiovascular Dynamics* CSDS Alberta, Canada, 2004, 48

This research has been supported by MŠMT grant No. MSM 210000012 and CTU grant No. CTU0416833.

Mobile Device for Diagnostic Measuring of Galvanic Cells in Oral Cavity

K. Hána, J. Procházková*, P. Smrčka, H. Kučerová*, J. Kašpar, M. Mikšovský*

hana@ubmi.cvut.cz

Institute of Biomedical Engineering, Czech Technical University, Zikova 4, 166 36 Prague 6, Czech Republic

*Institute of Dental Research 1st Medical Faculty and General Faculty Hospital, Charles University, Vinohradská 48, 120 21 Prague, Czech Republic

This work describes the construction of an appliance for measurement of galvanic cells electric parameters in the oral cavity, own developed method of measurement. The aim of the study is to create a theoretical model of galvanic cells' dislocation in the oral cavity.

The alloys of common or rare metals have been used in dentistry for a long time for their excellent physical conditions as pourment, malleability, tensillness or resistance. Last period they have been used in implantology for dental restorations as well. Metals from dental alloys are not the physiological part of the human organism in commonly used volumes. That is the reason for appearance of unwanted side effects in sensitive individuals after application of dental alloys. These side effects can be of physical or biological origin. During the interaction of the metallic denture with the aggressive environment of the oral cavity each alloy more or less corrodes. This corrosion is characterized not only by simple chemical one, but electrochemical one, on the base of galvanic features when the dental alloys function as electrodes and the oral liquids - saliva, crevicular and tissue fluids - as bath. The ions are released from one electrode and intercepted by the other one. Such a way the movement of metal elements is performed. These mechanisms together with abrasion caused by the mastication lead not only to the destruction of dental alloys but also to the ballast of the organism with the metal elements from the used materials. Both, the galvanic features and the exposition to released metal elements are able to evoke subjectively very unpleasant feelings in predisposed individuals while the objective findings using a large scale of serious diagnostic methods are rare. They can show both local or general symptoms. Galvanic voltage and currents function as tickler like any other physical irritant and the answer of the organism is characterized by standardly known features of inflammation: rubor, color, dolor, tumor and function laesa, depending on the health stage of organism and the intensity or irritation.

All negative influences are strictly individual and can be objectified only on the basis of measurement. In Czech Republic, there is the measurement of absolute maximal values of voltage and currents (going through the resistor 2200 ohm) performed and on the base of these values the mood of therapy is decided. The aim of our study is to create a theoretical model of galvanic cells' layout in the oral cavity. For this purpose the methodical tip for establishment of this model was proposed.

Due to this requests and to own experiences from the clinic practice we find out building of our own mobile device for the diagnostic measuring of current and voltage in the oral cavity accompanied with user's software. The mobile device enables the measuring voltage, current, their polarity, maximal value, internal resistance, capacity of galvanic cells, and the possibility to follow the effect of the loading of the one cell to the other cell. The single-chip microcomputer (Cygnal C8051F330) and A/D converter (Analog Devices

AD7738) built the substance of the equipment. The resistor 2200 ohm is automatically wired in mode of the measurement current by the relay. The values of measuring quality are transferred to PDA (Personal Digital Assistant) or PC in the real-time by the serial interface RS232. The data are processed on PDA or PC and by the rectangle method the capacity of galvanic cell are calculated.

We also found the new method of measuring, which should enable high repeatability, definiteness and reliability. The clinical practice has already showed us, that the metal systems (metal crowns and bridges, fillings) have inhomogeneous surface (different state of corrosion, internal inhomogeneity of material, etc...), which has a serious influence on the magnitude of measuring value. Recently the measuring is practised in this way. At first we gradually touch the surface of measuring metal system by the electrode, the measuring advice displays the max. value. After this first step we have to put the electrode on the place where we suppose max. value there we start the measuring of the current and we obtain its value by the similar way. This method is impossible to use for measurement of further parameters. It is necessary to find the place with the highest voltage while the actual value is being showed all the time, and the current and other parameters (internal resistance, cell capacity...) are measured in this place.

A new mobile system for identification of the electrical parameters of galvanic cells in the oral cavity was developed composed of the own appliance accompanied with user's software. Due to the current literature this problem has not been solved yet. We proposed our own measurement method as well. Our next aim is to measure a statistically significant sample of values for various dental metal materials and the correlation of gained data with the clinical stage of the patients. The final result should be the creation of a theoretic model by using the Finite Element Method (FEM) that enables to follow not studied potentially important dependences, and to make the diagnostic judgement of the physician in the clinical praxis easier using the graphical scan of measured parameters. Nowadays, when at least tens till hundreds of measured values in one patient are manually evaluated only on the base of the experience, this model will open a new age in the evaluation of data and will enable the thousands of measurements combine with further medical research (immunology...). This all would lead to the solving of the key problem: to the prevention of galvanic cells arise in the oral cavity for the concrete person or the prediction of voltage and currents decomposition in case of a new metal dental product added to older ones.

References:

- [1] CERTOSIMO, A. J. - O'CONNOR, R. P.: *Oral Electricity* Gen Dent, 1996, 44, 4, 324-326.
- [2] NOGI, N.: *Electric Current around Dental Metals as a Factor Producing Metal Ions in the Oral Cavity* Nippon Hifuka Gakkai Zasshi, 1989 99, 12, 1243-1254.
- [3] UJEC, E. – HLAVÁČOVÁ, M.: *Měření elektrické dráždivosti zubu a jeho elektrického odporu* Československá stomatologie, 1981 81, 6, 398-403.
- [4] ŠIMSA, J.: *Měření elektrických proudů na kovových náhradách v ústech*. Československá stomatologie, 1955 13-23.

This research has been supported by IGA MZ grant No. NK 7722-3.

Realistic Simulation in Joint Replacement of Human Joints

L. Franta*, J. Pražák**

frantal@biomed.fs.cvut.cz

*Department of Mechanics, Faculty of Mechanical Engineering, Czech Technical University, Technická 4, 166 00 Prague 6, Czech Republic

**Institute of Thermomechanics, Academi of Sciences of the Czech Republic, Dolejškova 5, 182 00 Prague 8, Czech Republic

Effective friction coefficient is among the main parameters influencing periods of survival in elaborating tasks aimed at joint replacements testing, mainly if mutual speed of friction areas of joint replacements are very low. Due to friction and consequently detritions, friction elements are releasing, and they can cause relieving of bone components of a replacement. Temperature [1] increases by dissipation of friction energy during motion in joint, which can cause increasing of friction, creep, degradation UHMWPE or even degradation of tissue [4], which is situated close to joint components. To minimize detritions of joint components increasing viability is necessary. When searching of optimal solution, which will lead to increased viability of joint replacements, the right way seems to be simulation of real conditions during experimenting by simulator. Real simulation of working conditions (mainly conditions, which significantly influence tribologic processes in joint replacements of big human joints) is done by simulator KKK [3]. A loading and kinematic simulator characteristic meets fundamentals requests.

In motion, joint components mutually roll away and push and pull, by which weight powers cause dynamic and cyclic exertion. Mutual motion depends on replaced joint connection and on replacement structure itself [2]. Pressure power significantly influences detritions and consequently endoprosthetics viability. That's why friction power and effective friction coefficient are important factors in evaluation of viability of joint replacements. By simulating working conditions of joint replacements ‚in vitro‘ it is possible to receive valuable knowledge to be used in applying of results ‚in vivo‘. Simulator KKK simulates variable loading of sinus course for knee joint replacement, where the force goes from 250 N to 1800 N. Fundamentals motion is determined by swing angle from 0° to 30°, then the motion is accompanied by along knee motion towards a base in the extent of 4 mm and rotation around vertical axis $\pm 2^\circ$. Motion frequency is adjustable from $0.25 \div 2$ Hz. Lubricate bath can be warmed by resistive heating unit up to the requested temperature similar to a temperature of human body. Contemporary, motion simulation of knee joint replacement is realized, experiments will be elaborated also in hip replacement.

Nowadays, tension is measured in tibia plateau in static loading is simulated. Static tension measurement is a preparatory phase before tension measurement during dynamic loading of tibial component, i.e. in working conditions of loading, similar to these by joint replacement after implantation.

The main effort is aimed to create universal simulator, where knee and hip joints can be tested after easy adjustments. Considering different anatomy of knee and hip joint, demands is laid down to regulate the extent of motion and loading. Loading of joint components enable realistic simulations of motion regimes according different working characteristics [1]. To solve various tasks in the field of biomechanics of joint replacements, it is necessary to know the extent of local tensions in different parts of joint replacements. Loading characteristics

varies in different kinds of motion, that's why differences shall be included into realistic simulation. The temperature approx. 37°C is necessary in measurement in long- and short-termed experiments [3], to provide lubrication by a liquid, which simulates real synovial liquid after implantation of joint replacement and to enable to set different regimes of loading. Based on relevant determined real loading, it will be possible to measure, eg. real tension in tibial plateau. These results can be compared to previously gained ones in exercises 'in vivo'. Following of thermic processes during simulation seems to be very important, mainly it is important to follow warming up close to slide areas [4]. Mainly a creation of friction elements is influenced by mutual activity of all mentioned factors.

It would have been possible to receive lubricant samples in real motion simulation, when these samples would have been enriched by friction elements, which would have been further assessed. Simulator will be further developed for increased function advantage. The goal is, to achieve changes in extent of motions according to requests, quickly, easily and of low cost. By this then to change simulation conditions to bring it closer to real conditions in joint space after implantation. In the second period, it is necessary to adjust a simulator in the sense to create a possibility to change loading's extent and characteristics.

Next important task is to close a joint space considering a real volume of lubricating liquid. Experiment shall be elaborate in space in simulator, which is filled with lubricant and both components are completely under the liquid-level. Mainstream testing is done in significantly higher volume of lubricant, compared to the volume of lubricant in a joint after implantation. The possibility how to achieve this is to construct artificial joint casing, which will guarantee, that in joint space will be the same volume of lubricant as in real joint implanted into human body.

After construct adjustments, there will be a possibility to elaborate experiments, i.e. friction measurement, measurement of thermic processes in motion or of extent of tension by tension meters, which will be done in conditions relevant to real environment in joint space in implanted joint replacement.

References:

- [1] G. BERGMANN, F. GRAICHEN, A. ROHLMANN: *Die Belastung des Hüftgelenkes [on-line]*, Med. Orthop. Technik 116, 1996, 143-150.
- [2] L. FRANTA, J. PRAŽÁK: *The Probleme of Effective Coefficient of Static Friction at Friction Surfaces of Joint Replacement* , In Engineering mechanic 2004:Book of extended Abstracts National Conference with International Participation IM 2004, I. Zolotarev et. al., Editor, IT AS CR 2004, pp. 85-86. ISBN 80-85918-88-9
- [3] L. FRANTA, J. PRAŽÁK: *Realistic Simulation of Wear Tribology in Joint Replacement of Human Joints* , In Summer Workshop of Applied Mechanics 2004, Department of Mechanics, Faculty of Mechanical Engineering, Czech Technical University 2004, pp. 116-122.
- [4] R. NĚMEČEK, J. PRAŽÁK: *Thermal Aspects of Friction in Joint Replacement*, In Engineering mechanic 2004:Book of extended Abstracts National Conference with International Participation IM 2004, I. Zolotarev et. al., Editor, IT AS CR 2004 pp. 209-210. ISBN 80-85918-88-9

This research has been supported by MSM 6840770012

Development of Algorithm for Analog Data Acquisition by the PDA in the Real-Time

K. Hána

hana@ubmi.cvut.cz

Institute of Biomedical Engineering, Czech Technical University, Zikova 4, 166 36 Prague 6, Czech Republic

Presented application project refers to formerly established one named „Sleeping driver, Vigilant car“, which was being solved within the framework of research project MSM 210000012 – Transdisciplinary research in biomedical engineering and, before that, under the „MSMT“ grant within the program „Support of the science and research at the undergraduate and graduate education system“ (250s) at UBMI (formerly CBMI) already in 1999.

The essential part of the project was the development of algorithms for digitalization and storing of data on the real time basis, its reliability, sturdiness, detection of the data flow interruption and other background computing options (fiber priority control, calculations of given attributes from the current data and its imaging) for the needs of the „Sleeping driver, Vigilant car“ project and also for ECOM Ltd., a domestic manufacturer of the liquid chromatography equipment that is used for all scanning and processing of the analog input signals in testing and burn-in of the products.

Should all the analog input signals be monitored and processed in real time and the imaging and parallel computing available (for alarm settings and other industrial purposes) with the possibility to change configurations, keep the whole system mobile and small in size, the solution is the use of one board PC with the appropriate operational system. At the moment, as a result of the computing technology development there are available fairly inexpensive PDA computers (Personal Digital Assistant) (priced from as little as 7000 CZK), containing Intel StrongArm processor (400MHz), several tens of MB of the memory (extendable by memory cards), operating system PocketPC 2002 on the MS Windows CE basis (others also available) and with plenty of peripheries from net interfaces to GSM, GPS modules and miniature hard discs. Although PDAs are due to its „commercial“ technical parameters not widely usable in common industrial practice and due to Windows CE not even for the true real time operations, its low price and wide accessibility makes them ideal for the one-purpose or intelligent monitoring unit use in the prevailing „office“ environments such as laboratories and service workshops.

In below described „Sleeping driver, Vigilant car“ project we faced the problem how to detect the steering wheel movements that carry the information about the driver's fatigue, how to calculate in real times all the parameters referring to the lack of vigilance symptoms and how to display it and inform the driver about any possible related danger.

Thanks to all above mentioned advantages and due to an absence of any rotating mechanical parts (sensitive to vibrations in moving vehicle) we decided to use PDA. This innovative solution found already its industrial use targets, an interest with the prospect of long-term cooperation was expressed by ECOM Ltd. (see <http://www.ecomsro.cz>), Czech manufacturer of the liquid chromatography equipment that is used for all scanning and processing of the analog input signals in testing and burn-in of the products.

Within the project there was a PDA based equipment developed that is readily able to scan and store analog signals in real time. It is derived from previously developed system that contained a standard PC component (notebook). The essential aspect was to implement algorithms resolving processing on the real time basis and to adopt the final solution for an industrial practice.

The proposed solution should be considered perspective mainly due to decreasing prices and improving performance of PDA units. Further development of algorithms for such analog signal scanning is determined by necessity to construct a HW module with A/D converter that would enable scanning, digitalization, wireless transmission and storing signals in PDA in real time. Such module was developed, tuned and constructed at the initial stage of the project. Also developed were the algorithms for digitalization and storing of data on the real time basis, its reliability, sturdiness, detection of the data flow interruption and other background computing options (fiber priority control, calculations of given attributes from the current data and its imaging). Finally, the SW for the purposes of „Sleeping driver, Vigilant car“ project (as well as for the company „ECOM Ltd.“) was composed.

The results are to be presented not only at the Workshop 2005 (presentation of achievements by Czech Technical University in Prague) but it has also contributed to the final version of modular measurement chain „ADVANCED PDA“ assigned for the research support in medicine and biomedical engineering. Its author's collective (K. Hána, R. Fiala, J. Kašpar a P. Smrčka) was granted with the Innovation 2004 Prize by the Innovative Enterprise Association of Czech republic, personally delivered by the Czech vice-prime minister Ing. Martin Jahn, MBA.

With respect to the common financing of the project by ECOM Ltd. and practical impact of the project results we consider our work as very prospective as it provides a solid example of mutually beneficial cooperation in which the scientific results are both used as a basis for further research and development activities as well as usefully implemented in practice.

References:

- [1] BITTNER, R. - SMRČKA, P. - VYSOKY, P. - HANA, K. - POUSEK, L. - SCHREIB, P.: *Detecting of Fatigue States of a Car Driver* Springer-Verlag, 2000, 260-273.
- [2] BITTNER, R. - SMRČKA, P. - PAVELKA, M. - VYSOKY, P. - POUSEK, L.: *Fatigue indicators of drowsy drivers based on analysis of physiological signals* Springer-Verlag, 2001, 137-142.
- [3] VYSOKY, P.: *Calibration of the driver's fatigue estimator with help of fuzzy aggregation function* VUTIUM Brno, 2000, 86-88.
- [4] RASMUSSEN, J.: *Skills, rules and knowledge, signals, signs and symbols and other distinctions in human performance models* IEEE trans. SMC, 1983, 2, 257-266.

This research has been supported by CTU grant No. CTU0416833.

Measuring and Processing of EEG Signal in the High Noise Environment

Jan Kašpar, Pavel Smrčka, Karel Hána, Jan Mužík

`kaspar@ubmi.cvut.cz`

Institute for Biomedical Engineering, NMR SISCO Laboratory, Studničkova 7,
120 00 Prague 2, Czech Republic

The manner of central nervous system in man is considerably complicated and learning all the underlining processes is a natural mankind's desire. Each process is in fact a system of more physical procedures that result in more or less measurable quantities. Monitoring of such quantities helps us to detect physiological or pathological principles. Many physical approaches could be used in general but monitoring of the electrical brain activity by EEG seems to be very promising, especially in combination with the functional MRI investigation.

Functional magnetic resonance (fMRI) enables the mapping of active brain areas with fine spatial resolution based on so called BOLD effect. The increase of the local blood flow in given area result in the change of T1, T2 and T2* constants, which is manifested by changes in the shades of gray in final image. By comparing and further processing prior to and after the activation, the areas can be later highlighted in 2D or 3D model for easier diagnostics.

The electrical activity of a brain is viewed by EEG. This method monitors brain with very fine time resolution of incoming signals and is ideal complement to the spatial information generated by fMRI. Problematic issue in this combination seems to be low level of EEG signals that are in addition under fMRI deformed and produce specific artifacts. These are caused by a strong magnetic field, radiofrequency pulses (RF) and also by alternation of gradient fields. All of these aspects can be expanded to more general environment, said to be with a high noise.

The EEG apparatus destined for operation in this high noise environment should therefore be specifically adapted. Elimination of the disturbing factors should be distinguished in two levels. Firstly at the level of the very signal acquisition, e.g. of measuring hardware (HW) and secondly at the level of the registration program and digitalized data processing.

Development and construction of such EEG device adapted for an operation in the high noise environment has started in Institute for Biomedical Engineering at Czech Technical University in Prague. Our team is focused on the development and construction of such acquisition hardware and control programs with incorporated numerical filters.

The protection from RF pulses is ensured by shielding and a special construction of the scanning electrodes. Further protection from the disturbance at the level of HW is replacing the classical metallic data transfer system by optical fibers or alternatively using wireless system that does not interfere with the RF noise. However, a substantial deal of the artifacts yet remains on the side of processing the signal by the measuring program. In case of MRI, precisely defined pulse sequence allows us to set the adaptive filtration of signals very effectively and eliminate thus the influence of RF and gradient fields. In other cases, further numerical filters and processing has to be implemented and thus we should eliminate also the

influence of ballistic-cardiographical artifacts (such as synchronization with ECG) and effects of movements of scanning electrodes and cables.

Scanning the EEG signals in the course of fMRI proves to be a beneficial combination for monitoring of time-spatial processes in human brain and it is a subject of further research, what are the diagnostic scopes of the correlation between these two methods. There are some results obtained especially in epileptic patients but it is quite possible that this approach will become very valued in the health care of the future.

References:

- [1] HANA, K.: *The impementation of EEG and Peripheral Biofeedback Processing in the Real-Time UWB in Pilsen* 2000 65-67.
- [2] HAUSDORF, J.M. – PENG, C.K.: *Multiscaled randomnes: A possible source of 1/f noise in biology* Physical Review E 1996 Vol. 54, No. 2.
- [3] SATORRAS, R.P.: *Multifractal properies of power-law time sequences: Application to rice piles* Physical Review E 1997 Vol. 56, No. 5.
- [4] KAULAKYS, B.: *Autoregressive model of 1/f noise* Physical Letters A 1999 Vol. 257, No. 1/2, p.37-42.

This research has been supported by MŠMT grant no. MSM 210000012 and CTU grant No. CTU0416833..

The Design of Architectures for Multiagents Systems for Health Service

P. Novák, M. Fejtová

fejtovam@k333.felk.cvut.cz

Department of Cybernetics, Faculty of Electrical Engineering, Czech Technical University, Technická 2, 166 27 Prague 6, Czech Republic

Modern health care is highly specialized. Many experts and laboratories have to be involved in a complex examination of a single patient. Modern medicine is characterized by distributed data, information, knowledge, and competence. Most often, the specialists exchange their conclusions in terms of high level concepts, but this approach makes it difficult to utilize complex relations among diverse symptoms namely in the early stages of a disease, when manifestations remain minor. Hopefully, such relations can be recognized if all measurements are evaluated by a single person. However, there is a number of reasons why this is hard to achieve. Most measurements do not produce a simple unique number, but they correspond to a time trace of some attribute (ECG, EEG, etc.). The resulting data is extensive, its interpretation is very demanding and it needs lot of special knowledge – consequently it must be ensured by a domain specialist. But most probably, a specialist in one domain is not a specialist in the other domain, which is vital for the patient at the very moment. That is why it is most important to search for solutions enabling flexible exchange of data or knowledge between specialists participating in reasoning process. The exchange should not restrict to high level concepts, but it should pay attention to minor signs which would otherwise go unnoticed. For predictive diagnostics, it would be useful to complement the present specialized view on the patient by a more complex picture reflecting the details recognised in independent measurements.

Recently there has been growing interest in the application of agent-based systems in health care. The most frequent medical domains in which agents have already been considered are: retrieval of medical knowledge from the Internet, decision support systems for monitoring and diagnostic tasks or for home care, distributed patient scheduling within a hospital.

Considering the whole cycle of patient treatment, we can identify (at least) five separate areas that can be computer supported, namely:

Diagnostics as a process of identifying a disease from its signs and symptoms is the most obvious area for application of computer support. The systems can help to focus attention on the most probable diseases, to suggest other special examinations of the patient, etc.

Prediction means inference regarding future disease development after application of a certain treatment. Prediction, likes diagnostics, requires a vast amount of knowledge and experience on the part of the doctor. Prediction may be supported by various tools, such as simulation systems or certain machine learning methods.

Monitoring is a life-critical activity in intensive care units, where delayed information can be decisive for the patient's survival. It therefore requires (at least partial) real-time data processing and evaluation. In this context, computer support offers significant time saving for personnel.

Distributed information processing represents a big problem. Isolated “island” solutions are typical in medicine. There is a high degree of distribution, a great volume of

knowledge, and heterogeneity of information (findings, images, treatment protocols, laboratory results). If this information is to be used efficiently in diagnostics and treatment, it must be easily accessible and must be as consistent as possible.

Workflow management and treatment planning requires a high degree of cooperation and communication, especially in hospitals and between different health care providers. As in classical industrial fields (production, sales), also in medicine computer supported solutions promise increased efficiency and decreased costs.

Is it possible to develop and set into life a large system covering and supporting all the above- mentioned areas? It seems plausible provided that hospital management is highly enthusiastic about such a plan. To simplify the task, we have decided to focus on diagnostics and monitoring first. There are several reasons for this: We have long-term practical experience with the development of diagnostic knowledge-based systems. Diagnostic data and knowledge are quite easily available for development and testing of the system. Several modules have already been developed that can be incorporated into a larger system. Thus we will concentrate in further description on diagnostic and monitoring tasks.

Diagnostic Tasks. Medical diagnostics in general is a complex process requiring a vast amount of specialised knowledge and experience. Depending on the patient's symptoms, the general practitioner (GP) is able to determine a probable diagnosis more or less precisely. If the symptoms are the same for several diseases he/she has to perform further examinations. Some examinations are based on measurement of signals or parameters. Most of this data needs interpretation (= explanation of the semantic content). Of course, it should be stressed that in any case the final decision will be taken by the medical doctor and not by a computer system. The computer system is always considered as a decision support tool.

Monitoring Tasks. Most bedside monitoring and patient-support devices, such as ventilators and physiological monitors, are microcomputer based. They have frequently different outputs because they come from different manufacturers. As a result, the responsible person has to read data from several displays and then to enter to another system for further processing. The urgent need for integration of the outputs is obvious. We can identify several categories of patients who need monitoring: patients with unstable physiological regulatory systems; patients with a suspected life-threatening condition and number of patient parameters has to be measured continuously, namely heart rate and rhythm, respiratory rate.

References:

- [1] M. FEJTOVÁ, J. FEJT, L. LHOTSKÁ, O. ŠTĚPÁNKOVÁ: *Architecture of multi-agent systems for healthcare*, In MIPRO 2004 - Computers in Technical Systems and Intelligent Systems. Chorvatsko: Mipro HU. ISBN 953-233-003-8. 2004, pp. 140-145.
- [2] M. FEJTOVÁ, P. NOVÁK, L. LHOTSKÁ: *Multiagentní systém pro podporu rozhodování*, In Inteligentní systémy ve zdravotní péči. Praha: ČVUT, Fakulta elektrotechnická. 2002, pp. 1-2.

This work is based upon work sponsored by the CTU grant No. CTU CTU0414613 "The design of architectures for multiagents systems for health service".

Ultrasonic Immersion Measurement of CFRP Composites Elastic Coefficients – Preliminary Study for Cortical Bone Elastic Properties Assignment

T. Goldmann, M. Landa*, H. Seiner*,**

goldmann@biomed.fsfd.cvut.cz

Laboratory of Biomechanics of Man, Department of Mechanical Engineering, Czech Technical University in Prague, Technická 4, 166 07 Prague 6, Czech Republic

*Institute of Thermomechanics, Academy of Sciences of the Czech Republic, Dolejškova 5, 182 00 Prague 8, Czech Republic

**Department of Materials, Faculty of Nuclear Sciences and Physical Engineering, Czech Technical University in Prague, Trojanova 13, 120 00 Prague 2, Czech Republic

The acquirement of elastic coefficients of bone is important mainly for micromechanical modelling that conduces to new findings concerning the microstructure of bone tissue. This knowledge may for example help to answer a bone tissue remodelling problem. Bone tissue is from mechanical point of view inhomogeneous, anisotropic and visco-elastic material. It is in principle composite material. Strain of bone tissue is compared to other tissues of the human body comparatively small, hence it is possible to assume linear dependence between stress and strain. Visco-elasticity of cortical bone is in terms of time dependency on material constants relatively small therefore it is possible to contemplate a cortical bone as a linear elastic material, which is approximately homogenous and anisotropic with orthotropic material symmetry [2].

Determination of elastic coefficients of bone tissue is very important for description of mechanical properties of bone. Static mechanical tests (for example tension, compressive, bending and torsional tests) are currently used for assessment of elastic coefficients of bone. Elastic coefficients are possible to detect experimentally by means of dynamics tests (ultrasonic tests).

The purpose of this study is a measurement of elastic coefficients of cortical bone as an orthotropic material [2] in its material symmetry via immersion technique. This experimental method consists in specimen positioning between transmitting and receiving ultrasonic transducers, whereas entire measuring configuration is immersed into a liquid. The specimen is rotated in various directions and phase velocities and broad range of directions are measured. This method is closely described in [1]. Elastic coefficients of specimen can be obtained either analytically from velocity measurements in different directions or the problem is possible to solve as multi dimensional optimization approach [4]. This optimization method is used for specimen elastic coefficients assessment in this study.

Ultrasonic immersion scanner was prepared in this project. It is mechanical-acoustic device for performing both reflection and transmission measurements. Design of this scanner assures various degrees of freedom among transducers and sample. Transmitting transducer is steady and receiving transducer is movable, since the position of both the target (sample) and transducers can be adjusted. Sample is fastened into goniometer, immersed in liquid between both transducers and enables rotation around goniometer axis. In particular, one can apply rotation to the target and move the receiver laterally. This makes it possible to monitor the

wave propagation occurring in a system, which obeys the Snell laws, and also measure shear waves and determine their velocities in planar directions.

Velocity measurements were performed on etalon composite specimen CFRP (Carbon Fiber Reinforced Plastic) by virtue of above described ultrasonic scanner. CFRP is homogenous and anisotropic (transversally isotropic material symmetry) material with principal directions identical to the fiber direction. The specimen were plate-shaped; the thickness is approximately 8 , 3.8 and 2 mm. Velocity of the wave propagating through specimen along various directions are well known from previous acoustic measurements as well as corresponding elastic constants [4] and they are in good agreement with immersion measurements. Further experiment will be performed on composite sample of pipe shape.

This study will follow on bone sample elastic constants observation. The measurement will be performed on immersion ultrasonic scanner and the results will be compared with the results from contact and RUS measurement, which is also scheduled into the future. General aim of this study is mapping of bone elastic constants in principal bones of human skeleton.

References:

- [1] GEISKE, J.H. - ALLRED, R.E.: *Elastic Constants of B-AI Composites by Ultrasonic Velocity Measurements*, Experimental Mechanics, April 1974, pp. 158-166.
- [2] RHO, J.Y.: *An ultrasonic method for measuring the elastic properties of human tibial cortical and cancellous bone*, Ultrasonics 34, May 1996, pp. 777-783.
- [3] LEVY, M. - BASS, H.E. - STERN, RR: *Handbook of Elastic Properties of Solids, Liquids and Gases. Vol.I: Dynamics Methods for Measuring the Elastic Properties of Solids*, Academic Press, San Diego, 2001.
- [4] SEINER, H. - LANDA, M.: *Sensitivity analysis of an inverse procedure for determination of elastic coe.cients for strong anisotropy*, Ultrasonics 43, 2005, pp. 253–263.

This research has been supported by CTU grant No. CTU0303612, GAČR grant No. GA 106/01/0396 and MŠMT grant No. MSM 6840770012.

Combination of Laser Fabricated ZrO₂ and HA Layers for Coating of Tooth Implants

P. Mašínová*, M. Jelínek**, T. Kocourek***, K. Jurek****, V. Studnička***,
W. Mróz*****, T. Dostálová******, K. Smetana*****

petrucham@seznam.cz

*Departement of Physical Electronics, Faculty of Nuclear Sciences and Physical Engineering, CTU, V Holešovičkách 2, 180 00 Prague 8, Czech Republic

**Institute of Physics, AS CR, Na Slovance 2, 182 21 Prague 8, Czech Republic
Institute for Biomedical Engineering, CTU, Sítňá 3105, 272 01 Kladno, Czech Republic

***Institute of Physics, AS CR, Na Slovance 2, 182 21 Prague 8, Czech Republic

****Institute of Physics, AS CR, Cukrovarnická 10/112, 162 53 Prague 6

*****Institute of Optoelectronics, Military University of Technology, 2 Kaliski Str.,
01-489 Warsaw 49, Poland

*****1st Medical Faculty, Charles University, Stomatological clinique, Kateřinská 32,
121 08 Prague, Czech Republic

*****1st Medical Faculty, Charles University, Institute of Anatomy, U nemocnice 3,
128 00 Prague 2, Czech Republic

Hydroxyapatite [HA; Ca₁₀(PO₄)₆(OH)₂] ceramics have been recognized as substitute materials for teeth in dentistry for long time. The method of pulsed laser deposition (PLD) was successfully used to create HA coatings and these were studied in vitro and in vivo [1]. HA-coated implants have shown good fixation to the host bones and increased bone ingrowth into the implants. However, there are still many concerns about the application of HA coatings due to their poor mechanical stability. Some previous studies have shown that mechanical properties of HA coatings can be improved by adding ZrO₂. One of the approaches is to create HA/ZrO₂ composite coatings. Alternatively, HA + ZrO₂ coatings are fabricated with the ZrO₂ layer as a bond coat.

To improve HA layer adhesion to the substrate the intermediate ZrO₂ layers were created. The depositions of HA and ZrO₂ films were carried out in two different deposition set-ups where KrF and ArF excimer lasers were used. The sample of an implant was a round pad made of titanium alloy Ti6Al4V with the diameter of 10 mm and the thickness of 2 mm. Film properties were characterized by XRD, SEM and WDX methods. The biological samples were tested of cytotoxicity, attachment and spreading and the immunohistochemical reaction was proceeded [2].

First, all ZrO₂ films were created by KrF excimer laser (LUMONICS PM 842) of 248 nm wavelength, frequency 10 Hz and energy 450 mJ. The target was fixed in the distance of 4 cm from the ZrO₂ substrate. The trace of the laser beam on the target was 7.6 mm². The energy density of the laser beam was 4 Jcm⁻². During the deposition, the oxygen pressure of 6.10⁻³ Pa was kept and the substrate temperature of 20°C was maintained. The number of pulses was 4000. Then HA films were created on titanium substrates coated with the ZrO₂ layers. The ArF excimer laser of 193 nm wavelength, working at repetition rate 50 Hz and output energy 330 mJ was used for deposition. The trace of the laser beam was 5.3 mm². The deposition was proceeded in the H₂O atmosphere at the pressure of 50 Pa. The target was fixed in the distance of 3 cm from the HA substrate and heated up to 600°C.

The film thickness was measured by Alpha Step 500. The ZrO₂ films of the thickness of 50 - 100 nm were grown. The thickness of the HA films varied from 6.0 μm to 16.7 μm. The crystalline structure of the deposited film was characterized by X-ray diffraction (XRD).
788

The XRD analysis proved the presence of the crystalline HA in the deposited films. The film morphology was observed by scanning electron microscopy (SEM) (JEOL JXA 733) using 15 kV electron beam and 400x magnification. Smooth surface covered by droplets of diameters of 5 – 20 μm was demonstrated. The Ca/P ratio was studied using an electron microprobe using wavelength dispersive X-ray analysis (WDX). The ratio was studied on droplets and on flat surfaces and it differed within the range 2.2 - 2.4. The Ca/P ratio of the droplets was lower. Measuring on the larger surface (40 μm x 40 μm), the value of 2.37 was reached.

The direct test of cytotoxicity was used to evaluate the biocompatibility of HA + ZrO₂ samples. Mice line and human fibroblasts were cultivated in the presence of different materials including the studied samples. The best results were reached for the HA + ZrO₂ samples. No morphology changes were observed during cultivation. The cytotoxicity of the HA + ZrO₂ samples was not proved. In the test of attachment, the amounts of attached fibroblasts onto the surface of the sample and onto the bottom of the dish were numbered. After 24 hours of cultivation, there were 53 % of cells attached onto the surface of the sample and 47 % of cells attached onto the bottom of the dish. In the test of spreading, the human fibroblasts were cultivated for 96 hours. There was 47 % growth of the cells on the surface of the sample and 53 % growth of the cells in the surroundings. Two of the HA + ZrO₂ samples were separated after 72 hours of the cultivation processed in the test of spreading to study the immunohistochemical reaction. The fibroblasts created subconfluent and confluent growth.

The thin films of HA were grown by pulsed laser deposition on the titanium alloy Ti6Al4V with the intermediate ZrO₂ layer. The HA + ZrO₂ coatings were well adhesive. The cytotoxicity of the films was not proved. The perspective of its implantation into the bone is open. Various modifications of the coatings can be used for future research, especially sole ZrO₂ coatings are expected to be deposited and studied for tooth prostheses.

References:

- [1] DOSTÁLOVÁ, T., HIMMLOVÁ, L., JELÍNEK, M., GRIVAS, C.: *Osseointegration of Loaded Denatal Implant with KrF Laser Hydroxylapatite Films on Ti6Al4V Alloy by Minipigs* Journal of Biomedical Optics 6 (2), 2001, pp. 239-234.
- [2] KOCOUREK T., JELÍNEK M., MAŠÍNOVÁ P., JUREK K., STUDNIČKA V., MRÓZ W., PROKOPIUK A., DOSTÁLOVÁ T., SEYDELOVÁ M., TEUBEROVÁ Z.: *ArF and KrF Excimer Laser Deposition of ZrO₂ - Hydroxyapatite for Tooth Prostheses* Nano '04 International Conference 2004 pp. 73.

This research has been supported by GA AV CR A1010110 and IGA MZD.

ATR BIOLAB - System for Achilles Tendon Reflex Measurement

P. Kneppo*, M. Tyšler**, V. Rosík**, J. Ždiňák**, J. Švehlíková**

kneppo@ubmi.cvut.cz

*Institute for Biomedical Engineering, Czech Technical University, Zikova 4, 166 36 Prague 6, Czech Republic

**Institute of Measurement Science, Slovak Academy of Sciences, Dúbravská cesta 9, 841 04 Bratislava, Slovakia

Integration of a biomedical measuring system using Ethernet as a standard interface between smart sensors and evaluating station offers the possibility to get local area or even wide area configurations of open, modular systems. They allow immediate acquiring of various types of medical information that was previously obtained off-line or by several independent systems.

Presented BIOLAB ATR device is a part of a BIOLAB project [1] intended to design a concept and develop necessary hardware and software components of a modular networked biomedical measuring system for biophysical examinations. Based on previous experience with the method [2], BIOLAB was designed to help in fast diagnostics of thyroid gland function by evaluating parameters of the cardiovascular, neuromuscular and thermoregulatory system as its peripheral indicators. In comparison with biochemical methods, such examinations are non-traumatizing and in many cases provide enough diagnostic information at much lower costs.

BIOLAB ATR was designed to help in fast diagnostics of thyroid gland function using a non-invasive measuring method revealing the effect of thyroid gland hormones on the neuromuscular system. Increased production of thyroid gland hormones induces faster actions of the neuromuscular system and vice versa. Based on this relation, dynamics of Achilles tendon reflex (ATR) is evaluated as one of peripheral indicators of thyroid gland function.

The reflex is initiated by a neurological hammer and the tendon jerk causes motion of the sole that is scanned by an IR optoelectronic system. Time course of the motion is recorded as the ATR signal, sampled at 1 kHz rate and transferred over the Ethernet into the data processing PC. From the measured ATR signal, time intervals of the contraction time T_K , relaxation time T_R and half-relaxation time T_{H1} are extracted and evaluated by the PC software.

Results from several measurements can be averaged, presented in numeric and graphical form and classified according preprogrammed known diagnostic criteria to assess the functional state of the thyroid gland. During the diagnostic classification, age and biometric parameters of the patient are taken into account.

Besides direct evaluation of the reflex time intervals, overall thyroxin T4 level can be estimated and classified using regression equation [3]: $\ln T4 = 8,62104 - 0,01169 *TH$.

If also indicators from the cardiovascular and thermoregulatory system are present (measured by BIOLAB STI and BIOLAB RHT devices), T4 level estimation can be based on other appropriate regression equations using additional measured parameters and/or their combinations. Results of the classification are displayed in a circular diagram showing values of all evaluated parameters and estimated T4 level relatively to a normal range.

Core of each BIOLAB smart sensor module is Analog Devices AD μ C812 microcontroller chip with a measuring unit and interface control and an RS 232C to TCP/IP converter with RJ45 Ethernet connector enabling connection of the module to a data processing PC via Ethernet network. For the patient safety, module is optically isolated from the Ethernet and is powered by Li-Ion battery enabling approximately 6 hours of measurement. Due to advanced power management, average battery operating time is about 5 working days, however, device can be operated also during the battery charging from an isolated charger.

Specific input module of the BIOLAB ATR sensor contains three infra red emitting diodes and a photo-transistor sensing the radiation reflected by the moving sole. Switching of the emitting diodes and sampling of the photo detector output is controlled directly by the AD μ C812 chip. Intensity of the reflected radiation depends on the distance between the photo sensor and the sole.

After the sensor module is initiated from the data processing PC, ATR signal recording starts automatically when a stimulus signal is detected. This signal is generated by an accelerometric sensor placed in the neurological hammer and its sensitivity is adjusted for precise synchronization of the measurement with properly strong stimulus.

Software for real time ATR measurement, communication with a PC and module power management is factory programmed and can be reprogrammed over the RS 232C interface if software is updated. Modular BIOLAB application software can run on any PC with Ethernet network adapter and is available on CD.

Presented device has been successfully used in the clinic for routine screening of thyroid gland patients as well as a learning tool in courses of biomedical engineering. It combines simplicity of the measuring method with advanced technology to obtain reliable measurements. Presented BIOLAB concept was proposed as open and modular one. From the users' point of view, main advantage of the solution is its variability, possibility to extend it to other examinations, including applications where information is acquired off-line. Modular concept cuts the cost and time for system development and implementation.

References:

- [1] ROSÍK, V. - TYŠLER, M. - ŽDINÁK, J. - RÁŠO, R.: Modular measuring system for biophysical examinations, In MEASUREMENT 2003. Institute of Measurement Science SAS, 2003, pp. 248–251.
- [2] KNEPPO, P. - KUŽMA, E. - ORAVEC, V. - ROSÍK, V.: Thyreomat, Lékař a technika 18, 1989, pp. 97–č. 104.
- [3] VÁŇA, S. - REISENAUER, R. - NĚMEC, J. - BEDNÁŘ, J.: Index obvodového tyreoidálního účinku v jednotkách odpovídajících celkovému tyroxynu v séru, Vnitřní lékařství 31, 1985, pp. 474–č. 481.

This research has been supported by grant 51-51-9014-00/2002 from the Slovak Academy of Sciences, grant 2/4089/24 from the VEGA Grant Agency (Slovak Republic) and grant TRP 04/59/1/a/a from the Ministry of Education, Youth and Sports (Czech Republic).

Evaluation of the Mechanical Loading Change Influence on the Hip Joint Osteoarthritis Development

Z. Horák, M. Stupka*, J. Martiník*, J. Vrána

horakz@biomed.fsi.cvut.cz

Laboratory of Human Biomechanics, Department of Mechanics, Faculty of Mechanical Engineering, Czech Technical University in Prague, Technická 4, 166 07 Prague 6

*Department of Anatomy and Biomechanics, Faculty of Physical Education and Sport, Charles University in Prague, Jose Martiho 31, 162 52 Prague 6

Mechanical loading of the hip joint is very important factor determining articular cartilage damage. One of osteoarthritis frequent reasons is an excessive mechanical overloading articular cartilage. Geometrical shape and mainly a mode of loading cause different stress and contact pressure magnitude and distribution in the hip joint. This paper specified contact stress and pressure distributions in the hip joint. Further, influence of changes in the loading modes and magnitudes on the contact pressure and stress distributions in the hip joint was evaluated.

Osteoarthritis (OA) is a very serious hip joint disease, which attacks mainly older population. OA causes a significant damage of human health connected with important social and economic problems. An OA prevention would contribute to early diagnoses and subsequent treatment of this disorder. It appears that one of important factors influencing a rise and development of OA in hip joint is a magnitude and mainly a mode of its loading. Geometrical shape and mainly a mode of loading cause different stress and contact pressure magnitude and distribution in the hip joint. This paper specified contact stress and pressure distributions in the hip joint. Further, influence of changes in the loading modes and magnitudes on the contact pressure and stress distributions in the hip joint was evaluated. The hip joint loading during walking has a cyclic character. This loading mode is for the articular cartilage advantageous not only from the mechanical, but as well as from the nutrition, viewpoints. Articular cartilage is nourished with the synovial fluid which is “sucked in” at unloading and “driven out” at loading. When this physiological situation is disrupted by a change of loading mode, a continuous local overloading of the articular cartilage occurs resulting in its primary and permanent damage since its physiological nutrition can not proceed. The primary degenerative region (PDR) occurs with every patient at different femur head areas depending on a way of his/her locomotion. Most often (60%) OA is found on the top of the femur head. At the PDR location, an increase of the articular cartilage stress and strain concentration occurs influenced with the multiplied mechanical loading. Thus the cartilage is again overloaded and its secondary degeneration occurs resulting in a progressive expansion of the degenerative area. The human organism tries to correct this adverse reaction by changes of its locomotion, but this causes further concentration of the mechanical loading into still smaller areas of the cartilage tissues, which results in a still more intensive overloading. Such an always developed cycle: *overloading – change of locomotion – overloading* (OCO) is one of main factors influencing a rise and development of osteoarthritis of the hip joint. This paper deals with the stress and strain analyses of the hip joint, how it is influenced by the loading mode changes during human walk, and aimed at the assessment of significant factors of the OCO cycle described above. To carry out the stress and strain analyses of a 3D model of the hip joint, the finite element method (FEM) was applied.

Next part of this work has been carrying out physiological study of several patients with OA first-degree. Further was design video-analysis of motion these patients namely with reference to a location of their stereotyped movement. Results of these clinical investigation together with videoanalysis was comparing with results of the simulation analyses described above. After complete study of all results has been designed an optimal physiotherapy treatment. With reference to long-time treatment the results of treatment are not known yet.

References:

- [1] BERGMANN, G., ET AL.: *Free University of Berlin, Benjamin Franklin School of Medicine, Biomechanics Laboratory, Berlin, Germany* <http://www.medizin.fu-berlin.de/biomechanik/Homeframe.htm>
- [2] TAYLOR, J.G., WALKER, P.S.: *Forces and moments telemetred from two distal femoral replacements during various activities* Journal of Biomechanics, 1997, pp. 839-848.
- [3] DUDA, G.N, SCHNEIDER, E., CHAO, E.Y.S.: *Internal forces and moments in the femur during walking* Journal of Biomechanics, 1993, pp. 933-941.
- [4] WANG, C.B., CHAHINE, N.O., HUNG, C.T., ATESHIAN, G.A.: *Optical determination of anisotropic material properties of bovine articular cartilage in compression* Journal of Biomechanics, 2003, pp. 339-353.

This research has been supported by CTU grant No. CTU0404712.

Non-linear Analysis of the Heart Rate Variability – a New Cybernetic Gate Into Central Nervous System

P. Smrčka, K. Hána, J. Kašpar,

`smrcka@ubmi.cvut.cz`

Institute for Biomedical Engineering, Czech Technical University, Technická 2, 166 27
Prague 6, Czech Republic

We would like to present the results obtained from the signal of heart rate variability (HRV) in experiments motivated by practical needs of distinguishing the sleep-deprived individuals and individuals with alcohol intoxication from vigilant individuals with no sleep deficit. In the experimental part, we have obtained 23 pairs of 80 minutes long ECG records. In each pair were one record from vigilant state and one record in alcohol deprivation or sleep deprivation. For the experimental and technical details see [2]. The experimental data were preprocessed (filtration, segmentation) and heart rate variability signal was extracted. The basic idea of the fractal analysis of time-series is in quantification of self-similarity of rescaled segments of the signal. The integration (or accumulation) is the step that can be interpreted as the mapping of the original (bounded) series to the integrated signal with fractal behavior. In fractal signals the distribution is scale dependent and this dependency can be quantified using so called self-similarity indexes; in monofractal signals the dependency is exponential and it is possible to calculate one and only self-similarity exponent; on the contrary for the multifractal signals it's not possible and we must characterize signal using more local exponents of self-similarity.

We have conducted classical statistical and spectral analysis and then fractal and multifractal analysis. For this purpose we have used 3 different methods: (A) the DFA-estimator - Detrended Fluctuation Analysis, Havlin and Goldberger 1994, (B) the WAV-estimator based on dispersion of the wavelet transform coefficients and (C) the WTMM-estimator - Wavelet Transform Modulus Maxima, which represents so-called multifractal formalism. Classical statistical and frequency domain methods of analysing HRV proved to be insufficient, mono and multi-fractal analysis allowed rather distinctive differentiation of both states. The best results were given by the multifractal descriptor derived from the 3rd order distribution function. Well-known Gaussian formalism with the 2nd order statistical moments gives only the suboptimal results in case of heart rate fluctuations. We have not found significant difference between the states of sleep deprivation and alcohol intoxication together. For the details concerning results see [4]. We believe this methodology can be utilized in practical situations, for example, in personal monitors of the alertness or vigilance in the traffic and industry. The main advantage of introduced methodology may be in an automatic, absolutely noninvasive procedure and relatively easy accessible source signal (heart rate). Proposed interpretation comes from the analysis of 23 independent datasets, so some (but no so far going) generalizations are convenient. In the near future it will be necessary to carry out more experiments in order to verify this methodology and, especially, its accuracy. For the first experimental group the results are quite promising.

Our interpretation of the results of multifractal analysis of the heart rate, which we would like to present here, concerns the configuration of biological regulatory systems. We used division into 3 levels of the control. This is not just theoretical construction but such procedure of multifractal analysis of the time arrays which makes possible to quantify the crucial aspects which is documented by the comments for each of the control levels.

1. **Strategic (planning) level.** Characteristic length of the fluctuations of heart rate is hundreds to thousands of heart beats. There is significant influence of sleep-deprivation and alcohol intoxication. No need for detail evidencing, long-term memory necessary. Possible localization: restricted areas in brain.

2. **Tactical (coordination) level.** Characteristic length of the fluctuations of heart rate is tens to hundreds of heart beats. Low influence of sleep-deprivation and alcohol intoxication. Need for more detailed evidencing, earlier forgetting. Physiological assignment: autonomous reflexive loops. Possible localization: medulla oblongata, spinal cord.

3. **Operational (executive) level.** Characteristic length of the fluctuations of heart rate is units to tens of heart beats. No significant influence of sleep-deprivation nor alcohol intoxication. Need for detail evidencing, immediate response in real time, early forgetting. Local feedback circuits, direct control mechanisms. Possible localization: pacemakers, transmission heart system.

This configuration leads to new understanding of physiological regulations different from compartment model for example, or from the homeostasis principle. In this new picture there would rather be the whole coordinated system of interrelated fluctuating regulatory loops that operates chaotically and far from the balance. There is a clear evidence that most physiological signals under healthy conditions may have a fractal temporal structure – time series generated by certain physiological control systems may be member of special class of complex processes, called multifractal (Ivanov , Thurner 1999). Though some physiological signals may contain an important information, classical methods (such a statistical or spectral analysis and also methods arising from low-dimensional deterministic chaos) do not imply unambiguous results. One of the most interesting questions is how the properties of heart rate fluctuations (or other physiological modalities) are altered in mentioned (or any other) physiological states. The multifractal analysis of HRV is a very convenient tool for inspecting the central nervous system, further investigations and development of this method will reveal more.

References:

- [1] I. PENG: *Fractal mechanism in neural control*, Nonlinear Dynamics, Cambridge University Press, 1999
- [2] R. BITTNER, P. SMRČKA, M. PAVELKA, P. VYSOKÝ *Fatigue Indicators of Drowsy Drivers Based on Analysis of Physiological Signals*, Medical Data Analysis, Lecture Notes on Computer Science, Springer Verlag, 2001
- [3] G. KATUL, B. VIDA KOVIC, J. ALBERTSON *Estimating global and local scaling exponents in turbulent flows using discrete wavellet transformation*, Physica of Fluids, Vol. 13, No. 1, 2001
- [4] P. SMRČKA *Fraktální a multifraktální analýza variability srdečního rytmu v extrémních stavech lidského organismu*, Disertační práce FEL ČVUT v Praze, 2002

E-learning Course Development to Support Teaching of Programming Tools

M. Fejtová*, J. Fejt*, P. Smrčka**

`fejtovam@k333.felk.cvut.cz`

*Department of Cybernetics, Faculty of Electrical Engineering, Czech Technical University, Technická 2, 166 27 Prague 6, Czech Republic

**Institute of Biomedical Engineering, Czech Technical University, Zikova 4, 166 36 Prague 6, Czech Republic

Due to the ever faster development of science and technology, the knowledge acquired during the study before entering the job market is not sufficient for the life-long career. The significance of life-long education is growing. Therefore there are being searched new forms of education that are accessible for broad public and enable individual approach and optimal utilization of precious time of employed people. These requirements can be reached by combination of classical methods with new information and communication technologies (ICT) – approach nowadays called blended e-learning. This approach is suitable for most of the topics relevant for the life-long learning – the only condition of its utilization is computer literacy of its users. Our aim has been to develop simple, illustrative, well-arranged, structured, and easily understandable teaching materials suitable for combined form of study and for self-study that can be efficiently used by all users who want to acquire practical skills for utilization of modern computer and information technologies.

During last decade in advanced countries stress has been laid on versatile satisfaction of one of the basic human rights – right education. However education is not limited to primary education (continuous education of an individual from kindergarten to university level); education must be offered during the whole life – then we speak about life-long learning. Developed systems of life-long learning enable to individuals to enter the process of self-education any time in their career corresponding with changing tasks or perceived needs in their jobs or personal interests. Lifelong learning means expansion of educational process out of schools.

Computers have become common working tools gradually during last decade. We cannot manage without them such operations, as for example launching a space rocket, controlling a NC machine tool or robot, creating magic film illusions of prehistoric animals or action tricks. Till recently we could perceive the presence of computers completely passively. However, that time is over. Nowadays, each of us meets computers daily – at school, library, bank, post office, local authorities or when ordering services of a travel agency. Number of jobs where computer skills are required is growing. We are witnessing revolutionary introduction of computers and information technologies into daily practice. Similarly to Guttenberg typography, this technology brings people unthought-of opportunities and danger at the same time. It opens gate of knowledge and increase of work effectively. However, the same gate may be a cause dividing society to those who can utilize offered advantages and those who cannot. It is obvious that ability to work with computers is becoming new literacy. It is not sufficient to teach pupils and students these skills. Most adults must manage them as well if they want to keep their jobs or to proceed in their career.

The content of the course is transparently structured into several teaching blocks that fully cover area of inevitable computer skills from entire fundamentals (switching on/off the computer, working with the mouse) over advanced document formatting to creation of user-

defined tables and queries. The course is divided into eight basic modules (basic management of PC for absolute laymen, Concepts of Information Technology, Using the Computer and Managing Files, Word Processing, Spreadsheet, Database, Presentation and Information and Communication).

Each module is developed according to the syllabus whose individual points are presented in detail and illustratively in the course. At the beginning of each teaching unit, the given problem is explained in its context. Then detailed description (step by step) of individual acts using both keyboard and mouse follows. The course contains a number of multimedia elements including visual representation of text (individual steps) in the form of video sequences. Since we plan to introduce printed version of the learning course for students, we have completed it with pictorial series that can replace the video sequences. Other multimedia elements are audio comments, clicking maps. Tests with automated evaluation are present as well.

Presented e-learning course is practically applicable to education of fundamentals of computer literacy in presented range. It is well-structured and illustrative. Chosen form introduces knowledge of computer literacy to persons interested in it in clear and attractive form and enables them to verify continuously level of knowledge acquisition. The course is interactive and contains a number of multimedia elements (figures, animations, sound tracks). Prepared modules significantly contribute to easier acquisition of new information, incorporation of this information into context and its successive natural fixation and refreshment. The course is implemented in the MultiPeS e-learning system [1]. Thanks to that the learning pages do not have usual rigorous layout but they have rich content and are user-friendly. Little figure of magician Merlin developed using Microsoft Agent technology cares for user-friendliness in the MultiPeS system. This figure is a guide to students in courses and study materials. It can offer explanation of terms or advice how to proceed in the course.

References:

- [1] M. FEJTOVÁ, J. FEJT, L. LHOTSKÁ: *E-learning System MultiPeS*, EUNITE 2003, Verlag Mainz, Aachen. ISBN 3-86130-194-6. 2003, pp. 377-383.
- [2] M. FEJTOVÁ, J. FEJT, L. SEDLÁČEK, L. LHOTSKÁ: *E-learning Courses in the MultiPeS System*, IADIS Press, Lisboa, 2003, vol. 1,2. ISBN 972-98947-0-1., 2003, pp. 949-952.
- [3] M. FEJTOVÁ, J. FEJT, P. SMRČKA, L. LHOTSKÁ: *E-learningový kurz základů počítačové gramotnosti v systému MultiPeS*, In E-learning v České a Slovenské republice. Praha: ČVUT, díl 1, ISBN 80-01-02923-9., 2004, pp. 184-189.
- [4] P. SMRČKA, M. FEJTOVÁ, J. FEJT, L. LHOTSKÁ: *for Supporting Education of Basics of Computer Literacy*, In Conference Proceedings ICETA 2004. Košice: ELFA. ISBN 80-89066-85-2. 2004 pp. 499-503

This work is based upon work sponsored by the CTU grants No. CTU0417413 and No. CTU0417433 "E-learning course development to support teaching of Programming tools" and University Development Foundation grant No. FRV 2015 "Fundamentals of computer literacy".

Unsteady Fluid Flow with Focus on Hemodynamics

J. Matěcha, H. Netřebská, J. Adamec

jan.matecha@fs.cvut.cz

Department of Fluid Dynamics and Power Engineering, Division of Fluid Dynamics and Thermodynamics, Faculty of Mechanical Engineering, Czech Technical University in Prague
Technická 4, 166 07 Praha 6, Czech Republic

Although a lot of research tries to find relation between hemodynamics and mechanisms which cause arterial diseases the influence of hemodynamics on arterial diseases has not been completely understood so far. The main cause of these ambiguities is the fact that the flow is very complex and the existing measurements are carried out in models which are approaching reality to a certain extent. Presently, the development of experimental methods together with the development of measurement technique make possible to measure in models which are closer to reality.

The aim of this project was to create tools which enable research of unsteady flow in models of parts of cardiovascular system (CVS), like bypass, bifurcation, aneurysm, stenosis, etc. The project solving was divided into several partial aims: design and construction of test circuit, the creation of measurement space, making of construction for holding the cameras and laser, design and putting the measurement chain for pressure measurement into operation, synchronization, creation of methodology, and verification of methodology. All of determined aims were accomplished and solving of the project was carried out as follows. The test circuit which allows obtaining velocity flow field by PIV (Particle Image Velocimetry) method in model of parts of CVS in required instants of unsteady flow period and allows synchronizing the flow field with data obtained from pressure transducers was designed and produced. The complete methodology of all measurement together with software for controlling experimental devices, software for saving experimental data and for processing measured data were created. The methodology was verified on trial experiments.

The test circuit comprises several parts. The peristaltic pump is used as a source of periodical unsteady flow. It is driven by stepping motor with 4 Nm moment. Mechanical connection with the pump is implemented with the help of elastic coupling which reduces vibration. The control electronics allows setting precise position with precision 1.8 degree. It is possible to increase stepping accuracy (pump rotation) by microstepping with the help of control electronics. In the software which controls the operation of motor stepping there is possible to define flow pulse shape and the shape of synchronization signal (0/5V). The synchronization signal has rectangular pulse in desired places. The device with optical sensor placed in the shaft between pump and motor which generates synchronization pulses (0/5V) was made for alternative drive.

The measured model is placed in the test circuit and is modified so that the optical access between camera chip and measured plane was minimally deformed. The transparent prismatic boxes (for 2D and 3D measurement) were made for thin-walled models which are placed into them. During measurement the box is full of working fluid. The box walls are parallel with the camera chip. The holders for pressure transducer were made, which allow measuring the static pressure upstream and downstream the model. In the circuit there is a reservoir which is also used for setting the required static pressure (by setting the fluid surface height towards the model). In order to enable appropriate placing of cameras and laser towards the measured plane in required places, the construction was made which allows fixed holding of model, cameras and laser in optimal position towards each others.

The measurement of unsteady flow field by PIV method is limited by parameters of the system used and by camera and laser frequency in the first instance. The cameras in our system have frequency 4.5 Hz in double-frame regime and laser frequency is 15Hz. The flow in CVS has average maximal values of frequency parameter which is defined as $\alpha = 0.5d\sqrt{2\pi f/\nu}$ where d is diameter, f is frequency and ν is kinematics viscosity $\alpha = 17$ for physiological state and $\alpha = 35$ for increased heart frequency. These values of α correspond with maximal frequency $f = 0.5$ Hz and $f = 1.9$ Hz for model of characteristic dimension $d = 20$ mm and for working fluid viscosity near to water viscosity and they correspond with maximal frequency $f = 1$ Hz and $f = 3.5$ Hz for working fluid viscosity near to blood viscosity.

Concerning these values of periodic flow frequency it is not possible to obtain the progress of flow field during one period by PIV method with sufficient resolution. For that reason periodic character of flow is used and measurement methodology is created which enables to obtain flow field in concrete instant of period for selected number of periods. These values enable to calculate mean values of flow field for individual instants of period and allow assembling the progress of mean flow field during whole period. The synchronization signal is used for obtaining images in the required instant and is connected to the control unit of PIV system. The control of PIV system is set so that the system saves double-image after coming of rectangular pulse. The double-image allows calculating the instantaneous flow field. Instantaneous flow fields are saved in structured variable of program MATLAB for next processing.

The pressure transducers XTM-190M-0.7BAR D made by Kulite company are used for pressure measurements. The signal from pressure transducers together with synchronization signal are connected to measurement card PCI-6024E made by National Instruments company. A program is created for recording and saving data in LabVIEW software. The data together with time recorded are saved in columns in files of ASCII format

The data from pressure transducers and instantaneous velocity field data are loaded in MATLAB where further processing is carried out. Data synchronization is carried out with the help of time of recording. Owing to this synchronization, the values of corresponding pressure from pressure transducers are linked with concrete velocity fields. The graphical user interface was created in MATLAB enabling synoptic graphic representation. The graphical user interface allows simultaneous looking over the process of pressures and velocity fields and other calculated characteristics as well.

The financial means were spent in required amount; their spending was in harmony with budget presented, transfer among particular cost items was not accomplished.

References:

- [1] MATĚCHA, J.; NETŘEBSKÁ, H.; ADAMEC, J. *Měření nestacionárního proudění metodou PIV*. In sborník příspěvků Colloquium fluid dynamics 2004, Praha 3.-5. 11. 2004, Institute of Thermomechanics AS CR, pp. 119-122. ISBN 80-85918-89-7.
- [2] MATĚCHA, J.; ČÍŽEK, J.; ADAMEC, J. *Vliv nepřesnost kalibrace na výsledky měření metodou PIV* In sborník příspěvků Colloquium fluid dynamics 2004, Praha 3.-5. 11. 2004, Institute of Thermomechanics AS CR, pp. 119-122. ISBN 80-85918-89-7.

Using the PIV Method for Blood Flow Investigation

J. Matěcha, K. Vališová, J. Adamec

jan.matecha@fs.cvut.cz

Department of Fluid Dynamics and Power Engineering, Division of Fluid Dynamics and Thermodynamics, Faculty of Mechanical Engineering, Czech Technical University in Prague
Technická 4, 166 07 Praha 6, Czech Republic

The project deals with using the PIV method for blood flow investigation. Experimental loops for measurement in models of cardiovascular system are made together with experimental loops for testing different types of model material, working fluid type and seeding particles type. The problems with choosing suitable material of model, type of working fluid and type of seeding particles are being solved. The methodology of measurement by PIV method (both 2D and stereo) is created. The methodology was verified on trial experiments. The experimental loops were adjusted for teaching. The laboratory tasks are prepared for two courses Fluid mechanics and Unsteady flow and hemodynamics. The manual for measuring by PIV system and manual for calculating 2D and 3D flow field are created.

For flow simulation in different parts of cardiovascular system by PIV method, experimental loops were built. These loops are made of variable components (i.e. measurement space for 2D or 3D PIV, pumps, flow meters, valves, pressure transducers, tanks, etc.). It is possible to change these components when necessary. If unsteady flow is to be investigated peristaltic pump is used as its source. Other experimental loops were made for testing different types of materials for models and different types of working fluids. Since it is necessary, during the measurement, to set the cameras and laser into optimal positions towards the measured model, both traverse constructions and camera stands and other different preparations enabling 2D and 3D measurement.

The models of a part of cardiovascular system have usually very complex geometry where most of the faces are curved. The curvature or the junction of two tubes can lead to severe optical distortions during flow imaging. Distortions can be reduced by refractive index matching or when the model is enclosed in a transparent fluid-filled box with flat faces so that the camera chip plane was parallel to the box wall and thus the transition from one optical environment to the other one is made by flat plane.

The most frequently used working fluid is water, which is cheap, easy available and bio-safety. The disadvantage is the difference between physical properties of water and human blood, but for the first approximation is usage of water adequate. To minimize optical distortion and optical noise at the model/fluid interface, the variant mixture of sodium-iodine (NaI) or glycerin are used. The fluid index of refraction is than close to the index of Plexiglas. Addition of glycerin also approximates the physical properties (density and kinematic viscosity) to human.

The quality of the measurement by PIV method is dependent on seeding particles properties and on their ability to follow the flow stream. The selection of particles is closely joined with selection of working liquid. Their density should be approximately the same as working fluid density. During measurement in transparent models made for example from Plexiglas, high reflections arise on the boundary between the model and liquid which makes the measurement close to the wall impossible. Except of using ordinary particles (polyamide or metal coated particles, wooden particles, air bubbles or dissolved milk, etc.) it is possible to use the fluorescent particles as well. If they are illuminated from monochromatic light they absorb luminous intensity in the range from $\lambda=520$ to 570 nm and they emit light with lower

energy from $\lambda=570$ to 650 nm. If these particles are illuminated with ND-YAG laser ($\lambda=532$ nm) and if the screen for camera (which transmits only the light with the wave length higher than $\lambda=580$ nm) is used then it is possible to scan only the light emitted from the particles and thus to filter out the reflections.

One of the suitable combinations is Plexiglas for model material, 60% NaI solution for working fluid and fluorescent particles for seeding particles. Frequent problem with optical distortions can be reduced when the model is enclosed in a transparent fluid-filled box with flat faces so that the camera chip plane was parallel to the box wall.

Measurements and data analysis by PIV method is partly the same both for 2D PIV (which measures flow field projection on the measured area) and for stereo PIV (which measures all velocity components in measured area). In case of stereo PIV a transforming matrix calculation is additionally carried out. With the help of this matrix it is possible to calculate the flow field with all velocity components from two projections of flow field obtained from two different places. The process can be summarized into several points: 1. Preparation of the experiment; 2. Calibrations; 3. Measurements; 4. Data analysis and evaluation. The preparation of the experiment requires several steps. That means to position the laser so that it illuminated the measurement area in the required place with sufficient intensity and with suitable light sheet thickness. Further it is necessary to select seeding of measured fluid. The following step is calibration during which real sizes are assigned to the image acquired with a camera (sometimes the image can be largely distorted).

During the measurement it is necessary to set the time between particular images according to flow velocity and size of the measured area. It comes out that suitable setup is when particles displacement between particular images is approximately five pixels. The basic analysis and data evaluation is carried out in FlowManager program. For further analysis, comparison and graphical presentation of the results of measured data Matlab program is used. A set of scripts was created for this program. FlowManager program enables direct data transfer to Matlab. For analysis of great amount of measured regimes the system of data saving was created so that it enabled data analysis and comparison in real time. One structured variable of one-dimensional type is created where index of the field is number of regime. All recorded values from FlowManager and all calculated values are saved in one variable.

References:

- [1] MATĚCHA, J.; VALIŠOVÁ, K.; ADAMEC, J. *Using the PIV Method for Blood Flow Investigation* In: Biomechanics of Man 2004 [CD-ROM]. Pilsen: University of West Bohemia, 2004, ISBN 80-7043-315-9.
- [2] MATĚCHA, J.; BÍČA, M.; ADAMEC, J. *Kapaliny pro modely SCS měřených metodou PIV* In: Aplikácia experimentálných a numerických metód v mechanike tekutín. Žilina: Žilinská univerzita, 2004, pp. 31–34, ISBN 80-8070-234-9.
- [3] BÍČA, M.; MATĚCHA, J.; ADAMEC, J. *Optimization of end-to-side anastomosis using PIV* n: Biomechanics of Man 2004 [CD-ROM]. Pilsen: University of West Bohemia, 2004, ISBN 80-7043-315-9.
- [4] NOVOTNÝ, J.; ČÍŽEK, J.; MATĚCHA, J.; ADAMEC, J. *Accuracy of Stereo - PIV Measurement* In: 21st Danubia-Adria Symposium on Experimental Methods in Solid Mechanics . Zagreb: Croatian Society of Mechanics, 2004, pp. 44–45, ISBN 953-96243-6-3.

This research has been supported by FRVŠ grant No.1996/2004

Experimental Line to the Self-excited Oscillation of the Thin-walled Elastic Tubes

H. Chlup*, **, F. Maršík**, S. Konvičková*

Chynek@seznam.cz

* Department of Mechanics, Faculty of Mechanical Engineering, Czech Technical University, Technická 4, 166 07 Prague 6, Czech Republic

** Institute of Thermomechanics, Academy of Sciences of the Czech Republic, Dolejškova 5, 182 00 Prague 8, Czech Republic

Many causes of the cardio-vascular system (CVS) behaviour, both under normal and under pathophysiological conditions, remain still unexplained and therefore great attention has been paid to this problem [1]. The thickening of the intima (part of the blood-vessel walling) at the regions where the low shear stress appears this effect may lead to the formation of the atherosclerotic plates. Theoretical analysis shows that the change of the shear stress (sudden increase or decrease) affects as a trigger of the chemical reactions. Consequently the dramatic decrease of the vessel elasticity is followed by the increase of the blood flow resistance in the vessel. The shear stress has thus the crucial impact on the cell's functions; it influences the cell morphology and the activity of the cell's organelles. The change of the arterial geometry leads consequently to the changes of blood flow conditions and thus even to the alterations of both the shear stress and the arterial wall deformation [2].

Aim task is to solve the blood flow through the elastic tubes analytically, numerically and experimentally and to analyze the context of the mechanical properties of the blood (viscosity) and of the vessel wall (elastic modules) with their instability (Korotkoff's sounds), all with the proper intention to biomechanics of the cardio-vascular system.

We consider the parallel theoretical and experimental research supported by the numerical simulation as inevitable. Is developed and constructed experimental hemodynamic line for simulation of the self-excited and enforcement oscillating in the thin-walled elastic tubes, both at continuous and pulsating liquid flow. All establishment with its characteristics will be constructed for biomechanics purposes. There will be followed up mechanical, and above all elastic, properties of the investigated wall's sample and its interaction with the liquid running through. Physical model will be promoted by mathematical systems modelling.

The dynamics of the CVS as whole is determined by the mechanical properties of its single parts and especially by the heart activity. The mechanical properties of the single components of the physical and mathematical model of the system characterize their compliance and resistance values under blood flow, fitted to the concrete patient [3] or particular problem. The physics and mathematics, especially the numerical mathematics, are presently in the stage be able to solve the problems of the blood flow several chemical reactions included and considering the geometry change and the elastic properties of the blood vessel wall. Especially encouraging is the analysis of the unsteady blood flow through vessels and the finding of the relations between the oscillations (Korotkoff's sounds) and the elastic properties of the blood vessel. It has been demonstrated that the frequency of these sounds depends not only on the blood flow type (laminar or turbulent), on its properties (viscosity), but on the elastic properties of vessels too. There exists great hope that these phenomena will be possible to simulate as well numerically [4] and to support results which

are obtained experimentally through the physical simulation in the near future. The suitable material parameters will be fitted in connection with the physical experiment (IP CAS, GRBB Montreal, Canada), and the consequential verification of the proposed model by the comparison with the manufactured material will thus be possible.

Laboratory of Biomechanics of Man (CTU in Prague) and Biomechanical Laboratory (Institute of Thermomechanics CAS in Prague) long-time pursued the biothermodynamic problems, especially to the experimental and theoretical modelling of the cardiovascular system function. By means of the operating models it is possible to study the flow in the elastic tubes (collapsible fluid flow) partly experimentally and partly simulating mathematically on the computer the hemodynamics of the human cardiovascular system.

Thanks to the computer simulation and physical modelling of this problem it is possible to contribute by improvement of the diagnostics process in the heart-vessel system. The already existing numerical methods and algorithms will be used for solving the viscous fluid flow, and they will be extended to the problem of the fluid structure interaction (the liquid with the elastic wall). The experimental research of the elastic properties of the flow through elastic tube under the regime of their oscillation will be carried out at the Laboratory of Biomechanics of Man and the mathematical modeling to the IT CAS. The project solution will contribute to understanding of the vascular disorder origin e. g. atherosclerosis formation in the large vessels and maybe even to the prevention of the one of the most dangerous diseases.

References:

- [1] ŠTEJFA, M. A KOL. : *Kardiologie* Grada Publishing, 1998,
- [2] GOUBERGRITS, L. - AFFELD, K. - FERNANDEZ-BRITTO, J. - FALCON, L.: *Atherosclerosis in the human common carotid artery. A morphological study of 31 specimens*. Pathology Research and Practice, 197 (12), 2001, pp. 803-809
- [3] PŘEVOROVSKÁ, S. - MUSIL, J. - MARŠÍK, F.: *Human cardiovascular systém with heart failure under baroreflex control (numerical model)* Acta of Bioengineering and Biomechanics Vol. 3, No 1, 2001, pp. 39-52
- [4] HAYASHI, S. - HAYASE, T. - KAWAMURA, H.: *Numerical Analysis for Stability and Self-Excited Oscillation in Collapsible Tube Flow* Transaction of the ASME, Vol. 120, 1998, pp. 468-475.

This research has been supported by GAČR 106/04/1181, MSM 6840770012.

System for Evaluation of Microwave Applicators

J. Herza, T. Martan*

xherza@fel.cvut.cz

Department of Electromagnetic Field, Faculty of Electrical Engineering, Czech Technical University in Prague, Technická 2, 166 27 Prague 6, Czech Republic

* Institute of Radio Engineering and Electronics, Academy of Sciences of the Czech Republic, Chaberská 57, 182 51, Prague 8.

Introduction

This paper deals with the system for optical applicator evaluation, that means measurement of the far-field radiation pattern nearby the aperture of the optical applicator. The measurement was realized with the fiber applicators, which were designed for photodynamic treatment of primary lesion.

This project is also focused on the design and testing of different shapes of the optical applicator. Different terminations of optical applicators were modified for obtaining the optimal radiation patterns. The radiation pattern represents the dependence of radiated power on the angle shift of the fiber termination.

Photodynamic Treatment Method

The photodynamic treatment method has been used for many years in advanced countries, in our country it is for about 15 years. The principle of this method is based on treatment of the tumor by the medicament, which is incorporated in the patient body and activated by the optical radiation of defined frequency and defined power. The advantage of this method is the activation of the medicament only in the area, which is irradiated by the optical radiation. For the medicament activation is used the special optical applicator with the accurately defined radiation pattern.

The medicament is activated only by the specific radiation of specific power, its wavelength is 630 nm (red light). The applicator has to be able to transfer the optical energy about hundreds of milliwatts.

Design and Construction of the Applicators

For the construction of the optical applicators we chose the plastic optical fiber, the diameter of the fiber cladding is 1 mm, the fiber core diameter is 200 μm . We molded the fiber terminations to achieve many different termination shapes. These fiber terminations we measured by a special device.

Device for Measurement of the Radiation Pattern

We used the system for measurement of the optical fiber numerical aperture, which was modified for purposes of mentioned radiation pattern measurement. We combined this measuring device with the water phantom of the biological tissue.

We used the LED (Light Emitting Diode) or the laser diode as the light source for applicator excitation, the wavelength of the radiation was 650 nm. The light source was not modulated. The quasi-monochromatic light was guided within the optical fiber to the optical applicator, which was located in the center of the rotation cylinder. This rotation cylinder was mechanically connected to the axis of the stepper motor, which was controlled by the computer.

The light from the applicator was emitted on the photodetector, located in the far-field zone in the fixed position (it is possible to change the distance between the applicator and the optical applicator). As the photodetector we used the PIN diode. The applicator was rotated in conjunction with the cylinder from -45° to $+45^\circ$ in front of the photodetector.

The electrical analog signal from the optical detector is converted by the A/D converter to the digital form and then processed by the computer.

The rotation cylinder together with the optical applicator and with the photodetector was placed in the black box. This box was closed for prohibition of penetration of the external light to the PIN diode.

The advantage of our system is the possibility to immerse the rotation cylinder with the applicator and the optical detector inside the liquid, so we can measure the radiation pattern in the loss media.

Conclusions

We modified the device for automatic measurement of numerical aperture of optical fiber and the system for evaluation of microwave applicator in the water phantom of the biological tissue for the needs of our measurements. It allows us to study different types of fiber terminations, which can be useful for tumor exposure. We designed and constructed some types of the optical applicators for cancer treatment and diagnostics.

References:

- [1] J. HERZA, T. MARTAN, J. CVEK, R. CHOVANEC, P. KUNSTAT: *Optical Applicators for Photodynamic Treatment*, Conference Proceedings of Radioelektronika 2004., Bratislava: Slovak University of Technology, 2004, pp. 510-512.
- [2] T. MARTAN, J. HERZA, P. KUNSTAT: *Measurement of Far-Field Radiation Patterns of Applicators for Photodynamic Treatment*, POSTER 2004 [CD-ROM], Praha: CVUT FEL Praha, 2004.
- [3] J. HERZA, T. MARTAN, P. KUNSTÁT: *Návrh a testování optických aplikátorů*, Sborník příspěvků konference RADEŠÍN 2004. Brno: FEKT VUT v Brně, 2004, pp. 48-49.

This research has been supported by CTU grant No. CTU0406613 ("System for Evaluation of Optical Applicators").

Physical model of the bloodstream systemic resistance of human.

H. Chlup*, **, S. Konvičková*

Chynek@seznam.cz

* Department of Mechanics, Faculty of Mechanical Engineering, Czech Technical University, Technická 4, 166 07 Prague 6, Czech Republic

** Institute of Thermomechanics, Academy of Sciences of the Czech Republic, Dolejškova 5, 182 00 Prague 8, Czech Republic

The element simulating the body tissue resistance changes represents the dominant part in the cardiovascular modeling circuit set-ups. The element simulating the distal resistance of system circuit of the bloodstream systemic resistance (SO) [1] was created. The total resistance of this apparatus is possible to change with connecting proper number of resistance segments (OS), in dependence of experiments. The element is made up of multiple embranchment flow liquids and resistance segments. The flow cross-section will be extended fivefold from input to output by full opening of SO.

The circulation in a human body represents closed hydrodynamic system, in view of technical details. It is structured from three main components, which are reciprocally interactively connected: heart, vascular system and blood. Vascular system is described, among others, by systemic resistance of the bloodstream, which generated functional ballast for human heart and aorta. It is dependent on diameter of blood vessels and blood's viscosity. General peripheral resistance in systemic circulation represents overall resistance of all parallel circuits together. Measurement of the flow capacity, like peripheral resistance, can be determined by Hagen-Poiseuille principle [2, 3, 4]. The blood flow is directly proportional and peripheral resistance of systemic circulation is indirectly proportional to fourth power of the blood vessel's internal radius. Systemic resistance (SO) of the bloodstream (total peripheral resistance) is about range $R = (\text{from } 77 \text{ to } 150) [MPa \cdot s \cdot m^{-3}]$ [4] at the healthy adult. Diastolic aortic pressure is between values $p_{ad} = (\text{from } 8 \text{ to } 13,3) [kPa]$. The middle minute cardiac distribution at the healthy adult about weight 70 kilogram's or superficies of their human body $1,73 \text{ m}^2$ is approximately $Q = 5,5 \cdot 10^{-3} [m^3 \cdot \text{min}^{-1}] \approx 5.5 [l \cdot \text{min}^{-1}]$ [4].

These experiments were realized with a continuous flow of liquid. The input pressure titled p_v and output pressure p_h to SO were scanned. The flow of this system was caused with hydrodynamic pump and was regulated by ball valve. This experimental line was closed. Measurements were carried out with 24, 18, 12 and 6 active OS. There was set proper value of input pressure p_v by ball valve in experimental circuit, which is matched up with value pressure p_h behind SO. After stabilization of this liquid circulation and compensation of pressures, we can find the value of the element simulating the body tissue resistance.

Our measurement was carried out with range of input pressure $p_v = (\text{from } 2 \text{ to } 24) [kPa]$. The flow was defined in extent $Q = (\text{from } 0,2 \text{ to } 4) [l \cdot \text{min}^{-1}]$. Developed SO is assembled from 24 resistance segments. Calculated values of the element simulating the body tissue resistance were in scale $R = (\text{from } 300 \text{ to } 800) [MPa \cdot s \cdot m^{-3}]$ for 24, 18, 12 a 6 active resistance segments of OS. The liquid flow is directly proportionate to internal cross-section S , velocity of flow c and tube radius r , which liquid flows. By means of approximation with method of the smallest square, used for calculated values R and Q , are

obtained relations of dependence R-Q for experiments with different number of active resistance segments of peripheral resistance.

Causes of high hydraulic resistance:

- The resistance of each element is composed of hydraulic resistance of bath with resistance segments of OS and multiple embranchments, which is moving liquid to OS. Resistance in embranchment can caused accumulation of total element resistance.
- There are 3500 capillaries with diameter 0,18 millimeters in resistance segments of OS. These are situated in tube. Their length could be the cause of total element resistance increment above area of physiological layout of peripheral resistance.

Potential ways of hydraulic resistance decrease:

- Functional simplification of multiple embranchment before bath of SO.
- Magnification of output cross-section of SO by adding another resistance segments with conservation of existing multiple input embranchment.
- Length reducing of resistance segment's capillaries of SO.

Function of the element simulating the peripheral body tissue resistance was demonstrated. The total resistance of element is dependent on cross-section, which is liquid funneling. When the flow cross-section is decreasing, a whole apparatus's resistance is increasing. With increasing distance from the compressive generator pv we can monitor escalation of hydraulic resistance. These facts are in harmony with physiology [2, 3, 4]. Acquired values of total resistance were higher and moved above area of range R, in accordance with literature. Present hydraulic resistances simulated suspiciously peripheral resistance of hyper tonic's cardiovascular system.

References:

- [1] CHLUP, H. – KONVIČKOVÁ, S.: *Evolution of the mock-line of cardiovascular system circuit*, Engineering mechanic 2004, ISBN 80-85918-88-9, 2004
- [2] KOŘEN, J. – ROSENBERG, J. – JANÍČEK, P.: *Biomechanika*, Vydavatelství západočeské univerzity, Plzeň, 1997
- [3] NEČAS, E. A SPOLUPRACOVNÍCI: *Patologická fyziologie orgánových systémů, Část I*, Nakladatelství Karolinum, Praha, 2003
- [4] [1]VALENTA, J. – KONVIČKOVÁ, S.: *Biomechanika srdečně cévního systému člověka*, Vydavatelství ČVUT, Praha, 1997,

This research has been supported by GAČR 106/04/1181, MSM 6840770012.

Methods and Technical Tools for an Analysis of Sudden Cardiovascular Death in the Horse

J. Holčík, K. Hána, P. Kozelek, M. Kohut, R. Fiala

holcik@ubmi.cvut.cz

Institute for Biomedical Engineering, CTU in Prague
nám. Sítná 3104, 272 01 Kladno, Czech Republic

High risk of sudden death associated with a general anaesthesia in horses is considered as one of serious problems of equine medicine. Clinical experience suggests that there exists a correlation between various phenomena as training conditions, feeding (generally a way of keeping the horse) and predisposition to sudden death by failing of the cardiovascular system (CVS) during anaesthesia - a high level of fitness can serve as an example. The correlation imposes a hypothesis about hidden system causes influencing capability of CVS control in horses that could be the reason of the lethal anaesthetic complications.

In order to verify or exclude this hypothesis it was necessary to develop methodological system for measuring proper physiological variables describing activity of CVS in horses under specific experimental and clinical conditions and design and construct appropriate measuring equipment. The signals measured by the developed measuring system should express dynamics of variables describing status in horses during anaesthesia and the hidden dependencies of the variables. The signals should also serve for a search of neurocardiovascular characteristics that could indicate a disposition to the sudden death caused by CVS failure. The choice of signals depends on the background of the analysed phenomenon and on technical capabilities to measure the signals under the given experimental conditions (respecting specificity of equine medicine and demands following from equine clinic management).

Required signals had to describe a neural component of the cardiovascular system control, heart activity and haemodynamics of blood flow through the vascular bed. The former two facts can be expressed by ECG signal and its parameters (heart rate variability, shape of ventricular waveforms as QRS complexes and T waves, resp., length of QT interval, etc.), the measuring of which is a standard diagnostic procedure even in equine medicine. This explains why the initial part of the work was oriented to study relationships between time parameters of ECG signals, in particular RR, QT, PQ, and QRS intervals respectively. The later properties can be described by parameters of phonocardiograms and chest bioimpedance signals.

The ECG signals were recorded at rest (at different places - stable, examination laboratory - and daytime - in morning during standard work at clinic and at night) and as response to electrical excitation (rectangular impulse 100 mA, 100 ms) applied at back of the horse. The signals were recorded for 10 minutes. If electrical excitation was applied, it was done in the middle of recording, i.e. cca 5 minutes after the beginning of the recording. Three bipolar ECG signals V_{46} , V_{26} , and V_{42} were recorded from standard chest lead positions V_2 , V_4 , and V_6 of the tetrahedron lead system used in equine electrocardiography. The ECG signal parameters were measured automatically, and afterwards inspected and if necessary, corrected manually.

Analysis of variations in equine heart activity revealed some unexpected and at present unexplainable behaviour in relationship between lengths of QT and RR intervals in equine ECG signals measured under different experimental conditions. It has been found out

that equine ECG records exhibit much more heterogeneous and complicated relationships between QT and RR intervals if compared with human ECGs.

Besides not very frequent shape of the QT/RR diagram similar to that usually found in humans, three dominant classes of the QT/RR interval dynamics can be recognized in equine ECG:

- Delayed shortening of QT intervals appears after instantaneous shortening of RR intervals. It is followed by slowly oscillating return to a steady state;
- Negligible QT variability with substantially variable heart rate;
- At first, QT intervals prolong with shortening of RR intervals and only after that their values return to the initial point - this kind of behaviour has not been found in human ECG signals yet.

The last mentioned inverse dependency between QT and RR intervals in equine heart can be caused by several hypothetical reasons, such as:

- Decrease of the vagal activity is not proportionally complemented by the sympathetic action;
- There is quite different innervation of heart in horses than in man;
- Greater dimensions of equine heart can substantially change propagation of the electrical excitation in various parts of the heart and these changes can result in different values of ECG signal parameters and their dynamics.

No relevant explanation of the described fact can be found in the literature, so it was necessary to confirm or exclude the suggested hypotheses either experimentally or by means of computer simulation.

Several mathematical models have been developed to analyse character and parameters of equine heart innervation. The models represent definitions of different relationships between parameters of the sympathetic and vagal activity, in particular intensity and time-delay. Simulation experiments with the developed models and their parameters demonstrated that in particular the additive model has the most suitable properties to express the behaviour of real equine ECG signals. It seems that the described model provided a good tool for generating hypothesis about background of the processes in equine heart. This is a necessary and useful starting point for investigation of the problems that can be a cause of fatal cardiovascular events in horses.

References:

- [1] HOLČÍK, J. ET AL.: *Mathematical Modelling as a Tool for Recognition of Causes of Disorders in QT/RR Interval Relationship in Equine ECG* Proc.7th Intern. Conf. PRIA 2004, vol.III, pp. 688–691.
- [2] HOLČÍK, J. ET AL.: *Pilot Study of the RR and QT Interval Relationship in Equine Electrocardiograms*. CD Proc. IFMBE Conf. MEDICON, 2004, 2p.

This research has been supported by GAČR grant No. GA102/04/0887 "Methods and Technical Tools for an Analysis of Sudden Cardiovascular Death in the Horse".

Calculation of the Knee Muscle Forces During Squatting.

Miloslav Vilimek, Miroslav Sochor

`vilimek@biomed.fsids.cvut.cz`

Department of Mechanics, Faculty of Mechanical Engineering, CTU in Prague

Technická 4, 16607 Prague 6, Czech republic

In order to perform stress analyses of bone or true loading of joint prostheses, muscle forces must be determined. The determination of musculotendon forces about knee actuators during squatting activities was chosen, because this functional movement pattern generates relatively high compressional stresses at the knee and squatting requires mechanical output at the hip and ankle in addition to the knee; consequently some of the knee actuators must be modeled as two joint muscles.

In this study, the average data of three experimental trials from one subject were used. The anatomical model of the knee joint actuators included 31 musculotendons. Two force platforms were used to obtain ground reaction forces (GRF) and a motion analysis system was simultaneously used to collect segment coordinate data, see for details [1]. All other input data, e.g. data about musculotendon attachment positions, and inertial and mass properties, maximal isometric muscle force F_0^M , were calculated or based on SIMM software (Musculographics Inc.; [2]), the lower limb anatomical model.

Lower limb joint kinematic data were used as input for the anatomical model to determine individual musculotendon lengths and velocities for the muscles. Additionally, moment arms for each muscle during the squatting movements were determined using the anatomical model. Input joint angles were flexion/extension for the hip, knee and ankle joint, as well as adduction/abduction and internal/external rotation of the hip. The last data processing requirement was to calculate the net moments at the ankle, knee and hip joints in sagittal plane.

For the solution a representation of the musculotendon complex (Hill type model) using idealized mechanical objects was used. Here is the basis for the physiological EMG-driven model [3, 4], and it considers factors related to force-velocity f_v , force-length f_l and activation level $a(t)$ of the contractile muscle component, force-length relation of passive muscle component f_{lp} , and pennation angle $\alpha(t)$. This model corresponds with a full Hill type musculotendon complex without tendon dynamics. The lower extremity musculoskeletal system is strongly redundant and the muscle forces were calculated by optimization technique and inverse dynamics approach.

It is evident that for a complicated musculoskeletal system such as the knee (a system which includes many double joint actuators), additional constraints associated with other joint mechanics (ankle and hip) must be applied. For this reason, it is difficult to use experimentally collected EMG data for complex force analysis of lower extremity, because it is near impossible to collect EMG data for all lower-extremity muscles, 31 muscles in this study. Our analysis was simplified by modeling squatting movements as uniplanar events.

One potential method of addressing these discrepancies is to use a optimization scheme which assumes that EMG and kinematic information are inherently imperfect, and the driven activation signal $a(t)$ (normalized EMG) is calculated by optimization method. Therefore, the unknown variable is now activation (for each muscle). The optimization of the driven - activation signal has been done for all 31 used muscles based on: first, sum of the cube of the ratio between current muscle forces and physiological cross section area must be minimum, and second, minimizing the sum of the muscle activation square. A third criterion used was,

the sum of maximal muscle activations must be minimum. The inequality constraints of activation signal $1 \geq a_i \geq 0$ were added.

For solving the problem of calculating the muscle forces of the knee actuators during squatting, three different optimization criteria were used. Results suggest that the shape of the knee actuator force curves is similar and the variance of values depended upon selected optimization criterion. Important finding is that the difference between optimized values of activation by criterion provides numerous potential solutions.

Here are two problems. At first, the net joint moments calculated from forces given by optimized activation signal differed in some cases from the net joint moments calculated from inverse dynamics. At second, the optimized activation signal do not agree with the measured flexor activation levels (normalized EMG's). Usage of the derived method with Hill-type muscle model is suitable for calculation of the muscle forces for both contractors and co-contractors and calculated data suggest that extensor activation is greater than flexor activation and these findings correspond with the orientation of the net knee moment.

In conclusion it appears that optimized EMG-driven muscle model provide similar results for analysis of squatting movements in used optimization criteria. Nevertheless, we suggest care in selecting appropriate optimization criteria which may be influenced by the type of movement studied, kinetic and kinematic characteristics of the movement (e.g. range of motion, rate of force development, and movement speed) and the co-contraction of antagonistic muscle groups.

References:

- [1] VILIMEK, M. – SONG, J-E. – SALEM, G.: *The Prediction of Knee Actuator Forces Using EMG-Driven Models and Static Optimization Techniques* In: Biomechanics of Man 2004 [CD-ROM], Pilsen: University of West Bohemia 2004, pp. 569–574.
- [2] DELP, S.L. – LOAN, J.P.: *A graphic-based software system to develop and analyze models of musculoskeletal structures* Comput. Biol. Med. 25 , 1997, pp. 21–34 strany.
- [3] LLOYD, B.G. – BESIER, T.F.: *An EMG-driven musculoskeletal model to estimate forces and knee joint moments in vivo* Journal of Biomechanics 36, 2003, pp. 765–776.
- [4] ZAJAC, F.E.: *Muscle and tendon: properties, models, scaling, and application to biomechanics and motor control* Critical Reviews in Biomedical engineering 17, 1989, pp. 359–411.

This research has been supported by MSM6840770012.

Is the Knowledge of the Real Activation Signal Necessary in the Muscle Forces Calculation?

Miloslav Vilímek, Miroslav Sochor

`vilimek@biomed.fs.cvut.cz`

Department of Mechanics, Faculty of Mechanical Engineering, CTU in Prague

Technická 4, 16607 Prague 6, Czech republic

Several methods are available for the muscle forces calculation. Most of the methods use the optimization techniques, according to the strong redundancy of the musculoskeletal system. Some authors use the processing of the EMG signals to the muscle force (EMG-driven methods). Its advantage is, that the EMG-driven methods give muscle forces with non zero values because every muscles, contractors and co-contractors are almost full time activated, and is not important to know complex information about the all joint actuators just as in optimization approaches. Almost is most important have information about muscle shortening and lengthening, suitable muscle model (for example Hill-type muscle model) and activation signal. The processed and normalized EMG signal is appropriate as the activation signal. One of physiological driving factor for muscle force is EMG, processed as muscle activation level $a(t)$.

The EMG-driven methods usually make use of the muscle model with respectation of an active muscle properties or both active and passive muscle properties.

The main problem of these methods is the processing of the normalized EMG signal to muscle activation signal. If the normalized EMG signal as activation signal to muscle models is used, in many cases the joint moments calculated from the forces estimated by raw EMG-driven models are different than net joint moments calculated by using inverse dynamics techniques. The joint moments calculated from forces based on raw EMG-driven models are usually much smaller than moments from inverse dynamics technique.

Such that the muscle forces estimated by using raw EMG-driven models are necessary to be optimized, or the activation (normalized EMG) signal in the Hill-type model is optimized. In our studies, [1, 2] the combined technique was used, the EMG-driven model with optimization approach for muscle force estimation in both elbow and knee problems. The activation input into EMG-driven model was unknown variable which was calculated from optimization. Therefore, the experimentally collected EMG signals were not used for muscle force estimation.

If the EMG-driven model with respectation of all active and passive properties as active and passive force-length relations, force-velocity relation and activation, as for example in [3], the activation signal is optimized and the estimated muscle forces seems authentic. This muscle model expresses the most of the physiological muscle properties, but without respectation the tendon dynamics.

Some authors, [3] [4], use the Hill-type models with the processed EMG directly as an activation signal (EMG-driven models). Question is: Is the prime necessity to know the muscle activation signal if the muscle forces are wanted results, especially if the driven signal (processed EMG) is optimized? The role of the muscle activation signal is to control the active muscle component.

If we compare both, the processed and normalized EMG's with the optimized activations, the measured signals are very small and different form the optimized signals. Also the forces calculated from the processed and normalized EMG's have usually very small magnitudes but the forces calculated from optimized signals seems more realistic and net joint moment

calculated from these forces usually agree with the net joint moment calculated by inverse dynamics approach.

The processed EMG signal is good to be used as activation signal only for the first approach. The findings of our studies and the answer for the above question is that for the EMG-driven models with the optimization technique is not necessary to know muscle activation and recorded and processed EMG, see results in [1] and [2], disregarding its difficult experimental collection for some muscles.

In conclusion, the knowledge of the real activation signal (based on measured EMG's) is not necessary for the muscle force calculation. Optimization techniques with respectation of the muscle active and passive properties give non-zero values for co-contractors. The EMG recording from the small and deep muscles is very difficult to record and the best appropriate usage is only for the timing of the muscle action. Finally it must be said that the Hill-type models, where the unknown activation signals are results from the optimization technique, are better than the raw static optimization without respectation of muscle mechanics mentioned above.

References:

- [1] VILIMEK, M.: *Muscle Forces in Elbow II - EMG-Driven Models [research report]* ČVUT FS, Ústav mechaniky, Laboratoř biomechaniky člověka , 2004, 33 pages.
- [2] VILIMEK, M.: *Muscle Forces in Knee during Squatting Motion [research report]* ČVUT FS, Ústav mechaniky, Laboratoř biomechaniky člověka , 2004, 23 pages.
- [3] BUCHANAN, T.S. – LOYD, D.G. – MANAL, K. – BESIER, T.F.: *Neuromusculoskeletal modeling: Estimation of muscle forces and joint moments and movements from measurements of neural command* Journal of Applied Biomechanics 20, 2004, pp. 367–395.
- [4] LLOYD, D.G. – BESIER, T.F.: *An EMG-driven musculoskeletal model to estimate forces and knee joint moments in vivo* Journal of Biomechanics 36, 2003, pp. 765–776.

This research has been supported by MSM6840770012.

An Artificial Neural Network in Prediction of Elbow Actuators Forces.

Jana Vejpusťková, Miloslav Vilímek, Miroslav Sochor

`vilimek@biomed.fs.cvut.cz`

Department of Mechanics, Faculty of Mechanical Engineering, CTU in Prague

Technická 4, 16607 Prague 6, Czech republic

It is difficult to directly examine the muscle force in living subjects. Many muscles are acting cooperatively in living subjects, therefore, computed simulation could be useful in analyzing the muscle force.

Consequently, in this study, prediction of the muscle force using the artificial neural network was described. Using the MATLAB neural network toolbox, the backpropagation neural network with learning algorithm was programmed. In Standard backpropagation is a gradient descent algorithm, in which the network weights are moved along the negative of the gradient of the performance function.

Properly trained backpropagation networks tend to give reasonable answers when presented with inputs that they have never seen. The architecture of the network that is commonly used with the backpropagation algorithm is the feedforward multilayer network, in this case consists of three layers (two hidden layers of sigmoid neurons followed by an output layer of linear neurons).

The proposed object of neural network simulated cooperation of 7 musculotendon actuators in elbow joint, four flexors: m.biceps brachii c. longum a c. breve; m. brachioradialis; m. brachialis, and three extensors: m. triceps brachii c. laterale, c. mediale a c. longum. The elbow joint was selected because it provides a good visual demonstration, the movement is uniplanar and uniarticular.

In the neural network for muscle forces estimation were used 14 input parameters, and was assumed that these parameters have influence on resulting muscle force. Input parameters were physiological characteristics of participating muscles of particular joint mechanism, further data about movement and electric activation of muscles. Parameters were obtained an experimentally, from the technical literatures [3] and calculation.

Elbow flexion/extension movements were recorded with the 6-camera 60Hz VICON Motion Analysis system across two movement speeds (slow, 1.1rad/sec and fast, 2.8rad/sec) and two loading conditions (unloaded and with 4.2kg bar-bell). Electric activation of watched muscles was recorded by EMG. Processed and normalized EMG signal were taken as muscle activation and history of muscle activation.[1] The used input parameters were: musculotendon length, L_{MT} , velocity of muscle shortening, v , pennation angle, α_0 , optimal muscle length, l_0 , physiological crosssectional area, $PCSA$, tendon slack length, L_{ST} , maximal isometric muscle force, F_0 , force-velocity factor, Fv , active force-muscle length factor, Fl_a , passive force-muscle length factor, Fl_p , muscle activation, $a(t)$ and three degrees of history of muscle activation, $a_{1H}(t+\Delta t)$, $a_{2H}(t+2\Delta t)$, $a_{3H}(t+3\Delta t)$.

The output parameter must be known for training as well. The training output parameter for a network object in the variant A was the muscle force and for its approaching to the real muscle force, the Virtual Muscle system was used, see [2].

For the problem of muscle forces estimation using neural network were proposed two variants of neural object, which were watched at different initial and boundary conditions.[4] In a first one, variant A, a network object for one general muscle was created. In a second

one, variant B, a network object for elbow joint system with 7 musculotendon actuators was created.

The Variant A, a network object for one general muscle was created. Generally, this network could be used for prediction of the muscle force for all of the muscles, not only about elbow joint, accuracy of predication depends on quality of training data of course. For the Variant B, the elbow torque, as training output parameter calculated by inverse dynamic, was used.

The variant B was created directly for 7 elbow joint actuators. A basic effort was the precise prediction of muscle forces. The network object was composed by 7 networks for each muscle (the same network as in variant A was used), enlarged on moment arms inputs. Synaptic weights were adjusted according to actual errors between learned torque and torque calculated by inverse dynamic. This solution had remove errors in results, which were obtained from system of Virtual Muscle. But it is impossible to set up the weights for example positive for flexors and negative for extensors. In this case the network is setting up the weights in each training process with different values and signs. Therefore, this type of artificial neural network, variant B, could not be used for this type of task.

The A variant of network object for general muscle was very difficult to learn and generalized for all of the muscles. The error was minimized, but for general using of this network for all of the muscles it was still enough high. Probably the error is due to the low number of training sets, and due to possible errors in muscle forces calculation by Virtual Muscle system, even if the input data to both methods were the same.

The artificial neural network, variant B, predict net moment on the whole very good. But this variant, could not be used for prediction of joint actuator forces. It is very difficult to use the network variant B for obtaining of values from inside the network, because the relations between the values inside of the network could not be guaranteed.

For the general usage the network variant A appears, with partly reduction of input parameters, as the best, but with higher number of good training sets.

References:

- [1] DE LUCA, C.L.: *The use of surface electromyography in biomechanics* Journal of Applied Biomechanics 13, 1997, pp. 135–163.
- [2] CHENG, E.J. – BROWN, I.E. – LOEB, G.E.: *Virtual muscle: a computational approach to understanding the effects of muscle properties on motor control* Journal of Neuroscience Methods 101, 2000, pp. 117–130.
- [3] GARNER, B.A. – PANDY, M.G.: *Estimation of musculotendon properties in the human upper limb* Annals of Biomedical Engineering 31, 2003 pp. 207–220.
- [4] VEJPUSTKOVÁ J. – VILÍMEK M.: *A muscle forces prediction using learning artificial neural network* Biomechanics of man 2004, 2004, pp. 94

This research has been supported by MSM6840770012.

The sensitivity of the muscular parameters to the muscle force prediction.

Jana Vejpustková, Miloslav Vilímek, Miroslav Sochor

`vilimek@biomed.fs.cvut.cz`

Department of Mechanics, Faculty of Mechanical Engineering, CTU in Prague

Technická 4, 16607 Prague 6, Czech republic

The muscle force in human subjects is affected by many effects. Based on observations of the important muscular parameters by the help of the artificial neural network, analyzing the muscle force can be simplified. Moreover, the muscle force is important considerations for orthopaedists, biomechanists, and physical therapists because joint contact forces, as well as muscle forces, must be estimated to understand joint and bone loading and pathology.

For analyzing and simplification the muscle force sensitivity analysis were studied on the artificial neural network [4]. By using the MATLAB neural network toolbox, the backpropagation neural network with learning algorithm was programmed. In standard backpropagation is a gradient descent algorithm, in which the network weights are moved along the negative of the gradient of the performance function.

The threelayer feedforward neural network with 14 input parameters and one output neuron was used for solving this problem. A degree of adaptation and generalization was possible to change by the change of number of neurons in the hidden layers. The topology of the network was consisting of three layers. Between input layer and first hidden layer, the sigmoidal transfer function was used. Also between first and second hidden layers the sigmoidal function was used. For transfer between second hidden layer and output layer was used linear function.

Input parameters were physiological characteristics of participating muscles of particular joint mechanism, further data about movement and electric activation of muscles. Parameters were obtained an experimentally, from the technical literatures [3] and calculation. Was assumed that these input parameters have influence on resulting muscle force. Changes in the network outputs, for training without input parameter, were described by correlation coefficient, C .

Elbow flexion/extension movements were recorded with the 6-camera 60Hz VICON Motion Analysis system across two movement speeds (slow, 1.1rad/sec and fast, 2.8rad/sec) and two loading conditions (unloaded and with 4.2kg bar-bell). Electric activation of watched muscles was recorded by EMG. Processed (after rectification, filtering and smoothing) and normalized EMG signal were taken as muscle activation and history of muscle activation.[1]

The used input parameters were: musculotendon length, L_{MT} , velocity of muscle shortening, v , pennation angle, α_0 , optimal muscle length, l_0 , physiological crosssectional area, $PCSA$, tendon slack length, L_{ST} , maximal isometric muscle force, F_0 , force-velocity factor, F_v , active force-muscle length factor, Fl_a , passive force-muscle length factor, Fl_p , muscle activation, $a(t)$ and three degrees of history of muscle activation, $a_{1H}(t+\Delta t)$, $a_{2H}(t+2\Delta t)$, $a_{3H}(t+3\Delta t)$.

The output parameter must be known for training as well. The training output parameter for a network object was the muscle force and for its approaching to the real muscle force, the Virtual Muscle system was used, [2].

The network object was used for estimation of sensitivity inputs. By the observation of the sensitivity of input parameters for each from the four movement conditions (slow and fast movement unloaded, slow and fast movement with weight) was the network object the same in every event, only one observed input parameter was zero or constant value.

The two most insensitive input parameters to results and network topology are velocity of muscle shortening, v and force-velocity factor, Fv . The most sensitive input parameters are length of musculotendon, L_{MT} and muscle activation, $a(t)$. It is evident, that muscle activation include information about muscle state and work, and can describe different situations as for example the same velocity of muscle shortening with different loading of muscle. This finding corresponds with knowledge, if a muscle activation parameter has zero value, muscle can not produce active force. All of the other input parameters have, in this case, similar influence on results and the neural network topology.

References:

- [1] DE LUCA, C.L.: *The use of surface electromyography in biomechanics* Journal of Applied Biomechanics 13, 1997, pp. 135–163.
- [2] CHENG, E.J. – BROWN, I.E. – LOEB, G.E.: *Virtual muscle: a computational approach to understanding the effects of muscle properties on motor control* Journal of Neuroscience Methods 101, 2000 pp. 117–130.
- [3] GARNER, B.A. – PANDY, M.G.: *Estimation of musculotendon properties in the human upper limb* Annals of Biomedical Engineering 31, 2003, pp. 207–220.
- [4] VEJPUŠTKOVÁ J. – VILÍMEK M.: *A muscle forces prediction using learning artificial neural network* Biomechanics of man 2004, 2004, pp. 94.

This research has been supported by MSM6840770012.

Corticothalamic Model of Human Brain

Radek Novák, Karel Hána*

novakr@fel.cvut.cz

Department of Radioelectronics, Faculty of Electrical Engineering, Czech Technical University in Prague, Technicka 2, 166 27 Prague 6, Czech Republic

*NMR laboratory, Institute of Biomedical Engineering of the Czech Technical University in Prague, Studnickova 7, 120 00 Prague 2, Czech Republic

Human brain is with no doubt one of the most complicated systems that mankind ever encountered. It integrates all somatic functions (metabolism, endocrinic regulations, immunity, cardiovascular and gastrointestinal systems, etc.), psychic functions (vigility, reactivness, sleep, memory, etc.) and its own systems.

Electrical activity is probably generated by synchronous and synphasic activity of electrical impulses of many neurons in cortex and deep brain centers. This synchronicity is ensured partially by the cortex itself but mainly thalamus and to certain extent even septal nuclei and hippocampus. The rythm generated by cortex is irregular and is expressed basicaly in slow waves area whereas more regular thalamic rythm is prominent in faster wave areas. Electrical activity is measurable by scanning the electroencephalogram (EEG) from the head surface.

The most interesting seems to be further study of EEG activity with the use of a model for prediction of the EEG spectre shape and for consequent design of EEG data compression, recognition of neurophysiological abnormalities incl. light brain disfunctions (ADHD) etc.

In our proposal we consider model simulations presented by Wright and Liley. Their investigations led to more advanced methods of implementation incl. wave equations mentioned by Robinson for instance.

In later years there were various improvements implemented into the mentioned models, in particular by adding more physiological parameters that describe the brain anatomy more precisely. (Liley, Wright and Rennie).

The model constructed by us is based on real human brain anatomy and physiology that was later reviewed and broaden by Rennie. The proposal consists from three basic structures (submodels) – main, thalamic and cortical. He main submodel comprises the manner of basic structures such as excitatory star and pyramidal neurons or inhibitory star neurons. In other submodels the manner of particular interconnections are specified, incl. local and global responses between cortex and thalamus.

References:

- [1] J.J.WRIGHT: *Simulation of EEG: dynamic changes in synaptic efficacy, cerebral rhythms, and dissipative and generative activity in cortex*, Biol Cybern 81, 1999 pp. 131-147
- [2] J.J.WRIGHT, D.T.J.LILEY: *A millimetric-scale simulation of electrocortical wave dynamics based on anatomical estimates of cortical synaptic density*, New Comput Neural 5, 1994 pp. 191-202

-
- [3] P.A.ROBINSON, P.N.LOXLEY, S.C.O'CONNOR, C.J.RENNIE: *Modal analysis of corticothalamic dynamics, electroencephalographic spectra, and evoked potentials*, Phy Rev E 63, 2001 041909
- [4] P.SUFFCZYNSKI, S.KALITZIN, G.PFURTSCHELLER, F.H.LOPES DA SILVA: *Computational model of thalamocortical networks: dynamical control of alpha rhythms in relation to focal attention*, Int J Psychophysiol 43, 2001 pp. 25-40

Intelligent Systems in Medicine

L. Lhotská, J. Macek, J. Rieger, V. Chudáček

lhotska@fel.cvut.cz

CTU, Faculty of Electrical Engineering, Dept. of Cybernetics
Technická 2, 166 27 Praha 6

Medical and biomedical applications are particularly suitable for successfully applying computational intelligence (CI) tools and techniques, due to the nature of the domain. Any relevant information about these problems is the prior domain knowledge, usually incomplete, and input-output instances of the system's behaviour, which is also incomplete. Therefore, in many cases, hybrid combinations are capable of describing an approximate reasoning for these domains. Hybrid computational intelligence is defined as any effective combination of intelligent techniques that performs in a superior or competitive way to simple standard intelligent techniques. Generally we could define two types of hybrid systems, namely systems that combine two or more well-known intelligent techniques in a methodological manner in order to obtain a superior intelligent performance in complex domains of application, and systems that combine a well-known intelligent technique and a standard mathematical or heuristic method, in order to effectively handle complex problems, still preserving the intelligence of the overall approach.

In the medical domain, data exists in various forms – single numerical values, non-numerical expressions, measured signals (e.g. ECG, EEG, EMG). In this research we have focused on automatized processing of long-term recordings of measured signals, in particular ECG and EEG. One of the most important aspects of the ECG and EEG classification systems is reliable analysis of ECG and EEG records respectively, which enables significant values to be identified on the measured signal. This analysis is a necessary condition for correct classification. In both cases we use hybrid intelligent systems combining several methods – mathematical transforms, clustering, soft computing and machine learning methods. The standard procedure is following: first step is application of mathematical transform (wavelet, Fourier) for extraction and/or calculation of characteristic attributes of the signal. Then clustering is used for class determination (in case we do not have a training set developed by an expert). Final step is development of models using one or several learning methods - in our study decision trees, fuzzy rules, neural networks, kNN and fuzzy kNN classifiers.

For ECG signal preprocessing we have used the wavelet transform. It has proven to be a good tool for ECG signal analysis. It achieves a sufficiently high level of reliability – about 80 per cent. It enables to detect required values of selected attributes in few steps, which is important from the point of view of time required for processing. The extracted values are then used as input values for a classification system. We have used decision tree induction and successive classification with the See5 program. We have verified the suitability of classification using decision trees for different numbers of attributes and classes. Then we have made a comparative study using fuzzy rules [1]. FURL (FUZZY Rule Learner), a theory revision approach to fuzzy rules learning based on the Hierarchical Prioritized Structures (HPS), has been used. FURL's natural tendency to produce a relatively large number of rules can be reduced in some specific domains by employing negated antecedents. While decision trees decompose the feature space by means of hypercubes, fuzzy rule sets represent classes through more complex membership functions. On the contrary of other interpolative approaches (i.e. neural networks) fuzzy rule sets employ a symbolic formalism that explains more clearly the learned knowledge. Moreover, they provide a soft classification that is suited to cope either with the uncertainty in the data or in the diagnostic knowledge. The initial

partitioning is decisive in obtaining more compact rule sets. Comparing results of both approaches the FURL reached lower classification error, on the other hand it generates greater number of rules than the decision tree.

The EEG signal is more complex, and thus it requires more steps of pre-processing. The first step is the adaptive segmentation that divides the EEG signal into stationary segments. When the signals are segmented, all attributes are calculated, some of them in time domain, some of them in frequency domain. In this step, we have employed the Fourier transform. The extracted values are used as input values of a classification system. In our case study we have used cluster analysis, neural network, kNN and fuzzy kNN classifiers. The developed system has been tested using real EEG signals. In the first experiment the signal has contained epileptic graphoelements [2]. Classification into two classes has been used. Based on individual experiments we can compare properties of applied methods for EEG processing. First test has been aimed on evaluation of impact of the value of constant k in k -NN algorithm and K in fuzzy k -NN with K -NN learning. The classifier reaches better results with higher value of k . However, if k exceeds a certain limit the classification error increases again. From the tests it has followed that the most suitable values of k are 5, 7 or 9. The system has reached very good results in detection of graphoelements. The whole processing has reached mean testing error of 6%. In the second experiment we have used real sleep EEG recording for which the classification has been known (in total 10 classes) [3]. For segmentation, combination of non-adaptive and adaptive segmentation has been used. Length of segments for non-adaptive segmentation has been set up to 32 seconds (at sampling rate of 256 Hz 8192 samples correspond to 32 seconds, this value has been selected with respect to successive computation of FFT). Intervals containing artefacts have been determined by adaptive segmentation. With respect to the character of the application we cannot expect 100% success rate. When requiring exact classification we reach success rate of approximately 80%. When allowing tolerance of one level of sleep depth the success rate increases to 90%. More exact evaluation of the error has no practical sense because the manual estimation of classification done by an expert is burdened by a non-zero error according to his view.

It is necessary to stress that not only the selection of a pre-processing method is a very important step in data mining process, especially when working with continuous signals, but also careful generation of the training set. In such complex tasks as classification of ECG or EEG records, experience of a human expert that can modify, for example, a training set generated by cluster analysis may contribute to more successful classification.

References:

- [1] MACEK, J. – LHOTSKÁ, L. - PERI, D.: *Evaluation of ECG: Comparison of Decision Tree and Fuzzy Rules Induction*. Cybernetics and Systems, ASCS, 2004 pp. 713-718
- [2] KOSAŘ, K. – LHOTSKÁ, L.- KRAJČA, V.: *Classification of Long-Term EEG Recordings* Biological and Medical Data Analysis, Springer Verlag, 2004, pp. 322-332.
- [3] RIEGER, J. – LHOTSKÁ, L., KRAJČA, V. - MATOUŠEK, M.: *Application of Quantitative Methods of Signal Processing to Automatic Classification of Long-Term EEG Records* Biological and Medical Data Analysis, Springer Verlag, 2004, pp. 333-343.

This research has been supported by MŠMT grant No. MSM 210000012.

Driver's Vigilance Identification by Means of RBF Neural Network - Influence of Artefacts

M. Mráz, K. Hána*, M. Šnorek

m.mraz@fel.cvut.cz

Department of Computer Science and Engineering, Faculty of Electrical Engineering, Czech Technical University, Technická 2, 166 27 Prague 6, Czech Republic

*Institute for Biomedical Engineering, Czech Technical University, Studničkova 7, 12800 Prague 8 - Albertov, Czech Republic

This paper is focused on the issue of the vigilant state (level of concentration) of a man based on EEG signal processing in neuronal network RBF. A specific area of interest is influence of preprocessing of training patterns for neuronal network on a quality and consequent recognition of the state of wakefulness in tested samples.

All experiments described in this paper are derived from the Vigilant car project conducted at Center for Biomedical Engineering of CTU in Prague and "Detection of a drop in drivers concentration" conducted at the Laboratory of System Reliability" at the Transport Faculty of CTU in Prague, both in 1999-2004.

The target of these experiments was to detect the state of fatigue of a driver from biological and other signals and warn him in case of the danger of a micro-sleep. There were always two long-distance rides (Prague-Pilsen) undertaken, one in vigilant state, the other after 24hours of sleep deprivation. The videorecordings of the driver were taken in both cases too beside the standard biological signal monitoring such as EEG, EKG, EOG, etc. From each experiment there are therefore 2 data files (d-files) available, one of the vigilant state drive and second of the fatigue state.

The state of the driver is detected from a spectral analysis of the EEG outcome together with the video recording in both drives. The procedure of the fatigue recognition consists of two steps: the first is the preparation of the training and testing samples for neuronal network based on the data acquired from vigilant and fatigue drives of some of the drivers, the second is the very training of of this network and testing of its capability to learn in samples that it did not learn beforehand. In preparation of the training samples the selected EEG channel is via FFT (with 2 or 4 sec frame) translated into a sequence of patterns comprising output or amplitude in frequential ranges delta, theta, alpha, beta with potential types of preprocessing none-percentage-norming, resulting in 4-element input vector that is evaluated by 2-element output vector (1.0) or (0.1) depending on the vigilant/fatigue state of the tested person. The state is determined based on the file with the time characteristics of the fatigue evaluated by the team of psychologists from the videorecording and was assessed once in each minute. The state of fatigue was evaluated by point ranging from 1 to 5 (1-vigilance, 5-fatigue) and the final decision about the state of the driver was judged according to passing beyond a given threshold value (e.g. 2.7 for instance).

The highest level of the recognition in tested samples (in one driver with one EEG channel) is 80%, in some cases only 60%, eventually even less. As far the ways of preprocessing of the training and testing samples are concerned, the combination of 2 main parameters were used: firstly the result type of FFT (4 element array of output values in delta-beta ranges or of amplitudes), secondly the type of preprocessing modes none (direct output or amplitudes in given ranges) / percentage (the sum of the 4 gives 100%) / norming (each of the numbers is presented in % related to min. and max. value of the number at this position in all file). There is an evidence that use of amplitudes is more successful in evaluation of testing samples rather than the use of output values and so is the use of norming and percentages rather than no preprocessing. The differences in various types of preprocessing are basically only in units of %. However, there are other possible ways of preprocessing available: for example the use of only theta, alpha and beta ranges (amplitude in delta is highest in all samples) or the use of coupled patterns delta+theta, alpha+beta, delta+theta/alpha+beta. Finally, it is necessary to mention that the level of vigilance assessed from EEG is rather complicated and is a subject for an experienced neurologist.

References:

- [1] R. BITTNER, K. HÁNA, L. POUŠEK, P. SMRČKA, P. SCHREIB, P. VYSOKÝ: *Detecting of Fatigue States of a Car Driver*, International symposium on Medical Data Analysis ISMDA 2000, Frankfurt am Main, Springer Verlag, 2000
- [2] M. NOVÁK, J. FABER, Z. VOTRUBA, T. TICHÝ, P. SVOBODA: *Problémy spolehlivosti interakce řidiče (pilota) a dopravního systému*, výzkumná zpráva č. LSS 104/2001, Společná Laboratoř spolehlivosti systémů, katedra řídicí techniky a telematiky, fakulta dopravní ČVUT Praha + Ústav informatiky AV ČR, 2001
- [3] J. FABER, Z. VOTRUBA, M. NOVÁK, M. HONCŮ: *Omezení spolehlivosti interakce řidiče s vozidlem a jeho technické, zdravotní a ekonomické důsledky*, Transportation and Telecommunication in the 3rd Millennium, 10th Anniversary of the Foundation of the Faculty Transportation Sciences, Prague, May 26-27, 2003
- [4] T. TICHÝ, Z. BUREŠ: *The problem of detection of micro-sleep on human operator*, Research Report No. LSS 113/2001, Orlando, Florida, USA, 2001

Method and Technological Tool for Early Non-Invasive Diagnostics of Bronchogenical Carcinoma by Means of Temperature Measuring in Air Passages

J. Holčík, K. Hána, P. Smrčka, J. Kašpar

holcik@ubmi.cvut.cz

Institute for Biomedical Engineering, Czech Technical University, Technická 2, 166 27
Prague 6, Czech Republic

Lung cancer is the leading cause of cancer-related mortality in the whole world. Non-small-cell lung cancer accounts for 80% of all cases, with the remaining 20% presenting as small-cell lung cancer. Non-small-cell lung cancer is composed of the following three major histologic subtypes: (1) squamous cell carcinoma, (2) adenocarcinoma, and (3) large-cell undifferentiated carcinoma. Adenocarcinomas can be further subdivided histologically into four less distinct subtypes: acinar, papillary, mucinous, and bronchioloalveolar carcinoma. The varied clinical and radiographic manifestations of bronchioloalveolar carcinoma often lead to an incorrect diagnosis of pneumonia and possibly significant delays in obtaining appropriate diagnosis.

In this paper we would like to present methods and experimental results concerning developed instrumentation and data processing methods for early and non-invasive diagnostical method for detection of bronchogenical Carcinoma by temperature measuring in air passages. On this place it is necessary to mention main methodology previously used – bronchoscopy. It is one of the diagnostical methods of bronchogenic carcinoma. In the past, bronchoscopy played a limited role in the staging of bronchogenic carcinoma, and the major use of bronchoscopy was to assess the T (tumor) status. Method proposed in this paper extends preliminary results obtained by Votruba et al. (2003) and may provide cheap and early diagnosis of Bronchogenical carcinoma. The method is based on measurement of surface temperature in lung cancer. Numerous reports have been published about the staging of lung cancer for example by CT scan, in particular about its usefulness in evaluating the nodal status. The general conclusion is that the CT scan, when used to evaluate the mediastinum, is very sensitive, but not too specific.

Bronchoscopy is an examination that allows a doctor to see inside the airway. During bronchoscopy, an instrument called a bronchoscope is used to look at the throat, larynx, trachea, and lower bronchial airways of the lungs. Bronchoscopy may be done to: (A) Identify problems that may be causing inflammation and bleeding. (B) Diagnose certain lung diseases. This is done by collecting samples of lung tissue for biopsy or by collecting mucus (sputum) samples to be examined in a lab for specific abnormalities or infections. (C) Diagnose and determine the extent of lung cancer – it is our case. (D) Remove foreign objects or thick mucus that may be blocking the airway. (E) Destroy growths in the airway.

Two different types of bronchoscopes may be used, depending on why the procedure is being done.

1) A flexible bronchoscope is a long, thin tube that contains many small, clear fibers or a small camera that can transmit light images as it bends. The flexible bronchoscope is used more often than the rigid bronchoscope because it is usually safer, does not require

general anesthesia, is more comfortable for the person, and offers a better view of the small airways. Small samples of tissue can also be removed using a flexible bronchoscope.

2) A rigid bronchoscope is a straight, hollow metal tube that is used when there is bleeding in the airway that could block the flexible scope's view, to remove large tissue samples for biopsy, to clear the airway of foreign bodies (such as a piece of food) that cannot be removed using a flexible bronchoscope. Special procedures, such as widening (dilating) the airway or destroying a growth using a laser, are usually done with a rigid bronchoscope.

Bronchoscopy may be used diagnostically to detect the cause of symptoms such as blood-tinged sputum (hemoptysis), wheezing, or difficulty breathing, evaluate abnormalities such as nodules or growths found on chest X-rays. Biopsies can help diagnose certain types of cancer or infection. Obtain samples of secretions or mucus in the airway to help diagnose certain lung problems, evaluate the airway after a traumatic chest injury and evaluate the extent of previously diagnosed lung cancer.

Using our equipment, it was measured (by dr. Votruba in hospital Na Homolce, Prague) the surface temperature of the tumors in patients with primary lung cancer, using a flexible bronchofiberscope (this is big advantage) and a thermometer BETATHERM. The thermometer was inserted into the aspiration channel of the bronchofiberscope, and temperature was studied under bronchofiberscop located in the various portions of the lung where the carcinoma provably was and provably was not (distinguishing by visual observation). Lung cancer showed a significantly higher surface temperature. The method is very promising and our technical equipment and data processing software is usable for this purposes. In the near future, much more work will be done in order to prove results on wide sample of patients.

References:

- [1] T. OGHIMI, S. AKIYMA, K. SHIMOKATA: *Measurement of surface temperature in lung cancer*, Lung Chest, January, No. 1, 1982, pp. 62-66.
- [2] T. SCHULTEK, J. BRAUN, K.J. WIESSMANN, W.G. WOOD *Bronchoalveolar lavage. The humoral parameter spectrum in bronchial carcinoma and chronic bronchitis* Dtsch Med Wochenschr, Feb 28, 1986, pp. 333-337
- [3] M. SHAHID, A. MALIK, R. BHARGAVA *Prevalence of aspergillosis in chronic lung diseases*, Journal of medical Microbiology, Vol. 19, No. 4, 2001, pp. 201-205
- [4] J. RÉMY, M. JARDIN, F. BONNEL, P. MASSON *La tomodensitométrie spiralee (hélicidale) en pathologie trachéobronchique*, Journal de radiologie, Vol. 81, 2000, pp. 201-216

This work is based upon work sponsored by the CTU grant No. CTU0416733

Wear Resistance Evaluation of Implants with DLC Coat

R. Sedláček, J. Rosenkrancová

radek.sedlacek@fs.cvut.cz

Laboratory of Biomechanics, Department of Mechanics, Faculty of Mechanical Engineering,
Czech Technical University, Technická 2, 166 27 Prague 6, Czech Republic

No known surgical implant material has ever been shown to be completely free of adverse reactions in the human body. However, long-time clinical experience of use of the biomaterials has shown that an acceptable level of biological response can be expected, when the material is used in appropriate applications. This article deals with very specific wear resistance testing of the bio-compatible and bio-stable materials used for surgical implants. The abrasion is indispensable parameter for evaluation of the mechanical properties. This type of testing is very important for appreciation of new directions at the joint replacement design (for example in total knee replacement). The special experiments were carried out in collaboration with company Walter Corporation - developing and producing bone-substitute biomaterials and implants.

The titanium alloy with DLC coat and UHMWPE is a new combination of materials used for surgical implants. The DLC coat (Diamond-like Carbon) was created by combination two methods – Plasma Assisted Chemical Vapour Deposition and Ion Beam Mixing. This surface coat was made in laboratory of Physics. The special wear resistance test with the first pair of these new materials was carried out according to ISO 6474:1994(E) Implants for surgery – Ceramic materials based on high purity alumina. International Standard deals with evaluation of biocompatible and bio-stable materials. These materials are used for production of bone and orthopaedic joint components replacements. The standard requires a long-time mechanical testing at which a complete volume of worn material is evaluated. The test conditions, requirements on the testing system and specimens' preparation are closely determined. For the specimens treatment and their evaluation, a procedure is assessed which ensures the testing objectivity.

The method is based on loading and rotating two pieces from biomaterials (fig. 1, 2). A ring from titanium alloy (Ti_6Al_4V) with DLC coat is loaded onto a flat plate from UHMWPE. The axial load that is applied on the ring is all the time constant. The ring is rotated through an arc of $\pm 25^\circ$ at a frequency of (1 ± 0.1) Hz for a given period of time (100 ± 1) hours. There is distilled water using as the surrounding medium.

The special jigs were used for fixing both specimens during testing. These jigs have to be able to undergo oscillatory rotation of the ring specimen about fixed axis using a sinusoidal or near-sinusoidal rate of change of angle. The disc-holding device is equipped with the especial joint to ensure the plane of the disc surface coincides with the plane of the ring surface at all times during the test.

As a measure of wear resistance is determined and used volume of the wear track on the disc. The wear track cross-sectional area is analysed from measured profile. The volume is calculated from this area. The profile measurement of the tested specimen was carried out using a specially adapted assembly. To determine the vertical position of points on the disc was used the digital drift sight MAHR EXTRAMESS 2001, with the sensibility of $0.2 \mu\text{m}$, placed in a sufficiently stiff stand. A positioning cross-table (ZEISS), containing a make-up piece (in which the disc was inserted), served for the disc shifting. The cross-table is movable in two axes by means of two micrometric screws. The shifting sensitivity is 0.01 mm . Measured data were registered in a table prepared in advance.

The experiment was carried out on the top quality testing system MTS 858 MINI BIONIX placed in “Laboratory of Biomechanics of Man” at the Czech Technical University in Prague.

The final parameters obtained in this test - the wear track on the discs and standard deviation - were calculated

Volume of the wear track is $6.61 \pm 0.21 \text{ mm}^3$.

The test was executed with only first pairs of specimens, because of obtaining objective information about wear resistance for this combination of materials. The resulting volume describes one from the mechanical properties and shows that this new combination of biomaterials is suitable for using as a surgical implants.

We obtained the objective information about wear resistance for these combinations of materials. The resulting wear volume indicates the amount of elements that are loosening during loading of the bone substitute implant in human body and describes one from the mechanical properties.

For next development is purposeful to finish the full test as is required in international standards – that means with five pairs of specimens. In near future is suitable to create database of this parameters for other combinations of bone-substitute materials.

References:

- [1] SEDLACEK, R. - ROSENKRANCOVA, J.: *The Wear Resistance Testing of Biomaterials Used for Implants*, In Bioceramics - 16, International Society for Ceramics in Medicine (ISCM), Porto, Portugal, 2003, pp. 703 – 706.
- [2] SEDLACEK, R. - ROSENKRANCOVA, J.: *Experimental Evaluation of Biomaterials – PolyEtherEtherKetone*, In 20th DANUBIA-ADRIA SYMPOSIUM on Experimental Methods in Solid Mechanics, Scientific Society of Mechanical Engineering, Győr, Hungary, 2003, pp. 164 - 165.
- [3] SEDLACEK, R.: *New Experimental Equipment in Mechanical Testing Laboratory*, Summer Workshop of AppliedMechanics, 2004 pp. 281 - 289.
- [4] SEDLACEK, R. - ROSENKRANCOVA, J.: *Experimental Analysis of Tribological Properties of Biomaterials Used for Orthopedical Implants*, Canadian Society for Biomechanics, Halifax, Nova Scotia, Canada, 2004, pp. 178-179.

This research has been supported by the Ministry of Education of Czech Republic project No. MSM 210000012.

Laser Beam Interaction with Material during the Production of Stents

Ing. Petr Císařovský, Prof. Ing. Jiří Dunovský, CSc.

petr.cisarovsky@fs.cvut.cz

Faculty of Mechanical Engineering CTU, Technická 4, 166 07 Praha 6

*Faculty of Transportation Science CTU, Horská 3, 128 03 Praha 2

This paper deals with the interaction of the laser beam and stent's material during their production. The stents are used in the case of perfusion defects in the whole cardiovascular system. The stents are produced by different technologies and from different materials. This work pays attention to the stents produced from the Ni-Ti alloy by Nd:YAG laser.

In these days, many more stents are needed, whether it concerns biliary, pancreatic or colonic stents. Their production is difficult and time consuming, and because of the high accuracy required manufacturers often turn to new progressive methods of production. One of them is the production with the help of lasers.

The use of lasers in the production of body implants has the advantage of the accuracy, great repeatability and a small heat affected zone.

Lasers are divided by different aspects. One of the main aspects is active medium; according to this, lasers are solid-state, semiconductor, gas and chemical. Most frequently used lasers in industry are Nd³⁺:YAG a CO₂.

The word stent derives from a dentist, Dr C.T. Stent, who in the late 1800's developed a dental device to assist in forming an impression of teeth. Nowadays, the term stent is reserved for devices used to scaffold or brace the inside circumference of tubular passages or lumens, such as the esophagus, biliary duct, and most importantly, a host of blood vessels including coronary, carotid, iliac, aorta and femoral arteries. Stenting in the cardiovascular system is most often used as a follow-up to balloon angioplasty, a procedure in which a balloon as placed in the diseased vessel and expanded in order reopen a clogged lumen (called a stenosis). These balloons are introduced percutaneously (non-surgically), most often through the femoral artery. Ballooning provides immediate improvement in blood flow, but 30% of the patients have restenosed within a year and need further treatment. The placement of a stent immediately after angioplasty has been shown to significantly decrease the propensity for restenosis.

Stents are also used to support grafts, e.g. in the treatment of aneurysms. An aneurysm is caused by the weakening of an arterial wall, that then balloons out and presents a risk of rupture. Surgical repairs are often difficult. With the endovascular approach, a graft is placed through the aneurysm and anchored in the healthy part of the artery at least at the proximal neck of the aneurysm. Thus, blood is excluded from the aneurysm sack. The grafts are typically supported and anchored by self-expanding stents structures.

Most stents today are 316L stainless steel, and are expanded against the vessel wall by plastic deformation caused by the inflation of a balloon placed inside the stent. Nitinol stents, on the other hand, are self-expanding – they are shape-set to the open configuration, compressed into a catheter, then pushed out of the catheter and allowed to expand against the vessel wall. Typically, the manufactured stent OD is about 10% greater than the vessel in order to assure the stent anchors firmly in place. Stents are made from knitted or welded wire, laser cut or photoetched sheet, and laser cut tubing.

Binary alloy TiNi, known also by the original name NITINOL is one of the series of metal systems, which embody formative memory phenomena. The nickel and titanium alloy or if needed its ternary variants doped by copper, iron, chromium etc., has the best combination of properties for practical purposes, the formative memory behaviour is a phenomenon connected with non-diffusion phase transformation of the martensitic type. The control of the relevant transformation characteristics creates the fundamentals of effective use of materials with these properties in technical practice.

From the mechanical point of view, the material exhibits the return to the original configuration only by change of temperature or in another variant by superelastic behaviour and during deformation the material is able to unfold relatively considerable forces. These characteristics, accompanied by excellent corrosion resistance and biocompatibility predetermine this material for a wide use in many branches of electrotechnics, mechanical engineering, robotics and not in the last in medicine.

It is possible to produce the NiTi alloy in several structural forms, which will differ by a slight difference of chemical composition and which are strongly affected by thermal and mechanical treatment. The deciding parameter for selecting a suitable structural type is the final object of application and the working temperatures at the point of setting. The temperature of termination of the austenitic transformation can vary at intervals $A_f = -200$ to $+150^\circ\text{C}$ depending on chemical composition.

The most evident property of superelastic Nitinol is its flexibility, which is 10 to 20 times higher than for stainless steel, this means that setouts, still elastic after an 11% deformation may be seen. This flexibility has its role for some near the surface application stents, as are carotides and femoral arteries, when vessels may be stressed by external pressure, which could cause warping of conventional stents. Such deformation has been observed in stainless steel stents and it may have serious effects.

References:

- [1] DUERIG, T., PELTON, A., STOCKEL, D.: *An overview of nitinol medical applications*, Elsevier Science S.A., 1999
- [2] BROWN, STANLEY A., LEMONS, JACK E.: *Medical applications of titanium and its alloys : The material and biological issues*, West Conshohocken : American Society for Testing and Materials, 2002
- [3] ČÍSAŘOVSKÝ, P., DUNOVSKÝ, J., KOLAŘÍK, L.: *The interaction of the laser beam and material during the production of stents*, CO-MAT-TECH 2004, Bratislava: STU Bratislava, 2004 vol. 1, s. 222-226

This research has been supported by CTU 1084062.

Our Experiences with Tensile Tests of Arterial Layers

L. Horny *, H. Chlup, R. Sedlacek, S. Konvickova

horny@biomed.fs.cvut.cz

*Department of Mechanics, Faculty of Mechanical Engineering, Czech Technical University, Technická 4, 166 07, Praha 6, Czech Republic

In the last few years there has been a significant growth in interest in the mechanical properties of arteries and some other parts of the cardiovascular system. The reason of this investigation is that diseases of cardiovascular system cause the most of deaths in the mature countries. The knowledge of the mechanical properties of the cardiovascular system is very important in development of new diagnostic techniques, artificial organs and therapeutic methods.

Realistic information about constitutive relations of a human tissue is one of the most important input to our engineering computing models. There are a many papers which describe constitutive equations for human aorta where is this artery assumed as homogenous continuum. This assumption is not so realistic because of its structure. If we do not consider composite structure of particular aortic layers, we can distinguish three basic parts of aortic wall if we do not consider composite structure of each layer – each layer is difficult system of elastin, collagenous and smooth muscle fibres. There are intima (very thin inner layer which is not so important from mechanical point of view), media (the thickest layer) and adventitia, respectively. Each of them has own individual substructure which is based on composite configuration. We do not consider this composite composition in our paper.

Passive mechanical properties and constitutive equation of the arterial wall was studied by many authors, Fung, Humphrey, and Vorp for example. They performed uniaxial tensile tests in 70th. They observed basic mechanical properties during experiments with arterial wall considered as continuum. So, we can find many papers which describe mechanical properties of components of arterial layers as are collagenous and elastin fibres, respectively. But we can not find papers which describe mechanical properties of each layer. So, this is the reason why we decided to perform uniaxial tensile tests with arterial layers, with media and adventitia respectively. We did not consider an intima as important from mechanical point of view because it is essentially one cells layer only and so can not take over important load.

We performed our experiments with 30 samples of human aortic arterial layers which we obtained from Department of Forensic Medicine of University Hospital Královské Vinohrady. We had 14 media layers and 10 adventitia layers. Because of viscoelastic properties of arteries, which include relaxation and creep, each experiment consists of two parts. First part was preloading; ten pre-cycles were performed in a rate 6 mm per minute. A loading to failure posed second part of experiment and loading rate was 4 mm per minute. The loading during pre-cycles was restricted by the value of axial force 1.8 N. Experiments were performed in axial and circumferential direction. Tests were performed on MTS 858 MINI BIONIX, MTS corp. USA, in our Mechanical Testing Laboratory accredited by ČIA.

Our results show that adventitia layer is more compliant than media layer. We do not observe important differences between male and female specimens. In case of media the mean maximum value of the strain was 35 pct but in one case of male media was achieved 60pct. Strain in circumferential direction. Linear regression with polynomial regression function was performed and we obtained as the most appropriate function a third degree multinomial. 6th degree multinomial was used in case of maximum strain 60 pct. A graph of 830

these functions has always distinct initial part with low value of slope and approximately linear part follows. This second part has higher values of the slope. A point of inflexion was found in at end of second part. Approximately similar results were found in case of adventitia. But we can say that adventitia layer is more compliant than media because here were achieved higher values of strain. We hope that our results and our constitutive equations will be useful in computing modelling. A comparison of the properties of the adventitia and media with all wall was performed too. We did not observed essential differences between them.

References:

- [1] ŠRÁMEK, B. - VALENTA, J. - KLIMEŠ, F.: *Biomechanics of the Cardiovascular System* Czech Technical University Press 1995.
- [2] VALENTA, J. - KONVIČKOVÁ, S.: *Biomechanika srdečněcévního systému* Vydavatelství ČVUT 1995,
- [3] BURŠA, J.: *Possibilities of Using Strain Energy Density Functions to Solve Stress State in Arterie* Biomechanics of Man 2000, 2000, pp. 141-145.
- [4] VAJDÁK, M. - BURŠA, J.: *Non-linear regression application in identification of hyperelastic constitutive models of soft tissues* National Conference with International Participation Engineering Mechanics 2003, 2003, pp. 284-289.

This research has been supported by GA CR 106/04/1181 and MSM 68 40 77 00 12.

New Approach to Evaluate Risk of Aneurysmatic Rupture

L. Horný*, J. Vtípil

horny@biomed.fsic.cvut.cz

*Departement of Mechanics, Faculty of Mechanical Engineering, Czech Technical University in Prague, Technická 4, Prague, 166 27, Czech Republic

Aneurysm of the abdominal aorta (AAA) is of the most serious cardiovascular diseases. It is described as a distortion of the sub renal part of the aorta by more than 50%. The most dangerous event accompanying the AAA is a rupture of the AAA (RAAA), which is a common cause of death in patients with AAA. Processes, which cause aneurysm, are influenced by many factors and the exact aetiology of all types of aneurysms is not yet known. Many factors play an important role during the development of the AAA, mainly heredity, hemo-dynamic factors, such as type of a blood flow, hypertension and other vascular diseases – arterioscleroses, vasculitis and various ischemic diseases. There is also a separate group of people with Marfan Syndrome or Erdheim disease. Currently in the cardiovascular surgery a definite indicator for a surgical solution (removal) or endo vascular therapy is the diameter of the AAA and the speed of growth of the aneurysm.

At this time a great interest is given to a calculation method (based specially on the method of end elements FEM or other methods of numerical mechanics), which should determine the stress state of the aorta's wall affected by the AAA. But calculating the tension so that the results can indicate accurately the borderline state of the aorta can be difficult with mainly material and geometrical difficulties. For this reason we have concentrated on other methods. Our goal is to find a method, which will predict the behavior of the AAA. The objective is to be able to answer this question: How is the aneurysm going to develop further? For this purpose we think it is possible to use the artificial neural network (ANN).

Neural network does not progress along classical algorithms but allows us to answer some questions, where there are no exact physical, chemical and other substances available. It manages to bypass this problem. In the propagator v1.0 program artificial network type back-propagation was created with these characteristics: Three layered ANN (one concealed layer), 7 entry neurons with linear transmission function, 1 entry neuron with sigmoid transmission function, 3 neurons in the concealed layer with sigmoid transmission function. The entry parameters for ANN learning were chosen from an average AAA selected from the last two measurements (with an interval between measurements of at least 100 days) and other information, which might influence the behavior of the AAA. (Age, ischemic heart disease, diabetes mellitus, hypertension, smoking, lung obstruction disease. The information about ICHS, DM, K, H, PP is entered with the help of logical 0 or 1. The value of the diameter of the aneurysm and the age appear in the model standardized from 0 to 1. From this information the patient receives an entry data vector. The exit model of the AAA is the scalar value of the diameter of the aneurysm 100 days after the last measurement, which was the entry to the ANN.

Mean difference between predictive values and real values was $m = 0.00015948$ [1] in the case of normalized values and $m = 0.0087714$ [mm] in the case of non-normalized data. We were obtained these results considering positive and negative values of predictive diameters. Another situation arises if we take the residue (deviation) only as a positive quantity. If we take non standardized residue (in mm) in their absolute value, we get for the

test file these parameters: $e=0,7404562 \approx 0,74$ mm chosen diameter Maximum network error was 1,94 mm and minimum 0,04 mm (non-normalized data).

References:

- [1] TŘEŠKA, V. A KOL.: *Aneurysma břišní aorty* Grada Publishing , 1999.
- [2] RAGHAVAN, M. L. - VORP, D. A. - FEDERÁLE, M. P. - MAKAROUN, M. S. - WEBSTER, M. W.: *Wall Stress Distribution on Three-Dimensionally Reconstructed Models of Human Abdominal Aortic Aneurysms* Jour. Vasc. Sur. 2000, pp. 760-769.
- [3] INZOLI, F. – BOSCHETTI, F. – KAPPA, M. – LONGO, T. – NUMERO, R.: *Biomechanical Factors in Abdominal Aortic Aneurysm Rupture* Eur. J. Vasc. Surg. 1993, pp. 667-674.
- [4] ELGER, D. F. – BLACKKETTER, D. M. – BUDWIG, R. S. – JOHANSEN, K. H.: *The Influence of Shape on the Stress in Model Abdominal Aortic Aneurysm* Jour. Biomech. Eng. 1996, pp. 326-332.

This research has been supported by MSM 68 40 77 00 12.

Determination of Mechanical Properties of Human Coronary Artery

J. Benes, L. Horny, S. Konvickova, H. Chlup*

horny@biomed.fsid.cvut.cz

Department of Mechanics, Faculty of Mechanical Engineering, Czech Technical University,
Technická 4, 166 07, Praha 6, Czech Republic

In a mature countries are diseases of cardiovascular system the most important cause of death. Major of this diseases has direct connection with coronary arteries and their mechanical behavior. In the last few years there has been a significant growth in interest in the mechanical properties of arteries and some other parts of the cardiovascular system. A number of publications focused on any mathematical models biological and chemical and mechanical behavior of some diseases was increased in the last few years too. The reason of this investigation is that diseases of cardiovascular system cause the most of deaths in the mature countries. The knowledge of the mechanical properties of the cardiovascular system is very important in development of new diagnostic techniques, artificial organs and therapeutic methods.

Realistic information about constitutive relations of a human tissue is one of the most important input to our engineering computing models. The most of papers which were published in the world is focused on the investigation of easy available animal samples, e.g. [1], [2]. If you want to use data obtained from experiments with human tissue in your computing model you usually have big problem to find them in the literature. It was the most reason why we decided to perform mechanical experiments with human coronary arteries to determine their constitutive relationships.

We built a special experimental system based on static pressure tests to measure deformations of arteries which are under loading. Basic loading were performed by internal pressure of liquid medium. The internal pressure was measured by pressure sensor. Loading was static during experiments. During our experiments we measured external diameter of artery by camera system. The measured artery was also subjected to an axial pre-stretch. An incompressibility condition was used to determine internal diameter of the artery.

Ordinary constitutive equation was replaced by a strain energy density function W . We used strain energy density function in Hayashi's shape (logarithmic), [3].

$$W = -C \ln(1 - \psi) \quad \psi = \frac{1}{2} (c_{11} E_1^2 + 2c_{12} E_1 E_2 + c_{22} E_2^2)$$

Where C , c_{11} , c_{12} , c_{22} are mechanical constants of constitutive equation and E_1, E_2 components of Green tensor of deformation. Parameters C , c_{11} , c_{12} , c_{22} were obtained by solution of equilibrium equation in radial direction in artery:

$$p_i = \int_{r_i}^{r_0} \lambda_r^2 \frac{\partial W}{\partial E_1} \frac{1}{r} dr$$

Where p_i is internal pressure, r_i, r_0 internal and external diameter and λ_l is circumferential stretch during loading. Material constants were obtained in this numerical values: $C = 10.6791$ kPa, $c_{\theta} = 8.9854$, $c_{zz} = 1.3872$, $c_{\theta z} = -0.0087$. Residual strain and stress were included to our computations.

References:

- [1] ŠRÁMEK, B. - VALENTA, J. - KLIMEŠ, F.: *Biomechanics of the Cardiovascular System* Czech Technical University Press, 1995.
- [2] FUNG, Y. – LIU, S.: *Changes of Zero-stress State of Rat Pulmonary Arteries in Hypoxic Hypertension* Journal of Applied Physiology, 1991, pp. 2455-2470.
- [3] MATSUMOTO, T. – HAYASHI, K.: *Stress and Strain Distribution in Hypertensive and Normotensive Rat Aorta Considering Residual Strain* Journal of Biomedical Engineering, 1996, pp. 62-73.

This research has been supported by GA CR 106/04/1181 and MSM 68 40 77 00 12.

Modelling of the Human Respiratory System

M. Rozanek, K. Roubik

rozanem@fel.cvut.cz

Czech Technical University in Prague, Department of Radioelectronics,
Faculty of Electrical Engineering, Technicka 2, Prague 6, 166 27, Czech Republic

Institute for Biomedical Engineering, Czech Technical University in Prague,
Zikova 4, Prague 6, 166 36, Czech Republic

Artificial lung ventilation (ALV) is a method that is often used in clinical practice. This technique is the most efficient method to treat acute respiratory failure. Despite the fact that conventional artificial lung ventilation (CV) is able to solve acute respiratory insufficiency in many cases, there still remain from 40 % to 60 % patients that do not take a profit from CV. Other ventilatory techniques are searched and studied in order to substitute CV especially as a "rescue" technique when CV fails. High-frequency ventilation (HFV) is one of the unconventional ventilatory regimens that is being tested in the treatment of acute respiratory distress syndrome (ARDS) in adult patients and is supposed to be more efficient in ARDS treatment than CV. These unconventional ventilatory strategies are very different from CV not only because of their principle, but also because of their totally different influence upon intrapulmonary conditions and gas exchange. Different effects of artificial ventilation can be observed when CV or HFV is used. Many parameters can influence the oxygenation, but it is very difficult to study their effect directly in the human body. Any direct measurements in the alveolar space, as well as measurements of ventilatory parameters changes along the bronchial tree, are practically impossible. Nevertheless, these parameters are essential for a rational control and further investigation of these unconventional ventilatory regimens. Investigation of the unconventional ventilatory strategies cannot be based on clinical trial studies only. Sophisticated and advanced methods of intrapulmonary conditions monitoring, the respiratory and chest wall mechanics measurement and evaluation of other parameters must be employed. These sophisticated methods comprise various modelling techniques of the human respiratory system that differs in the approach used. Therefore, deriving model of the respiratory system exactly corresponding with the reality can be the only possibility how to study influence of mechanical lung properties along the bronchial tree.

Our aim was to develop a model of the respiratory system in concordance with the anatomical structure of the lung with a possibility to study the effect of the inhomogeneous changes in the pulmonary mechanics upon the efficiency of both ventilatory techniques: CV and HFV. The model was supposed to be used for evaluation of intrapulmonary conditions and description of gas exchange, to assess them and evaluate their precision and suitability for use in the clinical investigation and practice. The airways begin with trachea and divide with each new generation by course of irregular dichotomy. It means that airways in the same generation have various length and diameter. The whole structure of the bronchial tree is very complex and not suitable for modelling because it is very difficult to describe this structure mathematically. Therefore the morphological model of Weibel [1] was used to gain the geometrical proportions of the airways. The irregularity in the dichotomy is considered as negligible thus the airways in the model have the uniform length and diameter in the same generation of the bronchial tree.

Most of the existing models of the respiratory system are very simple without any possibility to observe differences in the intrapulmonary conditions such as pressure and tidal

volume distributions inside the lung structure. Novel approach has been used to study the ventilatory parameters inside the lung structure for both CV and HFV. A mathematical model of the respiratory system has been developed as an electro-acoustic analogy of the respiratory system respecting its exact anatomical structure. All individual airways are represented by short acoustic capillaries with parameters computed using the common acoustic principles and the published lung morphometry measurements. Alveoli are represented by acoustic compliances computed from their proportions and the overall lung compliance. The final model has 23 airway generations and employs 67 108 859 individual components.

The following results were obtained from the conducted simulations. The airway resistance increase has no significant effect on the total lung impedance during CV, whereas the total lung impedance is substantially higher during HFV for the same airway resistance increase. The tidal volume distribution among the bronchial tree generations is worsted more during HFV compared with CV with increased airway resistance. It suggests that CV is more suitable ventilatory technique for the lung affected by the increased airway resistance in comparison with HFV. The alveolar compliance increase causes the total lung impedance growth during CV, whereas the resonant frequency is shifted during HFV. The total lung impedance remains unchanged during HFV and it is possible to maintain the tidal volume with the similar pressure amplitude applied to the airway opening in healthy lungs. HFV is more suitable technique to ventilate the lungs affected by the reduced alveolar compliance. The inhomogeneous changes in the pulmonary mechanics affects especially the tidal volume distribution along the bronchial tree compared with the changes in the total lung impedance. Several simulated parameters predicted by the models can be compared, as for example distribution of tidal volume among bronchial generations, distribution of airflow, etc. Approximately the same results (error is less than 4%) have been obtained from the presented model and a gas flow model [3]. In spite of the different modelling approach and methods of computation, both the models yield the same results.

The electro-acoustic analogy model is the first model suitable for the fast modelling of the intrapulmonary conditions along the real bronchial tree structure both during HFV and CV. The model is able to explain different behaviour of the respiratory system during these ventilatory regimens. Importance of the exact modelling occurs especially during HFV, where low tidal volumes are used and the mechanical parameters of the respiratory system play a significant role in efficacy of the artificial ventilation efficacy. The model is useful for introduction of HFV into the practice.

References:

- [1] JONGH, DE F.H.C.: *Ventilation modelling of the human lung* Delft University of Technology, 1995
- [2] ROŽÁNEK, M. - ROUBÍK, K.: *Influence of The Changes in Pulmonary Mechanics upon the Suitability of Artificial Lung Ventilation Strategy*. Acta Press, 2004, pp. 417-132.
- [3] ROŽÁNEK M, ROUBÍK K.: *Using the Simulations of the Human Respiratory System Model to Explain the Effects Observed in the Clinical Practice*. Orgit ltd., 2004, P4.16

This research has been supported by IGA CVUT No. CTU0410113 and GA CR 102/03/H086 and research program No. MSM 210000012 at CTU in Prague.

Section 13

CIVIL ENGINEERING

Limit States and Design of Materially Non-Homogenous Structures

J.Studnička, J.Macháček, J.Dolejš, A.Kuklíková

studnicka@fsv.cvut.cz

Department of Steel Structures, Faculty of Civil Engineering, Czech Technical University, Thákurova 7, 166 29 Prague 6, Czech Republic

The research project was focused on basic problems of behaviour of materially non-homogenous structures. The goals of project in theoretical modelling and experimental investigation of non-homogenous structures from steel, concrete and timber were achieved. The four main parts of research were:

- New types of shear connectors
- Integral bridges
- Timber and concrete structures
- Composite beams with undulated webs.

New Types of Shear Connectors

Perforated shear connector (perfbond) with circular openings have been originally developed in Germany twenty years before the end of last century. Very extensive experimental research into static load capacity was fulfilled during last years at CTU [4]. Now are commonly known and widely published all necessary formulas for calculation of characteristic and design load capacities for two basic types of perfbond connectors. Connectors can be and also are frequently used in practice of steel structures. The sophisticated computer model developed under frame of this research enables to calculate load capacity of any other type of perfbond connector [1].

For bridges is needed to know also fatigue load capacity of connector. The first experimental research was finished and computer model for fatigue behaviour of perfbond connector is under progress now.

New types of thin-walled shear connectors called Ribcon and Stripcon and fastened via powder actuated nails were tested in collaboration with Hilti CZ Company. Ribcon is a thin steel angle formed from 1.5 - 3 mm sheet, whose larger free leg is supplied with various perforations enabling penetrating of concrete and shorter leg is fastened by prescribed number of Hilti nails to a beam flange. Stripcon is made of cold formed steel strip of width 80 mm, with a shape corresponding to the wave of trapezoidal sheeting used as a formwork and fastened to a beam also by nails in its each valley. Based on series of push tests shear design resistances of Ribcon and Stripcon connectors were established, leading to certification of the connectors for use in the Czech Republic as the first country in the Europe.

Integral Bridges

Traditional beam-type bridges include expansion joints and bearings in order to accommodate the thermally induced movements. As practice shows, these structural members are the most vulnerable points in highway bridge construction. In case of integral bridges there are no expansion joints and no bearings between the superstructure and the substructure. The initial costs of these structures are therefore much lower and less demanding maintenance is required.

The analysis and the design of integral bridges are more sophisticated compared to traditional beam-type bridges because of the necessity of analysing the soil-structure interaction. Response of the structure is dependent on lateral earth pressure magnitude. And in turn, lateral earth pressure is a function of structure deformation. This means that the analysis of the structure must be iterative. In addition, there is non-linear relationship between horizontal earth pressures and deformations of a structure.

To analyse integral bridges it is possible to use many finite element methods. Computer program IM2004 being developed to simplify integral bridge analysis of these structures is shortly described in [3].

Timber and Concrete Structures

Timber beams can be connected with concrete deck into the non-homogenous composite structure. Moreover it is very advantageous solution especially for reconstructions and rehabilitations of old buildings with horizontal timber structures. Two advanced models for calculation of load capacity of timber-concrete beams were developed and verified compared with foreign experiments. New methods for testing of mechanical characteristics of old timber beams were established simultaneously. New type of shear connector was tested. Three composite beams will be tested having novel type of shear connector in short future.

Composite Beams with Undulated Webs

Novel structural forms in composite steel and concrete structures enlarge material base of modern structures and pertain to progressive trends in structural design. Recently some highly efficient elements were introduced into practice, namely steel girders with undulating web and thin-walled shear connectors called Ribcon or Stripcon, reported above.

Within the research project a joint use of both elements was investigated experimentally and theoretically. The investigation covered both full and partial shear connection to analyse full range of its use in structures. The possible application is envisaged in floor beams of multi-story buildings having larger spans (> 6 m) as contemporarily required for administrative buildings. Three real-size tests (7.5 m span) were performed, evaluated and compared with analytical results. Numerical non-linear analysis and further investigation into interaction of buckling of undulating web with a partial shear connection is under way.

The experimental investigation and evaluation of the results proved practical applicability of this new progressive structural element. While the strength of such girder corresponded well to common Standard design, the deflection was due to ductility and slip in the shear connection larger and needs a careful design. The results were fully published in [2].

References:

- [1] SAMEC, J. – STUDNIČKA, J.: *Model chování spřahovací lišty při statickém namáhání*, Stavební obzor 13, 2004, pp. 165–170.
- [2] MOTÁK, J. – MACHÁČEK, J.: *Experimental Behaviour of Composite Girders with Steel Undulating Web and Thin-walled Shear Connectors Hilti Stripcon*, Journal of Civil Engg. and Management, Vilnius,, 2004 pp. 45–49.
- [3] ROLLER, F. – STUDNIČKA, J.: *Soil-Structure Interaction of Integral Bridges*, IABSE Shanghai, 2004, pp. 206–207.
- [4] MACHÁČEK, J. – STUDNIČKA, J.: *Perforated shear connectors*, Steel and Composite Structures 2, 2002, pp. 51–66.

This research has been supported by grant 103/02/0008 of Czech Science Foundation.

Iron release from corroded iron pipes in drinking water distribution system

A. Grünwald, K. Slavíčková, M. Slavíček, B. Štátný

grunwald@fsv.cvut.cz

CTU, Faculty of Civil Engineering, Dept. of Sanitary and Ecology Engineering, Thákurova 7, 166 29 Praha 6

Drinking water distribution systems are primarily composed of iron and steel pipes that are subject to corrosion. Corrosion of system pipes has economic, hydraulic and aesthetic impacts, including water leaks, corrosion product buildup, increased pumping costs, high demand for chlorine and dissolved oxygen, biofilm growth and water quality deterioration (color, taste, turbidity). The corrosion scales present in corroded iron pipes restrict the flow of water, and can also deteriorate the water quality. The compounds usually found in iron corrosion scales include goethite (α -FeOOH), lepidocrite (γ -FeOOH), magnetite (Fe_3O_4), siderite (FeCO_3), ferrous hydroxide ($\text{Fe}(\text{OH})_2$), ferric hydroxide ($\text{Fe}(\text{OH})_3$), ferrihydrite ($5\text{Fe}_2\text{O}_3 \cdot 9\text{H}_2\text{O}$), green rusts (e.g. $\text{Fe}_4\text{Fe}_2(\text{OH})_{12}(\text{CO}_3)$) and calcium carbonate (CaCO_3) (1).

In the absence of any corrosion scales, corrosion of iron is the primary cause of iron release. The interaction of corroded iron surfaces with water quality are not completely understood. However, it is recognized that water quality parameters can influence iron release from corroded iron/steel pipes in distribution systems. Some of these factors include dissolved oxygen DO, pH, alkalinity, buffer capacity, water flow characteristics, temperature, water treatment practices, application of an inhibitor, and fluctuations in water quality.

Based upon circumstantial evidence linking elevated coliform bacteria counts in drinking water distribution systems, it was hypothesized that adsorption of humic substances by iron oxide containing corrosion products can stimulate and/or support biofilm development. The combination of humic substances and corrosion products led to an increase in biofilm biomass when free chlorine was not present, similar to conditions that occurs at distribution system dead-ends. The reaction between chlorine and iron oxide in corrosion products can reduce chlorine concentration in drinking water while also affecting the ability of chlorine to act on biofilm (2).

The development of bacteria in the biofilm is highly relevant for water quality, since these bacteria directly influence bacterial density in the bulk phase through detachment. Recent research suggest that using phosphate-based inhibitors for corrosion control contributes to improving the microbial quality of distributed water and enhancing compliance records, which may be the result of better maintenance of the chlorine residual along with the limitation of corrosion deposits. Phosphate, a bacterial nutrient like carbon and nitrogen, may also stimulate bacterial growth (3).

This research was conducted to assess the impact of different corrosion control programs on water quality. Specific objectives of the study were:

- To design a simple corrosion monitoring program
- To evaluate a current corrosion control program applied at a full scale conventional treatment plant

- To determine a corrosion control strategy that can minimize corrosion rates in a distribution system
- To evaluate its short term effects on bacterial water quality (bulk water and biofilm bacteria).

Three places were chosen as locations for corrosion monitoring and taken samples for the analysis of the main characteristics of the treated water from WTP Plav in South Bohemia.

The WTP Plav is a conventional water treatment plant that provides settling, coagulation, flocculation, sand filtration and disinfection with chloramines. Corrosion rates were measured using removable steel coupons and glass coupons to evaluate biofilm density. From pre-tests carried out, it was decided to use two exposure periods: 63 and 120 days. After this period the coupons were analyzed. Corrosion rate measured in crude water from Římov reservoir after 63 days exposition was $70 \mu\text{g.l}^{-1}$, in water after filtration $162 \mu\text{g.l}^{-1}$ and in final drinking water $60 \mu\text{g.l}^{-1}$.

References:

- [1] SARIN P., SNOEYINK V.L., BEBEE J., JIM K.K., BECKETT M.A., KRIVEN W.M., CLEMENT J.A.: *Iron release from corroded iron pipes in drinking water distribution systems: effect of dissolved oxygen*. Water Res. 38, 2004, pp. 1259 – 1269.
- [2] J. JUHA, J. KRÁSA, A. PRÁG, A. CEJNAROVÁ, D. CHVOSTOVÁ, J. KRAVÁRIK, HALLAM N.B., WEST J.R., FORSTER C.F., SIMMS J.: *The Potential for Biofilm Growth in Water Distribution System*. Water Res. 35, 2001, pp. 4063 – 4071.
- [3] BATTÉ M., KOUDJONOU B., LAURENT P., MATHIEU L., COALLIER J., PRÉVOST M.: *Biofilm responses to ageing to a high phosphate load in a bench-scale drinking water system*, Water Res. 37, 2003, pp. 1351 – 1361.

This work has been supported by the Czech Ministry of Agriculture grant No. 1G46036 and MŠMT grant MSM J04/98:211100002.

The Effect of Residence Time on the Biological Stability of Water in a Distribution System

A. Grünwald, N. Strnadová*, B. Šťastný, K. Slavičková, M. Slaviček

grunwald@fsv.cvut.cz

Department of Sanitary and Ecological Engineering, Faculty of Civil Engineering, Czech Technical University, Thákurova 7, 166 29 Prague 6, Czech Republic

*Department of Water Technology and Environmental Engineering, Institute of Chemical Technology in Prague, Technická 5, 166 28 Prague 6, Czech Republic

The basic function of water utilities is to provide uninterrupted supply of safe drinking water to the appropriate place. Water treatment and distribution systems have to be carefully designed and monitored to ensure the reliability of the quality of drinking water delivered to the users. Bacterial regrowth at the pipe walls of a distribution system can contribute to degrade this water quality. Many studies have been made to identify the principal factors influencing regrowth of heterotrophic bacteria in pipes of the distribution system. They have been identified as:

1. The concentration of organic substrate in the treated water that could be utilized by heterotrophic bacteria (BDOC),
2. The concentration of free residual chlorine in the distributed water,
3. The residence time of the drinking water in the distribution system from the treatment plant to the consumer
4. The water temperature
5. The characteristics of the material covering the distribution pipes.

Several papers have shown that the breakdown of organic matter in the pipes of water mains mainly take place at the interface between the water and the pipe surface, on which a high density of microorganisms accumulates (a biofilm). The increase in the number of bacteria in tap water may be explained by the growth and shear of the biofilm with transport of the detached organisms into the water. Proper monitoring of the microbiological quality of water in the distribution system also requires the development of hydraulic and biological models[1,2].

During the last years, different studies were carried out in full-scale distribution networks, focusing on the role of the biodegradable organic carbon (BDOC) in distribution systems. It was shown, that this parameter in the finished water was the major controlling factor of bacterial dynamics when free chlorine was depleted. The different studies agree to conclude that the control of biodegradable organic carbon remains one of the prime objectives to achieve biologically stable water. This solution, in addition to reduce bacterial growth by limiting the nutrient sources, offers two additional advantages: removal of organic matter initially reduces the formation of undesirable disinfection by-products (DBPs) during chlorination and also increases the stability of the chlorine residual in the distribution system by reducing chlorine demand.

This study was designed to monitor the water quality in the drinking water distribution system served by the Plav WTP. The sampling strategy chosen consisted of measuring two groups of parameters related to biomass, organic matter and residual chlorine concentration. To obtain a picture of the water quality, a large number of samples were collected from several points in the distribution system: WTP Plav, WT Hlavatce(inlet/outlet), WT Zdoba(inlet/outlet), WT Varta, Sudoměřice (inlet/outlet) and WT Hodušín(inlet/outlet).

BDOC parameter was used for evaluation of the biological stability of water in given distribution system. This parameter based on DOC analysis numerates the resistance of water to bacterial growth. BDOC concentrations were estimated as the difference of DOC concentrations measured before and after a 30 d incubation at 20°C with indigenous bacteria [2].

BDOC levels in raw water from WR Římov were between 0,19 and 1,07 mg.l⁻¹ (Ø 0,38 mg.l⁻¹) and at the outlet of the WTP Plav between 0,12 and 0,28 mg.l⁻¹ (Ø 0,20 mg l⁻¹), whereas in the outlet from WT Sudoměřice the values from 0,10 to 0,57 mg.l⁻¹ (Ø 0,36 mg.l⁻¹) were measured. It was shown, that the BDOC values in outlets from all water reservoirs were higher then in their inlets.

References:

- [1] MATHIEU L., BLOCK J.C., PRÉVOST M., MAUL A., DE BISCHOP R.: *Biological Stability of drinking water in the city of Metz distribution system*. J. Water SRT Aqua, 44, 5 1995, 230-239.
- [2] SERVAIS P., BILLEN G., LAURENT P., LEVI Y., RANDON G.: *Studies of BDOC and bacterial dynamics in the drinkung water distribution system of the northern parisian suburbs*. Sciences de l'Eau 5, 1992, 69 – 89.

This research has been supported by NAZV grant No. 1G46036 and MSM J04/98:211100002.

Application of Cooled Ceiling

V. Zmrhal

zmrhal@fsid.cvut.cz

Department of Environmental Engineering, Faculty of Mechanical Engineering, Czech Technical University, Technická 4, 166 07 Prague 6, Czech Republic

Radiant cooled ceiling is relatively efficient cooling system, which can be used to achieve optimal thermal comfort. Heat gains in rooms are dissipated by large-area water-cooled panels, which are installed into the soffit of the rooms. Airflow, which is supplied into the room, can be reduced to minimal amount of the fresh air. Theoretically, the radiant heat transfer between body and surroundings is preferable than convection heat transfer in the view of thermal comfort achieving and energy consumption. Paper deals with advantages and disadvantages of radiant cooled ceiling application. Especially paper presents cooled ceiling application in various type of buildings.

Sensible heat gains in spaces with thermal comfort requirement as offices, conference halls, museums, etc. is possible to remove by radiation cooling system. The minimum of fresh air is used for moisture reducing. Principal advantages and disadvantages of cooled ceiling systems are:

- Advantages:
- better comfort levels
 - low energy consumption
 - minimum fresh air supplying
 - less demands for air distribution
 - no noise
 - no risk of draft
- Disadvantages:
- capital cost
 - risk of condensation
 - the heat taken in vapour couldn't be drain of
 - capacity limitation

Inlet water temperature into the cooled ceiling has to be chosen to preserve condensation on surface (surface temperature of cooled ceiling have to be higher than dew point temperature of air). In principle the inlet water temperature t_{w1} is chosen ≥ 16 °C (Central Europe), maximally 20°C. Temperature difference between inlet and outlet cooling water is commonly $2 \leq \Delta T \leq 4$ K.

Cooling ceiling system is useful only for sensible heat gains removing. Latent heat gain is possible to remove by convection ventilation system only. Most often the cooled ceiling systems are combined with displacement ventilation. The air supply system is often 100% outdoor air system and works with minimum fresh air requirements.

Energy consumption is one of very discussed subjects in connection with higher energy cost. Many authors advert to energy saving possibility within the range 10 – 30 % in comparison with all air system.

The application of cooled ceiling system is limited. The limitations derive from advantages and disadvantages discussed above. Of course it's not possible to cover whole

ceiling. In practice it is possible to calculate with covering of 50 – 80 %. That's basic limitation of cooled ceiling application. Following paragraphs describes wide range application of cooled ceiling system in particular buildings.

Most frequent and optimal is application of cooled ceiling in offices. Offices in modern buildings with large glazing are exposed to heat gains from solar radiation. Also indoor heat gains like electrical appliances (PC, screen, copy devices, printers), lighting etc are present. Often, tempered air is supplied at a constant volume, and the room thermostat modulates the panel output. In some application, the panels are arranged for zone control, and the air system is designed to provide individual room control.

Over the last years the radiant panel systems are applied for hospital patient rooms. The system is well suited because it:

- provides thermally stable environment,
- is noiseless system,
- requires no mechanical equipment in the space,
- does not take up space within the room,
- is possible to use it for heating,
- does not pollute the space.

The piping system may have a two- or four- pipe design. Water control valves should be placed in the corridor outside the patient room so that they can be adjusted or serviced without entering the room. The system can be used in areas of the hospital occupied by mentally disturbed patients since no equipment is accessible to the occupant for destruction or self-inflicted injury.

Application of cooled ceiling panels in industry is not very common, but especially in Western Europe it is possible to found some using also in this area. Thermal comfort demands for people working in industry still increase and radiant cooled ceiling can be very efficient solution.

Cooled ceiling panels can be used in museums, airport terminals, convention halls etc. Over the last years the personalized ventilation was developed as a new ventilation system. Personalized ventilation is a ventilation system, where the minimum amount of fresh air is supplied directly into the breathing zone of people. But minimum amount of air doesn't satisfy to remove sensible heat gain in space. Therefore the system has to be combined with cooling system and cooled ceiling system could be a good alternative.

References:

- [1] V. ZMRHAL: *Thermal Comfort Evaluation in a Space with Cooled Ceiling (in Czech)*, In: Proc. of 16th National Conference Air-conditioning and ventilation 2004, 2004, pp. 108-115.
- [2] V. ZMRHAL, DRKAL F., HENSEN J., LAIN, M: *Low Energy Cooling Techniques for Retrofitted Office Buildings in Central Europe (in Czech)*, In: Proc. of 3rd National Conference SBTP 2004Proc. of, 2004, pp. 131-135.

Rotational Restraint Of Purlins – Effect Of Primary Loading

T.Vraný

vraný@fsv.cvut.cz

Department of Steel Structures, Faculty of Civil Engineering, Czech Technical University, Prague, Czech Republic

Cold-formed purlins are restrained by connected sheeting both laterally and rotationally. The stiffness of rotational restraint C_D , provided by connected sheeting to one flange of cold-formed beam, influences the behaviour of the beam: higher stiffness C_D leads to the reduction of stresses in the free flange and to the reduction of its buckling length in hogging moment areas. The stiffness C_D depends on primary loading of purlin q . Though, simple tests (recommended i.e. by [1]) do not cover influence of loading – they give the same C_D for gravity and uplift loading. The effect of loading on the purlin rotation can be determined by more complicated tests proposed and used by Lindner (e.g. [2]) or by presented theoretical method.

The proposed solution for determining the effect of the loading is based on analytical analysis, with relevant help of numerical modelling. FEM program ANSYS was applied for numerical calculations. The models compose of purlin (modelled by shell elements), the sheeting (modelled by beam elements in lateral direction) and their connection (modelled by contact and spring elements). The compression contact between the purlin and the sheeting is modelled by contact elements while the screw is modelled by the linear spring element. Contact elements are compression-only ones of infinite stiffness. The stiffness K_D of the linear spring element controls C_D - the relation was derived in [3]. Torsion at purlin supports is free in the model so that purlin rotation is controlled purely by stiffness C_D and it is constant along the purlin length. This model corresponds with standard test procedure.

Rotational stiffness C_D for zero loading q was set as input value by appropriate stiffness of spring connection elements. The aim of the study is to analyse the change of flange rotation and redistribution of contact forces in relation to the change of loading q . This redistribution causes the change of stiffness of rotational restraint. The results depend linearly on the ratios M_x/q and M_x/C_D where M_x is applied torsion moment per unit length of purlin.

Four different cases - Z- or C-sections under gravity or uplift loading - were defined and solved, and appropriate formulas were derived. The behaviour varies for listed cases and it is described in the following paragraphs.

Top flange of Z-shaped purlins is restrained against rotation by gravity loading so as the stiffness C_D needs not to be determined. The length of contact area between purlin and sheeting was determined and formula for determination was derived using numerical solution. Proposed new attitude gives favourable results compared to traditional approach.

Two different cases can occur for Z-shaped purlins under uplift loading: when lateral forces bring purlin into contact at the purlin web, the stiffness C_D is not influenced by loading; when contact takes place at the flange tip, the loading reduces C_D and the following formula was derived:

$$C_D = C_{D,0} \frac{k_h h}{b_a - k_h h} \quad (1)$$

where

$C_{D,0}$ is rotational stiffness C_D for zero loading q

k_h	ratio of lateral to primary loading, it is constant for each cross-section and it can be determined using [1]
h	depth of cross-section
b_a	width of top flange

For C-shaped purlins under the gravity loading it was found that loading q does not have any effect on force in the screws. Therefore loading q does not influence the stiffness C_D in this case. This consequence again gives favourable results compared to existing calculation methods.

For C-shaped purlins the uplift loading strongly reduces C_D . Formula (2) was derived:

$$C_D = C_{D,0} \frac{k_h h}{k_h h + b_a} \quad (2)$$

Proposed procedure can be used for determining the effect of loading on the stiffness C_D when basic value of C_D was determined by standard tests or by such calculation procedure that did not cover the effect of loading, e.g. author's method [3].

Modified model of real purlin with restraint of rotation in supports and without direct torsion load served for verification of basic results. Distribution of forces to supports corresponds to [4]. Purlin rotation is function of span length in this case but the principle of behaviour is the same as in basic analysed model.

References:

- [1] EN 1993-1-3 *Design of steel structures, Part 1.3: General rules, Supplementary rules for cold-formed thin gauge members and sheeting* CEN 2004.
- [2] LINDNER, J. - GREGULL, T.: *Torsional Restraint Coefficients of Profiled Sheeting*, IABSE Colloquium Thin-Walled Metal Structures in Buildings, Stockholm, 1986, pp.161-168.
- [3] VRANÝ, T.: *Torsional Restraint of Cold-Formed Beams Provided by Corrugated Sheeting For Arbitrary Input Variables*, Eurosteel - The Third European Conference on Steel Structures, Coimbra, 2002, pp. 733-742.
- [4] HÖGLUND, T.: *Beams restrained by sheeting – forces on fasteners*, Internal material of PT EN 1993-1-3, 2002.

This research has been supported by CTU 0413211.

Climatic Effects on Composite Steel and Concrete Bridges

J. Římal, V. Jelínek, J. Chod*, K. Maleček, A. Kovářová, V. Sopko**, J. Zaoralová,
H. Horká, S. Kasíková, L. Samek**

rimal@fsv.cvut.cz

CTU, Faculty of Civil Engineering,
Thákurova 7, 166 29 Prague 6, Czech Republic
* CTU, Faculty of Electrical Engineering,
Technická 2, 166 29 Prague 6, Czech Republic
** CTU, Faculty of Mechanical Engineering,
Technická 2, 166 29 Prague 6, Czech Republic

The correct determination of the loading of the bridge structure is one of the decisive problems in bridge design. While traffic load is being investigated in detail, traffic flows on roads are monitored and railway carriages are weighed, climatic loads have not been explored in such a detailed manner yet.

A railway bridge in Královské Poříčí was selected for the measurement of climatic effects on composite steel and concrete structures.

The aim of the measurements was to collect data on the real fluctuation of temperature fields and maximum temperature gradients in a composite bridge structure during different year seasons.

The bridge in Královské Poříčí has a continuous gravel bed. The superstructure of the bridge is made by two main plate girders connected with a monolithic reinforced concrete deck 200 mm thick. The deck is connected to the beams by stud shear connectors welded to the upper flange of the beams.

The applied measuring method involved temperature measurement with resistance platinum sensors.

As the measurements were conducted on a composite steel and concrete structure, two types of temperature sensors had to be developed. Based on commercially available resistance sensors MT 100, the following devices were constructed:

- contact sensors for temperature measurement of steel structures
- probes for temperature measurement inside concrete decks.

The basic demand on the construction of the contact sensor was to achieve the best possible heat transfer between the sensor and the measured structure (steel), while thermally insulating the sensor from the outside environment. Therefore, the sensor developed had a large contact area of 1260 mm² and the heat transfer was increased even more by the use of silicon oil. The whole sensor was forced down to the steel structure mechanically with suitable attachments.

Some sensors were placed on the steel structure. Others were placed inside the concrete deck at the depths of 55, 100, 130, and 150 mm, measured from the lower surface of the deck. In plan, the holes made corners of a square with 200 mm sides.

The sensors were connected with the measuring equipment situated in a caravan under the bridge by means of cables.

In order to achieve the highest possible measurement accuracy, each sensor in the thermostat was individually calibrated in connection with the same measuring equipment, which was also used for measurement in the field. The dependence of resistance of the platinum sensor on temperature was approximated with a linear function within the assumed temperature range. Based on the calibration results, calibration equations were determined for each sensor using linear regression.

Evaluations and Conclusion

The data collected in these experimental measurements have become the basis for ČSN 73 6203 facilitating development of a temperature distribution scheme in composite bridges. It is a favourable fact that the European preliminary standard for the temperature bridge load (part of ENV 1991-2-3) is similar to ČSN.

In this respect, it is necessary to state that climatic changes of the construction environment are generally known and are experimentally measurable without problems. Temperature field and temperature gradient measurements within e.g. a bridge structure itself, on the contrary, are rather difficult. They often involve the entire bridge structure, and measurements at various, hardly accessible points. Due to the nature of the problem, they are always long-term measurements setting high all-round demands.

The determination of gradients of temperature and moisture fields from surface temperatures and temperatures of the surrounding environment is not sufficient for the analysis of building structures. It can be misleading. It is necessary to gather data inside the structure experimentally. It is important to penetrate into the mass of the structure and determine the values inside the structure experimentally. It is also one of the key benefits of this experimental research.

This project is being conducted with the participation of Ph.D. student Ing. Jan Pytel and undergraduate student Jakub Římal.

References:

- [1] ŘÍMAL, J.: *Charles Bridge in Prague - Measurement of Moisture Fields*. International Journal for Restoration of Buildings and Monuments. 2004, vol. 10, no. 3, pp. 237–250.
- [2] ŘÍMAL, J.: *Charles Bridge in Prague - Measurements of Temperature Fields*. International Journal for Restoration of Buildings and Monuments. 2003, vol. 9, no. 6, pp. 585–602.
- [3] ŠEJNOHA, J. – BITTNAR, Z.: *Numerical Methods in Structural Analysis*. ASCE Press, New York/ Thomas Telford, London, 1996.
- [4] ŠEDIVÉC, J.: *Load Bridge Code*. ČSN 73 6203.

This research has been supported by the Grant Agency of the Czech Republic, grant No. 103/03/0290.

Prospects of Renewable Materials and Resources in Construction Industry

M. Hezl, P. Svoboda

`martinhezl@centrum.cz`

Department of Construction Technology, Faculty of Civil Engineering,
Czech Technical University
7 Thakurova, 166 29 - Prague 6, Czech Republic

INTRODUCTION

Renewable construction materials and other resources (energy, etc.) have recently become a very much-discussed topic. It is more than logical in times of dramatically increasing oil prices and notification of natural resources scarceness. General knowledge of renewable sources' advantages, disadvantages, and prices, especially in comparison with non-renewable substitutes, are the main factors to influence their rate of use.

The volume of world consumption of energy and raw materials being used in construction industry as well as in other branches of industry is continuously increasing. Depletion of these limited sources implies way of life and economic development of future generations. Current volume of consumption of non-renewable sources does not head towards so called **sustainable development** (i.e. situation when needs of present generation are met without compromising those of future generations) [1].

WAYS TO SUSTAINABILITY

How to make construction industry more sustainable and more effective from points of view of the environment and resources? We can analyse four main phases of the whole construction industry and lifecycle of construction production, and focus on each of them:

- Design phase
- Construction process
- Structure's life period
- Reconstruction (renovation) or Demolition

Ad A – Design phase is very important from architectural and material point of view. A skilled designer uses landscape settings and terrain to benefit from their advantages as well as specific materials (e.g. plated windows, thermal insulations, etc.) with respect to their characteristics.

Higher share of renewable and easily processible materials composed in a structure causes lower energy consumption, reduced labour needs within processing, and less irreversible depletion of limited resources. An example of this type of material is wood. Timber structures are lightweight, and moreover production process of timber as a construction material spends ten times less energy than production of steel.

Ad B – Construction process is generally the most important consumer of materials and energy in construction industry. It includes transport of material and construction processing. Usage of local and lightweight materials (see point A) reduces needs and costs of transport, which implies to lower energy consumption.

Innovative construction technologies and materials may make construction process itself easier and improve characteristics of the final structure. Furthermore they offer differentiation and combination of materials, higher share of mechanisation and prefabrication. It enables for example so-called "off-site way of construction" (certain way of

prefabrication), which is significantly more precise than on-site construction (concreting, building of bricks, etc.).

Ad C – Structure's life period represent a period demanding a volume of energy for operation (lighting, heating, etc.). An improvement to be achieved in energy consumption area is dependent on current rate of energy use efficiency. It requires making a survey and taking remarkable but relevant measures. The first step should be focused on possible reduction of energy consumption, e.g. with help of thermal insulation. Later, the structure of energy sources should be also considered with respect to renewable energy sources.

Ad D – Reconstruction (part of point C) or demolition need to be considered in initial phase of a project preparation. An energy audit should be carried out to assess needs of the structure during its entire life cycle. External costs and benefits analysis is, therefore, to be evolved with respect to future costs of energy and materials in their net present values. [2]

ECONOMIC EFFICIENCY

All measurements should be economically effective otherwise it is not reasonable to take them. How to motivate building firms to use environmental friendly technologies and materials for construction?

Motivation through a taxation system as one of the most effective instruments may be set up according to evaluation of external costs and benefits. Environmental taxation such as payments for energy, fuels, and other limited resources consumption, is an example of successful model applied for instance in several European countries. On the other hand, positive motivation may come with specific tax rebates on environmental friendly production.

ETUS I

ETUS is a doctoral project of PhD students of the Czech Technical University. It is titled Economics of Sustainable Constructing Based on Renewable Sources and Materials. Objectives of our team are the following: to support environmental friendly construction processing, to establish an economic assessment model, and to draft framework of sustainable production development in the Czech construction industry. [3]

At present we prepare construction of an experimental low energy structure mostly with use of renewable sources. In terms of cooperation with several companies we plan to establish a cluster agency in the year 2005. This organisation is about to support and manage development of low energy timber structures production in the Czech Republic.

References:

- [1] OECD: www.oecd.org
- [2] EUROPEAN COMMISSION: *Energy for the Future: Renewable Sources of Energy*
European Commission, 1997
- [3] ETUS I: <http://eko.fsv.cvut.cz/etus>

This research has been supported by GA ČR grant No. GA 103/03/H127.

Modelling of Impacts of Land Use and Technical Measures to Storage Capacity of the Basin

K. Uhlířová

uhlirova@fsv.cvut.cz

Department of Drainage, Irrigation and landscape Engineering, Faculty of Civil Engineering, Czech Technical University, Thákurova 7, 166 29 Prague 6, Czech Republic

The project focuses on studying the rainfall-runoff conditions of catchments. The research study should help to find possible ways of protection the Cesky Krumlov suburb from repeated flooding by Polecnice stream. The Polecnice watershed is located in South Bohemia, its area is 198 km² and outlet point of Polecnice stream is in UNESCO protected town Cesky Krumlov. There are two main streams in the basin – Polecnice stream and Chvalsinsky stream, their junction is located few kilometers upstream the town. Rainfall-runoff processes were simulated in hydrologic interface WMS 6.1 (Watershed Modeling System). For purposes of this study Curve Number Method, Method of Unit Hydrograph and Muskingum-Cunge Method for channel routing were used. The calculation was provided by HEC-1 model. Input data (digital elevation model, land use map, soil type map, hydrographical network) were prepared in GIS (ArcView, Idrisi). Flood situation from summer 2002 (precipitations from 6.-8.8., 11.-13.8. and 31.8.2002) was used for calibration. After the calibration the study focused on simulation of different scenarios that can influence runoff. There were following simulated scenarios – change of land use, transformation of the outflow wave by change of channel roughness and channel size and transformation by small reservoirs. For comparing the effects precipitation from 6.8.2002 (total head was 128,6 mm – that corresponds to precipitation with probability of repetition 1000 years) was used. Tendencies noticeable from model results were helpful for conclusion of knowledge which combination of influences would lead to solution of runoff problems.

By probing of land use changes influence five scenarios were simulated: all meadows and pastures assigned to arable land; actual land use interpreted from satellite image and terrain survey (year 2002); all arable land and bents assigned to pastures; all arable land and bents assigned to meadows; arable land, meadows, pastures and bents afforested. Results showed changes in runoff peak and runoff volume (the same order like above). The afforested scenario had the highest difference from real land use and the peak was lowered by 22%. Delays of runoff peaks weren't much remarkable.

Five scenarios were considered for change of hydraulic roughness of the channel - 5 various Manning's coefficients (0.180, 0.025, 0.040, 0.060 and 0.100) that represent real values for varied channel conditions. Shape (trapezoid) and size of the channel used for simulation is close to real conditions. The main importance of this separate effect is increased peak delay. The runoff peak did not change reasonably.

The next view was comparing transformation of waves caused by channels with various sizes combined with various hydraulic roughnesses of inundation fields. There were trapezoidal channel, wide inundation, 3 different channel sizes and 2 roughness scenarios considered. Results show that for the smaller channel there is bigger influence of inundation roughness because of larger spillage. Higher roughness of inundation also cause slowing down the outflow wave which corresponds to reality.

As the last separate effect transformation of outflow by reservoir was simulated. On both streams the reservoirs (model case) were considered upstream the Polecnice and Chvalsinsky stream junction. Graphic chart of inflow and outflow from the reservoirs (decrease and delay of peak) was one of the results. Other results were: total effects of various combinations involving the reservoirs in the outlet point of the basin. It was showed that reservoirs haven't very big influence because of filling up already before beginning of culmination. It's necessary to keep in mind that used precipitation invokes runoff that is corresponding to Q_{1000} thus inflow volume is 4 times higher than retention volume. It was only a model case; in practice the system of polders would be used. After the simulation of separated effects it was approached to combination of disposed influences to total decrease and delay of runoff peaks. It was simulated 6 scenarios (1 negative, 1 real, and 4 positive). The biggest influence (decrease of peak - 33% and time difference of peaks - almost 5 hours against real scenario) had forestation, meadows, pastures and bents, the channel with high roughness of inundation field and both reservoirs. The last effort was to break the outflow waves from sub-basins using disposed effects. The aim was to speed up one of the stream and slow down the second one above the junction. Possible delay without reservoir routing wasn't sufficient and the waves would encounter. Even the influence of designed reservoirs wasn't efficient enough. The reasons are that the precipitation is too high and that culmination of outflow wave lasts ca 9 hours. For smaller precipitation the influence would be bigger.

Conclusions are: Strong land use change influences runoff peak and runoff volume. Change of channel roughness influences especially time of peak. Delay of culmination may be caused by spillage to inundations, especially if they have high hydraulic roughness. Model case of reservoir showed the possibilities and reserves of impacts to runoff (particularly in case of extreme rainfalls). By combination of disposed effects the peak would decrease by one third and delay rose to 5h (even in case of this extreme precipitation and only model case of reservoirs). On the other hand it wasn't successful in separating runoff waves from sub-basin (without land use changes) not to come to encounter and redouble the runoff peak. It could be assumed that the simulated effects would have bigger influence in case of smaller rainfall.

Acquired results are the base for further research: To find trends and efficiency of simulated effects for lower probability precipitation and for precipitation with other continuance; involving of polder and comparing to reservoir; examination of influence of reservoir (polder) parameters changes; to project polder system including finding available locality and further proposing disposed scenarios to resolving problem of encounter outflow waves from sub-basins.

References:

- [1] UHLÍŘOVÁ, K. - DOSTÁL, T.: *Aplikace modelu WMS v povodí Polečnice: Sborník z Workshopu 2004 "Extrémní hydrologické jevy v povodích"* Praha, ČVUT v Praze a ČSVTS 2004 103-112
- [2] UHLÍŘOVÁ, K. - DOSTÁL, T.: *Aplikace modelu WMS v povodí Polečnice: Sborník 7. Odborné konference doktorského studia Juniorstav Akademické nakladatelství CERM, s.r.o. Brno 2005*

This research has been supported by CTU No. CTU0403611.

Low Temperature Bituminous Binders and Their Impact on Selected Rheological Properties of Asphalt Mixes

J. Valentin*

valentinj@post.cz

*Department of Road Structures, Faculty of Civil Engineering, Czech Technical University, Thákurova 7, 166 27 Prague 6, Czech Republic

The general trend of increasing the protection of environment and the efforts to minimize the energetic costs of production are apparent also in the production of asphalt mixes. The requirement to decrease the consumption of energy is a logical one as our goal is the most economic and sustainable use of non-renewable and renewable sources and minimization of produced emissions (CO₂, fumes and aerosols). There is a proven direct relationship among the volume of emissions of the CO, CO₂, or NO_x type, energy demands and the range of working temperatures as well as an economically clearly defined relationship between costs and consumed energy [2]. On the other hand following such requirements and developing technologies consuming less energy should not impact the performance and mechanical or rheological characteristics of pavement construction. The paper presents summarizes results of selected mechanical and rheological properties of compacted asphalt mixes with standard and low viscous bituminous binders, with respect to the influence of used additives on the properties of asphalt mix.

The additives for the production of low-temperature bitumen binders and their use in asphalt mixes that are produced, laid and compacted at lower temperatures are generally called bitumen liquefying agents or intelligent fillers. Some groups of these additives are called low molecular weight polymers. For research presented e.g. in [1, 3, 4] low molecular paraffin was used. FTP has higher softening and rigidifying point due to the longer hydrocarbon chains and specific structure. This is in the range of 70 to 120°C. The bitumen modified by FTP is characterized by relatively high softening point and medium penetration. The penetration index has the value PI > 3. The breaking point measured was the same as for the initial binder. The negative influence of FTP or Montana waxes on the breaking point has been observed only if more than 4% mass of wax had been added. The viscosity for the temperature range 100 – 120°C is an important parameter that demonstrates the difference between low-temperature binders and standard bitumen. This improves the workability and compactability of asphalt mixes with the binder containing low molecular paraffin. Due to higher stiffness modulus of the binder there is a negative influence on ductility because of higher fragility. Results of force ductility showed higher values of deformation work (E_s, E_r or E₂₀).

The ideal bitumen binder should have a good workability of the mix for the temperatures 130 – 140°C (decrease of the consumption of energy and to the lower quantity of released fumes). The binder should be characterized by the high elasticity on one side and the capacity of good relaxation on the other side. It should have a high strength and resistance to pavement deformation at 60°C. Its properties have to allow the decrease of binder content in the mix guarding his functional properties, [2]. During the research it was proven that the addition of 3% mass of synthetic waxes to the bitumen binder is optimal for the practice from the point of view of achieved effects and properties.

As appropriate mixes SMA (Stone Mastic Asphalt) for wearing course because of high-quality standards insisted on this type of asphalt mixture and ACHC (Asphalt Concrete High Coarse Grained) for binder course were used. The mix design was in all six variations of SMA the same with bitumen content of 6.2% mass. The mix design in three variations of ACHC was also the same too with bitumen content of 4.2% mass. For low temperature mixtures 0.3% mass of additive was calculated and added to the bitumen. Asphalt mixes with original modified binders have been produced and compacted at different temperatures. Each of the mixes was then tested on following mechanical and rheological characteristics [3, 4]:

- Marshall stability and Marshall deformation
- Stiffness modulus at 27°C (SMA) and at 15°C and 40°C (ACHC)
- Relaxation test at Nottingham Asphalt Tester
- Flexural strength
- Resistance against permanent deformation

Adding FT-paraffin into binder increased the resistance against permanent deformation of the asphalt mix and the stiffening effect of FT-paraffin was confirmed again. Mixtures where FTP was used show also higher value of flexural modulus of rigidity as well as higher values of stiffness modulus. The expected positive effect of binders with lower penetration and polymer modified bitumen could be evaluated.

It was possible to confirm the positive influence of synthetic wax additive on workability, compactability as well as on mechanical and rheological properties of asphalt mixes designed with low-temperature bitumen binders. The attention should be focused further on confirming the improvement of thermal resistance of asphalt courses under the service conditions without the impact on the low temperature properties as well as higher resistance against the fatigue. In the same time it is possible to determine on a broader scale the advantages of the combination of these additives and polymer modified binders – the use of higher resistance to permanent resistance and higher stiffness due to the FTP and elasticity of modified binders.

References:

- [1] DAMM, K.W., ABRAHAM, J., BUTZ, T., HILDEBRAND, G., RIEBESEHL, G.: *Asphaltverflüssiger als „intelligenter Füller“ für den Heißeinbau – ein neues Kapitel in der Asphaltbauweise*, Bitumen 1/02, Hamburg 2002 .
- [2] VALENTIN, J., MONDSCHNEIN, P.: *Comparison of Asphalt Mixtures with Standard and Low-Temperature Bitumen Binders*, TU Delft, 5th International PhD Symposium in Civil Engineering, 2004 .
- [3] VALENTIN, J.: *Survey on Environmentally Compatible Pavement Structures and Asphalt Pavement Technologies*, CTU Prague, Proceedings of 3rd International Seminar on ECS, 2002, pp. 504-509.
- [4] VALENTIN, J.: *Porovnání vlastností asfaltových betonů se standardními a nízkoteplotními asfaltovými pojivy* STU Bratislava, Sborník IX. seminára Ivana Poliačka 2004 pp. 127 - 133.

This work has been supported by the Czech Technical University Prague within the Ph.D. research grant (CTU grant No. CTU0402711). The author appreciates very much the support of CTU Prague.

Measurement of Temperature in Concrete Bridges

O. Tomaschko, V. Hrdoušek

ondrej.tomaschko@fsv.cvut.cz

Department of Concrete Structures and Bridges, Faculty of Civil Engineering,
Czech Technical University, Thákurova 7, 166 29 Prague 6, Czech Republic

Temperature measurements continued in two prestressed concrete bridges with one box girder during the year 2004. These temperature measurements started in 2003 thanks to support of CTU grant – always in one cross section of the two following bridges:

- Highway bridge (D8) across the Vltava river, the right bridge structure from Prague;
- Tramway bridge (Hlubočepy scaffold bridge) on tramway line from Hlubočepy to Barrandov.

Temperature measurements are running in connection with ČSN EN 1990 [1] and with currently introducing EN 1991-1-5 – Thermal actions [2]. This European Standard is devoted to temperature changes in structures including bridges and its National Annex (NA) which is being prepared will specify postulates referring to climatic conditions in the Czech Republic. Collections of obtained values will be given to authors of the NA.

In the case of the highway bridge across the Vltava river, the advantage of already inserted heat detectors was taken (they were buried in concrete during the time of building of the bridge), which were used by the Klokner Institute for measuring the development of hydration heat. In a cross section in the middle of a side span across the Vltava river, fifteen detectors are situated (four in the top slab, six in walls and five in the bottom slab), one measures outer shade air temperature. The temperature is measured periodically once an hour in every detector. The measurement was started in July 2003.

In the case of the tramway bridge, all preparatory works had been running during bridge building. Heat detecting elements were compiled and tested in cooperation with the Experimental Center of the Faculty of Civil Engineering. They were embedded by epoxy resin to be protected from wet concrete during the building of the bridge. The chosen cross section is in the stationing of km 0.600 of the new tramway line from Hlubočepy to Barrandov. The heat detectors were fixed to a conventional reinforcement shortly before the pouring of concrete to the particular section of the bridge. Thirteen heat detecting elements are buried in concrete in the cross section, one is measuring the values inside the box girder and one outer shade air temperature. Every hour's recording is processed by a program made by the Experimental Center of the Faculty of Civil Engineering. The measurement was started in December 2003 and after its recondition, which was made in April 2004, it is still running.

The following parameters of thermal load are determined from obtained values in both of measured bridge structures:

- An uniform temperature component with the minimum and maximum measured bridge temperature;
- A linearly varying temperature difference component (non-linear), which represents the vertical or horizontal temperature components in the cross section or in walls or in slabs;
- A shade air temperature and its relation to the measured bridge temperature.

The uniform temperature component depends on the minimum and maximum uniform bridge temperature component – $T_{e,min}/T_{e,max}$ [2]. The results of this temperature component are in length – element's changes in an unrestrained structure. $T_{e,min}/T_{e,max}$ is derived according to a type of bridge deck (steel deck, composite deck and concrete deck) from a correlation with the minimum and maximum shade air temperature – T_{min}/T_{max} . In the case of the highway bridge across the Vltava river, the minimum measured bridge temperatures

($T_{e,min}$ in [2]) haven't been recorded yet to compare them with values in [2] and [3], because of no occurrence of the extreme shade air temperatures. Values of the maximum measured bridge temperatures ($T_{e,max}$ in [2]) are between values, which are introduced in [2] and [3]. They are certainly near to lower value according to [3]. Both of the maximum and minimum measured bridge temperatures were recorded in the heat detector, which is located 20 mm from the top surface of the top slab in the axis of the box girder. In the case of the tramway bridge, the minimum measured bridge temperatures in winter 2004 aren't suitable for comparison with values according to [2] and [3] up to now. The maximum measured bridge temperatures are near to value in [3] as for the highway bridge. The bridge surface is made from ballast, which means a top slab is protected against sun and freeze. The temperature extremes were recorded in the heat detector, which is located under the top surface of the cantilever of the top slab, where is no ballast.

The linear temperature difference component is characterized by the heating or cooling of a bridge deck's upper surface, which leads to the maximum heating $\Delta T_{M,heat}$ – the top surface is warmer or to the maximum cooling $\Delta T_{M,cool}$ – the bottom surface is warmer [2]. The horizontal component is considered only in particular cases. In the case of the highway bridge across the Vltava river, values of vertical components are higher than values of horizontal components. This is why, that a bridge road is warm due to the sun and that the left bridge structure (from Prague) is located in south-west from measured bridge structure and it induces a shadow on the measured bridge structure. The maximum vertical temperature gradients are determined as maximum temperature differences measured in the top slab's heat detectors and in the bottom slab's heat detectors located always 20 mm from the outer surface of both slabs in the axis of the box girder. The location of heat detectors allows obtaining the vertical temperature gradients in the left wall of the box girder too. But these don't reach maximum values as those in the top slab and in the bottom slab. In the case of the tramway bridge, vertical temperature gradients in the axis of the box girder and in the left wall are negative influenced by the occurrence of ballast, which behaves as an insulation. The vertical temperature gradient is observed in the left cantilever of the top slab too, which thickness is only 180 mm. Prefabricated side walls, which are located outer of the walls with heat detectors caused the preventing of side sun of bridge structure. The values of the vertical temperature gradients are lower than values conforming with [2]. There aren't values for horizontal temperature gradients in [3]. The value of maximum heating gradient is attainable only in the summer season. On the other hand, the maximum cooling gradient occurs in the summer and winter season.

There are measured shade air temperatures near both cross sections too. For example in the case of the highway bridge, a temporal movement of process of temperatures between shade air temperature and temperature measured in the heat detector, which is located 20 mm from the top surface of the top slab in the axis of the box girder is three hours. Concrete structures don't heat and don't cool immediately with fluctuation of ambient temperature.

References:

- [1] ČSN EN 1990 - Eurocode - Basis of structural design ČSN, 2004.
- [2] prEN 1991-1-5 - Eurocode 1 - Action on Structures, Part 1.5: General Actions - Thermal Actions CEN, 2003, pp. 20–31.
- [3] ČSN 73 6203 - Action on Bridges ČSN, 1986, pp. 48–53.

This research has been supported by CTU grant No. 0401911.

Modelling of Chlorine Decay in a Part of South Bohemian Drinking Water Distribution System

K. Slavíčková, A. Grünwald, M. Slavíček, B. Šťastný, K. Štrausová

`katerina.slavickova@fsv.cvut.cz`

Department of Sanitary and Ecological Engineering, Faculty of Civil Engineering,
Czech Technical University, Thákurova 7, 166 29 Praha 6

Water quality modelling is an important tool for improving our understanding of the movement and fate of drinking water constituents within distribution systems. This paper describes chlorine decay modelling in EPANET 2 and its practical application in a part of South Bohemian drinking water distribution system.

The main objective of drinking water utilities is to guarantee safe water to all consumers connected to the distribution system. Microbiological and chemical deterioration of water may occur during the distribution process through pipelines even if the treatment is effective and the quality of the water, which leaves the water treatment plant, is acceptable. There are two commonly encountered problems with regard to water quality control in the drinking water distribution system. The first problem is that of taste, odour, and contaminants in water. The other is deterioration of bacteriological quality. To effectively control these problems, it is imperative to maintain a disinfectant residual in distributed water. Chlorine is the most widely employed disinfectant over the world. A drinking water utility must be able to predict the location at which the chlorine concentration drops below a certain minimum desired level to ensure low bacterial concentration in distributed water. The chlorine decay modelling is therefore a well-established tool for assisting in the operation of distributed system to achieve adequate water quality.

Hydraulic modelling of drinking water distribution systems can help in operation of the systems and also in assessment of drinking water quality. Program EPANET 2 tracks the flow of water in each pipe, the pressure at each node, the height of water at each tank and a concentration of a chemical species throughout the network during a simulation period comprised of multiple time steps. In addition to chemical species, water age and source tracing can also be simulated. It is possible to design and evaluate different variants and solutions and to optimise the operation of the network. Zero order growth is used in EPANET 2 to model water age, where with each unit of time the “concentration” (i.e. age) increases by one unit. It enables also to model the movement and fate of reactive material as it grows (e.g., a disinfection by-product or iron) or decreases (e.g., chlorine residual) with time. It is possible to model reactions both in the bulk flow and at the pipe wall with the use of n-th order kinetics for reactions in the bulk flow and zero or first orders kinetics for reactions at the pipe wall.

This paper is focused on modelling of free and total chlorine in a system which supplies drinking water from water treatment plant Plav through water tank Včelná and pumping stations Hlavatce and Sudoměřice to water tank Hodušín. The total length of this water distribution network is 89 km and hydraulic model contains 693 nodes, 7 distribution reservoirs, 661 pipes and 21 pumps. Some parts of this system are created by gravity water pipes Včelná – Hlavatce, Zdoba - Malá Varta and Malá Varta – Sudoměřice and parts of it are pressurised Plav – Včelná, Hlavatce - Zdoba and Sudoměřice – Hodušín.

In this contribution we present the results of chlorine decay models calibration and verification. Hydraulic model WTP Plav – Hodušín was created at our department in co-

operation with JVS company. Necessary total and free chlorine concentration data were measured and collected. These data were evaluated and used for calibration and verification of chlorine decay model in EPANET 2. Two models were used for free chlorine decay modelling – first was model of first order decay in bulk water and first order decay at the pipe wall and second was model of first order decay in bulk water and zero order decay at the pipe wall. The same approach was realised also for total active chlorine. In EPANET 2 the Lagrangian time-driven method is used for water quality modelling. Reaction coefficients k_b and k_w are different for each distribution network and they depend on input water quality, length of distribution system, pipe diameter, material and age and other factors.

The results of total active chlorine decay model calibration are reaction coefficients $k_b = -0,1 \text{ d}^{-1}$ a $k_w = -0,06 \text{ m/d}$ for model of first order decay in bulk water and first order decay at the pipe wall and first order decay in bulk water and zero order decay at the pipe wall these coefficients are $k_b = -0,18 \text{ d}^{-1}$ a $k_w = -2,2 \text{ mg/m}^2/\text{d}$. Both models showed relatively high correlation (0,96 and 0,95) of measured and computed values.

Calibration of free chlorine decay models was performed on the base of means of measured concentrations. The results are reaction coefficients $k_b = -0,03 \text{ d}^{-1}$ a $k_w = -0,008 \text{ m/d}$ for model of first order decay in bulk water and first order decay at the pipe wall and first order decay in bulk water and zero order decay at the pipe wall these coefficients are $k_b = -0,09 \text{ d}^{-1}$ a $k_w = -0,075 \text{ mg/m}^2/\text{d}$. Both models showed relatively high correlation (0,85 and 0,9) of measured and computed values.

Verification of models were realised with use of a set of independent measured data. Achieved results showed, that free and total chlorine decay in South Bohemian drinking water system can be predicted by these models. For some stages of system operation models of first order decay in bulk water and first order decay at the pipe wall are more suitable and for other stages models of first order decay in bulk water and zero order decay at the pipe wall give better results.

References:

- [1] GRÜNWARD, A. - MACH, M. - SLAVÍČKOVÁ, K. - SLAVÍČEK, M. - ŠŤASTNÝ, B. - KASAL, R. - ŠTRAUSOVÁ, K.: *Výzkum efektu úpravy vody na její jakost při prodlužujícím se zdržení v rozvodné síti, Závěrečná zpráva NAZV Č. 1003 ČVUT*, 2004, pp. 1-80.
- [2] SLAVÍČKOVÁ, K.: *Modelování změn kvality pitné vody v distribuční síti v programu EPANET 2 Soil and Water*, roč. 3, č. 3, ISSN 1213-8673 2004, pp. 189-195.
- [3] SLAVÍČKOVÁ, K.: *Změny kvality vody při dopravě a jejich modelování v programu Epanet 2 Sborník konference Voda Zlín 2002, Vodovody a kanalizace Zlín*, ISBN 80-238-8326-7, 2002, pp. 137-141
- [4] GRÜNWARD, A. - FOŠUMPAUR, P. - SLAVÍČKOVÁ, K. - SLAVÍČEK, M. - ŠŤASTNÝ, B. - ŠTRAUSOVÁ, K. - KASAL, R. - ČIHÁKOVÁ, I.: *Inovace procesu úpravy vody a zabezpečení vysoké kvality pitné vody v distribučních systémech, Výzkumná zpráva grantu NAZV 1G46036*. ČVUT, 2004, pp. 1-62.

This research has been supported by grant NAZV 1G46036.

Laboratory test of Reinforcing Grids in Compacted Asphalt Mixes

P. Mondschein

petr.mondschein@fsv.cvut.cz

CTU, Faculty of Civil Engineering, Dept. of Road Structures, Thákurova 7, 166 29, Prague 6

The problems of reinforcing elements exploitation in transportation engineering solutions are well known. There are plenty of examples of reinforcing elements application in steep soil slopes construction and in soft soil properties enhancement [1]. The further step in reinforcement elements transportation engineering application is the use of these elements in the pavement structure strengthening. The incorporation of reinforcing elements in the asphaltic layers of pavements prevents the crack propagation from the cement bound base layers and in the case of concrete road reconstruction from the cracked pavement slabs into the asphalt top courses. Further improvement of the pavement performance is the restriction of the permanent deformation development. It is, therefore, of prime interest to prove, theoretically and experimentally, the increase in performance and service life duration of the pavement due to the incorporation of the reinforcing element, or to certify the possible savings in the asphalt layers thicknesses for the pavement of the same service life.

The market activity in geosynthetics is very strong. The individual products differ in fibre material, the size of the warp, the fabric material and in overall mechanical properties of the whole product. It is, however, questionable, whether the classical methods of the transportation engineering are able to suggest which product is best suited for the given problem solution. This contribution aim is to present possible answers to these problems.

The assessment of the mechanical contribution of the reinforcing elements built in the asphaltic layers has been based on results of five well-known testing procedures, which had to be modified to recognize the effects of the reinforcement. The following laboratory measurements have been involved: (1) indirect tensile strength test, (2) resistance against rutting, (3) shear test of layer bonding, (4) bending strength test and (5) Marshall test. These tests have been performed on four reinforced samples and the resulting values were compared to those of the nonreinforced sample.

The reinforcing effects have been tested using asphalt mix ABS as a reference mix with binder 50/70 and binder content of 6,2%. The type of the binder and its content indicate that the mechanical properties of the mix would be under average, which fact is favourable for testing (now more evident) benefit effects of the reinforcement element installation.

The indirect tensile strength test was performed according to the prepared European Standard ČSN EN 12697-23 Asphalt mixes – Testing methods for hot asphalt mixes – Part 23: Determination of indirect tensile strength (in the execution time). The cylindrical specimen to be tested is fixed between loading strips and is loaded along the line parallel to the axis of cylinder under constant loading rate until failure of specimen. The indirect tensile strength (ITS) is the maximum tensile stress computed from the value of the failure loading and specimen dimensions. The result of the test is the indirect tensile strength ITS in kPa. At the same time, the type of failure mechanism is recorded.

The resistance against rutting has been tested in accordance with the methodology prescribed in the Technical Specifications TP109 „Asphalt compacted layers with enhanced resistance against rutting“, change 1. The manufacturing of specimens had to be modified due to the installation of the reinforcing grid in the specimen body. The specimen with dimensions 300x150x70 mm was manufactured in three stages. In the first stage, the first part of the specimen was made with the thickness of 4 cm. The top surface of the specimen was

sprayed with the asphalt binding coating and then the reinforcing geocomposite was placed (sticked). Then the second layer was placed in the thickness of 3 cm. The reference set of specimens (with no reinforcement) was manufactured in the same sequence of steps (of course without grid installation). In this way, the similar manufacturing conditions for reinforced and reference specimens were guaranteed in order to perform tests under comparable circumstances.

The flexural strength test is defined in the specifications TP 151 „Asphalt mixes with high stiffness modulus“, issued in september 2001. This test is one of the two tests concerning low-temperature properties of asphalt mixes. In order to verify mechanical contribution of reinforcing grids, the standard version of the flexural strength test had to be slightly modified. The test has been performed in a special climatized basin at the temperature $0\pm 1^{\circ}\text{C}$, the beam specimen having dimensions 75x80x300 mm. The flexural strength test results allow analogous conclusions to be made on the role of reinforcing grids as in four other laboratory tests. The moderate-only flexural strength increase should be attributed to the small distance of the geogrid placement from the neutral axis of the nonreinforced sample. This distance couldn't be increased owing to the sample limited dimensions and to the maximum aggregate grain size allowed in the ABS mix.

The Leutner shear test of layer bonding condition serves for determination of the maximum allowable shear force on the pavement asphaltic layers interface. The sample is loaded in shear at the layer interface under constant shear slip rate. The shear force and shear slip (deformation) determined in the test are used to assess the quality of layer bonding as an important design factor influencing dramatically the service life of the pavement.

In the Marshall test, the most important test parameter is the amount of energy necessary for specimen failure. Once again, the standard manufacturing of specimens had to be modified due to the installation of the reinforcing grid in the specimen body.

The results of the performed laboratory testing proved its ability to detect behavioural benefits of the reinforcing elements installation in the compacted asphalt layers. On the basis of the performed laboratory tests, using results of the theoretical analysis and multicriterial assessment of the laboratory results, the following conclusions may be drawn:

- the installation of each of the four tested geogrid types improved the utility value (mechanical performance) of the asphalt layer,
- the performance improvement is markedly influenced by the aperture size of the geogrid - the smaller the aperture size, the more pronounced is the geogrid material separation property with adverse effects on the layer performance,
- the arrangement with impregnated fibres seems more suitable.

References:

- [1] R. M. KOERNER: *Designing with geosynthetics*, 4th ed. Prentice Hall, New Jersey 1998

This research has been supported by GA 103/02/0396.

Soil Erosion Assessment in Larger Watersheds Using GIS Tools

J. Krása, T. Dostál, K. Vrána

josef.krasa@fsv.cvut.cz

Department of Irrigation, Drainage and Landscape Engineering, Faculty of Civil Engineering, Czech Technical University, Thákurova 7, 166 29 Prague 6, Czech Republic

From the collectivization period and landscape pattern destruction almost 50 years ago sediment transport from agricultural land into rivers and reservoirs remains problem within the Czech Republic. For erosion assessment at larger scale, robust and simple modelling tools are needed. USLE is commonly used in the Czech Republic for many years at a plot-scale but modern GIS tools in computer science allow using it (after a proper calibration) at larger scales. Another available approach is use of Watem/SEDEM model (developed at the Laboratory for Experimental Geomorphology of KU Leuven, Belgium).

Watem/SEDEM is a spatial distributed model of erosion and sediment transport processes. The model is RUSLE (Revised Universal Soil Loss Equation) based, applying sediment delivery routines at 2D topography scale. As empirically based model it is relatively less precision data demanding comparing to physically based erosion models. Its' relative simplicity leads to widespread usability and availability for larger catchment scale.

With Watem/SEDEM, the sediment transport assessment within a watershed is solved in three major steps. First – erosion rates are calculated using RUSLE and raster based GIS layers. Model uses Idrisi32 GIS formats and routines. Average annual soil loss ($t\ ha^{-1}\ year^{-1}$) by RUSLE is calculated as: $A = R K L S C P$. 2D topography routines are used for evaluating LS factor at DEM grid. As a second step, outflow pathways are derived for each pixel of the DEM (Landscape pattern, different crops and field borders are considered). Through these pathways eroded soil is then distributed toward the river streams, while at each pixel the amount of sediment is compared to the cell's trapping efficiency. When the cell's transporting capacity is exceeded, the proper part of transported soil amount deposits at the cell. After the sediment reaches the river stream, the sum of delivered amounts is compared to total soil loss within catchment resulting in the SDR (sediment delivery ratio) of the watershed. Total soil loss, total sediment transport and total sediment deposition in the catchment are the main simulation results. To these, third step is now implemented. Nowadays new and revised version of the model – Watem/SEDEM 2.1.0 – is available. This version uses different approach for sediment routing through the rivers. Now all the river segments are labelled and the river topology is included. All the sediment that reaches the rivers is continuing through the river scheme to the outlet of the whole catchment and the pond trapping efficiency is applied for considering the amount of sediment trapped in various reservoirs within a catchment.

For the first implementing of Watem/SEDEM model to Czech conditions, Vrchlice watershed (Middle Bohemia, $97\ km^2$) was chosen as appropriate. The sediment amount within the two main outlet reservoirs was measured in frame of previous projects at the Department of Irrigation, Drainage and Landscape Engineering and various data sources were available for the main GIS layers and maps. Sediment transport from the watershed was also previously calculated the traditional way using USLE, sediment delivery ratio (as a lumped approach – for 11 sub-watersheds separately) and trapping efficiency of the main watershed reservoirs and ponds using Brune's curves.

Various sources were used for data preparation and conversion to GIS layers. Twenty meters grid size was used for sediment transport assessment as appropriate to the sources accuracy. DEM based on 1:25000 vector contour maps (DMÚ25) with contours' interval 5 m was prepared. Land cover map was based on supervised classification of Landsat TM scene, completed together with terrain survey and orthophoto map digitalization. Soil map was taken from BPEJ – official detailed bohemian database in scale 1:5000. As a special input layers the Parcel map (calculated using Watem/SEDEM routine), the Rivers map (including river segments topology table) and the Ponds map (including Brune's trapping efficiency values) have to be prepared. Ponds are then given identifiers by program itself during computation and their identification according to river segments is provided. Ponds trapping efficiencies are then applied for proper river segments. Then various input parameters have to be set before the calculation can start. These were tested for Belgian watersheds but then different values after basic recalibration were selected for Czech conditions.

The main results are always taken from the final program output menu. Except for them, various Idrisi32 data layers and several tables are produced. Among these, the map of sediment export and deposition within the cells of the catchments is the most important. For the table of river sediment inputs many analyses may be done. When hillslope sediment input to each segment is normalized by its length, the most endangered river length units are derived showing where efficient river bank conservation measures could be done. From the table of sediment inputs, trapped values and outputs for every pond (and corresponding river segments) the sediment amounts trapped in the main reservoirs of the catchments can be compared with the measured values for the model output calibration and validation. Total sediment production of $31990 \text{ t year}^{-1}$ within catchments and total sediment deposition of $21562 \text{ t year}^{-1}$ within catchments was estimated. Total sediment deposition of 9324 t year^{-1} in all catchment's reservoirs lead to calculated 100015 m^3 of sediment laying within Vrchlice reservoir, while measured value is estimated being above 125000 m^3 . 40200 m^3 were predicted for Hamersky pond, where measured value reached 32470 m^3 . That shows partial correspondence, but model calibration and validation continues in other areas. The research also focuses on model suitability for prediction scenarios of land-use changes and landscape pattern development.

References:

- [1] KRÁSA, J.: *Hodnocení erozních procesů ve velkých povodích za podpory GIS*. Dizertační práce, Fakulta stavební ČVUT v Praze, 2004
- [2] KRASA, J., DOSTAL, T., VRANA, K.: *Empirical Modelling of Sediment Transport Processes in Czech Conditions* 12th International Conference on Transport & Sedimentation of Solid Particles joined with 12th International Symposium on Freight Pipelines, The Institute of Hydrodynamics, Academy of Sciences of the Czech Republic, Prague 2004, pp. 457-466.

This research has been supported by CTU grant No. CTU0403511 DPP.

Solving Gap in the Prefabricated Bearing Wall

Karel Sládek *

karel.sladek@fsv.cvut.cz

*Department of Concrete structures and Bridges, Faculty of Civil Engineering, Czech Technical University, Thákurova 7, 166 29 Prague 6, Czech Republic

Prefabricated buildings – phenomenon industrial architecture bring into our domain many new, good and poor. Greater peoples dislike their features, building physical properties elementary structures, disposition concept residential buildings and solitary housings or town planner estate. Prefabricated buildings will be here and 1,5 million housings make up 40 % housing stock Czech Republic. That means there is no at present pace renewal housing stock c. 40 thousand yearly possibility fast replace given prefabricated buildings. It led after a year 1990 to that initiation inquiry current place prefabricated buildings and to that design reconstruction unsuitable part. Use chiefly about activity concerted to thermal barrier peripheral and roof structures, repair, constructive changes roof jacket, renewal or changes service core, installation, ... Results single inquiry and concrete practical experience from same reconstructions will be publication in technical paper and present on technical discussion and conference. Regarding on necessity gradual renovation housing stock is need systematically deal with problems prefabricated buildings and from piece of knowledge take into account specifically properties there buildings step by step design more effectively and safety method there reconstruction.

In the course of inquiry make to in view that regarding technical, time and pocket severity impossible of achieve total information on object. Along analyze experience research make to take trough in a way it is possible partial piece of knowledge generalizing, or information obtained by sectional construction extract on all construction. Item make to explore as it would be use for useful design structure. Inquiry made out that prefabricated have to uniform experiences (geometric, reinforcement, concrete) while there joint are difference.

Cross wall system with small span withheld excessive lay-out scope. Change life activity and social differentiation society often leads to requirement lay-out flat, or their connection so need make a hole in gap in bearing wall.

Bearing wall are strengthening steel structures, problems is their activation and interaction regarding to rheology properties. For strengthening structures use frame with rolled beam, or bonding steel plates or FRP reinforcement.

Will be carrying out pilot project influence size gap in wall that is economic and exigent of minimal strengthening wall. Design has shown voltage buil-up in both lines that will be dependent on size gap. Tension force increases twice as much in horizontal or vertical line. Effect joint will be boot labefaction thickness wall.

Performed paper acknowledges possibility linear design, because results from linear or nonlinear calculation each other be differ about 3 – 5 %. Labefaction thickness wall for vertical joint 90-95%, horizontal joint 50 – 60 %.

Wider demand nonlinear calculation in engineering design it is impossible regarding to timing title and unnecessary difference in result. Nonlinear calculation is need for solving special details (simulation load test).

Elaborate study show that in the course of acceptable take into account behavior prefabricated structures in joint prefabricated. May be completed use for design internal

forces in structures net thickness gap apply linear calculation. Computer analysis structures and their load is only variant solution because verification results trough the use of load test real structures almost impossible in the face of big size structures and their heavy load carrying capacity structures.

Results from calculation that load carrying capacity horizontal joint have to influence into carrying capacity all structures at load take vertically. In case that decisive factor for carrying capacity prefabricated structures in gap is bearing resistance horizontal joint in pressure, we have to determine bearing resistance all structure as that the proportion of pressure horizontal joint and wall prefabricated. Effect vertical joint and neighboring prefabricated in carrying capacity prefabricated structures with gap declines after exponential curve with in growing distance from gap. Low carrying capacity make structures with minimal depth column next to gap or side jamb gap forms late joint prefabricates.

Result study acknowledge importance analysis size gap and location gap in structures for decision making about reality his performance, pointed also critical place structures that need devote advance attention.

References:

- [1] WITZANY, J. *Vady, poruchy a rekonstrukce panelových domů* Stavební ročenka 1998 1998
- [2] HORÁČEK, E., VADIM, I., PUME, D.: *Únosnost a tuhost styků panelových konstrukcí* SNTL 1983
- [3] HORÁČEK, E.: *Navrhování nosných styků panelových budov podle československých předpisů* Pozemní stavby 1997, 08/1987,
- [4] HORÁČEK, E.: *Panelové budovy – Navrhování a výpočet nosné konstrukce* SNTL, 1977

This research has been supported by CTU0401811.

Ensuring of a Pit, Underpinning of Existing Structures – on-Line Course

Z. Jeřichová, M.Dubnová, R.Mikula

jerichov@fsv.cvut.cz

Department of Technology of Construction, Faculty of Civil Engineering, Czech Technical University, Thákurova 7, 166 27 Prague 6, Czech Republic

Present time can be characterized as a time of inflow of knowledge and information – in many fields. Many standards, new technologies, many discoveries have come into being and many of them are still appearing. It is a problem for anybody to absorb such quantity. And also it is a problem for a teacher to prepare a valid long-term study material in a paper form. On the other hand there exists such medium as internet – enabling people to get information for instance from their homes. I suppose that those are some of the reasons why on-line study publications are becoming popular and also why some students will probably in not distant future choose to take a distant type of study and some of them can prefer a subject worked-out as on-line course in comparison with regular study.

We have worked out an on-line course concerning ensuring of a pit and excavation as a whole and underpinning of existing structures. It should enable students to get some information about used kinds of retaining walls – piles, micropiles, h-piles, cast-in-situ diaphragm walls, pre-cast diaphragm walls, jet-grouting, steel sheet piles, anchors – performed in hydro-geological and local conditions. It is quite an important matter for water, transport and civil engineers to be able to design convenient and performable ensuring of a pit, as most of constructions are performed in urban conditions with high density of neighbour structures. The design of retaining structures must reflect the way of their performing and needs. There exists a division into two parts during retaining structures: 1st part – retaining structures performed by means of big machines, usually not able to work in solid rock, 2nd part – retaining structures performed by means of smaller machinery plant – able to get into solid rocks. On the other hand the retaining structures can be divided from point of view of their permeability. Some of them can be performed as impermeable, some as permeable. The choice of convenient type of retaining structure so depends on local and hydro-geological conditions especially. The projector must also notice influence of aggressiveness on structures. Some stage of aggressiveness needs a secondary prevention – not performable for each type of retaining structure.

The text also contains information on the performing of this sheeting and simplified static survey – by means of static software GEO4.

In the text there are also described some ways of dewatering of excavations as pumping from wells, well-points, from sumps, simplified calculation of needed number of wells, design of their diameters and depths.

The study material is combined with answers concerning individual chapters and also six tasks – four for static survey of retaining structures, one for choice of convenient type of retaining structure and one for design of dewatering system. The static survey could be worked out by means of PC software intended to be installed in PC room of a school.

The course is worked-out in HTML form. The material consists of two columns - left with text and right with pictures, tabs and so on. CTU has been holding a licence on Class-server for preparing on-line teaching since 2004 year. It is in a tested stage now. After getting-know more of this system the communicative part of text may be converted into this system.

System of the on-line course:

Ensuring of a Pit and Excavations as a Whole, Underpinning of Existing Structures

1. Preface :
 - 1.1 Why just this theme and for whom is this course?
 - 1.2 What can we imagine under name ensuring of a pit and excavations as a whole (during this course)?
 - 1.3 Content of a course = what can we learn
 - 1.4 Contact
 - 1.5 Some technical data
2. Basic data
 - 2.1 Kinds of excavations and their definitions:
 - 2.2 What should we know before starting to design a way of ensuring the excavation
 - 2.3 Where is no need to have excavation with sheeted or battered faces?
 - 2.4 When retaining structure and when battered faces?
 - 2.5 Safety battered faces
3. Retaining structures
 - 3.1 Which retaining structures do we know and for which branches of building industry are they suitable
 - 3.2 Impermeable retaining structures
 - 3.2.1 Steel sheet piles
 - 3.2.2 Cast-in-situ diaphragm walls
 - 3.2.3 Over-bored piles
 - 3.2.4 Jet-grouting
 - 3.3 Permeable retaining structures
 - 3.3.1 H-piles
 - 3.3.2 Pile walls
 - 3.3.3 Pre-cast diaphragm walls
 - 3.3.4 Micropiles
4. Static survey
5. Aggressiveness on retaining structures
6. Excavation with level of the bottom under water surface
7. Occupational safety
8. Tasks
9. Literature
10. What to say in the end?

On-line course will be placed on web pages of Department of Technology of Construction. It should enable students to know more of ensuring of excavations and design of convenient retaining structures. Probably it will be offered as an eligible course.

References:

This research has been supported by FRVŠ grant FRV F1 1925

Application of Artificial Neural Network to Control the Coagulant Dosing in Water Treatment Plant

A. Grünwald, P. Fošumpaur*

`grunwald@fsv.cvut.cz`

Departement of Sanitary and Ecological Engineering, *Departement of Hydrotechnics,
Faculty of Civil Engineering, Czech Technical University,

Thákurova 7, 166 29 Prague 6, Czech Republic

Natural waters contain many different compounds, both natural and anthropogenic. Categories of these compounds include taste and odor causing compounds, synthetic organic chemicals, pesticides, herbicides, trihalomethanes precursors etc. Most of these chemicals are hazardous and must be removed from drinking water. The most common water treatment includes chemical coagulation followed by separation (sedimentation or flotation). Coagulation is a treatment process by which the physival or chemical properties of colloidal or suspended particles are altered such that agglomeration is enhanced to an extent that these solids will settle out of solution by gravity or will be removed by filtration. Coagulants change surface charge properties of solids to promote agglomeration and/or enmeshment od smaller particles into larger flocs.

Historically, most coagulation processes were primarily designed for particle and turbidity removal. However, some plants, especially those having to treat highly colored water, were designed to remove organic matter. The modification of the coagulation process to achieve greater natural organic matter removals is called „enhanced coagulation“.

Enhanced coagulation is a method for maximising the removal of dissolved organic carbon (DOC) which results in reduction of chlorine decay rates and THM formation in water distribution system. High doses of coagulant (typically Alum or Ferric Sulphate) are used, higher than those needed for the reduction of colour and turbidity alone. It has been well established that removal of DOV is strongly influenced by pH, with the optimum being about 5-6. Depending on the type of DOC and its concentration, usually more than about 50% of DOC can be removed by enhanced coagulation.

Improvement performance in operation and control of water treatment process plants depends on better understanding of the inter-relationships of process variables. Computer simulation is mainly based on principal models and has been widely used as a tool to capture the inter-relationships of process variables. If principal models are not available, neural networks can be employed to learn empirical models from databases. The main advantage of neural networks compared with more traditional data-driven approaches, such as regression analysis, is that they are highly non-linear, universal function approximators. In addition, the form of the model does not have to be chosen at the start of the modelling process, but is chosen so as to provide the best fit to the available data.

In some previous studies artificial neural networks were used to develop process inverse models for the prediction of optimum coagulant doses [1,2]. In all studies, the model inputs consisted of raw water parameters, whereas the model output was the optimal coagulant dose needed to achieve the desired treated water quality.

In this work, ANN model are developed that are capable of assisting treatment plant operators with determining optimal alum doses for water treatment plant Plav in southern Bohemia. This WTP provides settling, coagulation, flocculation sand filtration and disinfection with chloramines.

The inputs to the model predicting treated water quality parameters were the raw water quality parameters and the applied alum dose. The model outputs were the treated water quality parameters that are to be controlled by the addition of coagulant, namely turbidity, color and COD. The pH and residual coagulant concentration of the treated water were omitted.

References:

- [1] GAGNON C., GRANDJEAN B.P. A., THIBAUT J.: *Modelling of coagulant dosage in a water treatment plant*. Artificial Intelligence in Engineering. 11, 1997, pp. č. 401–č. 404.
- [2] JOO D.S., CHOI D.J., PARK H.: *The effects of data preprocessing in the determination of coagulant dosing rate*. Water Research 34, 13, 2000 pp. č. 3295-3302.

This research has been supported by NAZV grant No. 1G46036, No. QD1004, MSM J04/98:211100002 and GA ČR 103/02/D049.

Optimization of a Turbine Intake Structure

P. Fošumpaur, F. Čihák

fosump@fsv.cvut

Department of Hydrotechnics, Faculty of Civil Engineering, Czech Technical University,
Thákurova 7, 166 29 Prague 6, Czech Republic

A suitable design of the hydro power plant inlet belongs among the basic premises for the proper functioning of the plant and assists in increasing the overall efficiency, optimizing the operation of the plant. The hydraulic solution for the separating pier as well as other components of the inlet usually employs a method of mathematical modelling.

The objective of this study is the optimization of hydrodynamic conditions in the area of the inlet of a run-off river hydro power plant using a 2-D mathematical modelling of the flux. The main emphasis is placed on the design of the separating pier between the weir and the power plant since the wrong width and shape may cause detachment of the current from the face side of the pier infringing the flux. This disturbance then propagates to the inlet of the nearest aggregate. Measurements conducted on finished water works have demonstrated a decrease in the efficiency of such an aggregate by as much as 30% [3]. The above-mentioned methodology can also be used for the optimization of pier shapes, in order to direct the inlet flux towards the individual turbine blocks. These piers also serve as supports for the coarse screens and the footbridge.

The modelling was carried out on the premises of a stable two-dimensional flux of incompressible fluid. Both viscosity and density were considered equal within the whole area. The basic description of the fluid flux is given by the two Navier-Stokes equations and the continuity equation [4]. The above set of equations is used for the calculation of the laminar flux of real fluid. For real flows, the current must be considered turbulent. Mathematical modelling of a turbulent flow used the turbulent k - ε model [4], comprising modified Navier-Stokes equations with the Reynolds number, the continuity equation, transport equations and the diffusion of kinetic turbulent energy, and equations describing transport and diffusion of the speed of the dissipation of the kinetic energy of the turbulence. The above-specified equations for the 2-D turbulent flow were approximated by the Finite Element Method in the computing environment FEMLAB. Geometric limit conditions are given by the shape of the area of flux and are based on the layout solution of the inlet to the water power plant. The geometry of the inlet was estimated first, with the subsequent optimization of the geometrical solution with the aim of achieving the most uniform possible velocity profile between individual turbine blocks.

The case study of inlet optimization before turbine blocks is calculated for the project of the power plant on the Nemen River in Belarus. The flux area was derived from the layout solution of the power plant and the weir. The positioning of the power plant, weir fields and piers between individual turbine blocks was retained. The water power plant comprises a total of five turbine blocks, separated in the inlet by piers with elliptical pier heads. The number of finite elements in the area was 5,000 to 10,000 depending on the alternative and type of flow. A reliable description of the inlet flow to the power plant required the selection of a sufficiently large area for the solution. The power plant is located on the concave side of a curve of a diameter of approximately 340 m. The area of the solution starts at the beginning

of this curve in the vicinity of the upper dock of the lock chamber, where uniform distribution of velocities is assumed.

A total of five basic scenarios of the power plant inlet were examined. Four of them focused on the shape of the separating pier and one examined the effects of the shape of the side pier between the power plant and the riverbank. The circumfluence around the separating pier between the power plant and the weir is unsymmetrical; therefore the shape of the pier should be equally unsymmetrical and streamlined. A model research [1,2] demonstrated that the width of the separating pier is a function of turbine flow rates.

There are numerous empirical relations and recommendations for the optimum design of hydrodynamic shapes of elements subject to circumfluence in the area of the inlets of water power plants, usually based on physical research in laboratories. This paper utilises these recommendations in the formulation of the initial design scenarios, which are subsequently optimised using 2-D mathematical modelling of the laminar and turbulent flux. The advantage of this solution is above all in the low time and financial demands of the optimization of inlet elements of hydro-power plants.

References:

- [1] ČIHÁK, F., MEDŘICKÝ, V.: *Navrhování jezů*. Vydavatelství ČVUT, Praha, 1991.
- [2] GABRIEL, P., GRANDTNER, T., PRŮCHA, M., VÝBORA, P.: *Jezy*. SNTL, Praha, 1989.
- [3] HOLATA, M.: *Malé vodní elektrárny*. ed.: Pavel Gabriel, Academia, Praha, 2002.
- [4] WILCOX D.: *Turbulence Modeling for CFD*. 2nd edition, DCW Industries Inc., 1998.

This research has been supported by grant No. 103/02/D049 of the Grant Agency of the Czech Republic.

Adaptive Control of Water Resources in Climate Change Conditions

P. Fošumpaur, F. Klouček

`fosump@fsv.cvut.cz`

Departement of Hydrotechnics, Faculty of Civil Engineering, Czech Technical University,
Thákurova 7, 166 29 Prague 6, Czech Republic

Climate change significantly affects water resources which evokes demand of the new management and control strategies development. This contribution quantifies and discusses climate change impacts on water yield and on the value of the previously defined cost function which describes cumulative losses as an result of water supply failures. Recently, the research has shown that to mitigate adverse climate change impacts on water resources adaptive control models can be used to advantage. The paper deals with optimization of these adaptive models known from cybernetics in conditions of stochastic uncertainty with the use of synthetic series of daily flows affected and non-affected by the climate change.

Owing to the climate change, higher flow variability (while keeping the same average annual flows) is to assume. It could result in a decrease in minimum flow and an increase in value of flood flows. Reservoirs are usually designed to supply preferably constant releases for various demands, which are highly reliable. However, this reliability could not be achieved, if the above-mentioned change occurred. The active storage capacity of water reservoirs, which serve for fluent and continuous water supply, are unable to resist more frequent drought periods. Due to the emptying of active storage, the required amount of water could not be supplied to consumers and this would lead to economic losses. Indeed, these losses can be reduced by the application of adaptive control model.

The proposed Adaptive Control Model (ACM) is based on Patera and Nachazel [1] concept. ACM puts off the moment of water supply failure, which occurs in the hydrological drought period. This postponement can be reached by well-timed reduction of the releases. The current release restriction depends on the predicted inflow and on the condition of active storage. The lower the inflow and condition of active storage is, the more restricted the release will be. The actual release is given by the decision matrix and it depends on the actual storage and on river inflow forecast. ACM in the course of management restricts releases from reservoir, the function of which is described in the simulation model (SM). SM imitates the reservoir function by balance calculation of inflows and releases.

The discharge series used in the simulation model is given by the stochastic ARMA model which generates average annual discharges (1000 years long). These annual values of discharges are consecutively modified either by fragments of real daily discharges or by adjusted fragments which describe the favourable and unfavourable probable climate change.

The optimum way of management is defined by the minimum sum of economic losses evaluated by balance calculation of given flow series. It is impossible to express the problem analytically, the optimum point is reached by repeated calculations using varied parameters of ACM. Under these parameters, we understand elements of the decision matrix. We have taken into account two different methods for retrieving the restrictive coefficient :

- the restrictive coefficient is given by the set according to decision matrix [1],
- the restrictive coefficient is intermediately interpolated and acquires values ranging from C_{\min} to C_{\max} ,
- for comparison, the model without optimization was applied.

For optimization, the genetic algorithm (GA) method is used [2]. This method is one of the powerful stochastic optimization techniques, which belong to the group of artificial intelligence methods. Results are compared with standard procedures of non-linear programming. These methods are capable to find the global extremes of non-linear and multi-dimensional functions. Following figures show process of optimization. In case of optimization by GA method is evident stochastic manner of process. In case NP method the changes are fluently.

As a case study the adaptive control of the Rimov reservoir in the Czech Republic was accomplished. Control model was accomplished with the use of Matlab programming environment [3]. It was shown that the optimized adaptive control model can partly mitigate climate change impacts in comparison with standard release control.

References:

- [1] NACHÁZEL, K. – PATERA, A.: *Možnosti využití principu adaptivity pro řízení nádrží v reálném čase*. Vodohosp.čas., 36 1988 pp. č. 237–285.
- [2] GOLDBERG, D.E.: *Genetic algorithms in search*, Optimization and machine learning. Addison-Wesley Publishing Company, Inc. Reading Massachusetts, 1989 pp. 412
- [3] MATLAB *The Language of Technical Computing*. The Math Works, Inc. 2004.

This research has been supported by grant No. 103/04/0352 and No. 103/02/D049 of the Grant Agency of the Czech Republic.

A Neural Network Approach for the Optimisation of Water Treatment Plant Management

A. Grünwald, P. Fošumpaur*

grunwald@fsv.cvut.cz

Departement of Sanitary and Ecological Engineering, *Departement of Hydrotechnics,
Faculty of Civil Engineering, Czech Technical University,

Thákurova 7, 166 29 Prague 6, Czech Republic

Better controlling and optimising the plant's processes has become a priority for Wastewater Treatment Plant managers. The more and more strict standards for treatment plant effluents require better process control. The use of mathematical models is also crucial to elaborate optimised management strategies. The major aims of the control options in WWTPs can be summarised as follows:

- Avoiding discharge of biomass into the effluent
- Maintaining performance of the plant processes
- Meeting the overflow discharge and effluent standards
- Minimisation of operation and maintenance costs.

Dynamic simulation of wastewater treatment plants is generally used as a powerful tool to increase the detailed knowledge on the process and system behaviour, for optimisation studies (e.g. performance evaluation, operational optimisation, controller design and conceptual process design), for training and teaching, and for model-based process control. In the last years dynamic simulation not only became an important tool for the scientific community but also proved its usefulness in the general wastewater treatment practice.

The quality of simulation studies can vary strongly depending on the goal set, expertise available and resources spent. Different approaches and insufficient documentation make the quality assessment and comparability of these studies difficult or almost impossible.

The model-based diagnosis technique requires good mathematical models to represent WWTP under different conditions. Even though many different models such as IAWQ Activated-Sludge Model No.1 and 2. [1,2] have been developed, there are still weak points in applying these models to diagnosis and control problems of real activated – sludge WWTP. These weaknesses include: (1) they cannot provide an entirely satisfactory description of the cause-effect relationships within the activated-sludge WWTP, (2) the models require the specification of a large number of parameters, many of which are difficult to determine, (3) a large number of parameters included in this model need to respecify parameter values for different operational conditions [3].

In the recent years, intelligent monitoring and fault diagnosis to achieve good performance of WWTP using an artificial neural network-based pattern recognition technique has been a very active investigation area.

The aim of this work is to discover the interrelationships and response of the process variables and to analyse the system behaviour of the real activated-sludge WWTP using a neural network.

The Hostivice WWTP is located on the west of Prague and was originally built with the specification of the conventional activated-sludge process.

References:

- [1] HENZE M., GRADY JR CPL., GUJER W., MARAIS GR., MATSUO T.: *Activated Sludge Model No. 1*. IAWQ Scientific and Technical Report No. 1, IAWQ, London, UK 1987 .
- [2] HENZE M., GUJER W., TAKAHASHI M., MATSUO T., WENTZEL MC., MARAIS GR.: *Activated Sludge Model No. 2* IAWQ Scientific and Technical Report No. 3, IAWQ, London, UK, 1995 .
- [3] HONG YS., BHAMIDIMARRY SMR., CHARLESON T.A.: *A genetic adapted neural network analysis of performance of the butrient removal plant Rotorua* Institute of Professional Engineers New Zealand (IPENZ) Annual Conference. Simulation and Control Section, 1998 pp. č. 2-43.

This research has been supported by the NAZV grant No. QC 0244 and MŠMT grant MSM J04/98:211100002.

Fatigue of Composite Steel and Concrete Structures

J. Mareček, J. Studnička

jan.marecek@fsv.cvut.cz

Department of Steel Structures, Faculty of Civil Engineering, Czech Technical University, Thákurova 7, 166 29 Prague 6, Czech Republic

Steel and concrete composite structures consist of a steel section, concrete slab and a shear connector, that transfers longitudinal shear force acting at the steel-concrete interface. Among wide-spread shear connectors belong headed studs, *HILTI* brackets and perforated shear connector, that is made of a steel plate of certain height and thickness, through which holes are punched. Such connector is welded upright to upper flange of a steel section. So called “concrete dowels” formed in connector holes together with reinforcement of a concrete slab running through these holes transfer longitudinal shear force. Perforated shear connector was developed in 1985 in Germany and in 1987 performance analysis was published in [1]. Since this time development of different types of perforated connector began in many countries. Investigated connectors differed in dimensions and hole shapes. Experimental specimen configuration differed in amount of transversal reinforcement and in concrete strength. The aim of both experimental and theoretical research was to find relation between above mentioned variables and shear load capacity of the connector in terms of kilonewtons per connector length (kN/m).

At the Department of Steel Structures research of perforated connector started in 1994. Two connector shapes were developed. „Basic“ or sometimes called „low“ connector with height of 50 mm, thickness of 10 mm with holes 32 mm in diameter was termed as connector „CTU 50/10“. The second „high“ connector, termed as „CTU 100/12“, was 100 mm high, 12 mm thick and with holes 60 mm in diameter. Basic connector is to be used mainly for building construction, high connector for bridges and for heavily loaded structures.

Altogether 34 push-out tests and 3 beam tests with basic connector under static loading were carried out. Based on regression analysis of experimental results formula for shear load capacity of CTU 50/10 connector was derived [2]. This formula takes into account the two variables: amount of transversal reinforcement and concrete strength. Numerical analysis of push-out specimen under static loading based on finite element method was performed as well. Also different modifications of basic connector were arranged and tested (parallel connectors, heightened basic connector etc.).

As for high connector, 16 push-out tests under static loading with normal concrete and 9 with lightweight concrete were carried out. Formula for static shear load capacity of this connector was established as well.

Since high connector CTU 100/12 is proposed to be used mainly for bridge steel-concrete composite beams (simple supported or continuous) with concrete slab thickness of about 200 mm, also its behaviour under repeated loading, which is in bridges caused by traffic, has to be known. For this reason push-out tests under repeated loading had to be conducted. Altogether 3 push-out tests with cyclic loading of a specimen with connector CTU 100/12 have been carried out so far. These tests, conducted by CTU, were performed in 2001 – 2003 in „Dynamická zkušebna ŠKODA VÝZKUM s r.o.“ in Plzeň, Czech Republic. All the three specimens were identical with concrete cylindrical strength of 40 MPa and with reinforcement area of 0.25 mm²/mm. 1st, 2nd, 3rd specimens were loaded cyclically with frequency 3, 4.5 and 3 Hz respectively. Load amplitude (difference between maximal and minimal acting force), which was the most important variable, was 460, 300 and 450 kN respectively. Specimen was loaded either until its failure or until the number of cycles 2

million was reached. 1st and 3rd specimens failed after 808,000 and 1,909,000 cycles respectively. In both cases micro-cracks occurred on outer surfaces of concrete blocks just after first cycles and spread and joined into one magistral crack after further cycles. Fatigue fracture occurred in the connector at the outer opening in 1st as well as in 3rd specimen. 2nd specimen did not fail even after the number of cycles 2,400,000.

Based on these experimental results the following can be concluded. Fatigue load capacity (amplitude corresponding to the number of cycles 2,000,000) of perforated shear connector CTU 100/12 while using concrete with cylindrical strength 40 MPa and with area of transversal reinforcement $0.25 \text{ mm}^2/\text{mm}$ is approximately 375 kN/m. It is assumed, that increasing amount of transversal reinforcement will lead to higher fatigue load capacity of the connector, however it is necessary to verify this assumption either by other experiments or by a numerical model. Since the experiments with cyclic loading are extremely expensive, the only way to verify the results and to extend them for different specimen modifications is to prepare a theoretical model.

Due to large complexity of the problem (two different materials, cyclic loading) software based on finite element method ABAQUS was chosen for modeling. Symmetry along the two planes of the specimen allows to model only its quarter. Very important aspect of numerical modeling is to choose the right material model as well as to input corresponding material parameters. Concrete block was modeled by using "concrete damaged plasticity", one of many material models included in ABAQUS material model library. The "concrete damaged plasticity" model in ABAQUS uses concepts of isotropic damaged elasticity in combination with isotropic tensile and compressive plasticity to represent the inelastic behavior of concrete and is defined by using the concrete damaged plasticity, concrete tension stiffening and concrete compression hardening options. This model was designed among others for affecting behaviour of concrete under cyclic loading. Steel part of the specimen was modeled by using nonlinear isotropic/kinematic hardening model, one of the two material models for cyclic loading of metals in ABAQUS, which describes translation and expansion of yield surface in stress space. Constrain equations defined at nodes are applied, where translation in z-direction (along the connector) is enabled, while translations in other two (x-, y-) directions are restrained. Dividing the model into finite elements was performed using structured mesh technique provided by ABAQUS. Shell elements S4R are used for steel part of the model, while concrete is modeled with continuum C3D8R elements. Very important steps in this numerical modeling, that have not been performed yet, are defining loading and load steps relating to cyclic loading, final solving the problem and comparing obtained results with those from experiments together with subsequent calibration of the numerical model, which is supposed to be a powerful tool for the following parametric study.

Intensive effort is made to finish the numerical model successfully, however no certain results have been gained so far.

References:

- [1] LEONHARDT, F. – ANDRA, W. – ANDRA, H.P. – HARRE, W.: *Neues, vorteilhaftes Verbundmittel für Stahlverbund-Tragwerke mit hoher Dauerfestigkeit*, Beton-und Stahlbetonbau, 12, 1987, pp. 325–331.
- [2] MACHÁČEK, J. – STUDNIČKA, J.: *Perforated Shear Connectors*, Steel and Composite Structures, Vol.2, No.1, 2002, pp. 51–66.

This research has been supported by CTU grant No CTU0402211.

Using SAR Interferometry For Detecting Landslides And Subsidence In The Coal Basin In Northern Bohemia

J.Kianička, I. Čapková

jan.kianicka@fsv.cvut.cz

Remote Sensing Laboratory Department of Mapping and Cartography Czech Technical University, Faculty of Civil Engineering Thákurova 7 Praha 6 - Dejvice

This article describes the possibilities and applications of active remote sensing. It also considers using SAR interferometry techniques in geotechnical applications in northern Bohemia. First of all, is this problem connected with SAR (Synthetic Aperture Radar). This is the kind of radar that scans Earth surface by receiving and measuring not only delay and amplitude of reflected signal, but also frequency and phase. This helps resolving the problem of resolution in flight direction and it is possible to receive data in resolution about three orders higher. This radar is named coherent radar and it is the basic condition for using the SAR interferometry method. In principle, radar interferometry in digital processing is comparison of corresponding pixels in two images of the same area acquired in a very little different looking angles. Generating the interferogram involves only pixelwise subtraction of the phases of both images. Phase difference is closely connected with difference in distance between Earth surface and the satellite. The advantage of the method is the possibility of very accurate measurements of this phase difference.

The method can be applied for topographic mapping with relative precision of 10 – 15 m, deformation mapping with precision less than 1 cm, another possibility is thematic mapping based on change detection, and last one is measuring the atmospheric influence on satellite movements.

We can see wide use of this method but in practice, obtaining data with such high precision is difficult, because it's very sensitive on many events. For instance a wet surface, snow or vegetation has a significant influence on surface features in longer time periods, and the interferometry method is impossible to use due to decorrelation.

Our project is focused on using of the conventional interferometry for monitoring landslides and ground displacements caused by mining activities in northern Bohemia. We are using data from European satellites ERS 1 and ERS 2 (Earth Resource Satellite). Hence ERS 1 is over we plan to use data from the new biggest remote sensing satellite, ENVISAT. In our whole solution we wanted to use only free software products, but the step named SAR processing is not covered by this kind of service, so we used SAR processor developed in Indian Bombay University. For an interferometric processing, open-source product DORIS is used. A digital elevation model (DEM) was successfully derived from a tandem pair. This topographic information serves as input into so called three pass interferometry where three scenes are needed. One topographic pair and one differential one, which should already contain deformation. The purpose of our research is to test this method and compare the results with different ground based methods on specified area of the open brown coal mine Chabarovice. Unfortunately, deformation interferogram doesn't show good results in the place. Next step is to improve method using or developing different algorithms, and using data selected with different criteria.

Problems: There are several problems in our project. First of all, we don't have enough data to produce reliable estimates of deformations. For data selection, very strict criteria were used because of the fear of coherence lost due to vegetation and atmosphere. Fortunately, even the interferogram with temporal baseline longer than two months and spatial baseline of approx. 100 m shows good coherence in more than 50 % of the area. There is also another deformation pair selected, but there are some problems with coregistration so an

interferogram cannot be generated. This problem is probably caused by convergence of orbits and therefore the resampling step cannot be covered by the polynomial transformation.

Another problem of our application are the orbit and atmospheric errors which cannot be distinguished (their influence is very similar and both can be corrected by the same procedure – setting the „artificial“ baseline – see e.g. [3]).

Future work: First, we plan to order another data; the criteria for data selection should not be so strict now. We would like to process data with shorter perpendicular baseline (in order to prevent such a strong influence of errors) and different seasons (not just winter). We would also like to improve results by testing other algorithms.

We would also like to implement interferogram adjustment in order to eliminate the orbit errors: to adjust the measurements to a plane (but this procedure is dependent on the success of phase unwrapping which is not certain), implement some sophisticated methods both with and without use of tie points.

References:

- [1] KAMPES, B. - USAI, S: *Doris: The Delft Object-oriented Radar Interferometric software*. DEOS, 1999.
- [2] RABUS, B. - EINEDER, M. - ROTH, A. - BAMLER, R.: *The shuttle radar topography mission – a new class of digital elevation models acquired by spaceborne radar*. ISPRS Journal of Photogrammetry and Remote Sensing 57, 2003, pp. 241-262.
- [3] TARAYRE, H. - MASSONNET, D.: *Atmospheric Propagation Heterogeneities Revealed by ERS-1 Interferometry*. Geophysical Research Letters, vol. 23, No. 9, 1996 pp. 989-992.
- [4] HANSEN, R.: *Radar Interferometry, Data Interpretation and Error Analysis*. KLUWER ACADEMIC PUBLISHERS, 2001.

This research has been supported by CTU grant No. CTU0403811

Application of UMS and SISIM numerical models for classification of brownfields in the Czech Republic.

J. Hajaš, V. Kuráž

`j.hajas@centrum.cz`

CTU, Faculty of Civil Engineering, Dept. of Irrigation, Drainage and Landscape Engineering
Thákurova 7, 166 29 Praha 6

The Czech Republic is country with high loads due to point sources of pollution and, in general, there are large brownfield areas. However, considerable efforts have been made in the last decade to improve the situation. The removal of brownfields always leads an improvement in the environment, especially when it is a matter of dealing with present or potential sources of contamination that threaten water quality.

Approximately 80% of all decisions on brownfields are made on the basis of a risk evaluation for groundwater. This risk assessment is based on an estimation of the absorption and desorption matter in the soil, and also involves a prediction value for introducing improvements and anticipates the time period for which possible contamination of groundwater may continue. A basic starting point in brownfield remediation is to ascertain a socially acceptable value of ecological and health risks.

UMS/SISIM models were selected as software tools for classifying brownfields. The model was created in cooperation with the following institutions: Chemlog GbR, Focon GmbH and LFA RWTH Aachen. For this classification, the UMS System was chosen from the accessible software programs. It connects a transport simulation model of harmful substances SISIM and self-model UMS. UMS model derives a recommendation on how to use the locations at the present time or in the future, taking into account affected user groups, soil characteristics, concentration of contamination in contact media, the transport medium and soil, and also the background load. SISIM simulates transfer in the unsaturated zone and quantifies the extent and time of possible groundwater contamination. The calculations are carried out until the capillary zone is reached. Based on this information, the potential contamination in the aquifer can be determined and it can be established by means of a comparison with target levels whether a risk situation exist. The numerical model was tested on an area of about 0,7 ha situated in the former industrial park of CKD Prague (used in the past for burning solid fuels and for dumping municipal wastes, accumulator cells, barrels containing unknown liquids, chemicals, etc.) Verification of the model in the Czech Republic indicates that a small number of simple and efficient soft resources can lead to rapid and efficient determination of all factors that influence decision making on the re-use of brownfields.

Three soil sampling have been made on monitoring area or its vicinage. Laboratory analyses of soil samples proved exceeding of limits on one sample. Values were overrun by Arsenic (limit B) and non-polar extractives (limit C).

For these substances was done also simulation by UMS for determination of the best way for use of surveyed area. For Arsenic were used 8 of exposure scenario. After simulations we can determine final recommendation. Soil in this area with that concentration of pollution is possible safely use only for commercial building or like industrial areas, either as public green with the small risk. Such as places, where not direct contact with contaminated medium (soil) is and where is restricted frequency of risk-groups, especially small babies and children. Results from SISIM displays small amount of contamination in soil

profile and it is without influence on groundwater. Similar conclusion we get for non-polar exceeding namely, that the deposit of pollution is not extensive and it will not have influence on underground water. It means (in connection with the UMS), that after remediation (from-mining) of contaminated soil, will be possible make use of locality without restriction.

During this project - working with the UMS/SISIM models, the creating basics databases was finished and the comparison was done between obtained results (values of impact to groundwater and recommended using models) and values from the ecological audit. General handbook for using the UMS/SISIM program in the form of user manual translation arose during the solving project as a part of the methodology, and also it will be a part of dissertation thesis of this project author. The manual in Czech language will serve as a basis for the interrelated project.

Results:

- inserted databases were tested in research area and the results were compared with obtained values by ecological audit of Ekohydrogeo Zitny,
- the methodology for creating and creating extended databases are in process now,
- results will be used in dissertation thesis, which is going to be defended during of the year 2006

In the meantime was the UMS/SISIM program found as very available tool for determining to use contaminate areas. Its using is simple and purposeful. The results carried out by means of the UMS/SISIM model do not show any fundamental deviation in comparison with the values and the results obtained in ecological audit.

References:

- [1] P. DOETSCH: *Risikoquantifizierung mit dem UMS-System*, Chemlog/IfUA GmbH, 1998, pp. 2-60.
- [2] M. MACHTOLF, D. BERGMANN: *Das UMS Programm; Anwendungsbeispiele*, Chemlog/IfUA GmbH, 1998.
- [3] D. BERGMANN, P. DOETSCH, D. GRÜNHOF: *SISIM - Sickerwasser Simulation*, Chemlog/focon, 1998.,

This research has been supported by CTU grant No. CTU0403211

Connection of HDM 4 System with Current Statistic and Diagnostic Systems

O. Rynes

rynes@fsv.cvut.cz

Department of Road Structures, Faculty of Civil Engineering, Czech Technical University, Thákurova 7, 166 29 Prague 6, Czech Republic

The Highway Development and Management System - HDM-4 - is a software system for investigating choices in investing in road transport infrastructure. The Highway Design and Maintenance Standards Model (HDM III), developed by the World Bank, has been used for over two decades to combine technical and economic appraisals of road projects, to prepare road investment programmes and to analyze road network strategies. The International Study of Highway Development and Management ISO HDM has been carried out to extend the scope of the HDM model, and to provide a harmonized systems approach to road management, with adaptable and user-friendly software tools. This has produced the Highway Development and Management Tool HDM 4. The scope of HDM 4 has been broadened considerably beyond traditional project appraisals to provide a powerful system for the analysis of road management and investment alternatives. Emphasis was placed on collating and applying existing knowledge, rather than undertaking extensive new empirical studies, although some limited data collection was undertaken. Wherever possible, creative new approaches were developed for applying up to date knowledge to the technical problems and management needs of different countries. HDM 4 uses five basic mathematic models: Traffic, Road deterioration model, Road works model, Road users effects, Social and environmental effects. The results of economic analyses are quite sensitive to traffic data, and most benefits that justify road improvements arise from saving in road user costs (Road Users Effects). To perform economic analyses in HDM -4, traffic characteristics of road therefore need to be described and represented at an appropriate level of detail. Traffic characteristics need to be represented for project analysis. This requires a detailed representation of traffic characteristics on the road being analyzed. For each road section, the representation should include data items that describe the details of changing traffic composition and volumes, axle loading, capacity and speed-flow relationships, hourly traffic flows, traffic induced by road improvements and of demand shifts. Road deterioration is broadly a function of the original design, material types, construction quality, traffic volume, axle load characteristics, road geometry, environmental conditions, age of pavement, and the maintenance policy pursued. HDM 4 includes relationships for modeling Road Deterioration and Road Works Effects. These are used for the purpose of predicting annual road condition and for evaluating road works strategies. The relationship should link standards and costs for road construction and maintenance to road user costs through road user cost models. The modeling of Road User Effects comprises analysis of the motorized, non-motorized vehicle speed, operating costs, travel time and road safety. The vehicle classification system uses a flexible approach in which vehicles are divided into motorized and non-motorized categories, and each category is divided into vehicle classes. A class comprises several vehicle types or representative vehicles, which can be user specified based on one of several standard vehicle types. This approach suits the needs of many countries and satisfies all the analytical requirements in the system. The Social and Environmental Effects are for the analysis of energy balance and vehicle emissions. It is widely recognized that energy and environmental effects need to be

considered in the assessment of alternative investment policies and projects. By adopting projects and policies that minimize total life cycle energy use and vehicle exhaust emissions, related benefits such as reduced vehicle operating costs, reduced pollution, reduced dependency on imports of energy and reductions in the balance of payments deficits can be maximized. Planners and decision makers need to be able to understand the energy implications and environmental impacts of alternative road transport projects and policies. HDM 4 caters for three applications levels commonly used in decision making within the road sub-sector. Strategic planning – for estimating medium and long-term budget requirements for the development and preservation of a road network under various budgetary and economic scenarios. Programme analysis- for preparing single or multi-year work programmes under budget constraints, in which those sections of the network likely to require maintenance, improvement, of new construction, are identified in a tactical planning exercise. Project analysis – for estimating the economics of engineering viability of different road investment projects and associated environmental effects. Typical projects include the maintenance and rehabilitation of existing roads, widening or geometric improvement schemes, pavement upgrading and new road construction. In Czech Republic are now used only Project analysis. For analyzing by HDM 4 is needed calibrated workspace, which is issued by Technical Department of Ředitelství silnic a dálnic ČR. This workspace contains data of vehicle fleet, maintenance and improvement standards, and all calibrated parameters such as climate zone, traffic flow patterns, speed flow types etc. For entry of road network parameters can be used built in forms or data can be imported form file in dBase standard. This file and contains 159 fields for each section.

References:

- [1] H.G.R. KERALI: *HDM 4 Highway Development and Management*, PIARC 2000,
- [2] J. B. ODOKI, H.G.R. KERALI *HDM 4 Analytical Framework and Model Descriptions* PIARC 2002, pp. 1098-1105.
- [3] V. BOINA: *HDM 4 a možnosti importu stávajících databází proměnných parametrů a geometrie vozovky v ČR* Silniční obzor 4/2001 pp. 87-88
- [4] VUT BRNO *Navrhování vozovek pozemních komunikací* Technické podmínky 77 1995

This research has been supported by CTU0402611

Improvement of Concrete Surface Layer by Epoxide Coatings

L. Svoboda

svobodal@fsv.cvut.cz

CTU, Faculty of Civil Engineering, Dept. of Building Materials
Thákurova 7, 166 29 Praha 6

The common concrete is a considerably porous material. The rate of most of the degradation processes is controlled by the rate at which moisture, or any aggressive agent can penetrate the concrete.

The porosity of concrete has influence on freeze-thaw resistance too. Freeze-thaw degradation is a result of internal stresses caused by the freezing of water within concrete. The internal stresses are caused by the expansion of water as it freezes and pore pressure, which is developed in the capillaries of the concrete as water, moves through the concrete during freezing. Concrete, which remains dry in service, or is otherwise protected from water will be less susceptible to freezing damage.

Also strength, hardness, abrasives resistance and durability of concrete generally are limited by the porosity. One of ways for improvement lifetime of concrete is impregnation of concrete surface. Impregnation (surface treatment) with waterproof products (waterproof coatings) is firstly a barrier against the penetration of liquid water, into concrete, but suitable impregnant increases chemical resistance and strength of concrete surface layer. It is important namely in case of industrial floors.

All experience tells one that all concrete floors should have a surface protection. This way one will obtain an extended life and also a more aesthetic appearance. The choice of impregnant depends on many parameters concerning concrete (porosity, cleanliness, etc), the product and the local conditions for application (climatic conditions and purpose of service).

Concrete contains pores of varying types and sizes, and therefore the penetration some fluid substance into concrete can be considered as a flow through a porous medium. The rate of flow will not depend simply on the porosity, but on the degree of continuity of the pores at their sizes.

Flow can occur by movement of a fluid under a pressure differential (permeation), or by movement of a component under a concentration gradient (diffusion) and last but not least by capillary attraction of a liquid into empty or partially empty pores (sorption). The well selected impregnant must penetrate deeply and must act as a binder increasing mechanical properties of penetrated layer.

Strengthening of concrete is possible by epoxide coatings first of all. Epoxy resins based on epichlorohydrin and bisphenol A are well established materials used in a wide variety of applications. For surface treatment of concrete are used in diluted form. The viscosity of epoxy resins is too high for coating application and must be reduced by the addition of either nonreactive or reactive diluents.

Dibutyl phthalate, xylene, xylene-butanol, isopropanol or acetone can be used as nonreactive diluents and butyl glycidyl ether is a popular reactive diluent.

Common epoxide coatings for concrete surface treatment use acetone as solvent. A mixture of technical polyalkylene polyamines (containing mainly diethylenetriamine) is used as curing agent. Usual impregnation involves medium molecular weight epoxy resin. Total solid is 25 % by weight and epoxide group content is 3,0 – 3,8 mol/kg.

Nowadays are produced new types of epoxy resins (with lower molecular weight and lower viscosity) and new types of solvents appear either. It gives good preconditions for further development new concrete coatings.

A design of a better impregnating composition is possible as likely as not. The goal can be reached by using new resins, new hardeners, and new solvents. Additives improving capillary elevation and flow can help.

For testing of new epoxide impregnants a next method is developed. The method uses a layer of fine silica sand (with 100 mm thickness) as a model porous media. Pushing laboratory pestle into the sand layer does an indenture. Then a sample of tested impregnant (5 g) is dropped into the indenture. Glued piece of sand (conglomerate) is isolated from sand bed next day. Weight and cohesive strength of the conglomerate is rated by empirical scale (0 – 10 points).

Results can serve for further design. Using as data for formulation program based on flexible simplex algorithm seems be advantageous. Results obtained in dry sand bed must be completed with results in wet sand bed. It will necessary to compare results from sand bed with results from impregnated concrete samples. This contribution has therefore character of preliminary report only.

References:

- [1] I. KUČEROVÁ : *The solvent influence on penetration of Solakryl BMX solutions into wood* 35th International Conference on Coatings Technology, ČSCH, 2004, pp. 463-474.
- [2] J. NOVÁK: *Nátěry betonu* Sborník referátů z 31. mezinárodní konference o nátěrových hmotách, ČSCH 2000 pp. 79-85.
- [3] L. Hochmannová, J. Jarušek: *Snižování podílů organických rozpouštědel v epoxidových nátěrových hmotách* Sborník referátů z 33. mezinárodní konference o nátěrových hmotách, ČSCH, 2002, pp.76-84.
- [4] M. Sochůrek: *Nová i současná pojiva pro nátěrové hmoty sortimentu Spolchemie a.s.* Sborník referátů z 33. mezinárodní konference o nátěrových hmotách, ČSCH, 2002, pp.102-111.

This research has been supported by MŠMT grant No. MSM 210000030.

Risk Engineering and Reliability of Technical Systems

M. Holický*, J. Marková*, B. Novotný*, M. Sýkora*

holicky@klok.cvut.cz

*Department of Reliability, Klokner Institute, Czech Technical University in Prague, Solínova 7, 166 08 Prague 6, Czech Republic

The risk engineering and reliability are extremely important research topics, which are of a great interest of experts, state institutions, insurance and financial organizations as well as of the wide range of undertakings. The evident reasons for this are the recent accidents of technical systems including construction works for various purposes (structures and buildings for power production, public, administrative and service buildings, civil engineering works) constructed by investors in power industry, transportation, chemistry and other branches in all parts of the world.

The main goals of the presented research project include the development of reliability theory and methods of risk assessment taking into account uncertainties and vagueness of technical systems in accidental situations. In particular, theoretical models for unfavorable environmental effects are newly developed or re-examined for conditions of the Czech Republic.

Risk engineering methods based on the Bayesian concept [1] and probabilistic reliability methods are investigated and their application to risk analysis of complex structural and technical systems is discussed considering accidental design situations such as fire, impacts due to vehicles or trains [2], accidental actions caused by water, etc. It appears that theoretical models applied for the accidental actions can be improved using e.g. the Bayesian concept, sensitivity factors of the FORM method or experiments. Uncertainties in the theoretical models of actions and structural resistance are effectively described by the statistical models and uncertainties in the specified limit state are estimated by the fuzzy-probabilistic approach.

The newly introduced methods are applied in analyses of structural reliability and assessments of residual lifetime as well as in planning of maintenance and schedule of inspections. A special attention is paid to the methodology of risk assessment of technical systems under fire. It is emphasized that accidental actions and unfavorable impacts of the environment on technical systems should be analyzed by the developed procedures considering conditions of the Czech Republic.

Data for probabilistic models of accidental situations with regard to accidental actions in the Czech Republic are collected and theoretical models for various types of the actions are updated. The theoretical models for the behavior of existing as well as new structures under accidental situations are developed. Analyses of structures endangered by natural or technical seismicity and explosions are elaborated. Probabilistic models for accidental actions due to impacts of vehicles and trains together with models for estimates of damage caused by such actions are proposed. Database of probabilistic models for accidental actions in the Czech Republic and data for risk engineering is established, i.e. data are systematically gained, gathered and evaluated focusing on extreme environmental effects, e.g. fire actions, impacts of trains and vehicles, gas explosions, explosions caused by terrorists [3], etc. The collected data include common conditions of normal use of technical systems in persistent (design) situations and exceptional conditions in accidental (design) situations where both the existing and new structures are considered.

The project is partly focused on analysis of climatic actions considering conditions of the Czech Republic. Temperatures on bridges are measured and obtained data are used to specify the theoretical model. Stochastic analysis of wind speed in selected locations in the Czech Republic is carried out. Simulations of exceptional design situations of the wind actions on structures are generated using the boundary layer wind tunnel [4]. Results of numerous analyses clarify the reasons of changes in natural frequencies of structures with variations of temperature. Measurements of the snow load intensity in mountain regions are evaluated.

Response of footbridges to dynamic actions due to vandals is investigated and application of dynamic dampers is analyzed. It appears that effects of such dynamic actions are efficiently reduced by the dynamic dampers.

Part of the research is devoted to models of the layered structure of the pavement slab supporting system. The reliability of the computational model for concrete pavements is enhanced by the procedure allowing the layered structure to be fully accounted for. The procedure accomplishes a time-saving computation of layered system deflections under effect of the unit pyramidal loadings, from which the overall contact stress distribution in concrete-slab/subgrade contact problem may be constructed.

An important outcome of this research is implementation of the new findings into European and international standards and in their Czech national annexes. Background materials and recommendations for the development of the standards and regulations in the field of risk engineering and reliability are provided.

Within the framework of the newly implemented European standards, nationally determined parameters such as safety factors for actions and material properties are specified and design procedures are selected. Findings in reliability theory and probabilistic structural design are implemented in the European standard EN 1990 Basis of Structural Design. Results of analysis of dynamic actions on footbridges are used in EN 1991-2 Traffic Loads on Bridges. The measurements of the snow load intensity are used to determine the nationally determined parameters in EN 1991-1-3 Snow Loads. Extensive investigation of wind action on structures and its effects forms basis for the national annex of EN 1991-1-4 Wind Actions. Achievements of the research in reliability theory are included in JCSS Probabilistic Model Code where basic principles of probabilistic structural design are provided. Selected results are involved in the national annex of the international standard ISO 13822 Assessment of Existing Structures.

It is indicated that significant results are achieved within the development of six-year research project. The findings are applied in the construction industry and standardization as well as in the further research.

References:

- [1] M. HOLICKÝ: *Bayesian Assessment of Structural Risk under Fire Design Situation, Abnormal Loading on Structures*, E&FN spon., 2000, pp. 152-161.
- [2] M. HOLICKÝ, J. MARKOVÁ: *Reliability of Concrete Column Exposed to Accidental Action due to Impact*, Challenges of Concrete Construction, Dundee, UK, 2002.
- [3] M. STUDNÍČKOVÁ: *Dynamic Response of Building Loaded by a Terrorist Explosion Effect*, Theoretical and experimental research in structural engineering, 2004, pp. 139-144.
- [4] D. MAKVIČKA, J. KRÁL, D. MAKVIČKA: *Verification of Wind Response of a Stack Structure*, AED 2003, CTU Prague & University of Glasgow, Prague, 2003, 8p.

This research has been supported by the MŠMT grant No. MSM 210000029.

The Measuring of Hygric and Thermal Properties of Clay Plasters

R.Vejmelka, E.Mňahončáková, J.Toman, J.Drchalová

roman.vejmelka@fsv.cvut.cz

Department of Physics, Faculty of Civil Engineering, Czech Technical University, Thákurova 7, 166 29 Prague 6, Czech Republic

The topic of this paper is to describe the measuring of hygric and thermal properties of clay plasters, experimentally improved by polypropylene fibres or wool. The impact of this additives on thermal conductivity, moisture diffusivity and specific heat capacity has been studied. There was found, that the impact of additives on moisture diffusivity is very low. We was not able to determine the impact of fibre additives on thermal conductivity and specific heat capacity due to small quantity of until finished measuring steps.

The base material for the production of clay plasters was a clay obtained from a foundation excavation of a experimental single house in the village Únětice. The testing spoil was composed mainly of clay. The result of the granulometric test is shown in fig.1.

Fig.1: The composition of the tested soil

Dimensions of soil paticules [%]	0,001-0,063	0,063-0,25	0,25-0,5	0,5-01
Mass [%]	80	15	4	1

On the beginning of the experiment, there were made three mixtures named S-01, S-02 and S-03. The reference mixture named S-01 was made of basic soil and water only. The mixture named S-02 was made of basic soil, wool (2% of mass) and water. The mixture named S-03 was made of basic soil, polypropylene fibres (2% of mass) and water. The clay-water ratio of all mixtures was 0,3.

The dimensions of specimens were designed in relation to the type of the measuring. For the measuring of moisture diffusivity there were made specimens of dimensions 20x40x150 mm. For the measuring of thermal conductivity and specific heat capacity there were made specimens of dimensions 70x70x70 mm.

For the measuring of moisture diffusivity λ [m^2s^{-1}] was determined so-called Matano method. The moisture profiles were determined using a common capillary suction 1-D experiment in the horizontal position, lateral sides of specimens were water and vapor-proof insulated. Moisture meter reading along the specimen was done every 5 mm. The calibration curve was determined after the last moisture meter reading, when the moisture penetration front was at about one half of the length of the specimen, using this last reading and the standard gravimetric method after cutting the specimen into 1 cm wide pieces. The moisture profiles were then calculated from the calibration curve. The measurements were done at 25°C ambient temperature. For the mixtures named S01 and S02 were determined the values of moisture diffusivity in the range of moisture content between 3 to 23%, for the mixture named S03 between 3-22%.

There was found, that the values of moisture diffusivity of clay plasters is low, they are on the same level as values of moisture diffusivity of high performance concretes. The impact of fibre additives in the clay plasters is very low.

Thermal parameters, which is thermal conductivity λ [$\text{W m}^{-1}\text{K}^{-1}$] and specific heat capacity C [$\text{J m}^{-3}\text{K}^{-1}$], were measured using the commercial device ISOMET 2004. It is equipped with various types of optional probes, needle probes are for porous, fibrous or soft materials, and surface probes are suitable for hard materials. The measurement is based on analysis of the temperature response of the analyzed material to heat flow impulses. The heat flow is induced by electrical heating using a resistor heater having a direct thermal contact with the surface of the sample.

Before the measuring, the specimens were dried by the temperature 110°C in the kiln. In each step of the measuring, the moisture content was determined. In the fig.2 and 3 are shown until measured values of thermal conductivity and specific heat capacity.

Fig.2: Thermal conductivity ($\text{Wm}^{-1}\text{K}^{-1}$)

Mixture	Moisture content (% m)	
	0,0	2,5
S-01	0,835	1,028
S-02	0,846	0,959
S-03	0,901	1,062

Fig.3: Specific heat capacity ($\text{Jm}^{-3}\text{K}^{-1}$)

Mixture	Moisture content (% m)	
	0,0	2,5
S-01	1446	1527
S-02	1442	1502
S-03	1503	1557

There was found, that the values of moisture diffusivity of clay plasters is low, they are on the same level as values of moisture diffusivity of high performance concretes. The impact of fibre additives in the clay plasters is very low.

- [1] C. Matano: On the Relation between the Diffusion Coefficient and Concentration of Solid Metals. Jap. J. Phys.8, 1933, 109-113
- [2] R.W. Hamming: The Numerical Methods for Scientists and Engineers. New York, McGraw-Hill, 1962
- [3] J. Drchalová, R. Černý: Moisture Diffusivity of High Performance Concrete, Acta Polytechnica, 1999, Vol. 39, No.3, 39-45

Verification of Laser Scanning Systems Possibilities

T. Křemen

tomas.kremen@.fsv.cvut.cz

Department of Special Geodesy, Faculty of Civil Engineering, Czech Technical University,
Thákurova 7, 166 29 Prague 6, Czech Republic

Laser scanning systems are devices for collection of spatial information with contactless measurement, 3D modelling and visualisation [1]. We tested systems using spatial polar method for determination of the point spatial place. Two experiments were carried out [2-3]. The first experiment was verification of scanners possibilities to measure different materials under different angles. The second experiment was directed to object measurement under steep angles. They were tested these scanners: HDS 2500, Riegl LMS Z 360 and Mensi GS200.

The first experiment dealt with scanning systems' ability to measure various materials under various angles of incidence and linked up to the previous experiment with the HDS 2500 System [3]. There were 19 desks of various materials and colours used for the experiment. The desks were ranged under 5 angles of incidence. For each desk there was determined theoretical number of detailed points and real number of points ranged on the desk. From these two data, there was arranged number of per cent of really ranged points towards theoretical number of points. Tables 1, 2 and 3 state results of measuring materials, with which the scanners had certain troubles.

Tab. 1) Scanner GS 200

Incidence Angle [gon]	0	30	55	75	90
material	k[%]	k[%]	k[%]	k[%]	k[%]
Sheet - red	80	100	100	100	80
Sheet -dark blue	40	100	100	100	10
Metal sheet	0	100	100	100	0
Cuprum	10	100	100	90	0
Sheet - black	95	100	99	30	0
Clear glass	100	0	0	0	0
Smoke glass	100	0	0	0	0
Mirror	70	0	0	0	0

Tab. 2) Scanner HDS 2500

Incidence Angle [gon]	0	30	55	75	90
material	k[%]	k[%]	k[%]	k[%]	k[%]
Sheet - yellow	100	100	100	100	86
Sheet - red	100	100	100	19	0
Sheet -dark blue	100	100	100	25	0
Metal sheet	100	100	100	100	64
Cuprum	100	100	73	12	10
Sheet - black	100	13	2	0	0
Clear glass	100	0	0	0	0
Smoke glass	100	0	0	0	0
Mirror	100	6	0	0	0

Tab. 3) Scanner LMS Z 360

Incidence Angle [gon]	0	30	55	75	90
material	k[%]	k[%]	k[%]	k[%]	k[%]
Wood Light Blue	100	100	100	100	30
Zinc-coated	100	100	100	95	0
Sheet - green	100	100	100	100	0
Sheet -dark blue	100	100	100	100	10
Metal sheet	100	100	80	95	0
Cuprum	100	100	75	20	0
Sheet - black	100	100	20	0	0
Clear glass	0	0	0	0	0
Smoke glass	94	0	0	0	0
Mirror	20	10	10	10	0

It is possible to judge from the results of the experiments that the laser scanning systems are able to measure most materials even under large angles of incidence. The scanners can have troubles when scanning dark, highly reflexive or transparent materials.

The second experiment dealt with verification of abilities to determine position of plane edge that was scanned under very abrupt angles. It concerned determination of plane edge that lied further from the scanner in view of scanning. Experiment was carried out with the Riegl LMS-Z360 Scanner. 3 objects from 5 points of view (5 angles of incidence) were measured. Distance from the scanner was c. 7-8 m. The defined edges were modelled from the scanned points. Position of those edges was compared with position of control points ranged by the total station.

During verification of position of object edges measured under very abrupt angles it turned out that in some cases, the Riegl LMS-Z360 Scanner does not define position of the ranged edge precisely.

References:

- [1] KAŠPAR, M. - POSPÍŠIL, J. - ŠTRONER, M. - KŘEMEN, T. - TEJKAL, M.: *Laser Scanning in Civil Engineering and Land Surveying* Vega Hradec Králové 2004 pp. 104
- [2] KOSKA, B. - KŘEMEN, T. - ŠTRONER, M. - POSPÍŠIL, J. - KAŠPAR, M.: *Development of Laser and Optic Rotating Scanner, Testing of Terrestrial Laser Scanner* In: Proceedings INGENEO 2004, Section TS2 2004 pp. 1/10-10/10
- [3] KŘEMEN, T.: *Testování laserového skenovacího systému Cyrax 2500 JUNIORSTAV* 2004 - 6. Odborná konference doktorského studia 2004

This research has been supported by CTU grant No. CTU0404311.

Using of 3D Scanners in Geodesy and Historical Monuments Care

K. Pavelka, J.Pazdera, J.Záleská

pavelka@fsv.cvut.cz

Department of Mapping and Cartography, Faculty of Civil Engineering, Czech Technical University, Thákurova 7, 166 29 Prague 6, Czech Republic

Geodetic cultural heritage documentation tasks usually comprise close range recording applications. It means objects range from small artifacts over sculptures to buildings. Irregular shapes and surfaces are encountered frequently. Often, the time available for the measurements is limited. In the past, close range photogrammetry was the only method to meet these demands.

In the framework of co-operation between the Laboratory of Photogrammetry of Department Mapping and Cartography, Department of Special Geodesy and the Laboratory of Quantitative Methods of Monuments Research (Faculty of Nuclear Physics and Physical Engineering), new methods of 3D objects documentation are tested on school level. There are two base types of 3D scanners under developing: first type uses triangulation method: laser is used only as a point or profile marker (rotating platform system) and system with 2 cameras and image projector as a structured light source. Second type uses pure laser technology "time of flight". Three small devices for 3D object co-ordinates capturing are being developed at present on CTU in Prague. The aim of this research is to develop a small inexpensive device for special purposes of 3D documentation. Combining of several electronic parts such as CCD camera, laser marker, computer and distance measuring device and laser sensor head (time of flight) have been used for instrument development.

In last years, new methods for documentation of 3D objects were prepared. In the framework of co-operation of above mentioned subjects new methods of 3D objects documentation as a part of project are tested. Two devices for 3D object co-ordinates capturing are being developed at present. The aim of the project is to develop a small inexpensive device for special purposes of 3D documentation. By combining several electronic parts such as CCD camera, laser marker, computer and distance measuring device a new laser sensor has been developed. There are only few possibilities how to construct laser based 3D sensors. The principle of these devices is the same: the laser beam is used as an object point marker (single point or line on object) and the laser track is recorded by using of a small CCD camera. The camera and laser position are convergent to the object, 3D co-ordinates can be computed from laser-camera basis.

As the first is a laser system with CCD camera and rotating platform. For small objects such as small sculptures, vessels or models a system with rotating platform has been constructed. A laser beam optically modified to a thin line on the object is recorded from a basis with CCD camera. A maximum of 25 frames per second can be used. The measured object is situated on a rotating platform with a possibility to change the rotating velocity. All the images are stored on a PC and processed by using of special software. From the image co-ordinates of marked object points the real 3D co-ordinates are computed.

Second is system with two cameras and structured light source. This device uses the principle of image – correlation. The image projector sends structured light on the object and

the object is recorded by using of two CCD cameras from a known basis. This system can be combined with rotating platform for complete documentation of object (0-360deg). Every image pair must be post –processed by using image correlation for 3D co-ordinates of object point's determination.

The last is laser scanner based on laser head SICK. In the 2003-4 a small inexpensive laser 3D scanner based on "time of flight" was developed. The laser head SICK is the main part of 3D scanner. There are two possibilities for using: first one as a linear laser scanner and second one as a rotating head. In the linear scheme the SICK head was used as a 3D scanner for sculpture documentation, but the resolution on about 50cm was not very high (it is a good idea for more precision scanners). Next, the head was completed with motorized PC-controlled rotating part with incremental device for angle measurement. It is the "classical" laser scanner scheme. All with the control software was made on CTU Prague and will be used such a "school laser scanner". Technical details: laser head for technical using (security, working process control), relatively inexpensive (5000Euro), accuracy cca 8mm (0.1-10m), accuracy cca 8cm (10-80m). Disadvantage: wide laser beam = big laser trace (low detail resolution), without rotating or motion device for practical using (all must be „hand-made“), without control and processing software.

Examples of inexpensive systems based on simple digital camera and laser are discussed in the paper. All systems are under construction on Czech Technical University in Prague and they are used for the technology testing and teaching.

References:

- [1] K.PAVELKA: *Using of Laser and Digital Camera Based Systems for 3d Object Documentation* Proceedings of Symposium of Commission CIPA, WG 6, Korfu, Greece 2002 pp. 331-334
- [2] T.DOLANSKÝ, K.PAVELKA: *Using of non-EXPENSIVE 3D Scanning Instruments for cultural heritage documentation*, Symposium CIPA, WG 6, Antalya, Turkey, Proceedings of symposium, 2003, , pp. 152-157.
- [3] B.KOSKA, M.ŠTRONER, J.POSPÍŠIL: *An Algorithm of Determination of the General Plane Equation for Laser Scanning, Including Accuracy Analyses*, Stavební obzor No. 2, 2004, pp. 55 60
- [4] K.PAVELKA, E.ŠTEFANOVÁ, M.ŠTRONER: *Visualisation and Animation of Undiscovered Tomb Interior at the Prague Castle*, Phitsanulok, Thailand, ISPRS International Workshop on Processing and Visualization using High-Resolution Images Proceedings of workshop, The International Archives of the Photogrammetry, Remote Sensing and Spatial Information Sciences, Vol XXXVI-5/W1, ISSN 1682-1777, 2004 pp.112-118

This research has been supported by GA ČR grant No. GA 205/04/1398.

Semi-rigid Joint of Timber Frame

Rudolf Vyhňálek

vyhnalek@fsv.cvut.cz

Department of Steel Structures, Faculty of Civil Engineering, Czech Technical University, Thákurova 7, 166 29 Prague 6, Czech Republic

At present, the amount of energy used on manufacturing, usage, demolition and recoverability aspects of materials is going to be one of the judgement criteria of the future buildings quality. From this point of view, timber structures are one of the solutions for modern buildings. It is because of their cost, recoverability of timber and the low impact on the environment.

The most common structural form of timber structures is the wall system known as light skeleton as well. The disadvantage of this system is a small ability of changing the interior layout during the building's life. The need for a better flexibility of the interior leads to the heavy skeleton structure.

The behaviour of the building and its horizontal deformation due to the impact of horizontal forces depends on the space rigidity of the structure. The most significant influence to the rigidity of the structure has the stiffness of structural joints. The stiffness of modern timber skeleton joints used in housing is not sufficient enough to carry horizontal loads; therefore the construction has to be braced. The common bracing types are shear walls or diagonal bracing which constrain interior layout. To get minimal number of these constructions, we need to make an appropriate connection between the frames and the bracing. This connection is the fully rigid ceiling, which is hard to obtain for timber structures. The solution to the problem how to minimize the number of bracing constructions could be the rigid or semi-rigid frames. These constructions are able to carry particular load corresponding to their rigidity, so that the requirement for bracing is smaller. The current types of the rigid or the semi-rigid joints are not easy to assemble and the structural joints are usually very expensive. One of the cheap and easily performed joints is a joint with glued-in rods.

Joint with glued-in rods has been tested in CTU laboratories during author's diploma thesis. Assumptions based on this pilot research results has been implemented into the new research supported mainly by CTU0402511. The task of the news research is to specify real joints stiffness using experimental, analytical and numerical data.

Experiments

Tested specimens have been divided into three groups. The first group of specimens has been loaded mainly with bending moment, the second group mainly with shear force and the third one is a group of specimens which represents only a part of the whole joint, and the rod glued perpendicular to grain loaded with tensile force. All tests are now being performed.

The result of the first group specimen's tests will be a real joint stiffness represented by $M-\phi$ curve (relation between bending moment and rotation of the joint) and a ductility of the joint. Stiffness is needed when the rigidity of the building is calculated; ductility is a criterion for applicability of joint.

The tests of the second group of specimens are mainly focused on a failure mode. The knowledge of a failure mode is necessary for the applicability of this type of joint in constructions with short and heavy loaded beams.

Loading of these two types of tests represents common loading of timber frames. The test of the third group is focused only on a part of the joint and the results of this test will be used for verification of the analytical model.

Analytical model

For the analytical analysis component method has been used. The principle of this method is to simplify the real geometry of the structure by dividing the structure into parts (components) which have significant influence on the joint stiffness. Tested specimens have been divided into components as follows: the rod glued parallel to grain loaded with tensile/compression force, the rod glued perpendicular to grain loaded with tensile/compression force and the sway of the timber in the column and the beam. Every component is represented by a spring with specific stiffness. Knowing the geometry and stiffness of each component we are able to evaluate the rigidity of the whole joint. For this purpose, spreadsheet in MS Excel has been made. With this utility we are able to determine the stiffness of joint of various geometry. This utility has been verified by numerical model made in ANSYS.

Numerical model

Every numerical model has been made in ANSYS 8.0. For timber, SOLID64 has been used, for other materials SOLID45 was considered. Material characteristics for steel and glue have typical values for these materials. Characteristics of the timber were taken from [1], because we were not able to specify all parameters of tested timber until experiments were made. The first task of the numerical analysis was to verify analytical model. Two models have been made. The first model is simulating a rod glued perpendicular to grain, the second a rod glued parallel to grain. The distribution of strain energy in the volumes of both models was studied and it is now being evaluated. Due to the knowledge of strain energy distribution we are able to specify area or volume of the timber which has most significant influence on the rigidity of tested component [2]. This timber block with the steel rod represents the spring used in analytical model.

The second task of the numerical analysis is to simulate the behaviour of a whole joint. The reason for this simulation is unknown behaviour of mentioned timber blocks acting in groups. These blocks (areas) can affect each other so this aspect has to be taken into consideration in analytical model.

References:

- [1] VYHNÁLEK, R.- VAŠEK, M.: *Vliv návrhu budov na životní prostředí* Vysoké učení technické v Brně, Fakulta stavební, Brno 2004 str. 431.
- [2] VYHNÁLEK, R.- VAŠEK, M.: *Semi-rigid Joint of Timber Frame* A.A. Balkema Publishers, Leiden, The Netherlands, 2004, sborník Vol2 str. 849-855

This research has been supported by CTU0402511 and GAČR 103/03/H089.

Ecological Fly Ash-Sludge Composites

E. Pospíšilová

eva.pospisilova@email.cz

Department of Building Materials, Faculty of Civil Engineering, Czech Technical University, Thákurova 7, 166 29 Praha 6 - Dejvice

This paper informs the professional public about results of the experimental composites verifying process on the basis of the power station fly ash and sludge from the water purification plant with addition of the bentonite eventually of the cement and lime hydrate. Existing results show a brighter use in the praxis, although their research and development is only at the beginning.

1 Introduction

The period, in which we are living, confronts us with new problems and as every phase of the human being, also it brings new trends. There is speaking about a principles of the maintainable development more and more, which becomes a central theme between professionals, politics and managers and which is investigated in many views also in all economical, industrial and social areas of the society. It is no possible to develop a building activity and to search for new methods, trends and technologies without a responsible interest, how much is this activity compatible with a basic nature system and how much is this system maintainable in view of further development. One from awaited changes of building materials and products is the maximal use of existing, still not processed raw material sources, in particular wasted. In ecological view, we discern following main wastes:

- wastes during raw materials mining (e.g. nine times more of the waste earth than the lignite is stored during lignite mining),
- products during lignite burning (ash, fly ash etc.),
- solid communal waste (requiring deponies, disposal sites, incinerators),
- waste sediments

2 Input data

Following components were used for composite production:

Fine power station fly ash from the EMĚ III Mělník power station (traditional atmospheric lignite burning).

Waste sediment from the water purification plant in Praha 6 – Bubeneč.

Common bentonite sort B 70, Obrnice u Mostu

Slag Portland cement CEM II/B – S 32,5 R

Lime hydrate volume stable, class I. – fine, Ca (OH)₂:200

3 Partial experiment results

Nine sample sets (small balk 40x40x160 mm) were tested in proving tests in the laboratory of the Department of Building Materials, Faculty of Civil Engineering, Czech Technical University in Prague.

Significant hardening occurs at each mixture after 2 to 13 days after covering be PE foil during one week.

On the contrary, the mixture stability loss (after stiffening and hardening) by influence of the rising water (during the balk storing into the water, ranging up to one third of their high) does not occur after one exposition week.

The comparison of tested composite properties, namely the volume weight and the strength in a simple pressure (tested on balk fractions after 28 days since production) was made.

4 Conclusion

The paper refers to the fly ash and sediment use not only from the point of view of two separate wastes, but their combination. A mixture is created after addition of suitable sediment and stabilising binder amount into fly ash, which has such properties after stiffening and hardening, that it could be stored as stabilised, without the risk of environmental contamination [1]. The fly ash and sediment stabilisation could be secured by higher cement rate (more than 20% of their total weight). The research and development of the composites on fly ash and sediment base from Water Purification Plant is in the beginning and surely will be changed, because „if all would be loosed, no progress could occur.“ Prospectively, the investigated composites could be used as:

- underlying and protective roads, highways, airport areas, parking places etc. layers,
- holes, caverns, hollow dips, underground areas (incurred after floods or coal mining) fillings,
- material suitable for filling of areas after open cast mining and restoration of initial or balance of new land area,
- „concrete over“ sewerage and replacements of filling of areas about the ferro-concrete basis, collectors in particular there, where are difficult comprehensive conditions,
- material suitable for reclamation of anterior sludge places,
- technical reclamation layer of waste dumps, unloading yards etc. before covering by earth and final surface finishing,
- sealing material for waste dumps; it is possible, under certain conditions, by composite recipe modification and by its storing, to prepare a layer for sealing purposes, reaching the penetrability against water (values of the filtering coefficient) order of 10^{-9} to 10^{-11} m/s [2].

References:

- [1] *Zákon č. 100/2001 Sb. o posuzování vlivů na životní prostředí a o změně některých souvisejících zákonů (zákon o posuzování vlivů na životní prostředí), účinnost od 1.ledna 2002*
- [2] POSPÍŠILOVÁ, E.: *Snižování zátěže ekosystému úpravou kalů s využitím odpadů ze spalovacích zařízení. Diplomová práce. ČVUT v Praze, Fakulta stavební, Praha. 2001*

This research has been supported by CTU grant No. CTU0400711.

Soil Erosion and Surface Runoff Problems Assessment with GIS Tools Application

**K Vrána, T.Dostál, M.Dočkal, H.Nováková, P.Koudelka, V.David, J.Krásá,
J.Kolářčková, M.Bečvář**

vrana@fsv.cvut.cz

*Department of Irrigation, Drainage and Landscape Engineering, Faculty of Civil Engineering, Czech Technical University, Thákurova 7, 166 29 Prague 6, Czech Republic

The project presented is rather broad, as it has been declared as a “Support of successful teams from the funds of Rector of CTU Prague”. Therefore, there was not one particular problem solved within the project, but the support has been used for progress at more connected branches. There was also cooperation (not multiple support) with other projects or other supported activities in frame of other national and international projects.

Basically, the topic of the project has included following chapters:

- Data measurements concerning of surface runoff, soil erosion and sediment transport to have a material for mathematical models validation and calibration
- Structured approach definition and theory development for surface runoff, soil erosion and sediment transport in the landscape
- Individual mathematical simulation models of surface runoff, soil erosion and sediment transport validation and calibration for the conditions of the Czech Republic
- Preparation of new national and international project proposals for future development of the team’s activities.

As for the data measurement, the activities had concentrated mainly in two directions. At first, the measurements on laboratory rainfall simulator at hydraulic laboratory of Faculty of Civil Engineering, has been prolonged. Mainly surface roughness and soil erodibility has been measured this year, as referred at [2] and [3]. At second, a field experimental gauging station has been set up near of Neustupov village at the small stream. The station has been equipped by two rainfall gauging stations and two barometric discharge sensors to measure runoff response of the catchment (ca 1,5 km²) to storm event and flood wave transformation from artificial channel to revitalized stream bed, as can be seen at [2].

Within the chapter of structured approach, the main effort has been focused to the so called “global” and “regional” levels, as can be seen for instance at [1]. Method for soil loss and sediment transport assessment within large watersheds based on combination of USLE and SDR, with GIS assistance have been newly applied and precised at Svratka catchment. Concerning of USLE, as the most popular method of soil erosion risk assessment, the revision of rainfall erosivity and acceptable soil loss limits has been started, as can be seen for instance at [2].

Concerning of individual mathematical models testing, validation and calibration, the effort has concentrated mainly to validation of WATEM/SEDEM (model of soil loss and sediment transport) for the conditions of the Czech Republic in the branch of soil erosion [4]. Within the field of surface runoff, simple robust methods like CN-curves assisted by GIS

tools were tested. More sophisticated model, based on empirical relations Wet-Spa has been used and tested at Polečnice catchment in Southern bohemia. Furthermore, more detailed models like V-flo or WMS has been implemented for smaller catchments size in order tens of km².

The last topic covers an effort of the team to prepare new scientific projects at different levels and orientations. The international project EMTAL, managed by TU Bergakademie Freiberg in Germany, dealing with structured approach to flood protection, where Dept. Of Irrigation, Drainage and Landscape Engineering cooperates, continued in this year. The project proposal within Kontakt program together with VUB Brussels, dealing with surface runoff modeling within medium scale catchments has been accepted for 2004 – 2005 years and international project within AKTION program together with BOKU Wien for 2005 – 2006 has been prepared in 2004 year and accepted for funding since beginning of 2005. The staff of the Department of Irrigation, Drainage and Landscape Engineering has participated at the Management committee of international project COST Action 634 in Bratislava in October 2004 and coordinated national project COST Action 634. Also project proposal for grant agency of ministry of Environment of the Czech Republic has been prepared within 2004, dealing with GIS tools application for landscape stability assessment and the team also participated at project proposal to Brussels commission for science in the “Asia Pro Eco Programme”, together with Technical university of Suderburg in Germany, ministry of Environment of Nepal and University of Sannio, Benevento, which coordinates the project.

Generally, there can be claimed, that the support of the Rector of the CTU Prague has been used very effectively and that the head of the team believes, that it will improve the reputation of the Czech Technical University within the Czech Republic and also on the international field.

References:

- [1] K. VRÁNA, T.DOSTÁL: *Structured approach to soil erosion and transport processes assessment in the landscape*, Krajinotvorné programy, konference, 2004 pp. 9 - 21.
- [2] T.DOSTÁL, K.VRÁNA, J.KRÁSA, H.NOVÁKOVÁ, J.KOLÁČKOVÁ, M.BEČVÁŘ, V.DAVID, P.ROSENDORF, V.KVĚTOŇ: *Metody a způsoby predikce povrchového odtoku, erozních a transportních procesů v krajině*, Interrim report of COST Action 634 project, CTU Prague 2004, pp. 87.
- [3] J. KOLÁČKOVÁ, P.PAŘÍKOVÁ, T.DOSTÁL: *Soil Erodibility and its experimental determination*, 4. Mezinárodní vodohospodářská konference, 2004 pp. 239 - 243.
- [4] J.KRÁSA, K.VRÁNA,T.DOSTÁL *Empirical modelling of sediment transport processes in Czech conditions* 12th international conference on transport and sedimentation of soil particles 2004 pp. 457 - 466

This work was funded by the grant No. 111430104143, given by Rector CTU in Prague to successful scientific teams to support their activities in 2004 year.

Experimental Background for the Load Capacity Analysis of the Nature Stone Masonry

M. Vokáč, P. Bouška

vokac@klok.cvut.cz

Department of Measuring and Experimental Methods, Klokner Institute, Czech Technical University in Prague, Šolínova 7, 166 08 Prague 6, Czech Republic

It is well known that the advance methods of numerical analysis, not only in the field of masonry structures, require a lot of material properties. There are very few experimental results especially in the case of stone masonry. Consequently, the experimental research was focus on masonry made from nature stone units. In the Klokner Institute, a several tests of material properties of sandstone, cretaceous marl and some types of mortars were conducted. Further, the first pilot test of masonry specimen was carried out.

The tested sandstones were from the following localities: Kamenné Žehrovice, Božanov, Hořice, Vyšehořovice (all in the Czech Republic). Also, the cretaceous marl, so called golden Prague cretaceous marl from Přední Kopanina near Prague, was investigated. We pay attention to the sizable set of material properties including stress strength, tensile strength, three-points bending test, fracture energy, modulus of elasticity, Poisson's ratio, bulk density, water absorption and others. The tests were performed in two stages – on dry specimens and then on specimens saturated by water. The influence of moisture is dependent on the type of sandstone and the correlation with moisture absorption can be recognised. In case, that the orientation of layers was determined, it was also taken into account. Some results were presented in [1] [2] and [3].

It is necessary to obtained similar set of material properties which the mortars posses. First, the commercially sales types of mortar were investigated (MZŠY – grey mortar intended for brickwork produced by YTONG; MAY – universal plaster produced by YTONG; MVSJ – lime-cement mortar). The results of fracture energy (specimen dimensions 40 x 40 x 160 mm, span length 120 mm, notch 13 mm), compression strength (specimen dimensions 100 x 100 x 400 mm), strength in simple tension (specimen dimensions 40 x 40 x 160 mm) and modulus of elasticity (derived from stress-strain diagram in compression) are presented in table 1.

Table 1: Basic mechanical properties of mortars

mortar	MZŠY	MAY	MVSJ
fracture energy [N/m]	16,00	10,17	6,57
compression strength [MPa]	8,26	2,66	2,61
strength in simple tension [MPa]	0,85	0,34	0,40
modulus of elasticity [MPa]	6935	3177	3615

But it is not able to take from the real structure the specimen which dimensions are suitable to direct testing. So, the specimens should be prepared in the laboratory according to prescription gained by means of the analytical methods. Consequently, the chemical and mineralogical analyses of historical mortar were done. About 10 samples of historical mortar were obtained and investigated. Theses analyses were conducted by Mr. Rychard Štrouf (WTA CZ), who co-operated on renovation of plaster situated on the St. Vitus Cathedral and

on renovation of other monuments in Prague. With assistance provided by Mr. Štrouf, we determine the prescription of mortars, which will be taken into account in the next research. For this purpose, we obtained the mortar components (aggregate, trass cement and slack lime) from Mr. Ivan Vaněček (Baumit, Ltd.).

Finally, the pilot test of the masonry specimen was provided. It was uncoursed random rubble set in mortar (assembled from cretaceous marl and cement mortar). Dimensions were 600 x 600 x 10 mm. The specimen was loaded so that the combination of normal and shear stress was invoked in the bed joints. There are a lot of methods that invoke this state of stress. They are summarised in [4], but in all cases, it is not possible to achieve ideal shear stress distribution along the joint. We choose the test arrangement according to Samarasinghe et al. This arrangement was applied to many previous experimental and theoretical analysis of brickwork masonry. It is based on loading by diagonal compression load. The maximum value was 41,5 kN in this case. Of course, four potentiometric transducers measured the deformations and, further, strains were measured by two extensometers. So, we get data for next processing. Then another masonry specimens were prepared in laboratory of Klokner Institute including regular coursed rubble assembled from sandstone.

The unique data were obtained by experimental methods; especially in case of fracture energy such brittle materials like sandstones, cretaceous marl and mortar. The results will be applied to non-linear analysis of masonry structures.

References:

- [1] VOKÁČ, M. – BOUŠKA, P.: *Základní mechanické vlastnosti pískovce a opuky* In: CONSTRUMAT 2004, TU Košice, 2004, pp. 208–210.
- [2] BOUŠKA, P. – KLEČKA, T. – VOKÁČ, M. – ZÁRUBA, J.: *Experimental Investigation of Mechanical and Physical Properties of Sandstone* In: CTU Report, Special Issue, March 2004, Vol 8, 2004, pp. 972–973.
- [3] BOUŠKA, P. – VOKÁČ, M. – ZÁRUBA, J. – ŠTEMBERK, P.: *Experimental investigation on basic mechanical properties of the sandstone masonry* In: Engineering Mechanics 2004, Institute of Thermomechanics, AV ČR, 2004, pp. 47 – 48.
- [4] HOBBS, B. - ROMAN, H.: *Shear behaviour of mortar joints in brickwork subjected to non-uniform compressive stress* In: Brick and Block Masonry, Vol. 2, edited by John W. de Coury, 1988, pp. 676–685.

This research has been partially supported by GA ČR grant No. GA 103/04/1321 and by CTU grant No. CTU0412131. Also acknowledged is the assistance provided by Mr. Richard Štrouf (WTA CZ) and the mortar components (aggregate, trass cement and slack lime) provided by Mr. Ivan Vaněček (Baumit, Ltd.).

Determination of principles for design of small watercourses rehabilitation

P. Koudelka, T. Mrázková, K. Vrána

petr.koudelka@fsv.cvut.cz

Department of Irrigation, Drainage and Landscape Engineering, Faculty of Civil Engineering, Czech Technical University, Thakurova 7, 166 29 Praha 6

The article is divided to two parts corresponding to the research. The first part focuses on morphological characteristics of natural small watercourses and then on principles of design of small watercourses rehabilitation. The second part focuses on rehabilitation of small watercourses from the hydrobiological point of view.

Morphological Characteristics of Natural Watercourses

The former part of the project was focused on determination of morphological characteristics of natural small watercourses based on terrain measurements and the latter on finding relationships between measured characteristics and hydrological data of a watershed. The measured characteristics and the relationships will result in a handbook for designing of small watercourses revitalization.

Terrain measurements

Three reaches of natural streams were chosen for terrain measurements. Those were done during the year 2004:

- Polečnice stream, Český Krumlov district: reach length 450 m, river log 20.000 – 20.450 km, watershed area 18.03 km²,
- Polečnice stream, Český Krumlov district: reach length 350 m, river log 13.530 – 13.880 km, watershed area 57.41 km²,
- Chvalšinský stream, Český Krumlov district: reach length 570 m, river log 1.530 – 2.100 km, watershed area 89.83 km².

The stream reaches were chosen in relation to their: minimum interference by human activities, altitude, stream type, watershed area, and accessibility. Stream dimensions and the watershed area should correspond with dimensions and the watershed area of recently revitalized streams.

Terrain measurements were made in a way of a geodetic surveying. Theodolite Theo 010A and digital distance meter WILD 1000 + geodetic prism LEIKA were used for the surveying. The field measurement consisted of measuring of stream bed elevation and water depth in a centerline in a span of 1 – 5 m depending on stream segmentation. Furthermore longitudinal slope of alluvial plain and cross-sections of stream channel were measured in a span of 50 – 100 m.

Processing of measured data

Geodetic data were processed by geodetic software ZKGEO and the results were then used and processed in AutoCAD. Then stream morphologic data were imported to software HEC-RAS (River Analysis System) and channel flow was simulated. N-year-flood discharges (Q_1 , Q_5 , Q_{10} , Q_{50} and Q_{100}) were used like a design discharge for the flow simulation.

Results and conclusions

AutoCAD outputs are horizontal projections and longitudinal profiles of surveyed stream reaches and bend radius. HEC-RAS outputs are computed hydraulic data in a tabular form (flow velocity, water level, Froude number etc.) or in a graphic form (cross-sections, longitudinal profile, axonometric 3D view).

For the flow modeling the span of measured cross-section was too long. Shorter span will be used in next surveying (10 - 20 m – depend on the stream segmentation). HEC-RAS results correspond sufficiently with measurement and modeling which were done by Zuna in 1987, 1992 and 1994.

Hydro-biological principles of watercourses rehabilitation

One aim of the second project part is to work up a methodology of “evaluation of watercourses rehabilitations” based on hydro-biological and chemical indicators. Another aim is to find out which materials used for channel structures and stream revitalizations should be optimally used for settlement of benthic and attached organisms.

Terrain measurement

For terrain research Slupský stream (Benešov district) was chosen because the stream has been regulated in past and rehabilitated in the spring 2004. Four control sections on the stream were placed and monitoring started in June 2nd 2004 after the end of the rehabilitation. Measuring frequency is ones per month according to Czech standard ČSN 75 7221. The monitoring will go on in total 24 months.

Monitoring indicators are divided in to two parts:

- Hydro-chemical: alkalinity, acidity, carbon dioxide (free), $Ab_{S_{254}}$, total carbon, inorganic carbon, organic carbon, COD_{Mn} , bicarbonates, phosphates, ammonium ions, nitrite, nitrate, total inorganic phosphorus and total inorganic carbon.
- Biological: diversity and saprobity indexes of makrozoobenthos and phytobenthos, algal growth potential.

Processing of measured data

Up to now measured data were processed in MS EXCEL 97. Measured data will be imported to the biological software CONOCO where the gradient analyses will be used.

Results and conclusions

The monitoring started after finishing of the revitalization and during six months the benthic macroinvertebrates were evolving rapidly and positively. Benthic macroinvertebrates frequency and diversity was the highest and still is the highest at the first control section. The first way of benthic macroinvertebrates migration is drifting downstream to the revitalized stream reach and the second one is imago flyover. Exemplary sample of a quick migration is a migration of mayfly larvae (*Heptagenia lateralis*) that occurred initially only at the first control section (natural stream reach). After two month mayfly larvae occurred sporadically at the revitalized stream reach (control section three) and after six month its presence there was frequent.

References:

- [1] KOUDELKA, P. – MRÁZKOVÁ, T.: *Stanovení zásad pro navrhování revitalizací drobných vodních toků*. In: 5. odborná konference doktorského studia, Akademické nakladatelství CERM, 2005
- [2] KOUDELKA, P.: *Studie disertační práce na téma: Zásady revitalizace drobných vodních toků*, ČVUT, Fakulta stavební, 2004 pp. 35

This research has been supported by číslo grantu.

Functional Qualification and Optimization of Building Structures

**J. Witzany, J. Šejnoha, J. Procházka, J. Studnička, J. Jettmar, F. Lehovec, V. Vorel,
H. Krejčířiková, J. Jarušková**

witzany@fsv.cvut.cz

CTU, Faculty of Civil Engineering, Dept. of Building Structures
Thákurova 7, 166 29 Praha 6

The current trend in designing building constructions is characterized by efficient exploitation of physical and mechanical properties of materials and constructions and by minimizing their reserves. The development of numerical methods, material engineering and theoretic models describing the behaviour of materials and constructions allows a highly efficient practice in designing structures. The objective of the research plan, VZ No. 1, is to increase the functional qualification and reliability of structures, namely by reducing the risks of appearance of serious faults and failures of structures and their parts in the course of their use. In order to fulfil the above-mentioned objectives, the research carried out in 1999-2003 was focused, in particular, on the following areas:

- multi-criteria evaluation of reliability, safety, residual service life and serviceability of structures.
- development of reliability and durability theory of building materials and constructions with regards to time-dependent effects of loads and optimization of constructions.
- evaluation of reliability of structures exposed to extreme loading conditions (floods, fire, explosion, vehicle impacts).
- the effect of rheological changes, degradation and corrosive processes on the reliability and service life of structures.
- the effect of loading history on the reliability and service life of structures.
- reliability of joints of structural systems.
- interaction of constructions with sub-base and optimization.
- identification of accident localities and minimization of risks of road traffic accidents.
- quality control systems and innovations of diagnostic methods.
- decision-making methodology on the methods of building stock rehabilitation and renovation.
- development of suitable design models of concrete constructions with respect to an analysis of their safety, suitability and durability, monitoring of the effect of different parameters on plastic angular displacement of reinforced concrete slabs and beams, new methods of strengthening concrete and masonry constructions reinforced with metallic materials to ensure their reliability.
- experimental and theoretic research into steel and thin-walled planar units, development of design procedures and aids, new types of coupling, behaviour of timber truss plates and panels for housing design.
- exploitation of probability models of road construction response to structural data of random character ensuring a higher reliability level of roads.

In 2004, the research activity was focused, in particular, on the following areas:

- analysis of degradation of load-bearing pre-cast panel constructions and their individual parts exposed to non-stress effects and extreme loads,

- theoretic and experimental research into vaulted masonry structures, verification of reliability of existing design relations for the calculation of the load-bearing capacity of strengthened masonry pillars,
- formulation of partial conclusions for the assessment of the effect of increased moisture content on physical and mechanical properties of masonry constructions, development of design recommendations, preventative measures,
- elaboration of models for monitoring the effect of active depth below oversize foundation slabs,
- analysis of the appearance and development of cracks in foundation slabs,
- theoretical procedures for the homogenization of masonry with irregular texture,
- theoretical procedures based on chemo-nanomechanics,
- load-bearing capacity of arch bridges and problems of durability of concrete structures,
- monitoring of the effect of individual material parameters (of concrete, reinforcement, sub-base etc.) and geometric parameters (dimensional tolerances of slab thickness, reinforcement emplacement etc.) on the reliability of industrial concrete floors,
- problems of behaviour of thin-web joists connected with flanges by one-side welds,
- stability of frames, practical recommendations for frame design and assessment,
- fire resistance, on-going experiments and process simulations,
- composite beams with Stripcon connectors, execution of an experiment leading to interaction of web buckling with the behaviour of coupling using shot-fixed Stripcon connectors,
- research into the behaviour of composite timber-concrete structures,
- mathematical modelling of geotechnical structures,
- introduction of two alternatives of road pavement construction composition for two different sub-base bearing capacities,
- monitoring of selected properties of asphalt mixes with high moduli of rigidity (fatigue, relaxation), monitoring of the effect of temperature and asphalt binder type on these properties,
- detailed assessment of the effect of various noise-absorbing elements inserted in rail constructions,
- measurement and evaluation of shifts and strain of structures with a focus on historical monuments,
- application of GPS/RTK method in checking the condition of engineering line structures.

References:

- [1] WITZANY, J.- ČEJKA, T. - ZIGLER, R.: **Moisture Effects on Long-Term Masonry Strain**. In: 6th conference WTA, Rehabilitation and reconstruction of buildings 2004. Česká stavební společnost, WTA CZ, 2004, pp. 168-173.
- [2] PROCHÁZKA, P. - ŠEJNOHA, J.: **Extended Hashin Shtrikman Variational Principles**. In: Applications of Mathematics, 2004, pp. 357-372.
- [3] MOTÁK, J. - MACHÁČEK, J.: **Composite Girder with Steel Undulating Web and Shear Connectors Hilti Stripcon**. Composite Girder with Steel Undulating Web and Shear Connectors Hilti Stripcon, 2004, pp. 271-272.

This research has been supported by MSM 210000001.

On Flexible Pavement Design

F. Luxemburk, B. Novotný *

luxemburk@fsv.cvut.cz

CTU, Faculty of Civil Engineering, Dept. of Road Structures, Thákurova 7, 166 29, Prague 6

* CTU, Klokner Institute, Dept. of Reliability, Šolínova 7, 166 08, Prague 6

The design of flexible pavements is usually based on pavement fatigue life assessment evaluating the amount of cracking distress developed in the pavement during its exploitation period. The aim of the project GACR 103/02/0396 „Fatigue of asphalt mixes and flexible pavement design optimization“ was to gain new knowledge on the fatigue associated processes in asphaltic layers of flexible pavements and to use it in the innovation of the Czech design method. The combination of experimental testing and computational modelling was envisioned as a major tool of the projected research.

The laboratory monitoring of asphalt mix fatigue properties was performed on the NAT (Nottingham Asphalt Tester) device. NAT allows monitoring of selected rheological properties of asphalt mixes, besides fatigue the stiffness modulus as well as dynamic and static creep characteristics are determined. In the course of the project research more than 60 asphalt mixes were tested. Different types of mixes were examined (asphalt concrete of medium grading ABS I, coarse grading ABH I and very coarse grading ABVH I, asphalt mastic of medium grading AKMS I and coarse grading AKMH I, coated maccadam of coarse grading OKH I and asphalt mix VMT with high stiffness modulus) and the effect of different asphalt binders (road asphalt 50/70 and different types of modified binders) was also studied.

The conditions for implementation of fatigue experimental results in pavement design procedures changed during the project solution in context of changes associated with transition from the original version of the Czech design method TP 77 [1] to the currently prepared design method innovation TP 170 [2]. At the beginning, the aim was to verify details of the fatigue based evaluations of [1] in order to establish rational values of fatigue parameters for innovative types of asphalt mixes (such as VMT mixes with high stiffness modulus). The design method innovation [2] introduces formally principles of performance based pavement design allowing the laboratory determined stiffness modulus of asphalt mixes to be taken as characteristic value of their elastic modulus and laboratory determined fatigue parameters to be used in pavement fatigue life assessments. The problem arises to be answered, in which way the laboratory obtained fatigue results are to be transformed to provide reasonable projection of the actual pavement fatigue performance.

The recent results of international research in the field of pavement design indicate extreme complexity of the task to develop a coherent design method. In the theoretical part of this task, new complex models of construction materials behaviour should be solved demanding substantial calibration phase to be accomplished in order to verify derived design criteria. It is hardly conceivable that such solutions may be based on direct implementation of (restricted) laboratory determined material parameters as stipulated in [2]. In our current situation, the only rational way is to study results of international research (e.g. [3]) and to transform them in the manner compatible with the current Czech design method.

Substantial part of the research of the project GACR 103/02/0396 was devoted to the computational modelling of the structure of asphalt mixes in order to gain new information on processes associated with distress formation in asphaltic layers. To this end, the method of multivolume micromechanical analysis was used. The method considers asphalt mix as a periodic composite and analyzes mechanical behaviour of its characteristic volume. The complex structure of the asphalt mix requires a three-level modelling procedure. The first

level represents modelling of asphalt cement as a two-component composite (binder & filler), on the second level the asphalt mortar is modelled as a three-component composite (binder & asphalt cement & soft aggregate) and, finally, on the third level the asphalt concrete is modelled as a three-component composite (binder & asphalt mortar & coarse aggregate). The computerized version of this modelling procedure is denoted as program AB-model, the input being the material characteristics of binder and aggregate, the output representing the equivalent modulus of elasticity and Poisson's ratio of the asphalt mix. In progress are research activities taking into account the viscoelastic properties of the asphalt binder, the efforts on determining Wöhler curves of the asphalt mixes based on fatigue properties of asphalt binder and the elaboration of the procedure for determination of permanent deformation formation in asphalt mixes using viscoplastic characteristics of the binder mechanical behaviour.

The method of multivolume micromechanical modelling was used also for determination of the reinforcement parameter S_{mem} of geosynthetic grids. This quantity is used to describe mechanical performance of the geogrid built in the asphaltic layer. The micromechanical modelling procedure was used to study performance of the geocomposite ARMATEX with polyester material of the grid. In modelling mechanical performance of this geocomposite, the effort was focused on simulation of the locking effect of the geogrid – the aggregate grains being „locked“ in the grid apertures. The modelling procedure followed that of the AB-model, the first two levels of modelling being the same as when modelling asphalt mix structure. The third level modelled the structure of the geogrid and of the composite membrane wrapped up around the grid. The results of this theoretical analysis indicate possibility of saving up to 10-20% of asphaltic layers overall thickness in the flexible pavement structure.

Considerable attention was given also to the application of research results in pavement design praxis and diagnostics. Several cases of pavement structures with premature distress formation were analysed to find the causes of observed structural failure. In the year 2003 the failure of the Prague Radial (connecting highway D1 with Brno main road circle) was analyzed as well as Pilsen circumferential highway. In the year 2004, the new opened section of the highway D3 was examined as well as the reconstruction of the road I/35 Litomyšl-Gajer. The theoretical computations confirmed gravity of technological violations in course of road construction, but were unable to explain (confirm theoretically) full extent of the observed distresses. In this way it was confirmed that the Czech design method lacks reliable links with the reality of pavement deterioration and distress accumulation.

References:

- [1] TP 77 PAVEMENT DESIGN SPECIFICATIONS *Ministry of Transportation of the Czech Republic*, 1995.
- [2] TP 170 PAVEMENT DESIGN SPECIFICATIONS & CATALOGUE OF PAVEMENTS *Ministry of Transportation of the Czech Republic*, 2004.
- [3] WITCZAK, M.W.: *2002 Guide for Mechanistic Pavement Design*, International Conference on Highway Pavements. Data, Analysis and Mechanistic Design Applications Columbus, Ohio, 2003.

This research has been supported by GA ČR grant No. GA 103/02/0396.

Method of Optimal Alternative Selected Technological Method Realization of Underground Buildings from Technological-Economy Perspective

K. Štrobl

kamil.strobl@centrum.cz

Department of Construction Technology, Faculty of Civil Engineering, Czech Technical University, Thakurova 7, 166 29 Prague 6, Czech Republic

Procedure providing optimal selection of a technological method of underground structure realization (basement realization) in voids is described in the presented research. The procedure is based on comparison of two different technological methods of basement realization.

The first method, the so-called Standard Method or the Method of Full Excavation under Flooring Slab, is in principle a sequence of the following steps: (1) realization of underground walls, (2) complete excavation-mining of a foundation pit, (3) realization of foundations and (4) realization of horizontal and vertical structural members of an underground structure.

The second method involved in the submitted comparison, the newly introduced Method Top & Down, is based on simultaneous realization of basements together with upper floors. Apparently, this may reduce amount of time necessary for realization of the whole building.

However, selection between the discussed methods is dependent on a number of basements and upper floors. Parametric study is carried out for a building with a fixed number of upper floors (total number of 7 upper floors is considered) and with variable number of basements (being a parameter changing from 3 up to 7).

From a technological point of view, time required for basement realization and time needed for realization of the whole building is identified and recorded. Economical comparison of the two methods is based on determination of the total cost spent on the basements since the cost of upper floor realization remains, at least in approximation, of a constant value.

A considerable number of secondary effects may have influence on the optimal selection between these two methods. E.g. weather, quality of design and project, available technological procedures and geological conditions may significantly affect realization of the building. Sensitivity analysis is, therefore, carried out using probabilistic methods of reliability theory. Uncertainties in the secondary effects mentioned above are approximately described by the well-known normal (Gauss) probability distribution that seems to constitute a relatively appropriate theoretical model. It is noted that the theoretical models should be improved in the further research.

Assessment of the time required for basement realization and realization of the whole building, evaluation of the cost of basement realization and the sensitivity analysis yield the following conclusions and recommendations.

It is necessary to consider realization of the whole building. When comparing time needed for basement realization only, the obtained results are nearly the same. Differences are 1 or 2 months. As basements and upper floors are realized simultaneously in the Method Top & Down, time required for realization of the whole building by this method is significantly reduced. The difference corresponds to the time needed for realization of 5 or 6 upper floors compared with the Standard Method. Realization of the whole building with 7 upper floors and with 3 – 7 basements by the Method Top & Down is faster on average for 150 days.

The sensitivity analysis indicates that lower total cost for the Method Top & Down is obtained for 6 and more basements. For 5 basements, the total cost is similar for both the methods.

It appears that realization based on the Method Top & Down is incomparably faster than realization based on the Standard Method. Realization using the Method Top & Down remains a rather more expansive. However, differences in costs are nearly negligible.

References:

- [1] K. ŠTROBL: *Příspěvek k optimálnímu provádění spodní stavby (On Optimal Technological Procedure of Basement Realization - in Czech)*, doktorandské minimum (proposal of the Ph.D. thesis), Prague, 2003.
- [2] V. BERAN: *Dynamický harmonogram (Realization Schedule)*, Academia Praha, Prague, 2002.
- [3] Č. JARSKÝ: *Automatizovaná příprava a řízení realizace staveb (Automated Preparation and Construction Realization - in Czech)*, Contec Kralupy nad Vltavou, 2000.

This research was funded by the Czech Technical University, Grant CTU0400611.

Mankind and Their Environment

J. Šafránková, W. Droženová a kol.

`jana.safrankova@fsv.cvut.cz`

Department of Social Sciences, Faculty of Civil Engineering, Czech Technical University,
Thákurova 7, 166 29 Prague 6, Czech Republic

This publication presents the results of the studies of the Department of Social Sciences of the Faculty of Civil Engineering of the Czech Technical University, related to the research objects No. 5 The Environmental Aspects of Civil Engineering and No. 6 The Management of Sustainable Development of Buildings, Building Firms and Territories, concerning the broader contexts of these issues.

During the years of the political and economical transformation important value changes have appeared, but without any definite decision about the priorities of the society. The targets of education are based on the democratic values. The importance of the freedom of individuality should not, nevertheless, prevent solidarity and the respect of the common interest (to which the environment undoubtedly belongs) to exist. The education at the University needs a suitable combination of the value and the knowledge areas of approach.

The problems of sustainability and the environment from the point of view of social sciences are seen in the context of the conclusions of the documents of the UN international summits, namely Agenda 21 (accepted on the summit in Rio de Janeiro in 1992) and of the 16th summit in Johannesburg (2002) „People, Earth, Prosperity“, defining the three pillars of sustainable development: the social, the ecological, and the economical one. Social sciences aim to study each of these aspects and their mutual relations in the national and in the global levels.

The sub-heading of this publication “The Broader Contexts of the Sustainable Development in the Building Industry” gives some idea about the range of problems included in this book. The discourse of sustainability is grasped from the point of view of various disciplines represented at the Department of Social Sciences Faculty of Civil Engineering CTU and at the same time, of the various authors themselves. In this way, it should throw some light on the approach to the topic of the environment in the context of the research objects. The present publication concentrates especially on the questions which are relevant for the basis of the education at the Faculty of Civil Engineering CTU.

At first, the topic of sustainability is approached in its general theoretical and historical levels, in two different points of view, as are represented in the Chapter 1 and 2. In the first one, more stress is put on the origin and the history of the concept, nevertheless in both contexts the concept of sustainable development is proclaimed to be a concept with rather ambiguous content, not a closed and a static one. It has been subjected to many debates since its definition in Brundtland Report in the 1987, its interpretations being based on different philosophical backgrounds. To make a meaningful debate possible, it is necessary to identify the multidisciplinary nature of the concept, especially both its factual and normative aspects. At the same time, it is based on the anticipation of the future development with the aim to eliminate the potential crises. Sustainability is both the scientific concept and social strategy. In this context, it has been affected by the decline of science’s claims on “objective” knowledge.

The third chapter focuses on the difference and relationship between the spheres of nature and culture, important for formulating the relationship of man and society to nature and environment. The concept of culture is rooted in the metaphor of cultivation and tillage,

which grants to it a connotation of the anchorage of humankind in nature. During history, the relationship “culture“ - “nature“ has undergone important changes. The modern concept of culture emerged in Early Modern Times together with the beginnings of modern science and with the modern concept of nature.

In the contemporary Czech environmental philosophy, culture - nature relationship is interpreted by J. Šmajš as a necessary conflict. In contrast to it, E. Kohák explains that the conflict between nature and culture is not a fatal result of the culture itself, but the result of a certain direction of human action, or culture.

The following part of the book (chapters 4 - 5) already concentrates on the problems of the environment and sustainability in its relation to civil engineering, at first from the sociological point of view. Building activities are approached in the context of the whole society and the population influenced by them. This part of the text concentrates on information about social aspects of sustainable development in the educational system of civil engineering. In the Czech system of laws, general provisions for environmental impact assessment (EIA) are provided. The EIA process is established by the Act of the Czech National Council No.100/2001 Coll.

One of the most important practical tasks in relation to the building activities and its impacts on the environment is territorial planning. This topic is connected with the questions of the best way how to stimulate economically the use of the „brownfields“. Sustainable development in the building industry is only possible when re-use of large areas is realized.. At the same, time density, form and location of such development must be in line with sustainability principles.

The following part of the book concerns education at CTU in respect to sustainable development and the values related to it. In the system of education at the Czech Technical University, knowledge of environmental protection and sustainable development is vital.

We analyse mutual relations of the quality of life and sustainable development. One of the vital faculties of a graduate is his ability to communicate. Communication skills in a developed form might serve as a basis for penetration, development and sustainance of all human relations both in private and public area. Communication competency significantly contributes to the success in studies, business and leading of groups of people.

In the last part of the publication, we attempt to address events and issues which are central to the future direction the Czech Republic will follow. It highlights a number of shortcomings which have prevented society from creating critical feedback mechanisms (and which have not been sufficiently considered in political science and sociological studies).

In the conclusion, a concept of “common good” is analysed in the context of jurisprudence.

References:

- [1] J. ŠAFRÁNKOVÁ, W. DROZENOVÁ A KOL.: *Člověk a jeho životní prostředí. Širší souvislosti udržitelného rozvoje ve stavebnictví*. ČVUT v Praze, Fakulta stavební, 2004, 172 s.

This research has been supported by MSM211100005, MSM211100006.

Numerical Simulation of Fibre Concrete Members

A. Kohoutková, V. Křístek, I. Broukalová

akohout@fsv.cvut.cz

Department of Concrete Structures and Bridges, Faculty of Civil Engineering, Czech Technical University in Prague, Thakurova 7, 166 29 Prague 6, Czech Republic

The lack of design guidelines and design experience in FRC applications in structural concrete elements are responsible for a slow spread of FRCs in broader structural applications, despite their many advantages. Fibres are often used in controlling plastic and drying shrinkage cracks, instead of steel reinforcing bars or steel wire mesh. Application examples include floors and slabs, and concrete pavements. These structures and products have extensive exposed surface areas and movement constraints, resulting in high cracking potential. For such applications, fibres have a number of advantages over conventional steel reinforcements. Most structural design is based on empirically-obtained code equations that are loosely based on elasticity or plasticity theories and on experience-based serviceability criteria. Such tendencies greatly limit the usage of new and advanced materials or structures that generally fall outside the scope of the conventional approaches. The formulation and utilization of more rational approaches has led to modifications of existing design codes. Along these lines, fracture mechanics based methodologies seem to be promising but are not yet able to provide a complete basis for a new generation of design codes.

The most general structural analysis procedure is that based on the finite element method. However, due to the need for significant computing time and skill, such analysis is often restricted to special and non-conventional structures. Within this approach, the incorporation of the σ - w relation of FRC is straightforward through a discrete crack approach or an equivalent smeared crack approach. Alternatively, cracked FRC elements have been used, for example, where the crack is incorporated within special elements. Other FE implementations include the use of bar elements that represent fibres and elasto-plastic SFRC beam elements. The main aim is to find a stress-strain relationship that works with the method of FEA. As tests are used for validating the FE results a stress-strain relationship is derived from control specimens that belong to the specimens in to determine their characteristics. A special procedure is needed that allows transforming a load-deflection relationship into a ρ - w relation approach. The demanded ρ - ε relationship can be derived by dividing through a characteristic length L_{ch} . This length is assumed to relate narrowly to the element length L_{EL} . That is in case of calculating structural members of SFC/SFRC with finite element programs the post-cracking behaviour demands for an element size-dependent definition of the ρ - ε relationship. The characteristic length has to be restricted by a value that is strongly connected to the fibre length ($L_{ch} \leq L_{F/2}$).

Program systems based on FEA that enable modelling of non-linear behaviour and further parameters of concrete as cracking in approach as smeared or discrete crack model (e.g. ANSYS, ABAQUS, ATENA, DIANA) are suitable for simulation of fibre concrete to a limited extent.

The basic material characteristics were gained from laboratory tests on beams in four or three point bending and by an inverse analysis procedure the load-deflection relation was transformed into ε - σ relation used in simulation.

In the process of verification the main task was a simulation of a prescribed test using acquired material relation. The result of numerical modelling is load-deflection relation, which is compared with measurements. The test was simulated by means of a non-linear program system using a user-defined constitutive relation, which enables to model fibre

concrete. Constitutive relations in the program comprise parameters of concrete which could be used in modelling of fibre concrete: non-linear behaviour in compression including hardening and softening, fracture of concrete in tension based on the nonlinear fracture mechanics, biaxial strength failure criterion, reduction of compressive strength after cracking, tension stiffening effect, reduction of the shear stiffness after cracking (variable shear retention), two crack models: fixed crack direction and rotated crack direction. For post-peak response fracture mechanics approach is employed for softening behaviour, which is based on the crack band model and fracture energy. Such a model substantially reduces the mesh sensitivity. Discrete cracks and compression zones are modelled by means of strain localisation within bands. A test beam was modelled in 2D.

Constitutive models in commercial program systems comprise model for non-linear behaviour for concrete that can be used for modelling of fibre concrete. The model includes non-linear behaviour in compression with hardening and softening, brittle behaviour in tension resulting in cracks, failure reduction of compression strength after cracking, tensile stiffening, reduction of shear resistance after cracking, a model of strain softening based on fracture energy. Reinforcement can be modeled by means of smeared concept of layers in different directions. In a similar way modelling in ABAQUS was performed and also the material relation acquired was used in the non-linear analysis. The test beam was loaded by increments of deflection in simulation and load-deflection in midspan relation was observed. Comparison of results from simulation and from measurement proved a good agreement. The main contribution of the apparently simple applications (in fact it is quite complicated to gain post-peak response by means of current tools) was achievement of the harmony between the analysis and the tests. Effectiveness of used method was proved and an analysis of more complex structure could be carried out.

The non-linear finite element analysis is an advanced tool for design and development of concrete structures. The constitutive model based on the smeared cracks and fracture energy shows the low mesh sensitivity and good agreement with experiments in many investigated cases of fibre concrete members. The experience with the programs used indicates that non-linear analysis can be used for prediction of structural response of fibre concrete as well.

References:

- [1] KOHOUTKOVÁ, A.: *Design Methods of FRC Structural Members*, Proceedings of the International Conference Life Cycle Assessment, Behaviour and Properties of Concrete and Concrete Structures. Brno: Technical University in Brno, Faculty of Civil Engineering 2004 pp.199-204.
- [2] KOHOUTKOVÁ, A. - KŘÍSTEK, V. - BROUKALOVÁ, I.: *Material Model of FRC - Inverse Analysis*, Fiber reinforced concretes. Bagnaux: Rilem Publications s.a.r.l., 2004, pp. č. 857-864.
- [3] KOHOUTKOVÁ, A. - BROUKALOVÁ, I. - KŘÍSTEK, V.: *Aplikace numerického modelování v navrhování konstrukcí z vláknobetonu*, Česká betonářská společnost ČSSI, 2004, pp. 573-580.

This research has been supported by GA ČR grant No. GA 103/03/0838,, MŠMT grant No. MSM 210000003.

Testing of Behaviour of Fibre in Structure of Concrete

Oldřich Vlasák, Karel Trtík

oldrich.vlasak@centrum.cz

Department of Concrete Structures and Bridges, Faculty of Civil Engineering, Czech Technical University in Prague, Thakurova 7, 166 29 Prague 6, Czech Republic

Fibres in concrete structure affect its behaviour during tension stress generally after a development of the first crack. Fibres bridge the crack and carry the most of the tension stress. As the load increases, the crack gets wider and the cross-section absorbs certain amount of energy. The amount of absorbed energy depends on properties of concrete, properties of the material that the fiber is made of, and also on interaction between concrete and fiber. The interaction is influenced by the shape of fibre cross-section, and above all by the geometry of the fibre axis, and the anchor length.

Friction interaction is usually not sufficient, so the bond strength of the most used steel fibres is usually increased by bending, flattening or expansion of their ends, by corrugation or molding of the whole fibres or by combination of these modifications. The quality of the fiber material, shape of the fibre, and the anchor length determines whether the fiber is pulled out from the concrete or is teared.

The interaction of fibres and concrete is usually tested by the method of the Single Fibre Pull-out test. Usually one end of the fibre is embedded in concrete or cementitious matrix and the other one is fixed in a jaw and pulled out of the concrete specimen. The load and displacement is measured. It is also possible to embed both ends of the fibre into the concrete specimen, which is separated by a thin plastic film. The Single Fibre Pull-out test has several disadvantages. It is not easy to provide the correct fibre position during casting of the concrete specimen. The free part of the fibre between the surface of concrete and jaws has to be as small as possible and the loading has to be pure axial. When only one end of the fibre is embedded in concrete, the top concrete surface has different properties than concrete inside of the specimen. In case of both ends are embedded, the specimen has to be casted separately, which means it is made of two concretes with different ages. Also gripping of concrete specimens and their axial loading is even harder.

Because of above-mentioned disadvantages, the authors of this article developed a new testing method. This method is based on classical three point bending test of notched beams. Two fibres have been placed in the middle of each beam. The middle of the fibre was placed adjacently to the notch, so the crack was bridged by the fibre and the embedded length was the same. Some fibres were placed parallel with the bottom surface of the beam; other included an angle of 15, 30 or 45°. The used mixture proportion was invariable. Ten different types of steel fibres, two types of synthetic fibres and one glass fibre have been tested. Also the same steel fibres with different shapes have been tested. For example the expanded ends of twin cone fibre have been cut off or hooks of hooked fibre have been straighten. Overall 98 test have been carried out.

The load and displacement were recorded during testing and were put in load – displacement diagrams. The area under the load-displacement diagram is equal to the energy absorbed during the test. Absorbed energy at five points - displacement 1 to 5 mm has been compared.

The experiment proved, that it is possible to use the testing method based on three point bending test, and that in some aspects, it is comparable or even better than the standard single fibre pull out test.

The worst results have been achieved with synthetic, glass and straight steel fibres. These fibres were anchored only by friction force. They were simply pulled out and the amount of absorbed energy was very low.

Thin corrugated fibres, fibres with flat ends, and hooked fibres were pulled out too, but during this process these fibres were straightened which increased the absorbed energy. The maximum deflection was 5 mm and all these fibres were still able to carry indispensable load.

The highest amount of energy was absorbed during the test with thick corrugated fibres, and fibres with a cone on each end. From the load-displacement diagram it is also obvious, that these fibres were teared when the deflection reached approximately 2 to 4 mm. It means, that these fibres did not carry any load after the deflection reached certain point.

It is obvious, that the fibre geometry has a great influence on the amount of energy that is absorbed during fracture process of the concrete structure. Some fibres are able to carry the load even though the deflection is large, other can carry bigger load but only till the deflection reaches certain point. This has to be taken into consideration when the real concrete structure is designed.

References:

- [1] NAAMAN A.E. - NAMUR G. - ALWAN J.M., NAJM. H.: *Fiber pull-out and bond slip. Part I: Analytical study* ASCE Journal of Civil Engineering, 1991, pp. 2769-2790.
- [2] ALWAN J.M. - NAAMAN A.E. - GUERRERO P.: *Effect of mechanical clamping on the pull-out response of hooked steel fibres embedded in cementitious matrices* Concrete Science and Engineering, Vol.1 – No.1, 1999 pp. 15-25.
- [3] WEILER B. – GROSSE CH J.: *Pullout behaviour of fibers in steel fiber reinforced concrete* Otto-Graf-Journal 7, 1996, pp. 116 - 127.

This research has been supported by VZ MSM 210000004 .

Reliability of Timber Members and Joints

P. Kuklík, A. Kuklíková

kuklik@fsv.cvut.cz

Department of Steel Structures, Faculty of Civil Engineering, Czech Technical University, Thákurova 7, 166 29 Prague 6, Czech Republic

The European harmonisation of timber building codes, the determination of design values for loads and materials is the purpose for his study. Safety factors in building codes are traditionally based on long-term experience. Also, Eurocode states that, as the most common method, numerical values of partial safety factors can be determined on the basis of calibration to the long-term experience of the building industry. As an alternative, the use of statistical evaluation based on probabilistic reliability theory is mentioned. An international model code for probability-based assessment and design of structures is under preparation. However, it does not yet include information concerning timber and wood-based products resistance.

Timber structures

This study on the use of probabilistic methods in the development of timber building codes, which is a part of the Czech COST project, covers a study with a special emphasis on Eurocode 5, an analysis on material strength data to which CTU has access, and some reliability analyses to demonstrate the effect of selected distribution types and parameters on calculated failure probabilities. Also, a calculation is performed to demonstrate the dependence of safety factors on the coefficient of variation of strength.

When the number of experiments allows, determination of the 5% fractile of strength should be based on the function fitting on the lower tail of the strength values, for instance 10%. All smooth functions fitted to tail data gave good estimates of the 5% fractile. When the 5% fractile was determined from a function fitted to all data, up to 5% error occurred when compared to a non-parametric estimate. Three-parameter Weibull distribution gave, in all calculated cases, the 5% fractile within an accuracy of $\pm 3\%$.

The result of structural reliability analysis depends strongly on the load and strength distribution types used. When fitted functions are used in reliability analysis, it is essential that the fit is good in the lower tail area, the lowest values being most important. When fitted to the same data, a two-parametric Weibull distribution being next, and lognormal and three-parameter Weibull being the most optimistic. In an example, a two-parameter Weibull gave a failure probability 10 times higher than that of a three-parameter Weibull.

Reliability analysis with a permanent load and a variable load gives an interesting result: constant reliability level can be obtained by the same value of material safety factor γ_M , when partial load factors are $\gamma_G = 1.2$ and $\gamma_Q = 1.6$ and COV of lognormally distributed strength is not more than 20 %.

Timber-concrete composite structures

The study also deals in a complex way with the problems of timber-concrete composite structures.

The aim of this study is to determine design models for timber-concrete composite beams, that are applicable for computer simulations as well as for hand calculations.

The study is concerned with the investigation of the use of non-destructive testing methods for the evaluation of structural timber and for determination of the performance of structural timber elements.

The investigations dealt with the ultrasonic and stress wave methods and mainly with the penetration method. The usability of these methods was verified at samples with the structural dimensions. The principle of the work lies in the search for statistic relationships between parameters characterising the timber quality (e.g. bending strength, modulus of elasticity) and magnitudes measured by the above mentioned non-destructive methods (e.g. dynamic modulus of elasticity, density).

The study confirmed the important influence of the load-slip characteristics of the timber to concrete connection on the bending stiffness and load-bearing capacity of a composite beam.

The effect of an interlayer on the strength and slip modulus of the connector is also very important. General rules as to how to reduce strength and slip modulus are formulated. Calculation models (analytical and based on the FEM) were developed, since the non-linear behaviour of the timber, the concrete and the connectors up to failure could not be well described by analytical model.

The study provided an alternative solution relating modulus of rupture and tensile strength for structural timber with intermediate ratio of tensile to compressive strength, assuming that the timber member failed in tension but with some compression yielding.

The study revealed the importance of the timber tensile strength, the timber modulus of elasticity and the slip modulus and strength of the connectors.

The concrete quality hardly affects the behaviour of a composite beam.

The design models for the behaviour of timber-concrete composite beams, were implemented into design equations and can be used in practice.

References:

- [1] KUKLÍK, P. - KUKLÍKOVÁ, A.: *Methods for Evaluation of Structural Timber* Wood research 2001, pp. 1–10.
- [2] KUKLÍK, P. - KUKLÍKOVÁ, A.: *Evaluation of structural timber* ČVUT v Praze, 2002, pp. 97-106.
- [3] KUKLÍK, P. ET AL: *Dřevěné konstrukce* ČVUT v Praze, 2003, pp. 1-134.
- [4] KUKLÍK, P.: *The Potential of Wood as a Structural Material* ČVUT v Praze, 2004, pp. 23-28.

This research has been supported by MSMT grant No. OC E24.001.

Environmental Impact of Buildings - Life Cycle Assessment

M. Vonka

`martin.vonka@fsv.cvut.cz`

*Faculty of Civil Engineering, Department of Building Structures, Thakurova 7, 166 29
Prague 6, Czech Republic

The energy consumption in the building sector represents approximately 40% of the total energy use within the EU and the buildings produce about 30% of CO₂ emission and 40% of total waste. The predominant part of these indicators is related to the operational phase of buildings. The implications regarding the environment lead to an increased interest for energy and emissions in buildings during all phases of their lives. It is obvious that the more energy needed for operation decreases, the more important is to pay attention to the amount of embodied energy (and related embodied emissions). Therefore, the embodied values have become important research fields in order to minimize the environmental impact of the building sector.

The main goal of this paper and of the poster is to show one possible way of the environmental impact assessment applied to residential buildings in the Czech Republic. There are assessed environmental parameters such as consumption of non-renewable material sources, consumption of energy sources, waste production, emissions of CO₂ and SO₂, etc. in this evaluation process.

The environmental assessment models used for residential buildings presented in this paper are based on the principles of ISO 14040 international standard [1].

These used tools are:

- a) the tool, which is developed within the Martin Vonka's thesis "Life Cycle of Assessment of Buildings" (this tool is not for practical utilization at this moment, but for the research purposes only),
- b) a Canadian tool Athena [<http://www.athenasmi.ca/>] (this tool was used for two buildings to show differences between my tool and Athena).

There were calculated the flow of materials used for building and flow of the energy consumed during manufacturing of materials, transport and construction (embodied energy) for each building. Main groups and used criteria in the assessment process of the residential buildings are the following:

- (i) environmental criteria associated with material use: weight and volume of used materials, embodied energy, embodied CO_{2, eq.} and SO_{2, eq.}, material input (amount of renewable sources, use of recycled materials, primary natural sources), material output (amount of fully recyclable materials, partially recyclable materials and non-recyclable materials - waste),
- (ii) environmental criteria associated with utilisation phase: heating, DHW, cooling, primary energy consumption, CO_{2, eq.} and SO_{2, eq.} emissions associated with operation of building,
- (iii) other parameters: floor area, heated area, building size, number of occupants, etc.

The tool Athena calculates besides water pollution index and solid waste emissions.

There are a lot of possibilities to relate the values of each criterion. The best type of relation depends mainly on the purpose of the study:

- (i) values in absolute values (disadvantage: it is impossible to compare the assessed buildings),
- (ii) values related to comparative floor area (the calculating of this floor area = the net floor area without loggie, balcony, terrace + 0,1 x area of loggie, balcony, terrace),
- (iii) values related to volume of the building,
- (iv) values related to number of occupants.

It has been assessed 20 buildings from the environmental point of view – among evaluated buildings are for instance prefab buildings (structural system T06B or VVÚ ETA), old traditional buildings about 100 years old, new “standard” buildings, low-energy buildings, etc. (see the poster).

There are shown the primary energy consumption of these buildings and the embodied energy as well on the poster. It is possible to see quite interesting values in the 2D graphs of (i) embodied energy and primary energy consumption during use of building, (ii) embodied CO₂ (SO₂) and operating emissions of CO₂ (SO₂), (iii) amount of renewable sources + recycled materials and amount of nature sources.

References:

- [1] ISO 14 040: Environmental Management: Life Cycle Assessment International Organization for Standardization

This research has been supported by grant of IG ČVUT CTU0401011 “Environmental Impact of Buildings - Life Cycle Assessment”.

Structured Approach to Estimation of Surface Runoff from Small Watersheds

V. David

vaclav.david@fsv.cvut.cz

Department of Irrigation, Drainage and Landscape Engineering, Faculty of Civil Engineering, Czech Technical University in Prague, Thákurova 7, 166 29 Prague 6, Czech Republic

The grant project “Structured Approach to Estimation of Surface Runoff from Small Catchments” was a continuation of the project starting in the year 2003. The first year of the research (2003) focused on the classification of large areas according to their surface runoff production. This classification was tested on the area of Central Bohemian District. The main result of this research was the map of surface runoff production for the catchments of fourth hydrological order. This solution presents a so called global approach which is the first step of “Structured Approach”.

The year 2004 was aimed at the research connected with the second step of structured approach - a so called local approach. Within this part of complex solution small areas, which were evaluated in the first step as a big producer of surface runoff, are solved in detail. The analysis was tested on a small German catchment for which the data were available. It was a catchment of a stream Reichstädter Bach situated south from Dresden. The assessed catchment with a quite steep character and mainly agricultural use has 12,8 square kilometers. Hydrographic net of Reichstädter Bach is only a little developed and buildings are concentrated along the main stream.

All analyses were made using a hydrological software “Watershed Modeling System version 6.1” (WMS v. 6.1) - a complex environment for hydrological modeling which offers interface for different hydrological models (HEC-1, TR-20, TR-55, NFF, HSPF, Rational formula, etc.) and tools for pre- and post-processing of the data (digitizing of raster images, editing of vector data, creating of rainfall data, etc.).

Different analyses were made for Reichstädter Bach catchment. Surface runoff volumes and peak discharges of surface runoff were calculated for different conditions. These values were then compared and evaluated. For these calculations mainly spatially oriented data (land use map, soil map, hydrographic net, etc.) were used.

First, analyses of influence of land use changes were made. For this purpose five different land use scenarios were assumed including both real and theoretic conditions.

Tested scenarios were:

- All arable land covered with small grains and rape (present state)
- All arable land covered with crop residues (possible present state)
- All arable land not covered – bare soil (possible present state)
- All arable land changed into pasture or meadow (theoretical state)
- All arable land forested (theoretical state)

Calculations of runoff parameters were done for all possible combinations of land use and precipitation totals. Different soil conditions were also considered.

As a second type of analysis a comparison of runoff response of sub watersheds was made. For this purpose the watershed was divided in to six smaller sub watersheds. The runoff volumes were then calculated for each of them respectively and then mutually compared to see which of them is producing more surface runoff. Areas of sub watersheds had to be considered for comparability of calculated values. For this purpose unit runoff values for each sub catchment were calculated.

The main output from the presented research was that the software WMS v.6.1 was tested for application within a local step of “Structured Approach”. Also the analysis of land use changes influence on surface runoff was done. It was also necessary to find out a procedure how to prepare the data for the use in WMS v. 6.1. This procedure is described for the use of software ArcGIS 9.

References:

- [1] DAVID, V.: *Strukturovaný přístup k odhadu produkce povrchového odtoku z malých povodí*, in *Workshop Adolfa Patery 2004 - Extrémní hydrologické jevy v povodích*, České vysoké učení technické v Praze a Česká vědeckotechnická vodohospodářská společnost, 2005, s. 93 - 102.
- [2] DAVID, V. – DOSTÁL, T. - KRÁSA, J. - VRÁNA, K.: *Structured Approach to Estimation of Surface Runoff from Small Watersheds*, in *CTU Reports, Workshop 2004*, Czech Technical University in Prague, 2004, s. 870–871.

This research has been supported by CTU grant no. CTU0403111.

Determination of Crack Width of Fibreconcrete Elements

P. Machula, A. Kohoutková, I. Broukalová

iva.broukalova@fsv.cvut.cz

Department of Concrete Structures and Bridges, Faculty of Civil Engineering, Czech Technical University, Thákurova 7, 166 29 Prague 6, Czech Republic

Crack control is required in all structures. The design of conventionally reinforced flexural concrete members is often governed by the maximum crack width requirements in the serviceability limit state. The application of FRC could be a suitable way to fulfil these requirements. The calculation of the design crack width in fibre reinforced concrete is similar to that in normal reinforced concrete. The calculation of crack widths in fibreconcrete, as proposed by RILEM seems to be too conservative. An adaptation of the formula to calculate the final crack spacing and width should be proposed.

When a crack is formed in fibre reinforced concrete, the fibres will typically stay unbroken. The fibres crossing a crack will resist further crack opening and impose what is called crack closing or crack bridging effect on the crack surfaces. Different failure modes can result, depending on the effectiveness of the fibres, in providing crack bridging. If the fibres break or are pulled out during crack initiation, or if the fibres cannot carry more load after the formation of the first crack, then the first cracking strength is the ultimate strength and further deformation is governed by the opening of a single crack and fibres pulling out and/or breaking along the edges of the crack. This behaviour is also known as tension softening behaviour. If – on the other hand – the fibres are able to sustain more load after the formation of the first crack, more cracks will be formed and what is known as multiple cracking or pseudo-strain hardening will occur.

A crack propagating in concrete can be modelled by a zone of diffuse microcracking – the process zone and a localized crack. The localized crack can be divided into a part where aggregate interlock is present, and a traction free crack. First crack formation is calculated on the bases of stress-strain relationship. Crack width is calculated on the bases of bond between fibreconcrete and reinforcement. Owing to fibre activation the bond is higher. Bond has principal significance on structural behaviour of fibreconcrete. Without presence of bond the structure could not be able to carry loads together. Bond performance has an effect on flexural load bearing capacity and particularly on service ability behaviour. Tension stiffening, thus crack widths can be evaluated directly from an analysis based on bond and force transfer. Bond performance of reinforcing bars is usually represented by bond stress – slip responses. Phases of bond performance and failure are the followings: i) adhesion with zero slip, ii) mechanical interlocking microcracks are formed around the reinforcement and microcrushing occurs in the concrete highly stressed in front of ribs of the reinforcement.

If splitting failure is avoided failure of bond in the case of conventional reinforcement is always rebar pull-out with shearing the concrete lugs present between ribs. Surface failure of steel reinforcement never occurs, thus bond strength depends only on the strength of the concrete.

Cracks are formed in fibreconcrete members when principal tensile stress from loads reaches the tensile strength of concrete. Formation of cracks of flexural members can be distinguished into two phases: the crack formation phase and the stabilised cracking phase. During crack formation phase cracks form at random positions according to the locally weak sections. The compatibility of strains between concrete and reinforcement is no more maintained at a crack as concrete stress dropped to zero for normal reinforced concrete. However, it has to be taken into account that the tensile stress in steel fibre reinforced

concrete after cracking is not equal to zero. With increasing distance the compatibility of strains between concrete and reinforcement is again recovered. The better the bond properties of the reinforcing bar, the shorter the length for re-establishing strain compatibility. At the crack formation phase the disturbed zones are independent from each other and increase of load causes the decrease of the average crack spacing.

The so-called stabilised cracking phase is reached when no more cracks may form. Under this condition cracks are so close to each other that the disturbed zones can not be independent. At the stabilised cracking phase the average crack spacing remains constant. Increase of loads causes increase of only the crack widths. The average crack spacing at stabilised cracking phase is a function of bar diameter, bond properties, concrete tensile strength and effective reinforcement ratio.

During crack formation phase cracks form (independently from each other) at random positions in locally weak sections. When a crack is formed, stress in the concrete adjacent to the crack drops. At the section of a crack loads are carried by the reinforcement only. Compatibility of strains between concrete and reinforcement is no more maintained. With increasing the distance from the crack the tensile stress in the concrete increases as force is transferred by bond stresses. At some distance from the crack the compatibility of strains between concrete and reinforcement is again maintained. The better the bond characteristics of the reinforcing bar, the shorter the length for re-establishing strain compatibility.

In applications where conventional reinforcement is used with fibre concrete, FRC members exhibit multiple cracking until reinforcement yielding. At that point, one crack generally governs the member behaviour due to the softening nature of fibre concrete. The assumptions must enable modelling the member response at small and moderate crack opening. At small crack opening under service loads, both the maximum crack width and the stress level limits in the reinforcement can have a significant importance.

Despite a long time elapsed from the first applications of fibreconcrete elements, the use of FRC in load-carrying structural members is very limited. It might be because of the lack of clear understanding in how fibres contribute to better behaviour of a structure, lack of structural design guidelines for FRC members, uncertain cost benefit ratio, and insufficient material property specification, characterization, and test standards for novel materials. This paper intends to propagate favourable properties of fibreconcrete - convenient spreading and spacing of cracks and from it arising crack width. Fibres may increase a flexural load bearing capacity but main benefit of fibre content in FRC members shows itself primarily in analysis of serviceability limit state.

References:

- [1] KOHOUTKOVÁ, A. - KŘÍSTEK, V - BRUKALOVÁ, I.: *Material Model of FRC – Inverse Analysis*, BEFIB, 2004, pp. 857-864
- [2] RILEM COMITEE.: *Test and Design Methods for Steel Fibre Reinforced Concrete: Materials and Structures* RILEM TC-162 TDF 2000, pp. č. strany–č. strany.

This research has been supported by CTU grant No. CTU0401711 and by GA ČR grant No. GA 103/03/0838.

Determination of Material Characteristic of Fibreconcrete from Laboratory Tested Beams Behavior for Structural Analysis by Inverse Analysis

I. Broukalová, A. Kohoutková

iva.broukalova@fsv.cvut.cz

Department of Concrete Structures and Bridges, Faculty of Civil Engineering, Czech Technical University, Thákurova 7, 166 29 Prague 6, Czech Republic

Large research and development has been made in research on fibreconcrete behaviour. Even though benefits of fibreconcrete material properties are obvious, the use of fibre-reinforced concrete in load-bearing structural members is rare and sporadic. Reasons might be in a shortage of codes and guidelines with statement of FRC material properties as engineers get used to for structural analysis of reinforced concrete structures. That is in fact impossible, as fibre-reinforced concrete material properties strongly depend on the fibre type, i.e. material of fibres, fibre cross-section, ratio of fibre length and diameter and the amount of fibres in concrete mixture. It is necessary to determine material properties for a specific fibreconcrete used in a particular structural member.

Number of searched material properties depends on type of a structural analysis. For simple calculation of load bearing capacity Young elastic modulus, tensile and compressive strength are sufficient. For more sophisticated structural analysis performed on computer (e.g. finite element method) more data input is required. Except above-mentioned basic material characteristics an engineer has to determine a number of other material inputs and decide about a suitable material model.

There are two recommended approaches for modelling of FRC: model based on a stress-strain relationship and model based on non-linear fracture mechanics. In terms of these two approaches there are several possibilities for modelling behaviour after crushing and for modelling of tension softening. Tension softening might be based on fracture energy or exponential or linear crack opening law.

To gain material properties for FE analysis input a laboratory test must be carried out. Three or four point-bending test is simple to perform and sufficient for finding material inputs to FE simulation.

In this research work FRC with polypropylene fibres Forta Ferro (reinforcement ratio 0.5%) was investigated. A notched specimen 100 x 100 x 400 mm with was bent in three point bending laboratory test. The notch depth was 31mm. The load to the specimen was applied by deformation and a midspan deflection was measured. Elastic modulus, tensile and compressive strength were calculated from the load – deflection curve. Other material parameters – important points of stress-strain relationship were obtained by means of an inverse analysis.

In a former stadium of the research work an inverse analysis was performed by manually controlled input. The laboratory flexural test was simulated in a FE analysis. Material properties for the first run of computer analysis were estimated. Results of FE simulation were compared with experiment and material input was adjusted to approximate the load - deflection curve from FE simulation to that obtained in laboratory test. This procedure was repeated for several times until acceptable coincidence of the curves was reached. Favourable results of inverse analysis were obtained for two material models; first based on stress – strain relation with adopted fracture mechanics approach to prevent

influence of mesh size; second formulated with reference to the relationship stress – crack band opening, where fracture energy is one of the input material parameter.

In a latter analysing of material characteristics of polypropylene fibre reinforced concrete a more complex tool for inverse analysis is adopted. Material parameters are sought for by a random study. In a first run of such study deterministic calculation is performed. In a similar way as for the previous method for the first computer run of the analysis the material properties are defined and a deterministic FE analysis is performed. The material input parameters and other input parameters used in a deterministic analysis are used as mean values for random distributions of selected variables. Further stochastic parameters for selected material parameters are defined by their probability density functions. Selected material parameters are described by mean value, variance and other statistical parameters. The randomness of the input values reflects randomness regarding material properties. Correlation between random input variables can be introduced in form of the correlation matrix. Number of samples is selected according to complexity of the problem to be solved and required quality of expected results. Already a small number of samples could give a reasonable estimation of stochastic parameters of the structural response. For prepared sets of particular samples FE stimulations of bending test are performed. The resulting set from the whole simulation process is statistically evaluated. And the material parameters that satisfy the laboratory test in the best way are input for the last stage of analysis.

With material parameters obtained by means of inverse analysis FRC with steel bar reinforcement was analysed. Beam size 1800 x 150 x 100 mm, reinforced by two steel bars with 6 mm diameter. In a flexural test was a load bearing capacity determined. A curve load – deflection was monitored and recorded. Comparison of the relationship load versus deflection from the test and from FE simulation proved correctness of material parameters found by means of inverse analysis.

Comparing results of bending test of reinforced concrete and reinforced fibreconcrete we also proved benefits of fibreconcrete. Despite bigger compressive strength and elasticity modulus of reinforced concrete due to the confinement of the fibres the reinforced fibre concrete beam had bigger flexural load bearing capacity both in a laboratory test and in FE simulation.

References:

- [1] ČERVENKA, V. – JENDELE, L. - ČERVENKA, J.: *ATENA Program Documentation* Vydavatel, 2003, pp. 15–33.
- [2] KOHOUTKOVÁ, A. – BROUKALOVÁ, I - KRÍSTEK, V.: *Application of Numerical Simulation in Design of Fibreconcrete Structures* ČBS ČSSI Hradec Králové, ISBN 80-903501-3-5, 2004, pp. 573-580.
- [3] CERVENKA CONSULTING.: *SARA User's Manual* Cervenka Consulting, Prague, Czech Republic, r, pp. 3–26.

This research has been supported by CTU grant No. CTU04014111 and by GA ČR grant No. GA 103/03/0838.

Serviceability Limit State of Prestressed Concrete Bridges

V. Křístek, A. Kohoutková, J. L. Vítek

kristek@fsv.cvut.cz

Department of Concrete Structures and Bridges, Faculty of Civil Engineering, Czech Technical University of Prague, Thákurova 7, 166 29 Prague 6, Czech Republic

Prestressed concrete bridges are very sensitive to long-term increase of deflections. This phenomenon has paramount importance for serviceability, durability and long-time reliability of such bridges. This is why a reliable prediction of deformations of bridges during their construction as well as during their service life is extremely important.

Results of the experimental research and the developed analytical and design methods are necessary to create sufficient theoretical tools for reliable and economic structural design of prestressed concrete box girder bridges, enabling great economy of materials, energy and costs and their better utilisation and offer objective and effective tools increasing in the same time the level of durability and efficiency of prestressed concrete box girder bridges. The achieved results will enable not only to avoid excessive deflections resulting in long-time serviceability problems, but also possibly other serviceability impairments. Serviceability and durability belong to the main factors, which are evaluated at large concrete structures. Some years ago, the safety was considered as a main criterion of the correct design, however, many problems with reliable function of concrete structures lead to re-evaluation of the criteria of their reliability. Many large concrete bridges suffer from the steadily growing deflections. If such deflection exceeds a certain limit, the bridge has to be repaired, which results in the necessity to deviate the traffic outside the bridge and make usually expensive reconstruction. The costs may be rather high.

The underestimated or incorrectly calculated deflections of a bridge may introduce some doubt if the stresses and internal forces, which were calculated by the same analysis, are also correct. Since the analysis is usually performed by the method by which both - the internal forces and deflections are calculated, such doubts are really important. If there is some inaccuracy in deflections, there may be also an inaccuracy in stresses and the safety factor of the bridge may differ from that calculated as a proof showing that the safety of the bridge corresponds to the code requirements.

To avoid problems of serviceability, durability and long-time reliability of such bridges, the following recommendations can be formulated:

- Analysis – all important influencing factors must be taken into account (shear strains in webs as well as the shear lag), 3D FEM approach would be welcome, but it is - until now – rather exceptional.
- The statistical scatter of the material characteristics and other parameters is important, statistical methods are not still commonly used in the design practice – robust structure should be designed (uncertainty in calculated results must be respected, two analyses – lower and upper limit deflection estimate).
- Creep and shrinkage data for the analysis - based on the short-term measured values significantly improves the accuracy of the prediction.
- Prestressing design – the balancing factor for dead load should be taken into account
- Tendons in the cantilever stage – careful estimate of their efficiency.
- Tendons in the final stage – arrangement, which contributes to reduction of deflections.
- Prestress losses – reduction using ducts with low friction, monitoring of stress in selected tendons.

- Monitoring of deflections at bridges with large spans.
- Summarizing of measured results from different projects and drawing recommendations for improvement of future design methods.

It may be summarised that the excessive and with time increasing deflections of long-span prestressed bridges are caused by a combination of several simultaneously acting factors.

- The deflections cannot still be predicted with an accuracy, which would guarantee a reliable function of the bridge for a long time
- The role of the designer is important for a reasonable design
- The robust design is necessary to avoid future problems

The appropriate solutions have to be based on reliable experimental data and physical phenomena and have to take into account randomness of the input parameters. The application of numerical methods and development of new advanced computer software for the analysis of multi-dimensional structures will be necessary to obtain realistic prediction of the structural performance.

The research on this problem is extremely important, not only to avoid excessive deflections resulting in long-time serviceability problems, but also possibly in cracking, corrosion or other serviceability impairments. Such bridges have to be either closed or repaired well before the end of their initially designed service life. It also should be noted that a wrong prediction of the development of deflections means that also prediction of the distribution of internal forces, particularly in bridges changing the structural systems, can be quite far from the reality. Thus, it should be concluded that appropriate methods of analysis are needed to predict a realistic time variations of deflections as well as internal forces redistributions in long span prestressed concrete bridges.

References:

- [1] VÍTEK, J. L. - KRÍSTEK, V. - KOHOUTKOVÁ, A.: *Time Development of Deflections of Large Prestressed Concrete Bridges*, FIB Symposium 2004 on Segmental Construction in Concrete, Delhi, 2004, pp. 177-179.
- [2] KRÍSTEK, V. - VÍTEK, J.L. - HRDOUŠEK, V. - KOHOUTKOVÁ, A.: *Experimentální Výzkum Na Mostech Velkých Rozpětí A Doporučení Pro Navrhování*, Sborník 9. Mezinárodního Symposia Mosty 2004, Brno, Sekurkon Brno, 2004, pp. 184-188.
- [3] KRÍSTEK, V. - VÍTEK, J.L.: *Účinnost Předpětí Na Dlouhodobé Průhyby Předpjatých Mostů*, Beton Č.2, ČBS ČSSI Praha, 2001, pp. 38-42.
- [4] ŠMERDA, Z. - ŠMERDA, J.: *Influence Of Traffic Loads On Permanent Deflections Of Prestressed Concrete Bridges*. Journal Of Fib "Structural Concrete", Vol. 3, No.4, Thomas Telford, 2002, pp. 163-165.

This research has been supported by 103/02/1005.

Estimation of the Soil Hydraulic Properties in Headwater Territory

M. Dohnal, J. Dušek, T. Vogel, M. Šanda *

dohnalm@mat.fsv.cvut.cz

Department of Hydraulics and Hydrology, Faculty of Civil Engineering, Czech Technical University, Thákurova 7, 166 29 Prague 6, Czech Republic

*Department of Drainage, Irrigation and Landscape Engineering, Faculty of Civil Engineering, Czech Technical University, Thákurova 7, 166 29 Prague 6, Czech Republic

Headwater territories play significant role in problems of the flood protection and rainfall-runoff studies. To understand runoff formation, knowledge of shallow subsurface flow is crucial. Reliable prediction of water flow in natural porous systems most importantly relies on appropriate description of unsaturated hydraulic properties. Hydraulic functions of soils are varying in both time and space [1]. Estimation of the soil hydraulic parameters depends on adequacy and usability of parametric model, sensitivity and mutual dependence of parameters.

This contribution aims at quantifying the spatio-temporal variability of soil hydraulic characteristics at highly heterogeneous headwater watershed Uhlířská (total area 1.87 sq. km; average altitude 820 m above sea level, total annual precipitation 1229 mm; average annual temperature 4.7°C) in North Bohemia (Jizera Mountains). Jizera Mountains were extensively deforested in 80's. Currently, the forest openings are covered with the monoculture of young spruce. Well equipped experimental slope Tomšovka, typical for the Uhlířská watershed, provides a broad variety of measurements [2]. The soil profile typically consists of three layers under the sod layer: 20-cm deep Ah-horizon, 50-cm thick B-horizon, and a 5-cm thick C-horizon. At the depth of about 70 cm, the zone of transition between the soil and the granite bedrock is situated. Soils at the site of interest are classified as Dystric Cambisols. Pressure head data continuously recorded by tensiometers at four different locations within three consecutive years 2000, 2001 and 2002 were used in our comparative study. At each location, the nest of three sensors was set up. The observation depths of the sensors in the nest were chosen so as to represent the local soil horizons. Potential evapotranspiration, using Penman-Monteith formula, was determined on the basis of the available meteorological measurements.

Water regime in the soil profile was simulated with numerical code HYDRUS [3] based on Richards' equation. To simplify the description of spatial variability of hydraulic properties, the concept of linear variability of porous medium [4] is used. The initial set of soil hydraulic parameters for running the simulations was derived from measured retention curves. Observed rainfall data and calculated potential transpiration rates were employed. The initial soil water pressure head profile was set up in agreement with tensiometer measurements. The presented simulations cover the whole vegetation season in each of the three years.

Inverse modeling was performed in order to minimize discrepancies between the model response and measured pressure heads. Commercial software package PEST (Waterloo Hydrogeologic), based on the Levenberg-Marquardt algorithm, was used as a parameter estimator. The objective function was composed of the three separate contributions of tensiometric data (recorded during the vegetation season). This was done separately for each

of the four nests at the respective year – resulting in twelve individual optimizations. The scaling factors were used to upscale the reference van Genuchten's hydraulic parameters by means of inverse modeling. Four values of scaling factors, namely scaling factors of hydraulic conductivity and pressure head at the top and at the bottom of the soil profile, were optimized in the least-square sense.

Two separate scenarios were formulated to examine if hysteresis of soil hydraulic functions plays an important role in simulations of the soil water movement in the context of parameter optimization. In the first case, the hysteretic behavior of the retention curve was included while in the second case hysteresis was neglected. The hysteretic effects were included by setting the measured hydraulic parameters equal to the parameters of the main drying curve while the parameters of the main wetting curve of the hysteretic loop were estimated. In our particular case, the evaluation of individual optimizations proved insignificant effect of hysteresis on the results. Therefore, following analyses consider exclusively the model optimizations without hysteresis. Neglecting hysteretic behavior of the retention curve seems noteworthy, since the redistribution process takes place during the vegetation season.

Were the soil hydraulic properties invariant, both in time and horizontal location, we would obtain twelve equal parameter sets. However, the results from optimization procedures suggest significant spatio-temporal heterogeneity. Parameter sets estimated from each tensiometer nest and vegetation season were than used for simulations at the other locations and for the other years. In fact, permutations of optimized parameter sets, taken two at a time, were completed in order to resolve both spatial and temporal variability. For this purpose, we employed root mean square error criterion to compare performance of the optimizations.

From the numerical experiments, it follows that the spatial variability of the soil hydraulic characteristics prevails over temporal variations. Furthermore, the used upscaling method of the measurement-based parameter set allows considerable reduction of the objective function. The upscaling concept also reduces the amount of optimized parameters which consequently makes the inverse problem more robust and estimated parameters less prone to non-uniqueness. This results in substantial saving of time needed to run the optimization. Finally, we were able to characterize the most effective parametric sets for which the model performance was significantly higher than for the rest of the sets.

References:

- [1] OLYPHANT, G. A. *Temporal and spatial (down profile) variability of unsaturated soil hydraulic properties determined from a combination of repeated field experiments and inverse modeling*, Journal of Hydrology 281, 2003, 25-35.
- [2] M. ŠANDA *Subsurface runoff generation on a slope*, PhD. Thesis, Czech Technical University of Prague, 1999.
- [3] T. VOGEL, K. HUANG, R. ZHANG, M. TH. VAN GENUCHTEN *The HYDRUS Code for Simulating One-dimensional Water Flow, Solute Transport and Heat Movement in Variably-saturated Media - Version 5.0*, Research Report No. 140, U.S. Salinity Lab., ARS, USDA, Riverside, CA., 1996.
- [4] T. VOGEL, ČÍSLEROVÁ, M., AND J.W. HOPMANS *Porous media with linearly variable hydraulic properties*, Water Resources Research, 27, 1991, 2735–2741.

This research has been supported by CTU grant No. CTU0402911.

Competitive Corrugated Sheeting Through Connection Fire Resistance

Petra STUDECKA

petra.studecka@fsv.cvut.cz

Department of Steel Structures, Faculty of Civil Engineering, Czech Technical University, Thakurova 7, 166 27 Prague 6, Czech Republic

Cold-formed corrugated sheeting is widely used for different kind of buildings, especially for roofs and facades. The dominant technical culture considers that steel is not efficient in case of fire. However, in reality, steel is widely used for its good structural and architectural performances. For this, we focused our research interest on the steel resistance in case of fire. The structural behaviour of cold formed profiles is well described under normal conditions. The knowledge of their material properties evolution under high temperatures enables to predict their behaviour and bearing capacity with a good accuracy. This knowledge is integrated into European standard under its EN version. Thus, for joints, the full description of their behaviour is characterized by the prediction of the initial stiffness, the deformation capacity and the resistance. The influence of the joints on the structural elements behaviour under high temperatures is not negligible. The global analysis models using stress skin method allow the evaluation of the sheeting stiffness and resistance in the roof. The model, based on theoretical and experimental approaches, depends on the behaviour of thin walled elements and also on the stiffness of the connecting elements.

The paper presents the outputs of an experimental and theoretical research of the fire behaviour of the cold-formed corrugated sheeting held at Czech Technical University in Prague.

Five fire tests of the assembly performed at Institute PAVUS in Veselí n. L. are available for the study. The tests are loaded by the standard time-temperature experimental curve. Because of section factor $A_m/V [m^{-2}]$ up $1\ 000$ ($1\ 136$ in observed case) is heat transfer into the thin walled structures by conduction, convection and radiation so rapid that, may be for design expect the steel temperature θ_s equal to the gas temperature θ_g .

The accuracy of the experiments is limited by the boundary conditions, which are for the tests well described and developed in standard [3] but seldom reflect the behaviour in real structure. The knowledge of material properties of the cold-formed profiles under high temperatures, see [1], enables to predict the behaviour and the load bearing capacity with a good accuracy. The knowledge was integrated into European standard under its conversion, see [3]. The full description of the joint behaviour by prediction of initial stiffness as well as deformation capacity with the traditional good knowledge of joint resistance reflects today practice, see [4]. The influence of joints on behaviour of the structural elements under height temperatures exhibits its significant role into the behaviour.

The connections were tested at the Laboratory of the Czech Technical University in Prague under room temperature. Thirty tests were performed to check stiffness, resistance and deformation capacity of the bolted connection with one type of self-drilling screw of the diameter $5,5\ mm$ and the bolt head $7,2\ mm$. The frame stiff in bending simulates the behaviour of connection at support. The bearing of the plate was observed as the collapse at all tests. The mean value of test resistance ($4,48\ kN$) was reached with standard deviation of $18,5$. The characteristic value of resistance F_k was calculated from the values at 5% quintile as ($3,12\ kN$). The characteristic design value F_d ($2,71\ kN$) was calculated by reduction to steel yield strength f_y/f_u . The initial connection stiffness k_b was calculated as mean value from

deformation at $2/3$ of F_d , excluding the initial slip. The stiffness of $k_b = 32 \text{ kN/mm}$ was found. The minimum deformation capacity of the connection is $\delta_{Cd,min} = 1,5 \text{ mm}$ and mean value $\delta_{Cd,k} = 2 \text{ mm}$.

Finite element code ANSYS 5.7 was utilized for the modeling. Element with tension-compression and bending capabilities with three degrees of freedom at each node was used for the analysis, it is marked as BEAM 23 in the elements library. The bolted connection of the thin walled sheet to the supporting structure was modeled by non-linear spring element with one degree of freedom element (NONLIN39). Multi-linear isotropic material option without strain hardening was used for the calculation. The material properties of steel were temperature dependent. The stress-strain diagrams at elevated temperatures and the elongation of steel as temperature dependent were modeled as recommended in [3].

The load of the structure was applied in two steps. In the first step, uniformly distributed load representing dead load on the roof was applied. In the second step, the temperature of the structure was increased from 20°C until collapse. Only the span of the beam was heated, while the cantilever remained cold. The applied temperature was expected as uniform over the span of the beam and through depth of the steel sheeting. Properties of the bolted connection were idealized.

Simple engineering models for prediction of resistance of sheeting under high temperature are based on beam or membrane modeling. The material properties of steels in thin-walled structures are available for hot rolled as well as cold formed sections based on work [3]. The results are standardized in [4]. In case of the similar change of the modulus of elasticity and of strength may be assumed that the local buckling due to temperature and by neglecting.

The finite element and analytical prediction models are compared to tests. The beam analytical model and the membrane model is included to show the prediction accuracy. All models are calculated with measured material properties and partial safety factors $1,0$.

The FE simulation enables to predict the resistance of the cold-formed sheeting under high temperatures with good accuracy compared to available experiments. The analytical beam model shows a conservative approximation of the experimental behaviour.

The test of sheeting's with connections allowing the membrane action, the tests of ductile screw connections at high temperatures and the stress skin behaviour of the roofing under fire conditions are under progress at Czech Technical University in Prague to complete the work.

References

- [1] OUTINEN J., MÄKELÄINEN P.: *High-temperature strength of structural steel and residual strength after cooling down, in Stability and ductility of steel structures*, ed. Ivanyi M., Akadémiai Kiadó, Budapest 2002, pp. 751-760, ISBN 963-05-7950-2.
- [2] OUTINEN J., KAITILA O., MÄKELÄINEN P.: *High-temperature testing of structural steel and modelling of structures at fire temperatures*, Laboratory of steel structures publications, TKK-TER-23, HUT, Helsinki 2001.
- [3] PrEN - 1993-1-2: *Design of Steel Structures - Part 1.2: Structural Fire Design*, Fourth final draft, Document CEN/TC 250/SC 3, CEN, Brussels 2002, p. 74.
- [4] JASPART J.P.: *Recent advances in the field of steel joints – Column bases and further configurations for Beam-to Column Joints and Beam Splices*, Thesis, Université de Liège 1997, p. 134.

This research has been supported by CTU0402411.

Monitoring of Dynamic Behavior Changes of Two Types of Structures

T. Plachý, M. Polák

plachy@fsv.cvut.cz

CTU, Faculty of Civil Engineering, Dept. of Structural Mechanics
Thákurova 7, 166 29 Praha 6

In practice, various kinds of damage on reinforced concrete structures can be found. Undetected damage can lead to the failure of structural members or a structure at all. Therefore monitoring of a deterioration degree and damage detection of a structure at the earliest possible stage is very important. Current damage detection methods require that the vicinity of the damage is known a priori and that the portion of the structure being inspected is accessible. The need for methods that can be applied to complex structures led to the development of methods that examine changes in modal characteristics of the structure.

Methods and procedures, which use results of an experimental modal analysis for estimation of a degradation degree of a structure, are suitable to verify on simple structural elements or complex structures, where we know their damage state.

Tests of structural elements of two types were carried out in laboratories of Faculty of Civil Engineering CTU in Prague. The influence of damage increase of reinforced concrete beams and slabs on change of their modal characteristics was monitored.

Three reinforced concrete beams with dimensions 4.5 m x 0.3 m x 0.2 m were prepared for the purpose of the test. The beam was simply supported with the length of a span 4.0 m with cantilevered ends 0.25 m on both sides. The state deterioration of beams was done by static loading and dynamic fatigue loading. The beams were tested in four-point bending to get a constant bending moment in the mid-section of the beam. Before the test and after each load step the dynamical response of the beam was measured with a separate test arrangement.

The change of modal characteristics was monitored and confronted with the damage state of the beams. Modal characteristics of the beams, which were measured after each loading step, were mutually compared. Changes of natural frequencies $\Delta f_{(j)}$ were computed as well. For the comparison of natural modes, the modal assurance coefficient $\text{MAC}_{(j,j)}$, the coordinate modal assurance criterion $\text{COMAC}_{(p)}$, changes of a mode surface curvature $\text{CAMOSUC}_{(j),x}$, changes of a modal flexibility matrix $\Delta[\delta]$ and the second derivative of changes of diagonal members of a modal flexibility matrix $\Delta[\delta]''$ were used.

After the evaluation of the first test results of the beams, the second tests of the slabs were designed. Four reinforced concrete slabs with dimensions 3.2 m x 1.0 m x 0.1 m were made for the purpose of the test. Slabs were simply supported on two opposite sides with the span 3.0 m and cantilevered ends 0.1 m. Slabs were also loaded by static and dynamic fatigue loading and the change of modal characteristics was monitored and confronted with the damage state of the slabs using the same coefficients as for the beams.

For localization of places with crazing induced by load increase during experimental and theoretical studies on structural elements $\text{CAMOSUC}_{(j),x}$, $\Delta[\delta]$ and especially $\Delta[\delta]''$ seems to be most appropriate.

For acquisition of reliable data for appreciation of monitored structure based on $\text{COMAC}_{(p)}$, $\Delta[\delta]$ and $\Delta[\delta]''$, it is very important to consider carefully the character and the number of natural modes, which are used in their computation. For determination of $\text{CAMOSUC}_{(j),x}$ it is the most suitable to use the basic natural mode (the first vertical bending mode of natural

vibration), for higher natural modes CAMOSUC_{(j),x} does not give as good results as for the first one. For reliable analysis, it is important to obtain reference data about dynamic properties of investigated structure in the undamaged virgin state, optimally before starting its operation.

The investigation of the damage influence of the structure on change of its modal characteristics was done also on one bridge structure, where we knew its damaged state.

The tested bridge is situated across the highway D5 near the village Vráž in Czech Republic. The bearing structure of the composite bridge consists of four main steel I-girders and a reinforced concrete slab. It is a three-span continuous bridge (11.7m + 35.1m + 11.0m). In March 2001, the bridge was damaged by a crash. A heavy vehicle (excavator) ferried on D5 clashed into its two main girders. Consequences of this crash were permanent buckle of the main girder and damage of the connection between the main girder and the crossbeam.

The experimental modal analysis was carried out twice on this bridge – for the damaged state and for the state after the reconstruction.

Modal characteristics evaluated for the both verified states of the bridge were mutually compared. During the investigation of the influence of the bridge damage on its modal characteristics there were computed changes of natural frequencies and damping frequencies, for comparison of natural modes coefficients MAC_(j,j), COMAC_(p), CAMOSUC_{(j),x}, $\Delta[\delta]$ and $\Delta[\delta]''$ were used as for investigation on structural elements.

From evaluated results, there can be found that damage of the main girder and its reconstruction significantly influence the dynamic behavior of the investigated bridge. Ascertained changes of modal characteristics are significant and confirm the improvement of the structural state of the bridge after the reconstruction of the main girder.

The change of the mode shapes was so large that the coefficient MAC had to be used to find corresponding modes for comparison. For damage detection and localization on this bridge the use of natural frequency changes, CAMOSUC_{(j),x}, $\Delta[\delta]$ and $\Delta[\delta]''$ proved to be appropriate.

In contrary to the results obtained on simple structural elements it seems that for damage localization on complex structures using CAMOSUC_{(j),x} not only the first natural mode but also the higher ones can be used. Especially there is suitable to use combination of the values of CAMOSUC_{(j),x} computed in longitudinal and transversal direction of the bridge.

References:

- [1] BRINCKER, R. - ANDERSEN, P. - CANTIENI, R.: *Identification and Level I Damage Detection of the Z24 Highway Bridge* Experimental Techniques, 25 (6) 2001, pp. 51-57.
- [2] FRÝBA, L. – PIRNER, M.: *Localization of damages in concrete structures* Proceedings of the International Conference Computational Methods and Experimental Measurements X. 2001 pp. č. strany–č. strany.
- [3] PLACHÝ, T.: *Dynamic study of cracked reinforced concrete beams* Ph.D. Thesis, FCE CTU 2003 pp. 1-139.
- [4] PLACHÝ, T. – POLÁK, M.: *Influence of Damage of a Reinforced Concrete Beam on Changes of Its Behaviour* Proceedings of the 5th European Conference on Structural Dynamics EURODYN 2002 - Volume2, A.A.Balkema, Rotterdam, Netherlands, 2002, pp. 1451–1456.

This research has been supported by MŠMT grant No. MSM 210000030.

Stochastic Response and Stability of Imperfect Structures with Random Additive and Parametric Excitation

J. Náprstek*, A. Kohoutková**, V. Křístek**

kristek@fsv.cvut.cz

*ÚTAM ČSAV, Prosecká76/809, 190 00 Prague 9

**Department of Concrete Structures and Bridges, Faculty of Civil Engineering, Czech Technical University of Prague, Thákurova 7, 166 29 Prague 6, Czech RepublicKatedra

Response, stability, reliability and service life of structures are influenced significantly by unavoidable imperfections of their physical, properties (technology dispersion, successive material degradation, etc.) and geometric characteristics (shape and wall thickness deviations, corrosion, damage cumulation, etc.). These imperfections are of random character. They can be modelled mathematically as stochastic functions in space and time taking into account various scope of their mutual stochastic interaction. The behaviour of structures is influenced substantially by interacting environment. Properties of such environment, such as density, velocity field, stiffness, homogeneity and others are also of stochastic character, as a rule, whether primarily or as a consequence of mostly nonlinear interaction with the moving structure, producing various types of loads comprizing a strong stochastic component.

These phenomena are related with a number of other random processes which may yield significant information about state of the structure. They can assist in the prediction of approaching defect or failure, identify wear and initiate the start of repair or to be the source of warning signals before a dangerous event. Other random processes, resulting mostly from nonlinear interactions of a structure and a medium, may help to restabilize its response and to support its serviceability or, on the other hand, to stimulate its final collapse. Fluctuations of geometric and physical properties of systems and loads manifest themselves most markedly in combination with extreme static and particularly dynamic effects. Hence the defects of function and serviceability of the system and further nonconventional processes of crack propagation, degradation of the system material or of the ambient continuum (subgrade of transport ways, buildings, etc.). Therefore, modern approach to structural design must be based on stochastic principles which enable to take into account the scatter of real values of quantities considered in the analysis of the structure-load-environment system. This enables a subsequent determination of reliability of the structure expressed by the theoretical probability of failure. At the same time it makes it possible to explain the phenomena observed in practice, resulting from the stochastic character of the problem and to assess their significance with reference to the achievement of the 1st and 2nd limit states of the structure including a possibility of proposal of maintenance and reconstruction strategy.

The immediate applications are mostly oriented into the field of real civil engineering structures. With reference to serviceability and usability of large-span girder bridge structures, seems to be important the problem of permanent growth of deformations in time. To emphasize the seriousness of the problem it must be realized that should the deflection evolution in time follows a different way from that determined by structural analysis, then the internal forces being computed at a statically indeterminate structure will be heavily influenced, as they arise from their redistribution due to creep of concrete, occurring usually during the multiple change of the structural system in the course of the structure erection. The

increase of deformations of bridge superstructures is brought about by long-term effects depending on external load, prestress and of ambient environment.

A realistic description of the actual function of such composite structures as reinforced concrete members exposed to high level stresses, showing imperfections of shape and material characteristics, require the application of specially developed nonlinear methods. The model of material should be based on an idea of isotropic damage of concrete compressed before origin of cracks and on an orthotropic mechanism of damage as soon as cracks arise. The modelling of composite action of concrete and reinforcement must be truthful. The tensile toughness of concrete must be taken into account by means of achievements of nonlinear fracture mechanics. Experience with erected structures has shown that the absolute majority of defect impairing more or less the structures, reducing their service life and serviceability, increasing the requirements of repairs, maintenance and reconstruction, are due to the effect of volume changes in particular shrinkage and creep of concrete and temperature changes. On the other hand, it has been proved that concrete structures become more perfect reducing any influence of volume changes. Therefore a correct assessment of these phenomena already in the design and/or erection stages of the structure is necessary. Their correct prediction, however, is very difficult, as they include many parameters of random character influencing directly the shrinkage and creep of concrete effects. The research resulted in development and extensive testing of material models intended for theoretical analyses of real structures. As the shrinkage and creep of concrete are highly complicated phenomena, comprizing an interaction of a number of factors on several micro-structure levels, being influenced by numerous variable effects, the mathematical characterization of evolution of these phenomena was as comprehensive as possible. In the framework of the analysis of models for prediction of concrete creep and shrinkage it was necessary to compare various approaches with the purpose of recommending adequate relations for the computations on research as well as practical design levels. The incorporation of the influence of imperfections and that of successive degradation of the structure due to aggressive environment was necessary.

The principal significance of the proposed project for civil engineering practice consists in that the results of the appropriate solutions help creating the sufficiently broad theoretical prerequisites for reliable and economic structural design while respecting random character of most factors being decisive for their quality. The engineering practice, introducing stochastic approaches, acquires tools which are much more objective and effective to achieve a substantial economy of materials, energy and costs increasing in the same time the level of reliability, durability and efficiency of these structures. In the ever increasing international competition the results may assist in increasing the competitiveness of our civil engineering companies and facilitate their penetration to foreign markets.

References:

- [1] KOHOUTKOVÁ, A. - KRÍSTEK, V.: *Simulace chování vláknobetonových konstrukcí pomocí numerického modelování*, in: *Speciální betony*, Sekurkon Praha, 2004, pp. 65-72.
- [2] VÍTEK, J.L. - KRÍSTEK, V. - KOHOUTKOVÁ, A.: *Time Development of Deflections of Large Prestressed Concrete Bridges*, *Fib Symposium 2004 on Segmental construction in Concrete*, Fib, Munchen, 2004, CD-ROM.

This research has been supported by GA 103/02/0020.

Effect of Cladding on Stability Parameters of Framed Steel Structure

V. Hapl, T. Vraný

vitezslav.hapl@fsv.cvut.cz

Department of Steel Structures, Faculty of Civil Engineering, Czech Technical University, Thákurova 7, 166 29 Praha 6 - Dejvice

Introduction

The modern steel structures of industrial buildings take advantage of framed structures. Cladding is usually designed with thin-walled steel members. In most cases the cladding is in interaction with members of frame structure, but this interaction is not commonly considered in calculation. However, the inclusion of this interaction into the analysis of internal forces and/or into the checks of members could allow more accurate, and in many cases more economical design of the structure.

The influence of cladding on behaviour of steel bar under bending and/or compression can be simulated by structural model with elastic lateral (eventually rotational) supporting of frame members. This support must be applied with respect to geometry and rigidity of cladding. Increase of critical load in lateral and lateral-torsional buckling appears as a consequence of this interaction. But on the other hand, there are arising forces at cladding plane. These forces must be included in the design and check of connections between cladding and members of steel structure and cladding units together.

Today, there are methods leading to determination of rigidity of various types of cladding systems. However the impact of metal sheathing rigidity onto real resistance of bar structures is not thoroughly discovered these days. Correct method of solution must consider the fact that support by cladding usually affects in the plane of exterior flange of designed beam-column.

Numerical study of lateral support impact onto stability parameters of beams, columns and beam-columns

Classical hand methods of search for stability parameters of structure leads to solving the problem of eigen-values of differential equation systems. Solution of this problem is very difficult. Moreover, complexity of these systems rapidly increase due to inclusions of any new joint, whose establishing are necessary for consideration of nodal lateral supports. Because of that, the study has been performed by simulation using the scientific final element method software Ansys.

It has been performed for a simply supported beam for cross-sections IPE, HEA, HEB with dimensions of 100,200,300 and 500mm (sections have been considered as sharp angular for simplicity). The length of bars has been taken 2, 4, 6 and 8m. Girder has been loaded by one of 27 load cases with various moment distributions and various ratios of the compressive force and the maximal bending moment. This load cases represents several types of beams in the structure (a continuous beam, a frame stanchion or a crosspiece). Association of lateral supported points with bearing points has been assumed for the sake of simplicity (moreover this simplification corresponds with real situation for complete majority of standard structures). These points have been chosen at the top flange midpoint, at the centre of gravity of the cross-section and at the bottom flange midpoint. Rigidity of the lateral support has been taken 0 (without lateral support), 4, 8 and 16MN/m^2 for continuous support, or adequate rigidity of the point support (these values have been taken without relationship to real cladding rigidity).

Line element BEAM188 has been chosen for a numerical model for beam-columns. BEAM188 is a linear element in 3D space. This element has seven degrees of freedom at each of the end nodes including warping magnitude (warping must be considered for solving of lateral-torsional buckling problem). The element could be used with any beam cross-section (in case of this study I and H shaped sections have been used). BEAM188 enabled elastic and plastic material models, study of inelastic buckling of beam-columns in interaction with cladding is scheduled.

Element COMBIN39 has been chosen for numerical model for elastic support. COMBIN39 is an element with nonlinear force-deflection capability. The element has no bending or torsion capability, which has been supposed to be negligible low for a typical configuration of cladding (to include the effect, COMBIN7 or combination of COMBIN39 and an element with bending stiffness have to be used). For some types of panel cladding this effect may be involved.

Results of study

Study indicated that magnitude of buckling resistance is very strongly affected due to rigidity of lateral support. As was supposed, the increase of lateral supports rigidity of compressed flange of bended beam leads to full lateral stabilisation of beam. On the other hand, increasing of lateral supports rigidity of tensioned flange of bended beam leads to lateral-torsional buckling about imposed axis. For columns, in case when support points are positioned in the cross-section gravity center, involving of lateral support leads to the increase of critical load. Choice of support points at the flange midpoint leads to change of buckling mode: lateral-torsional mode becomes governing at higher magnitude of critical load. For beam-columns the increase of lateral support rigidity leads to the increase of critical load and to change of eigen shape of buckled structure.

Generalization of obtained results is the object of following research.

References:

- [1] HAPL, V. Tlačené a ohýbané ocelové pruty – zjednodušené metody posudku, CERM 2005 Sborník přednášek Juniorstav 2005 v tisku
- [2] Hapl V., Vraný T.: Tlačené a ohýbané ocelové pruty - přesnost zjednodušených metod EDIS – vydavatelství ŽU 2004 Zborník prednášok str. 167-172

This research has been supported by CTU grant No. CTU0402011

Sustainable development and concrete structures

B. Teplý*, A. Kohoutková*, P. Hájek**, V. Křístek*,

kristek@fsv.cvut.cz

*Department of Concrete Structures and Bridges, Faculty of Civil Engineering, Czech Technical University of Prague, Thákurova 7, 166 29 Prague 6, Czech Republic

**Department of Building Structures, Faculty of Civil Engineering, Czech Technical University of Prague, Thákurova 7, 166 29 Prague 6, Czech Republic

Providing the backup for the sustainable development (hereafter SD only) is becoming an imperative for mankind. In the last few years, the questions connected with this problem have been mentioned in many fields of human activities including the building industry – especially focusing on the concrete structures. Recently, the relations between SD and the building industry have become the matter of the increased attention in developed countries and as a result e.g. the thematic Network *Performance Based Building* has been established. Our project GA 103/02/1161 is partially based on its main ideas.

The concept is simple: “Performance Based Building (PBB) is the practice of thinking and working in terms of ends rather than means’, as applied to building and constructing.” Therefore, the basis of all building activities should be the performance of the building in use rather than the prescription of how the building is to be constructed! The stress is put on economy, ecology and innovations. The main objective of the Network is: “Stimulation and pro-active facilitation of international dissemination and implementation of Performance Based Building in building and construction practice”, and in that context to maximisation of the contribution to this by the international R&D community, through:

- Stimulation and facilitation of the international programming and coordination of research and implementation projects as concerns PBB as effectively as possible in order to make optimal use of limited available resources and to prevent unnecessary recurrences.
- Stimulation of actual investments in such research and implementation projects.
- Providing EU Network Members with an optimal access to knowledge and experience as available in non-EU countries in which respective developments have progressed further than in the EU.
- Coordinated dissemination and implementation of results of international research in the area of Performance Based Building.

The Network aims at combining fragmented knowledge in the area of Performance Based Building in order to build a systematic approach towards innovation of the building industry and applying user requirements throughout the building process. From this, white spots and a coherent future research agenda can be derived. End-users, policy makers, building industry and regulatory communities are closely involved in this development in order to facilitate dissemination and implementation of research results. The Network especially stimulates investments in research that may be expected to produce practical recommendations for the adoption and application of Performance Based Building throughout the building industry and in all phases of the building process. Let us enumerate the most important features/goals of the PBB strategy concerning the concrete structures:

- Putting the squeeze on investors, designers and producers so that they may subordinate their decisions and planning to the optimisation of the environmental impacts, taking into account the whole service life of the construction and the total costs;
- the decision on the strategy in constructing and maintaining the infrastructure to be supported by the evaluation of risks (and all the hitherto suggested questions);

- minimisation of energy consumption completely used in production, operation, reconstructions and structure removal or the minimisation of emissions connected with the building activities;
 - research in the field of demountable structures, i.e., with a possibility of the subsequent reuse of some parts even after the original structure service life has expired;
 - preferential use of recyclable materials and recycled materials;
 - problems of waste disposal of materials from demolitions;
 - recycling materials from demolitions, e.g., the production of concrete utilizing recycled aggregates;
 - problems of degradation of building materials (especially that of concrete and reinforcement) and the problems of durability and service life of structures;
 - promoting the principle that for large structures of assumed longer service lives, the designer's duty would also be to devise a certain "instruction" for the use of a building.
- Activities of the project:
1. the selection and evaluation of the most important activities which may favourably/unfavourably affect the efforts to fulfil the requirements of SD, and which are in connection with building activities, especially in the area of concrete structures;
 2. the creation of necessary methodological tools for the survey of the existing concrete structures and the appreciation of the whole life cycle of structures (the final, real and moral service life);
 3. the definition of the methodology of the evaluation of the effect of concrete structures on the environment (selection of relevant environmental criteria, eco-value, optimisation, multi-criteria evaluation and optimisation, sensitivity analysis, definition of quantified criteria system);
 4. the elaboration of comparative examples (case studies), parametric studies, selection of phenomena and characteristics for a long-term observation, the proposal of databases type;
 5. monitoring and evaluation of effects of some variables with respect to the degradation of concrete structures and materials, sensitivity analysis;
 6. information activities aimed at the professional community and relevant institutions (legislative, industrial, commercial and others) on the usefulness of methods and measures leading to SD;
 7. the development of "performance-based" processes;
 8. the proposal of measures for the promotion of SD in the construction of concrete structures, proposals and documents for the legislative modifications.

References:

- [1] KOHOUTKOVÁ, A. - HÁJEK, P.: *technologie recyklace betonu*, in: *Technologie, provádění a kontrola betonových konstrukcí 2004, 1. díl*, ČBS ČSSI, 2004, pp. 55-61.
- [2] KRÍSTEK, V: *Ekodukty - technické problémy a koncepční řešení*, in: *Betonové konstrukce a udržitelný rozvoj*, ČBS ČSSI, 2004, pp. 65-77.

This research has been supported by GA 103/02/1161.

Mapping of Recultivated Areas Using Remote Sensing

P. Junek

junek@gama.fsv.cvut.cz

Laboratory of Remote Sensing, Department of Mapping and Cartography,
Faculty of Civil Engineering, Czech Technical University,
Thákurova 7, 166 29 Prague 6, Czech Republic

Laboratory of Remote Sensing at Department of Mapping and Cartography, Faculty of Civil Engineering, CTU Prague is for many years involved in analysis of spaceborne and airborne data of various sensors and from different periods of time in order to provide monitoring of land use and vegetation dynamics in the Severočeská hnědouhelná pánev (SHP) - North Bohemian Brown Coal Basin (NBBCB) area.

NBBCB consist of 4 former districts (Chomutov, Most, Teplice, Ústí nad Labem) spread over 2 300 square km. This area is inhabited by 490 000 residents with high population density of 216 inhabitants per square km (average of the Czech Republic is 130 inhabitants per square). Environment of the area is strongly influenced by human activities – such as industrial air pollution caused by power stations, chemical factories and other kinds of heavy industry and by open cast brown coal mining. As a result of mining activities the landscape is changed, soil horizon is strongly or irrecoverably damaged and significant impact on water regimen is present. Landscape changes are caused not only by the mining itself but by thick overburden as well. Up to present area of 260 square km was affected by mining activities.

In order to reduce impact of mining activity affected areas are undergoing process of reclamation. Reclamation is long lasting process beginning with geotechnical phase (measures realized during preparatory development work and during mining in order to provide optimal conditions for following phases). After finishing geotechnical stage reclamation continues by biotechnical stage (e.g. reforestation, agricultural, hydrological reclamation etc.).

Owing to rapid dynamics of changes across the NBBCB area advanced mapping methods of these changes are needed to monitor and understand further development of reclaimed areas. The goal of the research project is to develop Geographic Information System (GIS) of selected abandoned opencast coal mines in order to carry out quality assessment of reclamation works undertaken during past decades (1970-2000). The GIS input data consist of original land reclamation design (earthworks and vegetation planting) and spatial data acquired by aerial and satellite imagery processing during presented project.

Towards obtaining the spatial data Landsat imagery from years 1988, 1992 and 1998 have been purchased and following steps have been carried out – evaluation of data preprocessing methods in order to normalize imagery prior change detection analysis, calculation of vegetation indices (VI) as represents of vegetation cover and their evaluation, GIS analysis of reclaimed areas using values of VI, multitemporal colour composite and object oriented analysis.

In the stage of data preprocessing the obtained data acquired as digital number (DN) values recorded by sensor had to be corrected in order to carry out multi-temporal change

detection. Various methods of absolute (no correction, at-sensor-radiance, at-sensor-reflectance) and relative (radiometric normalization) radiometric correction methods have been investigated. The resultant data have been tested using training areas in order to evaluate provided corrections and to select applicable method for change detection analysis.

In order to evaluate intensity of vegetation cover various VI have been calculated (RVI, NDVI, IPVI, DVI, PVI, WDVI, SAVI, TSAVI, MSAVI, MSAVI2, GEMI, ARVI, GVI and EVI). Average value of VI, standard deviation, maximum and minimum of pixels within each studied reclaimed area have been used to provide basic GIS analysis of vegetation cover evolution. The method is able to provide only basic evaluation of vegetation dynamics. Because of non-homogeneous vegetation cover located within these areas, the method of more detailed analysis is required.

According to this finding the multitemporal color composite of these images has been used – it means combination of VI images from different time periods into one RGB image. Interpretation of multitemporal colour composite is based on additive colour mixing. Areas showing no changes of VI values within studied period are in this composite shown as grey shades. Areas showing different values of VI in different years have various colours recording to the habit of the change, thus areas affected by changes are highlighted by different colours. Furthermore the saturation of colours is linked with the intensity of the change.

For purpose of providing output ready to use in GIS the object-oriented classification method has been used. This method consists of two steps – segmentation of the multitemporal colour composite into homogeneous areas and classification of these areas using their VI values providing information about vegetation dynamics during studied period and spatial characteristics. Segmentation and classification has been successfully carried out using eCognition software and in further development of the project the results will be evaluated in the GIS using contemporary data of study areas.

The methodology will be used by private companies designing reclamations and may be used by environmental governmental bodies and for the Environmental Impact Assessment (EIA) of prospective mining.

References:

- [1] JUNEK, P.: *Mapování rekultivovaných území pomocí DPZ* Sborník konference Aktuální problémy fotogrammetrie a DPZ, ČVUT Praha, 2004.
- [2] JUNEK, P.: *Geological Mapping in the Cheleken Peninsula, Turkmenistan Area Using Advanced Spaceborne Thermal Emission and Reflection (ASTER) Data* International Archives of Photogrammetry, Remote Sensing and Spatial Information Sciences, Vol. XXXV, part B4 2004.
- [3] JUNEK, P.: *Preliminary Results of Geological Mapping in the Cheleken Peninsula, Turkmenistan Area Using Advanced Spaceborne Thermal Emission and Reflection (ASTER) Data* GIS Ostrava 2004, 2004.

This research has been supported by CTU grant No. CTU0403711.

Research into Non-force Effects and Aggressive Environment Affecting the Ageing of Historical Structures with Special Emphasis on Charles Bridge in Prague.

J. Witzany, *M. Gregerová, **P. Pospíšil, **A. Materna, ***T. Klečka, ***J. Kolisko,
Š. Šilarová, E. Burgetová, T. Čejka, J. Pašek, Wasserbauer, R. Zigler, **P. Cikrle**

witzany@fsv.cvut.cz

CTU, Faculty of Civil Engineering, Dept. of Building Structures, Thákurova 7, 166 29 Praha 6

*Masaryk University, Faculty of Sciences, Dept. of Mineralogy, Kotlářská 2, 611 37 Brno

**TU, Faculty of Civil Engineering, Institute of Geotechnics, Veveří 95, 662 37 Brno

***CTU, Klokner Institute, Šolínova 7, 166 08 Praha 6

****TU, Faculty of Civil Engineering, Dept. of Building Structures,

17.listopadu, 708 33 Ostrava

In keeping with the project's targets and time schedule, research works in 2004 were focused in particular on the following problems:

- Within the planned field investigation stages of February, June and November 2004, systematic sampling was taken on three arches (III, IV and VI) for the complementation of material analyses of building materials from Charles Bridge in Prague, including samples of secondary minerals (efflorescence) from exposed parts of vault sandstone blocks within a grid of 25 points on one arch. At the same time, samples of outermost weathered parts of sandstone blocks of the stone construction and of joint mortars were taken. Sampling on individual construction elements was subject of detailed photo-documentation. The samples taken were used for making 70 microscopic preparations for study in a polarization microscope, 20 samples for chemical analyses and 20 for microanalyses. The data obtained was processed and published in professional periodicals and presented on conferences. The results of long-term testing of salt solution migration through different concrete samples of comparable concrete types to those used within the reconstruction of Charles Bridge were obtained and processed, together with a long-term monitoring of degradation processes in granolite rock types as part of a comparative analysis of material characteristics of stone constructions built of granolite rock types (e.g. bridge in Písek).
- As a follow-up to a continuous surface monitoring and systematic sampling on three arches it was proved that mineral associations of efflorescence depend on the changes in climatic conditions and fluctuate during the year. A drop in nitrogen salts was demonstrated. Studies of a material analysis of arenaceous marl types used as a component of the packing or arenaceous marl masonry of the bridge body were made. All outermost samples of the given historical origin studied differ from the original sandstones by the content of carbonate-sulphate cement.
- In addition to construction stone samples, samples of joint mortars were taken and evaluated. Joint mortars may be divided into mortars with cement and sand additions and cement pastes. Within a systematic investigation carried out in the last stage of the grant project, no historical lime mortars were identified among the samples taken on arch III, IV and VI, but only hydraulic mortars. On contact discontinuity surfaces of sandstone blocks damaged by rupture, development of secondary minerals was demonstrated. The most often presented were the needle crystals of sulphates, with less frequent increment forms of carbonates. Within the porous system of cement pastes, analogically to the foundation slab,

colcrete and expanded-clay concrete, pores filled in by ettringite, thaumasite and gypsum may be identified.

- The structural elements (construction stone blocks) are exposed to negative effects of namely secondary crystallized carbonates and Ca – sulphates where Ca leached from concrete elements implemented in the bridge within the last major reconstruction.
- The presence of the main groups of chemoautotrophic, chemoorganotrophic a ammonifying bacteria was demonstrated using the methodology by Barcelona Vero L. et al.: Proposal of a method of investigation for the study of presence of bacteria in exposed works of art in stone (Bologna 1976). Laboratory models were designed according to the principles valid for climatic modelling of natural destruction processes (velocity and magnitude of degradation of individual material properties, Arheni relationships for chemical equations, Richtera et al. 1974).
- Four stages of measurements of deformations and investigation (in winter, summer and autumn season) at a water level and continuous measurements at measuring points in the bridge deck in a total range of approximately 150 measuring points or 1500 readings were performed, plus cores from load-bearing and non-load-bearing parts of Charles Bridge were taken.
- Based on thermovision research, a numerical analysis of a section of the bridge construction loaded with temperature was made. The temperature field illustrating the temperature pattern on the surface of the stone construction of Charles Bridge was determined on the basis of thermovision measurements. Furthermore numerical analysis and mutual interaction of comparison within application of three-dimensional and shell finite elements were assessed. The numerical analyses of characteristic material models of the bridge construction (existing and design state) demonstrated sensitivity of the stone bridge construction to the effects of temperature forced strain (flood) and the consequences of repairs carried out within the last Major Repair of Charles Bridge.

References:

- [1] WITZANY, J. - ČEJKA T. - WASSERBAUER, R. - GREGEROVÁ, M. - POSPÍŠIL, P. - CIKRLE P.: *Theoretic and Experimental Investigation of Charles Bridg*. Stavební obzor, 13, 2004, pp. 97-111.
- [2] WITZANY, J.- ČEJKA, T.: *Analysis of Resistance and Safety of the Stone Bridge Structure in Floods*. The Second International Conference on Structural Engineering, Mechanics and Computation. Cape Town, JAR, 2004, pp. 5-7.
- [3] WITZANY, J. - GREGEROVÁ, M. - POSPÍŠIL, P. - ČEJKA, T. - WASSERBAUER, R. - CIKRLE, P. - MATERNA, A. - ZIGLER, R.: *Long-Term Monitoring and Theoretic Investigation of Charles Bridge*. Stavební obzor, 2005, in print.
- [4] WITZANY, J. - ČEJKA, T. - ZEMÁNEK, J.: *Chemical adn Biochemical Degradation of Charles Bridge, Analysis of Resistance and Safety of the Stone Bridge Structure in Floods, Exploration of Footing Masonry and Pier Footings*. Stavební obzor č. 6, 2003, pp. 161-180.

This research has been supported by GAČR 103/02/0990

Completing and Analysing of Experimental Geodetic Network for Movements Monitoring of Historical Structures

T. Jiříkovský

tomas.jirikovsky@fsv.cvut.cz

Department of Engineering Geodesy, Faculty of Civil Engineering, Czech Technical University, Thákurova 7, 166 29 Prague 6, Czech Republic

Historical buildings in the area of Prague Castle have high historical value; they are interesting in sense of arts, old construction technologies etc. Continual repairs and reconstructions are necessary for their long life. Monitoring of durable reliability includes verification of static situation; which means for example tests of verticality or horizontality of some measured parts of objects and evaluation of the changes. Many different parameters required for detecting of the geometrical changes must be obtained by various methods of measurement. Basically, geotechnical and geodetic measurements are applied. It is necessary to mention that real movements are very small; some tenths of millimeters usually (some millimeters maximally). Therefore the highest accuracy of measurements is required. In described research project was completed the reference geodetic-geotechnical network by the micro-network for securing of the main point.

METHODS OF THE MONITORING MEASUREMENT

Main geodetic observations are based on the precision levelling for the vertical displacements detection; for horizontal movements on trigonometry and optical or laser plumbing (local changes). In large scale (whole objects and areas) GPS (Global Positioning System) is successfully used. Geotechnical measurements, which are interesting for geometers are especially observation with sliding inclinometer for horizontal movement and deformer/micrometer for height changes in special equipped vertical measure-boreholes. Main geodetic result is change of relative position of the first and the last measuring mark in the borehole between two epochs. CTU in Prague dispose with the precise micrometer and the inclinometer probes Glötzel. Typical declared accuracy/mean error is 0.05mm/m in horizontal plane (xy) and 0.004mm/m in height (z). With the special designed centering device is possible to use the last measuring mark in the tube as an universal geodetic mark. It is suitable for both height measurement and for instrument centering. In addition the tribrach or the GPS antenna can be directly mounted at the top of this centering rod.

REFERENCE NETWORK

The reference geodetic-geotechnical network was established (before this project) including three main points/measuring boreholes. Independent main reference point TV01 is placed relatively far from monitored objects (1.8 km), near Czech Technical University buildings in Dejvice. Precise heights of the points are regularly measured by levelling (partly digital), horizontal relative position is observed by long static GPS measurement and postprocessing. The network is joined with other observation marks (including next 3 boreholes) by precise levelling and traverses.

NEW SECURE MICRO-NETWORK FOR THE POINT TV01

This research project allows completing the reference GPS network by the micro-network to secure the height and the relative position of the main point TV01. This micro-net will be very helpful for verification of the conformity of the results of geotechnical probes and high accurate geodetic measurement. Expected movements are nearly zero, so the top-946

class instruments are used in this task (like the robotic total station Leica TCA 2003 or the digital level Zeiss DiNi 12T).

For the independent height measurement with precise digital level was designed small net including 4 existing marks of the Czech Levelling Network. Measurement is carried out with the high precision digital level Trimble Zeiss DiNi 12T.

Second network was designed primary for plane measurement, but it is also usable for trigonometric monitoring of heights. The optimal configuration of points was analyzed and two types of the net were suggested. First, the regular pentagon fixed with ground marks around the TV01 point, and second as two perpendicular lines of sight, which intersects at TV01 and their closes fixed with marks at the walls of neighbouring buildings. On November 2004 was realized the modified second variant. Its main advantage is small influence of centering, optically centered is only instrument at the TV01 point, all other points are fixed with special hidden holders. The small holder equipped with the thread lies at the plane of the wall and allows temporary mounting of different target marks, levelling bolt-mark, target reflective prism etc. The same universal “invisible” holders are often used for various applications at historical objects. The holder is suitable even for application of ultra-accurate short-distance measurement with Kern DistoMeter equipment.

Measurement scheme for this type of the net is simple, only four distances and four directions are to measure. Accuracy is insured by fixing all target points and by using high precision automatic total station Leica TCA 2003. With suitable on-board software is the instrument able to perform all the measurement automatically (incl. tests and checks of observed values). The net can be used also for 3D monitoring after extending measurement by zenith angles. In addition there is necessary to find out exact height difference point—instrument (mounted at the tripod). For this whole new mechanical instrument height meter was designed and developed. It consists of steel tube, interchangeable steel sticks (for various heights) and shifting nonius scale (sensitivity 0.05mm). With this assembly and temperature-correcting chart is possible to read the instrument height with accuracy about 0.12mm (mean error).

RESULTS

New geodetic secure-micro-network was designed and established. The first regular geodetic measurement was performed. Important numerical results will be obtained after the next epochs of measurement. At this time only zero epoch (autumn 2004) has been measured. There is necessary to verify expected accuracy of movement and its proof. Important is joining next epochs with the geotechnical measurements for the time relation and an evaluating possibility.

References:

- [1] JIŘIKOVSKÝ, T.: *Lokální geodetické sítě – možnost společného polohového i výškového vyrovnání*. In. Proceedings of 5th Conference of PhD Study, Part 11, CERM Brno, 2003, pp. 45 – 48.
- [2] ZÁLESKÝ, J. – CHAMRA, S. – PRUŠKA, J.: *Projekt instrumentace pro měření prostorových deformací vybraných objektů Pražského hradu*. Stavební obzor, 2003, roč. 12, č. 8, pp. 225–228.

This research has been supported by CTU grant No. CTU0404111

Object Analysis of Mathematical Model of Geodetic Networks Adjustment

J. Pytel

pytel@gama.fsv.cvut.cz

Department of Mapping and Cartography, Faculty of Civil Engineering, CTU Prague,
Thakurova 7, 166 29 Prague

1. Introduction

Following the project of Object Geodetic Networks Adjustment GNU Gama was developed database of Global Positioning System (GPS) observations in collaboration with professor Kostelecky. WWW interface was implemented in order to access the GPS database.

In the Czech Republic there was a process called "GPS densification" from 1995 until 2003. The results (data) of this densification is a large number of the new densified stations and GPS observations. GPS observations from this densification are archived in the form of "database" files of the observation vectors (information about stations [coordinates, sketches, etc.] is collected in ORACLE type database maintained by the Land Survey Office in Prague.). These "database" files are transformed into a main database. The database was created in 2003/2004 based on PostgreSQL database.

2. Implementation and results

As mentioned above, the data from both densifications processes are archived in the form of "database" files of the observation vectors. This form is not suitable for the common/final users. Hence it follows demand to create database of GPS observations (observation vectors achieved from densification process) and internet (www) access to the database. GPS data are stored in relational database system PostgreSQL. We had chosen PostgreSQL in order to PostgreSQL fulfills all ours requirements and provides with many other useful features such as triggers, multiversion concurrency control, etc. The database is serve as: revision of observations, archive of observations, provision of free access of observations for all possible users.

The GPS observations data model, each item (line) of "data" files represents one vector with this information: campaign number, project number, epoch of observation, pair of stations, coordinate differences dx, dy, dz in [m], name of coordinate system., name of fieldworker, code of used software, code of used efemerid. The data model, consists of four tables. The tables are interconnected by using foreign keys: table Project - general information concerning projects, table Campaign - cover data about campaigns, table SysToGPS - list data including coordinate systems entity, table Software - list data including software entity and table Vector - main table, including observed vector data.

For creating access to the database via http protocol, we have used only C++ libraries released under GNU General Public License. The whole project is written in C++ language and is available for OS GNU/Linux (the main platform on which this project was developed). We have decided to get rid of www-like languages (like PHP) from the project, owing to possibility to run the project everywhere. The project is based on the two libraries:

- **library Gowl** is a small C++ object library for creating CGI and is released under GNU GPL license. The project Gowl has started at the Department of Mapping and Cartography, faculty of Civil Engineering, Czech Technical University in Prague about 2000. More information about this project are available

<http://gama.fsv.cvut.cz/~pytel/gowl>

- **library libpgxx** is a C++ frontend (API) to PostgreSQL and is released under the BSD license. This library contains Standard Template Library (STL)-conformant interface and makes extensive use of C++ language features such as exceptions, templates, and strings. Further information about this library can be found at either of web pages:
<http://gborg.postgresql.org/projects/libpqxx>

Final WWW interface, CGI scripts, is consist of pure C++ programs which are using both of previous libraries. CGI scripts generate html pages which are valid XHTML 1.0 (XHTML is a reformulation of HTML 4.0 in XML 1.0. XHTML is a language for building web pages that has recently been proposed as a W3C Recommendation). One of the main advantages of generating XHTML pages is accessibility via cell phones. In particular while operators working outside, they can obtain data through mobile connection instantly.

WWW interface can be found on homepage

<http://www.vugtk.cz/gpsdb>.

For working with GPS observations (vectors) WWW interface offers next possibilities: viewing/editing/adding/deleting of GPS observations, create XML input data format (selected observations) for program GNU Gama, browsing GPS campaign. To change (deleting, editing) data in database it is necessary to know and use a password.

WWW interface is very intuitive and simple to use. Because of using of database system PostgreSQL is possible to find appropriate observations by using a regular expression.

Conclusions

Using language C++ (with libraries Gowl and libpqxx) instead of pure "web" languages like PHP decreases requirements on software equipment dramatically. The database system and any support programs are released under the GNU General Public License (GPL). Although this database application is tailored to the specific Czech needs, it is a Free Software and it is available to the whole geodetic community. The database of GPS observations has internet access on homepage

<http://www.vugtk.cz/gpsdb>.

The results of work on this grant were presented on international conference FIG in Athens.

References:

- [1] PYTEL, J. - CHROMÝ, R. *Databáze GPS měření 6*. Odborná konference doktorského studia, VUT v Brně 2004
- [2] KOSTELECKÝ, J. - PYTEL, J. *Modern geodetic control in the Czech Republic based on the densification of EUREF network* The Olympic Spirit in Surveying (FIG Working Week) 2004
- [3] CHROMÝ, R. - PYTEL, J. - SOUCEK, P. *Databáze GPS měření* Konference GIS Seč 2004 - GIS ve veřejné správě 2004

This research has been supported by CTU grant No. CTU0403911

Fire Resistance of Timber Construction

P. Hejduk, P. Kuklík

pavel.hejduk@fsv.cvut.cz

Department of Steel Structures, Faculty of Civil Engineering, Czech Technical University in Prague, Thakurova 7, 166 29 Prague 6, Czech Republic

Timber construction is a good choice for the fast and ecological buildings. Light timber frame construction is widely used in the residential houses and multi-storey buildings (one to four storeys). This report is interested in the fire resistance of the wall of the light frame construction using timber. Light frame construction has excellent fire behaviour, provided by good construction from the appropriate material. Fire resistance is a resistance of complete assemblies of light frame construction, not the individual components.

Fire endurance is defined as a measure of the elapsed time during which a material or assembly exhibits fire resistance under specified conditions of test and performance until its collapse.

Because of the small size of timber used in this stile construction, fire resistance must be based on protective materials, by far the most common is gypsum board. The gypsum board is used as wall linings, where it provides a wearing surface as well as contributing to the acoustic, thermal and fire separation of the barrier. Other lining materials, used less often, include a variety of wood-based panel products, fibre cement panels and calcium silicate board. Gypsum board has fire-resisting properties superior to most other similar materials, because of the moisture in the gypsum crystal, described below.

Currently I have made an analytical model. In the program Excel I have made parametrical study of the wall construction. This model is in agreement with national standard ČSN P ENV 1995-1-2.

When the fire started in the construction, a first barrier is lining. If the gypsum board is dehydrated, the lining will burn. When the wood-based panel products are in the fire, fire decrease thickness of panel. Some thickness of the gypsum or wood base panel and his fire resistance are shown in Table 1.

	Density	15	25	30	40	50	t_p [mm]
OSB	600 kg/m ³	15	31	43	68	97	t_{pr} [min]
gypsum board F	600 kg/m ³	25	42	51	68	85	t_{pr} [min]

Table 1. Fire resistance of the lining

Light frame construction often contains insulation in the cavities, to improve thermal, acoustic or fire performance. The most common forms of insulation are glass fibre batts or mineral wool batts. Glass fibre batts are made from thin glass fibre bonded into a mat with an organic binder. Mineral wool batts are made of mineral or ceramics fibres which do not melt at fire temperatures. When the lining is disturbed, the insulation and wood stud are has been

evolved. If the insulation in the cavity between the studs has compatibility even after 1000°C protected side of the wood stud. Char layer is only in the front of the flame.

Result of my parametric study will be used from the numeric model. Parametric study will be compared with the finite element method.

References:

- [1] KUKLÍK P. - KUKLÍKOVÁ A. - HEJDUK P.: *Vícepodlažní budovy ze dřeva* VOŠ Volyně, 2004, pp. 51-54.
- [2] HEJDUK P.: *Požární bezpečnost nízkopodlažních obytných budov zedřeva* Vysoké učení technické v Brně, Fakulta stavební, 2004 pp. č. 135.

This research has been supported by CTU0402111

Quazi-random Numbers Generation Using Simulated Annealing

M. Lepš, Z. Vitingerová

leps@cml.fsv.cvut.cz

Department of Structural Mechanics, Faculty of Civil Engineering, Czech Technical University, Thákurova 7, 166 29 Prague 6, Czech Republic

This work is closely connected with several methods from the Artificial Intelligence area, namely with evolutionary optimization algorithms [1] and artificial neural networks [2]. The meet point of these methods is the generation of *independent* and/or *random vectors*, which, in the first case, help to discover new unexplored areas and, in the second case, create representative sets of data. The aim of this contribution is therefore to minimize the number of needed iterations of an appropriate optimization method or the improvements of a training process within the artificial neural networks (hereafter only neural networks) domain.

At this point, it is worthwhile to mention the meaning of the word *random*. Majority of scientific literature use this word only for several physical (natural) processes. Random numbers sequences given by mathematical expressions, which are usually used in computer programs, are missing “real” randomness (after several iterations the same numbers are created again in a given order) and therefore they are called *pseudo-random*. The typical example here is the standard function *rand()* that is available almost in all programming languages. Because we are dealing with generation of random numbers on common personal computers, hereafter we will use *pseudo-random* variants for all *random vectors* and *random numbers* generators.

The next important term is *quasi-random* sequences. They mimic some form of randomness, but, concurrently, they are aimed to uniformly cover the given space. These antagonistic constraints, i.e. randomness against uniformity, are fulfilled by several mathematical sequences like famous Sobolev’s sequences or algorithms based on the Monte Carlo method and their *quasi-* versions. The Latin Hypercube Sampling method (LHS) [3] used in this work is the example of the last mentioned algorithms.

Nowadays, applied sciences are often dealing with problems that are unmanageable in reasonable time with deterministic methods. Therefore, approximate, fuzzy and stochastic approaches are becoming popular. The artificial neural network can serve as an example of approximate approaches and every method that uses random numbers will be called as stochastic. This work deals with both above-mentioned areas.

For quazi-random numbers generation, the Latin Hypercube Sampling (LHS) is used. The proposed methodology can be divided into two parts. The first one is a common LHS method, which selects individual samples by the inverse transformation of a probability function in the middle point of uniformly distributed ranges of a distribution function. In the second part, the samples are swapped in order to satisfy the desired statistical independency between individual variables. In this stage, the Simulated Annealing (SA) method is used. The SA algorithm is based on an analogy with a cooling schedule in metal materials. At the beginning, new solution is created (usually randomly). If this solution is better than the old one, this new solution is automatically used instead of the old solution. In the opposite case, i.e. old solution is better, the new one is chosen only with some probability given by Boltzmann distribution and actual temperature (energy) of the solved system.

The method of random input data generation for neural networks can be described as follows: Firstly, the LHS method is used to produce the samples matrix with the *number of variables* columns and the *number of samples* rows. Next, the statistical independency

between samples is needed and therefore the difference between the actual correlation matrix and the elementary matrix is minimized using the Simulated Annealing method by changing samples position within all columns.

The obtained results are satisfactory, although the similar results were obtained by much simpler methods, see e.g. [4]. It is possible that for particular neural network, the LHS method with Simulated Annealing principle will produce better results, but, because of high computational demands, we cannot advise this methodology for practical use.

The second part of this project has been aimed at generation random numbers and random vectors for multi-modal optimization, where several solutions are already known during an optimization process. Therefore, the goal can be stated for instance as: Generate random numbers sequences with a uniform distribution but as much as possible different from the already known solutions and/or vectors. The solution procedure is the same as in the previous case. The LHS method is used to generate uniformly distributed samples and the SA method is used to fulfill given conditions. We have tested two objective functions – first is the statistical norm like in the previous case and the second is to minimize the distance between new and old solutions.

The use of statistical norm does not lead to tangible advantages. Good results were obtained with the norm based on geometrical properties of individual vectors. Here, the LHS method satisfactorily helps to cover uniformly the search space. The graphical outputs from this method are very promising, although the practical impact and use must be tested on real applications.

References:

- [1] LEPŠ, M.: *Single and Multi-objective Optimization in Civil Engineering with Applications*, CTU in Prague, 2005, PhD. Thesis.
- [2] LEHKÝ, D., NOVÁK, D.: *Identification of material model parameters using stochastic training of neural network*, Proceedings of 5th International PhD Symposium in Civil Engineering (Delft, Netherlands), 2004.
- [3] CAFLISCH, R.E.: *Monte Carlo and quasi-Monte Carlo methods*, Acta Numerica, 1998, 1–49.
- [4] TONG, F., LIU, X.L.: *On training sample selection for artificial neural networks using number-theoretic methods*, Proceedings of the Fourth International Conference on Engineering Computational Technology (B.H.V. Topping and C.A. Mota Soares, eds.), Civil-Comp Press, Stirling, Scotland, 2004.

This research has been supported by GA ČR grant No. GA 106/03/0180.

Progressive Composite Steel-concrete Element - Stage 2

J. Moták

jan.motak@fsv.cvut.cz

Dept. of Steel Structures, Faculty of Civil Engineering, Czech Technical University in Prague
Thákurova 7, 166 29 Prague 6, Czech Republic

The paper deals with analysis of composite steel and concrete T-shaped girder consisted of novel elements. These are represented by I-section plate steel girder WT with transversely undulated thin-walled web and shot-fired shear connector Stripcon made of cold-formed thin-walled perforated steel strip.

The experimental investigation includes three large-scale static tests of steel and concrete composite girders. The first two denominated EX1 and EX2 are described in [1], while the third denominated EX3 in this contribution. Furthermore, a numerical model employed in nonlinear finite element (FE) structural analysis is described.

The bending test EX3 of similar composite girder form as those two girders EX1 and EX2 [1] was carried out in Structural laboratory of Faculty of Civil Engineering of CTU in Prague. The simply supported girder with the span of 4500 mm was in configuration resulting in shear buckling of the undulating web. The Girder was designed with partial shear connection with level of $\eta = 58\%$ (in total 9 connectors per span of the girder).

The loading was placed in the thirds of the span and realized through a hydraulic jack PZ60 and distributing beam. The loading was controlled by displacement of the central load cell. The procedure of the loading followed the same two-phase pattern. In the first phase, given by elastic behaviour, each loading was followed by unloading. In the second phase, plastic one, the loading continued after settling down both of the deflections and stresses of the current loading up to the collapse.

Deflections, strains and slips in material interface were monitored and received data processing was performed in similar way as in case of the tests EX1 and EX2 [1]. In addition to this monitoring of the girder response five pairs of rosette strain gauges were used to record behaviour of the girder web in assumed area of buckling collapse in shear. In time of the testing the basic material characteristics for steel and concrete were evaluated.

In the test EX3 the calculated shear capacity $F_v = 459.2$ kN that value is critical for the girder strength was reached. Both buckling in shear of the undulating web and lateral cracking of the concrete deck in critical cross section (roughly at $L / 3$) took place at this load level. The shear buckling process was attended by local web buckling in place of concentrated load - distributing beam. The test was terminated due to extensive deflection appears after reaching and exceeding of calculated shear capacity and after approaching the calculated capacity of the partial shear connection (corresponding load $F = 508.2$ kN).

The theoretical shear strength of the girder web agrees well with the test collapse capacity. Strong nonlinearity of deflection appears after reaching approximately 85 % of the theoretical elastic loading. Before this value the measured deflection is in agreement with the elastic calculated one. This behaviour well corresponds with development of slip between slab and steel beam. The measured deflection at mid-span for value of theoretical collapse loading (approximately 97 % of the theoretical elastic loading) is roughly 2.5-times bigger in comparison with the calculated one.

Preliminary simple linear calculations on the basis of common standard design in accordance with Eurocode 4 [3] proved that experimental strength capacity of the girder is in good agreement with the calculated value. The buckling shear capacity of the undulating web was critical for the girder strength according to assumption. However, the deflections are due

to shear connector flexibility (slip in the shear interface) larger. The elastic calculation of deflections for the tested girder with partial shear connection was correct up to 85% of the elastic strength of the girder, while the real maximum deflection value for the elastic girder strength was roughly 2.5-times bigger than the commonly calculated one.

As a main part of analytical analysis of the composite girders under investigation the numerical modeling has been performed using general-purpose FE software package ANSYS. Pre- and post-processing are partially made in standard spreadsheet. Only a half of composite girder is modeled due to symmetry with respect to perpendicular plane transecting the mid-span. Material and geometrical nonlinearity due to large deformations are considered. All parts of a three-dimensional FE model are designed with full geometry except for following simplifications. Geometry of the sinusoidally corrugated web is substitute by triangular corrugation. The discretely distributed shear connection is idealized using nonlinear spring elements. A fully structured mesh is generated over the whole model to allow direct control over the shapes and sizes of elements.

Flanges and web of the steel girder are modeled using 4-node shell element, called SHELL43, with 6 degrees of freedom (DOF) in each node. The element allows simulating of plastic behaviour, stress stiffening and large strain theory. Concrete slab is modeled with 8-node hexahedral brick element, called SOLID65, with 3 DOF in each node. The element has plastic behaviour, stress stiffening, large strain theory, cracking-crushing capability and smeared reinforcing steel model embedded inside the element. Both elements support birth and death effect. Nonlinear spring element, called COMBIN39, is employed to simulate shear connector. This 2-node uniaxial tension-compression element with 3 DOF in each node has large displacement capability.

Material model for steel is trilinear elastic stress-strain relationship identical in tension and compression. Concrete is characterized by multilinear elastic stress-strain relationship with linear softening for uniaxial state of stress and combination of several plastic criterions (Drucker-Prager, Chen and Rankine criterion) for biaxial state of stress. Force-displacement (force-slip) relationship of shear connection model is derived on the basis of curves obtained from series of push tests of connectors Stripcon performed at CTU in Prague [2].

Preliminary evaluation of experimental investigation results confirmed practical applicability of the new composite girder having shear connectors Hilti Stripcon and steel girders with undulating web. At present, the three tested girders under static loading to failure are being considered for verification of the initial numerical model. Comparison of experimental and numerical simulation results will be followed to validate capability of the FE model to predict behaviour of such steel and concrete composite girders. All results will be published in author's PhD thesis.

References:

- [1] J. MOTÁK: *Progressive Composite Steel-concrete Element*, CTU Reports, Proceedings of Workshop 2004, Part B, Prague 22.-26.3. 2004, CTU in Prague, 2004, pp. 932–933.
- [2] J. STUDNIČKA, J. MACHÁČEK, P. BOUŠKA: *Shear connectors for composite steel and concrete beams*, Scientific Session VSU 2001, Vol. 1, May 2001, pp. 60–65.
- [3] *prEN 1994-1-1 Design of composite steel and concrete structures, Part 1.1, General rules and rules for buildings*, Final draft, CEN, 2002.

This research has been supported by CTU grant No. CTU0402311.

Influence of Climate Change over Water Management Systems

L. Satrapa

satrapa@fsv.cvut.cz

Stavební fakulta ČVUT, Katedra hydrotechniky, Thákurova 7, 166 29 Praha 6

Climate change

Problems of global but as well of local climate change are now very important for groups of specialist and scientists and for number of general people. Last two decades shows that some change in climate condition is very probable. The cause of it is not clear but it is not important from water management point of view.

Water management systems in changed conditions

For water management systems are not important that the causes of some changes in weather conditions are not clear. Proper function mainly of water resources is very important and demanded by public without deeper interest in real situation. The question for us is to find techniques applicable to management of hydraulic schemes under different conditions taking global and local climate change conditions into account. The main problem is to cover demands of drinking water supply. Nevertheless all hydraulic schemes with reservoirs are multi purpose so optimization and balancing of all purposes realization is important.

The grant was focused on following question coherent to climate change:

- 1 - influence of climate change over water resources with water management reservoirs,
- 2 - effects of climate change to real time operation for medium and large catchment areas,
- 3 - effects of climate change to real time operation for small catchment areas,
- 4 - influence of climate change over scenarios for management of reservoirs in dry seasons,
- 5 - influence of climate change over fish habitat and fish migration in rivers downstream reservoirs,
- 6 - possibilities of reallocation of reservoir volumes to increase the flood protection function of reservoirs taking the climate change into account,
- 7 - climate change effects to river bed stability and possibilities to overcome adverse effects.

Pilot areas for the research

Pilot areas were used during our work to present the results of the research as clear as possible. Following pilot areas were used:

theme 1 – hydraulic schema Římov,

theme 2 – catchment area of Teplá river with hydraulic elements Březová, Stanovice, Podhora (reservoirs)

theme 3 – catchment area of Botič river and Hostivař reservoir

theme 4 – hydraulic schema Římov

theme 5 – Malše river,

theme 6 – Římov reservoir

thema 7 – Litavka river near Beroun city, Olše river near Karviná city

Application of GIS technologies

All pilot areas and corresponding results of the research are visualized using GIS technology. Arc View model is used in the grant. Some additional functions were developed and added to GIS to perform necessary analysis directly inside GIS model.

Conclusion

The main problem of the analysis incorporating effects of climate change into the calculation of water management system is the selection of reliable scenarios of climate change. Specialists in climate sciences are not sure what is possible expect in near future but we have to be prepared to assure the maximum safety in functions of water management systems. Many analysis show that the only possibility how to cover demands in the future and how to balance among purposes of systems is operative management. It is necessary to develop robust forecast methods to support real time management of hydraulic systems with reservoirs.

References:

- [1] FOŠUMPAUR,P.-PŘENOSILOVÁ,E.: *Reservoirs in changing natural conditions* ČVUT-Fsv 1998
- [2] KOS,Z.: *Sensitivity of irrigationand water resources system to climate change* Vodohospodářský časopis 41 Praha 1993

This research has been supported by GA ČR grant No. 103/03/Z021.

Approach to Risk Evaluation for Water Management Systems

L. Satrapa

satrapa@fsv.cvut.cz

Stavební fakulta ČVUT, Katedra hydrotechniky, Thákurova 7, 166 29 Praha 6

Risk definition

Values defining risk consists in two main parameters, precisely by the product of them.

The first parameter is probability of the analyzed risky situation. Probability is calculated by statistical methods working with historical data describing the function of system.

The second parameter is consequence of risky situation. The best expression of consequence is any quantitative evaluation. Mainly are consequences expressed in monetary units but this evaluation is not every time appropriate (loss of life) or applicable (adverse ecological effects). In such situations with “non countable” consequences is necessary to use experts estimations, analogies etc.

Risk analysis was and today is often used in many branches affecting the human life. Known and accessible data of both groups of parameters are mainly in industry and energy supply. Specific situation is in branch of water management.

Risk in hydrotechnological and water management systems

We are very often able to analyze the second group of necessary parameters – consequences and theirs countable expression. The main problem in hydrotechnological and water management system is to evaluate probability. Causes of this problem are:

- low repeatability and in most cases no repeatability of construction elements, construction schemes and designs,
- long life span (and in contrary low failure rate) of construction elements and technological equipments and dam accessory,
- different surrounding conditions acting on hydraulic structures during their function life time,
- high variability of forces acting on hydraulic structures (extreme floods, extreme water levels, high temperatures in contrary to dry seasons and deep frost periods),
- high variability in purposes of hydraulic structures and combination of purposes for single structures and systems as well.

From specific features of hydraulic structures result very limited database to evaluate probability of risky situations. The analogy used in many other branches is for hydraulic structures because of above mentioned features not eligible.

Research project GA ČR 103/02/0606 is focused on the application of risk analysis methods for hydraulic structures and systems of hydraulic structures taking all specific conditions into account. The known method of risk analysis named “Preliminary risk analysis

(PRA)” is applied to 5 pilot areas. Pilot projects are used for the presentation of PRA method to show the technology and results to specialists working with operation and strategy of development for hydraulic systems.

Pilot study areas are:

- multi purpose water management system with Nechanice reservoir (North-West Bohemia, city Chomutov),
- water management system for drinking water supply with two reservoirs Josefův Důl and Souš (North Bohemia, city Liberec, Jablonec nad Nisou),
- multi purpose water management system with Římov reservoir (mainly drinking water supply, South Bohemia, city České Budějovice),
- Těrlicko water management system for industry water supply (North Moravia, city Havířov),
- multi purpose water management system of Dyje and Svratka catchment areas (South Moravia).

PRA technology is presented in grant for all pilot areas in the form of questionnaires describing, evaluating and combining risks for all purposes of water management systems. Questionnaires are used for the summarization of risk matrices. Following presented step is the simulation of different behaviour scenarios of system and analyzing risk using risk matrices.

Application of GIS technologies

All pilot areas and corresponding risk analysis and simulations are visualized using GIS technology. Arc View model is used in the grant. Some additional functions were developed and added to GIS to perform necessary analysis directly inside GIS model.

Open questions of risk analysis in water management systems

Actual question for research is the development of methods useful for transparent combination of risk with economically and non economically expressible consequences. It is not possible in all cases but the minimizing of non countable criteria is demanded.

References:

- [1] SATRAPA,L.-FOŠUMPAUR,P.: *Analysis of flood protection effect of Vltava cascade* ČVTVHS, Český přehradní výbor 2004 27-33
- [2] SATRAPA,L.-FOŠUMPAUR,P.: *Analysis of interaction of flood wave with Vltava river bed in august 2002* ČVTVHS, Český přehradní výbor 2004 33-39

This research has been supported by GA ČR grant No. 103/02/0606.

Local Buckling of Flange under Fire

J. Charvát, F. Wald

jan.charvat@fsv.cvut.cz

Department of Steel Structures, Faculty of Civil Engineering, Czech Technical University, Thákurova 7, 160 00 Prague 6, Czech Republic

The first assessments to fire safety were based on descriptions of the requirements for the structures, on the classifications of the different types of structures based on experiences. Next step was the establishment of fire compartments, the definition of the asked and the reaches safety based on the experimental works on the structural elements, which were the only solution for fire safety for a long time. In today practice are the tests used for the fire safety of products and the calculations for the fire safety of structures. The prediction models consist of the evaluation of the temperature development in the fire compartment, of the calculation of the heat transfer into the structure (and in the structural elements itself) and of the calculation of the structure under a high temperature. The basic levels of complexity may be distinguished: the simple models, the complex analytical models and the discrete methods. The simplest models are exploring the calculation under the room temperature and are improved of the changes of the major material properties only. The basic simplifications of the simple models compare to the complex ones are: i) The assumption of the constant temperature in an element and an unlimited heat-conduction. ii) The effects of the actions is taken in time $t = 0$ not including the changes during the fire. The member thermal elongation and the shortenings are neglected. iii) The structure is analysed elements by element and the interaction is neglected. By the complex methods are taken into account the non-linear effects of the material and the geometry as well as the large deformations.

The high temperatures affect the material properties. The most important is the reduction of the strength and the Young's modulus. The properties vary for the steel, which is alloy, based on the carbon and the impurities, but the safe predicted values are established. The knowledge of the material properties of connectors (welds and bolts) is available in last ten years.

The prediction of the connections behaviour in case of the room temperature is based on the component method [3], where is the beam flange included by the simple plastification neglecting the phenomena of the local instability, which is minimised by fixing of the flange in joint. For the beam design are the models of the resistance of the compressed flange based on a description of the plastic mechanism. We may be distinguished between the in-plane local buckling and the out-of-plane local buckling. The models are developed to illustrate the beam behaviour under loading by the seismic actions. Kato (1965) prepared the first description of the behaviour in plane. Kuhlman (1986, 1998) precised the complex analytical prediction model, which is used for beams in today design methodology in Europe. Gioncu at al (2000) reported the latest development based on the computer-code supports. Climenhaga a Johnson (1972) described an analytical model in case of out-of-plane buckling. Ivanyi (1985, 1993) published the complex prediction based on the yield line theory. The last contribution to the subject is included in the work of Gioncu and Mazolani (2002). The interaction of the internal force and the bending moment, which is mostly critical in case of the elevated temperatures, is solved extensively for the beams under a room temperature only. The complex prediction of the behaviour under a high temperature was not published yet.

When the fire is initializing, behaviour of a rotationally and axially restrained beam may be describe in few phases (see [1], [2]). When the longitudinal restrain acts on the thermal

expansion of the beam, the restrained part of thermal expansion of the beam will be converted into a compression force in the beam and unrestrained part of the beam will increase the length of the beam.

When the bending moment and additional compression force in the beam at the end are considerably growing, compression stresses will be generated in the beam which can cause local buckling in the lower flange near the ends.

After local buckling, the compressive force in the beam will be decreasing by the increasing in deflection of the beam and a reduction in the length of the beam. Due to initial bending moment in the beam, this will be a gradual process. The connection bending moment will also start to grow.

When lateral deflection in the beam become sufficiently large, the shortening in the beam length will overtake the beam's thermal expansion and a tensile force will develop in the beam and the beam is now under catenary action. In pure catenary action, the axial force in beam will follow the yield stress at increasing temperatures. The bending moment capacity of the beam will be negligible but the beam will still to resist the applied load and will not crash as in a simply supported beam. Though, the tensile force in the beam will be equal to the beam's decreasing tensile capacity at increasing temperatures and the beam will resist the applied load by growing of deflection. At this time, the beam is completely accounted for catenary sag. If very large deflections are acceptable, failure of the beam is likely to be governed by fracture of the connections to the adjacent structure.

The first set of test was finished to study the local buckling. The first test was created to the shear restrained and distribution of temperatures in beam and connections. The second test will study the restrained beam more carefully. The in situ test is prepared to check the structural integrity after the lost of beam action. The preliminary results are showing the possibility to explore the catenary for design purposes.

References:

- [1] WANG Y.C.: *Steel and composite structures-behaviour and design for fire safety* Spon Press 2002
- [2] YIN Y.Z., WANG Y.C. *Application of Catebary Action in Steel Beams under Fire Conditions* The 3rd International Conferece on Steel and Composite, Seoul, Korea 2004 pp. 636–651.
- [3] WALD F., CHLADNÁ M., MOORE M., SANTIAGO A., LENNON T.: *The Temperature distribution in a full-scale steel framed building subject to a natural fire* The second international conference of steel and composite structures 2-49/2004, ed. Chan-Koon Choi, Techno-Press, Seoul Korea Advanced Institute of Science and Technology 2004 pp. 218–219.
- [4] WALD F., SILVA S., MOORE D.B., LENNON T.: *Structural fire integrity test* 10th Nordic Steel Construction Conference 7-9/6/2004, Proceeding Book, ed. N.Gimsing, Danish Steel Institute, Copenhagen 2004 pp. 577–588.

This research has been supported by GA ČR grant No. GA 103/04/2100.

Comparison of Two Conceptually Different Pesticide Leaching Models in Vadose Zone

J. Dušek, T. Vogel, M. Dohnal, M. Šanda*

dusek@mat.fsv.cvut.cz

Department of Hydraulics and Hydrology, Faculty of Civil Engineering, Czech Technical University, Thákurova 7, 166 29 Prague 6, Czech Republic

*Department of Drainage, Irrigation and Landscape Engineering, Faculty of Civil Engineering, Czech Technical University, Thákurova 7, 166 29 Prague 6, Czech Republic

In order to be able to qualitatively compare two different conceptual numerical models a detail database must be available. Such database is supposed to include not only meteorological, hydrological and soil data but also chemical data when dealing with contaminant transport. Field-scale leaching experiment, conducted at Kunia site on island of Oahu, Hawaii State in 1989 [1, 2], offered only limited soil-water data, thus the water dynamics during the experiment was not sufficiently described.

The results of a few sample collecting campaigns can hardly provide complete insight into the soil water flow regime. In addition, field experiments often encounter many uncertainties. An interpretation of experimental boundary conditions, namely the solute application rates, may be done in an way, which is inappropriate for the purpose of numerical modeling. Other difficulties arise with soil heterogeneity which in principle can span several spatial scales. It is well known that soil heterogeneity may result in heterogeneity of processes, in case of solute transport particularly sorption and degradation. These two principle processes primarily govern the fate of pesticides in natural porous medium.

Despite above mentioned facts, the water flow and solute transport through the soil profile was simulated using two conceptually different numerical codes. The data from the field experiment, performed at Kunia site, serves for the comparison purposes. Previous studies suggested that aggregate structure of Hawaiian Oxisols at Kunia contributes to accelerated leaching of chemicals. For that reason, we had to apply a numerical model capable of simulating water movement and solute transport through the preferential pathways. The preferential flow hypothesis was subsequently proved by relatively deep penetration of bromide tracer in response to natural rainfall and irrigation.

In our comparative study, we used two models: S_1D_Dual code with dual-permeability based approach [3], and MACRO code. The latter is based on a kinematic wave equation for solving the water flow in the macropore domain [4]. The dual-permeability approach assumes that the porous medium consists of two domains with different hydraulic properties. The detailed model description can be found in [3, 4].

The soil water distribution simulated by MACRO reveals somewhat closer agreement with measured water content than S_1D_DUAL model. This is presumably due to different hydraulic parameters, the distinct fluid coupling term definition, and especially different approach in the macropore domain. Although soil-water data were fitted by similar expressions: van Genuchten & Mualem (S_1D_Dual) and Brooks-Corey & Mualem (MACRO), results from both analytical models deviated significantly. This may be caused by restricted soil-water samples used in the fitting procedure. The results of simulated concentration profiles show in most cases quite good agreement with the measured pesticide penetration. More specifically, the simulated resident concentrations in the soil profile match the measured values in terms of one order of magnitude. However, some uncertainties in

simulation of the pesticide leaching remain unexplained, e.g.: the bromide breakthrough simulation suggests clearly the necessity of including preferential flow effects in the model, on the other hand, in a few cases, classical Richards' single-permeability approach (without considering preferential flow) predicts deeper penetration of pesticides, compared to the measured breakthrough, indicating overestimation of the pesticide mobility. Regardless of numerical model, all simulation runs confirm the hypothesis that the pesticides can significantly decay in both phases: liquid and solid. Even when the pesticide is adsorbed on the solid phase, it may still biodegrade. The first-order biodegradation process was assumed in the simulations.

Besides the modeling part, a new research project was proposed with several improved features. The challenging research project was initiated partly by the Hawaii Department of Agriculture (HDOA) and the University of Hawaii because of recent findings of pesticide residues in selected drinking water wells in Hawaii. The project was carried out to elucidate the potential impacts of selected pesticides on groundwater and to understand pesticide behavior in tropical soils. The major outcome of the research project will be a recommendation to the HDOA whether to restrict or approve these pesticide products entering Hawaii's agricultural market. Three sites on Oahu, one on Maui, and one on Kauai were selected for field evaluation of leaching. The soil types on Oahu are Wahiawa Oxisol (Poamoho), Molokai Oxisol (Kunia), and Waialua Vertisol (Waimanalo). The soil at Kula, Maui is an Andisol (loam of Kula series) and that at Mana, Kauai is a Vertisol of Malama series. Three herbicides (S-metolachlor, imazaquin, sulfometuron methyl), one fungicide (trifloxystrobin), and one insecticide (imidacloprid) were used in our study. In addition, a commonly used herbicide (atrazine) and potassium bromide tracer were applied as reference chemicals. After spraying, the plots were covered with straw to decrease evaporation from bare soil surface and irrigated with aerial sprinklers for a period of 16 weeks. Disturbed soil samples from various depths were taken at regular intervals for chemical analysis. Water flow dynamics was monitored with TDR probes and tensiometers installed at three depths. Weather data were acquired simultaneously. Laboratory experiments of soil-water retention, as well as degradation, sorption, and column displacement experiments for the selected pesticides were conducted. Some laboratory experiments are still running, thus the data have not been processed and evaluated yet. It is anticipated that the final database will be utilized for detailed comparison study using both discussed numerical models in the near future.

References:

- [1] R.T. GAVENDA, R.E. GREEN, R.C. SCHNEIDER: *Leaching of pesticides in selected Hawaii Oxisols and Andisols as influenced by soil profile characteristics*, CTAHR Research Series 075, University of Hawaii, 1996, pp. 1-35.
- [2] J. DUŠEK, T. VOGEL: *Modeling Pesticide Leaching in Hawaii Oxisol*, Proceedings of CTU Workshop 2004 Part B, 2004, pp. 926-927.
- [3] C. RAY, T. VOGEL, J. DUSEK: *Modeling depth-variant and domain-specific sorption and biodegradation in dual-permeability media*, Journal of Contaminant Hydrology, 2004, pp. 63-87.
- [4] M.H. LARSSON, N.J. JARVIS: *Evaluation of a dual-porosity model to predict field-scale solute transport in a macroporous soil*, Journal of Hydrology, 1999, pp. 153-171.

This research has been supported by CTU grant No. CTU0403011.

Analysis of Clayey Soils Parameters Using Isotropic Consolidation Triaxial Tests

T. Janda*

tomas.janda@fsv.cvut.cz

*Department of structural mechanics, Faculty of Civil Engineering, Czech Technical University, Thákurova 7, 166 29 Prague 6, Czech Republic

Description of the mechanical behavior of soils requires suitable constitutive model and a technique to determine values of respective parameters. As an appropriate set of constitutive rules for clayey material can be chosen modified Cam clay model. Applying Cam clay model is convenient in particular for prediction mechanical response of collapsible soils i.e. materials that tends to relatively large volumetric deformation under applied load.

Although parameters of modified Cam clay model have well defined sense, there is no standard laboratory test leading to straightforward determination. Therefore a backward analysis of an isotropic consolidation as a standard test provided in triaxial apparatus is adopted for parameter extraction.

Assuming fully saturated soil the model accepts Terzaghi concept of effective stresses. The material is considered as two phases medium. The response of the solid phase to the mechanical loading corresponds to the bilinear consolidation line (BCL) [2, 6] which defines the relationship between mean effective stress and current void ratio. Since the deformation of the grains is neglected, change in void ratio defines also value of actual volumetric deformation of porous material. BCL diagram is defined by slope of elastic line κ , slope of elasto-plastic branch λ , initial void ratio e_0 and preconsolidation pressure p_{cp} . The value of preconsolidation pressure corresponds to the highest mean effective stress which the soil was exposed ever in history and form the yielding point for isotropic loading.

The interaction between solid and liquid phase is governed by Darcy's law. With respect to potentially significant volumetric deformation of the material the coefficient of permeability is assumed dependent on current void ratio. The exponential relationship between relative changes of coefficient of permeability and void ratio [3] proved useful in form $K/K_0 = (e/e_0)^m$, where K_0 is the initial coefficient of permeability, e_0 represents initial void.

The advantage of using isotropic consolidation test in the backward analysis consists in direct relation between effective mean stress and porous pressure, while the chamber pressure is keeping constant. Hence four-dimensional problem reduces to the two-dimensional. The solution of given problem is the time development of the field of porous pressures in the soil sample. In spite of significant simplification the governing equation can not be solved analytically. Thus finite volume method was implemented for the numerical solution.

As was stated before, the main goal is to suggest method for extracting material parameters of Cam clay model from single laboratory test. The proposed backward analysis is based as optimization problem on fitting numerical results into real experimental data gained from triaxial test. The optimization technique, called augmented simulated annealing (AUSA) [4], prove as an efficient tool for determining optimal set of material parameters. This method based on combination of genetic algorithm and simulated annealing finds global minimum of given function $F(\mathbf{X})$ on given interval. The optimized function is proportional to the difference between measured and calculated course of porous pressure and is defined as $F(\mathbf{X}) = \sum (p(t_i) - p'(t_i))^2$ where $\mathbf{X} = (e_0, K_0, p_{cp}, \kappa, \lambda, m)$ is the vector of unknown parameters, $p(t_i)$ is

the value of calculated porous pressure in i -th time step and $p'(t_i)$ represents the experimentally obtained value of porous pressure.

The outlined technique for extracting material parameters of modified Cam clay model with deformation dependent coefficient of permeability was tested on samples of Brazilian clay [1]. This type of soil has been subjected to a leaching process and the finest particles have been eroded. This phenomenon raises porosity and such type of soil tends to show significant volumetric strains. Therefore Brazilian clay represents appropriate material for parametric determination.

The tests were performed in three phases. First of all the porous pressure on the undrained base of the sample was measured in condition of isotropic consolidation until the process reaches steady state. Afterwards the sample was unloaded and the measurement of porous pressure under reconsolidation in the same loading conditions followed. The value of preconsolidation pressure changed to the highest effective stress the sample was exposed. Subsequently the values of void ratio and coefficient of permeability was actualized. This set of new parameters was used to predict the behavior in reconsolidation phase. The course of porous pressure computed with this actualized set of material parameters agree well with experimental data obtained by reconsolidation phase and confirms that the reconsolidation rate is relatively higher the rate of primary consolidation.

References:

- [1] CUNHA, R. P., KUKLÍK, P.: *Numerical evaluation of Pile Foundations in Tropical Soils of the Federal District of Brazil by Means of a Semi-Analytical Mathematical Procedure* Soils & Rocks, Vol. 26, No. 2, 2003, pp. 169–173.
- [2] JANDA, T., KUKLÍK, P., ŠEJNOHA, M.: *Mixed experimental and numerical approach to evaluation of material parameters of clayey soils* International Journal of Geomechanics, Vol. 4, Nu. 3, 2004, pp. 199–206.
- [3] KUKLÍK, P., MAREŠ, J., ŠEJNOHA, M.: *Evaluation of the modified Cam clay model with reference to isotropic consolidation* CTU Reports, Prague, 1999, pp. 47–54.
- [4] LEPŠ, M., MATOUŠ, K., ŠEJNOHA, M., ZEMAN, J.: *Applying genetic algorithm to selected topics commonly encountered in engineering practice* Comput. Methods Appl. Mech. Eng., 119, 2000, pp. 1600–1620.
- [5] KREJČÍ, T., NOVÝ, T., SEHNOUTEK, L., ŠEJNOHA, J.: *Structure - subsoil interaction in view of transport processes in porous media* CTU Reports, Prague, 2001, pp. 27–60.
- [6] POTTS, D. M., ZDRAVKOVIC, L.: *Finite element analysis in geotechnical engineering* Thomas Telford, London, 1999, pp. 160–165.

This research has been supported by GA 103/02/0688.

Modelling of Hydraulic Jump in Closed Conduit

P. Fatka, J. Pollert, Z. Koniček

fatkap@lermo.cz

Laboratory of Ekological Risks in Urban Drainage,
Faculty of civil Engineering, Czech technical University,
Thákurova 7, 166 29 Prague 6, Czech Republic

At present, the rate of urban development in city agglomerations put great demands on a function of sewer systems. Considerable quantities of polluted waters run off the catchment surface especially during rain events. This water is usually drained by the system of sewer system.

Increasing flow in system subsequently causes several, usually negative, hydraulic phenomena. One of these phenomena is a hydraulic jump as a result of energy transformation. Such occurrence of the jump is not included in design procedure of the sewer system.

By the term hydraulic jump one understands the transition from supercritical to subcritical flow accompanied by considerable local turbulence production and associated with energy dissipation. The hydraulic jump can, for example, occur in pipe of the sewer which slope becomes flatter or for supercritical flow falling suddenly down to a pool of still water [1]. While the stilling basin is a standard structure dealing with the hydraulic jump under all conditions of flow, in sewer system that kind of structure does not exist. With small flow rates the stilling basin would be clogged by shifted substance as mud or sand and its operation would be inefficient [4]. In sewers, the hydraulic jump is not implemented into design procedure and depending on the conditions in the upstream and downstream; it shifts along the pipe to the stabilizing position.

Together with hydraulic jump there can occur rather negative phenomena as a cavity, clogging or pressure fluctuations [3]. Then the interaction of these phenomena cause faster degradation of material, excess of inner stress and increased hydraulic load of sewers that can finally lead to break down of sewer structure and to a local not only ecological accident due to the wastewater outflow into environment. Regarding extent of present sewer systems in major urbanized areas, the definition of such critical places is both expensive and time consuming.

Project focuses on a free surface flow conditions when the hydraulic jump occurs in place of the change of the pipe bottom slope. Understanding and description of the behaviour of the jump on the pipe fracture would lead to more accurate definitions of these critical places and consequently to their better maintenance.

Project takes place in hydraulic laboratory at the CTU in Prague, Faculty of Civil Engineering. To determine parameters of hydraulic jump the approach using a physical modelling was applied. Laboratory experiments were carried out in an acrylic circular pipe of 15 m long with inner diameter 242 mm (outer 250 mm) and with exact change of bed slope from 19 ‰ to 0 ‰. During the experiments, the discharge was measured with a help of calibrated measurement weir placed in a tank attached to the pipe upstream. Hydraulic jump were generated with a moving clack valve at the end of the pipe and located at the change of the slope. This physical model enables flow rates from 0 to 50 l/s. The upstream and downstream water depths of the hydraulic jump were measured with ultrasonic sensors. The pressure fluctuations at the bottom change were measured with four pressure inductive

differential sensors connected to Spider transducer. These sensors were placed on each side of the pipe 100 mm and 300 mm from the bottom change in order to measure fluctuation changes properly.

All measured results were obtained at the model with exact bottom change of the pipe from 19 ‰ to 0 ‰. At the beginning the testing and tuning of the model were carried out. In this step all sensors were calibrated and installed to the model. For each sensor its characteristic calibration curve was obtained. After that Q-h curves for the upstream depth were derived. These curves served mainly for the verification of measurement.

Then experiments for hydraulic jump with Froude numbers ranging from 1,5 to 2,8 were carried out. In each case the flow rate and upstream and downstream depth was measured. Then the upstream Froude number and other parameters important for hydraulic jump as (sequent depth ratio etc.) were counted and, if possible, compared with values published in literature. Results achieved denote good agreements with published ratios. Some new relations characterizing a movement of the jump in dependence of slope change and a ratio of Froude numbers upstream and downstream were derived.

Along with depth measurements the pressure fluctuations were also measured as well. Unfortunately the first assumption, that pressure fluctuations due to energy transformation in hydraulic jump are measurable directly with sensors, was disproved. Presently it seems to be evident, that the pressure fluctuations could be estimated using tools of spectral analysis. According to [2] the presumption of the roller formation – advection model was assumed. This presumption was tested on the model and partial agreement was achieved. In first steps several sampling rates were tested as well as number of sample acquired at each measurement to cope with the application of FFT. Unfortunately the evaluation of energy spectra did not bring satisfactory results so far.

These results should be extended with results for several defined bottom changes in order that it would be possible to describe the movement of the jump in whole range.

References:

- [1] HAGER, W.H.: *Wastewater Hydraulics* Springer - Verlag, 1999, 173–208.
- [2] MOK, K.M.: *Relation of surface roller eddy formation and surface fluctuation in hydraulic jumps* IAHR-Journal of Hydraulic Research, 2004, 207-212.
- [3] HAINDL, K.: *Prstencový skok a přechodové jevy proudění* Akademia Praha, 1975, 13-19, 98-107
- [4] HAINDL, K.: *Energy Dissipation and Wateroxidation in Sewers* Conference on Topical Problems in Urban Drainage, 1989.

This research has been supported by CTU0404511.

Masonry Arch Bridges

T.Dvorský, V.Kukaň, P.Řeřicha

tomas.dvorsky@fsv.cvut.cz

Department of Concrete Structures and Bridges, Faculty of Civil Engineering,
Czech Technical University in Prague, Thákurova 7, 166 29 Prague 6, Czech Republic

The project Masonry Arch Bridges compares the results of experimental test on masonry arches with several analytic solutions. The results from the comparison will serve as the input data for development of an analytical model for determination of the load bearing capacity of arches and vaults and for suggesting a methodology of assessment of load bearing capacity of arch structures, since there is no specific method of determination of load bearing capacity of arches and vaults. There are several methods of such determination in use these days in the Czech Republic and also abroad. Also, as for the assessment of the load bearing capacity at collapse, there are numerous methods which are essentially different.

In the experimental part of the project, three sets, where each set contained three arches were built. The shape of each arch was that of a circular arch band. The arch bands were made of full firebrick of the type P15 and cement-lime mortar, M2. The width of the arch bands was 29 cm, corresponding to the length of the firebrick. The thickness of the arch band was 14cm, corresponding to the width of the firebrick. The span of the arch bands was 3 m with the height of 1.2 m, 1.0 m and 0.75 m.

The static border conditions were secured with steel beams. The vertical displacement of arches was arrested by anchors attached to the floor. The horizontal displacements were arrested by a steel beams fix to the rear side of the foot of the arch. There beams were also anchored to the floor.

The arch bands were loaded at a quarter of the span with a hydraulic press. The force acting at the arch band was transferred though a distributing device. The loading was continuous increased with a step of 0.1 kN, until the force reached the collapse force level – until the fourth hinge formed. Time interval between each loading step was 60 seconds.

During the experiment, deformations of arches and stresses in the arches were monitored. The stresses, measured through the relative deformations, were recorded by strain gauges, the vertical and horizontal deformations were recorded by potentiometers and at the point where the load was applied deformations were recorded by an inductive sensor. At one experiment, there were seven vertical deformations and two horizontal deformations recorded. The stresses are recorded at different six locations. For a better monitoring of crack formation the surface of arches was painted with gypsum grout.

The program CTAP [1] was used as one of the analytical methods for calculation of the load bearing capacity at collapse. This program was developed at the University of Wales, Cardiff, Great Britain. The computations of collapse capacity were performed on an arch with a width of 1 m and subsequently the computed results were reduced for arches with the width of 0.29 cm.

The second method was developed by the British Army's Engineering Experimental base (MEXE) [2]. The MEXE is a simple empiric method for estimation of load bearing capacity of masonry circular arches for army purposes. The method allows for consideration geometric properties of circle arches. The method is also used for civilian purposes.

The method uses a monogram, or equations, e.g. $PAL = \frac{740(d+h)^2}{L^{1.3}}$, for preliminary determination of permissible axle loading (PAL), which depends on the span, the axial length of an arch and the height of a mound. The PAL value can be modified by various coefficients

regarding the geometric and other condition of an arch. The MEXE method is limited by the arch span of 18 m.

The program developed at the Department of Structural Mechanics of CTU (DSM) represents the third analytical method used in this project. The method is based on the model which is described in [3]. The plane strain condition is assumed. The circle is modeled as a layered beam with five layers. The material of the layers is considered elasto-plastic with Rankin's condition and with linear softening. The fracture energy valid for mortar was estimated with the assumption that the crack occurs in mortar.

The ADINA [4] program is the fourth and last method. The program works with the Drucken-Prager condition with an additional limitation surface in tension and with tensile softening. The nine-point isoperimetric elements are used in five layers in combination with the Newton-Raphson and the arc-length methods for solving the nonlinear equation system.

In the next part of the project, the experimental tests will be finished and further comparative calculation of the load bearing capacity at collapse will be performed. The conformity of the analytical solutions and the experimental results was not acceptable. However, the considered analytical methods (DSM, ADINA) have some free parameters. The calibration of these free parameters is one of the next goals of the project. Further, development of an analytical model for determination of the load bearing capacity of arches will be pursued with subsequent verification of the developed 2D model, or preferably 3D model, with the experimental test results.

References:

- [1] *CTAP Masonry arch assessment package, University of Wales, Cardiff, UK*
- [2] *BA 21/97 The Assessment of Highway Bridges and Structures (Incorporating Amendment No. 1 dated August 1997) and BA 16/97 The Assessment of Highway Bridges and Structures (Incorporating Amendment No. 1 dated November 1997)*
- [3] P. ŘEŘIČHA: *Statistic and Dynamic Limit Loads of Reinforced Concrete Structures*, CTU Report Praha, 2000
- [4] *Theoretical manual ADINA ADINA R&P, Inc., 71 Elton Avenue, Watertown, MA 02172 USA*

This research has been supported by CTU grant No. 0401511.

Accuracy Evaluation of Wire Strain Gages for Dynamic Measurements of Engineering Structures

M. Černý

cerny@klok.cvut.cz

Klokner Institute CTU, Šolínova 7, 166 08 Praha 6

Introduction

Aim of the present study was to assess an accuracy of dynamic measurement by wire strain gages in low frequency range (0-10 Hz). The assessment of the wire strain gage accuracy is of most importance for measurements on most structures in civil and transport engineering (e.g. buildings and bridges).

Measurement Setup

The accuracy of wire strain gage made in Klokner Institute has been evaluated. The wire strain gage consists of pretensioned steel wire, excited by electromagnetic system to carrying frequency approximately 1 kHz. The sensor has been tested in special setup for calibration which has been constructed at Klokner Institute. The parameters of setup are as follows: amplitude 0-10 mm, frequency 0-50 Hz, distortion max 0.1%. A wire strain gage body has been fixed to base of the setup and wire strain gage connected to the moving plate of the setup. The wire frequency is changing on dependence of moving of the plate. Output dynamic signal in range 0.5 - 10 Hz has been measured by high speed voltmeter HP 44704A (16 bits, 100 kSa/sec) and digitized data have been transferred to PC Pentium. A range 10.24 V of input voltage has been considered.

Evaluation of Dynamical Accuracy of Frequency Measurement

Signal from wire strain gage has been analyzed by software LabWindows CVI 5.01. Output signal from wire strain gage is distributed in the range 500 Hz to 2 kHz and depends on the corresponding mechanical frequency 0.5 to 10 Hz. Frequency output from the sensor has been measured and then mechanical frequency calculated from the measured time of signals' passage through its mean value (comparative level).

The dependence of noise on mechanical frequency has been calculated and the corresponding Effective Numbers of Bits (ENOB) representing a dynamical accuracy were evaluated. The dynamic signal has been processed by Chebyshev low pass digital filter with max. frequency 100 Hz.

In the range 10.24 V the Effective Number of Bits (ENOB) 6.05- 7.03 for nonfiltered signal and 6.23- 7.30 for filtered signal has been found. The results are shown in Table 1.

Table 1 Measurement with wire strain gage, evaluation of ENOB, range 10.24 V

Input Frequency Hz	ENOB	
	Without Filter	Filter DP 500 kHz
10	6.05	6.23
5	6.55	6.64
2	6.79	7.24
0.5	7.03	7.30

Conclusions

A good dynamical accuracy of wire strain gages has been achieved, which is comparable with the accuracy of LVDT sensors. The increased mechanical frequency causes lower accuracy of measurement, as the number of samples in a period decreases. Described method of calculation can be applied only for low frequency mechanical signals.

References:

- [1] ČERNÝ, M.: *Dynamic Testing of LVDTs and WS Gauges* Proceedings of the Czech Technical University Workshop, CTU in Prague, 2000
- [2] ČERNÝ, M.: *Accuracy Evaluation of Accelerometers for Dynamic Measurements of Engineering Structures* Proceedings of the Czech Technical University Workshop, CTU in Prague, 2002
- [3] ČERNÝ, M.: *Accuracy Evaluation of LVDTs and Strain Gages for Dynamic Measurements of Engineering Structures* Proceedings of the Czech Technical University Workshop, CTU in Prague, 2003
- [4] ČERNÝ, M.: *Accuracy Evaluation of HP3852 for Measurement of Engineering Structures* Proceedings of the Czech Technical University Workshop, CTU in Prague, 2003

This research has been supported by project MSM6840770015 and MD ČR 1F55B/120/120.

Standardization of the Validation Criteria's for the Dynamic Landscape Development and the Landscape Management

A.Vokurka

vokurka@fsv.cvut.cz

Department of Irrigation, Drainage and Landscape Engineering, Faculty of Civil Engineering, Czech Technical University, Thákurova 7, 166 29 Praha 6

The project was focused to evaluate an importance of aerial photo coverage's for landscape planning, dynamic landscape development criteria assessment, landscape quality criteria assessment and for determinating a current landscape status.

Specific territories aerial photo coverage's, taken in period of 1945 to 2001 were selected as a basis for the dynamic landscape evaluation. Scenic development and anthropogenic activities impacts were checked in 4 different time periods:

- first moderate postwar photography,
- photos territory of 70's,
- photos of the end of 80's,
- photos from contemporary period.

Each aerial photograph was scanned, adjusted by using the ortho-photograph map, GEOREF (World Geographic Reference System) and processed by implementing GIS tools.

Aerial photo coverage's were taken at different Czech Republic locations to describe various impacts of human activities on the landscape development. For that reason, the following areas were selected - territories of former "behind the iron curtain" borderline area with strictly excluded human impacts on natural ecosystems, territories of agricultural landscape with meadows and grassland dominating, territories of high-powered agricultural landscape with superiority of arable soil and territories of watershed of the Botič stream, etc.

Based on aerial photograph, gradual changing of selected areas were described – both changes of the landscape being under direct human influence, and succession of the nature in case of leaving the slots free of human activities, on the other hand.

The selected periods of time and photographs of the borderline areas made it possible to compare characteristics of Czech and German pieces-of-lands and thus to compare a scenic development in neighbouring territories with differend forms of possesion and relations to them (German parts represented with private land-holders and active farming, Czech parts of restricted borderline areas - now National park Šumava – with excluded human activities and natural succession).

In other locations, it was possible to observe ongoing trends in agricultural lots farming such as consolidation of plots into large fields, studio floodlight drainage systems, changes of watercourse and way meshes characters. Gradual changes and development of various seats was also observed. In recent years, change of proprietary relations to a piece-of-lands, has been presented by growing number of fallow arable soil, bows and grassland with gradual natural succession and growth.

Based on the presented project, it was verified, that aerial photograph coverage's is suitable and fit basis for landscape assessment. Together with other maps they are objective enough for analyzing and comparing territory characteristics in different period of times. The aerial photographs can also be used for landscape and seats development planning.

Based on that project, a proposal for external grant agencies will be elaborated and presented. Other project will be focused to evaluate and define limits of acceptable human

impacts on landscape development, and to determine admissible conditions and limits for incorporating man and possible thrifty farming into a natural landscape.

References:

This research has been supported by CTU grant No. CTU0413311

Experimental Research of Structural Materials and Technologies

F. Luxemburk, B. Novotný *, P. Bouška** P. Mondschein

luxemburk@fsv.cvut.cz

CTU, Faculty of Civil Engineering, Dept. of Road Structures, Thákurova 7, 166 29, Prague 6

* CTU, Klokner Institute, Dept. of Reliability, Šolínova 7, 166 08, Prague 6

** CTU, Klokner Institute, Dept. of Experimental and Measurement Methods, Šolínova 7,
166 08, Prague 6

In the year 2004, the last year of the project MSM 210000004 solution, the research was conducted by the research teams from the departments of Physics, Building Structures, Structural Mechanics, Concrete Structures and Bridges, Steel Structures, Geotechnics, Road Structures and from Experimental Center and Center of Experimental Geotechnics of the Faculty of Civil Engineering of CTU as well as by the researchers from the Klokner Institute of CTU.

The research project covers the whole scope of scientific activities of both Faculty of Civil Engineering and Klokner Institute and is divided in the following main topic groups:

- aging and durability of concrete,
- biological degradation of structural materials,
- micromechanical properties of the concrete structures and concrete reinforced by fibres,
- experimental research in steel, timber and composite materials and their technologies,
- research on bentonite (construction of underground radioactive wastes deposits),
- self-compacting concrete,
- geotechnical properties of mixtures of soils and brown coal combustion fallouts,
- rheological properties of road materials.

The aim of the project is to stimulate research in materials based on our natural resources in order to develop innovative construction materials for advanced engineering structures. The research is focussed on minimization of the energy consumption, recycling and use of waste materials. In the year 2004, the most notable contributions are the following:

1. In the field of non-destructive methods for determination of strength and stiffness parameters of structural timber, the combination of the penetration and ultrasonic methods was tested in order to obtain most accurate values of timber strength and elastic modulus. The research in the steel and concrete composite structures has been concentrated into the experimental investigation of innovative shear connectors. Especially, the new thin-walled powder actuated shear connectors and modification of perforated shear connectors have been investigated. The experimental research in structural joints was focused on working diagrams under repeated, accidental (fire, explosion etc.) and combined loadings, description of joints of composite and mixed structures and more reliable prediction of their deformation capacity.

2. The complex set of experiments and computer simulations of material, thermal, hygric and other physical properties of concrete and cementitious composites was carried out. The new methodology was developed for determination of concrete elastic modulus in compression with material softening, for measuring concrete permeability, for material testing under exposition to cyclic changes of temperature. Non-standard methods have been developed and tested for measurement of heat capacity, moisture content, coefficients of

thermal conductivity, linear and volume heat expansion, moisture conductivity and water vapour diffusivity. Original results have been achieved concerning nanoporosity changes and its influence on mechanical properties of cement-based materials.

3. The correlation between limit indent depth and the homogeneity of physical nanocharacteristics of concrete internal structure was investigated, this problem having basic importance for possibility of using the nanoindentation as a tool for assessment of concrete structure properties.

4. The experimental method for assessment of the single fiber behaviour in the concrete structure was enhanced by elaborating specific process of test specimen manufacturing, the properties of specimen having significant effect on the measurement results. The effects of fibre material, geometrical shape and finish were studied. The model of fibre-reinforced concrete volumetric changes was elaborated.

5. The research of self compacting concrete was focused on testing of long-term strength and deformation properties of concrete mixtures prepared from raw materials available in the Czech Republic with plasticizing admixtures being prepared on the carboxyl ethers base.

6. In the Centre of Experimental Geotechnics the research connected with disposal of radioactive waste was continued with evaluation of two physical models: the MOCK-UP-CZ model and the model of prefabricated wall composed of bentonite blocks. The performed research is expected to bring new knowledge on changes in material properties of barriers caused by long-term exposition to elevated temperature and moisture.

7. The catalogue of asphalt and block pavements was prepared taking into account different subgrade characteristics, design levels of deterioration, traffic loads and different materials of pavement base layers. The performances of all the proposed pavement structures were theoretically evaluated using innovative versions of design criteria. The catalogue of pavements comprises also pavement structures with layers of R-material (recycled material).

8. The laboratory procedures for testing of shear strength, compressibility and permeability of saturated samples of recultivated soils were elaborated and practically verified by the computer controlled three-axial shear device and hydraulic oedometer. The failure mechanisms of the clodded soil with double porosity was studied in detail.

References:

- [1] DRCHALOVÁ, J. - MŇAHONČÁKOVÁ, E. - VEJMELKA, R. - KOLÍSKO, J. - BAYER, P. *Hydric and Mechanical Properties of Carbon Fiber Reinforced Cement Composites Subjected to Thermal Load* In: Construction and Building Materials 2004 p. 567-570
- [2] KONVALINKA, P. *Changes of Material Characteristics of Concrete under Freeze-thaw Loading* Progress in Structural Engineering, Mechanics and Computation 2004 p. 224-228
- [3] VODIČKA, J.- SPŮRA, D. – KRÁTKÝ, J. *Homogeneity of steel fiber reinforced concrete (SFRC)* BEFIB 2004, Sixth International RILEM Symposium 2004 p. 537 – 544
- [4] WALD F. - SOKOL Z. - MOAL M. - MAZURA V. - MUZEAU J. P. *Stiffness of cover plate connections with slotted holes* Journal of Constructional Steel Research, Issues 3-5, Vol 60 2004 p. 321-327

This research has been supported by MSM grant No. 210000004.

Uncertainty in Open Channel Analyses under Extreme Flow Conditions

P. Sklenář, M. Salaj

sklenar@fsv.cvut.cz

Department of Hydraulics and Hydrology, Faculty of Civil Engineering, Czech Technical University, Thákurova 7, 166 29 Prague 6, Czech Republic

Estimation of channel and floodplain conveyance and similarly prediction of flood water level and associated extent of inundation is assumed to be one of the most important tasks in operational management of floods or in design of efficient flood protection measures. Post-flood reconstruction of flood peak flow based on field evidence computation is equally important when discharge data is not available at observation stations failing their proper functioning or being destroyed during flood event. It is also difficult to correctly assess flow resistance in floodplains. Mostly it is generated by vegetation roughness (there is a strong effect of seasonal change in vegetation or an effect of characteristic stiffness of tree stems or branches) or by resistance associated with improper functioning of watercourse structures (affected by floating debris clogging or ice packing at the throat of embankment openings). Assessment of active or passive areas in flow sections causes difficulties as well. Nature of these factors, especially occurrence of unpredictable phenomena (run of floating debris or ice drift and its packing, obstruction of flow area etc.), is a reason of process uncertainty. Deterministic approach to analysis can't reflect stochastic nature in modification of conditions of flow during flood event. Another field of uncertainty is connected with reliability in statistical evaluation of input discharge (probability of occurrence), however it is not question for computation methodology itself. This issue becomes more important when flood risk analysis is applied and probability of stage exceedance is reviewed with actual potential losses due to flooding. In that case it is necessary to provide a river manager, responsible for implementation of safe and efficient flood protection measures, with estimation of mean water stage supplemented with confidence intervals in resultant value expressing its uncertainty. During the first year of the project dealing with uncertainty issues research team focused on following problems:

- Assessment of uncertainty in determination of the extent of flood affected areas [1], and consequently in analysis of flood protection measures effectiveness [2].
- Assessment of uncertainty in estimation of the balance inflow in reservoir of the Orlik dam [3].

The first issue is connected with a fact that conditions of flow in flood plain are excessively vague both due to probabilistic nature of inundation and due to temporal changes in roughness, terrain geometry and way of land use. The most promising attitude is to use of Monte Carlo (MC) technique. Probabilistic methods, such as the Monte Carlo Method, make a many times repeated use of the deterministic 2D flood flow models and the statistical characteristics of the model input. The probabilistic method aims at the estimation of the statistical characteristics of the model outputs like the mean value, the variance, the percentile values and the probability distribution type. These probabilistic methods requires a derivation of random generator of input data with statistical characteristics identical to real data. These techniques are rather computation-intensive. For practical use research team seeks a simpler and less computation-intensive stochastic meta-model, which would be able to reproduce stochastic behaviour in same manner.

In the second issue the balance inflow in reservoir of the Orlik dam can be used as an estimate in determination of run-off from upper part of the Vltava river basin entering reservoir of the

Orlík dam. At present a reservoir characteristics is used to obtain balance inflow. The adjective “balance” means that the inflow is not the true discharge entering reservoir, but the value of discharge, which completes the balance between change in impounding volumes in increment of time and discharge released within the same time increment. This balance value assessed in this way refers strictly to the site of the dike, nevertheless it gives the best estimate of the real inflow entering the reservoir of the dam. However, the problem is that the water stage at the whole extent of reservoir can be hardly assumed as perfectly horizontal (static) as it is assumed in reservoir characteristics. Usually the hydrodynamic backwater effect is present even for small reservoir inflows at the real tail of the reservoir and is limited in its extent. For more extreme hydraulic situations with significantly unsteady inflows a disagreement between hydrodynamic and static water stage in reservoir might be considerable and between corresponding impounds as well. Research team set a hypothesis, that the hydrodynamic drawback effects might considerably influence the assessment of balance inflow at dike of the Orlík dam. It can be concluded from a few of the water marks recorded on the periphery of the Orlík dam during flood in August 2002. For this reason it is inevitable to provide discrete values of balance inflow derived with uncertainty limits, especially for reviewing

In frame of the second issue the researchers co-operate with operational bodies of the Vltava River Authority and have agreed with them on the common procedure how and where to collect the real time data (water stages) in order to facilitate a further research work and secure its progression.

References:

- [1] SKLENÁŘ, P. – SALAJ, M.: *Význam prvku nejistoty v technicko-ekonomické a rizikové analýze při návrhu preventivních protipovodňových opatření*. VRV Praha, a.s. & ČVTVHS, 2004, pp. 12–19.
- [2] HAVLÍK, A., SATRAPA, L., SALAJ, M., HORSKÝ, M., FOŠUMPAUR, P.: *Riziková a finanční analýza na horní Opavě*. VRV Praha, a.s. & ČVTVHS, 2004, pp. 32–37.
- [3] MAREŠ, K.: *Nejistoty při hodnocení kulminačních průtoků extrémních povodní*. VRV Praha, a.s. & ČVTVHS, 2004, Přednáška konference Vodní toky.

This research has been supported by GA ČR No. GA 103/04/1328.

Testing of RC Beams Strengthened by CFRP in Bending

M. Černý

cerny@klok.cvut.cz

Klokner Institute CTU, Šolínova 7, 166 08 Praha 6

Introduction

In recent years, the innovative rehabilitation and strengthening methods for reinforced concrete structures are developed. The development of strengthening techniques is requested to extend the life time or to increase load bearing capacity of many existing bridges. Some of the methods that are being considered, make use of composite materials. The usually used method of strengthening by composites is application of externally bonded CFRP (carbon fibre reinforced) strips on bridge structures subjected to bending. Several studies of RC bridges strengthened by CFRP strips are reported in the literature. Carbon fibres have been successfully used for strengthening of T beams, box beams, plates and bridge piers.

The work presented here follows other work previously done at Klokner Institute on the testing of carbon fibre strips and adhesives in frame of grant Ministry of Transport of the CR. This paper presents some results of testing of strengthened reinforced concrete beams in bending. The beams of rectangular cross-section 140x 215 mm with length 1200 mm have been strengthened by externally bonded carbon fibre strips 50 (60) x 1.2 mm. The testing program was prepared to investigate failure mechanisms of reinforced concrete beams strengthened by CFRP strips, to compare load capacity strengthened and nonstrengthened tested beams and to assess the performance of products (systems) from various suppliers available in the CR.

Experiments

An experimental program for 12 beams has been prepared for testing at CTU Klokner Institute. Beams were 1200 mm long, with cross-section 140x215 mm, reinforced by steel rods 2R8 at lower and 2R6 at upper part of the beam. Concrete grade was 25/30. Total 4 types of beams, reinforced by C- strips Sika 512 (produced by Sika AG) size 50x1,2 mm, MBT 200/1000 (produced by Degussa MBT) 50x 1,2 a experimental pultruded C-strips (2x30x1,2) and adhesives Sika a MBT were tested. The carbon fibre strips have been manually applied by means of cold cured adhesive bonding at temperature 21^oC and relative humidity 43% in testing hall of Klokner Institute. The beams have been conditioned before application 72 h at temperature 20^oC.

MBT-Mbrace Epoxikleber 220 (produced by Degussa MBT) and Sikadur 30 (produced by Sika) have been used for the bonding of CFRP strips to concrete. The beams have been tested in electronic testing machine Instron 1273 (200 kN loading capacity) which has been equipped with loading table and a system of steel supporting beams. Loading rate for all tests was 1 mm.min⁻¹. Analog signals (load and displacement of upper clamp) from testing machine and vertical displacements in the middle of the beam have been measured by data acquisition system HP 3852 (USA), digitized data transferred through GPIB to PC Pentium and analyzed by software LabWindows CVI 5.01 (National Instruments) adapted for measurement at Klokner Institute. The vertical displacements have been measured by two LVDT sensors of type Lucas-Schaevitz E300 (USA). The results are given in Table 1.

Testing of unstrengthened beam

The unstrengthened beam has been loaded in the middle of the length up to failure. Two LVDTs have been used for measurement of vertical displacements in the middle of the length. Two levels can be distinguished from load- displacement curve: load P_r corresponding to crack inicialization and load P_y corresponding to point of plasticized concrete.

Testing of strengthened beams

A set of strengthened beams (CFRP strips Sika S512, MBT 200/1000 and experimental) have been tested. Recorded load- displacement curves show that after inicialization of cracks the load has increased without plasticized concrete, but the failure occured at anchorage of CFRP strip and in cause of cracks inicialization and propagation the load has decreased. At beam strengthened by MBT strip a peeling-off effect before reaching P_r load was observed.

Conclusions

The beams were subjected to monotonic bending load up to failure. Four types of strengthened beams have been tested: C-strips Sika 512 (50x1,2 mm), MBT 200/1000 (50x 1,2) a experimental (2x30x1,2) bonded with adhesives Sika and MBT. The results of testing show that the best performance have strengthening C-strips Sika (adhesive Sika) and experimental C-strips bonded with adhesive MBT. Max. load due to strengthening has increased by 44% (Sika) and 29% (experimental C-strip), load on cracks limit has increased by 20%. The influence of strengthening on displacement at failure is low.

Tab.1 Results of static testing of RC beams

Beam	P_r [kN]	P_y [kN]	P_{max} [kN]	w_{max} [mm]
Nonstrengthened	15	40	45	7
Strengthened Sika	20	-	65	8
Strengthened Exp.Sika adhesive	18	-	48	6
Strengthened, Exp.MBT adhesive	18	-	58	5

References:

- [1] ČERNÝ M. AT AL.: *Use of Fibre Composites for Strengthening of Bridges* Technical Report (in Czech) KI CTU, 2003.
- [2] ČERNÝ M.: *Mechanical Properties of Composites and Adhesives for Strengthening of RC Structures* Proceedings of Workshop, CTU in Prague, 2003
- [3] ČERNÝ M.: *Experimental Evaluation of Mechanical Properties of Carbon Fibre Composites for Strengthening of Engineering Structures (in czech)* Proceedings of the Conference Reinforced Plastics, Karlovy Vary 2003

This research has been supported by project MSM6840770015 and MD ČR 1F55B/120/120.

Thermal-Moisture Problems of External Skins of Civic Building-Distribution-Effect of Moisture and Temperature on Biodeterioration

P. Bednářová, D. Bedlovičová

bednarov@fsv.cvut.cz, bedlovic@fsv.cvut.cz

Department of Building Structures, Faculty of Civil Engineering, Czech Technical University, Thákurova 7, 166 29 Prague 6, Czech Republic

To build and live healthily is an everyday demand of our time. If it is to be fulfilled, great care must be taken in selecting building materials. A proper function of the roof envelope depends not only on a suitable composition of the multi-layer roof structure, but also on an appropriate selection of the building material for the ceiling construction. A large scope of materials used for the bottom covering of sloping roof constructions have fairly different parameters, both in terms of thermal technological, acoustic, fire properties and biodegradation risks.

In roof constructions, biodegradation occurs very often, and the cause of its appearance is either already on the design level, or it results from improper technological procedures applied during the construction process.

Among fundamental causes of biodegradation of roof constructions, the following ones may be mentioned:

- drop in surface temperatures of ceiling constructions, which is due to:
 - ❑ thermal bridges – incorrect design of the composition of a padded roof construction, workmanship error etc.
 - ❑ penetration of cool air inside an enclosed air cavity at the point of the ceiling construction – improper design of the composition of a padded roof construction, workmanship error etc.

- non-standard temperatures and relative air humidity in the interior, which are due to:
 - ❑ increased moisture content of newly built structures
 - ❑ transfer of wet processes
 - ❑ reduced infiltration
 - ❑ change in a heating system

All these factors may be referred to as risk factors in relation to the growth of micromycetes. The main research objectives include assessment of the resistance of individual materials used in the construction of ceiling constructions of sloping padded roofs in terms of biodegradation appearance and determination of the boundary conditions interval, which is a limiting factor for the risk of biodegradation appearance.

Research is carried out on three levels:

1. In-situ measurements – measurements of temperatures and relative moisture content values in interiors and exteriors, measurements of temperature, relative humidity and air flow velocity in an enclosed air cavity, and measurements of surface temperatures on the bottom face of roof constructions. Materials have been selected so as to characterize a wide spectrum of compositions and ceiling constructions applied presently in sloping roofs.
2. Computer simulation of a thermal and moisture regime in the respective roof construction, and computation of surface temperatures for individual thermal bridges.
3. Laboratory simulation of biodegradation appearance, including determination of the boundary conditions interval within which the respective material is susceptible to biodegradation appearance.

Research implemented on more levels allows specification of the presumed behaviour of a construction and successive comparison of the presumed and actual state.

Due to the fact that the research indicates considerable hazards of biodegradation of roof constructions in terms of health safety of structures (the majority of fungi are allergens and facultative pathogens), the problems considered are of highly topical nature. A drop in the surface temperature on the bottom face of a roof construction is most often caused by air infiltration from an open air cavity into an enclosed cavity, which is situated at the point of the load-bearing construction of the ceiling. This infiltration occurs due to imperfect tightness of thermal insulation, poor-quality workmanship of vapour-barrier joints, incorrect design of individual details. This fairly common implementation defect may be eliminated by a suitable composition of the construction, i.e. the composition of the construction should be designed without air cavities, which dramatically increase the risks of failures and successive biodegradation. It is advisable to exploit ceiling constructions with a lower coefficient of heat transfer (e.g. woodwool panels) as in this way even if thermal bridges arise, we may eliminate a drop in surface temperatures reaching an interval of values within which biodegradation arises. In some ceiling constructions, e.g. gypsum wallboard implies the appearance of some types of fungi, e.g. *paecilomyces*, and the necessity of replacement of all infested parts as this type of mould cannot be removed from the gypsum wallboard either by grinding or by chemical sprays. As can be clearly seen, there exists a fair number of economic and user reasons for the elimination of biodegradation appearance on ceiling constructions of padded sloping roof envelopes.

References:

- [1] BEDNÁŘOVÁ, P.: *Tepelně vlhkostní režim dvouplášťových konstrukcí*. Disertační práce, 2002.
- [2] BEDLOVIČOVÁ, D.: *Rozložení vlhkosti ve zdivu s konstantním zateplením ve vztahu k výskytu fakultativně patogenních plísní*. Disertační práce, 2004.
- [3] SVOBODA, Z.: *Area*. Svoboda software, 2004.
- [4] SVOBODA, Z.: *Mezera*. Svoboda software, 2004.

This research has been supported by CTU 0412711.

The Automatic Classification of B&W Aerial Photos

L. Halounová

halounov@fsv.cvut.cz

Remote Sensing Laboratory, Faculty of Civil Engineering, Czech Technical University
Prague

Thakurova 7, 166 29 Prague 6, Czech Republic

Automatic classification of two remote sensing data types is analyzed in this habilitation. This data type has not been either classified (B&W) or too successfully automatically classified (radar data).

There are more possibilities to perform automatic classification of remote sensing image data. However, these methods do not offer good results if used for monochromatic aerial photographs or radar data.

Method of automatic classification of B&W aerial photographs and radar data processed within this work comprises three processing steps. The first one is image division into base types of land cover existing both in image, and in data. It was forest areas extraction e.g., from agricultural and urban areas. This basic step avoids partly from the problem of similar image data value from different land cover types.

The second step of B&W aerial photograph automatic classifications is new channel calculations offering new land cover non-redundant information. Object-oriented classification is the third step after segmentation into such called primitives, image parts representing thematically homogenous areas or their parts of the study area. Classification used in the work is a part of object-oriented analysis applying fuzzy classification

The processed workflow for radar data automatic classification does not comprise the basic image division into base land cover types. Radar data with their typical „pepper and salt“ outlook do not differ substantially for various land cover types. One case suitable for the image division application could be a land area with large water surface. They differ seriously by their radiometric values from the rest of land cover under certain conditions. It would be suitable to separate them by higher-level segmentation from other areas.

Classifications of individual image data were performed for various numbers of calculated channels by image filtration and Haralick functions for image texture within the work. The methodology was tested on parts of an aerial photograph – one comprised forest regions, the main part of the second one was formed by urban areas – and on the complete aerial photograph.

Evaluating classification accuracies, the best classification was always the classification using the highest number of channels. The best classification of forest areas reached 0.915 value that is kappa coefficient equal to 0.892. The lowest accuracy classification was 0.565 with kappa coefficient 0.446. The urban area classification was equal to 0.897 for the best case and 0.760 with kappa coefficient equal to 0.693 for the worst case. The orthophoto accuracy was 0.920 for the best classification where kappa coefficient was 0.869 and the accuracy of the worst classification was 0.915 where kappa coefficient was 0.859.

The reason of the high orthophoto accuracy was due to smaller details of thematic classes, which the image was classified into. Forest areas were divided only into coniferous and deciduous forest, e.g., and into forest areas with age younger than 7 years on the whole orthophoto, while for the detailed forest classification higher number of classified classes was 982

applied. Difference in resulting accuracy for various numbers of channels is higher for detailed classifications than for the whole orthophoto classification.

Individual orthophoto classes were classified (for the best classification) with accuracy from 82 % to 99 % in case of forest areas, the accuracy of urban area classes varied from 51 % to 100% for the detailed urban classification and from 43% to 100% for the orthophoto.

Evaluating the accuracy of radar data classification, the highest accuracy of radar data appeared in case of the highest number of channels (the whole accuracy was 0.629, kappa coefficient was equal to 0.556). The individual class classification accuracy of radar data varied in 48% -88% range for the best classification.

The mentioned methodology brings satisfying results for aerial photographs. Application of calculated channel by median filter and of three channels calculated by texture measures (using Haralick functions) is a condition of good results.

It is necessary to use additional measured radar data – multitemporal or multipolarizational data – to improve classification results.

References:

[1] HALOUNOVÁ, L.: *Automatic classification of forest areas from B&W aerial orthophotos*, conference GGRS, Goettingen - Německo, 2004

*This research has been supported by CTU0413411
číslo grantu.*

Section 14

**ARCHITECTURE, TOWN PLANNING,
GEODESY, CARTOGRAPHY**

Optimum Laser Systems in Industrial Metrology (part 6)

M. Kašpar, R Blažek, P. Hánek, J. Pospíšil, M. Štroner, L. Línková

`kaspar@fsv.cvut.cz`

CTU, Faculty of Civil Engineering, Dept. of Special Geodesy, Thákurova 7, 166 29, Praha 6
CTU, Faculty of Civil Engineering, Dept. of Geodesy and Land Adjustment, Thákurova 7, 166
29, Praha 6

Atmosphere Influence on Geodetic Measurement The second experimental verification of accessible accuracy was accomplished in the scientific-research network "Stare Mesto pod Sneznikem" in the year 2004 [1]. Attained results confirmed availability and competency of using this method during precise determination of height-differences and consequently also altitudes in mountain fields with big height-differences. This is possible due to better determination of refraction influence on measured vertical angles and accurate determination of slope lengths by the GPS method. Refraction coefficients were determined by three different models in the interval 0.105 to 0.252. The known constant value defined by C. F. Gauss is valid neither as an average one (0.169).

The resaearch team of Ass. Prof. P. Hánek is solving a problem of disposal possibilities of self-adhesive code scales for digital levelling instruments. An experimental field was put up at Faculty of civil engineering and temporal stability of these scales is proved by measurements in this field. External surrounding effect on changes of scales divisions contrast is also monitored. This long time research has not been finished yet. [2]

There was also solved the specific problems of measuring to virtual boundary surface of two parallel planes using total stations with passive reflection. There was made a theoretic analysis of distance determinations using total stations with passive reflection in case of simultaneous measuring to two parallel planes that are situated in different distances from source of telemetric bundle. The experimental testing of theoretical analyses using tool "kneed plate at optical bench" which represents two parallel vertical planes perpendicular to line of sight with different distances from source of bundle and which forms (view from source of bundle) virtual boundary surface between that planes was also performed and it confirmed the theoretic analysis. Theoretic analysis of testing the total stations with passive reflection in case of measuring to an edge formed by two mutually perpendicular planes was made and accompanied by succesful experimental testing of theoretical analyses using a tool which represents the edge and by means of measuring to two experimental edges of the pillars too. Research solves the specific problems of measuring to objects edge using total stations with passive reflection in civil engineering. [3]

The documentation of the current state of the gothic arches in Sloupová síň of Prague castle was made out this year. The total station Leica 307 TCR was used for this purpose. A theory about construction of these arches was proved true on the basis of performed measurements. The main part of this research stage is testing of the laser scanning system Cyrax 2500. This is camera-type scanner with the capability of surveying objects up to a distance of 100 m. The system Cyrax 2500 was used for geodetic measurements of the road bridge near Chomutov. Results of these measurements were compared with results obtained from measurement with a total station.

Laser scanning systems are devices for collection of spatial information with contactless measurement, 3D modelling and visualisation. We tested systems using spatial polar method for determination of the point spatial place. Two experiments were carried out. The first experiment was verification of scanners possibilities to measure different materials under different angles. The second experiment was directed to object measurement under steep angles. They were tested these scanners: HDS 2500, Riegl LMS Z 360 and Mensi GS200. [4]

References:

- [1] BLAŽEK, L. - SKOŘEPA, Z.: *Snížení vlivu refrakce na měřené zenitové úhly (Sanchezova metoda)* Stavební obzor 2005 v tisku.
- [2] CHLUP, J.: *Provozní zkoušky ručního laserového dálkoměru DISTO pro2* Stavební obzor 2005 v tisku.
- [3] ŠTRONEROVÁ, J. - POSPÍŠIL, J.: *Testování stanic s pasivním odrazem II.* GaKo 7 2004 pp. 138 - 144.
- [4] KOSKA, B. - KŘEMEN, T. - ŠTRONER, M. - POSPÍŠIL, J. - KAŠPAR, M.: *Development of Rotation Scanner, Testing of Laser Scanners* In Proc. INGEO 2004 Bratislava 2004 p.p.1/8 - 8/8.

This research has been supported by CTU Grant No. J04-098:21000022.

Development of the Laserscanner, Testing of the Influence of the Materials and the Configuration

J. Pospíšil, M. Štroner, B. Koska, T. Křemen, M. Kašpar

bronislav.koska@fsv.cvut.cz

CTU, Faculty of Civil Engineering, Dept. of Special Geodesy
Thákurova 7, 166 29 Praha 6

3D LASER SCANNING SYSTEM LORS

The 3D laser scanning system LORS (Laser and Optic Rotating Scanner) is being developed to be suitable for scanning of small archaeological artifacts. The system is composed of three hardware components, there is a digital camera, the laser module, which forms a laser plane, and a rotating platform. The calibration of the digital camera on a theodolite was designed and realized so the elements of inner and outer orientation are known. The digital camera JVC TK-C1380E (physical resolution 752x548 pixels) is being used at present. The camera is mounted on the theodolite Zeiss Theo 010B (ŠTRONER, M., 2003). Laser module DPGL-3005L-45 (power 5mW, wave length 532nm) which makes directly the laser plane is used at present as a light source. The rotating platform has a constant rotation velocity (in accordance with required accuracy). It is necessary to level it to the horizontal plane and to determine the position of the center of rotation before measuring. A 3D point is defined by intersection of the laser plane and an optic line. The laser plane crosses a measured object and creates a laser mark which is scanned by the digital camera. The optic line is determined from corrected image coordinates of the laser mark. Each section (image) is independently transformed to the model coordinate system (rotating system). The issue is closely described in (KOSKA, B., 2004). The software system consists of several programs which provide computing of all necessary configurations parameters, automatic scanning of image coordinates and finally computing of the 3D coordinates of the points on a scanned object. The first group of programs provides computing of all configurations parameters (parameters of plane, coordinates of the rotating platform). A least square method is used for adjusting of these parameters. The issue is closely described in (KOSKA, B. - ŠTRONER, M. - POSPÍŠIL, J., 2004). The second component is the program POWOK which provide treating images from the digital camera. It consists of a few modules and allows automatic evaluation of the image coordinates from scanned pictures. The last component is the program "SKENER". This program computes 3D coordinates of points on a scanned object from configuration parameters of the system and from image coordinates of the laser mark.

TESTING OF THE INFLUENCE OF THE MATERIALS AND THE CONFIGURATION

This research is a follow-up to the previous one already published (KAŠPAR, M. - POSPÍŠIL, J. - ŠTRONER, M. - KŘEMEN, T., 2003). Prior to the measuring process itself, it is quite necessary to carefully check the subject and to focus, among other things, on the types of its surface available on the given subject since the quality of surface is one of the most important factors affecting scanning results. A majority of laser scanners used in civil engineering for measuring distances within 100 meters use the polar spatial method for determination of the detail point position – a laser distance meter is used for length measuring. In order to measure the distance between a detail point and a laser distance meter (scanner), it is necessary to make sure that the laser distance meter -generated signal bounces back from the detail point and returns to the laser distance meter with an intensity sufficient for determining the distance. Whether the signal bounces back and its intensity depend,

988

among other factors, on the reflection capabilities of the surface hit by the signal and the angle under which the signal hit the surface. Reflection capabilities of the surface depend on qualities like its color, roughness, dispersion, wavelength used by the laser distance meter, etc. Scanners must be able to handle different types of material reflection capabilities and different laser distance meter beam angles. That is why the goal of the following experiments was to find out how specific scanners handle that requirement. For the purpose of the experiments, plates (150 x 300 mm) with various types of surface were produced (metals, wood, colors, glass, etc.).

The Cyrax 2500 scanner owned by the Stavební geologie a geotechnika company was used at first. The plates were positioned on a vertical wall and scanned from 5 positions from a distance of 25 m. These positions were selected in order to make sure that the laser distance meter-generated beam hit the wall with the plates under approximately the following angles: 0gon, 30gon, 55gon, 75gon, 90gon. The density of scanning was 5 mm x 5 mm. Based on the obtained clouds of points, the program assigned particular colors to the individual points in accordance with the returned radiation intensity. According to the results it is clear that the Cyrax 2500 system is not suitable for the scanning of clear glass, black shiny color and the mirror surface. The second measuring was conducted via the Riegl Z360 scanner owned by the Geodis Brno Company. The plates were again scanned from a distance of 25 m. This time, the scanner's position remained the same during the whole measuring process. The different hit angles (0gon, 30gon, 55gon, 75gon, 90gon) of the laser distance meter-generated beam were produced by the turning of individual scanned plates under precise angles. The density of scanning was 5 mm x 5 mm. The evaluation showed that the selected method of plate measuring was not the best one, therefore, it was not possible to simply produce a similar table as with during the measuring of the Cyrax 2500 scanner. Despite that small handicap, the evaluation showed that the Riegl Z360 scanner was able to scan a majority of materials without problems, however, it faces troubles during the scanning of clear and smoke glass, mirror, and shiny black color – similar to the Cyrax 2500 scanner. Another phenomenon that was detected during the measuring with the Riegl Z360 scanner was the quite clear spread or noise of points.

It is clear from both of the conducted experiments, that the scanning of transparent and shiny materials causes substantial difficulties. That is why we recommend avoiding the scanning of those materials or at least being aware of potential complications associated with their scanning. Due to the very interesting results, the experiments will continue with the CALLIDUS and Mensi GS200 scanners.

References:

- [1] ŠTRONER, M.: *Návrh a kalibrace měřicího systému tvořeného teodolitem a digitální kamerou*. Stavební obzor, 2003, č. 2, pp. 56 – 60.
- [2] KOSKA, B.: *Laserový a optický rotační skener*. In : JUNIORSTAV, Brno : VUT, 2004 [CD-ROM]
- [3] KOSKA, B - ŠTRONER, M. - POPÍŠIL, J.: *Algoritmus určování rovnice obecné roviny pro laserové skenování včetně rozborů přesnosti*. Stavební obzor, 2004, No. 2, pp. 55 - 60.
- [4] KAŠPAR, M. - POPÍŠIL, J. - ŠTRONER, M. - KŘEMEN, T. - TEJKAL, M.: *Laser Scanning in Civil Engineering and Land Surveying*. Vega s.r.o., 2004, 103 p.

This research has been supported by GA ČR grant No. GA 103/02/0357

Rainfall Simulator Aided Research of Soil Erosion Using Field Data

J. Koláčková, T. Dostál

jarka.kolackova@mat.fsv.cvut.cz

Czech Technical University in Prague, Faculty of Civil Engineering, Department of Irrigation, Drainage and Landscape Engineering, Thákurova 7, Praha 6, 166 29, Czech Republic

Soil erosion characteristics are determined in laboratory conditions using the nozzle type of rainfall simulator. The results are used for the calibration of simulation models of erosion processes. The aim of the work is to set up the most suitable erodibility factors for the soils in the Czech Republic to be used for predicting the intensity of soil erosion.

The amount of surface runoff, soil loss and percolation water was measured in 5-minutes time interval during the rainfall events. The basic soil characteristics such as the soil density, moisture, grain size distribution and organic carbon are also observed. The rainfall intensities varied between 40 to 60 mm/h and the slope was 4° to 8°. The experiments were run with two types of initial soil surface: loose or sealed and crusted. Till now, two soils were tested, the clay-loam soil and the sandy-loam soil. The later soil sample was taken from the field plot of the Research Institute of Ameliorations and Soil Conservation and the laboratory results can be compared with the field data. The testing of this soil is still in process.

The results show very different amount of surface runoff between the loose and the crusted experiments. It means that the soil erodibility is not constant in time, but it is higher after the tillage. Later, as the process of sealing and crusting continues, the soil erodibility is lower and after several storms become constant.

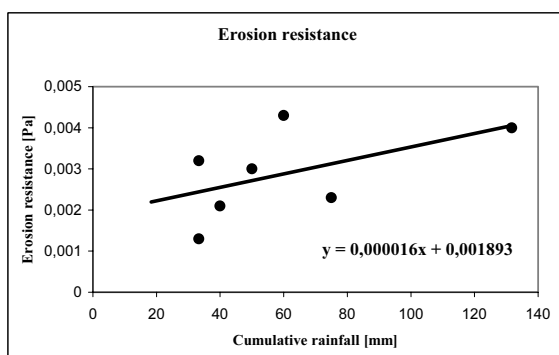


Figure 1: Erosion resistance for the model Erosion 2D/3D.

Several soil erodibility factors were calculated based on the simulation results: K-factor for the Universal Soil Loss Equation (USLE), interrill erodibility K_i for the Water Erosion Predicting Project (WEPP) and the erosion resistance and skin factor for the physically based model Erosion 2D/3D. The model Erosion 2D/3D was also calibrated as described below.

The erosion resistance for the Erosion 2D/3D was at first set from the particle size distribution of the soil. Then, the skin factor was optimised according to the measured surface runoff. Finally, the erosion resistance was established to fit the soil loss data. As the skin factor and erosion resistance are not constant, the regression equations show their time distribution, see figures 1 and 2. The calibrated values of the erosion resistance and the skin factor were validated using independent dataset of the rainfall simulation results.

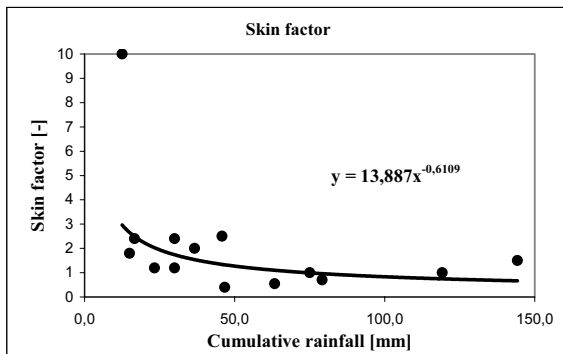


Figure 2: Skin factor for the model Erosion 2D/3D

The erosion resistance values recommended in the Erosion 2D/3D model catalogue for given soil are 0.0015 to 0.0023 for the loose soil and 0.0032 to 0.0040 for the sealed and crusted soil. Particularly for the crusted soil, the predicted soil loss fits very well to the measured data. The model Erosion 2D/3D is suitable for assessing of soil erosion on the clay-loam soil.

References:

- [1] KOLACKOVA, J. - DOSTAL, T.: *Use of rainfall simulator research results as input data for simulation models* In: 25 Years of Assessment of Erosion, International Symposium, Ghent, Belgium, Proceedings. Ghent : International Centrum for Eremology (ICE) of Ghent University, 2003, p. 99.
- [2] KOLÁČKOVÁ, J. - PAŘÍKOVÁ, P. - DOSTÁL, T.: *Chování půdy při extrémních srážkách* In: Workshop 2003 - Extrémní hydrologické jevy v povodích. Praha : ČVUT v Praze, Fakulta stavební, 2003, pp. 199-206.
- [3] KOLÁČKOVÁ, J. - PAŘÍKOVÁ, P. - DOSTÁL, T.: *Erodovatelnost půdy a její experimentální stanovení* In: 4. Vodohospodářská konference 2004 s mezinárodní účastí, Brno: ECON Publishing, 2004, pp. 239 - 243.

This research has been supported by the CTU grantNo. 0403311.

Generalization and Intergation of Geodata

J. Zaoralová

jana.zaoralova@fsv.cvut.cz

Department of Mapping and Cartography, Faculty of Civil Engineering,
Czech Technical University in Prague,
Thákurova 7, 166 29 Prague 6, Czech Republic

Abstract

This article is about generalisation and integration process, rules for integration and about project that are solving in Europe. There are some facts about EuroGeographics and Expert Group on Quality and their projects too.

Fundamentals rule for unequal accuracy precision data integration

Element with most exact localization must have priority and we must use a MasterCard. The MasterCard makes sure relative position one element compared with other elements. The MasterCard for topographic data can be an orthophoto and for administrative boundaries can be an administrative boundaries database.

The next important rule is for updating of existing databases. We can't changing element position if we know that the element don't change its location in terrain and our database is more accurate as another, even thought this element is in another database in another place.

European projects solving generalization and integration of geodata

Solving problems with integration and generalization of geodata is very considerable, because every geoinformation system needs some generalisation and integration processes. These problems solve many European's projects:

- INSPIRE
- ABDS
- EuroGlobalMap, EuroRegionalMap
- Sabe
- Benchmarking meetings

EuroGeographics' Expert Group on Quality

EuroGeographics represents nearly all European National Mapping and Cadastral Agencies (NMCAs). It is the official and united voice of Europe's NMCAs, promotes the NMCAs national and pan-European products and services, and their leadership in building the European Spatial Data Infrastructure (ESDI) and it promotes collaboration and sharing of best practice between our members.

Expert Group on Quality is team that looks into data quality and quality management issues and has produced several benchmarking reports on these topics.

Benchmarking about Generalisation Processes

EuroGeographics' Expert Group on Quality (EGQ) organises benchmarking visits to a member or other organisation in order to identify good practices.

The fourth benchmarking visit of the EGQ was held in Paris on 27th and 28th September 2004 at the Institut Géographique National (IGN), which is the National Mapping Agency representing France at EuroGeographics.

The main topic was a generalization process. The study was focused on automatic generalisation from three different and complementary points of view, according to the experience of IGN: research, project management and production.

The Benchmarking Group Recommendation in Generalisation

The benchmarking group identified following good practices at the IGN that would be beneficial to other European mapping organizations:

- To have resources available for long-term strategic research guided by long-term needs of production
- Outstanding results from the in-house research department were developed and implemented efficiently in production
- Cooperation between the researchers and commercial software vendors
- Willingness to share the fruits of research with other NMAs
- Update information collected in a separate database and used for maintaining several different datasets
- Management of object history (ids, time stamps, linking the current and history records) in the database to enable retrieval of change information (new, altered and deleted objects during a given period of time) for in-house and possible customer needs
- Separation between cartographic databases (based on product specifications and data models) and the master database that supports them
- Use of identifiers to link map names to objects
- Automatic name placement that gives a good starting point for final interactive placement
- Use of a seamless database to produce overlapping sheets and to manage automatic generalisation

References:

- [1] BARROT, D. – ZAMBON, M. – LESKINEN, T. – GOWER, R. – WASSTRÖM, CH.: *Generalisation processes. A benchmark study of the Expert group on Quality.* EuroGeographics, France, 2004, pp. 31.
- [2] ZAORALOVÁ, J.: *Solving of Particular Problems Regarding ZABAGED Update* Proceeding of Workshop 2004, CTU, Prague, 2004, pp. 922-923.
- [3] HNOJIL, J. – ZAORALOVÁ, J.: *Řešení vybraných problémů spojených s aktualizací ZABAGED.* Výzkumný ústav geodetický, topografický a kartografický, Zdičky, 2003, pp. 19.
- [4] ROBINSON, A. – MORISSON, J. – MUEHRCKE, P. – KIMERLING, A. – GUPTILL, S.: *Elements of Cartography.* John Wiley & Sons, inc., New York, 1995, pp. 674.

Railway Heritage in the Czech Republic

T. Šenberger, M. Zlámaný

zlamany@vc.cvut.cz

Research Centre for Industrial Heritage, Czech Technical University, Prague, Pod Juliskou 4,
166 07 Prague 6, Czech Republic

Since 2002 the Research Centre for Industrial Heritage at the Czech Technical University in Prague has actively been participating in the development of the field of industrial archaeology in the Czech Republic. One of the main research projects is the “Documentation and Assessment of Sites at Risk in Selected Sectors”. Currently two sub-projects are under way aimed at documenting and assessing sites in the sugar refining and brewing industries. Thanks to the involvement of doctoral students at the Czech Technical University in the activities of the VCPD it has been possible to prepare other specialised projects within the framework of this research. One of them is a sub-project on “Railway Heritage in the Czech Republic”. Preparation for the project was initiated in 2004 and focused mainly on expanding the literary sources available in the VCPD’s library. Other activities included coordinating a central register of industrial and technical monuments on the territory of the Czech Republic, which is also one of the main projects of the VCPD, along with a register of protected sites according to information from the database of the National Heritage Office and records of other sites that are not yet protected. In cooperation with the National Technical Museum, employees of the VCPD have also participated in the preparation of commentary and opinion statements on proposals for according monument status to railway depots, workshops and stations in Prague-Bubny for the Ministry of Culture of the Czech Republic. The work on the project has been presented in the Czech Republic and abroad [1] and contacts have been established with institutions and professionals working in this field. Industrial heritage, as defined in the charter of the International Committee for the Conservation of Industrial Heritage (TICCIH), comprises the remains and surviving elements of industrial culture that have a historical, technological, social, architectural, or scientific value. Railways without question meet such criteria. Railways and the buildings and sites associated with them represent a significant component in industrial heritage, which is as equally important a part of human history as any other artefact from other times. During the times of the greatest boom in technology, from the very onset of the industrial revolution, which the railways were both a product of and instrumental in furthering, the railways have had a significant impact on human history. Railway heritage is a broad subject that encompasses many fields, even within the Czech Technical University it relates to the activities of most parts of the university, and it relates equally to fields in the humanities, not just history, but also interdisciplinary fields such as the history of technology, technology assessment, and social ecology. The main field through which the VCPD approaches the subject is industrial archaeology and the conservation of industrial heritage. It is essential to view these issues from multiple perspectives in order to satisfy to the maximum degree requirements that are essentially contradictory – preserving historically valuable elements and at the same time achieving the operational parameters of modern railways. The requirements of travel culture have changed quite radically over the more than 150 years that the railways have been operating on Czech territory. The travel cars or the safety features are on an entirely different technological level today. It is logical that contemporary railway transportation puts entirely different demands on sites that often date from the period when the railways were just emerging and which were designed to meet the needs of their time. On the other hand, the majority of these sites and

buildings are of unquestionable architectural quality. Many prominent Czech and foreign architects worked on the construction of railway stations in the country. From an urbanist perspective the railways represent an important catalyst for the growth of urban centres, but at the same time a source of many problems. One big problem that is not just an urban issue is the enormous amount of ground they take up, often on the edge of historical town centres or in what were formerly peripheral areas, but are now suitable locations for further urban growth. Owing to the integrated character and the genius loci of railways, the sites that have been preserved, such as depots or workshops, have been able to have a profound impact on history, and they are tightly linked to the development of towns. These sites, like abandoned factories and other spaces and like the so-called brownfields, offer possibilities for conversion and revitalisation, which are many times more appropriate and provide greater advantages than the construction of new buildings. Conserving other larger sections as a whole, as coherent sets of unified buildings, from the smallest engineer's hut to the station buildings at large railway junctions, accords the railway sites even greater historical value. One of the main tasks of this project is to coordinate various approaches to the issue of railway heritage. Extending the discussion to include the broadest spectrum of experts and specialists should help create a platform for determining and unifying the methodology applied to working with such historical artefacts and for formulating options for the revitalisation or conversion of railway sites and buildings. By gathering information from abroad and in the domestic environment, by conducting independent research, documentation, and assessments of selected sites, and even by preparing the materials and documents required for declaring a site a cultural monument, the VCPD is carrying the work it has been pursuing in this field even further. The VCPD also aims to establish links between ongoing or prepared doctoral projects and study programmes. It is on this basis that the research project intends to include the broadest spectrum of post-secondary institutions that deal with or are otherwise involved in the issue of railway heritage. In addition to the project's collective results, that is, the elaboration and extension of the central register of industrial buildings and sites, and the documentation and assessment of individual buildings and sites, the project outcome should be the formation of a platform for the further development of research in this direction and the dissemination of such information in specialised and professional publications, international conferences, and independent publications.

References:

- [1] ZLÁMANÝ, M.: *Railway Heritage of the Czech Republic and Its Future in the EU* International Scientific Student Workshop: "Technology in the History of Civilisation – Thinking into the Future", University of Technology Wrocław, 2004, pp. 195–200

Testing Possibilities of Using a Standard Digital Camera at Laser and Optic Rotating Scanner. Investigating Method to Evaluate Accuracy of 3D Scanning Systems.

B. Koska

`bronislav.koska@fsv.cvut.cz`

Department of Special Geodesy, Faculty of Civil Engineering, Czech Technical University, Thákurova 7, 166 29 Prague 6 - Dejvice, Czech Republic

Suggestion, realization and testing results of the 3D scanning system LORSM (modified) is presented in the proceeding. This system is modification of the system LORS [1]. The main change is using of another digital camera and different determination method of inner and outer orientation elements (DLT).

The disadvantage of the system LORS is very expensive hardware equipment (digital camera JVC TK-C1380E with special video card frame grabber X-Press plus). Therefore the using of commercial digital camcorder was suggested.

The basic demands for digital camcorder were: progressive scanning, manual control, remote control, stability of inner orientation elements and quality optics. None of financial accessible camcorders had progressive scanning. After wide market research has been chosen camcorder Panasonic NV-GS120EG. The hyperfocal distance was determined.

At first the stability of inner orientation elements was verified by repeated reading of points image coordinates (after defocusing and repeated focusing on a given distance). The mean square error (MSE) of repeated reading is 0.18 pixel for column and 0.16 pixel for row. The stability seems to be sufficient.

The next problem is non-progressive scanning of camcorder and rectangle shape of pixel.

The program AviSynth 2.08 and VirtualDub 1.5.10 (both GNU GPL) was used for solving these problems. The internal filter SeparateFields of AviSynth was used to separate original 25fps interlaced images to 50fps half-images (deinterlaced images). The external VirtualDub filter deinterlace-smooth 1.1 was used for refilling half-images to 50fps full images and the internal filter resize was used for changing video resolution to ratio 4x3 (exactly from original 720x576 to 768x576). The output video was saved as image sequence.

The same image material as from the digital camera with progressive scanning and square pixel was obtained by this procedure. The maximal error is 0.5 new pixel in row.

The computing algorithms from LORS have to be changed for LORSM. The elements of inner and outer orientation are determined by direct linear transformation (DLT) at LORSM. For this reason was made calibration cage with 20 points. The program DLT3k made by Ing. M. Štroner, Ph.D. was used for computing DLT parameters. The mean standard error of DLT was 0.2 pixel. The intersection of optic line (determined from corrected image coordinates of the laser mark) and the laser plane is computed by program DLTR2XYZ.

The configuration of calibration cage (and of the whole system LORS too) was determined by spatial forward intersection from angles with using of the total station Topcon GPT 2006 (mean square error of direction is 0.0020gon). The mean square error estimation of intersection point and of points distance ($m_d=0.08\text{mm}$) was computed by accuracy analysis.

The suitability of DLT method was verified by image coordinates computing of points which has't been used for computation of transformation key (MSE. is 0.29 pixel).

The calibration model for accuracy assessing of the system LORSM was suggested and created. It consists of six identical spheres (table tennis balls). These balls are fixed on

duralumin poles. For determination of calibration model configuration was again used spatial forward intersection from angles.

The accuracy of the whole system LORSM was tested by measuring of calibration model. The created point cloud was fitted with spheres with fixed radius by library SPATFIG (see below). The most suitable method for determining of reached spatial accuracy seems to be using of Helmert transformation in space (using the spheres centers of calibration model). The mean standard error of this transformation is $m_0=0.44\text{mm}$ (mean square distance between points is 0.76mm). Expected mean square errors were smaller. It is probably brought out by unexpected constant errors (irregularity of rotating platform angular velocity or irregularity of its axis motion). The applicability of this system was demonstrated anyway.

The application of the same method on another digital camera with higher physical resolution is planned. The accuracy results of both cameras will be compared.

For accuracy assessing of 3D scanner is often necessary fitting point cloud with geometrical primitives. There is none accessible free-software or freeware for this work. The accessible commercial software is very expensive, doesn't compute accuracy analysis, doesn't work with covariant matrix of measuring and its computation algorithm is unknown.

Therefore the development of the public library (GNU GPL) of classes and functions SPATFIG (Spatial Figure) has started. The main function of SPATFIG is fitting of primitives in 3D space (2D primitives: **straight line**, **plane**, circle; 3D: **sphere**, cone, cylinder ...) by the least square method (LMS). There are solved estimations of mean square errors of adjusted variables and their covariant matrix and there are considered the covariant matrix of measuring. The bold printed primitives are implemented at present. SPATFIG has been already used for evaluation of presented experiments and for determination of the system LORSM configuration (laser plane determination [2]).

Suggestion, realization and testing results of the 3D scanning system LORSM is presented in the proceeding. The digital camera was chosen and tested. The conversion from video format PAL to the format of video recorded with progressive scanning camera was solved. The theoretical and software solution of 3D point computation was solved and tested. The procedure of practical solution was presented and the calibration model was created. The accuracy assessing of the system LORSM was done by measuring of the calibration model. The library of classes SPATFIG for fitting of geometrical primitives by LSM was presented in the last paragraph.

References:

- [1] KOSKA, B. – KAŠPAR, M. – POSPÍŠIL, J. – ŠTRONER, M. – KŘEMEN, T.: *Development of Rotation Scanner, Testing of Laser Scanners*. In Proceedings of the 6th International Conference on Engineering Surveying and FIG Regional Conference for Central and Eastern Europe INGE0 2004 in Bratislava, Slovakia, 2004.
- [2] KOSKA, B. – ŠTRONER, M. – POSPÍŠIL, J.: *Algoritmus určování rovnice roviny pro laserové skenování (An Algorithm of Determination of the Plane Equation for Laser Scanning)* Stavební obzor, 2003, No. 12, 309-313.

This research has been supported by CTU grant No. CTU0404211.

Information System Dikat-P

J. Zaoralová

`jana.zaoralova@fsv.cvut.cz`

Department of Mapping and Cartography, Faculty of Civil Engineering,
Czech Technical University in Prague,
Thákurova 6, 166 29 Prague 6, Czech Republic

Abstract

DIKAT-P is specialized information system. It was developed in Research Institute of geodesy, Topography and Cartography for National Institute for the Protection and Conservation of Monuments and Sites.

Digitalized historical maps can be modified and we can integrate these historical maps into the information system for specification of detailed localization of real estate cultural monuments DIKAT-P.

Information System DIKAT-P

Today the information system for specification of detailed localization of real estate cultural monuments named DIKAT-P makes possible administration and refreshing digital map of real estate cultural monuments, interactive creating, complementing, revising and deleting thematic layer of digital map, importing data to the coordinate system in old exchange format, map layout ascertaining by defined scale, choosing raster data and working with them, differentiating real estate cultural monuments by colour and displaying photographic representation of real estate cultural monuments.

This system with function for inclusion of historical map series can help us with detailed localization of real estate cultural monuments and we will be able to differ protects margins for each real estate cultural monument. Detailed localization of real estate cultural monuments is aggravated by different maps, different coordinate systems, and different way of cartographical map editing and by shrinkage of map paper.

There are some specialised functions for working with raster historical maps such as:

- Attaching historical maps
- File manager
- Raster manager
- Territory manager
- Raster transformation

Attaching historical maps

This is the function that can attach colour raster maps; there are supported two colour maps, 256 and true colour maps. Operator can choose a transparent colour for much data visibility and can choose maps sort order. The function is also able to localize non-georeferenced graphic formats into a coordinate system.

File manager

File manager is a function working with reference files. Operator can with this function attach vector maps and the review maps too. All operations are very simple, because the operations are graphical and interactive.

Raster manager

Raster manager is for attaching and working with raster data. You don't attach raster interactive but in accordance with their scale and name. It is better if you have a lot of raster located in one place and interactive attaching isn't inspectional. You can choose a different colour for each raster with this function too.

Territory manager

This manager is for working with cadastral district and with other administrative districts. You can find concrete district in accordance with its name or number. This function also can switch into another district by its name or number or interactive.

Raster transformation

The function is for transforming one bit raster. There are supported these transformation algorithms: advancement, affine, Helmert, bicubic Coons plate and the Jung transformation.

Data source

The basic data source for this information system are digital cadastral maps, raster actual cadastral maps, old cadastral maps and finally old raster map as maps from stable cadastre and old military maps.

The system can work with all of map together, you must only transform these maps in to the Czech state coordinate system and after it you can attach many maps with the basic digital map.

Conclusion

DIKAT-P is information system oriented at working with raster map. We can work with actual digital cadastral maps, actual raster cadastral maps and with historical raster maps too. There were a lot of specialized functions for simplification work. This function organized used maps, make possible finding in archive and so on and operator can be concentrate on his work.

Digitalization of historical map series and their inclusion into the information system DIKAT-P makes possible better and more elementary access to these maps. And these historical maps will be better protecting against damage because all people will work with digital copy of map not with analogue original.

References:

- [1] KOCÁB, M. – ROUBÍK, F. – ZAORALOVÁ, J.: *Začlenění historických mapových děl do systému DIKAT-P pro upřesnění podrobné lokalizace nemovitých kulturních památek*. Výzkumná zpráva VÚGTK č. 1179/03, VÚGTK, Zdíby, 2003, pp. 49.
- [2] OGRISSEK, R.: *Problems of Historic Maps and Old Maps in Historic Research*. Proceeding of the 8th International Cartographical Conference, Moscow, 1976. pp.13-14.
- [3] SOUKUP, L.: *Spojování sousedních katastrálních území při transformaci digitalizovaných katastrálních map*. Výzkumná zpráva VÚGTK č. 1052/03, VÚGTK, Zdíby, 2003, pp. 35.
- [4] ZAORALOVÁ, J.: *Inclusion of Historical Map Series into DIKAT-P System for Specification of Detailed Localization of Real Estate Cultural Monuments*. Proceeding of Workshop 2004, CTU, Prague, 2004, pp. 920-921.

Exhibitions and Presentations in the Atrium of the Faculty of Civil Engineering and Architecture

K.Kroftová *, V.Šlapeta **

Klara.Kroftova@seznam.cz

* Department of Architecture, Faculty of Civil Engineering, Czech Technical University, Thákurova 7, 166 28 Prague 6, Czech Republic

** Faculty of Architecture, Czech Technical University, Thákurova 7, 166 28 Prague 6, Czech Republic

The educational environment should offer the complementary activities within the university buildings in general. This is represented for example by different exhibition and presentation actions that in the final effect motivate students to a better study results as well as it activates their cooperation with the university.

As the representatives of the Faculty of Civil Engineering, Department of architecture, and Faculty of Architecture, that are in their educational activities very close, we have agreed that the development and improvement of the common “working aids” will bring bilateral benefits. In accordance with the experiences from previous years we have focused on the new and more suitable exhibition and presentation aids, such are the exhibitions panels and frames. Since for the students with architectural orientation (such as the students of Department of architecture, Faculty of Civil Engineering, and of Faculty of Architecture) it is especially needed to present their works.

According to this idea we have bought new set of exhibition panels that are light, easily relocatable, general-purpose and easy to operate and store (the size of the exhibition area is 95x125cm, the complete height of the panel is 180cm, the surface is made of a special material called “velcro textil” which makes it possible to fix the exhibition material by pin, tack or by “dry” zip without demolishing the surface). Next to the exhibition panels we also have bought a set of steel frames (size of 70x100cm, the front cover is made of polystyrene plastic) that might improve the level of instalment of the works. Both, the exhibition panels and frames, are mainly to be used in the common atrium of the Faculty of Civil Engineering and the Faculty of Architecture, so it serve to the students of the Czech Technical University.

With the support of the internal grant we also have organised few students (and doctorate students) exhibitions.

In March 2004 there was an exhibition called “Reconstruction of the Meisterhaus Muche/Schlemmer, Dessau” which took place first in the atrium of the Faculty of Civil Engineering and Architecture and then it was placed in the Goethe Institut, Prague. This exhibition introduced the main principles of the unique reconstruction of the Bauhaus building in Dessau, Germany.

In October 2004 the Department of Architecture, Faculty of Civil Engineering, organised a small exhibition of student’s works of the prospectus “Architecture and Engineering” with the stress placed on the diploma works. This exhibition was well appreciated by the European Evaluation Committee that visited the university in the mean time.

At the end of November 2004 a group of students has prepared interesting exhibition of photographs called “New Berlin 2004”, which introduced their personal view on the newly

built Berlin's Potsdammer Platz and its surroundings. (The posters, made for the university exhibition, are now showed in the Museum of the city Pardubice.)

Since the middle of December 2004 there were two parallel exhibitions in the atrium of the Faculties of Civil Engineering and Architecture.

The bigger one with the name "Architecture of the Central Asia – Uzbekistan 2004" focused on the interesting historical, architectural and natural places of Uzbekistan. Next to the various pictures it also offered detail description of the areas and cities. This exhibition was complemented by a lecture on the same theme.

The second, smaller exhibition, which took place in the same time, was called "Sacral buildings of Croatia 2004". This exhibition introduced few important representatives of sacral buildings, from the point of view of historical, architectural and constructional value, located in the centre of the Zagreb county.

With the support of the internal grant were also started the preparation works of the yearly big exhibition "Students of the prospectus "Architecture and Engineering" and their guests", which is organised by the Department of Architecture, Faculty of Civil Engineering, and take place in January and February 2005.

The year 2004 proved that the possibility to show, to exhibit the student's knowledge is very attractive. It plays important role in the student's motivation and cooperation between students and university.

References:

This research has been supported by CTU internal grant No. CTU 04 17211.

Buildings in Decline in the Textile Industry – Possible New Uses

M. Koiš

`koiš@vc.cvut.cz`

Research Centre for Industrial Heritage, Czech Technical University, Prague, Pod Juliskou 4,
166 07 Prague 6, Czech Republic

In the region of Central and Eastern Europe the concept of “industrial heritage” essentially did not exist for a long time. Historical industrial buildings or technical monuments from the period between the 18th and the 20th centuries survived for the most part only owing to their long tradition or owing to their continued operation and usability for different production. Many of them have been affected by reconstruction, additions and even in many cases by demolition work. Among the professional community dealing with history this trend has been met with considerable disagreement and became the impetus for the emergence of various initiatives focusing on this subject. One of these is the Research Centre for Industrial Heritage (VCPD), operating as part of the Czech Technical University in Prague.

For 2005, as part of its systematic documentation of production sectors and their buildings and sites at risk, one of the priority areas of the VCPD is the textile industry. The methodology and content of this project are consistent with the other similar projects already under way, focusing on the documentation of specific branches of industry that have had a significant influence on the life and character of the Czech countryside. The textile industry, along with the documented sectors of sugar refineries and breweries, is among just such industries.

The inclusion of the project on mapping the textile industry heritage as part of the programme of the VCPD was preceded in 2004 by preparatory work, the objective of which was to gather primary information on well-known locations and to gradually seek out suitable sites for further research work. The lists of localities and buildings compiled as such are used to complement the existing information database in the central register of the VCPD and to validate the register entries. The preparation also included a search for possible contacts prepared to collaborate on work in this area. In addition to doctoral students at the Czech Technical University already cooperating with the VCPD, other individuals and specialists in the regions in which a considerable portion of the relevant sites are located were invited to cooperate. Additional direct cooperation has also been agreed with some heritage institutes and museums that focus on and deal with textile industry heritage.

Activities in 2004 also included the presentation of results to date among the professional community [1] and to the public, and consequently the development of additional contacts at home and abroad. Papers on the evolution and contemporary status of the textile industry on the territory of the Czech Republic were presented at an international conference in Poland in the town of Dzierżonow on 3-5 September 2004. The presentations at this conference were part of the overall presentation of the VCPD. The individual papers presented at the conference and published in a volume of conference papers were prepared by doctoral students working in cooperation with the VCPD on the various objectives that form part of the VCPD's overall mission. There were four papers presented, thematically focused on the following topics: 1) Railway heritage on the territory of the Czech Republic and its future in the European Union; 2) Czech industrial heritage in the textile industry – potential new uses; 3) The transformation of historical industrial architecture in Prague; 4) An introduction to the Research Centre for Industrial Heritage, a presentation of its work to date and its objectives.

On the basis of the research and the data processed in 2004, the objectives for 2005 were defined and integrated into the research programme of the VCPD. These objectives are set at several levels. In addition to the systematic and ongoing work on recording and documenting sites and buildings in the textile industry, especially those at risk, as extended entries in the register or in the form of detailed passports, the VCPD's research agenda targets three basic areas: 1) Creating platforms for cooperation; 2) Outlining the evolution of architectural forms and creating a typology of buildings and sites – and foreign comparisons; 3) Searching for new functions and uses and new conservation procedures for textile architecture. The research objective of creating platforms for cooperation focuses especially on connecting with tradition. The number of enthusiasts interested in the history of textile factories is not as large as those interested in the more popular area of breweries, but their contribution is certainly a notable help to the study of this subject. The ambition of the VCPD in this area is to assume the professional leadership of these activities with the aim of examining and processing the information that is gathered and interpreting it correctly. Cooperation with contemporary textile manufacturers has also proven beneficial, some of which attempt to connect with the tradition of the original enterprise and, especially in relation to changes introduced to the building stock, try to respect the historical value of the original buildings and consult with experts on implementing changes. However, there are still relatively few such cases.

Outlining the evolution of architectural forms and creating a typology of buildings and sites in the Czech Republic is an area that focuses mainly on comparing the as yet insufficiently studied relationship to developments abroad.

Finally, no less significant an objective of the VCPD is the search for new functions and uses for historical buildings and sites and in this way facilitating their survival and conservation. The goal of this area of work is to continue in recording already completed projects targeting buildings or industrial sites, but especially in assessing their strengths and weaknesses of the elected solutions. The intention is to transform these assessments into a unified document as a set of recommendations for working with historical buildings in the textile industry. Such a document is to include a subject index of appropriate, less appropriate, and even inappropriate functions for various types of buildings or situations and a simple methodology for assessing historical classifications and the technical status of sites.

References:

- [1] KOIŠ, M.: *Czech Textile Industrial Heritage – Potentials for New Uses* International Scientific Student Workshop: "Technology in the History of Civilisation – Thinking into the Future", University of Technology Wrocław, 2004, pp. 165–174

Bohemian and Moravian Breweries

Š. Jiroušková, L. Doležal, T. Kužel

jirousko@vc.cvut.cz

Research Centre for Industrial Heritage, Czech Technical University, Prague, Pod Juliskou 4,
166 07 Prague 6, Czech Republic

Beer is a product that figures importantly in Czech industry, one with centuries of history on the territory of the country. Beer became a common beverage among all social levels of the population and over time it has been brewed in increasingly larger quantities. This growth brought about the construction of breweries, and at the turn of the last century, it could be said that every town had its brewery. The network of breweries in Bohemia, Moravia and Silesia was therefore evenly distributed. The World Wars led to a decline in the beer industry and many breweries terminated production. There were fewer breweries, and it was not possible to find satisfactory uses for the sites that were shut down. The communist period was the next painful era; all production was united and smaller breweries served the purposes of storage supply. This led to the deterioration of the breweries that remained unused. Changes were introduced in the 1990s, when industrial heritage began to be considered important. While the funds necessary to finance the conservation and conversion of these sites are not always easy to find, historical and cultural awareness of the value of industrial buildings is spreading.

“Bohemian and Moravian Breweries” is a topic that is intended to initiate the conservation of abandoned breweries as sites representative of national industry. The study is divided into three stages: recording information on all sites and buildings and entering the information into the database; outlining the structural history of the breweries; addressing options for the conservation of breweries and the possibilities for their conversion to new uses and property revitalisation. These aspects will be considered with regard to the infrastructure and social circumstances of the site and possible developments in the locality. Contributing to the conservation of industrial heritage sites at risk in the Czech Republic is one of the main objectives of the Research Centre for Industrial Heritage at the CTU in Prague. The project titled “Bohemian and Moravian Breweries” is one project that targets the field of industrial heritage in the brewing industry. The project was initiated in October 2003 and will be completed in June 2006.

Project outline, stages and objectives

The work on this project has been divided into three main stages. The objective in the first stage of the work is to create a catalogue of existing breweries, which will include not only abandoned sites but also historical breweries that are still in use, and converted breweries, i.e. breweries that are no longer in operation and now have a new function. Priority is given to documenting breweries about which it is known that there exists an intention to target them for demolition. An altogether separate group is made up of those breweries that are designated protected heritage sites. The main items of information in the catalogue pertain to the identification of the site (name, address, location), and photo-documentation. At present (December 2004) the catalogue contains 700 verified sites. The objective of the second stage is to create a detailed study of roughly 100 selected architecturally or otherwise interesting sites as representative from the historical and structural perspectives of the development of breweries. Basic identification data for this group of sites are compiled from archive and especially draft documentation, period photographs, and specialised literature. An example of a site studied and documented in this manner is the brewery in Semín u Přelouče, where a

unique type of malting house facility was discovered. One of the sub-goals of this stage of the project is to create a typological overview of the interior spaces of the breweries and malting houses, their typical structural elements, and the structural development of the individual parts in relation to the modernisation of the technology used in the production of malt and the brewing of beer. Another sub-goal in this stage is to focus on the development of one part of the malting house – the malt kiln – a component indicative of the function of the entire site typified by its characteristic chimney and often also its architectural composition and integration into the site as a whole. In the third stage of the work the most interesting representative examples will be assessed and materials relating to them prepared with the aim of proposing their designation as cultural monuments. Authors of the work will appeal to relevant bodies and bureaus and draw attention to the valuable aspects and elements of the sites, which warrant greater attention and renewed integration into the life of the town, village and locality. This outcome will also include an overview of the most successful examples of converted breweries, in the Czech Republic and abroad, where considerable consideration has been given to finding appropriate uses and functions for the sites while at the same time preserving their historical authenticity. The outcome of the project will be specially presented at the Biennial “Vestiges of Industry” in 2005, the third such Biennial to be held, aimed at professionals and the lay public interested in technical monuments, industrial heritage, and brownfields.

Conclusion

Abandoned breweries comprise a large group of unused industrial sites in decline in the Czech Republic. As sites that feature spaces designed for housing the technology required for beer production, they offer very diverse environments, with the potential to be used in various manners according to the needs of the towns and communities around them or for private activities, etc. There are approximately 1500 breweries of this kind in the Czech Republic, located in small communities, where it is more difficult to find new uses for converted sites, and in larger towns and cities, and even in the historical centres of some cities. Using these sites in new functions offers numerous advantages. The transformation and development of old buildings provides large open spaces for use, while augmenting the value of old art and craftsmanship, the authenticity of the original structures is preserved, and this is also an advantage for urban planning in the local environment, as the sites are frequently accompanied by natural structural elements of such diversity that would require years to achieve in the case of new construction sites. In some cases these sites are examples of exceptional architectural work of significance from the perspective of heritage conservation and important for the cultural heritage passed on to future generations. The renewal of historical industrial buildings should never be a part of sustainable development projects alone, but should also figure in other activities contributing to the conservation and conversion of industrial heritage for new uses

References:

- [1] DOLEŽAL, L. – KUŽEL, T.: *Czech and Moravian breweries* International Scientific Student Workshop: “Technology in the History of Civilisation – Thinking into the Future”, University of Technology Wrocław, 2004, pp. č. strany–č. strany.

The Electronic Interactive Textbook / Publication “Technical and Industrial Buildings in Prague”

Fragner, B.

Jiroušková, Š. - Popelová, L. - Valchářová, V. - Vorlík, P. - Zlámaný, M.

fragner vc.cvut.cz

Výzkumné centrum průmyslového dědictví ČVUT, Pod Juliskou 4, 166 34 Praha 6

This project is a model example of how to take the results of the research on technical and industrial buildings and sites conducted as part of the main activities of the Research Centre for Industrial Heritage at the Czech Technical University in Prague (ČVUT) with the involvement of doctoral students, and to make use of these results for pedagogical purposes.

The history of technology and industry in Prague is presented using the examples of buildings and sites that have survived to date and others that have not. Information is provided under entry headings that describe the buildings, and searches can be made according to the criteria of location, type of building or site, or name. Altogether 350 entries for buildings have been prepared, along with 85 profiles of important figures or firms, 22 entries on the urban development of the administrative districts in the greater Prague area, brief outlines on the development of individual fields of industry, and a chronology of important dates of relevance.

The data entered into the central registry of industrial heritage at ČVUT is integrated and elaborated to include additional information and the result is that users are able to obtain an easily accessible and solid outline of information on their entry of choice. Each entry that describes a building or site includes basic information on the particular site (address, authors/architects, heritage status, etc.), a brief outline of the site's structural history to date, along with a description of the technology or production connected with the site, relevant literature, and illustrations. The entries are linked through an index that contains profiles of firms and in some cases also institutions and important figures (architects, builders, industrialists, entrepreneurs, experts in technology, inventors, teachers, etc.).

The textbook is intended to serve the needs of students in all fields of technology, but is especially aimed at the students at the Faculty of Architecture and the Faculty of Civil Engineering. Emphasis is consequently placed on the structural aspects of sites, and the profiles of important figures are primarily associated with industrial and technical structures. The textbook also serves as a unique guidebook to the City of Prague, and in reference to the technological and industrial developments that took place in the city over time it facilitates an

understanding of the city's urban development. The textbook also largely serves as a source of information for the practical decision-making relating to the future transformations of the various parts of the City of Prague and the changes introduced within them and often also in reference to the conversion of abandoned industrial sites.

* * *

This interdisciplinary project arose with the support of a grant from the Ministry of Education, Youth and Sport within the framework of the development programmes for creating multimedia educational aids. The project is run by the Research Centre for Industrial Heritage ČVUT. The electronic form of the textbook involved the participation of a team of specialists from ČVUT Publishers – the Centre for Educational Support.

References:

- [1] FRAGNER, B. (ED.) *Industrial Prague. A Brief Guide to Technological Monuments and Industrial Architecture in Prague* ABF - Nadace pro rozvoj architektury a stavitelství, Praha 1999

This research has been supported by MŠMT 04427-2004

Research of Historical and Contemporary Architecture - 6th Phase (Year 2004)

P. Urlich, M. Ebel, B. Fanta, E. Fantová, B. Filsaková, M. Hauserová, K. Kibic, P. Kalina, M. Rykl, O. Ševčík, J. Škabrada, P. Škranc, P. Vlček, P. Vorlík.

urlich@fa.cvut.cz

CTU, Fac. of Architecture,

Dept. of History of Arch. & Fine Arts

Thákurova 7, 166 34 Praha 6

During last years the research of the history of architecture that has been developed during whole period of existence of the Institute for History of Architecture of the Faculty of History at Czech Technical University in Prague and has been more and more systematically concentrated on these aspects of technical knowledge, interpretation and the evaluation of the architectural work of the past, which are most influenced by a strange character of architecture as a work of art, expressed by a design form significantly fixed by both requirements on the service of the purpose function and incorruptible technical constructive, technological and other patterns of construction. The research aim involves 9 partial subjects following the suggested issue from various points of views. The selection of these subjects at the basic level contributes to the filling in of the white places in knowledge and to the evaluation of our historical architecture. Its importance inheres in the development and enrichment of the variety of research approaches (study of historical constructions, history of displaying ways of the works of art, deepen the research methodology of historical engineering, research of historical functions of constructions and function construction types, treatise of the architect and his work, study of social cultural context of the production etc.), which systematic development leads to a more and more complex and objective view at the construction culture of the past and view at the importance of the heritage for the current society. It is obvious that the individual „case studies“ do not exhaust the issue indicated by the name of the aim and they even cannot do so. They manifest the range of the work field and the level of the reached knowledge and its depth in particular parts of the research and they indicate indirectly the range of the future task in the branch, which transcend the official framework of this research aim.

Workload of the final stage of solution:

P. Kalina: *Cathedral and Monastic Architecture; the Work of Benedikt Ried*. Initial research field later enlarged on interdisciplinary research of the Prague and Italy gothic architecture. Both the edit of the previous results (the book Prague 1310 – 1419), and research of the work of Benedikt Ried in 2004.

M. Hauserová: *Room and Functional Structure of a Municipal Residential House in the Middle Age and in the Early Modern Time*. A special room structure of some house dispositions sporadically handed down from early Renaissance was interpreted as a result of the need to face the deterioration of light proportion in the case of the volume growth on narrow plot. We succeeded in proving the mass expansion of the traces of this effect in historical construction fond of our towns this year.

M. Rykl: *Residential Middle Age Typology in Bohemia – Disposal and Construction Arrangement, Ground and Reverberation*. The basic thesis of the function and disposal housing requirements in the Middle Ages verified by a detail research of some Prague gothic

houses. Exemplary cooperation with archaeology, which contribute to the desirable clasp of both disciplines and to practical and theoretical maturing of the constructional historical research methodology.

K. Kibic: *Evolution of the School Buildings*. On the basis of a large collection of documentation materials made rich in this stage prepared the selection of objects, which prove best the discovered evolution trends for the publication in a special journal.

P. Vlček: *Johann Philipp Joendl and Czech Classicist Architecture*. The Encyclopaedia of architects, constructors and stonemasons came out in 2004, where the author created all entries of the classicist architects and constructors. The journal Umění (Art) was delivered article about the garden architecture in Veltrusy.

M. Ebel - J. Škabrada: *Historical Constructions and Projects*. A lot of historical construction plans from 16th-13th century, from which is possible to draw information on evolution of historical construction in Bohemia, excel all expectations. Except of the final summary, which is possible to use as an outline for a large publication, it has been published several detailed studies and hold presentations devoted to selected construction types.

M. a E. Fanta: *Czech Architectonic Drawing among the Historism and Modernism*. The selection of the best drawings from the Czech architects inspired by the late 19th century Italian architecture has been presented in the frame of expositions arranged under the auspices of the Czech Embassy in many Italian cities.

P. Škranc: *Rondocubism*. There has been done searches and researches concentrated on the inheritance of the representatives of this art stream. There has been finished the chapters on nationalism and officialities and historism for the publication under preparation. The chapter on the connection with the folk art has been enlarged and completed. Other chapters have been developed in a frame. An enlarged text for the journal Umění (Art) has been composed in the stage of final technical redaction.

The solving team under management of P. Urlich: *Sixties in the Czech architecture*. Research concentrated on the identification of the most decisive trend in the Czech architecture of this period with the stress on the comparison with the evolution in Europe and North America vented in a range of publication activities, which theoretical background sums up the prepared study of P. Urlich and O. Ševčík *Zlatá šedesátá léta v české architektuře* (Golden sixties in the Czech architecture).

Professional community became acquainted with the most serious new and not yet published results of the research work from this period on the seminar Transformation of the historical and current architecture hold by the solving workplace on 12 November this year in the National Technical Museum in Prague.

References:

- [1] KALINA, P. – KOŤÁTKO, J.: *Praha 1310-1419. Kapitoly o vrcholné gotice* Libri 2004.
- [2] ŠKABRADA, J. – KYNCL, T.: *Datování gotických krovů na Starém Městě v Praze* Dějiny staveb, 2004, 198–225.
- [3] EBEL, M.: *Terminologie okenních a dveřních kování ve střední Evropě* Svorník, 2/2004, 217–238.
- [4] RYKL, M.: *Různá okna v těžé době na jednom domě* Svorník, 2/2004, 181–192.

This research has been supported by CEZ: J04/98:21450027

Model Methods of Design, Model and Presentation Techniques in Architecture

M. Fischer, R. Hanus, J. Pospíšil, D. Smitka, T. Šenberger

vmlab@seznam.cz

Faculty of Architecture, Czech Technical University, Thákurova 7 166 27 Prague 6, Czech Republic

Institute of Model Design and Projection, Jugoslávských partyzánů 1580/3, 166 27 Prague 6, Czech Republic

Research Assignment MSM 210000028 deals with the wide spectrum of disciplines of presentation techniques and modelling in architecture. This assignment includes research and its application to the areas of structural design itself, where these methods serve as the fundamental means in the architectural creation process.

We are using in process of projection model categories first:

1/ **model of basic idea**

- **conceptual**, is the first spontaneous concept of the design idea, its sketch-like improvised formulation that is only rarely executed in a particular scale. The material for construction of these models is chosen with the intention to express the structure idea; the reality is not the priority aspect.
- **in scale**, represents the next stage of space articulation.

2/ **draft (sketch) model**

Serves the designer in further creative process to achieve the optimal solution by means of tests, variants and comparisons.

3/ **final model (facsimile)**

Focuses upon 2 fields. It is an important aid and basis for managing, administrative and investment compounds for the purposes of optimum decision and situational assessment.

Physical presentation methods are compared with those of visual simulation, with relation to two-dimensional graphical methods, in standard model type, in digital shape, and with digital modelling methods as well. The research assignment observes the possibilities of interconnection and mutual complementation between these two trends. At the same time the research assignment deals with the utilisation possibilities of a special scanning technique. The solution of the structural task usually issues from a volume dispositional programme, which determines the necessary plan area. The chosen, imaginary organisation of spatial structure conceived in accordance with functional aspects (i.e. mutual and outer relationships of spaces) leads towards the first sketch. At this moment we have achieved the stage in which, besides handling two-dimensional areas and planes, the spatial design, i.e. three-dimensional form of the structural body and the space, must start.

New Methods of Model Design

Our architectural model workshop has been equipped with machines that can be used for 3-dimensional digitising and rapid prototyping too. This method include next proceeding:

1. Two dimensional sketches on paper
2. Conceptual model of basic idea (without scale) made by hands
3. Transformation of this physical model into the computer by 3D scanner
4. Working on idea a sculpture like kind of work and design the PC-model in scale in program RHINO
5. Transformation of PC model to the physical form by 3D printer

Our workshop for modelling is using this type of machines:

A/ 3D – scanner - Immersion MicroScribe G2 is a powerful tool for performing 3-dimensional digitising. This machine communicates a host computer through a standard USB port or RS-232 serial port. The system includes the digitising arm unit, which houses the internal electronics, a USB cable a serial cable, an input device, and an external power module.

B/ 3D – printer - Dimension is the first modeller designed with ultimate simplicity in mind, which will build models quickly. The system models with ABS plastic, so modelled parts will be strong and durable. ABS also ensures you'll be able to drill, tap, sand, and paint your creations. Dimension builds models, including internal features, directly from CAD STL files.

Methods of Computer Models Design

Research assignment deals with the wide spectrum of disciplines like relationship between digital and physical models used in teaching processes in ateliers of architectural creation.

Another direction of research is a question about light problems in render technology of computer modelling. It compares simulation of reality with its illusion and works with radiozity backgrounds, environments, model /figure/ and its ground. A combination of three or more kind of light use /key light/ in angle of 45 0 from the top with a combination of another kind of light like frontal light, fill light, unidirectional illumination, point light or sometimes parallel light.

Last but not least is a question about discipline of architectural and historical field research. This subject is a base for creation of digital models of architecture, especially czech cubist architecture well known all on the world.

References:

- [1] J. POSPÍŠIL *Model-creative mean in the process of design*, Čs. čas. Forum 6 2002, .
- [2] D. SMITKA, T. ŠENBERGER *Conceptual model* Čs. čas. Forum 6 2002,
- [3] R.HANUS AND COLLECTIVE: *Exhibition about model design and model methods of projection*, Old town hall of Prague, 2004 june-september, Hall of Architects.
- [4] M. FISCHER *Digital czech cubism* Digital Design, CAADe conference Graz Austria 2003

This work was funded by the Czech Ministry of Education as a Research Assignment

MSM 210000028

Brownfields and Their Consequences

Z. Kramářová

`z.kramarova@seznam.cz`

Department of Urban Development and Regional Planning, Faculty of Civil Engineering,
Czech Technical University in Prague, Thakurova 7, 166 29 Prague 6, Czech Republic

The process of the rise of brownfields (lit.[1]) apparently has many consequences for the locality itself, its closest surroundings and the town. The consequences of the rise of the brownfields can be divided into two types - direct and indirect. As direct consequences can be considered unemployment and the overall degeneration of the environment. As indirect consequences can be seen the departure of population, the capital investment outflow, the cutdown of the population's ability to buy, price fall in real estates, downfall of the small and middle business especially in the sector of services, population separation leading to the genesis of slum area, the increase of crime and the reduction of the aesthetical and the ethical feeling of the population.

A derelict area is not often in good technical state, because its owner usually does not have enough funds for the required maintenance. The buildings will slowly start to fall apart, wild trees will grow over the areas – it comes to an aesthetical and functional degradation of the environment.

The problem of unemployment after the birth of the brownfields would have to be of utmost priority. At the same time it is one of the big differences in the way of solving brownfields in small towns and large agglomerations. Especially small towns would stress out the anticipation of the rise of brownfields. All this can be shown on a simple example of two towns – Pardubice, Nova Paka. It makes a great difference when 1000 people lose job in Pardubice (the population is at about 94 000) or in Nova Paka (the population is at about 9500). In Pardubice, it is “a trouble“ if the town but unemployment increases only about 1 % (only in case that nobody of them finds a new job). If Nova Paka is in the same situation, unemployment will increase about 10,5 % and it will be a great “disaster“ for the town. Moreover the probability of finding a new job in Pardubice is much more higher than in Nova Paka. There is a higher probability to find a new job outside the original domicile (most often in a bigger town).

If the inhabitants have to commute to job, they are forced to spend money for transportation and it decreases their ability to buy. Therefore the shoppings are frequently realized outside the original domicile which causes the outflow of money from the area. The inhabitants go back to their domicile only to sleep, their domicile becomes a satellite (see more details in the issue of estates, which is not a part of this work).

The town can take in question the variant of the population's commuting to work – inhabitants do not commute, they move quite out of their residence. If residents leave the town, they sell their flats or houses, provided that number of outgoings rises up over the maximum limit, the market with real estates will become oversaturated the prices will fall. At the same time the exceeding of the limits can result in all probability in such a great decline in the number of inhabitants, that it will turn out to a surplus in the capacity of civil facilities, especially services. As a result of the market economy middle and small business will be ruined.

In some period of the cease of services it comes to important demographic-social changes in the locality. People of high and middle social-economy layers leave the locality and it comes to

the social-economic inflow of weaker and problematic groups of inhabitants (drug addict, gangs, ...) – a slum is born. The crime will rise among these problematic groups of people, in the time the area will become an isolated ghetto, where „only the strongest ones will survive, the others just will slum“.

In such environment it is very difficult to get or retain the aesthetical and the ethical feeling. Through the time it comes to blunting and their lost is unavoidable. It is given also in the so-called Maslow's pyramid of values, where there is proven, that man is able to anticipate values situated at no more than four levels higher than their own existence.

It's necessary to avoid the rise of brownfields or we have to take measures to eliminate their growth. This can occur only when fulfilling some prerequisites.

The first premises are the multidisciplinary educated state officials and town councilmembers, who will identify the problems in time and solve it in its beginnings. Multidisciplinary education is meant to be the professionalism not only in one field, but other in interrelated fields too, for example: sociology, law, economy, building, ecology, regional planning.

The second presumption is the formation of index brownfields, which would serve as the list of brownfield localities, of which investors can choose the areas appropriate for their capital investments and they do not take over other greenfields. Necessary condition is however its reasonable updating – at minimum once a year.

The last longtime premise is the complete optimization of conditions in the locality for entrepreneurship – it means especially creating an economically stable environment.

References:

- [1] KRAMÁŘOVÁ, Z.: *Issue of Born of the Brownfields in Small Towns* Juniorstav 2004, 2004, 417.
- [2] KRAMÁŘOVÁ, Z.: *Brownfields and Their Consequences in the Small Towns* Workshop W1-410, 2004, 33-38.

This research has been supported by GA ČR grant No. GD 103/03/H089 and by MŠMT grant No. MSM6840770005.

Brownfields and Industrial Heritage – the Tools for the Revival of Towns and Landscapes.

T. Šenberger, F. Štědrý

senberger@fa.cvut.cz

Research Centre for Industrial Heritage, Czech Technical University, Prague, Pod Juliskou 4,
166 07 Prague 6, Czech Republic

The preparation of a course on Brownfields and Industrial Heritage comes as a direct reaction to the current situation in the Czech Republic, where the impact of transformation and of the reduction of production in the industrial sector since 1990 is compounded by the high degree of industrialisation and urbanisation in the country. The fact that the Czech Republic contains a large proportion of territory on which there are abandoned industrial, military, or transportation-related sites, which as so-called urban brownfields are insufficiently or inappropriately used, is one of the factors that has a negative influence on the country's future development. In addition to the environmental, property, and economic obstacles there also arises then the problem of sustainable development and the potentially negative social and cultural consequences associated with the problem.

In the context of the experiences in the countries of the European Union this educational course makes use of the contacts and information concentrated at the Research Centre for Industrial Heritage to summarise the available knowledge and information in this area that can be employed as a practical tool for solving specific problems at the state-wide, regional and local levels. Examples of industrial regions in the country that have experienced or are currently experiencing similar processes of restructuring in the industrial sector provide tested and proven approaches and opportunities: targeted initiatives and managed approaches set up by the state and local administration, investment and construction activities in the towns and regions, and the creation of new opportunities in the labour market.

This course emerged as a project in cooperation with a number of other institutions, and it offers a topical, methodological and organisational curriculum of a post-graduate course aimed at employees in state administration and regional administration, architects and urban specialists, employees in the national heritage conservation bureaus, and regional territorial planners and designers. The purpose of the course is to broaden and complete the education of these employees in the area of the rehabilitation and revival of decaying and inappropriately used parts of towns, with sites abandoned by industry, the military or the railway industry. The objective of the course is to explain and provide a rudimentary understanding of what brownfields are in the Czech Republic, compare the possibilities and methods for newly integrating these areas into the urban area of towns and into the rural landscape, with a view to the reasonable conservation of industrial heritage, as is the case in the countries of the EU, e.g. in the United Kingdom, Germany, France, Austria, and elsewhere. The course provides information and knowledge that is useful not only from the perspective of environmental rehabilitation, urbanism, and heritage conservation, but also in connection with the legislative, social and technological aspects related to determining practical solutions to the problem of finding new uses for brownfields and the conversion of industrial sites to new functions.

The course includes almost 60 hours worth of lectures presented by 17 lecturers, and it is divided into seven thematic blocks:

1 Brownfields as a Part of the Heritage of Industrial Civilisation

Urban brownfields are a concomitant phenomenon of the post-industrial stage of the

evolution of society. Determining the sources of their origin, their general context and their social context is one of the necessary preconditions for determining possible new ways in which to use their spatial, economic and cultural potential for other functions and to create programmes and concepts for their regeneration.

2 Regeneration Strategies as Part of the Development of Settlements and Regions

The concept of sustainable development leads to the promotion of policy and strategic principles that prioritise the development of settlements through the revitalisation of brownfields in an urban environment as opposed to the advancement of suburbanising elements on greenfields, i.e. at the expense of the expansion of urban agglomerations on undeveloped ground and the undesired appropriation of public land and the countryside.

3 The Obstacles and Risks Involved in Regeneration

The circumstances in the Czech Republic are such that the largest obstacles to putting urban brownfields to new use are property-rights issues, insufficient initiative on the part of the state's political bodies, especially at the local level, environmental difficulties and the obstacles to solving environmental problems, inadequate conceptual, organisational, and territorial-planning preparation for the implementation of regeneration projects. The activities and cooperation of partner components at all levels of addressing the problems of the revitalisation of brownfields is a necessary precondition for the successful implementation of any such project.

4 Tools for Regeneration

Finding new uses for the areas facing these kinds of developmental difficulties and their reintegration requires the formation of new economic tools and multiple-source financial resources. The methodological approaches and legislative tools of regional planning also offer some specific possibilities. Examples from the Czech Republic and abroad offer a comparison of approaches and results with countries that have more long-term experience with the processes of regeneration.

5 The Conversion and Conservation of Industrial Monuments

Industrial heritage also includes sites that are of sufficient value to warrant protection as monuments, and other sites that for various reasons are worth conserving and putting to use in new ways. This requires specific forms of assessment of such sites from architectural and technological perspectives, the use of methodology based on structural-historical studies, and documentation on industrial or technical monuments.

6 Planning the Implementation of Projects

The developmental potential of particular territories is the basic precondition for any regeneration project, for establishing goals and policies, and for developing urban plans designed for the transformation of a particular area. The involvement of communities and regions in the process of developing solutions for urban brownfields through state and European programmes supporting transformation operations is the basic precondition for any realistic project.

7 Excursions, Final Report

The aim of the excursions is to verify theoretical assumptions in specific locations and applying proposed solutions to models.

The course organisers summarised their lectures in a volume published on paper and in electronic format. The course was introduced in November 2004 at a seminar titled "Brownfields - Projects and Research", which was part of the research project of the Ministry for Local Development titled "The Revitalisation of Zones for Public Administration WB-41-04". Information on the course is available at: <http://vcpd.cvut.cz> and <http://www.brownfieldsinfo.cz>.

Formation of Planners in the Next Decade – Trends and Strategy

I. Horký, A. Mansfeldová

horkyi@fsv.cvut.cz

Alena.mansfeldova@fsv.cvut.cz

CTU, Faculty of Civil Engineering

Department of Planning and Regional Development

Thákurova 7, 166 29 Prague 6, Czech Republic

To learn complex and not only technical and technological problem – solutions is especially important for those, who form man-made environment through design, building and construction processes.

1. Body of knowledge and contextual sensibility.

As a response to current needs, the Department provides a complex of courses of City- and Regional-planning, Urban Design and Settlements' Development for all students of the Faculty of Civil Engineering and guarantees a professional module of Urban and Rural Areas Planning. It offers at the same time the advanced, postgraduate studies in the subjects described above. The teaching concept is based on the fact that the interdisciplinary character of development and management of human settlements and regions requires conceptual specialists with interdisciplinary professional orientation, who will be able to design and make qualified decisions both on the basic level of state administration, that is in Local Authorities' councils, as well as on higher levels of state administration, and who will be able to set and process the planning documentation of the area. Moreover, they should be able to identify and assess cultural values of environment, needs of preservation of nature and cultural monuments, integrate proposed new developments into existing environment and last, but not least to make distinction between the real needs of citizens on one hand and particular interests of lobbying groups and corporations.

2. Project – problem based education of Planners.

Since the very beginning of the reformed study of Urban Planning and Regional Development at the Faculty of Civil Engineering in C.T.U., Prague, the programs are project – problem oriented. Every student willing to pass, has to produce a series of designs and projects assigned on current tasks of development or redevelopment of selected Czech and Moravian cities and villages. Referring to our experience, we are convinced that problem based education of Planners should be above all the opportunity how explain philosophies, approaches, policies and principles using the typical sets of problems of urban and regional developments

3. Understanding of a “problem” in the Education of Planning and Regional Development.

The concept of project-problem based education leads us to some hesitations about what the “problem” means in Civil Engineering?

Is the complexity of current world's reality sufficiently reflected in Civil Engineers' education? After all, even for two Civil Engineers of different profession the same specific task to design, let's say a new motorway through the city may represent “problem” of two very different kinds: destruction of existing structure of the city for a Planner on one hand and squeezed space available for Transportation Engineer on the other. What Planner and Architect consider be a problem of major importance is not seen as a problem by Civil Engineers at all! So, relativity of “problem” in Civil Engineering is a real problem. We are convinced, that complex processing of

“problem” in Civil Engineering: identification - assessment - structuring - proposal of adequate means for solution - choice of optimal solution - evaluation of results is actually one of the most important issues of education.

4. From Project – problem based learning to Project – value oriented Education of Planners.

Creative approach, alternative solutions, complex assessment are therefore prerequisites for appropriate identification and reflection of real values of existing environment on one hand and proposed problem-solutions on the other. Here, the following questions might be raised:

1. “Are the categories of „friendly cities“, „pleasant environment“ and „preserved landscapes“ meaningful to Civil Engineers? “
2. “How increase the sensibility of Civil Engineers to esthetical values of buildings, urban space and landscapes?”

5. Implementation of sustainable development strategy in the Education of Planners.

The education in interdisciplinary professional modules was considerably extended. One of such modules is „Planning of settlements and regions“ and is fully practised by the Department of Planning and Regional Development with the aim to form Communal Engineers, Planners and Communal Politicians, who would promote the following rules of man’s behaving in the environment :

- to change the man’s behaving in environment from exploitation of natural resources towards careful cultivation and in conformity with biological cycle
- to optimize the economy of limited natural resources and environmental potential
- to suppress the sectorial approach in favour of the complex creation of environment
- to forecast the relations rather than target values in different time – horizons
- to produce alternative proposals of problem – solutions, tools and means for development of settlements and regions
- to contribute to reinstallation of natural balance in areas
- to collect information on territory and develop methodology of data base treatment as means for realistic prognosis, long-bearing plans and development programs.

It is obvious, that these newly profiled Professionals need not only the technical formation, but also the basic knowledge of humanities (philosophy, politology, sociology), of planning and architecture and also be sufficiently informed about economical, legal aspects of building and construction, financing and management of territory and settlements.

References:

- [1] Madows, D. H. and collaborators: *Beyond the limits*. Chelsea Green Publishing Company, 1992.
- [2] Horký I.: *Principals of Settlements’ Environmental Transformation in the Current Practice of Planning*. Proceedings of the International Seminar on Environmentally Compatible Structures and Structural Materials, Prague – C.T.U. Press, 2001
- [3] Broadbent G.: *Emerging Concepts in Urban Space Design*. Van Nostrand Reinhold Int., New York, London, 1990
- [4] Ortega y Gasset, J.: „La rebelion de las masas“, Revista de Okcidente, Madrid, 1930
- [5] Lorenz, K.: „Eight lethal sins of a civilized man“, Munich, 1973
- [6] Mansfeldová, A. – Moos, P.: „Creation of Human Settlements and Synergic Phenomenas“, Stavební obzor č.3, 1997
- [8] Horký I. – Mansfeldová A.: „Education of Professional in Sustainable Urban and Regional Development – Philosophy behind“, AECEF Symposium, Porto, 2002

Section 15

**TRANSPORTATION, LOGISTICS,
ECONOMY, MANAGEMENT**

Reliability Aspects in Contemporary Management

R. Flegl

flegl.isq@nextra.cz

CTU, Faculty of Mechanical Engineering,
Department of Management and Economics,
Horská 3 128 00 Praha2

Enterprise reliability is necessary for making good products in time specified in contract. Reliability of supplies (goods delivery) to customer as well as quality of product and price is criterion of competitiveness. Process reliability is therefore important for organization if it wants to survive and have a success on the market. Especially in automotive industry time point of view is fundamental and very actual in present because of production planning by JIT (Just - in -Time) method, which is widely used in the branch. In JIT system producer minimizes its production stores and has only operational stock for very short time of production. Therefore it is necessary to deliver supplies punctually in time (specified in the contract) directly to assembly line. Delayed supply is serious threat for customer production (it can stop whole assembly line). If delay cause losses customer exact compensation by supplier. Premature delivery on the other hand is not desirable as well, because of absence of customer storage capacities. Non-satisfaction and subsequent loss of important customer may cause serious economical problems or breakdown of supplier.

How to comply increasing emphasis on time accuracy in supplying?

Under pressure of decreasing the price on the market it is not possible to solve the problem by production stores, as it was usual in the past. Production stores, as is known from the economics, lead to increasing the costs and make operational capital unavailable. Only one right response to this contemporary challenge is optimalization of processes from reliability point of view, so as we were sure (with some level of residual risk) that inputs will be transformed to the outputs (products) in specified time and customer will be satisfied.

Reliability theory has been widely used in the sphere of technical objects and systems reliability. Pioneers in this field were branches as aerospace, nuclear power and automotive industries, where possible failure of product has social non-acceptable affects, or electronics, where reliability is serious problem because of high complexity of electronic products. Process reliability has been at the edge of interest.

For improving reliability of whole suppliers process, i.e. production and delivery of products to customers, it is necessary to leave perceiving of organization as only "black box", which transforms inputs into the outputs and look into its internal structure - complex cybernetic system. Whole process is result of connection of a number of subprocesses. Reliability of the whole process is influenced by reliability of these subprocesses. Right connection of subprocesses has also significant importance.

It is possible to identify a number of factors, which play the important role in process reliability. To succeed in process reliability analysis it is necessary to categorize these factors using for example Ishikawa diagram. In list bellow are defined main process factors in relation to basic manager questions:

- Human factor: Who does it?
- Environment: Where is it done?
- Procedures: How is it done?

- Machines: Which machines and tools are needed?
- Material: What is it made from/of?
- Information: What information is needed?

To succeed in process reliability improving it is necessary to apply a systematic approach - for example realization of following steps:

1. Analyze the whole process and divide it into subprocesses.
2. Divide these processes into categories according to their function: main processes, supporting processes, processes of management.
3. Analyze sequence and connections among subprocesses: inputs and outputs of subprocesses, time point of view (sequence, parallel subprocesses and serial subprocesses).
4. Identify critical subprocesses: importance (e.g. by FMEA method), time (e.g. by CPM method), replaceability / possibility of reserves.
5. Analyze reliability factors of critical subprocesses (e.g. by Ishikawa diagram method): reliability of production machines and equipment, human factor reliability, quality of material inputs, reliability and quality of information inputs.
6. Identify which of these factors are significant (or critical).
7. Choose appropriate methods for analysis of possibilities of critical factors reliability improvements in process.
8. Plan and realize improvements.
9. Verify effectiveness.

Improving process reliability needs systematic approach and never ending effort. The good news is that the effort is rewarded by better market position and economic success.

References:

- [1] GARSCHA, J.B.: *Rozvoj organizace pomocí managementu procesů* Česká společnost pro jakost, 2003.
- [2] MELAN, E.H.: *Process Management. Methods for Improving Products and Service*. Mc.Graw-Hill, Inc., 1993.
- [3] MYKISKA, A.: *Spolehlivost technických systémů* Vydavatelství ČVUT, 2004.
- [4] PANDE, P.S. - NEUMAN, R.P. - CAVANAGH, R.R.: *Zavádíme metodu Six Sigma* TwinsCom, 2002.

Decision Making for Production

M. Kavan

kavan@kar.net.fsih.cvut.cz

Department of Enterprise Management and Economics, Faculty of Mechanical Engineering,
Czech Technical University, Horská 3, 120 00 Prague 2, Czech Republic

It is characteristic of the production environment, due to its dynamic nature, that the decisions have to be made with imperfect information. Over the years there have been various degrees of interest in the techniques and tools which could aid the executive in gathering and quantifying information in the decision-making process.

Early efforts in the use of quantitative techniques for decision making were almost always oriented toward operational problems. While a particular example may seem trite and unspectacular to us in this day of computers and sophisticated mathematical models, it does illustrate an important point. There was the need for isolating and treating quantitatively all the variables involved in a given operating problem. We recognised that to fill the barrow with different materials required different amounts of time. We recognised that in order to have a quantitative base on which to make a decision it is important to measure. It has been only in the last few years that our technology in computer data collection, storage, and retrieval and the development of quantitative operations research techniques have enabled the business community to base decisions on facts rather than intuition.

Almost all approaches to quantitative decision making generally involve some common underlying characteristics including:

- A well-defined objective
- A mathematical and/or logical model
- Optimisation process

The objective of most quantitative analysis is usually associated with either the improvement of the organisation's profits or the reduction of its costs. In the field of production, however, mathematical models may be classified either by the form they take or by the method of solution. If we are to classify models by the method of solution, we would specify those models which can be solved in closed form and those which can be solved by simulation. Closed-form models are those for which the state of the art is such that the equations can be solved mathematically. Simulation models, on the other hand, are those for which a solution is obtained by assuming certain values for some of the variables to obtain values for the variables of interest. To achieve its full usefulness the model should capture the essence of the problem and be solvable. However, developing a model which leaves out a significant variable or relationship may well lead to more damaging results than if this approach were not used in the first place.

Once a mathematical expression or model is obtained for a problem, the model is generally manipulated in an attempt to achieve an optimum solution. The best possible solution considering the variables, costs, and relationships in the model is desired. Optimisation in the broadest sense will often apply in balancing the cost of seeking better and better solutions against the potential benefits of these better solutions.

Expected value is a criterion frequently used in quantitative decisions for making a choice between alternative courses of action. However, considerable care should be taken in using expected value as our decision criterion. Utility is simply a way of representing the intrinsic value of money. For example, a company may evaluate a potential loss of \$1,00,000 as quite different than just double the loss of \$500,000 if the larger loss would result in bankruptcy. On the other hand, a very large gain may allow a further spectacular investment. It is possible

that a small, consistent profit is more important than large profits one year followed by losses in the following year. It is the answers to questions of the preceding type which allows a firm to develop a utility function or determine some of the important characteristics of the utility function that it will use. Therefore, we shall refer to "utility" as the subjective value that a person or firm obtains from a particular return in a given situation involving risk.

Forecasts are essential in formulating inventory policy. Every business uses a forecast of some kind in planning its buying and manufacturing program and in planning expansion and cutbacks. The forecast may be only the statement that next year will be like this year, or it may result from a long analysis of the economy, the industry, birth rates, etc., or it may be only the result of wishful thinking. The efficiency of the inventory policy will depend on the accuracy of the forecast and the knowledge of the market. There are forecasting methods which act as servomechanisms, i.e., new forecasts are regenerated, say, monthly, as information on the market is gathered. Forecasts generally fall into two classes:

- Continuous
- One shot

Both classes of forecast, and indeed, any forecast, are probabilistic statements expressed with a degree of reliability.

There are many industries where there is an opportunity for making only a single buy decision due to the highly seasonal nature of the business. This occurs quite frequently in the retail industry in "high style" and "fad" items. If the buyer purchases too many of the items, he will have a loss due to obsolescence. On the other hand, if he buys too few of the items, he will have lost sales. It is possible to develop quantitative rules which prescribe optimum ordering quantities based on expected-profit considerations. The measure of effectiveness of the buying policy is the expected profitability of the last item, which is defined as the expected gain minus the expected loss. One should buy an amount such that the expected profitability on the last unit is positive.

A key function of the production manager is decision making. Every manager is continuously faced with choices among various alternatives.

ANOTACE: Rozhodování ve výrobě má svá nesporná specifika, daná například náhodností poruch strojů a zařízení. Vzniká dynamická rozhodovací situace, kupříkladu řešitelná v článku uvedenými způsoby.

References:

- [1] VANIŠ, L.: *Decision Alternatives Evaluation Under Risk With Incomplete Information on the Probabilities of Scenarios*. Czech Technical University, 2004, pp.126–128.
- [2] ZELENK, A. – PRECLÍK, V.: *Realisation of the Leonardo Project-Effective Production Management*. Czech Technical University, 2004, pp. 122–125.
- [3] ZRALÝ, M. – PLACHÝ, M.: *IT Support for ABM Oriented Planning*. Czech Technical University, 2004, pp. 86–90.
- [4] DAUN, CH.: *Service Engineering-How to develop New Services*. Czech Technical University, 2004, pp. 15–18.

Effectivity of Research

H. Nassereddine

M. Ayoubi *

Houssam@seznam.cz

Majed@seznam.cz *

CTU, Faculty of Mechanical Engineering, Dept. of Economics and Management

Horská 3, 128 03 Prague 2

It is possible to characterize effectiveness as rate of success of the transformation between inputs and outputs.

In economic science, it is possible to express the effectiveness, for example, Investment as ratio of income to investment. In production operation effectiveness can be viewed in the light of invested and gamed time.

In scientific areas it is possible to calculate the effectiveness, like the interpolation and acquire of the information, like the graduation of the science information. Here is necessary to solve the problem of tranformation of the information. Steer sometimes like social time, sometimes like price, another time like utility.

Research is then generally accounted as priming stone of future innovation, into is necessary first to input substance in definite shape. Their deposit presents regarding to the production, interference of that deposit into research can account as achievement and mutual relate ratio means the effectiveness of research.

Output-input relation in its moneywise representation presents the economic effectiveness.

When investigation the degree of economic effectiveness, as a rule is used this relation relation:

$$K_E = (N_0 - N_1) / I$$

Where,

K_E ... coefficient of economic effectiveness,

I ... addition interpolation costs,

N_0 ... prime cost starting period,

N_1 ... prime cost further period as a rule decrease owing to innovation.

Time, under which additional amount incurred on innovation cover from reducing the costs of production, it is possible calculate by the :

Doba, za kterou se navíc vynaložené prostředky na inovaci uhradí ze snížení výrobních nákladů, lze spočítat podle vzorce:

$$T_E = I / K_E = I / (N_0 - N_1)$$

Where,

T_E ... is backflowf period in addition exercise substance.

Economic effectiveness (E) is then defined by relation:

$$E = I_1 - I_0 - V (N_0 - N_1)$$

Where,

V ... volume of production under operating time innovation.

References :

- [1] JIRÁSEK, J.:Řízení výzkumu – vedení výzkumu, díl 1, Institut řízení, Praha 1974.
- [2] JIRÁSEK, J.:Řízení výzkumu – výzkumní proces, díl 2, Institut řízení, Praha 1976.

Defining and Assessing E-learning

Ing. Darina Tvrđíková

darcat@centrum.cz

Department of Management and Economics, Czech Technical University, Horská 2, 120 00
Prague 2, Czech Republic

Computer-based training, learning-management systems, and synchronous or asynchronous learning conducted over the Internet, an intranet, or extranet, are all forms of E-learning if they include a tailored multimedia experience offered individually at any location. That experience lets learners work at their own speed, better retain information, and repeat exercises as needed to build usable skills. It focuses not only on how well employees master critical material, but also on how that mastery is applied in on-the-job performance. By far, the best E-learning efforts include the involvement of CEOs, CIOs, and COOs who relentlessly link interactive education to bottom-line, real-life business drivers. This is a hands-on undertaking in every sense. When executive-level support is present, E-learning can show a quick ROI and help business audiences accomplish their goals. Industry analysts generally agree that done correctly companies can enjoy 40% reductions in training time and expenses using E-learning versus traditional classroom delivery. As a guideline for spending, first identify the real cost of the business problem at hand. Development of successful E-learning also requires an initial investment of time at every level, including the executive suite.

E-learning is a growing trend among many higher educational institutions. Learners and teaching professionals are attracted by the many benefits of e-learning, such as the flexibility of learning anywhere, at any time and at an individualized pace. The question of the effectiveness of e-learning should be reviewed before adopting e-learning on a large scale. This paper presents, how to evaluate the effectiveness of e-learning.

Evaluations try to establish the value of objects, service—and e-learning courses. Taking an organization into e-learning is a major undertaking. And e-learning can be expensive, upsetting and challenging. It makes sense to establish the value of your move into e-learning. You may have more specific reasons for evaluating e-learning: Your organization has been using e-learning for a few months and you would like to get a handle on how successful it has been, or not been. You've heard rumors and wish to verify their accuracy.

E-Learning courses replaced conventional classroom classes and you would like to establish the relative costs and benefits of the classroom version compared to the virtual classroom version.

You promised that e-learning would lead to anytime, anywhere training. Now you wish to determine whether it has delivered as promised. Management bought into e-learning because they were told it is 50% faster, 50% cheaper and 50% more effective. You wonder whether there is any truth to these claims. An evaluation should help to shed some light on the question.

Your organization has had a few e-learning pilot courses and now you are considering developing additional courses. Before you move ahead, it would be a good idea to know what level of success you have had with the pilots. Were they as effective as classroom sessions?

You do things right. You know that evaluations are crucial to performance improvement. You always evaluate. So you will also evaluate e-learning activities. It's expected in your organization.

Evaluation is a discipline where many earn a living and most do this in specialized fields such as accounting, education and general program and project evaluation. However, specialists are just that. Frequently the evaluation that you get is based on the particular model that the evaluators are expert in.

The word evaluation sounds definitive. When you hold an evaluation document in your hand, you would like to be able to say with certainty that it is accurate. Is it? How do you know? What can you do to increase confidence in evaluation studies? The Institute for Higher Education Policy (IHEP) developed an evaluation framework for e-learning that is a useful overview of areas you may wish to consider for e-learning evaluation in your organization. In a review of the literature IHEP identified 45 areas for evaluation or benchmarks and grouped them into seven categories.

In most departments within a corporation, determining the return on a given investment is a straightforward accounting exercise that produces a factual and typically uncontested result. But when it comes to e-learning, computing ROI suddenly becomes a complicated procedure requiring thoughtful chin-stroking, serious seminar time, and earnest input from consultants and vendors. Easily determined hard savings include reduction in training budgets and materials, travel, instructors, physical facilities, administrative time, and hours of lost productivity when employees are off-site - among other savings. But what about improved productivity and proficiency, learning curve, and employee retention, satisfaction, and maybe even morale? They are not always so easily measured. In some cases, they are not even relevant. Fortunately for training professionals, there is no shortage of opinions or expertise. Indeed, an army of e-learning vendors stands ready to assist any perplexed executive on the nuances of ROI and the benefits to be gained by their particular products.

Evaluation is fundamental to grasping the value of an e-learning program. Evaluation is fundamental to pinpointing ways to improve an e-learning program. You have access to a wide variety of e-learning evaluation models. They vary according to what counts in an organization and the budget assigned to evaluation. Armed with the information in this article you will have a better idea of the central evaluation issues and you will be able to work more closely with evaluation specialists to generate a successful e-learning evaluation.

References:

- [1] TVRDÍKOVÁ, D: *Structure of Budget for E-learning Education* CTU, 2004, pp. č. strany-č. strany.
- [2] WILSON, H. W.: *Evaluating the Effectiveness of e-Learning* Computer Science Education, 2003, 123 - 123.
- [3] BROADBENT, B., COTTER, C.: *Evaluating e-learning* Pfeiffer Annual: Training, 2003,
- [4] ALLEN, M: *The lessons of E-learning* Optimize. Manhasset, 2003, pp 51 - 51

The Risk Modified Strategy Modeling

P. Dlask, V. Beran

dlask@fsv.cvut.cz, beran@fsv.cvut.cz

Department of Economics and Management in Civil Engineering Czech Technical University, Thákurova 7, 166 29 Prague 6, Czech Republic

Technical and economical professionals have a long tradition in using quantifications. There is a good reason for it. Any decision that was materialized does inevitably have many observers and materialized existence create any time new ones. Long-term existence of technical goods will always be an object of potential reviewer of past decision(s). And *vice versa*, late critics are usually right, having the information the designer has never been able to get in the past.

In these terms, there are decisions that have long memory (records). There are decisions that are irreversible and have a very high critical mass of energy needed to change the path the decision has and will have in the future. We might speak about inventions, innovations, lost opportunities, disasters, crisis, accidents or other events, very briefly about strategic decisions, or better about long memory decisions and data. The economy and technical skill will be an ineluctable witness and arbitrator of chosen solutions. Moreover, during the live cycle, the criteria scheme will very probably be changed and shaped to the fresh requirements and past decisions made will get a criticism from experience that the decision maker might never get on a natural basis. In spite of this, there exists a dynamic modeling and dynamic simulations. This technique is able to see future developments based on current mechanisms and judgments. Some insight, how the problem solved behaves, will be developed by means of simulations, simulation under risk conditions, parameterization of input data etc. There is a tool how to create documentation for intelligent and difficult decisions. There is a productive tool for professional and experienced *decision making with a long future validity* even for long live cycle goods as the technical projects usually are.

For the future risk modified strategy modeling, we can use Modified Dynamic Model (referred to [2]). The basic calculation method used for the standard calculation is published in [1] (see equation (1, 2, 3)):

$$X_i(t + \Delta t) = X_i(t)^{\Phi_i(t)}, \quad (1)$$

$$\Phi_i(T) = \frac{1 + \frac{\Delta t}{2} \sum_{j=1}^m [a_{ij} + B_{ij}] - (a_{ij} + B_{ij}) X_j(t)}{1 + \frac{\Delta t}{2} \sum_{j=1}^m [a_{ij} + B_{ij}] + (a_{ij} + B_{ij}) X_j(t)}, \quad (2)$$

where:

$$B_{ij} = b_{ij} \frac{d(\ln(X_i(t)))}{dt} \quad (3)$$

t internal model time

Δt time increment

a_{ij} interaction between two model element's (the element of the matrix \mathbf{A})

b_{ij} element of the management matrix \mathbf{B}

$X_i(t)$ standard for concrete model element in t

The Modified Dynamic Model is modifying the equation (1), (2) and (3) in sphere of the risk. The targets of the risk influence (risk attack) are single interaction between model elements.

The user has to determine position of the risk interaction in the interaction matrix \mathbf{A} for equation (4), (5), (6):

$$X_i^{Risk}(t + \Delta t) = X_i^{Risk}(t)^{\Phi_i^{Risk}(t)}, \quad (4)$$

$$\Phi_i^{Risk}(T) = \frac{1 + \frac{\Delta t}{2} \sum_{j=1}^m \left[\left(a_{ij} \pm R(a_{ij})_{Min}^{Max} \right) + B_{ij} \right] - \left(\left(a_{ij} \pm R(a_{ij})_{Min}^{Max} \right) + B_{ij} \right) X_j(t)}{1 + \frac{\Delta t}{2} \sum_{j=1}^m \left[\left(a_{ij} \pm R(a_{ij})_{Min}^{Max} \right) + B_{ij} \right] + \left(\left(a_{ij} \pm R(a_{ij})_{Min}^{Max} \right) + B_{ij} \right) X_j(t)}, \quad (5)$$

$$\text{where: } B_{ij} = b_{ij} \frac{d(\ln(X_i(t)))}{dt} \quad (6)$$

t internal model time

Δt time increment

a_{ij} interaction between two model elements (the element of the matrix \mathbf{A})

b_{ij} element of the management matrix \mathbf{B}

$X_i^{Risk}(t)$ the risk standard for concrete model element in t

$\Phi_i^{Risk}(t)$ coefficient for depreciation of the $X_i(t)$ under the risk attack

$R(a_{ij})_{Min}^{Max}$ the risk attack in interval $\langle Min, Max \rangle$

Risk interactions $a_{ij} \pm R(a_{ij})_{Min}^{Max}$ are created by means of a random number generator. The generator needs several characteristics for its process. Risk and uncertainty exist in different time periods. The model has to be able to describe the risk in these periods. Risk description contains the following information:

- Starting time (beginning of interval)
- Ending time (end of interval)
- Type of random number (type of distribution)
- Parameters of distribution
- Original value of risk interaction
- Decision about using (YES/NO symptom)

The risk parameters described above are basic for method solving under risk and uncertainty. The system is open and it is possible to add next missing type of a random number distribution.

References

- [1] HOLLING, C., S. *Adaptive Environmental Assessment and Management* International Series on Applied Systems Analysis 1978
- [2] DLASK, P. *Modifikovaný dynamický model pro řešení technicko-ekonomických úloh s použitím rizik a nejistot* ČVUT, Fakulta stavební, 2002,
- [3] BERAN V. A KOL. *Dynamický harmonogram, elektronické rozvrhování technicko ekonomických procesů* Academia, Praha 2002

This research has been supported by grant OC A17.001.

Simulation and Value at Risk

V. Beran, P. Dlask

beran@fsv.cvut.cz, dlask@fsv.cvut.cz

Department of Economics and Management in Civil Engineering Czech Technical University, Thákurova 7, 166 29 Prague 6, Czech Republic

Introduction

The term *risk* is used in economic and business applications through out the whole last century. The New York Stock Exchange applied to member firms risk around 1922. Risk is nowadays a substantial part of entrepreneurship. Even the definition of entrepreneurship is in some countries connected to existence of risk. However the calculation of risk may be evaluated satisfactory the situation in risk management seems to need some improvement. Since 1960 and 1970 we see that organizations were exploring alternatives, risk reduction through safety, quality control and other technicalities enabling risk evaluation and risk reduction. The academic and practitioners seek for more comprehensive tools and methods. The technical tools for evaluation of risks developed in last years still show very turbulent development. The frame of mind is that there is desirable to develop more comprehensive methods and advanced computer software for evaluation of risk and his origin roots in organizational structure. However, the priority for more risk management seems to be more urgent that technical indicators itself.

There are three fundamental approaches to risk evaluation a) parametric methods, b) simulation on the basis of classical input-output observations, c) Monte Carlo method on the basis of pseudo random numbers. The approach presented in this paper is linked to last one methodology mentioned. In this context it is important to emphasize, that risk evaluation and risk technical indicator are only prerequisite for risk management as methodology for risk maneuvering into a harmonized process.

Risk evaluation

A simplified time scheduling example and cost flow will show how to evaluate risk by very moderate calculation on the basis of spreadsheets. The calculation enables deterministic specification of time and cost for every activity. The *Duration* and *Start* and *End* of every activity we will get on the basis of *Costs*. The process of calculation will be called spreadsheet *mapping*. Costs column matrix C is transformed by means of speed matrix ξ to duration matrix D . Costs C are again calculated by means of quantity vector Q and their vector of prices π . In the mapping of the chain *quantities - prices - costs - speed - durations* are advanced information in the chain initiated from independent matrixes Q and π . These values play the role of key inputs. The first risk signals in calculation have his origin (are formed from) in design as Q and in economical origin π , or say are formed by means of market. Dependent values are costs C and durations D . We may follow matrix calculation of *duration* as $D=C*\xi$ or better as $D=(Q*\pi)*\xi$. The further mapping of D in to *Start* and *End* of partial activities (t_{Start} , t_{End}) are given as transformation on the basis of organizational consequences Δ_1 . The symbol Δ_1 expresses rule for time scheduling of processes on the basis of existing vector D . From D there will be derived t_{Start} , t_{End} . The *derivation* algorithm Δ_2 enables calculation of cash-flows $c_{Start,End}$ from existing C . The derivations Δ_1 and Δ_2 are in this case calculations by means of spreadsheet (see [1], CD table *Harmgen1.xls*). The attempt to construct a spreadsheet (TAB) is the same as develop *derivative algorithm* for decomposition of C into time D calculated by means of production speed ξ . *Integrative algorithm* enables on the basis of partial durations D enumerate the total project duration TD .

However, the origins of all parameters (indicators) data are by project design proposed quantities Q . The testify power of may be compressed to expression

$$Q \xrightarrow{TAB} (t_{End}, t_{Start}) \text{ and } c_{Start,End} \quad (1)$$

Where $t_{End} - t_{Start}$, are activity durations and $c_{Start,End}$ are partial activity costs flow conditioned by D .

For practical management there are important technical indicators t_{Start} , t_{End} and cash-flow $c_{Start,End}$. The activities *start* and *end* are evident. These data play substantial role in practical scheduling of process. Differences between planed data and real flow of process are scope of management. However there exists a strong lack of information about *sensitivity* of given data and potential risk exposition.

Risk analysis

For the advanced risk management we start in background from a time schedule and seek for additive information for management. For starting information we have information about cash-flow and divided information about cash-flow intensity. The changes will be called *virtual management momentum*. However we may seek for many others management momentums as D' and D'' or π' and π'' and so on. The calculation conditioned by risk is based on simulation and is again virtual oriented. The risk of Cash-Flow is evident and is connected to partial activities. For practical approach it is necessary respect time schedule and probability in prospect schedule. If probability will not be in the realistic belt (say between 0,65 to 0,90) it has to be considered as activity at risk. The regulations by management will be foreseeable, read it additional costs will be on the way.

Conclusion

The risk management is management about value at risk. There is necessary to thing in terms possible changes of values (parameters) or *virtual shifts*. The methodology that might be useful is methodology about potential change or better *virtual momentums*. Every quantitative value has only limited potential to be changed. The risk as measure of future exposure to conditions that violently change the project realization is an important representation of this category. The development of comprehensive virtual momentums for management reasons is not only theoretical but also practical task. It is core management task.

References:

- [1] BERAN, V. A KOL. *Dynamický harmonogram* Academia 2002
- [2] SYDSAETER K., HAMMOND P., J. *Mathematics for Economic Analysis* Prentice Hall International, Inc. 1995

This research has been supported by grant OC A17.001.

The Investigation of the Unexacting Restructuring of Basic Internal Relations in Small and Medium Enterprises

G. Tomek, V. Vávrová

tomek@fel.cvut.cz, vavrovav@fel.cvut.cz

Department of Economics, Management and Humanities, Faculty of Electrical Engineering, Czech Technical University, Technická 2, 166 27 Prague 6, Czech Republic

1. Background

The new manufacturing philosophies come up as a response to the dynamic of the competitive environment, with the aim to offer the capacity of a company based on the orientation towards a customer. It is the solution that responds to the definite movement towards the individualization of market relations. It also necessitates new approaches to the interpretation of marketing, option of marketing strategies and utilization of instruments of marketing mix. If some stagnation starts to manifest within the framework of a company, the company usually offers an additional service. The global solution requires the analysis of all the aspects that lead to the increase in utility value for a customer. No falling, on the contrary rising significance of the market segmentation also bears upon that. It is impossible to offer the same to everybody. Thus, step by step the company comes to the realization of the marketing type “one to one”. Also this has to be comprehended as the search for a higher flexibility of an offer in order to satisfy the requirements of a customer.

2. The Encounters of the Marketing Conception

The requirement to apply the marketing conception in the practice of large enterprises and also middle and small companies may bring along a number of latent and also actual discrepancies between the basic components of the value forming chain. These components are represented by primary functions on the one side and on the other side by subsidiary functions. The reasons of the origin of these discrepancies might be miscellaneous:

- the tough hierarchical structure of control, which is consequent upon the distinct division of functional zones that excludes any overlapping,
- the unsatisfactory comprehension of the importance of the company orientation towards marketing by non-marketing divisions,
- the negotiating power of some representatives of the individual functional areas that makes it impossible to create company objectives as the consensus of all the “competitive” relationships inside a company.

The discrepancies and numerous “points of friction” in horizontal and vertical lines originate newly in the management during the implementation of the “marketing entrepreneurial conception”, when a new managerial principle with a special purpose starts up and operates in a company. They increase the number of strained relationships, e. g. between the production control and purchasing control, the preparation and start of manufacturing and manufacturing itself, the manufacturing control and quality control, as well as between the control of subsidiary and service procedures, and others. The discrepancies between the production and the financial or economic division and the other subsystems are also very frequent. The production has to conform to a greater extent to the basic requirement, which is the necessity of manufacturing marketable articles. Furthermore, the relationships towards the market and towards the actual and potential customers should result not only in maintaining the position on the market, but also in its continuing improvement, and in raising market share and the efficiency of sale. Purchasing, which is accountable for the complete, good

quality and economically optimal assurance of material inputs has larger space for making decisions. If purchasing may choose from more competing suppliers, they can do it regardless whether the supplier is domestic or foreign. Also its function changes as to the relationship to the preparation and start of manufacturing and the production control. The greater initiative and participation is as well expected at the choice of material, process of standardization, at the effort to utilize material economically and to recover waste ecologically, and others. The higher accountability concerns also deliveries in due time and the assurance of their highest quality.

The encounters of marketing with the other sectors within the framework of a company are not the only ones that arise during the creation of a product and its utility value. At the one end, the enterprise is joined to the value forming chains of suppliers, at the other end to the chains of customers, logistics links, and others, which results in the rise of the discrepancies at the boundary-line supplier – manufacturing enterprise, and also manufacturing enterprise – customer.

Thus, the encounters of marketing may be analysed as:

- encounters within the scope of the value forming chain of a company (manufacturing enterprise),
- encounters within the scope of the supplier-customer chain, which comprises supplier – manufacturer – customer (supply chain).

3. Methods of Solving an Actual or Latent Contravention from the Standpoint of Interplant Relations

- **The Adoption of Marketing Philosophy by Whole Company**
- **The Implementation of the Idea of Product Management**
- **The Implementation of Global Integrated Standardization**
- **The Operational Production Control**
- **Transition to Process Management**

4. The External Linking of the Value Forming Chain - Supply Chain Management

If we resume the outlined control of processes viewing from the standpoint of internal customers and in the scope of the SCHM, it is the controlled co-operation. This co-operation overlaps the enterprise in such a way, that the suppliers at the one end and the customers at the other end of value forming chain are co-ordinated at creating the relevant entrepreneurial processes. It concerns the interconnection of the value forming chain inside a company with the supplier-consumer chain.

References:

- [1] G.TOMEK, V.VÁVROVÁ: *Strěty marketingu* C.H. Beck, 2004, ISBN 80-7179-887-8.

This work was funded by Czech Science Foundation, No. 402/02/0160.

The Effect of Transport Infrastructure on Regional Development

F. Lehovec

lehovec@fsv.cvut.cz

CTU, Faculty of Civil Engineering, Dept. of Road Structures
Thákurova 7, 166 29 Praha 6

With regards to exceptional financial demands given by the construction, modernization and maintenance of transport infrastructure, a qualified and objective assessment of its attainable benefits becomes a dominating factor.

The principles designed for use in complex assessment of projects of integrated transit routes of transport structures are usable in determining their urgency within the implementation time prospective. They allow us to extend the evaluation of alternatives not only in terms of economic expression of direct benefits, but by including indirect benefits they may, in a principal way, affect setting the priorities in the implementation phase.

The principle of overall benefit determination further allows assessment of profitability of reconstruction (or modernization) projects of existing roads in comparison with a new road construction in a different route.

The expression of urgency and benefits of projects of line structures provides positive argumentation not only for the representatives of state administration and district authorities, but also for awareness building and active cooperation with the general public.

Based on the specification of relevant indicators, it is desirable to develop successive studies assessing the impact of line structures on regional development by using the “before“ and “after“ method, as background for decision making on the development of road infrastructure network.

Complex (overall) benefits of transport infrastructure projects may be expressed by the following relation:

$$U_{\text{total}} = \sum_{i=1}^n U_{\text{pr}} + \sum_{j=n+1}^m U_{\text{nepř}}$$

where U_{pr} equals direct benefits of monitored factors, direct benefits assessment $i=1, \dots, n$
 $U_{\text{nepř}}$ equals indirect benefits of monitored factors, indirect benefits assessment, $j=n+1, \dots, m$.

In order to express direct benefits, economic (cost-benefit analysis) project assessment is used in comparison with zero-alternative (application of HDM – 4 assessment model).

This allows monetary expression within standard categories, i.e.:

- overall net economic benefit discounted at the end of monitored period (NPV)
- setting internal return rate (IRR)
- expression of a ratio of net present value to costs (cost return, BCR)

In order to determine indirect benefits, evaluation of the following 4 aggregated indicators has been designed:

- increase in the number of job opportunities – F_1
- mobility effect on economic growth – F_2
- increase in territorial value – F_3
- environmental effects on the territory and population – F_4

The designed evaluation procedure respects differentiation and changes in the conditions along the line structure route.

A prominent evaluation factor is implementation of the time dependency principle in the form of

$$U_i(t) = \sum F_i(t)^{existing} - F_i(t)^{design}$$

$$U_j(t) = \sum F_j(t)^{existing} - F_j(t)^{design}$$

- where U_i are evaluative effects of direct benefits $i=1, \dots, n$
 U_j are evaluative effects of indirect benefits $j=1, \dots, m$.
 t design period length
 F function of evaluative effect time course

which provides the expression of the benefits' growth within a time interval of the design period of the respective structure.

The analysis performed makes it clear that the present-day evaluation methods allow us to express, by means of standard procedures, only economic benefits of direct effects. In order to monitor indirect socioeconomic effects, an illustration solution has been developed for the territory affected by the construction of the D8 motorway in the Praha – Lovosice section. Expressions of factors F_1 , F_2 and F_3 were developed separately for individual exits (6 in total), which allows us to define overall indirect benefits in monetary terms.

References:

[1] LEHOVEC, F.: *Hodnocení vlivu silniční infrastruktury na rozvoj území, Silniční konference 2004 Hradec Králové*, 2004, Sborník pp. 52–54.

This research was supported by the research grant No. MSM 210000001.

Upgrading the Communication Skills and Managerial Abilities of PhD Students of the Czech Technical University in Prague

B. Duchoň, V. Soyková

soykova@fd.cvut.cz

Department of Economics and Management of Transportation and Telecommunication, Faculty of Transportation of the Czech Technical University in Prague, Horská 3, 128 03 Prague 2, Czech Republic.

Good communication is a basic skill for achieving success in any senior position. Unfortunately, the study programs at the Czech technical universities, including the Czech Technical University in Prague (CTU), do not place emphasis on this important topic. Graduates freshly employed by industrial companies are often highly appreciated for their technical knowledge and skills, but they are criticized for their lack of communicativeness and for their unread ness for making business decisions. We have therefore we decided to contribute to the education of PhD students in fields related to industrial control and management by introducing a course to improve their communication skills and extend their managerial abilities.

The aim of this course for PhD students at CTU is to improve participants' awareness, know-how and performance in the area of communication, presentation and self-management. The course will include traditional class work, development of awareness, and practical exercises.

The main accent is on developing and deepening students' communication and self-management skills. Students will work on their own personal development, on the principle that the deeper they reach the greater the gain. Systematic work will be done in a small team, making use of simulation techniques and case studies. This approach will help students to explore and extend their own abilities in the area of decision-making, and to discover their own self-management abilities. This course will encourage PhD students to think and act with managerial attitudes suitable for the 21st century.

This course originated as a follow up to the courses Personal Management I and Personal Management II, in response to students' requests to extend and deepen their work on personal management. When considering a proposal for such a course, we were confronted with fact that presentation skills are not systematically dealt with anywhere in the educational system. We therefore decided to offer training in selected areas of management skills, involving personal experience, teamwork and feedback. The course covers both verbal and non-verbal communication.

At universities abroad, a course such as this regarded as an aspect of management and self-management training as a whole, and communication skills form an integral part of the whole pedagogical process. The accent is on practical training running through all levels of education, from elementary schooling education through to life long learning courses.

Good presentation of scientific projects plays an increasingly important role in obtaining grants, and presentation of results can determine whether they will be developed and implemented in industrial or commercial practice. A course in presentation skills can surely help scientists to “sell” more effectively the results of high quality research that they have carried out.

The course will be offered to PhD Students within the individual study programs that they are required to take. It will be offered on a non-commercial basis, and PhD students will be required to put in time and effort, but not to make any extra payment. Students will be invited to negotiate in the design of the course, which will involve communicating effectively about the progress of the scientific work that they are engaged in.

Participants will gain an insight into their own personal capacities and managerial abilities from the viewpoint of psychology of personality. The accent is on identifying capacities and abilities that can be further developed, and helping participants to make the most of the abilities that they have. Strict ethical conditions must be kept to, as psychological tests and questionnaires will be used and very sensitive parts of the human psyche will be exposed.

It is very important to formulate and transfer all information from facilitator to student and vice versa in a positive and supportive way – this is the “*conditio sine qua non*” for this course. Feedback will be given on a strictly personal basis, and the privacy of each individual in the sensitive sphere of personal feelings must be respected.

Important aspects of presentation are conciseness, clarity and an appreciation of the listener’s requirements. These important interpersonal skills need to be taught sensitively, taking into account the personality of the learner.

Training in decision-making plays a key role in the whole learning schema. Simulations of real-life situations and case studies will form the basis of the learning process. Decision-making is the key to successful management.

The course is offered to PhD students throughout the University, and can form a useful part of the program of students not specializing in management. All students, regardless of their field of specialization, need to apply the skills obtained in this course, for example in presentations at conferences, or when presenting and defending projects. In general, all PhD graduates of CTU need to be prepared to become managers of projects, research groups, departments or institutes. In the modern world, communication skills are a necessary part of the intellectual equipment every academically educated person.

This research has been supported by internal grant No. CTU0419016. The authors appreciate very much the given support.

The Questions of Effectiveness Evaluation of R&S Activities

M.Soukup, M.Rejha*, Houssam Nassereddine**

Soukupm2@centrum.cz

M.Rejha@seznam.cz *

Houssam@seznam.cz **

CTU, Faculty of Mechanical Engineering, Dept. of Economics and Management
Horská 3, 128 03 Prague 2

Problems of evaluation research R & D:

Creation of evaluation methods and figures mustn't still mean objective evaluation. Like in all majors as well here, we hit human factor and basic obstacles, which can influence the R&D evaluation.

- Fear from detection of low efficiency, incompetence of research, worker progress and formation.
- Limited accesses and measuring data.
- Incofidence in effective and credible evaluation of research efficiency and progress is not possible.
- Overcomplication and subjectivity of classification, respectively unbelief resulting from negative experience with measuring efficiency experimental and evolutionary working in the past.

Another finding rearranging evaluation of „economical effectiveness“ is that it has no sense to express expenses of R&D in absolute numbers, because predicative ability of that is so low, unless we know the size, character and history of such project. Meaningful might be only proportion indices, which can help to compare single experimental projects with each other and which are worth to study their development during the years..

From the mentioned reasons the main points for R&D evaluation are:

- Determination of all factors influencing R&D evaluation, research workers and institutions.
- Setup of determination and relation definition in frame process of research project itself and evaluation of its effectiveness.
- Integration of single methods to the particular content of experimental projects for reaching higher effectiveness of not only classification, but above all experimental activity by using feedback and reciprocal interaction these action.

Generally, there are used these typical models for R&D evaluation:

Scoring models: to assess the R&D figures, are used sets of quantification and qualification criteria with associated importance.

Decision models: to assess the R&D values, are used for example theory of utilities, decision tree, risk analysis and decision theory.

Portfolio models: Allows allocation sources from standpoint of maximum contribution within whole group of projects.

Financial models: for determination of R&D projects values are used financial criteria, e.g. ROI, NPV, etc..

Peer review: special examination R & D activity of chosen systems.

Brief characteristic of selected methods:

Scoring model:

One of the most important aspects of this model is its utility for three broad areas, which can be defined:

- Basic research
- Applied research
- Experimental development

Each area has its own properties, such as costs, timesplan, funding source etc.

The main benefit of the scoring model is its ability to include qualitative and quantitative data. Determination of criteria and their weight is possible by several procedures. We can use a techniques as Delphi or peer review, or less formal methods (e.g. by the help of questionnaire).

Financial analysis:

To well know tools of financial analyses belongs the cost analysis and the discount cash-flow (DCF). This analysis is suitable especially for applied research, where is a presumable less accuracy for estimation of future cash flow. It is possible use DCF for these projects, which were added to experimental development and have broader available spectrum of information. Although DCF could be effected by time factor, various methods of calculation DCF are suitable for various examination of situation:

- Index of present values (PVI) is independent on project sizes; e.g the project with smaller outputs can demonstrate higher PVI, than big project with bigger outputs.
- Internal rate of return (IRR), is contributive for project classification, which where realized in the same time period. This method prefers projects with a shorter life cycle.
- Net present value (NPV) is independent of the time period, but using this method becomes evident the effect of extension of individual projects.

Regarding above mentioned presentation and consideration to essential characters of the individual projects, which differ in timespan and size, NPV seems to be optimal method.

R&D projects come through its life cycle, which consists of selection phase, executing phase and phase of implementation.

Essential, but not only precondition hypothesis of R&D projects is achievement of required efficiency in all three phases of projects life cycles.

Generally, it could be said, that the purposes of research in any area is to maximize positive impacts and to minimize negative impacts.

It is impossible quantify, or qualify all effects immediately in select (mostly too short) time period.

Assigned methodology can be founded on estimation of publication, quotation and their comparison with similar types of research in our country and in the foreign countries as well. This classification of projects would have further appear and be closely connected with the area of effects. Utilization and determination of correct effects can help us not only to estimation of this research, but we are able to use it for the other research projects, because we will know detail identification of their requirements on source of information and next analyses.

References:

- [1] S.COLDRICK: An R&D options selection model for investment decisions,2003
- [2] M.E.McGARTH,M.N.ROMERI:The R&D Effectiveness:A Metric for Product Development Performance
- [3] A.BAŠTA: Kvantifikace a měření ve společenských vědách, Praha 1986

Computer Based Training of Air Transport Pilots at CTU

P. Hvězda, B. Sravovčík, T. Míkl

xhvezda@fd.cvut.cz

Department of Air Transport, Faculty of Transportation Sciences, Czech Technical University, Konviktská 20, 110 00 Prague 1, Czech Republic

The main purpose of this project was to implement a new worldwide used philosophy of air transport pilots education - Computer Based Training (CBT) and so enhance the quality of pilots' theoretical preparation and bring our university into front pilot theoretical knowledge providers. The aim was to inspect current system of education, identify parts of syllabus suitable for enhancement or potential replacement by CBT, analyze optimal means of CBT implementation, find appropriate software in accordance with Joint Aviation Authority Requirements, modify current syllabus and finally obtain Czech Aviation Authority certification for computer supported study program.

The first project phase concerned inspection of air transport pilots educating system at the Department of Air Transport and identification of possible ways of enhancement by using Computer Based Training. Although majority of aircraft systems have become computerized and there have been many supporting software products developed, the system of educating pilots at our university is still very traditional – so called chalk and talk. It was shown, that with the increased access to computer-based tutoring programs, students are moving away from passive reception of information to more active engagement in the acquisition of knowledge. Additionally, personal computer-based training helps provide the educational components in multiple learning styles, thereby meeting more individuals' learning needs than are provided by classroom lecture alone.

The syllabus for Air Transport Pilot (ATP) students is given by JAR FCL 1 regulation issued by Joint Aviation Authority. Required knowledge is divided into 14 areas and each is covered by appropriate subject with relevant number of hours. To analyze possibilities of CBT implementation in each subject, detailed syllabus specifications and learning objectives were studied and parts suitable for supporting by CBT were highlighted. All suggestions were consequently discussed with the tutors and representatives of flight training providers and specifications for concrete software product were identified.

Two possible ways of CBT implementations were concerned. The first counted on purchase of suitable ab initio training product from some renowned provider like Wicat or The Roach Organisation (TRO). These products use the latest in multimedia technologies, including audio and full-motion video, to enhance pilot training and increase retention, while reducing the time associated with ab initio ground school. However, two significant disadvantages of this solution were discovered. These products are based on self study, each student goes at his own pace and so these products are suitable rather for selfstudy purposes than for university use and do not cover requirement on supporting lectures. The other limitation is its price. After communication with the ab initio training providers we realized, that price of these products highly exceeds our financial capabilities and it was decided to create some supporting software from our resources, less sophisticated, but tailored for our needs. So far, following steps were achieved:

System of testing:

1040

ATP candidates must prove their theoretical knowledge at the appropriate Civil Aviation Authority by passing computer test from each subject. The tests usually contain around 50 questions with a choice of four answers and cover subject syllabus defined in JAR FCL 1 regulation. In order to prepare students for these tests, testing software was purchased and tutors asked to create similar database of questions from each subject. Computer test is now considered as a mandatory part of an exam and a very good performance of our students at CAA ATP exams proved the efficiency of this system.

Multimedia annexes to lectures:

Instead of using expensive ab initio CBT software it was preferred to create a kind of multimedia annex for each subject. These annexes are tailored to fit particular requirements of each subject and should have a form of an interactive powerpoint application containing explanatory text, pictures, videos and sounds. All tutors have been asked to prepare syllabus and relevant material for these supporting files and now it is being transformed into powerpoint files mainly by students. The tutors are supposed to use this explanatory material during lectures via data projector. All annexes will be available for students in advance via intranet. So far, annexes for Avionics 1 and 2 and Radiocommunication have been made.

Other supporting software:

Jeppview – viewer of Jeppesen maps, that are necessary both for flight planning and performing. Maps are periodically updated and contain standard instrument arrivals, departures, instrument approach and airport charts for all IFR airports in EUR region. This program is shared with F-air company – provider of practical pilot training for CTU pilots.

Meteorology and principles of flight CBT – this CBT is primarily made for ATC controllers by Eurocontrol, nevertheless it is fully sufficient for practising purposes for student pilots. For exercises, two computer labs and multimedia classroom are available.

References:

- [1] KARP, M. : *Theoretical aviation training for future airline pilots*, Doctoral Dissertation, Walden University, Minneapolis, MN. UMI 9713644 1996.
- [2] H. FABISCH, J. BOHN: *Integration of Modern Training Methodologies in Ab Initio Courses*, Inter Cockpit, EATS Frankfurt, 2003.
- [3] UNITED STATES DEPARTMENT OF TRANSPORTATION FEDERAL ADVISORY COMMITTEE : *Pilots and aviation maintenance technicians for the twenty-first century: Assessment of availability and quality*, Washington D.C.: U.S. Government Printing Office 1993.

This research has been supported by CTU grant No. CTU0411916.

The Analysis of Traffic Networks and Attended Region Interaction

L. Týfa, M. Vachtl

tyfa@fd.cvut.cz

Department of Transportation Systems, Faculty of Transportation Sciences,
Czech Technical University in Prague, Konviktská 20, 110 00 Prague 1, Czech Republic

Each traffic system of passenger transport is in interaction with locality, through which it passes, as these regions generate the passengers-clients for transport contractors, which use particular traffic network. Objects of interest of the project in question are common features and differences mainly of two systems, whose implementation in Czech Republic is still awaiting, i.e. High-Speed Railway Lines (HSRL) with regard to the NUTS 1 territorial entities (the Czech Republic), resp. NUTS 2 (county associations), and tram-train systems with regard to the NUTS 4 territorial entities (districts) and NUTS 5 (municipalities). However, also the other related rail transport systems have to be considered, i.e. municipal high-speed tracks (e.g. underground, S-Bahn) in large municipal agglomerations, and the network of traditional railway lines, which are with the systems in question in close relationship, both direct (vehicles transitivity) and indirect (interchange points). However, nor the rail transport as a whole is isolated from the other transport means, therefore the linkages to trackless haulage must be also reviewed; i.e. above all to road car traffic in the Czech Republic conditions. There is linkage between those two means of transport in traffic and transport market.

The High-Speed Railway Lines are up-to-date railway lines, which distinguishes from the traditional railway line above all by their track speed, which must be designed for each new HSRL at least 250 km per hour according to the Directive No. 96/48/EC on interoperability of Trans-European High-Speed Railway System. HSRL are built either only for passenger trains, or for mixed traffic; presently the trend of HSRL network creation only for passenger traffic predominates, particularly due to easier layout of the lines (higher longitudinal slope and smaller radiuses of direction curves). In important agglomerations, the HSRL are introduced into city centres in such manner, that in edges of urban units is the HSRL linked to existing railway network, and the high-speed trains then enter the stations located directly in city centres in lower speeds. In cases of the centres of lower importance, new HSRL stations are built on agglomeration edges or even in rural zones, and the interchange points between various kinds of transport are established there. In the Czech Republic, there is no HSRL, only corridors in planned lines of HSRL are territorially protected. The most modern and dense HSRL networks are established and developed in Germany, France and Japan.

The traffic system for passenger transport, the vehicles of which can be used both for the railway and tram line, and consequently to use advantages of both kinds of transport, is called tram-train. As the railway system and the tram system were developed independently, there are many technical differences, which have to be unified by linking of both traffic systems (different wheel profile, traction, platform elevation, etc.). Service of the territory by tram/trains will be solved either by the manner, that through the city the vehicle moves as a tram and in the city border it passes into the railway line, on which it continues and serves the suburban areas around the railway line, or, in very large cities, the railway line in rural zone is used for the tram-trains (segregated traffic route), and in satellite towns the vehicle then

moves as a tram. The most developed tram-trains are in Germany, their development in our country is considered above all in the area of Liberec, Most and Žatec.

Just for the reason, that the projects both of HSRL and tram-trains in the Czech Republic are only at the solution outset, it is not possible to be based on any existing methodology for their network design with regard to exact procedures, the decision of the construction of such systems even abroad stems from the acute need to solve existing bottlenecks of traffic network of their pure quality. Interconnection of these systems anticipates during design solution of vehicles, traffic route, and traffic control, also ensuring of full interoperability.

The HSRL network must be interconnected with the traditional railway network to ensure the usage the advantages of both high-speed on HSRL, and location of station in city centres and the network density of traditional railway lines. Similarly, in case of tram-trains, the interconnection of the two systems will be realised to minimise a walking distance to the stations and also minimise the travelling time. In both cases, it is necessary to solve the problem of optimal location of the stations / halting stations on existing and proposed traffic network and to decide, which train categories will stop for entrainment and getting-out of passengers in what stations. On one hand, there is effort for maximal travelling speed (i.e. to minimise the number of halting), and on the other hand, the attractiveness of public transport for passengers diminishes with reducing the number of stations (necessity of interchange to other transport means, increase of walking distance). It is therefore necessary to develop real territory model, to mutually determine the attractiveness of particular locations, optimal lay-out of tariff points, and the line intervals with regard to train set loading. Therefore, the draft of optimal locality service by particular public transport means will be proposed in last stage.

The project is realised in frame of the „Traffic Service of Territory“ dissertation thesis of two doctorands and monitors also their teamwork. The existing public transport systems (i.e. mainly tram-trains and HSRL), their parameters, and both technical and transport interconnection will be monitored in Germany and Austria; the project results should be used during elaboration of realisation studies for high-speed routes and tram-train systems in the Czech Republic.

References:

- [1] KUBÁT, B. – TÝFA, L.: *Relationship Between Modernisation of the Railway Lines and Building of the High Speed Railway Lines in the Czech Republic*, XII. International Conference „High-Speed Railway Lines“ The Modernisation of the Railway Lines, Žilina, 2002, pp. 93-98.
- [2] KUBÁT, B. – VACHTL, M. – TÝFA, L.: *The Growth of Railway Traffic Share in the Integrated Transport System in Prague*, 6th International Conference „Public Passenger Transport“, Bratislava, 2003, pp. 132-137.
- [3] VACHTL, M.: *Possibilities and Opportunities to Build of Systems Tram-Train in the Czech Republic*, Conference Transport in Euroregions, Děčín, 2002.

This research has been supported by CTU grant No. CTU 0411816.

Public Orders in the Praxis - software

R. Schneiderová Heralová*, J. Franěk**

Sch.heralova@seznam.cz

*Katedra Ekonomiky a řízení ve stavebnictví, Fakulta stavební, ČVUT, Thákurova 7, 166 29
Praha 6

**Stavební a inženýrská společnost, s.r.o., Národní 10, 110 00 Praha 1

Act no 40/2004 Coll., treat of public orders and its executive public notices, made more restrictive regime for public orders competition and brought European terminology and legislation in local law system. Software Public Order in Practise is answer to this reality. Can be apply for the **above the threshold and below the threshold public contracts for supplies, services and construction works.**

The product is selected in following sections:

- Guide
- Contracting Entity
- Tenderer
- General Section

Guide provides user by dialog windows through public contracts. Guide is prepared for users-beginners and advanced users (contracting entity or tenderers) can not use it.

Section determined for tenderer is focused on proper consideration, evaluation and assignment of public tender. This section is solved separately for individual methods of the award. The public contract may be awarded by open award procedure (all interested suppliers may submit a tender), restricted award procedure (only the candidates selected by the contracting entity are entitled to submit a tender), negotiated procedure with publication (only selected candidates submit a tender, and are subsequently invited by the contracting entity to negotiate) and negotiated procedure without publication (the contracting entity directly invites one or more suppliers of its choice to negotiate).

Most of all is concerned creation and sending out of notice of award on the central address – Indicative Notice and Publication of the Notice of Procedure (open, restricted or negotiated), further than creation of order for the central address. It is important to respect procedures defined for receiving and opening of envelopes with tenders – here sample documents help (sample documents: List of Tenders, Attendance List, Protocol on Opening of Envelopes, Request of the Tenderer Written Justification of the Abnormally Low Tender Price, Request of the Written Explanation of Confusion). Exclusion of competitors occurs, the reason for exclusion are determined by law.

It is important to respect procedures relevant for consideration and evaluation of tenders. It was the reason why **evaluating module** was prepared. This module helps with received offers evaluation. Evaluating module can be used for tenders evaluated based on one criterion – the lowest tender price, but also for tenders evaluated based on more partial criteria. The contracting entity shall be obligated to accord a relative weight to individual partial criteria, expressed in terms of percentage. Outcome is Rang-order of tenders in accordance with the amount of tender price, respective Rang-order of tenders in accordance with the amount of economic advantage of the tender. Next Decision of the Assignment of a

Public Contract, Written Report of Contracting Entity, Report of Consideration and Evaluation of Tenders and Advertisement of Outcome of Award Procedures. The Software helps with release of information concerning public contracts on the central address, with distribution of letters to competitors.

Working Schedule is important function of software. Working Schedule controls time keeping and highlights in time.

The Part Tenderer is defined for Suppliers, Candidates and Tenderers. This part helps with selection and filter public contracts, that are for tenderer interested, from the central address. Key function is submission of tender and creation of draft of contract. Samples of documents are involved - Request of the Contract Documentation, Request of the Additional Information Relating to Contract Documentation, The Fulfilment of Qualifications, Demonstration of the Financial and Economics Standing, Demonstration of the Technical Capability, Written Justification of the Abnormally Low Tender Price, Written explanation of Confusion in Tender, Request of Applicant in Restricted Procedure, Request of Applicant in Negotiated Procedure with Publication and Complaint.

Another option is creation of simple offer calculation. Working schedule is also quit important part (it is the same as in part determined for tenderer).

General Section involves Basic Information, Legal Regulation and Directory. This section is determined for users that miss detailed information related to public offers. Section Legal regulation is legislative background of software. All legal regulations related to mentioned topics are involved. Directory offer not only addresses of important companies, products, certificated institutions, ministry, board of works, etc., but also section Own Contacts, where is possible to input contacts important for user and for job order.

References:

- [1] SCHNEIDEROVÁ HERALOVÁ, R. – FRANĚK, J.: *Veřejné zakázky v praxi*, Verlag Dashöfer, 2004
- [2] SCHNEIDEROVÁ HERALOVÁ, R.: *5. medzinárodné vedecké sympóziu Ekonomické a riadiace procesy v stavebníctve a investičných projektoch. Bratislava, : Veřejné zakázky - Posuzování a hodnocení nabídek : Katedra ekonomiky a riadenia stavebníctva, Stavebná fakulta STU v Bratislave, 2004, 188–191.*
- [3] HERALOVÁ, R.: *Model hodnocení výběrů variant stavebního díla*, ČVUT Praha, 2000
- [4] LADRA, J., MIKŠ, L. A KOL.: *Stavební , autorský a technický dozor investora*, Verlag Dashöfer, 2004, kap.11/1-11/7.

Analysing and Measuring Quality in Services

B. Košetická, J. Kožíšek

`koseticka@yahoo.fr`

CTU, Faculty of Mechanical Engineering, Department of Enterprise Management, Horská 3,
128 00 Prague 2

Competition in the case of service organisation is sometimes considered more demanding than in the case of manufacturing industries. We can't handle with unsatisfied customers in the same way we handle with bad product. That's why is crucial for service organisation to have functional system of quality and it can't be achieved without effective measurement.

Defining quality is the starting point for measuring it. It's necessary to answer four questions:

1. *What is quality in our business?*

To clarify what quality means for one's own business and to find relevant definitions is an important first phase of quality improvement. The danger is that service providers use their own definitions of quality – of what they think that the customers wants. Copying the quality definitions of others companies it supposed to be dangerous too – they can be irrelevant in other conditions.

It is also important to involve the customers in determining the level of quality. One way of achieving this is to make visible parts of co-service process (the creation of the service). The right quality is achieved when expectations are fulfilled, needs satisfied and demands met: those of the customers, staff and owners.

2. *What languages and what concepts should we use?*

We need a language and concepts that everybody understands. We have some quality concepts which are general in character and applicable to all types of service company (e.g. Gummesson's model 1987: *Production quality* - how the service is produced; *Delivery quality* – the way in which a service is delivered; *Finally relational quality* – quality in the interaction with the customer).

On the other hand, the concepts must be specified and given a content which is adapted to the specific activities of the company.

3. *What are the most important quality factors in our development work?*

It is quality factors that produce the customer's perception of the quality service. There are some common factors for all services: ability and willingness to serve of the staff of the service company, reliability and trust, empathy, handling of critical incidents and customer complaints (the effects of this may be significant and very costly).

There are several studies which describe different factors that affect customer's perceived quality (e.g. Berry et al. (1988) – five quality determinants in services: tangibles, reliability, responsiveness, assurance and empathy.) We can see that the role of staff in services is irreplaceable – a customer's trust is often more related to personal than to companies – that's why the quality of personal contact is supposed to be the main factor which influenced ability of the service organisation to competition.

4. *Are there suitable models which people in business can use for analysing quality?*

The choice of model depends on the purpose of the analysis, the type of company and market situation. There are many models for analysing quality and may be divided into three groups, according to the focus on

- customer-perceived quality,
- the process in the creation of the service
- the whole service (systems models).

(e.g. Gronroos 1983 model, The 4 Q model, An integrated model, Vicious and virtuous circles, The consistency model Expected and Perceived quality Zone of Tolerance, The gap model

Quality in the service encounter, The Wel-Qual framework)

Which model is the best to use? It is significant to exercise two or three models that together cover all these aspects and at the same time, the concept must be adapted to the customers', staffs' and owners' needs.

Of course, the models in service quality improvement must envelop also every of three fundamental parts of services. These are:

- the service concept,
- the co-service process which create the service – the customers pathway process, and the internal support processes,
- the co-service system, as it designed to resource the creation of the service.

For measuring quality in services is eligible to combine quantitative and qualitative methods. Quantitative methods we utilize for objective facts and explicit measures (e.g. number of errors per 1000 transactions, number of delays and time delays can measure service precision).

Qualitative measurement involves listening, studying, analysing and interpreting customers' statements. Another method of quality measurement is the focus group interview (between six and ten) – they discuss the problems of a particular field and usually it's easier for them to express their views than in case of traditional interview. Nowadays studies examined question order effects on service quality measurement (DeMoranville, Bienstock 2003). Examples of methods for measuring quality in services:

Various quality measurements systems are based on a number of quality factors, which are divided into a number of variables (e.g. Total Quality Index – Telia Swedish Telecom, availability – successful calls).

A different method - Servqual method consist of customers reacting to 22 statements based on five quality dimensions (tangibles, reliability, responsiveness, assurance and empathy). There is a scale with seven intervals ranging from “fully agree” to “do not agree at all” (Described in Zeithamal et al. 1990).

Certainly it is essential to start quality measurement with the customer, but other internal measures are also important to be considered (quality of support services in the service chain and as well as professional and management quality).

We can use several criteria of some models to evaluate status of the company, to decide where to make investments in the company to improve quality (e.g. EFQM – Model Excellence - Policie ČR, 2004).

References:

- [1] EDVARDSON B. – THOMASSON B. – B.OVRETVEIT J.: *Quality of Service* McGRAW-HILL Book Comany Europe, England, 1996, pp. 75–208.
- [2] NENADÁL, J.: *Měření v systémech managementu jakosti* Management Press, Praha, 2001, pp. 55–118.
- [3] DEMORANVILLE C. – WBIENSTOCK C. C.: *Question order effects in measuring service quality* International Journal of Research in Marketing, Volume 20 Issue 3, 2001, pp. 271–281.

Input-Output Models as the Tool of Target Costing Method

L. Zeman, K. Macik

`lukasekzeman@seznam.cz`

CTU, Faculty of Mechanical Engineering, Dept. of Management and Economics, Horská 2,
128 03 Praha

Costs calculation is one of the most important parts in a managerial system of a company. In most cases setting the price is dependent on costs calculation of activities. This sequence induces that prompt decrease in the price of product is possible only by decreasing the profit margin.

Target costing is a method which reverses this sequence. The basis for this method are market requirements, i.e. needs and price required by consumers of target products. Companies have to create The Survival Triplet, which represents the relation: price-quality-functions and try to be better than competitors. The market research ensures that the condition of economies of scale is fulfilled and the company reaches the preliminary optimization of production process, because only products demanded by consumers will be produced. Therefore, the primary task is to set the sale price. If the required profit margin is subtracted from this price, the company gets its maximum target costs called drifting costs. This is the reason why this method is often called the method of determining the target costs. Consequently, in a broad definition, the drifting costs consist of total costs of all activities occurring in an enterprise.

Drifting costs involve not only the manufacturing costs and the non-manufacturing part of costs, but also the pre-manufacturing costs as research and development and design works.

Each member of the team participating on the construction of a product has particular drifting costs assigned, which it mustn't exceed. (This requirement is crucial for products consisting of great number of components, whose realization or delivery takes place in different company divisions or from different suppliers, e.g. in automobile industry.) This fact supports searching for new technologies and their implementation. The great advantage of this method is based on lowering costs already in the stage of research and development. The by-product of the method is also the fact that inventories and production processes don't become outdated. Such assessment of target costs can be considered as the first stage of the Target Costing Method.

The second stage of the Target Costing rests on keeping the height of target costs in realized production and evaluation of the differences between plan and reality. It is important to identify and classify these differences according to their cause. This control part of Target Costing (tracking the differences) has to proceed continuously during the whole production process. The inevitable element of the method is the effort for product innovations.

The essential condition for using Target Costing is its integration into all parts of the company. The company has to be perceived as a system and company processes as system processes. The system analysis must be done in order to describe precisely the system. Such analysis disintegrates the system into particular subsystems and expresses links and causalities between them. The analysis can also establish the isolation of some subsystems.

These disintegrated subsystems have to cooperate by obeying a prearranged company goal. The system's inputs and outputs can be divided into endogenous and exogenous ones.

The endogenous inputs occur between particular company subsystems. The exogenous inputs occur between the company system and environment.

In the company information system it is possible to find two isolated subsystems: accountancy and the statistical information subsystem. . The accountancy uses double-entries in the form of balances while the statistical information subsystem uses indicators recorded in the form of tables. These isolated subsystems can be integrated into a one consistent complex by means of the Input-Output Models method.

Therefore, the Input-Output Models appear to be an appropriate tool for the Target Costing method. These models can integrate company's subsystems and show endogenous and exogenous inputs and outputs. In the Input-Output Model endogenous inputs and outputs are represented by the internal turnover and exogenous inputs and outputs by gross production (production of goods and the change in state of unfinished production)

Input-Output Models can be expressed in organisational configuration or in product configuration. These two types can be combined. For Target Costing it is appropriate to create a Product Input-Output Model. With regards to this model it is important to express the links between particular products correctly. In this context single parts components, subassemblies and assemblies are all comprehended as products.

Drifting costs have been defined as total cost of an activity. This means that all the manufacturing, administrative, marketing and supply costs must be assigned to the particular product. In practice, however, it is not easy to do so, especially when the company produces a lot of different products which are produced collectively by a number of centres. This problem can be solved by means of an Input-Output Model creation with fixed costs for the considered production volumes. The fixed costs can be then rescheduled by means of an organisational Input-Output Model with utilization of an hour overhead rate.

The research was carried out in the company MESIT přístroje spol. s r.o., where hypotheses set at the beginning of the research have been proved.

The still faster growing market environment requires producing only products that are characterised by great demand. In spite of this the most of companies do not use the principles of Target Costing yet. Input-Output Models enable to use linear algebra and simulate various situations exactly and quickly as well as compare these situations. E.g. when introducing new technologies, these models can affect the change in primary inputs or the change in the size of the market and so affect the relevant change in primary returns. Thanks to this method companies can react faster to the changes in their own system and in their environment.

References:

- [1] MACÍK, K.: The Input-Output Model for Product Target Cost Determination, Department of Enterprise Management and Economics CTU in Prague, Faculty of Mechanical Engineering, Congress Centre Brno 2003, pp. 90-97.
- [2] MACÍK, K.: Target Costing and Absorbtion Cost Calculation in Product Cost Models CTU in Prague, Proceedings of Workshop March, 2004 pp. 1096-1097.

This research has been supported by the Czech Ministry of Education MSM 212200008..

Size Effect in the Risk Theory

P. Erben

pavel.erben@fsv.cvut.cz

Department of Economics and Management in Civil Engineering, Faculty of Civil Engineering, Czech Technical University, Thákurova 7, 166 29 Prague 6, Czech Republic

The principles of risks in economical and technological systems are the same as the principles in other systems, e.g. constructed facilities, mechanical engineering systems. *The risk theory* is still strongly phenomenological – it is based on the description of facts observed in the human society and nature, and also on estimation of development and changes of these facts. Yet patterns, which risk systems are following, are neither known nor suggested, however, it seems that a kind of *risk mechanics* is possible to be built up. This mechanics should be analogous to e.g. solid mechanics or soil mechanics and should enable to generalize lots of isolated information (Tichý, 2004). One of the most important effects influencing the system of risk is the *size effect*.

One of many possible definitions of risk presents: the risk is the probable value of damage of risk-bearer during realization of hazard scenario, expressed in currency or other units (Tichý, 2004). In the risk analysis three basic classes of object (process) parameters should be distinguished: *geometric* parameters – describing shape and size of object (process) and its changes; *physical* parameters – e.g. solidity, elasticity, fragility, tensibility, temperature of materials, products or systems (including age) and its changes; *time* – either as an absolute value describing the time point of analysis, or as a reference time with its location on the time axis.

For the risk analysis mostly *time* is important. Concerning the *dimension* usually one- to three-dimensional spaces and *nets* are investigated. *Net* is a hyperspace over spaces defined by edges and nodes. As dimensions are meant in the risk analysis for example: “curve” (1D) – steel rod (tension failure), highway (traffic jam), telephone line (connection failure), chain (chain link failure); “area” (2D) – sea (an accident on a stormy sea), frozen pond (slumping through the ice), athletic stadium (javelin hit), forest (fire); “space” – shopping centre (loss of a child), skyway (crash of two aircrafts), concrete structure (stress failure; Novák, 2002), stock market (development of stock price), construction company (communication in the organization); “net” (1D, 2D, 3D) – concrete skeleton armature, road system, town water-supply system, company communication system. It is always useful to consider the sense of integration of object (process) into a space-complex (1-3 dimensional) or a net, because it strongly changes the final risk impacting the object (process).

The hazard, which threatens to the investigated object (process), depends on the *stress* (outer and inner). Object (process) always breaks down in the weakest point. The larger the object (process) is, the more probable is a failure, e.g. a long chain with many links is more probable to fail than a short chain, a stormy sea causes more ship accidents than a water tank, in a large concrete facility there is a higher probability of hair-cracks than in a small one, big company works with more risky projects than a small one. In other words, the probability of existence of “weak” element by small objects (processes) is less than by larger ones.

Other definition of risk describes the risk as the volatility of a financial quantity (portfolio value, profit, stock price) about a prospected value as a consequence of circumstances changes, or as the possibility of a profit or a loss by investing (enterprising) (Tichý, 2004).

The risk is in economical systems usually evaluated by *beta coefficient* in CAPM model (Capital Assets Pricing Model); this is neither β nor β^{HL} index (Tichy, 1993) which is used in construction reliability. The core of CAPM is the idea of the balance – future returns (but also losses) are proportional to the risk (beta coefficient) of an investment.

Stocks with a high beta coefficient do not have to come to the profit, which corresponds to the empirical expected value. Problems arising during practical empirical evaluation of beta coefficient lead to a wrong opinion that CAPM model is not significant. Actually only the assumption that *empirical records* are applicable to evaluation of the *real* beta coefficient is not significant. The beta coefficient formula is not *statistical robust* and only one “off day” on a stock market may distort the coefficient assessment.

On the other hand, many empirical studies have demonstrated that small companies *reach the better-than-average rate of stock return*. This for a long time not explained economical abnormality was named as *size effect*. This unexpected difference, illusion of size effect, results from a different statistical distribution of the beta coefficient and the long-term stock return – beta coefficient distribution is not symmetric, while the stock return distribution is (Kohout, Hlušek, 2002).

In the past more significant mistakes have appeared, e.g. the fact that it is possible to ignore the company size by the evaluation of the beta coefficient. For example Nokia represents two thirds of the total capitalization of Helsinki stock market. The consequence is, that beta coefficient evaluated on the basis of Finnish stock market cannot have any practical utility. Such a phenomenon is typical for all stock markets over the world except for the US stock market, where the CAPM model was born. The authors of the model did not come across the size influence, so they did not count with the size effect during the model creation. As conclusion, in the present time, distorted beta coefficients are used in many countries. Beta coefficients evaluated for non-American stocks are not recommended for a usage in the financial practice.

References:

- [1] KOHOUT, P. – HLUŠEK, M.: *Peníze, výnosy a rizika: příručka investiční strategie*. 2. vyd. Praha: Ekopress, 2002. 216 s. ISBN 80-86119-48-3.
- [2] NOVÁK, D.: *Modelování spolehlivosti a vlivu velikosti betonových konstrukcí*. Brno: Vutium, 2002. 28 s. ISBN 80-214-2101-0.
- [3] TICHY, M.: *Applied Methods of Structural Reliability*. Dordrecht: Kluwer, 1993. 402 s. ISBN 0-7923-2349-1.
- [4] TICHÝ, M.: *Rizikové inženýrství a management rizika*. Praha: [b.j.], 2004. pprukopis rozpracované knihy.

This research has been supported by CTU grant No. CTU0401211.

Problems of the Traffic Safety Evaluation Objectivity

P. Slabý, M. Hála, P. Karlicý

slaby@fsv, cvut. cz

CTU, Faculty of Civil Engineering, Dept. of Road Structures, Thákurova 7, 166 29, Prague 6

Results of the real state of accidents are presented on the base of statistical parameters worked out at the Police Presidium on the Ministry of Interior of the Czech Republic. Detailed analysis of accident types, their causes, etc. are given there in global parameters for individual districts and as a summary. These global results do not enable entire traffic engineering analysis necessary for objective proposal of improving measures in practice.

Our department has been working for many years, especially in the last decade, on systematic research of traffic-engineering characteristics under various construction and transport conditions as well as on the occurrence of conflict situations or real traffic accidents.

We have been working on the research project [1]. Conclusion of this demanding work (from the viewpoint of using existing databases, in the necessity of assuring a couple of topical traffic analysis, monitoring of conflict situations and in the development of impartial statistical analysis) can be given even today. For unbiased conclusions of general impact it is necessary to study this problem continuously and calibrate and update step-by-step the application in various branches.

Progression and partial results of the related research project [2] have been presented during the work on following tasks:

- I. State of the official database of traffic accidents
- II. Statistical analysis of traffic accidents
- III. Analysis of accidents according monitored factors. Traffic experiments
- IV. Efficiency and evaluation of realized measures

Brief characteristics of the conclusions and recommendations of individual tasks

Ad I) The innovation of the traffic accidents evidence system was proposed. It was based on detailed analysis of the present state of traffic accident databases (in the competence of the Ministry of Interior) together with databases of roads and traffic (in the competence of the Ministry of Transport) and on the close cooperation with the traffic police. The new system of the traffic accident evidence would permit to construct so called “collisions diagram” that is indispensable for impartial traffic engineering analysis.

Ad II) Various statistical methods and tools were used and tested when analyzing traffic accidents. The database containing all traffic accidents on Prague signalized intersections during the time period 1995-2003 served us as raw data. We have used records on traffic volumes on these intersections together with detailed schemes, etc., too. Our main goal was searching for relations between accident rates and traffic volumes; objective detection of unsafe intersections, etc. We have started with standard descriptive statistical tools, which gave us first insight into the problem. Time series analysis provided also interesting findings. Nevertheless the main stress was put on the use of regression and correlation tools. First we derived regression models for the total count of accidents on the given intersection (for a chosen time period) where the total traffic volume served us as the regressor. The regressor seems to be statistically significant; the models helped us to detect unsafe intersections. In the second part of the research we tried to apply regression methods when looking for the relationship between the number of accidents on a given intersection related to specified

maneuvers of the cars involved and the traffic volumes related to the approaches to the intersection used by these cars. We derived very interesting and helpful results. The classification of accidents with respect to 15 typical patterns gives us very detailed insight. On the contrary the classification as such was very laborious, we have met many technical problems when specifying the traffic volumes related to these patterns. The quality of the regression models was sometimes lower than we had expected. Therefore the use of multiple regression seems to be slightly debatable.

Ad III) This task was focused on the analysis of the impact of selected constructional and traffic characteristics on the accidents. Attention was given mainly to the intersections, through roads and juvenile drivers.

Road network in the Czech Republic is very dense; it connects all towns and villages. Traffic of automobiles complicates there pedestrian and cyclist movement, so danger of street accident increases. The accident rates were calculated from numbers of accidents and traffic volumes on 26 sections of 2nd class highways in 9 towns of Central Bohemia region. These data can be used as a starting point for determination of adequate measures to increase traffic safety on main roads in small urban areas.

Ad IV) The efficiency of traffic measures on the traffic accidents rate was evaluated by comparison of the states before and after realisation. Both states were monitored in relation to the traffic loads – intensities of traffic streams.

The important conclusions are:

- Proposal of the new system of traffic accidents evidence.
 - Detailed statistical analysis of accidents on traffic light controlled intersections did not improve sufficient statistical reliability of regression relation between accidents and traffic loads in comparison to the results published in [1].
 - Similar analysis for the file of non controlled intersections was relatively more favourable
 - The parameter of „safe distance“ for profile measurements is an important factor for the description of traffic streams under various constructional and traffic conditions.
- It will be necessary to pay attention especially to the traffic states with columns of cars and possibly with congestion.

References:

- [1] SLABÝ P., JIRAVA P., HÁLA M., KARLICKÝ P.: *Traffic engineering analysis and possibilities of the elimination of accident's sites, (In Czech) Final report GACR* Vydavatel, 1996-1998, 120 pages .
- [2] SLABÝ P., HÁLA M., KARLICKÝ P.: *Problems the traffic safety evaluation objectivity (In Czech) Partial reports* Vydavatel, 2002-2004, pp. .
- [3] SLABÝ P.: *Identification and Forecasting of the Road Safety 11th International Scientific Conference* , University of Zilina, 2003, pp. č. strany–č. strany.
- [4] SLABÝ P., MALÝ M., ŠPAČEK P.: *Accident Rate of Young People* Doprava , 2003, pp. 20-21.

This work was funded by the National Research Center (Grant 103/02/0065/A)

Application of Balanced Scorecard in Siska printing works

J. Beneš, M.Volf

benes_jiri@seznam.cz

volfurbo@volny.cz

CTU, Faculty of Mechanical Engineering, Dept. of Economics and Management
Horská 3, 128 03 Prague 2

Nowadays many enterprises have defined its strategy, but many top managers of these enterprises solve problem, what exactly do we have to do, to fill out our strategy. Or they ask themselves, how our actions are connected with strategy and how do they fill it? These are frequently asked questions. Balanced Scorecard (BSC) is the way, how to answer these questions.

In our case, we solved similar problem. Printing works Siska had defined strategy. Management was interested in implementation of strategy in everyday enterprise live, so that every employee would know, what to do to fill strategy and enterprise successfully.

We used BSC for our case. BSC is method, which translate enterprise strategy into "action". We used Horvát & Partners method of implementation BSC in our case. Further on we demonstrate implementation of strategy by BSC in our case.

On beginning of the case, we learned enterprise history and intradepartmental processes. After that we did financial analysis of Siska for evaluating previous activity and as one of starting points of our next work.

The next step was analysis of neighborhood. For this task, we chose SWOT analysis. We defined enterprise strength and weakness, opportunities and threats of the market. Based on SWOT analysis, we set up four cross strategies (SO, ST, WO and WT).

In following steps we acceded to implementation of strategy by BSC method. First of all we had to define strategic targets. Strategic targets were defined on workshop with top management, for each of cross strategies, which were defined by SWOT analysis. After definition of strategic targets we step to creation of strategic map of targets. We searched binding between particular targets for creation strategic map of targets. There were used cause and consequence analysis. The result of this process was to find significant bindings between targets and figure these bindings in strategic map of targets. This process was applied for each of cross strategies.

Final solution result up from selection of the most important targets from cross strategic targets. Those targets, which were not used into final strategic map, where used as measures or as projects of the final strategic targets.

Measures are used for clear and nonchangable visions of strategic targets and they are able to monitor their level. Measuring of strategic targets could affect behavior on the right way. Every strategic target has been described and has final value.

Projects are realising strategic targets. It says, which activites could make good strategic targets. Dead line, budget and the chief of projects define whole project.

With this block definition of strategic activities and projects, part of definition and creation of strategy with Balanced Scorecard is finished. The second part of implementation starts here. We control and evaluate, how succesful this implementation is in main strategy. Where are the errors, size and reasons. We have to look for resolutions, how to repair these errors. It can not vergot connection of strategic and tactic plan. The main dates from strategic plan will be the most important dates for us to build Tactical Years Plan. That is the best resolution, the definated strategy will drive each individual plan. They are prepared in company. For example: business plan, processing plan, financial plan, etc.

Aplication of method Balanced Scorecard shows not only the implementation to constrution of company, but to the area of service too. There is the most important part of modern strategical driving company. Every part of company has specifical function from the main targets, measures and projects, which have consequently to do it and complement datas to the central place. This place exists for evaluation of succesful projects. For methodology Balanced Scorecard is very useful and it is a main measure for driving and evaluating of culture of company.

Implementation of Balanced Scorecard was successful. Strategy was converted into concrete action in company. We defined strategical targets, measures and projects and told what we wanted, we can measure it and if we did it and specified concrete people for the most important projects and targets.

References:

- [1] KAPLAN, S. R. – NORTON, P. D.: Balanced Scorecard – Strategický systém měření výkonnosti podniku, Management Press, Praha 2000
- [2] HORVÁT & PARTNERS : Balanced Scorecard v praxi, Profess Consulting, Praha 2002
- [3] PORTER, E. M.: Konkurenční strategie, Victoria Publishing, Praha 1994

Utilization of Picocell Nets for Transmission Information in Transportation

J. Bláha, Z. Bělinová, J. Kazda

xjblaha@fd.cvut.cz

Department of Control and Telematics, Faculty of Transportation Sciences, Czech Technical University, Konviktská 20, 110 00 Prague 1, Czech Republic

This paper deals with the utilization of the wireless technologies (DECT, Bluetooth) in the transport telematic systems. The monitoring of the current movement of modes of transport, technological maintenance vehicles, and transportation units (containers, goods, and persons) and system parameters are defined. It is described the measuring and testing of the wireless networks. It was used a standard statistical method for processing of results, which utilize the probability density.

Wireless technologies in transportation will have above all chief meaning for drivers. Possibilities appear above all in offered services. The solution, how to get needed information to drivers, is by means of radio ways. This is the question of sending actual traffic information, dynamic navigation, localization position, etc. Next utilize appears in preferred rescue or police cars on the crossing. As well it will need to communicate inside vehicles with whole series electronic devices.

DECT works in band 1880 - 1900 MHz. This band is divided into ten channels, which they are divided further into strings 24 repeating timeslots. Twelve of those timeslots operate traffic from Base Transceiver Station to Mobile Station and second twelve slots use for reverse direction. DECT uses as well as GSM modulation GMSK. Perhaps substitution of cable for data transmission afloat until the distance about 50 meters in building and 300 meters in opening free space. Data transmission is characterized by very low error rate.

Bluetooth is universal radio system in band 2.4 - 2.48 GHz. It consists of very small network segments (piconet). Data flow is maximum 723 kbit/sec. The guaranteed reach of device is 10 meters. The network topology "ad hoc" is applied in the Bluetooth system. The first device, which sets up the connection, serves the function of the control section (Master). Other data stations constitute Slave units. The function of the Master segment is merely temporary and it wears off after-nullification given nets. Arbitrary data station can communicate at the same time with several piconets. This network topology is called "Scattered ad hoc". Data station Bluetooth uses transmission with Spread Spectrum (with coded multiplexer). It reduces possibility of mutual interference among single devices, which are working in this band. Radio transmission is protected in system Bluetooth against error rate.

The system requirements are availability of > 99.7 %, integrity of < 2 s, response dynamism of < 10 s, localization (by type of transport) of < 2 m, safety of SW, HW, and data.

The wireless networks are measured by means of notebook, server, mobile phones and wireless modules. It is used the own measurement software. The measurement proceed in the following way. At first it is sent out the demand on server about the sized file with the random data content. After it is received data in the mobile data station. Data acceptance runs to the moment of receiving the last sign. It is possible to measure statically or dynamically. Dynamic measurement allows to evaluate dependence the transfer rate on the car speed. It is reduced the transfer rate by higher speed of vehicle movement. It is happened to connection faults more frequently. These connection faults are random and it depends on many factors (e.g. net overload, atmospheric influence, dependence on position transmitter / receiver). The

transfer rate increases with the higher data size. On the other hand it is happened connection faults and data transmission take longer. Then given measurements have different numbers of measured samples.

It was used a standard statistical method for processing of results, which utilize probability density. This probability density is approached by rates of measurement data. The linear interpolation is implemented among of measurement data. The next statistical parameters will be used for measurement data processing. It is possible to calculate the mean value estimation experimentally as a moment of the probability density. The maximum likelihood estimation is the value of a parameter, in which the probability density function has a maximum value. It means in praxis that measurements occur around this value (likelihood) the most frequently. The advantage of this estimation is especially in that it is remote values resistant. Selection standard deviation uses for evaluation of the measurement values reliability. The measurement value will be in defined interval by the theoretical normal distribution with the probability 95 %.

It was proved by measurement that the transfer rate increases with higher data size and by movement was connection stability much lower. Switching channels and influences caused the biggest variations in transmission, which isn't possible to specify (reflection signal, randomly disturbance of radio signal, etc.). The measuring notebook didn't have the influence on accuracy of measurement. It wasn't proved the influence of operating system with measuring program. It wasn't proved the distance influence on the transfer rate of technology DECT, while Bluetooth is high dependent.

References:

- [1] V. VODRÁŽKA, M. SVÍTEK: *Measurement of Data Transfer Speed in GSM/GPRS Net of Radiomobile a.s.*, Department of Control and Telematics, Faculty of Transportation Sciences, CTU in Prague, 2001, pp. 1-11.
- [2] M. KOPECKÝ, M. PÍCHL, M. SVÍTEK: *Transport relies on telematics*, Technologies & Prosperity, 2000, pp. 30-31.
- [3] Z. BĚLINOVÁ: *Analysis of Communications Systems in Transport Telematics*, Thesis, Department of Control and Telematics, Faculty of Transportation Sciences, CTU in Prague, 2003, pp. 40-60.

This research has been supported by FRVŠ grant No. FRV 2110/G1.

Human Factor in Production Management

J. Lastivková, Z. Molnár

jlastivkova@yahoo.com

Department of Management and Economics, Faculty of Electrical Engineering, Czech Technical University, Horská 3, Praha 2, 128 03

Gap between academic field and real factories in the area of planning and scheduling give a lot of questions that have not yet satisfying answers. Observations in factories clearly display that plans created by APS information system often hadn't qualities required by planners for immediate plan launches. Since APS system used mathematic algorithms for creation of optimal plans, is necessary to asked what the reason for such inadequate plans is, what does make existence of human planner necessary.

A better understanding of planning methods in factories and problems connected with effective usage of APS information systems is necessary. Therefore research based on study of factories in Japan continues to study information system effectiveness in Czech Republic. In Japan it started to address problems of APS information systems and planning methods. Together with Global Survey on Manufacturing Management Practice (McKay) research is too interested in global impact of different cultural background on planning styles, methods and solutions of problems.

Researches on planning and scheduling point out that it is difficult to find difference between planning and scheduling and that often planning, scheduling and dispatching tasks are described as black boxes with no exact specification for how these functions are carried out and that un-transparency of functions in practice, combination of planning, scheduling and dispatching tasks and functions appeared to be varied almost with every company or factory and their meaning is interpreted differently [3].

A number of researchers consider that the influence of human scheduler in the production process of factories is not possible to omit or ignore, because the human scheduler significantly influences scheduling decisions. Present automated solutions to scheduling process approach scheduling as well defined mathematical problem in contrast to the reality and solving of arising problems is left to human scheduler. [1]

The planning process in the plant is at a higher level influenced by many factors. Human and material resources impact planning as do the environment, infrastructure in plant, and weather outside the plant. The evaluation and recognition of these and other factors is believed to be a necessary and tough part of planner's work and forms the basis of this research.

If planners choose key work in a way similar to schedulers and dispatchers, there must exists at least some inner system of classification for importance of tasks in the plant that the human planner is working with. Understanding these categories and how the planner deals with them will assist in understanding how planning is performed, what support is necessary in planning tools used within the plant, and what issues need to be addressed by supply chain planning software. Analysis of these categories and roles in the planner's decision process is critical for unravelling the planning and scheduling problematic and care is required to identify the connections, intersections, cross-connections, and so forth between the categories.

Obviously, not all of the variables and information used by planners can be included in any information system. However, it is likely possible that some of the key information can be included as can the processes of filtering, pre-selection, and anchoring. Part of present research will identify subsets of the planner's knowledge base and information gathering that should be considered for inclusion in the decision support systems used by the planner.

In addition to the human issues, there are machine or physical resource issues. For example, there are bottlenecks machines, recently damaged machines, and machines that are extremely sensitive to weather or skill of operators. There are also cultural events (national holidays and resulting traffic patterns) and plant infrastructure (e.g., maintenance schedules) and weather to consider.

Hence, it is likely that information used by the planner will include data about the plant, what is in the plant, how well things are going in the plant, and the environment in which the plant operates. It is also possible that the planner will need increased or enlarged information sources to include knowledge about customers and vendors. For example, is some serious production problem occurring at an important vendor? How does it impact the plant? If the planner is thinking at the system level and considering the overall supply chain, the importance and priority of such information has to be evaluated. It must be placed into the general context of the production plan in the plant.

The creation of an optimal plan (based on the plant's objective measures) that is not necessary to modify and that can be followed for the foreseeable future can be considered as the optimal goal. In an academic sense, this is achieved with deterministic scheduling models in which everything is known in advance and no uncertainty exists in the execution. In contrast, the basic premise for plan creation in real factories is the planner's experience with the plant and the detailed knowledge of production – real factories are not deterministic, nor are they free of uncertainty. Thus, in real factories the idealistic goal of a totally optimal plan is not possible to meet and in practice compromises are made to create plans that attempt to balance demand with available capacity [1]. The question is how such compromised and balanced plans are made – what special decisions are made by the planner to create the balance?

Problems connected with gap are not only APS software; another problem can be language, because of difference in using technical term about planning and scheduling tasks. Therefore in present consultants often play important role during processes of APS software implementation and help to obtain of mutual understanding of requirements between customer and vendor, between management and planner. That is too reason why thorough introduction of APS software to planners before usage in factories and determination of information is necessary and can be crucial for obtaining planner's knowledge for using of APS software.

References:

- [1] S. CRAWFORD, V. C. S. J. WIERS *From Anecdotes to Theory: A review of Existing Knowledge on Human Factors of Planning and Scheduling* In B.L. MacCarthy & J.R. Wilson (Eds.), *Human Performance in Planning and Scheduling: Fieldwork Studies, Methodologies and Research Issues*, Taylor & Francis 2001 pp. 15-43
- [2] K. N. MCKAY, J. A. BUZACOTT *The Application of Computerized Production Control Systems in Job Shop Environments* *Computers In Industry* 42 (2-3) 2000 pp. 79-97
- [3] K. N. MCKAY., V. C. S. J. WIERS *Integrated Decision Support for Planning, Scheduling, and Dispatching Tasks in a Focused Factory* *Computers in Industry*, 50 (1) 2003 pp. 5-14
- [4] V. C. S. J. WIERS, T. W. SCHAAF *A Framework for Decision Support in Production Scheduling Tasks* *Production Planning and Control*, 8(6) 1997 pp. 533-544

Two Special Transformations of Linear Programs Used to Decision Making under Incomplete Information about Scenarios Probabilities

L Vaniš

Ladislav Vaniš@Fs.cvut.cz

Department of Management and Economics, Faculty of Mechanical Engineering, Czech Technical University, Horská 3, 128 00 Prague 2, Czech Republic

Decision making under risk is concerning at this time a large number of decision-making processes, above all namely in strategic planning. In this decision making it is possible to use the technique of scenario writing, which in addition is able under definite presumption to derive benefit from mathematical modelling just with the view of algorithm development of strategic planning.

Scenario is a mathematical intersection of risk factors levels. Single risk factors activity results in events, which may or may not occur, or occur in different modifications. Risk factors may be for example unemployment, inflation, demand, etc.

In using decision making under risk there is characteristic an incomplete information about scenarios occurrence. Information on scenarios probabilities are incomplete. That means it is impossible to determine probability of each scenario as point estimates.

From different possible forms of information incompleteness on scenario probability it is possible to meet most often the following cases:

- 1) scenarios probabilities are assessed as interval estimates,
- 2) scenarios are ordered ordinally according to their probabilities.

On the bases of a decision table with rows representing alternatives of decision making and columns representing scenarios and where table values are the corresponding assessments, for solving of such situation mathematical models of linear programming are used.

For both cases it is possible to create linear programming mathematical model with linear restrictions and goal function. The restrictions of such models are so simple as to make possible to solve the models by an appropriate transformation without using the simplex method.

For illustration we choose the case 1).

Denoting \underline{p}_k the lower limit of probability p_k of scenario k and, \overline{p}_k the upper limit of probability p_k of scenario k , then every probability p_k satisfies the inequalities.

$$0 \leq \underline{p}_k \leq p_k \leq \overline{p}_k \quad (k = 1, \dots, s)$$

conditioned by the inequalities

$$\sum_{k=1}^s \underline{p}_k \leq 1, \quad \sum_{k=1}^s \overline{p}_k \geq 1.$$

Values of probabilities p_k , maximizing or minimizing the expected final assessment $E(h_i)$ for alternative I , form optimum solution of linear programming model with restrictions

$$\sum_{k=1}^s p_k = 1$$

$$\begin{aligned} p_k &\leq \bar{p}_k \\ p_k &\geq \underline{p}_k \end{aligned} \quad (k = 1, \dots, s)$$

and goal function $\sum_{k=1}^s h_{ik} p_k \stackrel{!}{=} \max$ resp. $\sum_{k=1}^s h_{ik} p_k \stackrel{!}{=} \min$.

Then

$$\underline{E}(h_i) = \max E(h_i) \quad \text{a} \quad \underline{E}(h_i) = \min E(h_i)$$

After probabilities transformation by the relation the modified model

$$d_k = p_k - \underline{p}_k \quad (k = 1, \dots, s)$$

takes the form

$$\sum_{k=1}^s d_k = 1 - \sum_{k=1}^s \underline{p}_k$$

$$d_k \leq \bar{p}_k - \underline{p}_k \quad \text{a} \quad d_k \geq 0 \quad (k = 1, \dots, s)$$

$$\sum_{k=1}^s h_{ik} \cdot d_k = \begin{cases} \text{MAX} \\ \text{MIN} \end{cases}$$

In decision making under risk, where's necessary in some cases to solve even several tens of linear programming models, these transformation very profitably accelerates work in solving these models.

References:

[1] Z. W. KMIETOWITZ, A. D. PERMON: *Decision Theory and Incomplete Knowledge* Gower, Aldershot 1981

This work has not been supported.

The Role of Foreign Direct Investment in Restructuring of Manufacturing Industry

H. Pačesová

Hana.Pacesova@Fs.cvut.cz

Department of Management and Economics, Faculty of Mechanical Engineering, Czech Technical University, Horská 3, 128 00, Praha 2, Czech Republic

There is a broad agreement that foreign direct investment is playing an important role in restructuring of manufactory. The impact of FDI rises with the technology intensity of exports especially in the case of developing countries.

The analythics have found that a 1% rise in FDI per capital leads to a 0.8% increase in high technology exports. In countries without strong national innovation systems and exports led by national enterprises, the question is how to cope with the pace of technical change and make inroads into markets held by more advanced countries. Moreover, when the evolution of dynamic comparative advantage is assisted by FDI there is a problem of sustainability and upgrading, especially as wages rise and cheaper competitors apper. The question of spillovers between foreign-owned and domestic sectors has to be tackled in order to avoid that isolated points of advancement develop while the rest of the economy falls behind.

Foreign direct investment has been one of the driving forces of industrial restructuring. Countries middle and east Europe have inherited from the past a largely obsolete capital stock that frequently turned out to be non-viable in the conditions of a market economy. And, contrary to frequently held opinions, there is some recent evidence that transition economies lag behind advanced market economies also in terms of the quality of their workforce. Despite achievements in formal education, the skills – especially at the level of managerial and other skilled employment – required in a market economy are deficient. The modernization of existing assets and the training of human resouces require extensive efforts and huge financial resources that are generally scarce. That is why foreign investment, especially FDI, has been seen to play a prominent role in upgrading both human and capital stocks. However, the evidence for direct links between FDI performance and growth or restructuring and productivity spillovers in transition economies is mixed, partly also due to the scarcity of reliable.

Manufacturing industry has been an important target of FDI in the countries of central and east Europe, attracting nearly half of all inward FDI stock as of end – 1999 (except for the Baltic states where the shares are lower). FDI penetration in the manufacturing industry (FDI stock per employee) is high in the Czech Republic, Hungary, Poland and in Slovenia. All these countries display a similar pattern – an uneven FDI distribution across branches, reflecting not only the varying attractiveness of individual branches for foreign investors and their investment motives, but also the different privatization policies. FDI inflows have been high in both domestically oriented branches such as the food, beverages and tobacco industry (especially in the Czech Republic, Hungary, Poland Slovenia) and pulp and paper, as well as in predominantly export – oriented branches such as the chemicals and especially the transport equipment industries.

FDI helps to speed up restructuring. There is a clearly positive link between foreign penetration and various components of international competitiveness at both the aggregate and sectoral levels of manufacturing. There were many cases of investigation the branch specific relationship between FDI stock per employee and various branch perfomance indicators

during 1993 – 1999 for the countries of middle and east Europe. Robust regressions (all variables in log – linear form with country specific dummies show statistically significant impact of sectoral FDI penetration on output growth, as well as on labour productivity growth and the estimated coefficient is significant at 10% level on unit labour costs improvements. All parameters have the expected signs and are statistically significant. Higher FDI penetration is associated with faster growth of output, with bigger productivity increases and with lower growth of unit labor costs.

After the trade liberalization and re-orientation starting at beginning of the 1990s, the most important trading partner for above mentioned countries is EU. The shares of the EU in total manufacturing exports range from 40% (Bulgaria) to more than 70% (Hungary), import shares range from 40% (Bulgaria) to nearly 70% (Slovenia) and the manufacturing industry accounts for more than 90% of EU trade. Manufacturing exports of these countries to the EU increased by more than 50%, in current euro terms, between 1995 and 2000, much faster than exports of the other competitors on the EU market (total extra – EU manufacturing imports grew by 30%). Hungary, Estonia and the Czech Republic – all attractive FDI destinations – recorded the faster export growth. The market share of these countries in extra EU imports reached nearly 12% in 2000, about half of the US market share in the EU and surpassing the share of Japan. EU manufacturing export to these countries grew with nearly equal speed during this period also much faster than overall extra – EU manufacturing industry exports (+15%). The importance of EU market for above mentioned countries manufacturing exports and imports are thus already roughly comparable to that of the internal market for the current EU member states.

References:

- [1] R. BARREL, D. HOLLAND: *Foreign Direct Investment and Enterprise Restructuring in Central Europe. Economics of Transitions* , 2000,
- [2] R. DOBRINSKY: *Economics Transformation and the Changing Patterns of European East. West Trade* 2002
- [3] P. HAVLIK: *Restructuring of Manufacturing Industry in the Central and East European Countries* 2003

This work has not been supported.

Recruitment Process

T. Šulcová

tereza.sulcova@fs.cvut.cz

Department of Management and Economics, Faculty of Mechanical Engineering, Czech Technical University in Prague, Horská 3, 128 00 Prague 2, Czech Republic

The recruitment of new staff is a very important and necessary part of human resources management. The main question is why? Because the management can achieve aims only by force of motivated, qualified employees.

Human Resources Managers can choose different kinds of recruitment methods and techniques – for example application forms (CVs), interviews, personality, and ability, job knowledge and graphology tests or Assessment Centre etc.

This contribution is focused on the way of recruiting oriented to middle and top management - executive search. The choice of recruitment process is determined by the level of the position in an organization structure. If the organization would like to search the candidates for middle and top management it can be used the method of executive search.

Executive search was appointed as a most suitable form of recruiting management. It was identified these main reasons: 1. Managers are approached directly 2. The communication and recruiting process is strictly confidential 3. The searching process is focused only on most suitable candidates for appointed position.

The definition of executive search is: the process of looking for new managers for organizations, usually by approaching managers in their existing jobs and asking them if they want to work for different companies. More polite term for executive search is headhunting. Executive search is a special process of human resources recruiting and it's better to use external special consultancy company due to these reasons: 1. Detailed information about the situation on the market 2. Experienced team of consultant specialized in branch and detailed understanding of the labor market 3. Definition of client needs via personal meeting with client 4. Selection of most useful tools and best execution of the searching project.

It's a long-term cooperation with Consultancy Company because of providing confidential information. The project usually consists of following parts: 1. Pre-Project 2. Project Planning and Preparation 3. Research Strategy 4. Interviews with Consultant 5. Short-list of candidates 6. Interviews with Client 7. Candidate Review and Feedback 8. Offer and Acceptance.

The process of executive search is applicable in different sectors. The trend during nineties ages of last century on the Czech market was appointed as following continuance: 1. Sector of Sales - FMCG (Fast Moving Consumer Goods) 2. Pharmaceutical Sector 3. IT/Telecommunication sector 4. Financial Sector 5. Investment and Manufacturing Sector.

The differences between executive search and "classical" way of searching candidates was identified as the following: Executive search – 1. Know – how 2. Networking 3. Tailor-made approach 4. Best-fit selection 4. Preparation of Success Profile 5. Description of Opportunities. "Classical" way of searching – 1. Systems Process 2. Database of candidates 3. In-Mass Approach 4. Elimination incompetent candidates 5. Preparing Job Description 6. Description of Candidates Requirements.

References:

- [1] ŠULCOVÁ, T - ŠVEDOVÁ, M.: *The Executive Search Process Application*. Vox a.s., 12/2004 Conference Human Resources Management, Training and Devedlopment.

The Aerodynamic Characteristics of Helicopter Main Rotor

R.Pohl, J.Šesták

jan.sestak@email.cz

Department of Transportation Technology, Faculty of Transportation Sciences, Czech Technical University, Na Florenci 25, 110 00 Praha 1, Czech Republic

The main rotor produces a lift, it is an aerodynamic force needed for flight. An ability of lift generating is given by the rotor aerodynamic characteristics. These characteristics are set by the flight tests. The aerodynamic forces which influence to a helicopter during the flight, are the lift (vertical force), the propulsion (horizontal direct-axis force) and the side thrust (transverse force). The total force is vector sum the above-mentioned forces.

In the aircraft coordinates system the main rotor lift is defined by its direct-axis and transverse component forces. The lift acts in rotor axis and it depends on the parameters: lift coefficient – it formulates the rotor aerodynamic characteristics and the maximal loading during hovering flight, it depends on the collective blades angle and the rotor power; rotor disk area; air density; square root of blade tip velocity.

In the aerodynamic coordinates system there are defined the rotor uplift force and propulsion force and transverse force. The uplift depends on the parameters: uplift coefficient – it depends on the blade angle of attack, the collective blades angle, the aircraft speed and the rotor disk angle of attack; rotor disk solid coefficient; rotor disk area; air density; square root of blade tip velocity.

The aerodynamic forces formulation in the aerodynamic coordinates system is the transformation of the formulation in the aircraft coordinates system, it flows from the above-mentioned characteristics. The turns ratio is formulated by the rotor disk solid coefficient, which depends on the blade central chord length ratio on the rotor radius.

The helicopter main rotor works at the harder conditions during the directional flight than during the vertical flight. The helicopter can do directional move at engine flight, when the gyroscopic moment is transmitted to rotor axis (horizontal and vertical flight), or it can do directional move at nonengine flight – autorotation. These situations are different, because they are done at different aerodynamic conditions; the main difference is rotor disk angle of attack: it is negative angle at engine flight and it is positive angle at autorotation. The directional flight is done on negative angle of attack, the air flows down from top trough the rotor disk area – at autorotation it is backward.

Aerodynamic dissymmetry of helicopter main rotor lift is caused by the physical principle of flight. It has to be appointed the rotor blades airspeed at the azimuthal location. During the directional flight the helicopter is rotating (round the rotor axis) and it is moving forward (translation move). Dissymmetry of lift is difference in lift that exist between the advancing half of the rotor disk and the retreating half. It is caused by the fact that in the directional flight the aircraft relative wind is added to the rotational relative wind on the advancing blade, and subtracted on the retreating blade. The blade passing the tail and advancing around the right side of the helicopters (left moving rotors) has an increasing airspeed which reaches maximum at the 3 o'clock position. As the blade continues, the airspeed reduces to essentially rotational airspeed over the nose of the helicopter. Leaving the nose, the blade airspeed progressively decreases and reaches minimum airspeed at the 9 o'clock position. The blade

airspeed then increases progressively and again reaches rotational airspeed as it passes over the tail at the 6 o'clock position.

The cyclic changes of airspeed at the azimuth positions cause the changes of aerodynamic force, which effect on the blade. The forces are higher on the advancing side than on the retreating side. This difference causes the cant moment, which is transmitted to an airframe of helicopter. If the distribution of blade lift (along the blades at 3 and 9 o'clock position) is substituted by one vector, this vector will not act at the axis of rotation, it will act out of the axis and it will cause the cant moment, which cants the helicopter to the retreating side. This moment makes oneself felt furthest in case of 2-blades rotors. These rotors are reaching the maximal cant moment two-time per one revolution. The situation improves with increasing number of the rotor blades.

To compare the lift of the advancing half of the disk area to the lift of the retreating half, the lift equation can be used. In forward flight, two factors in the lift formula, density ratio and blade area, are the same for both the advancing and retreating blades. The airfoil shape is fixed for a given blade. The only remaining variables are changes in blade angle of attack and blade airspeed. These two variables must compensate for each other during forward flight to overcome dissymmetry of lift. Two factors, rotor RPM and aircraft airspeed, control blade airspeed during flight. Both factors are variable to some degree, but must remain within certain operating limits. Angle of attack remains as the one variable that may be used by the pilot to compensate for dissymmetry of lift.

The blade is changing an effective angle of attack at all azimuth positions of rotation move. At 3 o'clock azimuth position the blade is at the low effective angle of attack (it corresponds to up motion of the blade), on the retreating blade side there is the situation opposite. At 9 o'clock azimuth position the blade is moving down and this motion increases the effective angle of attack. The blade, which is entering this azimuth position, is at the higher effective angle of attack depending on the increasing forward speed. The retreating blade is working with higher and higher effective angle of attack and this angle is coming near to the critical angle of attack (at this angle the blade is entering blade stall). If the critical angle of attack is exceeded in the increasing velocity, the blade will stall. This fact is formulated at the dependence of the lift coefficient on the angle of attack. The blade stall causes decrease of the lift and increase of the blade air resistance. A tendency for retreating blade to stall in forward flight is inherent in all present day helicopters and is a major factor in limiting their forward speed. Just as the stall of an airplane wing limits the low speed possibilities of the airplane, the stall of a rotor blade limits the high speed potential of a helicopter.

The centrifugal force influences more in the specific azimuth range, depending on a decrease of lift. It causes the increasing vibrations of the controls and whole helicopter airframe. It is the reason of a low maximal speed of the helicopters. The second reason of the low maximal speed is the blade stall. The blade stall can be moved to the higher speed by the change of rotor decreasing. In this case the rotor blades work at the lower angle of attack. The conditions of the rotor blades work and the directional flight are challenge and they are changing in flight regimes. These changes cause aerodynamic dissymmetry of lift and it is the reason for the constructional modification of the rotor blades suspension and controls.

References:

- [1] POHL, R. – KOCÁB, J. – ŠESTÁK, J.: *Vrtulníky a letadlové pohonné jednotky*
Vydavatelství ČVUT, 2005,

The Sociological Research on the CTU Students Opinions

J. Šafránková

jana.safrankova@fsv.cvut.cz

Department of Social Sciences, Faculty of Civil Engineering, Czech Technical University, Thákurova 7, 166 29 Prague 6, Czech Republic

Today, there are many discussions about further development directions of the Czech Technical University and its component faculties in the context of the transformations under way in the Czech society and with regard to the accession of the Czech Republic into the European Union. One of the sources of information is also the knowledge about the opinions of the CTU students on their studies. The subject of this survey is connected to four representative surveys realized within the Czech Technical University, namely the survey of students in the 2nd to the 5th year of their program in 2001, students in the 1st year of their program (2001) and students, who did not enroll after they had been accepted in 2002. In these surveys, the opinions of existing students as regards the instruction, motivation to study, and identification with a selected course of studying, etc., are being uncovered. The survey in 2003 was about chances of the graduates from component faculties of Czech Technical University on a labour market., for that reason, a survey gathering information about graduates from 1994 to 2001 of all six faculties of Czech Technical University was realized.

The information of the survey of students in the 2nd to the 5th year of their program in 2004 describes their opinions on their study conditions. The survey regarded these basic questions: the satisfaction with a study on CTU faculties, as well as a general satisfaction, as valuation study conditions (a satisfaction with schedule, with lessons number, with tuitions, with availability of literature and textbooks for individual courses.

Further, it was observed the evaluation of education process. Into this evaluation there belongs a structure of taught courses, a proportion of optional courses in education, professional and pedagogical level of lectures and recitations, and the recitation range. The other contentual part covered the information where of the students obtain knowledges, how much they use the information obtained from lectures, seminars, textbooks, university books, foreign language publications, Internet etc. The students had also the possibility to evaluate their work contribution to projects, their knowledge obtained from education, and the relationship among teachers and students. The list of questions contained also many supplemental information, which were related to students satisfaction and dissatisfaction with study organization and with faculties technical equipment.

A few questions were focused on students opinion of future use, as well as in employment, jobs in CR or abroad and type of work

The important factor was also a students interest of a faculty they study at and their study program, mainly from the viewpoint that the part of students enter a faculty of CTU because of their failure of an entrance examination at another preferred faculty, and during their study they realize, if they are interested in their study field or they are not.

The information about view of study and about type of students accommodation of particular faculties of the CTU are also an important observed area out of study.

All these information are an important feedback for all CTU faculty administrations, since they give not only information about students satisfaction, but also about students view of other questions, that are connected to their study and that increase or decrease general

students satisfaction, in our case CTU students, and that can help as topics for further CTU study improvement, also from the point of having a prestige in competition with other technical universities and universities in general. What is very important is the feedback information about the instruction.

The sociological survey from 2nd to 5th year students of all six faculties was representative. The lists of questions were filled up by more than 2 300 students.

It was proved relatively high identification with study at particular CTU faculties. 80% students were satisfied with their study option. Half of enquired were satisfied with study at CTU and the other half of them were generally satisfied. Two thirds were satisfied with schedule, with the number of course, and more than half of them were satisfied with teachers. There was less satisfaction with textbook availability, third of them was satisfied and the other third was generally satisfied.

Three quarters of students were satisfied with technical level of courses, and one half with their pedagogical level; there was no distinctive dissatisfaction.

The students during their study use mainly their notes from seminars, recitations, lectures, and textbooks. It was proved again, that the usage of foreign literature is minimal.

The results of representative survey from 2nd to 5th year CTU students brought many important information. The students satisfaction was proved from many statements, on the other hand some questions showed persisting problems, such as inefficient exploitation of abroad scholarship intership possibility.

The results of the survey were hand over to the CTU administrations for further analysis.

References:

- [1] J. ŠAFRÁNKOVÁ: *The CTU students opinion on study and CTU study condition. The sociological CTU students survey report in 2004. CTU 2004, Internal material CTU, Prague 2004.*

This work was funded by the Czech Technical University Prague.

Interactive Model of Feasibility Study

J. Frková

frkova@fsv.cvut.cz

CTU, Faculty of Civil Engineering, Department of Economics and Management in
Construction, Thakurova 7, 166 29 Praha 6

The aim of the project was to create the complex study material, which provides the students with the manual for disposing the Feasibility study. The manual is especially focused on Finance and Economic Analysis in that way: to obtain co-financing from the public funds and EU financial resources. An interactive model of the Feasibility study provides the students with an unmistakable guideline for working up a project according to the manual by UNIDO. The model is located on the CTU net. The model is actually manual, whereby students step by step generate the Feasibility study as it is UNIDO standards. Parts of the model are interactive calculation tables of cash flow and financial indicators. The model was programmed by Kontis, by means of design tools CDS / Publisher. The tools facilitate developed compatible courses by the standard Scorm 1.2. The model is able to run from the local net without implementation LMS system. The model can be run from the web pages <http://eko.fsv.cvut.cz/studieproveditelnosti/>

The presented model can develop in a creative way a narrow look at the students of technical discipline to economic cogitation. This good technical solution of project must be the good economical solution, too.

The teaching model consists of many additional examples of specific project solutions. A calculation part includes 12 tables scheme, which are interconnected through. An output value from one table is a load to the next table as input data. Distinguishing colors inform student about which array is used for putting in data and which are programmed for output data. A calculation part is finished by automatic calculation of financial and economic indicators.

References:

- [1] BUKOVSKÝ J. – FRKOVÁ, J.: *Finanční a ekonomická analýza veřejně prospěšných projektů*. ČVUT Praha, 2004, pp. 1–187.
- [2] FRKOVÁ, J.: *Vybrané problémy integrace ČR do EU*. ČVUT Praha, 2003, pp. 1-174.
- [3] FRKOVÁ, J.: *Malé a střední podnikání*. ČVUT Praha, 2004, pp. 1–180.

This research has been supported by FRVŠ 3341260.

Integration of Utility Characteristics of Engineering Products for Determination of Their Market Prices

J. Trkal

jan.trkal@fs.cvut.cz

Department of Management and Economics, Faculty of Mechanical Engineering,
Czech Technical University, Horská 3, 128 03 Prague 2, Czech Republic

The goal of this issue is to propose a method for determination of an integrated utility characteristic (consumer value) which we suppose to have the essential influence on the pricing of engineering products.

When making the pricing decision, we will concentrate just on determining the initial price level. There are several steps that are necessary to proceed:

- Identification of the global business targets that have to be supported by pricing
- Definition of elasticity and factors that affect it
- Calculation of the costs
- Market research for competitive offer and price
- Determination of the consumer perceived value (different pricing methods)
- Choice of a pricing method - focus will be especially on the method of complex pricing as a result of several market factors thus making it the only virtually acceptable one in competitive environment
- Final price determination

Studying of this problem leads among others to product strategies, market price evaluation, conjoint analysis (the combination of attributes creating the maximum satisfaction) or the use of multidimensional scaling – the aggregation to a single parameter.

The goal of any conjoint survey is to assign specific values to the range of options buyers consider when making a purchase decision. Conjoint analysis presents choice alternatives between products/services defined by sets of attributes. Conjoint analysis attempts to break the task into a series of choices or ratings. These choices or ratings, when taken together, allow us to compute the relative importance of each of the attributes studied. Instead of “stated importance,” conjoint analysis uses “derived importance” values for each attribute or feature. Equipped with this knowledge, marketers can focus on the most important features of products or services and design messages to impact the target buyers.

In multidimensional scaling models, we suppose the existence of an underlying multidimensional space that describes the items displayed in the space. It may represent e.g. the stimuli (concepts such as brands) and the attributes that describe them, or the similarities between the objects themselves, or even between the objects and groups of respondents that scale them. The objects in such models are represented in a two or more dimensional space. The dimensions of the space represent attributes that are perceived as characterizing the stimuli or respondents. Multidimensional scaling is generally characterized by respondent judgments concerning either the degree of similarity of pairs of stimuli, or the preference for a stimuli as measured on attributes describing the stimuli.

The task is to analyze the influence of respective parameters, determine the significance and intensity of incidence of these arguments on price and to quantify the technical, operational and marketing capability of the product.

References:

No references available.

Problematic of Reconstruction of Diesel Locomotives on Compressed Natural Gas Operation

B. Drápal, C. Novotný *

drapal@fd.cvut.cz

Department of Transportations Technologies, Faculty of Transportations Sciences,
Czech Technical University in Prague, Horská 3, 128 00 Praha 2 - Nové Město

* Czech Railways - Railway Research Institute Prague, Novodvorská 1698,
142 00 Praha 4 - Braník

In last years goes the traffic and vehicles on the line to high ecology and economy. But on the rails can we see very old diesel locomotives, which fall short of this "new" ecological standards and economical standards. For example: in the time, when "on street" has been valid norm Euro 3, "on railways" has been not valid for new built vehicles even analogy of norm Euro 1. Possible solutions are modernization of olds rail vehicles – the motorization with use of new ecological diesel motor or gasification services. Unfortunately it has been make only some experiments with gasification in '90 years in Germany and Russia – the gas operation of engines is more environmentally friendly than diesel operation.

On railway we have specific and hard operation conditions for locomotives. Gas working is principle different as a diesel working, but safety and another standards are the same or more hard. Some of the basic limits, from which get we the basic concept of the modernized locomotive, are this:

- 1) The modernized locomotive can't overstep the vehicle gauge.
- 2) The quality of use from the viewpoint of locomotive driver, another people of railway service and passengers can't decrease.
- 3) The fueling of locomotive must be fluent and simple.
- 4) It is not possible to reduce interval between two charging times.
- 5) It is good; when on the locomotive are minimal gas compression installations.
- 6) It is favourable retain emergency diesel working of locomotive.
- 7) The price of modernization must be minimal.

From these limits price is for investors the most famous. All railways vehicles and modernized components must be approved from national railway office or ministry. And the homologation can be very expensive. So it is good to take for modernization components that are from this office already approved.

On the locomotive is very problematic to "find a place" for gas tanks - volume of compressed natural gas can be even 7 m³ (commensurate with power of locomotive). The locomotive so must have a special wagon with gas container - so we get something similar as has been a steam locomotive with tender. On the railways be used in transport of dangerous gases special multiple element gas container (MEGC). Basic component of MEGC is a bomb vessel from steel or composite materials. The maximal pressure in bomb vessel is 30 MPa. On basis of MEGC is constructed the wagon for gas locomotive. On the wagon are two independent MEGC that are connected per pressure valve and pressure reducer with feeding pipeline of motor on the locomotive. On the locomotive also aren't high-pressure gas components. The gas pipes on locomotive and "gas container wagon" are coupled through

special quick-acting coupling. On one end is equip wagon furthermore of locomotive driver stand. So it is guaranteed ample breadth of views for locomotive driver by the back run of gas locomotive (for example by shutting). The fueling of gas containers is in the meantime long. Consequently is advantageous to have more "gas container wagons" as gas locomotives: Locomotive can change a full "gas container wagon" instead of empty. For quickly and easy changing are between locomotive and "gas container wagon" quick-acting coupling.

The motor will be rebuilt to dual-operation. In principle commingle in blender a natural gas (on normal pressure) with air. Gas-air mixture we bring across supercharger and intercooler to the cylinder and there we this mixture fired with Ignition dose of diesel. Ignition dose of diesel is determinate of type and power of diesel motor and is just about from 10 to 40 percent of amount diesel by normal diesel operation. Mixing proportion is determinate in control member from momentary and predicted power. This concept of motor rebuilding guaranteed among other things emergency return to diesel operation of locomotive. Together with reconstruction of motor is good to modernize other parts of locomotive - suspension, stand of locomotive driver, cooling system, buffers and alternatively even the traction with machine control system.

Rail tank car loading station for gas locomotive must be build as requested on buildings on the railway. Must be respected id est structure gauge, fire regulations and service requirements of railways operators. Next must be created service regulations, fueling regulations, plan of control and maintenance and practice training for locomotive driver and another people of railway service.

The modernized locomotive must be tested minimal in this range: Traction test, measure of quasi-static safety contra derailment on the limit state of rail track (by curse of report ERRI B 55 RP 8), test of fastening points of MEGC on "gas container wagon" and test of "gas container wagon" on hunt (by curse of report ERRI B 12 RP 17 paragraph 3.1). Minimal after there testes can railway office approved modernized locomotive to normal working.

The economical and ecological savings are not such a big as by gasification of cars. Is possible to achieved (by the dual working of locomotive) cost savings between 25 and 45 percents. The cost savings are followed with corresponding ecology savings on exhalations.

References

Two Models Supporting Cost Decision-Making

M. Zralý, M. Plachý, O. Šmíd

`martin.zraly@fs.cvut.cz`, `plachy.m@worldonline.cz`, `ondrasmid@centrum.cz`

Department of Enterprise Management and Economics, Faculty of Mechanical Engineering,
Czech Technical University, Horská 3, 128 00 Prague 2, Czech Republic

Company management on different hierarchical levels requires the accurate enough information supporting decision making in order to achieve to goals of the company. Nowadays, economic steering applications provide this information, which covers the whole area of decision making within the company. This paper deals with the description of two models applicable also in practice of the company, which enable to calculate both: the productive and non-productive costs in order to evaluate the profitability of each product, in other words to set optimal portfolio of products from the profitability point of view. These models make also possible to predict (or simulate) the resources of the processes under investigation, so that the models enable to simulate different production processes in order to reach target costs. Both models make use of the hour overhead tariffs (HOT) method, moreover, the second model makes use multistage contribution margin method, which represents different approach to costing.

As the major advantages of HOT method, it is the possibility to merge consideration of capacity utilization into cost calculation, integration of process characteristics into cost calculation and using of information from technological procedures. Thus, each change in the manufacturing process (not only the changes in the product design items) influences the process costs and the HOT method calculation is the true reflection of this dependency

The first cost model (Model-3F) covers the pre-production, production and post-production stages, which are linked with manufacturing of the particular product (the model was used for the Paddle Wheel Fan D1000). For this reason the cost model was divided into three main modules.

The module of pre-production stages considers of costs, which have arisen by the activities of analytical, designing, engineering and prototype departments. These departments have been chosen as the representatives of departments, which can be taken into account in the pre-production stages in case that the engineering product should be manufactured. The structure of costs in each department is two-fold. First, there arise the costs of employees who work in these departments (wage, health insurance, option money and others) and second there are costs of particular department (rent cost, energy, communications and others) linked with the existence of the department. As was mentioned above, a vertical version of hour overhead tariffs method was used for costing (as the first level it is possible to mention hour overhead tariff of employee whereas the second level is hour overhead tariff of department). Later on, hour overhead tariffs (HOT itself is mostly calculated when total costs of center, workplace or employee per year are divided by the yearly capacity of this center, workplace or employee) are multiplied by the number of hours, which are indispensable in order to develop the product. As a result, the overhead costs, which are linked with the pre-production stages, are determined. The same approach is used in the following two modules.

Module of production stages covers the whole area of the manufacturing processes; this module embodies the costs of manufacturing. The basic idea of this module is the same as it was in the previous case; however, hour overhead tariff of employees was substituted by hour overhead tariff of workplaces. In accordance with the data of manufacturing processes

(the important information for costing is operating time and batch time of the manufacturing operations) overhead costs of manufacturing are determined. Direct costs (raw material, costs of purchased parts and others) are assigned directly to the product.

The third part of the cost model includes the post-production activities; the main departments (parts) of post-production module are shipping, warehouse, sales and distribution departments. There are also two additional departments (complaints department and department of guarantee repair) just in case of some breakdown in the warranty period. These costs can (or do not have to) be included in the total cost summarization.

The final part of each module represents cost summarization; total costs of all the stages are summarized at one additional sheet.

The other cost model (Model-P) is divided into two main parts – cost of manufacturing centers (center of assembly, machines, welding and components) and cost of non-manufacturing center (IT, development, maintenance and administration). The costing system was based on two different approaches, the first is representing by using of vertical version of hour overhead tariffs method (it is alike as it was in the costing Model-3F). The multistage contribution margin method represents the other costing approach.

Generally speaking, decision - making is getting more and more difficult and complicated, processes within the company are so comprehensive that IT support of these processes is inevitable, even for the small and smallest companies (from the long-run viewpoint). The two cost models mentioned above were created in the software based on Microsoft Excel. These models are interactive. Each change (for instance in technological procedure, in cost or capacity utilization of centers and workplaces, in a number of manufactured pieces, etc.) will have the impact in the total costing. If we take into consideration all the products manufactured by particular company we can determine (and simulate) the impact of those changes into the balance sheet profit. These pieces of information are the most important ones for enterprise management, in other words they enable to know the impact of decisions (or changes) in enterprise management ahead of time (Ex-Ante information). Comparison of planned values and actual values and the variances, which have arisen, represents Ex-Post information.

The cost models, which were introduced in this paper, offer both Ex-Ante and Ex-Post information. The models represent one of the possible solution of IT support that is required by managers for effective and accurate decision - making.

References:

- [1] M. ZRALÝ: *Methodology of Activity Set for product Set (AS/PS) Contributes to Product Strategy Application* In: Proceedings from 3. International Conference on “Integrated Engineering in Enterprise Management”, FME CTU in Prague, Brno 2002, pp. 124-128.
- [2] M. ZRALÝ *Integration in Enterprise Controlling Application* In: Proceedings from 10. International Conference on “Business and Economic Development in Central and Eastern Europe”, BBS-TUB, Brno 2002, pp. 522-527.
- [3] M. ZRALÝ *Marketing and Cost Factors in the Sophisticated Machine Tools Development Process* In: Proceedings from “New Trends in Industrial Development”, BBS-TUB, Brno 2001, pp. 103-112.
- [4] P. HORVÁTH *Controlling* Vahlen Munchen 2002

This work has been supported by research grant No. 402/03/1386

Barriers to IT Outsourcing in Czech Manufacturing Enterprises

Jaroslav Zahradník

jaraza@atlas.cz

Department of Management and Economics,
Faculty of Machinery Engineering, Czech Technical University,
Horská 3, 128 00 Prague, Czech Republic

As the business environment moves towards a knowledge-based economy, enterprises are facing ever more challenges in their management of information technology (IT) operations for business success. Thus, organisations are trying to gain competitive advantages by cutting costs through IT outsourcing and focusing more of their internal resources on core activities. On the other hand, service outsourcing in the Czech Republic is not so developed as in Western Europe.

As a part of our research, we have conducted a survey focusing on use of IT outsourcing in the Czech Republic. The target of the survey of the study consisted of manufacturing enterprises in the Czech Republic. The primary industry sectors included in the sample were industrial goods, cable, and metal sectors. The sample of the present study was partly drawn from the directory of CzechInvest and partly from the database of manufacturing enterprises at Department of Management and Economics at CTU. The list of enterprises contained in both databases included 220 firms. The information about survey was sent to companies in October 2004. It was important to have respondents who had a good understanding of both IT and strategy. Therefore, whenever possible, the questionnaire was primarily targeted at managers who were responsible for IT development at the enterprises. The questionnaire consisted of 27 statement-style scaled items and 41 various other types of questions, 68 questions altogether. 51 companies actually returned the questionnaire. This resulted to the response rate of 23 %.

In our research, we have been interested which barriers to IT outsourcing exist in the Czech Republic. One of the barriers could be a high price of services provided by Czech suppliers. However, first we have to ask, whether the price is the most crucial factor for Czech companies. It was documented that outsourcing decisions are rarely taken within a thoroughly strategic perspective. Hence, many companies adopt a short-term perspective, being motivated primarily by search for direct cost reductions. But while in the past companies emphasized low cost as their main objective in outsourcing activities, today many companies are expanding the traditional role of outsourcing relationships to include improved services, improved financial performance, and even the development of new lines of business.

The recent survey of supply side in the Czech Republic /1/ has shown that suppliers see as the main factor in the process of selecting suppliers the level of service quality (72 %). The price was designated as the most significant factor only by 11 % of suppliers. This would lead to the conclusion that the Czech Republic is already at the stage when outsourcing is used as the means for better performance of the companies. On the contrary, the extent of services is the most crucial factor for 50 % of client companies requested in our survey. The price is the most important factor for nearly a third of companies (29 %) which is different to suppliers' opinion. The quality of services and the reputation of supplier are the most significant factors for only 20 % respondents. Though the results of both surveys are to some extent different, the price does not seem to be the most important factor and consequently we can argue high price is not the fundamental barrier to IT outsourcing in the Czech Republic.

Further, we have focused on other factors that could influence behaviour of potential clients in the IT outsourcing market. Most of these factors are connected with Williamson's transaction cost economics. Transaction cost economics proposes that managers need to consider production and transaction co-ordination costs, for example, the costs of monitoring, controlling, and managing transactions when making decisions about outsourcing. As transaction costs increase, organisations tend to internalise the production through hierarchy instead of procuring the transactions from the market, unless the market enjoys significant production economies. The real cost of buying an output rather than making it must include the costs of identifying suitable suppliers, communicating needs to them, monitoring their progress and outputs, avoiding predatory behaviour by them and so on.

All statement items representing the factors were measured on a seven-point Likert-scale, where the choices were labelled as 1 = strongly disagree to 7 = strongly agree. According to the survey, respondents feel that outsourcing increases dependence on supplier (mean 5.0; variance 1.6). The great disadvantages seem to be that transfer of activities back to home is difficult (mean 4.8; variance 1.7) and that change of supplier is time demanding (mean 4.6; variance 1.6). On the other hand, managers do not see as a problem searching for the acceptable supplier ("Searching for the right suppliers is costly" with the mean 3.7 and variance 1.6). According to these results and with respect to transaction cost economics, we can conclude that the transaction costs are barriers to IT outsourcing in the Czech Republic.

The quite important issue in transition economies is the supplier presence, which is sometimes limited [2]. Greater supplier presence reduces bargaining problems and declines opportunism. Respondents feel that the amount of trustful suppliers is sufficient (mean 4.3; variance 1.5) and services offered in the Czech Republic are on sufficient level (mean 4.2; variance 1.5). Managers also mostly disagree with the statements that supplier is not able to provide services in requested quality on time (mean 3.0; variance 1.6). Therefore, the supply of services is perceived to be adequate and it does not seem to be the barrier to IT outsourcing.

According to the survey, we can argue that outsourcing barriers often stem from fear of locking into outsourcing relationship. Nevertheless this problem is standard in all developed countries. The price of services as well as the sufficiency of services are not seen to be critical problems in the Czech Republic, however, these factors are still important. With respect to the importance of IT outsourcing phenomenon to researchers and practitioners in the developed countries, the evaluation and assessment of the benefits and risks of outsourcing services in transition economies is also an area which requires further and vigorous research.

References:

- [1] ZAHRADNÍK, J. – SMETANA, A.: *Pánové, zadejte se. Outsourcing v České republice*. Business World 10, 2004, 10-15.
- [2] ZAHRADNÍK, J.: *Outsourcing Challenges in Transition Economy* In Proceedings of the 10th Annual International Scientific and Technical Conference Radio-Electronics, Electrical and Power Engineering REEPE, Moscow, 2-3 March 2004, 213.

Opportunities and Threats of the Czech Industry Connected with Progress of the Electricity Prices

Zdeněk Jobánek

jobanek@argonaut.cz

CTU, Faculty of Mechanical Engineering, Dept. of Economics and Management

Horská 3, 128 03 Prague 2

Nowadays it takes place dramatic growth of the world consumption of the Energy resources in the last few years. Accessible Energy resources are stunted and unevenly distributed across the planet Earth. Different regions embody different Energy consumption and this consumption is often enabled because of the transport of Energy resources from undeveloped regions with moderate resources of energy to rich regions which are depending on imports and which this energy resources feed on. Prices and availability of the energy resources can not be perceived as a solid and unchanging for the future. Dependency of the world economic on fossil fuels mainly on crude oil is alarming. Only small part of the world population consumes most of energy resources.

Fossil fuels are representative of the exhaustible energy resources which fundamentally participate on the global warming and with this connected change of climate. This state will be one of the biggest problems and also dare for the 21st century.

World reserves of crude oil are estimated on 50 years, reserves of coal on 100 years and reserves of natural gas on 150 years. But this numbers are very approximate and nobody knows exactly world reserves of the energy resources. Distribution of the energy resources crosswise world countries is very unequal. From the point of view Czech Republic is situation unfriendly except of lignite.

The economy of each state is depending on sure-footed supply of energy because of it needs energy for producing its output. Growth of GDP (Gross Domestic Product) is affected by the energy consumption in the production of goods and services and also depends on Energy intensity of the concrete economy.

For the all countries is important the structure of the Energy production and the Energy consumption in different sectors of the economy and also there is important the availability of the natural resources which are used for Energy production.

Just the Czech Republic has got problems with Energy intensity of its economy but Energy efficiency is growing up. Indicator of Energy intensity is worse in the Czech Republic than in the western countries of the European Union.

Czech machine industry consumes great deal of energy and has great Energy intensity. But competition advantage based on low wages and skilled labor is wearing of. This is big threat. Higher wages, great Energy intensity and products without bigger value added will be competition disadvantage. Price of raw materials is approximately the same anywhere.

Czech machine industry has to trace not only technical parameters of production but also value added, Energy intensity and many others parameters. World growing consumption of the energy is opportunity for those who are target these sectors: mining of energy resources, transport of energy, efficient energy production and consumption, research and innovation which are friendly for environment. Also sector of transport and its dilemma of nowadays combustion engines and their replacement is great opportunity.

It stands to reason that prices of energy as well as the Energy consumption will grow in the long-period. Fixation on the electricity and nuclear energy with renewable resources can be stabilization element in the development of economics because nuclear energy is quite cheap and reasonable.

References:

- [1] JOBÁNEK, Z. *Prognóza spotřeby elektrické energie v Evropě do roku 2020* diplomová práce 2003
- [2] JOBÁNEK, Z.: *The Long-Term Forecast of the Electricity Consumption and the Electricity Prices in Europe* Workshop 2004 Czech Technical University in Prague; Prague, 2004, pp.1032-1033

Problematics of Digital Toll in Czech Republic

J.Svoboda, P.Mačat*

josef.svoboda@fsv.cvut.cz

Department of Road Structures, Faculty of Civil Engineering, Czech Technical University,
Thákurova 7, 166 29 Prague 6, Czech Republic

*Department of Applied Informatics, Faculty of Civil Engineering, Czech Technical
University, Thákurova 7, 166 29 Prague 6, Czech Republic

This paper contains aspects of the current roads and highways situation and the theme of this issue is looking for new resources of financing road and highway net in Czech Republic. The goal of Czech government is to provide digital toll during next year. This paper will find out couple of answers to many questions about digital toll.

Today is the situation of the Czech traffic system really bad, worse than for example 15 years ago. There are many damages on the surface of roads and highways, especially after winter season. Traffic intensity of overloaded vehicles and trucks is getting higher every year and Czech roads and highways are not designed for these forces. Danger comes mostly from foreign truck, which use often our republic like the through traffic country. Our government is looking for new resources of roads and highways financing. Digital toll seems like the best way, how to find new reserves for our traffic system. Sample of using this system we can find really close to our country. Our neighbors – Germany and Austria - are already experienced in digital toll system and every country has little bit different type of a toll.

The satellite identification and the land static identification is the main difference between these two system solutions. It is about one year ago, when the Austria started a land static digital system. The priority is, that this system type has an exact localizing of the potential car payer. There are many gates around Austria, which are usually at the beginning and at the end of the road or highway. Vehicle or truck, which wants to use a paid section, must have activated the “Go – box”.

This is the box, where every user of the road has a money account and a detector, which provides connection with the gate. When you drive through the gate, signal of box connects the gate, which sends the information of your payment to the center. If you did not pay, system connects the police. Costs of providing of this system are higher than satellite system. Otherwise the German system has already started on 1st of January and it evidently works.

Germans started little earlier than Austrians, but their system of digital toll is more complicated. Everybody knows the GPS satellites placed on earth orbit. This is an American system. Europeans want to finish their own satellite system “Galileo” close to year 2008. German system of digital toll is based on the Galileo satellites.

Germans tried to start their digital toll system in 2003, but especially errors of localizing were the cause of failure during next couple years. The biggest problems are with roads, which are close to highways. Satellite system is not able to tell apart the main road – paid road (accuracy +/- 5m). Car, which is using the non-paid road section, could be detected like the car on the paid road. Uniformity of the digital toll system all around the Europe is not

provided and it means next problem for the German satellite system, which is the first in the world in this category. Galileo satellites are the main part of German system. It means, that operating of German toll is cheaper than Austrian, but anyway Germans need to provide checking centers and this is the same for both systems. Cars and trucks need to be provided by “boxes” and “gates” in Germany also, because it is necessary to find out vehicles, which are not in database or they did not pay, by checkpoints and send it to checking center or inform a police. Problems of coordination of “boxes”, “gates” and satellites are very topical at this time in Germany, because Toll Collect Company providing the system is responsible for the start on 1st of January 2005. It is about third attempt how to start the system. If they would have time delays, company could pay high financial penalties.

Czech Republic is looking for the most appropriate solution for our conditions. We have great samples around – Germany and Austria – and we want to start realization at the beginning of year 2006. We must decide, which of these systems is more credible and financially practicable. Of course it depends on many other circumstances. That is why, we would like to design the system for our republic and we want to find appropriate theme of research.

The multi-critical evaluation is one interesting solution, how to design the optimal variant of digital toll system in Czech Republic. It is important to include all of factors like traffic intensity, economic effects and prices, development of vehicle industry, development of digital systems and computers, natural effects (climate, water effects), casual effects, environmental effects and so one. Next thing is to compare some of European (worldwide) toll systems, take the best of and to design special version for our country. This is the theme we would like to research during year 2005.

Experiences from Austria and Italy show us, that advantageous type of financing is the PPP financing (PPP – public – private – projects). PPP means, that public sector is dependent on the “money” of private sector. Private sector sponsors everything about the construction and technical equipment of the road or highway and also works like the manager of the road – include the functional working of Digital Toll system.

Czech Republic is financed from the state budget. There is many resources of financing – fuel taxes, highway marks, State Fund of Transportation Infrastructure (this fund is supported from the Fund of National Assets – privatization finances), Department of Transport – percentage of budget and so one in Czech Republic. System of Digital Toll means next great resource for our country, that is why we have to design optimal Czech version.

References:

System Dynamics Models in Teaching Process

D. Vytlačil

vytlacil@fsv.cvut.cz

Department of Engineering Informatics, Faculty of Civil Engineering, Czech Technical University, Thákurova 7, 166 29 Prague 6, Czech Republic

There are many environmental, economic and social changes that we meet every day. The complexity of socio-economic systems is growing very fast. It is more and more complicated to do correct decisions. The possible solution is to develop models describing a dynamic behavior of an investigated systems. It allows us to understand the problem that is in the beginning of all projects and makes possible to test different policies before an implementation [1,2].

The methodology for describing the complex system behavior is system dynamics. This methodology helps to create tools called management flight simulators. Computer simulation programs and adequate developed models make it possible to understand the behavior of the systems in very short time. Teaching process based on the described methodology allows us to gain an experience that can be gained only in real live but with all consequences of an unsuccessful implementation. Therefore, the result, in the form of the computer program, reached on the basis of this methodology is called flight simulator. Airline companies train their pilots before the first flight but in management it is very typical to implement an important decision without testing the consequences of the decisions [3].

The development of the models and solutions can be described by two loops:

Virtual world: Analysis possible scenarios of the solution → Model creation → Simulation → Comparison outputs from the simulation with the description of problem definition →

Real world: Problem definition → Analysis → Analysis possible scenarios of the solution → Select strategy → Implement strategy → Response of real world →

The loops are connected by common element *Analysis possible scenarios of the solution* and include internal connections between *Comparison* element and *Problem definition* element.

In the beginning we have only verbal description of the system or often problem and in the end we need a set of difference equations. The connection between these two stages is the development of the causal loop diagram. The system is described by causal loop diagrams and then drawing a level-rate diagram with equations. It is the change from a *structural qualitative model* to a *mathematical quantitative model*.

For understanding the dynamics of the complex systems we use system dynamics games such as *Beer distribution* game and *Fish banks* game. The games are used as the introduction to the problem of the dynamic behavior. Students learn how is difficult to predict in the beginning the behavior of simple systems. The difficulty is caused by the system complexity that depends on the existence of loops.

Group of problems that can be solved by system dynamics approach and that are investigated by students in different subjects in department of engineering informatics:

- Design of the capacity (production, services)
- Optimization of health service (capacity, waiting time)
- Policy testing in the field of housing problem
- Behavior of systems dealing with renewable resources
- Distribution systems
- Consequences of population grow

Project management problems (capacity, productivity)
Simulation of production chain
Management of human resources

It is possible to write a system dynamics simulation program in a general-purpose programming language such as Fortran or C. Graphical outputs are very important at the end of the simulation when a designed model is used for finding the solution of some practical problems. Therefore, using a general-purpose language is not recommended [4]. For the investigation of the behavior of simple system dynamics models spread-sheet programs are suitable. These programs can generate graphs with little effort but they are not recommended for large-scale or complicated models. An advantage is availability of the software in the university. The best solution is using specialist system dynamics software with in-built functions for all kinds of models. Forrester introduced in sixties the Dynamo programming language. Since this time many other software have been developed for the simulation of dynamic behavior of socio-economic systems. The most spread programs are *Stella* and *Powersim*. Both programs are user friendly and include all functions for developing models and investigating problems. The graphical environment is used not only for the development but also for the presentation of the investigated problem, the model structure and the presentation of the calculated results. By means of these programs can be designed above mentioned "flight simulators" for testing different policies. These programs are available also for universities for lower price and it is possible to use them in computer laboratories.

References:

- [1] STERMAN, J., D.: *Business dynamics - System thinking and modeling for a complex world* McGraw-Hill, 2000.
- [2] RICHMOND, B.: *An Introduction to systems thinking* High Performance systems, 2001.
- [3] MEADOWS, D., H. – MEADOWS, L., M. - RANDERS, J.: *Beyond the limits* Chelsea Green Publishing Company, 1992.
- [4] PIDD, M.: *Computer simulation in management science* Wiley, 1992.

This research has been supported by CTU grant 0417611.

New Technical Specifications TP 170 for Road Pavements Design

L. Vébr

vebr@fsv.cvut.cz

Department of Road Structures, Faculty of Civil Engineering, Czech Technical University, Thákurova 7, 166 29 Prague 6, Czech Republic

The technical regulations TP 77 Designing Road Pavements developed by TU Brno and TP 78 Catalogue of Road Pavements developed by CTU in Prague have been in force since 1996. Although TP 77 and TP 78 existed parallel to each other in the past period as well, their mutual compatibility for a certain spectrum of structural road pavement types never existed as some structural types of flexible pavements specified in TP 78, when assessed in accordance with TP 77, came out as underdimensioned, while others were markedly overdimensioned. For the reason of putting both design regulations TP 77 and TP 78 in harmony, in 1996 the Ministry of Transport ČR formulated a research project S301/120/601 "Improving the condition of road pavements" one of whose outputs were the innovated technical conditions TP 77, including the Catalogue of recommended road pavement constructions.

Revision of TP 77 and TP 78

The first version of revised TP 77 was submitted for expert opinions after the project completion in 2002. Since then, several rounds of expert opinions have passed, which, however, did not lead to fulfilling the presumed target. In November 2003, therefore, a "working group" of experts was established and coordinated by the SSŽ Company whose task was to reach the desired opinion consensus, namely among the researchers from TU Brno and CTU in Prague, and complete successfully the revised regulation. Within a nearly one-year negotiations, prominent changes in the content of TP 77 against their original version were reached, namely in the part dealing with the road pavement catalogue, and the opinions of all participating parties on the problems to solve came much closer to each other. Based on a decision of the Ministry of Transport ČR, the last stage of TP 77 revision ended up in merging them with the Road Pavement Catalogue (described in technical conditions of the Ministry of Transport ČR TP 78) to form one technical regulation, referred to as TP 170. Discussions on the final version of these technical conditions TP 170 were successfully completed in November 2004. By a decision of the Ministry of Transport ČR, TP 170 has been in force since 1st December 2004.

Contributions of new TP 170 against TP 77 and TP 78

Due to the fact that the presumed focus of the new TP 170 for the absolute majority of its potential future users may be seen in the innovated road pavement catalogue, this catalogue must be mentioned in the first place. The newly developed catalogue, as compared to the TP 78 catalogue in force to-date, contains the following positive features:

- Extension of catalogue sheets of rigid and flexible road pavements by including constructions related to the newly introduced class of traffic load (hereinafter referred to as TDZ) "Super" (hereinafter referred to as "S"), which was caused by actual traffic volumes of heavy trucks on our roads,
- Implementation of modern technologies (AKT, VMT, asphalt mixes in accordance with TP 109) allowing reduction of the cover thickness or the total road pavement thickness,

- Introduction of technical requirements allowing exploitation of recycled materials obtained either by milling or removing and successive recrushing of old degraded layers of asphalt mixes,
- Classification of road pavement sub-base types in terms of their mechanical and physical properties into three unambiguously defined types (including demands for sub-base final acceptance – see Table) and development of an alternative solution of catalogue road pavement constructions for 3 (for constructions for design failure level D0) or 2 (for NÚP D1 and D2) types of road pavement sub-base. This solution allows optimum exploitation of specific design conditions given in particular by the sub-base quality,
- Introduction of a system of determination of control values of the moduli of deformability $E_{def,2}$, required for individual non-consolidated structural road pavement layers, depending on the material and layer thickness and the modulus of deformability of an underlying layer.

Sub-base type	Design modulus of elasticity E_{pd} (MPa)	Minimum modulus of deformability $E_{def,2}$ (MPa)	Sub-base frost susceptibility
P I	120	90	non-frost susceptible
P II	80	60	slightly frost susceptible to frost susceptible
PIII	50	45 (30) ¹⁾	extremely frost susceptible

¹⁾ The value of 30 MPa is valid for road pavements and constructions in design failure level D2, or D1 for traffic loading of class VI

The catalogue constructions in TP 170 were designed with the aim of observing the logical “cross links“(between constructions for individual TDZ, for different materials of sub-base layers and sub-base types) and, at the same time, reaching the values of relative failure within a range of 0.6 and 0.8. In developing the catalogue constructions, the design failure level was considered in a corresponding way. For defined versions of road pavement sub-base P I to P III, road pavement constructions were designed so that the blankets and usually also the base courses for all sub-base types would be identical, and the difference in the sub-base quality would be compensated by the designed thickness of the protective layer or for P I sub-base by eliminating the protective layer at all. In practice, this will allow a more economical and, for the user (designer and builder), a simpler design of road pavement constructions.

References:

- [1] VÉBR, L. – LUXEMBURK, F. - NOVOTNÝ, B.: *TP 78 Catalogue of Road Pavements*, MD ČR + ŘSD ČR, 1995, 1-98.
- [2] KUDRNA, J.: *TP 77 Design of Road Pavements*, MD ČR, 1995, 1-66.
- [3] KUDRNA, J. - VÉBR, L. – LUXEMBURK, F.: *TP 170 Design of Road Pavements*, MD ČR, 2004, 1-108.

This research has been supported by research project MSM 210000001 and 210000004.

The Problems of Concrete Road Pavements

L. Vébr

vebr@fsv.cvut.cz

Department of Road Structures, Faculty of Civil Engineering, Czech Technical University, Thákurova 7, 166 29 Prague 6, Czech Republic

A rapid growth in the volumes of heavy truck traffic provokes questions what technology to choose for the construction of a new and the repair of the existing road network. Exploitation of more demanding – in terms of construction - road pavements with cement-concrete covers reduces total expenses related to the overall length of the service life of constructions increasing the safety of the road pavement use. In order that a road pavement with a concrete cover may perfectly serve for the whole time of its presumed service life and provide all its benefits, however, not only modern building technologies, but also first-rate technological design methods are necessary. These problems, in particular, were subject of detailed research. The aim was to compare the results of the rigid road pavement assessment obtained by using two different design methods, and evaluate the results achieved. The background data considered within the assessment were constructions of rigid road pavements sharing a common protective and base course, and possessing a cement-concrete slab of variable thickness and a variable sub-base bearing capacity. The design conditions chosen for the assessment were such which would in current practice correspond to conditions on highways. The following input data was considered in the computations:

- traffic load – a load of 3000 TNV per 24 h, and a road pavement design period length of 25 years were considered. The design level of road pavement failure considered was D 0,
- climatic conditions – a territory with an altitude of 450 m and a corresponding average annual air temperature of +8 °C was considered,
- sub-base conditions – a spectrum of 5 alternatives of geological conditions characterized by the values of the design module of sub-base elasticity $E_{pd} = 50, 60, 80, 100$ and 120 Mpa was considered. The soils included in the computations were considered as frost susceptible, and the sub-base water regime considered was unfavourable,
- road pavement constructions assessed – a cement-concrete slab CB I with a thickness graded by 20 mm from 200 mm up to 280 mm was considered. Further more, two structural layers of constant thickness were considered, a layer of mechanically consolidated aggregates (MZK) 200 mm in thickness, and a layer of partially crushed gravel (ŠD) 220 mm in thickness.

Road pavement assessment

Each load causes stress in the construction – relative strain or stress. In cemented layers and in the sub-base where this strain is irreversible, proportionally to the magnitude of loading degradation of the layer occurs. In the area exposed to the highest repetitive stresses, a microcrack in the layer structure arises, and under subsequent repetitive loading the microcrack starts propagating through the layer in a horizontal and vertical direction. The road pavement assessment determines whether a layer or sub-base is loaded proportionally to the required amount of repetitive loading so that a crack in the design period is manifested only with the required probability of occurrence in accordance with the design failure level. The assessment was performed for the longitudinal as well as transverse edge of a cement-concrete slab with their longitudinal and transverse joints reinforced with tie bars or anchors in accordance with the relevant ČSN standard. The assessment of the correctness of the road

pavement construction design was performed for maximum cement-concrete slab dimensions of $L_x = 5,5$ m and $L_y = 4,25$ m.

The computations within the assessment were made using the two following procedures:

- procedure in accordance with the TP 77 design method,
- procedure in accordance with the TSm design method.

Assessment conclusions

- TP 77 design method:

In order that this design method when used for the road pavement assessment by computation may provide „reasonable“ results, some limiting conditions expressing the links between the cement-concrete slab thickness and the sub-base bearing capacity must be introduced, e.g. for $E_{pd} \leq 80$ MPa it must hold true that $220 \text{ mm} \leq h \leq 260 \text{ mm}$. In the case of non-observance of these conditions, the assessment by computation provides such values of the relative road pavement degradation which do not correspond to real facts and have no evidential strength with respect to the correctness of the road pavement construction overdimensioning. The results confirm the fact that the TP 77 design method is able to assess suitability or unsuitability of a designed construction, but when the specified conditions are not respected, its results are misleading and do not correspond to actual state.

- TSm design method:

The results of computations show that with a growing thickness of the cement-concrete slab or the sub-base bearing capacity the road pavement overdimensioning also increases. Thus we may state that for any real design bearing capacity of the sub-base and the cement-concrete slab thickness, the results correspond to presumed reality.

- Comparison of both design methods:

For a very high sub-base quality ($E_{pd} = 120$ MPa) the results of both design methods are fairly similar, namely for greater thicknesses of the cement-concrete slab. On the contrary, for the sub-base with a low bearing capacity ($E_{pd} = 50$ MPa) the results obtained by using the method in accordance with TP 77 absolutely deviate from real values presumed (the road pavement was approximately 57x underdimensioned, but also the road pavement was approximately 380x overdimensioned). The results coming from the TSm method, on the contrary, remain real for any input values, and in a situation where the design does not comply, they allow a fast and simple remedy quite evident from the values obtained.

To conclude, we may state that in the case of non-observance of the limiting criteria for input values, the values obtained by the assessment using the TSm method are more reliable.

References:

- [1] VÉBR, L. – LUXEMBURK, F. - NOVOTNÝ, B.: *TP 78 Catalogue of Road Pavements*, MD ČR + ŘSD ČR, 1995, 1-98.
- [2] KUDRNA, J.: *TP 77 Design of Road Pavements*, MD ČR, 1995, 1-66.
- [3] DOPRAVOPROJEKT BRATISLAVA, *TSm Catalogue of Rigid and Flexible Road Pavements*, MD ČR, 1984.

This research has been supported by research project MSM 210000001 and 210000004.

Innovation of a Specialized Workplace for AIP Systems Training in Road Pavement Engineering

L. Vébr

vebr@fsv.cvut.cz

Department of Road Structures, Faculty of Civil Engineering, Czech Technical University,
Thákurova 7, 166 29 Prague 6, Czech Republic

Within the project of the University Development Fund “Innovation of a specialized workplace for AIP systems training in road pavement engineering“ the major project target was principal innovation of the existing training workplace of the Department of Road Structures, both in terms of software and hardware. The objective of the project holder was to establish and run a top-level training workplace focused on teaching modern road application software for a fully interactive design of roads, including road pavement dimensioning and economic evaluation of investments, alternative solutions etc. The workplace innovation presumed consisted in its equipment with modern software systems of a fully interactive design of road routes in the environment of the ROADPAC system allowing creation of standard (2D) graphic supplements in accordance with ČSN standards, but also of 3D models of road routing, displays of perspective views, including animations of vehicle travel along the designed route (this is of importance namely in assessing the road traffic safety or in assessing designs of various types of traffic calming elements and measures).

The AIP workplace was established at the Faculty of Civil Engineering, CTU, in Room No. B 216 administered by the Department of Road Structures. The workplace is equipped with the total of six graphic stations BRAVE BlueLine P 950 in a basic configuration with an Intel Pentium IV processor, RAM 512 MB, a 200 GB hard disc, CD/CD RW burning mechanics + other standard devices and accessories. For solving graphic problems in the AutoCAD (Microstation) environment, the stations needed to be fitted with a large top-quality monitor – the type selected was Samsung SyncMaster 19“. In order to process mapping background data for the digitalization and creation of DTM, the workplace is further equipped with a colour scanner Hewlett Packard 7450C, which, together with accessories and user software, allows top-quality colour-depth scanning (with a resolution of up to 2400 dpi). In order to provide printouts of the resulting large-format drawings from all graphic stations, the workplace is equipped with a large-format network colour printer HP DesignJet 500ps with a resolution of up to 1200 dpi and a printing size of up to 610 mm.

In order to provide the presumed application software, within an agreement with the Pragoprojekt a.s. Company, the workplace was equipped with a newly modified software package ROADPAC 2004, allowing creation of a digital terrain model and a successive fully interactive design of roads, including final graphic modifications and development of own design documentation. This software package in its newly updated version comprises three basic modules, i.e. DTM'04 module (multi-layer digital terrain model, complete interactive terrain and field measurement data processing, including DTM interpretation), ROADPAC'04 module (complex automatic system of road and highway design, including interactive design of directional routing, longitudinal and vertical section alignment and cross sections) and ROADCAD'04 module (interactive graphic system as an extension to AUTOCAD R2002/2004 system for creating or making final touches of final drawings).

To provide computer support for solving road mechanics problems, the graphic stations were equipped with LAYMED-D software serving for road pavement dimensioning and allowing modelling of multi-layer structural systems of road pavements, including 1090

computation of stress and strain from input traffic load. This software is part of a Czech design method in force allowing designing and assessment in accordance with TP 77. This computer application was originally developed for the WIN '98 operation system. Based on negotiations with its developer, a newly updated version for WIN XP was made and supplied.

The establishment of the AIP workplace itself consisted of several linked-up steps. In the first project stage, minor building and technical adaptations of the departmental workplace were made so that the room would meet the demands for the teaching activities presumed. Immediately after delivery, all new hardware was installed in the AIP workplace and put into operation. Then, all application software was implemented in individual graphic stations, and successively tested in its correct function. As the hardware purchase, installation and putting into operation was delayed against the original plans, the fact that the operating staff training for all application software had been completed earlier proved to be a great benefit. This dramatically shortened the total time necessary for the final putting of the workplace into operation in teaching conditions. The main project objective was to establish and put into operation an AIP workplace and to successively partially provide the teaching of selected compulsory and compulsory optional courses or to fully provide the teaching of optional departmental courses with narrow specialization. The newly established AIP workplace is presumed to be used namely by the students of the Bachelor's and Master's degree programmes specialized in transportation or road structures. The originally planned date of putting the AIP workplace into teaching operation - October 2004 - was not observed, but despite this delay at least part of the teaching process at the newly equipped AIP workplace has been successfully accomplished. The workplace is presently also used by the departmental diploma students for the development of their diploma projects and by the doctoral degree students. A more extensive exploitation of the newly established AIP workplace for teaching other selected courses specialized in transportation or road structures has been postponed until the start of the spring semester of the 2004/2005 academic year. The teaching of all selected courses oriented on a complex development and assessment process of road construction projects or their parts at the AIP workplace will be fully provided by the Department staff members.

Despite the fact that by its size (it comprises only six graphic stations) the newly established AIP workplace is relatively very small with a relatively narrow professional orientation, i.e. it has a potential ability of "addressing" only a narrow spectrum of future school graduates, its contribution may be seen namely in the fact that the graduates of the respective teaching programme or at least some of its part will leave the Faculty with practical skills for working with modern software systems of fully interactive road route design (the majority of design companies are presently already equipped with similar systems), or for executing demanding tasks related to designing, assessing and optimization of road pavement constructions. We believe that this new knowledge will help to raise the credit of not only the professional workplace, but the Faculty as a whole.

This research has been supported by grant No. FRV A 1913-Vébr, L.

Using Modern Methods for Urban Roads Design

L. Vébr

vebr@fsv.cvut.cz

Department of Road Structures, Faculty of Civil Engineering, Czech Technical University, Thákurova 7, 166 29 Prague 6, Czech Republic

In the last years, the implementation of traffic calming principles in our towns and cities has been on the increase, which leads not only to higher road traffic safety, but also to environmental improvements, including the living conditions for the inhabitants of surrounding built-up areas. The design of traffic calming measures is easier when designing new territorial units than when these are introduced within existing, often historic built-up areas. There, on the contrary, the conflicts of vehicles and pedestrians, vehicles and the surrounding environment are more frequent and more likely to occur as the existing development does not always allow radical solutions by traffic diversion outside the territory limits and servicing the area from the perimeter. Implementation of traffic calming principles, however, implies one drawback, i.e. usually somewhat higher investment costs accompanying the above-standard technological solution. For this reason, such technological solutions are sometimes successfully enforced as part of investment plans of municipal governments only with difficulties. As one of the examples where the respective local government authority was persuaded to support such measures, is a developed study of Castle roads reconstruction in the historic centre of the town of Brandýs nad Labem.

The designed local roads are located in the historic centre of Brandýs n. L., they presently serve in a two-directional traffic regime carrying mostly service and delivery traffic – e.g. for the inhabitants of adjoining houses, visitors to the Castle, tourists and Castle deliveries. On two sides, Castle roads are connected to minor roads carrying local traffic, while in the other two directions, the roads are blinded. In the east direction, the road debouches into the Castle Park, in the north direction there is presently only a pedestrian passage into Na Celné Street. The traffic volumes are relatively low, the traffic flow composition corresponds to the number and type of structures serviced. On the east side, the roads border on a vast Castle Park, and on the south and west side on low-rise housing development (blocks of flats on the south side and family houses on the west side). On the north side, there are Castle premises, including adjoining structures and gardens.

In accordance with ČSN 73 6110 “Designing local roads“, Castle roads may be classified as “service local roads“ of functional group C. Due to the fact that one of the targets of the development of a reconstruction study of Castle roads was to provide the lowest possible traffic volume within the solved locality (in particular by eliminating heavy or through traffic), following negotiations with the local government representative it was decided to solve the whole locality of Castle roads as a “dwelling zone” (i.e. with “a special traffic regime“). For this reason, all design elements used had to comply with the conditions of TP 103 – Dwelling zones. Act No. 361/2000 Sb., on operation on roads, also sets a maximum speed for a dwelling zone of 20 km/h.

Connection to local road network

The designed dwelling zone consisting of Castle roads had to be connected to two local roads of major traffic importance (local distribution roads). This connection was solved by designing wide road humps 4.0 m in length, integrated with a pedestrian crossing 3.0 m in width. In order to distinguish it from the adjoining local distribution roads, which have an

asphalt cover, and highlighting the entrance into the dwelling zone (territory with “a special traffic regime”), both road humps were designed as paved. The entrance into the dwelling zone was marked by the respective road traffic signs placed immediately behind both humps.

Castle roads

The design of the roads within the dwelling zone was based on a philosophy of “traffic calming” of the whole area solved, i.e. application of such road design parameters which would motivate (or force) drivers to drive at an adequate speed acting, at the same time, in the manner to eliminate all through traffic. With respect to the dwelling zone character, a design speed of 20 km/h was considered. Although TP 103 prescribes observance of a minimum width of a traffic lane of 3.50 m, the specific case had to take into account potential Castle deliveries using light to medium-size lorries. That is why (in accordance with recommendations of model sheets of MD ČR VL-7), the minimum traffic lane width was designed with respect to allowing mutual passing of design vehicles. Here, the alternative considered was mutual passing of either two passenger cars or a medium-size lorry with a passenger car. For these conditions, the suitable width of two-directional traffic lane is 4.50 m for which the roads were designed.

So that the designed Castle roads are, at the same time, able to fulfil the required function of still traffic (parking), parallel or ninety-degree parking was designed on individual roads (in dependence on local conditions). The parking strips and lanes thus designed were subdivided into smaller areas for max. 5 ninety-degree and/or 3 parallel parking spaces by planting greenery, which highlighted the planned effect of “road narrowing” increasing the proportion of greenery in the total area. A different way of using individual areas was also stressed by designing their cover where asphalt and paved covers were alternatively used, and in some cases both covers were paved, but markedly different colour shades were used. In order to ensure safety and provide free space for pedestrian traffic, the ninety-degree parking spaces adjoining pedestrian pavements were designed using regulation posts connected by chains whose function was both functional and aesthetic.

The Castle road reconstruction project has presently been developed in a “study” form only, but according to the latest information the municipality presumes development of the following design document stage and successively also the construction of these roads.

References:

- [1] VÉBR, L. & KOL: *TP 132 The Principles of Traffic Calming Design on Urban Roads*, MD ČR, 2000, 1-58.
- [2] VÉBR, L. & KOL: *VL 7 Selected Elements of Urban Roads for Traffic Calming*, MD ČR, 2002, 1-136.
- [3] VÉBR, L. - KARLICKÝ, P.: *Traffic Calming on Urban Roads in Design Regulations of the Czech Republic*, Specialised seminar SEKURKON, 2001,
- [4] VÉBR, L. - KARLICKÝ, P.: *Traffic Calming on Urban Roads*, Informační centrum ČKAIT, 2004, 1-22.

This research has been supported by research project MSM 210000001.

Profiling of Approaches to Project Management

L. Michalík, M. Prajer

michalik@karnet.fsih.cvut.cz,

prajer@karnet.fsih.cvut.cz

Department Management and Economics, Faculty of Mechanical Engineering,
Czech Technical University,
Horská 3, 128 00 Prague 2

Economic results engineering company they are to a certain extent dependent on the effectiveness of development and productions new products. High-level development new products and new technology creates expectations for achievement competitive advantage, hence it's possibly apply to development and productions new product significant attention. For raising the effectiveness of development and productions new products is necessary look for also new method management. Significant tasks in project management new products they have managerial activities, above all planning and determination. It was showed, that for project planning new products is best apply CPM and for decision making method multicriterial valuation.

In terms of research in the area integrated engineering, which is solving on Faculty Mechanical CVUT in Prague, is designed new method planning and decision making for management development and productions new product. Method connecting and integrating planning method CPM with method multicriterial valuation.

Proposed method makes it possible watch time path development and productions new products, pursue analyses financial and human resources for development and productions new products and at the same time in project new products looking for best variant solution sub layer project, so step by step optimize general solution development new products.

At present it is important for maintenance competitive advantage possibly process projects new products always in variant solution for all factory activities. Between basic activities projection product behove:

1. Market research and communication with consumer - actions in company
2. Proposal variant conception product development - action academic team
3. Selection optimal variant concept product development - cooperation company and academic team
4. Integration constructive, technical and technological variant solution - activity academic team
5. Project and pursuance productions - action in company
6. Sell and financial analysis successful project - action in company
7. Conception subsequent innovation - cooperation company and academic team

For supports management project new products it is possible use software Microsoft Project, in which it is possible variant compile whole project and display him by the help of network diagram, which it is possible operative after changes enters data change in dependencies on requirement consumer and conditions on market.

Further it is possible solve problems management human resources and following load in all action project. That makes it possible quicker decision making and acceptable setting all expense and source, which they are key for healthy function company.

Process planning and decision making in project new product has been applied on collection actions handling construction, technology and productions mix machinery. For the next application is possibly ensure acceptable connection software tool network analyses and software product management information system. Introduced model will modifying for use at other engineering products.

On basis monitoring industrial process it is possible identify all business activities and with them related information. These information creating data for processing method CPM by the help of software Microsoft Project. Subsequently on basis previous analyses activity at projection mix machinery was programmed critical place for decision making so, to consumer and responsible manager company have had conception of separate variation solution. Selection best-fit variation solution is provided method multicriterial valuation.

Utilizations program Microsoft Project as tool for solution critic path method at proposal development and productions new products gives data managing unit pursue edits action, which under certain conditions, make possible abbreviating total period project new products. Front office thereby acquires more accurately view of allocation his moderate resources in each of action project and at his implementation unique trace up swing from plan or if need be is able to operative hit such, to minimized aftermath those deviations. Introduced method planning it can be farther modify and connect through with method multicriterial valuation, which makes it possible select acceptable variation solution and increases effectiveness project management new products.

References:

- [1] ZAHRADNÍK, J. – PRAJER, M.: *Model of Product Projecting in Concurrent Engineering* Workshop CVUT 2002

Optimization Of Flight Plannig Process At General Aviation Operator

T. Míkl

J. Chmelík, M. Kameník, P. Hvězda

`xmik1@fd.cvut.cz`

CTU, Faculty of Transportation Sciences,
Department of Air Transport,
Horská 3, 128 03 Praha 2

Flight planning and preparation is one of the most difficult processes for an aviation operator both from the point of view of understanding the theoretical part and from the point of view of practical application.

Because of this reason it is becoming more and more important to find an optimized method of flight planning that is closely connected to the practical flight planning process. This is one of the research projects held at Department of Air Transport, Faculty of Transportation Sciences, Czech Technical University in Prague.

The basic aim of this project was to find an effective flight planning, which has been created in compliance with European aviation requirements JAR-FCL and JAR-OPS. Effectiveness of the flight planning process is meant as a cost/time optimization. This method is to be used primarily by a small general aviation operator. In the Czech Republic, such a typical operator is an aviation company F-Air, Ltd. Working environment of small aviation operators includes some typical features, such as:

- a need of a quick reaction to customer wishes,
- limited amount of specialized workers/crew,
- compliance with particular requirements and aviation regulations,
- preservation or if possible increasing an adequate level of safety,
- preservation of a pre-defined level of customer service.

From these points of view, a quick and quality processing of flight planning needs is one of the most critical factors in the meaning of an ability of the operator to deal with competition.

The secondary aim of the project was to finish the “Flight Planning and Preparation Laboratory” that was built at the Department of Air Transport and that was supported by grant projects in recent years as well. The laboratory is a part of highly specialized workstations serving as the theoretical knowledge and ground training improvement of educational process of professional pilots and as a research and development platform at the Department of Air Transport. The heart of the laboratory is created by three computer workstations that allow:

- collection of meteorological data (METAR, TAF, SIGMET, CHMI information – forecasts, forecasted maps, satellite and radar data, etc.),
- flight planning and pre-flight preparation using a sophisticated software Jeppesen FliteStar,
- aircraft mass and balance computations, center of gravity assessment.

The creation of the flight planning method was characterized by several phases. First phase was to finish the “Flight Planning and Preparation Laboratory”.

During the second phase it was necessary to collect information, learning materials and knowledge sources regarding the flight planning process. The members of the project team went through educational courses and software training as well. The main stress was laid on collection of requirements for optimization computations that follow the pre-defined inputs and create requested outputs.

The third phase was characterized by creation of the optimized method for flight planning. The practical impact of this method was tested in laboratory conditions at the “Flight Planning and Preparation Laboratory” at Department of Air Transport and at real conditions at F-Air, Ltd. aviation company.

The process of flight planning is a very dynamic one and its optimization depends on several factors and aspects. Because of forthcoming changes in Air Traffic Management it is very likely to see a variety of significant changes in a near future that could be resolved in advance.

References:

- [1] TÝBL, M. – MIKL, T. – DANĚK, V.: *Flight Planning and Monitoring* CERM 2002 pp. 88.
- [2] MIKL, T. *Impact of Flight Planning on Aviation Safety* Žilinská univerzita v Žilině v EDIS 2004 pp. 146

This research has been supported by grant CTU0412016.

Management and Economics of Post and Delivery Services

O. Hölzl*, P. Stejskal*

xstejskal@fd.cvut.cz

**Department of Economy and Management of Transport and Telecommunications,
Faculty of Transportations Sciences, Czech Technical University in Prague, Horská 3,
128 03, Praha 2, Česká republika**

Post and delivery services have in spite of development modern electrical communications and informational technologies unsubstituting function and stay one of the basic subserviences of communications and trade and as a part of infrastructure are important for all social and economical activity.

Material way of transport messages and things, unique work with originals in a real time, safety (it's not possible to intercept, copy and change), documentary, economical and simply of servicing, guarantee of undistorting transmission to partial addressee, availability each of addressee (without classifications limits to the net) are characteristics, which will find their users, who will prefer this characteristics before electrical services not only in a sphere of transporting goods but also correspondences – agreements, trade invoices, court's files and summons, verdicts etc., by direct – mail (advertisement, goods offer, contests), by press media (newspapers, special magazines), etc.

The end of this project is to innovate the learning of subject Management and Economics of Post and Delivery Services and complete the possibilities of graduates to acquaint with the specifics of manage tools, spheres of regulation including legislative acts (with directions EC relating to post services) and deepen knowledge from another sphere of traffic infrastructure.

Also the end is to create attractive offer of study facultative subject the segment, which is employing over 42 thousand people and gives possibility to:

- understand problems of this sector with it's activity they'll meet both professional and personal life with
- use knowledge to exercise in this sector (otherwise special prepared graduates can invoke interest of big operators with strong part at employment market with cooperation with faculty).

Courses are structured to six parts:

1. excursion to economical history of post
2. stance and function post as a infrastructure sector in social-economical system of state
3. market post services
4. prize regulation (tariff policy as a regulation tool)
5. quality as a attribute of service
6. development vision in sphere of post services

Within these courses graduate will acquaint with main trends of development in sphere (liberalization), dimension and market structure of post services, active subjects at this market, forms of regulation and legislative limiting working both business subjects and users at this market.

References:

- [1] HOLEMÝ, J. + kol.: *Analýza rizik poštovního trhu v ČR a definice regulačního rámce v souvislosti s liberalizací trhu* Testcom, 2003
- [2] MADLEŇÁKOVÁ, L.: *Kvalita služby – fenomén spokojenosti zákazníka* Pospoint, 2003

This research has been supported by CTU0419116.

Personal Vehicle Occupancy in Relation to the Season, the Day of Week and the Hour of Day

Z. Čarská

`carska@fd.cvut.cz`

Department of Transport Systems, Faculty of Transport Engineering, Czech Technical University, Konviktská 20, 110 00 Prague 1, Czech Republic

The first impulse for lower described traffic observations of the private motor vehicle occupancy by passengers was the missing information about passenger number of vehicles participated in a road accident, that we can find in the database of road accidents that happened on so called "main road network of the capital Prague" (HUS). This database for every year is provided by the Ministry of Interior of Czech Republic for next statistical analyses. The information about number of vehicle passengers and their localization inside a vehicle would be possible to get only directly from complete forms of the evidence of a road traffic accident. For our aims i.e. for approximate determination of influence of number of vehicle passengers and their seat localization on number of killed, slightly and seriously injured persons, that are important for counting of so called total social losses [1], will be sufficient basic information about passenger numbers in relation on time period.

To get some data about passenger numbers in vehicles we (our department of CTU FTS) organized traffic observations of motor vehicle occupancy on selected profiles of Prague road network, which we realized with help of a group of students. The first part of observations realized from autumn 2003 till the beginning of year 2004. The other one realized from spring 2004 till the beginning of summer 2004.

The observations were realized on all kinds of mostly main town roads in various time periods of a day (from 0:00 till 23:59) and various kinds of days (Monday, ..., Sunday). The vehicle occupancy on selected road profile in any day and time was observed always 10 till 20 minutes during the day-peak period and 15 till 30 minutes during the other day times. For this reason the exact beginnings and the ends of peak periods in the 24 hours for all days of the whole week was defined.

From November 2003 till February 2004 the first part of vehicle occupancy observations was realized in total time 34 hours and 40 minutes long. From April till June 2004 the rest observations were realized in total time 37 hours and 15 minutes long. The first part of observations includes 15 hours and 37 minutes of day-peak periods and the second part of observations includes 18 hours and 48 minutes of day-peak periods. Similarly the first part of observations includes 9 hours and 46 minutes from weekend time periods and the second part of observations includes 10 hours and 19 minutes from weekends [2].

The results of these solitary observations are interesting also generally for most of people, which on their ways by personal vehicles or public mass transport take notice to very low occupancy (above all) personal motor vehicles. This is so important above all with regard on everyday traffic jams, which culminate especially during morning peak periods of working days. The transport efficiency of people by personal vehicles represented by number of transferred persons per time and space units has the least efficiency in comparing with the all other town kinds of transport. For example the number of transferred persons by personal vehicle for total transport speed 15 till 25 km per hour is 120 till 220 persons per 1 meter of road width and 1 hour. But already the number of transferred persons by bicycles for total transport speed 10 till 14 km per hour is 1500 persons per 1 m width and 1 hour. For the

different kinds of public mass transport these numbers of transferred persons increase from 2700 persons till 5200 persons per 1 m road width and 1 hour in relation with increasing total transport speed [3].

In comparing with the other kinds of transport the personal vehicle transport is the worse way of transport from standpoint of environment, amount of exhalations and emissions, usage of fuel per person per 1 km etc. [4].

From the results of observations it was appeared, that the year season (summer, winter etc.) has not significant influence on average passenger number in vehicles. During winter season there is possible to see a little less average numbers of passengers per vehicle that during spring. More significant there is the difference of average passenger number per vehicle between the peak period and the rest hours of days, also because they include above all weekends.

The most significant difference of average passenger number per vehicle was found in comparing of working days and weekends. The one of reasons for this result can be the fact that during working days the traffic flows contain plenty of non-private personal vehicles and small vans. On the other hand during weekend plenty of people travel with whole families by private vehicles.

References:

- [1] ANDRES J., ROKYTOVÁ J., HRUBÝ Z., SKLÁDANÝ P.: *Metodika identifikace a řešení míst častých dopravních nehod* CDV Brno, 2001, pp. 12–14.
- [2] ČARSKÁ Z.: *Obsazenost motorových vozidel ve vztahu k analýze dopravní nehodovosti* In: International Conference "Věda o dopravě 2004".CTU Prague, 2004, pp. 5-10. ISBN 80-01-03047-4.
- [3] ČARSKÝ J.: *Problems in Progress of Cycle Ways Infrastructure in Czech Towns* In: 5th International Conference "Environmental Engineering" Program and abstracts. Vilnius Gediminas Technical University, 2002, pp. 179-180. ISBN 9986-05-524-5
- [4] NEUBERGOVÁ K.: *Metody posuzování vlivů dopravy na životní prostředí a jejich vstupní parametry* In: Silniční obzor. 2004, vol. 65, num. 5, 2004, pp. 121-125. ISSN 0322-7154

This research has been supported by MSM 212600025.

System for Monitoring of Hazardous Goods Transport

M. Svítek

svitek@lss.fd.cvut.cz

Department of Control Engineering and Telematics, Czech Technical University,
Konviktská 20, 110 00 Prague 1, Czech Republic

The paper presents the result of national ITS project "Monitoring and control of dangerous goods transport with help of GNSS (Global Navigation Satellite System)" within which the practical pilot trial on different traffic infrastructure is tested. Presented solution relates to route selection of the dangerous goods transport, so monitoring and control of real movement on selected route is automatically reported.

The Fig. 1 describes the architecture of system for dangerous transport control and monitoring.

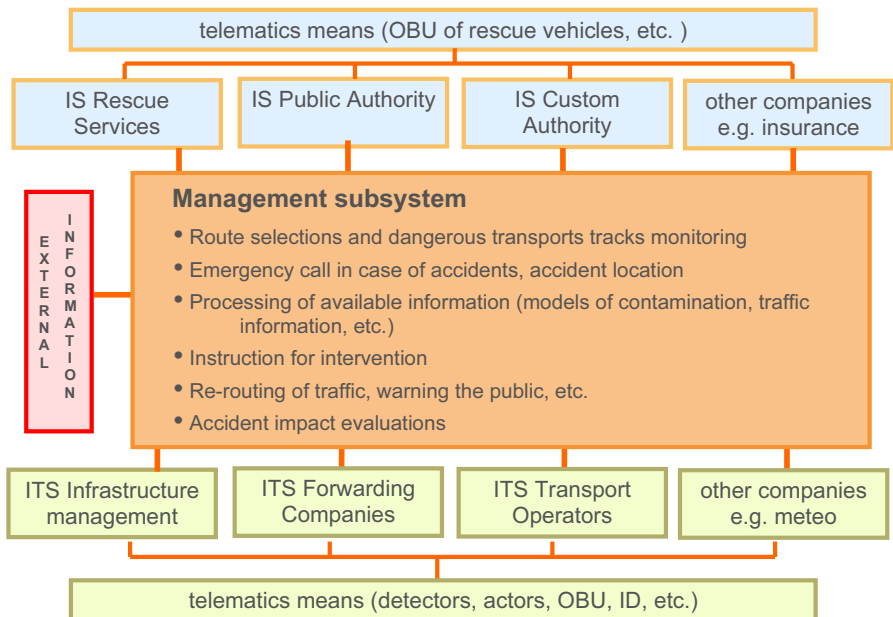


Fig 1. Architecture of system for dangerous transport control and monitoring

The system must be designed in such a way that following individual systems parameters must be guaranteed:

- Safety (risk analysis, risk classification, risk tolerability matrix, etc.),
- Reliability (the ability to perform required function under given conditions for a given time interval),

- Availability (the ability to perform required function at the initialisation of the intended operation),
- Integrity (the ability to provide timely and valid alerts to the user when a system must not be used for the intended operation),
- Continuity (the ability to perform required function without non-scheduled interruption during the intended operation),
- Accuracy (the degree of conformance between a platform's true parameter and its estimated value), etc.

Substantial part of the systems parameters analysis regarding telematics application Monitoring of hazardous goods is represented by a decomposition of systems parameters to individual subsystems of the telematics chain, including a proposal for macro-functions of individual subsystems and information relations between macro-functions. Part of the analysis is the establishment of requirements on individual functions and information linkage so that the whole telematics chain should comply with the above defined systems parameters. Requirements on GNSS locator in road transport (example of performance parameters analyses) could be summarize in following table:

Level of Security	Horizontal	Integrity		Service	Max. Service	Service	Sampling [s]
	Accuracy	Alert	Time to	Continuity	Loss	Availability	
	[m]	Limit [m]	alert [s]	[%]	[s]	[%]	
I.	1	3	< 1	> 99,98	< 5	> 99,98	1
II.	4	12	< 1	> 99,9	< 6	> 99,9	1
III.	10	30	< 1	> 99,9	< 10	> 99,9	1

References:

- [1] M. SVÍTEK: *Towards to e-Transport, international conference SSGRR2002 - Advances in Infrastructure for Electronic Business, Science, Education and Medicine on the Internet*, . Roma 2002 2002, ISBN 88-85280-63-3
- [2] M. SVÍTEK, F. KOPECKÝ, M.PICHL: *Vision of Galileo Project Technology and Prosperity 6/02 2002*, pp. 17-19.
- [3] M. SVÍTEK: *Architecture of Intelligent Transport Systems and Services*, Transport Systems Telematics TST03 Katowice 2003, ISBN 83-917156-1-2
- [4] M. SVÍTEK *Architecture of the Transport Telematics Applications Using the GNSS* International MultiConference in Computer Science & Engineering, International Conference on Information and Knowledge Engineering (IKE'03) Las Vegas, USA 2003.

This work was funded by the Czech Ministry of Transport within the framework of the program 802-210-112

ITS Architecture of the Czech Republic

M. Svítek

svitek@lss.fd.cvut.cz

Department of Control Engineering and Telematics, Czech Technical University,
Konviktská 20, 110 00 Prague 1, Czech Republic

The presented results were created within the "TEAM project", the goal of which is to develop the national ITS architecture and support the strategy for ITS development in the Czech Republic (organizational and legislative analysis of ITS applications, etc.) with respect to current and future transport-telecommunication environment of the Czech Republic.

The architecture reflects several different views of the examined system and can be divided into:

- Reference architecture - defines the main terminators of ITS system (the reference architecture yields to definition of boundary between ITS system and environment of ITS system),
- Functional architecture - defines the structure and hierarchy of ITS functions (the functional architecture yields to the definition of functionality of whole ITS system),
- Information architecture - defines information links between functions and terminators (the goal of information architecture is to provide the cohesion between different functions),
- Physical architecture - defines the physical subsystems and modules (the physical architecture could be adopted according to the user requirements, e.g. legislative rules, organisation structure, etc.),
- Communication architecture - defines the telecommunication links between physical devices (correctly selected communication architecture optimises telecommunication tools),
- Organisation architecture - specifies competencies of single management levels (correctly selected organisation architecture optimises management and competencies at all management levels).

The instrument for creating ITS architecture is the process analysis shown on Fig.1. The processes are defined by chaining system components through the information links. The system component carries the implicit system function (F1, F2, F3, G1, G2, G3, etc.). The terminator (e.g. driver, consignee, emergency vehicle) is often the initiator and also the terminator of the selected process.

The chains of functions (processes) are mapped on physical subsystems or modules (first process is defined with help of functions F1, F2 and F3 on Fig.1, second process is defined by chaining the functions G1, G2 and G3) and the information flows between functions that specify the communication links between subsystems or modules. If the time, performance, etc. constrains are assigned to different functions and information links, the result of the

presented analysis is the table of different, often contradictory, system requirements assigned to each physical subsystem (module) and physical communication link between subsystems.

From the viewpoint of the construction of the selected subsystem it is possible to consider a single universal subsystem fulfilling the most exacting system parameters, the creation of several subsystem classes according to a set of system parameters, creation of a modular subsystem where the addition of another module entails the increase of system parameters, etc.

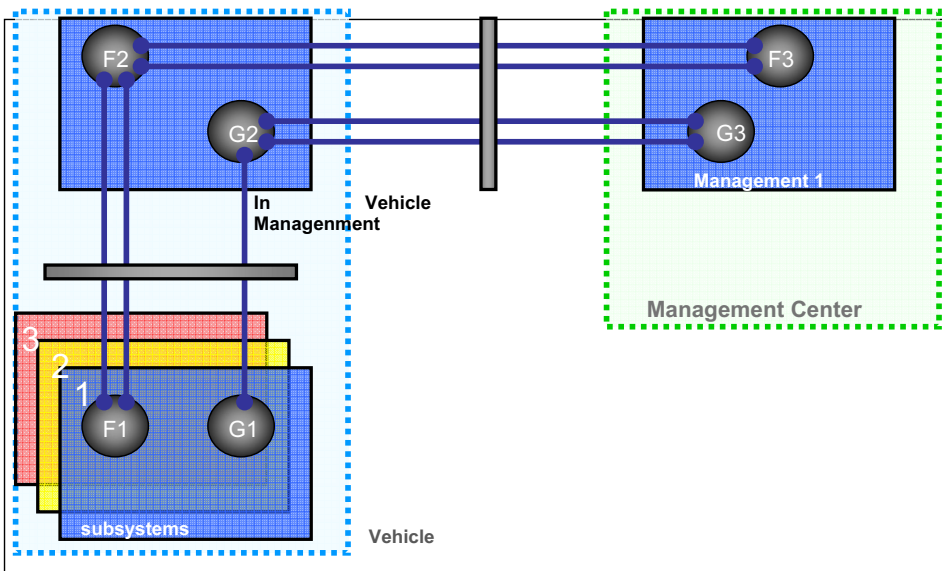


Fig.1. The principle of process analysis

References:

- [1] M. SVÍTEK: *Towards to e-Transport, international conference SSGRR2002 - Advances in Infrastructure for Electronic Business, Science, Education and Medicine on the Internet*, . Roma 2002 2002, ISBN 88-85280-63-3
- [2] M. SVÍTEK, F. KOPECKÝ, M.PICHL: *Vision of Galileo Project Technology and Prosperity* 6/02 2002, pp. 17-19.
- [3] M. SVÍTEK: *Architecture of Intelligent Transport Systems and Services*, Transport Systems Telematics TST03 Katowice 2003, ISBN 83-917156-1-2
- [4] M. SVÍTEK *Architecture of the Transport Telematics Applications Using the GNSS* International MultiConference in Computer Science & Engineering, International Conference on Information and Knowledge Engineering (IKE'03) Las Vegas, USA 2003.

This work was funded by the Czech Ministry of Transport within the framework of the program 802-210-108

INDEX

- Adamec, J., 578, 582, 798, 800
 Adámek, P., 84
 Altmann, J., 222
 Andreovský, J., 626
 Atanasov, P., 116
 Aubrecht, L., 144
 Ayoubi, M., 1024

 Becvar, J., 628
 Balagurov, A., 516
 Balda, M., 624
 Balík, L., 538
 Baloun, J., 232
 Barvir, P., 158
 Barviř, P., 68, 70
 Bařta, J., 618, 622
 Bayer, J., 398
 Bečvář, M., 262, 312, 900
 Bedlovičová, D., 980
 Bednář, B., 608
 Bednářová, P., 980
 Belas, E., 710
 Belda, K., 170, 580, 616
 Bendová, P., 340
 Benes, J., 834
 Beneš, J., 1054
 Beneš, P., 734, 736, 740
 Bensch, J., 542
 Beran, V., 1028, 1030
 Berka, L., 530, 534
 Berka, Z., 690
 Bernas, M., 188
 Bezpalec, P., 230
 Bělinová, Z., 1056
 Birol, Y., 466
 Bílek, T., 362
 Blaha, J., 688
 Blazek, K., 694
 Blažej, J., 140, 340, 342
 Blažek, R., 986
 Bláha, J., 1056
 Bláhová, I., 124, 146
 Bláhová, O., 534

 Bodnár, M., 160
 Borecká, L., 744
 Bořík, M., 226, 238
 Bosáček, V., 516
 Bouřa, A., 386, 416
 Bouřka, P., 902, 974
 Brabec, T., 262, 280
 Brandejsova, E., 690
 Brich, M., 626
 Brothánek, M., 146
 Broukalová, I., 914, 924, 926
 Brož, K., 610, 622
 Bryknar, Z., 80
 Břeh, D., 132
 Buček, J., 282
 Burcík, J., 270
 Bureš, P., 120
 Bureš, Z., 352
 Burget, P., 284, 398
 Burgetová, E., 944
 Burian, Z., 448, 452
 Bušek, K., 380
 Buřata, M., 748, 758
 Böhm, J., 170

 Cabalka, M., 740
 Cechak, T., 692
 Cejp, J., 446, 462, 464, 524
 Chalupecký, V., 34
 Charvát, J., 960
 Cháb, V., 698, 700
 Chichev, A., 494, 516
 Chlup, H., 802, 806, 830, 834
 Chmelík, J., 1096
 Chmelík, V., 442, 648
 Chod, J., 850
 Christescu, R., 128
 Chudáček, V., 820
 Chyský, J., 260
 Čiahotný, K., 152
 Cikrle, P., 944
 Cisařovský, P., 828
 Crenn, J., 492
 Cudzik, L., 116

 Čadík, M., 300
 Čambál, M., 260
 Čapek, M., 772
 Čapková, I., 880
 Čarská, Z., 1100
 Čechák, T., 670, 674, 720
 Čejka, T., 944
 Čelikovský, S., 324
 Čermák, P., 142
 Černý, F., 758
 Černý, J., 26
 Černý, M., 970, 978
 Černý, R., 420, 422, 424, 426, 428, 430, 432, 444, 460, 468, 470, 472, 474, 476, 478, 480, 482, 486, 488, 518, 522
 Čerňovský, Z., 656
 Čihák, F., 872
 Čuba, V., 728, 742, 746, 748, 752, 758
 Čulík, J., 762
 Čuprová, D., 524

 Drkal, F., 628
 Dalíková, K., 544
 Daněk, M., 194
 David, V., 900, 922
 Demchenko, N., 104
 Denk, T., 500, 502, 504
 Dione, M., 150
 Divoký, M., 112, 136
 Dlask, P., 1028, 1030
 Dlouhá, M., 114, 290, 494, 510, 514, 516
 Dobiáš, R., 218
 Dobšiček, M., 266
 Dočkal, M., 900
 Dohnal, M., 930, 962
 Dolanský, J., 728, 740
 Dolejš, J., 840
 Dolejš, O., 236
 Doležal, L., 1004
 Doležel, T., 540
 Dostál, T., 864, 900, 990

- Dostálová, T., 788
Doubrava, K., 662
Doubrava, M., 150
Draessler, M., 646
Drahoš, V., 452
Dráb, M., 290
Drápal, B., 1074
Drchalová, J., 890
Drkal, F., 604, 622
Drozenová, W., 912
Drška, L., 82, 84
Drtinová, B., 728, 740
Dubnová, M., 868
Duchoň, B., 1036
Duda, F., 222
Dunovský, J., 828
Dušek, J., 224, 930, 962
Dušek, K., 650
Duška, M., 588
Dvorský, T., 968
Dvořák, M., 138
Dvořák, R., 382
Dynda, V., 196, 198, 200, 250
Dündar, M., 466
- Ebel, M., 1008
Erben, P., 1050
- Fanta, B., 1008
Fantová, E., 1008
Fatka, P., 966
Fay, J., 688
Fábera, V., 412
Fejt, J., 298, 796
Fejtová, M., 220, 298, 784, 796
Fiala, O., 222
Fiala, R., 774, 808
Fidler, V., 138
Filip, J., 176
Filsaková, B., 1008
Finger, M., 688, 688
Fischer, J., 382
Fischer, M., 1010
Fišer, J., 272
Flegl, R., 1020
Fliegel, K., 376
Flígl, S., 256
Fojtík, A., 64
Foltýn, L., 222
- 1107
- Forstová, K., 496
Fořt, I., 524
Fošumpaur, P., 870, 872, 874, 876
Fragner, B., 1006
Franěk, J., 1044
Franta, L., 778
Friedlová, L., 428
Frková, J., 1070
Froňka, A., 722
Frýda, M., 240
Fuka, J., 308, 322
Fukuda, T., 74
Fumin, Y., 340
- Galuška, M., 150
Ganev, N., 526, 546
Gascon-Shotkin, S., 688
Gazdo, M., 474, 476
Gerndt, J., 720
Goldmann, T., 770, 786
Gorodynskyy, V., 76
Gosmanová, G., 546
Gregerová, M., 944
Grišin, A., 514
Grünwald, A., 730, 732, 842, 844, 860, 870, 876
Gurovič, J., 440, 442
Guskov, S., 104
- Haindl, M., 176
Hajaš, J., 882
Halounová, L., 248, 982
Hamal, K., 62, 340, 342
Haméček, J., 448
Hampl, P., 640, 642
Hanus, R., 1010
Hao, C., 24
Hapl, V., 938
Hargaš, L., 604
Hartman, K., 204, 644
Hauserová, M., 1008
Haušild, P., 434, 436, 490, 492
Havel, P., 652
Havlan, M., 372
Havlena, V., 172, 174
Havliková, R., 64
Havlíček, R., 242, 580, 616
Hazdra, P., 162, 348, 354, 358
Hájek, P., 940
- Hála, M., 1052
Hána, K., 774, 776, 780, 782, 794, 808, 818, 822, 824
Hánek, P., 986
Hejduk, P., 950
Hejman, M., 614
Hemerka, J., 622
Hemzal, K., 622, 630
Heralová, R., 1044
Herman, A., 608
Herza, J., 804
Hezl, M., 852
Himmelová, L., 770
Hlaváč, J., 244
Hodakova, L., 80
Hoffmann, K., 370
Hofreiter, M., 316
Holčík, J., 808, 824
Holický, M., 888
Homola, P., 520
Honzík, P., 208, 400
Honzík, V., 226, 238
Horaždovský, T., 442
Horák, Z., 792
Horká, H., 850
Horký, I., 1016
Horný, L., 830, 832, 834
Hořejší, J., 462
Hospodka, J., 378
Hovorková, Z., 638
Hozman, J., 392
Hrdoušek, V., 858
Hromčík, M., 336
Hříbek, P., 160
Hubený, T., 278
Hudousek, O., 212, 372
Hulicius, E., 348
Hurák, Z., 336
Husák, M., 386, 394, 416
Husník, L., 188, 352, 360, 362
Hvězda, P., 1040, 1096
Hykšová, M., 44, 46, 48
Hözl, O., 1098
Hüttel, I., 448, 450, 452
- Ille, B., 688
- Jančárek, A., 64
Janda, T., 964
Jandera, D., 294

- Jareš, P., 274
Jarušková, J., 906
Javůrek, R., 252
Jánský, B.,
Jeanneret, P., 152
Jelinek, I., 438
Jelínek, I., 334
Jelínek, M., 116, 128, 788
Jelínek, V., 850
Jeřábek, V., 388, 410
Jeřichová, Z., 868
Jettmar, J., 906
Jiroušková, Š., 1004, 1006
Jirout, T., 524
Jiříčková, M., 422, 424, 472, 474, 476, 478, 482, 488, 518
Jiříkovský, T., 946
Jiříček, O., 146, 148
Jobánek, Z., 1080
John, J., 750, 754, 756
Junek, P., 942
Jurč, R., 148
Jurek, K., 788
Juříček, Z., 466
Juříčková, M., 696, 698

Kačer, M., 302, 304
Kačmařík, P., 406
Kadlec, F., 352
Kadlec, J., 194, 208
Kadleček, D., 206, 222
Kafka, J., 640
Kafka, L., 258
Kaizr, V., 126
Kalina, P., 1008
Kalvoda, L., 290, 494, 510, 512, 514
Kameník, M., 1096
Karel, F., 76
Karliclý, P., 1052
Karlík, M., 434, 436, 466, 490, 492, 520
Karovičová, I., 508
Kasíková, S., 850
Kasperczuk, A., 104
Kašpar, J., 774, 776, 782, 794, 824
Kašpar, M., 986, 988
Kašpar, P., 414

Katovský, K., 702, 704, 714
Kavan, M., 1022
Kazda, J., 1056
Kálal, M., 104
Khun, J., 72
Kianička, J., 880
Kibic, K., 1008
Kirchmann, B., 284, 398
Kirchner, G., 62
Klečka, T., 944
Klepáček, R., 512
Kléma, J., 296
Klír, D., 158
Klíma, M., 188
Klír, D., 68, 70, 78
Klouček, F., 874
Kešner, D., 544
Klusoň, J., 674, 692
Kluth, O., 80
Kneppo, P., 790
Kniže, M., 320
Knob, M., 578, 582
Kobliha, D., 758
Kobylka, D., 684
Kocourek, T., 128, 788
Kočandrlová, M., 30
Kohout, K., 222
Kohoutková, A., 914, 924, 926, 928, 936, 940
Kohut, M., 808
Koidl, F., 62
Koiš, M., 1002
Koláčková, J., 900, 990
Kolář, J., 266
Kolesnikov, D., 346
Kolisko, J., 944
Koller, J., 134
Koloros, P., 294
Kolros, A., 702, 708, 714, 716, 718
Komarnitskyy, V., 162, 354
Komínková, D., 726
Koniček, Z., 966
Koničková, J., 36
Konvalinka, P., 540
Konvickova, S., 830, 834
Konvičková, S., 802, 806
Kopecký, L., 460
Kopelent, V., 764

Kopřiva, P., 458
Kosek, P., 372
Koska, B., 988, 996
Košetická, B., 1046
Koudelka, P., 900, 904
Kovařík, P., 746
Kovář, D., 400
Kovář, P., 390, 406
Kovářová, A., 850
Kozelek, P., 808
Kožišek, J., 1046
Koňářík, D., 140
Kramářová, Z., 1012
Kraus, I., 526, 546
Kravárik, J., 158
Kravárik, J., 68, 70, 78
Krákora, J., 314, 404
Králová, D., 670
Krása, J., 864, 900
Kreidl, M., 384
Krejčířiková, H., 906
Kroftová, K., 1000
Kropík, M., 696, 700
Kroupa, S., 288
Krouský, E., 104
Křemen, T., 892, 988
Křístek, V., 914, 928, 936, 940
Kubalík, J., 296
Kubalík, P., 214
Kubart, T., 118, 532
Kubátová, H., 214, 218
Kubes, P., 158
Kubeš, P., 68, 70, 78
Kubešová, M., 678
Kubínová, L., 772
Kuchařík, M., 120
Kučera, J., 382, 756
Kučera, M., 602, 620
Kučerová, A., 586
Kučerová, H., 776
Kudrman, J., 458
Kukaň, V., 968
Kuklík, P., 918, 950
Kuklíková, A., 840, 918
Kulha, P., 386, 394, 416
Kunca, A., 522
Kunčar, R., 598
Kuneš, M., 254
Kunka, A., 694

- Kunz, J., 458
Kuráz, V., 882
Kutil, M., 308
Kužel, T., 1004
Kytka, M., 434, 436
- Lahoda, J., 246
Landa, M., 456, 490, 786
Langr, D., 302
Lastivková, J., 1058
Lauschmann, H., 454, 484, 508
Láník, O.,
Lehovec, F., 906, 1034
Lepš, M., 586, 952
Leso, M., 412
Lettl, J., 256
Lhotská, L., 296, 298, 362, 820
Limpouch, J., 104
Linhart, V., 710
Liska, R., 104, 120, 130
Línková, L., 986
Lojík, V., 232
Lorencz, R., 32
Lučaníková, M., 756
Lukeš, M., 400
Luxemburk, F., 908, 974
Lórencz, R., 244, 266, 280, 282, 328
- Macek, J., 820
Macek, K., 446
Mach, M., 222
Macháček, J., 840
Machovič, V., 448, 744
Machula, P., 924
Macík, K., 1048
Mačat, P., 1082
Maděra, J., 468, 470, 486
Malá, Z., 52, 54, 58, 60
Maleček, K., 850
Maly, P., 694
Mann, H., 330
Mareček, J., 878
Mareš, L., 620
Mareš, T., 662
Marková, J., 888
Maroušek, L., 608
Maršík, F., 802
- Martan, T., 402, 804
Martinez, M., 114
Martini, M., 74
Martiník, J., 792
Masarik, J., 368
Mašek, K., 104
Mašínová, P., 788
Materna, A., 500, 502, 504, 944
Matěcha, J., 590, 798, 800
Matějka, K., 676, 680, 684, 696, 704, 708
Matějka, M., 594
Matoušek, R., 194, 208, 258
Matyáš, P., 268
Matz, V., 384
Mayer, P., 38
Máca, J., 592
Medek, O., 192
Melichar, B., 202, 228, 246, 264
Melichar, J., 626
Mestres, L., 114
Michalík, L., 1094
Michálek, P., 472
Michl, M., 138
Mikl, T., 1040, 1096
Mikš, A., 86, 88, 90, 92, 94, 96, 98, 100, 102, 106
Mikšovský, M., 776
Mikula, R., 868
Mikyška, J., 28
Milka, D., 690
Mindl, P., 656
Mířejovský, J., 464
Mizera, J., 744
Mizerová, G., 744
Molnár, Z., 1058
Mondschein, P., 862, 974
Moták, J., 954
Moucka, L., 694
Moučka, L., 722
Mráz, M., 822
Mrázková, T., 904
Mróz, W., 788
Murafa, N., 530, 534
Musílek, L., 712, 670
Mansfeldová, A., 1016
Mužík, J., 782
Můčka, V., 74, 748, 752, 758
- Mňahončáková, E., 422, 444, 518, 890
- Nahodil, P., 206, 222
Nassereddine, H., 1024, 1038
Nábělková, J., 726
Náprstek, J., 936
Nedbal, I., 454
Nepraš, M., 138
Nesvadbová, S., 610
Netřebská, H., 798
Neufuss, S., 742
Němec, M., 750
Němeček, J., 460, 496
Němeček, P., 318
Němečková, J., 460
Nikl, M., 74
Notaristefani, F., 694
Novák, J., 86, 88, 90, 92, 94, 96, 98, 100, 102, 106, 344
Novák, L., 712
Novák, M., 260
Novák, P., 86, 88, 90, 92, 94, 100, 102, 106, 784
Novák, R., 118, 532, 818
Novák, V., 456
Nováková, D., 52, 54, 58, 60, 532
Nový, Z., 544
Nováková, H., 900
Nováková, L., 286
Novotná, L., 676
Novotný, B., 888, 908, 974
Novotný, C., 1074
Novotný, J., 590, 626
Nový, R., 602, 610, 622
Nožička, J., 590
- Oliva, V., 500, 502, 504
Olivík, S., 30
Ondráčková, J., 450
Oswald, J., 76, 448, 450
- Pacherová, O., 440
Pachner, D., 288
Pačesová, H., 1062
Padevět, P., 460
Paluska, P., 702
Pangrác, J., 348
Papuga, J., 624
Pašek, J., 944
- 1109

- Pavelka, J., 658
 Pavelka, K., 248, 894
 Pavelka, M., 116
 Pavlík, Z., 420, 424, 426, 472, 474, 476, 478, 480, 482
 Pavlov, S., 714
 Pazdera, J., 894
 Pánek, D., 138
 Pánek, M., 468, 486
 Páta, P., 188
 Pech, Z., 288
 Peicheng, H., 340
 Pejchal, J., 74
 Pekař, J., 174
 Pekárek, L., 76
 Pekárek, S., 72, 164, 166
 Peřina, V., 448
 Pešek, P., 434, 436
 Pěnička, R., 614
 Pisarczyk, T., 104
 Pitter, J., 462
 Pichal, J., 108
 Plachý, M., 1076
 Plachý, T., 934
 Plihal, M., 368
 Pluphrach, G., 446, 528
 Podaný, J., 642
 Pohl, K., 592
 Pohl, R., 1066
 Polák, M., 934
 Polcar, T., 52, 54, 58, 60, 202, 532
 Pollert, J., 966
 Ponec, M., 508
 Popelka, L., 594
 Popelová, L., 1006
 Poruba, A., 80
 Pospíšil, J., 1010
 Pospíšil, J., 986, 988
 Pospíšil, M., 728, 742, 746, 752
 Pospíšil, P., 944
 Pospíšilová, E., 898
 Pošík, P., 296
 Prahl, J., 492
 Prajer, M., 450, 1094
 Prajzler, V., 448, 450, 452
 Pražák, J., 778
 Procházka, I., 62, 140, 340, 342
 Procházka, J., 906
 Procházková, J., 776
 Pšenička, J., 398
 Pultarová, I., 22
 Puričer, P., 390, 406
 Purkert, M., 366
 Pytel, J., 948
 Radil, T., 382
 Rataj, J., 678, 704, 706, 708
 Rech, B., 80
 Reháč, B., 324
 Rejha, M., 1038
 Remsa, J., 128
 Renner, O., 84
 Ridziková, A., 722
 Rieger, F., 524
 Rieger, J., 820
 Rosenkrancová, J., 826
 Rosík, V., 790
 Roubal, J., 172
 Roubík, K., 836
 Roubík, K., 188, 764
 Rovnaníková, P., 444, 522
 Rozanek, M., 836
 Růžička, M., 614, 624
 Růžička, T., 636
 Rybár, P., 478
 Rydlo, P., 250, 276
 Rykl, M., 1008
 Ryneš, O., 884
 Řehoř, D., 222
 Řeřicha, P., 968
 Římal, J., 850
 Salaj, M., 976
 Samek, L., 110, 506, 850
 Satrapa, L., 956, 958
 Schmidt, J., 292
 Scholtz, V., 122
 Scholzová, L., 64
 Schroeder, J., 138
 Schröfel, J., 380
 Schwarzer, J., 630
 Sedlacek, R., 830
 Sedláček, R., 826
 Sedlák, P., 456, 510
 Seidenglanz, M., 386, 416
 Seidl, L., 390, 406
 Seiner, H., 456, 786
 Sejk, K., 466
 Sekerešová, Z., 484
 Semenko, S., 440, 442
 Semerák, P., 100
 Shim, J., 74
 Siegl, J., 458, 542
 Silber, R., 742, 748, 752
 Skalský, M., 452
 Sklenář, P., 976
 Sklenka, L., 682, 704
 Skoček, J., 586
 Skvor, Z., 370
 Slabý, P., 1052
 Slaviček, M., 730, 732, 842, 844, 860
 Slavičková, K., 730, 732, 842, 844, 860
 Slavík, P., 326
 Sládek, A., 596
 Sládek, K., 866
 Slámová, M., 466, 520
 Slunečka, M., 688
 Smetana, K., 788
 Smitka, D., 1010
 Smišek, O., 234
 Smrčka, P., 220, 774, 776, 782, 794, 796, 824
 Smrž, M., 112, 136
 Sochor, M., 810, 812, 814, 816
 Sodomka, J., 710
 Sokol, V., 374
 Solovieva, N., 74
 Somolová, A., 584
 Sopko, B., 710, 758
 Sopko, V., 110, 506, 850
 Součková, N., 594
 Soukup, M., 1038
 Soukup, P., 210
 Soyková, V., 1036
 Springer, J., 80
 Stavovčík, B., 1040
 Stejskal, J., 452
 Stejskal, P., 1098
 Stoklasová, D., 488
 Straka, P., 112, 136
 Strnadová, N., 844
 Studecká, P., 932
 Studnička, J., 840, 878, 906

- Studnička, V., 116, 788
 Stunová, B., 608
 Stupka, M., 792
 Surovec, Z., 138
 Svítek, M., 1102, 1104
 Svoboda, J., 222, 624, 1082
 Svoboda, L., 498, 538, 886
 Svoboda, P., 852
 Svrček, A., 222
 Synek, L., 356, 660
 Syrovatka, B., 658
 Sýkora, M., 888
 Szabó, Z., 766
- Šafařík, P., 578
 Šafránková, J., 912, 1068
 Šanda, M., 930, 962
 Šebela, P., 676
 Šebera, J., 738
 Šebesta, F., 754, 756
 Šedlbauer, M., 682
 Šejnoha, J., 906
 Šenberger, T., 994, 1010, 1014
 Šesták, J., 1066
 Ševčík, O., 1008
 Šilarová, Š., 944
 Šimeček, I., 178, 180, 182,
 184
 Šiška, F., 454
 Šittner, P., 456
 Šiňor, M., 104
 Škabrada, J., 1008
 Škandera, D., 56
 Škranc, P., 1008
 Škvor, Z., 362
 Šlapeta, V., 1000
 Šmíd, O., 1076
 Šmíd, R., 384, 768
 Šnorek, M., 822
 Šoch, M., 216, 328
 Šolcová, A., 40
 Šourek, B., 632
 Špaček, J., 390, 406
 Španiel, M., 662
 Špírková, J., 448, 450, 452
 Štamberg, K., 734
 Štaubr, R., 718
 Štekl, I., 142, 152
 Štědrý, F., 1014
 Štěpánek, I., 534
- Štrausová, K., 860
 Štrobl, K., 910
 Štroner, M., 986, 988
 Štukjunger, P., 312
 Šulcová, T., 1064
 Šumbera, J., 454
 Šuláková, J., 754
 Švehlíková, J., 790
 Švihla, M., 334
 Šťastný, B., 730, 732, 842,
 844, 860
- Teplý, B., 940
 Tesárek, P., 430, 432, 474,
 476, 478, 486
 Thinova, L., 690, 692, 694
 Thinová, L., 674
 Tichý, P., 462
 Tischler, D., 76, 440, 442,
 530, 758
 Tolar, J., 66
 Toman, J., 444, 890
 Tomaschko, O., 858
 Tomek, G., 1032
 Trinkewitz, J., 310
 Trkal, J., 1072
 Trnka, M., 366
 Trojek, T., 670, 672, 692, 694
 Trtík, K., 916
 Trubačová, M., 630
 Třebický, T., 396
 Tvrdlík, P., 178, 180, 192
 Tvrdlíková, D., 1026
 Tydlitát, V., 432, 522
 Tyšler, M., 790
 Týfa, L., 1042
- Uhlíř, I., 260
 Uhlířová, K., 854
 Urban, P., 332
 Urbánek, J., 650
 Urlich, P., 1008
- Vacek, K., 76
 Vacek, V., 150, 154, 156
 Vachtl, M., 1042
 Vacková, S., 76, 442
 Valášek, M., 170
 Valchářová, V., 1006
 Valentin, J., 856
- Vališová, K., 582, 764, 800
 Vančata, P., 186
 Vanecek, M., 80
 Vanek, T., 306
 Vaněk, F., 322, 394
 Vaniš, L., 1060
 Vavříčka, R., 618
 Váchal, P., 130
 Vávrová, V., 1032
 Včelák, J., 320, 414
 Vecková, J., 26
 Vedda, A., 74
 Vejmelka, R., 890
 Vejputsková, J., 814, 816
 Vejražka, F., 406
 Veselý, R., 730
 Věbr, L., 1086, 1088, 1090,
 1092
 Vičan, M., 406
 Vilímeck, M., 810, 812, 814,
 816
 Vimmrová, A., 498
 Vinš, V., 154
 Vítíngerová, Z., 952
 Vitek, J., 928
 Vítek, K., 662, 664
 Vítek, S., 408
 Vítů, T., 532
 Vlasák, O., 916
 Vlček, A., 738
 Vlček, P., 1008
 Vlčková, K., 732
 Vobecký, J., 346, 358
 Vobecký, M., 718
 Vodrážka, J., 190, 278
 Vogel, T., 930, 962
 Vokáč, M., 902
 Vokál, A., 742
 Vokurka, A., 972
 Vokurka, L., 462
 Volf, M., 1054
 Voloshinovskii, A., 74
 Vondřích, J., 580, 616
 Vonka, M., 920
 Vopálka, D., 686, 740
 Voráček, M., 264
 Voráčková, Š., 42
 Vorel, V., 906
 Vorlík, P., 1006, 1008
 Votlučka, J., 620

- Voves, J., 348, 396
Vozár, V., 284
Vrabec, M., 640
Vraný, T., 848, 938
Vratislav, S., 114, 290, 494,
510, 514, 516
Vrána, J., 792
Vrána, K., 864, 900, 904
Vrba, P., 64
Vrbová, M., 64
Xтвѣтъ. 'XO'768
Vtípil, J., 832
Vuilleumier, J., 152
Vybíral, P., 612
Výdra, D., 658
Výhnálek, R., 896
Vysoký, O., 318
Výtlačil, D., 1084
Výborný, Z., 394
- Wagener, P., 138
Wald, F., 960
- Wasserbauer, R., 944
Winklerová, A., 464
Witzany, J., 906, 944
- Yoon, D., 74
Yoshikawa, A., 74
- Zahradnický, T., 32
Zahradník, J., 1078
Zahradník, P., 350
Zaoralová, J., 850, 992, 998
Záleská, J., 894
Záliš, S., 738
Závodný, V., 370
Zbořil, V., 630
Zdenek, J., 368
Zdimal, V., 690
Zeman, J., 584, 678, 680, 684
Zeman, L., 1048
Zendulka, J., 124, 146
Zerbs, J., 138
- Zhongping, Z., 340
Zigler, R., 944
Zib, A., 676
Zítek, P., 272
Zlámaný, M., 994, 1006
Zmrhal, V., 846
Zralý, M., 1076
Zvánovec, S., 364
Zýka, J., 536
- Žáček, J., 646
Ždiňák, J., 790
Žďánský, K., 76
Žďárek, J., 228
Ženka, R., 326